Hans Lambers · Rafael S. Oliveira

Plant Physiological Ecology

Third Edition

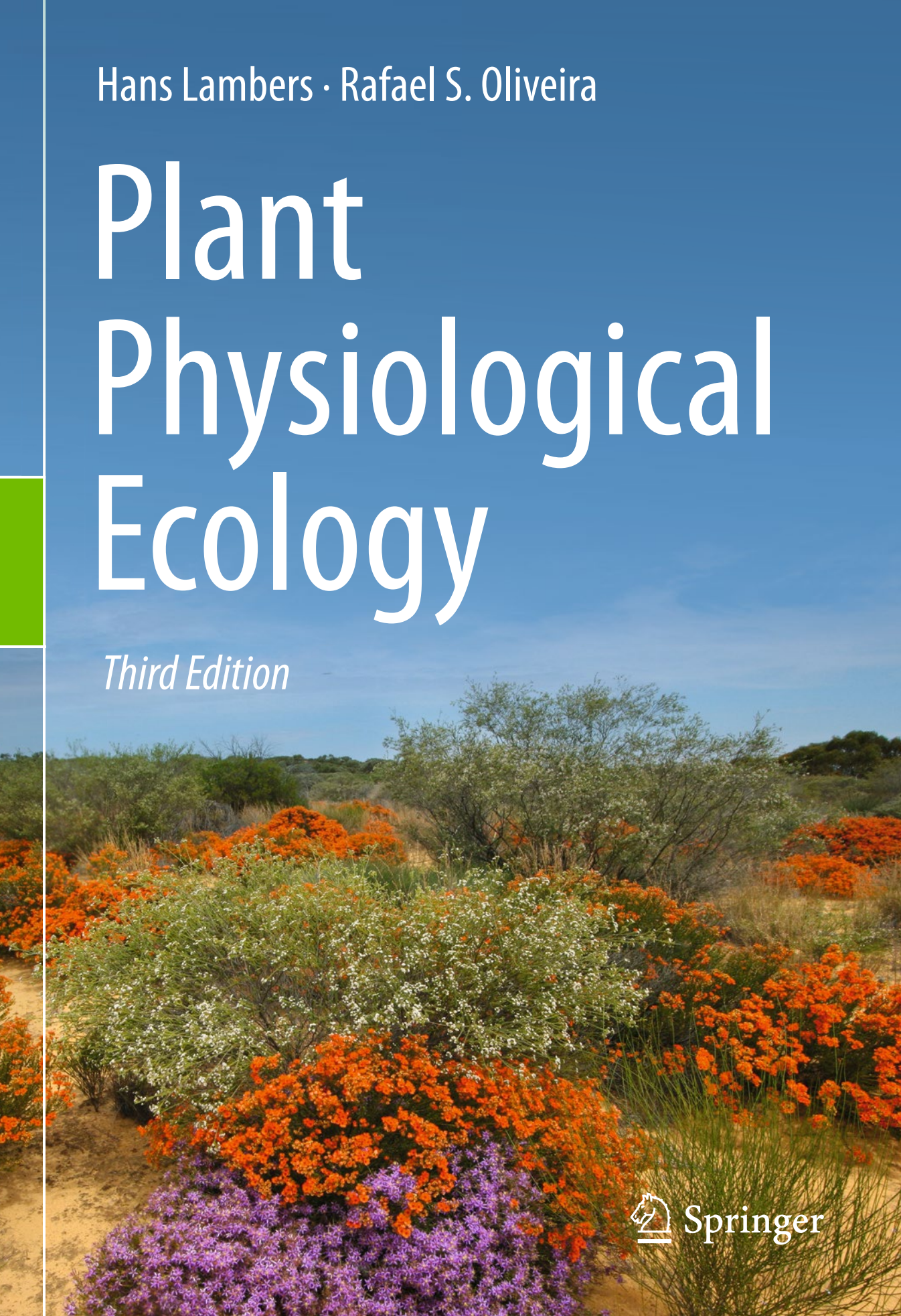

Springer

Plant Physiological Ecology

Hans Lambers • Rafael S. Oliveira

Plant Physiological Ecology

Third Edition

Springer

Hans Lambers
School of Biological Sciences
University of Western Australia
Crawley, WA, Australia

Rafael S. Oliveira
Institute of Biology
University of Campinas
Campinas, Brazil

ISBN 978-3-030-29638-4 ISBN 978-3-030-29639-1 (eBook)
https://doi.org/10.1007/978-3-030-29639-1

Cover Illustration: Photo credit: Hazel Dempster.

This Springer imprint is published by the registered company Springer Nature Switzerland AG.
The registered company address is: Gewerbestrasse 11, 6330 Cham, Switzerland

Foreword Third Edition

How do and will 'plants cope' in the face of global environmental change? Temperatures, carbon dioxide, and other trace gases are rising at an unprecedented rate. Urbanization, with its expanding and destructive human footprint, continues to sweep across and impact all ecosystems. Climatic extremes, like hurricane- or typhoon-associated floods, deep frosts and even deeper snows, and the most extreme droughts ever recorded are now part of every day, every year, and in every place. These are, Earth's 'new normals'. And as alarming as these facts are, the field of *plant physiological ecology* (P^2E) thrives, because it is a field of science that is and will provide some of the most critical evidence and fundamental understanding about how the diversity of plant adaptations, at the center of its investigations, will allow plants to handle the conditions of the Anthropocene. Such understanding will also reveal how we can best use the information gathered from basic ecophysiological research to help stakeholders – humanity – 'change course' and take new roads to crafting solutions for preserving biodiversity and the planet that harbors it *writ large*.

Investigations focused on the physiological adaptations plants have come to possess over their long evolutionary history can teach us not only about the nature of the adaptation-environment nexus, but also reveal what to expect when plants are challenged by the conditions they now face on Earth that are outside of their previous (evolutionary) experiences. Since the last addition of this book, the aforementioned issues have become the centerpiece around which modern plant ecophysiological investigations often hinge. The data plant physiological ecologists gather on how plants function and cope with environmental challenges also serve to inform other types of plant research at levels of biological organization, both below at the cellular and molecular scales and above at the population, community, and ecosystem levels. Plant ecophysiological information also continues to be integral to the study of biological evolution, as it helps to reveal how adaptations are identified and how they serve the plants that possess them. For me, I have long advocated for the central role that plant physiological ecology has, can, and should play in our fundamental understanding of plant adaptations (*e.g.*, the field of physiological ecology is essentially studying the 'basis' of plant adaptations to their biotic and abiotic environments). But plant ecophysiology is also likely to play a greater and greater role in designing best practices for mitigating humanity's assault on the organisms that sustain us and Earth – plants.

As the third edition of this textbook emerges, the students and scientists who will build upon the information it contains have a new responsibility, a new weight, and new opportunities to add their voices in new ways. As a community, plant ecophysiologists also have a frontier of new prospects to not just build upon our fundamental knowledge, but to also innovate and surprise 'science' and the academy. New technological advances in microscopic imaging, in quantifying fluxes into and out of plants (at scales from the sub-cellular to the globe), in characterizing with much more rigor plant interactions with their microbiome, and in modeling form-function relationships and how they inform plant trait evolution and ecosystem functions are firmly part of the 'new toolkit' of modern plant ecophysiology. Healthy debate on best (new) methods and best practices still marshals on and this is good – good for the credibility of the information we as a community are providing to the plant sciences and for those who are adding their talents and ideas on how we can deepen our understanding of plant functions. Without debate and opinions, we cease to have a productive dialogue, and our science becomes 'comfortable', even complacent and risks becoming less relevant. But plant physiological ecology is very relevant in the many ways highlighted above, and may more ways.

Students continue to ponder the age-old questions of – what will I do in my life ahead, how can I make a difference with my profession or vocation, and how can I, we, make our planet a better place? Such questions move to answer – through knowledge, understanding, a belief in evidence, a passion for 'place', and then participating in *doing* plant physiological ecology (P^2E). P^2E is a hub around which the plant world and the Earth revolves – onwards.

Berkeley, CA, USA Todd Dawson
May 2019

Acknowledgments

Numerous people have contributed to the text and illustrations in this book. Most importantly, Terry Chapin and Thijs Pons provided significant input into chapters that appeared in earlier editions and formed the basis of revised texts in this third edition. Others commented on sections and chapters, provided photographic material, or made electronic files of graphs and illustrations available. In addition to those who wrote book reviews or sent us specific comments on the first and second edition of *Plant Physiological Ecology*, we wish to thank the following colleagues, in alphabetical order, for their valuable input into the third edition: Felipe Albornoz, Paulo Bittencourt, Dev Britto, Brendan Choat, Tim Colmer, Elaine Davison, Wenli Ding, Cleiton Eller, Patrick Hayes, Bethany Huot, Hamlyn Jones, Ulrike Mathesius, Ian Max Møller, Francis Nge, Ko Noguchi, Ole Pedersen, Luciano Pereira, Kenny Png, Rafael Ribeiro, Megan Ryan, Lucas Silva, Fernando Silveira, Christiana Staudinger, Ichiro Terashima, François Teste, Robert Turgeon, Erik Veneklaas, and Rafael Villar.

The authors

Contents

About the Authors

Hans Lambers is an Emeritus Professor of Plant Biology at the University of Western Australia, in Perth, Australia, and a Distinguished Professor at China Agricultural University, in Beijing, China. He did his undergraduate degree at the University of Groningen, the Netherlands, followed by a PhD project on effects of hypoxia on flooding-sensitive and -tolerant *Senecio* species at the same institution. From 1979 to 1982, he worked as a postdoc at the University of Western Australia, Melbourne University, and the Australian National University in Australia, working on respiration and nitrogen metabolism. After a postdoc at his alma mater, he became Professor of Ecophysiology at Utrecht University, the Netherlands, in 1985, where he focused on plant respiration and the physiological basis of variation in growth rate among herbaceous plants. In 1998, he moved to the University of Western Australia, where he focused on plant mineral nutrition, especially in legume crops and native species occurring on severely phosphorus-impoverished soils in a global biodiversity hotspot in southwestern Australia and southeastern Brazil. He has been Editor-in-Chief of the journal *Plant and Soil* since 1992 and featured on the first ISI list of highly cited authors in the field of animal and plant sciences (since 2002), and on several other ISI lists more recently. He was elected Fellow of the Royal Netherlands Academy of Arts and Sciences in 2003, and Fellow of the Australian Academy of Science in 2012. He received Honorary Degrees from three Universities and from the Academy of Sciences in China.

Rafael S. Oliveira is a Professor of Ecology at the University of Campinas (UNICAMP), Brazil. He did his undergraduate degree at the University of Brasília, Brazil, followed by a PhD on water relations of Amazonian and savanna trees at the University of California, Berkeley, USA. He worked as a postdoc from 2005 to 2007 at the National Institute of Space Research and the University of São Paulo in Brazil to improve the representation of key vegetation processes on climate models, followed by a project on the ecohydrology of tropical montane cloud forests. In 2007, he became Professor at UNICAMP. His research focuses on plant hydraulics, vegetation-climate feedbacks, and mineral nutrition of tropical plants. He is an Associate Editor for the journal *Functional Ecology* and Section Editor for *Plant and Soil*.

Abbreviations

a	radius of a root (a_r) or root plus root hairs (a_e)
A	rate of CO_2 assimilation; also total root surface
A_n	net rate of CO_2 assimilation
A_f	foliage area
A_{max}	light-saturated rate of net CO_2 assimilation at ambient C_a
A_s	sapwood area
ABA	abscisic acid
ADP	adenosine diphosphate
AM	arbuscular mycorrhiza
AMP	adenosine monophosphate
APAR	absorbed photosynthetically active radiation
ATP	adenosine triphosphate
b	individual plant biomass; buffer power of the soil
B	stand biomass
c_s	concentration of the solute
C	nutrient concentration in solution; also convective heat transfer
C_3	photosynthetic pathway in which the first product of CO_2 fixation is a 3-carbon intermediate
C_4	photosynthetic pathway in which the first product of CO_2 fixation is a 4-carbon intermediate
C_a	atmospheric CO_2 concentration
C_c	CO_2 concentration in the chloroplast
C_i	intercellular CO_2 concentration
C_{li}	initial nutrient concentration
C_{min}	solution concentration at which uptake is zero
C:N	carbon:nitrogen ratio
CAM	crassulacean acid metabolism
CC	carbon concentration
CE	carbohydrate equivalent
chl	chlorophyll
CPF	carbon dioxide production value
d	plant density; also leaf dimension
D	diffusivity of soil water
D_e	diffusion coefficient of ion in soil
DHAP	dihydroxyacetone phosphate
DM	dry mass
DNA	deoxyribonucleic acid

e	water vapor pressure in the leaf (e_i; or e_l in section 2.5 of the plant's energy balance) or atmosphere (e_a); also emissivity of a surface
E	transpiration rate
f	tortuosity
F	rate of nutrient supply to the root surface; also chlorophyll fluorescence, minimal fluorescence (F_0), maximum (F_m), in a pulse of saturating light (F_m'), variable (F_v)
$FAD(H_2)$	flavin adenine dinucleotide (reduced form)
FM	fresh mass
FR	far-red
g	diffusive conductance for CO_2 (g_c) and water vapor (g_w); boundary layer conductance (g_a); mesophyll conductance (g_m); stomatal conductance (g_s); boundary layer conductance for heat transport (g_{ah})
GA	gibberellic acid
GE	glucose equivalent
GOGAT	glutamine 2-oxoglutarate aminotransferase
HCH	hydroxycyclohexenone
HIR	high-irradiance response
I	irradiance, above (I_o) or beneath (I) a canopy; irradiance absorbed; also nutrient inflow
I_{max}	maximum rate of nutrient inflow
IAA	indoleacetic acid
IR_s	short-wave infrared radiation
J	rate of photosynthetic electron flow
J_{max}	maximum rate of photosynthetic electron flow measured at saturating I and C_a
J_v	water flow
k	rate of root elongation; extinction coefficient for light
K	carrying capacity (*e.g., K* species)
k_{cat}	catalytic constant of an enzyme
K_i	inhibitor concentration giving half-maximum inhibition
K_m	substrate concentration at half V_{max} (or I_{max})
l	leaf area index
L	rooting density; also latent heat of evaporation; also length of xylem element
L_p	root hydraulic conductance
LAI	leaf area index
LAR	leaf area ratio
LFR	low-fluence response
LHC	light-harvesting complex
LMA	leaf mass per unit area
LMR	leaf mass ratio
LR	long-wave infrared radiation that is incident (LR_{in}), reflected (LR_r), emitted (LR_{em}), absorbed (SR_{abs}), or net incoming (LR_{net}); also leaf respiration on an area (LR_a) and mass (LR_m) basis

mRNA	messenger ribonucleic acid
miRNA	micro ribonucleic acid
M	energy dissipated by metabolic processes
ME	malic enzyme
MRT	mean residence time
N_w	mol fraction, that is, the number of moles of water divided by the total number of moles
NAD(P)	nicotinamide adenine dinucleotide(phosphate) (in its oxidized form)
NAD(P)H	nicotinamide adenine dinucleotide(phosphate) (in its reduced form)
NAR	net assimilation rate
NDVI	normalized difference vegetation index
NEP	net ecosystem production
NIR	near-infrared reflectance; net rate of ion uptake
NMR	nuclear magnetic resonance
NP	nitrogen productivity, or nutrient productivity
NPP	net primary production
NPQ	nonphotochemical quenching
NUE	nitrogen-use efficiency, or nutrient-use efficiency
p	vapor pressure
p_o	vapor pressure of air above pure water
P	atmospheric pressure; also turgor pressure
P_{fr}	far-red-absorbing configuration of phytochrome
Pi	inorganic phosphate
P_r	red-absorbing configuration of phytochrome
PAR	photosynthetically active radiation
PC	phytochelatins
PEP	phosphoenolpyruvate
PEPC	phosphoenolpyruvate carboxylase
PEPCK	phosphoenolpyruvate carboxykinase
pH	hydrogen ion activity; negative logarithm of the H^+ concentration
PGA	phosphoglycerate
pmf	proton-motive force
PNC	plant nitrogen concentration
PNUE	photosynthetic nitrogen-use efficiency
PQ	photosynthetic quotient; also plastoquinone
PR	pathogenesis-related protein
PS	photosystem
PV′	amount of product produced per gram of substrate
q_N	quenching of chlorophyll fluorescence due to nonphotochemical processes
*q*P	photochemical quenching of chlorophyll fluorescence
Q	ubiquinone (in mitochondria), in reduced state (Q_r = ubiquinol) or total quantity (Q_t); also quinone (in chloroplast)
Q_{10}	temperature coefficient
Q_A	primary electron acceptor in photosynthesis

r	diffusive resistance, for CO_2 (r_c), for water vapor (r_w), boundary layer resistance (r_a), stomatal resistance (r_s), mesophyll resistance (r_m); also radial distance from the root axis; also respiration; also growth rate (in volume) in the Lockhart equation; also proportional root elongation; also intrinsic rate of population increase (*e.g., r* species)
r_i	spacing between roots
r_o	root diameter
R	red
R	radius of a xylem element; also universal gas constant
R_a	molar abundance ratio of $^{13}C/^{12}C$ in the atmosphere
R_d	dark respiration
R_{day}	dark respiration during photosynthesis
R_e	ecosystem respiration
R_p	whole-plant respiration; also molar abundance ratio of $^{13}C/^{12}C$ in plants
R_h	heterotrophic respiration
$R*$	minimal resource level utilized by a species
RGR	relative growth rate
RH	relative humidity of the air
RMR	root mass ratio
RNA	ribonucleic acid
RQ	respiratory quotient
RR	rate of root respiration
RuBP	ribulose-1,5-bisphosphate
Rubisco	ribulose-1,5-bisphosphate carboxylase/oxygenase
RWC	relative water content
S	nutrient uptake by roots
$S_{c/o}$	specificity of carboxylation relative to oxygenation by Rubisco
SHAM	salicylichydroxamic acid
SLA	specific leaf area
SMR	stem mass ratio
SR	short-wave solar radiation that is incident (SR_{in}), reflected (SR_r), transmitted (SR_{tr}), absorbed (SR_{abs}), used in photosynthesis (SR_A), emitted in fluorescence (SR_{FL}), or net incoming (SR_{net}); also rate of stem respiration
SRL	specific root length
$t*$	time constant
tRNA	transfer ribonucleic acid
T	temperature
T_L	leaf temperature
TCA	tricarboxylic acid
TR	total radiation that is absorbed (TR_{abs}) or net incoming (TR_{net})
u	wind speed
UV	ultraviolet
V	volume

V_c	rate of carboxylation
V_o	rate of oxygenation
V_{cmax}	maximum rate of carboxylation
$V_w{}^o$	molar volume of water
VIS	visible reflectance
VLFR	very low fluence response
V_{max}	substrate-saturated enzyme activity
VPD	vapor pressure deficit
w	mole fraction of water vapor in the leaf (w_i) or atmosphere (w_a)
WUE	water-use efficiency
Y	yield threshold (in the Lockhart equation)
γ	surface tension
Γ	CO_2-compensation point
$\Gamma*$	CO_2-compensation point in the absence of dark respiration
δ	boundary layer thickness; also isotopic content
Δ	isotopic discrimination
ΔT	temperature difference
ε	elastic modulus; also emissivity
η	viscosity constant
θ	curvature of the irradiance response curve; also volumetric moisture content (mean value, θ', or at the root surface, θ_a)
λ	energy required for transpiration
μ_w	chemical potential of water
μ_{wo}	chemical potential of pure water under standard conditions
σ	Stefan-Boltzmann constant
ϕ	quantum yield (of photosynthesis); also yield coefficient (in the Lockhart equation); also leakage of CO_2 from the bundle sheath to the mesophyll; also relative yield of de-excitation processes
Ψ	water potential
Ψ_{air}	water potential of the air
Ψ_m	matric potential
Ψ_p	pressure potential; hydrostatic pressure
Ψ_π	osmotic potential

Introduction: History, Assumptions, and Approaches

1

1.1 What Is Ecophysiology?

Plant ecophysiology is an experimental science that seeks to describe the **physiological mechanisms** underlying ecological observations. In other words, ecophysiologists, or physiological ecologists, address ecological questions about the controls over the growth, reproduction, survival, mortality, abundance, and geographical distribution of plants, as these processes are affected by interactions between plants with their physical, chemical, and biotic environment. These ecophysiological patterns and mechanisms can help us understand the functional significance of specific plant traits and their evolutionary heritage. Ecophysiological studies also provide the basis for a mechanistic understanding of community assembly and ecosystem functioning.

The questions addressed by ecophysiologists are derived from a higher level of integration, *i.e.* from 'ecology' in its broadest sense, including agriculture, horticulture, forestry, and environmental sciences. However, the ecophysiological explanations often require mechanistic understanding at a lower level of integration (physiology, biochemistry, biophysics, molecular biology). It is, therefore, quintessential for an ecophysiologist to have an appreciation of both ecological questions and biophysical, biochemical, and molecular methods and processes. In addition, many societal issues, often pertaining to agriculture, environmental change, or nature conservation, benefit from an ecophysiological perspective. A modern ecophysiologist thus requires a good understanding of both the molecular aspects of plant processes, the functioning of the intact plant in its environmental context, and the links of plant functioning with broader ecological processes.

1.2 The Roots of Ecophysiology

Plant ecophysiology aims to provide mechanistic explanations for ecological questions relating to survival, distribution, abundance, interactions of plants with other organisms, and the organization of communities and the functioning of ecosystems. Why does a particular species live where it does? How can it grow there successfully, and why is it absent from other environments? These questions were initially asked by geographers who described the global distributions of plants (Schimper 1898; Walter 1974). They observed consistent patterns of morphology associated with different environments, and concluded that these differences in morphology must be important in explaining plant distributions. Geographers, who know climatic patterns, could therefore predict the predominant life forms of plants (Holdridge 1947). For example, many desert plants have small, thick leaves that minimize the heat load and danger of overheating in hot environments, whereas shade plants often have large, thin leaves that maximize light interception. These observations of

H. Lambers, R. S. Oliveira, *Plant Physiological Ecology*, https://doi.org/10.1007/978-3-030-29639-1_1

morphology provided the impetus to investigate the physiological traits of plants from contrasting physical environments (Blackman 1919; Pearsall 1938; Ellenberg 1953).

Although ecophysiologists initially emphasized physiological responses to the abiotic environment [*e.g.*, to calcareous *vs.* acidic substrates (Tansley 1917; Clarkson 1966) or dry *vs.* flooded soils (Conway 1940; Crawford 1978)], physiological interactions with other plants, animals, and microorganisms also benefit from an understanding of ecophysiology. As such, ecophysiology is an essential element of every ecologist's training.

A second impetus for the development of ecophysiology came from agronomy. Even today, agricultural production in industrialized nations is limited to 25% of its potential by drought, infertile soils, and other environmental stresses (Boyer 1985). A major objective of agricultural research has always been to develop crops that are less sensitive to environmental stress so they can withstand periods of unfavorable weather or be grown in less favorable habitats. For this reason, agronomists and ecophysiologists have studied the mechanisms by which plants respond to or resist environmental stresses. Because some plants grow naturally in extremely infertile, dry, or salty environments, ecophysiologists were curious to know the mechanisms by which this is accomplished.

Plant ecophysiology is the study of physiological responses to the environment. The field developed rapidly as a relatively unexplored interface between ecology and physiology. Ecology and agronomy provided the questions, and physiology provided the tools to determine mechanism. Techniques that measured the microenvironment of plants, their water relations, and their patterns of carbon exchange became typical tools of the trade in plant ecophysiology. With time, these studies have explored the mechanisms of physiological adaptation at ever finer levels of detail, from the level of the whole plant to its biochemical and molecular bases. For example, initially plant growth was described in terms of changes in plant mass. Development of portable equipment for measuring leaf gas exchange enabled ecologists to measure rates of carbon gain and loss by individual leaves (Wright et al. 2004). Growth analyses documented carbon and nutrient allocation to roots and leaves, and rates of production and death of individual tissues. These processes together provide a more thorough explanation for differences in plant growth in different environments (Lambers and Poorter 1992). Studies of plant water relations and mineral nutrition provide additional insight into controls over rates of carbon exchange and tissue turnover. More recently, we have learned many details about the biochemical basis of photosynthesis and respiration in different environments, and, finally, about the molecular basis for differences in key photosynthetic and respiratory proteins. This mainstream of ecophysiology has been highly successful in explaining why plants are able to grow where they do. Ecophysiological studies have also been instrumental in providing new insights about the mechanisms of species coexistence through niche differentiation, the conservation of natural communities, and the scaling of physiological processes to ecosystems.

1.3 Physiological Ecology and the Distribution of Organisms

Although there are 285,000 species of vascular plants (Magallón and Hilu 2009), a series of **filters** eliminates most of these species from any given site, and restricts the actual vegetation to a relatively small number of species (Fig. 1.1). Many species are absent from a given plant community for **historical reasons**. They may have evolved in a different region and never dispersed to the site under consideration. For example, the tropical alpines of South America and Africa have few species in common, despite similar environmental conditions, whereas eastern Russia and Alaska have very similar species composition because of extensive migration of species across a land bridge connecting these regions when Pleistocene glaciations lowered sea level 20,000–100,000 years ago (Graham 2018).

Of those species that arrive at a site, many lack the physiological traits to survive the physical

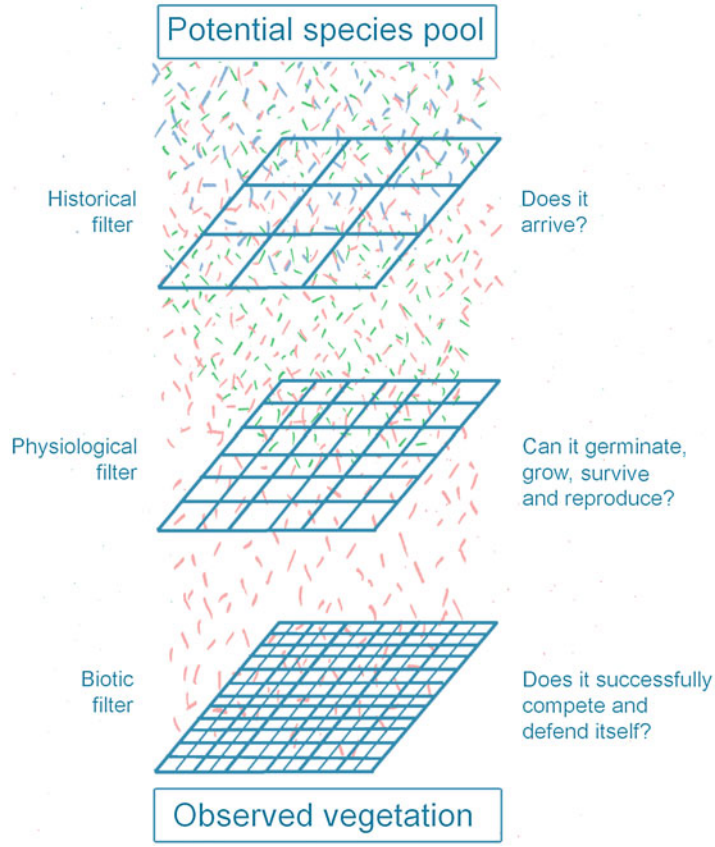

Fig. 1.1 Historical, physiological, and biotic filters that determine the species composition of vegetation at a particular site.

environment. For example, whalers inadvertently brought seeds of many weedy species to Svalbard, north of Norway, and to Barrow, in northern Alaska. However, in contrast to most temperate regions, there are currently no exotic weed species in these northern sites (Billings 1973). Clearly, the **physical environment** filtered out many species that may have arrived, but lacked the physiological traits to grow, survive, and reproduce in the Arctic.

Biotic interactions exert an additional filter that eliminates many species that may have arrived and are capable of surviving the physical environment. Most plant species that are transported to different continents as ornamental or food crops never spread beyond the areas where they were planted, because they cannot compete with native species (a biotic filter). Sometimes, however, a plant species that is introduced to a new place without the diseases or herbivores that restricted its distribution in its native habitat becomes an aggressive invader. For example, *Opuntia ficus-indica* (prickly pear) in Australia, *Solidago canadensis* (golden rod) in Europe, *Melinis minutiflora* (molasses grass) in Brazil, *Cytisus scoparius* (Scotch broom) in North America and *Acacia saligna* (orange wattle) in South Africa. Because of biotic interactions, the actual distribution of a species (realized niche, as determined by **ecological amplitude**) is more restricted than the range of conditions where it can grow and reproduce (its fundamental niche, as determined by **physiological amplitude**) (Fig. 1.2).

Historical, physiological and biotic filters are constantly changing and interacting. Human and natural introductions or extinctions of species, chance dispersal events, and extreme events

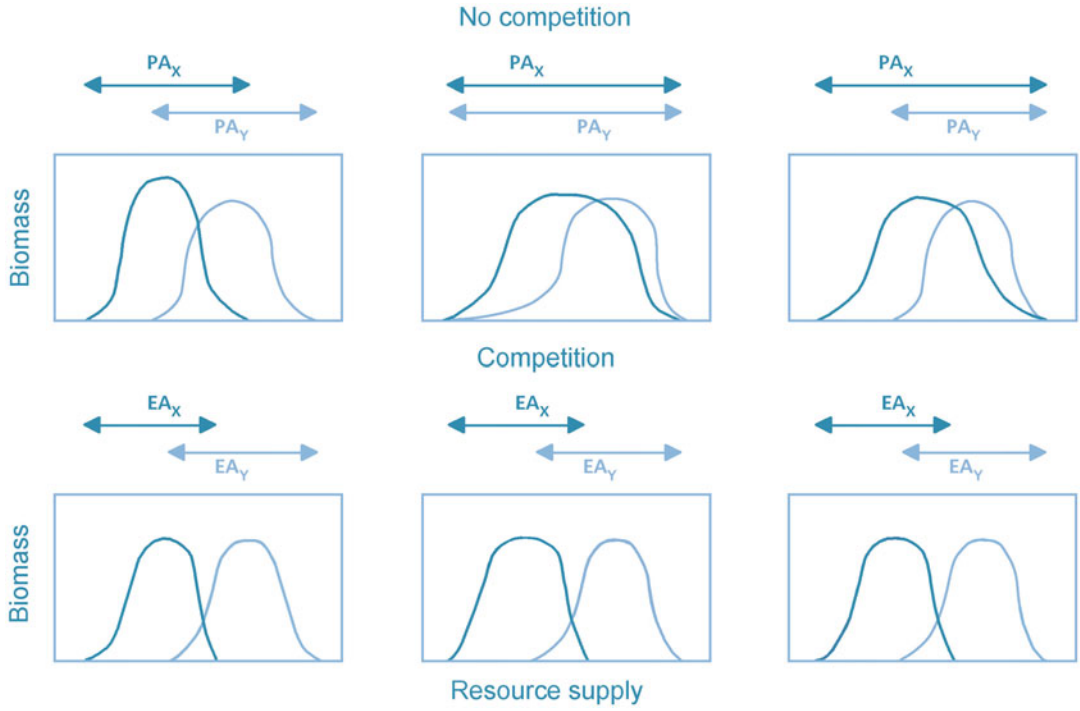

Fig. 1.2 Biomass production of two hypothetical species (x and y) as a function of resource supply. In the absence of competition (upper panels), the physiological amplitude of species x and y (PA_x and PA_y, respectively) define the range of conditions over which each species can grow. In the presence of competition (lower panels), plants grow over a narrower range of conditions (their ecological amplitude, EA_x and EA_y) that is constrained by competition from other species. A given pattern of species distribution (*e.g.*, that shown in the bottom panels) can result from species that differ in their maximum biomass achieved (left-hand pair of graphs), shape of resource response curve (center pair of graphs), or physiological amplitude (right-hand pair of graphs). Adapted from Walter (1974).

such as volcanic eruptions or floods change the species pool at a site. Changes in climate, weathering of soils, and introduction or extinction of species change the physical and biotic environment. Those plant species that can grow and reproduce under the new conditions or respond evolutionarily so that their physiology provides a better match to this environment will persist. Because of these interacting filters, the species present at a site are simply those that arrived, survived, and reproduced. There is no reason to assume that the species present at a site attain their maximal physiologically possible rates of growth and reproduction (Vrba and Gould 1986). In fact, controlled-environment studies typically demonstrate that a given species is most common under environmental conditions that are distinctly suboptimal for most physiological processes, because biotic interactions prevent most species from occupying the most favorable habitats (Fig. 1.2).

Given the general principle that species that are present at any site reflects their arrival and survival, why does plant species diversity differ among sites that differ in soil fertility (Huston 1980), especially soil phosphorus availability (Lambers et al. 2010)? To answer this question, we need detailed ecophysiological information on the various mechanisms that allow plants to compete and co-exist in different environments (Laliberté et al. 2015). The information that is required will depend on which ecosystem is studied. In biodiverse (*i.e.* species-rich), nutrient-poor, tropical rainforests, with a wide variation in light climate, plant traits that enhance the conversion of light into biomass or conserve carbon

are likely important for an understanding of plant diversity. In the biodiverse, nutrient-impoverished habitats of South Africa, Australia, and Brazil, however, variation in root traits that are associated with efficient nutrient acquisition and use offers clues to understanding plant species diversity (Lambers et al. 2010; Oliveira et al. 2015).

1.4 Time Scale of Plant Response to Environment

We define **stress** as an environmental factor that reduces the rate of some physiological process (*e.g.*, growth or photosynthesis) below the maximum rate that the plant could otherwise sustain. Stress can be generated by abiotic and/or biotic factors, but is stress only for species that evolved in its absence. Examples of stress include low nitrogen availability, toxic metals, high salinity, and shading by neighboring plants. The immediate response of the plant to stress is a reduction in performance (Fig. 1.3). Plants compensate for the detrimental effects of stress through many mechanisms that operate over different time scales, depending on the nature of the stress and the physiological processes that are affected. Together, these compensatory responses enable the plant to maintain a relatively constant rate of physiological processes, despite occurrence of stresses that periodically reduce performance. If a plant is going to be successful in a stressful environment, there must be some degree of stress **resistance**. Mechanisms of stress resistance differ widely among species. They range from **avoidance** of the stress, *e.g.*, in deep-rooting species growing in a low-rainfall area, to stress **tolerance**, *e.g.*, in Mediterranean species that can cope with a low leaf water content.

Physiological processes differ in their sensitivity to stress. The most meaningful physiological processes to consider are growth and reproduction, which integrate the stress effects on fine-scale physiological processes as they relate to fitness, *i.e.* differential survival and reproduction in a competitive environment. To understand the mechanism of plant response, however, we must consider the response of individual processes at a finer scale (*e.g.*, the response of photosynthesis or of light-harvesting pigments to a change in light intensity). We recognize at least three distinct time scales of plant response to stress:

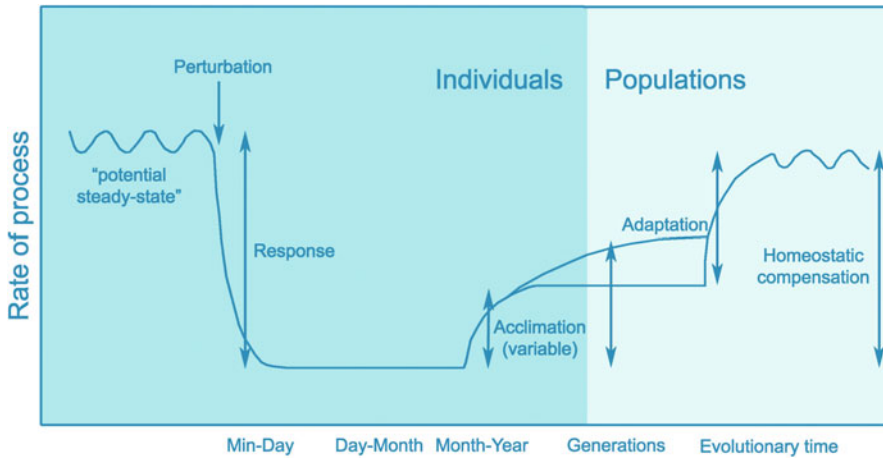

Fig. 1.3 Typical time course of plant response to environmental stress. The immediate response to environmental stress is a reduction in physiological activity. Through *acclimation*, individual plants compensate for this stress such that activity returns toward the control level. Over evolutionary time, populations *adapt* to environmental stress, resulting in a further increase in activity level toward that of the unstressed unadapted plant. The total increase in activity resulting from acclimation and adaptation is the *in situ* activity observed in natural populations and represents the total homeostatic compensation in response to environmental stress.

1. The **stress response** is the immediate detrimental effect of a stress on a plant process. This generally occurs over a time scale of seconds to days, resulting in a decline in performance of the process.
2. **Acclimation** is the morphological and physiological adjustment by individual plants to compensate for the decline in performance following the initial stress response. Acclimation occurs in response to environmental change through changes in the activity or synthesis of new biochemical constituents such as enzymes, often associated with the production of new tissue. These biochemical changes then initiate a cascade of effects that we can observe at other levels, such as changes in rate or environmental sensitivity of a specific process (*e.g.*, photosynthesis), growth rate of whole plants, and morphology of organs or the entire plant. Acclimation to stress always occurs within the lifetime of an individual, usually within days to weeks. Acclimation can be demonstrated by comparing genetically similar plants that are growing in different environments. The acclimation responses may be reversible (*e.g.*, concentrations of compatible solutes in response to water stress), or irreversible (*e.g.*, changes in the vascular system). None of these phenotypic changes involve any genotypic changes in the population.
3. **Adaptation** is the evolutionary response resulting from genetic changes in populations that compensate for the decline in performance caused by stress. The physiological mechanisms of response are often similar to those of acclimation, because both require changes in the activity or synthesis of biochemical constituents and cause changes in rates of individual physiological processes, growth rate, and morphology. In fact, adaptation may alter the potential of plants to acclimate to short-term environmental variation. Adaptation, as we define it, differs from acclimation in that it requires genetic changes in populations. It, therefore, typically requires many generations to occur. We can study adaptation by comparing genetically distinct plants grown in a common environment.
4. More recently **epigenetic** effects are receiving attention. These involve changes in the DNA of individuals, for example, as a result of methylation (Yong-Villalobos et al. 2015). This methylated DNA may be transferred to the next generation, blurring the difference between acclimation and adaptation (Preite et al. 2015).

Not all genetic differences among populations reflect adaptation. Evolutionary biologists have often criticized ecophysiologists for promoting the 'Panglossian paradigm', *i.e.* the idea that just because a species exhibits certain traits in a particular environment, these traits must be beneficial and must have resulted from natural selection in that environment (Gould and Lewontin 1979). Plants may differ genetically because their ancestral species or populations were genetically distinct before they arrived in the habitat we are studying, or other historical reasons may be responsible for the existence of the present genome.

There are at least two additional processes that can cause particular traits to be associated with a given environment:

1. Through the quirks of history, the ancestral species or population that arrived at the site may have been pre-adapted, *i.e.* exhibited traits that allowed continued persistence in these conditions. These 'pre-adaptations' are generally referred to as '**exaptations'** (Gould and Vrba 1982). Natural selection for these traits may have occurred under very different environmental circumstances. For example, traits that allow plants to cope with fire, are not necessarily adaptations, but may be exaptations (Bradshaw et al. 2011). Similarly, the tree species that currently occupy the mixed deciduous forests of Europe and North America were associated with very different species and environments during the Pleistocene, 100,000 years ago. They co-occur now because they migrated to the same place some

time in the past (the **historical filter**), can grow and reproduce under current environmental conditions (the **physiological filter**), and outcompeted other potential species in these communities and successfully defended themselves against past and present herbivores and pathogens (the **biotic filter**).

2. Once species arrive in a given geographic region, their distribution is fine-tuned by ecological sorting, in which each species tends to occupy those habitats where it most effectively competes with other plants, and defends itself against natural enemies (Vrba and Gould 1986).

1.5 Conceptual and Experimental Approaches

Documentation of the correlation between plant traits and environmental conditions is the raw material for many ecophysiological questions. Plants in the high alpine of Africa are strikingly similar in morphology and physiology to those of the alpine of tropical South America and New Guinea, despite very different phylogenetic histories. The similarity of physiology and morphology of shrubs from Mediterranean regions of western parts of Spain, South Africa, Chile, Australia, and the United States suggests that the distinct floras of these regions have undergone **convergent evolution** in response to similar climatic regimes (Mooney and Dunn 1970). For example, evergreen shrubs are common in each of these regions. These shrubs have small, thick leaves, which continue to photosynthesize under conditions of low water availability during the warm, dry summers, characteristic of Mediterranean climates.

Documentation of a correlation of traits with environment can never determine the relative importance of adaptation to these conditions, and other factors such as exaptation of the ancestral floras and ecological sorting of ancestral species into appropriate habitats. Moreover, traits that we measure under field conditions reflect the combined effects of differences in magnitude and types of environmental stresses, genetic differences among populations in stress response, and acclimation of individuals to stress. Thus, documentation of correlations between physiology and environment in the field provides a basis for interesting ecophysiological hypotheses, but can rarely test these hypotheses without complementary approaches such as growth experiments or phylogenetic analyses. Growth experiments allow one to separate the effects of **acclimation** by individuals and genetic differences among populations. We can document acclimation by measuring the physiology of genetically similar plants grown under different environmental conditions. Such experiments show, for example, that plants grown at low temperature generally have a lower optimum temperature for photosynthesis than warm-grown plants (Billings et al. 1971). By growing plants collected from alpine and low-elevation habitats under the same environmental conditions, we can demonstrate genetic differences: with the alpine plant generally having a lower temperature optimum for photosynthesis than the low-elevation population. Thus, many alpine plants photosynthesize just as rapidly as their low-elevation counterparts, due to both acclimation and **adaptation**. Controlled-environment experiments are an important complement to field observations. Conversely, field observations and experiments provide a context for interpreting the significance of laboratory experiments.

Both acclimation and adaptation reflect complex changes in many plant traits, making it difficult to evaluate the importance of changes in any particular trait. Ecological modeling and molecular modification of specific traits are two approaches to explore the ecological significance of specific traits. Ecological models can range from simple empirical relationships (*e.g.*, the temperature response of respiration) to complex mathematical models that incorporate many indirect effects, such as negative feedbacks of sugar accumulation to photosynthesis. A common assumption of these models is that there are both **costs** and **benefits** associated with a particular trait, such that no trait enables a plant to perform

best in all environments (*i.e.* there are no 'super-plants' or 'Darwinian demons' that are superior in all components). That is, presumably, why there are so many fascinating physiological differences among plants. These models seek to identify the conditions under which a particular trait allows superior performance or compares performance of two plants that differ in traits. The theme of **trade-offs** (*i.e.* the costs and benefits of particular traits), is one that will recur frequently in this book (Lambers et al. 2018).

A second, more experimental approach to the question of optimality is **molecular modification** of the gene that encodes a trait, including the regulation of its expression. In this way, we can explore the consequences of a change in photosynthetic capacity, sensitivity to a specific hormone, or response to shade. This molecular approach is an extension of comparative ecophysiological studies, in which plants from different environments that are as similar as possible except with respect to the trait of interest are grown in a common environment. Molecular modification of single genes allows evaluation of the physiological and ecological consequences of a trait, while holding constant the rest of the biology of the plants.

1.6 New Directions in Ecophysiology

Plant ecophysiology has several new and potentially important contributions to make to biology. The rapidly growing human population requires increasing supplies of food, fiber, and energy, at a time when the best agricultural land is already in production or being lost to urban development and land degradation (Pellegrini and Fernández 2018). It is thus increasingly critical that we identify traits or suites of traits that maximize sustainable food and fiber production on both highly productive and less productive land. The development of varieties that grow effectively with inadequate supplies of water and nutrients is particularly important in less developed countries that often lack the economic and transportation resources to support high-intensity agriculture. Molecular biology and traditional breeding programs provide the tools to develop new combinations of traits in plants, including GMOs (genetically modified organisms). Ecophysiology is perhaps the field that is best suited to determine the costs, benefits, and consequences of changes in these traits, as whole plants, including GMOs, interact with complex environments.

Past ecophysiological studies have described important physiological differences among plant species and have demonstrated many of the mechanisms by which plants can live where they occur. These same physiological processes, however, have important effects on the environment, shading the soil, removing nutrients that might otherwise be available to other plants or soil microorganisms, transporting water from the soil to the atmosphere, thus both drying the soil and increasing atmospheric moisture. These plant effects can be large, and provide a mechanistic basis for understanding processes at larger scales, such as community, ecosystem, and climatic processes. For example, forests that differ only in species composition can differ substantially in productivity and rates of nutrient cycling. Simulation models suggest that species differences in stomatal conductance and rooting depth could significantly affect climate at regional and continental scales (Foley et al. 2003; Field et al. 2007). As human activities increasingly alter the species composition of large portions of the globe, it is critical that we understand the ecophysiological basis of community, ecosystem and global processes.

1.7 The Structure of the Book

We assume that the reader already has a basic understanding of biochemical and physiological processes in plants. Chapters 2, 3 and 4 in this book deal with the primary processes of carbon metabolism and transport. After introducing some biochemical and physiological aspects of photosynthesis (Chap. 2), we discuss differences in photosynthetic traits among species, and link these with the species' natural habitat. Trade-offs are discussed, like that between a high

water-use efficiency and a high efficiency of nitrogen use in photosynthesis (Chap. 2). In Chap. 3 we analyze carbon use in respiration, and explore its significance for the plant's carbon balance in different species and environments. Species differences in the transport of photosynthates from the site of production to various sinks are discussed in Chap. 4. For example, the phloem transport system in climbing plants involves an interesting trade-off between transport capacity and the risk of major damage to the system. A similar trade-off between capacity and safety is encountered in Chap. 5, which deals with plant water relations. Subsequently, the plant's energy balance (Chap. 6) and the effects of radiation and temperature (Chap. 7) are discussed. Following these chapters on photosynthesis, water use and energy balance in individual leaves and whole plants, we then scale the processes up to the level of an entire canopy, demonstrating that processes at the level of a canopy are not necessarily the sum of what happens in single leaves, due to the effects of surrounding leaves (Chap. 8). Chapter 9 discusses the plant's mineral nutrition and the numerous ways in which plants cope with soils with low nutrient availability or toxic metal concentrations (*e.g.*, sodium, aluminum, metals). These first chapters emphasize those aspects that help us to analyze ecological problems. Moreover, they provide a sound basis for later chapters in the book that deal with a higher level of integration.

The following chapters deals with patterns of growth and allocation (Chap. 10), life-history traits (Chap. 11), and interactions of individual plants with other organisms: symbiotic microorganisms (Chap. 12), ecological biochemistry, discussing allelopathy and defense against herbivores (Chap. 13), microbial pathogens (Chap. 14), parasitic plants (Chap. 15), interactions among plants in communities (Chap. 16), and animals used as prey by carnivorous plants (Chap. 17). These chapters build on information provided in the earlier chapters.

The final chapters deal with ecophysiological traits that affect decomposition of plant material in contrasting environments (Chap. 18), and with the role of plants in ecosystem and global processes (Chap. 19). We address many topics in the first two series of chapters again in this broader context. For example, allocation patterns and defense compounds affect decomposition. Photosynthetic pathways and allocation patterns affect to what extent plant growth is enhanced at elevated levels of carbon dioxide in the atmosphere.

Throughout the text, we use 'boxes' to elaborate on specific problems, without cluttering up the text. They are meant for students seeking a deeper understanding of problems discussed in the main text. A glossary provides quick access to the meaning of technical terms used in both this book and the plant ecophysiological literature. The references at the end of each chapter are an entry point to relevant literature in the field. We emphasize review papers that provide broad synthesis, but also include key experimental papers in rapidly developing areas ('the cutting edge'). In general, this book targets students who are already familiar with basic principles in ecology, physiology, and biochemistry. It should provide an invaluable text for both undergraduates and postgraduates, and a reference for professionals.

References

Billings WD. 1973. Arctic and alpine vegetation: similarities, differences, and susceptibility to disturbance. *BioScience* **23**: 697–704.

Billings WD, Godfrey PJ, Chabot BF, Bourque DP. 1971. Metabolic acclimation to temperature in arctic and alpine ecotypes of *Oxyria digyna*. *Arct Alp Res* **3**: 277–289.

Blackman VH. 1919. The compound interest law and plant growth. *Ann Bot* **33**: 353–360.

Boyer JS. 1985. Water transport. *Annu Rev Plant Physiol* **36**: 473–516.

Bradshaw SD, Dixon KW, Hopper SD, Lambers H, Turner SR. 2011. Little evidence for fire-adapted plant traits in Mediterranean climate regions. *Trends Plant Sci* **16**: 69–76.

Clarkson DT. 1966. Aluminium tolerance in species within the genus *Agrostis*. *J Ecol* **54**: 167–178.

Conway VM. 1940. Aeration and plant growth in wet soils. *Bot Rev* **6**: 149–163.

Crawford RMM. 1978. Biochemical and ecological similarities in marsh plants and diving animals. *Naturwissenschaften* **65**: 194 201.

Ellenberg H. 1953. Physiologisches und ökologisches Verhalten derselben Pflanzanarten. *Ber Deutsch Bot Ges* **65**: 351–361.

Field RH, Benke S, Bádonyi K, Bradbury RB. 2007. Influence of conservation tillage on winter bird use of

arable fields in Hungary. *Agric Ecosyst Environ* **120**: 399–404.

Foley JA, Costa MH, Delire C, Ramankutty N, Snyder P. 2003. Green surprise? How terrestrial ecosystems could affect Earth's climate. *Front Ecol Evol* **1**: 38–44.

Gould SJ, Lewontin RC. 1979. The spandrels of San Marco and the Panglossian paradigm: a critique of the adaptationists programme. *Proc R Soc Lond B* **205**: 581–598.

Gould SJ, Vrba ES. 1982. Exaptation-a missing term in the science of form. *Paleobiology* **8**: 4–15.

Graham A. 2018. *Land Bridges: Ancient Environments, Plant Migrations, and New World Connections*. Chicago: University of Chicago Press.

Holdridge LR. 1947. Determination of world plant formations from simple climatic data. *Science* **105**: 367–368.

Huston M. 1980. Soil nutrients and tree species richness in Costa Rican forests. *J Biogeog* **7**: 147–157.

Laliberté E, Lambers H, Burgess TI, Wright SJ. 2015. Phosphorus limitation, soil-borne pathogens and the coexistence of plant species in hyperdiverse forests and shrublands. *New Phytol* **206**: 507–521.

Lambers H, Albornoz F, Kotula L, Laliberté E, Ranathunge K, Teste FP, Zemunik G. 2018. How belowground interactions contribute to the coexistence of mycorrhizal and non-mycorrhizal species in severely phosphorus-impoverished hyperdiverse ecosystems. *Plant Soil* **424**: 11–34.

Lambers H, Brundrett MC, Raven JA, Hopper SD. 2010. Plant mineral nutrition in ancient landscapes: high plant species diversity on infertile soils is linked to functional diversity for nutritional strategies. *Plant Soil* **334**: 11–31.

Lambers H, Poorter H. 1992. Inherent variation in growth rate between higher plants: a search for physiological causes and ecological consequences. *Adv Ecol Res* **22**: 187–261.

Magallón S, Hilu K 2009. Land plants (Embryophyta). In: Hedges SB, Kumar S eds. *The Timetree of Life*. New Yorl: Oxford University Press, 133–137.

Mooney HA, Dunn EL. 1970. Convergent evolution of mediterranean-climate sclerophyll shrubs. *Evolution* **24**: 292–303.

Oliveira RS, Galvão HC, de Campos MCR, Eller CB, Pearse SJ, Lambers H. 2015. Mineral nutrition of *campos rupestres* plant species on contrasting nutrient-impoverished soil types. *New Phytol* **205**: 1183–1194.

Pearsall WH. 1938. The soil complex in relation to plant communities. *J Ecol* **26**: 180–193.

Pellegrini P, Fernández RJ. 2018. Crop intensification, land use, and on-farm energy-use efficiency during the worldwide spread of the green revolution. *Proc Natl Acad Sci USA* **115**: 2335–2340.

Preite V, Snoek LB, Oplaat C, Biere A, Putten WH, Verhoeven KJF. 2015. The epigenetic footprint of poleward range-expanding plants in apomictic dandelions. *Mol Ecol* **24**: 4406–4418.

Schimper AFW. 1898. *Pflanzengeographie und physiologische Grundlage*. Jena: Verlag von Gustav Fischer.

Tansley AG. 1917. On competition between *Galium saxatile* L. (*G. hercynicum* Weig.) and *Galium sylvestre* Poll. (*G. asperum* Schreb.) on different types of soil. *J Ecol* **5**: 173–179.

Vrba ES, Gould SJ. 1986. The hierarchical expansion of sorting and selection: sorting and selection cannot be equated. *Paleobiology* **12**: 217–228.

Walter H. 1974. *Die Vegetation der Erde*. Jena: Gustav Fischer Verlag.

Wright IJ, Reich PB, Westoby M, Ackerly DD, Baruch Z, Bongers F, Cavender-Bares J, Chapin T, Cornelissen JHC, Diemer M, Flexas J, Garnier E, Groom PK, Gulias J, Hikosaka K, Lamont BB, Lee T, Lee W, Lusk C, Midgley JJ, Navas M-L, Niinemets Ü, Oleksyn J, Osada N, Poorter H, Poot P, Prior L, Pyankov VI, Roumet C, Thomas SC, Tjoelker MG, Veneklaas EJ, Villar R. 2004. The worldwide leaf economics spectrum. *Nature* **428**: 821–827.

Yong-Villalobos L, González-Morales SI, Wrobel K, Gutiérrez-Alanis D, Cervantes-Peréz SA, Hayano-Kanashiro C, Oropeza-Aburto A, Cruz-Ramírez A, Martínez O, Herrera-Estrella L. 2015. Methylome analysis reveals an important role for epigenetic changes in the regulation of the Arabidopsis response to phosphate starvation. *Proc Natl Acad Sci USA* **112**: E7293-E7302.

2 Photosynthesis, Respiration, and Long-Distance Transport: Photosynthesis

2.1 Introduction

Approximately 40% of a plant's dry mass consists of carbon, fixed in photosynthesis. This process is vital for growth and survival of virtually all plants during the major part of their growth cycle. In fact, life on Earth in general, not just that of plants, totally depends on current and/or past photosynthetic activity. Leaves are beautifully specialized organs that enable plants to intercept light necessary for photosynthesis. The light is captured by a large array of chloroplasts that are in close proximity to air and not too far away from vascular tissue, which supplies water and exports the products of photosynthesis. In most plants, CO_2 uptake occurs through leaf pores, the stomata, which are able to rapidly change their aperture (Sect. 5.5.4). Once inside the leaf, CO_2 diffuses from the intercellular air spaces to the sites of carboxylation in the chloroplast (C_3 species) or in the cytosol (C_4 and CAM species).

Ideal conditions for photosynthesis include an ample supply of water and nutrients to the plant, and optimal temperature and light conditions. Even when the environmental conditions are less favorable, however, such as in a desert, alpine environments, or the understory of a forest, photosynthesis, at least of adapted and acclimated plants, continues (for a discussion of the concepts of **acclimation** and **adaptation**, see Fig. 1.3; Chap. 1.4). This chapter addresses how such plants manage to photosynthesize and/or protect their photosynthetic machinery in adverse environments, what goes wrong in plants that are not adapted and fail to acclimate, and how photosynthesis depends on a range of other physiological activities in the plant.

2.2 General Characteristics of the Photosynthetic Apparatus

2.2.1 The 'Light' and 'Dark' Reactions of Photosynthesis

To orient ourselves, we imagine zooming in on a chloroplast: from a tree, to a leaf, to a cell in a leaf, and then to the many chloroplasts in a single cell, where the primary processes of photosynthesis. In C_3 plants, most of the chloroplasts are located in the mesophyll cells of the leaves (Fig. 2.1). Three main processes are distinguished:

1. Absorption of photons by pigments, mainly chlorophylls, associated with two photosystems. The pigments are embedded in internal membrane structures (**thylakoids**) and absorb a major part of the energy of the photosynthetically active radiation (PAR; 400–700 nm). They transfer the excitation energy to the reaction centers of the photosystems where the second process starts.

H. Lambers, R. S. Oliveira, *Plant Physiological Ecology*, https://doi.org/10.1007/978-3-030-29639-1_2

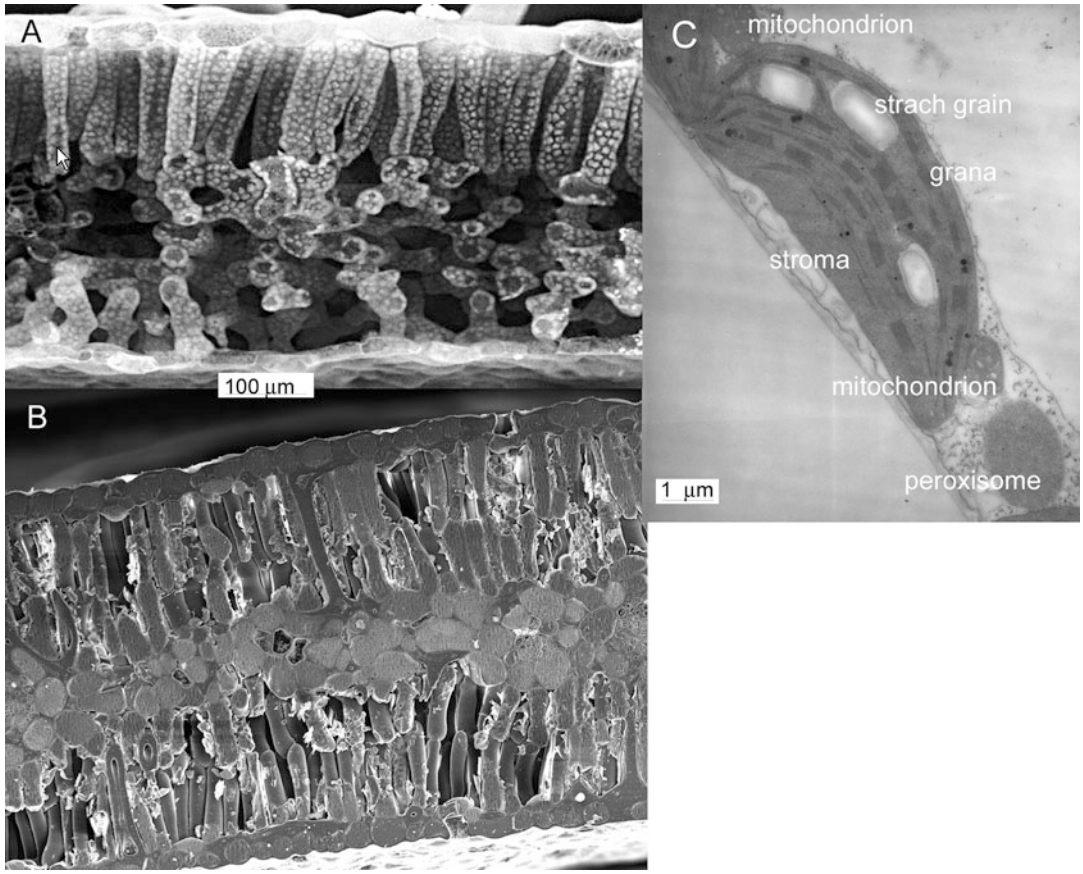

Fig. 2.1 (**A**) Scanning electron microscope cross sectional view of a dorsiventral leaf of *Nicotiana tabacum* (tobacco), showing palisade tissue beneath the upper (adaxial) epidermis, and spongy tissue adjacent to the (lower) abaxial epidermis. (**B**) Scanning electron microscope cross sectional view of an isobilateral leaf of *Hakea prostrata* (harsh hakea). (**C**) Transmission electron microscope micrograph of a tobacco chloroplast, showing appressed (grana) and unappressed regions of the thylakoids, stroma, and starch granules. Note the close proximity of two mitochondria (top and bottom) and one peroxisome (scale bar is 1 µm) (*Nicotiana tabacum:* courtesy J.R. Evans, Australian National University, Canberra, Australia; *Hakea prostrata:* courtesy M.W Shane, University of Western Australia, Australia).

2. Electrons derived from the splitting of water with the simultaneous production of O_2 are transported along an electron-transport chain embedded in the thylakoid membrane. NADPH and ATP produced in this process are used in the third process. Since these two reactions depend on light energy, we call them the '**light reactions'** of photosynthesis.
3. The NADPH and ATP are used in the photosynthetic carbon-reduction cycle (Calvin-Benson cycle), in which CO_2 is assimilated leading to the synthesis of C_3 compounds (triose-phosphates). These processes can proceed in the absence of light and are referred to as the '**dark reactions'** of photosynthesis. As discussed in Sect. 2.3.4.2, however, some of the enzymes involved in the 'dark' reactions require light for their activation, and hence the difference between 'light' and 'dark' reaction is somewhat blurred.

2.2.1.1 Absorption of Photons

The **reaction center** of **photosystem I** (PS I) is a chlorophyll dimer with an absorption peak at 700 nm, hence called P_{700}. There are about 110 'ordinary' chlorophyll a (chl a) molecules

per P_{700} as well as several different protein molecules, to keep the chlorophyll molecules in the required position in the thylakoid membranes (Lichtenthaler 2015). The number of PS I units can be quantified by determining the amount of P_{700} molecules, which can be assessed by measuring absorption changes at 830 nm.

The **reaction center** of **photosystem II** (PS II) contains redox components, including a pair of chlorophyll a molecules with an absorption peak at 680 nm, called P_{680}, pheophytin, which is like a chlorophyll molecule but without the Mg atom, and the first quinone acceptor of an electron (Q_A) (Baker 2008). Redox cofactors in PS II are bound to the structure of the so-called **D1/D2 proteins** in PS II. PS I and PS II core complexes do not contain chl b (Lichtenthaler and Babani 2004). Several protein molecules keep the chlorophyll molecules in the required position in the thylakoid membranes. *In vitro*, P_{680} is too unstable to be used to quantify the amount of PS II. The **herbicide** atrazine binds specifically to one of the complexing protein molecules of PS II, however; when using ^{14}C-labeled atrazine, this binding can be quantified and used to determine the total amount of PS II. Alternatively, the quantity of functional PS II centers can be determined, *in vivo*, by the O_2 yield from leaf disks, exposed to 1% CO_2 and repetitive 'single turnover' light flashes. A good correlation exists between the two assays. The O_2 yield per flash provides a convenient, direct assay of PS II *in vivo* when conditions are selected to avoid limitation by PS I (Chow et al. 1989).

A large part of the chlorophyll is located in the **light-harvesting complex** (LHC). These chlorophyll molecules act as antennae to trap light and transfer its excitation energy to the reaction centers of one of the photosystems. The reaction centers are strategically located to transfer electrons along the electron-transport chains. The ratio of chl a/chl b is about 1.1–1.3 for LHC (Lichtenthaler and Babani 2004).

Leaves appear green in white light, because chlorophyll absorbs more efficiently in the blue and red than in the green portions of the spectrum; beyond approximately 720 nm, there is no absorption by chlorophyll at all. The **absorbance spectrum** of intact leaves differs from that of free chlorophyll in solution, and leaves absorb a significant portion of the radiation in regions where chlorophyll absorbs very little *in vitro* (Fig. 2.2).

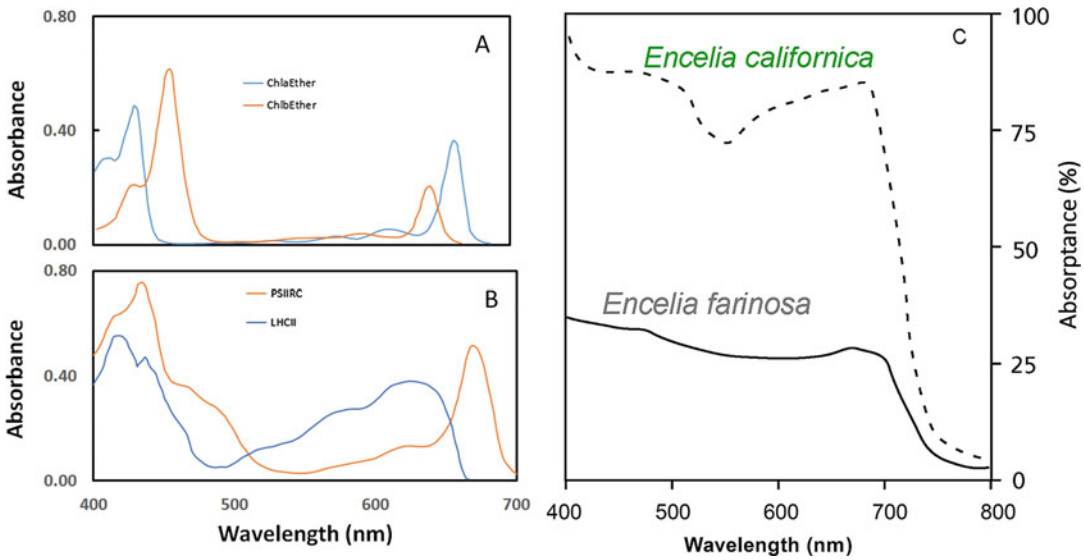

Fig. 2.2 (**A**) The relative absorbance spectrum of chlorophyll *a* and chlorophyll *b*; absorbance = -log (transmitted light/incident light) (Zscheile and Comar 1941). (**B**) The relative absorbance spectrum of pigment-protein complexes: PS II reaction centre and PS II light-harvesting complex (Lichtenthaler 1986). (**C**) Absorption spectrum of an intact green leaf of *Encelia californica*; for comparison the absorption spectrum of an intact white (pubescent) leaf of *Encelia farinosa* (brittlebush) is also given (after Ehleringer et al. 1976).

This is due to (1) the modification of the absorbance spectra of the chlorophyll molecules bound in protein complexes *in vivo*, (2) the presence of accessory pigments, such as carotenoids, in the chloroplast, and, most importantly, (3) light scattering within the leaf (Sect. 2.3.2.2).

2.2.1.2 Fate of the Excited Chlorophyll

Each quantum of red light absorbed by a chlorophyll molecule raises an electron from a ground state to an excited state. Absorption of light of shorter wavelengths (*e.g.*, blue light) excites the chlorophyll to an even higher energy state. In the higher-energy state after absorption of blue light, however, chlorophyll is unstable and rapidly gives up some of its energy to the surroundings as heat, so that the elevated electron immediately falls back into the orbit of the electron excited by red light. Thus, whatever the wavelength of the light absorbed, chlorophyll reaches the same excitation state upon photon capture. In this excitation state, chlorophyll is stable for 10^{-9} s, after which it disposes of its available energy in one of three ways (Krause and Weis 1991; Baker 2008):

1. The primary pathway of excitation energy is its highly efficient transfer to other chlorophyll molecules, and ultimately to the reaction center where it is used in **photochemistry**, driving biochemical reactions.
2. The excited chlorophyll can also return to its ground state by converting its excitation energy into **heat**. In this process, no photon is emitted.
3. The excited chlorophyll can emit a photon and thereby return to its ground state; this process is called **fluorescence**. Most fluorescence is emitted by chl a of PS II. The wavelength of fluorescence is slightly longer than that of the absorbed light, because a portion of the excitation energy is lost before the fluorescence photon is emitted. Chlorophylls usually fluoresce in the red; it is a deeper red (the wavelength is about 10 nm longer) than the red absorption peak of chlorophyll. Fluorescence increases when photochemistry and/or dissipation are slow relative to photon absorption, but the process is not regulated as such. This can occur under conditions of excessive light, severely limiting CO_2 supply, or stresses that inhibit photochemistry.

The primary photochemical reactions of PS II and PS I occur at a much faster rate than subsequent electron transport (Sect. 2.2.1.3), which in turn occurs faster than carbon reduction processes (Sect. 2.2.1.4). Since the three compartments of the photosynthetic apparatus operate in series, they are each tightly regulated to coordinate their activity under changing conditions.

2.2.1.3 Membrane-Bound Photosynthetic Electron Transport and Bioenergetics

The excitation energy captured by the pigments is transferred to the reaction centers of PS I and PS II, which are associated with different regions of the thylakoid membrane. PS I is located in the stroma-exposed **unappressed** regions, and PS II is largely associated with the **appressed** regions where thylakoids border other thylakoids (grana) (Fig. 2.1). In PS II, an electron, derived from the splitting of water into O_2 and protons, is transferred to pheophytin, and then to plastoquinone (Q_A, bound to D2 protein, a one-electron carrier), followed by transfer to Q_B (bound to D1 protein, a two-electron carrier), and then to free plastoquinone (PQ). Reduced PQ subsequently transfers an electron to the cytochrome b/f complex.

In the process of electron transfer down the photosynthetic electron transport chain, protons are transported across the membrane into the thylakoid lumen (Fig. 2.3). The protons acidify and charge the thylakoid lumen positively. The **electrochemical potential gradient** across the thylakoid membrane, representing a **proton-motive force**, is subsequently used to phosphorylate ADP, thus producing **ATP**. This reaction is catalyzed by an ATPase, or coupling factor, located in the stroma-exposed, unappressed regions of the thylakoids. In **linear electron transport**, electrons are transferred from the

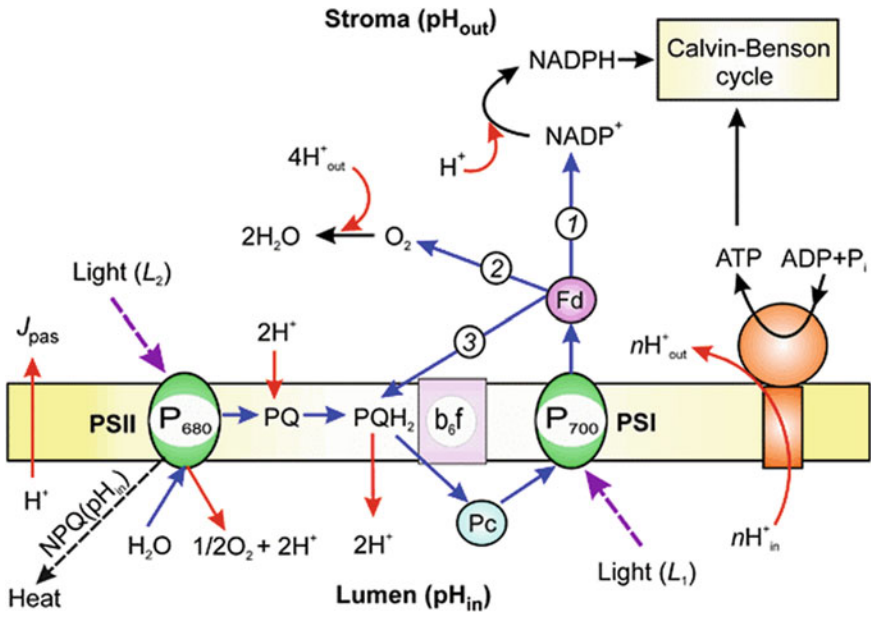

Fig. 2.3 A scheme of electron transfer and proton transport processes considered in the model and the arrangement of protein complexes (PSI, PSII, the Cyt b_6f, and the ATP synthase complexes) in the thylakoid membrane. Two electrons extracted from the water molecule in PSII are used to reduce PQ to PQH_2. Electrons from PQH_2 are transferred through the cytochrome b_6f complex to reduce plastocyanin (Pc). PSI oxidizes Pc on the lumen side of the thylakoid membrane, and reduces a mobile electron carrier ferredoxin (Fd) on the stromal side of the membrane. Reduced Fd molecules pass electrons to $NADP^+$ (pathway 1). Reduced NADPH molecules and ATP are consumed in the Calvin–Benson cycle. Along with the linear electron flow from H_2O to $NADP^+$, the model takes into account alternative routes of electron transport: electron transfer from PSI to O_2 (pathway 2), and cyclic electron transport around PSI (pathway 3). The trans-thylakoid proton transport processes (shown by red arrows) coupled to the light-induced electron transport reactions (shown by blue arrows) provide generation of ΔpH (Tikhonov and Vershubskii 2017). Copyright © 2017, Springer Science Business Media Dordrecht.

cytochrome b/f complex to PS I through plastocyanin (PC) that migrates through the thylakoid lumen. NADP is reduced by ferredoxin as the terminal acceptor of electrons from PS I which results in formation of NADPH. In **cyclic electron transport**, electrons are transferred from PS I back to cytochrome b/f through plastoquinone, thus contributing to proton extrusion in the lumen and subsequent ATP synthesis. NADPH and ATP are used in the carbon-reduction cycle that is located in the stroma. Linear electron transport is the principal pathway, whereas the engagement of cyclic electron transport is tuned to the demand for ATP relative to NADPH. Other components of the photosynthetic membrane are also regulated, particularly with respect to the prevailing light conditions.

2.2.1.4 Photosynthetic Carbon Reduction

Ribulose-1,5-bisphosphate (RuBP) and CO_2 are the substrates for the principal enzyme of the carbon-reduction or Calvin-Benson cycle: ribulose-1,5-bisphosphate carboxylase/oxygenase (**Rubisco**) (Fig. 2.4). The first product of carboxylation of RuBP by Rubisco is phosphoglyceric acid (**PGA**; the ionic form is phosphoglycerate) a compound with three carbon atoms, hence, the name **C_3 photosynthesis** (Pottier et al. 2018). With the consumption of the ATP and NADPH produced in the light reactions, PGA is reduced to a **triose-phosphate** (triose-P), some of which is exported to the cytosol in exchange for inorganic phosphate (Pi). In the cytosol, triose-P is used to produce sucrose

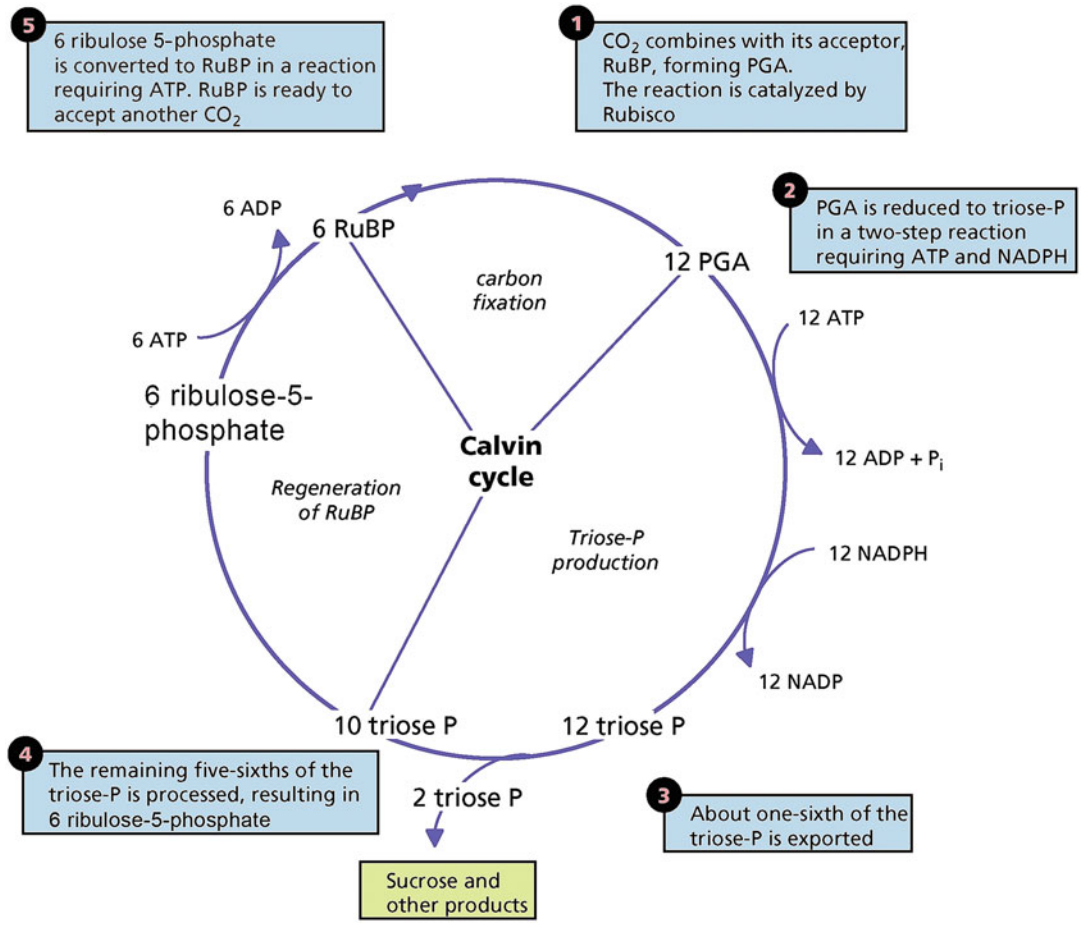

Fig. 2.4 Schematic representation of the photosynthetic carbon reduction cycle (Calvin-Benson cycle) showing major steps: carbon fixation, triose-P production and regeneration of RuBP. 1: CO_2 combines with its substrate, ribulose-1,5-bisphosphate (RuBP), catalyzed by ribulose bisphosphate carboxylase/oxygenase (Rubisco), producing phosphoglyceric acid (PGA; the anion component of this is called phosphoglycerate). 2: PGA is reduced to triose-phosphate (triose-P), in a two-step reaction; the reaction for which ATP is required is the conversion of PGA to 1,3-bisphosphoglycerate, catalyzed by phosphoglycerate kinase. 3 and 4: Part of the triose-P is exported to the cytosol, in exchange for P_i; the remainder is used to regenerate ribulose-5-phosphate. 5: ribulose-5-phosphate is phosphorylated, catalyzed by ribulose-5-phosphate kinase, producing RuBP.

and other metabolites that are exported via the phloem or used in the leaves. Five out of six triose-P remaining in the chloroplast are used to regenerate RuBP through a series of reactions that are part of the **Calvin-Benson cycle** in which ATP and NADPH are consumed (Fig. 2.4). Instead of exporting triose-P to the cytosol, it may remain in the chloroplast to produce **starch**, which is stored inside the chloroplast. During the night, starch may be hydrolyzed, and the product of this reaction, triose-P, is exported to the cytosol. The photosynthetic carbon-reduction cycle has various control points and factors that function as stabilizing mechanisms under changing environmental conditions.

2.2.1.5 Oxygenation and Photorespiration

Rubisco catalyzes not only the **carboxylation** of RuBP, but also its **oxygenation** (Fig. 2.5). The ratio of the carboxylation and the oxygenation reaction strongly depends on the relative concentrations of CO_2 and O_2 and on leaf

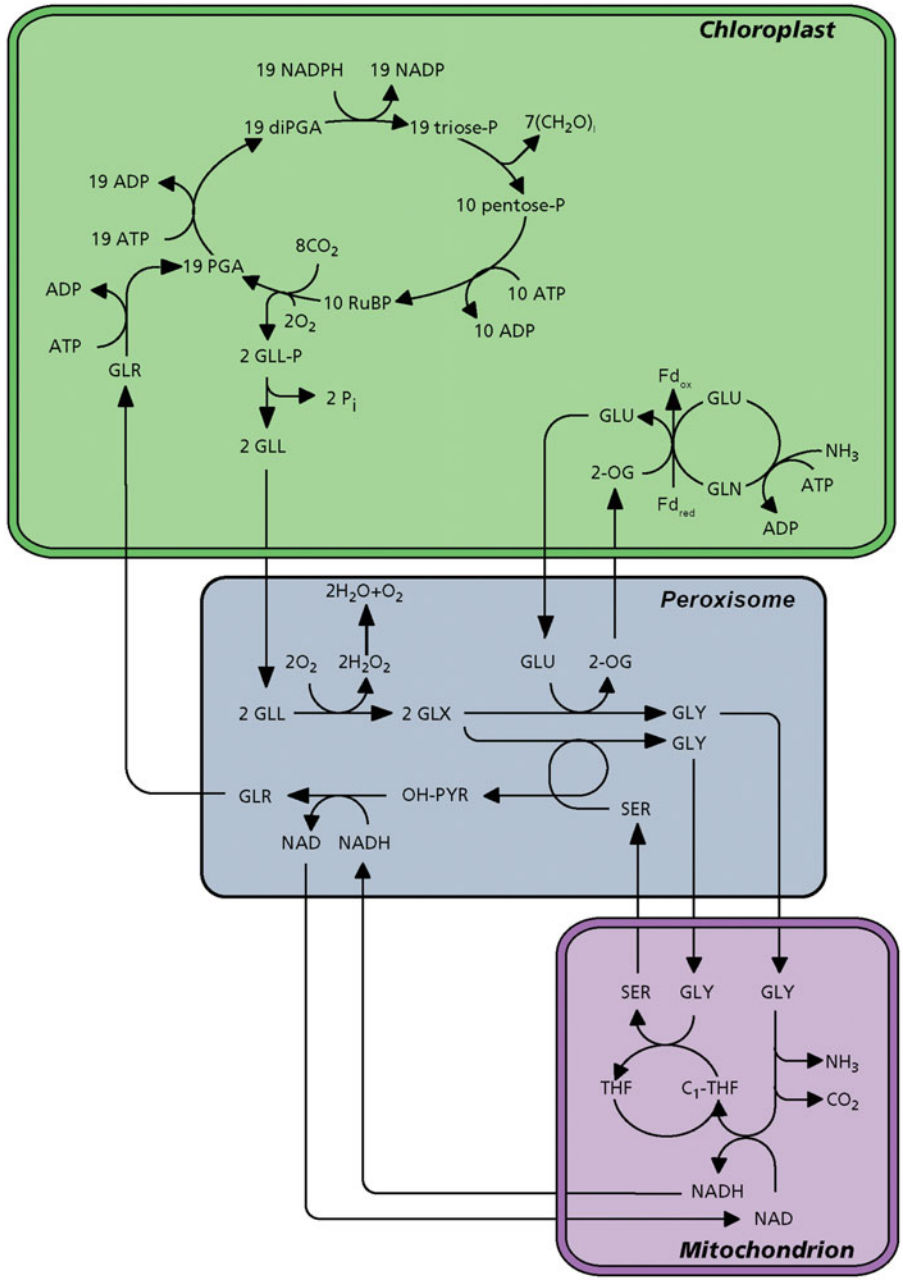

Fig. 2.5 Reactions and organelles involved in photorespiration. In C_3 plants, at 20% O_2, 0.035% CO_2, and 20 °C, two out of ten RuBP molecules are oxygenated, rather than carboxylated. The oxygenation reaction produces phosphoglycolate (GLL-P), which is dephosphorylated to glycolate (GLL). Glycolate is subsequently metabolized in peroxisomes and mitochondria, in which glyoxylate (GLX) and the amino acids glycine (GLY) and serine (SER) play a role. Serine is exported from the mitochondria and converted to hydroxypyruvate (OH-PYR) and then glycerate (GLR) in the peroxisomes, after which it returns to the chloroplast (after Ogren 1984).

temperature. The products of the carboxylation reaction are two C_3 molecules (PGA), whereas the oxygenation reaction produces only one PGA and one C_2 molecule: phosphoglycolate. This C_2 molecule is first dephosphorylated in the chloroplast, producing glycolate (Fig. 2.5),

which is exported to the peroxisomes, where it is metabolized to glyoxylate and then **glycine**. Glycine is exported to the mitochondria where two molecules are converted to produce one serine with the release of one molecule of CO_2 and one NH_3. Serine is exported back to the peroxisomes, where a transamination occurs, producing one molecule of hydroxypyruvate and then glycerate. Glycerate moves back to the chloroplast, to be converted into PGA. Therefore, out of two phosphoglycolate molecules, one glycerate is made and one C-atom is lost as CO_2. The entire process, starting with the oxygenation reaction, is called **photorespiration**, as it consumes O_2 and releases CO_2; it depends on light, or, more precisely, on photosynthetic activity. The process is distinct from 'dark respiration' that largely consists of mitochondrial decarboxylation processes that proceed independent of light. We discuss dark respiration in Chap. 3.

2.2.2 Supply and Demand of CO_2 in the Photosynthetic Process

The rate of photosynthetic carbon assimilation is determined by both the supply of and demand for CO_2. The **supply of CO_2** to the chloroplast is governed by diffusion in the gas and liquid phases and can be limited at several points in the pathway from the air surrounding the leaf to the site of carboxylation inside. The **demand for CO_2** is determined by the rate of processing the CO_2 in the chloroplast which is governed by the structure and biochemistry of the chloroplast (Sect. 2.2.1), by environmental factors such as irradiance, and factors that affect plant demand for carbohydrates (Sect. 2.4.2). Limitations imposed by either supply or demand can determine the overall rate of carbon assimilation, as explained below.

2.2.2.1 Demand for CO_2 - the CO_2-Response Curve

The response of photosynthetic rate to CO_2 concentration is the principal tool to analyze the demand for CO_2 and partition the limitations imposed by demand and supply (Warren 2007; Flexas et al. 2008; Fig. 2.6). The graph giving net CO_2 assimilation (A_n) as a function of CO_2 concentration at the site of Rubisco in the chloroplast (C_c) is referred to as the **A_n-C_c curve**. With rising CO_2, there is no net CO_2 assimilation, until the production of CO_2 in respiration (mainly photorespiration, but also some dark respiration occurring in the light) is fully compensated by the fixation of CO_2 in photosynthesis. The CO_2 concentration at which this is reached is the **CO_2-compensation point** (Γ). In C_3 plants, this is largely determined by the kinetic properties of Rubisco, with values for Γ in the range 40-50 μmol (CO_2) mol^{-1} (air) (at 25 °C and atmospheric pressure).

Two regions of the CO_2-response curve above the compensation point can be distinguished. At C_c, values, below those normally found in leaves (approximately 170 μmol mol^{-1}), photosynthesis increases steeply with increasing CO_2 concentration. This is the region where CO_2 limits the rate of functioning of Rubisco, whereas RuBP is present in saturating quantities (**RuBP-saturated** or **CO_2-limited region**). This part of the A_n-C_c relationship is also referred to as the **initial slope** or the **carboxylation efficiency**. At light saturation and with a fully activated enzyme (Sect. 2.3.4.2 for details on 'activation'), the initial slope governs the carboxylation capacity of the leaf which in turn depends on the amount of active Rubisco.

In the region at high C_c, the increase in A_n with increasing C_c levels off, and CO_2 no longer restricts the carboxylation reaction. Now the rate at which RuBP becomes available limits the activity of Rubisco (**RuBP-limited region**). This rate, in turn, depends on the activity of the Calvin-Benson cycle, which ultimately depends on the rates at which ATP and NADPH are produced in the light reactions; in this region, photosynthetic rates are limited by the rate of electron transport. This may be due to limitation by light or, at light saturation, by a limited capacity of electron transport (Box 2.1). Even at a high C_c, in the region where the rate of electron transport, J, no longer increases with increasing C_c, the rate of net CO_2 assimilation continues to increase slightly. This is because the oxygenation reaction

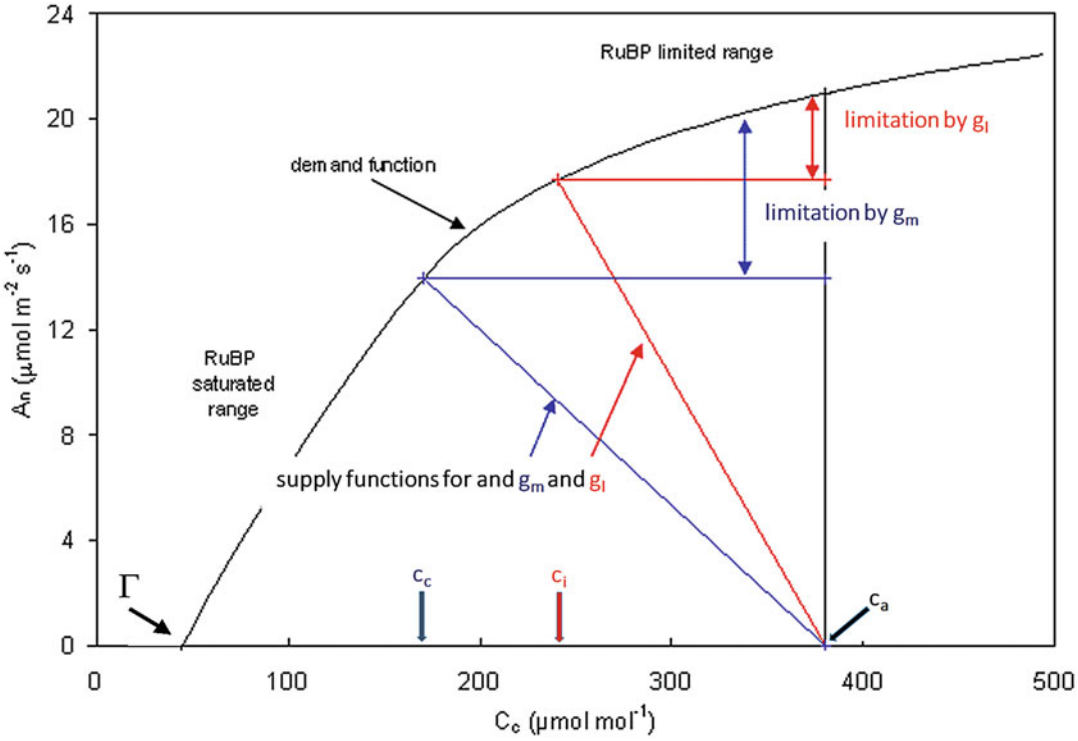

Fig. 2.6 The relationship between the rate of net CO_2 assimilation (A_n) and the CO_2 concentration at the site of Rubisco in the chloroplasts (C_c) for a C_3 leaf: the 'demand function'. The concentration at which $A_n = 0$ is the CO_2-compensation point (Γ). The rate of diffusion of CO_2 from the atmosphere to the intercellular spaces and to Rubisco in the chloroplast is given by the 'supply functions' (the red and blue lines). The slopes of these lines are the leaf conductance (g_l) and mesophyll conductance (g_m), respectively. The intersection of the 'supply functions' with the 'demand function' is the actual rate of net CO_2 assimilation at a value of C_i and C_c that occurs in the leaf intercellular spaces (C_i) and at the site of Rubisco (C_c) for C_a in normal air (indicated by the vertical line). The difference in A_n described by the demand function and the two horizontal lines depicts the degree of limitation imposed by the mesophyll resistance and leaf resistance.

of Rubisco is increasingly suppressed with increasing CO_2 concentration, in favor of the carboxylation reaction. At a normal atmospheric concentration of CO_2 (C_a) and O_2 (*ca.* 400 and 210,000 µmol mol^{-1}, respectively) and at a temperature of 20 °C, the ratio between the carboxylation and oxygenation reaction is about 4:1. How exactly this ratio and various other parameters of the A_n-C_c curve can be assessed is further explained in Box 2.1. Typically, plants operate at a C_c where **CO_2** and **electron transport co-limit** the rate of CO_2 assimilation (*i.e.* the point where the Rubisco-limited / RuBP-saturated and the RuBP-limited part of the CO_2-response curves intersect). This allows effective utilization of all components of the light and dark reactions.

Box 2.1: Modeling C_3 Photosynthesis

Thijs L. Pons
Department Plant Ecophysiology, Institute of Environmental Biology, Utrecht University, Utrecht, The Netherlands

Based on known biochemical characteristics of Rubisco and the requirement of $NADPH_2$ and ATP for CO_2 assimilation, Farquhar et al. (1980) and Farquhar and von Caemmerer (1982) developed a model of photosynthesis in C_3 plants. This model was further developed, based on the CO_2 concentration in the chloroplast (C_c)

(continued)

Box 2.1 (continued)

rather than the intercellular CO_2 concentration (C_i) (Sharkey et al. 2007). It is widely used in ecophysiological research and in global change modeling. The model elegantly demonstrates that basic principles of the biochemistry of photosynthesis explain physiological properties of photosynthesis of intact leaves.

Net CO_2 assimilation (A_n) is the result of the rate of carboxylation (V_c) minus photorespiration and other respiratory processes. In photorespiration, one CO_2 molecule is produced per two oxygenation reactions (V_o) (Fig. 2.5). The rate of dark respiration during photosynthesis may differ from dark respiration at night, and is called day respiration' (R_{day}):

$$A_n = V_c - 0.5V_o - R_{day} \qquad (2.1)$$

The CO_2-limited and O_2-limited rates of carboxylation and oxygenation by Rubisco are described with standard Michaelis-Menten kinetics. When both substrates are present, however, they competitively inhibit each other. An effective Michaelis-Menten constant for the carboxylation reaction (K_m) that takes into account competitive inhibition by O_2 is described as:

$$K_m = K_c \times (1 + O/K_o) \qquad (2.2)$$

where K_c and K_o are the Michaelis-Menten constants for the carboxylation and oxygenation reaction, respectively, and O is the oxygen concentration.

The rate of carboxylation in the CO_2-limited part of the CO_2-response curve of *A*n (Box Fig. 2.1) can then be described as:

$$V_c = \frac{V_{cmax} \times C_c}{C_c + K_m} \qquad (2.3)$$

where V_{cmax} is the rate of carboxylation at saturating C_c

The ratio of oxygenation and carboxylation depends on the specificity of Rubisco for CO_2 relative to O_2 ($S_{c/o}$) which varies

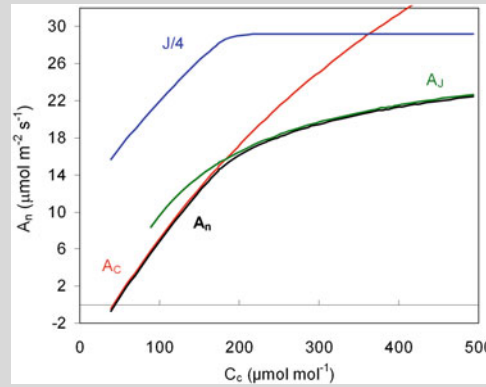

Box Fig. 2.1 The response of net photosynthesis (A_n) to the CO_2 concentration in the chloroplast (C_c) at 25 °C and light saturation (solid black line). Calculations were made as explained in the text, with values for V_{cmax}, J_{max}, and R_{day} of 90, 117, and 1 μmol m^{-2} s^{-1}, respectively. The lower part of the A_n-C_c relationship (A_c; red line) is limited by the carboxylation capacity (V_{cmax}) and the upper part (A_j; green line) by the electron-transport capacity (J_{max}; blue line). The rate of electron transport (*J*/4; blue line) is also shown.

widely among photosynthetic organisms (von Caemmerer 2000), but much less so among C_3 higher plants (Galmés et al. 2005). Increasing temperature decreases the specificity, partly because K_c increases faster with increasing temperature than K_o does (Fig. 2.35).

The CO_2-compensation point in the absence of R_{day} (Γ^*) depends not only on the specificity factor and the O_2 concentration (O) in air, but also on the solubilities of CO_2 (s_c) and O_2 (s_o) in water:

$$\Gamma^* = \frac{0.5O}{S_{c/o} + s_c/s_o} \qquad (2.4)$$

Γ^* increases more strongly with rising temperature than would be expected from the decrease in $S_{c/o}$, because s_c decreases more strongly with increasing temperature than does s_o. Γ^* shows little variation among C_3 angiosperms as follows from the similarity of $S_{c/o}$. Γ^* can be derived from gas exchange measurements (Brooks and Farquhar 1985) and is used to

(continued)

Box 2.1 (continued)

calculate the ratio of carboxylation and oxygenation as dependent on $[CO_2]$ in the chloroplast:

$$\frac{V_o}{V_c} = \frac{2\Gamma^*}{C_c} \tag{2.5}$$

This avoids the need for incorporating the specificity factor and solubilities (Eq. 2.4).

In the lower range of C_c, ribulose bisphosphate (RuBP) is available at saturating levels. Photosynthesis is limited by $[CO_2]$ (A_c; Box Fig. 2.1) and can be calculated using Eqs 2.1, 2.3, and 2.5 as:

$$A_c = \frac{V_{cmax} \times (C_c - \Gamma^*)}{C_c + K_m} - R_{day} \tag{2.6}$$

In the higher range of C_c where $[CO_2]$ is saturating, photosynthesis is limited by the supply of RuBP (A_j, Fig. 2.1). The rate of electron transport (J) is constant, and increasing C_c increases the rate of carboxylation at the expense of the rate of oxygenation. There is a minimum requirement of four electrons per carboxylation or oxygenation reaction. Hence, the minimum electron transport rate (J) required for particular rates of carboxylation and oxygenation is:

$$J = 4 \times (V_c + V_o) \tag{2.7}$$

At light intensities below saturation, J and thus the supply of RuBP is limited by light. At light saturation, J is limited by the capacity of electron transport and is called J_{max}.

Using Eqs 2.5 and 2.6, the rate of carboxylation can then be expressed as:

$$V_c = \frac{J}{4(1 + 2\Gamma^*/C_c)} \tag{2.8}$$

The RuBP-limited rate of photosynthesis (A_j) can be calculated using Eqs 2.1, 2.5, and 2.8 as:

$$A_j = \frac{J \times (C_c - \Gamma^*)}{4(C_c + 2\Gamma^*)} - R_{day} \tag{2.9}$$

The minimum of Eqs 2.8 and 2.9 describes the full CO_2-response curve as shown in Box Fig. 2.1.

In the above equations, gas concentrations are expressed as molar fraction (mol mol^{-1}). If required, partial pressure can be converted to molar fraction by dividing it by atmospheric pressure (P). It is, therefore, important to mention P when reporting gas exchange measurements.

From gas exchange measurements, the intercellular $[CO_2]$ (C_i) can be calculated (Box 2.5). When CO_2 is taken up during photosynthesis, C_c is lower than C_i, because of the resistance (r_m) for diffusion in the liquid phase from the surface of the mesophyll cell walls to the site of carboxylation in the chloroplast. The conductance for CO_2 diffusion in the mesophyll ($g_m = 1/r_m$) and $[CO_2]$ in the chloroplast (C_c) are related to the gas exchange parameters A_n and C_i as:

$$A_n/g_m = C_i - C_c \tag{2.10}$$

We can estimate C_c and g_m from ^{13}C fractionation or chlorophyll fluorescence in combination with gas exchange measurements (Pons et al. 2009). However, values for g_m and C_c may not always be available. As an approximation, the same model can be used assuming that $C_c = C_i$. We should then use parameter values specific for that scenario (see below).

Parameter values for the above equations are normally given for 25 °C. Values for other temperatures can be calculated from their temperature dependencies, as described by the generic equation:

$$\text{parameter} = \exp(c - \Delta H_\alpha / R \times T_L) \tag{2.11}$$

where T_L is leaf temperature (K), R is the molar gas constant, c is a dimensionless constant, and ΔH_α is the activation energy

(continued)

Box 2.1 (continued)

(kJ mol^{-1}). Parameter values estimated for *Nicotiana tabacum* (tobacco) for the CO_2 response at 25 °C, an atmospheric pressure, of 99.1 kPa, and an infinite ($C_c = C_i$) and a finite g_m, together with the temperature dependencies for the latter scenario (Bernacchi et al. 2001, 2002) are:

	$C_c = C_i$	finite g_m ($C_c < C_i$)		
CO_2-response parameter	at 25 °C	at 25 °C	c	ΔH_α
$\Gamma*$ (μmol mol^{-1})	42.75	37.43	19.02	24.46
K_c (μmol mol^{-1})	404.9	272.4	38.28	80.99
K_o (mmol mol^{-1})	278.4	165.8	14.68	23.72

Temperature dependencies of model parameters describing the rates of metabolic processes that are leaf specific (J_{max}, V_{cmax}, R_{day}) are calculated in a similar manner, but Eq. (2.11) must then be multiplied by the rates at 25 °C. For constants and activation energies, see Bernacchi et al. (2001, 2003).

Values of C_c depend on the balance between supply and demand for CO_2. The demand function is described above. Supply of CO_2 goes through the stomata; the function is described in Sect. 2.2.2.2. Electron-transport rates depend on irradiance when not saturated (Sect. 2.3.2.1), where the equation describing net CO_2 assimilation as a function of irradiance can be used to calculate J by substituting J and J_{max} for A_n and A_{max}, respectively. A combination of these mathematical equations makes it possible to model C_3 photosynthesis over a wide range of environmental conditions.

2.2.2.2 Supply of CO_2—Stomatal and Boundary Layer Conductances

The supply of CO_2 by way of its diffusion from the surrounding atmosphere to the intercellular spaces (this CO_2 concentration is denoted as C_i) and to the site of carboxylation in the chloroplasts (this CO_2 concentration is described as C_c) represents a limitation for the rate of photosynthesis. The magnitude of the limitation can be read from the A_n-C_c curve as the differences in photosynthetic rate at C_a and C_i and C_c, respectively (Fig. 2.6). To analyze diffusion limitations, it is convenient to use the term **resistance**, because we can sum resistances to arrive at the total resistance for the pathway. When considering fluxes, however, it is more convenient to use **conductance**, which is the reciprocal of resistance, because the flux varies in proportion to the conductance.

In a steady state, the rate of net CO_2 assimilation (A_n) equals the rate of CO_2 diffusion into the leaf. The rate of CO_2 diffusion can be described by **Fick's first law**. Hence:

$$A_n = g_c(C_a - C_c) = (C_a - C_c)/r_c \qquad (2.12)$$

where, g_c is the leaf conductance for CO_2 transport; C_a and C_c are the mole or volume fractions of CO_2 in air at the site of carboxylation and in air, respectively; r_c is the inverse of g_c (*i.e.* the leaf resistance for CO_2 transport).

The leaf conductance for CO_2 transport, g_c, can be derived from measurements on leaf transpiration, which can also be described by Fick's first law in a similar way:

$$E = g_w(w_i - w_a) = (w_i - w_a)/r_w \qquad (2.13)$$

where g_w is the leaf conductance for water vapor transport; w_i and w_a are the mole or volume fractions of water vapor in air in the intercellular spaces and in air, respectively; r_w is the inverse of g_w (*i.e.* the leaf resistance for water vapor transport); and E is the rate of leaf transpiration. We can measure E directly. The water vapor

concentration in the leaf can be calculated from measurements of the leaf's temperature, assuming a saturated water vapor pressure inside the leaf. Under most conditions, this is a valid assumption. Therefore, the leaf conductance for water vapor transport can be determined.

The total leaf resistance for water vapor transfer, r_w, is largely composed of two components that are in series: the **boundary layer resistance**, r_a, and the **stomatal resistance**, r_s. The boundary layer is the thin layer of air adjacent to the leaf that is modified by the leaf (Fig. 6.6). Turbulence is greatly reduced there, and transport is largely via diffusion. Its limit is commonly defined as the point at which the properties of the air are 99% of the values in ambient air. The boundary layer resistance can be estimated by measuring the rate of evaporation from a water-saturated piece of filter paper of the same shape and size as that of the leaf. Conditions that affect the boundary layer, such as wind speed, should be identical to those during measurements of the leaf resistance. The stomatal resistance for water vapor transfer (r_s) can now be calculated since r_w and r_a are known:

$$r_w = r_a + r_s \tag{2.14}$$

The resistance for CO_2 transport (r_c, as used in Eq. 2.12) across boundary layer and stomata can be calculated from r_w, taking into account that the diffusion coefficients of the two molecules differ. The ratio H_2O diffusion/CO_2 diffusion in air is approximately 1.6, because water is smaller and diffuses more rapidly than CO_2. This value pertains only to the movement of CO_2 inside the leaf air spaces and through the stomata. For the boundary layer above the leaf, where both turbulence and diffusion influence flux, the ratio is approximately 1.37.

$$r_c = (r_a \times 1.37) + (r_s \times 1.6) = 1/g_c \tag{2.15}$$

C_i can now be calculated from Eq. 2.12, after substitution of C_i for C_c. If calculated according to this, C_i is the CO_2 concentration at the point where evaporation occurs inside the leaf (*i.e.* largely the mesophyll cell walls bordering the substomatal cavity), but higher than C_c, the CO_2 concentration at the point where Rubisco assimilates CO_2 (Sect. 2.2.2.3).

In C_3 plants, C_i is generally maintained at around 250 μmol mol^{-1}, but may increase to higher values at a low irradiance and higher humidity of the air, and decrease to lower values at high irradiance, low water availability, and low air humidity. For C_4 plants, C_i is around 100 μmol mol^{-1} (Osmond et al. 1982).

Under most conditions, the stomatal conductance is considerably less than the boundary layer conductance (g_a is up to 10 mol m^{-2} s^{-1}, at wind speeds of up to 5 m s^{-1}; g_s has values of up to 1 mol m^{-2} s^{-1} at high stomatal density and widely open stomata), so that stomatal conductance strongly influences CO_2 diffusion into the leaf. For large leaves in still humid air, where the boundary layer is thick, however, the situation is opposite. In a dense canopy, the wind speed decreases drastically with increasing distance from the canopy surface. Taking measurements *in situ* at full ambient air agitation, it is not possible to measure the true *in situ* photosynthesis rate of leaves deep in a canopy.

2.2.2.3 The Mesophyll Conductance

For the transport of CO_2 from the substomatal cavity to the chloroplast, a **mesophyll conductance** (also called **internal conductance**), g_m (or resistance, r_m) should be considered. Hence, we can describe the net rate of net CO_2 assimilation by:

$$A_n = (C_a - C_c)/(r_a + r_s + r_m) \tag{2.16}$$

Until fairly recently, the mesophyll conductance was assumed to be large and often ignored in analyses of gas-exchange measurements. However, this is not justified (Warren 2007; Flexas et al. 2008). In fact, g_m changes with environmental conditions, and often quite rapidly, compared with changes in stomatal conductance (Flexas et al. 2007; Warren 2007).

Two types of measurements are commonly employed for the estimation of C_c, which is subsequently used to calculate g_m. **Carbon-isotope**

fractionation (Box 2.2) during gas exchange, and simultaneous measurement of **chlorophyll fluorescence** and gas exchange. The two methods rely on a number of assumptions that are largely independent, but they yield similar results (Evans and Loreto 2000). From the estimates made so far, it appears that g_m is of similar magnitude as g_s; whilst g_m is generally somewhat higher, the opposite can also be observed (Galmés et al. 2007a). Consequently, C_c is substantially lower than C_i (the CO_2 concentration in the intercellular spaces); a difference of about 80 μmol mol^{-1} is common, as compared with C_a - C_i of about 100 μmol mol^{-1}. The mesophyll conductance varies widely among species and correlates with the photosynthetic capacity (A_{max}) of the leaf (Fig. 2.7). Interestingly, the relationship between mesophyll conductance and photosynthesis is rather similar for scleromorphic and mesophytic leaves, but scleromorphs tend to have a somewhat larger drawdown of CO_2 between intercellular space and chloroplast ($C_i - C_c$) (Warren and Adams 2006).

Box 2.2: Fractionation of Stable Carbon Isotopes in Plants

CO_2 in the Earth's atmosphere is composed of different carbon isotopes. The majority is $^{12}CO_2$; approximately 1% of the total amount of CO_2 in the atmosphere is $^{13}CO_2$. Both are stable isotopes; a much smaller fraction is the radioactive species $^{14}CO_2$, which we will not deal with in the present context. Ecophysiological research makes abundant use of the fact that the isotope composition of plant biomass differs from that of the atmosphere. Carbon stable isotopes are a crucial tool in estimating time-integrated measures of photosynthetic performance of individual plants or plant communities, information that would be difficult or impossible to obtain from direct physiological measurements. Carbon-isotope composition differs among plants with different photosynthetic pathways or water-use efficiency. How can we account for that?

The molar abundance ratio, R, of the two carbon isotopes is the ratio between ^{13}C and ^{12}C. The constants k^{12} and k^{13} refer to the rate of processes and reactions in which ^{12}C and ^{13}C participate, respectively. The 'isotope effect' is:

$$R_{source}/R_{product} = k^{12}/k^{13} \qquad (2.17)$$

where the source in the case of photosynthesis is CO_2 in air (R_a) and the product of the photosynthesis process is the carbon in the plant (R_p). Since isotope effects are small, data are commonly expressed as fractionation values, $\Delta^{13}C$ (capital delta), defined as

$$\Delta^{13}C = \left(R_a/R_p - 1\right) \times 1000\ (‰) \quad (2.18)$$

Fractionation is to a small extent due to the slower diffusion in air of $^{13}CO_2$. However, most of the fractionation during photosynthesis of C_3 plants is due to the biochemical properties of Rubisco, which reacts more readily with $^{12}CO_2$ than it does with $^{13}CO_2$. As a result, Rubisco discriminates against the heavy isotope with values estimated between 27 and 30 ‰ (Farquhar et al. 1982). Smaller fractionation values are found for this enzyme from bacteria (Guy et al. 1993).

On the path from intercellular spaces to Rubisco, a number of additional steps take place, where some further isotope fractionation can occur. The intercellular CO_2 concentration (C_i) is easily estimated from gas exchange measurements (Box 2.5). The C_i/C_a ratio, where C_a is the CO_2 concentration of the air surrounding the leaf can be used for approximating the discrimination against $^{13}CO_2$ during photosynthesis by the simplified formula (Farquhar et al. 1982):

(continued)

Box 2.2 (continued)

$$\Delta^{13}C = a \times (C_a - C_i)/C_a + b\,(C_i/C_a) = a + (b - a) \times C_i/C_a \quad (2.19)$$

where a is the discrimination due to diffusion through the stomata (4.4 ‰) and b the discrimination by Rubisco (27 ‰). A rather low value is used as the net effect of Rubisco, which accounts for the additional fractionation processes, but excluding the effect of the mesophyll conductance (g_m). The equation thus assumes infinite g_m ($C_c = C_i$). The significance of a finite g_m for ^{13}C discrimination is discussed below and shown in Box Fig. 2.2.

The isotope composition of C in a sample is described as $\delta^{13}C$ ('lower case delta'):

$$\delta^{13}C\ (‰) = \left(R_{sample}/R_{standard} - 1\right) \times 1000 \quad (2.20)$$

Values for $\Delta^{13}C$ and $\delta^{13}C$ are related as:

$$\Delta = \left(\delta_{source} - \delta_{plant}\right)/\left(1 + \delta_{plant}\right) \quad (2.21)$$

where $\delta_{source} \cong -8‰$ if the source is CO_2 in air (δ_{air}) which decreases gradually due to fossil fuel burning. A $\delta^{13}C$ value of -27‰, therefore, converts to a Δ value of 19.5‰. The standard is a cretaceous limestone consisting mostly of the fossil carbonate skeletons of *Belemnitella americana* (referred to as PDB-belemnite). By definition, it has a $\delta^{13}C$ value equal to 0‰. Plant $\delta^{13}C$ values are negative, because they are depleted in ^{13}C compared with the fossil standard. Diffusion and carboxylation discriminate against $^{13}CO_2$; δ-values for C_3 plants are approx. -27‰, showing that Rubisco is the predominant factor accounting for the observed values and that diffusion is less important.

For C_4 plants, the following simplified equation has been derived (Evans et al. 1986):

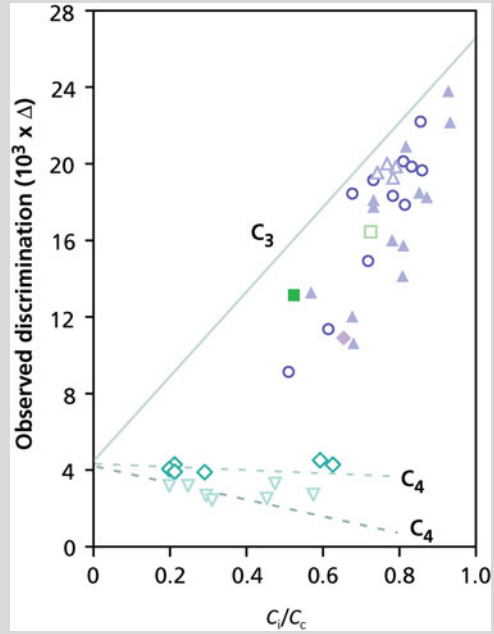

Box Fig. 2.2 The relationship between the ratio of the intercellular and the atmospheric CO_2 concentration of 340 µmol mol^{-1} (C_i/C_a). The solid line is modeled using Eq. (2.19) for C_3 plants. The hatched lines with Eq. (2.22) for C_4 plants with ϕ=0.21 (lower line) and ϕ=0.34 (upper line). $\Delta^{13}C$ was measured 'online' on CO_2 entering and leaving a gas-exchange cuvette. Data points refer to measured values for different species and measurement conditions. The lower $\Delta^{13}C$ measured compared to modelled values for the C_3 plants illustrates the lower C_c than C_i as caused by a finite g_m (Evans et al. 1986, *Australian Journal of Plant Physiology* **13**: 281–292). Copyright CSIRO, Australia.

$$\Delta^{13}C = a + (b_4 + b \times \phi - a) \times C_i/C_a \quad (2.22)$$

where ϕ is the fraction of CO_2 fixed by PEP carboxylase that leaks from the bundle sheath cells, and b4 (-5.7) is the net effect of CO_2 dissolving, hydrating to HCO_3^- and then being fixed by PEP carboxylase

Where do these equations lead us? Within C_3 plants, the $\delta^{13}C$ of whole-plant biomass gives a better indication of C_i over a longer time interval than can readily be obtained

(continued)

Box 2.2 (continued)

from gas-exchange measurements. The value of C_i in itself is a reflection of stomatal conductance (g_s), relative to photosynthetic activity (A). As such, $\delta^{13}C$ provides information on a plant's water-use efficiency (WUE) (Sect. 2.5.2). How do we arrive there? As can be derived from Eq. (2.18), the extent of the fractionation of carbon isotopes depends on the intercellular partial pressures of CO_2, relative to that in the atmosphere. If C_i is high, g_s is large relative to A, and much of the $^{13}CO_2$ discriminated against by Rubisco diffuses back to the atmosphere; hence the fractionation is large. If C_i is low, then relatively more of the accumulated $^{13}CO_2$ inside the leaf is fixed by Rubisco, and therefore the fractionation of the overall photosynthesis process is less. Comparison of WUE calculated on the basis of $\delta^{13}C$ is only valid at constant vapor pressure difference (Δw) and is called intrinsic WUE (A/g_s; iWUE). Under many situations $\delta^{13}C$ is a good proxy for WUE and it can be used for, *e.g.*, paleoclimatic studies and genetic screening for drought-tolerant varieties. However, under conditions where Δw varies or g_s and g_m are not strongly correlated, $\delta^{13}C$ may not be a good predictor of WUE.

Carbon-isotope fractionation values differ between C_3, C_4, and CAM species (Sects. 2.9 and 2.10). In C_4 plants, little of the $^{13}CO_2$ that is discriminated against by Rubisco diffuses back to the atmosphere. This is prevented, first, by the diffusion barrier between the vascular bundle sheath and the mesophyll cells. Second, the mesophyll cells contain PEP carboxylase, which scavenges most of the CO_2 that escapes from the bundle sheath (Box Table 2.1). Fractionation during photosynthesis in C_4 plants is, therefore dominated by fractionation during diffusion (4.4‰). There is also little fractionation in CAM plants, where the heavy isotopes discriminated against cannot readily diffuse out of the leaves, because the stomata are closed for most of the day. The actual $\delta^{13}C$ of CAM plant biomass depends on the fractions of the carbon fixed by CAM and C_3 photosynthesis.

Aquatic plants show relatively little fractionation due to unstirred layers surrounding the leaf, rather than to a different photosynthetic pathway (Sect. 2.11.6). The unstirred boundary layers cause diffusion to be a major limitation for their photosynthesis, so that fractionation in these plants tends toward the value found for the diffusion process.

Box Table 2.1 The magnitude of fractionation during CO_2 uptake.

Process or enzyme	Fractionation (‰)
Diffusion in air	4.4
Diffusion through the boundary layer	2.9
Dissolution of CO_2	1.1
Diffusion of aqueous CO_2	0.7
CO_2 and HCO_3^- in equilibrium	−8.5 at 30 °C
	−9.0 at 25 °C
CO_2 - HCO_3^- catalysed by carbonic anhydrase	1.1 at 25 °C
HCO_3^- - CO_2 in water, catalysed by carbonic anhydrase	10.1 at 25 °C
PEP carboxylase	2.2
Combined process	−5.2 at 30 °C
	−5.7 at 25 °C
Rubisco	30 at 25 °C

Source: Henderson et al. (1992)

The mesophyll conductance is a complicated trait, involving diffusion of CO_2 in the intercellular spaces in the gas phase, dissolving of CO_2 in the liquid phase, conversion of CO_2 into HCO_3^- catalyzed by carbonic anhydrase, and diffusion in the liquid phase and across membranes. The resistance in the gas phase is low and considered as normally not a limiting factor (Bernacchi et al. 2002). Diffusion in the liquid phase is much slower (10^4 times less), and the path length is

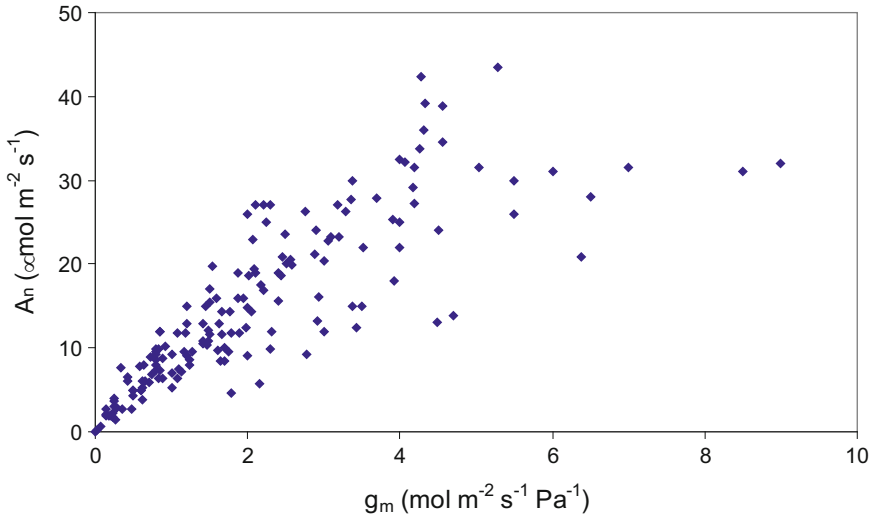

Fig. 2.7 The relationship between the rate of photosynthesis (A_n) and maximum mesophyll conductance (g_m), determined for a wide range of species. Values for scleromorphic leaves are at most 2.1 mol m^{-2} s^{-1} Pa^{-1} (g_m) and 22.9 μmol m^{-2} s^{-1} (A_n), whereas those for mesomorphic leaves span the entire range shown here. The units of conductance as used in this graph differ from those used elsewhere in this text. The reason is that when CO_2 is dissolving to reach the sites of carboxylation, the amount depends on the partial pressure of CO_2 and conductance has the units used in this graph. For air space conductance the units could be the same as used elsewhere: mol m^{-2} s^{-1}, if CO_2 is given as a mole fraction (based on data compiled in Flexas et al. 2008). Courtesy, J. Flexas, Universitat de les Illes Balears, Palma de Mallorca, Spain.

Table 2.1 The area of the chloroplast in palisade (P) and spongy (S) mesophyll ($Area_{chlor}$) expressed per unit leaf area ($Area_{leaf}$) for species from the mountain range of the East Pamirs, Tadjikistan (3500–4500 m)*.

	$(Area_{chlor})/Area_{leaf}$				
	P	S	P+S	Lowest (P+S)	Highest (P+S)
Perennial dicotyledonous herbs (54)	12	9	18	3	41
Cushion plants (4)	20	11	26	12	40
Dwarf shrubs (12)	16	6	21	5	48
Wintergreen semi-dwarf shrubs (8)	9	7	15	7	24

Source: Pyankov and Kondratchuk (1995, 1998)

*The number of investigated species is given in brackets. The sum P+S differs from P+S, because data pertain to both dorsiventral (P+S) and isopalisade (P) species

minimized by chloroplast position against the cell wall opposite intercellular spaces (Fig. 2.1). This component likely represents a large fraction of total r_m, and **carbonic anhydrase** is important for minimizing it (Gillon and Yakir 2000). Evidence for an important role for the area of chloroplasts bordering intercellular spaces as a determinant of g_m stems from a positive relationship with this parameter per unit leaf area (Evans and Loreto 2000). Data about a similar parameter, chloroplast area per leaf area, are more widely available and vary by an order of magnitude among species (Table 2.1) which is likely associated with g_m. There is evidence that specific **aquaporins** facilitate transport of CO_2 across membranes (Groszmann et al. 2017). Their role in the transport of CO_2 might account for rapid modulation of g_m in response to environmental factors such as temperature, CO_2, and desiccation (Flexas et al. 2006b). The mesophyll conductance

is proportional to chloroplast surface area within a given functional group. The difference in g_m between functional groups is associated with mesophyll cell wall thickness, which varies from 0.1 μm in some annuals, but they may be 0.2–0.3 μm in *Arabidopsis thaliana* (Mizokami et al. 2019), 0.2–0.3 μm in deciduous, broad-leaved species, and 0.3–0.5 μm in evergreen, broad-leaved species (Terashima et al. 2006). Leaves with more rigid structures (thicker cell walls) should also have a lower bulk module of elasticity (ε). A meta-analysis compiling data from all major plant growth forms shows a negative correlation between gas exchange parameters (mainly A_n and g_m) and ε (Nadal et al. 2018).

When stomatal and mesophyll conductance are considered in conjunction with the assimilation of CO_2, the 'supply function' (Eq. 2.12) tends to intersect the 'demand function' in the region where carboxylation and electron transport are co-limiting (Fig. 2.6).

2.3 Response of Photosynthesis to Light

The level of irradiance is an important ecological factor on which all photoautotrophic plants depend. Only the photosynthetically active part of the spectrum (PAR; 400–700 nm) directly drives photosynthesis. Other effects of radiation pertain to the photoperiod, which triggers flowering and other developmental phenomena in many species, the direction of the light, and the spectral quality, characterized by the red/far-red ratio, which is of major importance for many aspects of morphogenesis. We discuss these effects in Chaps 10 and 11, and effects of infrared radiation in Chap. 6; its significance through temperature effects on photosynthesis in Sect. 2.7. Effects of ultraviolet radiation are treated briefly in Sect. 7.2.2.

Low light intensities pose stresses on plants, because irradiance limits photosynthesis and thus net carbon gain and plant growth. Responses of the photosynthetic apparatus to shade can be at two levels: either at the structural level, or at the level of the biochemistry in chloroplasts. Leaf anatomy, and structure and biochemistry of the photosynthetic apparatus are treated in Sect. 2.3.2.2; aspects of morphology at the whole plant level are discussed in Sect. 10.5.1.

High light intensities may also be a stress for plants, causing damage to the photosynthetic apparatus, particularly if other factors are not optimal. The kind of damage to the photosynthetic apparatus that may occur and the mechanisms of plants to cope with excess irradiance are treated in Sect. 2.3.3.

To analyze the response of photosynthesis to irradiance, we distinguish between the dynamic response of photosynthesis to light (or any other environmental factor) and the steady-state response. A steady-state response is achieved after exposure of a leaf to constant irradiance for some time until a constant response is reached. Dynamic responses are the result of perturbations of steady-state conditions due to sudden changes in light conditions resulting in changes in photosynthetic rates.

Certain genotypes have characteristics that are adaptive in a shady environment (shade-adapted plants). In addition, plants may acclimate to a shady environment, to a greater or lesser extent, and form a shade plant phenotype (shade form). The term **shade plant** may therefore refer to an 'adapted' genotype or an 'acclimated' phenotype. Similarly, the term **sun plant** normally refers to a plant grown in high-light conditions, but is also used to indicate a shade-avoiding species or ecotype. The terms sun leaf and shade leaf are used more consistently; they refer to leaves that have developed at high and low irradiance, respectively.

2.3.1 The Light Climate Under a Leaf Canopy

The average **irradiance** decreases exponentially through the plant canopy, with the extent of light attenuation depending on both the amount and arrangement of leaves (Monsi and Saeki 1953; Monsi and Saeki 2005):

$$I = I_o e^{-kL} \tag{2.23}$$

where I is the irradiance beneath the canopy; I_o is the irradiance at the top of the canopy; k is the

extinction coefficient; and L is the cumulative leaf area index from the top to the given depth of the canopy. The extinction coefficient is low for vertically inclined leaves (for example 0.3-0.5 for grasses), higher for a more horizontal leaf arrangement, and approaching 1.0 for randomly distributed, small, perfectly horizontal leaves. A low extinction coefficient allows more effective light transfer through canopies dominated by these plants. Leaves are more vertically inclined in full sun than in cloudy or shaded environments. This minimizes the probability of photoinhibition and increases light penetration to lower leaves in high-light environments, thereby maximizing whole-canopy photosynthesis (Terashima and Hikosaka 1995). Leaf area index ranges from less than 1 in sparsely vegetated communities like deserts or tundra to 5–7 for crops to 5–10 for forests (Schulze et al. 1994).

The **spectral composition** of shade light differs from that above a canopy due to the selective absorption of photosynthetically active radiation by leaves. Transmittance of photosynthetically active radiation is typically less than 10%, whereas transmittance of far-red (FR, 730 nm) light is substantial (Fig. 11.6). As a result, the ratio of red (R, 660 nm) to far-red (the R/FR ratio) is lower in canopy shade. This affects the photoequilibrium of **phytochrome**, a pigment that allows a plant to perceive shading by other plants (Box 10.2), and requires adjustment of the photosynthetic apparatus.

Another characteristic of the light climate in and under a leaf canopy is that direct sunlight may arrive as 'packages' of high intensity: **sunflecks**, short spells of high irradiance against a background of low irradiance. Such sunflecks are due to the flutter of leaves, movement of branches and the changing angle of the sun. Their duration ranges from less than a second to minutes. Sunflecks typically have lower irradiance than direct sunlight due to penumbral effects, but large sunflecks can approach irradiances of direct sunlight. Since sunflecks are a critical component of seasonal carbon gain for shaded leaves, sunfleck regimes and physiological responses to sunflecks should be incorporated into models to more accurately capture forest and crop carbon dynamics (Way and Pearcy 2012). Even at the top of the canopy, fluctuating light due to clouds perturbs photosynthesis greatly (Yamori 2016).

2.3.2 Physiological, Biochemical, and Anatomical Differences Between Sun and Shade Leaves

Shade leaves exhibit a number of traits that make them quite distinct from leaves that developed in full daylight. We first discuss these traits and then some of the problems that may arise in leaves from exposure to high irradiance. In the last Section, we discuss signals and transduction pathways that allow the formation of sun *vs.* shade leaves.

2.3.2.1 The Light-Response Curve of Sun and Shade Leaves

The steady-state rate of CO_2 assimilation increases asymptotically with increasing irradiance. Below the **light-compensation point** ($A_n = 0$), there is insufficient light to compensate for respiratory carbon loss due to photorespiration and dark respiration (Fig. 2.8). At low light intensities, A_n increases linearly with irradiance, with the light-driven electron transport limiting

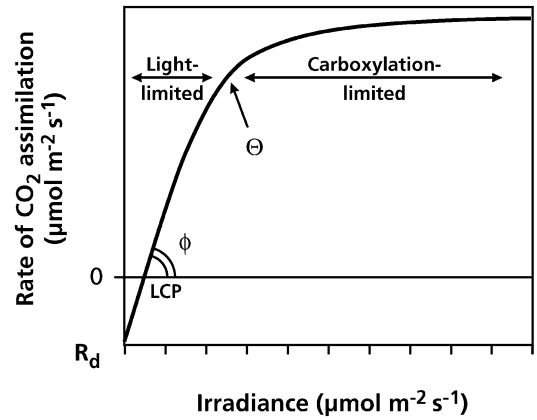

Fig. 2.8 Typical response of net photosynthesis to irradiance, drawn according to Eq. 2.24. The intercept with the x-axis is the light-compensation point (*LCP*), the initial slope of the line gives the quantum yield (ϕ) and the intercept with the y-axis is the rate of dark respiration (R_d). The curvature of the line is described by θ. At low irradiance, the rate of CO_2 assimilation is light-limited; at higher irradiance A_n is carboxylation limited. A_{max} is the light-saturated rate of CO_2 assimilation at ambient C_a.

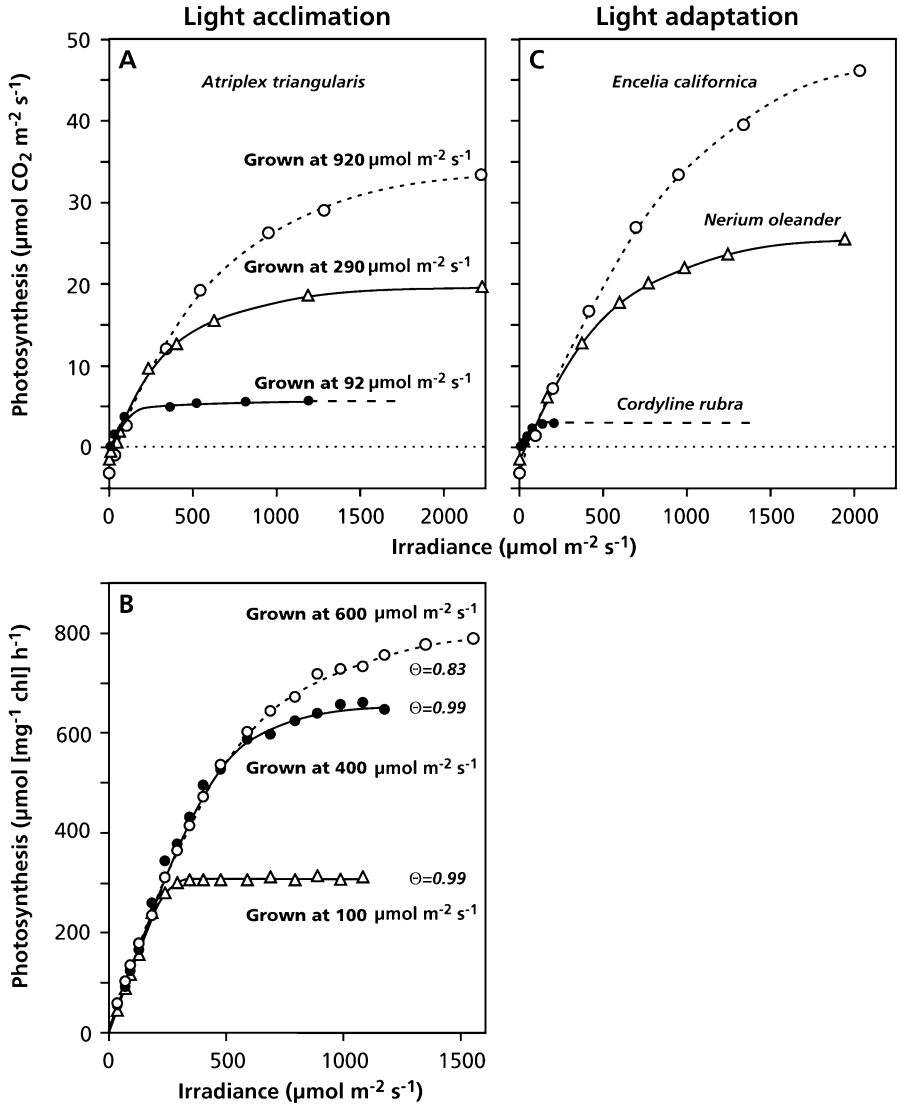

Fig. 2.9 Photosynthesis as a function of irradiance for different species and growing conditions. Light acclimation: (**A**) for *Atriplex triangularis* (Björkman 1981) and (**B**) for a thin algal culture (*Coccomyxa* sp.) grown at different levels of irradiance 100, 400, or 600 µmol m^{-2} s^{-1} (**B**) note the difference in 'curvature', for which the Θ values (Eq. 2.24) are given in B, between the three curves (after Ögren 1993). Copyright American Society of Plant Biologists. Light adaptation: (**C**) for species which naturally occur at a high, intermediate, or low irradiance (after Björkman 1981).

photosynthesis. The initial slope of the light-response curve based on *absorbed* light (**quantum yield**) describes the efficiency with which light is converted into fixed carbon (typically about 0.06 moles CO_2 fixed per mole of quanta under favorable conditions and a normal atmospheric CO_2 concentration). When the light-response curve is based on *incident* light, the leaf's absorbance also determines the quantum yield; this initial slope is called the **apparent quantum yield**. At high irradiance, photosynthesis becomes light-saturated and is limited by carboxylation rate, which is governed by some combination of CO_2 diffusion into the leaf and carboxylation capacity. The shape of the light-response curve can be described by a nonrectangular hyperbola (Fig. 2.9):

$$A_n = \frac{\phi x I + A_{max} - \left\{ (\phi \times I + A_{max})^2 - 4 \times \Theta x \phi x I \, x A_{max} \right)^{0.5} \}}{2\Theta} - R_d \quad (2.24)$$

where A_{max} is the light-saturated rate of gross CO_2 assimilation (net rate of CO_2 assimilation + dark respiration) at infinitely high irradiance, ϕ is the (apparent) quantum yield (on the basis of either incident or absorbed photons), Θ is the curvature factor, which can vary between 0 and 1, and R_d is the dark respiration during photosynthesis. Equation 2.24 can also be used to describe the light dependence of electron transport, when A is replaced by J and A_{max} by J_{max} (Box 2.1). This mathematical description is useful, because it contains variables with a clear physiological meaning that can be derived from light-response curves and used to model photosynthesis.

Sun leaves differ from shade leaves primarily in their faster light-saturated rates of photosynthesis (A_{max}) (Fig. 2.9). The rate of dark respiration typically covaries with A_{max}. The initial slope of the light-response curves of light-acclimated and shade-acclimated plants (the **quantum yield**) is the same, except when shade-adapted plants become inhibited or damaged at high irradiance (photoinhibition or photodestruction), which reduces the quantum yield. The apparent quantum yield (*i.e.* based on incident photon irradiance) may also vary with variation in absorptance due to differences in chlorophyll concentration per unit leaf area. This is typically not important in the case of acclimation to light (Sect. 2.3.2.3), but cannot be ignored when factors such as nutrient availability and senescence play a role. The transition from the light-limited part to the light-saturated plateau is generally abrupt in shade leaves, but more gradual in sun leaves (higher A_{max} and lower Θ in sun leaves). Although shade leaves typically have a low A_{max}, they have lower light-compensation points and faster rates of photosynthesis at low light, because of their slower respiration rates per unit leaf area (Fig. 2.9).

Just as in acclimation, most plants that have evolved under conditions of high light have higher light-saturated rates of photosynthesis (A_{max}), higher light-compensation points, and slower rates of photosynthesis at low light than do shade-adapted plants when grown under the same conditions.

2.3.2.2 Anatomy and Ultrastructure of Sun and Shade Leaves

One mechanism by which sun-grown plants, or sun leaves on a plant, achieve a high A_{max} (Fig. 2.9) is by producing **thicker** leaves (Fig. 2.10) which provides space for more chloroplasts per unit leaf area. The increased thickness is largely due to the formation of longer palisade cells in the mesophyll, and, in species that have this capacity, the development of multiple palisade layers in sun leaves (Hanson 1917). Plants that naturally occur in high-light environments (*e.g.*, *Eucalyptus* and *Hakea* species) may have palisade parenchyma on both sides of the leaf (Fig. 2.1). Such leaves are naturally positioned (almost) vertically, so that both sides of the leaf receive a high irradiance, except at peak irradiance in the middle of the day. Anatomy constrains the potential of leaves to acclimate, *e.g.*, the acclimation potential of shade leaves to a high-light environment is limited by the space in mesophyll cells bordering intercellular spaces (Oguchi et al. 2005). Full acclimation to a new light environment, therefore, typically requires the production of new leaves.

The spongy mesophyll in dorsiventral leaves of dicotyledons increases the **path length** of light in leaves by reflection at the gas-liquid interfaces of these irregularly oriented cells. The relatively large proportion of spongy mesophyll in shade leaves, therefore, enhances leaf absorptance, due to greater internal light

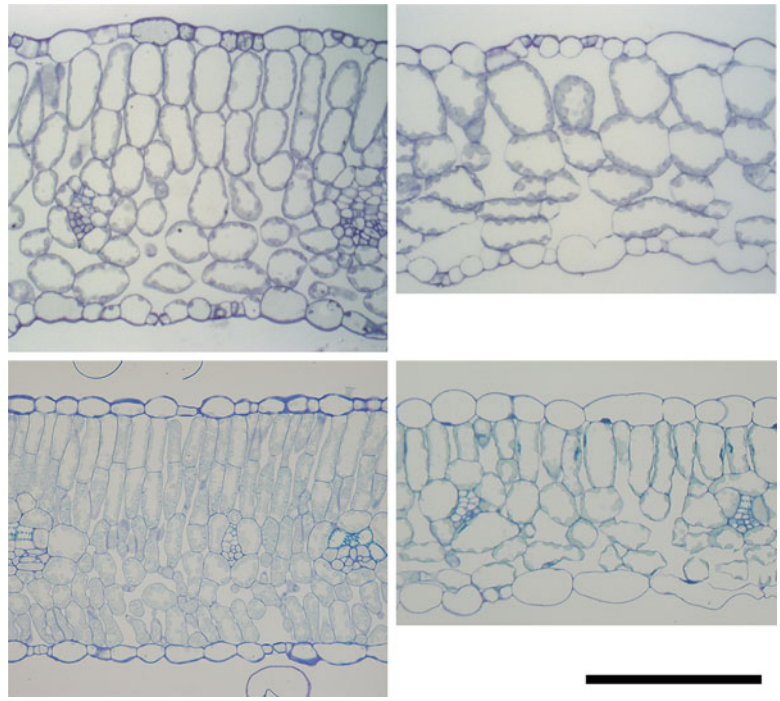

Fig. 2.10 Light-microscopic transverse sections of sun and shade leaves of two species: (Top) *Arabidopsis thaliana* (thale cress) and (Bottom) *Chenopodium album* (pigweed). Note that the sun leaves of *Arabidopsis thaliana* have two cell layers for the palisade tissue while those of *Chenopodium album* have only one layer. Shade leaves of both species have only one cell layer. Scale bar = 100 µm (courtesy S. Yano, National Institute for Basic Biology, Okazaki, Japan).

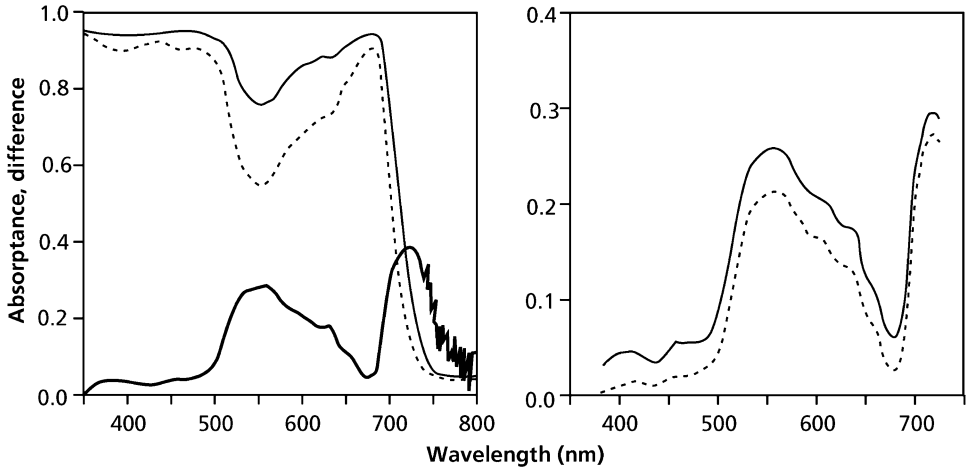

Fig. 2.11 (**A**) Light absorptance in a shade leaf of *Hydrophyllum canadense* (broad-leaved waterleaf). The solid line gives the absorptance of a control leaf. The broken line shows a leaf infiltrated with mineral oil, which reduces light scattering. The difference between the two lines is given as the thick solid line. (**B**) The difference in absorptance between an oil-infiltrated leaf and a control leaf of *Acer saccharum* (sugar maple). The solid line gives the difference for a shade leaf, the broken line for a sun leaf (after DeLucia et al. 1996).

scattering (Vogelmann et al. 1996). When air spaces of shade leaves of *Hydrophyllum canadense* (broad-leaved waterleaf) or *Asarum canadense* (Canadian wild-ginger) are infiltrated with mineral oil to eliminate internal light scattering, light absorptance at 550 and 750 nm is reduced by 25 and 30%, respectively (Fig. 2.11). In sun leaves, which have relatively less spongy

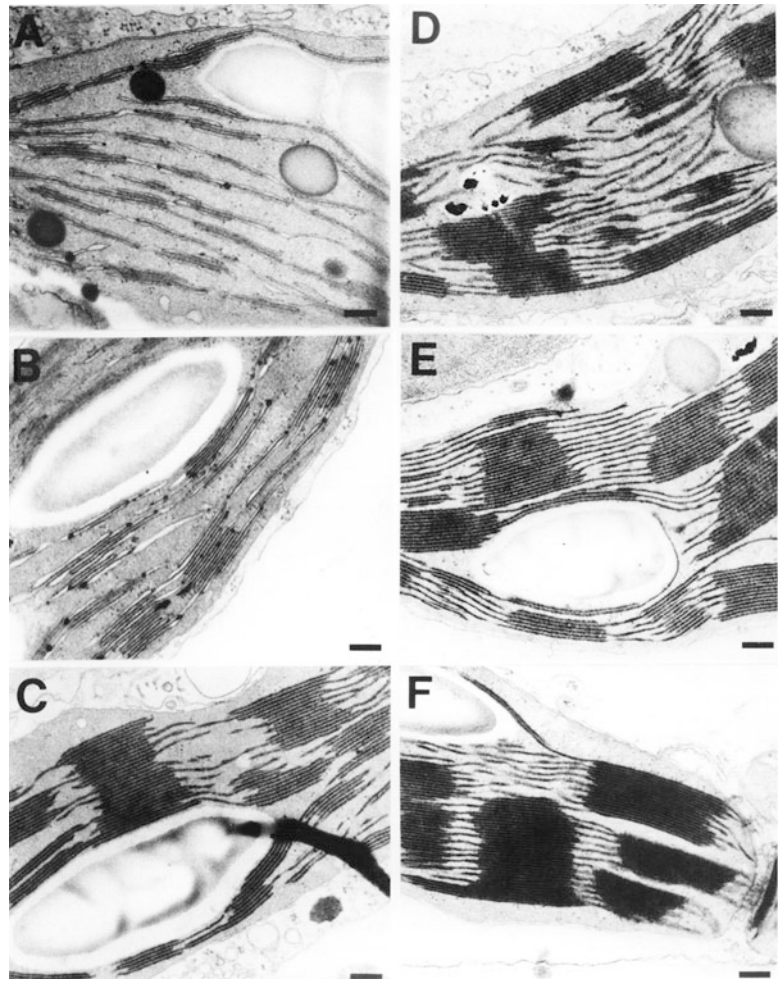

Fig. 2.12 Electron micrographs of chloroplasts in sun (**A**–**C**) and shade (**D**–**F**) leaves of *Schefflera arboricola* (dwarf umbrella plant). Chloroplasts found in upper palisade parenchyma tissue (**A**, **D**), lower palisade parenchyma tissue (**B**, **E**) and spongy mesophyll tissue (**C**, **F**). Note the difference in grana between sun and shade leaves and between the upper and lower layer inside the leaf. Scale bar = 0.2 μm (courtesy A.M. Syme and C. Critchley, Department of Botany, The University of Queensland, Australia).

mesophyll, the effect of infiltration with oil is much smaller. The optical path length in leaves ranges from 0.9 to 2.7 times that of an equivalent amount of pigment in an organic solvent, partly because not all light may intercept a chloroplast. The path length is greatly increased in thin leaves of shade plants, enhancing the effectiveness of light absorption (Rühle and Wild 1979).

There are fewer chloroplasts per unit area in shade leaves as compared with sun leaves due to the reduced thickness of mesophyll. The **ultrastructure** of the chloroplasts of sun and shade leaves shows distinct differences (Fig. 2.12). Shade chloroplasts have a smaller volume of stroma, where the Calvin-Benson-cycle enzymes are located, but larger grana, which contain most of the chlorophyll. Such differences are found both between plants grown under different light conditions and between sun and shade leaves on a single plant, as well as when comparing chloroplasts from the upper and lower side of one, relatively thick, leaf of *Schefflera arboricola* (dwarf umbrella plant) (Fig. 2.12). The adaxial (upper) regions have a chloroplast ultrastructure like sun leaves, whereas shade acclimation is found in the abaxial (lower) regions of the leaf (Box 2.3).

Box 2.3: Carbon-Fixation and Light-Absorption Profiles inside Leaves

We are already familiar with differences in biochemistry and physiology *between* sun and shade leaves (Sect. 2.3.2). If we consider the gradient in the level of irradiance inside a leaf, however, then should we not expect similar differences *within* leaves? Indeed, palisade mesophyll cells at the adaxial (upper) side of the leaf tend to have characteristics associated with acclimation to high irradiance: a high Rubisco/chlorophyll and chl a/chl b ratio, high levels of xanthophyll-cycle carotenoids, and less stacking of the thylakoids (Fig. 2.13; Terashima and Hikosaka 1995). On the other hand, the spongy mesophyll cells at the abaxial (lower) side of the leaf have chloroplasts with a lower Rubisco/chlorophyll and chl a/chl b ratio, characteristic for acclimation to low irradiance. What are the consequences of such profiles within the leaf for the exact location of carbon fixation in the leaf?

To address this question we first need to know the light profile within a leaf which can be measured with a fiberoptic microprobe that is moved through the leaf, taking light readings at different wavelengths (Vogelmann 1993). Chlorophyll is not homogeneously distributed in a cell; rather, it is concentrated in the chloroplasts that may have a heterogeneous distribution within and between cells. In addition, inside the leaf, absorption varies because of scattering at the air-liquid interfaces that modify pathlength (*e.g.*, between palisade and spongy mesophyll) (Sect. 2.3.2.4). How can we obtain information on light absorption?

After a period of incubation in the dark, chlorophyll fluorescence of a healthy leaf is proportional to the light absorbed by that leaf (Box 2.4). Vogelmann and Evans (2002) illuminated leaves at the adaxial side and at the side of a transversal cut, and measured the distribution of fluorescence over the cut surface using imaging techniques. Fluorescence obtained with adaxial light represents light absorption, whereas lighting the cut surface represents chlorophyll concentration. In leaves of *Spinacia oleracea* (spinach), going from the upper leaf surface deeper into the leaf, the chlorophyll concentration increases to 50 μmol m^{-2} over the first 250 μm in the palisade layer, remains similar deeper down in the palisade and spongy mesophyll, but then declines steeply toward the lower surface over the last 100 μm of the spongy mesophyll layer (Fig. 2.3). As expected from the absorption characteristics of chlorophyll (Fig. 2.2), green light is less strongly absorbed than blue and red, penetrates deeper into the leaf, and, consequently, shows there a higher absorption (Box Fig. 2.3A). The data on light absorption and chlorophyll concentration allow the calculation of an extinction coefficient, which varies surprisingly little across a leaf. Differences in scattering between the two mesophyll layers are apparently not very important as is also evident from measurements of infiltrated leaves (Fig. 2.11; Vogelmann and Evans 2002).

What are the consequences of the profiles of absorption and chlorophyll concentration for the distribution of photosynthetic activity across section a leaf? The profile of photosynthetic capacity (A_{max}) can be measured following fixation of $^{14}CO_2$ ensuring light saturation for all chloroplasts (Evans and Vogelmann 2003); alternatively, the profile of Rubisco concentration can be used (Nishio et al. 1993). Both techniques require making thin sections parallel to the leaf surface. A_{max} peaks where chlorophyll reaches its maximum in the palisade mesophyll, and declines to a lower value in the spongy mesophyll (Fig. 2.3). A_{max} per chlorophyll

(continued)

Box 2.3 (continued)

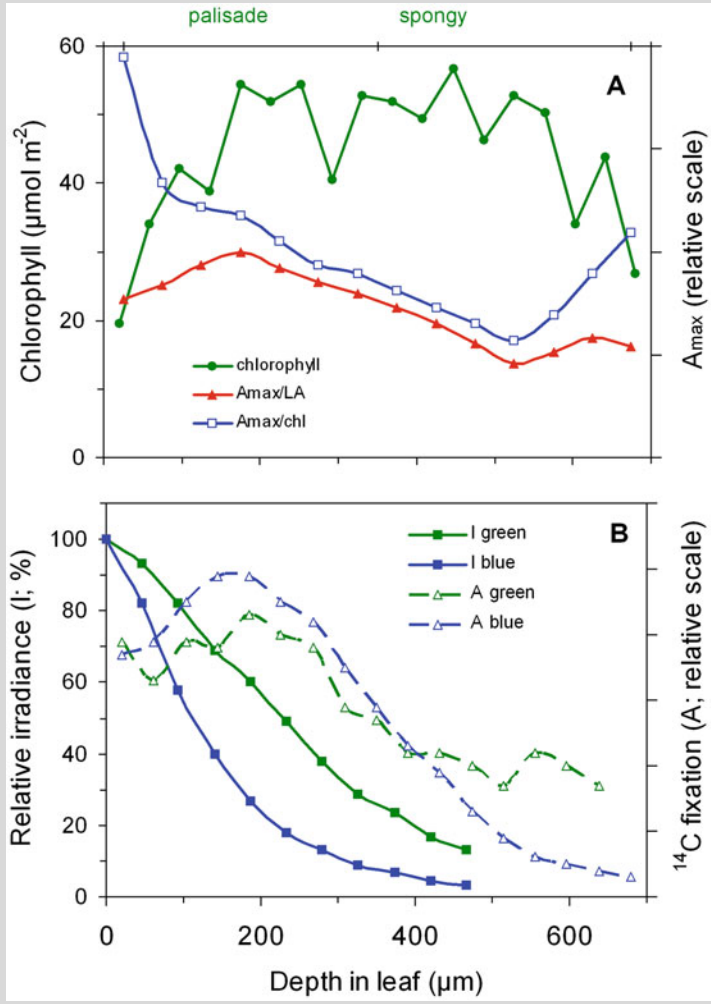

Box Fig. 2.3 Profiles of chlorophyll and light absorption (**A**), and photosynthesis (**B**) in a leaf of *Spinacia oleracea* (spinach). The distribution of chlorophyll was derived from measurements of chlorophyll fluorescence, using a light source to illuminate the cut surface of a transversal section of the leaf. The absorption of green and blue light was also measured with chlorophyll fluorescence, but with light striking the upper leaf surface. The light-saturated photosynthetic electron transport rate (A_{max}) was derived from ^{14}C-fixation profiles and photosynthetic activity at and irradiance of 500 and 50 µmol m^{-2} s^{-1} in green and blue light were calculated using Eq. (2.25) (Vogelmann and Evans 2002; Evans and Vogelmann 2003).

decreases similarly from the palisade to the spongy mesophyll. We can use the profiles of A_{max} and absorbed irradiance to calculate photosynthetic activity (A) in each layer from the light-response curve, using virtually the same equation as introduced in Section 2.3.2.1 (the only difference being that R_{day} is left out):

$$A = \frac{\phi \times I + A_{max} - \left\{(\phi \times I + A_{max})^2 - (4 \times \theta \times \phi \times I \times A_{max})^{0.5}\right\}}{2\theta} \quad (2.25)$$

where ϕ is the maximum quantum yield, I is the absorbed irradiance and θ describes the curvature. The calculated light-response

(continued)

Box 2.3 (continued)

curves of the adaxial layers are like those of sun leaves, whereas those of the abaxial layers are like the ones of shade leaves. Photosynthetic activity peaks close to the adaxial surface in low light, but the maximum shifts to deeper layers at higher irradiances (Fig. 2.3). Since green light has a lower absorptance, *A* in that spectral region is more homogeneously distributed across the leaf profile, whereas blue light causes a sharp peak closer to the upper surface. Calculated profiles of *A* show a close match with the experimental data of the ^{14}C-fixation profile.

2.3.2.3 Biochemical Differences Between Shade and Sun Leaves

Shade leaves **minimize light limitation** through increases in capacity for light capture and decreased carboxylation capacity and mesophyll conductance, but this does not invariably lead to higher chlorophyll concentrations per unit leaf area which determines their absorptance (Terashima et al. 2001). Some highly shade-adapted species [*e.g.*, *Hedera helix* (ivy) in the juvenile stage], however, may have substantially higher chlorophyll levels per unit leaf area in shade. This might be due to the fact that their leaves do not get much thinner in the shade; however, there may also be some photodestruction of chlorophyll in high light in such species. In most species, however, higher levels of chlorophyll per unit fresh mass and per chloroplast in shade leaves are compensated for by the smaller number of chloroplasts and a lower fresh mass per area. This results in a rather constant chlorophyll level per unit area in sun- and shade leaves.

The **ratio** between **chlorophyll a** and **chlorophyll b** (chl a/chl b) is lower in shade-acclimated leaves. These leaves have relatively more chlorophyll in the **light-harvesting complexes**, which contain large amounts of chl b (Lichtenthaler and Babani 2004). The decreased chl a/chl b ratio is therefore a reflection of the greater investment in LHCs. The larger proportion of LHC is located in the **larger grana** of the shade-acclimated chloroplast (Fig. 2.12). Sun leaves also contain more xanthophyll carotenoids, relative to chlorophyll (Box 2.3; Esteban et al. 2015).

Sun leaves have larger amounts of Calvin-Benson-cycle enzymes per unit leaf area due to more cell layers, a larger number of chloroplasts per cell, and a larger volume of stroma, where these enzymes are located, per chloroplast, compared with shade leaves. Sun leaves also have more stroma-exposed thylakoid membranes, which contain the b_6f cytochromes and ATPase (Fig. 2.13). All these components enhance the **photosynthetic capacity** of sun leaves. Since

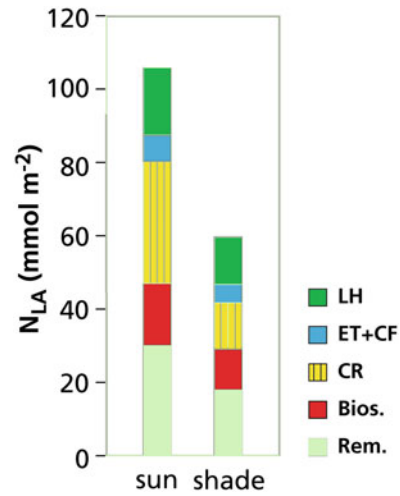

Fig. 2.13 Nitrogen partitioning among various components in shade- and sun-acclimated leaves. Most of the leaf's N in herbaceous plants is associated with photosynthesis. Some of the fractions labeled Bios. (Biosynthesis) and Rem. (Remainder) are indirectly involved in synthesis and maintenance processes associated with the photosynthetic apparatus. LH = light harvesting (LHC, PS I, PS II), ET+CF = electron transport components and coupling factor (ATPase), CR = enzymes associated with carbon reduction (Calvin-Benson cycle, mainly Rubisco), Bios = biosynthesis (nucleic acids and ribosomes), Rem = remainder, other proteins and N-containing compounds (*e.g.*, mitochondrial enzymes, amino acids, cell wall proteins, alkaloids) (after Evans and Seemann 1989).

the amount of chlorophyll per unit area is similar among leaf types, sun leaves also have a higher photosynthetic capacity per unit chlorophyll. The biochemical gradients for Rubisco/chlorophyll across a leaf are similar to those observed within a canopy, with adaxial (upper) cells having more Rubisco, but less chlorophyll than abaxial (lower) cells (Terashima and Hikosaka 1995).

2.3.2.4 The Light-Response Curve of Sun and Shade Leaves Revisited

Table 2.2 summarizes the differences in characteristics between shade-acclimated and sun-acclimated leaves (Esteban et al. 2015). The higher A_{max} of sun leaves as compared with shade leaves is associated with a greater amount of compounds that determine photosynthetic capacity which are located in the greater number of chloroplasts per area and in the larger stroma volume and the stroma-exposed thylakoids in chloroplasts. The increase of A_{max} with increasing amount of these compounds is almost linear (Evans and Seemann 1989). Hence, investment in compounds determining photosynthetic capacity is proportional to photosynthetic rate at high irradiance levels.

The faster rate of dark respiration in sun leaves is not only due to a greater demand for respiratory energy for the maintenance of the larger number of leaf cells and chloroplasts, because respiration rates drop rapidly upon shading, whereas A_{max} is

Table 2.2 Overview of generalized differences in characteristics between shade- and sun-acclimated leaves.

	Sun	Shade
Structural		
Leaf dry mass per area	high	low
Leaf thickness	thick	thin
Palisade parenchyma thickness	thick	thin
Spongy parenchyma thickness	similar	similar
Stomatal density	high	low
Chloroplast per area	many	few
Thylakoids per stroma volume	low	high
Thylakoids per granum	few	many
Biochemical		
Chlorophyll per chloroplast	low	high
Chlorophyll per area	similar	similar
Chlorophyll per dry mass	low	high
Chlorophyll a/b ratio	high	low
Light-harvesting complex per area	low	high
Electron transport components per area	high	low
Coupling factor (ATPase) per area	high	low
Rubisco per area	high	low
Nitrogen per area	high	low
Xanthophylls per area	high	low
Gas exchange		
Photosynthetic capacity per area	high	low
Dark respiration per area	high	low
Photosynthetic capacity per dry mass	similar	similar
Dark respiration per dry mass	similar	similar
Carboxylation capacity per area	high	low
Electron transport capacity per area	high	low
Quantum yield	similar	similar
Curvature of light-response curve	gradual	acute

still high (Pons and Pearcy 1994). Much of the demand for ATP is probably associated with the export of the products of photosynthesis from the leaf and other processes associated with a high photosynthetic activity (Sect. 3.4.4).

The preferential absorption of photons in the red and blue regions of the spectrum by a leaf is not a simple function of its irradiance and chlorophyll concentration. A relationship with a negative exponent is expected, as described for monochromatic light and pigments in solution (Lambert-Beer's law). The situation in a leaf is more complicated, however, because preferential absorption of red light by chlorophyll causes changes in the spectral distribution of light through the leaf. Moreover, the path length of light is complicated, due to reflection at the interface of cells and inside the leaf and to changes in the proportions of direct and diffuse light. Empirical equations, such as a hyperbole, can be used to describe light absorption by chlorophyll. For a healthy leaf, the quantum yield based on incident light is directly proportional to the amount of photons absorbed.

The cause of the decrease in convexity (Eq. 2.24) of the light-response curve with increasing growth irradiance (Fig. 2.9) is probably partly associated with the level of light-acclimation of the chloroplast in the cross section of a leaf in relation to the distribution of light within the leaf (Leverenz 1987).

A high A_{max} per unit area and per unit chlorophyll (but not per unit biomass) of sun leaves is beneficial in high-light conditions, because the prevailing high irradiance can be efficiently exploited, and photon absorption per unit photosynthetic capacity is not limiting photosynthetic rates. Such a high A_{max}, however, would be of little use in the shade, because the high irradiance required to utilize the capacity occurs only infrequently, and a high A_{max} is associated with fast rates of respiration and a large investment of resources. On the other hand, a high chlorophyll concentration per unit photosynthetic capacity and per unit biomass in thin shade leaves maximizes the capture of limiting photons in low-light conditions which is advantageous at low irradiance. There is a trade-off between investment of resources in carbon-assimilating capacity and in light harvesting as reflected in the ratio of photosynthetic capacity to chlorophyll concentration. This ratio represents light acclimation at the chloroplast level.

Although A_{max} per unit chlorophyll responds qualitatively similar to growth irradiance in all plants, there are differences among species (Fig. 2.14; Murchie and Horton 1997; Oguchi et al. 2018). There are four functional groups:

1. Shade-avoiding species such as pioneer trees have a high A_{max}/chlorophyll ratio. This ratio, however, does not change much with growth irradiance.
2. Fast-growing herbaceous species from habitats with a dense canopy and/or a variable light availability have high A_{max}/chlorophyll ratios, which decrease strongly with decreasing irradiance.

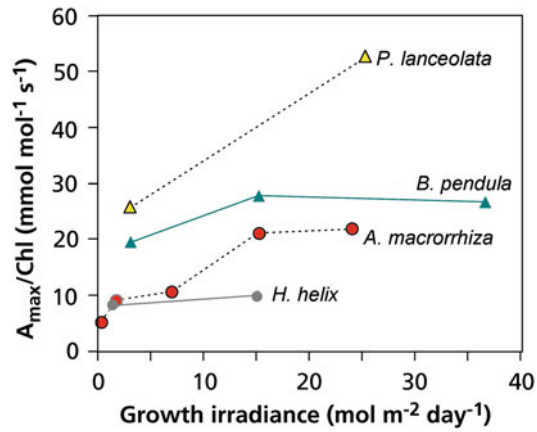

Fig. 2.14 Light-saturated rate of CO_2 assimilation (A_{max}) per unit chlorophyll in relation to growth irradiance for four different species. *Plantago lanceolata* (snake plantain) (Poot et al. 1996), *Betula pendula* (European white birch, Bp) (Öquist et al. 1982), *Alocasia macrorrhiza* (giant taro, Am) (Sims and Pearcy 1989) and *Hedera helix* (ivy, Hh) (T.L. Pons, unpublished data).

3. A plastic response is also found in shade-adapted plants such as herbaceous understory species [*Alocasia macrorrhiza* (giant taro)] that depend on gaps for reproduction, and forest trees that tolerate shade as seedlings. The A_{max}/chlorophyll ratio, however, is much lower over the entire range of irradiance levels.
4. A low A_{max}/chlorophyll ratio that changes little with growth irradiance is found in woody shade-adapted species, such as juvenile *Hedera helix* (ivy).

2.3.2.5 The Regulation of Acclimation

As mentioned in previous Sections, light acclimation consists of changes in leaf structure and chloroplast number at the leaf level, and changes in the photosynthetic apparatus at the chloroplast level. Some aspects of leaf anatomy, including morphology of epidermal cells and the number of stomata, are controlled by **systemic signals** originating in mature leaves (Lake et al. 2001; Coupe et al. 2006). Chloroplast properties are mostly determined by the **local light environment** of the developing leaves (Yano and Terashima 2001). This local environment affects the rate of transpiration and the delivery of signaling molecules such as cytokinins which affect acclimation of leaves in a canopy (Pons 2016).

Studies of regulation at the chloroplast level have yielded significant insights. Each of the major components of the photosynthetic apparatus has part of their subunits encoded in the chloroplast and others in the nucleus. Acclimation of chloroplast composition thus likely entails coordinated changes in transcription of both genomes. The abundance of mRNAs encoding photosynthetic proteins, however, does not respond clearly during acclimation which suggests that post-transcriptional modifications play an important role (Walters 2005). Several perception mechanisms of the spectral and irradiance component of the light climate have been proposed.

When leaves of *Oryza sativa* (rice) are kept in darkness and **far-red-light** conditions for several days, there is an initial lag in chlorophyll concentration, Chl a/b ratio, and maximum PS II photochemistry (Yamazaki 2010). In contrast, Rubisco rapidly disappears under low-light conditions. The PSII and PSI reaction centers are regulated by light quality, but cytochrome f is regulated by light intensity. An imbalance between PSII and PSI induces the generation of reactive oxygen species (**ROS**), although these are scavenged by stromal enzymes such as superoxide dismutase, ascorbate peroxidase, and glutathione reductase. The activities of these stromal enzymes are also regulated by light quality. Thus, although the photosynthetic apparatus is regulated differently depending on light quality, light quality may play an important role in the regulation of the photosynthetic apparatus (Yamazaki 2010). **Systemic signals** play a role in the effect of the light environment of mature leaves on the acclimation of young, growing leaves, irrespective of their own light environment (Yano and Terashima 2001).

2.3.3 Effects of Excess Irradiance

All photons absorbed by the photosynthetic pigments result in excited chlorophyll, but at irradiance levels beyond the linear, light-limited region of the light-response curve of photosynthesis, not all excited chlorophyll can be used in photochemistry (Figs 2.8 and 2.15). The fraction of excitation energy that cannot be used increases with irradiance and under conditions that restrict the rate of electron transport and Calvin-Benson-cycle activity such as extreme temperatures and desiccation. This is potentially harmful for plants, because the excess excitation may result in serious damage, if it is not dissipated, but plants have mechanisms to safely dispose of this excess excitation energy. When these mechanisms are at work, the quantum yield of photosynthesis is

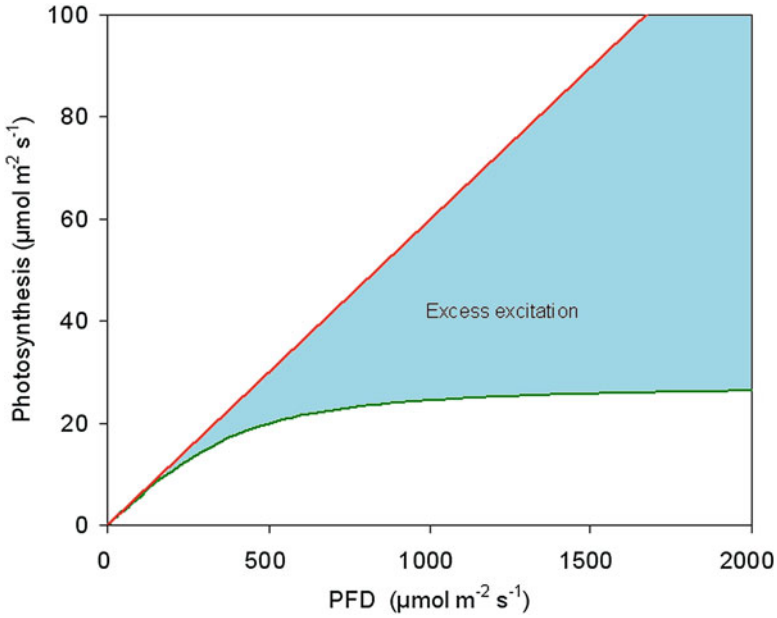

Fig. 2.15 Response of photosynthesis to light intensity. Photosynthesis increases hyperbolically with irradiance, but photon absorption, and thus the generation of excited chlorophylls, increases linearly. The difference (blue area) between the two processes increases with increasing irradiance and represents the excess excitation energy.

temporarily reduced (minutes), a normal phenomenon at high irradiance. The excess excitation energy, however, may also cause damage to the photosynthetic membranes if the dissipation mechanisms are inadequate. This is called **photoinhibition**, which is due to an imbalance between the rate of photodamage to PS II and the rate of repair of damaged PS II. Photodamage is initiated by the direct effects of light on the O_2-evolving complex and, thus, photodamage to PS II is unavoidable (Nishiyama et al. 2006). We refer to this as the **excess-energy hypothesis** (Ögren et al. 1984; Demmig and Björkman 1987). The alternative, the **two-step hypothesis**, suggests that the excitation of manganese (Mn) in the oxygen-evolving complex by photons is the primary cause, while the subsequent excitation of chlorophyll by photons leads to secondary damage to the reaction center of PSII (Hakala et al. 2005; Ohnishi et al. 2005). Experimental evidence support both hypotheses, but the two-step mechanism appears to be the most important (Oguchi et al. 2011).

A reduction in quantum yield that is re-established within minutes to normal healthy values is referred to as **dynamic photoinhibition** (Osmond 1994; Teixeira et al. 2015); it is predominantly associated with changes in the xanthophyll cycle (Sect. 2.3.3.1). More serious damage that takes hours to revert to control conditions leads to **chronic photoinhibition**; it is mostly related to temporarily impaired D1 (Sect. 2.2.1.1; Long et al. 1994; Kitao et al. 2018). Even **longer-lasting** photoinhibition (days) can be referred to as **sustained photoinhibition** (Sect. 2.7.2; Míguez et al. 2015). A technique used for the quantification of photoinhibition is the measurement of quantum yield by means of **chlorophyll fluorescence** (Box 2.4).

Box 2.4: Chlorophyll Fluorescence

When chlorophyllous tissue is irradiated with photosynthetically active radiation (PAR; 400–700 nm) or wavelengths shorter than 400 nm, it emits radiation of longer wavelengths (approx. 680–760 nm). This fluorescence originates mainly from chlorophyll a associated with photosystem II (PS II). The measurement of the kinetics of chlorophyll fluorescence has been developed into a sensitive tool for probing state variables of the photosynthetic apparatus *in vivo*. In an ecophysiological context, this is a useful technique to quantify effects of stress on photosynthetic performance. It is also applicable under field conditions.

Photons absorbed by chlorophyll give rise to (1) an excited state of the pigment which is channelled to the reaction center and may give rise to photochemical charge separation. The quantum yield of this process is given by ϕ_p. Alternative routes for the excitation energy are (2) dissipation as heat (ϕ_D) and (3) fluorescent emission (ϕ_F). These three processes are competitive. This leads to the assumption that the sum of the quantum yields of the three processes is unity:

$$\phi_P + \phi_D + \phi_F = 1 \qquad (2.26)$$

Since only the first two processes are subject to regulation, the magnitude of fluorescence depends on the added rates of photochemistry and heat dissipation. Measurement of fluorescence, therefore, provides a tool for quantification of these processes.

Basic Fluorescence Kinetics

When a leaf is subjected to strong white light after incubation in darkness, a characteristic pattern of fluorescence follows, known as the Kautsky curve (Bolhàr-Nordenkampf and Ögren 1993; Schreiber et al. 1995a). It rises immediately to a low value (F_0), which is maintained only briefly in strong light, but can be monitored for a longer period in weak intermittent light (Box Fig. 2.4, left). This level of fluorescence (F_0) is indicative of open reaction centers due to a fully oxidized state of the primary electron acceptor Q_A. In strong saturating irradiance, fluorescence rises quickly to a maximum value (F_m) (Box Fig. 2.4, left) which indicates closure of all reaction centers as a result of fully reduced Q_A. When light is maintained, fluorescence decreases gradually (quenching) to a stable value as a result of induction of photosynthetic electron transport and dissipation processes.

After a period of illumination at a sub-saturating irradiance, fluorescence stabilizes at a value F, somewhat above F_0 (Box Fig. 2.4, right). When a saturating pulse is given under these conditions, fluorescence does not rise to F_m, but to a lower value called F_m'. Although reaction centers are closed at saturating light, dissipation processes compete now with fluorescence which causes the quenching of F_m to F_m'.

Since all reaction centers are closed during the saturating pulse, the photochemical quantum yield (ϕ_P) is practically zero and, therefore, the quantum yields of dissipation at saturating light (ϕ_{Dm}) and fluorescence at saturating light (ϕ_{Fm}) are unity:

$$\phi_{Dm} + \phi_{Fm} = 1 \qquad (2.27)$$

It is further assumed that there is no change in the relative quantum yields of dissipation and fluorescence during the saturating pulse:

$$\frac{\phi_{Dm}}{\phi_{Fm}} = \frac{\phi_D}{\phi_F} \qquad (2.28)$$

Photochemical quantum yield (ϕ_p) is also referred to as ϕ_{II} because it originates mainly from PSII. It can now be expressed in fluorescence parameters only, on the basis of Eqs (2.26), (2.27), and (2.28).

$$\phi_{II} = (\phi_{FM} - \phi_{IF})\phi_{FM} \qquad (2.29)$$

The fluorescence parameters F_0 and F_m can be measured with time-resolving equipment, where the sample is irradiated in

(continued)

Box 2.4 (continued)

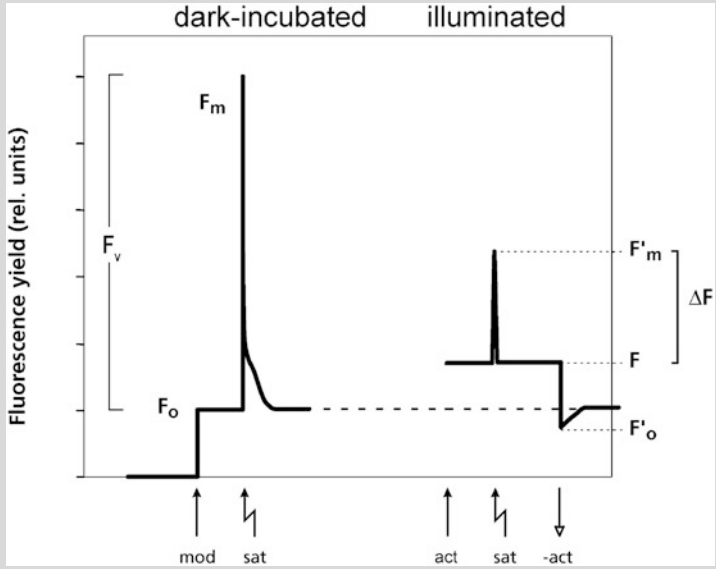

Box Fig. 2.4 Fluorescence kinetics in dark-incubated and illuminated leaves in response to a saturating pulse of white light. mod = modulated measuring light on; sat = saturating pulse on; act=actinic light on for a prolonged period together with modulated measuring light; -act = actinic light off. For explanation of fluorescence symbols see text (after Schreiber et al. 1995b).

darkness with $\lambda < 680$ nm and fluorescence is detected as emitted radiation at $\lambda > 680$ nm. White light sources, however, typically also have radiation in the wavelength region of chlorophyll fluorescence. For measurements in any light condition, systems have been developed that use a weak modulated light source in conjunction with a detector that monitors only the fluorescence emitted at the frequency and phase of the source. A strong white light source for generating saturating pulses (> 5000 μmol m^{-2} s^{-1}) and an actinic light source typically complete such systems. The modulated measuring light is sufficiently weak for measurement of F_0. This is the method used in the example given in Box Fig. 2.4. The constancy of the measuring light means that any change in fluorescence signal is proportional to ϕ_F. This means that the maximum quantum yield (ϕ_{IIm}) as measured in dark-incubated leaves is:

$$\phi_{IIm} = (F_m - F_0)/F_m = F_v/F_m \quad (2.30)$$

where F_v is the variable fluorescence, the difference between maximal and minimal fluorescence. In illuminated samples the expression becomes:

$$\phi_{II} = (F_m' - F)/F_m' = \Delta F/F_m' \quad (2.31)$$

where ΔF is the increase in fluorescence due to a saturating pulse superimposed on the actinic irradiance. $\Delta F_v/F_m$ has values equal to or lower than F_v/F_m; the difference increases with increasing irradiance.

(continued)

Box 2.4 (continued)

The partitioning of fluorescence quenching due to photochemical (qP) and nonphotochemical (qN) processes can be determined. These are defined as:

$$qP = (F_m' - F)/(F_m' - F_0') = \Delta F/F_v' \quad (2.32)$$

$$qP = (F_m' - F)/(F_m' - F_0') = \Delta F/F_v' \quad (2.33)$$

F_0 may be quenched in light, and is then called F_0' (Box Fig. 2.4, right). The measurement of this parameter may be complicated, particularly under field conditions. We can also use another term for nonphotochemical quenching (NPQ) which does not require the determination of F_0':

$$\text{NPQ} = (F_m - F_m')/F_m' \quad (2.34)$$

The theoretical derivation of the fluorescence parameters as based on the assumptions described above is supported by substantial empirical evidence. The biophysical background of the processes, however, is not always fully understood.

Relationships with Photosynthetic Performance

Maximum quantum yield after dark incubation (F_v/F_m) is typically very stable at values around 0.8 in healthy leaves. F_v/F_m correlates well with the quantum yield of photosynthesis measured as O_2 production or CO_2 uptake at low irradiance (Box Fig. 2.5). In particular, the reduction of the quantum yield by photoinhibition can be evaluated with this fluorescence parameter. A decrease in F_v/F_m can be due to a decrease in F_m and/or an increase in F_0. A fast- and a slow-relaxing component can be distinguished. The fast component is alleviated within a few hours of low light or darkness and is therefore only evident during daytime; it is supposed to be involved in protection of PS II

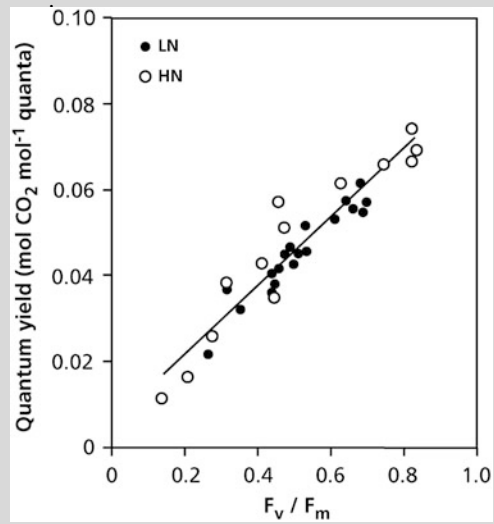

Box Fig. 2.5 The relationship between quantum yield, as determined from the rate of O_2 evolution at different levels of low irradiance, and the maximum quantum yield of PS II determined with chlorophyll fluorescence (F_v/F_m, ϕ_{IIm}). Measurements were made on *Glycine max* (soybean) grown at high (open symbols) and low (filled symbols) nitrogen (N) supply and exposed to high light for different periods prior to measurement (after Kao and Forseth 1992).

over-excitation. The slow-relaxing component remains several days and is considered as an indication of (longer-lasting) damage to PS II. Such damage can be the result of sudden exposure of shade leaves to full sun light, or a combination of high irradiance and extreme (high or low) temperature. The way plants cope with this combination of stress factors determines their performance in particular habitats where such conditions occur.

Quantum yield in light ($\Delta F/F_m'$) can be used to derive the rate of electron transport (ETR or J_F).

$$J_F = I \times \Delta F/F_m' \times \text{abs}\ 0.5 \quad (2.35)$$

where I is the irradiance and abs is the photon absorption by the leaf and 0.5 refers to the equal partitioning of photons between the two photosystems (Genty et al. 1989). For comparison of J_F with photosynthetic gas-exchange rates, the rate of the carboxylation

(continued)

Box 2.4 (continued)

(V_c) and oxygenation (V_o) reaction of Rubisco must be known. In C_4 plants and in C_3 plants at low O_2 and/or high CO_2, V_o is low and can be ignored. Hence, the rate of electron transport can also be derived from the rate of O_2 production or CO_2 uptake (J_c). For a comparison of J_F with J_c in normal air in C_3 plants, V_o must be estimated from the intercellular partial pressure of CO_2 (Box 2.1). Photosynthetic rates generally show good correlations with J_F (Box Fig. 2.6). J_F may be somewhat higher than J_c (Box Fig. 2.6). This can be ascribed to electron flow associated with nonassimilatory processes, or with assimilatory processes that do not result in CO_2 absorption, such as nitrate reduction. Alternatively, the chloroplast population monitored by fluorescence is not representative for the functioning of all chloroplasts across the whole leaf depth. The good correlation of gas exchange and fluorescence data in many cases indicates that J_F is representative for the whole-leaf photosynthetic rate, at least in a relative sense. Hence, J_F is also referred to as the relative rate of electron transport.

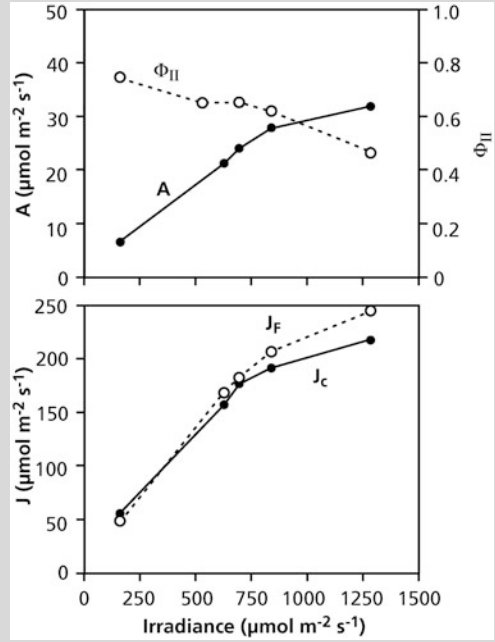

Box Fig. 2.6 Relationship of chlorophyll fluorescence parameters and rates of CO_2 assimilation in the C_3 plant *Flaveria pringlei*. A = rate of CO_2 assimilation; ϕ_{II} = quantum yield of PS II in light (F/F_m'); J_F = electron-transport rate calculated from ϕ_{II} and irradiance; J_c = electron-transport rate calculated from gas-exchange parameters (after Krall and Edwards 1992). Copyright Physiologia Plantarum.

2.3.3.1 Photoinhibition—Protection by Carotenoids of the Xanthophyll Cycle

Plants that are acclimated to high light, dissipate excess energy through reactions mediated by a particular group of **carotenoids** (Fig. 2.16). This dissipation process is induced by accumulation of protons in the thylakoid lumen which is triggered by excess light. Acidification of the lumen induces an enzymatic conversion of the carotenoid violaxanthin into antheraxanthin and zeaxanthin (Sacharz et al. 2017). The dissipation process also requires a special **photosystem II subunit S** (**PsbS**). Mutants of *Arabidopsis thaliana* (thale cress) that are unable to convert violaxanthin to zeaxanthin in excessive light exhibit greatly reduced nonphotochemical quenching, and are more sensitive to photoinhibition than wild-type plants (Niyogi et al. 1998). Similarly, PsbS-deficient mutants have a reduced fitness at intermittent, moderate levels of excess light (Külheim et al. 2002).

Zeaxanthin triggers a kind of 'lightning rod' mechanism. It is involved in the induction of conformational changes in the light-harvesting antennae of PS II which facilitates the dissipation of excess excitations (Fig. 2.17; Pascal et al. 2005). This energy dissipation can be measured by chlorophyll fluorescence (Box 2.4) and is termed high-energy-dependent or pH-dependent

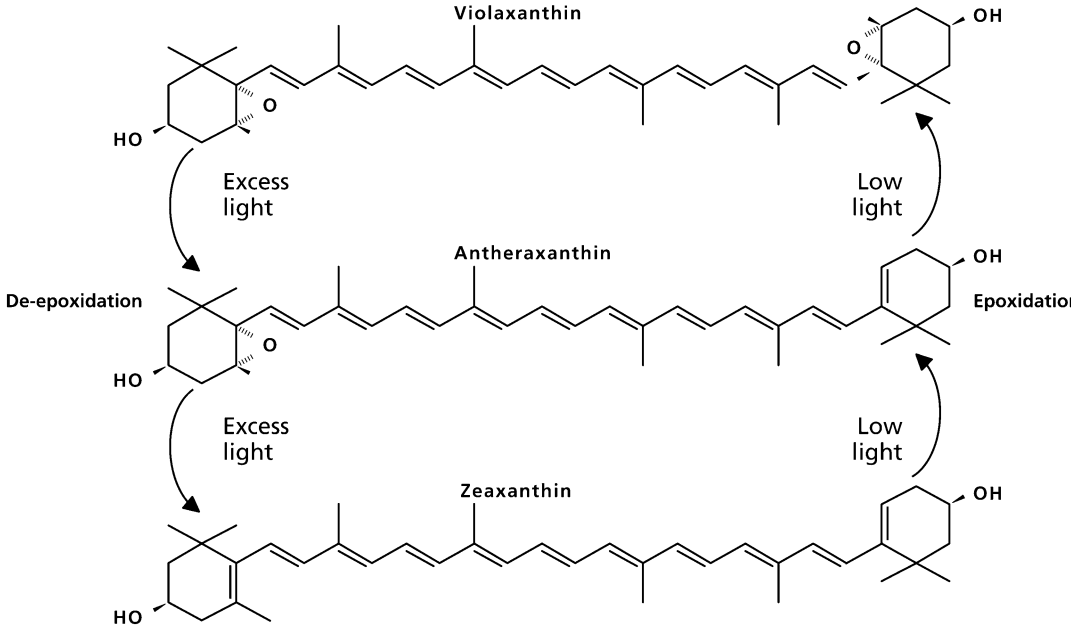

Fig. 2.16 Scheme of the xanthophyll cycle and its regulation by excess or limiting light. Upon exposure to excess light, a rapid stepwise removal (de-epoxidation) of two oxygen functions (the epoxy groups) in violaxanthin takes place; the pH optimum of this reaction, which is catalyzed a de-epoxidase, is acidic. This de-epoxidation results in a lengthening of the conjugated system of double bonds from 9 in violaxanthin 10 and 11 in antheraxanthin and zeaxanthin, respectively. The de-epoxidation step occurs in minutes. Under low-light conditions, the opposite process, epoxidation, takes place. It may take minutes, hours, or days, depending on environmental conditions (Demmig-Adams and Adams 1996, 2006).

fluorescence quenching. In the absence of a properly functioning **xanthophyll cycle**, excess energy could, among others, be passed on to O_2. This leads to photooxidative damage when scavenging mechanisms cannot deal with the resulting **reactive oxygen species** (ROS). For example, **herbicides** that inhibit the synthesis of carotenoids cause the production of vast amounts of ROS that cause chlorophyll to bleach and kill the plant (Wakabayashi and Böger 2002). In the absence of any inhibitors, ROS inhibit the repair of PS II, in particular the synthesis of the **D1 protein** of PS II, by their effect on mRNA translation. It is a normal phenomenon when plants are exposed to full sunlight even in the absence of other stress factors (Nishiyama et al. 2006). However, when shade plants are exposed to full sunlight, or when other stresses combine with high irradiance (*e.g.*, desiccation, high or low temperature), then more excessive damage can occur, involving destruction of membranes and oxidation of chlorophyll (bleaching), causing a longer-lasting reduction in photosynthesis.

In sun-exposed sites, diurnal changes in irradiance are closely tracked by the level of **antheraxanthin** and **zeaxanthin**. In shade conditions, sunflecks lead to the rapid appearance of antheraxanthin and zeaxanthin and reappearance of **violaxanthin** between subsequent sunflecks. This regulation mechanism ensures that no competing dissipation of energy occurs when light is limiting for photosynthesis, whereas damage is prevented when light is absorbed in excess. Typically, sun-grown plants not only contain a larger fraction of the carotenoids as zeaxanthin in high light, but their total pool of **carotenoids** is larger also (Fig. 2.18; Adams et al. 1999). The pool of reduced **ascorbate**, which plays a role in the xanthophyll cycle (Fig. 2.17), is also several-fold greater in plants acclimated to high light (Logan et al. 1996).

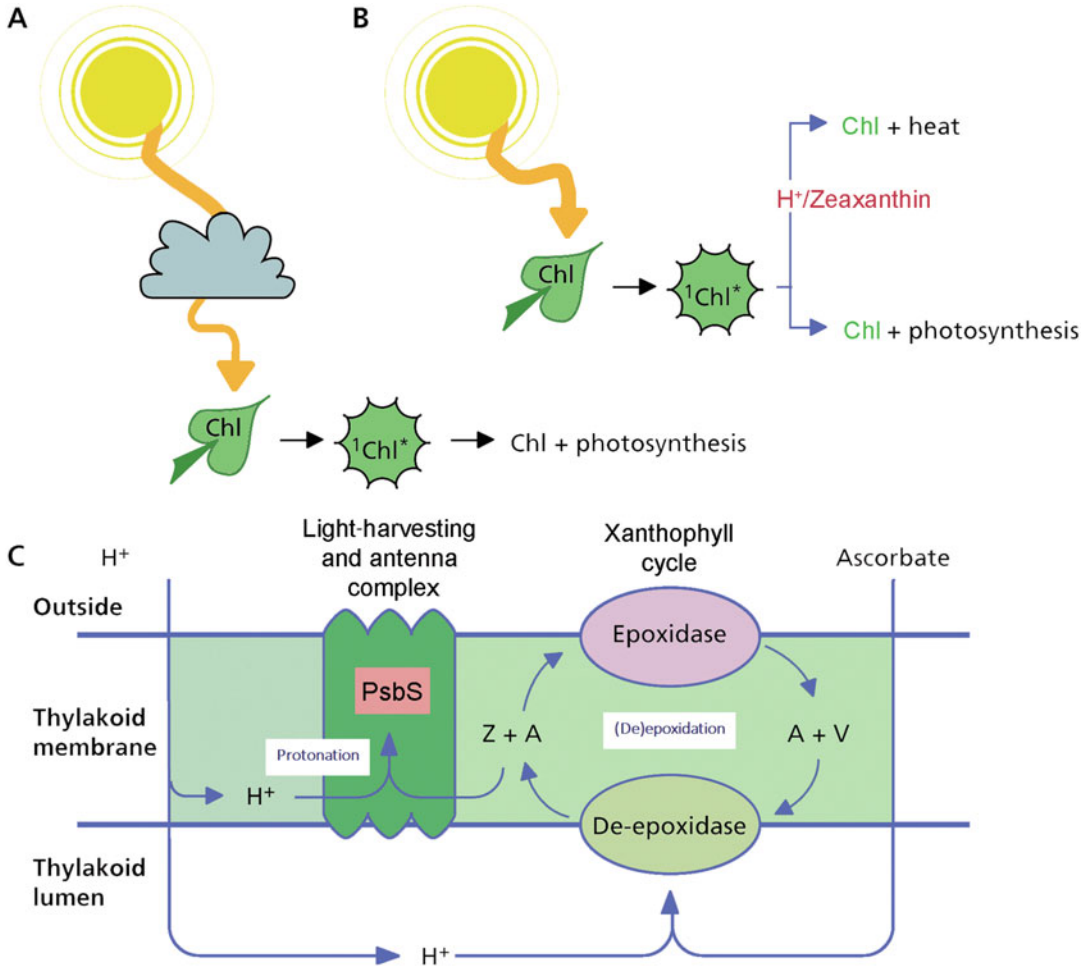

Fig. 2.17 Top: Depiction of the conditions where (**A**) all or (**B**) only part of the sunlight absorbed by chlorophyll within a leaf is used for photosynthesis. Safe dissipation of excess energy requires the presence of zeaxanthin as well as a low pH in the photosynthetic membranes. The same energized form of chlorophyll is used either for photosynthesis or loses its energy as heat. Bottom: Depiction of the regulation of the biochemistry of the xanthophyll cycle as well as the induction of xanthophyll-cycle-dependent energy dissipation by pH. De-epoxidation to antheraxanthin (A) and zeaxanthin (Z) from violaxanthin (V), catalyzed by a de-epoxidase with an acidic pH optimum, takes place at a low pH in the lumen of the thylakoid as well in the presence of reduced ascorbate. Protonation of a residue of a photosystem II subunit S (PsbS) is essential for the functioning of the cycle. In addition, a low pH of certain domains within the membrane, together with the presence of zeaxanthin or antheraxanthin, is required to induce the actual energy dissipation. This dissipation takes place within the light-collecting antenna complex of PS II (modified after Demmig-Adams and Adams 1996).

2.3.3.2 Chloroplast Movement in Response to Changes in Irradiance

Plants may reposition chloroplasts within their cells in response to changes in light intensity and quality (Senn 1908; Banaś et al. 2012). **Light-induced movements** of chloroplasts are affected blue and/or red light, depending on the plant group (Banaś et al. 2012). High intensities in this wavelength region cause the chloroplasts to line up along the walls, parallel to the light direction, rather than along the cell walls, perpendicular to the direction of the radiation. Chloroplasts are anchored with **actin networks**

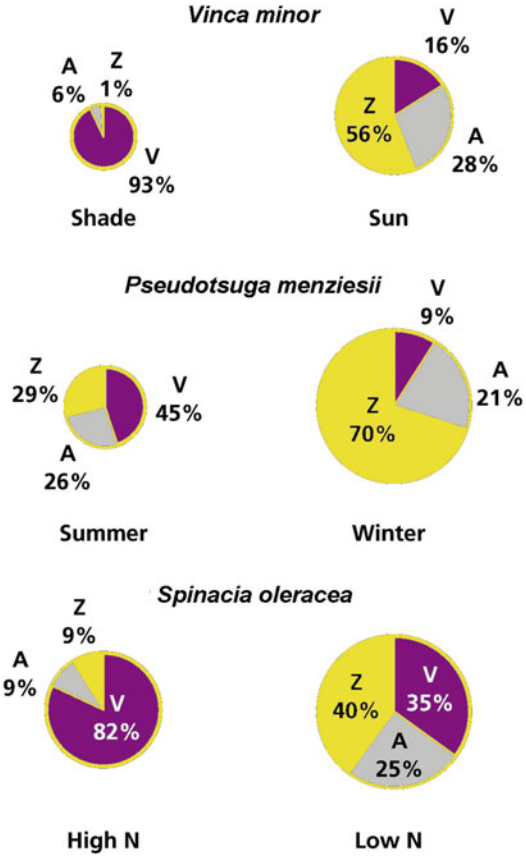

Fig. 2.18 Differences in zeaxanthin (Z), violaxanthin (V) and antheraxanthin (A) contents of leaves upon acclimation to the light level [*Vinca minor* (periwinkle)], season [*Pseudotsuga menziesii* (Douglas fir)] and N supply [*Spinacia oleracea* (spinach)]. The total areas reflect the concentration of the three carotenoids relative to that of chlorophyll (after Demmig-Adams and Adams 1996).

and their final positioning relies on connections to actin. Chloroplast movements are pronounced in aquatic plants such as *Vallisneria gigantea* (giant vallis) and shade-tolerant understory species such as *Tradescantia albiflora* (wandering Jew), where they may decrease the leaf's absorptance by as much as 20%, thereby increasing both transmittance and reflectance (Banaś et al. 2012). Many climbing species [*e.g.*, *Cayratia japonica* (Vitaceae, bushkiller)] show very low or no chloroplast photorelocation responses to either weak or strong blue light (Higa and Wada 2016). Chloroplast movements in shade plants exposed to high light avoid photoinhibition (Brugnoli and Björkman 1992).

2.3.4 Responses to Variable Irradiance

So far, we have discussed mostly steady-state responses to light, meaning that a particular environmental condition is maintained until a constant response is achieved. Conditions in the real world, however, are typically not constant, irradiance being the most rapidly varying environmental factor. Since photosynthesis primarily depends on irradiance, the dynamic response to variation in irradiance deserves particular attention.

The irradiance level above a leaf canopy changes with time of day and with cloud cover, often by more than an order of magnitude within seconds. In a leaf canopy, irradiance, particularly direct radiation, changes even more. In a forest, direct sunlight may penetrate through holes in the overlying leaf canopy, casting **sunflecks** on the forest floor. These move with wind action and position of the sun, thus exposing both leaves in the canopy and shade plants in the understory to short periods of bright light. Sunflecks typically account for 40-60% of total irradiance in understory canopies of dense tropical and temperate forests and are quite variable in duration and intensity (Chazdon and Pearcy 1991).

2.3.4.1 Photosynthetic Induction

When a leaf that has been in darkness or low light for hours is transferred to a saturating level of irradiance, the photosynthetic rate increases only gradually over a period of up to one hour to a new steady state rate (Fig. 2.19), with stomatal conductance increasing in parallel. We cannot conclude, however, that limitation of photosynthesis during induction is invariably due to stomatal opening (Allen and Pearcy 2000). If stomatal conductance limited photosynthesis, the intercellular CO_2 concentration (C_i) should drop immediately upon transfer to high irradiance, but, in fact, there is a more gradual decline over the first minutes, and then a slow increase until full induction (Fig. 2.19). Stomatal patchiness might play a

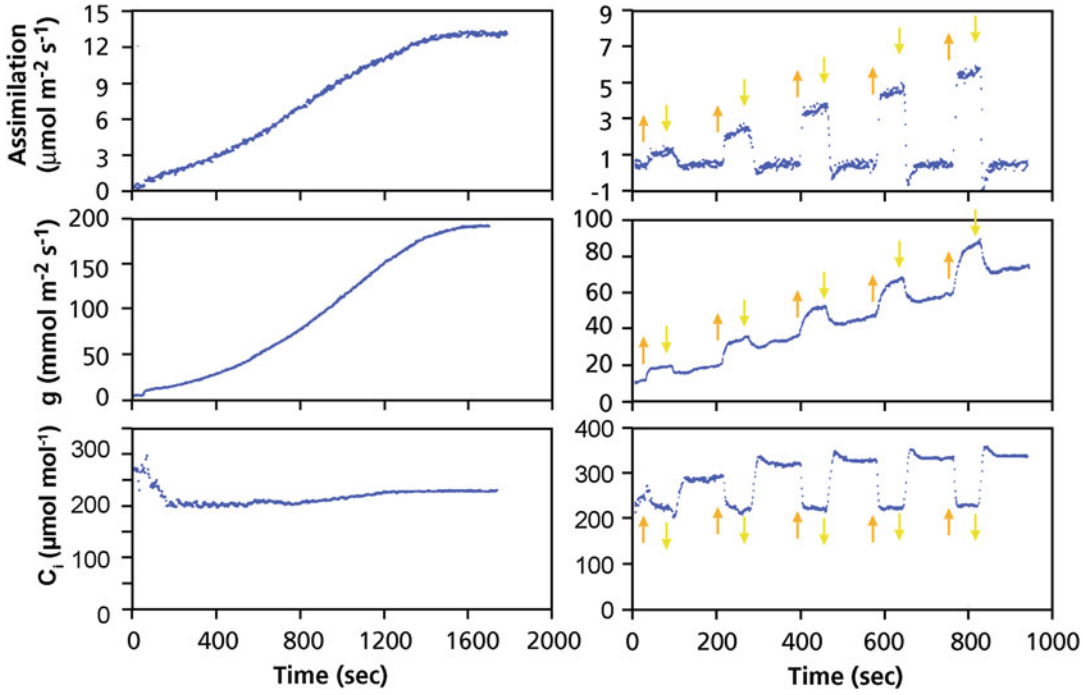

Fig. 2.19 Photosynthetic induction in *Toona australis*, which is an understory species from the tropical rainforest in Australia. (Left panels) Time course of the rate of CO_2 assimilation (A_n) (top), stomatal conductance (g_s) (middle), and the intercellular CO_2 concentration (C_i) (bottom) of plants that were first exposed to a low irradiance level and then transferred to high saturating irradiance. (Right panels) Leaves are exposed to five 'sunflecks', indicated by arrows, with a low background level of irradiance in between (Chazdon and Pearcy 1986).

role (Sect. 2.5.1), but there are also additional limitations at the chloroplast level. The demand for CO_2 increases faster than the supply in the first minutes, as evident from the initial decline in C_i. Its subsequent rise indicates that the supply increases faster than the demand, as shown in Fig. 2.20, where A_n is plotted as a function of C_i during photosynthetic induction. During the first one or two minutes there is a fast increase in demand for CO_2 (fast induction component) which is due to fast light induction of some Calvin-Benson-cycle enzymes and build-up of metabolite pools (Sassenrath-Cole et al. 1994). The slower phase of increase in demand until approximately 10 minutes is dominated by the **light-activation of Rubisco**. After that, C_i increases, and A_n increases along the A_n-C_i curve, indicating that a decrease in stomatal limitation dominates further rise in photosynthetic rate (Fig. 2.20).

Loss of photosynthetic induction occurs in low light, but at a slower rate than induction in high light, particularly in forest understory species. Hence, in a sequence of sunflecks, photosynthetic induction increases from one sunfleck to the next, until a high induction state is reached, when sunflecks can be used efficiently (Fig. 2.19).

2.3.4.2 Light Activation of Rubisco

Rubisco, as well as other enzymes of the Calvin-Benson cycle, are **activated by light**, before they have a high catalytic activity (Fig. 2.21; Carmo-Silva et al. 2015). The increase in Rubisco activity, due to its activation by light, closely matches the increased photosynthetic rate at a high irradiance, apart from possible stomatal limitations. Two mechanisms are involved in the activation of Rubisco (Bracher et al. 2017). Firstly, CO_2 binds covalently to a lysine residue at the enzyme's active site (**carbamylation**), followed

by binding of Mg^{2+} and RuBP. In this activated state, Rubisco is able to catalyze the reaction with CO_2 or O_2. Rubisco is **deactivated** when (1) RuBP binds to a decarbamylated Rubisco, (2) 2-**carboxy-D-arabinitol 1-phosphate** (CA1P), an analogue of the extremely short-lived intermediate of the RuBP carboxylation reaction, binds to the carbamylated Rubisco, and (3) a product produced by the catalytic 'misfire' of Rubisco ('misprotonation'), xylulose-1,5-bisphosphate (Salvucci and Crafts-Brandner 2004), binds to a carbamylated Rubisco. Secondly, **Rubisco activase** plays a role in catalyzing the dissociation of inhibitors from the active site of Rubisco; its activity increases with increasing rate of electron transport (Fig. 2.21). The activity of Rubisco activase is regulated by ADP/ATP and redox changes mediated by thioredoxin in some species.

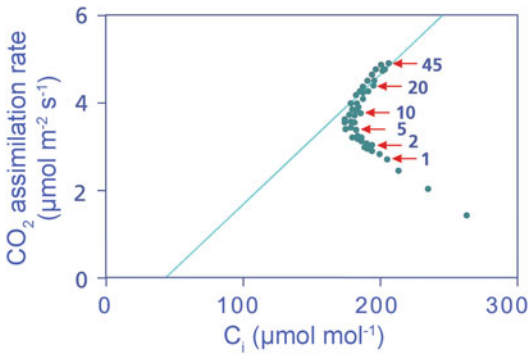

Fig. 2.20 Photosynthetic response of *Alocasia macrorrhiza* (giant taro) to intercellular CO_2 concentration (C_i) during the induction phase after a transition from an irradiance level of 10–500 µmol m^{-2} s^{-1} (light saturation). The solid line represents the A_n-C_i relationship of a fully induced leaf calculated as Rubisco-limited rates. Numbers indicate minutes after transition (after Kirschbaum and Pearcy 1988).

Light activation of Rubisco, a natural process that occurs at the beginning of the light period in all plants, is an important aspect of the regulation (fine-tuning) of photosynthesis. In the absence of such light activation, the three phases of the Calvin-Benson cycle (carboxylation, reduction, and regeneration of RuBP) may compete for substrates, leading to oscillation of the rate of CO_2 fixation upon the beginning of the light period. It may also protect active sites of Rubisco during inactivity in darkness (Portis 2003), but the regulation mechanism occurs at the expense of slow rates of CO_2 assimilation during periods of low induction.

2.3.4.3 Post-illumination CO_2 Assimilation and Sunfleck-Utilization Efficiency

The rate of O_2 evolution, the product of the first step of electron transport, stops immediately after a sunfleck, whereas CO_2 assimilation continues for a brief period thereafter, referred to as **post-illumination CO_2 fixation** (Fig. 2.22). CO_2 assimilation in the Calvin-Benson cycle requires both NADPH and ATP, which are generated during the light reactions. Particularly in short

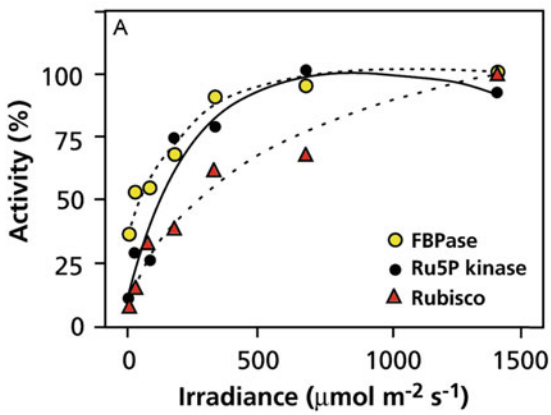

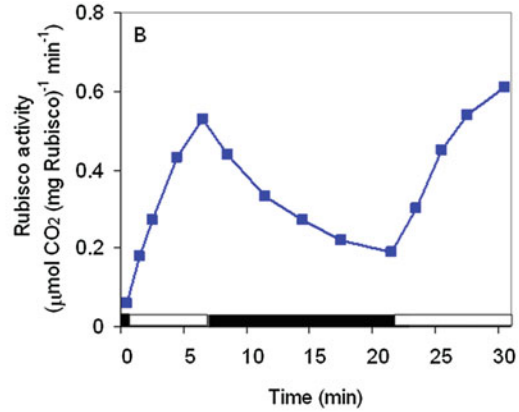

Fig. 2.21 (**A**) Light activation of Rubisco and two other Calvin-Benson cycle enzymes, Ribulose-5-phosphate kinase and fructose-bisphosphatase (Salvucci 1989). Copyright Physiologia Plantarum. (**B**) Time course of Rubisco activation level during sequential light (open bars) and dark (filled bars) periods (after Portis et al. 1986). Copyright American Society of Plant Biologists.

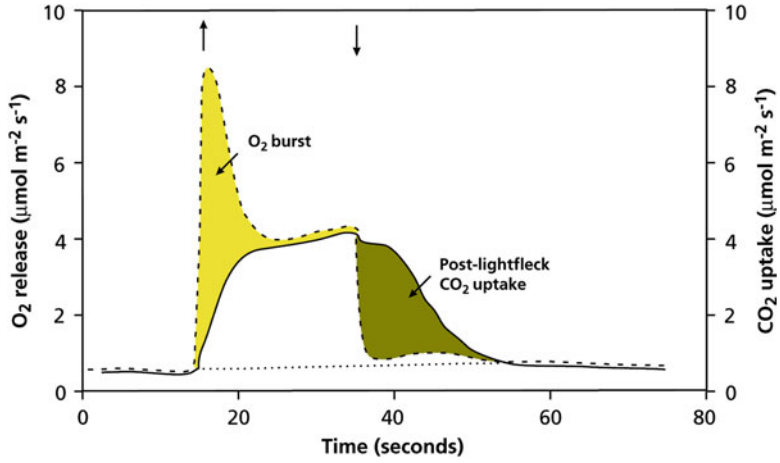

Fig. 2.22 CO_2 uptake and O_2 release in response to a 'sunfleck'. Arrows indicate the beginning and end of the 'sunfleck' (after Pearcy 1990).

sunflecks, this post-illumination CO_2 fixation is important relative to photosynthesis during the sunfleck, thus increasing total CO_2 assimilation due to the sunfleck above what would be expected from steady-state measurements (Fig. 2.23).

CO_2 assimilation due to a sunfleck also depends on **induction state**. Leaves become increasingly induced with longer sunflecks of up to a few minutes (Fig. 2.19). At low induction states, sunfleck-utilization efficiency decreases below what would be expected from steady-state rates (Fig. 2.23). Forest understory plants tend to utilize sunflecks more efficiently than plants from short vegetation, particularly flecks of a few seconds to a few minutes. Accumulation of larger Calvin-Benson-cycle metabolite pools and longer maintenance of photosynthetic induction are possible reasons. Efficient utilization of sunflecks is crucial for understory plants, since most radiation comes in the form of relatively long-lasting sunflecks, and half the plant's assimilation may depend on these short periods of high irradiance (Slattery et al. 2018).

2.3.4.4 Metabolite Pools in Sun and Shade Leaves

As explained in Sect. 2.2.1.3, the photophosphorylation of ADP depends on the proton gradient across the thylakoid membrane. This gradient is still present immediately following a sunfleck, and ATP can therefore still be generated for a brief period. The formation of NADPH, however, directly depends on the flux of electrons from water, via the photosystems and the photosynthetic electron-transport chain, and therefore comes to an immediate halt after the sunfleck. Moreover, the concentration of NADPH in the cell is too low to sustain Calvin-Benson-cycle activity. Storage of the reducing equivalents takes place in **triose-phosphates** (Table 2.3), which are intermediates of the Calvin-Benson cycle.

To allow the storage of reducing power in intermediates of the Calvin-Benson cycle, the phosphorylating step leading to the substrate for the reduction reaction must proceed. This can be realized by regulating the activity of two enzymes of the Calvin-Benson cycle which both utilize ATP: phosphoglycerate kinase and ribulose-phosphate kinase (Fig. 2.4). When competing for ATP *in vitro*, the second kinase tends to dominate, leaving little ATP for phosphoglycerate kinase. If this were to happen *in vivo* as well, no storage of reducing equivalents in triose-phosphate would be possible, and CO_2 assimilation would not continue beyond the sunfleck. The concentration of triose-phosphate at the end of a

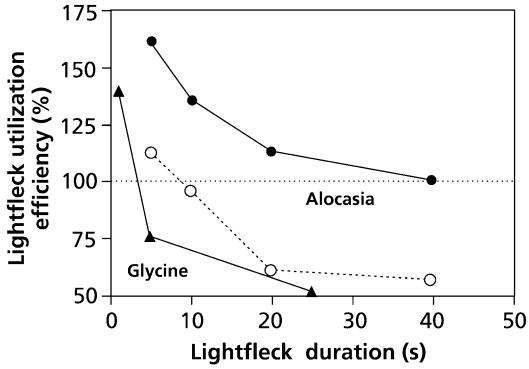

Fig. 2.23 Efficiency of 'sunfleck' utilization as dependent on duration of the 'sunfleck' and induction state in two species. *Alocasia macrorrhiza* (giant taro, an understory species) measured at high (closed symbols) and low induction state (open symbols). Induction state of *Glycine max* (soybean, a sun species) is approximately 50% of maximum. Efficiencies are calculated as total CO_2 assimilation due to the sunfleck relative to that calculated from the steady state rates at the high irradiance (sunfleck) and the low (background) irradiance (Pearcy 1988; Pons and Pearcy 1992).

sunfleck is relatively greater in shade leaves than in sun leaves, whereas the opposite is found for ribulose-1,5-bisphosphate (Table 2.3). This indicates that the activity of the steps in the Calvin-Benson cycle leading to ribulose-phosphate is suppressed. Thus, competition for ATP between the kinase is prevented, and the reducing power from NADPH can be transferred to 1,3-bisphosphoglycerate, leading to the formation of triose-phosphate. Storage of reducing power occurs in species that are adapted to shade, *e.g.*, *Alocasia macrorrhiza* (giant taro), as well as in leaves acclimated to shade, *e.g.*, shade leaves of common bean (*Phaseolus vulgaris*) (Sharkey et al. 1986a).

2.3.4.5 Net Effect of Sunflecks on Carbon Gain and Growth

Although most understory plants can maintain a positive carbon balance with diffuse light in the absence of sunflecks, daily carbon assimilation and growth rate in moist forests correlates closely with irradiance received in sunflecks (Fig. 2.24). Moreover, sunflecks account for an increasing proportion of total carbon gain (9–46%) as their size and frequency increase. In dry forests, where understory plants experience both light and water limitation, sunflecks may reduce daily carbon gain on cloud-free days (Allen and Pearcy 2000). Thus, the net impact of sunflecks on carbon gain depends on both cumulative irradiance and other potentially limiting factors.

2.4 Partitioning of the Products of Photosynthesis and Regulation by Feedback

2.4.1 Partitioning Within the Cell

Most of the products of photosynthesis are exported out of the chloroplast to the cytosol as **triose-phosphate** in exchange for Pi. Triose-phosphate is the substrate for the synthesis of sucrose in the cytosol (Fig. 2.25) and for the formation of cellular components in the **source** leaf. Sucrose is largely exported to other parts (**sinks**) of the plant, via the phloem (Chap. 3).

Partitioning of the products of the Calvin-Benson cycle within the cell is controlled by the concentration of Pi in the cytosol. If this concentration is high, rapid exchange for triose-phosphate allows export of most of the products of the Calvin-Benson cycle. If the concentration of Pi drops, the exchange rate will decline, and the concentration of triose-phosphate in the chloroplast increases. Inside the chloroplasts, the triose-phosphates are used for the synthesis of **starch**, releasing Pi within the chloroplast. So, the partitioning of the products of photosynthesis between export to the cytosol and storage compounds in the chloroplasts is largely determined by the availability of Pi in the cytosol. This regulation can be demonstrated by experiments using leaf discs in which the concentration of cytosolic Pi is manipulated (Table 2.5).

In intact plants, the rate of photosynthesis may be reduced when the plant's demand for carbohydrate (sink strength) is decreased, for example by the removal of part of the fruits or 'girdling' of the petiole (Table 2.5). [Girdling involves damaging

Table 2.3 The potential contribution of triose-phosphates and ribulose-1,5-bisphosphate to the post-illumination CO_2 assimilation of *Alocasia macrorrhiza* (giant taro) and *Phaseolus vulgaris* (common bean), grown either in full sun or in the shade*.

	Alocasia macrorrhiza		*Phaseolus vulgaris*	
	Shade	Sun	Shade	Sun
RuBP (μmol m^{-2})	2.0	14.5	2.9	5.3
Triose-phosphates (μmol m^{-2})	16.3	18.0	19.8	10.5
Total potential CO_2 fixation (μmol m^{-2})	12	25	15	12
Potential efficiency (%)	190	204	154	120
Triose-P/RuBP	4.9	0.7	4.1	1.2
Post-illumination ATP required (μmol g^{-1} Chl)	13	22	63	29

Source: Sharkey et al. (1986a)

*The values for the intermediates give the difference in their pool size at the end of the lightfleck and 1 min later. The total potential CO_2 assimilation is RuP_2 + 3/5 triose-P pool size. The potential efficiency was calculated on the assumption that the rate of photosynthesis during the 5 s lightfleck was equal to the steady state value measured after 20 min in high light

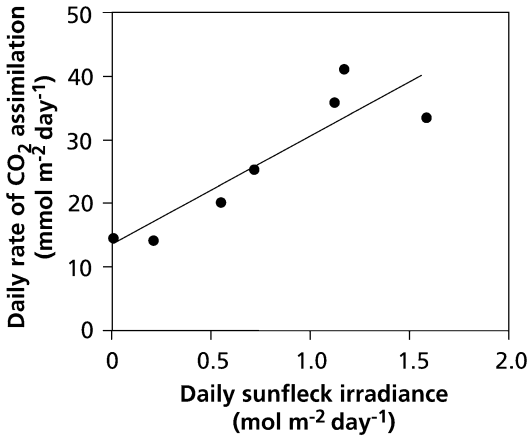

Fig. 2.24 Total carbon gain of *Adenocaulon bicolor* as a function of daily photon flux contributed by sunflecks in the understorey of a temperate redwood forest (after Chazdon and Pearcy 1991).

the phloem tissue of the stem, either by a temperature treatment or mechanically, leaving the xylem intact.] Restricting the export of assimilates by reduced sink capacity or more directly by blocking the phloem, sequesters the cytosolic Pi in phosphorylated sugars, leading to **feedback inhibition** of photosynthesis. When the level of Pi in the cytosol is increased, by floating the leaf discs on a phosphate buffer, the rate of photosynthesis may also drop ([*e.g.*, in *Cucumis sativus* (cucumber) Table 2.5], but there is no accumulation of starch. This is likely due to the very rapid export of triose-phosphate from the chloroplasts, in exchange for Pi, depleting the Calvin-Benson cycle of intermediates.

2.4.2 Short-Term Regulation of Photosynthetic Rate by Feedback

Under conditions of feedback inhibition (Sect. 2.4.1), phosphorylated intermediates of the pathway leading to sucrose accumulate, decreasing the cytosolic Pi concentration. In the absence of sufficient Pi in the chloroplast, the formation of ATP is reduced, and the activity of the Calvin-Benson cycle declines. Less intermediates are then available and less RuBP is regenerated, so that the carboxylating activity of Rubisco and hence the rate of photosynthesis drops.

How important is feedback inhibition in plants whose sink has not been manipulated? To answer this question, we can determine the **O_2 sensitivity** of photosynthesis. Normally, the rate of net CO_2 assimilation increases when the O_2 concentration is lowered from a normal 21% to 1 or 2% due to the suppression of the oxygenation reaction. When the activity of Rubisco is restricted by the regeneration of RuBP, lowering the O_2 concentration enhances the net rate of CO_2 assimilation to a lesser extent. Feedback inhibition is found at a high irradiance, and also at a low temperature, which restricts phloem loading. Under these conditions, the capacity to assimilate CO_2

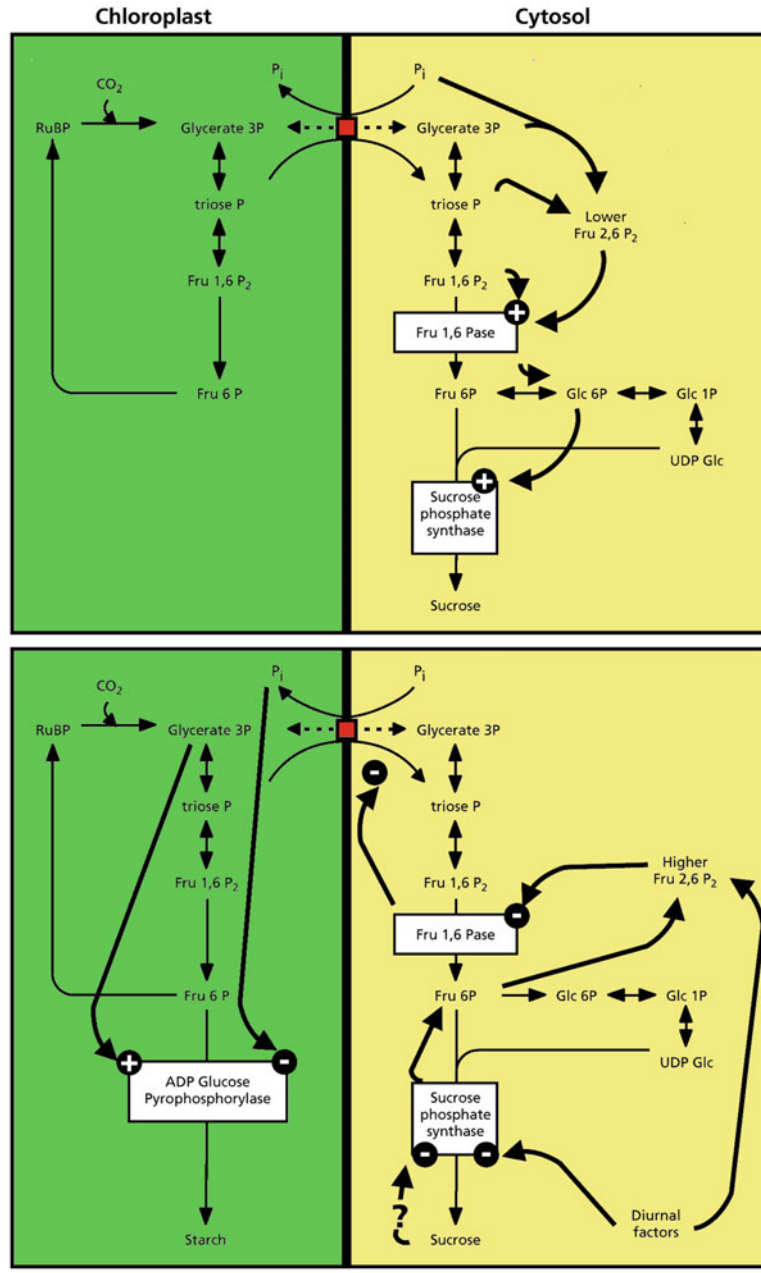

Fig. 2.25 The formation of triose-phosphate in the Calvin-Benson cycle. Triose-P is exported to the cytosol, in exchange for inorganic phosphate (Pi), or used as a substrate for the synthesis of starch in the chloroplast.

exceeds the capacity to export and further metabolize the products of photosynthesis. Consequently, phosphorylated intermediates of the pathway from triose-phosphate to sucrose accumulate which sequesters phosphate. As a result, Pi_i starts to limit photosynthesis, and the rate of photosynthesis declines as soon as the capacity to channel triose-phosphate to starch is saturated. Figure 2.26, showing the response of the net rate of CO_2 assimilation to $N_2 + CO_2$ at four levels of irradiance and a leaf temperature of 15 °C, illustrates this point.

Table 2.5 Rates of CO_2 assimilation (μmol m^{-2} s^{-1}) and the accumulation of ^{14}C in soluble sugars ('ethanol-soluble') and starch ('$HClO_4$-soluble') (^{14}C as % of total ^{14}C recovered) in leaf discs of *Gossypium hirsutum* (cotton) and *Cucumis sativus* (cucumber) floating on a Tris-maleate buffer, a phosphate buffer, or a mannose solution*.

	Control			Girdled		
	CO_2 fixation	Ethanol-soluble	$HClO_4$-soluble	CO_2 fixation	Ethanol-soluble	$HClO_4$ soluble
Cotton						
Tris-maleate	18	83	17	12	76	24
Phosphate	18	87	13	10	83	17
Mannose	12	54	46	10	76	24
Cucumber						
Tris-maleate	13	76	24	6	40	60
Phosphate	9	82	18	5	76	24
Mannose	9	55	45	4	40	60

Source: Plaut et al. (1987)

*Leaves were taken from control plants ('control') or from plants whose petioles had been treated in such a way as to restrict phloem transport ('girdled'). The concentration of cytosolic Pi can be decreased by incubating leaf discs in a solution containing mannose. Mannose is readily taken up and enzymatically converted into mannose phosphate, thus sequestering some of the P_i originally present in the cytosol. Under these conditions starch accumulates in the chloroplasts. At extremely low cytosolic P_i concentrations, the rate of photosynthesis is also reduced. When leaf discs are taken from plants with reduced sink capacity, the addition of mannose has very little effect, because the cytosolic P_i concentration is already low before mannose addition

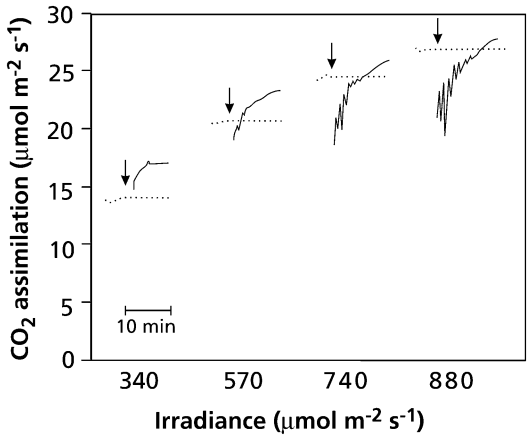

Fig. 2.26 The response of the CO_2 assimilation rate to a change in O_2 concentration at four levels of irradiance. The broken lines give the steady-state rate of CO_2 assimilation. The gas phase changes from air to N_2 + CO_2 at the time indicated by the arrows. The CO_2 concentration in the atmosphere surrounding the leaf is maintained at 550 μmol mol^{-1} and the leaf temperature at 15 °C. At a relatively low irradiance (340 μmol m^{-2} s^{-1}) the rate of CO_2 assimilation is rapidly enhanced when the O_2 concentration is decreased, whereas at high irradiance (880 μmol m^{-2} s^{-1}), CO_2 assimilation first decreases and is only marginally enhanced after several minutes, indicative of feedback inhibition (after Sharkey et al. 1986b)). Copyright American Society of Plant Biologists.

The assessment of feedback inhibition of photosynthesis using the O_2 sensitivity of this process is complicated by the fact that the relative activities of the carboxylating and oxygenating reactions of Rubisco also depend on temperature (Sect. 2.7.1). To resolve this problem, a mathematical model of photosynthesis has been used (Box 2.1). This model incorporates biochemical information on the photosynthetic reactions and simulates the effect of lowering the O_2 concentration at a range of temperatures. Comparison of the observed effect of the decrease in O_2 concentration (Fig. 2.27, lower middle and right panels) with the experimental observations (Fig. 2.27, lower left panel), allows conclusions on the extent of feedback inhibition in plants under normal conditions. The lower right panels show distinct feedback inhibition for *Solanum lycopersicum* (tomato) and *Populus fremontii* (Fremont cottonwood) at low temperatures, and less feedback inhibition for *Phaseolus vulgaris* (common bean), *Capsicum annuum* (pepper), *Scrophularia desertorum* (figwort), and *Cardaria draba* (hoary cress). Comparison of the modeled results in the lower left panel with the experimental results in the other lower panels in Fig. 2.27 shows that

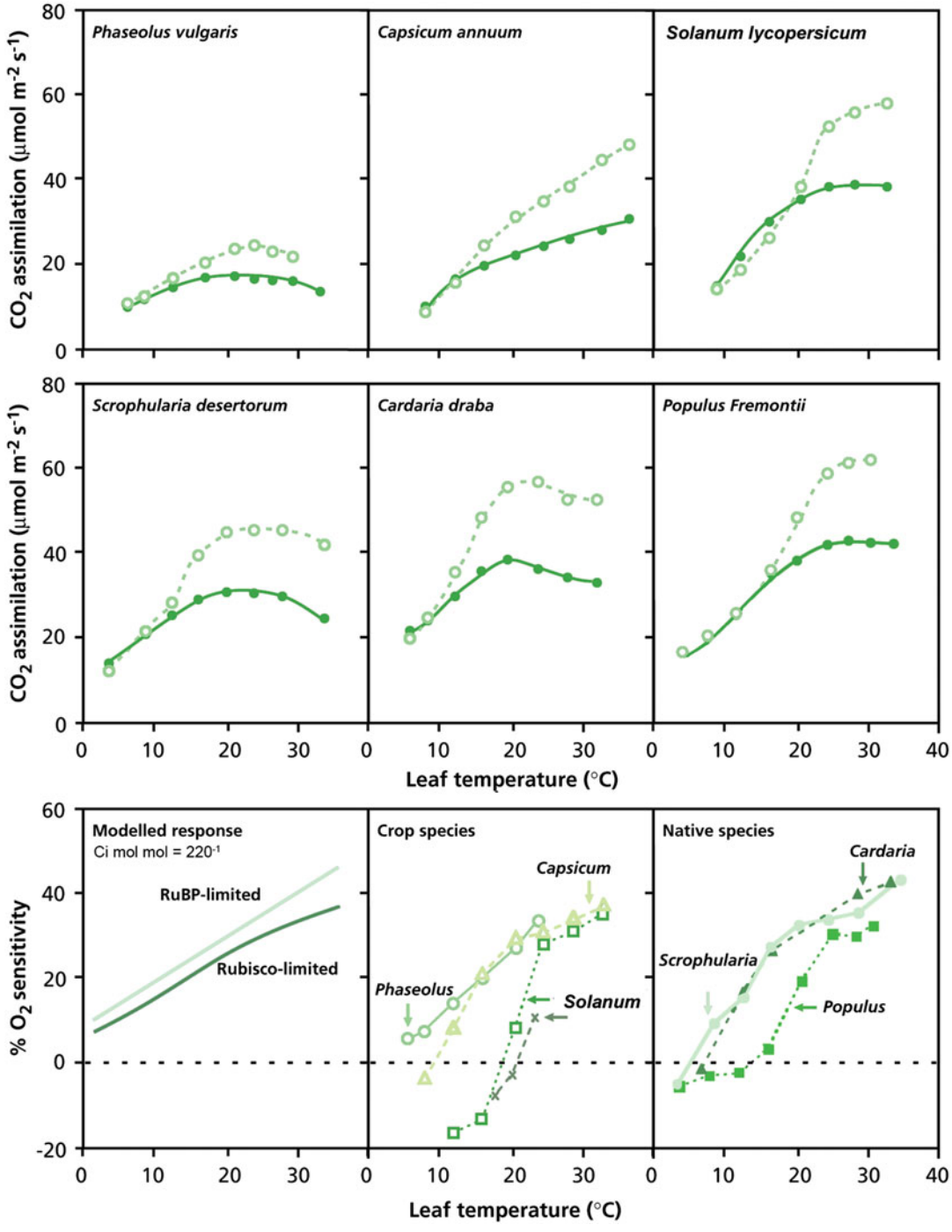

Fig. 2.27 The effect of temperature on the net rate of CO_2 assimilation at 18% (v/v; filled symbols) and 3% (v/v; open symbols) O_2 (top), and the O_2 sensitivity of photosynthesis (bottom) for a number of species. All plants were grown outdoors. Replicate measurements were made for one of the depicted species, *Solanum lycopersicum* (after Sage and Sharkey 1987). Copyright American Society of Plant Biologists.

photosynthesis of plants growing under natural conditions is commonly restricted by feedback, especially at relatively low temperatures. Some species are better at tolerating end-product inhibition. For example, panicle removal or antisense suppression of sucrose transporters involved in phloem loading in *Oryza sativa* (rice) results in accumulation of carbohydrates in leaves. Yet, their photosynthetic capacity is almost unaltered (Chang and Zhu 2017). Overexpression of a tonoplast monosaccharide transporter in *Arabidopsis thaliana* leads to increased monosaccharide import into mesophyll vacuoles. Overexpressor mutants grow faster than wild-type plants and produce larger seeds and greater seed yield, which is associated with increased sugar export from source leaves. Glucose suppresses a gene that encodes a sucrose transporter (SUC2) involved in phloem loading in leaves. Increased transport of monosaccharides into vacuoles modifies subcellular sugar compartmentation, alters cellular sugar sensing, affects assimilate allocation, increases seed weight, and accelerates early plant development (Wingenter et al. 2010).

2.4.3 Sugar-induced Repression of Genes Encoding Calvin-Benson-Cycle Enzymes

The feedback mechanism outlined in Sect. 2.4.2 operates in the short term, adjusting the activity of the existing photosynthetic apparatus to the capacity of export and sink activity, but mechanisms at the level of **gene transcription** play a more important role in the long term (Smeekens and Hellmann 2014). Developmental transitions in plants result in changes in the **source-sink relationship**. If carbon availability is insufficient, there is a risk of premature carbon depletion, resulting, for example, in abortion of fruit or seed development. Sugar signals regulate developmental transitions and signal if sufficient carbon is available for successful completion of a developmental program. The response to sugars and involvement of individual signaling pathways varies throughout the plant life cycle, because sugar signals interact with other developmental and environmental factors (Wingler 2018).

Hexose accumulation in response to high carbon availability results in the downregulation of photosynthetic gene expression. This prevents overinvestment of nitrogen (N) in the photosynthetic apparatus. Plants can sense hexose accumulation using a **hexokinase** (Granot et al. 2013, 2014). A mutant with catalytically inactive hexokinase forms still has a signaling function, indicating that the role of hexokinase in signaling high sugar availability is independent of its role in glucose metabolism (Wingler 2018). Hexokinase also mediates **stomatal closure**, thereby contributing to the feedback effect of sugar accumulation on photosynthesis (Kelly et al. 2013). In addition to hexokinase, trehalose-6-phosphatase and Snf1-related protein kinase-1 are involved in signaling a plant's high and low sugar status, respectively (Wingler 2018). Regulation at the level of gene transcription also plays a role in acclimation of the photosynthetic apparatus to elevated concentrations of atmospheric CO_2 (Sect. 2.12).

2.4.4 Ecological Impacts Mediated by Source-Sink Interactions

Many ecological processes affect photosynthesis through their impact on plant demand for carbohydrates (Sect. 2.4.2). In general, processes that increase carbohydrate demand increase the rate of photosynthesis, whereas factors that reduce demand reduce photosynthesis (Wingler 2018).

Defoliation generally reduces carbon assimilation by the defoliated plant by reducing the biomass of photosynthetic tissue, but it may cause a **compensatory increase** in photosynthetic rate of remaining leaves through several mechanisms (von Caemmerer and Farquhar 1984). The increased sink demand for carbohydrate generally leads to an increase in A_{max} in the remaining leaves. Defoliation also reduces environmental constraints on photosynthesis by increasing light penetration through the canopy, and by increasing the biomass of roots available

to support each remaining leaf. The resulting increases in light and water availability may enhance photosynthesis under shaded and dry conditions, respectively.

Growth at elevated atmospheric [CO_2] may lead to a downregulation of photosynthesis, involving sugar sensing (Sect. 2.12.1), and other ecological factors discussed here act on photosynthesis in a similar manner. Box 2.5 provides a brief overview of gas-exchange equipment, especially portable equipment that can be used in the field for ecological surveys.

Box 2.5: The Measurement of Gas Exchange

The uptake and release of CO_2 in photosynthesis and respiration and the release of H_2O during transpiration of plants or leaves is measured using gas-exchange systems. Several types exist (*e.g.*, Field et al. 1989; Long and Hällgren 1993). Here we briefly address the operation of so-called open systems and potential complications with their use, with particular attention to the commonly used portable systems that are commercially available.

The essence of a gas-exchange system is a transparent chamber that encloses the photosynthetically active tissue. Air enters the chamber at a specified flow rate (f_m) measured and controlled by a flow-controller. The leaf changes the concentrations of CO_2 and H_2O inside the chamber. The magnitude of the difference in CO_2 and H_2O concentration between the air entering the chamber (C_e and W_e) and at the outlet (C_o and W_o) depends on its gas-exchange activity. The net photosynthetic rate (A_n) is then calculated using the simplified formula:

$$A_n = \frac{F_m \times (C_e - C_o)}{L_a} \tag{2.36}$$

However, the increase in W_o as a result of transpiration is so large that its diluting effect cannot be ignored. Correction is done following von Caemmerer and Farquhar (1981).

$$A_n = \frac{f_m\{C_e - C_o(1 - W_e)/(1 - W_o)\}}{L_a} \tag{2.37}$$

E is calculated in an analogous manner, but with opposite sign.

$$E = \frac{f_m\{-W_e + W_o(1 - W_e)/(1 - W_o)\}}{L_a} \tag{2.38}$$

A_n and E are expressed per unit leaf area (L_a), but particularly for A_n, another basis, *e.g.*, dry mass can also be used. When leaf temperature is also measured, stomatal conductance (g_s) can be calculated using E and assuming a saturated vapor pressure in the intercellular spaces of the leaf. From g_s and A_n, intercellular CO_2 concentration (C_i) can be calculated. The principle is explained in Sect. 2.2.2.2, but corrections are necessary (von Caemmerer and Farquhar 1981). The calculations assume homogeneity of parameter values across the measured area. A powerful analysis of photosynthetic performance can be made when these four gas-exchange parameters are available, as explained in the text. A further development is the combination of gas-exchange with the measurement of chlorophyll fluorescence (Box 2.4) that gives a measure of electron-transport rate allowing estimates of the CO_2 concentration in the chloroplast (C_c), conductance for CO_2 transport in liquid phase of the mesophyll (g_m), photorespiration, and possible engagement of alternative electron sinks (Long and Bernacchi 2003).

A typical leaf chamber contains a fan that homogenizes the air which makes C_o and W_o representative of the air around the leaf (C_a and w_a, respectively). The fan further increases the boundary layer conductance (Chap. 6), which reduces the rise of

(continued)

Box 2.5 (continued)

leaf temperature (T_L) at high photon flux densities (PFD), allows a better control of T_L and reduces possible errors associated with the estimation of g_s associated with the assumption of homogeneity. It further contains a sensor for leaf and/or air temperature, and a light sensor is attached. Many portable systems are also equipped with temperature control and a mixing system for CO_2 with CO_2-free air that controls C_e. Control of W_e is not always accurate in these systems. In addition, a light source can be part of it. Concentrations of CO_2 and H_2O at the inlet and outlet of the leaf chamber (C_e, C_o, W_e, W_o) are measured with an infra-red gas analyzer (IRGA). The systems are completed with computerized control, data-acquisition and data-processing. We can use this versatile equipment to measure photosynthetic performance in ambient conditions and for measuring the response of gas-exchange activity to environmental factors such as humidity, CO_2, temperature and light.

The ease of gas-exchange measurement brings the danger of less critical use. Long and Bernacchi (2003) discuss some sources of error and guidelines for their avoidance; here, we address the most important problems. Most systems have small chambers that clamp with gaskets on a leaf, thus limiting the measurement to a part of the leaf. This has the advantage that we can also easily measure small leaves, and that the condition of homogeneity mentioned above is more easily met. However, the use of a small area has its draw-backs. In these chambers, a significant part of the leaf is covered by the gasket. The leaf area under the gasket continues to respire, and part of the CO_2 produced diffuses to the leaf chamber where it results in overestimation of respiration rates (Pons and Welschen 2002). In homobaric leaves, air can escape through the intercellular spaces depending on the overpressure in the chamber which complicates matters further (Jahnke and Pieruschka 2006). CO_2 and H_2O can also diffuse through the gasket, and more likely along the interface between gasket and leaf. This is particularly important when concentrations inside and outside the chamber are different, such as when measuring a CO_2 response and at high humidity in a dry environment (Flexas et al. 2007; Rodeghiero et al. 2007). Large errors can be caused by these imperfections at low gas-exchange rates, particularly when using small chambers. The cited references give suggestions to minimize and correct these errors, but that is not always straightforward and sometimes impossible. To avoid these errors, we should enclose whole leaves in larger chambers.

Other sources of error arise when estimates of gas exchange parameters are made for ambient conditions in the field, glasshouse, or growth chamber. Light is attenuated, particularly around the edges, which reduces A_n. Ambient air is often used for such measurements. The uptake of CO_2 results in a decreased CO_2 concentration in the chamber, causing a further underestimation of A_n compared with *in situ* rates. The reading for E deviates also from *in situ* rates due to a chamber climate in terms of humidity, temperature, and turbulence that differs from outside. When temperature is controlled, E causes an increase in w_a, with the magnitude depending on E itself. Hence, measured E is not representative for *in situ* values. When temperature is not controlled, T_L tends to rise in sunlight, which further affects E and A_n. When using short periods of enclosure, g_s is probably not affected by the chamber climate. Estimates of E under ambient conditions can best be obtained from g_s and *in situ* measurements of T_L and w_a. Corrections for A_n can be made from separately measured short-term T_L, PFD, and CO_2 effects, and using *in situ* measurements of these environmental parameters.

2.4.5 Petiole and Stem Photosynthesis

Most of the data discussed above referred to photosynthesizing leaves. However, many *Acacia* (Fabaceae) species tend to switch from photosynthesis using bipinnate compound leaves in juveniles to using modified petioles (**phyllodes**) in adults (Eamus and Cole 1997). Leaves of *Acacia koa* (koa) have faster mass-based gas exchange rates, while the water storage tissue in phyllodes contributes to greater capacitance per area. Phyllodes also show stronger stomatal closure at high *VPD* (Pasquet-Kok et al. 2010).

Stem photosynthesis is common in many desert succulents. Photosynthetic and hydraulic traits are coordinated in photosynthetic stems of 11 plant species from three desert locations in California (Ávila-Lovera et al. 2017). The relationship between mass-based stem photosynthetic CO_2 assimilation rate and specific stem area (stem surface area to dry mass ratio) is statistically indistinguishable from the **leaf economics spectrum**. Stem photosynthesis can contribute significantly to woody plant carbon balance, particularly in times when leaves are absent or in crowns allowing sufficient light penetration, for example in *Prunus ilicifolia* (holly-leaved cherry), *Umbellularia californica* (California laurel) and *Arctostaphylos manzanita* (whiteleaf manzanita) in California (Savveyn et al. 2010). Long-term light exclusion results in a reduction in chlorophyll concentration and radial growth, demonstrating that trunk assimilates contribute to trunk carbon income. Stem photosynthesis may be especially important for maintaining physiological activity in woody tissues of drought-stressed trees, as the supply of photosynthate from leaves declines due to stomatal closure (Vandegehuchte et al. 2015).

2.5 Responses to Availability of Water

The inevitable loss of water, when the stomata are open to allow photosynthesis, may lead to a decrease in leaf relative water content (RWC), if the water supply from roots does not match the loss from leaves. The decline in RWC may directly or indirectly affect photosynthesis. In this Section, we describe effects of the water supply on photosynthesis, and discuss genetic adaptation and phenotypic acclimation to water shortage.

2.5.1 Regulation of Stomatal Opening

Stomatal opening tends to be regulated such that photosynthesis is approximately **co-limited** by CO_2 diffusion through stomata and light-driven electron transport. This is seen in Fig. 2.6 as the intersection between the line describing the leaf's conductance for CO_2 transport (**supply function**) and the A_n-C_c curve (**demand function**). A higher conductance and higher C_c would only marginally increase CO_2 assimilation, but would significantly increase transpiration, since transpiration increases linearly with g_s, as a result of the constant difference in water vapor concentration between the leaf and the air ($w_i - w_a$) (Sect. 2.2.2.2; Fig. 2.28). At lower conductance, water loss declines again linearly with g_s; however, C_c also declines, because the demand for CO_2 remains the same, and the difference with C_a increases. This increased CO_2 concentration gradient across the stomata counteracts the decrease in g_s. Hence, photosynthesis declines less than does transpiration with decreasing C_c and C_i. The result is an increasing **water-use efficiency** (*WUE*) (carbon gain per water lost) with decreasing g_s. Less of the total

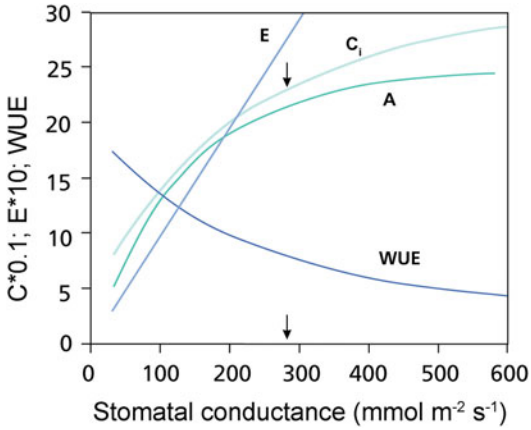

Fig. 2.28 The effect of stomatal conductance (g_s) on the transpiration rate (E, mmol m^{-2} s^{-1}), rate of CO_2 assimilation (A, μmol m^{-2} s^{-1}), intercellular CO_2 concentration (C_i, μmol mol^{-1}) and photosynthetic water-use efficiency (WUE, mmol CO_2 (mol H_2O)$^{-1}$ s^{-1}) as a function of stomatal conductance. Calculations were made assuming a constant leaf temperature of 25 °C and a negligible boundary layer resistance. The arrow indicates g_s at the co-limitation point of carboxylation and electron transport. For the calculations, Equations as described in Box 2.1 and Sect. 2.2.2.2 have been used.

photosynthetic capacity is used at a low C_c and C_i, however, leading to a reduced **photosynthetic N-use efficiency** (*PNUE*) (carbon gain per unit leaf N; Sect. 2.6.1).

Plants tend to reduce stomatal opening under water stress so that *WUE* is maximized at the expense of *PNUE*. Under limited availability of N, stomata may open further, increasing *PNUE* at the expense of *WUE* (Table 2.4). This trade-off between efficient use of water or N explains why perennial species from lower-rainfall sites in eastern Australia have higher leaf N concentration, lower light-saturated photosynthetic rates at a given leaf N concentration, and lower stomatal conductance at a given rate of photosynthesis (implying lower C_i) when compared with similar species from higher-rainfall sites (Wright et al. 2001). By investing heavily in photosynthetic enzymes, a larger drawdown of C_i is achieved, and a given photosynthetic rate is possible at a lower stomatal conductance. The benefit of the strategy is that dry-site species reduce water loss at a given rate of photosynthesis, down to levels similar to wet-site species, despite occurring in lower-humidity environments. The cost of high leaf N concentrations is higher costs incurred by N acquisition and possibly increased costs of phosphorus (P) invested in ribosomal RNA required for protein synthesis as well as herbivory risk.

When a plant is subjected to water stress, stomata tend to close. This response is regulated by **abscisic acid** (ABA), a phytohormone that is produced by roots in contact with dry soil and transported to the leaves (Sect. 5.5.4.1; Box 10.2). In addition to ABA, a **small peptide** travels from the roots to leaves, and leaves produce ABA in response to this peptide signal (Takahashi et al. 2018). Moreover, both electrical and hydraulic signals control stomatal conductance in response to soil moisture availability (Grams et al. 2007; Tombesi et al. 2015). Stomatal conductance may also decline in response to increasing vapor pressure deficit (*VPD*) of the air (Sect. 5.5.4.3). The result of these regulatory mechanisms is that, in **isohydric** plants, transpiration is constant over a range of *VPD*s, and leaf water potential is constant over a range of soil water potentials. Water loss is therefore restricted when dry air imposes water stress (a **feedforward response**) or when the plant experiences incipient water stress (a **feedback response**). In water-limited environments, responses to dry air or a low soil water potential often cause midday stomatal closure, and therefore a decline in photosynthesis (Fig. 5.33).

We have long assumed that stomata respond homogeneously over the entire leaf, but leaves of water-stressed plants exposed to $^{14}CO_2$ show often a heterogeneous distribution of fixed ^{14}C or starch. This shows that some stomata close completely (there is no radioactivity or iodine staining of starch close to these stomata), whereas others hardly change their aperture (label and staining is located near these stomata) (Downton et al. 1988; Terashima et al. 1988). This patchy stomatal closure can also be visualized nondestructively with thermography and gas exchange (Sweet et al. 2017); patches with closed stomata are identified by their high temperature. **Patchiness** of stomatal opening complicates the calculation of C_i (Sect. 2.2.2.2), because the calculation

Table 2.4 Intrinsic water-use efficiency (i*WUE*, A/g_s) and nitrogen-use efficiency of photosynthesis (*PNUE*, A_n/N_{LA}) of leaves of *Helianthus annuus* (sunflower), growing in a field in the middle of a hot, dry summer day in California*.

	N_{LA}	A_n	g_s	C_i	i*WUE*	*PNUE*
	mmol m^{-2}	μmol m^{-2} s^{-1}	mol m^{-2} s^{-1}	μmol mol^{-1}	mmol mol^{-1}	μmol mol^{-1} s^{-1}
High N + W	190	37	1.2	240	31	195
Low W	180	25	0.4	200	63	139
Low N	130	27	1.0	260	27	208

Source: Fredeen et al. (1991)
*Plants were irrigated and fertilized (high N + W), only irrigated but not fertilized (low N), or only fertilized but not irrigated (low W). Since transpiration is approximately linearly related to g_s, A/g_s is used as an approximation of i*WUE*

assumes a homogeneous distribution of gas exchange parameters across the leaf lamina.

2.5.2 The A_n–C_c Curve as Affected by Water Stress

Water stress alters both the **supply** and the **demand** functions of photosynthesis, but the main effect is on stomatal and mesophyll conductance, unless the stress is very severe (Fig. 2.29; Galmés et al. 2007b). When only the conductance declines with plant desiccation, the slope of the A_n-C_c curve is unaffected (Fig. 2.29B). Because high irradiance and high temperature often coincide with drought, however, photoinhibition may be involved which reduces the demand function.

The effects of water stress on **leaf growth** are stronger than those on photosynthesis (Hsiao 1973). Expansive growth is one of the processes most sensitive to water deficit in leaves, internodes, or reproductive organs (Tardieu 2013). As a result, nonstructural carbohydrates tend to accumulate under water stress (Zhang et al. 2015). The reduced demand of the sink will then lead to the kind of feedback inhibition of photosynthesis we discussed in Sect. 2.4. The net effect of the downregulation of photosynthetic capacity under severe water stress is that C_c is higher than would be expected if a decrease in conductance were the only factor causing a reduction in CO_2 assimilation in water-stressed plants. The reduction in photosynthetic capacity allows photosynthesis to continue operating near the break point between the RuBP-limited and the CO_2-limited regions of the A_n-C_c curve. Thus, drought-acclimated plants maximize the effectiveness of both light and dark reactions of photosynthesis under dry conditions at the cost of reduced photosynthetic capacity under favorable conditions. The decline in photosynthetic capacity in water-stressed plants is associated with declines in all biochemical components of the photosynthetic process.

2.5.3 Carbon-Isotope Fractionation in Relation to Water-Use Efficiency

Carbon-isotope composition of plant tissues provides an integrated measure of the photosynthetic water-use efficiency ($WUE = A/E$) or, more precisely, the intrinsic *WUE* (A/g_s) during the time when the carbon in these tissues was assimilated (Fig. 2.30). As explained in Box 2.2, air has a $\delta^{13}C$ of approximately -8‰, and the major steps in C_3 photosynthesis that fractionate are diffusion (4.4‰) and carboxylation (30‰, including dissolution of CO_2). The isotopic composition of a leaf will approach that of the process that most strongly limits photosynthesis. If stomata are almost closed and diffusion is the rate-limiting step, $\delta^{13}C$ of leaves would be −12.4‰ (*i.e.* −8 + −4.4); if carboxylation is the only limiting factor, we expect a $\delta^{13}C$ of −38‰ (*i.e.* −8 + −30). A typical range of $\delta^{13}C$ in C_3 plants is −25 to −29‰, indicating co-limitation by diffusion and carboxylation (O'Leary 1993); however, $\delta^{13}C$ values vary among plant species and environment depending on the rate of CO_2 assimilation and stomatal and mesophyll conductance. The fractionation, $\Delta^{13}C$, is defined as (Box 2.2):

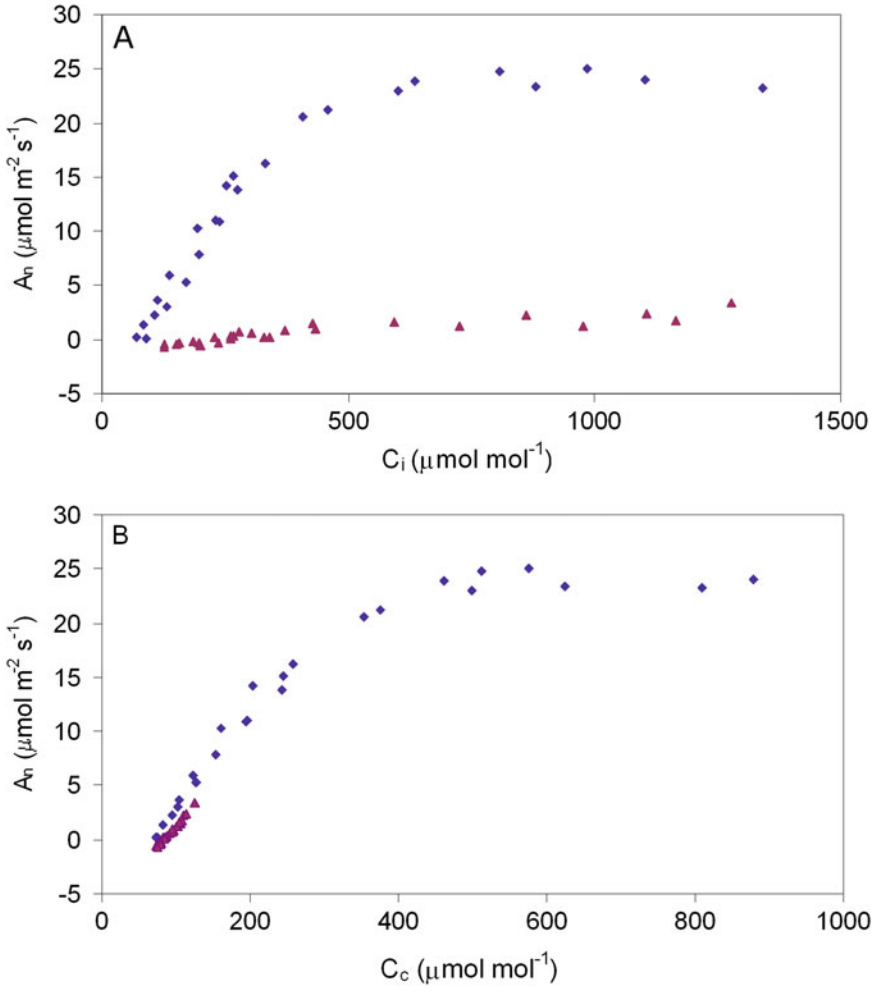

Fig. 2.29 The response of net photosynthesis to (**A**) intercellular CO_2 concentration (C_i), and (**B**) CO_2 concentration in the chloroplasts (C_c), for well-watered (blue symbols) and severely water-stressed *Vitis vinifera* (grapevine) plants (purple symbols) (after Flexas et al. 2006a).

$$\Delta^{13}\mathrm{C} = [4.4 + 22.6\ (C_i/C_a)] \times 10^{-3},$$

or:

$$\delta^{13}\mathrm{C_{air}} - \delta^{13}C_{\mathrm{leaf}} = 4.4 + 22.6\ (C_i/C_a), \quad (2.39)$$

which indicates that a high C_i/C_a (due to high stomatal conductance or low rate of CO_2 assimilation) results in a large fractionation (strongly negative $\delta^{13}C$). We can now use this information to estimate an integrated *WUE* for the plant, but we must be aware of one significant problem: Eq. 2.39 uses $\boldsymbol{C_i}$, and does not take **mesophyll conductance** into account; it uses $\boldsymbol{C_i}$, and assumes that the mesophyll conductance scales with stomatal conductance. Evergreen Mediterranean *Quercus* (oak) species with rapid rates of photosynthesis function at a high mesophyll conductance, without changes in stomatal conductance. This adaptation allows evergreen oaks to achieve photosynthetic rates similar to congeneric deciduous species (Peguero-Pina et al. 2017). Therefore, some of the fractionation data have to be interpreted with great care, because they may

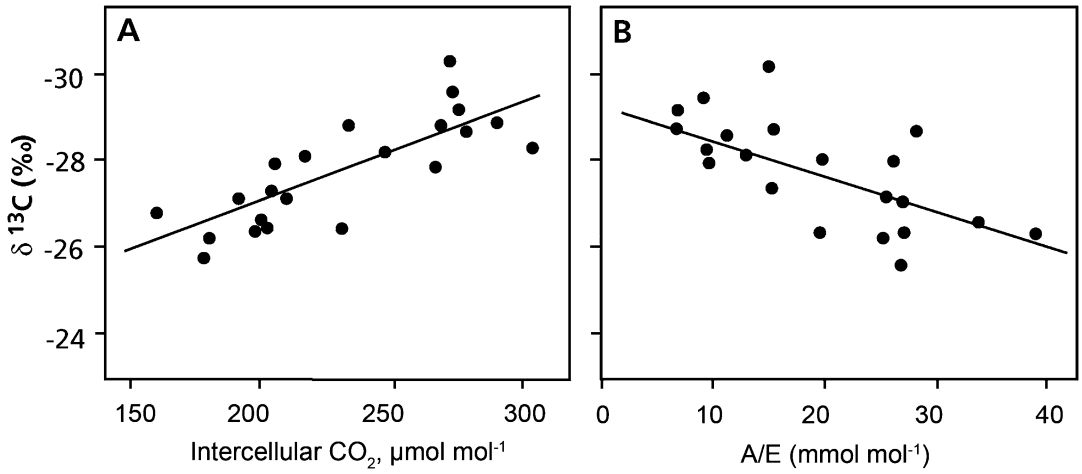

Fig. 2.30 The relationship between carbon-isotope composition ($\delta^{13}C$) and (**A**) average intercellular CO_2 concentration, and (**B**) daily photosynthetic water-use efficiency, assimilation/transpiration (A/E). The data points refer to mistletoes and host plants in central Australia (after Ehleringer et al. 1985).

reflect differences in mesophyll conductance, rather than (only) stomatal conductance (Warren and Adams 2006).

The water-use efficiency ($WUE = A_n/E$) is given by:

$$WUE = A_n/E = g_c(C_a\text{-}C_i)/g_w(w_i\text{-}w_a) = C_a(1\text{-}C_i/C_a)/1.6(w_i\text{-}w_a) \quad (2.40)$$

given that $g_w/g_c = 1.6$ (the molar ratio of diffusion of water vapor and CO_2 in air). Eq. 2.40 tells us that the *WUE* is high, if the conductance is low in comparison with the capacity to assimilate CO_2 in the mesophyll. Under these circumstances, C_i (and C_i/C_a) will be small. The right-hand part of Eq. 2.40 then approximates $[C_a/(1.6(w_i - w_a)]$ and diffusion is the predominant component determining fractionation of carbon isotopes and approaches a value of 4.4‰. On the other hand, if the stomatal conductance is large, *WUE* is small, C_i approximates C_a and the right-hand part of Eq. 2.39 approaches 27‰. Fractionation of the carbon isotopes is now largely due to the biochemical fractionation by Rubisco. Values for *WUE* thus obtained can only be compared at the same vapor pressure difference (w_i - w_a), *e.g.*, within one experiment or a site at the same atmospheric conditions. Therefore, the *WUE* derived from $\delta^{13}C$ of plant carbon is mostly referred to as **intrinsic *WUE*** (A_n/g_s), which is equivalent to a value normalized at a constant *VPD* of 1 mol mol^{-1}.

As expected from the theoretical analysis above, there is a good correlation between *WUE* and the carbon-isotope fractionation (Fig. 2.30). *Triticum aestivum* (wheat) grown under dry conditions has a higher *WUE* and a lower carbon-isotope fractionation than do wheat plants well supplied with water (Farquhar and Richards 1984). Correlation among parameters under different water treatments suggests that improvements in the (A/g_s) are possible among Mediterranean accessions of *Solanum lycopersicum* (tomato), without negative impacts on yield. A higher A/g_s does not reflect differences in Rubisco-related parameters, but correlates with the ratio between the leaf mesophyll and stomatal conductances (g_m/g_s) (Fig. 2.31A, B). A similar correlation between *WUE* and $\delta^{13}C$ has been found for cultivars of other species (Farquhar et al. 1989).

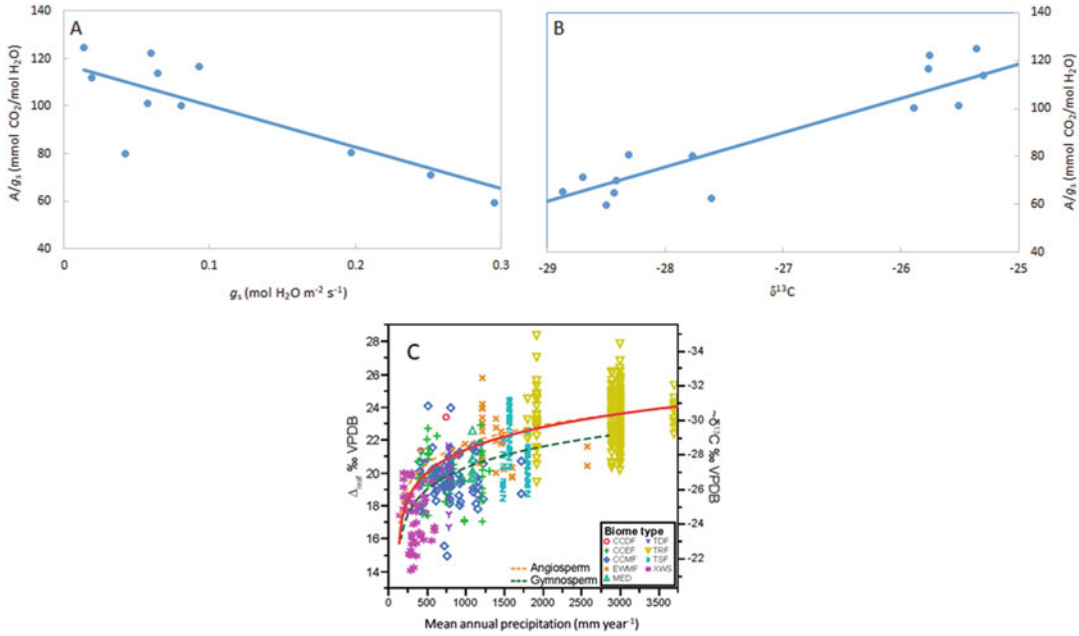

Fig. 2.31 Relationship between intrinsic leaf water-use efficiency (A/g_s) and (**A**) stomatal conductance (g_s) and (**B**) leaf $\delta^{13}C$ in *Solanum lycopersicum* (tomato). The symbols refer to three accessions with the common divided tomato leaf morphology, three with the potato leaf morphology, and two outgroup accessions (Galmés et al. 2011). Copyright John Wiley and Sons. (**C**) A compilation of leaf fractionation (Δ_{leaf}) values as a function of mean annual precipitation (MAP), using a total of 570 species-site combinations, 334 species and 75 families at 105 geographic sites. MAP accounts for 55% of the variability in Δ_{leaf}. Altitude is also an important predictor of Δ_{leaf}. The relationship between MAP and Δ_{leaf} is shown for angiosperms and gymnosperms and indicates higher average Δ_{leaf} in angiosperms. The right y-axis indicates the corresponding approximate $\delta^{13}C$ values. Points are coded by biome: tropical rain forest (TRF), evergreen warm mixed forest (EWMF), tropical seasonal forest (TSF), cool-cold deciduous forest (CCDF), cool-cold evergreen forest (CCEF), cool-cold mixed forest (CCMF), tropical deciduous forest (TDF), xeric woodland scrubland (XWS) (Diefendorf and Freimuth 2017); © 2016 Elsevier Ltd. All rights reserved. (2010).

2.5.4 Other Sources of Variation in Carbon-Isotope Ratios in C_3 Plants

Given the close relationship between *WUE* and $\delta^{13}C$, carbon-isotopic composition can be used to infer average *WUE* during growth (Fig. 2.30; Sect. 5.6). For example, $\delta^{13}C$ is higher (less negative) in **desert plants** than in **mesic plants**, and it is higher in biomass produced during dry seasons (Smedley et al. 1991) or in dry years. This indicates that, on a global scale, plants growing in dry conditions have a lower C_i than those in moist conditions (Fig. 2.31C; Diefendorf et al. 2010). Other factors can alter isotopic composition without altering *WUE*. For example, $\delta^{13}C$ of plant matter is higher at the bottom than at the top of the canopy. This is to a limited extent due to the contribution of ^{13}C-depleted CO_2 from soil respiration, but mostly to the lower C_i of sunlit top leaves compared with the shaded understory leaves (Buchmann et al. 1997). A complicating factor with the derivation of *WUE* from $\delta^{13}C$ is that isotope fractionation is operating at the level of Rubisco in the chloroplast, whereas the theoretical model is based on C_i. Possible variation in the drawdown of CO_2 from the intercellular spaces to the chloroplast (Sect. 2.2.2.3) due to the mesophyll resistance is not taken into account, but may cause variation in $\delta^{13}C$ that is not associated with *WUE*.

Evergreen gymnosperms discriminate more strongly against ^{13}C than other woody plant functional types (Diefendorf et al. 2010; Diefendorf

and Freimuth 2017). **Annuals** fractionate more than **perennials**; forbs fractionate more than grasses, and **root parasites** [*e.g.*, *Comandra umbellata* (pale bastard toadflax)] more than any of the surrounding species (Smedley et al. 1991). These patterns indicate a high stomatal conductance and low *WUE* in deciduous wooody plants, annuals, herbs, and hemiparasites (Fig. 2.31c). The low *WUE* of hemiparasitic plants is important for their nutrient acquisition (Sect. 15.3).

2.6 Effects of Soil Nutrient Supply on Photosynthesis

2.6.1 The Photosynthesis-Nitrogen Relationship

Since the photosynthetic machinery accounts for more than half of the N in a leaf (Fig. 2.13) and much of the remainder is indirectly associated with its photosynthetic function, N availability strongly affects photosynthesis. A_{max} increases linearly with leaf N per unit area (Fig. 2.32), regardless of whether the variation in leaf N is caused by differences in soil N availability, growth irradiance, or leaf age, and holds also when different species are compared (Fig. 2.32). The slope of this relationship is much steeper for C_4 plants than for C_3 plants (Sect. 2.9.5), and differs among C_3 plants (Sect. 9.4.2.1; Evans 1989). When we compare leaves of different N concentration of plants grown at different N availability, the photosynthetic rate per unit N (**photosynthetic N-use efficiency**; *PNUE*) at the growth irradiance is highest in leaves with low N concentrations. This is due to the higher degree of utilization of the photosynthetic apparatus (Fig. 2.33); hence, a higher efficiency at the expense of photosynthetic rate.

The strong A_{max} *vs.* N relationship cannot be due to any simple direct N limitation of photosynthesis, because both carbon-isotope studies and A_n-C_c curves generally show that photosynthesis is co-limited by CO_2 diffusion and photosynthetic capacity. Rather, the entire photosynthetic process is downregulated under conditions of N limitation, with declines in Rubisco, chlorophyll, and stomatal conductance (Sect. 2.5.1, Table 2.4). Results on a tropical pioneer tree, *Ficus insipida* (Moraceae), suggest that variation in plant N

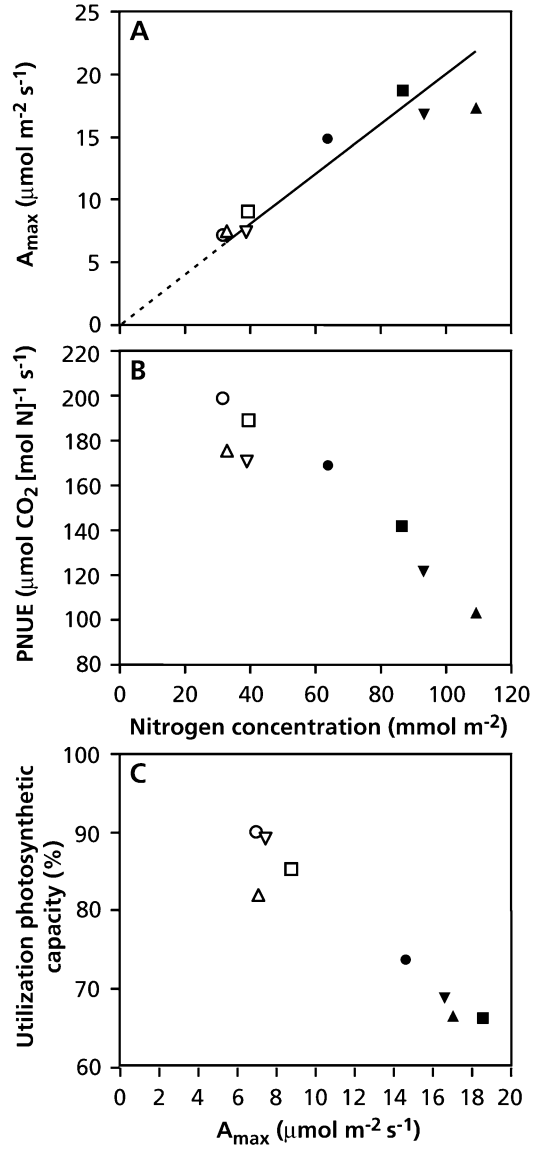

Fig. 2.32 The light-saturated rate of photosynthesis (A_{max}) of four grasses grown at high (filled symbols) and low (open symbols) N supply (**A**) and their photosynthetic N-use efficiency (*PNUE*) determined at growth irradiance (**B**) plotted against leaf N per unit area. Note the higher *PNUE* for plants grown at a low N supply. (**C**) The proportional utilization of the total photosynthetic capacity at growth irradiance, calculated as the ratio of the rate at growth irradiance and A_{max} in relation to A_{max} (Pons et al. 1994). Copyright SPB Academic Publishing.

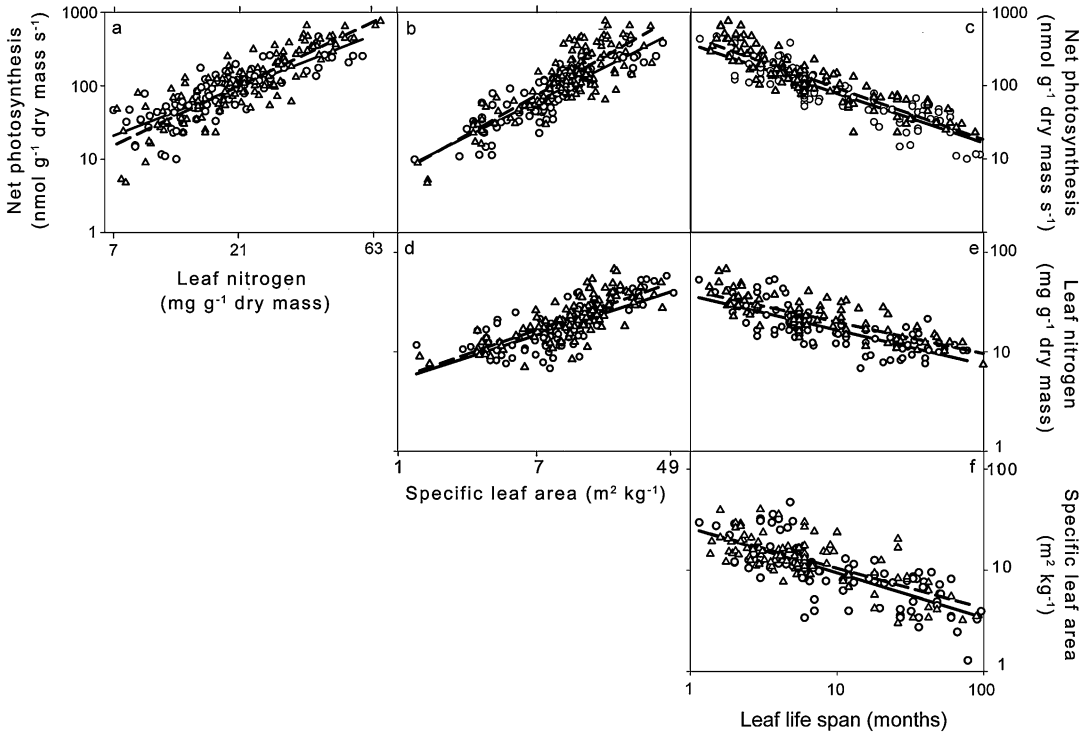

Fig. 2.33 Relations of (**A**) mass-based maximum rate of CO_2 assimilation, (**B**) leaf N concentration, and (**C**) specific leaf area of young mature leaves as a function of their expected leaf life span. The symbols refer to a data set for 111 species from six biomes (after Reich et al. 1997).

status affects coupling between CO_2 and water exchange in tropical forest trees. The pronounced variation in *WUE* results from a combination of a strong response of C_i/C_a to leaf [N], and inherently high values of C_i/C_a in this species (Cernusak et al. 2007).

In some field studies, especially in conifers, which often grow on low-P soils, photosynthesis may show little correlation with leaf N concentration, but a strong correlation with leaf P concentration (Reich and Schoettle 1988). The slow photosynthetic rate of plants grown at low P supply may reflect feedback inhibition due to slow growth and low concentrations of Pi in the cytosol (Sect. 2.4.1) or low concentrations of Rubisco and other photosynthetic enzymes, as their synthesis requires ribosomal RNA, which is a major organic P fraction in leaves (Veneklaas et al. 2012).

2.6.2 Interactions of Nitrogen, Light, and Water

Because of the coordinated responses of all photosynthetic processes, any environmental stress that reduces photosynthesis will reduce both the diffusional and the biochemical components (Table 2.4). Therefore, N concentration per unit leaf area is typically highest in sun leaves, and declines toward the bottom of a canopy (Pons 2016). In canopies of *Nicotiana tabacum* (tobacco), this partially reflects faster rates of CO_2 assimilation of young, high-N leaves in high-light environments. In multi-species canopies, however, the low leaf N concentration per area in understory species clearly reflects the adjustment of photosynthetic capacity to the reduced light availability (Table 2.4; Niinemets 2007).

2.6.3 Photosynthesis, Nitrogen, and Leaf Life Span

As discussed in Chaps 9 and 10, plants acclimate and adapt to low soil N and low soil moisture availability by producing long-lived leaves that are thicker and have a high leaf mass density, a low specific leaf area (SLA; *i.e.* leaf area per unit leaf mass) and a low leaf N concentration. Both broad-leafed and conifer species show a single strong negative correlation between leaf life span and either leaf N concentration or mass-based photosynthetic rate (Fig. 2.33; Reich et al. 1997). The low SLA in long-lived leaves relates to structural properties required to withstand unfavorable environmental conditions (Chap. 10). There is a strong positive correlation between SLA and leaf N concentration for different data sets (Fig. 2.33). Together, the greater leaf thickness and low N concentrations per unit leaf mass result in slow rates of photosynthesis on a leaf-mass basis in long-lived leaves (Fig. 2.33). Maximum stomatal conductance correlates strongly with leaf N concentration, because g_s scales with A_{max} (Wright et al. 2004). However, species that naturally occur on severely nutrient-impoverished soils tend to exhibit a high *PNUE* (Sulpice et al. 2014; Guilherme Pereira et al. 2019). This is largely driven by a very high photosynthetic P-use efficiency (PPUE) (Denton et al. 2007; Guilherme Pereira et al. 2019), which is partly accounted for by very low leaf ribosomal RNA levels (Sulpice et al. 2014).

2.7 Photosynthesis and Leaf Temperature: Effects and Adaptations

Temperature has a major effect on enzymatically catalyzed reactions and membrane processes, and therefore affects photosynthesis. Because the **activation energy** of different reactions often differs among plants acclimated or adapted to different temperature regimes, photosynthesis may be affected accordingly (for a discussion of the concepts of **acclimation** and **adaptation**, see Fig. 2.3; Sect. 1.4). In this Section, temperature effects on photosynthesis will be explained in terms of underlying biochemical, biophysical, and molecular processes.

Differences among plants in their capacity to perform at extreme temperatures often correlate with the plant's capacity to photosynthesize at these temperatures. This may reflect both the adjustment of photosynthesis to the demand of the sinks (Sect. 2.4) and changes in the photosynthetic machinery during acclimation and adaptation.

2.7.1 Effects of High Temperatures on Photosynthesis

Most plants show considerable capacity to adjust their photosynthetic characteristics to their growth temperatures (**temperature acclimation**). The most typical case is a shift in the optimum temperature for photosynthesis, which can maximize the photosynthetic rate at the growth temperature (Dusenge et al. 2019). These plastic adjustments can allow plants to photosynthesize more rapidly at their new growth temperatures (Fig. 2.34). C_3 species tend to maintain the same photosynthetic rate at their growth condition across a range of growth temperatures (Yamori

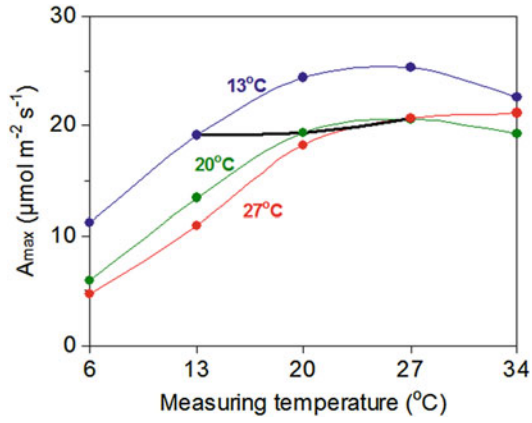

Fig. 2.34 Temperature dependence of light-saturated rates of photosynthesis of *Plantago major* (common plantain) grown at three temperatures. The black line connects measurements at the growth temperatures (after Atkin et al. 2006). Copyright John Wiley and Sons.

et al. 2014). Below optimum temperature, enzymatic reaction rates, primarily associated with the '**dark reactions'**, are temperature-limited. At high temperatures the **oxygenating** reaction of Rubisco increases more than the **carboxylating** one so that photorespiration becomes proportionally more important. This is partly because the **solubility** of CO_2 declines with increasing temperature more strongly than does that of O_2. Part of the effect of temperature on photosynthesis of C_3 plants is due to the effects of temperature on **kinetic properties** of Rubisco. V_{max} increases with increasing temperature, but the K_m-values increase also, and more steeply for CO_2 than for O_2 (Fig. 2.35). This means that the affinity for CO_2 decreases more strongly than that for O_2. Additionally, electron transport (Cen and Sage 2005) and g_m (Yamori et al. 2006a; Warren 2007) may decline at elevated temperatures. The combined temperature effects on solubility, affinity, and mesophyll conductance cause a proportional increase in **photorespiration**, resulting in a decline in net photosynthesis at high temperature when electron-transport rates cannot keep up with the increased inefficiency.

Adaptation to high or low temperature typically causes a shift of the temperature optimum for net photosynthesis to higher or lower

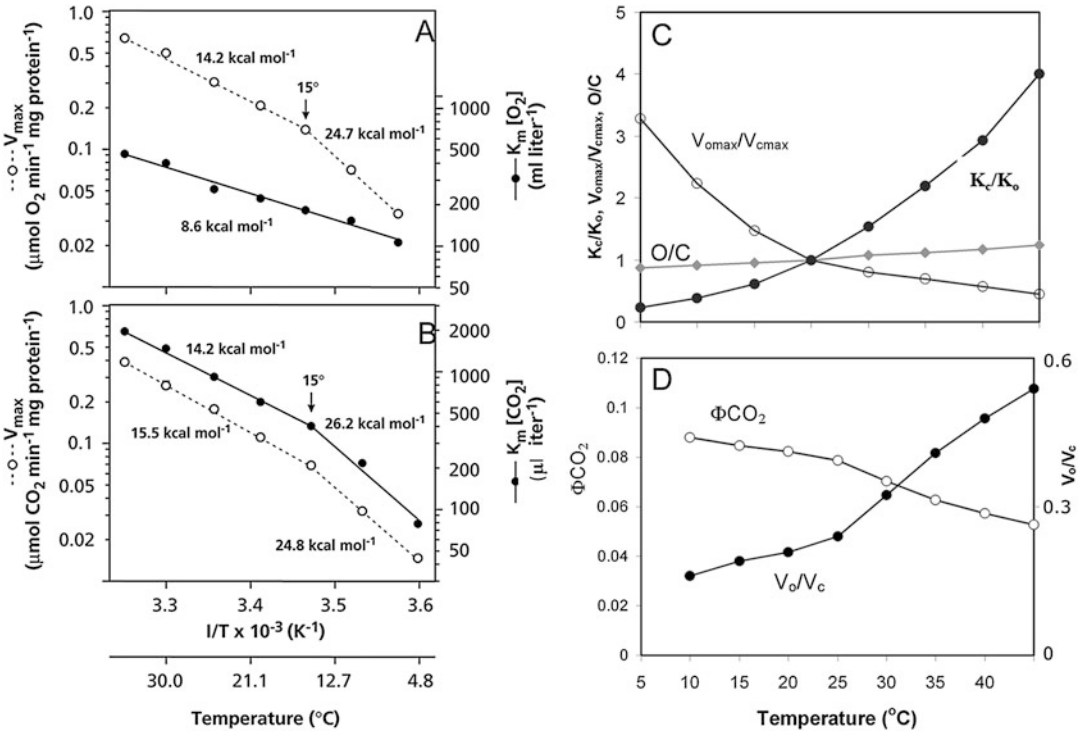

Fig. 2.35 Temperature dependence of V_{max} and the K_m of (**A**) the oxygenating and (**B**) the carboxylating reaction of Rubisco. V_{max} is the rate of the carboxylating or oxygenating reaction at a saturating concentration of CO_2 and O_2, respectively. The K_m is the concentration of CO_2 and O_2 at which the carboxylating and oxygenating reaction, respectively, proceed at the rate which equals $1/2V_{max}$. Note that a logarithmic scale is used for the y-axis and that the inverse of the absolute temperature is plotted on the x-axis ('Arrhenius-plot'). In such a graph, the slope gives the activation energy, a measure for the temperature dependence of the reaction (Berry and Raison 1981). (**C**) The combined effects of temperature on kinetic properties as shown in (**A**) and (**B**) and relative solubility of O_2 and CO_2 (O/C) have been modeled, normalized to values at 20 °C. (**D**) Relative rates of the oxygenation and carboxylation reactions of Rubisco (V_o/V_c) and quantum yield (ΦCO_2) modeled using the same parameter values as in (**C**). For calculation of V_o/V_c and ΦCO_2, it was assumed that partial pressures of CO_2 and O_2 in the chloroplast were 27 Pa and 21 kPa, respectively. Kinetic parameters used were calculated from Jordan and Ogren (1984) (courtesy I. Terashima, The University of Tokyo, Japan).

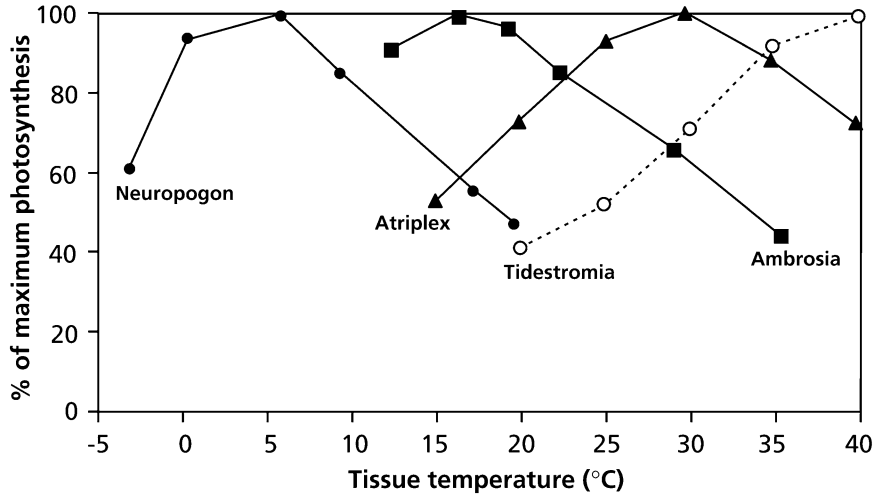

Fig. 2.36 Photosynthetic response to temperature in plants from contrasting temperature regimes. Curves from left to right are for *Neuropogon acromelanus*, an Antarctic lichen, *Ambrosia chamissonis*, a cool coastal dune plant, *Atriplex hymenelytra*, an evergreen desert shrub, and *Tidestromia oblongifolia*, a summer-active desert perennial (after Mooney 1986).

temperatures (Fig. 2.36). Similarly, the temperature optimum for photosynthesis shifts to higher temperatures when coastal and desert populations of *Atriplex lentiformis* **acclimate** to high temperatures (Pearcy 1977).

Apart from the increase in photorespiration discussed above, there are several other factors important for determining **acclimation** and **adaptation** of photosynthesis to temperature. In leaves of *Spinacia oleracea* (spinach) the **Rubisco activation state** decreases with increasing temperatures above the optimum temperatures for photosynthesis, irrespective of growth temperature, while the activation state remains high at lower temperatures. Rubisco thermal stabilities of spinach leaves grown at low temperature are lower than those of leaves grown at high temperature. Photosynthetic performance in spinach is largely determined by the Rubisco kinetics at low temperature and by Rubisco kinetics and Rubisco activation state at high temperature (Yamori et al. 2006b). Species adapted to hot environments often show temperature optima for photosynthesis that are quite close to the temperature at which enzymes are inactivated (Fig. 2.36). The lability of **Rubisco activase** plays a major role in the decline of photosynthesis at high temperatures (Salvucci and Crafts-Brandner 2004; Hikosaka et al. 2006). Thermal acclimation of *Acer rubrum* (red maple) from Florida in comparison with genotypes from Minnesota, United States, is associated with maintenance of a high ratio of Rubisco activase to Rubisco (Weston et al. 2007). In *Gossypium hirsutum* (cotton), expression of the gene encoding Rubisco activase is influenced by post-transcriptional mechanisms that probably contribute to acclimation of photosynthesis during extended periods of heat stress (DeRidder and Salvucci 2007). Increases in activation energy of V_{cmax} with increasing temperature appear to be most important for the shift of optimal temperature of photosynthesis (Hikosaka et al. 2006).

High temperatures also require a high degree of **saturation of the membrane lipids** of the thylakoid for integrated functioning of its components and prevention of leakiness (Sharkey 2005; Zhu et al. 2018b). Therefore, not only

Rubisco activity, but also membrane-bound processes of electron transport may be limiting photosynthesis at high temperatures.

2.7.2 Effects of Low Temperatures on Photosynthesis

When plants grown at a moderate temperature are transferred to a lower temperature, but within the range normal for the growing season, photosynthesis is initially reduced (Fig. 2.34). Temperature does not affect photon absorption, but the rate of electron transport and biochemical processes are slower at the lower temperature. Particularly, sucrose metabolism and/or phloem loading can become limiting for photosynthesis, causing feedback inhibition (Fig. 2.27). Acclimation to the lower growth temperature involves upregulation of the limiting components of the photosynthetic apparatus. Hence, the capacity for electron transport (J_{max}) is increased, and Rubisco levels increase as well, with a proportional increase in carboxylation capacity (V_{cmax}) (Atkin et al. 2006). Feedback inhibition is alleviated by increased expression of enzymes of the sucrose synthesis pathway (Stitt and Hurry 2002). Acclimation comprises therefore an increase in photosynthetic capacity, which is associated with an increase in leaf thickness, whereas chlorophyll concentrations remain similar, thus causing an increase in A_{max} per unit chlorophyll. The change is accompanied by a decrease in antenna size of PS II. Hence, acclimation to low temperature resembles acclimation to high irradiance (Hüner et al. 1998, 2016). In *Plantago major* (common plantain), the result of acclimation is that, just as with respiration (Fig. 3.17), photosynthetic rates are virtually independent of growth temperature (Fig. 2.34).

When cold is more extreme, damage likely occurs. Many (sub)tropical plants grow poorly or become damaged at temperatures between 10 and 20 °C. Such damage is called **chilling injury**, and differs from frost damage, which only occurs below 0 °C. Part of the chilling injury is associated with the photosynthetic apparatus. The following aspects play a role:

1. Decrease in membrane fluidity;
2. Changes in the activity of membrane-associated enzymes and processes, such as photosynthetic electron transport;
3. Loss of activity of cold-sensitive enzymes.

Chilling resistance probably involves **reduced saturation** of membrane fatty acids which increases membrane fluidity and so compensates for the effect of low temperature on membrane fluidity (Chap. 7).

Chilling often leads to **photoinhibition** and **photooxidation**, because temperature affects the biophysical reactions of photosynthesis (photon capture and transfer of excitation energy) far less than the biochemical steps, including electron transport and activity of the Calvin-Benson cycle (Sect. 2.3.3). The leaves of evergreen plants in cold climates typically develop and expand during the warm spring and summer months, and are retained during the winter months when growth ceases. Upon exposure to low temperature and high irradiance, the conversion of the light-harvesting **violaxanthin** to the energy-quenching **zeaxanthin** (Sect. 2.3.3.1) occurs within minutes. In addition to this ubiquitous process of flexible dissipation, several forms of **sustained dissipation** exist. The sustained dissipation does not relax upon darkening of the leaves, but it is still ΔpH-dependent; it is flexible in the sense that, *e.g.*, warming of leaves allows this state to quickly reverse (Demmig-Adams and Adams 2006). Therefore, under lasting stress conditions and in some plant species, the flexible ΔpH-independent engagement and disengagement of zeaxanthin in dissipation is replaced by a highly effective, but less flexible continuous engagement of zeaxanthin in dissipation, that does not require a ΔpH (Table 2.6). Recent data support an indirect role of zeaxanthin in pH-independent nonphotochemical quenching, rather than a specific direct function of zeaxanthin. Such an indirect function might be related to an allosteric regulation of quenching processes by zeaxanthin (*e.g.*, through interaction of zeaxanthin at the surface of proteins) or a general photoprotective function of zeaxanthin in the lipid phase of the

Table 2.6 Differences in the response of photosynthesis and photoprotection between crops/weeds and evergreens. Typical changes in intrinsic photosynthetic capacity, ΔpH-independent dissipation, zeaxanthin and antheraxanthin (Z + A) retention, in annual crops/biennial weeds *vs.* evergreen species in response to transfer of shade-acclimated plants to high light or in response to the transition from summer to winter conditions.

	Shade to sun transfer		Summer to winter transition	
			Tropical annual/biennial	
	Annual crop	Evergreen	Crop/weed	Temperate evergreen
Photosynthetic capacity	↑	↓	↑	↓↓
ΔpH-independent dissipation	*	↑↑	*	↑↑
Z+A retention	*	↑↑	*	↑↑

Source: Demmig-Adams and Adams (2006)
*Seen only transiently and at moderate levels upon transition

membrane (*e.g.*, by modulation of the membrane fluidity or by acting as antioxidant). This regulation supports the view that zeaxanthin can be considered as a kind of light stress memory in chloroplasts, allowing a rapid reactivation of photoprotective quenching processes in case of recurrent light stress periods (Kress and Jahns 2017).

Hardening of *Thuja plicata* (western red cedar) seedlings (*i.e.* acclimation to low temperatures) is associated with some loss of chlorophyll and increased levels of carotenoids, giving the leaves a red-brown color. Exposure to low temperatures causes a decline in photosynthetic capacity and the quantum yield of photosynthesis, as evidenced by the decline in chlorophyll fluorescence (*i.e.* in the ratio F_v/F_m; Box 2.4). The carotenoids prevent damage that might otherwise occur because of photooxidation (Sect. 2.3.3.1). Upon transfer of the seedlings to a normal temperature (dehardening) the carotenoids disappear within a few days (Weger et al. 1993). Other temperate conifers such as *Pinus banksiana* (jack pine) exhibit 'purpling', which is caused by the accumulation of anthocyanin in epidermal cells which protects the needles against photoinhibition of PS II through screening of irradiance (Hüner et al. 1998). Accumulation of photoprotective anthocyanins gives rise to typical **autumn colors** in deciduous plants, *e.g.*, in *Cornus stolonifera* (red-osier dogwood) (Feild et al. 2001) as well as evergreen Mediterranean shrubs (George 2002) and an evergreen tree (*Acmena acuminatissima*) in winter (Zhu et al. 2018a).

In the alpine and arctic species *Oxyria digyna* (alpine mountain sorrel), an increased resistance to photoinhibition is caused by an increased capacity to repair damaged PS II reaction centers and increased nonphotochemical quenching. Maximum rates of photosynthesis by arctic and alpine plants measured in the field are similar to those of temperate species, but are reached at lower temperatures - often 10–15 °C (Fig. 2.36). These substantial photosynthetic rates at low temperatures are achieved in part by high concentrations of Rubisco, as found in acclimation of lowland plants. This accounts for high leaf N concentration of arctic and alpine plants despite low N availability in soils (Körner and Larcher 1988). Although temperature optima of arctic and alpine plants are 10–30 °C lower than those of temperate plants, they are still 5–10 °C higher than average summer leaf temperatures in the field.

2.8 Effects of Air Pollutants on Photosynthesis

Many air pollutants reduce plant growth, partly through their negative effects on photosynthesis (Adrees et al. 2016). Pollutants like SO_2 and ozone (O_3) that enter the leaf through stomata, directly damage the photosynthetic cells of the leaf. In general, any factor that increases stomatal

conductance (*e.g.*, high supply of water, high light intensity, high N supply) increases the movement of pollutants into the plant, and therefore their impact on photosynthesis. At low [O_3], decreased production in *Glycine max* (soybean) corresponds to a decrease in leaf photosynthesis, but at higher [O_3] the larger loss in production is associated with decreases in both leaf photosynthesis and leaf area (Morgan et al. 2003). Different cultivars of Glycine max (soybean) vary considerably in their sensitivity to O_3. Estimated yield loss due to O_3 ranging from 13% for the least sensitive cultivar to 38% for the most sensitive, at a 7-h mean O_3 concentration of 55 ppb, a level that is frequently observed in regions of the USA, India and China in recent years (Osborne et al. 2016). Rates of net photosynthesis and stomatal conductance in *Fagus sylvatica* (beech) are about 25% lower when the O_3 concentration is double that of the background concentration in Kranzberg Forest (Germany), while V_{cmax} and g_m are not affected (Warren 2007).

2.9 C_4 Plants

2.9.1 Introduction

The first Sections of this chapter dealt primarily with the characteristics of photosynthesis of C_3 species. There are also species with photosynthetic characteristics quite different from these C_3 plants. These so-called **C_4 species** belong to widely different taxonomic groups (Table 2.7); the C_4 syndrome is very rare among tree species; *Chamaesyce olowaluana* (Euphorbiaceae) is a canopy-forming C_4 tree from Hawaii (Sage 2004; Sage and Sultmanis 2016). Although their different anatomy has been well documented for over a century, the biochemistry and physiology of C_4 species has been elucidated more recently. It is hard to say who first discovered the C_4 pathway of photosynthesis (Hatch and Slack 1998), but Hatch and Slack (1966) certainly deserve credit for combining earlier pieces of

Table 2.7 The 19 families containing members with the C_4 photosynthetic pathway*.

Family	Number of genera	Subtypes
Monocots		
Poaceae	20–23	NADP-ME, NAD-ME, PCK
Cyperaceae	6	NADP-ME, NAD-ME
Hydrocharitaceae	2	Single-cell NADP-ME
Eudicots		
Acanthaceae	1	–
Aizoaceae	4	NADP-ME
Amaranthaceae	10	NADP-ME, NAD-ME
Asteraceae	8	NADP-ME
Boraginaceae	1	NAD-ME
Capparidaceae	3	–
Caryophyllaceae	1	NAD-ME
Chenopodiaceae	10–13	NADP-ME, NAD-ME and single-cell NAD-ME
Euphorbiaceae	1	NADP-ME
Gisekiaceae	1	NAD-ME
Molluginaceae	1	NAD-ME
Nyctaginaceae	2	NAD-ME
Polygonaceae	1	–
Portulacaceae	1–2	NADP-ME, NAD-ME
Scrophulariaceae	1	–
Zygophyllaceae	1–2	NADP-ME

Source: Sage (2004, 2016)

*The biochemical subtypes (not known for all species) are as defined in Table 2.8 and Fig. 2.37. Single-cell C_4 is explained in the text

Table 2.8 Main differences between the three subtypes of C_4 species*.

Subtype	Major decarboxylase in BSC	Decarboxylation occurs in	Major substrate moving from		Photosystems in BSC
			MC to BSC	BSC to MC	
NADP-ME	NADP-malic enzyme	chloroplasts	malate	pyruvate	I and II[a]
NAD-ME	NAD-malic enzyme	mitochondria	aspartate	alanine	I and II
PCK	PEP carboxykinase	cytosol	aspartate + malate	alanine + PEP	I and II

*MC is mesophyll cells; BSC is vascular bundle sheath cells
[a]Some NADP-ME monocots, including *Zea mays* (corn) have only PS I in BSC chloroplasts

information with their own findings, and proposing the basic pathway as outlined in this Section.

None of the metabolic reactions or anatomical features of C_4 plants are unique to these species; however, they are linked in a manner quite different from that in C_3 species. Based on differences in biochemistry, physiology, and anatomy, three subtypes of C_4 species are discerned (Table 2.8). In addition, there are intermediate forms between C_3 and C_4 plants (Sect. 2.9.6).

2.9.2 Biochemical and Anatomical Aspects

The anatomy of C_4 plants differs strikingly from that of C_3 plants (Fig. 2.37; Christin and Osborne 2014). C_4 plants exhibit a **Kranz anatomy**, a sheath of thick-walled cells surrounding the vascular bundle ('Kranz' is the German word for 'wreath'). These thick walls of the bundle sheath cells may be impregnated with suberin, but this does not appear to be essential to reduce the gas diffusion between the bundle sheath and the mesophyll. In some C_4 species (NADP-ME types), the cells of the bundle sheath contain large chloroplasts with mainly stroma thylakoids and very little grana. The bundle sheath cells are connected via **plasmodesmata** with the adjacent thin-walled mesophyll cells, with large intercellular spaces.

CO_2 is first assimilated in the mesophyll cells, catalyzed by **PEP carboxylase**, a light-activated enzyme, located in the cytosol. PEP carboxylase uses phospho*enol*pyruvate (PEP) and HCO_3^- as substrates. HCO_3^- is formed by hydratation of CO_2, catalyzed by **carbonic anhydrase**. The high affinity of PEP carboxylase for HCO_3^- reduces C_i to about 100 µmol mol^{-1}, less than half that in C_3 plants (Sect. 2.2.2.2). PEP is produced in the light from pyruvate and ATP, catalyzed by pyruvate Pi-dikinase, a light-activated enzyme located in the chloroplast. The product of the reaction catalyzed by PEP carboxylase is oxaloacetate, which is reduced to malate. Alternatively, oxaloacetate may be transaminated in a reaction with alanine, forming aspartate. Whether malate or aspartate, or a mixture of the two, are formed, depends on the subtype of the C_4 species (Table 2.8). Malate (or aspartate) diffuses via plasmodesmata to the vascular bundle sheath cells, where it is decarboxylated, producing CO_2 and pyruvate (or alanine). CO_2 is then fixed by Rubisco in the chloroplasts of the **bundle sheath cells**, which have a normal Calvin-Benson cycle, as in C_3 plants. Rubisco is not present in the mesophyll cells, which do not have a complete Calvin-Benson cycle and only store starch when the bundle sheath chloroplasts reach their maximum starch concentrations.

Fixation of CO_2 by PEP carboxylase and the subsequent decarboxylation occur relatively fast, allowing the build-up of a high concentration of CO_2 in the vascular bundle sheath. When the outside CO_2 concentration is 400 µmol mol^{-1}, that at the site of Rubisco in the chloroplasts of the vascular bundle is 1000–2000 µmol mol^{-1}. The C_i, that is the CO_2 concentration in the intercellular spaces in the mesophyll, is only about 100 µmol mol^{-1}. With such a steep gradient in

CO_2 concentration, it is inevitable that some CO_2 diffuses back from the bundle sheath to the mesophyll, but this is only about 30%. Therefore, C_4 plants have a mechanism to enhance the CO_2 concentration at the site of Rubisco to an extent that its **oxygenation** reaction is virtually fully inhibited. Consequently, C_4 plants have negligible rates of **photorespiration**.

Based on the enzyme involved in the decarboxylation of the C_4 compounds transported to the vascular bundle sheath, there are three groups of C_4 species: NADP-malic enzyme-, NAD-malic enzyme- and PEP carboxykinase-types (Table 2.8, Fig. 2.37). The difference in biochemistry is closely correlated with anatomical features of the bundle sheath and mesophyll of the leaf blade as viewed in transverse sections with the light microscope (Ellis 1977; Edwards and Voznesenskaya 2011). In NAD-ME-subtypes, which decarboxylate malate (produced from imported aspartate) in the bundle sheath mitochondria, the mitochondrial frequency is several-fold higher than that in NADP-ME-subtypes. The specific activity of the mitochondrial enzymes involved in C_4 photosynthesis is also greatly enhanced (Hatch and Carnal 1992). The only phenotypic characters that are common to all C_4 plants are a high activity of **carbonic anhydrase** and **PEP carboxylase** in the cytosol of the **mesophyll** cells, and a high activity of **Rubisco** within chloroplasts in the **vascular-bundle** cells (Fig. 2.37), and most other traits vary among C_4 lineages (Christin and Osborne 2014).

Decarboxylation of malate occurs only during assimilation of CO_2, and *vice versa*, because the NADP needed to decarboxylate malate is produced in the Calvin-Benson cycle, during the assimilation of CO_2. At least in the more 'sophisticated' NADP-ME C_4 plants such as *Zea mays* (corn) and *Saccharum officinale* (sugar cane), the NADPH required for the photosynthetic reduction of CO_2 originates from the activity of NADP malic enzyme. Since two molecules of NADPH are required per molecule of CO_2 fixed by Rubisco, this amount of NADPH is not sufficient for the assimilation of all CO_2. Additional NADPH is required to an even larger extent if aspartate, or a combination of malate and aspartate, diffuses to the bundle sheath. This additional NADPH can likely be imported via a 'shuttle', involving PGA and dihydroxyacetone phosphate (DHAP). Part of the PGA that originates in the

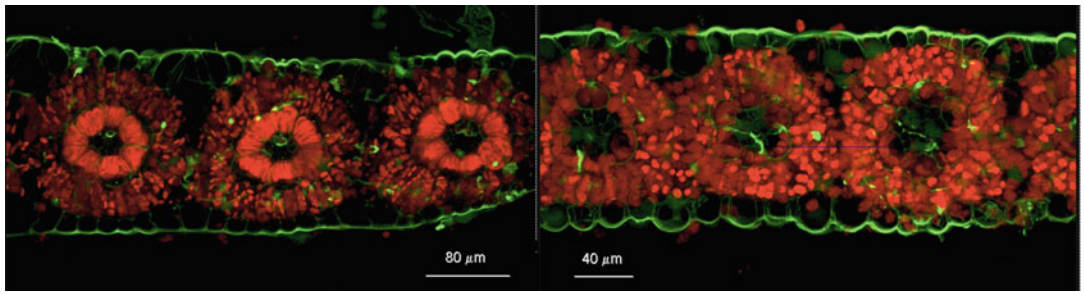

Fig. 2.37 (Facing page) Schematic representation of the photosynthetic metabolism in the three C_4 types distinguished according to the decarboxylating enzyme. NADP-ME, NADP-requiring malic enzyme; PCK, PEP carboxykinase; NAD-ME, NAD-requiring malic enzyme. Numbers refer to enzymes. 1) PEP carboxylase, 2) NADP-malate dehydrogenase, 3) NADP-malic enzyme, 4) pyruvate P_i-dikinase, 5) Rubisco, 6) PEP carboxykinase, 7) alanine aminotransferase, 8) aspartate amino transferase, 9) NAD-malate dehydrogenase, 10) NAD-malic enzyme (after Lawlor 1993). (Above) Cross sections of leaves of monocotyledonous C_4 grasses (Ghannoum et al. 2005). Chlorophyll *a* autofluorescence of a leaf cross section of (Left) *Panicum miliaceum* (French millet, NAD-ME), and (Right) *Sorghum bicolor* (millet, NADP-ME). The images were obtained using confocal microscopy. Cell walls are shown in green and chlorophyll *a* autofluorescence in red. Most of the autofluorescence emanates from bundle sheath cells in the NAD-ME species (Left) and from the mesophyll cells in the NADP-ME species (Right), showing the difference in photosystem II distribution between the two subtypes (courtesy O. Ghannoum, Centre for Horticulture and Plant Sciences, University of Western Sydney, Australia). Copyright American Society of Plant Biologists.

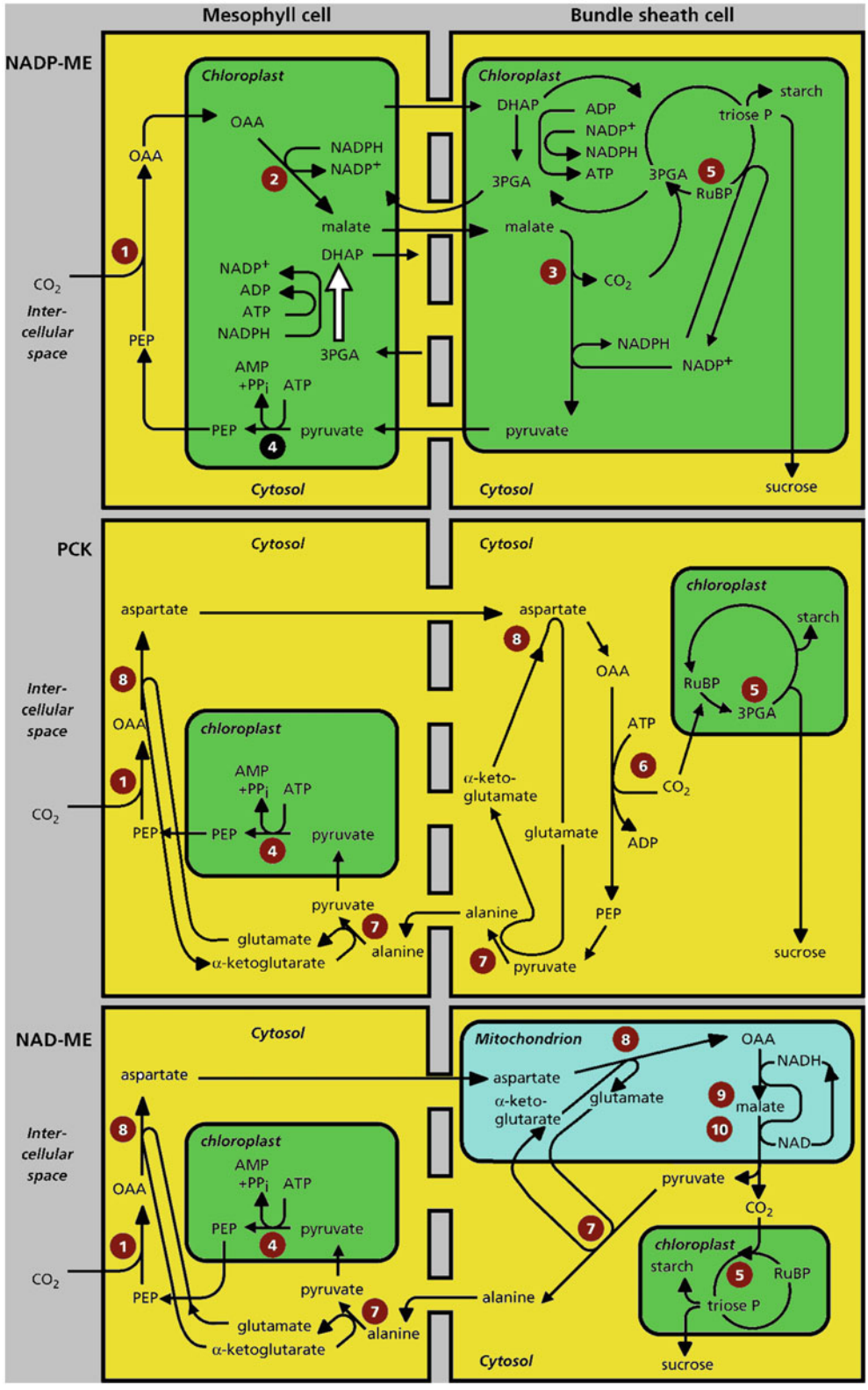

Fig. 2.37 (continued)

bundle-sheath chloroplasts returns to the mesophyll. Here it is reduced, producing DHAP, which diffuses to the bundle sheath. Alternatively, NADPH required in the bundle sheath cells might originate from the removal of electrons from water. This reaction requires the activity of PS II, next to PS I. PS II is only poorly developed in the bundle sheath cells, at least in the 'more sophisticated' C_4 species. The poor development of PS II activity in the bundle sheath indicates that very little O_2 is evolved in these cells that contain Rubisco, which favors the carboxylation reaction over the oxygenation.

The formation of PEP from pyruvate in the mesophyll cells catalyzed by pyruvate Pi-dikinase, requires one molecule of ATP and produces AMP, instead of ADP; this corresponds to the equivalent of two molecules of ATP per molecule of PEP. This represents the metabolic costs of the **CO_2 pump** of the C_4 pathway. It reduces photosynthetic efficiency of C_4 plants, when compared with that of C_3 plants under nonphotorespiratory conditions. In summary, C_4 photosynthesis concentrates CO_2 at the site of carboxylation by Rubisco in the bundle sheath, but this is accomplished at a metabolic cost.

2.9.3 Intercellular and Intracellular Transport of Metabolites of the C_4 Pathway

Transport of the metabolites that move between the two cell types occurs by **diffusion** through **plasmodesmata**. The concentration gradient between the mesophyll and bundle sheath cells is sufficiently high to allow diffusion at a rate that readily sustains photosynthesis, but for the movement of pyruvate additional mechanisms exist.

How can we account for rapid transport of pyruvate from the bundle sheath to the mesophyll if the concentration gradient is insufficient? Uptake of pyruvate in the chloroplasts of the mesophyll cells is a light-dependent process, requiring a specific energy-dependent carrier. Active uptake of pyruvate into the chloroplast reduces the pyruvate concentration in the cytosol of these mesophyll cells to a low level, creating a concentration gradient that drives diffusion from the bundle sheath cells (Flügge et al. 1985). In C_4 species, a novel gene has been identified (BASS2), encoding a protein that is located in the chloroplast envelope membrane. It is highly abundant in C_4 plants that have a Na^+-dependent pyruvate transporter. It shows Na^+-dependent pyruvate uptake activity, and the Na^+ influx is balanced by a Na^+: H^+ antiporter (NHD1) (Furumoto et al. 2011).

In the chloroplasts of the mesophyll cells, pyruvate is converted into PEP, which is exported to the cytosol in exchange for Pi. The same translocator that facilitates this transport is probably also used to export triose-phosphate in exchange for PGA. This translocator operates in the reverse direction in mesophyll and bundle sheath chloroplasts, in that PGA is imported and triose-phosphate is exported in the mesophyll chloroplasts, while the chloroplasts in the bundle sheath export PGA and import triose-phosphate.

The chloroplast envelope of the mesophyll cells also contains a translocator for the transport of dicarboxylates (malate, oxaloacetate, aspartate, and glutamate) (Flügge and Heldt 1991). Transport of these carboxylates occurs by exchange. The uptake of oxaloacetate, in exchange for other dicarboxylates, is competitively inhibited by these other dicarboxylates. Such a system does not allow rapid import of oxaloacetate. A special transport system, transporting oxaloacetate without exchange against other dicarboxylates, facilitates rapid import of oxaloacetate into the mesophyll chloroplasts (Hatch et al. 1984).

2.9.4 Photosynthetic Efficiency and Performance at High and Low Temperatures

The differences in anatomy and biochemistry result in strikingly different A_n-C_i curves between C_3 and C_4. First, the **CO_2-compensation point** of C_4 plants is only 0–5 μmol mol^{-1} CO_2, as compared with 40–50 μmol mol^{-1} in C_3 plants (Fig. 2.38). Second, this compensation point is not affected by O_2 concentration, as opposed to that of C_3 plants which is considerably less at a

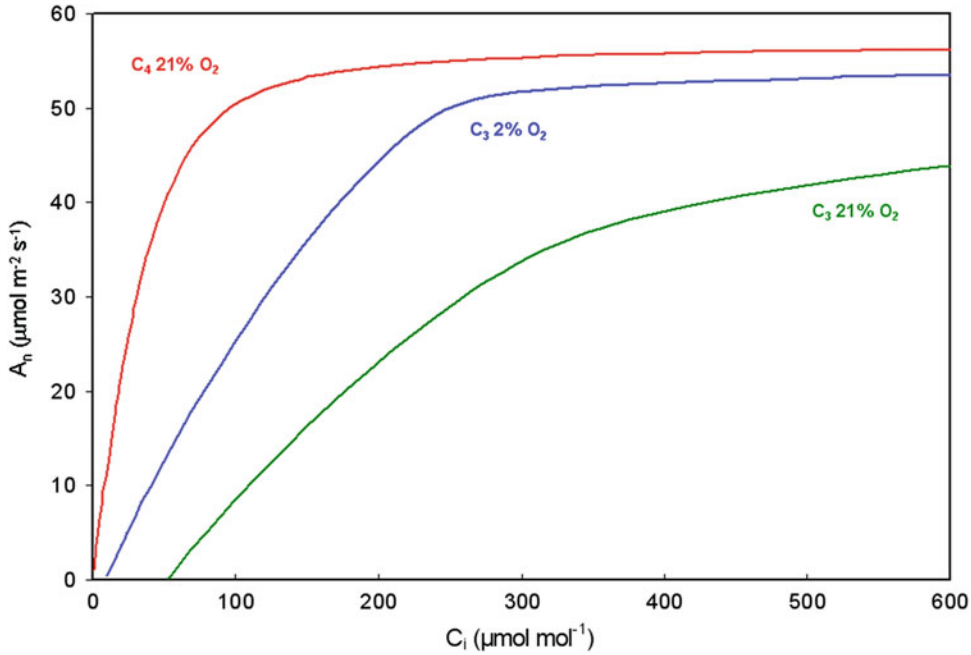

Fig. 2.38 Response of net photosynthesis (A_n) to intercellular CO_2 concentration in the mesophyll (C_i) of C_3 and C_4 plants. C_3 plants respond strongly to O_2 as shown by the lines for normal atmospheric (21%) and low (2%) O_2 concentrations, whereas C_4 plants do not. The CO_2-response curves were calculated based on models described by von Caemmerer (2000). Parameter values for the C_3 model were: V_{cmax} = 150 and J_{max} = 225 µmol m^{-2} s^{-1} (see Box 2.1), and in the C_4 model V_{cmax} = 60 and V_{pmax} = 120 µmol m^{-2} s^{-1}, where V_{pmax} is the maximum PEP carboxylase activity. Arrows indicate typical C_i values at 380 µmol CO_2 mol^{-1} air.

low O_2 concentration (*i.e.* when photorespiration is suppressed). Thirdly, the C_i (the internal concentration of CO_2 in the mesophyll) at a C_a of 400 µmol mol^{-1} is only about 100 µmol mol^{-1}, compared with approximately 250 µmol mol^{-1} in C_3 plants (Fig. 2.38).

There are also major differences in the characteristics of the light-response curves of CO_2 assimilation of C_3 and C_4 species. The initial slope of the light-response represents the light-limited part and is referred to as the **quantum yield**. Photochemical activity is limited by the rate of electron transport under these conditions. Changes in quantum yield are thus caused by changes in the partitioning between carboxylation and oxygenation reactions of Rubisco. When measured at 30 °C or higher, the quantum yield is considerably higher for C_4 plants and independent of the O_2 concentration, in contrast to that of C_3 plants. Therefore, at relatively high temperatures, the quantum yield of photosynthesis is higher for C_4 plants, and is not affected by **temperature**. By contrast, the quantum yield of C_3 plants declines with increasing temperature, due to the proportionally increasing oxygenating activity of Rubisco (Fig. 2.39). At an atmospheric O_2 and CO_2 concentration of 21% and 350 µmol mol^{-1}, respectively, the quantum yield is higher for C_4 plants at high temperatures due to photorespiration in C_3 species, but lower at low temperatures due to the additional ATP required to regenerate PEP in C_4 species. When measured at a low O_2 concentration (to suppress photorespiration) and a C_a of 350 µmol mol^{-1}, the quantum yield is invariably higher for C_3 plants.

The rate of CO_2 assimilation of C_4 plants typically saturates at higher irradiance than that of C_3 plants, because A_{max} of C_4 plants is generally higher. This is facilitated by a high C_c, the CO_2 concentration at the site of Rubisco. In C_3 plants with their generally lower A_{max}, the light-

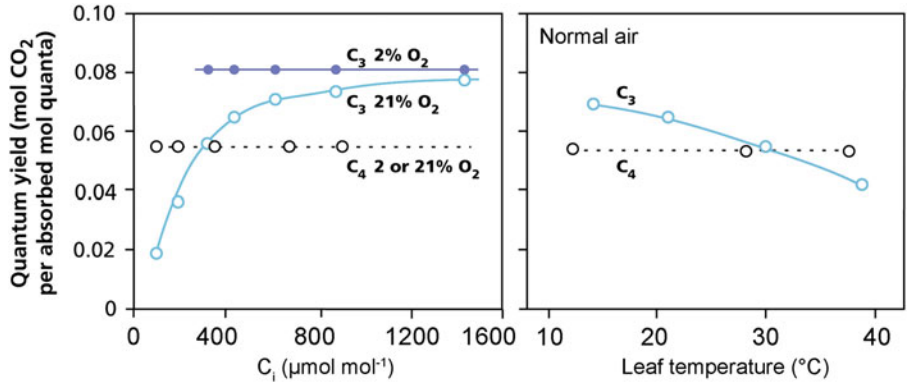

Fig. 2.39 The effect of temperature and the intercellular CO_2 concentration (C_i) on the quantum yield of the photosynthetic CO_2 assimilation in a C_3 and a C_4 plant (after Ehleringer and Björkman 1977).

Table 2.9 Variation in kinetic parameters of the ubiquitous carboxylating enzyme Rubisco at 25 °C for eight species in four groups.

		$K_m(CO_2)$		k_{cat}
		in water	in air	
	Presence of CCM	µM	µmol mol^{-1}	s^{-1}
Cyanobacteria				
Synechococcus	+	293	–	12.5
Green algae				
Chlamydomonas reinhardtii	+	29	–	5.8
C_4 terrestrial plants				
Amaranthus hybridus	+	16	480	3.8
Sorghum bicolor	+	30	900	5.4
Zea mays	+	34	1020	4.4
C_3 terrestrial plants				
Triticum aestivum	–	14	420	2.5
Spinacia oleracea	–	14	420	3.7
Nicotiana tabacum	–	11	330	3.4

Source: Tcherkez et al. (2006)

*Shown are the Michaelis-Menten constant $K_m(CO_2)$, inversely related to substrate (CO_2) affinity, and the catalytic turnover rate at saturating CO_2 (k_{cat}, mol CO_2 (mol catalytic sites)$^{-1}$. $K_m(CO_2)$ in air is calculated from the value provided for water using the solubility of CO_2 at 25 °C (33.5 mmol L^{-1} at standard atmospheric pressure). CCM = carbon-concentrating mechanism

response curve levels off at lower irradiances, because CO_2 becomes the limiting factor for the net CO_2 assimilation. At increasing atmospheric CO_2 concentrations, the irradiance at which light saturation is reached shifts to higher levels also in C_3 plants.

The high concentration of CO_2 in the vascular bundle sheath of C_4-plants, the site of Rubisco, allows different kinetic properties of Rubisco. Table 2.9 shows that indeed the $K_m(CO_2)$ of Rubisco from terrestrial C_3 plants is lower than that from C_4 plants. A high K_m, that is a low affinity, for CO_2 of Rubisco is not a disadvantage for the photosynthesis of C_4 plants, considering the high C_c in de the bundle sheath. For C_3 plants a low K_m for CO_2 is vital, since the C_i is far from saturating for Rubisco in their mesophyll cells.

The advantage of the high K_m of the C_4 Rubisco is indirect in that it allows a high **maximum rate** per unit protein of the enzyme (V_{max} or k_{cat}). That is, the tighter CO_2 is bound to Rubisco, the longer it takes for the carboxylation to be completed. In C_3 plants, a high affinity is essential, so that k_{cat} cannot be high. C_4 plants, which

do not require a high affinity, do indeed have an enzyme with a high k_{cat}, allowing more moles of CO_2 to be fixed per unit Rubisco and time at the high C_c (Table 2.9). Interestingly, the alga *Chlamydomonas reinhardtii*, which has a CO_2-concentrating mechanism (Sect. 2.11.3), also has a Rubisco enzyme with a high K_m (low affinity) for CO_2 and a high V_{max} and k_{cat} (Table 2.9). There is a trade-off in Rubisco between CO_2 specificity [a low $K_m(CO_2)$] and catalytic capacity (a high k_{cat}).

Interestingly, in alpine plants and cold-resistant C_3 Poaceae, the catalytic turnover rate (k_{cat}) of Rubisco shows a 1.1- to 2.8-fold higher k_{cat} than that in *Oryza sativa* (rice). Likewise, Rubisco with the highest k_{cat} also show a k_m for CO_2 (Kc) that is higher than that of rice (Ishikawa et al. 2009). This indicates that there is a similar trade-off as discussed for C_3 and C_4 species: Rubisco enzymes that have a high activity have a lower affinity for CO_2.

The biochemical and physiological differences between C_4 and C_3 plants have important ecological implications. The abundance of C_4 monocots in regional floras correlates most strongly with growing season temperature, whereas C_4 dicot abundance correlates more strongly with aridity and salinity (Ehleringer and Monson 1993). At regional and local scales, areas with **warm-season rainfall** have greater C_4 abundance than regions with cool-season precipitation. Along local gradients, C_4 species occupy microsites that are warmest or have driest soils. In communities with both C_3 and C_4 species, C_3 species are most active early in the growing season when conditions are cool and moist, whereas C_4 activity increases as conditions become warmer and drier. Together these patterns suggest that fast photosynthetic rates at high temperature (due to **lack of photorespiration**) and high water-use efficiency (*WUE*) (due to the **low C_i**, which enables C_4 plants to have a **lower stomatal conductance** for the same CO_2 assimilation rate) are the major factors governing the ecological distribution of the C_4 photosynthetic pathway. However, this pattern is partly accounted for by a phylogenetic effect, with C_4 eudicots that are extremely well adapted to arid conditions having evolved from C_3 ancestors that already inhabited dry conditions, and, in several groups of eudicots, the distributions of related C_3 and C_4 lineages along environmental gradients largely overlap (Christin and Osborne 2014). Similarly, in the Chenopodiaceae group, C_3 plants that were more tolerant of salinity gave rise to C_4 halophytes (Kadereit et al. 2012). Early studies failed to detect an overall relationship between the distribution of C_4 grasses and rainfall (Hattersley 1983; Ehleringer et al. 1997), despite the clear differences in water relations between C_4 and C_3 grass species. A phylogenetic perspective has resolved this paradox by revealing a complex picture in which both physiological innovation and subsequent ecological radiation have played important parts (Edwards et al. 2010).

C_4 plants generally have lower tissue N concentrations, because they have 3-6 times less Rubisco than C_3 plants and very low levels of the photorespiratory enzymes, though some of the advantage is lost by the investment of N in the enzymes of the C_4 pathway. C_4 plants also have equivalent or faster photosynthetic rates than C_3 plants, resulting in a faster rate of photosynthesis per unit leaf N (**photosynthetic N-use efficiency**, *PNUE*), especially at high temperatures (Fig. 2.40). The higher *PNUE* of C_4 plants is accounted for by: (1) suppression of the oxygenase activity of Rubisco, so that the enzyme is only used for the carboxylation reaction; (2) the lack of photorespiratory enzymes; (3) the higher catalytic activity of Rubisco due to its high k_{cat} and the high C_c (Table 2.9). Rubisco represents up to one third of all leaf soluble proteins and 20% of the total nitrogen budget (Evans and Poorter 2001). Just as in a comparison of C_3 species that differ in *PNUE* (Sect. 9.4.2.1), there is no consistent tendency of C_4 species to have increased abundance or a competitive advantage in low-N soils (Sage and Pearcy 1987b). This suggests that the high *PNUE* of C_4 species is less important than their high optimum temperature of photosynthesis in explaining patterns of distribution.

One of the key enzymes of the C_4 pathway in *Zea mays* (corn), **pyruvate Pi-dikinase**, readily loses its activity at low temperature and hence the

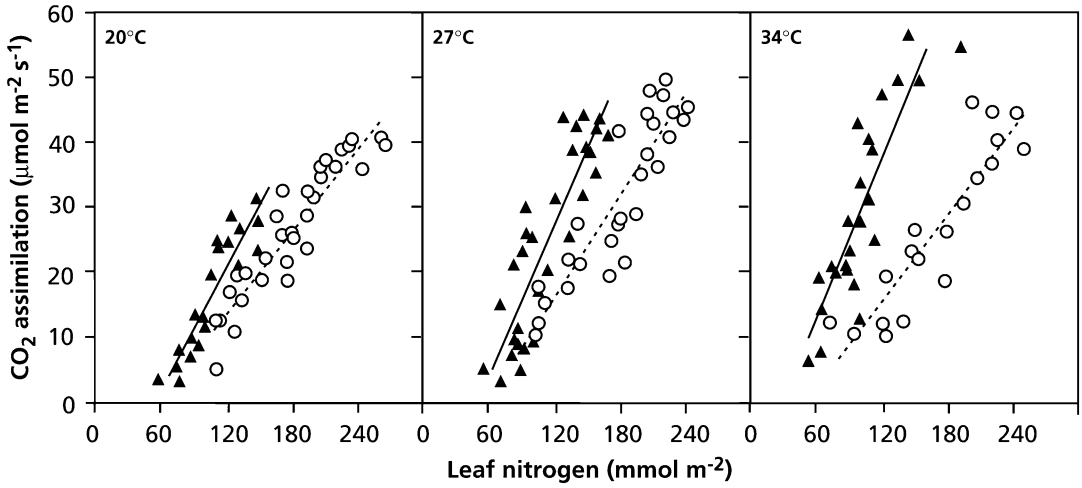

Fig. 2.40 The rate of CO_2 assimilation as a function of the organic N concentration in the leaf and the temperature, as measured for the C_3 plant *Chenopodium album* (pigweed, circles) and the C_4 plant *Amaranthus retroflexus* (triangles) (after Sage and Pearcy 1987a). Copyright American Society of Plant Biologists.

leaves' photosynthetic capacity declines. The bioenergy feedstock grass *Miscanthus* × *giganteus* (giant miscanthus) is exceptional among C_4 species for its high productivity in cold climates. It can maintain photosynthetically active leaves at temperatures 6 °C below the minimum for *Zea mays* (maize). When plants of these two species are grown at 25 °C and then transferred to 14 °C, their rate of light-saturated CO_2 assimilation and quantum yield of PS II declines by 30% and 40%, respectively. The decline continues in maize, but stops and then partially recovers in giant miscanthus. Within 24 h of the temperature transition, the pyruvate Pi-dikinase protein content per leaf area transiently declines in giant miscanthus, but then steadily increases, such that after a week, the enzyme level is significantly higher than that in leaves growing in 25 °C. By contrast, it declines throughout the chilling period in maize leaves. Rubisco levels remain the same in giant miscanthus, but decline in maize. The rate of light activation of pyruvate Pi-dikinase is also slower in cold-grown maize than in giant miscanthus. These results indicate that of the two enzymes known to limit C_4 photosynthesis, increase of pyruvate Pi-dikinase, rather than Rubisco, corresponds to the recovery and maintenance of photosynthetic capacity. Functionally, increased enzyme concentrations increase the stability of pyruvate Pi-dikinase in giant miscanthus at low temperature. Either RNA transcription of pyruvate Pi-dikinase and/or the stability of this RNA are important for the increase in pyruvate Pi-dikinase protein content and activity in giant miscanthus under chilling conditions (Wang et al. 2008).

2.9.5 C_3–C_4 Intermediates

In the beginning of the 1970s, when the C_4 pathway was unraveled, there were attempts to cross C_3 and C_4 species of *Atriplex* (saltbush). This was considered a useful approach to enhance the rate or efficiency of photosynthesis and yield of C_3 parents. The complexity of anatomy and biochemistry of the C_4 plants, however, is such, that these crosses have not produced any useful progeny (Brown and Bouton 1993). More recently, an international consortium started working toward introducing the C_4 pathway into *Oryza sativa* (rice) to increase crop yield. The goal is to identify the genes necessary to install C_4 photosynthesis through different approaches, including genomic and transcriptional sequence

comparisons and mutant screening (von Caemmerer et al. 2012). The fundamental assumption on which these efforts are based is that photosynthesis is the key limiting factor for crop yield. An increased photosynthetic capacity might simply lead to increased **feedback inhibition** (Sect. 2.4), unless the sink demand is increased proportionally.

Over 20 plant species exhibit photosynthetic traits that are intermediate between C_3 and C_4 plants (*e.g.*, species in the genera *Alternanthera*, *Flaveria*, *Neurachne*, *Moricandia*, *Panicum*, and *Parthenium*). We can consider C_3-C_4 intermediates ancestral to true C_4 species (Hylton et al. 1988; Lundgren and Christin 2017). Some of these show **reduced** rates of **photorespiration** and **CO_2-compensation points** in the range of 8–35 μmol mol^{-1}, compared with 40–50 μmol mol^{-1} in C_3 and 0–5 μmol mol^{-1} in C_4 plants (Table 2.10). They have a weakly developed Kranz anatomy, compared with the true C_4 species, but Rubisco is located both in the mesophyll and the bundle sheath cells (Brown and Bouton 1993). An important evolutionary step towards C_4 photosynthesis was an increased vein density (Lundgren et al. 2019), which first increased during the early diversification of angiosperms (Feild et al. 2011). A high density of major veins provides a greater capacity for water transport in case of xylem embolism and might confer greater drought tolerance (Sack et al. 2013). In addition, higher densities of minor veins enable rapid rates of photosynthesis and are advantageous in productive environments, such as high irradiance conditions (Brodribb et al. 2010). High vein density, therefore, allows rapid rates of photosynthesis and a lower risk of xylem embolism. However, vein density is only indirectly relevant to C_4 photosynthesis, because the absolute distance between veins is less important than the number of mesophyll cells separating consecutive vascular bundles (Hattersley and Watson 1975).

C_3–C_4 taxa tend to occur in warm climates, but the precipitation component of the C_3–C_4 niche is lineage specific, and correlates with that of closely related C_3 and C_4 taxa (Lundgren and Christin 2017). A large-scale analysis suggests that C_3–C_4 lineages converged toward warm habitats which may have facilitated the transition to C_4 photosynthesis, effectively bridging the ecological gap between C_3 and C_4 plants. The intermediates retained some precipitation aspects

Table 2.10 The number of chloroplasts and of mitochondria plus peroxisomes in bundle sheath cells compared with those in mesophyll cells (BSC/MC) and the CO_2-compensation point (Γ, μmol mol^{-1}), of C_3, C_4, and C_3-C_4 intermediates belonging to the genera *Panicum, Neurachne, Flaveria*, and *Moricandia*.

Species	Photosynthetic pathway	BSC/MC		Γ
		chloroplasts	mitochondria+ peroxisomes	
P. milioides	C_3-C_4	0.9	2.4	19
P. miliaceum	C_4	1.1	8.4	1
N. minor	C_3-C_4	3.1	20.0	4
N. munroi	C_4	0.8	4.9	1
N. tenuifolia	C_3	0.6	1.2	43
F. anomala	C_3-C_4	0.9	2.3	9
F. floridana	C_3-C_4	1.4	5.0	3
F. linearis	C_3-C_4	2.0	3.6	12
F. oppositifolia	C_3-C_4	1.4	3.6	14
F. brownii	C_4-like	4.2	7.9	2
F. trinerva	C_4	2.2	2.4	0
F. pringlei	C_3	0.5	1.0	43
M. arvensis	C_3-C_4	1.4	5.2	32
M. spinosa	C_3-C_4	1.6	6.0	25
M. foleyi	C_3	1.5	3.3	51
M. moricandioides	C_3	2.0	2.8	52

Source: Brown and Hattersley (1989)

of the habitat of their C_3 ancestors, and likely transmitted them to their C_4 descendants, contributing to the diversity among C_4 lineages seen today (Lundgren and Christin 2017).

In addition to the C_3-C_4 intermediate species, there are some species [*e.g.*, *Eleocharis vivipara* (sprouting spikerush) and *Nicotiana tabacum* (tobacco)] that are capable of either C_3 or C_4 photosynthesis in different tissues (Ueno 2001). Tobacco, a typical C_3 plant, shows characteristics of C_4 photosynthesis in cells of stems and petioles that surround the xylem and phloem; these cells are supplied with carbon for photosynthesis from the vascular system, and not from stomata. These photosynthetic cells possess high activities of enzymes characteristic of C_4 photosynthesis which allows the decarboxylation of four-carbon organic acids from the xylem and phloem, thus releasing CO_2 for photosynthesis (Hibberd and Quick 2002).

A C_4 photosynthetic pathway has ben found in the developing grains of *Triticum aestivum* (wheat) that is absent in leaves. Genes specific for C_4 photosynthesis are preferentially expressed in the photosynthetic pericarp tissue. The chloroplasts exhibit dimorphism that corresponds to chloroplasts of mesophyll- and bundle sheath-cells in leaves of classical C_4 plants (Rangan et al. 2016).

2.9.6 Evolution and Distribution of C_4 Species

C_4 species represent approximately 5% of all higher plant species, C_3 species accounting for about 85% and CAM species (Sect. 2.10) for 10%. C_4 photosynthesis first arose in grasses, near 30 million years ago (Sage 2016). However, it took several millions of years before the C_4 pathway spread on several continents and became dominant over large areas, between 8 and 6 million years ago, as indicated by changes in the carbon-isotope ratios of fossil tooth enamel in Asia, Africa, North America, and South America (Cerling et al. 1997). A decreasing **atmospheric CO_2 concentration**, as a result of the photosynthetic activity of plants and possibly much more so due to tectonic and subsequent geochemical events, has been a significant factor contributing to C_4 evolution. Briefly, the collision of the Indian subcontinent after the breakup of Gondwana caused the uplift of the Tibetan Plateau. With this, Earth crust consuming CO_2 became exposed over a vast area. The reaction $CaSiO_3 + CO_2 <--- > CaCO_3 + SiO_2$ is responsible for the dramatic decline in atmospheric CO_2 concentration (Ehleringer and Monson 1993). Since CO_2 levels were already low when the first C_4 plants evolved, other factors must have been responsible for the rapid spread of C_4 plants many millions of years after they first arose.

The universal carboxylating enzyme Rubisco does not operate efficiently at the present low CO_2 and high O_2 atmospheric conditions. Low atmospheric CO_2 concentrations would increase photorespiration and thus favor the **CO_2-concentrating mechanisms** and **lack of photorespiration** that characterize C_4 species. In at least 19 different families of widely different taxonomic groups, C_4 plants evolved from C_3 ancestors independently at least 66 times on different continents within the past 35 million years (**convergent evolution**) (Table 2.7; Sage et al. 2012).

C_4 photosynthesis originated in **arid regions** of low latitude, where **high temperatures** in combination with **drought** and/or **salinity**, due to a globally drying climate and increased **fire frequency**, promoted the spread of C_4 plants (Beerling and Osborne 2006). A major role for climatic factors as the driving force for C_4 evolution is also indicated by C_4 distributions in Mesoamerican sites that have experienced contrasting moisture variations since the last glacial maximum. Analyses of the carbon-isotope composition of leaf wax components indicate that regional climate exerts a strong control over the relative abundance of C_3 and C_4 species, and that in the absence of favorable moisture and temperature conditions a low atmospheric CO_2 concentration alone does not favor C_4 expansion (Huang et al. 2001).

Low altitudes in tropical areas continue to be centers of distribution of C_4 species. Tropical and temperate lowland grasslands, with abundant

warm-season precipitation, are dominated by C_4 species. At higher elevations in these regions, C_3 species are dominant, both in cover and in composition, for example on highland plains in a temperate arid region of Argentina (Cavagnaro 1988).

The high concentration of CO_2 at the site of Rubisco, allows net CO_2 assimilation at relatively high temperatures, where photorespiration results in low net photosynthesis of C_3 species due to the increased oxygenating activity of Rubisco. This explains why C_4 species naturally occur in warm, open ecosystems, where C_3 species are less successful (Figs 2.41 and 2.42). There is no *a priori* reason, however, why C_4 photosynthesis could not function in cooler climates. The lower

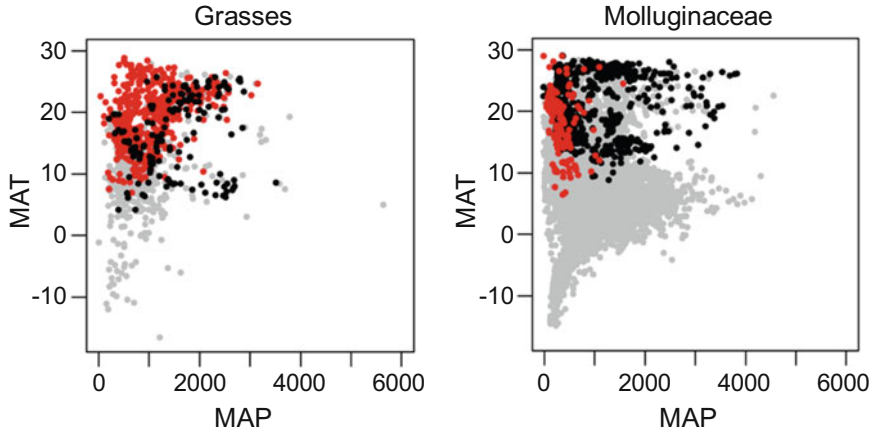

Fig. 2.41 Ecological distribution of some C_4 taxa compared to their C_3 relatives. For two distantly related groups that contain C_4 taxa (grasses and Molluginaceae), the mean annual temperature (MAT; in °C) is plotted against the mean annual precipitation (MAP; in mm $year^{-1}$). Grey points represent localities for C_3 species that belong to the sister-group of the clade with C_4 species. Localities for C_3 species that are closely related to C_4 taxa are in black, and those C4 taxa in each group are in red (Christin and Osborne 2014). With permission of the New Phytologist Trust.

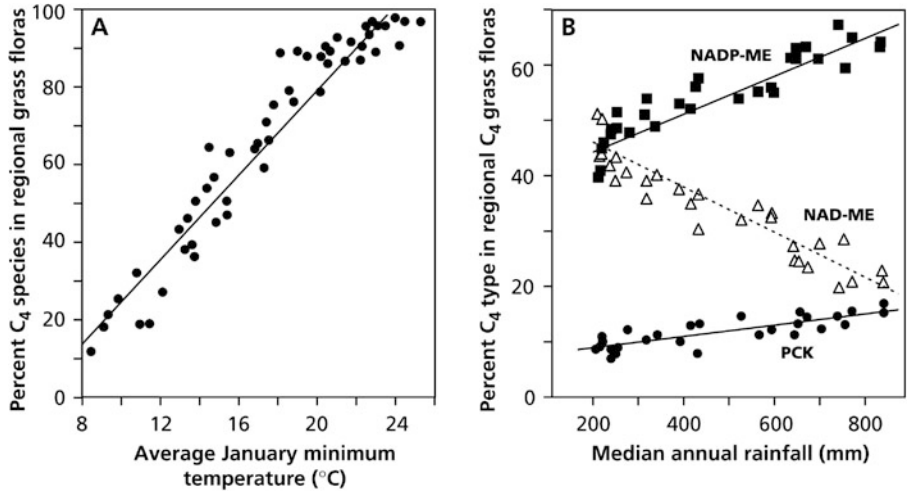

Fig. 2.42 (**A**) The percentage occurrence of C_4 metabolism in grass floras of Australia in relation to temperature in the growing season (January). (**B**) The percentage occurrence of C_4 grass species of the three metabolic types in regional floras in Australia in relation to median annual rainfall (Henderson et al. 1995).

quantum yield of C_4 species at low temperature would be important in dense canopies where light limits photosynthesis (and where **quantum yield** is therefore important). Quantum yield, however, is less important at higher levels of irradiance, and there is quite a wide temperature range where the quantum yield is still high compared with that of C_3 plants (Fig. 2.39). The high sensitivity to low temperature of pyruvate Pi-dikinase, a key enzyme in the C_4 pathway is likely the main reason why C_4 species have rarely expanded to cooler places (Sect. 2.7.2). Compatible solutes can decrease the low-temperature sensitivity of this enzyme and this could allow the expansion of C_4 species into more temperate regions in the future. Alternatively, rising atmospheric CO_2 concentration may offset the advantages of the CO_2-concentrating mechanism of C_4 photosynthesis (Sect. 2.12).

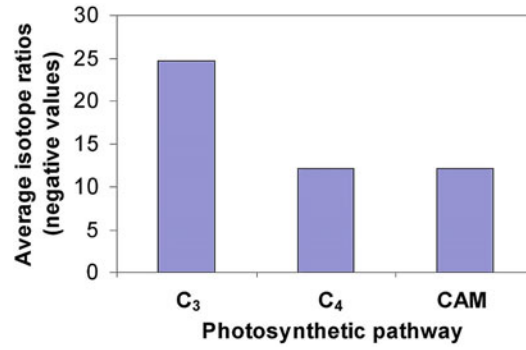

Fig. 2.43 The carbon-isotope composition of C_3, C_4, and CAM plants (Sternberg et al. 1984).

2.9.7 Carbon-Isotope Composition of C_4 Species

Although Rubisco of C_4 plants discriminates between $^{12}CO_2$ and $^{13}CO_2$, just like that of C_3 plants, the fractionation in C_4 species is considerably less than that in C_3 plants. This is explained by the small extent to which inorganic carbon **diffuses back** from the vascular bundle to the mesophyll (Sect. 2.9.2). Moreover, the inorganic carbon that does diffuse back to the mesophyll cells will be **refixed** by PEP carboxylase, which has a very high affinity for bicarbonate (Box 2.2). Most of the $^{13}CO_2$ that accumulates in the bundle sheath is ultimately assimilated; hence, the isotope fractionation of CO_2 is very small in C_4 species (Fig. 2.43).

The isotopic differences between C_3 and C_4 plants (Fig. 2.43) are large compared with isotopic changes occurring during digestion by herbivores or decomposition by soil microbes. This makes it possible to determine the relative abundance of C_3 and C_4 species in the diets of animals by analyzing tissue samples of animals ("You are what you eat") or as sources of soil organic matter in paleosols (old soils). These studies have shown that many generalist herbivores show a preference for C_3 rather than C_4 plants (Ehleringer and Monson 1993). C_3 species, however, also tend to have more toxic secondary metabolites, which cause some herbivores to show exactly the opposite preference.

2.9.8 Growth Rates of C_4 Species

Although C_4 photosynthesis has the potential to drive **faster growth rates**, experimental comparisons have surprisingly failed to show a clear difference in growth between C_3 and C_4 species. Snaydon (1991) compared the aboveground productivity data for 34 herbaceous species across 88 sites, and found no significant difference between C_3 and C_4 species when latitude was taken into account. In general, direct comparisons between C_3 and C_4 plants have failed to show consistently faster growth in C_4 species under controlled environments, natural climate conditions, or in comparisons between closely related C_3 and C_4 species (Christin and Osborne 2014). This is problematic because differential growth is a crucial element of research to increase C_3 crop productivity by introducing C_4 photosynthesis (von Caemmerer et al. 2012).

A comparison of the **relative growth rate** (*RGR*; Sect. 10.3) of 382 grass species, accounting for ecological diversity and evolutionary history, shows that plants that exhibit C_4 photosynthesis have a *RGR* that is 19–88% greater than that of C_3

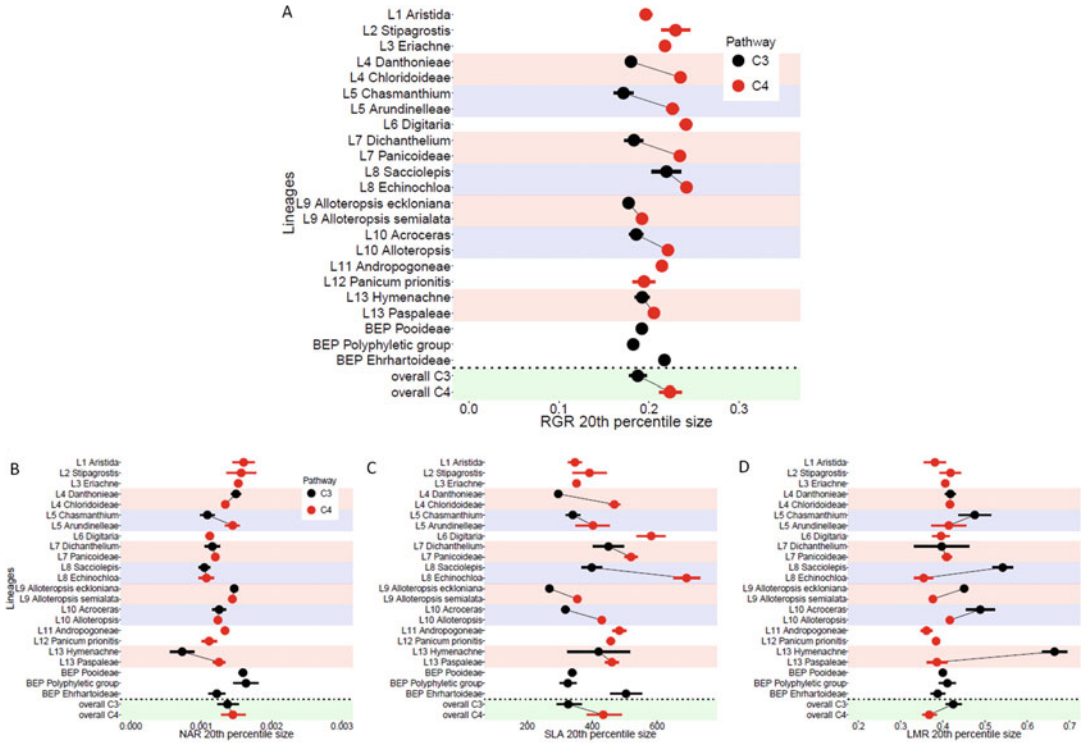

Fig. 2.44 (**A**) Relative growth rate (*RGR*) of sister C_3 (black) and C_4 (red) lineages, highlighted by colored shading and linked points. For each lineage, means and standard errors were calculated from raw data. Error bars are not visible in some cases because they are smaller than the symbol, whereas in other cases lineages are represented by a single species. The overall difference between C_3 and C_4 species calculated in a phylogenetic analysis is shown at the bottom of the panel. (**B**–**D**) Components of *RGR*. (B) Net assimilation rate (*NAR*), (**C**) specific leaf area (*SLA*) and (**D**) leaf mass ratio (*LMR*) (Atkinson et al. 2016). Copyright © 2016, Springer Nature.

plants (Fig. 2.44). However, unexpectedly, a high **leaf area ratio** (*LAR*), rather than fast growth per unit leaf area (**net assimilation rate**, *NAR*) drives this faster growth. C_4 leaves have less dense tissues (**low dry matter content**, *DMC*), allowing more leaves to be produced for the same carbon cost (Atkinson et al. 2016).

2.10 CAM Plants

2.10.1 Introduction

In addition to C_3 and C_4 species, there are many succulent plants with another photosynthetic pathway: **Crassulacean Acid Metabolism** (CAM) (Winter et al. 2015). This pathway is named after the Crassulaceae, a family in which many species show this type of metabolism. CAM, however, also occurs in Cactaceae, Euphorbiaceae, Orchidaceae, and Bromeliaceae [*e.g.*, *Ananas comosus* (pineapple)]. There are about 10,000 CAM species from 25 to 30 families (Table 2.11), all angiosperms, with the exception of a few fern species that also have CAM characteristics (Kluge and Ting 1978).

The unusual capacity of CAM plants to fix CO_2 into organic acids in the dark, causing **nocturnal acidification**, with de-acidification during the day, has been known for almost two centuries. A full appreciation of CAM as a photosynthetic process was greatly stimulated by analogies with C_4 species (Osmond et al. 1982).

The productivity of most CAM plants is low, but this is not an inherent trait of CAM species,

Table 2.11 Taxonomic survey of flowering plant families known to have species showing crassulacean acid metabolism (CAM) in different taxa.

Agavaceae = Asparagaceae	Commelinaceae	Oxalidaceae
Aizoaceae	Crassulaceae	Passifloraceae
Alismataceae	Cucurbitaceae	Piperaceae
Anacampserotaceae	Didieraceae	Plantaginaceae
Apiaceae	Euphorbiaceae	Polypodiaceae
Apocynaceae	Geraniaceae	Portulacaceae
Araceae	Gesneriaceae	Ruscaceae = Asparagaceae
Asphodelaceae = Xanthorrhoeaceae	Hydrocharitaceae	Vitaceae
Rubiaceae	Asteraceae	Isoetaceae
Vittariaceae	Bromeliaceae	Lamiaceae
Welwitschiaceae	Cactaceae	Montiaceae
Zamiaceae	Clusiaceae	Orchidaceae

Source: Medina (1996); Silvera et al. (2010)

because some cultivated CAM plants (*e.g.*, *Agave mapisaga* and *Agave salmiana*) may achieve an average aboveground productivity of 4 kg dry mass m^{-2} $year^{-1}$. An even higher productivity has been observed for irrigated, fertilized, and carefully pruned *Opuntia amyclea* and *Opuntia ficus-indica* (prickly pears): 4.6 kg m^{-2} $year^{-1}$ (Nobel et al. 1992). These are among the highest productivities reported for any species. In a comparison of two succulent species with similar growth forms, *Cotyledon orbiculata* (pig's ear) (CAM) and *Othonna opima* (C_3), during the transition from the rainy season to subsequent drought, the daily net rate of CO_2 assimilation is similar for the two species. This shows that rates of photosynthesis of CAM plants may be as high as those of C_3 plants, if morphologically similar plants adapted to the similar habitats are compared (Eller and Ferrari 1997).

As with C_4 plants, none of the enzymes or metabolic reactions of CAM are unique to these species. The reactions proceed at different times of the day, however, quite distinct from C_3 and C_4 species. Based on differences in the major decarboxylating enzyme, two subtypes of CAM species are discerned (Sect. 2.10.2). In addition, there are intermediate forms between C_3 and CAM, as well as facultative CAM plants (Sect. 2.10.4).

2.10.2 Physiological, Biochemical, and Anatomical Aspects

CAM plants are of great ecological significance, and there is increasing interest for their water-use efficiency and drought resistance (Males and Griffiths 2017). CAM plants are characterized by their **succulence** (but this is not pronounced in epiphytic CAM plants; Sect. 2.10.5), the capacity to fix CO_2 at night via **PEP carboxylase**, the accumulation of **malic acid** in the vacuole, and subsequent de-acidification during the day, when CO_2 is released from malic acid and fixed in the Calvin-Benson cycle, using Rubisco.

CAM plants show a strong fluctuation in pH of the cell sap, due to the synthesis and breakdown of malic acid (Borland and Griffiths 1997). The concentration of this acid may increase to 100 mM. By isolating vacuoles of the CAM plant *Kalanchoe daigremontiana* (devil's backbone), it was shown that at least 90% of all the acid in the cells is in the vacuole. The kinetics of malic acid efflux from the leaves of *Kalanchoe daigremontiana* provides further evidence for the predominant location of malic acid in the vacuole.

At night, CO_2 is fixed in the cytosol, catalyzed by **PEP carboxylase**, producing oxaloacetate (Fig. 2.45). PEP originates from the breakdown of glucose in glycolysis; glucose is formed from

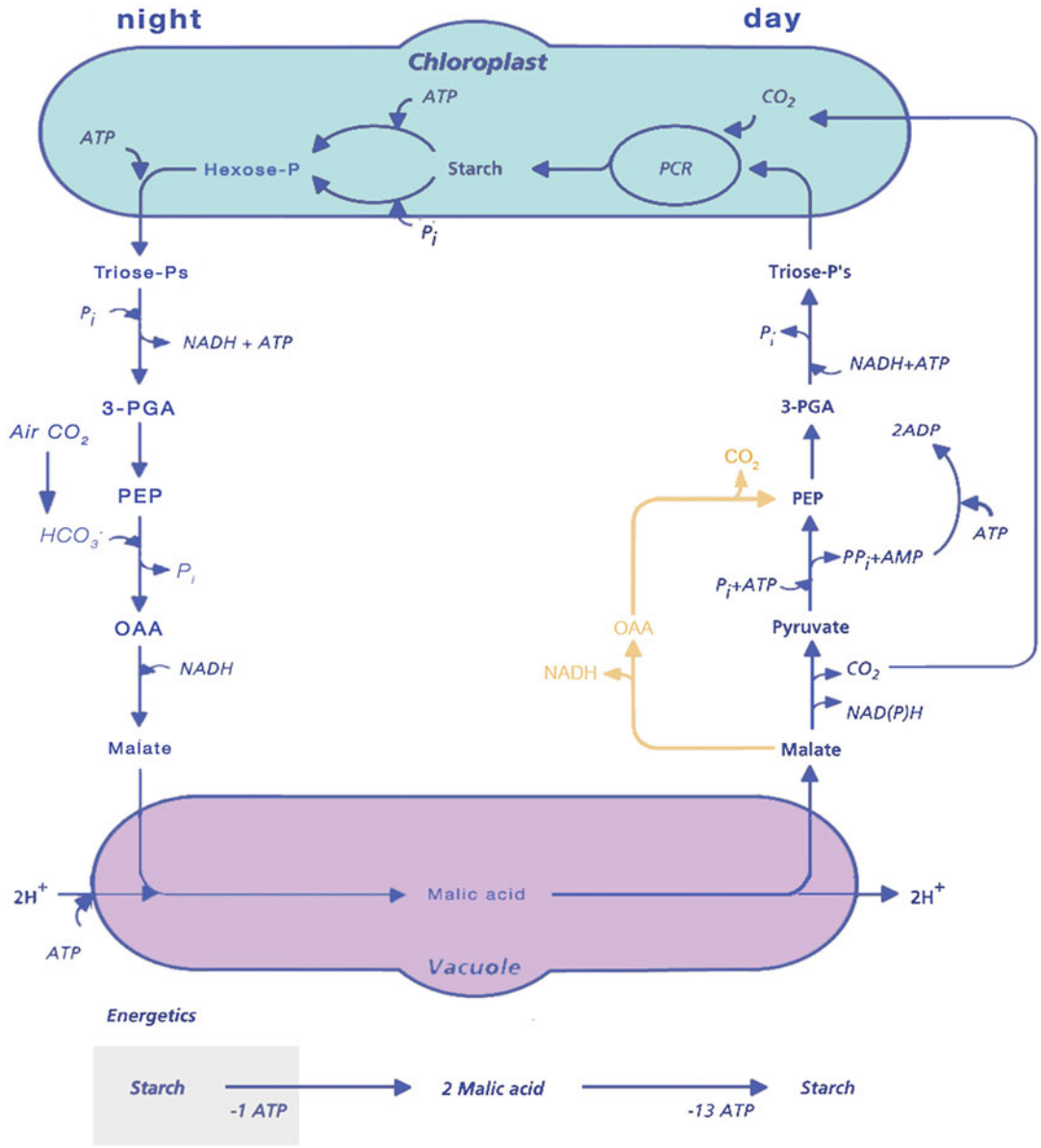

Fig. 2.45 Metabolic pathway and cellular compartmentation of Crassulacean Acid Metabolism (CAM), showing the separation in night and day of carboxylation and decarboxylation. The steps specific for PEPCK-CAM plants are depicted in red.

starch. Oxaloacetate is immediately reduced to malate, catalyzed by malate dehydrogenase. Malate is transported to the large vacuoles in an energy-dependent manner (Smith et al. 1996). A H^+-ATPase and a H^+-pyrophosphatase pump H^+ into the vacuole, so that malate can move down an electrochemical potential gradient (Sect. 9.2.2.2). In the vacuole, it will be present as malic acid.

The release of malic acid from the vacuole during the day is supposedly passive (Kluge and Ting 1978). Upon release, it is decarboxylated, catalyzed by **malic enzyme** (NAD- or NADP-dependent), or by **PEP carboxykinase** (PEPCK). Like C_4 species, CAM species are subdivided depending on the decarboxylating enzyme. The malic enzyme subtypes (ME-CAM) have a

cytosolic NADP-malic enzyme, as well as a mitochondrial NAD-malic enzyme; they use a chloroplast pyruvate Pi-dikinase to convert the C_3 fragment originating from the decarboxylation reaction into carbohydrate *via* PEP. PEPCK-type CAM plants have very low malic enzyme activities (as opposed to PEPCK-C_4 plants) and no pyruvate Pi-dikinase activity, but high activities of PEP carboxykinase.

The C_3 fragment (pyruvate or PEP) that is formed during the decarboxylation is converted into starch and **Rubisco** fixes the CO_2 that is released, like in C_3 plants. During the decarboxylation of malic acid and the fixation of CO_2 by Rubisco in the Calvin-Benson cycle, the stomata are closed. They are open during the nocturnal fixation of CO_2.

We can summarize the CAM traits as follows (Kluge and Ting 1978):

1. Fluctuation of organic acids, mainly of malic acid, during a diurnal cycle;
2. Fluctuation of the concentration of sugars and starch, opposite to the fluctuation of malic acid;
3. A high activity of PEP carboxylase (at night) and of a decarboxylase (during the day);
4. Large vacuoles in cells containing chloroplasts;
5. Some degree of succulence;
6. The CO_2 assimilation by the leaves occurs predominantly at night.

Four 'phases' in the diurnal pattern of CAM are discerned (Fig. 2.46). **Phase I**, the carboxylation phase, starts at the beginning of the night. Toward the end of the night, the rate of carboxylation declines and the malic acid concentration reaches its maximum. The stomatal conductance and the CO_2 fixation change more or less in parallel. During phase I, carbohydrates are broken down. **Phase II**, at the beginning of the day, is characterized by a high rate of CO_2 fixation, generally coinciding with an increased stomatal conductance. CO_2 fixation by PEP carboxylase and malic acid formation coincide with the fixation of CO_2 by Rubisco. Gradually, fixation by PEP carboxylase is taken over by fixation by Rubisco. In the last part of phase II, C_3 photosynthesis predominates, using exogenous CO_2 as substrate. Phase II typically occurs under

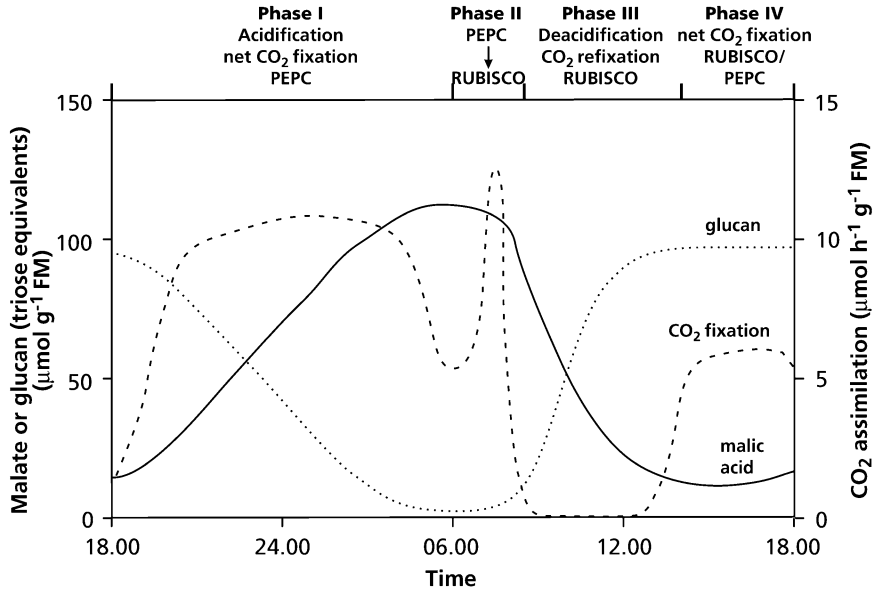

Fig. 2.46 CO_2 fixation in CAM plants, showing diurnal patterns for net CO_2 assimilation, malic acid concentration and carbohydrate concentrations (PEPC is PEP carboxylase). Four phases are distinguished, as described in Sect. 2.10.2 (after Osmond and Holtum 1981).

laboratory conditions, following an abrupt dark-to-light transition, but is not apparent under natural conditions. In **phase III** the stomata are fully closed, and malic acid is decarboxylated. The C_i may then increase to values above 10,000 μmol mol^{-1}. This is when normal C_3 photosynthesis takes place and when sugars and starch accumulate. When malic acid is depleted, the stomata open again, possibly because C_i drops to a low level (Males and Griffiths 2017); this is the beginning of **phase IV**. Gradually more exogenous and less endogenous CO_2 is being fixed by Rubisco. In this last phase, CO_2 may be fixed by PEP carboxylase again, as indicated by the photosynthetic quotient (PQ), *i.e.* the ratio of O_2 release and CO_2 uptake. Over an entire day the PQ is 1 (Table 2.12), but deviations from this value occur, depending on the carboxylation process (Fig. 2.47).

In phase III, when the stomata are fully closed, malic acid is decarboxylated, and the C_i is very high, **photorespiration** is suppressed, as indicated by the relatively slow rate of O_2 uptake (as measured using $^{18}O_2$; Fig. 2.47). In phase IV, when malic acid is depleted and the stomata open again, photorespiration does occur, as demonstrated by increased uptake of $^{18}O_2$.

How do CAM plants regulate the activity of the two carboxylating enzymes and decarboxylating enzymes in a coordinated way to avoid futile cycles? Rubisco is inactive at night for the same reason as it is in C_3 plants: this enzyme is part of the Calvin-Benson cycle that depends on the light reactions and is inactivated in the dark

Table 2.12 Cumulative daily net CO_2 and O_2 exchange in the dark and in the light periods (12 hour eacht) and the daily Photosynthetic Quotient for the entire 24 hour period of a shoot of *Ananas comosus* (pineapple)*.

	Cumulative daily net CO_2 and O_2 exchange (mmol $shoot^{-1}$]				
	Dark		Light		
	CO_2 assimilation	O_2 consumption	CO_2 assimilation	O_2 release	Daily Photosynthetic Quotient
Day 1	10.6	6.4	10.4	27.1	0.99
Day 2	11.1	6.3	10.7	27.5	0.98

Source: Coté et al. (1989)

*Photosynthetic Quotient is the ratio of the total net amount of O_2 evolved to the net CO_2 fixed in 24 hours (*i.e.* the total amount of O_2 evolved in the light period minus the total amount of O_2 consumed in the dark period) to the total amount of CO_2 fixed in the light plus dark period. Measurements were made over two consecutive days

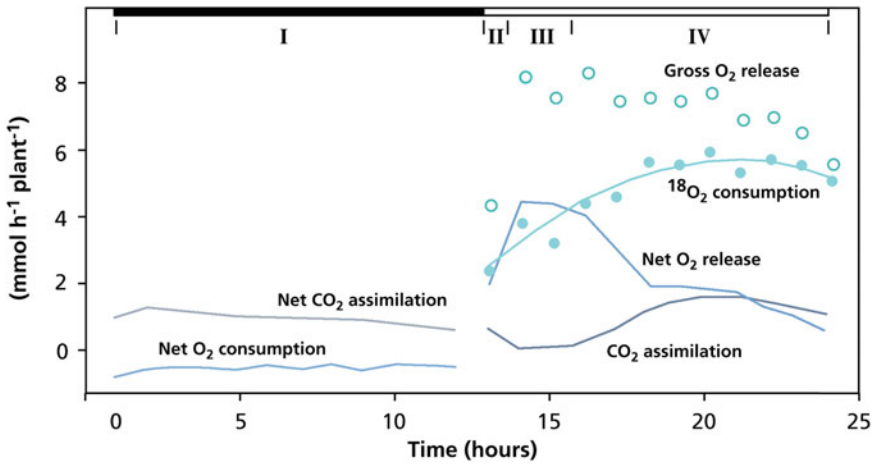

Fig. 2.47 Gas exchange of *Ananas comosus* (pineapple) during the dark and light period. O_2 consumption during the day is measured using the stable isotope $^{18}O_2$. Gross O_2 release is the sum of net O_2 production and $^{18}O_2$ consumption. The phases are the same as those shown in Fig. 2.45 (after Coté et al. 1989). Copyright American Society of Plant Biologists.

(Sect. 2.3.4.2). In addition, the kinetic properties of PEP carboxylase are modulated. In *Mesembryanthemum crystallinum* (ice plant) and in *Crassula argentea* (jade plant), PEP carboxylase occurs in two configurations: a day-configuration and a night-configuration. The night-configuration is relatively insensitive to malate (the K_i for malate is 0.06–0.9 mM, depending on pH) and has a high affinity for PEP (the K_m for PEP is 0.1–0.3 mM). The day-configuration is strongly inhibited by malate (the K_i for malate is 0.004–0.07 mM, again depending on the pH) and has a low affinity for PEP (the K_m for PEP is 0.7–1.25 mM). Therefore, when malate is rapidly exported to the vacuole at night in phase I, the carboxylation of PEP readily takes place, whereas it is suppressed during the day in phase III. The modification of the kinetic properties involves the **phosphorylation** and **de-phosphorylation** of PEP carboxylase (Nimmo et al. 2001).

Through modification of its kinetic properties, the inhibition of PEP carboxylase prevents a futile cycle of carboxylation and concomitant decarboxylation reactions (Nimmo et al. 2001). Further evidence that such a futile cycle does not occur comes from studies on the labeling with ^{13}C of the first or fourth carbon atom in malate. If a futile cycle were to occur, doubly labeled malate should appear, as fumarase in the mitochondria would randomize the label in the malate molecule. Such randomization only occurs during the acidification phase, indicating rapid exchange of the malate pools of the cytosol and the mitochondria, before malate enters the vacuole.

Next to malate, glucose 6-phosphate is also an effector of PEP carboxylase (Table 2.13). The physiological significance of this effect is that glucose 6-phosphate, which is produced from glucose, during its conversion into PEP thus stimulates the carboxylation of PEP (Kluge et al. 1981).

Temperature has exactly the opposite effect on the kinetic properties of PEP carboxylase from a CAM plant and that from a C_4 plant (Fig. 2.48; Wu and Wedding 1987). These temperature

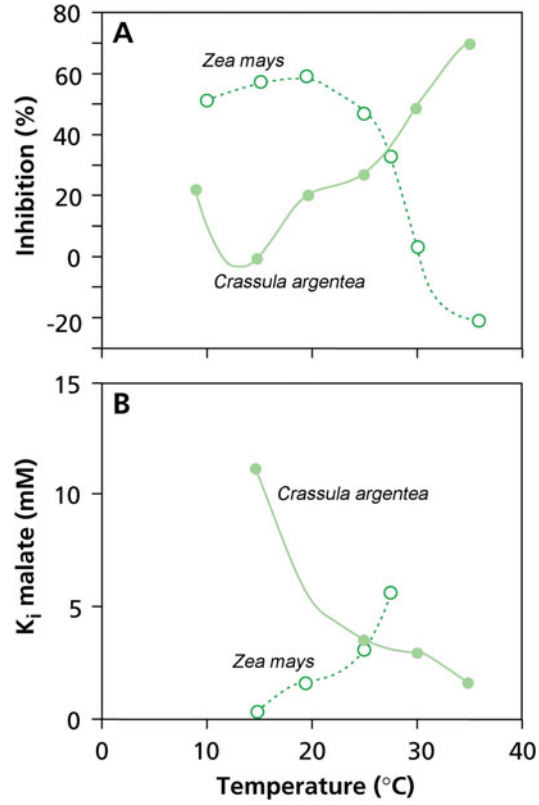

Fig. 2.48 The effect of temperature on kinetic properties of PEP carboxylase from leaves of a *Crassula argentea* (jade plant, a CAM plant) and *Zea mays* (corn, a C_4 plant). (**A**) Effect on percent inhibition by 5 mM malate. (**B**) Effect on the inhibition constant (K_i) for malate (Wu and Wedding 1987). Copyright American Society of Plant Biologists.

Table 2.13 Effects of malate and glucose-6-phosphate (G6P) on the kinetic parameters of PEP carboxylase*.

	V_{max}	Ratio	K_m	Ratio
	mmol mg^{-1} (Chl) min^{-1}		mM	
Control	0.42	1.0	0.13	1.0
+ 1 mM G6P	0.45	1.07	0.08	0.61
+ 2 mM G6P	0.47	1.12	0.05	0.39
+ 5 mM malate	0.31	0.74	0.21	1.60
+ 5 mM malate and 2 mM G6P	0.34	0.81	0.05	0.39

Source: Kluge and Ting (1978)

*The ratio gives the ratio of the values in the presence and absence of effectors

effects help to explain why a low temperature at night enhances acidification.

2.10.3 Water-Use Efficiency

Since CAM plants keep their stomata closed during the day when the vapor pressure difference (w_i - w_a) between the leaves and the surrounding air is highest, and open at night when w_i - w_a, is lowest, they have a very high **water-use efficiency** (Males and Griffiths 2017). As long as they are not severely stressed, which leads to complete closure of their stomata, the *WUE* of CAM plants tends to be considerably higher than that of both C_3 and C_4 plants (Table 5.8).

Populations of the leaf-succulent *Sedum wrightii* (Crassulaceae) differ greatly in their leaf thickness, $\delta^{13}C$ values (ranging from -13.8 to -22.9‰), the proportion of day *vs.* night CO_2 uptake, and growth. The largest plants exhibit the greatest proportion of day *vs.* night CO_2 uptake and hence the lowest *WUE*, suggesting an inverse relation between the plants' ability to conserve water and their ability to gain carbon (Kalisz and Teeri 1986).

2.10.4 Incomplete and Facultative CAM Plants

When exposed to severe desiccation, some CAM plants may not even open their stomata during the night (Bastide et al. 1993), but they may continue to show a diurnal fluctuation in malic acid concentration, as first found in *Opuntia basilaris* (prickly pear). The CO_2 they use to produce malic acid at night does not come from the air, but is derived from respiration. It is released again during the day, allowing some Rubisco activity. This metabolism is termed **CAM idling**. Fluorescence measurements have indicated that the photosystems remain intact during severe drought. CAM idling can be considered as a modification of normal CAM. *Guzmania monostachia* is an epiphytic tank bromeliad that shows such an increase in its nocturnal organic acid accumulation and a variable CAM behavior when exposed to water deficit (Pikart et al. 2018).

Some plants show a diurnal fluctuation in the concentration of malic acid without a net CO_2 uptake at night, but with normal rates of CO_2 assimilation during the day. These plants are capable of **recapturing** most of the CO_2 derived from dark respiration at night, and to use this as a substrate for PEP carboxylase. This is termed **CAM cycling** (Patel and Ting 1987). In *Peperomia camptotricha*, 50% of the CO_2 released in respiration during the night is fixed by PEP carboxylase. At the beginning of the day, some of the CO_2 that is fixed at night becomes available for photosynthesis, even when the stomatal conductance is very low. CAM cycling is typically expressed in the dry season by terrestrial and epiphytic plants of *Clusia arrudae* (Scarano et al. 2016).

In a limited number of species, CAM only occurs upon exposure to drought stress: **facultative CAM plants**. For example, in plants of *Agave deserti*, *Clusia uvitana, Mesembryanthemum crystallinum* (ice plant), and *Portulacaria afra* (elephant's foot), irrigation with saline water or drought can change from a virtually normal C_3 photosynthesis to the CAM mode (Fig. 2.49; Winter et al. 1992). We know of one genus containing C_4 species that can shift from a normal C_4 mode under irrigated conditions, to a CAM mode under water stress: *Portulaca grandiflora* (moss rose), *Portulaca mundula* (hairy purslane), and *Portulaca oleracea* (common purslane) (Koch and Kennedy 1982; Mazen 2000). The transition from the C_3 or C_4 to the CAM mode coincides with an enhanced PEP carboxylase activity and of the mRNA encoding this enzyme. Upon removal of NaCl from the root environment of *Mesembryanthemum crystallinum* (ice plant), the level of mRNA encoding PEP carboxylase declines in 2–3 hours by 77%. The amount of the PEP carboxylase enzyme itself declines more slowly: after 2–3 days the activity is half its original level (Vernon et al. 1988). *Mesembryanthemum crystallinum* has a competitive

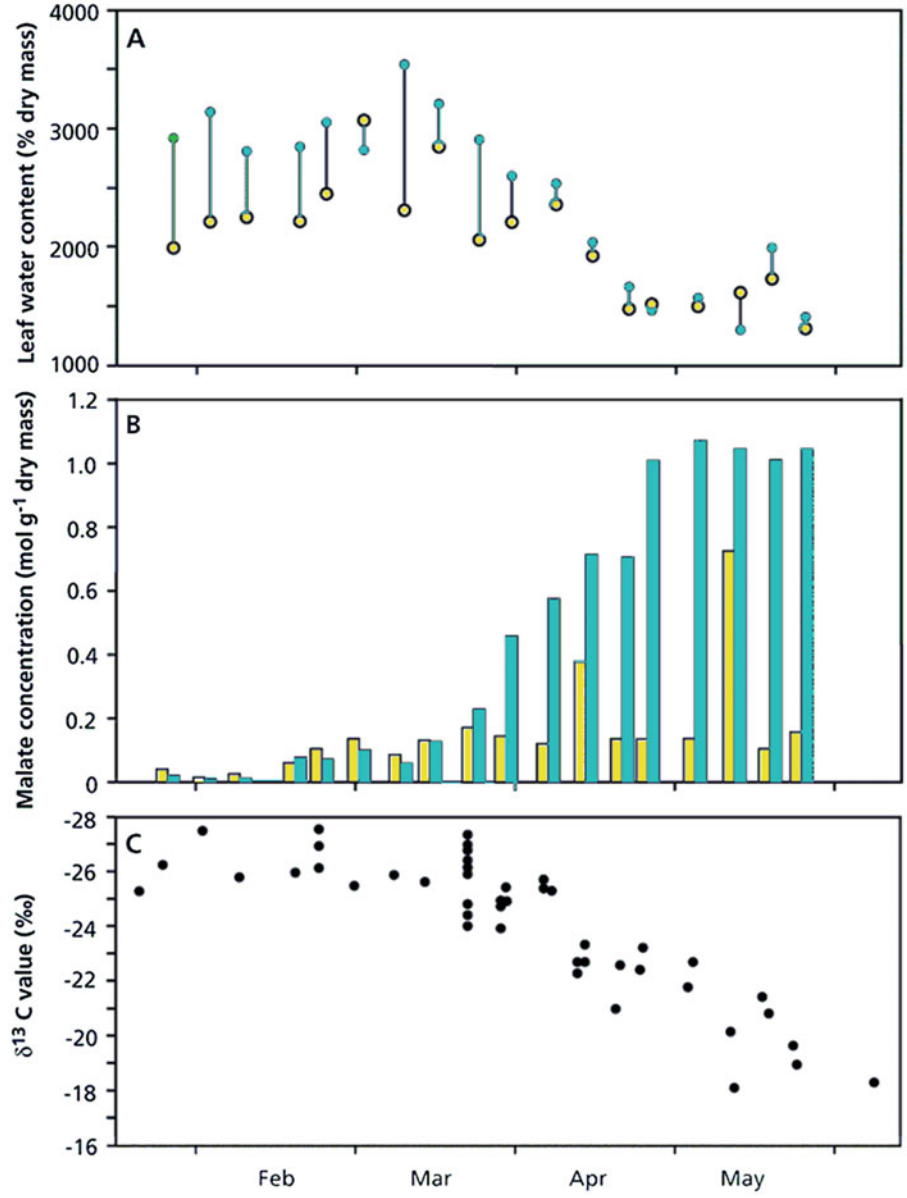

Fig. 2.49 Induction of CAM in the facultative CAM species *Mesembryanthemum crystallinum* (ice plant), growing in its natural habitat on rocky coastal cliffs of the Mediterranean Sea. Upon prolonged exposure to drought, the leaf water content (**A**) declines, and the nocturnal malate concentration (**B**) increases (yellow symbols and bars, day; turquoise symbols and bars, night). There is a shift from the C_3 mode to CAM, coinciding with less carbon-isotope fractionation (**C**) (Osmond et al. 1982).

advantage over the C_3 grass *Bromus mollis* (syn. *Bromus hordeaceus*, soft brome) in drought and saline conditions, while soft brome exerts strong competitive effects on ice plant when the water availability is favorable (Yu et al. 2017).

2.10.5 Distribution and Habitat of CAM Species

CAM is undoubtedly an adaptation to drought, since CAM plants close their stomata during most of the day. This is illustrated in a survey of epiphytic bromeliads in Trinidad (Fig. 2.50). There are two major ecological groupings of CAM plants: **succulents** from arid and semiarid regions and **epiphytes** from tropical and subtropical regions (Earnshaw et al. 1987; Ehleringer and Monson 1993). In addition, there are some submerged aquatic plants exhibiting CAM (Sect. 2.11.5). Although CAM plants are uncommon in cold environments, this may reflect their evolutionary origin in warm climates, rather than a temperature sensitivity of the CAM pathway (Nobel and Hartsock 1990). Roots of some leafless orchids may also show CAM (Winter et al. 1985).

In alpine habitats worldwide, CAM plants, or species showing incomplete or facultative CAM, *e.g.*, *Sempervivum* species occur on shallow rocky soils with low water availability (Osmond et al. 1975). Likewise, in temperate regions *Agave tequilana* shows appreciable daily net CO_2 uptake when the soil water content was relatively low, indicating that this CAM plant can sequester carbon even during prolonged dry periods (Pimienta-Barrios et al. 2001).

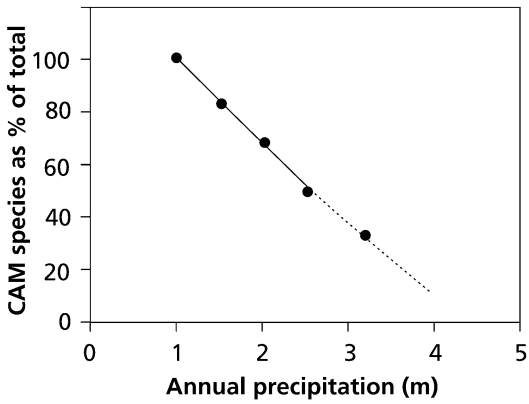

Fig. 2.50 The relationship between percentage of epiphytic bromeliad species with CAM in a tropical forest and mean annual rainfall across the north-south precipitation gradient in Trinidad (Winter and Smith 1996).

2.10.6 Carbon-Isotope Composition of CAM Species

Like Rubisco from C_3 and C_4 plants, the enzyme from CAM plants discriminate against $^{13}CO_2$, but, the fractionation at the leaf level is considerably less than that of C_3 plants and similar to that of C_4 species (Fig. 2.44). This is expected, as the stomata are closed during malate decarboxylation and fixation of CO_2 by Rubisco. Hence, only a small amount of CO_2 diffuses back from the leaves to the atmosphere, and Rubisco processes the accumulated $^{13}CO_2$ (Sects 2.9.3 and 2.9.4).

Upon a shift from C_3 to CAM photosynthesis in **facultative CAM plants**, the stomata are closed during most of the day and open at night, and the **carbon-isotope fractionation** decreases (Fig. 2.49). Hence, the carbon-isotope composition of CAM plants can be used as an estimate of the employment of the CAM pathway during past growth.

2.11 Specialized Mechanisms Associated with Photosynthetic Carbon Acquisition in Aquatic Plants

2.11.1 Introduction

Contrary to the situation in terrestrial plants, in submerged aquatic plants chloroplasts are frequently located in the **epidermis**. In terrestrial plants, CO_2 diffuses from the air through the stomata to the mesophyll cells. In aquatic plants, where diffusion is directly through the outer epidermal cell walls, the rate of this process is often limiting for photosynthesis. A thick boundary layer around the leaves, and slow diffusion of CO_2 in water limit the rate of CO_2 uptake. How do aquatic plants cope with these problems? To achieve a reasonable rate of photosynthesis and avoid excessive photorespiration, special mechanisms are required to allow sufficient diffusion of CO_2 to match the requirement for photosynthesis. Several specialized mechanisms have evolved in different species adapted to specific

environmental conditions. Another feature of the habitat of many submerged aquatics is the low irradiance. Leaves of many aquatics have the traits typical of shade leaves (Sect. 2.3.2).

2.11.2 The CO_2 Supply in Water

In fresh water, molecular CO_2 is readily available. Between 10 and 20 °C, the partitioning coefficient (that is, the ratio between the molar concentration of CO_2 in air and that in water) is about 1. The equilibrium concentration in water at an atmospheric CO_2 concentration of 412 μmol mol^{-1} is 14 μM (at 25 °C, but rapidly decreasing with increasing temperature). Under these conditions, leaves of submerged aquatic macrophytes experience about the same CO_2 concentration as those in air. The **diffusion** of dissolved gasses in water, however, is approximately 10^4 times slower than that in air, leading to rapid depletion of CO_2 inside the leaf during CO_2 assimilation. In addition, the O_2 concentration inside photosynthesizing leaves may increase. Decreasing CO_2 concentrations, especially in combination with increasing O_2, lead to conditions that restrict the **carboxylating** activity and favor the **oxygenating** activity of Rubisco (Mommer et al. 2005).

The transport of CO_2 through the unstirred **boundary layer** is only by diffusion. The thickness of the boundary layer is proportional to the square root of the leaf dimension, measured in the direction of the streaming water, and inversely proportional to the flow of the streaming water (Sect. 6.2.4). It ranges from 100 μm in well-stirred media, to 500 μm in nonstirred media. The slow diffusion in the boundary layer is often a major factor limiting photosynthesis of aquatic macrophytes.

CO_2 dissolved in water interacts as follows:

$$\begin{aligned} H_2O + CO_2 &\Leftrightarrow H_2CO_3 \\ &\Leftrightarrow H^+ + HCO_3^- \\ &\Leftrightarrow 2H^+ + CO_3^{2-} \end{aligned} \qquad (2.41)$$

$$HCO_3^- \Leftrightarrow OH^- + CO_2 \qquad (2.42)$$

Since the concentration of H_2CO_3 is very low in comparison with that of CO_2, the two are commonly combined and indicated as $[CO_2]$.

The interconversion between CO_2 and HCO_3^- is slow, at least in the absence of **carbonic anhydrase**. The presence of the dissolved inorganic carbon compounds strongly depends on the pH of the water (Fig. 2.51). In ocean water, as pH increases from 7.4 to 8.3, the contribution of dissolved inorganic carbon species shifts as follows: CO_2 as a fraction of the total inorganic carbon pool decreases from 4 to 1%, that of HCO_3^- from 96 to 89%, and that of CO_3^{2-} increases from 0.2 to 11%.

During darkness, the CO_2 concentration in ponds and streams is generally high, exceeding the concentration that is in equilibrium with air, due to respiration of aquatic organisms and the slow exchange of CO_2 between water and the air above it (Maberly 1996). The high CO_2 concentration coincides with a relatively low pH. During

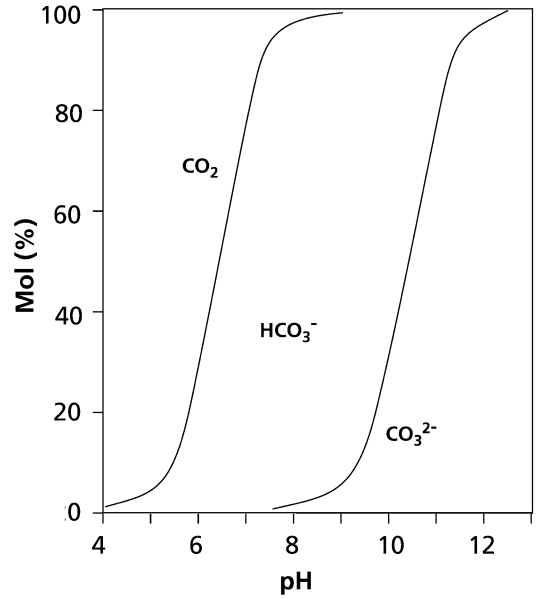

Fig. 2.51 The contribution of the different inorganic carbon species as dependent on the pH of the water (Osmond et al. 1982).

the day, the CO_2 concentration may decline rapidly due to photosynthetic activity, and the pH rises accordingly. The rise in pH, especially in the boundary layer, represents a crucial problem for CO_2 availability in water at a neutral pH. While the concentration of all dissolved inorganic carbon (*i.e.* CO_2, HCO_3^-, and CO_3^{2-}) may decline by a few percent only, the CO_2 concentration declines much more, since the high pH shifts the equilibrium from CO_2 to HCO_3^- (Fig. 2.51). This adds to the diffusion problem, and further aggravates the limitation by supply of inorganic carbon for assimilation in submerged leaves that only use CO_2 and not HCO_3^- (Klavsen et al. 2011).

2.11.3 The Use of Bicarbonate by Aquatic Macrophytes

Many aquatic macrophytes, cyanobacteria, and algae can use HCO_3^-, in addition to CO_2, as a carbon source for photosynthesis (Maberly and Madsen 2002). This might be achieved by **active uptake** of HCO_3^- itself, or by **proton extrusion**, commonly at the abaxial side of the leaf, thus lowering the pH in the extracellular space and boundary layer shifting the equilibrium towards CO_2 (Elzenga and Prins 1988). In some species [*e.g.*, *Elodea canadensis* (common waterweed)] the conversion of HCO_3^- into CO_2 is also catalyzed by an extracellular **carbonic anhydrase**. In *Ranunculus penicillatus* spp. *pseudofluitans* (a stream water crowfoot), the enzyme is closely associated with the epidermal cell wall (Newman and Raven 1993). Active uptake of HCO_3^- also requires proton extrusion, to provide a driving force.

Aquatic plants that use HCO_3^- in addition to CO_2 have a mechanism to concentrate CO_2 in their chloroplasts. Although this **CO_2-concentrating mechanism** differs from that of C_4 plants (Sect. 2.9.2), its effect is similar: it suppresses the oxygenating activity of Rubisco and lowers the CO_2-compensation point. In *Elodea canadensis* (common waterweed), *Potamogeton lucens* (shining pondweed), and other aquatic macrophytes, the capacity to acidify the abaxial side of the leaves, and thus to use HCO_3^-, is expressed most at high irradiance and low dissolved inorganic carbon concentration in the water (Elzenga and Prins 1989). The capacity of the carbon-concentrating mechanism also depends on the N supply: the higher the supply, the greater the capacity of the photosynthetic apparatus as well as that of the carbon-concentrating mechanism (Madsen and Baattrup-Pedersen 1995). Acidification of the lower side of the leaves is accompanied by an increase in extracellular pH at the adaxial side of the leaves. The leaves become 'polar' when the carbon supply from the water is less than the CO_2-assimilating capacity (Prins and Elzenga 1989). There are also anatomical differences between the adaxial and abaxial side of polar leaves: the abaxial epidermal cells are often **transfer cells**, characterized by ingrowths of cell-wall material which increases the surface area of the plasma membrane. They contain numerous mitochondria and chloroplasts. At the adaxial side of the leaves, the pH increase leads to precipitation of calcium carbonates (Fig. 2.52).

Fig. 2.52 Biogenic $CaCO_3$ precipitation on the adaxial surface of the leaves of *Cryptocoryne crispatula* (Araceae). Photo: Ole Pedersen.

This process plays a major role in the geological sedimentation of calcium carbonate (Sect. 2.11.7).

Due to the use of HCO_3^-, the internal CO_2 concentration may become much higher than it is in terrestrial C_3 plants. This implies that they do not need a Rubisco enzyme with a high affinity for CO_2. Interestingly, just like C_4 plants (Sect. 2.9.4), they have a Rubisco with a relatively high K_m for CO_2. The values are approximately twice as high as those of terrestrial C_3 plants (Yeoh et al. 1981). This high K_m is associated with a high maximum catalytic activity (k_{cat}) of Rubisco, as in the HCO_3^--using green alga, *Chlamydomonas reinhardtii*, and in C_4 species. For the Rubisco of the cyanobacterium *Synechococcus* that also has a carbon-concentrating mechanism, even higher $K_m(CO_2)$ and k_{cat} values are reported. (Table 2.9).

Hydrilla verticillata (water thyme) has an inducible CO_2-concentrating mechanism, even when the pH of the medium is so low that there is no HCO_3^- available. This monocotyledonous species predates modern terrestrial C_4 monocots and may represent an ancient form of C_4 photosynthesis (Magnin et al. 1997). The species has an inducible single-cell C_4-type photosynthetic cycle (Table 2.7; Sect. 2.9.5). This mechanism is induced at high temperatures and when the plants are growing in water that contains low concentrations of dissolved inorganic carbon (Reiskind et al. 1997). There appears to be a clear ecological benefit to this CO_2-concentrating mechanism when the canopy becomes dense, the dissolved O_2 concentration is high, and the CO_2 supply is low. Under these conditions, photorespiration decreases photosynthesis of a C_3-type plant by at least 35%, whereas in *Hydrilla verticillata* this decrease is only about 4% (Bowes and Salvucci 1989).

2.11.4 The Use of CO_2 from the Sediment

Macrophytes like water lilies that have an internal ventilation system assimilate CO_2 arriving from the roots due to pressurized flow (Sect. 3.4.1.4). The use of CO_2 from the sediment is only minor for most emergent wetland species such as *Scirpus lacustris* (bull rush) and *Cyperus papyrus* (papyrus), where it approximates 0.25% of the total CO_2 uptake in photosynthesis (Farmer 1996). *Stylites andicola* is a vascular land plant without stomata that derives nearly all its carbon through its roots (Keeley et al. 1984).

Submerged macrophytes of the isoetid life form receive a very large portion of their carbon for photosynthesis directly from the sediment via their roots: 60–100% (Table 2.14). This capability is considered an adaptation to growth in low-pH, carbon-poor (soft-water) lakes, where

Table 2.14 Assimilation of $^{14}CO_2$ derived from the air or from the rhizosphere by leaves and roots of *Littorella uniflora* (quillwort)*.

	$^{14}CO_2$ assimilation [μg C g^{-1} (leaf or root DM) h^{-1}]			
	Leaves		Roots	
Source:	Air	Rhizosphere	Air	Rhizosphere
CO_2 concentration around the roots (mM)				
0.1	300	340	10	60
	(10)	(50)	(0.3)	(70)
0.5	350	1330	10	170
	(5)	(120)	(0.3)	(140)
2.5	370	8340	10	570
	(4)	(1430)	(0.3)	(300)

Source: Nielsen et al. (1991)

*$^{14}CO_2$ was added to the air around the leaves or to the water around the roots (rhizosphere). Measurements were made in the light and in the dark; values of the dark measurements are given in brackets

these plants are common. *Lobelia dortmanna* (water lobelia), *Lilaeopsis macloviana* (Argentinian grass plant), *Ludwigia repens* (creeping primrose-willow), *Vallisneria americana* (water-celery), and *Hydrocotyle verticillata* (whorled pennywort) support their photosynthesis supplied by uptake of CO_2 from the sediment (Winkel and Borum 2009). In aquatic rosette plants, CO_2 diffuses from the sediment, via the lacunal air system to the submerged leaves. These leaves are thick with thick cuticles, have no functional stomata when growing submerged, but large air spaces inside, so that gas exchange with the atmosphere is hampered, but internal exchange is facilitated. Emergent leaves have very few stomata at the leaf base, and normal densities at the leaf tips (Fig. 2.52). The chloroplasts in leaves of isoetids (small rosette species) are concentrated around the lacunal system. The air spaces in the leaves are connected with those in stems and roots, thus facilitating the transport of CO_2 from the sediment to the leaves where it is assimilated. During the dark period, for *Lobelia dortmanna* (water lobelia, C_3), the leaf tissue CO_2 partial pressure (pCO_2) increases to 3.5 kPa, whereas for *Littorella uniflora* (quillwort, CAM) the pCO_2 is mostly below 0.05 kPa, because of CO_2 assimilation into malate (Pedersen et al. 2018). Upon darkness, the CAM plant shows an initial peak in pCO_2 (approx. 0.16 kPa) which then declines for several hours and then pCO_2 increases toward the end of the dark period. Upon illumination, leaf pCO_2 declines and pO_2 increases in both species.

2.11.5 Crassulacean Acid Metabolism (CAM) in Aquatic Plants

Though aquatic plants by no means face the same problems connected with water shortage as desert plants, some of them [for example, *Isoetes* (quillwort) species] have a similar photosynthetic metabolism: Crassulacean Acid Metabolism (CAM) (Keeley and Busch 1984; Klavsen et al. 2011). A CAM pathway has also been discovered in other genera of aquatic vascular plants (Maberly and Madsen 2002). They accumulate **malic acid** during the night, and have rates of CO_2 fixation during the night that are similar in magnitude as those during the day, when the CO_2 supply from the water is very low (Fig. 2.53). The aerial leaves of *Isoetes howellii*, in contrast to the submerged leaves of the same plants, do not show a diurnal fluctuation in the concentration of malic acid.

Why would an aquatic plant have a similar photosynthetic pathway as is common in species from arid habitats? CAM in *Isoetes* is considered an adaptation to very low levels of CO_2 in the water, especially during the day (Fig. 2.53; Keeley and Busch 1984), and allows the plants to assimilate additional CO_2 at night. This nocturnal CO_2 fixation gives them access to a carbon source that is unavailable to other species. Though some of the carbon fixed in malic acid comes from the surrounding water, where it accumulates due to the respiration of aquatic organisms, some is also derived from the plant's own respiration during the night.

2.11.6 Carbon-Isotope Composition of Aquatic Plants

There is a wide variation in carbon-isotope composition among aquatic plant species, as well as a large difference between aquatic and terrestrial plants (Fig. 2.54). A low carbon-isotope fractionation might reflect the employment of the C_4 pathway of photosynthesis, although the typical Kranz anatomy is usually lacking. Only about a dozen aquatic C_4 species have been identified, and very few have submersed leaves with a well-developed Kranz anatomy (Bowes et al. 2002). A low carbon-isotope fractionation in aquatic plants might also reflect the CAM pathway of photosynthesis. *Ottelia alismoides* (duck lettuce) is a constitutive C_4 plant and uses bicarbonate; it exhibits facultative CAM at low CO_2 availability (Shao et al. 2017). Its ratio of PEPC to Rubisco (>5) is in the range of that of typical C_4 plants. Isoetids often have rather negative $\delta^{13}C$ values, due to the isotope composition of the substrate (Table 2.15). Four factors account for

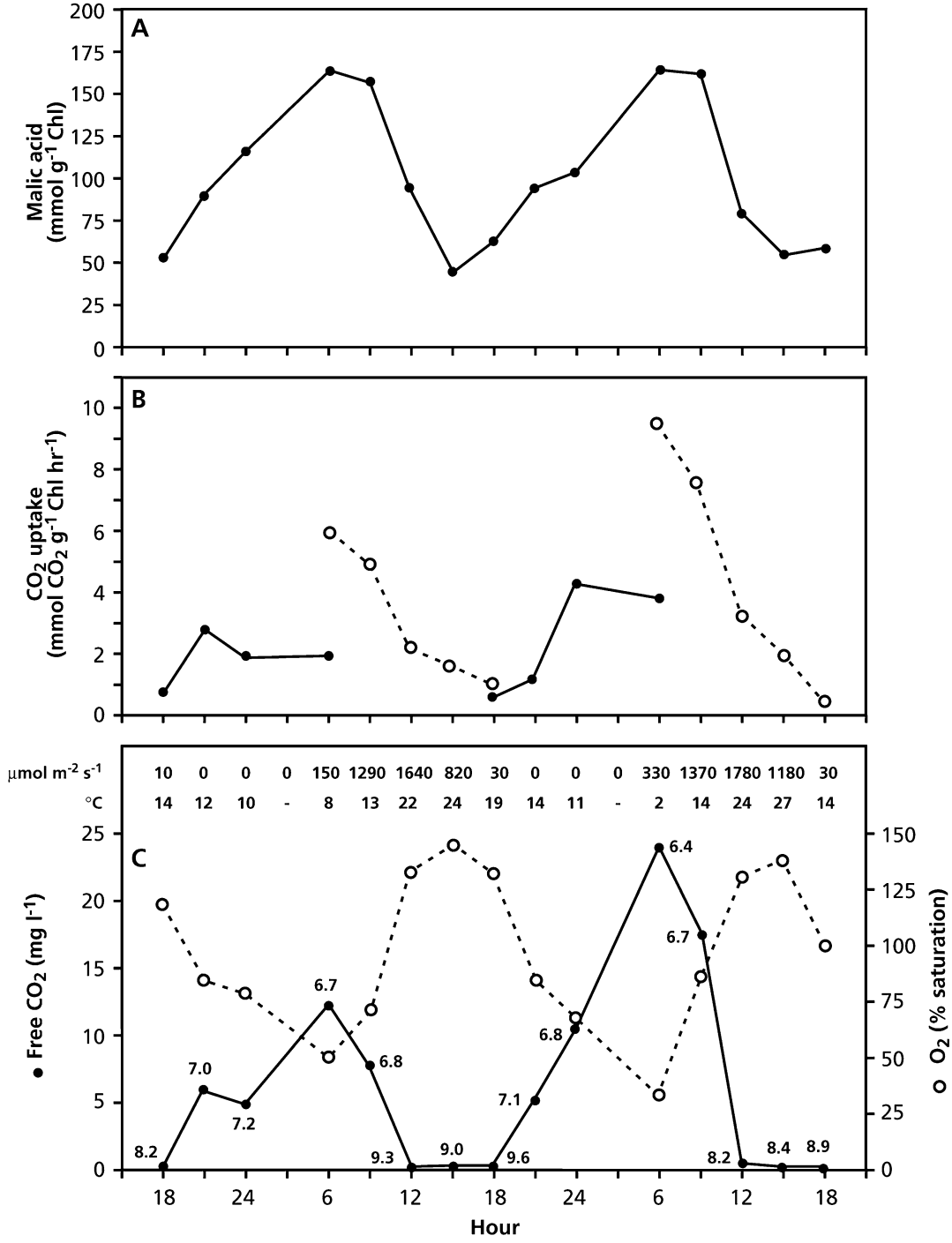

Fig. 2.53 CAM photosynthesis in submerged leaves of *Isoetes howellii* (quillwort) in a pool. (**A**) Malic acid levels, (**B**) rates of CO_2 uptake, and (**C**) irradiance at the water surface, water temperatures, and concentrations of CO_2 and O_2; the numbers near the symbols give the pH values. Open and filled symbols refer to the light and dark period, respectively (after Keeley and Busch 1984). Copyright American Society of Plant Biologists.

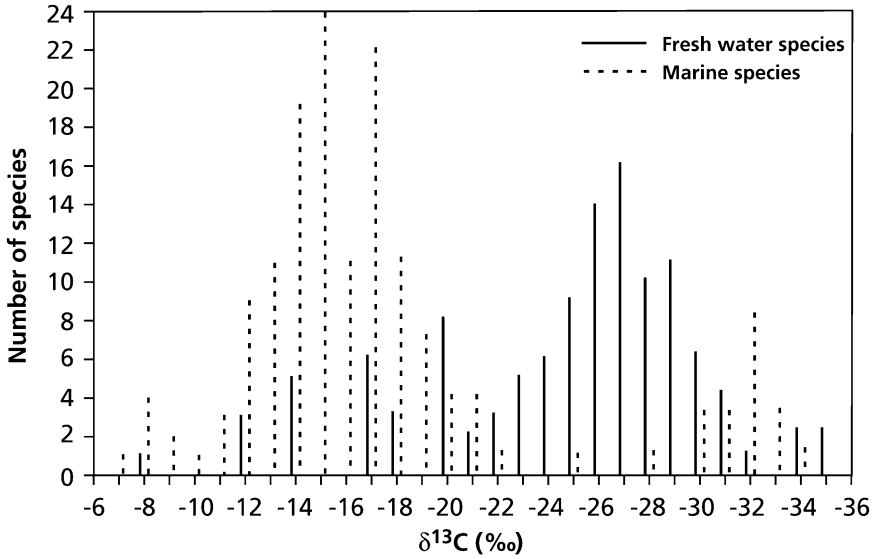

Fig. 2.54 Variation in the carbon-isotope composition ($\delta^{13}C$) of freshwater and marine aquatic species. The observed variation is due to variation in $\delta^{13}C$ values of the substrate and in the extent of diffusional limitation (Osmond et al. 1982).

Table 2.15 Carbon-isotope composition ($\delta^{13}C$ in ‰) of submerged and emergent *Isoetes howellii* plants*.

Pondwater carbonate	−15.5 to −18.6
Submerged	
Leaves	−27.9 to −29.4
Roots	−25.8 to −28.8
Emergent	
Leaves	−29.4 to −30.1
Roots	−29.0 to −29.8

Source: Keeley and Busch (1984)
*Values are given for both leaves and roots, as well as for the pond-water carbonate

the observed variation in isotope composition of freshwater aquatics (Keeley and Sandquist 1992):

1. The isotope composition of the carbon source varies substantially, ranging from a $\delta^{13}C$ value of +1‰, for HCO_3^- derived from limestone, to -30‰, for CO_2 derived from respiration. The average $\delta^{13}C$ value of CO_2 in air is -8‰. The isotope composition also changes with the water depth (Osmond et al. 1982).
2. The species of inorganic carbon fixed by the plant; HCO_3^- has a $\delta^{13}C$ that is 7 to 11‰ less negative than that of CO_2.
3. Resistance for diffusion across the unstirred boundary layer is generally important (except in rapidly streaming water), thus decreasing carbon-isotope fractionation (Box 2.2).
4. The photosynthetic pathway (C_3, C_4, and CAM) that represent different degrees of fractionation.

The isotope composition of plant carbon is dominated by that of the source (see 1 and 2 above), because diffusional barriers are strong (see 3). This accounts for most of the variation as described in Fig. 2.54, rather than biochemical differences in the photosynthetic pathway (Osmond et al. 1982).

2.11.7 The Role of Aquatic Plants in Carbonate Sedimentation

The capacity of photosynthetic organisms [*e.g.*, *Chara* (musk-grass), *Potamogeton* (pondweed), and *Elodea* (waterweed)] to acidify part of the apoplast and use HCO_3^- (Sect. 2.11.3) plays a major role in the formation of calcium

precipitates in fresh water, on both an annual and a geological time scale (Sand-Jensen et al. 2018). Many calcium-rich lake sediments contain plant-induced carbonates, according to:

$$Ca^{2+} + 2HCO_3^- \rightarrow CO_2 + CaCO_3 \qquad (2.43)$$

This reaction occurs in the alkaline compartment that is provided at the upper side of the polar leaves of aquatic macrophytes (Sect. 2.11.3). Similar amounts of carbon are assimilated in photosynthesis and precipitated as carbonate. If only part of the CO_2 released in this process is assimilated by the macrophyte, as may occur under nutrient-deficient conditions, CO_2 is released to the atmosphere. On the other hand, if the alkalinity of the compartment is relatively low, there is a net transfer of atmospheric CO_2 to the water (McConnaughey et al. 1994).

Equation 2.43 shows how aquatic photosynthetic organisms play a major role in the global carbon cycle, even on a geological time scale. On the other hand, rising atmospheric CO_2 concentrations have an acidifying effect and dissolve part of the calcium carbonate precipitates in sediments, and thus contribute to a further rise in atmospheric [CO_2] (Sect. 2.12).

2.12 Effects of the Rising CO_2 Concentration in the Atmosphere

Vast amounts of carbon are present in carbonates in the Earth's crust. Also stored in the Earth's crust is another major carbon pool: the organic carbon derived from past photosynthesis. This is a key factor in the development of the present low CO_2 / high O_2 atmosphere. Some CO_2 enters the atmosphere when carbonates are used for making cement, but apart from that, carbonates are only biologically important on a geological time scale. Far more important for the carbon balance of the atmosphere is the burning of fossil fuels (coal, oil, and natural gas) that represent a CO_2 input into the atmosphere of 9.9×10^{15} g of carbon per year in 2016 (10^{15} g equals 1 petagram, Pg) (Le Quéré et al. 2017). Changes in land-use contributed a further 1.3 Pg of carbon per year in 2016. Compared with the total amount of carbon present in the atmosphere, 780 Pg (Houghton 2007), such inputs are substantial and inevitably affect the CO_2 concentration in the Earth's atmosphere (Le Quéré et al. 2017). CO_2 is, by far, the largest contributor to the anthropogenically enhanced **greenhouse effect** (Houghton 2007).

Since the beginning of the industrial revolution in the late eighteenth century, the atmospheric CO_2 concentration has increased from about 290 μmol mol^{-1} to the current level of over 400 μmol mol^{-1} (Le Quéré et al. 2017). The concentration continues to rise by about 1.5 μmol mol^{-1} per year (Fig. 2.55). Measurements of CO_2 concentrations in **ice cores** indicate a pre-industrial value of about 280 μmol mol^{-1} during the past 10,000 years, and about 205 μmol mol^{-1} some 20,000 years ago during the last ice age. Considerable quantities of CO_2 have also been released into the atmosphere as a result of **deforestation**, **ploughing of prairies, drainage of peats**, and other land-use changes that cause oxidation of organic compounds in soil and, to a lesser extent, biomass. **Combustion of fossil fuel** adds far greater amounts of carbon per year (Fig. 2.56). Combined anthropogenic fluxes to the atmosphere amount to 11.2 Pg of carbon in 2016 (Le Quéré et al. 2017). Yet, the increase in the atmosphere is only 6 Pg of carbon per year (2016). About 2.6 Pg of the 'missing' carbon is taken up in the oceans and a similar amount (2.7 Pg) is fixed by terrestrial ecosystems (Le Quéré et al. 2017). Analysis of atmospheric CO_2 concentrations and its isotopic composition shows that north-temperate and boreal forests are the most likely sinks for the missing carbon. There is also strong uptake by tropical forests, but this is offset by CO_2 release from deforestation in the tropics. This increased terrestrial uptake of CO_2 has many causes, including stimulation of photosynthesis by elevated [CO_2] (about half of the increased terrestrial uptake) or by N deposition in N-limited ecosystems and regrowth of northern and mid-latitude forests (Houghton 2007).

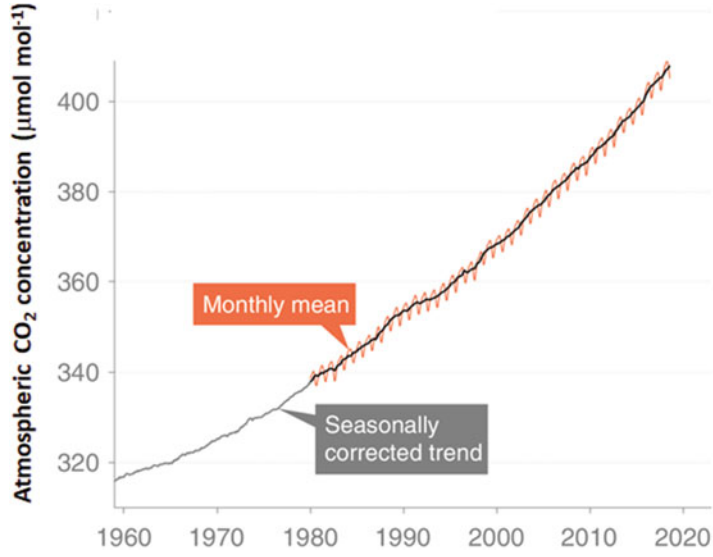

Fig. 2.55 Surface average atmospheric CO_2 concentration (ppm = µmol mol^{-1}) (Le Quéré et al. 2018). Reproduced with the author's permission.

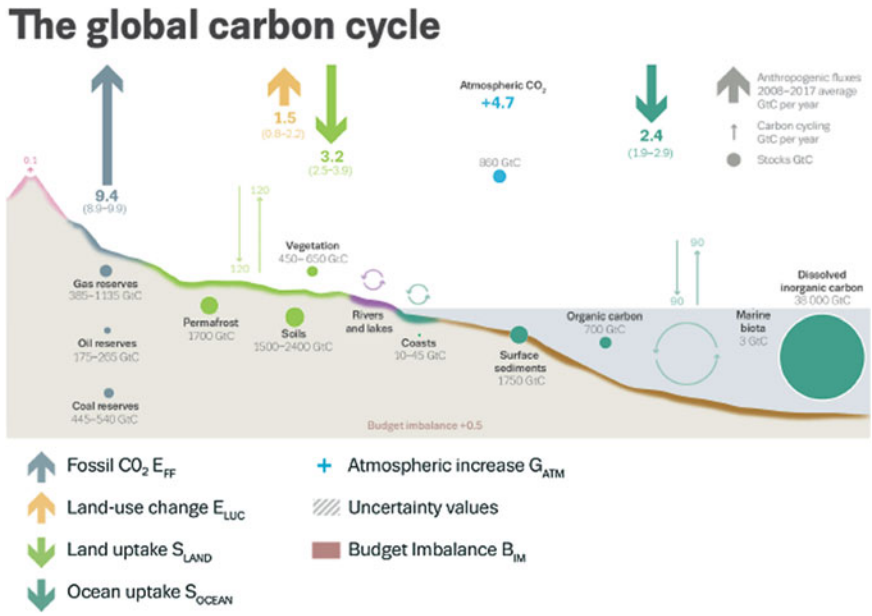

Fig. 2.56 Schematic representation of the overall perturbation of the global carbon cycle caused by anthropogenic activities, averaged globally for the decade 2008–2017. The anthropogenic perturbation occurs on top of an active carbon cycle, with fluxes and stocks represented in the background (Le Quéré et al. 2018). Reproduced with the author's permission.

Since the rate of net CO_2 assimilation is not CO_2-saturated in C_3 plants at 400 µmol mol^{-1} CO_2, the rise in CO_2 concentration is more likely to enhance photosynthesis in C_3 than in C_4 plants, where the rate of CO_2 assimilation is virtually saturated at a CO_2 concentration of 400 µmol

mol^{-1} (Fig. 2.38). The consequences of an enhanced rate of photosynthesis for plant growth are discussed in Sect. 10.5.8.

2.12.1 Acclimation of Photosynthesis to Elevated CO_2 Concentrations

Upon long-term exposure to 700 μmol CO_2 mol^{-1}, almost twice the present atmospheric CO_2 concentration, there may be a reduction of the photosynthetic capacity, associated with reduced levels of Rubisco and organic N per unit leaf area. This **downregulation** of photosynthesis increases with increasing duration of the exposure to elevated [CO_2] and is most pronounced in plants grown at low N supplies. By contrast, water-stressed plants tend to increase net photosynthesis in response to elevated [CO_2] (Wullschleger et al. 2002). Herbaceous plants consistently reduce **stomatal conductance** in response to elevated [CO_2], so that C_i does not increase as much as would be expected from the increase in C_a, but their intrinsic ***WUE*** tends to be increased (Long et al. 2004). Tree photosynthesis continues to be enhanced by elevated [CO_2], except when seedlings are grown in small pots, inducing nutrient limitation (Norby et al. 1999). The decrease in stomatal conductance of C_3 plants often indirectly stimulates photosynthesis in dry environments by reducing the rate of soil drying, and therefore the water limitation of photosynthesis (Hungate et al. 2002). C_3 and C_4 plants, however, benefit equally from increased water-use efficiency and water availability, reducing the relative advantage that C_3 plants gain from their greater CO_2 responsiveness of photosynthesis (Sage and Kubien 2003).

Why would acclimation of photosynthesis to elevated [CO_2] be more pronounced when N supply is poor? This could be a direct effect of N or an indirect effect by limiting the development of sinks for photoassimilates. This question can be tested by growing *Lolium perenne* (perennial ryegrass) in the field under elevated and current atmospheric CO_2 concentrations at both low and high N supply. Cutting of this herbage crop at regular intervals removes a major part of the canopy, decreasing the ratio of photosynthetic area to **sinks for photoassimilates**. Just before the cut, when the canopy is relatively large, growth at elevated [CO_2] and low N supply decreases in carboxylation capacity and the amount of Rubisco protein. At a high N supply, there are no significant decreases in carboxylation capacity or proteins. Elevated [CO_2] results in a marked increase in leaf carbohydrate concentration at low N supply, but not at high N supply. This acclimation at low N supply is absent after a harvest, when the canopy size is small. Acclimation under low N is, therefore, most likely caused by limitation of sink development rather than being a direct effect of N supply on photosynthesis (Rogers et al. 1998).

How do herbaceous plants sense that they are growing at an elevated CO_2 concentration and then downregulate their photosynthetic capacity? Acclimation is not due to sensing the CO_2 concentration itself, but sensing the concentration of sugars in the leaf cells, more precisely the soluble hexose sugars (Sect. 2.4.2), mediated by a specific **hexokinase** and other sugar-sensing systems (Sect. 2.4.3). In transgenic plants in which the level of hexokinase is greatly reduced, downregulation of photosynthesis upon prolonged exposure to high [CO_2] is considerably less. Via a signal-transduction pathway, which also involves phytohormones, the **sugar-sensing mechanism** regulates the transcription of nuclear encoded photosynthesis-associated genes (Rolland et al. 2006). Among the first photosynthetic proteins that are affected are the small subunit of **Rubisco** and **Rubisco activase**. Upon longer exposure, the level of thylakoid proteins and chlorophyll is also reduced (Table 2.16).

The downregulation of photosynthesis at elevated [CO_2] has led to the discovery of sugar-sensing in plants, but it has recently become clear that the signaling pathway is intricately involved in a network regulating acclimation to other environmental factors, including light and nutrient availability as well as biotic and abiotic stress (Rolland et al. 2002, 2006). Downregulation of photosynthesis in response to long-term exposure to elevated [CO_2] has important global

Table 2.16 Light-saturated rate of photosynthesis (A_{max}, measured at the CO_2 concentrations at which the plants were grown), *in vitro* Rubisco activity, chlorophyll concentration and the concentration of hexose sugars in the fifth leaf of *Solanum lycopersicum* (tomato) at various stages of development*.

Leaf expansion (% of full expansion)	Exposure time (days)	A_{max} (μmol m^{-2} s^{-1})		Rubisco activity (μmol m^{-2} s^{-1})		Chlorophyll (mg m^{-2})		Glucose (mg m^{-2})		Fructose (mg m^{-2})	
		Control	High	Control	High	Control	High	Control	High	Control	High
2	0	16.3	21.3	22.6	–	270	–	750	–	500	–
60	11	18.9	28.7	20.5	25.1	480	520	1000	1200	1400	1400
95	22	15.0	25.1	15.7	12.7	540	500	1100	1250	1800	2100
100	31	9.3	18.0	9.5	4.9	450	310	1100	2100	1800	4200

Source: Van Oosten and Besford (1995); Van Oosten et al. (1995)
*Plants were grown at different atmospheric CO_2 concentrations: control, 350 μmol CO_2 mol^{-1}; high, 700 μmol CO_2 mol^{-1}

implications. The capacity of terrestrial ecosystems to **sequester carbon** appears to be saturating, leaving a larger proportion of human carbon emissions in the atmosphere, and accelerating the rate of global warming (Canadell et al. 2007).

2.12.2 Effects of Elevated CO_2 on Transpiration - Differential Effects on C_3, C_4, and CAM Plants

Different types of plants respond to varying degrees to elevated CO_2. For example, C_4 plants, whose rate of photosynthesis is virtually saturated at 400 μmol mol^{-1}, generally respond less to elevated CO_2 concentrations than do C_3 plants.

Opuntia ficus-indica (prickly pear), a CAM species cultivated worldwide for its fruits and cladodes, also responds to the increase in CO_2 concentration in the atmosphere. The rate of CO_2 assimilation is initially enhanced, both at night and during the day, but this disappears upon prolonged exposure to elevated CO_2 (Cui and Nobel 1994). CAM species show, on average, a 35% increase in net daily CO_2 uptake which reflects increases in both Rubisco-mediated CO_2 uptake during the day and PEP carboxylase-mediated CO_2 uptake at night (Drennan and Nobel 2000).

2.13 Summary: What Can We Gain from Basic Principles and Rates of Single-Leaf Photosynthesis?

We have given numerous examples on how differences in photosynthetic traits enhance a genotype's performance in a specific environment. These include specific biochemical pathways (C_3, C_4, and CAM) as well as more intricate differences between sun and shade plants, aquatic and terrestrial plants, and plants differing in their photosynthetic N-use efficiency and water-use efficiency. Information on photosynthetic traits is also highly relevant when trying to understand effects of global environmental changes in temperature and atmospheric CO_2 concentrations. For a physiological ecologist, a full appreciation of the process of leaf photosynthesis is quintessential.

What we *cannot* derive from measurements on photosynthesis of **single leaves** is what the rate of photosynthesis of an **entire canopy** will be. To work out these rates, we need to take the approach discussed in Chap. 8, dealing with scaling-up principles. It is also clear that short-term measurements on the effect of atmospheric CO_2 concentrations are not going to tell us what will happen in the long term. Acclimation of the photosynthetic apparatus (downregulation) may occur, reducing the initial stimulatory effect. Most importantly, we cannot derive plant growth

rates or crop yields from rates of photosynthesis of a single leaf. Growth rates are not simply determined by rates of single-leaf photosynthesis per unit leaf area, but also by the total leaf area per plant and by the fraction of daily produced photosynthates required for plant respiration, issues that we deal with in later chapters.

References

Adams WW, **Demmig-Adams** B, **Logan** BA, **Barker** DH, **Osmond** CB. **1999.** Rapid changes in xanthophyll cycle-dependent energy dissipation and photosystem II efficiency in two vines, *Stephania japonica* and *Smilax australis*, growing in the understory of an open Eucalyptus forest. *Plant Cell Environ* **22**: 125–136.

Adrees M, **Saleem** F, **Jabeen** F, **Rizwan** M, **Ali** S, **Khalid** S, **Ibrahim** M, **Iqbal** N, **Abbas** F. **2016.** Effects of ambient gaseous pollutants on photosynthesis, growth, yield and grain quality of selected crops grown at different sites varying in pollution levels. *Arch Agron Soil Sci* **62**: 1195–1207.

Allen MT, **Pearcy** RW. **2000.** Stomatal behavior and photosynthetic performance under dynamic light regimes in a seasonally dry tropical rain forest. *Oecologia* **122**: 470–478.

Atkin OK, **Scheurwater** I, **Pons** TL. **2006.** High thermal acclimation potential of both photosynthesis and respiration in two lowland *Plantago* species in contrast to an alpine congeneric. *Glob Change Biol* **12**: 500–515.

Atkinson RRL, **Mockford** EJ, **Bennett** C, **Christin** P-A, **Spriggs** EL, **Freckleton** RP, **Thompson** K, **Rees** M, **Osborne** CP. **2016.** C4 photosynthesis boosts growth by altering physiology, allocation and size. *Nat Plants*: 16038.

Ávila-Lovera E, **Zerpa** AJ, **Santiago** LS. **2017.** Stem photosynthesis and hydraulics are coordinated in desert plant species. *New Phytol* **216**: 1119–1129.

Baker NR. **2008.** Chlorophyll fluorescence: a probe of photosynthesis *in vivo*. *Annu Rev Plant Biol* **59**: 89–113.

Banaś AK, **Aggarwal** C, **Łabuz** J, **Sztatelman** O, **Gabryś** H. **2012.** Blue light signalling in chloroplast movements. *J Exp Bot* **63**: 1559–1574.

Bastide B, **Sipes** D, **Hann** J, **Ting** IP. **1993.** Effect of severe water stress on aspects of Crassulacean Acid Metabolism in *Xerosicyos*. *Plant Physiol* **103**: 1089–1096.

Beerling DJ, **Osborne** CP. **2006.** The origin of the savanna biome. *Glob Change Biol* **12**: 2023–2031.

Bernacchi CJ, **Pimentel** C, **Long** SP. **2003.** *In vivo* temperature response functions of parameters required to model RuBP-limited photosynthesis. *Plant Cell Environ* **26**: 1419–1430.

Bernacchi CJ, **Portis** AR, **Nakano** H, **von Caemmerer** S, **Long** SP. **2002.** Temperature response of mesophyll conductance. Implications for the determination of Rubisco enzyme kinetics and for limitations to photosynthesis *in vivo*. *Plant Physiol* **130**: 1992–1998.

Bernacchi CJ, **Singsaas** EL, **Pimentel** C, **Portis Jr** AR, **Long** SP. **2001.** Improved temperature response functions for models of Rubisco-limited photosynthesis. *Plant Cell Environ* **24**: 253–259.

Berry JA, **Raison** JK **1981.** Responses of macrophytes to temperature. In: Lange OL, Nobel PS, Osmond CB, Ziegler H eds. *Physiological Plant Ecology*. Berlin: Springer, 277–338.

Björkman O **1981.** Responses to different quantum flux densities. In: Lange OL, Nobel PS, Osmond CB, Ziegler H eds. *Physiological Plant Ecology*. Berling: Springer, 57–107.

Bolhàr-Nordenkampf HR, **Öquist** G **1993.** Chlorophyll fluorescence as a tool in photosynthesis research. In: Hall DO, Scurlock JMO, Bolhàr-Nordenkampf HR, Leegood RC, Long SP eds. *Photosynthesis and Production in a Changing Environment*. London: Chapman and Hall, 193–206.

Borland AM, **Griffiths** H. **1997.** A comparative study on the regulation of C_3 and C_4 carboxylation processes in the constitutive crassulacean acid metabolism (CAM) plant *Kalanchoë daigremontiana* and the C_3-CAM intermediate *Clusia minor*. *Planta* **201**: 368–378.

Bowes G, **Rao** SK, **Estavillo** GM, **Reiskind** JB. **2002.** C_4 mechanisms in aquatic angiosperms: comparisons with terrestrial C_4 systems. *Funct Plant Biol* **29**: 379–392.

Bowes G, **Salvucci** ME. **1989.** Plasticity in the photosynthetic carbon metabolism of submersed aquatic macrophytes. *Aquat Bot* **34**: 233–266.

Bracher A, **Whitney** SM, **Hartl** FU, **Hayer-Hartl** M. **2017.** Biogenesis and metabolic maintenance of Rubisco. *Annu Rev Plant Biol* **68**: 29–60.

Brodribb TJ, **Feild** TS, **Sack** L. **2010.** Viewing leaf structure and evolution from a hydraulic perspective. *Funct Plant Biol* **37**: 488–498.

Brooks A, **Farquhar** GD. **1985.** Effect of temperature on the CO_2-O_2 specificity of ribulose–1,5-bisphosphate carboxylase/oxygenase and the rate of respiration in the light. *Planta* **165**: 397–406.

Brown HR, **Bouton** JH. **1993.** Physiology and genetics of interspecific hybrids between photosynthetic types. *Annu Rev Plant Biol* **44**: 435–456.

Brown RH, **Hattersley** PW. **1989.** Leaf anatomy of C_3-C_4 species as related to evolution of C_4 photosynthesis. *Plant Physiol* **91**: 1543–1550.

Brugnoli E, **Björkman** O. **1992.** Chloroplast movements in leaves: Influence on chlorophyll fluorescence and measurements of light-induced absorbance changes related to ΔpH and zeaxanthin formation. *Photosyn Res* **32**: 23–35.

Buchmann N, **Guehl** J-M, **Barigah** TS, **Ehleringer** JR. **1997.** Interseasonal comparison of CO_2 concentrations, isotopic composition, and carbon dynamics in an Amazonian rainforest (French Guiana). *Oecologia* **110**: 120–131.

Canadell JG, **Le Quéré** C, **Raupach** MR, **Field** CB, **Buitenhuis** ET, **Ciais** P, **Conway** TJ, **Gillett** NP, **Houghton** RA, **Marland** G. **2007.** Contributions to accelerating atmospheric CO_2 growth from economic

activity, carbon intensity, and efficiency of natural sinks. *Proc Natl Acad Sci USA* **104**: 18866–18870.

Carmo-Silva E**, Scales** JC**, Madgwick** PJ**, Parry** MAJ**. 2015.** Optimizing Rubisco and its regulation for greater resource use efficiency. *Plant Cell Environ* **38**: 1817–1832.

Cavagnaro JB**. 1988.** Distribution of C_3 and C_4 grasses at different altitudes in a temperate arid region of Argentina. *Oecologia* **76**: 273–277.

Cen Y-P**, Sage** RF**. 2005.** The regulation of Rubisco activity in response to variation in temperature and atmospheric CO_2 partial pressure in sweet potato. *Plant Physiol* **139**: 979–990.

Cerling TE**, Harris** JM**, MacFadden** BJ**, Leakey** MG**, Quade** J**, Eisenmann** V**, Ehleringer** JR**. 1997.** Global vegetation change through the Miocene/Pliocene boundary. *Nature* **389**: 153–158.

Cernusak LA**, Winter** K**, Aranda** J**, Turner** BL**, Marshall** JD**. 2007.** Transpiration efficiency of a tropical pioneer tree (*Ficus insipida*) in relation to soil fertility. *J Exp Bot* **58**: 3549–3566.

Chang T-G**, Zhu** X-G**. 2017.** Source–sink interaction: a century old concept under the light of modern molecular systems biology. *J Exp Bot* **68**: 4417–4431.

Chazdon RL**, Pearcy** RW**. 1986.** Photosynthetic responses to light variation in rainforest species. *Oecologia* **69**: 524–531.

Chazdon RL**, Pearcy** RW**. 1991.** The importance of sunflecks for forest understory plants. *BioSci* **41**: 760–766.

Chow WS**, Hope** AB**, Anderson** JM**. 1989.** Oxygen per flash from leaf disks quantifies photosystem II. *Biochim Biophys Acta Bioenerg* **973**: 105–108.

Christin P-A**, Osborne** CP**. 2014.** The evolutionary ecology of C_4 plants. *New Phytol* **204**: 765–781.

Coté FX**, Andre** M**, Folliot** M**, Massimino** D**, Daguenet** A**. 1989.** CO_2 and O_2 exchanges in the CAM plant *Ananas comosus* (L.) Merr: determination of total and malate-decorboxylation-dependent CO_2-assimilation rates; study of light O_2-uptake. *Plant Physiol* **89**: 61–68.

Coupe SA**, Palmer** BG**, Lake** JA**, Overy** SA**, Oxborough** K**, Woodward** FI**, Gray** JE**, Quick** WP**. 2006.** Systemic signalling of environmental cues in *Arabidopsis* leaves. *J Exp Bot* **57**: 329–341.

Cui M**, Nobel** PS**. 1994.** Gas exchange and growth responses to elevated CO_2 and light levels in the CAM species *Opuntia ficus-indica*. *Plant Cell Environ* **17**: 935–944.

DeLucia EH**, Nelson** K**, Vogelmann** TC**, Smith** WK**. 1996.** Contribution of intercellular reflectance to photosynthesis in shade leaves. *Plant Cell Environ* **19**: 159–170.

Demmig-Adams B**, Adams** WW**. 1996.** The role of xanthophyll cycle carotenoids in the protection of photosynthesis. *Trends Plant Sci* **1**: 21–26.

Demmig-Adams B**, Adams** WW**. 2006.** Photoprotection in an ecological context: the remarkable complexity of thermal energy dissipation. *New Phytol* **172**: 11–21.

Demmig B**, Björkman** O**. 1987.** Comparison of the effect of excessive light on chlorophyll fluorescence (77K) and photon yield of O_2 evolution in leaves of higher plants. *Planta* **171**: 171–184.

Denton MD**, Veneklaas** EJ**, Freimoser** FM**, Lambers** H**. 2007.** *Banksia* species (Proteaceae) from severely phosphorus-impoverished soils exhibit extreme efficiency in the use and re-mobilization of phosphorus. *Plant Cell Environ* **30**: 1557–1565.

DeRidder BP**, Salvucci** ME**. 2007.** Modulation of Rubisco activase gene expression during heat stress in cotton (*Gossypium hirsutum* L.) involves post-transcriptional mechanisms. *Plant Sci* **172**: 246–254.

Diefendorf AF**, Freimuth** EJ**. 2017.** Extracting the most from terrestrial plant-derived n-alkyl lipids and their carbon isotopes from the sedimentary record: A review. *Org Geochem* **103**: 1–21.

Diefendorf AF**, Mueller** KE**, Wing** SL**, Koch** PL**, Freeman** KH**. 2010.** Global patterns in leaf ^{13}C discrimination and implications for studies of past and future climate. *Proc Natl Acad Sci USA* **107**: 5738–5743.

Downton WJS**, Loveys** BR**, Grant** WJR**. 1988.** Stomatal closure fully accounts for the inhibition of photosynthesis by abscisic acid. *New Phytol* **108**: 263–266.

Drennan PM**, Nobel** PS**. 2000.** Responses of CAM species to increasing atmospheric CO_2 concentrations. *Plant Cell Environ* **23**: 767–781.

Dusenge ME**, Duarte** AG**, Way** DA**. 2019.** Plant carbon metabolism and climate change: elevated CO_2 and temperature impacts on photosynthesis, photorespiration and respiration. *New Phytol* **221**: 32–49.

Eamus D**, Cole** S. **1997.** Diurnal and seasonal comparisons of assimilation, phyllode conductance and water potential of three *Acacia* and one *Eucalyptus* species in the wet–dry tropics of Australia. *Aust J Bot* **45**: 275–290.

Earnshaw MJ**, Winter** K**, Ziegler** H**, Stichler** W**, Cruttwell** NEG**, Kerenga** K**, Cribb** PJ**, Wood** J**, Croft** JR**, Carver** KA**, Gunn** TC**. 1987.** Altitudinal changes in the incidence of crassulacean acid metabolism in vascular epiphytes and related life forms in Papua New Guinea. *Oecologia* **73**: 566–572.

Edwards EJ**, Osborne** CP**, Strömberg** CAE**, Smith** SA**. 2010.** The origins of C_4 grasslands: integrating evolutionary and ecosystem science. *Science* **328**: 587–591.

Edwards GE**, Voznesenskaya** EV **2011.** C_4 Photosynthesis: Kranz forms and single-cell C_4 in terrestrial plants. In: Raghavendra AS, Sage RF eds. *C_4 Photosynthesis and Related CO_2 Concentrating Mechanisms*. Dordrecht: Springer Netherlands, 29–61.

Ehleringer J**, Björkman** O**. 1977.** Quantum yields for CO_2 uptake in C_3 and C_4 plants. Dependence on temperature, CO_2, and O_2 concentration. *Plant Physiol* **59**: 86–90.

Ehleringer J**, Björkman** O**, Mooney** HA**. 1976.** Leaf pubescence: effects on absorptance and photosynthesis in a desert shrub. *Science* **192**: 376–377.

Ehleringer JR**, Cerling** TE**, Helliker** BR**. 1997.** C_4 photosynthesis, atmospheric CO_2, and climate. *Oecologia* **112**: 285–299.

Ehleringer JR**, Monson** RK**. 1993.** Evolutionary and ecological aspects of photosynthetic pathway variation. *Annu Rev Ecol Syst* **24**: 411–439.

Ehleringer JR**, Schulze,** E.-D.**, Ziegler,** H.**, Lange,** O.L.**, Farquhar,** G.D.**, Cowan,** I.R. **1985.** Xylem-tapping mistletoes: water or nutrient parasites? *Science* **227**: 1479–1481.

Eller BM**, Ferrari** S**. 1997.** Water use efficiency of two succulents with contrasting CO_2 fixation pathways. *Plant Cell Environ* **20**: 93–100.

Ellis RP**. 1977.** Distribution of the Kranz syndrome in the Southern African Eragrostoideae and Panicoideae according to bundle sheath anatomy and cytology. *Agroplantae* **9**: 73–110.

Elzenga JTM**, Prins** HBA**. 1988.** Adaptation of *Elodea* and *Potamogeton* to different inorganic carbon levels and the mechanism for photosynthetic bicarbonate utilisation. *Funct Plant Biol* **15**: 727–735.

Elzenga JTM**, Prins** HBA**. 1989.** Light-induced polar pH changes in leaves of *Elodea canadensis.* Effects of carbon concentration and light intensity. *Plant Physiol* **91**: 62–67.

Esteban R**, Barrutia** O**, Artetxe** U**, Fernández-Marín** B**, Hernández** A**, García-Plazaola** JI**. 2015.** Internal and external factors affecting photosynthetic pigment composition in plants: a meta-analytical approach. *New Phytol* **206**: 268–280.

Evans JR**. 1989.** Photosynthesis and nitrogen relationships in leaves of C_3 plants. *Oecologia* **78**: 9–19.

Evans JR**, Loreto** F **2000.** Acquisition and diffusion of CO_2 in higher plant leaves. In: Leegood RC, Sharkey TD, von Caemmerer S eds. *Photosynthesis: Physiology and Metabolism*. Dordrecht: Springer Netherlands, 321–351.

Evans JR**, Poorter** H. **2001.** Photosynthetic acclimation of plants to growth irradiance: the relative importance of specific leaf area and nitrogen partitioning in maximizing carbon gain. *Plant Cell Environ* **24**: 755–767.

Evans JR**, Seemann** JR **1989.** The allocation of protein nitrogen in the photosynthetic apparatus: costs, consequences, and control. In: Briggs WR ed. *Photosynthesis*. New York: Alan Liss, 183–205.

Evans JR**, Sharkey** TD**, Berry** JA**, Farquhar** GD**. 1986.** Carbon isotope discrimination measured concurrently with gas exchange to investigate CO_2 diffusion in leaves of higher plants. *Funct Plant Biol* **13**: 281–292.

Evans JR**, Vogelmann** TC**. 2003.** Profiles of ^{14}C fixation through spinach leaves in relation to light absorption and photosynthetic capacity. *Plant Cell Environ* **26**: 547–560.

Farmer AM **1996.** Carbon uptake by roots. In: Waisel Y, Eshel A, Kafkaki U eds. *Plant Roots: The Hidden Half*. New York, : Marcel Dekker, 679–687.

Farquhar G**, Richards** R**. 1984.** Isotopic composition of plant carbon correlates with water-use efficiency of wheat genotypes. *Funct Plant Biol* **11**: 539–552.

Farquhar GD**, Ehleringer** JR**, Hubick** KT**. 1989.** Carbon isotope discrimination and photosynthesis. *Annu Rev Plant Physiol Plant Mol Biol* **40**: 503–537.

Farquhar GD**, O'Leary** MH**, Berry** JA**. 1982.** On the relationship between carbon isotope discrimination and the intercellular carbon dioxide concentration in leaves. *Funct Plant Biol* **9**: 121–137.

Farquhar GD**, von Caemmerer** S **1982.** Modelling of photosynthetic response to environmental conditions. In: Lange OL, Nobel PS, Osmond CB, Ziegler H eds. *Physiological Plant Ecology II: Water Relations and Carbon Assimilation*. Berlin: Springer, 549–587.

Farquhar GD**, von Caemmerer** S**, Berry** JA**. 1980.** A biochemical model of photosynthetic CO_2 assimilation in leaves of C_3 species. *Planta* **149**: 78–90.

Feild TS**, Brodribb** TJ**, Iglesias** A**, Chatelet** DS**, Baresch** A**, Upchurch** GR**, Gomez** B**, Mohr** BAR**, Coiffard** C**, Kvacek** J**, Jaramillo** C. **2011.** Fossil evidence for Cretaceous escalation in angiosperm leaf vein evolution. *Proc Natl Acad Sci USA* **108**: 8363–8366.

Feild TS**, Lee** DW**, Holbrook** NM**. 2001.** Why leaves turn red in autumn. The role of anthocyanins in senescing leaves of red-osier dogwood. *Plant Physiol* **127**: 566–574.

Field CB**, Ball** T**, Berry** JA **1989.** Photosynthesis: principles and field techniques. In: Pearcy RW, Ehleringer JR, Mooney HA, Rundel PW eds. *Plant Physiological Ecology; Field Methods and Instrumentation*. London: Chapman and Hall, 209–253.

Flexas J**, Bota** J**, Galmés** J**, Medrano** H**, Ribas-Carbó** M**. 2006a.** Keeping a positive carbon balance under adverse conditions: responses of photosynthesis and respiration to water stress. *Physiol Plant* **127**: 343–352.

Flexas J**, Diaz-Espejo** A**, Galmés** J**, Kaldenhoff** R**, Medrano** H**, Ribas-Carbo** M**. 2007.** Rapid variations of mesophyll conductance in response to changes in CO_2 concentration around leaves. *Plant Cell Environ* **30**: 1284–1298.

Flexas J**, Ribas-Carbó** M**, Diaz-Espejo** A**, Galmés** J**, Medrano** H**. 2008.** Mesophyll conductance to CO_2: current knowledge and future prospects. *Plant Cell Environ* **31**: 602–621.

Flexas J**, Ribas-Carbó** M**, Hanson** DT**, Bota** J**, Otto** B**, Cifre** J**, McDowell** N**, Medrano** H**, Kaldenhoff** R**. 2006b.** Tobacco aquaporin NtAQP1 is involved in mesophyll conductance to CO_2 *in vivo*. *Plant J* **48**: 427–439.

Flügge U-I**, Heldt** HW**. 1991.** Metabolite translocators of the chloroplast envelope. *Annu Rev Plant Biol* **42**: 129–144.

Flügge U**, Stitt** M**, Heldt** HW**. 1985.** Light-driven uptake of pyruvate into mesophyll chloroplasts from maize. *FEBS Lett* **183**: 335–339.

Fredeen AL**, Gamon** JA**, Field** CB**. 1991.** Responses of photosynthesis and carbohydrate-partitioning to limitations in nitrogen and water availability in field-grown sunflower. *Plant Cell Environ* **14**: 963–970.

Furumoto T**, Yamaguchi** T**, Ohshima-Ichie** Y**, Nakamura** M**, Tsuchida-Iwata** Y**, Shimamura** M**, Ohnishi** J**, Hata** S**, Gowik** U**, Westhoff** P**, Bräutigam** A**, Weber** APM**, Izui** K**. 2011.** A plastidial sodium-dependent pyruvate transporter. *Nature* **476**: 472.

Galmés J**, Conesa** MÀ**, OchogavÍA** JM**, Perdomo** JA**, Francis** DM**, Ribas-Carbó** M**, Savé** R**, Flexas** J**, Medrano** H**, Cifre** J**. 2011.** Physiological and morphological adaptations in relation to water use efficiency in

Mediterranean accessions of *Solanum lycopersicum*. *Plant Cell Environ* **34**: 245–260.

Galmés J, Flexas J, Keys AJ**, Cifre J, Mitchell** RAC**, Madgwick** PJ**, Haslam** RP**, Medrano** H**, Parry** MAJ**. 2005.** Rubisco specificity factor tends to be larger in plant species from drier habitats and in species with persistent leaves. *Plant Cell Environ* **28**: 571–579.

Galmés J, Flexas J, Savé R**, Medrano** H**. 2007a.** Water relations and stomatal characteristics of Mediterranean plants with different growth forms and leaf habits: responses to water stress and recovery. *Plant Soil* **290**: 139–155.

Galmés J, Medrano H**, Flexas J. 2007b.** Photosynthetic limitations in response to water stress and recovery in Mediterranean plants with different growth forms. *New Phytol* **175**: 81–93.

Genty B**, Briantais** J-M**, Baker** NR**. 1989.** The relationship between the quantum yield of photosynthetic electron transport and quenching of chlorophyll fluorescence. *Biochimica et Biophysica Acta - General Subjects* **990**: 87–92.

George AS**. 2002.** *The long dry: bush colours of summer and autumn in south-western Australia*. Kardinya: Four Gables Press.

Ghannoum O**, Evans** JR**, Chow** WS**, Andrews** TJ**, Conroy** JP**, von Caemmerer** S**. 2005.** Faster rubisco is the key to superior nitrogen-use efficiency in NADP-malic enzyme relative to NAD-malic enzyme C4 grasses. *Plant Physiol* **137**: 638–650.

Gillon JS**, Yakir** D**. 2000.** Internal conductance to CO_2 diffusion and $C^{18}OO$ discrimination in C_3 leaves. *Plant Physiol* **123**: 201–214.

Grams TEE**, Koziolek** C**, Lautner** S**, Matyssek** R**, Fromm J. 2007.** Distinct roles of electric and hydraulic signals on the reaction of leaf gas exchange upon re-irrigation in Zea mays L. *Plant Cell Environ* **30**: 79–84.

Granot D**, David-Schwartz** R**, Kelly** G**. 2013.** Hexose kinases and their role in sugar-sensing and plant development. *Front Plant Sci* **4**.

Granot D**, Kelly** G**, Stein** O**, David-Schwartz** R**. 2014.** Substantial roles of hexokinase and fructokinase in the effects of sugars on plant physiology and development. *J Exp Bot* **65**: 809–819.

Groszmann M**, Osborn** HL**, Evans** JR**. 2017.** Carbon dioxide and water transport through plant aquaporins. *Plant Cell Environ* **40**: 938–961.

Guilherme Pereira C**, Hayes,** P.E.**, O'Sullivan,** O.**, Weerasinghe,** L.**, Clode,** P.L.**, Atkin,** O.K.**, Lambers,** H. **2019.** Trait convergence in photosynthetic nutrient-use efficiency along a 2-million year dune chronosequence in a global biodiversity hotspot. *J Ecol* **107**: 2006–2023.

Guy RD**, Fogel** ML**, Berry** JA**. 1993.** Photosynthetic fractionation of the stable isotopes of oxygen and carbon. *Plant Physiol* **101**: 37–47.

Hakala M**, Tuominen** I**, Keränen** M**, Tyystjärvi** T**, Tyystjärvi** E**. 2005.** Evidence for the role of the oxygen-evolving manganese complex in photoinhibition of Photosystem II. *Biochim Biophys Acta* **1706**: 68–80.

Hanson HC**. 1917.** Leaf structure as related to environment. *Am J Bot* **4**: 533–560.

Hatch MD**, Carnal** NW **1992.** The role of mitochondria in C_4 photosynthesis. In: Lambers H, Van der Plas LHW eds. *Molecular, Biochemical and Physiological Aspects of Plant Respiration*. The Hague: SPB Academic Publishing, 135–148.

Hatch MD**, Dröscher** L**, Flügge** UI**, Heldt** HW**. 1984.** A specific translocator for oxaloacetate transport in chloroplasts. *FEBS Lett* **178**: 15–19.

Hatch MD**, Slack** CR**. 1966.** Photosynthesis by sugarcane leaves. *Biochem J* **101**: 103–111.

Hatch MD**, Slack** CR **1998.** C_4 photosynthesis: discovery, resolution, recognition, and significance. In: Yang S-Y, Kung S-D eds. *Discoveries In Plant Biology*. Hong Kong: World Scientific Publishing, 175–196.

Hattersley PW**. 1983.** The distribution of C3 and C4 grasses in Australia in relation to climate. *Oecologia* **57**: 113–128.

Hattersley PW**, Watson** L. **1975.** Anatomical parameters for predicting photosynthetic pathways of grass leaves: the'maximum lateral cell count'and the'maximum cells distant count. *Phytomorphology* **25**: 325–333.

Henderson S**, Hattersley** P**, von Caemmerer** S**, Osmond** CB **1995.** Are C_4 pathway plants threatened by global climatic change? In: Schulze E-D, Caldwell MM eds. *Ecophysiology of Photosynthesis*. Berlin: Springer, 529–549.

Henderson SA**, von Caemmerer** SV**, Farquhar** GD**. 1992.** Short-term measurements of carbon isotope discrimination in several C_4 species. *Aust J Plant Physiol* **19**: 263–285.

Hibberd JM**, Quick** WP**. 2002.** Characteristics of C_4 photosynthesis in stems and petioles of C_3 flowering plants. *Nature* **415**: 451.

Higa T**, Wada** M**. 2016.** Chloroplast avoidance movement is not functional in plants grown under strong sunlight. *Plant Cell Environ* **39**: 871–882.

Hikosaka K**, Ishikawa** K**, Borjigidai** A**, Muller** O**, Onoda** Y**. 2006.** Temperature acclimation of photosynthesis: mechanisms involved in the changes in temperature dependence of photosynthetic rate. *J Exp Bot* **57**: 291–302.

Houghton RA**. 2007.** Balancing the Global Carbon Budget. *Annual Review of Earth and Planetary Sciences* **35**: 313–347.

Hsiao TC**. 1973.** Plant responses to water stress. *Annu Rev Plant Physiol* **24**: 519–570.

Huang Y**, Street-Perrott** FA**, Metcalfe** SE**, Brenner** M**, Moreland** M**, Freeman** KH**. 2001.** Climate change as the dominant control on glacial-interglacial variations in C_3 and C_4 plant abundance. *Science* **293**: 1647–1651.

Hüner NPA**, Dahal** K**, Bode** R**, Kurepin** LV**, Ivanov** AG**. 2016.** Photosynthetic acclimation, vernalization, crop productivity and 'the grand design of photosynthesis'. *J Plant Physiol* **203**: 29–43.

Hüner NPA**, Öquist** G**, Sarhan** F**. 1998.** Energy balance and acclimation to light and cold. *Trends Plant Sci* **3**: 224–230.

Hungate BA**, Reichstein** M**, Dijkstra** P**, Johnson** D**, Hymus** G**, Tenhunen** JD**, Hinkle** CR**, Drake** BG**.**

2002. Evapotranspiration and soil water content in a scrub-oak woodland under carbon dioxide enrichment. *Glob Change Biol* **8**: 289–298.

Hylton CM**, Rawsthorne** S**, Smith** AM**, Jones** DA**, Woolhouse** HW**. 1988.** Glycine decarboxylase is confined to the bundle-sheath cells of leaves of C_3-C_4 intermediate species. *Planta* **175**: 452–459.

Ishikawa C**, Hatanaka** T**, Misoo** S**, Fukayama** H**. 2009.** Screening of high k_{cat} Rubisco among Poaceae for iprovement of photosynthetic CO_2 assimilation in rice. *Plant Prod, Sci* **12**: 345–350.

Jahnke S**, Pieruschka** R. **2006.** Air pressure in clamp-on leaf chambers: a neglected issue in gas exchange measurements. *J Exp Bot* **57**: 2553–2561.

Jordan DB**, Ogren** WL**. 1984.** The CO_2/O_2 specificity of ribulose 1,5-bisphosphate carboxylase/oxygenase. *Planta* **161**: 308–313.

Kadereit G**, Ackerly** D**, Pirie Michael** D**. 2012.** A broader model for C_4 photosynthesis evolution in plants inferred from the goosefoot family (Chenopodiaceae s.s.). *Proc R Soc B Biol Sci* **279**: 3304–3311.

Kalisz S**, Teeri** JA**. 1986.** Population-level variation in photosynthetic metabolism and growth in *Sedum wrightii*. *Ecology* **67**: 20–26.

Kao W-Y**, Forseth** IN**. 1992.** Dirunal leaf movement, chlorophyll fluorescence and carbon assimilation in soybean grown under different nitrogen and water availabilities. *Plant Cell Environ* **15**: 703–710.

Keeley JE**, Busch** G**. 1984.** Carbon assimilation characteristics of the aquatic CAM plant, *Isoetes howellii*. *Plant Physiol* **76**: 525–530.

Keeley JE**, Osmond** CB**, Raven** JA**. 1984.** *Stylites*, a vascular land plant without stomata absorbs CO_2 via its roots. *Nature* **310**: 694–695.

Keeley JE**, Sandquist** DR**. 1992.** Carbon: freshwater plants. *Plant Cell Environ* **15**: 1021–1035.

Kelly G**, Moshelion** M**, David-Schwartz** R**, Halperin** O**, Wallach** R**, Attia** Z**, Belausov** E**, Granot** D**. 2013.** Hexokinase mediates stomatal closure. *Plant J* **75**: 977–988.

Kirschbaum MUF**, Pearcy** RW**. 1988.** Gas exchange analysis of the relative importance of stomatal and biochemical factors in photosynthetic induction in *Alocasia macrorrhiza*. *Plant Physiol* **86**: 782–785.

Kitao M**, Harayama** H**, Han** Q**, Agathokleous** E**, Uemura** A**, Furuya** N**, Ishibashi** S**. 2018.** Springtime photoinhibition constrains regeneration of forest floor seedlings of Abies sachalinensis after a removal of canopy trees during winter. *Sci Rep* **8**: 6310.

Klavsen SK**, Madsen** TV**, Maberly** SC**. 2011.** Crassulacean acid metabolism in the context of other carbon-concentrating mechanisms in freshwater plants: a review. *Photosyn Res* **109**: 269–279.

Kluge M**, Brulfert** J**, Queiroz** O**. 1981.** Diurnal changes in the regulatory properties of PEP-carboxylase in Crassulacean Acid Metabolism (CAM). *Plant Cell Environ* **4**: 251–256.

Kluge M**, Ting** IP**. 1978.** *Crassulacean Acid Metabolism: Analysis of an Ecological Adaptation*. Berlin: Springer-Verlag.

Koch KE**, Kennedy** RA**. 1982.** Crassulacean Acid Metabolism in the succulent C_4 dicot, *Portulaca oleracea* L under natural environmental conditions. *Plant Physiol* **69**: 757–761.

Körner C**, Larcher** W. **1988.** Plant life in cold climates. *Symp Soc Exp Biol* **42**: 25–57.

Krall JP**, Edwards** GE**. 1992.** Relationship between photosystem II activity and CO_2 fixation in leaves. *Physiol Plant* **86**: 180–187.

Krause GH**, Weis** E. **1991.** Chlorophyll fluorescence and photosynthesis: the basics. *Annu Rev Plant Biol* **42**: 313–349.

Kress E**, Jahns** P**. 2017.** The dynamics of energy dissipation and xanthophyll conversion in *Arabidopsis* indicate an indirect photoprotective role of zeaxanthin in slowly inducible and relaxing components of non-photochemical quenching of excitation energy. *Front Plant Sci* **8**: 2094.

Külheim C**, Ågren** J**, Jansson** S. **2002.** Rapid regulation of light harvesting and plant fitness in the field. *Science* **297**: 91–93.

Lake JA**, Quick** WP**, Beerling** DJ**, Woodward** FI**. 2001.** Plant development: signals from mature to new leaves. *Nature* **411**: 154–154.

Lawlor DW**. 1993.** *Photosynthesis; Molecular, Physiological and Environmental Processes*. London: Longman.

Le Quéré C**, Andrew** RM**, Friedlingstein** P**, Sitch** S**, Hauck** J**, Pongratz** J**, Pickers** PA**, Korsbakken** JI**, Peters** GP**, Canadell** JG**, Arneth** A**, Arora** VK**, Barbero** L**, Bastos** A**, Bopp** L**, Chevallier** F**, Chini** LP**, Ciais** P**, Doney** SC**, Gkritzalis** T**, Goll** DS**, Harris** I**, Haverd** V**, Hoffman** FM**, Hoppema** M**, Houghton** RA**, Hurtt** G**, Ilyina** T**, Jain** AK**, Johannessen** T**, Jones** CD**, Kato** E**, Keeling** RF**, Goldewijk** KK**, Landschützer** P**, Lefèvre** N**, Lienert** S**, Liu** Z**, Lombardozzi** D**, Metzl** N**, Munro** DR**, Nabel** JEMS**, Nakaoka** S-i**, Neill** C**, Olsen** A**, Ono** T**, Patra** P**, Peregon** A**, Peters** W**, Peylin** P**, Pfeil** B**, Pierrot** D**, Poulter** B**, Rehder** G**, Resplandy** L**, Robertson** E**, Rocher** M**, Rödenbeck** C**, Schuster** U**, Schwinger** J**, Séférian** R**, Skjelvan** I**, Steinhoff** T**, Sutton** A**, Tans** PP**, Tian** H**, Tilbrook** B**, Tubiello** FN**, Van der Laan-Luijkx** IT**, Van der Werf** GR**, Viovy** N**, Walker** AP**, Wiltshire** AJ**, Wright** R**, Zaehle** S**, Zheng** B. **2018.** Global Carbon Budget 2018. *Earth System Science Data (Online)*: Medium: ED; Size: 2141–2194.

Le Quéré C**, Andrew** RM**, Friedlingstein** P**, Sitch** S**, Pongratz** J**, Manning** AC**, Korsbakken** JI**, Peters** GP**, Canadell** JG**, Jackson** RB**, Boden** TA**, Tans** PP**, Andrews** OD**, Arora** VK**, Bakker** DCE**, Barbero** L**, Becker** M**, Betts** RA**, Bopp** L**, Chevallier** F**, Chini** LP**, Ciais** P**, Cosca** CE**, Cross** J**, Currie**, Gasser T**, Harris** I**, Hauck** J**, Haverd** V**, Houghton** RA**, Hunt** CW**, Hurtt** G**, Ilyina** T**, Jain** AK**, Kato** E**, Kautz** M**, Keeling** RF**, Klein Goldewijk** K**, Körtzinger** A**, Landschützer** P**, Lefèvre** N**, Lenton** A**, Lienert** S**, Lima** I**, Lombardozzi** D**, Metzl** N**, Millero** F**, Monteiro** PMS**, Munro** DR**, Nabel** JEMS**,** Nakaoka **S-i, Nojiri** Y**, Padin** XA**, Peregon** A**, Pfeil** B**, Pierrot**

D, **Poulter** B, **Rehder** G, **Reimer** J, **Rödenbeck** C, **Schwinger** J, **Séférian** R, **Skjelvan** I, **Stocker** BD, **Tian** H, **Tilbrook** B, **Tubiello** FN, **Van der Laan-Luijkx** IT, **Van der Werf** GR, **Van Heuven** S, **Viovy** N, **Vuichard** N, **Walker** AP, **Watson** AJ, **Wiltshire** AJ, **Zaehle** S, **Zhu** D. **2017.** Global Carbon Budget 2017. *Earth Syst Sci Data* **10**: 405–448.

Leverenz JW. **1987.** Chlorophyll content and the light response curve of shade-adapted conifer needles. *Physiol Plant* **71**: 20–29.

Lichtenthaler H **1986**. Laser-induced chlorophyll fluorescence of living plants.In. *ESA Proceedings of the 1986 International Geoscience and Remote Sensing Symposium(IGARSS'86) on Remote Sensing: Today's Solutions for Tomorrow's Information Needs*.

Lichtenthaler HK. **2015.** Fifty five years of research on photosynthesis, chloroplasts and stress physiology of plants 1958–2013. *Progr Bot* **76**: 3–42.

Lichtenthaler HK, **Babani** F **2004.** Light adaptation and senescence of the photosynthetic apparatus. Changes in pigment composition, chlorophyll fluorescence parameters and photosynthetic activity. In: Papageorgiou GC, Govindjee eds. *Chlorophyll a Fluorescence: A Signature of Photosynthesis*. Dordrecht: Springer Netherlands, 713–736.

Logan BA, **Barker** DH, **Demmig-Adams** B, **Adams** WW. **1996.** Acclimation of leaf carotenoid composition and ascorbate levels to gradients in the light environment within an Australian rainforest. *Plant Cell Environ* **19**: 1083–1090.

Long SP, **Ainsworth** EA, **Rogers** A, **Ort** DR. **2004.** Rising atmospheric carbon dioxide: plants FACE the Future. *Annu Rev Plant Biol* **55**: 591–628.

Long SP, **Bernacchi** CJ. **2003.** Gas exchange measurements, what can they tell us about the underlying limitations to photosynthesis? Procedures and sources of error. *J Exp Bot* **54**: 2393–2401.

Long SP, **Hällgren** JE **1993.** Measurement of CO_2 assimilation by plants in the field and the laboratory. In: Hall DO, Scurlock JMO, Bolhàr-Nordenkampf HR, Leegood RC, LONG SP eds. *Photosynthesis and Production in a Changing Environment*. London: Chapman and Hall, 129–167.

Long SP, **Humphries** S, **Falkowski** PG. **1994.** Photoinhibition of photosynthesis in nature. *Annu Rev Plant Physiol Plant Mol Biol* **45**: 633–662.

Lundgren MR, **Christin** P-A. **2017.** Despite phylogenetic effects, C_3–C_4 lineages bridge the ecological gap to C_4 photosynthesis. *J Exp Bot* **68**: 241–254.

Lundgren MR, **Dunning** LT, **Olofsson** JK, **Moreno-Villena** JJ, **Bouvier** JW, **Sage** TL, **Khoshravesh** R, **Sultmanis** S, **Stata** M, **Ripley** BS, **Vorontsova** MS, **Besnard** G, **Adams** C, **Cuff** N, **Mapaura** A, **Bianconi** ME, **Long** CM, **Christin** P-A, **Osborne** CP. **2019.** C_4 anatomy can evolve via a single developmental change. *Ecol Lett* **22**: 302–312.

Maberly SC. **1996.** Diel, episodic and seasonal changes in pH and concentrations of inorganic carbon in a productive lake. *Freshwater Biology* **35**: 579–598.

Maberly SC, **Madsen** TV. **2002.** Freshwater angiosperm carbon concentrating mechanisms: processes and patterns. *Funct Plant Biol* **29**: 393–405.

Madsen TV, **Baattrup-Pedersen** A. **1995.** Regulation of growth and photosynthetic performance in *Elodea canadensis* in response to inorganic nitrogen. *Funct Ecol* **9**: 239–247.

Magnin NC, **Cooley** BA, **Reiskind** JB, **Bowes** G. **1997.** Regulation and localization of key enzymes during the induction of Kranz-less, C_4-type photosynthesis in *Hydrilla verticillata*. *Plant Physiol* **115**: 1681–1689.

Males J, **Griffiths** H. **2017.** Stomatal biology of CAM plants. *Plant Physiol* **174**: 550–560.

Mazen AMA. **2000.** Changes in properties of phosphoenolpyruvate carboxylase with induction of Crassulacean Acid Metabolism (CAM) in the C_4 plant *Portulaca oleracea*. *Photosynthetica* **38**: 385–391.

McConnaughey TA, **LaBaugh** JW, **Rosenberry** D, **Striegl** RG, **Reddy** MM, **Schuster** PF, **Carter** V. **1994.** Carbon budget for a groundwater-fed lake: calcification supports summer photosynthesis. *Limnol Oceanogr* **39**: 1319–1332.

Medina E **1996.** CAM and C_4 plants in the humid tropics. In: Mulkey SD, Chazdon RL, Smith AP eds. *Tropical Forest Plant Ecophysiology*. New York: Chapman and Hall, 56–88.

Míguez F, **Fernández-Marín** B, **Becerril** JM, **García-Plazaola** JI. **2015.** Activation of photoprotective winter photoinhibition in plants from different environments: a literature compilation and meta-analysis. *Physiol Plant* **155**: 414–423.

Mizokami Y, **Sugiura** D, **Watanabe** CKA, **Betsuyaku** E, **Inada** N, **Terashima** I. **2019.** Elevated CO_2-induced changes in mesophyll conductance and anatomical traits in wild type and carbohydrate metabolism mutants of *Arabidopsis thaliana*. *J Exp Bot*.

Mommer L, **Pons** TL, **Wolters-Arts** M, **Venema** JH, **Visser** EJW. **2005.** Submergence-induced morphological, anatomical, and biochemical responses in a terrestrial species affect gas diffusion resistance and photosynthetic performance. *Plant Physiol* **139**: 497–508.

Monsi M, **Saeki** T. **1953.** Uber den Lichtfaktor in den Pflanzengesellschaften und seine Bedeutung fur die Stoffproduktion. *Japanes Journal of Botany* **14**: 22–52.

Monsi M, **Saeki** T. **2005.** On the factor light in plant communities and its importance for matter production. *Ann Bot* **95**: 549–567.

Mooney HA **1986.** Photosynthesis. In: Crawley MJ ed. *Plant Ecol*. Oxford: Blackwell Scientific Publications, 345–373.

Morgan PB, **Ainsworth** EA, **Long** SP. **2003.** How does elevated ozone impact soybean? A meta-analysis of photosynthesis, growth and yield. *Plant Cell Environ* **26**: 1317–1328.

Murchie EH, **Horton** P. **1997.** Acclimation of photosynthesis to irradiance and spectral quality in British plant species: chlorophyll content, photosynthetic capacity and habitat preference. *Plant Cell Environ* **20**: 438–448.

Nadal M, **Flexas** J, **Gulías** J. **2018.** Possible link between photosynthesis and leaf modulus of elasticity among vascular plants: a new player in leaf traits relationships? *Ecol Lett* **21**: 1372–1379.

Newman JR**, Raven** JA**. 1993.** Carbonic anhydrase in *Ranunculus penicillatus* spp. *pseudofluitans*: activity, location and implications for carbon assimilation. *Plant Cell Environ* **16**: 491–500.

Nielsen SL**,** Gacia **Ea, Sand-Jensen** K**. 1991.** Land plants of amphibious *Littorella uniflora* (L.) Aschers. maintain utilization of CO_2 from the sediment. *Oecologia* **88**: 258–262.

Niinemets Ü**. 2007.** Photosynthesis and resource distribution through plant canopies. *Plant Cell and Environment* **30**: 1052–1071.

Nimmo HG**, Fontaine** V**, Hartwell** J**, Jenkins** GI**, Nimmo** GA**, Wilkins** MB**. 2001.** PEP carboxylase kinase is a novel protein kinase controlled at the level of expression. *New Phytol* **151**: 91–97.

Nishio JN**, Sun** J**, Vogelmann** TC**. 1993.** Carbon fixation gradients across spinach leaves do not follow internal light gradients. *Plant Cell* **5**: 953–961.

Nishiyama Y**, Allakhverdiev** SI**, Murata** N**. 2006.** A new paradigm for the action of reactive oxygen species in the photoinhibition of photosystem II. *Biochim Biophys Acta Bioenerg* **1757**: 742–749.

Niyogi KK**, Grossman** AR**, Björkman** O**. 1998.** *Arabidopsis* mutants define a central role for the xanthophyll cycle in the regulation of photosynthetic energy conversion. *Plant Cell* **10**: 1121–1134.

Nobel PS**, García-Moya** E**, Quero** E**. 1992.** High annual productivity of certain agaves and cacti under cultivation. *Plant Cell Environ* **15**: 329–335.

Nobel PS**, Hartsock** TL**. 1990.** Diel patterns of CO_2 exchange for epiphytic cacti differing in succulence. *Physiol Plant* **78**: 628–634.

Norby RJ**, Wullschleger** SD**, Gunderson** CA**, Johnson** DW**, Ceulemans** R**. 1999.** Tree responses to rising CO2 in field experiments: implications for the future forest. *Plant Cell Environ* **22**: 683–714.

O'Leary MH **1993.** Biochemical basis of carbon isotope fractionation. In: Ehleringer JR, Hall AE, Farquhar GD eds. *Stable isotopes and plant carbon-water relations*. San Diego: Academic Press, 19–28.

Ögren E**. 1993.** Convexity of the photosynthetic light-response curve in relation to intensity and direction of light during growth. *Plant Physiol* **101**: 1013–1019.

Ögren E**, Öquist** G**, Hällgren** J-E**. 1984.** Photoinhibition of photosynthesis in *Lemna gibba* as induced by the interaction between light and temperature. I. Photosynthesis *in vivo*. *Physiol Plant* **62**: 181–186.

Ogren WL**. 1984.** Photorespiration: pathways, regulation, and modification. *Annu Rev Plant Physiol* **35**: 415–442.

Oguchi R**, Douwstra** P**, Fujita** T**, Chow** WS**, Terashima** I**. 2011.** Intra-leaf gradients of photoinhibition induced by different color lights: implications for the dual mechanisms of photoinhibition and for the application of conventional chlorophyll fluorometers. *New Phytol* **191**: 146–159.

Oguchi R**, Hihosaka** K**, Hirose** T**. 2005.** Leaf anatomy as a constraint for photosynthetic acclimation: differential responses in leaf anatomy to increasing growth irradiance among three deciduous trees. *Plant Cell Environ* **28**: 916–927.

Oguchi R**, Onoda** Y**, Terashima** I**, Tholen** D **2018.** Leaf anatomy and function. In: Adams WW, Terashima I eds. *The Leaf: A Platform for Performing Photosynthesis*. Cham: Springer International Publishing, 97–139.

Ohnishi N**, Allakhverdiev** SI**, Takahashi** S**, Higashi** S**, Watanabe** M**, Nishiyama** Y**, Murata** N**. 2005.** Two-step mechanism of photodamage to photosystem II: step 1 occurs at the oxygen-evolving complex and step 2 occurs at the photochemical reaction center. *Biochemistry* **44**: 8494–8499.

Öquist G**, Brunes** L**, Hällgren** J**. 1982.** Photosynthetic efficiency of *Betula pendula* acclimated to different quantum flux densities. *Plant Cell Environ* **5**: 9–15.

Osborne SA**, Mills** G**, Hayes** F**, Ainsworth** EA**, Büker** P**, Emberson** L**. 2016.** Has the sensitivity of soybean cultivars to ozone pollution increased with time? An analysis of published dose–response data. *Glob Change Biol* **22**: 3097–3111.

Osmond CB **1994.** What is photoinhibition? Some insights from comparisons of shade and sun plants. In: Baker NR, Bowyer JR eds. *Photoinhibition of Photosynthesis from Molecular Mechanisms to the Field,*. Oxford: Bios Scientific Publishers, 1–24.

Osmond CB**, Holtum** JAM **1981.** Crassulacean acid metabolism. In: Stumpf PK, Conn EE eds. *The Biochemistry of Plants A Comprehensive Treatise*. New York: Academic Press.

Osmond CB**, Winter** K**, Ziegler** H **1982.** Functional significance of different pathways of CO 2 fixation in photosynthesis. In: Lange OL, Nobel PS, Osmond CB, Ziegler H eds. *Physiological Plant Ecology*. Berlin: Springer, 479–547.

Osmond CB**, Ziegler** H**, Stichler** W**, Trimborn** P. **1975.** Carbon isotope discrimination in alpine succulent plants supposed to be capable of crassulacean acid metabolism (CAM). *Oecologia* **18**: 209–217.

Pascal AA**, Liu** Z**, Broess** K**, van Oort** B**, van Amerongen** H**, Wang** C**, Horton** P**, Robert** B**, Chang** W**, Ruban** A**. 2005.** Molecular basis of photoprotection and control of photosynthetic light-harvesting. *Nature* **436**: 134.

Pasquet-Kok J**, Creese** C**, Sack** L**. 2010.** Turning over a new 'leaf': multiple functional significances of leaves versus phyllodes in Hawaiian *Acacia koa*. *Plant Cell Environ* **33**: 2084–2100.

Patel A**, Ting** IP**. 1987.** Relationship between respiration and CAM-cycling in *Peperomia camptotricha*. *Plant Physiol* **84**: 640–642.

Pearcy R**. 1988.** Photosynthetic utilisation of light-flecks by understory plants. *Funct Plant Biol* **15**: 223–238.

Pearcy RW**. 1977.** Acclimation of photosynthetic and respiratory carbon dioxide exchange to growth temperature in *Atriplex lentiformis* (Torr.) Wats. *Plant Physiol* **59**: 795–799.

Pearcy RW**. 1990.** Sunflecks and photosynthesis in plant canopies. *Annu Rev Plant Biol* **41**: 421–453.

Pedersen O**, Colmer** TD**, Revsbech** NP**, Garcia-Robledo** E**. 2018.** CO_2 and O_2 dynamics in leaves of aquatic plants with C_3 or CAM photosynthesis – application of a novel CO_2 microsensor. *Ann Bot* **122**: 605–615.

Peguero-Pina JJ**, Sisó** S**, Flexas** J**, Galmés** J**, García-Nogales** A**, Niinemets** Ü**, Sancho-Knapik** D**, Saz** MÁ**, Gil-Pelegrín** E**. 2017.** Cell-level anatomical characteristics explain high mesophyll conductance and photosynthetic capacity in sclerophyllous Mediterranean oaks. *New Phytol* **214**: 585–596.

Pikart FC**, Marabesi** MA**, Mioto** PT**, Gonçalves** AZ**, Matiz** A**, Alves** FRR**, Mercier** H**, Aidar** MPM**. 2018.** The contribution of weak CAM to the photosynthetic metabolic activities of a bromeliad species under water deficit. *Plant Physiol Bochem* **123**: 297–303.

Pimienta-Barrios E**, Robles-Murguia** C**, Nobel** PS**. 2001.** Net CO_2 Uptake for *Agave tequilana* in a warm and a temperate environment. *Biotropica* **33**: 312–318.

Plaut Z**, Mayoral** ML**, Reinhold** L**. 1987.** Effect of altered sink: source ratio on photosynthetic metabolism of source leaves. *Plant Physiol* **85**: 786–791.

Pons TL **2016.** Regulation of leaf traits in canopy gradients. In: Hikosaka K, Niinemets Ü, Anten NPR eds. *Canopy Photosynthesis: From Basics to Applications*. Dordrecht: Springer Netherlands, 143–168.

Pons TL**, Pearcy** RW**. 1992.** Photosynthesis in flashing light in soybean leaves grown in different conditions. II. Lightfleck utilization efficiency. *Plant Cell Environ* **15**: 577–584.

Pons TL**, Pearcy** RW**. 1994.** Nitrogen reallocation and photosynthetic acclimation in response to partial shading in soybean plants. *Physiol Plant* **92**: 636–644.

Pons TL**, Ribas-Carbo** M**, Flexas** J**, Evans** JR**, von Caemmerer** S**, Genty** B**, Brugnoli** E**. 2009.** Estimating mesophyll conductance to CO_2: methodology, potential errors, and recommendations. *J Exp Bot* **60**: 2217–2234.

Pons TL**, Van der Werf** A**, Lambers** H **1994.** Photosynthetic nitrogen use efficiency of inherently slow and fast growing species: possible explanations for observed differences. In: Roy J, Garnier E eds. *A Whole Plant Perspective of Carbon Nitrogen Interactions*. The Hague: SPB Academic Publishing, 61–77.

Pons TL**, Welschen** RAM**. 2002.** Overestimation of respiration rates in commercially available clamp-on leaf chambers. Complications with measurement of net photosynthesis. *Plant Cell Environ* **25**: 1367–1372.

Poot P**, Pilon** J**, Pons** TL**. 1996.** Photosynthetic characteristics of leaves of male-sterile and hermaphrodite sex types of *Plantago lanceolata* grown under conditions of contrasting nitrogen and light availabilities. *Physiol Plant* **98**: 780–790.

Portis A. **2003.** Rubisco activase - Rubisco's catalytic chaperone. *Photosyn Res* **75**: 11–27.

Portis AR**, Salvucci** ME**, Ogren** WL**. 1986.** Activation of ribulosebisphosphate carboxylase/oxygenase at physiological CO_2 and ribulosebisphosphate concentrations by Rubisco activase. *Plant Physiol* **82**: 967–971.

Pottier M**, Gilis** D**, Boutry** M**. 2018.** The hidden face of Rubisco. *Trends Plant Sci* **23**: 382–392.

Prins HBA**, Elzenga** JTM**. 1989.** Bicarbonate utilization: function and mechanism. *Aquat Bot* **34**: 59–83.

Pyankov VI**, Kondratchuk** AV**. 1995.** Specific features of structural organization of photosynthetic apparatus of the East Pamirs plants. *Proc Russ Acad Sci* **344**: 712–716.

Pyankov VI**, Kondratchuk** AV**. 1998.** Structure of the photosynthetic apparatus in woody plants from different ecological and altitudinal groups in Eastern Pamir. *Russ J Plant Physiol* **45**: 481–490.

Rangan P**, Furtado** A**, Henry** RJ**. 2016.** New evidence for grain specific C_4 photosynthesis in wheat. *Sci Rep* **6**: 31721.

Reich PB**, Schoettle** AW**. 1988.** Role of phosphorus and nitrogen in photosynthetic and whole plant carbon gain and nutrient use efficiency in eastern white pine. *Oecologia* **77**: 25–33.

Reich PB**, Walters** MB**, Ellsworth** DS**. 1997.** From tropics to tundra: global convergence in plant functioning. *Proc Natl Acad Sci USA* **94**: 13730–13734.

Reiskind JB**, Madsen,** T.V.**, Van Ginkel,** L.C.**, Bowes,** G. **1997.** Evidence that inducible C_4-type photosynthesis is a chloroplastic CO_2-concentrating mechanism in *Hydrilla*, a submersed monocot. *Plant Cell Environ* **20**: 211–220.

Rodeghiero M**, Niinemets** Ü**, Cescatti** A**. 2007.** Major diffusion leaks of clamp-on leaf cuvettes still unaccounted: how erroneous are the estimates of Farquhar et al. model parameters? *Plant Cell Environ* **30**: 1006–1022.

Rogers A**, Fischer** BU**, Bryant** J**, Frehner** M**, Blum** H**, Raines** CA**, Long** SP**. 1998.** Acclimation of photosynthesis to elevated CO_2 under low-nitrogen nutrition is affected by the capacity for assimilate utilization. Perennial ryegrass under free-air CO_2 enrichment. *Plant Physiol* **118**: 683–689.

Rolland F**, Baena-Gonzalez** E**, Sheen** J**. 2006.** Sugar sensing and signaling in plants: conserved and novel mechanisms. *Annu Rev Plant Biol* **57**: 675–709.

Rolland F**, Moore** B**, Sheen** J. **2002.** Sugar sensing and signaling in plants. *Plant Cell* **14**: S185.

Rühle W**, Wild** A**. 1979.** The intensification of absorbance changes in leaves by light-dispersion. *Planta* **146**: 551–557.

Sacharz J**, Giovagnetti** V**, Ungerer** P**, Mastroianni** G**, Ruban** AV**. 2017.** The xanthophyll cycle affects reversible interactions between PsbS and light-harvesting complex II to control non-photochemical quenching. *Nat Plants* **3**: 16225.

Sack L**, Scoffoni** C**, John** GP**, Poorter** H**, Mason** CM**, Mendez-Alonzo** R**, Donovan** LA**. 2013.** How do leaf veins influence the worldwide leaf economic spectrum? Review and synthesis. *J Exp Bot* **64**: 4053–4080.

Sage RF**. 2004.** The evolution of C_4 photosynthesis. *New Phytol* **161**: 341–370.

Sage RF**. 2016.** A portrait of the C_4 photosynthetic family on the 50th anniversary of its discovery: species number, evolutionary lineages, and Hall of Fame. *J Exp Bot* **67**: 4039–4056.

Sage RF**, Kubien** DS**. 2003.** Quo vadis C_4? An ecophysiological perspective on global change and the future of C4 plants. *Photosyn Res* **77**: 209–225.

Sage RF**, Pearcy** RW**. 1987a.** The nitrogen use efficiency of C_3 and C_4 pants. II. Leaf nitrogen effects on the gas exchange characteristics of *Chenopodium album* (L.) and *Amaranthus retroflexus* (L.). *Plant Physiol* **84**: 959–963.

Sage RF**, Pearcy** RW**. 1987b.** The nitrogen use efficiency or C_3 and C_4 plants. I. Leaf nitrogen, growth, and biomass partitioning in *Chenopodium album* (L.) and *Amaranthus retroflexus*. *Plant Physiol* **84**: 954–958.

Sage RF**, Sage** TL**, Kocacinar** F**. 2012.** Photorespiration and the evolution of C_4 Photosynthesis. *Annu Rev Plant Biol* **63**: 19–47.

Sage RF**, Sharkey** TD**. 1987.** The effect of temperature on the occurrence of O_2 and CO_2 insensitive photosynthesis in field grown plants. *Plant Physiol* **84**: 658–664.

Sage RF**, Sultmanis** S. **2016.** Why are there no C_4 forests? *J Plant Physiol* **203**: 55–68.

Salvucci ME**. 1989.** Regulation of Rubisco activity *in vivo*. *Physiol Plant* **77**: 164–171.

Salvucci ME**, Crafts-Brandner** SJ**. 2004.** Relationship between the heat tolerance of photosynthesis and the thermal stability of Rubisco activase in plants from contrasting thermal environments. *Plant Physiol* **134**: 1460–1470.

Sand-Jensen K**, Jensen** RS**, Gomes** M**, Kristensen** E**, Martinsen** KT**, Kragh** T**, Baastrup-Spohr** L**, Borum** J**. 2018.** Photosynthesis and calcification of charophytes. *Aquat Bot* **149**: 46–51.

Sassenrath-Cole GF**, Pearcy** RW**, Steinmaus** S**. 1994.** The role of enzyme activation state in limiting carbon assimilation under variable light conditions. *Photosyn Res* **41**: 295–302.

Savveyn A**, Steppe** K**, UBIERNA** N**, Dawson** TE**. 2010.** Woody tissue photosynthesis and its contribution to trunk growth and bud development in young plants. *Plant Cell Environ* **33**: 1949–1958.

Scarano FR**, de Mattos** EA**, Franco** AC**, Cavalin** PO**, Orthen** B**, Fernandes** GW**, Lüttge** U**. 2016.** Features of CAM-cycling expressed in the dry season by terrestrial and epiphytic plants of *Clusia arrudae* Planchon and Triana in two rupestrian savannas of southeastern Brazil in comparison to the C3-species *Eremanthus glomerulatus* Less. *Trees* **30**: 913–922.

Schreiber U**, Bilger** W**, Neubauer** C **1995a.** Chlorophyll fluorescence as a non-intrusive indicator for rapid assessment of in vivo photosynthesis. In: Schulze ED, Caldwell MM eds. *Ecophysiology of Photosynthesis*. Berlin: Springer-Verlag, 49–70.

Schreiber U**, Hormann** H**, Neubauer** C**, Klughammer** C. **1995b.** Assessment of photosystem II photochemical quantum yield by chlorophyll fluorescence quenching analysis. *Funct Plant Biol* **22**: 209–220.

Schulze E-D**, Kelliher** FM**, Körner** C**, Lloyd** J**, Leuning** R**. 1994.** Relationships among maximum stomatal conductance, ecosystem surface conductance, carbon assimilation rate, and plant nitrogen nutrition: a global ecology scaling exercise. *Annu Rev Ecol Syst* **25**: 629–662.

Senn G. **1908.** *Die Gestalts-und Lageveränderung der Pflanzen-Chromatophoren: mit einer Beilage: Die Lichtbrechung der lebenden Pflanzenzelle*. Leipzig: W. Engelmann.

Shao H**, Jiang** HS**, Li** W**, Cao** Y**, Huang** WM**, Gontero** B**, Maberly** SC**. 2017.** Responses of *Ottelia alismoides*, an aquatic plant with three CCMs, to variable CO_2 and light. *J Exp Bot* **68**: 3985–3995.

Sharkey TD**. 2005.** Effects of moderate heat stress on photosynthesis: importance of thylakoid reactions, rubisco deactivation, reactive oxygen species, and thermotolerance provided by isoprene. *Plant Cell Environ* **28**: 269–277.

Sharkey TD**, Bernacchi** CJ**, Farquhar** GD**, Singsaas** EL**. 2007.** Fitting photosynthetic carbon dioxide response curves for C_3 leaves. *Plant Cell Environ* **30**: 1035–1040.

Sharkey TD**, Seemann** JR**, Pearcy** RW**. 1986a.** Contribution of metabolites of photosynthesis to postillumination CO_2 assimilation in response to lightflects *Plant Physiol* **82**: 1063–1068.

Sharkey TD**, Stitt** M**, Heineke** D**, Gerhardt** R**, Raschke** K**, Heldt** HW**. 1986b.** Limitation of photosynthesis by carbon metabolism: II. O_2-insensitive CO_2 uptake results from limitation of triose phosphate utilization. *Plant Physiol* **81**: 1123–1129.

Silvera K**, Neubig** KM**, Whitten** WM**, Williams** NH**, Winter** K**, Cushman** JC**. 2010.** Evolution along the crassulacean acid metabolism continuum. *Funct Plant Biol* **37**: 995–1010.

Sims DA**, Pearcy** RW**. 1989.** Photosynthetic characteristics of a tropical forest understory herb, *Alocasia macrorrhiza*, and a related crop species, *Colocasia esculenta* grown in contrasting light environments. *Oecologia* **79**: 53–59.

Slattery RA**, Walker** BJ**, Weber** APM**, Ort** DR**. 2018.** The impacts of fluctuating light on crop performance. *Plant Physiol* **176**: 990–1003.

Smedley MP**, Dawson** TE**, Comstock** JP**, Donovan** LA**, Sherrill** DE**, Cook** CS**, Ehleringer** JR**. 1991.** Seasonal carbon isotope discrimination in a grassland community. *Oecologia* **85**: 314–320.

Smeekens S**, Hellmann** H**. 2014.** Sugar sensing and signaling in plants. *Front Plant Sci* **5**: 113.

Smith JAC**, Ingram** J**, Tsiantis** MS**, Barkla** BJ**, Bartholomew** DM**, Bettey** M**, Pantoja** O**, Pennington** AJ **1996.** Transport across the vacuolar membrane in CAM plants. In: Winter K, Smith JAC eds. *Crassulacean Acid Metabolism: Biochemistry, Ecophysiology and Evolution*. Berlin: Springer, 53–71.

Snaydon RW**. 1991.** The productivity of C_3 and C_4 plants: a reassessment. *Funct Ecol* **5**: 321–330.

Sternberg LOR**, Deniro** MJ**, Ting** IP**. 1984.** Carbon, hydrogen, and oxygen isotope ratios of cellulose from plants having intermediary photosynthetic modes *Plant Physiol* **74**: 104–107.

Stitt M**, Hurry** V**. 2002.** A plant for all seasons: alterations in photosynthetic carbon metabolism during cold acclimation in *Arabidopsis*. *Curr Opin Plant Biol* **5**: 199–206.

Sulpice R**, Ishihara** H**, Schlereth** A**, Cawthray** GR**, Encke** B**, Giavalisco** P**, Ivakov** A**, Arrivault** S**, Jost**

R, **Krohn** N, **Kuo** J, **Laliberté** E, **Pearse** SJ, **Raven** JA, **Scheible** WR, **Teste** F, **Veneklaas** EJ, **Stitt** M, **Lambers** H. **2014.** Low levels of ribosomal RNA partly account for the very high photosynthetic phosphorus-use efficiency of Proteaceae species. *Plant Cell Environ* **37**: 1276–1298.

Sweet KJ, **Peak** D, **Mott** KA. **2017.** Stomatal heterogeneity in responses to humidity and temperature: Testing a mechanistic model. *Plant Cell Environ* **40**: 2771–2779.

Takahashi F, **Suzuki** T, **Osakabe** Y, **Betsuyaku** S, **Kondo** Y, **Dohmae** N, **Fukuda** H, **Yamaguchi-Shinozaki** K, **Shinozaki** K. **2018.** A small peptide modulates stomatal control via abscisic acid in long-distance signalling. *Nature* **556**: 235–238.

Tardieu F. **2013.** Plant response to environmental conditions: assessing potential production, water demand, and negative effects of water deficit. *Frontiers in Physiology* **4**: 17.

Tcherkez GGB, **Farquhar** GD, **Andrews** TJ. **2006.** Despite slow catalysis and confused substrate specificity, all ribulose bisphosphate carboxylases may be nearly perfectly optimized. *Proceedings of the National Academy of Sciences, USA* **103**: 7246–7251.

Teixeira MC, **de Oliveira Vieira** T, **de Almeida** TCM, **Vitória** AP. **2015.** Photoinhibition in Atlantic Forest native species: short-term acclimative responses to high irradiance. *Theor Exp Plant Physiol* **27**: 183–189.

Terashima I, **Hanba** YT, **Tazoe** Y, **Vyas** P, **Yano** S. **2006.** Irradiance and phenotype: comparative eco-development of sun and shade leaves in relation to photosynthetic CO_2 diffusion. *J Exp Bot* **57**: 343–354.

Terashima I, **Hikosaka** K. **1995.** Comparative ecophysiology of leaf and canopy photosynthesis. *Plant Cell Environ* **18**: 1111–1128.

Terashima I, **Miyazawa** S-I, **Hanba** YT. **2001.** Why are sun leaves thicker than shade leaves? -- Consideration based on analyses of CO_2 diffusion in the leaf. *J Plant Res* **114**: 93–105.

Terashima I, **Wong** S-C, **Osmond** CB, **Farquhar** GD. **1988.** Characterisation of Non-Uniform Photosynthesis Induced by Abscisic Acid in Leaves Having Different Mesophyll Anatomies. *Plant Cell Physiol* **29**: 385–394.

Tikhonov AN, **Vershubskii** AV. **2017.** Connectivity between electron transport complexes and modulation of photosystem II activity in chloroplasts. *Photosyn Res* **133**: 103–114.

Tombesi S, **Nardini** A, **Frioni** T, **Soccolini** M, **Zadra** C, **Farinelli** D, **Poni** S, **Palliotti** A. **2015.** Stomatal closure is induced by hydraulic signals and maintained by ABA in drought-stressed grapevine. *Sci Rep* **5**: 12449.

Ueno O. **2001.** Environmental regulation of C_3 and C_4 dfferentiation in the amphibious sedge *Eleocharis vivipara*. *Plant Physiol* **127**: 1524–1532.

Van Oosten J-J, **Besford** RT. **1995.** Some relationships between the gas exchange, biochemistry and molecular biology of photosynthesis during leaf development of tomato plants after transfer to different carbon dioxide concentrations. *Plant Cell Environ* **18**: 1253–1266.

Van Oosten J-J, **Wilkins** D, **Besford** RT. **1995.** Acclimation of tomato to different carbon dioxide concentrations. Relationships between biochemistry and gas exchange during leaf development. *New Phytol* **130**: 357–367.

Vandegehuchte MW, **Bloemen** J, **Vergeynst** LL, **Steppe** K. **2015.** Woody tissue photosynthesis in trees: salve on the wounds of drought? *New Phytol* **208**: 998–1002.

Veneklaas EJ, **Lambers** H, **Bragg** J, **Finnegan** PM, **Lovelock** CE, **Plaxton** WC, **Price** C, **Scheible** W-R, **Shane** MW, **White** PJ, **Raven** JA. **2012.** Opportunities for improving phosphorus-use efficiency in crop plants. *New Phytol* **195**: 306–320.

Vernon DM, **Ostrem** JA, **Schmitt** JM, **Bohnert** HJ. **1988.** PEPCase transcript Levels in *Mesembryanthemum crystallinum* decline rapidly upon relief from salt stress. *Plant Physiol* **86**: 1002–1004.

Vogelmann TC. **1993.** Plant tissue optics. *Annu Rev Plant Biol* **44**: 231–251.

Vogelmann TC, **Evans** JR. **2002.** Profiles of light absorption and chlorophyll within spinach leaves from chlorophyll fluorescence. *Plant Cell Environ* **25**: 1313–1323.

Vogelmann TC, **Nishio** JN, **Smith** WK. **1996.** Leaves and light capture: Light propagation and gradients of carbon fixation within leaves. *Trends Plant Sci* **1**: 65–70.

von Caemmerer S. **2000.** *Biochemical Models of Leaf Photosynthesis*. Collingwood: CSIRO Publishing.

von Caemmerer S, **Farquhar** GD. **1981.** Some relationships between the biochemistry of photosynthesis and the gas exchange of leaves. *Planta* **153**: 376–387.

von Caemmerer S, **Farquhar** GD. **1984.** Effects of partial defoliation, changes of irradiance during growth, short-term water stress and growth at enhanced p(CO2) on the photosynthetic capacity of leaves of Phaseolus vulgaris L. *Planta* **160**: 320–329.

von Caemmerer S, **Quick** WP, **Furbank** RT. **2012.** The development of C_4 rice: current progress and future challenges. *Science* **336**: 1671–1672.

Wakabayashi K, **Böger** P. **2002.** Target sites for herbicides: entering the 21st century. *Pest Manage Sci* **58**: 1149–1154.

Wang D, **Portis** AR, **Moose** SP, **Long** SP. **2008.** Cool C_4 photosynthesis: pyruvate P_i dikinase expression and activity corresponds to the exceptional cold tolerance of carbon assimilation in *Miscanthus* × *giganteus*. *Plant Physiol* **148**: 557–567.

Warren CR. **2007.** Stand aside stomata, another actor deserves centre stage: the forgotten role of the internal conductance to CO_2 transfer. *J Exp Bot* **59**: 1475–1487.

Warren CR, **Adams** MA. **2006.** Internal conductance does not scale with photosynthetic capacity: implications for carbon isotope discrimination and the economics of water and nitrogen use in photosynthesis. *Plant Cell Environ* **29**: 192–201.

Way DA, **Pearcy** RW. **2012.** Sunflecks in trees and forests: from photosynthetic physiology to global change biology. *Tree Physiol* **32**: 1066–1081.

Weger HG, **Silim** SN, **Guy** RD. **1993.** Photosynthetic acclimation to low temperature by western red cedar seedlings. *Plant Cell Environ* **16**: 711–717.

Weston DJ**, Bauerle** WL**, Swire-Clark** GA**,** Moore **Bd, Baird** WV**. 2007.** Characterization of Rubisco activase from thermally contrasting genotypes of *Acer rubrum* (Aceraceae). *Am J Bot* **94**: 926–934.

Wingenter K**, Schulz** A**, Wormit** A**, Wic** S**, Trentmann** O**, Hoermiller** II**, Heyer** AG**, Marten** I**, Hedrich** R**, Neuhaus** HE**. 2010.** Increased activity of the vacuolar monosaccharide transporter TMT1 alters cellular sugar partitioning, sugar signaling, and seed yield in *Arabidopsis*. *Plant Physiol* **154**: 665–677.

Wingler A**. 2018.** Transitioning to the next phase: the role of sugar signaling throughout the plant life cycle. *Plant Physiol* **176**: 1075–1084.

Winkel A**, Borum** J**. 2009.** Use of sediment CO_2 by submersed rooted plants. *Ann Bot* **103**: 1015–1023.

Winter K**, Holtum** JAM**, Smith** JAC**. 2015.** Crassulacean acid metabolism: a continuous or discrete trait? *New Phytol* **208**: 73–78.

Winter K**, Medina** E**, Garcia** V**, Luisa Mayoral** M**, Muniz** R**. 1985.** Crassulacean Acid Metabolism in roots of a leafless orchid, *Campylocentrum tyrridion* Garay and Dunsterv. *J Plant Physiol* **118**: 73–78.

Winter K**, Smith** JAC **1996.** An introduction to crassulaceaen acid metabolism. Biochemical principles and ecological diversity. In: Winter K, Smith JAC eds. *Crassulacean Acid Metabolism, Biochemistry, Ecophysiology and Evolution Ecological Studies,* Berlin: Springer-Verlag, 1–13.

Winter K**, Zotz** G**, Baur** B**, Dietz** K-J**. 1992.** Light and dark CO_2 fixation in *Clusia uvitana* and the effects of plant water status and CO_2 availability. *Oecologia* **91**: 47–51.

Wright IJ**, Reich** PB**, Westoby** M. **2001.** Strategy shifts in leaf physiology, structure and nutrient content between species of high- and low-rainfall and high- and low-nutrient habitats. *Funct Ecol* **15**: 423–434.

Wright IJ**, Reich** PB**, Westoby** M**, Ackerly** DD**, Baruch** Z**, Bongers** F**, Cavender-Bares** J**, Chapin** T**, Cornelissen** JHC**, Diemer** M**, Flexas** J**, Garnier** E**, Groom** PK**, Gulias** J**, Hikosaka** K**, Lamont** BB**, Lee** T**, Lee** W**, Lusk** C**, Midgley** JJ**, Navas** M-L**, Niinemets** Ü**, Oleksyn** J**, Osada** N**, Poorter** H**, Poot** P**, Prior** L**, Pyankov** VI**, Roumet** C**, Thomas** SC**, Tjoelker** MG**, Veneklaas** EJ**, Villar** R**. 2004.** The worldwide leaf economics spectrum. *Nature* **428**: 821–827.

Wu M-X**, Wedding** RT**. 1987.** Temperature effects on phosphoenolpyruvate carboxylase from a CAM and a C4 plant : a comparative study. *Plant Physiol* **85**: 497–501.

Wullschleger SD**, Tschaplinski** TJ**, Norby** RJ**. 2002.** Plant water relations at elevated CO_2– implications for water-limited environments. *Plant Cell Environ* **25**: 319–331.

Yamazaki J-Y**. 2010.** Is light quality involved in the regulation of the photosynthetic apparatus in attached rice leaves? *Photosyn Res* **105**: 63–71.

Yamori W**. 2016.** Photosynthetic response to fluctuating environments and photoprotective strategies under abiotic stress. *J Plant Res* **129**: 379–395.

Yamori W**, Hikosaka** K**, Way** DA**. 2014.** Temperature response of photosynthesis in C_3, C_4, and CAM plants: temperature acclimation and temperature adaptation. *Photosyn Res* **119**: 101–117.

Yamori W**, Noguchi** K**, Hanba** YT**, Terashima** I**. 2006a.** Effects of internal conductance on the temperature dependence of the photosynthetic rate in spinach leaves from contrasting growth temperatures. *Plant Cell Physiol* **47**: 1069–1080.

Yamori W**, Suzuki** K**, Noguchi** K**, Nakai** M**, Terashima** I**. 2006b.** Effects of Rubisco kinetics and Rubisco activation state on the temperature dependence of the photosynthetic rate in spinach leaves from contrasting growth temperatures. *Plant Cell Environ* **29**: 1659–1670.

Yano S**, Terashima** I**. 2001.** Separate localization of light signal perception for sun or shade type chloroplast and palisade tissue differentiation in *Chenopodium album*. *Plant Cell Physiol* **42**: 1303–1310.

Yeoh HH**, Badger** M**, Watson** L**. 1981.** Variations in kinetic properties of ribulose–1,5-bisphosphate carboxylases among plants. *Plant Physiol* **67**: 1151–1155.

Yu K**, D'Odorico** P**, Li** W**, He** Y**. 2017.** Effects of competition on induction of crassulacean acid metabolism in a facultative CAM plant. *Oecologia* **184**: 351–361.

Zhang T**, Cao** Y**, Chen** Y**, Liu** G**. 2015.** Non-structural carbohydrate dynamics in *Robinia pseudoacacia* saplings under three levels of continuous drought stress. *Trees* **29**: 1837–1849.

Zhu H**, Zhang** T-J**, Zheng** J**, Huang** X-D**, Yu** Z-C**, Peng** C-L**, Chow** WS**. 2018a.** Anthocyanins function as a light attenuator to compensate for insufficient photoprotection mediated by nonphotochemical quenching in young leaves of *Acmena acuminatissima* in winter. *Photosynthetica* **56**: 445–454.

Zhu L**, Bloomfield** KJ**, Hocart** CH**, Egerton** JJG**, O'Sullivan** OS**, Penillard** A**, Weerasinghe** LK**, Atkin** OK**. 2018b.** Plasticity of photosynthetic heat tolerance in plants adapted to thermally contrasting biomes. *Plant Cell Environ* **41**: 1251–1262.

Zscheile FP**, Comar** CL**. 1941.** Influence of preparative procedure on the purity of chlorophyll components as shown by absorption spectra. *Bot Gaz* **102**: 463–481.

3 Photosynthesis, Respiration, and Long-Distance Transport: Respiration

3.1 Introduction

Plants use a large portion of the carbohydrates that they assimilate each day in respiration in the same period (Table 3.1). If we seek to explain the carbon balance of a plant and to understand plant performance and growth in different environments, it is imperative to obtain a good understanding of respiration. Plant need **dark respiration** to produce energy and carbon skeletons to sustain plant growth; however, a significant part of respiration may proceed via a **nonphosphorylating pathway**. This is a cyanide-resistant pathway that generates less ATP than the **cytochrome pathway**, which is the primary energy-producing pathway in both plants and animals. We present several hypotheses in this chapter to explore why plants have a respiratory pathway that is not linked to ATP production (Del-Saz et al. 2018).

The types and rates of plant respiration are controlled by a combination of **respiratory capacity**, **energy demand**, **substrate availability**, and **O_2 supply** (Covey-Crump et al. 2002, 2007). At low levels of O_2, respiration cannot proceed by normal aerobic pathways, and fermentation starts to take place, with **ethanol** and **lactate** as major end-products. The ATP yield of fermentation is considerably less than that of normal aerobic respiration. In this chapter, we discuss the control over respiratory processes, the demand for respiratory energy, and the significance of respiration for the plant's carbon balance, as these are influenced by species and environment.

3.2 General Characteristics of the Respiratory System

3.2.1 The Respiratory Quotient

The respiratory pathways in plant tissues include **glycolysis**, which is located both in the cytosol and in the plastids, the **oxidative pentose phosphate pathway**, which is also located in both the plastids and the cytosol, the **tricarboxylic acid** (TCA) or **Krebs cycle**, in the matrix of mitochondria, and the **electron-transport pathways**, which reside in the inner mitochondrial membrane.

The **respiratory quotient** (*RQ*, the ratio between the number of moles of CO_2 released and that of O_2 consumed) is a useful index for the types of substrates used in respiration and the subsequent use of respiratory energy to support biosynthesis (Hanf et al. 2015). In the absence of biosynthetic processes, we expect the *RQ* of respiration to be 1.0, if sucrose is the only substrate for respiration and is fully oxidized to CO_2 and H_2O. When **leaves** of *Phaseolus vulgaris* (common bean) are exposed to an extended dark period or to high temperatures, their *RQ* declines, due to a shift from **carbohydrates** as the main substrate for respiration to **fatty acids** (Tcherkez et al. 2003). Likewise, shaded *Pinus sylvestris*

H. Lambers, R. S. Oliveira, *Plant Physiological Ecology*, https://doi.org/10.1007/978-3-030-29639-1_3

Table 3.1 Utilization of photosynthates in plants, as dependent on the nutrient supply*.

Item	Utilization of photosynthates % of C fixed	
	Free nutrient availability	Limiting nutrient supply
Shoot growth	40∗–57	15–27∗
Root growth	17–18∗	33∗–35
Shoot respiration	17–24∗	19–20∗
Root respiration	8–19∗	38∗–52
growth	3.5–4.6∗	6∗–9
maintenance	0.6–2.6∗	?
ion acquisition	4–13∗	?
Volatile losses	0–8	0–8
Exudation	negligible	<23
N_2-fixation	negligible	4–14
Mycorrhiza	negligible	4–16

Sources: Van der Werf et al. (1994); Kaschuk et al. (2009)
∗, inherently slow-growing species; ?, no information available

Table 3.2 The respiratory quotient (*RQ*) of root respiration of a number of herbaceous species*.

Species	*RQ*	Special remarks
Allium cepa	1.0	Root tips
	1.3	Basal parts
Dactylis glomerata	1.2	
Festuca ovina	1.0	
Galinsoga parviflora	1.6	
Helianthus annuus	1.5	
Holcus lanatus	1.3	
Hordeum distichum	1.0	
Lupinus albus	1.4	
	1.6	N_2-fixing
Oryza sativa	1.0	NH_4^+-fed
	1.1	
Pisum sativum	0.8	NH_4^+-fed
	1.0	
	1.4	N_2-fixing
Zea mays	1.0	Fresh tips
	0.8	Starved tips

Source: Various authors, as summarized in Lambers et al. (2002)
*All plants were grown in nutrient solution, with nitrate as the N-source, unless stated otherwise. The *Pisum sativum* (pea) plants were grown with a limiting supply of NH_4^+, so that their growth matched that of the symbiotically grown N_2-fixing plants

(Scots pine) trees shift from **carbohydrate**-dominated to **lipid**-dominated respiration and show progressive carbohydrate depletion (Fischer et al. 2015). Protein degradation and associated amino acid catabolism under stress conditions also leads to a decrease in *RQ* (Araújo et al. 2011). For **roots** of young seedlings, measured in the absence of an N source, values are close to 1.0, but most experimental *RQ* values differ from unity (Table 3.2). *RQ* values for germinating **seeds** depend on the storage compounds in the seeds. For seeds of *Triticum aestivum* (wheat), in which **carbohydrates** are major storage compounds, *RQ* is close to unity, whereas for the **fat**-storing seeds of *Linum usitatissimum* (flax) *RQ* values as low as 0.4 are found (Stiles and Leach 1936).

Both the nature of the respiratory substrate and biosynthetic reactions strongly influence *RQ*. The *RQ* can be greater than 1.0, if **organic acids** are an important substrate, because these are more oxidized than sucrose, and, therefore, produce more CO_2 per unit O_2. On the other hand, *RQ* will be less than 1, if compounds that are more reduced than sucrose (*e.g.*, **lipids** and **protein**) are a major substrate, as occurs during starvation of leaves and excised root tips (Table 3.2). In **shoots** of *Hordeum vulgare* (barley) that receive $\mathbf{NH_4^+}$ as their sole N source, respiratory fluxes of O_2 equal those of CO_2. By contrast, shoots exposed to $\mathbf{NO_3^-}$, show a greater CO_2 evolution than O_2 consumption in the dark (*RQ* = 1.25). These results show that a substantial portion of respiratory electron transport generates reductant for NO_3^- assimilation, producing an additional two molecules of CO_2 per molecule of NO_3^- reduced to NH_4^+. Substrates available to support root respiration depend on processes occurring throughout the plant. For example, organic acids (malate) that are produced during the reduction of NO_3^- in leaves can be transported and decarboxylated in the roots, releasing CO_2 and increasing *RQ* (Ben Zioni et al. 1971). If $\mathbf{NO_3^-}$ **reduction** proceeds in the roots, then the *RQ* is also expected to be greater than 1.0. Values of *RQ* are therefore lower in plants that use NH_4^+ as an N source

than in plants grown with NO_3^- or, symbiotically, with N_2 (Table 3.2).

Biosynthesis influences *RQ* in several ways. Carboxylating reactions consume CO_2, reducing *RQ*, whereas decarboxylating reactions produce CO_2 and, therefore, increase *RQ*. In addition, synthesis of oxidized compounds such as organic acids decreases *RQ*, whereas the production of reduced compounds such as lipids leads to higher *RQ* values. The average molecular formula of the biochemical compounds typical of plant biomass is more reduced than sucrose, so *RQ* values influenced by biosynthesis should be greater than 1, as generally observed (Table 3.2; for further information, see Table 3.11 in Sect. 3.5.2.2).

RQ values of root respiration increase with increasing potential **growth rate** of a species (Fig. 3.1). This results from fast rates of biosynthesis, relative to rates of ATP production; as explained above, ATP production associated with sucrose breakdown is associated with an *RQ* of 1.0, whereas biosynthesis yields *RQ* values greater than 1.0 (Scheurwater et al. 2002).

In summary, the patterns of *RQ* in plants clearly demonstrate that in roots it depends on the plant's growth rate. For all organs, it depends on the predominant respiratory substrate, integrated whole-plant processes, and ecological differences among species.

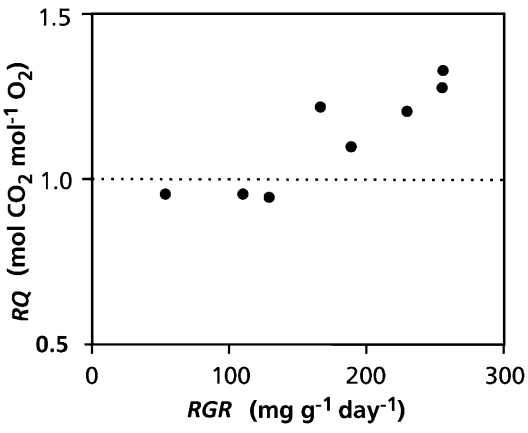

Fig. 3.1 The respiratory quotient (*RQ*) of a number of fast- and slow-growing grass species, grown with free access to nutrients and with nitrate as the source of nitrogen (Scheurwater et al. 1998).

3.2.2 Glycolysis, the Pentose Phosphate Pathway, and the Tricarboxylic (TCA) Cycle

The first step in the production of energy for respiration occurs when glucose, or starch or other storage carbohydrates are metabolized in glycolysis or in the oxidative pentose phosphate pathway (Fig. 3.2). **Glycolysis** involves the conversion of glucose, via phospho*enol*pyruvate (PEP), into malate and pyruvate. In contrast to mammalian cells, where virtually all PEP is converted into pyruvate, in plant cells, malate is the major end-product of glycolysis, and thus the major substrate for the mitochondria. Key enzymes in glycolysis are controlled by adenylates (AMP, ADP, and ATP), in such a way as to speed up the rate of glycolysis when the demand for metabolic energy (ATP) increases (Plaxton and Podestá 2006).

Oxidation of one glucose molecule in glycolysis produces two **malate** molecules, without a net production of ATP. When **pyruvate** is the end-product, there is a net production of two ATP molecules and two NADH molecules in glycolysis. Despite the production of NADH in one step in glycolysis, there is no net production of NADH when malate is the end-product, due to the need for NADH in the reduction of oxaloacetate, catalyzed by malate dehydrogenase.

Unlike glycolysis, which is predominantly involved in the breakdown of sugars and ultimately in the production of ATP, the **oxidative pentose phosphate pathway** plays a more important role in producing intermediates (*e.g.*, amino acids, nucleotides) and NADPH. There is no evidence for a control of this pathway by the demand for energy.

The malate and pyruvate that are formed in glycolysis in the cytosol are imported into the mitochondria, where they are oxidized in the **tricarboxylic acid (TCA) cycle**. Complete oxidation of one molecule of malate, yields four molecules of CO_2, five molecules of NADH and one molecule of $FADH_2$, as well as one molecule of ATP (Fig. 3.2). NADH and $FADH_2$ subsequently donate their electrons to the electron-transport chain (Sect. 3.2.3.1).

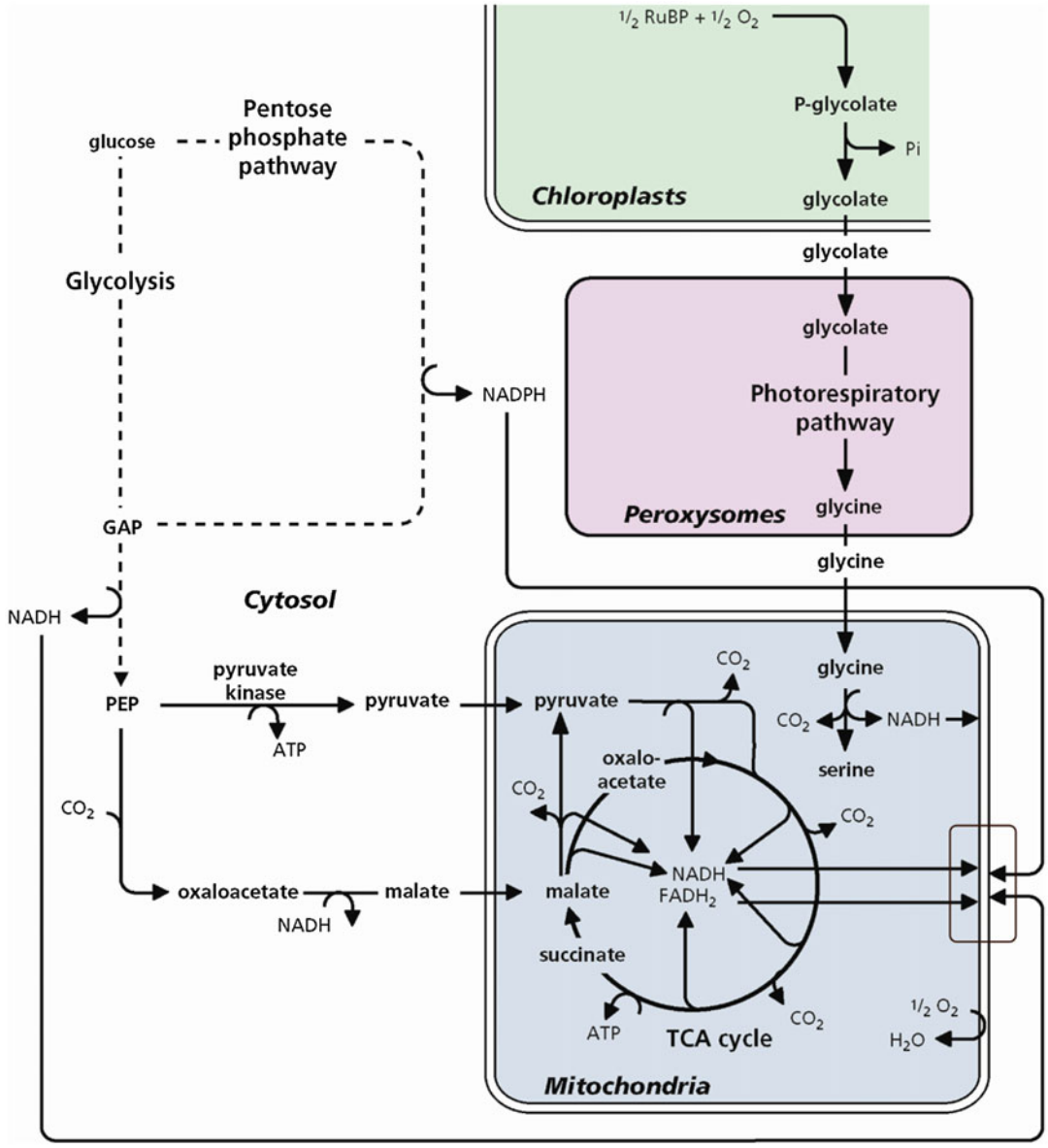

Fig. 3.2 The major substrates for the electron transport pathways. Glycine is only a major substrate in photosynthetically active cells of C_3 plants when photorespiration plays a role.

3.2.3 Mitochondrial Metabolism

The malate formed in glycolysis in the cytosol is imported into the mitochondria and oxidized partly via **malic enzyme**, which produces pyruvate and CO_2, and partly via **malate dehydrogenase**, which produces oxaloacetate. Pyruvate is then oxidized so that malate is regenerated (Fig. 3.2). In addition, pyruvate can be produced in the cytosol and imported into the mitochondria. Oxidation of malate, pyruvate, and other NAD-linked substrates is associated with complex I and other NADH dehydrogenases (Sect. 3.2.3.1). In mitochondria there are four major complexes associated with **electron transfer** and one associated with **oxidative**

phosphorylation, all located in the inner mitochondrial membrane. In addition, there are two small redox molecules, **ubiquinone** (Q) and **cytochrome c**, which play a role in electron transfer. In plant mitochondria there is also a cyanide-resistant, nonphosphorylating, **alternative oxidase**, located in the inner membrane (Fig. 3.3). Finally, there are additional NAD(P)H dehydrogenases in the inner mitochondrial membrane that allow electron transport without ATP formation as well as **uncoupling proteins** that converts energy that could have been used for ATP production into heat.

In the mitochondrial **matrix** the imported substrates are oxidized in a metabolic cycle (**Krebs** or **TCA cycle**), releasing three $\mathbf{CO_2}$ molecules per pyruvate in each cycle and generating reducing power (**NADH** and $\mathbf{FADH_2}$) in several reactions (Fig. 3.2). The pyruvate dehydrogenase complex (PDC) converts pyruvate into **acetyl-CoA**, which then reacts with oxaloacetate to produce citrate, is a major control point for entry of carbon into the TCA cycle.

3.2.3.1 The Complexes of the Electron-Transport Chain

Complex I is the main entry point of electrons from NADH produced in the **TCA cycle** or in **photorespiration**. Complex I generates a proton motive force (i.e. an electrochemical potential gradient across a membrane) and is the **first coupling site** or **site 1** of proton extrusion from the matrix into the intermembrane space which is linked to ATP production. Succinate is the only intermediate of the TCA cycle that is oxidized by a membrane-bound enzyme: succinate dehydrogenase (Fig. 3.3). Electrons enter the respiratory chain via complex II, and are transferred to ubiquinone. NAD(P)H that is produced outside the mitochondria also feeds electrons into the chain at the level of ubiquinone (Fig. 3.3). The external dehydrogenases are also not connected with the translocation of H^+ across the inner mitochondrial membrane. Hence, less ATP is produced per O_2 when succinate or external NAD(P)H are oxidized in comparison with that of glycine, malate, or citrate, which enter at complex I. Complex III transfers electrons from

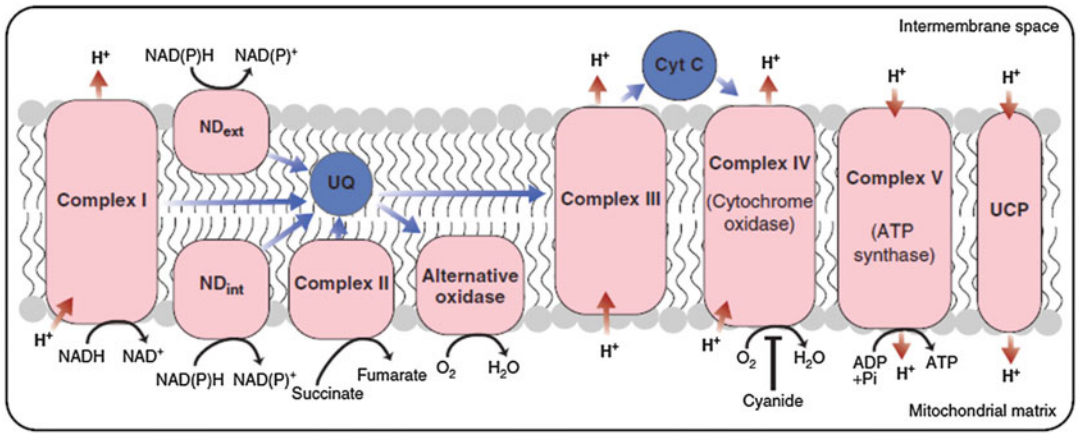

Fig. 3.3 Organization of electron transport processes occurring within the inner membrane of plant mitochondria. This illustration provides details of the phosphorylating cytochrome pathway (electrons flow to complex IV), which generates the proton-motive force for ATP synthesis by ATP synthase, and the nonphosphorylating alternative pathway (electrons pass directly to O_2 via the alternative oxidase, AOX). Complex I oxidizes NADH and complex II (succinate dehydrogenase of the TCA cycle) oxidizes succinate via $FADH_2$. Alternative, NAD(P)H dehydrogenases bypassing complex I exist on the external (ND_{ex}) and internal (ND_{in}) side of the inner membrane. Uncoupling protein (UCP) allows dissipation of the proton-motive force without ATP synthesis. Abbreviations: UQ, ubiquinone; Cyt c, cytochrome c (after O'Leary and Plaxton 2016);

ubiquinone to cytochrome c, coupled to the extrusion of protons to the intermembrane space; it is **site 2** of proton extrusion from the matrix into the intermembrane space. Complex IV is the terminal oxidase of the cytochrome pathway, accepting electrons from cytochrome c and donating these to O_2, and **site 3** of proton extrusion. The five complexes (complexes I–V) can be extracted in the form of active supercomplexes. Single-particle electron microscopy has provided two- and three-dimensional images showing interactions between complexes (Dudkina et al. 2010).

3.2.3.2 A Cyanide-Resistant Terminal Oxidase

Mitochondrial respiration of many tissues from plants is not fully inhibited by inhibitors of the cytochrome path (*e.g.*, KCN), because of the presence of a cyanide-resistant, alternative electron-transport pathway. This pathway consists of a single enzyme, the **alternative oxidase**, embedded in the inner leaflet of the inner mitochondrial membrane (Del-Saz et al. 2018). The branching point of the alternative path from the cytochrome path is at the level of ubiquinone, a component common to both pathways. Transfer of electrons from ubiquinone to O_2 via the alternative path is not coupled to the extrusion of protons from the matrix to the intermembrane space. Hence, the transfer of electrons from NADH produced inside the mitochondria to O_2 via the alternative path bypasses two sites of proton extrusion, and therefore yields considerably less ATP than is produced when complex I and the cytochrome path are used.

3.2.3.3 Substrates, Inhibitors, and Uncouplers

Figure 3.2 summarizes the major substrates for mitochondrial O_2 uptake as well as their origin. Oxidation of glycine is of quantitative importance only in tissues exhibiting **photorespiration**. Glycolysis may start with glucose, as depicted here, or with starch, sucrose, or any major transport carbohydrate or sugar alcohol imported via the phloem (Sect. 4.2).

A range of respiratory inhibitors have helped to elucidate the organization of the respiratory pathways. To give just one example, **cyanide** effectively blocks complex IV and has been used to demonstrate the presence of the alternative path. **Uncouplers** make membranes, including the inner mitochondrial membrane, permeable to protons and hence prevent oxidative phosphorylation. Many compounds that inhibit components of the respiratory chain or have an uncoupling activity occur naturally as **secondary compounds** in plant and fungal tissues; they may protect these tissues from being grazed or infected by other organisms or be released from roots and act as allelochemicals (Sects 13.2 and 13.3.1). A more recent addition to the complexity of the plant mitochondrial electron-transport chain is the discovery of **uncoupling protein** (UCP) (Figueira and Arruda 2011). UCP is a homologue of thermogenin, a protein responsible for thermogenesis in mammalian brown fat cells. Both uncoupling protein and thermogenin allow protons to diffuse down their concentration gradient from the intermembrane space into the matrix, circumventing the ATP synthase complex and thus uncoupling electron transport from ATP production (Plaxton and Podestá 2006).

3.2.3.4 Respiratory Control

To learn more about the manner in which plant respiration responds to the demand for metabolic energy, we first describe some experiments with **isolated mitochondria**. Freshly isolated intact mitochondria in an appropriate buffer that lacks substrates, a condition referred to as ‘state 1’, do not consume an appreciable amount of O_2; *in vivo* they rely on a continuous import of respiratory substrate from the cytosol (Fig. 3.4). Upon addition of a respiratory substrate (‘state 2’) there is some, but still not much O_2 uptake; for rapid rates of respiration to occur *in vivo*, import of additional metabolites is required. As soon as ADP is added, a rapid consumption of O_2 can be measured. This ‘state’ of the mitochondria is called ‘state 3’. *In vivo,* rapid supply of ADP will occur when a large amount of ATP is required to drive biosynthetic and transport processes. Upon conversion of all ADP into ATP

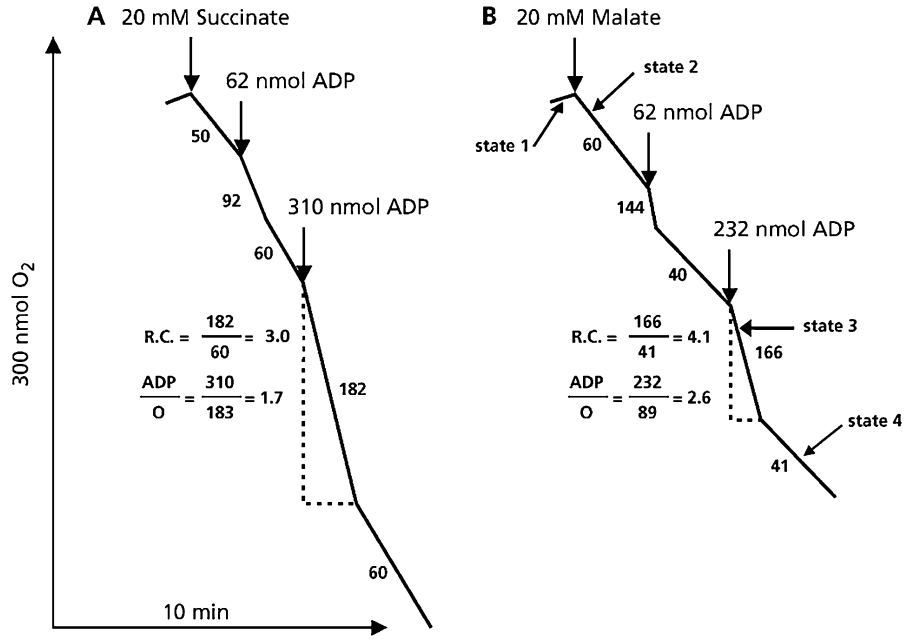

Fig. 3.4 The respiratory 'states' of isolated mitochondria. The ADP:O ratio (also called ATP:O ratio or P:O ratio) is calculated from the O_2 consumption during the phosphorylation of a known amount of added ADP (state 3). The amount of ADP consumed equals the amount that has been added to the cuvette (310 and 232 nmol in A and B, respectively); since the total amount of O_2 in the cuvette is known (300 nmol), the amount consumed during the consumption of the added ADP can be derived (dashed vertical lines, with values of 183 and 89 nmol of O atoms in **A** and **B**, respectively). The respiratory control ratio (RC) is the ratio of the rate of O_2 uptake (in nmol O_2 mg^{-1} protein min^{-1}; values written along the slopes) in state 3 and state 4. State 1 refers to the respiration in the absence of respiratory substrate and ADP, and state 2 is the respiration after addition of respiratory substrate, but before addition of ADP (based on unpublished data on potato mitochondria from A.M. Wagner, Free University of Amsterdam).

('state 4'), the respiration rate of the mitochondria declines again to the rate found before addition of ADP (Fig. 3.4). Upon addition of more ADP, the mitochondria go into state 3 again, followed by state 4 upon depletion of ADP. This can be repeated until all O_2 in the cuvette is consumed. Thus the respiratory activity of isolated mitochondria is effectively controlled by the availability of ADP: **respiratory control**, quantified in the 'respiratory control ratio' (the ratio of the rate at substrate saturation in the presence of ADP and that under the same conditions, but after ADP has been depleted; Fig. 3.4). The same respiratory control occurs in intact tissues, and is one of the mechanisms ensuring that the rate of respiration is enhanced when the demand for ATP increases.

3.2.4 A Summary of the Major Points of Control of Plant Respiration

We briefly discussed the control of glycolysis by 'energy demand' (Sect. 3.2.2) and a similar control by 'energy demand' of mitochondrial electron transport, termed respiratory control (Sect. 3.2.3.4). The effects of **energy demand** on dark respiration are a function of the metabolic energy that is required for **growth**, **maintenance**, and **transport** processes; therefore, when organs grow quickly, take up ions rapidly and/or have a fast turnover of proteins, they generally have a fast rate of respiration (Smith and Dukes 2018). At low levels of **respiratory substrate supply** (carbohydrates, organic acids), however, the activity of respiratory pathways may be

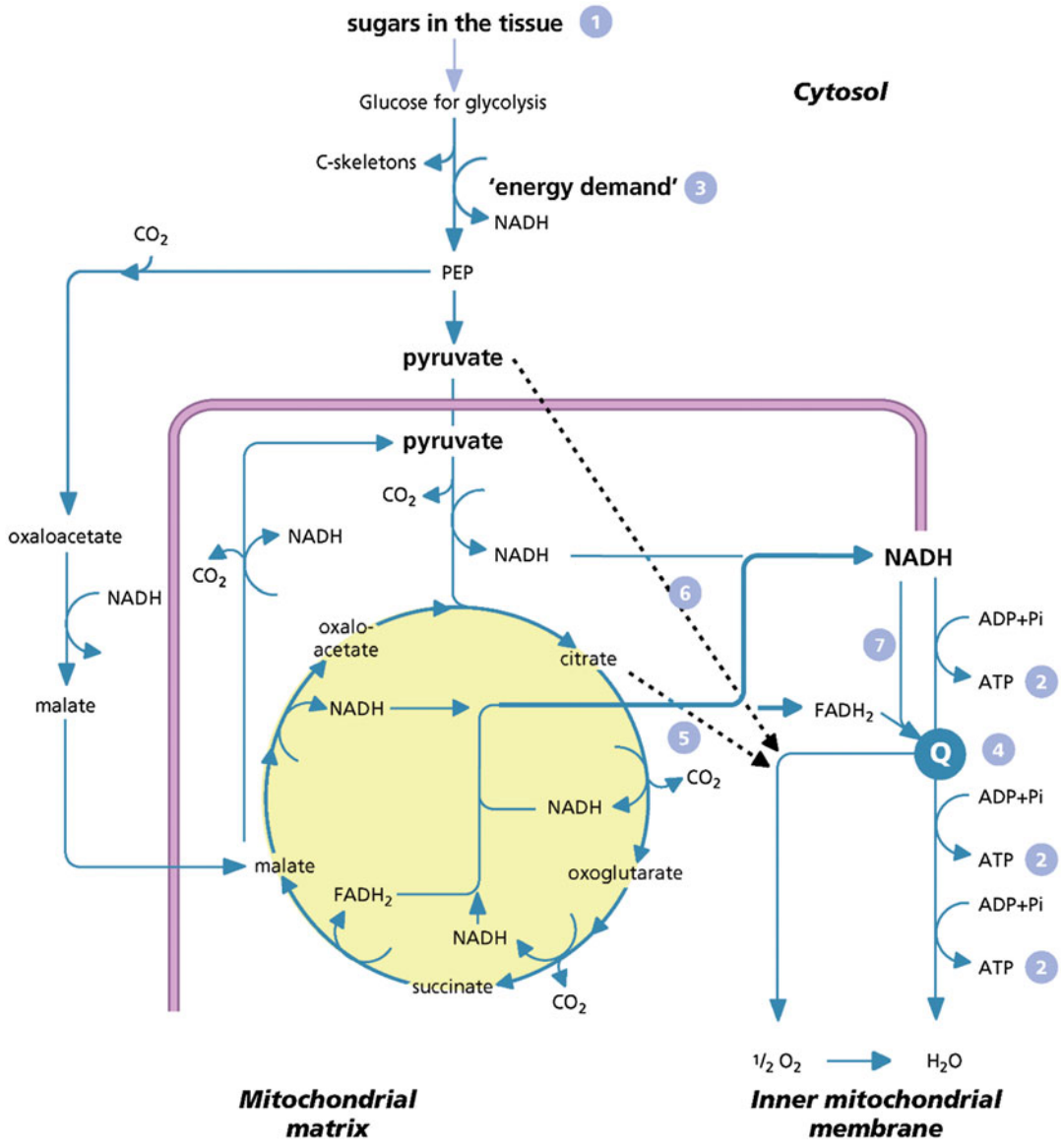

Fig. 3.5 A simplified scheme of respiration and its major control points. Controlling factors include the concentration of respiratory substrate [*e.g.*, glucose (1)] and adenylates (2, 3). Adenylates may exert control on electron transport via a constraint on the rate of oxidative phosphorylation (2) as well as on glycolysis, via modulation of the activity of key enzymes in glycolysis, phosphofructokinase and pyruvate kinase ('energy demand', 3). When the input of electrons into the respiratory chain is very high, a large fraction of ubiquinone becomes reduced and the alternative path becomes more active (4). When the rate of glycolysis is very fast, relative to the activity of the cytochrome path, organic acids may accumulate (5, 6). Accumulation of citric acid may lead to reduction of the sulfide bonds of AOX and thus enhance the capacity of the alternative path (5). Accumulation of pyruvate or other 2-oxoacids may increase the V_{max} of the alternative oxidase, and, hence, allow it to function at a low level of reduced ubiquinone (6). There is increasing evidence that the nonphosphorylating rotenone-insensitive bypass (7) operates in concert with the alternative path, when the concentration of NADH is very high.

substrate-limited. When substrate levels increase, the respiratory capacity is enhanced and adjusted to the high substrate input, through the transcription of specific genes that encode respiratory enzymes. Figure 3.5 summarizes these and several other points of control. Plant respiration is

clearly quite flexible and responds rapidly to the demand for respiratory energy as well as the supply of respiratory substrate. The production of ATP, which is coupled to the oxidation of substrate, may also vary widely, due to the presence of both nonphosphorylating and phosphorylating paths [alternative oxidase and NAD(P)H dehydrogenases other than complex I] as well as the activity of an uncoupling protein.

3.2.5 ATP Production in Isolated Mitochondria and *in Vivo*

The rate of O_2 consumption during the phosphorylation of ADP can be related to the total ADP that must be added to consume this O_2. This allows calculation of the **ADP:O ratio** *in vitro*. This ratio is around 2.5 for NAD-linked substrates (*e.g.*, malate, citrate) and around 1.5 for succinate and external NAD(P)H. Nuclear Magnetic Resonance (NMR) spectroscopy has been used to estimate ATP production in intact tissues, as outlined in Sect. 3.2.5.2.

3.2.5.1 Oxidative Phosphorylation: The Chemiosmotic Model

During the transfer of electrons from various substrates to O_2 via the cytochrome path, protons are extruded into the space between the inner and outer mitochondrial membranes. This generates a **proton-motive force** across the inner mitochondrial membrane which drives the synthesis of ATP. The basic features of this **chemiosmotic model** are (Mitchell 1961, 1966; Nicholls and Ferguson 2013):

1. Protons are transported outwards, coupled to the transfer of electrons, thus giving rise to both a **proton gradient** (ΔpH; more acid outside) and a **membrane potential** (ΔΨ; negative inside) across the inner mitochondrial membrane;
2. The inner membrane is **impermeable to protons** and other ions, except by special transport systems;
3. There is an **ATP synthetase** (ATPase), which transforms the energy of the electrochemical gradient generated by the proton-extruding system into ATP.

The pH gradient, ΔpH, and the membrane potential, ΔΨ, are interconvertible. It is the combination of the two that forms the **proton-motive force** (Δp), the driving force for ATP synthesis, catalyzed by an ATPase:

$$\Delta p = \Delta\Psi - 2.3(RT/F) \times \Delta\mathrm{pH} \qquad (3.1)$$

where R is the gas constant (J mol^{-1} K^{-1}), T is the absolute temperature (K) and F is Faraday's number (Coulomb). Both components in the equation are expressed in mV.

3.2.5.2 ATP Production in Vivo

ATP production *in vivo* can be measured using **NMR spectroscopy**. This technique relies on the fact that certain nuclei, including ^{31}P, possess a permanent magnetic moment, because of nuclear spin. Such nuclei can be made 'visible' in a strong external magnetic field, in which they orient their nuclear spins in the same direction. It is just like the orientation of a small magnet in response to the presence of a strong one. NMR spectroscopy allows us to monitor the absorption of radiofrequency by the oriented spin population in the strong magnetic field. The location of the peaks in a NMR spectrum depends on the molecule in which the nucleus is present and on the 'environment' of the molecule (*e.g.*, pH). Figure 3.6 illustrates this point for a range of P-containing molecules (Roberts 1984).

The resonance of specific P-containing compounds can be altered by irradiation with radiofrequency power. If this irradiation is sufficiently strong ('saturating'), then it disorientates the nuclear spins of that P-containing compound, so that its peak disappears from the spectrum. Figure 3.7A illustrates this for the γ-ATP P-atom, the P atom that is absent in ADP. Upon hydrolysis of ATP, the γ-ATP P atom becomes part of the cytoplasmic inorganic phosphate (Pi) pool. For a brief period, therefore, some of the Pi molecules also contain disoriented nuclear spins; specific radiation of the γ-ATP peak decreases the Pi peak. This phenomenon is called 'saturation transfer' (Fig. 3.7). Saturation transfer has been used to estimate the rate of ATP hydrolysis to ADP and Pi *in vivo*.

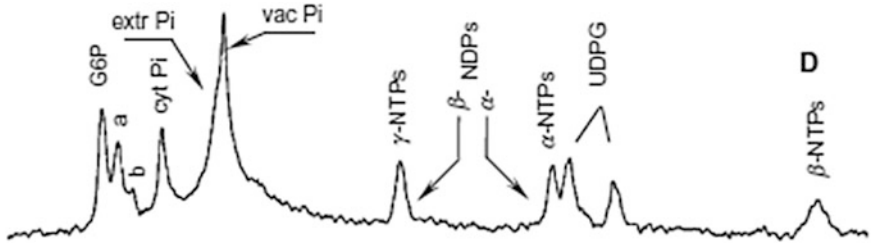

Fig. 3.6 *In vivo* ^{31}P nuclear magnetic resonance spectra of compressed *Nicotiana tabacum* (tobacco) cells treated with inorganic phosphorus (Pi). Pi-starved cells were first equilibrated with continuously aerated Pi-free perfusion medium to reach a semi-metabolic steady state. The cells were subsequently pulsed with 1 mm Pi. Peak assignment: G6P, glucose-6-phosphate; peak a, position of fructose-6-phosphate, ribose-5-phosphate, other sugar phosphates and phosphomonoesters; cyt Pi, cytoplasmic Pi; extr Pi, extracellular Pi, vac Pi, vacuolar Pi; α-, β- and γ-NTPs, α-, β- and γ-nucleoside triphosphates; UDPG, uridine-5-′-diphosphate-α-D-glucose (Danova-Alt et al. 2008).

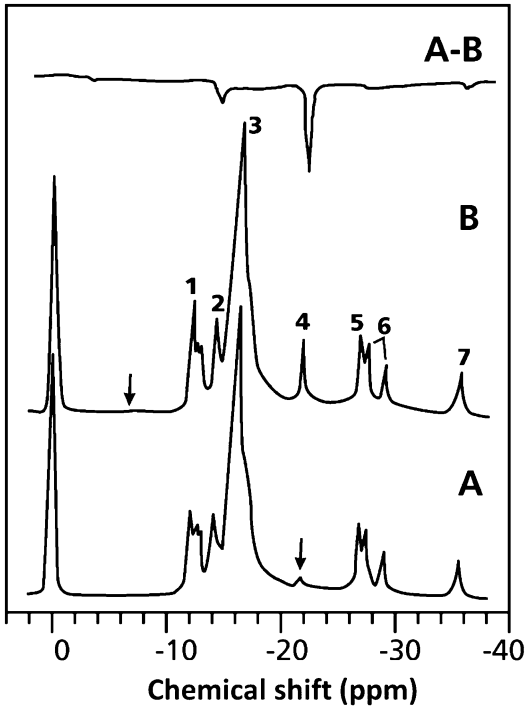

Fig. 3.7 Saturation transfer from γ-ATP phosphate to cytosolic P_i in root tips of *Zea mays* (maize). Spectrum A was obtained with selective presaturation of the γ-ATP peak. Spectrum B was obtained with selective presaturation of a point equidistant from the cytosolic Pi peak, Spectrum A-B gives the difference between the two spectra, showing the transfer of saturation from γ-ATP to cytosolic Pi (after Roberts et al. 1984).

If the rate of disappearance of the saturation in the absence of biochemical exchange of phosphate between γ-ATP and Pi is known, then the rate of ATP hydrolysis can be derived from the rate of loss of saturation. This has been done for root tips for which the O_2 uptake was measured in parallel experiments. In this manner ADP:O ratios in *Zea mays* (maize) root tips exposed to a range of conditions have been determined (Table 3.3).

The ADP:O ratios for the root tips supplied with 50 mM glucose are remarkably close to those expected when glycolysis plus TCA cycle are responsible for the complete oxidation of exogenous glucose, provided the alternative path does not contribute to the O_2 uptake (Table 3.3). KCN decreases the ADP:O ratio of glucose oxidation by two-thirds in a manner to be expected from mitochondrial studies. SHAM, an inhibitor of the alternative path, has no effect on the rate of ATP production. So far, maize root tips are the only intact plant material used for the determination of ADP:O ratios *in vivo*. We cannot assume, therefore, that the ADP:O ratio *in vivo* is invariably 3. In fact, the ratio under most circumstances is probably far less than 3 (Sect. 3.2.6.2).

In sensor lines of *Arabidopsis thaliana*, it is possible to use an assay for ATP changes in living plants using a fluorescent protein biosensor

Table 3.3 The *in vivo* ADP:O ratios in root tips of *Zea mays* (corn) determined with the saturation transfer ^{31}P NMR technique and O_2 uptake measurements.

Exogenous substrate	O_2 concentration	Inhibitor	Rate of O_2 uptake	Rate of ATP production	ADP:O ratio
Glucose	100	None	22	143	3.2
Glucose	0	None	0	<20	–
None	100	None	15	93	3.0
Glucose	100	KCN	14	26	1.0
Glucose	100	KCN +SHAM	4	<20	–
Glucose	100	SHAM	21	137	3.2

Source: Roberts et al. (1984)

*The O_2 concentration was either that in air (100) or zero. Rates of ATP production and O_2 consumption are expressed as nmol g^{-1} FM s^{-1}. Exogenous glucose was supplied at 50 mM. The concentration of KCN was 0.5 mM and that of SHAM was 2 mM; this is sufficiently high to fully block the alternative path in maize root tips

(De Col et al. 2017). An ATP map of seedlings highlights differences in ATP concentrations between tissues and within individual cell types, such as root hairs.

3.2.6 Regulation of Electron Transport *via* the Cytochrome and the Alternative Paths

The existence of two respiratory pathways, both transporting electrons to O_2, in plant mitochondria, raises the question if and how the **partitioning of electrons** between the two paths is regulated. This is important because the cytochrome path is coupled to proton extrusion and the production of ATP, whereas transport of electrons via the alternative path is not, at least not beyond the point where both pathways branch to O_2 (Del-Saz et al. 2018).

3.2.6.1 Competition or Overflow?

Under specific conditions, the activity of the cytochrome path *in vitro* increases linearly with the fraction of ubiquinone (Q, the common substrate with the alternative path) that is in its reduced state (Q_r/Q_t). By contrast, the alternative path shows no appreciable activity until a substantial (30–40%) fraction of the Q is in its reduced state, and then the activity increases exponentially (Fig. 3.8). This would suggest that the alternative path functions as an 'energy overflow'; however, this is an over-simplification, as outlined below.

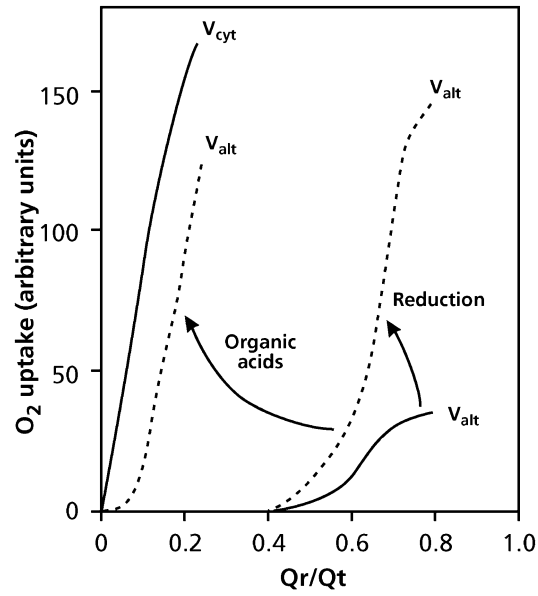

Fig. 3.8 Dependence of the activity of the cytochrome path and of the alternative path on the fraction of ubiquinone that is in the reduced state (Q_r/Q_t). When the alternative oxidase (AOX) is in its 'reduced' (higher-activity) configuration, it has a greater capacity to accept electrons. In its reduced state, AOX can be affected by 2-oxoacids, which enhance its activity at low levels of Q_r. Based on Dry et al. (1989); Umbach et al. (1994); Day et al. (1995); Hoefnagel et al. (1997).

3.2.6.2 The Intricate Regulation of the Alternative Oxidase

Depending on metabolic state, the activity of the alternative pathway changes, so that it competes with the cytochrome pathway for electrons. When embedded in the inner mitochondrial membrane,

the alternative oxidase (AOX) exists as a **dimer**. When an intersubunit disulfide bond covalently links the two subunits, AOX is inactive. When this bond is broken by reduction of the disulfide to dithiols, then the AOX subunits become noncovalently associated. This results in a **higher-activity state**, as opposed to the **lower-activity state** when the subunits are covalently linked (O'Leary and Plaxton 2016).

Roots of *Glycine max* (soybean) seedlings initially have a very rapid respiration rate, and almost all of this respiration occurs *via* the cytochrome path (Fig. 3.9A). At this stage, the activity of the alternative path is very low and the enzyme is in its lower-activity state. Within a few days, the growth rate and the cytochrome oxidase activity decline by about 75%, and the contribution of the alternative path to root respiration increases to more than 50%. At that stage, all the dimers are in their higher-activity state, suggesting that the transition from partly oxidized to fully reduced is responsible for the increased AOX activity (Millar et al. 1998). A similar change from oxidized to reduced occurs in leaves

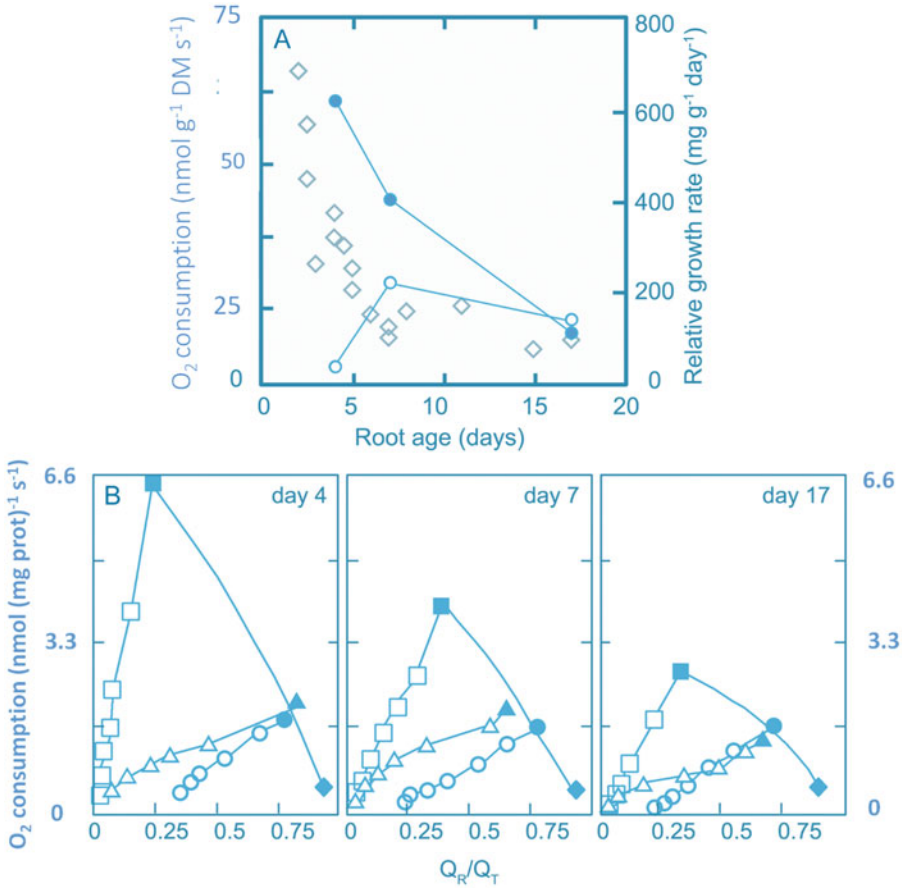

Fig. 3.9 Root respiration, growth and the activity of isolated mitochondria for young *Glycine max* (soybean) seedlings. (**A**) O_2 consumption via the cytochrome path (filled circles) and the alternative path (open circles), and the relative growth rate (diamonds). (**B**) Succinate-dependent O_2 consumption and Q-pool reduction state in isolated mitochondria (4-, 7-, and 17-days old seedlings). Data points are in the presence (squares) and in the absence (triangles) of ADP, and in the presence of myxothiazol with (circles) or without (diamonds) added pyruvate. Filled symbols denote data in the absence of malonate; open symbols are data from malonate titration of succinate oxidation (modified after Millar et al. 1998).

of *Alocasia odora* (Asian taro) upon exposure to high-light stress (Sect. 3.4.4). In intact roots of *Poa annua* (annual meadow-grass) and other grasses, however, AOX is invariably in its reduced, higher-activity configuration (Millenaar et al. 1998, 2000). There is, therefore, no clear evidence that changes in redox state of AOX play an important regulatory role *in vivo* during plant development.

The capacity of AOX to oxidize its substrate (Q_r) increases in the presence TCA-cycle intermediates that act in an isoform-specific manner (Selinski et al. 2018). As a result, in the presence of the potent activator **pyruvate**, the alternative path shows significant activity, even when less than 30% of ubiquinone is in its reduced state, when the cytochrome pathway is not fully saturated (Fig. 3.8; Millar et al. 1998). In intact tissues, pyruvate levels appear to be sufficiently high to fully activate AOX. That is, changes in the level of activating organic acids may not play a significant regulatory role *in vivo* (Del-Saz et al. 2018).

Whenever AOX is in its higher-activity state and active at low levels of Q_r, there will be competition for electrons between the two pathways, both *in vitro* (Millar et al. 2011) and *in vivo* (Atkin et al. 1995). Does competition for electrons between the two pathways really occur at the levels of Q_r that are commonly found *in vivo* (about 55% reduced) (Millar et al. 1998)? *In vitro* studies with mitochondria isolated from tissues of which we know that the alternative path contributes to respiration provides the answer (Fig. 3.9B). In the presence of succinate, but no ADP (state 4; Fig. 3.4), most of Q is reduced. Upon addition of ADP (state 3; Fig. 3.4), Q becomes more oxidized, until ADP is depleted. Activation of AOX by pyruvate oxidizes Q to a level similar to that found *in vivo*. Blocking the cytochrome path leads to Q being more reduced again. Since AOX contributes substantially to root respiration at a Q_r level of 55%, the activation mechanisms must operate. Because Q_r levels *in vivo* are similar to those in state 4, Fig. 3.8B also suggests that mitochondrial electron transport in roots is probably restricted by ADP (Fig. 3.5).

Decreasing expression of a single AOX isoform commonly leads to reduced plant performance, particularly under adverse conditions, indicating that AOX is not simply a 'wasteful pathway'. The question of why other AOX isoforms cannot compensate when a single AOX has been suppressed remains to be further investigated (Selinski et al. 2018). The finding that TCA-cycle intermediates differentially activate different AOX isoforms and that the extent and operation of the TCA cycle differ between tissues renders correct tissue- and cell-specific regulation of AOX an essential feature.

3.2.6.3 Mitochondrial NAD(P)H Dehydrogenases That Are Not Linked to Proton Extrusion

In addition to AOX (Sect. 3.2.3.2) and uncoupling proteins (Sect. 3.2.3.3), there are **NAD(P)H dehydrogenases** that allow electron transport without proton extrusion (Rasmusson et al. 2008; Fig. 3.3). A network of mitochondrial dehydrogenases supplies electrons for the respiratory chain. Entry of electrons via various pathways depends on the metabolic state of the plant cell. The regulation of electron entry pathways into the respiratory chain might depend on the formation of supramolecular structures (Schertl and Braun 2014).

Addition of NO_3^- to N-limited seedlings of *Arabidopsis thaliana* (thale cress) decreases the transcript abundance of NAD(P)H dehydrogenase and **AOX** genes, while addition of NH_4^+ increases the expression of the same gene families. Switching between NO_3^- and NH_4^+ in the absence of N stress leads to very similar results. Corresponding changes in alternative respiratory pathway capacities are exhibited in seedlings supplied with either NO_3^- or NH_4^+ as an N source and in mitochondria purified from the seedlings (Escobar et al. 2006). The parallel changes in both respiratory bypasses suggests that the NAD(P) dehydrogenases play a similar role as AOX (Sect. 3.3).

3.3 The Ecophysiological Function of the Alternative Path

Why should plants produce and maintain a pathway that supports nonphosphorylating electron transport in mitochondria? Do they really differ fundamentally from animals in this respect, or do animals have functional alternatives? Plants that have an AOX perform better under adverse growth conditions (Selinski et al. 2018). This Section discusses the merits of some of the hypotheses put forward to explain the presence of the alternative path in plants. Testing of these hypotheses involved the use of transgenics lacking or overexpressing alternative path activity.

3.3.1 Heat Production

An important consequence of the lack of coupling to ATP production in the alternative pathway is that the energy produced by oxidation is released as **heat**. de Lamarck (1778) described heat production in *Arum italicum* (Italian arum), and much later **thermogenesis** was linked to **cyanide-resistant respiration** (Meeuse 1975). Floral thermogenesis occurs in 11 families of extant angiosperms, with three families (five genera) in the first three branches of the angiosperm phylogenetic tree, and only two families in the eudicots (Thien et al. 2009). This **heat production** is ecologically important in, *e.g.*, *Macrozamia macleayi* cycad cones, to attract pollinators (Terry et al. 2016). An exponential rise in ß-myrcene emission only occurs after a major increase in respiration. When respiration during thermogenesis is interrupted by anoxic conditions, ß-myrcene emissions decrease. The increased emission rates are not a result of increased cone temperature *per se*, but depend on biosynthetic pathways associated with increased respiration during thermogenesis that provide the carbon, energy (ATP), and reducing compounds (NADPH) required for ß-myrcene production. These findings establish the significant contribution of respiration to thermogenesis and volatile production during thermogenesis to facilitate the movement of the specialist *Cycadothrips* pollinator out of cones (Terry et al. 2014, 2016).

Heat production also occurs in the flowers of several South American *Annona* species, *Victoria amazonica* (Amazon water lily) and *Nelumbo nucifera* (sacred lotus), clearly linked to activity of the alternative path (Fig. 3.10). These flowers regulate their temperature with remarkable precision (Wagner et al. 2008). When the air temperature varies between 10 and 30 °C, the flowers remain between 30 and 35 °C. The stable temperature is a consequence of increasing respiration rates in proportion to decreasing temperatures. Such a phenomenon of thermoregulation in plants is known for only a few species, *e.g.*, *Philodendron selloum* (heart-leaf philodendron), *Symplocarpus foetidus* (skunk cabbage) (Knutson 1974; Seymour 2001). Heat production in lotus is likely an energetic reward for **pollinating beetles**. These are trapped overnight, when they feed and copulate, and then carry the pollen away (Seymour and Schultze-Motel 1996).

Seed dispersal in the dwarf mistletoe *Arceuthobium americanum* in North America occurs by explosive discharge (Sect. 11.4.1). Slight warming of ripe fruit in the laboratory can trigger explosions. **AOX** is present in the dwarf mistletoe fruit. Infrared thermographs reveal that ripe fruits display an anomalous increase in surface temperature by 2.1 °C over 103s before dehiscence. These results support thermogenesis-triggered seed discharge, never before observed in any plant (deBruyn et al. 2015).

Can AOX also play a significant role in increasing the temperature of leaves, for example during exposure to low temperature? There is indeed some evidence for increased heat production (7–22% increase) in low-temperature resistant plants (Moynihan et al. 1995). It can readily be calculated, however, using an approach outlined in Chap. 6, that such an increase in heat production *cannot* lead to a significant temperature rise in leaves (less than 0.1 °C), and hence is unlikely to play a role in any cold-resistance mechanism. To explain the contribution of the

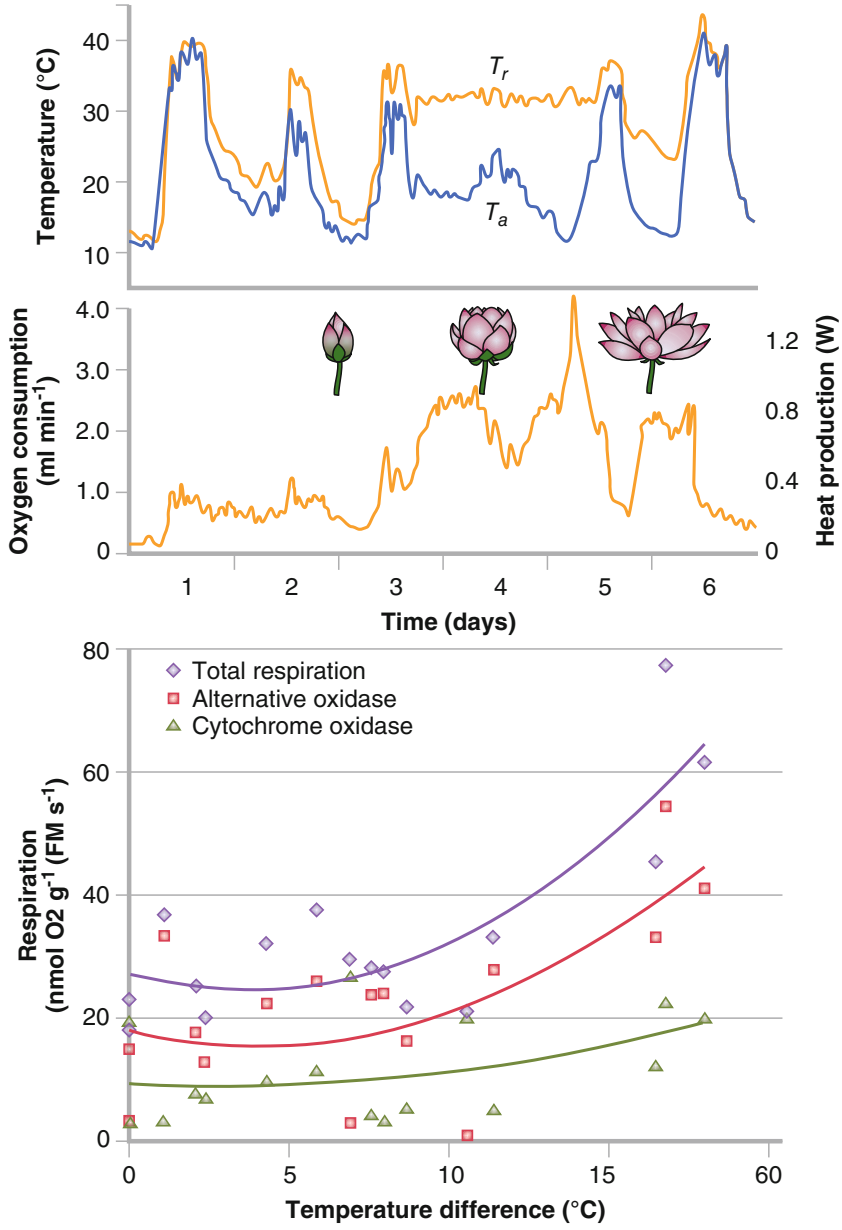

Fig. 3.10 (Top) Temperature of the receptacle (T_r) and ambient air T_a) and (Middle) rates of O_2 consumption throughout the thermogenic phase in *Nelumbo nucifera* (sacred lotus). O_2 consumption is converted to heat production assuming 21.1 J per ml of O_2. Shaded areas indicate the night period (Seymour and Schultze-Motel 1996); copyright © 1996, Springer Nature. (Bottom) Total respiratory flux and fluxes through the alternative and cytochrome pathways in lotus receptacle tissues as a function of the difference between receptacle temperature and temperature of an adjacent nonheating receptacle. Partitioning of electron transport between the two respiratory pathways was determined on the basis of ^{18}O-isotope fractionation of intact tissues, as described in Box 3.1 (modified after Watling et al. 2006).

Table 3.4 A comparison of the KCN-resistance of respiration of intact organs of a number of species and of O_2 uptake by mitochondria isolated from these organs*.

		Cyanide- resistance (%)	
Species	Organ	Whole tissue	Mitochondria
Gossypium hirsutum	Roots	36	22
Phaseolus vulgaris	Roots	61	41
Spinacia oleracea	Roots	40	34
Triticum aestivum	Roots	38	35
Zea mays	Roots	47	32
Pisum sativum	Leaves	39	30
Spinacia oleracea	Leaves	40	27

Source: Lambers et al. (1983)

*The percentage KCN-resistance of intact organ respiration was calculated from the rate measured in the presence of 0.2 mM KCN and that measured in the presence of 0.1 μM FCCP, an uncoupler of the oxidative phosphorylation; this was done to obtain a rate of electron transfer through the cytochrome path closer to the state 3 rate (Fig. 3.4). KCN-resistance of isolated mitochondria was calculated from the rate in the presence and absence of 0.2 mM KCN. Mitochondrial substrates were 10 mM malate plus 10 mM succinate and a saturating amount of ADP. KCN-resistant O_2 uptake by isolated mitochondria was fully inhibited by inhibitors of the alternative path; in the presence of both KCN and SHAM approximately 10% of the control respiration proceeded in some of the organs ('residual respiration')

alternative path in respiration of nonthermogenic organs, we must invoke other ecophysiological roles.

3.3.2 Can We Really Measure the Activity of the Alternative Path?

Does the alternative path also play a role in the respiration of 'ordinary' organs, such as roots and leaves? The application of specific inhibitors of the alternative path suggests that the alternative path does contribute to the respiration of roots and leaves of at least some species (Tables 3.4 and 3.5). The decline in respiration, however, upon addition of an inhibitor of the alternative path tends to underestimate the actual activity of the alternative path. Because the two pathways compete for electrons, inhibition is less than the activity of the alternative path (Table 3.5). Thus, any observed inhibition of respiration following the addition of an alternative pathway inhibitor indicates that some alternative pathway activity was present prior to inhibition, but provides no quantitative estimate of its activity (Del-Saz et al. 2018).

Table 3.5 KCN-resistance, expressing the total respiratory electron flow through the alternative path under the conditions of measurement, and SHAM-inhibition of root respiration*.

Species	KCN-resistance (%)	SHAM-inhibition (%)
Carex diandra	66	29
Festuca ovina	53	1
Hordeum distichum	34	0
Pisum sativum	40	11
Phaseolus vulgaris	57	4
Plantago lanceolata	53	45
Poa alpina	41	1
Poa costiniana	61	0

Source: Atkin et al. (1995)

*Values are expressed as percentage of the control rate of respiration. KCN and SHAM (salicylhydroxamic acid) are specific inhibitors of the cytochrome path and the alternative path, respectively. Only if the cytochrome path is saturated, SHAM inhibition would equal the activity of the alternative path. Since the cytochrome path is rarely saturated, SHAM-inhibition is usually less than the activity of the alternative path; in fact its activity may be as high as the KCN-resistant component of root respiration. Because the two pathways generally compete for electrons, inhibitors cannot provide information on the actual activity of the two pathways in root respiration

Stable isotopes can be used to estimate alternative path activity without the complications caused by use of inhibitors, because the alternative oxidase and cytochrome oxidase discriminate to a different extent against the heavy oxygen isotope (Box 3.1). The isotope method shows that the alternative pathway may account for over 40% of all respiration. If the role of the alternative path in roots and leaves cannot be that of heat production, what might be its role in these organs?

Box 3.1: Measuring Oxygen-Isotope Fractionation in Respiration

Plants have a cyanide-insensitive respiratory pathway in addition to the cytochrome pathway (Sect. 3.2.3). Unlike the cytochrome pathway, the transport of electrons from ubiquinol to O_2 through the alternative path is not linked to proton extrusion, and, therefore, not coupled to energy conservation. The alternative oxidase and cytochrome oxidase discriminate to a different extent against the heavy isotope of oxygen (^{18}O) when reducing O_2 to produce water (Guy et al. 1989). This allows calculation of the partitioning of electron flow between the two pathways in the absence of added inhibitors, also in intact tissues. For many years, studies of electron partitioning between the two respiratory pathways were performed using specific inhibitors of the two pathways [*e.g.*, cyanide for the cytochrome path, and SHAM (salicylhydroxamic acid) for the alternative path] (Møller et al. 1988). Electrons were considered available to the alternative pathway only when the cytochrome pathway was either saturated or inhibited; however, we now know that both pathways compete for electrons (Sect. 3.2.6.1). The only reliable technique to study electron partitioning between the cytochrome and alternative pathway is by using oxygen-isotope fractionation (Day et al. 1996). Although the methodology employed has changed, the theoretical basis of the oxygen-isotope fractionation technique remains that described by Guy et al. (1989).

The origin of the oxygen-fractionation methodology can be found in Bigeleisen and Wolfsberg (1957) and Mariotti et al. (1981). Oxygen-isotope fractionation is measured by examining the isotope fractionation of the substrate O_2 as it is consumed in a closed, leak-tight cuvette. The energy needed to break the oxygen-oxygen bond of a molecule containing ^{18}O is greater than that to break the molecule $^{16}O = {}^{16}O$. Therefore, both terminal oxidases of the plant mitochondrial electron-transport chain react preferentially with $^{16}O_2$, but they produce different isotope effects (Hoefs 1987). This allows determining the relative flux through each terminal oxidase. If α is the ratio of the rate of the reaction with ^{18}O to that with ^{16}O, then:

$$R_p = R \times \alpha \tag{3.1}$$

where R_p is the $^{18}O/^{16}O$ ratio of the product (H_2O), and R is that of the substrate (O_2). Since α generally differs from unity by only a few percent, fractionation is usually given by D, where:

$$D = (1 - \alpha) \times 1000 \tag{3.2}$$

and the units of D are parts per mil (‰). D is generally obtained directly from Eq. (3.1) by measurements of the isotope ratio of the substrate and product, but since the product of both mitochondrial oxidases is H_2O, which is either the solvent for these reactions (liquid-phase) or very difficult to obtain (gas-phase), this is not feasible in this case. Instead, changes in the isotope ratio of the O_2 in the substrate pool are measured (Box Fig. 3.1). If there is any isotopic fractionation during respiration, the oxygen-isotope ratio (R) of the remaining O_2 increases as the reaction proceeds. The respiratory isotope fractionation can be obtained by measuring R, and the fraction of molecular O_2 remaining at different times during the course of the reaction.

Therefore, if we define the following terms:

R_o = initial $^{18}O/^{16}O$
R = $^{18}O/^{16}O$ at time t
f = fraction of remaining oxygen at time t:
$f = [O_2]/[O_2]_o$
then the change in R through time is:

(continued)

Box 3.1 (continued)

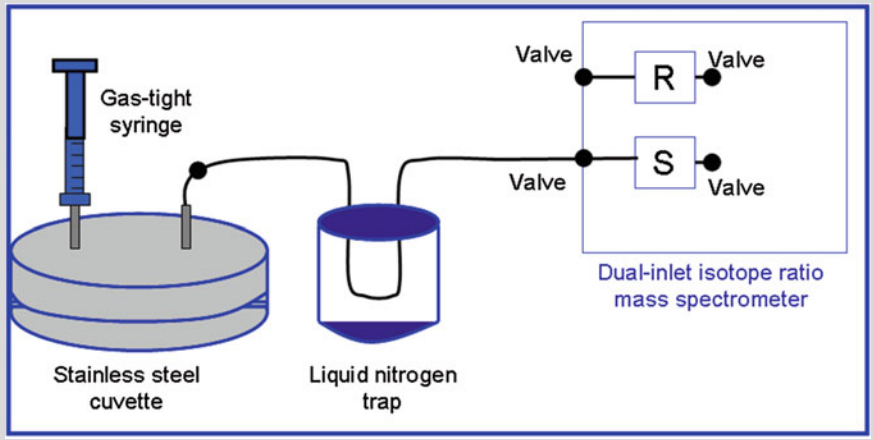

Box Fig. 3.1 Diagram of an on-line oxygen-isotope fractionation system, with a gas-tight syringe, a stainless steel cuvette, a liquid nitrogen trap to remove CO_2 and H_2O, a reference bellow, and a sample bellow (Ribas-Carbó et al. 2005).

$$\delta R/\delta t = \frac{\left[{}^{16}\mathrm{O}\left(\delta {}^{18}\mathrm{O}/\delta t\right) - {}^{18}\mathrm{O}\left(\delta {}^{16}\mathrm{O}/\delta t\right)\right]}{\left({}^{16}\mathrm{O}\right)^2} \tag{3.3}$$

Since

$$\delta {}^{18}\mathrm{O}/\delta t = R \times \alpha \left(\delta {}^{16}\mathrm{O}/\delta t\right) \tag{3.4}$$

we obtain:

$$\delta R/R = \delta {}^{16}\mathrm{O}/{}^{16}\mathrm{O} \times (1-\alpha) \tag{3.5}$$

which, upon integration, yields:

$$\ln\, R/R_\mathrm{o} = -\ln {}^{16}\mathrm{O}/{}^{16}\mathrm{O}_\mathrm{o} \times (1-\alpha) \tag{3.6}$$

Since only 0.4% of the O_2 contains ^{18}O, the ratio $^{16}O/^{16}O_o$ is a good approximation of $[O_2]/[O_{2o}]$ (f), and hence we may write:

$$D = \ln\, (R/R_\mathrm{o})/ - \ln f \tag{3.7}$$

and D can be determined by the slope of the linear regression of a plot of $\ln R/R_o$ *vs.* $-\ln f$, without forcing this line through the origin (Henry et al. 1999). The standard error (SE) of the slope is determined as:

$$\mathrm{SE} = \frac{D(1-r^2)^{1/2}}{r(\mathrm{n}-2)^{1/2}} \tag{3.8}$$

and indicates the precision of the measurement of isotopic fractionation (D). This error should be less than 0.4‰, because the fractionation differential between the cytochrome pathway (18–20‰) and the alternative pathway (24–31‰) is between 6‰ and 12‰, for roots and green tissues, respectively (Robinson et al. 1995). In most cases, accurate determinations of D can be achieved with experiments comprising six measurements, providing the r^2 of the linear regression is 0.995 or higher (Ribas-Carbó et al. 1995; Henry et al. 1999). Because it is common practice in the plant literature to express isotope fractionation in 'Δ' notation, the fractionation factors, D, are converted to Δ:

$$\Delta = \frac{D}{1-(D/1000)} \tag{3.9}$$

The partitioning between the cytochrome and the alternative respiratory pathways (τ_a) is (Ribas-Carbó et al. 1997):

(continued)

Box 3.1 (continued)

$$\tau_a = \frac{\Delta n - \Delta c}{\Delta a - \Delta c} \qquad (3.10)$$

where Δn is the oxygen-isotope fractionation measured in the absence of inhibitors, and Δc and Δa are the fractionation by the cytochrome and alternative pathway, respectively. These 'end-points' for purely cytochrome or alternative pathway respiration are established for each experimental system using inhibitors of the alternative oxidase and cytochrome oxidase, respectively. The cytochrome oxidase consistently gives a Δc between 18‰ and 20‰, while Δa is more variable, with values ranging from 24–25‰ in roots and nongreen tissues, and 30–32‰ in cotyledons and green leaves (Ribas-Carbó et al. 2005).

3.3.3 The Alternative Path as an Energy Overflow

The activity of the alternative path may increase when the production of NADH is not matched by its oxidation, *e.g.*, when the source of N is changed from nitrate to ammonium (Hachiya and Noguchi 2011). When nitrate is depleted, and NADH is no longer required to reduce nitrate, there is an excess of NADH. In some species this is associated with an increased expression of genes encoding AOX (Escobar et al. 2006). These kind of conditions led to the 'energy overflow hypothesis' (Lambers 1982). It considers the alternative path as a **coarse control** of carbohydrate metabolism, but not as an alternative to the finer control by adenylates (Sects 3.2.1 and 3.2.2).

The continuous employment of AOX under normal 'nonstress' conditions may ensure a rate of carbon delivery to the roots that enables the plant to cope with 'stress'. If the carbon demand of an organ suddenly increases, there is sufficient carbon import to meet these demands, if respiration were to switch entirely to supporting ATP synthesis. For example, a decrease in soil water potential increases the roots' carbon demand for synthesis of compatible solutes for osmotic adjustment. Similarly, attack by pathogens may suddenly increase carbon demands for tissue repair and the mobilization of plant defenses. AOX activity may also prevent the production of superoxide and/or hydrogen peroxide under conditions where electron transport through the cytochrome path is restricted (*e.g.*, due to low temperature or desiccation injury).

The plant mitochondrial electron transfer chain is a major source of other **reactive oxygen species** (**ROS**), even under unstressed conditions. Under normal steady-state conditions, ROS are scavenged by a complex array of antioxidant enzymes and small molecules that limit mitochondrial and cellular damage. However, under some conditions, these defenses can be overwhelmed and ROS accumulate, leading to damage of proteins, lipids and DNA (Fig. 3.11). Superoxide is produced by single electron transfers from reduced components in the electron transport chain to O_2 and is the main ROS produced by mitochondria. The main sites of superoxide production are the ubiquinone pool and components in complex I and complex III. Complex II also produces significant superoxide. Up to 5% of O_2 consumption by plant mitochondria may be from single electron reduction of O_2 to superoxide, with the remainder of O_2 consumption occurring at the terminal oxidases, complex IV and AOX, by four-electron reduction of O_2 to water (Jacoby et al. 2018). A major role of AOX appears to be prevention of too much ROS production, particularly during abiotic and biotic stress (Vanlerberghe et al. 2009).

3.3.4 NADH Oxidation in the Presence of a High Energy Charge

If cells require a large amount of carbon skeletons (*e.g.*, 2-oxoglutarate or succinate), but do not have a high demand for ATP, then the operation of the alternative path could prove useful in

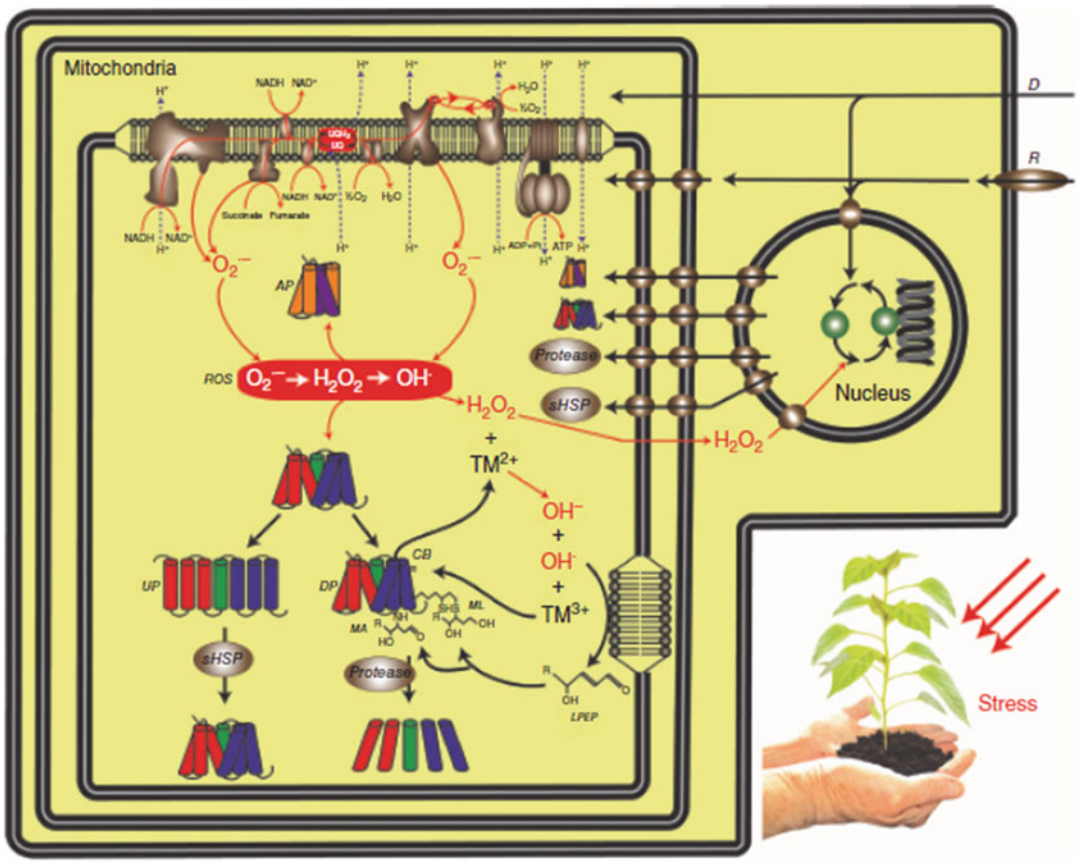

Fig. 3.11 Interaction of reactive oxygen species (ROS), proteins, metal ions and lipid peroxidation endproducts in plant mitochondria exposed to environmental stresses. When a plant is exposed to an environmental stress, this exposure must be sensed either by a receptor (R) on the plasma membrane or directly (D) inside the cell. This is then probably signaled to the nucleus and/or the mitochondria. Inside the mitochondria, ROS are produced by the electron transport chain at complex I, II, and III, and their production can increase during exposure to environmental stresses. These ROS can accumulate within the mitochondria when the antioxidant systems and antioxidant proteins (AP) are overwhelmed. This can lead to the production of lipid peroxidation end-products (LPEP), damaged proteins (DP), unfolded proteins (UP) and release of transition metal ions (TM). The accumulated ROS can directly inhibit proteins, while accumulated LPEP can modify amino acids directly (MA), and modify proteins via lipoic acid co-factors (ML). Accumulated transition metal ions can facilitate metal-catalyzed oxidation leading to the formation of carbonyl groups (CB). The mitochondria may also signal the accumulation of ROS to the nucleus. Either the external sensing of stress or mitochondrial signaling by ROS leads to the production of new proteins by the nucleus, including replacement proteins, small heat shock proteins (sHSPs), proteases and antioxidant proteins (AP). These are then involved in the refolding of UP or the degradation of DP (Jacoby et al. 2018); reprinted with permission from John Wiley & Sons, Inc.

oxidizing the NADH that would otherwise accumulate; considering the pool size of NADH, this would then stop respiration within minutes. However, can we envisage such a situation *in vivo*? Whenever the rate of carbon skeleton production is fast, there tends to be a great need for ATP to further metabolize and incorporate these skeletons. When plants are infected by pathogenic microorganisms, however, they tend to produce **phytoalexins** (Sect. 14.3). This generates substantial amounts of NAD(P)H without major ATP requirements, and hence might require engagement of the alternative path (Sect. 3.4.8).

There are also other circumstances where the production of carbon skeletons does not entail a need for ATP. **Cluster roots** of *Hakea prostrata* (harsh hakea) accumulate large amounts of carboxylates (*e.g.*, citrate), which they subsequently release to mobilize sparingly available P in the rhizosphere (Sect. 9.2.2.5). During the phase of rapid carboxylate synthesis, the alternative path is upregulated, presumably allowing re-oxidation of NADH that is produced during citrate synthesis (Shane et al. 2004). The O_2 isotope-fractionation technique (Sect. 3.3.2) shows that **cluster roots** of *Lupinus albus* (white lupin) have a greater *in vivo* alternative path activity when malate and citrate concentrations are also high (Florez-Sarasa et al. 2014).

There may be a need for a nonphosphorylating path to allow rapid oxidation of malate in plants exhibiting crassulacean acid metabolism (**CAM plants**) during the day (Sect. 2.10.2). If measurements are made in the dark, during the normal light period, then malate decarboxylation in CAM plants is indeed associated with increased engagement of the alternative path (Table 3.6). Malate decarboxylation, however, naturally occurs in the light (Sect. 2.10.2). Unfortunately, there are no techniques available to assess alternative path activity in the light, and it therefore remains to be confirmed that the alternative path plays a vital role in CAM.

Table 3.6 Respiration, oxygen-isotope fractionation, and partitioning of electrons to the cytochrome and the alternative pathway in leaves of *Kalanchoe daigremontiana*.

Parameter	Acidification	Deacidification
Respiration μmol O_2 m^{-2} s^{-1}	1.8	2.6
Discrimination o/oo	22.4	25.0
Cytochrome path μmol O_2 m^{-2} s^{-1}	1.3	1.4
Alternative path μmol O_2 m^{-2} s^{-1}	0.5	1.2

Source: Robinson et al. (1992)
Note: Measurements were made in the dark, during the normal dark period (acidification phase) and the normal light period (deacidification phase, when rapid decarboxylation occurs)

3.3.5 NADH Oxidation to Oxidize Excess Redox Equivalents from the Chloroplast

In illuminated leaves, mitochondria may play a role in optimizing photosynthesis. Inhibition of either the cytochrome or the alternative path, using specific inhibitors (Sect. 3.2.3.3), reduces photosynthetic O_2 evolution and the redox state of the photosynthetic electron transport chain in *Vicia faba* (broad bean) leaves under various light intensities (Yoshida et al. 2006). Under saturating photosynthetic photon flux density, inhibition of either pathway causes a decrease in the steady-state levels of the photosynthetic O_2 evolution rate and the PSII quantum yield. Obviously, both respiratory pathways are essential for maintenance of rapid photosynthetic rates at saturating light. At low light intensity, however, only inhibition of the alternative path lowers the photosynthetic rate. This suggests that inhibition of the alternative path causes over-reduction of the photosynthetic electron transport chain, even at low light levels.

An important function of AOX may be to prevent chloroplast over-reduction through efficient dissipation of excess reducing equivalents (Noguchi et al. 2005). This hypothesis was tested using *Arabidopsis thaliana* mutants defective in cyclic electron flow around PSI, in which the reducing equivalents accumulate in the chloroplast stroma due to an unbalanced ATP/NADPH production ratio. These mutants show enhanced activities of the enzymes needed to export the reducing equivalents from the chloroplasts. Interestingly, the amounts of AOX protein and cyanide-resistant respiration in the mutants are also greater than those in the wild-type. After high-light treatment, AOX, even in the wild-type, is upregulated, concomitant with accumulation of reducing equivalents in the chloroplasts. These results indicate that AOX can dissipate excess reducing equivalents that are exported from the chloroplasts, and that it plays a role in photosynthesis (Yoshida et al. 2007). Leaves of *Arabidopsis thaliana* without activity of a specific AOX isoform, show a reduced plastoquinol pool after high-light stress (Yoshida et al. 2011).

Leaves of similar mutants of *Nicotiana tabacum* (tobacco) show reduction of photosynthetic electron transport, but only after exposure to moderate water stress (Dahal et al. 2014).

3.3.6 Continuation of Respiration When the Activity of the Cytochrome Path Is Restricted

Naturally occurring **inhibitors** of the cytochrome path (*e.g.*, cyanide, sulfide, carbon dioxide, and nitric oxide) may reach such high concentrations in plant tissues that respiration via the cytochrome path is partially or fully inhibited (Palet et al. 1991; Martin et al. 2015). Similarly, mutants of that lack **complex I** and hence must use the nonphosphorylating bypass, produce less ATP than the wild-type, if respiring at the same rate. Under these circumstances the alternative pathway may be important in providing energy, even though it yields much less ATP than the cytochrome path does. This has indeed been shown to be the case for a *Nicotiana sylvestris* (flowering tobacco) mutant that lacks complex I, using the oxygen-isotope fractionation technique (Box 3.1; Vidal et al. 2007).

Many plants contain **cyanogenic** compounds, such as cyanohydrin, cyanogenic glycosides, and cyanogenic lipids (Sect. 13.3.1). Such compounds liberate free HCN after hydrolysis, *e.g.*, during imbibition or attack by herbivores. A mitochondrial β-cyanoalanine synthase detoxifies HCN (Machingura et al. 2016). Despite this detoxifying mechanism, some HCN may be present inside the cells, and hence requiring a cyanide-resistant path.

Some plants produce **sulfide**, *e.g.*, Cucurbitaceae species (gourd family) (Rennenberg and Filner 1983). Sulfide is also produced by anaerobic sulfate-reducing microorganisms. It may occur in high concentrations in the phyllosphere of aquatic plants or the rhizosphere of waterlogged plants. In waterlogged soils, **carbon dioxide** levels are also high. Since both sulfide and high concentration of carbon dioxide inhibit the cytochrome path (Palet et al. 1991), there may be a need for the alternative path under these conditions also.

When the activity of the cytochrome path is restricted by **low temperature**, the alternative path activity might also increase to provide energy needed for metabolism. *Arabidopsis thaliana* plants with altered AOX abundance show that it plays a role in supporting growth at low temperature, and double mutants of plants with less cyclic electron transport and AOX display reduced growth, while the single mutants are apparently unaffected (Fiorani et al. 2005). AOX plays a role in shoot acclimation to low temperature by preventing excess ROS formation (Sect. 3.3.3; Millar et al. 2011).

In transgenic *Nicotiana tabacum* (tobacco) plants lacking AOX, inhibition or restriction of the activity of the cytochrome path leads to the accumulation of fermentation products (Vanlerberghe et al. 1995). In addition, it might cause the ubiquinone pool to become highly reduced which might lead to the formation of reactive oxygen species and concomitant damage to the cell (Millar et al. 2011). The activity of AOX provides both metabolic and signaling stability (Vanlerberghe 2013).

3.3.7 A Summary of the Various Ecophysiological Roles of the Alternative Oxidase

AOX is widespread and can serve a wide variety of physiological functions These range from providing ATP when the cytochrome pathway is restricted, *e.g.*, at low temperature, to balancing the physiological rates of a range of processes, *e.g.*, organic acid synthesis and ATP production, to prevent metabolism from getting severely unbalanced. In plants, the alternative pathway is just as much entrained in all aspects of metabolism as is the cytochrome path. In addition to the alternative path, plants have bypasses of complex I and uncoupling proteins.

3.4 Environmental Effects on Respiratory Processes

3.4.1 Flooded, Hypoxic, and Anoxic Soils

Plants growing in flooded soil are exposed to **hypoxic** (low-O_2) or **anoxic** (no-O_2) conditions in the root environment, and experience a number of conditions, including an insufficient supply of O_2 and accumulation of CO_2 (Sect. 3.4.7), and changes in plant water relations (Sect. 5.3).

3.4.1.1 Inhibition of Aerobic Root Respiration

The most immediate effect of soil **flooding** on plants is a decline in the O_2 concentration in the soil. In water-saturated soils the air that is normally present in the soil pores is almost completely replaced by water. The **diffusion** of gases in water is approximately 10,000 times slower than in air. In addition, the O_2 **concentration** in water is much less than that in air (at 25 °C approximately 0.25 mmol O_2 dissolves per liter of water, whereas air contains approximately 10 mmol). The O_2 supply from the soil, therefore, decreases to the extent that aerobic root respiration, and hence ATP production, is restricted. During hypoxia, the activities of **pyruvate decarboxylase** and **alcohol dehydrogenase** increases (Herzog et al. 2015).

3.4.1.2 Fermentation

When insufficient O_2 reaches the site of respiration, such as in seeds germinating under water and submerged rhizomes, ATP may be produced through **fermentative processes**. These tissues generate energy in **glycolysis**, producing ethanol, and sometimes lactate. **Lactate** tends to be the product of fermentation immediately after the cells are deprived of O_2. Lactate accumulation decreases the pH in the cytosol (Sect. 3.4.1.3), which inhibits **lactate dehydrogenase** and activates the first enzyme of ethanol fermentation: pyruvate decarboxylase. When lactate accumulation does not stop, **cytosolic acidosis** may lead to cell death (Rivoal and Hanson 1994).

It was initially believed that root metabolism cannot continue in flooded conditions, due to the production of toxic levels of **ethanol**. Ethanol, however, does not really inhibit plant growth until concentrations are reached that far exceed those found in flooded plants (Table 3.7), and hence ethanol plays only a minor role in flooding injury to roots and shoots (Jackson et al. 1982). As long as there is no accumulation of **acetaldehyde**, which is the product of pyruvate decarboxylase and the substrate for alcohol dehydrogenase, which reduces acetaldehyde to ethanol, alcoholic fermentation is unlikely to cause plant injuries. If **acetaldehyde** does accumulate, however, for example upon re-aeration, then this may cause injury, because acetaldehyde is a potent toxin, giving rise to the formation of **reactive oxygen species** (Blokhina et al. 2003). It is the low potential for **ATP production** and its metabolic consequences, rather than the toxicity of the products of fermentative metabolism that constrain the functioning of plants under anoxia (Sect. 3.4.1.3).

Continued fermentation requires the mobilization of a large amount of reserves, such as starch. Seeds of most species fail to germinate under anoxia, but those of *Oryza sativa* (rice) are an exception (Magneschi and Perata 2009). Rice

Table 3.7 The effect of supplying ethanol in aerobic and anaerobic nutrient solutions to the roots of *Pisum sativum* (garden pea) at a concentration close to that found in flooded soil (*i.e.* 3.9 mM) or greater than that.

	Aerobic control	Aerobic + ethanol	Anaerobic control	Anaerobic + ethanol
Ethanol in xylem sap (mM)	37	540	90	970
Stem extension (mm)	118	108	94	74
Final fresh mass (g)				
shoot	11.9	11.9	10.7	11.4
roots	7.8	9.7	5.7	6.1

Source: Jackson et al. (1982)

seeds can germinate anaerobically by means of coleoptile elongation. This is mediated through coleoptile rather than root emergence. The **energetic efficiency** of ethanol formation is low, producing only two molecules of ATP in glycolysis ('substrate phosphorylation') per molecule of glucose. This is considerably less than that of aerobic respiration, especially if the most efficient mitochondrial electron-transport pathways are used (Sects 3.2.2 and 3.2.3). Moreover, a large fraction of the **lactate** that is produced in fermentation may be lost from the plants by secretion into the rhizosphere [*e.g.*, in some *Limonium* (statice) species] (Rivoal and Hanson 1993). A pivotal activity of cells under anoxia must be energy production, even when an anaerobic machinery produces insufficient amounts of ATP. Therefore, it appears that a new pH is set to ensure a proper functioning of the involved enzymes (Felle 2005). The anoxic pH is not experienced as an error signal and is not reversed to the aerobic level.

3.4.1.3 Cytosolic Acidosis

A secondary effect of the decline in root respiration and ATP production under anoxia is a decrease in the pH of the cytosol (**cytosolic acidosis**), due in part to accumulation of organic acids in fermentation and the TCA cycle. Moreover, in the absence of O_2 as a terminal electron acceptor, ATP production decreases, so there is less energy available to maintain ion gradients within the cell. Acidification of the cytosol reduces the activity of many cytosolic enzymes, whose pH optimum is around 7, and hence severely disturbs the cell's metabolism, so that protons leak from the vacuole to the cytosol (Felle 2005). Cytosolic acidosis also reduces the functioning of aquaporins, thus restricting water transport (Sect. 5.5.2).

The extent of cytosolic acidification is less in the presence of NO_3^- (Fig. 3.12). Reduction of NO_3^- leads to the formation of hydroxyl ions (Sect. 9.2.2.6.1), which partly neutralize the protons and prevent severe acidosis. Moreover, NO_3^- reduction requires the oxidation of NADH, producing NAD. This allows the continued oxidation of organic acids in the TCA cycle, thus

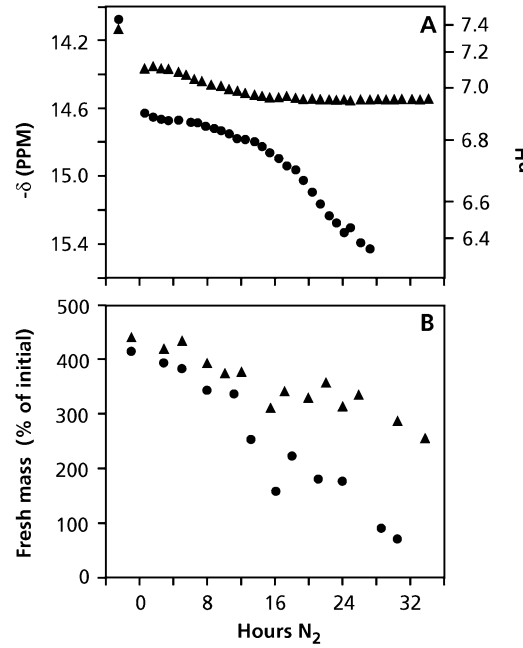

Fig. 3.12 The effect of hypoxia on root tips of *Zea mays* (maize), in the presence (triangles) and absence (circles) of nitrate. (**A**) the effect on the pH of the cytosol, as measured in experiments using ^{31}P-NMR spectroscopy; (**B**) the increase in fresh mass during 48 h in air, after the indicated period of hypoxia. The location of the inorganic phosphate (Pi) peaks in an NMR spectrum depends on the 'environment' of the molecule (*e.g.*, pH) (Fig. 3.6). NMR spectroscopy can therefore be used to determine the peak wavelength at which P_i absorbs the magnetic radiation and hence the pH in the cytosol as well as in the vacuole (after Roberts et al. 1985).

preventing their accumulation and associated decrease in pH. Nitrate reductase in the cytosol and nitrite reduction in mitochondria also produce **NO** (Hebelstrup and Møller 2015). In addition, NO is produced by Complex I and rotenone-insensitive NAD(P)H dehydrogenases, and complex I also participates in the formation of a supercomplex with complex III under hypoxia. Complex II is a target for NO, which, by inhibiting Fe–S centers, regulates ROS generation. Complex III is one of the major sites for NO production, and the maintenance of the redox level and limited energy production under hypoxia. Expression of AOX is induced by NO under various stress conditions, and AOX may regulate mitochondrial NO production. Complex IV is another major site for NO production.

Inhibition of complex IV by NO can prevent O_2 depletion when O_2 levels decline. The NO production and action on various complexes play a major role in NO signaling and energy metabolism (Gupta et al. 2018).

3.4.1.4 Avoiding Hypoxia: Aerenchyma Formation

Wetland plants, including crop species such as *Oryza sativa* (rice), have evolved mechanisms to prevent the problems associated with flooded soils. The most important adaptation to flooded soils is the development of a functional **aerenchyma**, a continuous system of air spaces in the plant that allows diffusion of O_2 from the shoot or the air to the roots (Colmer et al. 2014). Aerenchyma avoids inhibition of respiration due to lack of O_2 which is inevitable for plants that are not adapted to wet soils. In many species, other special structures allow the diffusion of O_2 from the air into the plant: the pneumatophores of mangroves, lenticels in the bark of many wetland trees, and, possibly, the knee roots of *Taxodium distichum* (bald cypress).

Because there is a gradient in partial pressure within the aerenchyma, O_2 will move by **diffusion** to the roots. In aquatic plants, however, like *Nuphar lutea* (yellow water lily) and *Nelumbo nucifera* (sacred lotus) there is also a **pressurized flow-through** system, which forces O_2 from young emergent leaves to the roots and rhizomes buried in the anaerobic sediment (Dacey 1980). Such a mass flow requires a difference in atmospheric pressure between leaves and roots. The diurnal pattern of the mass flow of air to the roots suggests that the energy to generate the pressure comes from the sun; however, it is not the photosynthetically active component of radiation, but the long-wave region (heat) that increases the atmospheric pressure inside young leaves by as much as 300 Pa. How can these young leaves draw in air against a pressure gradient? The sacred lotus, *Nelumbo nucifera*, possesses a complex system of gas canals that channel pressurized air from its leaves, down through its petioles and rhizomes, before venting this air back to the atmosphere through large stomata in the center of every lotus leaf. These large stomata lie over a gas canal junction that connects with two-thirds of the gas canals within the leaf blade, and with the larger of two discrete pairs of gas canals within the petiole that join with those in the rhizome. The lotus presumably regulates the pressure, direction and rate of airflow within its gas canals by opening and closing these large stomata. The large stomata are open in the morning, close at midday and reopen in the afternoon. The periodic closure of the large stomata during the day coincides with a temporary reversal in airflow direction within the gas canals. The conductance of the large stomata decreases in response to increasing light level which ventilates the rhizome and possibly directs benthic CO_2 towards photosynthesis in the leaves (Matthews and Seymour 2014).

Aerenchymatous plants often transport more O_2 to the roots than is consumed by root respiration. The **outward diffusion of O_2** into the rhizosphere implies a loss of O_2 for root respiration. Plants adapted to flooded conditions, *e.g.*, *Oryza sativa* (rice), *Phragmitis australis* (common reed) and *Glyceria maxima* (reed mannagrass) develop a **flooding-induced O_2 barrier** in basal root zones, thus reducing radial O_2 loss (Soukup et al. 2007). On the other hand, outward diffusion of O_2 also allows the oxidation of potentially harmful compounds. This can readily be seen when excavating a plant from a reduced substrate. The bulk substrate itself is black, due to the presence of FeS, but the soil in the immediate vicinity of the roots of such a plant will be brown or red, indicating the presence of oxidized iron (Fe^{3+}, 'rust'), which is less soluble than the reduced Fe^{2+}. Induction of a barrier reducing radial O_2 loss is not a unmitigated benefit to plants. The basal O_2 barrier, which involves both quantitative and qualitative differences in **suberin** composition and distribution within exodermal cell walls (Soukup et al. 2007), probably also decreases the roots' capacity for nutrient and water uptake.

Aerenchyma also serves as a conduit of soil gases to the atmosphere, including methane, ethylene, and carbon dioxide. **Methane** (CH_4) is a bacterial product commonly produced in anaerobic soils (Pangala et al. 2017). In rice paddies and natural wetlands, most CH_4 is transported to the

atmosphere through plant aerenchyma. Experimental removal of sedges from wetland substantially reduces CH_4 flux and causes CH_4 to accumulate in soils. CH_4 production and transport to the atmosphere is a topic of current concern, because CH_4 is a '**greenhouse gas**' that absorbs infrared radiation 20 times stronger than does CO_2. Increased methane production can warm the Earth, which can in turn cause methane to be produced at a faster rate - this is called a positive climate feedback (Dean et al. 2018). The expansion of rice agriculture and associated CH_4 transport via aerenchyma from the soil to the atmosphere is an important contributor to atmospheric CH_4.

3.4.2 Salinity and Water Stress

Sudden exposure of sensitive plants to salinity or water stress often enhances their respiration. For example, the root respiration of *Hordeum vulgare* (barley) increases upon exposure to 10 mM NaCl (Bloom and Epstein 1984). This may either reflect an increased **demand for respiratory energy** or an increased activity of the alternative path, when carbon use for growth is decreased more than carbon gain in photosynthesis (Sect. 10.5.3). Long-term exposure of sensitive plants to salinity or desiccation gradually decreases respiration as part of the general decline in carbon assimilation and overall metabolism associated with slow growth under these conditions (Galmés et al. 2007; Sect. 10.5.3). Generally, specific rates of leaf respiration at 25 °C are fastest in plants growing in hot, dry habitats, reflecting acclimation and/or adaptation to such habitats (Wright et al. 2006). Additional declines in root respiration of *Triticum aestivum* (wheat) plants upon exposure to dry soil may reflect a specific decline in the alternative path. The decline correlates with the accumulation of **osmotic solutes**, reducing the availability of sugars and hence providing less 'grist for the mill' of the alternative path.

Leaves also show a decline in respiration, as leaf water potential declines. The decline is most likely associated with a decrease in the energy requirement for growth or the export of photoassimilates. In *Glycine max* (soybean), net photosynthesis decreases by 40% under mild and by 70% under severe water stress, whereas the total respiratory O_2 uptake does change significantly in the leaves. However, severe water stress causes a significant shift of electrons from the cytochrome to the alternative pathway. The electron partitioning through the alternative pathway increases from about 11% under well-watered or mild water-stress conditions to 40% under severe water stress (Fig. 3.13). Consequently, the calculated rate of mitochondrial ATP synthesis decreases by 32% under severe water stress (Ribas-Carbó et al. 2005). With increasing severity of water stress, AOX overexpression in *Nicotiana tabacum* (tobacco) increases respiration in

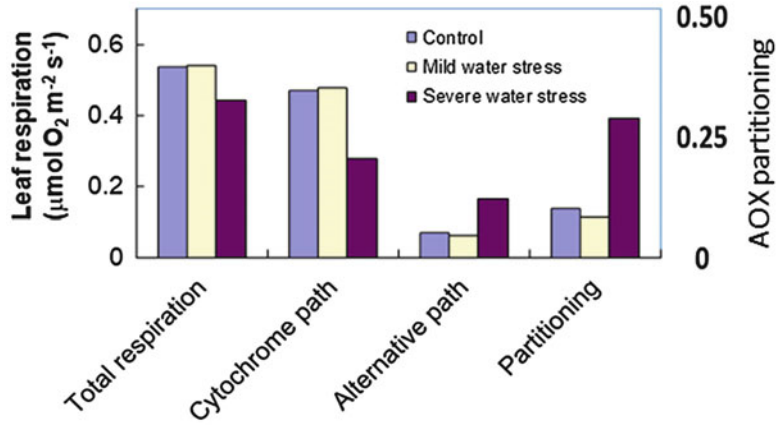

Fig. 3.13 Effect of different levels of water stress on total respiration (V_t), the activities of the cytochrome (v_{cyt}), and alternative (v_{alt}) pathways and the partitioning through the alternative pathway (τ_a) (after Ribas-Carbó et al. 2005).

the light, relative to that of wild-type, and improves photosynthetic performance, as the severity of water stress increases (Dahal et al. 2015). AOX overexpression dampens photosystem stoichiometry adjustments and losses of key photosynthetic components that occur in wild-type tobacco (Dahal et al. 2014).

Species differ in their respiratory response to water stress, primarily due to differences in sensitivity of growth to desiccation. When salt-adapted plants are exposed to mild salinity stress, they accumulate **compatible solutes** such as sorbitol (Sect. 5.3). Accumulation of these sugar alcohols requires glucose as a substrate, but does not directly affect the concentration of carbohydrates or interfere with growth. Studies of root respiration, using an inhibitor of the alternative path, suggested that sorbitol accumulation is associated with a reduction in activity of the nonphosphorylating alternative respiratory pathway. However, further experimentation using the oxygen-isotope fractionation technique (Box 3.1) is required to confirm this. Interestingly, the amount of sugars that are 'saved' by the decline in root respiration is the same as that used as the substrate for the synthesis of sorbitol, suggesting that accumulation of compatible solutes by drought-adapted plants may have a minimal energetic cost (Lambers et al. 1981).

Prolonged exposure of salinity-adapted species (**halophytes**) to salt concentrations sufficiently low not to affect their growth has no effect on the rate of root respiration. This similarity in growth and respiratory pattern under saline and nonsaline conditions suggests that the respiratory costs of coping with mild salinity levels are negligible in salt-adapted species. The respiratory costs of functioning in a saline environment for adapted species that accumulate NaCl are likely also relatively small, because of the low respiratory costs of absorbing and compartmentalizing salt when grown in saline soils. For salt-excluding **glycophytes**, however, there may be a large respiratory cost associated with salt exclusion.

3.4.3 Nutrient Supply

Root respiration generally increases when roots are suddenly exposed to increased ion concentrations in their environment, a phenomenon known as **salt respiration** (Lundegårdh 1955). The stimulation of respiration is at least partly due to the increased **demand for respiratory energy** for ion transport. The added respiration may also reflect a replacement of osmotically active sugars by inorganic ions, leaving a large amount of sugars to be respired via the **alternative path**. Oxygen uptake rates are increased in shoots of *Arabidopsis thaliana*, when **ammonium** instead of **nitrate** is used as sole N source (Hachiya et al. 2010). The capacity of the cytochrome pathway and its related genes are upregulated when ammonium is the sole N source, whereas AOX is not affected. The ammonium-dependent increase of the O_2 uptake rate via the cytochrome path may be related to the ATP consumption by the plasma-membrane H^+-ATPase.

When plants are grown at a low supply of N, their rate of **root respiration** is slower than that of plants well supplied with mineral nutrients (Atkinson et al. 2007). This is expected, because their rates of growth and ion uptake are greatly reduced (Fig. 3.14). Rates of root respiration, however, per ion absorbed or per unit root biomass produced at a low NO_3^- supply are relatively fast, if we compare these rates with those of plants that grow and take up ions at a *much* faster rate. This suggests that **specific costs** of growth (that is cost per unit biomass produced), maintenance (cost per unit biomass to be maintained), or ion transport (cost per unit nutrient absorbed) increase in plants grown at a limiting nutrient supply (Sect. 3.5.2.4).

There is also a correlation between **leaf respiration** and **leaf N concentration** in global comparisons, with some differences among functional types (Fig. 3.15; Atkin et al. 2015). Leaf respiration measured at 25 °C at any given leaf [N] is faster in C_3 forbs and grasses than in C_3 shrubs and trees. These faster rates probably reflect greater relative allocation of leaf N to metabolic processes, rather than to structural or defensive roles, combined with high demands for respiratory products.

In Sect. 3.3.4, we discussed *in vivo* respiratory activities of the cytochrome oxidase pathway and AOX in different root sections of *Lupinus albus*

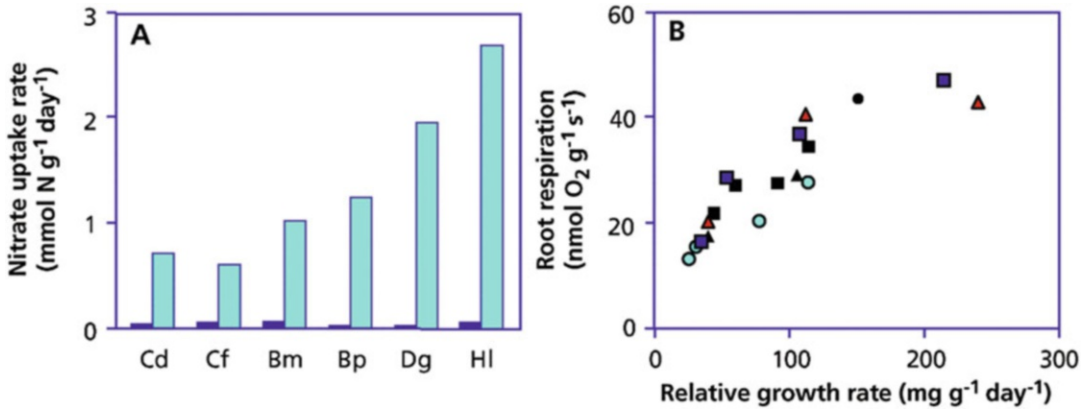

Fig. 3.14 (**A**) Rates of net inflow of nitrate of six grass species grown at two nitrogen addition rates, allowing a near-maximum relative growth rate (light blue columns) or a *RGR* well below RGR_{max} (dark blue columns). (**B**) Root respiration of the same inherently fast- and slow-growing grasses as shown in A, now compared at a range of nitrogen addition rates allowing a near-maximum relative growth rate or a relative growth rate below RGR_{max}, the lowest *RGR* being 38 mg g^{-1} day^{-1}. Cd, *Carex diandra* (lesser panicled sedge) (light blue circles); Cf, *Carex flacca* (blue sedge) (black triangles); Bm, *Briza media* (quacking grass) (blue squares); Bp, *Brachypodium pinnatum* (Tor grass) (black circles); Dg, *Dactylis glomerata* (cocksfoot) (blue squares); Hl, *Holcus lanatus* (common velvet grass) (red triangles) (Van der Werf et al. 1992b); copyright SPB Academic Publishing.

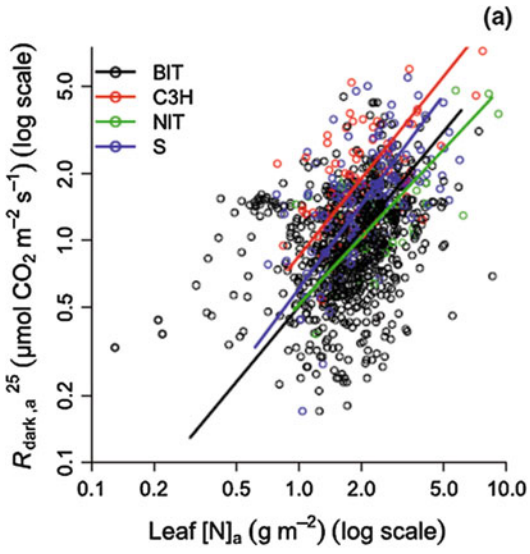

Fig. 3.15 Pattern of area-based rates of leaf respiration as a function of area-based leaf nitrogen (N) concentrations for different plant functional types The pattern is similar when both respiration and [N] are expressed on a leaf mass basis. BlT, broadleaved tree; C3H, C_3 herb/grass; NlT, needle-leaved tree; S, shrub (Atkin et al. 2015); with permission of the New Phytologist Trust.

(white lupin) grown with and without P. The AOX activity is greater at a low P availability, when malate and citrate concentrations are also high, confirming a role of AOX in oxidizing excess amounts of NADH (Florez-Sarasa et al. 2014).

3.4.4 Irradiance

The respiratory response of plants to light and assimilate supply depends strongly on time scale. The immediate effect of low light is to reduce the **carbohydrate status** of the plant, and, therefore, the supply of substrate available for respiration (Fig. 3.16A). Interestingly, in the shade species *Alocasia odora* (Asian taro) addition of sucrose does not increase the rate of leaf respiration of plants transferred to the shade (Fig. 3.16C), but addition of an uncoupler (Sect. 3.2.3.3) does increase respiration to a major extent (Fig. 3.16B; Noguchi et al. 2001b). This shows that respiration is controlled by **energy**

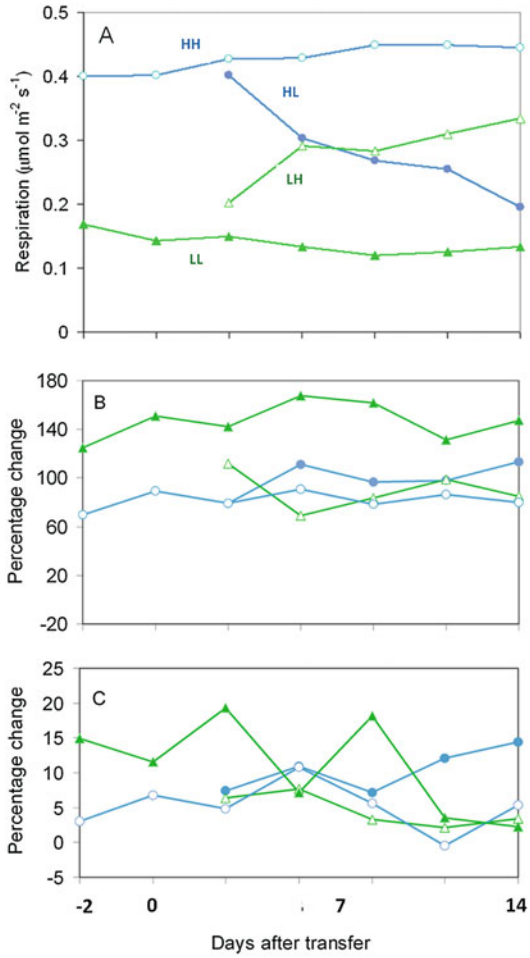

Fig. 3.16 Leaf respiration in the shade species *Alocasia odora* (Asian taro) as dependent on light availability. (**A**) Changes in the rate of O_2 uptake. Effects of (**B**) the addition of an uncoupler (FCCP) and (**C**) a respiratory substrate (sucrose) on the rate of O_2 uptake. Plants that were originally grown in high light (HH, open blue symbols) or low light (LL, filled green triangles) were subsequently transferred to low light (LH, filled blue circles) or high light (HL, open triangles) on day 0 (redrawn after Noguchi et al. 2001b).

demand, rather than **substrate supply** (Sect. 3.2.4; Fig. 3.5), and that the energy demand is downregulated in shade conditions. In the leaves of *Alocasia odora*, the contribution of the **alternative path** is less than 10% of the total respiratory rate, irrespective of growth irradiance. For the sun species *Spinacia oleracea* (spinach) and *Phaseolus vulgaris* (common bean) grown at high light intensity, the contribution of the alternative path in the leaves is about 40% early in the night, but decreases dramatically late in the night. When spinach is grown at low light intensity, however, the contribution of the alternative path in the leaves declines. The low activity of the alternative path in the leaves of the understory species *Alocasia odora* shows that the efficiency of ATP production (ADP:O ratio) of this species is high. This may be especially important in shade environments. In the leaves of sun species, the ADP:O ratio changes depending on conditions (Noguchi et al. 2001b).

To further investigate why the understory species *Alocasia odora* (Asian taro) consistently shows low alternative path activity, Noguchi et al. (2005) grew *Alocasia odora* and *Spinacia oleracea* (spinach) plants under both high and low light intensities. On a mitochondrial protein basis, *Spinacia oleracea* leaves show a greater cytochrome pathway capacity than do *Alocasia odora* leaves. Despite a low *in vivo* activity of the alternative path, *Alocasia odora* has a greater AOX capacity on a mitochondrial protein basis. In the low-light environment, most of the AOX protein in *Alocasia odora* leaves is in its inactive, **oxidized dimer** form (Sect. 3.2.6.2), but it is converted to its **reduced**, active form when plants are grown under high light (Fig. 3.17). This shift may prevent over-reduction of the respiratory chain under photo-oxidative conditions.

Roots and leaves that are subjected to an increased or decreased carbohydrate supply gradually **acclimate** over several hours by adjusting their respiratory capacity. Upon transfer of *Poa annua* (annual meadow-grass) from high-light to low-light conditions, and at the same time from long-day to short-day conditions, the **sugar concentration** in the roots decreases by 90%. Both the rate of root respiration and the *in vitro* **cytochrome oxidase** capacity decrease by about 45%, relative to control values. The absolute rate of O_2 uptake via the **alternative pathway**, as determined using the isotope fractionation technique (Box 3.1), does not change, but the cytochrome pathway activity decreases. Interestingly, there is no change in the concentration of AOX protein or in the reduction state of the protein. In addition, there is no change in the reduction state of the

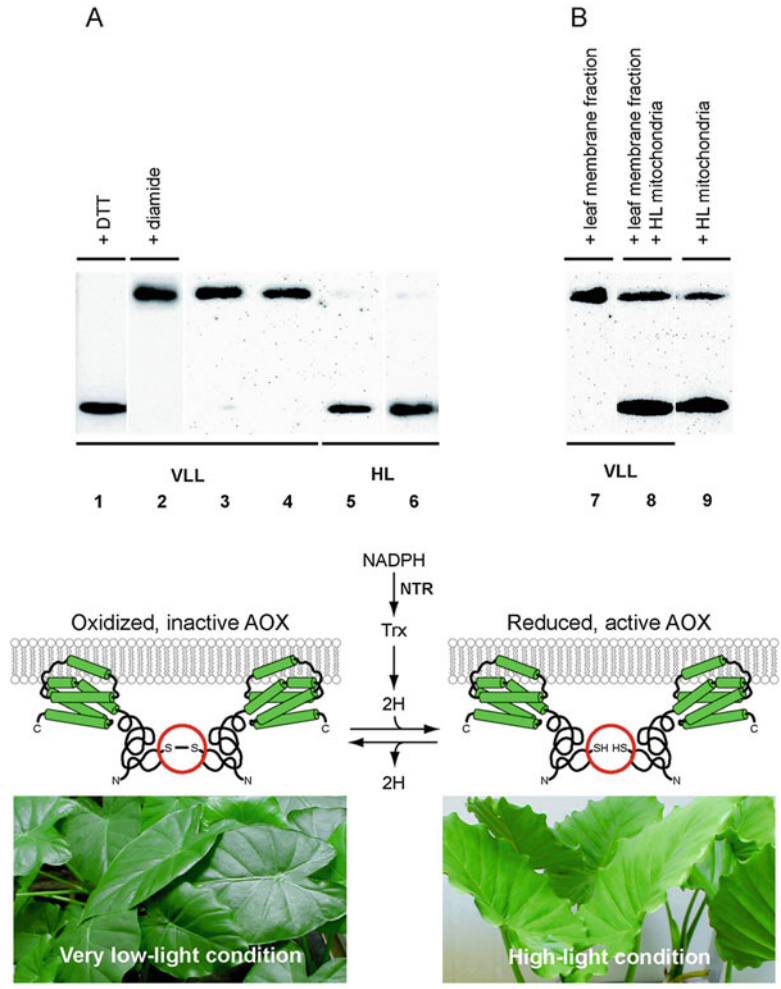

Fig. 3.17 (**A**) Immunoblots of the alternative oxidase (AOX) in extracted membrane fractions isolated from *Alocasia odora* (Asian taro) leaves. Extractions were made very rapidly, so as to maintain the activation state of AOX and determine its *in vivo* state. Lane 1, a sample of leaves of plants grown at very low light intensities (VLL) treated in the presence of 50 mM DTT (dithiothreitol, which renders AOX in its reduced and active state, irrespective of its state *in vivo*). Lane 2, a sample of VLL leaves treated in the presence of 5 mM diamide (which oxidizes and inactivates the AOX dimer, irrespective of its state *in vivo*). Lanes 3 and 4, samples consisted of only VLL leaf membrane fractions; the immunoblots show that AOX is in its oxidized, inactive state in leaves of plants grown at very low light intensity. Lanes 5 and 6, samples consist of only high-light grown (HL) leaf membrane fractions; these immunoblots show that AOX is in its reduced, active state in leaves of plants grown at high light intensity. (**B**) Immunoblots of AOX in rapidly extracted membrane fractions and/or mitochondria isolated from *Alocasia odora* leaves. Lane 7, a sample consist of only VLL leaf membrane fractions; AOX is in its oxidized, inactive state. Lane 8, a sample of VLL leaf membrane fractions, added with a mitochondrial extract from HL leaves just before the extraction; Lane 9, mitochondrial sample isolated from HL leaves; during isolation some AOX is reduced and activated (Noguchi et al. 2005). (**C**) Under very low light conditions, AOX is in its inactive, oxidized form (left). It is converted to its reduced, active form (right) when plants are exposed to high-light conditions. This shift may prevent over-reduction of the respiratory chain under photo-oxidative conditions. The structural model for AOX has been deduced from derived amino acid sequences and is reprinted with permission of the American Society of Plant Biologists. Photographs by K. Noguchi; copyright Blackwell Science Ltd.

ubiquinone pool. These results show that neither the amount nor the activity of the AOX change under severe light deprivation (Millenaar et al. 2000), suggesting an important role for this apparently wasteful pathway; this role is most likely avoiding production of reactive oxygen species, as discussed in Sect. 3.3.3. The results also point to acclimation of respiration as a result of changes in **gene expression**. Also, after pruning of the shoot to one leaf blade, both the soluble sugar concentration and the respiration of the seminal roots decrease. These effects on respiration reflect the **coarse control** of the respiratory capacity upon pruning or sucrose feeding (Bingham and Farrar 1988; Williams and Farrar 1990). This illustrates the adjustment of the respiratory capacity to the root's carbohydrate level.

Changes in respiratory capacity induced by changes in **carbohydrate status** reflect acclimation of the respiratory machinery. The protein pattern of the roots of pruned plants is affected within 24 h (Williams et al. 1992). Glucose feeding to leaves enhances the activity of several glycolytic enzymes in these leaves, due to regulation of **gene expression** by carbohydrate levels (Krapp and Stitt 1994). Clearly, the capacity to use carbohydrates in respiration is enhanced when the respiratory substrate supply increases, and declines with decreasing substrate supply. The plant's potential to adjust its respiratory capacity to environmental conditions is ecologically significant. Individual plants acclimated to low light generally have slow leaf respiration rates. Thus, acclimation accentuates the short-term declines in respiration due to substrate depletion.

As with acclimation, species that are **adapted** to low light generally exhibit slower respiration rates than high-light adapted species. For example, the rainforest understory species *Alocasia odora* (Asian taro) has slower rates of both photosynthesis and respiration than does the sun species *Spinacia oleracea* (spinach), when the two species are compared under the same growth conditions (Table 3.8). The net daily carbon gain of the leaves (photosynthesis minus respiration) is rather similar for the two species, when expressed as a proportion of photosynthesis. Similarly, understory species of *Piper* (pepper) have slower respiration rates than species from shaded and exposed habitats, when both are grown in the same environment (Fredeen and Field 1991). Because rates of photosynthesis and respiration show parallel differences between sun and shade species (both slower in shade species), differences in the carbon balance between sun and shade species probably reflect different patterns of biomass allocation, rather than differences in photosynthesis and respiration.

Respiration rates tend to be faster in plants grown at higher light intensity. Acclimation to higher levels of irradiance involves upregulation of genes involved in the metabolism of carbohydrates and in energy-requiring processes (**coarse control**). In the short term, respiration may respond to irradiance because this affects the availability of respiratory substrate (**control by supply**). Sudden exposure of shade plants to a high light intensity may require a change in activation state of the AOX, associated with accumulation of reactive oxygen species (**stress response**).

Table 3.8 The daily carbon budget (mmol g^{-1} day^{-1}) of the leaves of *Spinacia oleracea* (spinach), a sun species, and *Alocasia odora* (Asian taro), a shade species, when grown in different light environments*.

Irradiance	Photosynthesis		Leaf respiration		Net leaf carbon gain	
	Spinacia oleracea	*Alocasia odora*	*Spinacia oleracea*	*Alocasia odora*	*Spinacia oleracea*	*Alocasia odora*
500	26	nd	3.4 (13)	nd	23 (87)	nd
320	21	11	2.4 (12)	1.1 (10)	18 (88)	9.4 (90)
160	15	9	1.7 (11)	0.82 (9)	14 (89)	8.2 (91)
40	nd	4.5	nd	0.76 (17)	nd	3.7 (83)

Source: Noguchi et al. (1996); K. Noguchi, pers. comm.
*Irradiance is expressed in μmol m^{-2} s^{-1}. Percentages of the photosynthetic carbon gains have been indicated in brackets; nd is not determined; in the original paper the species name is erroneously given as *Alocasia macrorrhiza.*

Acclimation of respiration is relatively fast (hours to days), when compared with that of photosynthesis (days to weeks). This is largely accounted for by the fact that some aspects of photosynthetic acclimation require the production of new leaves with a different structure, whereas acclimation of respiration requires only production of new proteins.

3.4.5 Temperature

Respiration increases as a function of temperature, with the magnitude of increase depending on the **temperature coefficient** (Q_{10}) of respiration. This temperature effect on respiration is characteristic of most heterothermic organisms, and is a consequence of the temperature sensitivity of the enzymatic reactions involved in respiration. The temperature stimulation of respiration also reflects the increased demand for energy to support faster rates of biosynthesis, transport, and protein turnover at higher temperatures (Sect. 3.5.2).

Adverse temperatures are a major constraint to plant productivity, including global crop production, and the frequency and severity of temperature extremes are expected to worsen in the future (Long and Ort 2010). Temperature-mediated changes in plant respiration are an important component of the biosphere's response to global climate change. The Q_{10} is often modeled to be 2 (*i.e.* respiration doubles per 10 °C rise in temperature), but upon longer-term exposure to a different temperature, the Q_{10} may decrease. The long-term Q_{10} declines predictably with increasing temperature across diverse plant taxa and biomes (Fig. 3.18A), due to **thermal acclimation**, *i.e.* the adjustment of respiration rates to compensate for a change in temperature (Huntingford et al. 2017). The temperature dependence of Q_{10} is linked to shifts in the control by maximum **enzyme activity** at low temperature and **substrate limitations** at high temperature (Fig. 3.18B). In the long term, acclimation of respiration to temperature is common, reducing the temperature sensitivity of respiration to changes in thermal environment (Kruse et al. 2014).

Temperature acclimation results in a tendency toward **homeostasis** of respiration, such that warm-acclimated (temperate, lowland) and cold-acclimated (alpine or high-arctic) plants display similar rates of respiration when measured at their respective growth temperatures (Atkin and Tjoelker 2003). A comparison of the temperature dependence of respiration of cold-sensitive and cold-tolerant species suggests that a similar process limits respiration at different growth temperatures, and that the lower capacity of the respiratory system in cold-sensitive species may explain their slow growth rate at low temperature (Noguchi et al. 2015). Analyzing measurements for 231 species spanning seven biomes, temperature-dependent increases in leaf respiration do not follow a commonly used exponential function. Instead, they show a decelerating function with increasing leaf temperature, reflecting a declining sensitivity to higher temperatures that is uniform across all biomes and plant functional types (Heskel et al. 2016a, 2016b).

High-temperature tolerance in plants is important in a warming world. To assess whether there are global patterns in high-temperature tolerance of leaf metabolism, both the high temperature where photosystem II is disrupted (T_{crit}), and the temperature where leaf respiration in darkness is maximal, beyond which respiratory function rapidly declines (T_{max}) were determined for upper canopy leaves of 218 plant species spanning seven biomes (O'Sullivan et al. 2017). Mean site-based T_{crit} values range from 41.5 °C in the Alaskan arctic to 50.8 °C in lowland tropical rainforests of Peruvian Amazon. For T_{max}, the equivalent values are 51.0 and 60.6 °C in the Arctic and Amazon, respectively. T_{crit} and T_{max} follow similar biogeographic patterns, increasing ~8 °C from polar to equatorial regions. Such increases are much less than the 20 °C span in high-temperature extremes across the globe. With only modest high-temperature tolerance, despite high summer temperature extremes, species in mid-latitude (~20–50°) regions have the narrowest thermal safety margins in upper canopy leaves. These regions are at the greatest risk of damage due to extreme heat-wave events. Using predicted heat-wave events for 2050, and accounting for possible thermal acclimation of

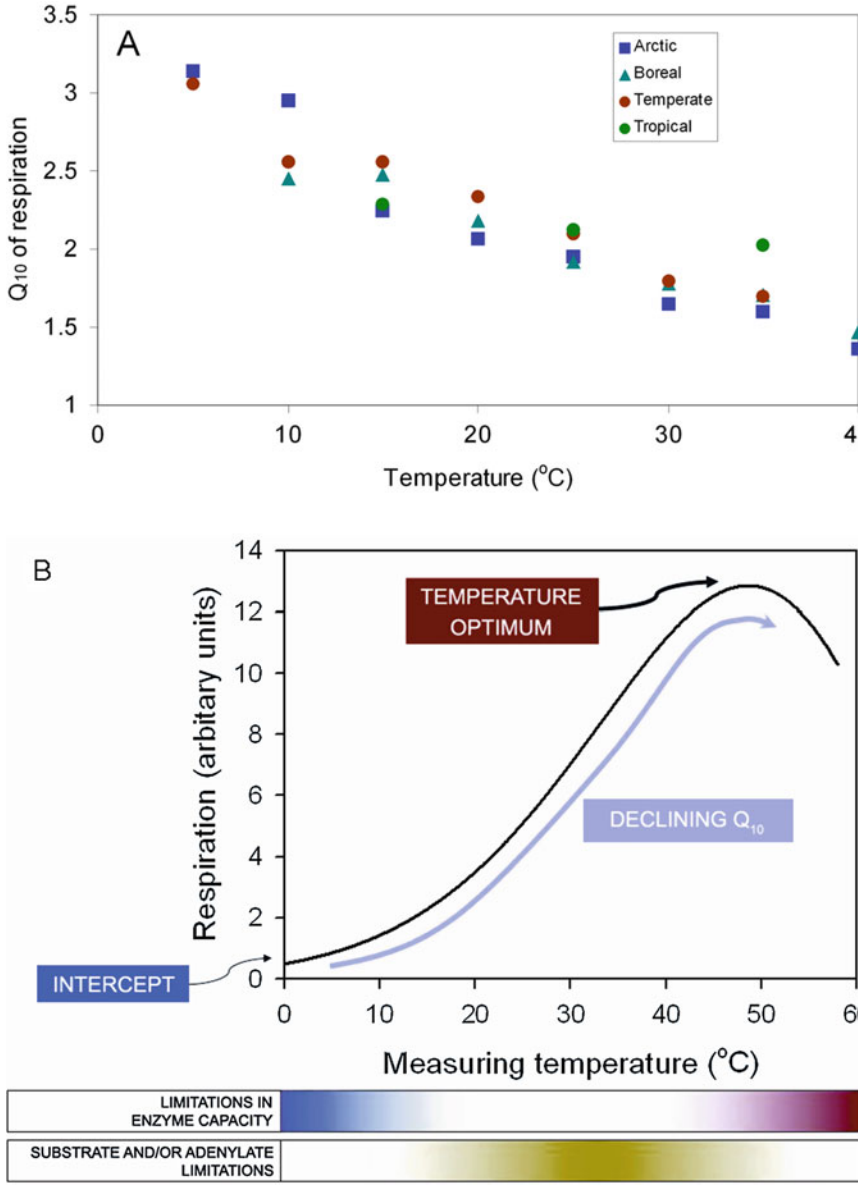

Fig. 3.18 Effects of temperature on plant respiration. (**A**) Q10 of foliar respiration rates in relation to short-term measurement temperature. Symbols are the mean Q10 of species of arctic (blue squares; 49 species), boreal (indicated green triangles; 24 species), temperate (brown circles; 50 species), and tropical (green circles; 3 species). (**B**) Assuming a rate of respiration of 0.5 at 0 °C (arbitrary units), respiration at other temperatures was predicted using the linear decline in Q10 with increasing temperature (shown in A). Both the intercept (i.e. R at 0 °C) and the temperature optimum of respiration (i.e. temperature where respiration rates are maximal) are shown. The lower panels indicate the degree to which respiratory flux is likely limited by enzyme capacity versus substrate supply and adenylates. The temperatures where respiratory flux is likely be limited by maximum catalytic enzyme activity (i.e. Vmax) are indicated in blue (limitations in the cold) and red (limitations at supra-optimal temperatures). At moderate temperatures, respiratory flux is likely regulated by the availability of substrate and/or adenylates (i.e. the absolute concentration of ADP and the ratio of ATP:ADP) (after Atkin and Tjoelker 2003); copyright Elsevier Science, Ltd.

T_{crit} and T_{max}, these safety margins could shrink in a warmer world, as rising temperatures will likely exceed thermal tolerance limits (Fig. 3.18). Thus, increasing numbers of species in many biomes may be at risk as heat-wave events become more severe with climate change (O'Sullivan et al. 2017).

At low measurement temperatures (*e.g.*, 5 °C), respiratory flux is probably limited by the V_{max} (Covey-Crump et al. 2002; lower panels in Fig. 3.19) of the respiratory apparatus [*i.e.* glycolysis, the TCA cycle, and mitochondrial electron transport (Sects 3.2.2 and 3.2.3)]. At moderately high temperatures (*e.g.*, 25 °C), respiratory flux is less limited by enzymatic capacity, because of increases in the V_{max} of enzymes in soluble and membrane-bound compartments; here, respiration is likely limited by substrate availability and/or adenylates. Increased leakiness of membranes at high temperatures may further contribute to substrate limitations. Fine-root respiration of *Acer saccharum* (sugar maple) acclimates to soil warming, particularly when ambient soil temperature are high or soil moisture availability is low. Enzyme or substrate limitation does not account for this acclimation, but adenylate control does, because addition of an uncoupler (Sect. 3.2.3.3) causes a 1.4 times greater stimulation of respiration in roots from warmed soil (Jarvi and Burton 2018). Fine-root respiration in warmed soil is partially constrained by adenylate use, helping constrain respiration to that needed to support work being performed by the roots.

The net result of temperature-mediated shifts in control from **capacity** (at low temperatures) to **substrate** or **adenylate** limitation (at moderately high temperatures) (Fig. 3.19) is that a rise in measurement temperature has less impact on respiratory flux at moderate-high temperatures than it does in the cold. As a result, the calculated Q_{10} is lower when calculated across a high measurement temperature range than at a range of low measurement temperatures. To firmly establish if respiratory enzyme capacity limits respiratory

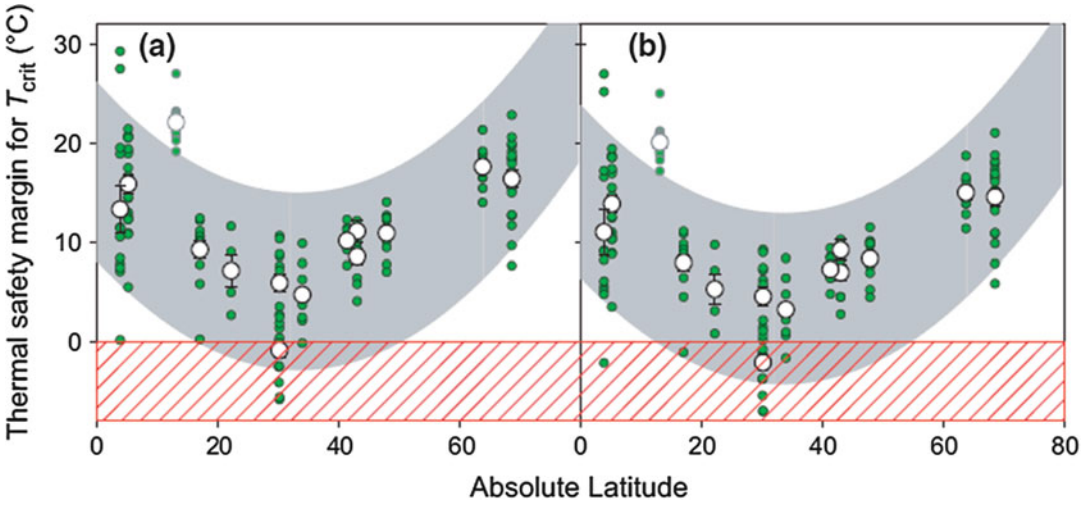

Fig. 3.19 Thermal safety margins of the high temperature outside which photosystem II is disrupted (T_{crit}). Thermal safety margins were determined in A, using measured values of T_{crit} and mean maximum daily temperature (T) over the warmest consecutive 3-day period from 2001 to 2010. Thermal safety margins were determined in B, using predicted future values of T_{crit} and estimated future mean maximum 3-day heat-wave temperatures. Grey shading indicates 95% confidence interval of thermal safety margins across latitudes. Red hatched box refers to thermal safety margins < 0, and so corresponds to the leaf injury zone at which T_{crit} has been exceeded. Green/closed circles indicate individual species-mean values for thermal safety margins at each site. Site-mean values for a high-altitude site in the Peruvian Andes (excluded from regression analysis) are shown with an open, grey circle (O'Sullivan et al. 2017); reprinted with permission from John Wiley & Sons, Inc.

flux in the cold, data are needed on the maximum potential flux of the respiratory apparatus in intact tissues at low temperatures. These can be obtained via measurements of respiration in isolated mitochondria, in the presence of saturating substrates and ADP (Fig. 3.4). Mitochondrial rates can then be scaled up to the whole-plant level (Atkin and Tjoelker 2003). Thermal acclimation may require changes in the expression of genes that encode respiratory enzymes or levels of substrates (Sect. 3.4.4). Acclimation of leaf respiration in field-grown *Eucalyptus pauciflora* (snow gum) occurs without changes in carbohydrate concentrations in leaves (Atkin et al. 2000). Temperature acclimation may also be associated with changes in leaf N concentration, which may affect photosynthesis (Sect. 2.6.1) and, consequently, the respiratory energy requirement for phloem loading (Sect. 3.5; Tjoelker et al. 1999). Acclimation to higher temperatures in leaves of *Arabidopsis thaliana* is associated with an increase in rates of O_2 uptake per unit mitochondrial protein in mesophyll cells (Armstrong et al. 2006).

In addition to acclimation of total respiration, acclimation may also change the partitioning of electrons between the cytochrome and alternative pathways and the activity of **uncoupling proteins**. Using roots of *Triticum aestivum* (wheat) and *Oryza sativa* (rice) cultivars with different degrees of respiratory acclimation shows that high-acclimation cultivars maintain shoot and root growth at low temperature (Kurimoto et al. 2004a). Irrespective of a cultivar's capacity to maintain homeostasis, **cytochrome path capacity** of intact roots and isolated root mitochondria are greater for plants grown at low temperature, and the maximal activity of cytochrome oxidase shows a similar trend. In contrast, **alternative respiration** of intact roots and relative amounts of AOX protein in mitochondria isolated from those roots, are lower in high- acclimation plants grown at low temperature. In the roots of low- acclimation cultivars, relative amounts of AOX protein are greater at low growth temperature. Relative amounts of **uncoupling protein** show similar trends. Maintenance of growth rates in high-acclimation plants grown at low temperature is obviously associated with both respiratory homeostasis and a high efficiency of respiratory ATP production (Kurimoto et al. 2004b).

Needles or leaves of cold-hardened plants that maintain relatively slow rates of respiration when exposed to higher temperatures maintain higher concentrations of soluble sugars which confers greater **frost tolerance**. During a 5 °C warmer-than-average winter in northeast Sweden, *Vaccinium myrtillus* (bilberry) may suffer lethal injuries due to the progressive respiratory loss of **cryoprotective sugars** from their leaves. Initial leaf carbohydrate reserves last four months only if tissue water content remains high due to frequent misty and rainy days; when dehydrated, the leaves' cold tolerance increases (Ögren 1996). Climate warming may impact significantly on cold hardiness of some northern European woody plants such as *Picea abies* (Norway spruce), *Pinus sylvestris* (Scots pine), and *Pinus contorta* (lodgepole pine). In *Pinus contorta* seedlings, climate warming may decrease needle sugar concentrations by 15% which makes them more sensitive to frost. If the seedlings contain unusually large carbohydrate reserves, as found for *Pinus sylvestris*, these may buffer respiratory expenditure of sugars, and thus avoid frost damage. A strong, linear relationship exists between levels of cold hardiness and leaf sugar concentrations (Ögren 2001).

3.4.6 Low pH and High Aluminum Concentrations

Root respiration rate increases as the **pH** in the rhizosphere decreases to a level below that at which growth is no longer possible (Yan et al. 2002). Net H^+ release from roots by H^+-ATPase activity is a prerequisite for continued root growth and limits root growth at very low pH values (Schubert et al. 1990). One way of coping with excess H^+ uptake at a low pH is to increase H^+ pumping by plasma-membrane ATPases. This increases the **demand for respiratory energy**. Increased respiration rates can, therefore, allow plants to maintain root growth at noncritical low

pH values, by increasing the supply of ATP for H^+ pumping by plasma-membrane ATPases.

At very low pH values, root growth, net H^+ release, and respiration rates decline (relative to rates at pH 7.0). The increased entry of H^+ into the roots under these circumstances appears to be responsible for these effects (Yan et al. 1992). Such increased uptake of H^+ tends to disturb cytosolic pH, and ultimately root growth. The decrease in root respiration at very low pH might, therefore, result from the decreased respiratory demand for growth.

A low pH may also affect respiration due to the increased solubility of **aluminum** (Sect. 9.3.1). Respiration of intact roots increases in response to aluminum in both aluminum-resistant and sensitive cultivars of *Triticum aestivum* (wheat) (Collier et al. 1993). Aluminum (Al) stress inhibits mitochondrial respiration and produces **reactive oxygen species** (ROS). Mitochondrial AOX uncouples respiration from mitochondrial ATP production and may improve plant performance under Al stress by preventing excess accumulation of ROS. Overexpression of *AOX* confers aluminum tolerance in *Nicotiana tabacum* (tobacco). This is associated with decreased respiratory inhibition and reduced **ROS** production (Panda et al. 2013). Similar results have been obtained in *Arabidopsis thaliana* (Liu et al. 2014). These results demonstrate that AOX plays a critical role in Al-stress tolerance by enhancing respiratory capacity, thereby reducing mitochondrial oxidative stress.

3.4.7 Partial Pressures of CO_2

When *Arabidopsis thaliana* plants are grown at atmospheric CO_2 concentration that were common in the Pleistocene, their respiration rate is slower than that of plants grown at Holocene CO_2 concentrations; the fastest rates occur in plants grown at elevated [CO_2] (Gonzàlez-Meler et al. 2009). The effects is strongest on the AOX activity, so that the rate of ATP production is similar in plants, irrespective of atmospheric [CO_2].

CO_2 concentrations in air pockets in soil are up to 10- to 100-fold greater than those in the atmosphere. Although respiration rates are fastest in the topsoil where root biomass is concentrated, the CO_2 concentration increases with increasing profile depth, due to the restricted diffusion of gases in soil pores (Oh et al. 2005). The CO_2 concentration in the soil may increase substantially upon **flooding** of the soil. Values of 2.4 and 4.2 mmol CO_2 mol^{-1}, respectively) occur in flooded soils supporting the growth of desert succulents, as opposed to 0.54 and 1.1 mmol mol^{-1} in the same soils, when well-drained (Nobel and Palta 1989). CO_2 concentrations in silt loam supporting the growth of *Fraxinus pennsylvanica* (green ash) and *Quercus nigra* (water oak) are 56 and 38 mmol CO_2 mol^{-1}, respectively (Good and Patrick 1987). Do such high CO_2 concentrations affect root respiration?

Root respiration is reversibly inhibited by 5 mmol CO_2 mol^{-1} in two cacti [*Opuntia ficus-indica* (prickly pear) and *Ferocactus acanthodes* (compass barrel cactus)] (Nobel and Palta 1989). Complete inhibition occurs at 20 mmol CO_2 mol^{-1} (2%) which is irreversible if lasting for at least four hours. Root respiration of *Pseudotsuga menziessii* (Douglas fir) and *Acer saccharum* (sugar maple) is also inhibited at soil CO_2 levels in a range normally found in soil (Qi et al. 1994; Burton et al. 1997), whereas no such inhibition occurs for a range of other species (*e.g.*, Bouma et al. 1997; Scheurwater et al. 1998). Because respiration is only affected by **CO_2**, and *not* by **bicarbonate** (Palet et al. 1991), the pH of the root environment will greatly affect experimental results (Fig. 2.51).

How can we account for effects of very high CO_2 concentration on respiration? The effects of soil CO_2 concentrations on root respiration is probably *indirect*, due to inhibition of energy-requiring processes. There may also be *direct* effects of a high concentration of CO_2 on respiration (*i.e.* inhibition of **cytochrome oxidase**) (Sect. 3.3.6). Other mitochondrial enzymes are also affected by high concentrations of inorganic carbon (Bruhn et al. 2007). Malic enzyme, which oxidizes malate to form pyruvate and CO_2, is strongly inhibited by HCO_3^- in a range that may well account for inhibition of respiration by CO_2 as found in some studies (Chapman and

Hatch 1977). Some of the effects *in vitro* for several mitochondrial enzymes, however, only appear at CO_2 concentrations that are much higher than expected to occur in intact roots.

The information in the literature does not allow a robust conclusion that CO_2 levels that normally occur in well-drained soil have a *direct* inhibitory effect on root respiration (Lambers et al. 2002). After much discussion on inhibition of **leaf respiration** by elevated atmospheric CO_2 concentrations due to **global change**, there is now a consensus that these are mostly artifacts of the methodology (Jahnke and Krewitt 2002; Davey et al. 2004). However, there are *indirect* effects of long-term exposure of plants to elevated [CO_2] (Smith and Dukes 2013). These effects involve transcriptional reprogramming of metabolism (Leakey et al. 2009a) and changes in, *e.g.*, allocation, plant growth rate, chemical composition of the biomass (Tjoelker et al. 1999; Davey et al. 2004). Across all studies, mass-based leaf dark respiration is reduced by 18%, while area-based leaf respiration is marginally increased (8%) under elevated [CO_2] (Wang and Curtis 2002). Area-based leaf respiration of **herbaceous** species increases by 28%, but is unaffected in **woody** species. Mass-based reductions in leaf respiration tend to increase with prolonged exposure to elevated [CO_2]. In cladodes of *Opuntia ficus-indica* (prickly pear), reductions in respiration are associated with a decrease in **mitochondrial number** and cytochrome path activity, and an increase in activity of the alternative path (Gomez-Casanovas et al. 2007). A **meta-analysis** of published results suggests that the amount of carbon used in leaf dark respiration will increase in a higher-[CO_2] environment, This is because of faster area-based leaf respiration rates and a proportionally greater leaf biomass increase than reductions in mass-based leaf respiration (Wang and Curtis 2002). Growth of *Glycine max* (soybean) at elevated [CO_2] (550 μmol mol^{-1}) under field conditions stimulates the rate of nighttime leaf respiration by 37%, driven by greater abundance of transcripts encoding respiratory enzymes (Leakey et al. 2009b). Stimulated respiration is supported by additional carbohydrates available from enhanced photosynthesis at elevated [CO_2]. This is one of the reasons why the stimulation of yield by elevated [CO_2] in crop species is much smaller than expected (Leakey et al. 2009a).

3.4.8 Effects of Nematodes and Plant Pathogens

Attacks on roots or leaves increase their respiration, but the pattern of this respiratory response may differ between sensitive and resistant plant varieties. For example, **nematode** infection of roots of a susceptible variety of *Solanum lycopersicum* (tomato) causes root respiration first to increase, but then to return to the level of uninfested plants. By contrast, the resistant variety shows no initial change in root respiration in response to nematode attack, but after eight days the respiration rate exceeds that of control plants (Zacheo and Molinari 1987).

Just as with tomato roots, leaves of a susceptible variety of *Hordeum distichum* (barley) show a large increase in respiration when infested with the **fungus** causing powdery mildew. This is expected, as both fungus and host have high demands for energy (the fungus for growth, the host for defense). In the case of barley, most of the respiration is accounted for by host respiration (Farrar and Rayns 1987).

Both the levels of **mRNA** that encode AOX and the amount of **AOX protein** strongly increase in leaves of *Arabidopsis thaliana* that are infiltrated with the leaf-spotting bacterium *Pseudomonas syringae* (Simons et al. 1999). What could be the functional significance for an increase of this pathway? Pathogenic fungi may produce **ethylene** and enhance the concentration of **salicylic acid** and **reactive oxygen species** in the plant (Overmyer et al. 2003). These compounds may trigger the increased activity of the alternative path. In ripening fruits, ethylene enhances alternative respiration; salicylic acid induces the large increase in respiration in the spadix of thermogenic *Arum* species (Sect. 3.3.1); reactive oxygen species trigger expression of AOX in a range of species (Considine et al. 2001). Quite likely, the enhanced synthesis of

defense-related compounds (phytoalexins and other phenolics; Sect. 14.3) requires a large production of NADPH in the **oxidative pentose phosphate** pathway (Fig. 3.2; Shaw and Samborski 1957). This pathway, unlike glycolysis (Fig. 3.3), is not regulated by the demand for metabolic energy. Products of the oxidative pentose phosphate pathway can enter glycolysis, bypassing the steps controlled by energy demand. Additional NADPH can be produced by a cytosolic **NADP-malic enzyme**, which oxidizes malate, producing pyruvate and CO_2. This enzyme is induced upon addition of elicitors (*i.e.* chemical components of a microorganism that induces the synthesis of defense compounds in plant cells) (Sect. 14.3; Schaaf et al. 1995). The increased activity of the oxidative pentose pathway and of NADP-malic enzyme probably leads to the delivery of a large amount of pyruvate and malate to the mitochondria, without there being an increased need for ATP. As a result, the cytochrome path becomes saturated with electrons, AOX is activated (Sect. 3.2.6.2), and much of the electron transport occurs via the alternative pathway (Sect. 3.3.3; Simons and Lambers 1999).

3.4.9 Leaf Dark Respiration as Affected by Photosynthesis

Both photosynthesis and mitochondrial respiration ('dark' respiration, as opposed to photorespiration) produce ATP and NAD(P)H to meet demands for plant growth and maintenance. The light reaction in photosynthesis provides ATP and NAD(P)H for biosynthesis in a leaf cell during illumination, but mitochondrial respiration in the light is necessary for biosynthetic reactions in the cytosol, such as sucrose synthesis (Krömer 1995). Respiratory activity in the light can be considered part of the photosynthetic process, because it is needed to regulate the redox state of the stroma in the chloroplast during photosynthesis (Foyer and Noctor 2000) and to maintain the cytosolic ATP pool (Krömer 1995). Under conditions where ATP demand for photosynthetic CO_2 fixation is sufficiently high, the mitochondria supply the bulk of ATP for the cytosol. In contrast, under stress conditions where CO_2 fixation is severely limited, ATP will build up in chloroplasts and it can then be exported to the cytosol, by metabolite shuttle mechanisms (Gardeström and Igamberdiev 2016). Thus, depending on the conditions, either mitochondria or chloroplasts can supply the bulk of ATP for the cytosol. Light inhibits leaf dark respiration, but the extent of inhibition and its effect on O_2 *versus* uptake and CO_2 release depends on species and environmental conditions. Leaf day respiration should be regarded as a central actor of plant carbon-use efficiency (Tcherkez et al. 2017).

In leaves of *Eucalyptus pauciflora* (snow gum), respiration is inhibited most at very low light intensities and moderate temperatures, and considerably less at higher irradiance. The irradiance necessary to maximally inhibit respiration at 6–10 °C is lower than that at 15–30 °C (Atkin et al. 2000). In leaves of *Xanthium strumarium* (common cocklebur), respiration is inhibited at both ambient and elevated CO_2 concentrations, but to a lesser degree for plants grown at elevated (17–24% inhibition) than for those grown at ambient (29–35% inhibition) CO_2 concentrations, presumably because elevated CO_2-grown plants have a higher demand for energy and carbon skeletons (Wang et al. 2001). Variation in light inhibition of leaf respiration can have a substantial impact on the proportion of carbon fixed in photosynthesis that is respired.

The metabolic origin of the CO_2 production in leaf dark respiration during photosynthesis can be analyzed by feeding ^{13}C-enriched glucose or pyruvate to intact leaves. Using metabolites that are ^{13}C-enriched in different positions, reveals that in leaves of *Phaseolus vulgaris* (common bean) the activity of the TCA cycle is reduced by 95% in the light; pyruvate dehydrogenase activity, however, is reduced much less (27%). Glucose molecules are scarcely metabolized to liberate CO_2 in the light, because glycolysis is downregulated. Instead, glucose is mainly used for sucrose synthesis. Several metabolic processes (glycolysis, TCA cycle) are downregulated, leading to a light-dependent inhibition of mitochondrial respiration (Tcherkez et al. 2005). Using an analytical model for

nonphotorespiratory CO_2 release to evaluate causes for suppression of respiration by light, Buckley and Adams (2011) predict engagement of nonphosphorylating pathways at moderate to high light, or concurrent with processes that yield ATP and NADH, such as fatty acid or terpenoid synthesis.

3.5 The Role of Respiration in Plant Carbon Balance

3.5.1 Carbon Balance

Approximately half of all the photosynthates produced per day are respired in the same period, depending on species and environmental conditions (Table 3.1). Globally rising temperatures tend to increase the proportion of carbon gained in photosynthesis that is subsequently used in respiration (Atkin et al. 2007). The level of irradiance and the photoperiod affect the carbon balance of acclimated plants to a relatively small extent, but factors such as a limiting nutrient supply and water stress may greatly increase the proportion of photosynthates used in respiration. This is accounted for by a much stronger effect of nutrients on biomass allocation, when compared with that of irradiance and photoperiod (Chap. 10). Root temperature likely also affects the plant carbon balance, because this has a major effect on biomass allocation (Sect. 10.5.2.2).

3.5.1.1 Root Respiration

Root respiration accounts for approximately 10–50% of the total carbon assimilated each day in photosynthesis (Table 3.1), and is a major proportion of the plant's carbon budget (Fig. 3.20). This percentage is much higher in slow-growing than in fast-growing plants. This is true for a comparison of species that vary in their **potential growth rate** (Poorter et al. 1991) and for plants of the same species that vary in growth rate, due to variation in **nutrient supply** (Van der Werf et al. 1992b). Root temperatures

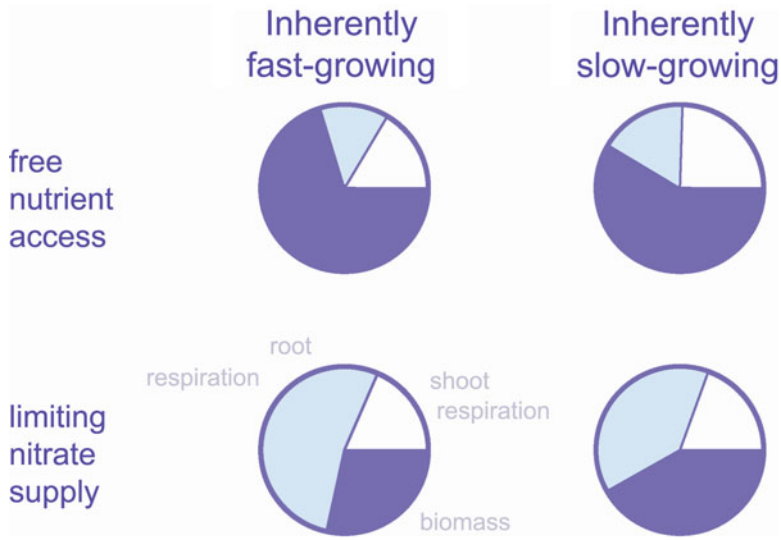

Fig. 3.20 The fraction of all carbohydrates produced in photosynthesis per day that is consumed in respiration as dependent on species and the nitrogen supply. Measurements were made on inherently fast-growing (pies on the left) and slow-growing (pies on the right) grass species grown with free nutrient availability (pies at the top) and at a nitrogen supply that allowed a relative growth rate of approximately 40 mg g^{-1} day^{-1} (pies at the bottom). The purple section of the pie refers to carbon invested in biomass; the other two sections refer to carbon used in shoot respiration (white sector), and in root respiration (light blue) pie (Van der Werf et al. 1992b); copyright SPB Academic Publishing.

that enhance biomass allocation to roots (Sect. 10.5.2.2) probably also increase the proportion of carbon required for root respiration. When slow growth is due to exposure to low light levels, however, no greater respiratory burden is incurred (Sect. 3.4.4). To some extent the proportionally greater carbon use in slow-growing plants is accounted for by their relatively low carbon gain per unit plant mass (Sect. 10.3; Poorter et al. 1995). This does not explain the entire difference, however; variation in respiratory efficiency and/or respiratory costs for processes like ion transport may play an additional role (Sect. 3.5.2.3).

Root respiration provides the driving force for root growth and maintenance and for ion absorption and loading into the xylem. The percentage of total assimilates that is used in root respiration tends to decrease as plants age. Such a decrease may be due to a decrease in the demand for respiratory energy, when the energy required for root growth and ion uptake decreases. Furthermore, the root mass ratio tends to decrease with increasing age, thus decreasing the respiratory burden of roots.

The fraction of carbohydrates used in root respiration, including the respiration of symbionts, if present, is affected by both abiotic and biotic environmental factors (Table 3.1). Root respiration is faster in the presence of an **N_2-fixing symbiont** than when nonnodulated roots are supplied with NO_3^- as an N source. This reflects the greater energy requirement for N-assimilation during N_2-fixation compared with NO_3^--assimilation (Sect. 12.3). The fraction of carbohydrates used in root respiration is also greater in the presence of a symbiotic **mycorrhizal fungus** than in nonsymbiotic plants (Table 3.1).

The *proportion* of the carbohydrates translocated to roots that is used in respiration, rather than root biomass accumulation, increases with plant age. This is primarily due to the increasing role of maintenance respiration, as root growth slows down and as the *quantity* of assimilates translocated to roots declines (Sect. 3.5.2). Low nutrient supply also increases the proportion of carbohydrates respired in the roots. At a high nutrient supply, plants respire approximately 40% of the carbon imported into the roots. This fraction increases to 60% at very low nutrient supply (Van der Werf et al. 1992b). This increase is largely accounted for by a relatively high carbon requirement for maintenance processes compared with that in growth processes. An additional factor is the proportionally low requirement for root growth (relative to maintenance) under these low-nutrient conditions. Finally, specific costs for maintenance or ion uptake might increase when nutrients are in short supply (Sect. 3.5.2; Van der Werf et al. 1994).

3.5.1.2 Respiration of Other Plant Parts

Leaf respiration provides some of the metabolic energy for leaf growth and maintenance, for ion transport from the xylem and export of solutes to the phloem. Leaf respiration, expressed as a fraction of the carbon gain in photosynthesis, however, varies much less than root respiration, because photosynthesis, leaf respiration and biomass allocation are affected similarly by changes in nutrient supply. This differs from the situation for roots, where a major cause of the large variation found for root respiration (Table 3.1) is the effect of nutrient supply and genotype on **biomass allocation** to roots.

Rates of photosynthesis and leaf respiration often vary in a similar manner with changes in environment (*e.g.*, N supply and growth irradiance) (Reich et al. 1998). This may be explained by greater respiratory costs of export of photosynthates from leaves which vary with the carbon gained in photosynthesis. There may also be greater maintenance costs in leaves with rapid rates of photosynthesis and high protein concentrations. Specific costs for major energy-requiring processes (*e.g.*, for transport of assimilates from the mesophyll to the sieve tubes) may also vary among species and environmental conditions (Cannell and Thornley 2000).

The respiration of other plant parts (*e.g.*, fruits) is largely accounted for by their growth rate and the respiratory costs per unit of growth. The maintenance component also plays a role. In green fruits, a substantial proportion of this

energetic requirement may be met by photosynthesis in the fruit (DeJong and Walton 1989; Blanke and Whiley 1995). Respiration of the flowers of *Citrus paradisi* (grapefruit) shows a distinct peak about 42 days after emergence, after a peak in respiration associated with growth of the flower. A major part of the respiration of the grapefruit flowers is probably accounted for by the alternative path (Bustan and Goldschmidt 1998; Considine et al. 2001).

3.5.2 Respiration Associated with Growth, Maintenance, and Ion Uptake

The rate of respiration depends on three major energy-requiring processes: **maintenance** of biomass, **growth,** and (ion) **transport**, as summarized in the following overall equation:

$$r = r_m + c_g \times RGR + c_t \times TR \qquad (3.2)$$

where r is the rate of respiration (normally expressed as nmol O_2 or CO_2 g^{-1} s^{-1}, but to comply with the units in which *RGR* is expressed, we use here μmol g^{-1} day^{-1}); r_m is the rate of respiration to produce ATP for the maintenance of biomass; c_g (μmol O_2 or CO_2 g^{-1}) is the respiration to produce ATP for the synthesis of cell material; *RGR* is the relative growth rate of the roots (mg g^{-1} day^{-1}); c_t (mol O_2 or CO_2 mol^{-1}) is the rate of respiration required to support *TR*, the transport rate (μmol g^{-1} day^{-1}). In roots *TR*, equals the net ion uptake rate and the rate of xylem loading; in photosynthesizing leaves *TR* equals the rate of export of the products of photosynthesis (from mesophyll to sieve tubes). Although respiration can be measured as either O_2 uptake or as CO_2 release, the measurements do not yield exactly the same values. First, *RQ* may not equal 1.0 (Sect. 3.2.1); second, the rate of CO_2 release varies with the rate of NO_3^- reduction, whereas rates of O_2 consumption do not. For this reason, **O_2 consumption** is preferred as a basis to compare plants when we are interested in **respiratory efficiency**, whereas **CO_2 release** is preferred when comparing the **carbon budgets** of different plants.

By examining these three requirements for respiratory energy, we can estimate how the ATP produced in respiration is used for major plant functions. This equation assumes a tight correlation between the rate of respiration and the rates of major energy-requiring processes; there is no implicit assumption that respiration controls the rate of the energy-requiring processes, or *vice versa*.

3.5.2.1 Maintenance Respiration

Once biomass is produced, energy must be expended for repair and maintenance. Estimates of the costs of maintaining biomass range from 35 to 80% of the photosynthates produced per day (Amthor 2000), higher values pertaining to plants that grow very slowly (Lambers et al. 2002) and lower values to shade-adapted species (Noguchi et al. 2001a). The energy demands of the individual maintenance processes *in vivo* are not well known and reliable estimates of individual maintenance costs are scarce. A major part of the maintenance energy costs is associated with **protein turnover** (Hachiya et al. 2007) and with the maintenance of **solute gradients** across membranes. These costs of maintenance have been estimated from basic biochemical principles (Penning de Vries 1975; Bouma 2005).

In plants, approximately 2–5% of all the proteins are replaced daily, with extreme estimates being as high as 20% (Van der Werf et al. 1992a; Bouma et al. 1994). It is quite likely that **protein turnover** rates vary among plant organs, species and with growth conditions, but the data are too scanty to make firm statements. The cost of synthesizing proteins from amino acids is estimated at 4.7–7.9 ATP, and possibly double that, per peptide bond, or approximately 0.26 (possibly 0.52) g glucose g^{-1} protein (Amthor 2000). Approximately 75% of amino acids from degraded proteins are recycled (Davies 1979). The remaining 25% must be synthesized from basic carbon skeletons, at a cost of 0.43 g glucose g^{-1} protein. The total cost of protein turnover is about 28–53 mg glucose g^{-1} day^{-1}, or 3–5% of dry mass per day. Similar calculations

for lipids suggest that membrane turnover constitutes a much lower energy requirement, approximately 1.7 mg glucose g^{-1} day^{-1}, or 0.2% of dry mass per day. Based on an experimentally determined protein half-life of 5 days, the respiratory energy requirement to sustain protein turnover is approximately 1 mmol ATP g^{-1} (dry mass) day^{-1} [*i.e.* 7% of the total respiratory energy produced in roots of *Dactylis glomerata* (cocksfoot)]. Expressed as a fraction of the total maintenance requirement as derived from a multiple regression analysis (Sect. 3.5.2) [*i.e.* 2.7 mmol ATP g^{-1} (dry mass) day^{-1} for *Carex* (sedge) species], the maintenance requirement for protein turnover is quite substantial (Van der Werf et al. 1992a).

Maintenance of **solute gradients** is also an important maintenance process. Some estimates suggest that the cost of maintaining solute gradients are up to 30% of the respiratory costs involved in ion uptake, or approximately 20% of the total respiratory costs of young roots (Bouma and De Visser 1993).

Other processes (*e.g.*, cytoplasmic streaming and turnover of other cellular constituents) are generally assumed to have a relatively small cost. Based on these many (largely unproven) assumptions, the total estimated maintenance respiration is approximately 30–60 mg glucose g^{-1} day^{-1} (3–6% of dry mass day^{-1}). Measured values of maintenance respiration (8–60 mg glucose g^{-1} day^{-1}) suggest that these rough estimates are reasonable. These experimental values for maintenance respiration suggest that protein turnover and the maintenance of solute gradients are by far the largest costs of maintenance in plant tissues. If true, then this conclusion has important implications for plant carbon balance, because it suggests that any factor that increases protein concentration or turnover or the leakiness of membranes will increase maintenance respiration.

The positive correlation of respiration rate with N concentration (Reich et al. 2006) is consistent with the prediction that maintenance respiration depends on protein concentration. Thus, leaves that have a high N investment in Rubisco and other photosynthetic enzymes have a correspondingly high maintenance demand. Faster respiration rates might reflect greater costs for the loading of photosynthates in the phloem, which is an ATP-requiring process (Sect. 4.3.3). Whatever the explanation for the faster leaf respiration rates, they do contribute to their higher light-compensation point (Sect. 2.3.2.1), and, therefore, place a higher limit on the irradiance level at which these leaves can maintain a positive carbon balance. Thus, there is a **trade-off** between high metabolic activity (requiring high protein concentrations and rapid loading of the phloem) and the associated increase in cost of maintenance and transport. However, no single universal scaling relationship accounts for variation in leaf dark respiration across a large biogeographical space; variability among sites in rates of leaf respiration and the ratio of respiration to photosynthesis is driven by variation in N- and P-use efficiency (Rowland et al. 2016).

The stimulation of maintenance respiration by temperature is a logical consequence of the increased leakage and of protein turnover that occurs at high temperature (Rachmilevitch et al. 2006; Hachiya et al. 2007). This provides a conceptual framework for studies that seek to explain why different organs and species differ in their Q_{10} of respiration. Perhaps this reflects differences in membrane properties upon prolonged exposure to higher temperatures or in thermal stability of proteins, with corresponding differences in protein turnover. It might also reflect a difference in contribution of the cytochrome and the alternative pathways.

Increased maintenance respiration is often assumed to be the cause of declines in forest productivity in late succession (Waring and Schlesinger 1985). Maintenance respiration remains relatively constant through succession, however, while growth and growth respiration decline. The more likely cause of reduced growth in old forest stands is a reduced carbon gain caused by loss of leaf area and loss of photosynthetic capacity associated with reduced hydraulic conductance, and in some cases with reduced nutrient availability (Ryan et al. 1997).

3.5.2.2 Growth Respiration

Production of biomass (**biosynthesis**) requires the input of carbohydrates, partly to generate ATP and NAD(P)H for biosynthetic reactions and partly to provide the carbon skeletons present in biomass (Fig. 3.21; Table 3.9). Plant biomass is, in general, more reduced than the carbohydrates from which it is produced, and the cost of biosynthesis from primary substrates must therefore include the carbohydrates necessary to supply reducing power, for example for the reduction of NO_3^-. If a more reduced source of N is absorbed instead (*e.g.*, NH_4^+ or amino acids) (Sect. 9.2.2), then biosynthetic costs are less. When an organ senesces, most of the chemical constituents are lost to the plant, but some are resorbed and can be used in the production of new organs. The **final cost** of producing biomass is the **initial cost** minus **resorption** (Fig. 3.22).

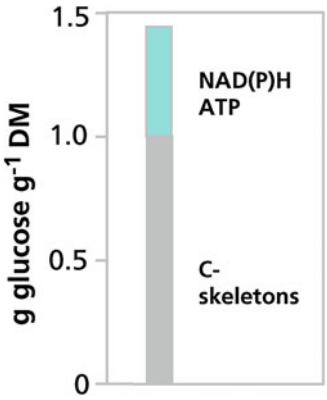

Fig. 3.21 Construction costs of leaf biomass. Most of the glucose required for biomass production ends up in the carbon compounds in the biomass. Because the average carbon compound biomass is more reduced than the carbohydrates from which it is produced, some glucose is required to produce NADPH. Some of the glucose is required to produce ATP that drives many energy-requiring biosynthetic reactions in the cell. The data are for an 'average' leaf.

In photosynthetically active leaves, some of the metabolic energy (ATP and NAD(P)H) may come directly from photosynthesis. In heterotrophic organs such as roots, and in leaves in the dark, respiration provides all the required energy. The amount of respiratory energy that is required for biosynthesis can be calculated from the composition of the biomass in several ways, as discussed in this Section.

First, costs for biosynthesis can be derived from detailed information on the **biochemical composition**, combined with biochemical data on the costs of synthesis of all the major compounds: protein, total nonstructural

Table 3.9 Values for characterizing the conversion of substrates to products during biosynthesis, excluding costs of substrate uptake from the environment*.

Compound	*PV′*	*ORF′*	*CPF′*	RQ′	*HRF*	*ERF*
Amino acids with NH_4^+	700	169	5772	34	−11.2	−1.4
Amino acids with NO_3^-	700	169	5772	34	26.7	39.0
Protein with NH_4^+	604	163	5727	35	−12.9	34.9
Protein with NO_3^-	604	163	5727	35	31.4	82.0
Carbohydrates	853	0	1295	–	−3.6	12.2
Lipids	351	0	10,705	–	−10.1	51.0
Lignin	483	1388	5545	4	−4.3	18.7
Organic acids	1104	0	−1136	–	16.9	−4.5

Source: De Visser et al. (1992)

*Production Value, *PV′*: mg of the end product per g of substrate required for carbon skeletons and energy production, without taking into account the fate of excess or shortage of NAD(P)H and ATP (the term Production Value, *PV*, is used when *PV′* is corrected for this component); Oxygen Requirement Factor, *ORF′*: μmol of O_2 consumed per gram of substrate required for carbon skeletons and energy production, without taking into account the fate of excess or shortage of NAD(P)H and ATP; Carbon dioxide Production Factor, *CPF′*: μmol of CO_2 produced per g of substrate required for carbon skeletons and energy production, without taking into account the fate of excess or shortage of NAD(P)H and ATP (the term Carbon dioxide Production Factor, *CPF*, is used when *CPF′* is corrected for this component); *RQ′* is the ratio of *CPF′* and *ORF′*; Hydrogen Requirement Factor, *HRF*: moles of NAD(P)H required (−) or produced (+) per gram of end product; Energy Requirement Factor, *ERF*: moles of ATP required (−) or produced (+) per gram of end product (Penning de Vries et al. 1974). More recent findings, for example on the importance of targeting sequences of proteins which are required to 'direct' the synthesized proteins to a specific compartment in the cell, indicate that the costs for protein synthesis are likely to be substantially higher, possibly even double the value presented in this table

carbohydrates (*i.e.* sucrose, starch, fructans), total structural carbohydrates (*i.e.* cellulose, hemicellulose), lignin, lipid, organic acids, minerals. This can be extended to include various other compounds, *e.g.*, soluble amino acids, nucleic acids, tannins, lipophilic defense compounds, alkaloids, but these are mostly ignored and generally combined with the major ones. Taking glucose as the standard substrate for biosynthesis, one can estimate the amount of glucose required to provide the carbon skeletons, reducing equivalents and ATP for the biosynthesis of plant compounds in tissues (Table 3.9; Poorter and Villar 1997).

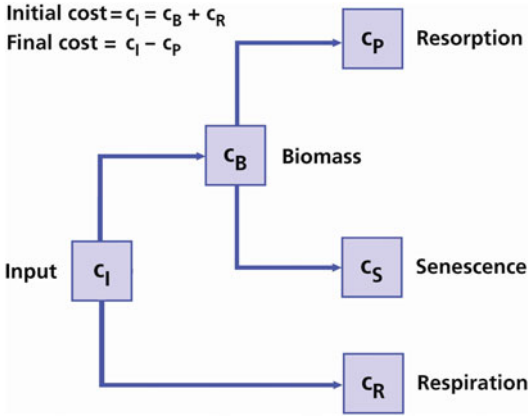

Fig. 3.22 Fate of carbon that is initially invested (C_I) in synthesizing a structure. Some of the carbon is retained in the biomass (C_B), the remainder is required for respiration (C_R). Of the carbon in the biomass (C_B), most is lost or respired when a plant part is shed (C_S) but some is resorbed (C_P) for subsequent use (after Chapin 1989).

The amount of product produced per unit carbon substrate (production value, *PV*') varies nearly threefold among chemical constituents (Table 3.10), with lipid and lignin being most expensive (*i.e.* requiring greatest glucose investment per gram of product), and organic acids least expensive. Compounds like proteins and lipids are very costly in terms of ATP required for their biosynthesis, whereas carbohydrates and cellulose are not. There are both expensive and cheap ways to produce structure in plants (lignin and cellulose/hemicellulose, respectively) and to store energy (lipid and sugars/starch, respectively) (Chapin 1989). Plants generally use energetically cheap structural components (cellulose/hemicellulose) and energy stores (sugars and starch). By contrast, mobile animals and small seeds, where mass is an important issue, often use lipids as their energy store. Immobile animals, like plants, use carbohydrate (glycogen) as their primary energy store. Knowing the costs and concentrations of the major compounds in plant biomass, we can calculate the costs for a gram of biomass. As for individual compounds, these costs can be expressed in terms of glucose, O_2 requirement, CO_2 release, requirement for reducing power and ATP (Table 3.10).

The major assumption underlying the approach based on the biochemical composition of the biomass is that glucose is the sole substrate

Table 3.10 An example of a simplified calculation of the variables characterizing biosynthesis of biomass from glucose, nitrate and minerals.

Compound	Concentration in biomass required (mg g^{-1} dry mass)	Glucose for synthesis	O_2 required for synthesis (μmol)	CO_2 production during synthesis (mmol)	NAD(P)H required for synthesis (mmol)	ATP required for synthesis (mmol)
N-compounds	230	371	65	2100	7.14	17.83
Carbohydrates	565	662	0	857	−2.03	6.92
Lipids	25	71	0	807	0.25	1.27
Lignin	80	166	230	918	−0.34	1.50
Organic acids	50	45	0	−52	−0.84	−0.23
Minerals	50	0	0	0	0	0
Total	1000	1315	295	4630	3.68	27.29

Source: Penning de Vries et al. (1974)

for all ATP, reductant, and carbon skeletons. When some of these resources are derived directly from photosynthesis, costs may be lower. Costs may be higher when the alternative path, rather than the cytochrome path plays a predominant role in respiration. If we restrict this approach to nonphotosynthetic organs in which the contribution of the cytochrome and alternative respiratory pathway is known, then there is still a source of error, if these organs import compounds other than glucose, for example amino acids, as a substrate for biosynthesis.

A second method for estimating the construction cost is based on information on the **elemental composition** of organs: C, H, O, N, and S (McDermitt and Loomis 1981). The constructions costs that are not covered by this equation include costs of mineral uptake and transport of various compounds in the plant, costs for providing ATP for biosynthetic reactions, and reductant required to reduce molecular O_2 in some biosynthetic reactions. This method is less laborious than the first method, which requires detailed chemical analysis; however, it is based on the observations of the first method (*i.e.* that expensive compounds are generally more reduced than glucose, whereas cheap compounds are more oxidized) (Poorter 1994). Although this method, based on elemental analysis of plant biomass, may seem a crude approach, the approach is surprisingly effective. First, this is because two thirds of the construction costs are costs to provide carbon skeletons, rather than for respiration. Second, most of the carbon that does not end up in the carbon skeletons of biomass is required to reduce carbon skeletons, and not for the production of ATP. So, even in the absence of detailed information on respiratory pathways, construction costs can be estimated rather accurately. In fact, the second method can be simplified even further, taking into account only the **carbon and ash content** of biomass and ignoring minor constituents that have only a small effect on the production value (Vertregt and Penning de Vries 1987).

The level of reduction of plant biomass is approximately linearly related to its **heat of combustion** as well as its costs of construction (McDermitt and Loomis 1981). For example, lipids are highly reduced compounds and have a high heat of combustion. A third method, therefore, uses this approximation to arrive at costs for providing carbon skeletons and reductant for biosynthesis (Williams et al. 1987).

Given the three-fold range in the cost of producing different organic constituents in plants and the large range in concentrations of these constituents among plant parts and species [often 2–10-fold (Fig. 3.23)], we might expect large differences in costs of synthesizing plant biomass of differing chemical composition. A given organ, however, tends to have *either* a high concentration of proteins and tannins (allowing high metabolic activity and chemical defense of these organs) *or* a high concentration of lignin and lipophilic secondary metabolites (Chapin 1989). The negative correlation between the concentrations of these two groups of expensive constituents is seen in the comparison of leaves *vs.* stems or in the comparison of leaves of fast-growing species (*e.g.*, forbs) and slow-growing species (evergreen shrubs) (Fig. 3.23). The net result of this trade-off between expensive components allowing rapid metabolic activity (proteins) *vs.* those allowing persistence (lignin and lipophilic defensive compounds) is that the cost of all plant species and plant parts are remarkably similar: approximately 1.5 g glucose per gram of biomass (Fig. 3.24). Another important correlation that explains the similarity of construction costs across species and organs is that organs of fast-growing species that have high protein concentrations (an expensive constituent) also have high concentrations of minerals (cheap constituents) (Poorter 1994; Villar et al. 2006). This explains why simple relationships are good predictors of costs of synthesis.

Small seeds are an exception to the generalization that all plant biomass has a similar cost of synthesis. Seed lipids are primarily an energy store (rather than an antiherbivore compound), and are positively associated with protein concentration, leading to a high carbon cost. The similarity among species and organs in carbon cost of synthesis has the practical consequence that biomass is a good predictor of carbon cost. A probable explanation is that the negative correlations

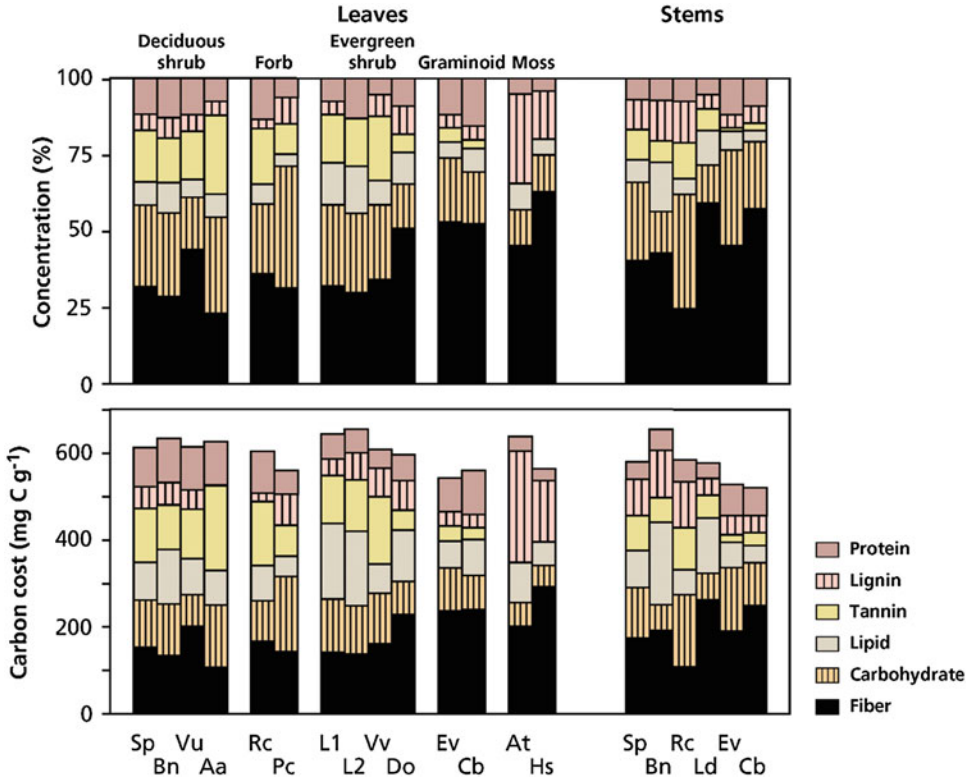

Fig. 3.23 The chemical composition and carbon cost of producing leaves and stems of 13 species of tundra plants. Note that these carbon costs do not include the respiratory costs associated with their synthesis, unlike the costs presented in Fig. 3.24 and Table 3.10. Species shown are *Salix pulchra* (willow, Sp), *Betula nana* (dwarf birch, Bn), *Vaccinium uliginosum* (blueberry, Vu), *Arctostaphylos alpina* (bearberry, Aa), *Rubus chamaemorus* (cloudberry, Rc), *Pedicularis capitata* (wooly lousewort, Pc), *Ledum decumbens* (Labrador tea, Ld, including 1-year-old, L1, and 2-year-old, L2, leaves), *Vaccinium vitis-idaea* (low-bush cranberry, Vv), *Dryas octopetala* (mountain avens, Do), *Eriophorum vaginatum* (tussock cottongrass, Ev), *Carex bigelowii* (Bigelow sedge, Cb), *Aulocomnium turgidum* (turgid aulacomnium moss, At), and *Hylocomium splendens* (feathermoss, Hs) (after Chapin 1989).

among expensive constituents and the positive correlation between protein and minerals have a basic physiological significance that, by coincidence, leads to a similar carbon cost of synthesis in most structures. For example, lignin and protein concentrations may be negatively correlated, because young expanding cells have a high protein concentration, but cell expansion would be prevented by lignin, or heavy lignification might render cell walls less permeable to water and solutes which would be disadvantageous in organs with high metabolic activity (as gauged by high protein concentration). In general, currently available data suggest that costs of synthesis differ much less within (10–20%) and among (25%) ecosystems than do other causes of variation in carbon balance, such as respiration and allocation (Chapin 1989; Villar et al. 2006).

3.5.2.3 Respiration Associated with Ion Transport

Ion transport across membranes may occur via ion channels, if transport is down an electrochemical potential gradient, or via ion carriers, which allow transport against an electrochemical potential gradient (Sect. 9.2.2.2). Because cation **transport from the rhizosphere** into the symplast mostly occurs down an electrochemical potential

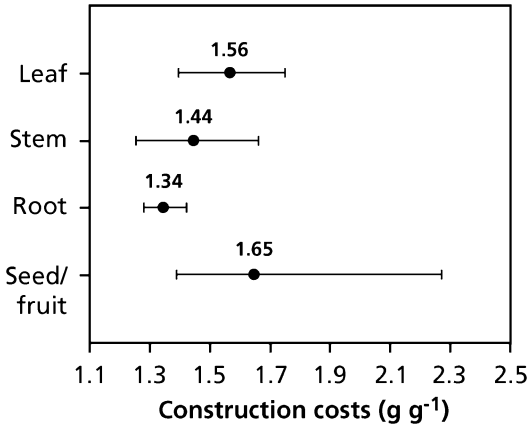

Fig. 3.24 Range of construction costs for a survey of leaves (n = 123), stems (n = 38), roots (n = 35), and fruits/seeds (n = 31). Values are means and 10th and 90th percentiles (Poorter 1994); copyright SPB Academic Publishing.

gradient, cation channels are often involved in this transport. This requires respiratory energy to extrude protons into the apoplast and create an **electrochemical potential gradient**. Transport of anions from the rhizosphere into the symplast almost invariably occurs against an electrochemical gradient and hence requires respiratory energy, mostly because such anion transport is coupled to proton re-entry into the cells (Sect. 9.2.2.2).

The situation is exactly the opposite for the transport of ions from the symplast to the xylem (**xylem loading**). Anions might enter the xylem via channels, as this transport is mostly down an electrochemical gradient; however, we know little about such a mechanism (De Boer and Wegner 1997). The transport of most cations is against an electrochemical gradient, and hence the transport of cations to the xylem depends directly on metabolic energy. Release of anions into the xylem may be passive, but it still depends on the presence of an electrochemical potential gradient, which is maintained by the expenditure of metabolic energy. On the other hand, resorption of anions must be active (involving carriers) whereas that of cations may occur via channels (De Boer and Wegner 1997; Zhu et al. 2007).

When NO_3^- is the major source of N, this will be the major anion absorbed, because only 10% and 1%, respectively, as much P and S compared with N are required to produce biomass (Fig. 9.33 in Sect. 9.4.1.1). Uptake of amino acids will also be against an electrochemical potential gradient, and hence require a proton-cotransport mechanism similar to that for NO_3^-. Like the uptake of NO_3^- and amino acids, P uptake also occurs via a proton symport mechanism (Sect. 9.2.2.2). When P availability is low, however, P acquisition may require exudation of carboxylates (Sect. 9.2.2.5) which will incur additional carbon expenditure (Raven et al. 2018). Similarly, P acquisition through a symbiotic association with mycorrhizal fungi requires additional carbon (Sect. 12.2.6).

As long as there is an electrochemical potential gradient, which is a prerequisite for the uptake of anions, cations can enter the symplast passively. In fact, plants may well need mechanisms to excrete cations that have entered the symplast passively, to avoid excessive uptake of some cation (*e.g.*, Na^+) (Sect. 9.3.4.2). When NH_4^+ is the predominant N source for the plant, such as in acid soils where rates of nitrification are slow, this can enter the symplast via a cation channel. Rapid uptake of NH_4^+, however, must be balanced by excretion of H^+, so as to maintain a negative membrane potential. Hence, NH_4^+ uptake also occurs with expenditure of respiratory energy.

When NO_3^- is the predominant N-source, rather than NH_4^+ or amino acids, there are additional costs for its reduction. These show up with carbon costs and CO_2 release, but not in O_2 uptake (Table 3.9), because some of the NADH generated in respiration is used for the reduction of NO_3^-, rather than reduction of O_2. As a result, the *RQ* strongly depends on the source of N (NH_4^+ or NO_3^-; Table 3.2) and on the rate of NO_3^- reduction. Costs associated with NO_3^- acquisition are less when the reduction of NO_3^- occurs in leaves exposed to relatively high light intensities, as opposed to reduction in the roots, because the reducing power generated in the light reactions exceeds that needed for the reduction of CO_2 in the Calvin-Benson cycle under these conditions (Sect. 2.3.2.1).

Given that N is a major component of plant biomass, most of the respiratory energy

associated with nutrient acquisition in plants with free access to nutrients will be required for the uptake of this nutrient.

3.5.2.4 Experimental Evidence

Measurements made with roots provide an opportunity to test the concepts of maintenance respiration, growth respiration, and respiration associated with transport. We assume that the rate of respiration for maintenance of root biomass is linearly related to the root biomass to be maintained. Second, we assume that the rate of respiration for ion transport is proportional to the amount of ions taken up, whereas that for root growth is proportional to the relative growth rate of the roots, provided the chemical composition of the root biomass does not change in a manner that affects the specific costs of biomass synthesis; superimposed is the maintenance respiration. Third, we assume that the contribution of the alternative path to total respiration is constant. Based on these assumptions, which are largely untested, the rate of ATP production per gram of roots and per day can be related to the relative growth rate of the roots and the rate of anion uptake by the roots. We can improve the approach by assessing the contribution of the **alternative path** (Box 3.1), and correct for any changes during plant development (Florez-Sarasa et al. 2007; Del-Saz et al. 2018). The costs of the three processes can then be estimated by **multiple regression analysis**, presented graphically in a three-dimensional plot (Fig. 3.25, left). If a plant's relative growth rate and rate of anion uptake are very closely correlated, which is common, then a multiple regression analysis cannot separate the costs of growth from those of ion uptake (Fig. 3.25, right).

Using the analysis depicted in Fig. 3.25A, respiratory costs for growth, maintenance, and ion uptake have been obtained for a number of species (Table 3.11A). Quite often, the correlation between *RGR* and nutrient uptake is so tight, that a linear regression analysis, as depicted in Fig. 3.25B, is the only approach possible (Table 3.11B). There is quite a large variation in

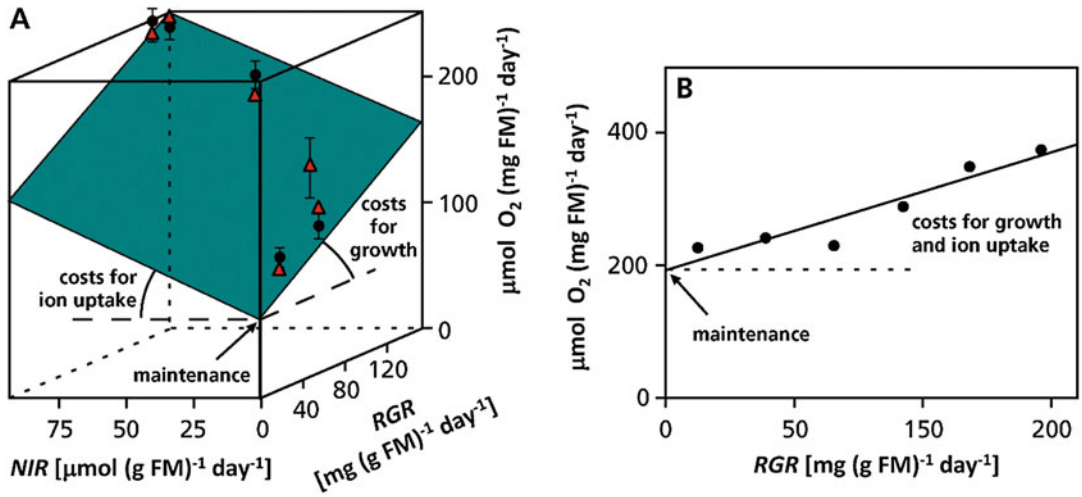

Fig. 3.25 (**A**) Rate of O_2 consumption per unit fresh mass (FM) in roots as related to both the relative growth rate (*RGR*) of the roots and their net rate of anion uptake (NIR). (**B**) Rate of O_2 consumption per unit fresh mass in roots as related to the relative growth rate of the roots. The plane in (**A**) and line in (**B**) give the predicted mean rate of O_2 consumption. The intercept of the plane in (**A**) and the line in (**B**) with the y-axis gives the rate of O_2 consumption in the roots which is required for maintenance. The slope of the projection of the line on the y-z plane gives the O_2 consumption required to produce one gram of biomass. When projected on the x-y plane, the slope gives the specific respiratory costs for ion transport. In (**B**) the slope gives costs for growth including ion uptake (after Lambers et al. 2002).

Table 3.11 (**A**) Specific respiratory energy costs for the maintenance of root biomass, for root growth and for ion uptake. (**B**) Specific respiratory energy costs for the maintenance of root biomass and for root growth including costs for ion uptake.

(A)	*Carex* species	*Solanum tuberosum*	*Zea mays*
Growth, mmol O_2 (g dry mass)$^{-1}$	6.3	10.9	9.9
Maintenance, nmol O_2 (g dry mass)$^{-1}$ s^{-1}	5.7	4.0	12.5
Anion uptake, mol O_2 (mol ions)$^{-1}$	1.0	1.2	0.53

(B)	*Dactylis glomerata*	*Festuca ovina*	*Quercus suber*	*Triticum aestivum*
Growth + ion uptake, mmol O_2 (g dry mass)$^{-1}$	11	19	12	18
Maintenance, nmol (g dry mass)$^{-1}$ s^{-1}	26	21	6	22

Sources: (**A**) The values were obtained using a multiple regression analysis, as explained in Fig. 3.25A [Van der Werf et al. (1988): average values for *Carex acutiformis* (pond sedge) and *Carex diandra* (lesser panicled sedge); Bouma et al. (1996): *Solanum tuberosum* (white potato); Veen (1980): *Zea mays* (maize)]. (**B**) The values were obtained using a linear regression analysis, as explained in Fig. 3.25B [Scheurwater et al. (1998): *Dactylis glomerata* (cocksfoot) and *Festuca ovina* (sheep's fescue); (Mata et al. 1996): *Quercus suber* (cork oak); Van den Boogaard, as cited in Lambers et al. (2002): *Triticum aestivum* (wheat)]

experimental values among species. This may reflect real differences between species; however, the variation may also indicate that the statistical analysis 'explained' part of respiration by ion uptake in one experiment and by maintenance in another. For example, a costly process like ion leakage from roots, followed by re-uptake, may show up in the slope or in the y-intercept in the graph, and suggest large costs for ion uptake or for maintenance, respectively. At the fastest rates of growth and ion uptake (young plants, fast-growing species) these data suggest that respiration for growth and ion uptake together account for about 80% of root respiration, and that maintenance respiration is relatively small. With increasing age, when growth and ion uptake slow down, maintenance respiration accounts for an increasing proportion of total respiration (over 85%).

The specific costs for *Carex* (sedge) species (Table 3.11A) were used to calculate the rate of root respiration of 24 other herbaceous species of differing potential growth rate whose rates of growth and ion uptake were known. These calculations greatly over-estimate the rate of root respiration of fast-growing species, when compared with measured values (Fig. 3.26). This suggests that either the efficiency of respiration is greater (*e.g.*, relatively more cytochrome path and less alternative path activity) in fast-growing species, or that the specific costs for growth, maintenance or ion uptake are lower for fast-growing species. Is there any evidence to support either hypothesis?

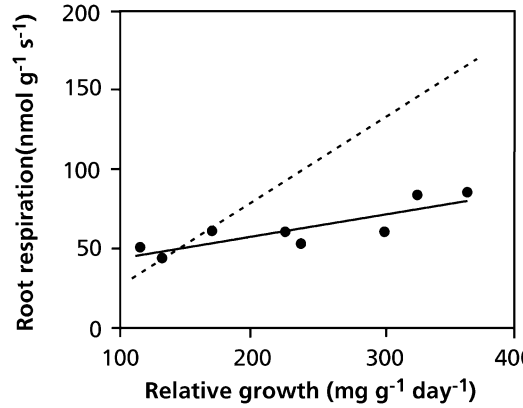

Fig. 3.26 The rate of root respiration of fast-growing and slow-growing herbaceous C_3 species. The broken line gives the calculated respiration rate, assuming that specific costs for growth, maintenance, and ion uptake are the same as those given in Table 3.11 and identical for all investigated species (Poorter et al. 1991); © Scandinavian Plant Physiology Society.

Roots of fast-growing grass species exhibit faster rates of alternative path activity than slow-growing grasses (Millenaar et al. 2001), and hence there is no evidence for a more efficient respiration in roots of fast-growing species. Specific respiratory costs for root growth are

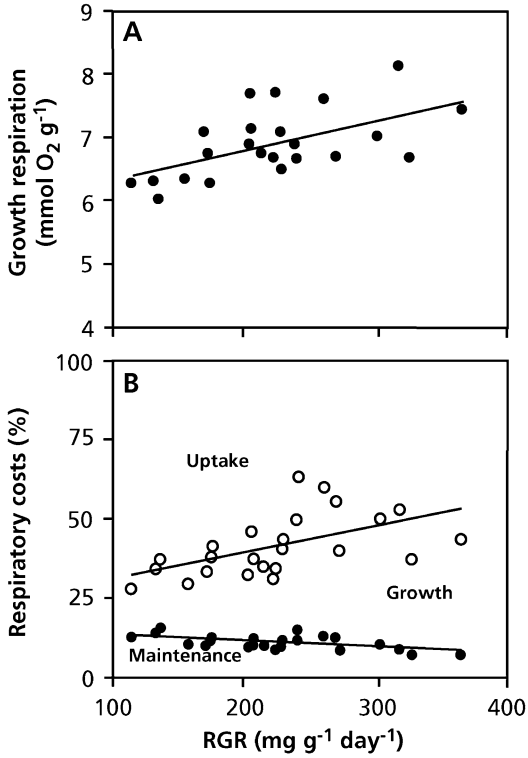

Fig. 3.27 Characteristics of root respiration of inherently fast- and slow-growing herbaceous species, grown at free nutrient availability. (**A**) Respiratory cost for growth, as derived from an analysis of the roots' chemical composition and known cost for the synthesis of the various plant compounds. (**B**) Assuming similar respiratory efficiencies and maintenance costs for all species and using the costs for growth as given in (**A**), the specific costs for ion uptake were calculated. It is suggested that these costs are substantially higher for slow-growing herbaceous species than for fast-growing ones (Poorter et al. 1991); © Scandinavian Plant Physiology Society.

somewhat higher for fast-growing species (Fig. 3.27A), and maintenance costs, if anything, are higher, rather than lower, for roots of fast-growing species, possibly be due to their higher protein concentrations and associated turnover costs (Scheurwater et al. 1998, 2000). If neither a low respiratory efficiency nor higher costs for growth or maintenance can account for unexpectedly fast respiration rates of slow-growing plants, then the discrepancy between the expected and measured rates of root respiration (Fig. 3.26) must be based on higher **specific costs** for ion uptake in the inherently slow-growing species (Fig. 3.27).

These higher specific costs when plants are grown with free access to NO_3^- are accounted for by a large **efflux of NO_3^-** (Sect. 9.2.2.2; Scheurwater et al. 1999). It should be noted that many slow-growing species naturally grow in a low-NO_3^- environment, and hence would rarely be exposed to the experimental conditions as referred to here. The question that remains to be addressed is whether NO_3^- efflux also plays a role when NO_3^- availability limits plant growth. Given that root respiration rates are also unexpectedly fast for plants grown at a severely limiting NO_3^- supply (Fig. 3.14), this is a likely possibility.

The rate of root respiration of plants grown with a limiting nutrient supply is slower than that of plants grown with free access to nutrients, but not nearly as slow as expected from their very slow rates of growth and nutrient acquisition (Sect. 3.4.3). This again suggests increased specific costs, possibly for ion uptake. Further experimental evidence is needed to address this important question concerning the carbon balance and growth of slow-growing plants.

In summary, experimental data show that the concept of respiration associated with growth, maintenance, and ion uptake is a valuable tool in understanding the carbon balance of plants, and that the partitioning of respiration among these functions differs substantially with environment and the type of plant species.

3.6 Plant Respiration: Why Should It Concern Us from an Ecological Point of View?

A large number of measurements have been made on the gas exchange (*i.e.* rates of photosynthesis, respiration, and transpiration) of different plants growing under contrasting conditions (O'Leary et al. 2019). Those measurements have yielded fascinating experimental results, some of which have been discussed in Chap. 2. There is often the (implicit) assumption, however, that rates of photosynthesis provide us with vital information on plant growth and productivity. Certainly, photosynthesis is essential for most of the gain in plant biomass; however, can we really derive essential

information on growth rate and yield from measurements on photosynthesis alone?

Rates of photosynthesis per unit leaf area are poorly correlated with rates of growth (Poorter et al. 1990), let alone crop yield (Gifford et al. 1984). One of the reasons that emerged in this chapter is that the fraction of all carbohydrates that are gained in photosynthesis and subsequently used in plant respiration varies considerably. First, slow-growing genotypes require relatively more of their photoassimilates for respiration. Second, many environmental variables affect respiration more than photosynthesis. This is mainly because the size of nonphotosynthetic plant parts, relative to that of the photosynthetically active leaves depends on the environment, as we discuss in Chap. 10. Clearly, an important message from this chapter is that measurements of leaf photosynthesis by themselves cannot provide sound information on a plant's growth rate or productivity.

A second message is that respiration and the use of respiratory energy [NAD(P)H, ATP] are not tightly linked. Respiration may proceed via pathways that do not yield the respiratory products needed for growth, but produce heat instead. These components of respiration can be substantial, at least in some plants under some conditions. In reproductive organs, the production of heat may be important to attract pollinators or disperse seeds, but the ecophysiological significance of nonphosphorylating pathways in other organs is different.

A challenge for the future will be to explore to what extent respiration scales with other plants traits, as has been done for photosynthesis (Sect. 2.6). There is clear evidence that leaf respiration rates scale with their N concentration, as photosynthesis does (Atkin et al. 2015).

References

Amthor JS. 2000. The McCree-de Wit-Penning de Vries-Thornley respiration paradigms: 30 years later. *Ann Bot* **86**: 1–20.

Araújo WL, Tohge T, Ishizaki K, Leaver CJ, Fernie AR. 2011. Protein degradation – an alternative respiratory substrate for stressed plants. *Trends Plant Sci* **16**: 489–498.

Armstrong AF, Logan DC, Tobin AK, O'Toole P, Atkin OK. 2006. Heterogeneity of plant mitochondrial responses underpinning respiratory acclimation to the cold in *Arabidopsis thaliana* leaves. *Plant Cell Environ* **29**: 940–949.

Atkin OK, Bloomfield KJ, Reich PB, Tjoelker MG, Asner GP, Bonal D, Bönisch G, Bradford M, Cernusak LA, Cosio EG, Creek D, Crous KY, Domingues T, Dukes JS, Egerton JJG, Evans JR, Farquhar GD, Fyllas NM, Gauthier PPG, Gloor E, Gimeno TE, Griffin KL, Guerrieri R, Heskel MA, Huntingford C, Ishida FY, Kattge J, Lambers H, Liddell MJ, Lloyd J, Lusk CH, Martin RE, Maksimov AP, Maximov TC, Mahli Y, Medlyn BE, Meir P, Mercado LM, Mirotchnick N, Ng D, Niinemets Ü, O'Sullivan OS, Philips OL, Poorter L, Poot P, Prentice IC, Salinas N, Rowland LM, Ryan MG, Sitch S, Slot M, Smith NG, Turnbull MH, VanderWel MC, Valladares F, Veneklaas EJ, Weerasinghe LK, Wirth C, Wright IJ, Wythers K, Xiang J, Xiang S, Zaragoza-Castells J. 2015. Global variability in leaf respiration in relation to climate, plant functional types and leaf traits. *New Phytol* **206**: 614–636.

Atkin OK, Evans JR, Ball MC, Lambers H, Pons TL. 2000. Leaf respiration of snow gum in the light and dark. Interactions between temperature and irradiance. *Plant Physiol* **122**: 915–924.

Atkin OK, Scheurwater I, Pons TL. 2007. Respiration as a percentage of daily photosynthesis in whole plants is homeostatic at moderate, but not high, growth temperatures. *New Phytol* **174**: 367–380.

Atkin OK, Tjoelker MG. 2003. Thermal acclimation and the dynamic response of plant respiration to temperature. *Trends Plant Sci* **8**: 343–351.

Atkin OK, Villar R, Lambers H. 1995. Partitioning of electrons between the cytochrome and alternative pathways in intact roots. *Plant Physiol* **108**: 1179–1183.

Atkinson LJ, Hellicar MA, Fitter AH, Atkin OK. 2007. Impact of temperature on the relationship between respiration and nitrogen concentration in roots: an analysis of scaling relationships, Q10 values and thermal acclimation ratios. *New Phytol* **173**: 110–120.

Ben Zioni A, Vaadia Y, Lips SH. 1971. Nitrate uptake by roots as regulated by nitrate reduction products of the shoot. *Physiol Plant* **24**: 288–290.

Bigeleisen J, Wolfsberg M. 1957. Theoretical and experimental aspects of isotope effects in chemical kinetics. *Adv Chem Phys* **1**: 15–76.

Bingham IJ, Farrar JF. 1988. Regulation of respiration in roots of barley. *Physiol Plant* **73**: 278–285.

Blanke MM, Whiley AW. 1995. Bioenergetics, respiration cost and water relations of developing avocado fruit. *J Plant Physiol* **145**: 87–92.

Blokhina O, Virolainen E, Fagerstedt KV. 2003. Antioxidants, oxidative damage and oxygen deprivation stress: a review. *Ann Bot* **91**: 179–194.

Bloom A, Epstein E. 1984. Varietal differences in salt-induced respiration in barley. *Plant Sci Lett* **35**: 1–3.

Bouma TJ 2005. Understanding plant respiration: separating respiratory components versus a process-based approach. In: Lambers H, Ribas-Carbó M eds. *Plant Respiration: From Cell to Ecosystem*. Dordrecht: Springer, 177–194.

Bouma TJ, Broekhuysen AGM, Veen BW. 1996. Analysis of root respiration of *Solanum tuberosum* as related to growth, ion uptake and maintenance of biomass. *Plant Physiol Bochem* **34**: 795–806.

Bouma TJ, De Visser R. 1993. Energy requirements for maintenance of ion concentrations in roots. *Physiol Plant* **89**: 133–142.

Bouma TJ, De Visser R, Janssen JHJA, De Kock MJ, Van Leeuwen PH, Lambers H. 1994. Respiratory energy requirements and rate of protein turnover *in vivo* determined by the use of an inhibitor of protein synthesis and a probe to assess its effect. *Physiol Plant* **92**: 585–594.

Bouma TJ, Nielsen KL, Eissenstat DM, Lynch JP. 1997. Estimating respiration of roots in soil: Interactions with soil CO_2, soil temperature and soil water content. *Plant Soil* **195**: 221–232.

Bruhn D, Wiskich JT, Atkin OK. 2007. Contrasting responses by respiration to elevated CO2 in intact tissue and isolated mitochondria. *Funct Plant Biol* **34**: 112–117.

Buckley TN, Adams MA. 2011. An analytical model of non-photorespiratory CO_2 release in the light and dark in leaves of C_3 species based on stoichiometric flux balance. *Plant Cell Environ* **34**: 89–112.

Burton AJ, Zogg GP, Pregitzer KS, Zak DR. 1997. Effect of measurement CO_2 concentration on sugar maple root respiration. *Tree Physiol* **17**: 421–427.

Bustan A, Goldschmidt EE. 1998. Estimating the cost of flowering in a grapefruit tree. *Plant Cell Environ* **21**: 217–224.

Cannell MGR, Thornley JHM. 2000. Modelling the components of plant respiration: some guiding principles. *Ann Bot* **85**: 45–54.

Chapin FS. 1989. The cost of tundra plant structures: evaluation of concepts and currencies. *Amer Nat* **133**: 1–19.

Chapman KSR, Hatch MD. 1977. Regulation of mitochondrial NAD-malic enzyme involved in C_4 pathway photosynthesis. *Arch Biochem Biophys* **184**: 298–306.

Collier DE, Ackermann F, Somers DJ, Cummins WR, Atkin OK. 1993. The effect of aluminum exposure on root respiration in an aluminum-sensitive and an aluminum-tolerant cultivar of *Triticum aestivum*. *Physiol Plant* **87**: 447–452.

Colmer TD, Armstrong W, Greenway H, Ismail AM, Kirk GJD, Atwell BJ. 2014. Physiological mechanisms of flooding tolerance in rice: transient complete submergence and prolonged standing water. *Progr Bot* **75**: 255–307.

Considine MJ, Daley DO, Whelan J. 2001. The expression of alternative oxidase and uncoupling protein during fruit ripening in mango. *Plant Physiol* **126**: 1619–1629.

Covey-Crump EM, Attwood RG, Atkin OK. 2002. Regulation of root respiration in two species of *Plantago* that differ in relative growth rate: the effect of short- and long-term changes in temperature. *Plant Cell Environ* **25**: 1501–1513.

Covey-Crump EM, Bykova NV, Affourtit C, Hoefnagel MHN, Gardeström P, Atkin OK. 2007. Temperature-dependent changes in respiration rates and redox poise of the ubiquinone pool in protoplasts and isolated mitochondria of potato leaves. *Physiol Plant* **129**: 175–184.

Dacey JWH. 1980. Internal winds in water lilies: an adaptation for life in anaerobic sediments. *Science* **210**: 1017–1019.

Dahal K, Martyn GD, Vanlerberghe GC. 2015. Improved photosynthetic performance during severe drought in Nicotiana tabacum overexpressing a nonenergy conserving respiratory electron sink. *New Phytol* **208**: 382–395.

Dahal K, Wang J, Martyn GD, Rahimy F, Vanlerberghe GC. 2014. Mitochondrial alternative oxidase maintains respiration and preserves photosynthetic capacity during moderate drought in *Nicotiana tabacum*. *Plant Physiol* **166**: 1560–1574.

Danova-Alt R, Dijkema C, De Waard P, Köck M. 2008. Transport and compartmentation of phosphite in higher plant cells – kinetic and ^{31}P nuclear magnetic resonance studies. *Plant Cell Environ* **31**: 1510–1521.

Davey PA, Hunt S, Hymus GJ, DeLucia EH, Drake BG, Karnosky DF, Long SP. 2004. Respiratory oxygen uptake is not decreased by an instantaneous elevation of [CO2], but is increased with long-term growth in the field at elevated [CO_2]. *Plant Physiol* **134**: 520–527.

Davies DD 1979. Factors affecting protein turnover in plants. In: Hewitt EJ, Cutting CV eds. *Nitrogen Assimilation of Plants*. London: Academic Press, 369–396.

Day DA, Krab K, Lambers H, Moore AL, Siedow JN, Wagner AM, Wiskich JT. 1996. The cyanide-resistant oxidase: to Inhibit or not to inhibit, that is the question. *Plant Physiol* **110**: 1–2.

Day DA, Whelan J, Millar AH, Siedow JN, Wiskich JT. 1995. Regulation of alternative oxidase in plants and fungi. *Aust J Plant Physiol* **22**: 497–509.

De Boer AH, Wegner LH. 1997. Regulatory mechanisms of ion channels in xylem parenchyma cells. *J Exp Bot* **48**: 441–449.

De Col V, Fuchs P, Nietzel T, Elsaesser M, Voon CP, Candeo A, Seeliger I, Fricker MD, Grefen C, Møller IM. 2017. ATP sensing in living plant cells reveals tissue gradients and stress dynamics of energy physiology. *Elife* **6**: e26770.

de Lamarck JB. 1778. *Flore Française*. Paris: L'Imprimerie Royale.

De Visser R, Spitters CJT, Bouma T 1992. Energy costs of protein turnover: theoretical calculation and experimental estimation from regression of respiration on protein concentration of full-grown leaves. In: Lambers H, Van der Plas LHW eds. *Molecular,*

Biochemical and Physiological Aspects of Plant Respiration. The Hague: SPB Academic Publishing, 493–508.

Dean JF, Middelburg JJ, Röckmann T, Aerts R, Blauw LG, Egger M, Jetten MSM, Jong AEE, Meisel OH, Rasigraf O, Slomp CP, Zandt MH, Dolman AJ. 2018. Methane feedbacks to the global climate system in a warmer world. *Rev Geophys* **56**: 207–250.

deBruyn RAJ, Paetkau M, Ross KA, Godfrey DV, Church JS, Friedman CR. 2015. Thermogenesis-triggered seed dispersal in dwarf mistletoe. *Nat Comm* **6**: 6262.

DeJong TM, Walton EF. 1989. Carbohydrate requirements of peach fruit growth and respiration. *Tree Physiol* **5**: 329–335.

Del-Saz NF, Ribas-Carbo M, McDonald AE, Lambers H, Fernie AR, Florez-Sarasa I. 2018. An *in vivo* perspective of the role(s) of the alternative oxidase pathway. *Trends Plant Sci* **23**: 206–219.

Dry I, Moore A, Day D, Wiskich J. 1989. Regulation of alternative pathway activity in plant mitochondria: nonlinear relationship between electron flux and the redox poise of the quinone pool. *Arch Biochem Biophys* **273**: 148–157.

Dudkina NV, Kouřil R, Peters K, Braun H-P, Boekema EJ. 2010. Structure and function of mitochondrial supercomplexes. *Biochim Biophys Acta Bioenerg* **1797**: 664–670.

Escobar MA, Geisler DA, Rasmusson AG. 2006. Reorganization of the alternative pathways of the *Arabidopsis* respiratory chain by nitrogen supply: opposing effects of ammonium and nitrate. *Plant J* **45**: 775–788.

Farrar JF, Rayns FW. 1987. Respiration of leaves of barley infected with powdery mildew: increased engagement of the alternative oxidase. *New Phytol* **107**: 119–125.

Felle HH. 2005. pH regulation in anoxic plants. *Ann Bot* **96**: 519–532.

Figueira TRS, Arruda P. 2011. Differential expression of uncoupling mitochondrial protein and alternative oxidase in the plant response to stress. *J Bioenerg Biomembr* **43**: 67–70.

Fiorani F, Umbach AL, Siedow JN. 2005. The alternative oxidase of plant mitochondria is involved in the acclimation of shoot growth at low temperature. A study of *Arabidopsis OX1a* transgenic plants. *Plant Physiol* **139**: 1795–1805.

Fischer S, Hanf S, Frosch T, Gleixner G, Popp J, Trumbore S, Hartmann H. 2015. *Pinus sylvestris* switches respiration substrates under shading but not during drought. *New Phytol* **207**: 542–550.

Florez-Sarasa ID, Bouma TJ, Medrano H, Azcón-Bieto J, Ribas-Carbó M. 2007. Contribution of the cytochrome and alternative pathways to growth respiration and maintenance respiration in *Arabidopsis thaliana*. *Physiol Plant* **129**: 143–151.

Florez-Sarasa ID, Lambers H, Wang X, Finnegan PM, Ribas-Carbó M. 2014. The alternative respiratory pathway mediates carboxylate synthesis in white lupin cluster roots under phosphorus deprivation. *Plant Cell Environ* **37**: 922–928.

Foyer CH, Noctor G. 2000. Oxygen processing in photosynthesis: regulation and signalling. *New Phytol* **146**: 359–388.

Fredeen AL, Field CB. 1991. Leaf respiration in *Piper* species native to a Mexican rainforest. *Physiol Plant* **82**: 85–92.

Galmés J, Ribas-Carbó M, Medrano H, Flexas J. 2007. Response of leaf respiration to water stress in Mediterranean species with different growth forms. *J Arid Environ* **68**: 206–222.

Gardeström P, Igamberdiev AU. 2016. The origin of cytosolic ATP in photosynthetic cells. *Physiol Plant* **157**: 367–379.

Gifford RM, Thorne JH, Hitz WD, Giaquinta RT. 1984. Crop productivity and photoassimilate partitioning. *Science* **225**: 801–808.

Gomez-Casanovas N, Blanc-Betes E, Gonzalez-Meler MA, Azcon-Bieto J. 2007. Changes in respiratory mitochondrial machinery and cytochrome and alternative pathway activities in response to energy demand underlie the acclimation of respiration to elevated CO_2 in the invasive *Opuntia ficus-indica*. *Plant Physiol* **145**: 49–61.

Gonzàlez-Meler MA, Blanc-Betes E, Flower CE, Ward JK, Gomez-Casanovas N. 2009. Plastic and adaptive responses of plant respiration to changes in atmospheric CO_2 concentration. *Physiol Plant* **137**: 473–484.

Good B, Patrick W. 1987. Gas composition and respiration of water oak (*Quercus nigra* L.) and green ash (*Fraxinus pennsylvanica* Marsh.) roots after prolonged flooding. *Plant Soil* **97**: 419–427.

Gupta KJ, Kumari A, Florez-Sarasa I, Fernie AR, Igamberdiev AU. 2018. Interaction of nitric oxide with the components of plant mitochondrial electron transport chain. *J Exp Bot* **69**: 3413–3424.

Guy RD, Berry JA, Fogel ML, Hoering TC. 1989. Differential fractionation of oxygen isotopes by cyanide-resistant and cyanide-sensitive respiration in plants. *Planta* **177**: 483–491.

Hachiya T, Noguchi K. 2011. Integrative response of plant mitochondrial electron transport chain to nitrogen source. *Plant Cell Rep* **30**: 195–204.

Hachiya T, Terashima I, Noguchi K. 2007. Increase in respiratory cost at high growth temperature is attributed to high protein turnover cost in *Petunia* × *hybrida* petals. *Plant Cell Environ* **30**: 1269–1283.

Hachiya T, Watanabe CK, Boom C, Tholen D, Tajahara K, Kawai-Yamada M, Uchimiya H, Uesono Y, Terashima I, Noguchi K. 2010. Ammonium-dependent respiratory increase is dependent on the cytochrome pathway in *Arabidopsis thaliana* shoots. *Plant Cell Environ* **33**: 1888–1897.

Hanf S, Fischer S, Hartmann H, Keiner R, Trumbore S, Popp J, Frosch T. 2015. Online investigation of respiratory quotients in *Pinus sylvestris* and

Picea abies during drought and shading by means of cavity-enhanced Raman multi-gas spectrometry. *Analyst* **140**: 4473–4481

Hebelstrup KH, Møller IM 2015. Mitochondrial signaling in plants under hypoxia: use of reactive oxygen species (ROS) and reactive nitrogen species (RNS). In: Gupta KJ, Igamberdiev AU eds. *Reactive Oxygen and Nitrogen Species Signaling and Communication in Plants*. Cham: Springer, 63–77.

Henry BK, Atkin OK, Farquhar GD, Day DA, Millar AH, Menz RI. 1999. Calculation of the oxygen isotope discrimination factor for studying plant respiration. *Funct Plant Biol* **26**: 773–780.

Herzog M, Striker GG, Colmer TD, Pedersen O. 2015. Mechanisms of waterlogging tolerance in wheat – a review of root and shoot physiology. *Plant Cell Environ* **39**: 1068–1086.

Heskel MA, Atkin OK, O'Sullivan OS, Reich P, Tjoelker MG, Weerasinghe LK, Penillard A, Egerton JJG, Creek D, Bloomfield KJ, Xiang J, Sinca F, Stangl ZR, Martinez-de la Torre A, Griffin KL, Huntingford C, Hurry V, Meir P, Turnbull MH. 2016a. Reply to Adams et al.: Empirical versus process-based approaches to modeling temperature responses of leaf respiration. *Proc Natl Acad Sci USA* **113**: E5996–E5997.

Heskel MA, O'Sullivan OS, Reich PB, Tjoelker MG, Weerasinghe LK, Penillard A, Egerton JJG, Creek D, Bloomfield KJ, Xiang J, Sinca F, Stangl ZR, Martinez-de la Torre A, Griffin KL, Huntingford C, Hurry V, Meir P, Turnbull MH, Atkin OK. 2016b. Convergence in the temperature response of leaf respiration across biomes and plant functional types. *Proc Natl Acad Sci USA* **113**: 3832–3837.

Hoefnagel M, Rich PR, Zhang Q, Wiskich JT. 1997. Substrate kinetics of the plant mitochondrial alternative oxidase and the effects of pyruvate. *Plant Physiol* **115**: 1145–1153.

Hoefs J. 1987. *Stable Iisotope Geochemistry*. Berlin: Springer-Verlag.

Huntingford C, Atkin OK, Martinez-de la Torre A, Mercado LM, Heskel MA, Harper AB, Bloomfield KJ, O'Sullivan OS, Reich PB, Wythers KR, Butler EE, Chen M, Griffin KL, Meir P, Tjoelker MG, Turnbull MH, Sitch S, Wiltshire A, Malhi Y. 2017. Implications of improved representations of plant respiration in a changing climate. *Nat Comm* **8**: 1602.

Jackson MB, Herman B, Goodenough A. 1982. An examination of the importance of ethanol in causing injury to flooded plants. *Plant Cell Environ* **5**: 163–172.

Jacoby RP, Millar AH, Taylor NL 2018. Mitochondrial biochemistry: stress responses and roles in stress alleviation. In: Logan DC ed. *Annual Plant Reviews, Volume 50: Plant Mitochondria, Second Edition*. Chicester: John Wiley & Sons Ltd, 227–268.

Jahnke S, Krewitt M. 2002. Atmospheric CO_2 concentration may directly affect leaf respiration measurement in tobacco, but not respiration itself. *Plant Cell Environ* **25**: 641–651.

Jarvi MP, Burton AJ. 2018. Adenylate control contributes to thermal acclimation of sugar maple fine-root respiration in experimentally warmed soil. *Plant Cell Environ* **41**: 504–516.

Kaschuk G, Kuyper TW, Leffelaar PA, Hungria M, Giller KE. 2009. Are the rates of photosynthesis stimulated by the carbon sink strength of rhizobial and arbuscular mycorrhizal symbioses? *Soil Biol Biochem* **41**: 1233–1244.

Knutson RM. 1974. Heat production and temperature regulation in eastern skunk cabbage. *Science* **186**: 746–747.

Krapp A, Stitt M. 1994. Influence of high carbohydrate content on the activity of plastidic and cytosolic isoenzyme pairs in photosynthetic tissues. *Plant Cell Environ* **17**: 861–866.

Krömer S. 1995. Respiration during photosynthesis. *Annu Rev Plant Physiol Plant Mol Biol* **46**: 45–70.

Kruse J, Gao P, Honsel A, Kreuzwieser J, Burzlaff T, Alfarraj S, Hedrich R, Rennenberg H. 2014. Strategy of nitrogen acquisition and utilization by carnivorous Dionaea muscipula. *Oecologia* **174**: 839–851.

Kurimoto K, Day DA, Lambers H, Noguchi K. 2004a. Effect of respiratory homeostasis on plant growth in cultivars of wheat and rice. *Plant Cell Environ* **27**: 853–862.

Kurimoto K, Millar AH, Lambers H, Day DA, Noguchi K. 2004b. Maintenance of growth rate at low temperature in rice and wheat cultivars with a high degree of respiratory homeostasis is associated with a high efficiency of respiratory ATP production. *Plant Cell Physiol* **45**: 1015–1022.

Lambers H. 1982. Cyanide-resistant respiration: a nonphosphorylating electron transport pathway acting as an energy overflow. *Physiol Plant* **55**: 478–485.

Lambers H, Atkin OK, Millenaar FF 2002. Respiratory patterns in roots in relation to their functioning. In: Y. Waisel, A. Eshel, Kafkaki U eds. *Plant Roots: The Hidden Half*. New York: Marcel Dekker Inc., 521–552.

Lambers H, Blacquière T, Stuiver B. 1981. Interactions between osmoregulation and the alternative respiratory pathway in *Plantago coronopus* as affected by salinity. *Physiol Plant* **51**: 63–68.

Lambers H, Day DA, Azcón-Bieto J. 1983. Cyanide-resistant respiration in roots and leaves. Measurements with intact tissues and isolated mitochondria. *Physiol Plant* **58**: 148–154.

Leakey ADB, Ainsworth EA, Bernacchi CJ, Rogers A, Long SP, Ort DR. 2009a. Elevated CO_2 effects on plant carbon, nitrogen, and water relations: six important lessons from FACE. *J Exp Bot* **60**: 2859–2876.

Leakey ADB, Xu F, Gillespie KM, McGrath JM, Ainsworth EA, Ort DR. 2009b. Genomic basis for stimulated respiration by plants growing under elevated carbon dioxide. *Proc Natl Acad Sci USA* **106**: 3597–3360.

Liu J, Li Z, Wang Y, Xing D. 2014. Overexpression of *ALTERNATIVE OXIDASE1a* alleviates mitochondria-dependent programmed cell death induced by aluminium phytotoxicity in *Arabidopsis*. *J Exp Bot* **65**: 4465–4478.

Long SP, Ort DR. 2010. More than taking the heat: crops and global change. *Curr Opin Plant Biol* **13**: 240–247.

Lundegårdh H. 1955. Mechanisms of absorption, transport, accumulation, and secretion of ions. *Annu Rev Plant Physiol* **6**: 1–24.

Machingura M, Salomon E, Jez JM, Ebbs SD. 2016. The β-cyanoalanine synthase pathway: beyond cyanide detoxification. *Plant Cell Environ* **39**: 2329–2341.

Magneschi L, Perata P. 2009. Rice germination and seedling growth in the absence of oxygen. *Ann Bot* **103**: 181–196.

Mariotti A, Germon JC, Hubert P, Kaiser P, Letolle R, Tardieux A, Tardieux P. 1981. Experimental determination of nitrogen kinetic isotope fractionation: Some principles; illustration for the denitrification and nitrification processes. *Plant Soil* **62**: 413–430.

Martin N, Kobayashi Y, Maricle B. 2015. Species-specific enzymatic tolerance of sulfide toxicity in plant roots and comparative susceptibility between plant and catfish tissue. *FASEB J* **29**: 887.886.

Mata C, Scheurwater I, Martins-Loucao M-A, Lambers H. 1996. Root respiration, growth and nitrogen uptake of *Quercus suber* seedlings. *Plant Physiol Bochem* **34**: 727–734.

Matthews PGD, Seymour RS. 2014. Stomata actively regulate internal aeration of the sacred lotus *Nelumbo nucifera*. *Plant Cell Environ* **37**: 402–413.

McDermitt DK, Loomis RS. 1981. Elemental composition of biomass and its relation to energy content, growth efficiency, and growth yield. *Ann Bot* **48**: 275–290.

Meeuse BJD. 1975. Thermogenic respiration in aroids. *Annu Rev Plant Physiol* **26**: 117–126.

Millar AH, Atkin OK, Menz IR, Henry B, Farquhar G, Day DA. 1998. Analysis of respiratory chain regulation in roots of soybean seedlings. *Plant Physiol* **117**: 1083–1093.

Millar AH, Whelan J, Soole KL, Day DA. 2011. Organization and regulation of mitochondrial respiration in plants. *Annu Rev Plant Biol* **62**: 79–104.

Millenaar FF, Benschop JJ, Wagner AM, Lambers H. 1998. The role of the alternative oxidase in stabilizing the *in vivo* reduction state of the ubiquinone pool and the activation state of the alternative oxidase. *Plant Physiol* **118**: 599–607.

Millenaar FF, Gonzalez-Meler MA, Fiorani F, Welschen R, Ribas-Carbó M, Siedow JN, Wagner AM, Lambers H. 2001. Regulation of alternative oxidase activity in six wild monocotyledonous species. An *in vivo* study at the whole root level. *Plant Physiol* **126**: 376–387.

Millenaar FF, Roelofs R, Gonzalez-Meler MA, Siedow JN, Wagner AM, Lambers H. 2000. The alternative oxidase in roots of *Poa annua* after transfer from high-light to low-light conditions. *Plant J* **23**: 623–632.

Mitchell P. 1961. Coupling of phosphorylation to electron and hydrogen transfer by a chemi-osmotic type of mechanism. *Nature* **191**: 144–148.

Mitchell P. 1966. Chemiosmotic coupling in oxidative and photosynthetic phosphorylation. *Biol Rev* **41**: 445–501.

Møller IM, Bérczi A, van der Plas LHW, Lambers H. 1988. Measurement of the activity and capacity of the alternative pathway in intact plant tissues: Identification of problems and possible solutions. *Physiol Plant* **72**: 642–649.

Moynihan M, Ordentlich A, Raskin I. 1995. Chilling-induced heat evolution in plants. *Plant Physiol* **108**: 995–999.

Nicholls DG, Ferguson SJ. 2013. *Bioenergetics4*. London: Academic Press.

Nobel PS, Palta JA. 1989. Soil O_2 and CO_2 effects on root respiration of cacti. *Plant Soil* **120**: 263–271.

Noguchi K, Go C-S, Terashima I, Ueda S, Yoshinari T. 2001a. Activities of the cyanide-resistant respiratory pathway in leaves of sun and shade species. *Funct Plant Biol* **28**: 27–35.

Noguchi K, Nakajima N, Terashima I. 2001b. Acclimation of leaf respiratory properties in *Alocasia odora* following reciprocal transfers of plants between high- and low-light environments. *Plant Cell Environ* **24**: 831–839.

Noguchi K, Sonoike K, Terashima I. 1996. Acclimation of respiratory properties of leaves of *Spinacia oleracea* L., a sun species, and of *Alocasia macrorrhiza* (L.) G. Don., a shade species, to changes in growth irradiance. *Plant Cell Physiol* **37**: 377–384.

Noguchi K, Taylor NL, Millar AH, Lambers H, Day DA. 2005. Response of mitochondria to light intensity in the leaves of sun and shade species. *Plant Cell Environ* **28**: 760–771.

Noguchi K, Yamori W, Hikosaka K, Terashima I. 2015. Homeostasis of the temperature sensitivity of respiration over a range of growth temperatures indicated by a modified Arrhenius model. *New Phytol* **207**: 34–42.

O'Leary BM, Asao S, Millar AH, Atkin OK. 2019. Core principles which explain variation in respiration across biological scales. *New Phytol* **222**: 670–686.

O'Leary BM, Plaxton WC 2016. Plant Respiration. *eLS*. Chichester: John Wiley & Sons, Ltd, 1–11.

O'Sullivan OS, Heskel MA, Reich PB, Tjoelker MG, Weerasinghe LK, Penillard A, Zhu L, Egerton JJG, Bloomfield KJ, Creek D, Bahar NHA, Griffin KL, Hurry V, Meir P, Turnbull MH, Atkin OK. 2017. Thermal limits of leaf metabolism across biomes. *Glob Change Biol* **23**: 209–223.

Ögren E. 1996. Premature dehardening in *Vaccinium myrtillus* during a mild winter: a cause for winter dieback? *Funct Ecol* **10**: 724–732.

Ögren E. 2001. Effects of climatic warming on cold hardiness of some northern woody plants assessed from simulation experiments. *Physiol Plant* **112**: 71–77.

Oh N-H, Kim H-S, Richter DD. 2005. What regulates soil CO_2 concentrations? A modeling approach to CO_2

diffusion in deep soil profiles. *Environ Eng Sci* **22**: 38–45.

Overmyer K, Brosché M, Kangasjärvi J. 2003. Reactive oxygen species and hormonal control of cell death. *Trends Plant Sci* **8**: 335–342.

Palet A, Ribas-Carbó M, Argiles J, Azcon-Bieto J. 1991. Short-term effects of carbon dioxide on carnation callus cell respiration. *Plant Physiol* **96**: 467.

Panda SK, Sahoo L, Katsuhara M, Matsumoto H. 2013. Overexpression of alternative oxidase gene confers aluminum tolerance by altering the respiratory capacity and the response to oxidative stress in tobacco cells. *Mol Biotechnol* **54**: 551–563.

Pangala SR, Enrich-Prast A, Basso LS, Peixoto RB, Bastviken D, Hornibrook ERC, Gatti LV, Marotta H, Calazans LSB, Sakuragui CM, Bastos WR, Malm O, Gloor E, Miller JB, Gauci V. 2017. Large emissions from floodplain trees close the Amazon methane budget. *Nature* **552**: 230–234.

Penning de Vries FWT. 1975. The cost of maintenance processes in plant cells. *Ann Bot* **39**: 77–92.

Penning de Vries FWT, Brunsting AHM, Van Laar HH. 1974. Products, requirements and efficiency of biosynthesis a quantitative approach. *J Theor Biol* **45**: 339–377.

Plaxton WC, Podestá FE. 2006. The functional organization and control of plant respiration. *Crit Rev Plant Sci* **25**: 159–198.

Poorter H 1994. Construction costs and payback time of biomass: a whole plant perspective. In: Roy J, Garmier E eds. *A Whole Plant Perspective on Carbon-Nitrogen Interactions*. The Hague: SPB Academic Publishing, 111–127.

Poorter H, Remkes C, Lambers H. 1990. Carbon and nitrogen economy of 24 wild species differing in relative growth rate. *Plant Physiol* **94**: 621–627.

Poorter H, Van de Vijver C, Boot R, Lambers H. 1995. Growth and carbon economy of a fast-growing and a slow-growing grass species as dependent on nitrate supply. *Plant Soil* **171**: 217–227.

Poorter H, Van der Werf A, Atkin OK, Lambers H. 1991. Respiratory energy requirements of roots vary with the potential growth rate of a plant species. *Physiol Plant* **83**: 469–475.

Poorter H, Villar R 1997. Chemical composition of plants: causes and consequences of variation in allocation of C to different plant compounds. In: Bazzaz FA, Grace J eds. *Resource Allocation in Plants, Physiological Ecology Series*. San Diego: Academic Press, 39–72.

Qi J, Marshall JD, Mattson KG. 1994. High soil carbon dioxide concentrations inhibit root respiration of Douglas fir. *New Phytol* **128**: 435–442.

Rachmilevitch S, Lambers H, Huang B. 2006. Root respiratory characteristics associated with plant adaptation to high soil temperature for geothermal and turf-type *Agrostis* species. *J Exp Bot* **57**: 623–631.

Rasmusson AG, Geisler DA, Møller IM. 2008. The multiplicity of dehydrogenases in the electron transport chain of plant mitochondria. *Mitochondrion* **8**: 47–60.

Raven JA, Lambers H, Smith SE, Westoby M. 2018. Costs of acquiring phosphorus by vascular land plants: patterns and implications for plant coexistence. *New Phytol* **217**: 1420–1427.

Reich PB, Tjoelker MG, Machado J-L, Oleksyn J. 2006. Universal scaling of respiratory metabolism, size and nitrogen in plants. *Nature* **439**: 457–461.

Reich PB, Walters MB, Tjoelker MG, Vanderklein D, Buschena C. 1998. Photosynthesis and respiration rates depend on leaf and root morphology and nitrogen concentration in nine boreal tree species differing in relative growth rate. *Funct Ecol* **12**: 395–405.

Rennenberg H, Filner P. 1983. Developmental changes in the potential for H_2S emission in cucurbit plants. *Plant Physiol* **71**: 269–275.

Ribas-Carbó M, Berry JA, Yakir D, Giles L, Robinson SA. 1995. Electron partitioning between the cytochrome and alternative pathways in plant mitochondria. *Plant Physiol* **109**: 829–837.

Ribas-Carbó M, Lennon AM, Robinson SA, Giles L, Berry JA, Siedow JN. 1997. The regulation of electron partitioning between the cytochrome and alternative pathways in soybean cotyledon and root mitochondria. *Plant Physiol* **113**: 903–911.

Ribas-Carbó M, Taylor NL, Giles L, Busquets S, Finnegan PM, Day DA, Lambers H, Medrano H, Berry JA, Flexas J. 2005. Effects of water stress on respiration in soybean leaves. *Plant Physiol* **139**: 466–473.

Rivoal J, Hanson AD. 1993. Evidence for a large and sustained glycolytic flux to lactate in anoxic roots of some members of the halophytic genus *Limonium*. *Plant Physiol* **101**: 553–560.

Rivoal J, Hanson AD. 1994. Metabolic control of anaerobic glycolysis (overexpression of lactate dehydrogenase in transgenic tomato roots supports the Davies-Roberts hypothesis and points to a critical role for lactate secretion. *Plant Physiol* **106**: 1179–1185.

Roberts JKM. 1984. Study of plant metabolism in vivo using NMR spectroscopy. *Annu Rev Plant Physiol* **35**: 375–386.

Roberts JKM, Andrade FH, Anderson IC. 1985. Further evidence that cytoplasmic acidosis is a determinant of flooding intolerance in plants. *Plant Physiol* **77**: 492–494.

Roberts JKM, Wemmer D, Jardetzky O. 1984. Measurement of mitochondrial ATPase activity in maize root tips by saturation transfer ^{31}P nuclear magnetic resonance. *Plant Physiol* **74**: 632–639.

Robinson SA, Yakir D, Ribas-Carbó M, Giles L, Osmond CB. 1992. Measurements of the engagement of cyanide-resistant respiration in the crassulacean acid metabolism plant *Kalanchoe daigremontiana* with the use of on-line oxygen isotope discrimination. *Plant Physiol* **100**: 1087–1091.

Robinson SA, Ribas-Carbó M, Yakir D, Giles L, Reuveni Y, Berry JA. 1995. Beyond SHAM and cyanide: opportunities for studying the alternative oxidase in plant respiration using oxygen isotope discrimination. *Aust J Plant Physiol* **22**: 487–496.

Rowland L, Zaragoza-Castells J, Bloomfield KJ, Turnbull MH, Bonal D, Burban B, Salinas N, Cosio E, Metcalfe DJ, Ford A, Phillips OL, Atkin OK, Meir P. 2016. Scaling leaf respiration with nitrogen and phosphorus in tropical forests across two continents. *New Phytol* **214**: 1064–1077.

Ryan MG, Binkley D, Fownes JH. 1997. Age-related decline in forest productivity: pattern and process. *Adv Ecol Res* **27**: 213–262.

Schaaf J, Walter MH, Hess D. 1995. Primary metabolism in plant defense (regulation of a bean malic enzyme gene promoter in transgenic tobacco by developmental and environmental cues). *Plant Physiol* **108**: 949–960.

Schertl P, Braun H-P. 2014. Respiratory electron transfer pathways in plant mitochondria. *Front Plant Sci* **5**: 163.

Scheurwater I, Clarkson DT, Purves JV, Van Rijt G, Saker LR, Welschen R, Lambers H. 1999. Relatively large nitrate efflux can account for the high specific respiratory costs for nitrate transport in slow-growing grass species. *Plant Soil* **215**: 123–134.

Scheurwater I, Cornelissen C, Dictus F, Welschen R, Lambers H. 1998. Why do fast- and slow-growing grass species differ so little in their rate of root respiration, considering the large differences in rate of growth and ion uptake? *Plant Cell Environ* **21**: 995–1005.

Scheurwater I, Dünnebacke M, Eising R, Lambers H. 2000. Respiratory costs and rate of protein turnover in the roots of a fast-growing (*Dactylis glomerata* L.) and a slow-growing (*Festuca ovina* L.) grass species. *J Exp Bot* **51**: 1089–1097.

Scheurwater I, Koren M, Lambers H, Atkin OK. 2002. The contribution of roots and shoots to whole plant nitrate reduction in fast- and slow-growing grass species. *J Exp Bot* **53**: 1635–1642.

Schubert S, Schubert E, Mengel K. 1990. Effect of low pH of the root medium on proton release, growth, and nutrient uptake of field beans (*Vicia faba*). *Plant Soil* **124**: 239–244.

Selinski J, Scheibe R, Day DA, Whelan J. 2018. Alternative oxidase is positive for plant performance. *Trends Plant Sci* **23**: 588–597.

Seymour RS. 2001. Biophysics and physiology of temperature regulation in thermogenic flowers. *Biosci Rep* **21**: 223–236.

Seymour RS, Schultze-Motel P. 1996. Thermoregulating lotus flowers. *Nature* **383**: 305.

Shane MW, Cramer MD, Funayama-Noguchi S, Cawthray GR, Millar AH, Day DA, Lambers H. 2004. Developmental physiology of cluster-root carboxylate synthesis and exudation in harsh hakea. Expression of phospho*enol*pyruvate carboxylase and the alternative oxidase. *Plant Physiol* **135**: 549–560.

Shaw M, Samborski DJ. 1957. The physiology of host-parasite relations. III. The pattern of respiration in rusted and mildewed cereal leaves. *Can J Bot* **35**: 389–407.

Simons BH, Lambers H 1999. The alternative oxidase: is it a respiratory pathway allowing a plant to cope with stress. In: Lerner HR ed. *Plant Responses to Environmental Stresses: From Phytohormones to Genome Reorganization*. New York: Plenum Press, 265–286.

Simons BH, Millenaar FF, Mulder L, Van Loon LC, Lambers H. 1999. Enhanced expression and activation of the alternative oxidase during infection of *Arabidopsis* with *Pseudomonas syringae* pv *tomato*. *Plant Physiol* **120**: 529–538.

Smith NG, Dukes JS. 2013. Plant respiration and photosynthesis in global-scale models: incorporating acclimation to temperature and CO_2. *Glob Change Biol* **19**: 45–63.

Smith NG, Dukes JS. 2018. Drivers of leaf carbon exchange capacity across biomes at the continental scale. *Ecology* **99**: 1610–1620.

Soukup A, Armstrong W, Schreiber L, Franke R, Votrubova O. 2007. Apoplastic barriers to radial oxygen loss and solute penetration: a chemical and functional comparison of the exodermis of two wetland species, *Phragmites australis* and *Glyceria maxima*. *New Phytol* **173**: 264–278.

Stiles W, Leach W. 1936. *Respiration in Plants*. London: Methuen & Co.

Tcherkez G, Cornic G, Bligny R, Gout E, Ghashghaie J. 2005. *In vivo* respiratory metabolism of illuminated leaves. *Plant Physiol* **138**: 1596–1606.

Tcherkez G, Gauthier P, Buckley TN, Busch FA, Barbour MM, Bruhn D, Heskel MA, Gong XY, Crous KY, Griffin K, Way D, Turnbull M, Adams MA, Atkin OK, Farquhar GD, Cornic G. 2017. Leaf day respiration: low CO_2 flux but high significance for metabolism and carbon balance. *New Phytol* **216**: 986–1001.

Tcherkez G, Nogues S, Bleton J, Cornic G, Badeck F, Ghashghaie J. 2003. Metabolic origin of carbon isotope composition of leaf dark-respired CO_2 in French bean. *Plant Physiol* **131**: 237–244.

Terry IL, Roemer RB, Booth DT, Moore CJ, Walter GH. 2016. Thermogenic respiratory processes drive the exponential increase of volatile organic compound emissions in *Macrozamia* cycad cones. *Plant Cell Environ* **39**: 1588–1600.

Terry LI, Roemer RB, Walter GH, Booth D. 2014. Thrips' responses to thermogenic associated signals in a cycad pollination system: the interplay of temperature, light, humidity and cone volatiles. *Funct Ecol* **28**: 857–867.

Thien LB, Bernhardt P, Devall MS, Chen Z-d, Luo Y-b, Fan J-H, Yuan L-C, Williams JH. 2009. Pollination biology of basal angiosperms (ANITA grade). *Am J Bot* **96**: 166–182.

Tjoelker MG, Oleksyn J, Reich PB. 1999. Acclimation of respiration to temperature and CO_2 in seedlings of boreal tree species in relation to plant size and relative growth rate. *Glob Change Biol* **5**: 679–691.

Umbach A, Wiskich J, Siedow J. 1994. Regulation of alternative oxidase kinetics by pyruvate and

intermolecular disulfide bond redox status in soybean seedling mitochondria. *FEBS Lett* **348**: 181–184.

Van der Werf A, Kooijman A, Welschen R, Lambers H. 1988. Respiratory energy costs for the maintenance of biomass, for growth and for ion uptake in roots of *Carex diandra* and *Carex acudformis*. *Physiol Plant* **72**: 483–491.

Van der Werf A, Poorter H, Lambers H 1994. Respiration as dependent on a species' inherent growth rate and on the nitrogen supply to the plant. *A Whole Plant Perspective on Carbon–Nitrogen Interactions*. The Hague: SPB Academic Publishing, 91–110.

Van der Werf A, Van den Berg G, Ravenstein HJL, Lambers H, Eising R 1992a. Protein turnover: a significant component of maintenance respiration in roots? In: Lambers H, van der Plas LHW eds. *Molecular, Biochemical and Physiological Aspects of Plant Respiration*. The Hague: SPB Academic Publishing, 483 492.

Van der Werf A, Welschen R, Lambers H 1992b. Respiratory losses increase with decreasing inherent growth rate of a species and with decreasing nitrate supply: a search for explanations for these observations. In: Lambers H, Van der Plas LHW eds. *Plant Respiration Molecular, Biochemical and Physiological Aspects*. The Hague: SPB Academic Publishing, 421–432.

Vanlerberghe GC. 2013. Alternative oxidase: a mitochondrial respiratory pathway to maintain metabolic and signaling homeostasis during abiotic and biotic stress in plants. *Int J Mol Sci* **14**: 6805–6847.

Vanlerberghe GC, Cvetkovska M, Wang J. 2009. Is the maintenance of homeostatic mitochondrial signaling during stress a physiological role for alternative oxidase? *Physiol Plant* **137**: 392–406.

Vanlerberghe GC, Day DA, Wiskich JT, Vanlerberghe AE, McIntosh L. 1995. Alternative oxidase activity in tobacco leaf mitochondria: dependence on tricarboxylic acid cycle-mediated redox regulation and pyruvate activation. *Plant Physiol* **109**: 353–361.

Veen BW 1980. Energy costs of ion transport. In: Rains DW, Valentne RC, Holaender C eds. *Genetic Engeneering of Osmoregulation Impact on Plant Productivity for Food, Chemicals and Energy,* New York: Plenum Press, 187–195.

Vertregt N, Penning de Vries FWT. 1987. A rapid method for determining the efficiency of biosynthesis of plant biomass. *J Theor Biol* **128**: 109–119.

Vidal G, Ribas-Carbo M, Garmier M, Dubertret G, Rasmusson AG, Mathieu C, Foyer CH, De Paepe R. 2007. Lack of respiratory chain complex I impairs alternative oxidase engagement and modulates redox signaling during elicitor-induced cell death in tobacco. *Plant Cell* **19**: 640–655.

Villar R, Ruíz-Robleto J, De Jong Y, Poorter H. 2006. Differences in construction costs and chemical composition between deciduous and evergreen woody species are small as compared to differences among families. *Plant Cell Environ* **29**: 1629–1643.

Wagner AM, Krab K, Wagner MJ, Moore AL. 2008. Regulation of thermogenesis in flowering Araceae: The role of the alternative oxidase. *Biochimica et Biophysica Acta - Bioenergetics* **1777**: 993–1000.

Wang X, Curtis P. 2002. A meta-analytical test of elevated CO_2 effects on plant respiration. *Plant Ecol* **161**: 251–261.

Wang X, Lewis JD, Tissue DT, Seemann JR, Griffin KL. 2001. Effects of elevated atmospheric CO_2 concentration on leaf dark respiration of *Xanthium strumarium* in light and in darkness. *Proc Natl Acad Sci USA* **98**: 2479–2484.

Waring RH, Schlesinger WH. 1985. *Forest Ecosystems: Concepts and Management*. Orlando: Academic Press.

Watling JR, Robinson SA, Seymour RS. 2006. Contribution of the alternative pathway to respiration during thermogenesis in flowers of the sacred lotus. *Plant Physiol* **140**: 1367.

Williams JHH, Farrar JF. 1990. Control of barley root respiration. *Physiol Plant* **79**: 259–266.

Williams JHH, Winters AL, Farrar JF 1992. Sucrose: a novel plant growth regulator. In: Lambers H, Van der Plas LHW eds. *Molecular, Biochemical and Physiological Aspects of Plant Respiration*. The Hague: SPB Academic Publishing, 463–469.

Williams K, Percival F, Merino J, Mooney HA. 1987. Estimation of tissue construction cost from heat of combustion and organic nitrogen content. *Plant Cell Environ* **10**: 725–734.

Wright IJ, Reich PB, Atkin OK, Lusk CH, Tjoelker MG, Westoby M. 2006. Irradiance, temperature and rainfall influence leaf dark respiration in woody plants: evidence from comparisons across 20 sites. *New Phytol* **169**: 309–319.

Yan F, Schubert S, Mengel K. 1992. Effect of low root medium pH on net proton release, root respiration, and root growth of corn (*Zea mays* L.) and broad bean (*Vicia faba* L.). *Plant Physiol* **99**: 415–421.

Yan F, Zhu Y, Muller C, Zorb C, Schubert S. 2002. Adaptation of H^+-pumping and plasma membrane H^+ ATPase activity in proteoid roots of white lupin under phosphate deficiency. *Plant Physiol* **129**: 50–63.

Yoshida K, Terashima I, Noguchi K. 2006. Distinct roles of the cytochrome pathway and alternative oxidase in leaf photosynthesis. *Plant Cell Physiol* **47**: 22–31.

Yoshida K, Terashima I, Noguchi K. 2007. Up-regulation of mitochondrial alternative oxidase concomitant with chloroplast over-reduction by excess light. *Plant Cell Physiol* **48**: 606–614.

Yoshida K, Watanabe CK, Hachiya T, Tholen D, Shibata M, Tersahima I, Noguchi K. 2011. Distinct responses of the mitochondrial respiratory chain to long- and short-term high-light environments in *Arabidopsis thaliana*. *Plant Cell Environ* **34**: 618–628.

Zacheo G, Molinari S. 1987. Relationship between root respiration and seedling age in tomato cultivars infested by *Meloidogyne incognita*. *Ann Appl Biol* **111**: 589–595.

Zhu J, Raschke K, Köhler B. 2007. An electrogenic pump in the xylem parenchyma of barley roots. *Physiol Plant* **129**: 397–406.

4 Photosynthesis, Respiration, and Long-Distance Transport: Long Distance Transport of Assimilates

4.1 Introduction

The evolution of cell walls allowed plants to solve the problem of osmoregulation in freshwater environments; however, cell walls restrict motility and place constraints on the evolution of long-distance transport systems. Tissues are too rigid for a heart-pump mechanism; instead, higher plants have two systems for long-distance transport. The dead elements of the xylem allow transport of water and solutes between sites of different water potentials. We discuss that transport system in Chap. 5. The other transport system, the phloem, allows the mass flow of carbohydrates and other solutes from a **source** region, where the **hydrostatic pressure** in the phloem is relatively high, to a **sink** region with lower pressure (Münch 1930).

Plants differ markedly in the manner in which the products of photosynthesis pass from the mesophyll cells to the sieve tubes (**phloem loading**) through which they are then transported to a site where they are unloaded and metabolized (Fig. 4.1). Plants also differ with respect to the major carbon-containing compounds that occur in the sieve tubes of the **phloem**, which is the complex consisting of **sieve elements** and **companion cells**. For reasons that are explained in this chapter, there is a close association between the type of phloem loading (symplastic or apoplastic) and the type of major carbon compound (sucrose or oligosaccharides) transported in the phloem. Sucrose is a sugar composed of two hexose units, whereas an oligosaccharide comprises more than two units. There is much to be learned about the phloem loading strategies of individual species in different physiological, developmental, and ecological contexts. The concepts outlined in this chapter, based on fundamental anatomical and thermodynamic principles, provide a foundation for this discovery process (Zhang and Turgeon 2018).

Phloem transport is important to consider in the context of **crop yield**, since higher-yielding newer varieties often have similar rates of photosynthates, but transport a greater fraction of their assimilates to harvestable sinks (Patrick and Colyvas 2014).

4.2 Major Transport Compounds in the Phloem: Why Not Glucose?

In animals, glucose is the predominant transport sugar, albeit at much lower concentrations than those of predominant sugars in the sieve tubes of higher plants. In plants, **sucrose** is a major constituent of phloem sap, whereas glucose and other monosaccharides are found only in trace concentrations. Why not glucose?

A comparison of the physical properties of glucose and sucrose does not provide a compelling reason for the predominance of sucrose. A good long-distance transport compound, however, should be **nonreducing**, so as to avoid a

H. Lambers, R. S. Oliveira, *Plant Physiological Ecology*, https://doi.org/10.1007/978-3-030-29639-1_4

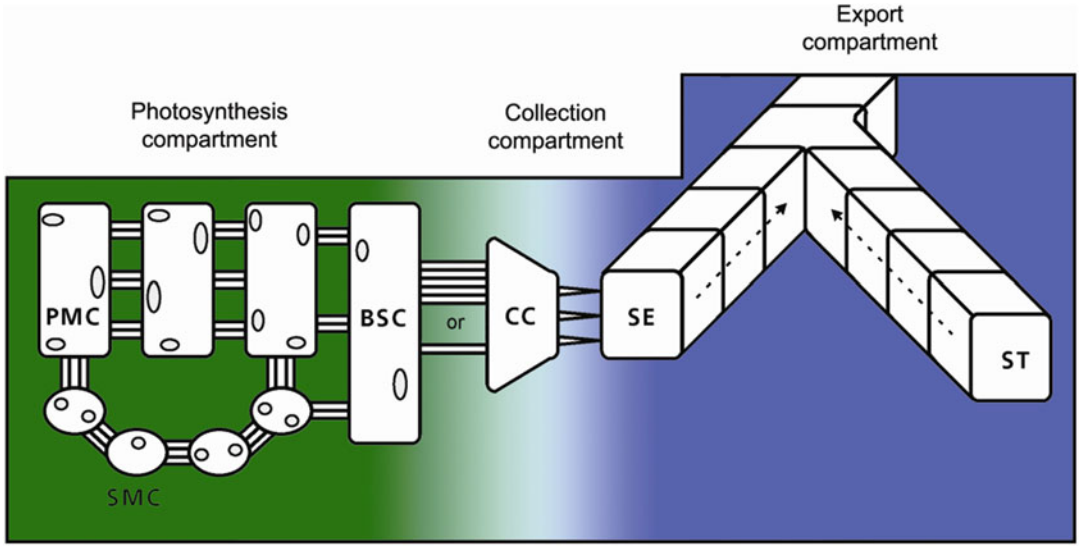

Fig. 4.1 Sucrose and other products of photosynthesis (photosynthates) are generated in palisade (PMC) and spongy (SMC) mesophyll cells. They are either symplastically (top) or apoplastically (bottom) moved to the companion cells (CC) and/or sieve elements (SE) of the minor vein phloem and are subsequently exported to sink regions of the plant. Plasmodesmata connect all cell types, but the roles they play in the various transport steps differ in different species. In particular, the number of plasmodesmata connecting bundle sheath cells (BSC) to companion cells varies greatly. In some plants there are many, as depicted at the top. In others there are relatively few, as shown at the bottom. The ultrastructure and biochemistry of the companion cells in minor veins also differs considerably in different plants, an indication of different loading strategies (as discussed in the text). The plasmodesmata between companion cells and sieve elements are especially wide and accommodate the passage of much larger molecules. Once inside the sieve elements, photosynthates are carried away in the export stream. The minor veins merge to create larger veins with connected sieve tubes (ST). Though not depicted here, all sieve elements have adjoining companion cells.

nonenzymatic reaction with proteins or other compounds during its transport. This excludes compounds such as glucose and fructose, which contain an aldehyde group, which is readily oxidized to a carboxylic acid group; hence they are known as **reducing sugars**. A good transport compound should also be protected from enzymatic attack until it arrives at its destination. In this way the flow of carbon in plants can be controlled by the presence of key hydrolyzing enzymes in appropriate sink tissues. Thus, **sucrose** appears to be a preferred compound because it is '**protected**'.

Other 'protected' sugars include the oligosaccharides of the raffinose family: raffinose, stachyose, verbascose. These sugars are formed by the addition of one, two or three galactose molecules to a sucrose molecule (Fig. 4.2). They are major transport sugars in a wide range of species. Other transport compounds are the sugar alcohols (sorbitol, mannitol, dulcitol) (Fig. 4.2), *e.g.*, in Apiaceae [*e.g.*, *Apium graveolens* (celery)], Rosaceae [*e.g.*, *Prunus persica* (peach)], Combretaceae, Celastraceae, and Plantaginaceae, and oligofructans [*e.g.*, in *Agave deserti* (century plant)] (Wang and Nobel 1998). Despite the diversity in composition of the phloem transport fluid among species, nearly all species are similar in their very low concentrations of monosaccharides (glucose, fructose) (Turgeon and Wolf 2009).

In addition to sugars, phloem sap contains a range of organic acids, amino acids, and inorganic ions. Concentrations of calcium (Ca), iron (Fe), and manganese (Mn) in the phloem sap are invariably low; these nutrients tend to precipitate

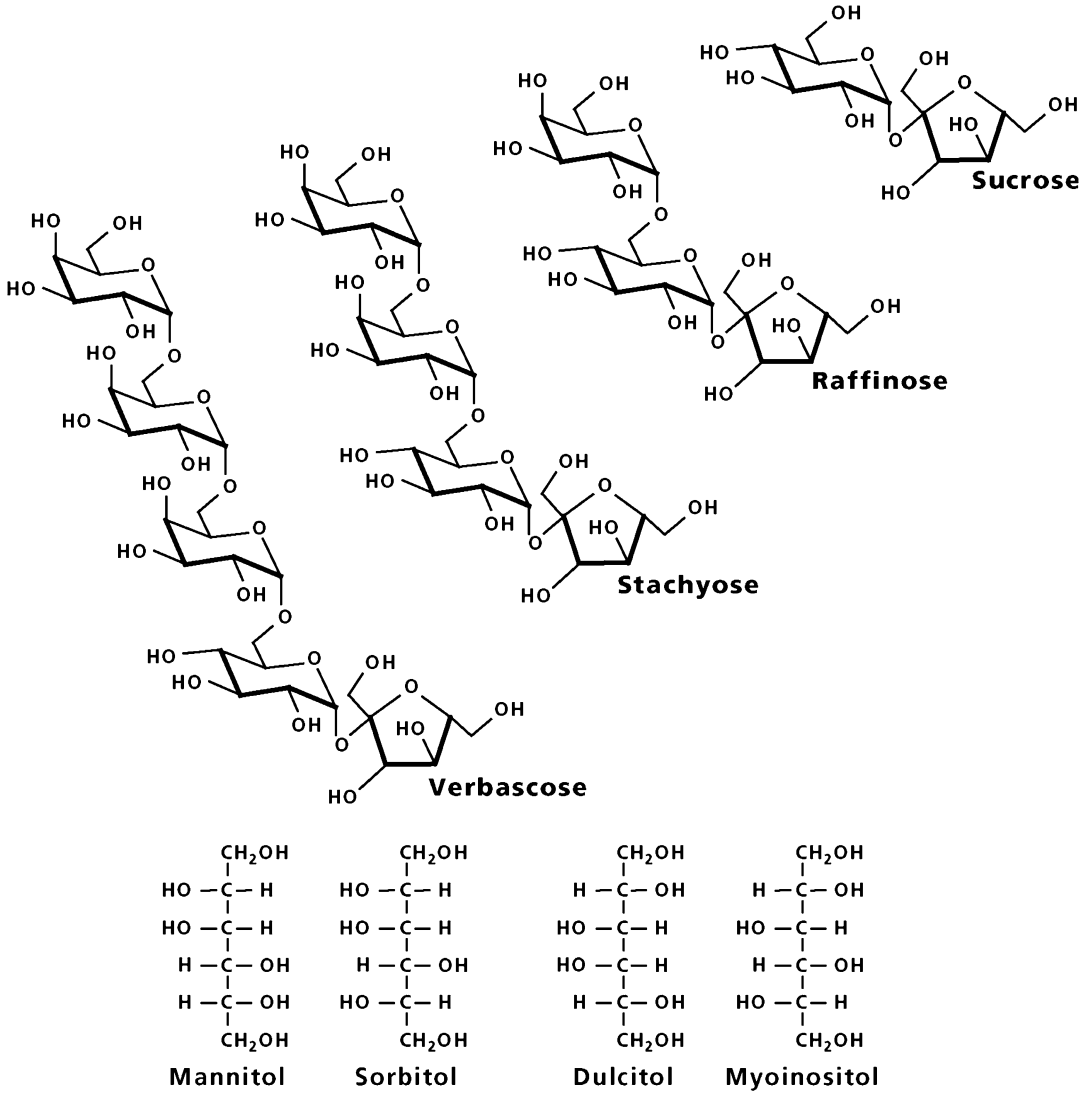

Fig. 4.2 The chemical structure of the major sugars and some sugar alcohols transported in sieve tubes. Note that not all of these compounds occur in the phloem sap of every species.

at the relatively **high pH** that characterizes phloem sap (Fig. 9.1B). As a result, growing leaves and fruits must predominantly import these nutrients via the xylem. Calcium deficiency and the so-called Ca deficiency-related disorders, such as tip-burn in lettuce, blossom end rot in tomato, and bitter pit in apple, are therefore widespread (White 2012). Similarly, legume seeds may show seed disorders when the import of Mn becomes too low, and calcifuge species show yellowing of their youngest leaves, due to a restricted uptake of Fe at high soil pH (Sect. 9.2.2.6). That is, plant organs that predominantly import specific nutrients via the xylem may show **deficiency symptoms** when transpiration rates are slow, when the concentration of these specific nutrients in the xylem is very low, due to restricted uptake, or both.

Most plant viruses can also move over long distances in the phloem (*e.g.*, Roberts et al. 1997). Moreover, alarm signals involved in induced systemic resistance, hormones, and microRNA

(miRNA) molecules, which are a class of developmental signaling molecules, are also transported via the phloem (Van Bel 2003; Juarez et al. 2004; Lough and Lucas 2006).

4.3 Phloem Structure and Function

In the process of transporting assimilates from the site of their synthesis (the **source**) to the site where they are used (the **sink**), the products of photosynthesis must move from the mesophyll cells to the transport system: the **sieve elements**. Sieve elements are living cells with greatly reduced cytoplasmic content and characteristic sieve areas in their cell walls. When pores connect adjacent cells, they are commonly differentiated into **sieve plates**, with pores ranging in diameter from 1 to 15 μm. The sparsity of the cytoplasm and the presence of pores in the walls allows flow through the phloem to occur with minimal obstruction.

In the gymnosperm *Sequoiadendron giganteum* (giant redwood) the source-sink distance of the phloem path can be as much as 110 m, due to the enormous height of the tree. This example is extreme, because sinks mostly receive assimilates from adjacent source leaves, but it illustrates the point that transport sometimes occurs over vast distances, for example to growing root tips far removed from source leaves. Long-distance transport in the phloem occurs by **mass flow**, driven by a difference in **hydrostatic pressure**, created by phloem loading in source leaves and unloading processes in sink tissues. In trees, **hydraulic resistance** in the phloem scales inversely with plant height, because of a shift in sieve element structure along the length of individual trees. This scaling relationship is robust across multiple species despite large differences in plate anatomy (Savage et al. 2017).

When sieve tubes are damaged and the pressure drops, sieve plates tend to be blocked. Short-term sealing mechanisms are triggered by Ca and involve proteins, *e.g.*, **forisomes** in legumes (Furch et al. 2007). Long-term sealing involves blocking the sieve pores with a glucose polymer, **callose**. **Aphids** can successfully puncture sieve tubes with their piercing mouthparts (stylets) and ingest phloem sap without eliciting the sieve tubes' normal occlusion response to injury. Occlusion mechanisms may be prevented by chemical constituents in aphid saliva injected into sieve tubes before and during feeding (Will et al. 2007). **Resistance** of a *Cucumis melo* (melon) line to the aphid *Aphis gossypii* is based on preventing aphids from ingesting phloem sap (Garzo et al. 2018). Stylectomy with aphids on susceptible and resistant plants while the stylet tips are phloem inserted shows the coagulation of phloem proteins inside the stylet canals and the punctured sieve elements (Garzo et al. 2018). A clear example of the **arm's race** that we discuss in Sect. 13.3.3.

4.3.1 Symplastic and Apoplastic Transport

How are the products of photosynthesis in the mesophyll loaded into the sieve tubes? There are two ways in which solutes (ions and small molecules) can pass from one cell to another. These transport pathways are used throughout the plant, depending on the specific functions of the tissues in question. One route is through **plasmodesmata** (Van Bel 2018). This is **symplastic** (or symplasmic) transport. (The symplast is the internal space of cells, surrounded by plasma membrane.) Since plasmodesmata are lined by the plasma membrane, cells connected by plasmodesmata form a symplastic continuum. Solute passage through plasmodesmatal channels is thought to be unassisted by proteins that mediate active transport and symplastic transport is therefore **passive** (without energy input). Passive transport through plasmodesmata has two components: **diffusion** (net movement down a concentration gradient as a result of random molecular motion) and **convection** (mass transfer due to bulk movement, like a flowing river). Since symplastic transport is passive it cannot, by itself, establish a solute concentration gradient.

Solutes can also move from one cell to another by **apoplastic** (or apoplasmic) transport (the apoplast is the space outside the plasma

membranes, including the cell walls and the xylem conduits. Clearly, if molecules pass from one cell type to another through the apoplast they must first exit (efflux) from a cell, and then be taken up again by another one (influx), across plasma membranes. This requires membrane-localized **transporter** proteins. Some transporters mediate passive transport, down a concentration gradient, and therefore do not use energy, while others drive solute against a gradient, an energy requiring step. Transporters are specific, to a greater or lesser extent, for a given solute.

In some species, but not all, transfer across the plasma membranes of specific cell types is augmented by extensive invaginations of the cells wall that increase the surface area of the plasma membrane and therefore uptake capacity. Cells with such cell wall elaborations are known as **transfer cells**. In species where they occur, transfer cells can be present at a number of locations in the plant body, including the phloem, where solute flux is high.

Which combination of pathways and mechanisms do individual species use to load the phloem with sugar? Minor vein anatomy provides important clues.

4.3.2 Minor Vein Anatomy

The veins in leaves of dicotyledonous species branch progressively to form a reticulate network. Up to six or seven branching classes (orders) can be recognized in some species. The largest vein is the **midrib** (class I) and the smallest few classes are called **minor veins**. Minor veins are much more extensive than the major veins, and thoroughly permeate the mesophyll tissue. Few mesophyll cells are more than 6 or 8 cells away from a minor vein. Clearly, the minor venation is responsible for most, if not all, phloem loading of photoassimilates.

Since structure is often a meaningful guide to function, the comparative anatomy of the minor veins should provide clues to the mechanisms of the loading process in different species. Gamalei and coworkers studied the minor-vein anatomy of over 1000 higher plant species. He recognized different degrees of **plasmodesmatal connectivity** between the mesophyll cells and the minor vein phloem in different species (Gamalei 1989, 1991; Batashev et al. 2013). In the herb *Senecio vernalis* (eastern groundsel) the frequency is around 0.03 plasmodesmata μm^{-2} interface area, against 60 in the tree *Fraxinus ornus* (manna ash). Gamalei grouped plants into arbitrarily defined types. **Type 1** plants exhibit about three orders of magnitude more plasmodesmatal contacts than **type 2,** while intermediates between the two extremes (types 1-2a) differ by about one to two orders of magnitude in plasmodesmatal frequency. Within Gamalei's types, there are subgroups. Some type 1 plants with the highest plasmodesmatal counts have specialized **companion cells** known as **intermediary cells** (Fig. 4.3). Intermediary cells are especially large, with many small vacuoles and extremely large numbers of asymmetrically branched plasmodesmata connecting them to bundle sheath cells. They almost always are present as a single pair of cells in the smallest veins (Fig. 4.3). Species with intermediary cells are so different in many respects from the rest of the type 1 plants that they should probably be treated as a separate group. Type 2 is also heterogeneous. Type 2a **companion cells** have smooth cell walls, whereas those of type 2b have transfer cells with highly invaginated plasma membranes.

Plasmodesmatal frequency is usually a strong family characteristic; for example, all studied species in the Magnoliaceae (magnolia family) are type 1, those in the Aceraceae (maple family) are type 1-2a; and those in the Liliaceae (lily family) are type 2. The minor veins of most monocots have low plasmodesmatal frequencies. Trees tend to have more plasmodesmata in the loading pathway than herbaceous plants, but this is not a strict correlation, because both herbaceous and tree species are found in some families. For example, *Fragaria* (strawberry) and *Malus* (apple) are both in the Rosaceae (rose family) and both are type 1-2a plants (Gamalei 1989, 1991).

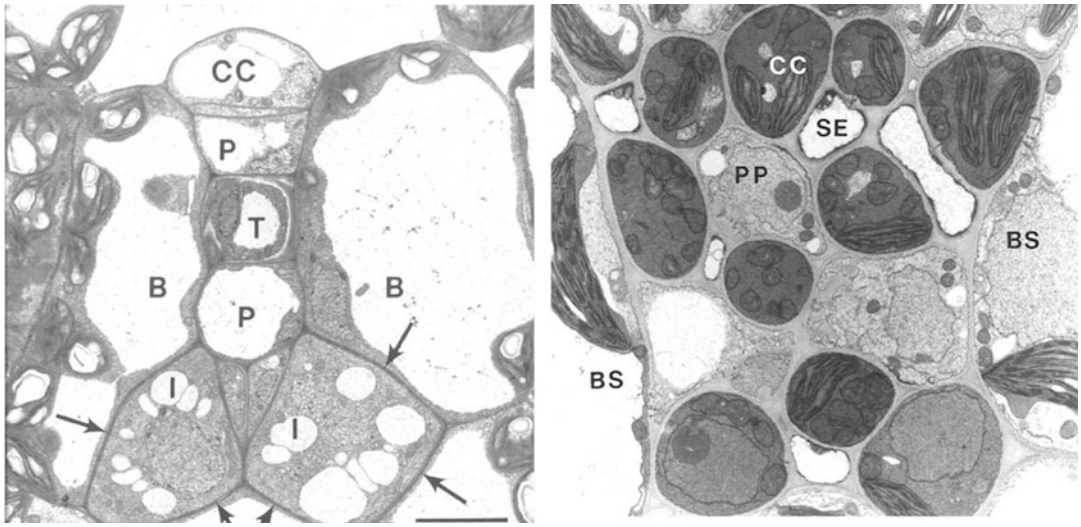

Fig. 4.3 (Left) Minor vein from sink-source transition region of a leaf of *Cucumis melo* (melon). Abaxial phloem contains two intermediary cells (I) and immature sieve elements (not labeled) adjacent to a parenchyma cell (P). The interface of intermediary cells and bundle-sheath cells is indicated by *arrows*. A developing tracheid (T) and adaxial companion cell (CC) with its immature sieve element (not labeled) are also present. Bar = 5 μm (Volk et al. 1996). (Right) Transverse section of a typical *Arabidopsis thaliana* (thale cress) minor vein, with five sieve elements. BS, bundle sheath cell; CC, companion cell; PP, phloem parenchyma cell; SE, sieve element; T, tracheary element; VP, vascular parenchyma cell. Bar = 2 μm (Haritatos et al. 2000).

4.3.3 Phloem-Loading Mechanisms

Given information on sugar transporters and phloem anatomy it is possible to identify (with more confidence in some cases than in others) how sugar passes from mesophyll cells into the phloem. Consider the plants in which there are many plasmodesmata at all interfaces. Sucrose, and by the same argument sugar alcohols, are likely to move passively into the phloem through the symplast (Reidel et al. 2009; Figs 4.4A, B). For passive movement to occur, the concentrations of these compounds must be higher in the mesophyll than in the phloem. As expected, high concentrations of transport compounds in leaves are a feature of plants that load passively (Fu et al. 2011). For example, *Salix babylonica* (weeping willow), a type 1 species with numerous plasmodesmata, has a high concentration of sucrose in leaves, but a lower concentration in the phloem of the stem (Turgeon and Medville 1998). Apple (*Malus domestica*), which transports more sorbitol than sucrose, is also type 1, and both compounds appear to move passively into the phloem (Fig. 4.4B). Almost all species that load passively are trees.

In species with intermediary cells, the mechanism is more complex (Fig. 4.4C). Interestingly, all plants with intermediary cells studied to date transport raffinose and stachyose (tri- and tetrasaccharides, respectively; Fig. 4.2), with much lower amounts of sucrose, suggesting that the synthesis of these larger sugars is part of the loading mechanism. A model put forward to explain this is known as **polymer trapping** (Turgeon and Wolf 2009). According to this model, sucrose diffuses into the intermediary cells from the bundle sheath through the numerous plasmodesmata that connect these two cell types. Inside the intermediary cells, most of the sucrose is converted to raffinose and stachyose, which accumulate to high concentrations, because these sugars are too large to diffuse back through the plasmodesmata. This raises the sugar concentration in the phloem, and thus its hydrostatic pressure, considerably (Fig. 4.5).

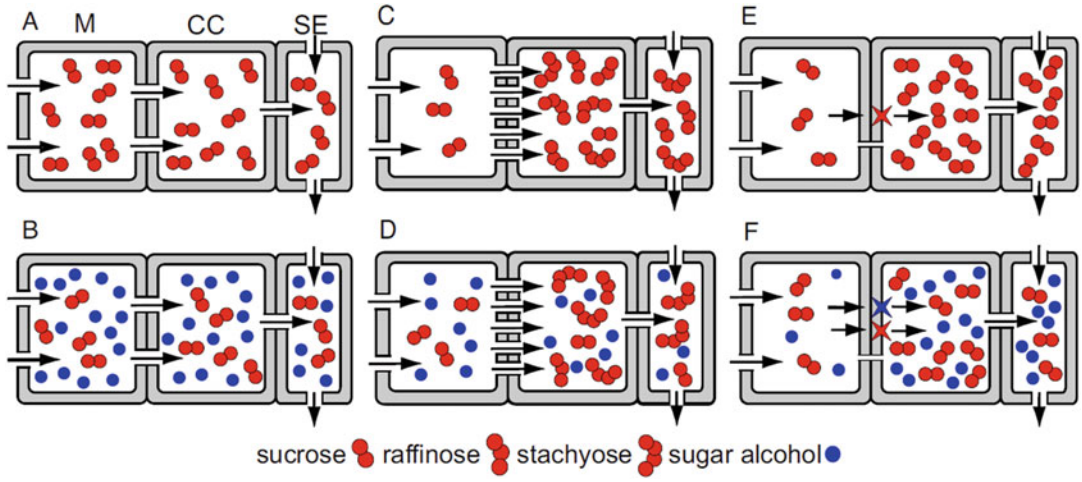

Fig. 4.4 Phloem loading strategies for sucrose (**A**, **C**, **E**) and sucrose plus sugar alcohols (**B**, **D**, **F**). Represented cell types are mesophyll (M), companion cells (CC), and sieve elements (SE). Sucrose loading may be passive, requiring abundant plasmodesmata (gaps in walls) and high sucrose concentrations in the cytosol of mesophyll cells (**A** and **B**), or energized, either by polymer trapping (**C** and **D**) or by active transport from the apoplast mediated by sucrose transporters (red stars on membranes) (**E** and **F**). Sugar alcohol may load passively through available plasmodesmata (**B** and **D**) or from the apoplast, mediated by specific transporters (blue star) (**F**). Rennie EA, Turgeon R. 2009. A comprehensive picture of phloem loading strategies. *Proc Natl Acad Sci USA* **106**: 14162–14167.

Conversion to other sugars keeps the sucrose concentration lower in the intermediary cell than in the mesophyll, and allows continued diffusion. Thus, the plasmodesmata between bundle sheath cells and intermediary cells act as valves. The plasmodesmata between the intermediary cells and the sieve elements are larger, which permits entry of the sugars into the long-distance transport stream. As with purely passive loading, sugar alcohols can enter intermediary cells down their concentration gradient through the plasmodesmata (Fig. 4.4D). Fewer plants use polymer trapping than purely passive loading but it is the loading mechanism common to several families of trees, vines and herbs. Cucurbits (pumpkin, squash etc.), known for their high productivity, are polymer trapping plants.

It turns out that minor veins in dicotyledonous species that do not use the polymer trap mechanism and do not produce galactinol nevertheless have a specialized pair of minor vein companion cells that are capable of activating the galactinol synthase gene if it is introduced by genetic engineering techniques. In *Arabidopsis thaliana* (thale cress) and *Nicotiana tabacum* (tobacco), these cells are the ones that express the gene *FLOWERING LOCUS T* (*FT*), which encodes a systemic signaling molecule that is a key component of the long-sought florigen (Sect. 11.3.3.1; Chen et al. 2018). It is thought that the polymer trap plants co-opted these FT cells to make the transport sugars.

As noted above, many plants have only a limited number of plasmodesmatal connections between the mesophyll and phloem, making passive loading or polymer trapping unlikely. In these species, there is a wealth of evidence that sucrose loads via the apoplast (Rennie and Turgeon 2009; Fig. 4.4E). The first step in this mechanism is passive sucrose efflux from mesophyll cells into the apoplast mediated by Sugar Will Eventually be Exported Transporters (SWEETs) (Chen et al. 2012). Once in the apoplast, sucrose is driven into phloem cells by SUTs (SUcrose Transporters). SUTs are H^+/sucrose symporters located in the plasma membranes of the **companion cells** and/or **sieve elements** (Fig. 4.4E); they use the **proton**

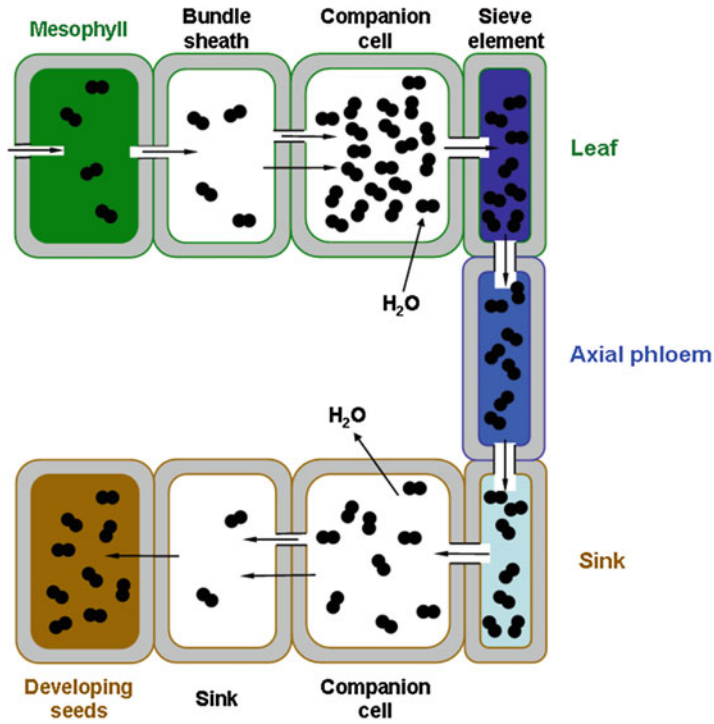

Fig. 4.5 Phloem transport. Cell walls are shown in gray. Sucrose molecules (double circles) are produced in mesophyll cells by photosynthesis and diffuse into bundle sheath cells of the minor veins through plasmodesmata. In the minor veins they enter the companion cells and sieve elements by one of several mechanisms, either through plasmodesmata, or across the apoplast (see Fig. 4.4). Water enters the phloem due to the low water potential, keeping the hydrostatic pressure above that in the sink phloem. Bulk flow of water carries sucrose, and other solutes, from the source leaf to sink tissues where it unloads into sink cells, either through plasmodesmata or via the apoplast. In some sinks, such as embryos of developing seeds, sucrose enters the apoplast after it is unloaded from the phloem and is actively pumped into the sink cells. (Courtesy R. Turgeon, Cornell University, Ithaca, USA).

gradient across the plasma membrane to load the sucrose into the cells against a concentration gradient by secondary active transport. By taking advantage of the steep proton gradient between the apoplast and the cytosol of the sieve elements, with pH values of approximately 5 and 9, respectively, sucrose is continually pumped into the phloem, maintaining a concentration several times that found in mesophyll cells. Since the symplastic pathway is almost entirely closed, species that load sucrose via the apoplast also load sugar alcohols by this route (Fig. 4.4F). In some apoplastic loading species, for example members of the pea family, uptake from the apoplast is facilitated by transfer cell ingrowths, which increase plasma membrane area considerably. Most herbaceous species, including the majority of crop plants load via the apoplast and for that reason most effort in this field has been devoted to apoplastic loading. Since H^+/sucrose symporters are found in the plasma membranes of most plant cells, apoplastic loading may have evolved from a general retrieval mechanism that returns to the cytoplasm sucrose that has leaked out of cells. We know rather little about the way in which other organic compounds and ions enter the phloem. Unraveling these mechanisms is an ongoing research effort (Turgeon 2010).

4.4 Evolution and Ecology of Phloem Loading Mechanisms

The ancestral mechanism of phloem loading in flowering plants is not known for certain, because

we cannot be sure that 'basal' groups (those that diverged early in the evolution of the angiosperms) have retained their ancestral characteristics (Fig. 4.6). However, most basal plants have numerous minor vein plasmodesmata (type 1) (Gamalei 1989; Turgeon et al. 2001). Type 2 plants, and plants with intermediary cells, are more phylogenetically derived; these traits having evolved independently on a number of occasions (Turgeon et al. 2001). The strategies employed by other vascular plants, including the gymnosperms, are not known.

What do the differences between phloem-loading types signify? The absence of type 1 plants in the arctic is probably due to the fact that there are very few woody species of any kind in those extremely cold environments, for reasons that have nothing to do with phloem loading. In addition, laboratory experiments do not support the concept of cold sensitivity in type 1 species with intermediary cells (Schrier et al. 2000). Although plants with intermediary cells seem to be favored in the tropics, there are many correlates of life in the tropics that need to be considered.

Sugar alcohols present another problem. Plants from many families produce **sugar alcohols** in their leaves, though only a few appear to transport significant amounts of these compounds in the phloem. There is convincing evidence that sugar alcohols confer tolerance to **boron** (B) deficiency, because they complex and solubilize this otherwise insoluble mineral and allow it to be transported in the phloem from leaves to meristematic regions, where it is needed for growth (Hu et al. 1997). However, B is also transported in the phloem *Lupinus albus* (white lupin), which does not transport polyols (Huang et al. 2008). Various Rosaceae show a relationship of sorbitol accumulation with tolerance of abiotic stresses including drought, salt, cold, and micronutrient deficiency stresses (Suzuki 2015).

4.5 Phloem Unloading

Phloem unloading represents a series of cell-to-cell transport steps transferring phloem-mobile constituents from phloem to **sink** tissues/organs to fuel their development or resource storage (Milne et al. 2018). When considering how sugars and other materials unload from the phloem, it is useful to make the distinction between **axial sinks** (tissues adjacent to the axial, long-distance transport phloem in shoots and roots) and **terminal sinks** (tissues that are either actively growing or storing large quantities of photoassimilates, such as shoot and root tips, growing leaves, and growing fruits) (Fig. 4.7).

In terminal sinks, where the unloading rate is generally high, solutes unload from the phloem through **plasmodesmata**. Water must follow through **aquaporins**, which are strongly expressed in sink tissues such as the seed coat of *Phaseolus vulgaris* (common bean) (Zhou et al. 2007). The unloading rate is apparently controlled by the radii of the plasmodesmata and by solute concentration and/or hydrostatic pressure differences between the phloem and surrounding cells. In some terminal sinks, the unloaded solute passes **symplastically** through a number of sink cells. It is subsequently released into the apoplast, from which it is actively retrieved by recipient cells. This is the route necessarily taken by sugars in **seeds** since the maternal plant and embryo are different generations and have no connecting plasmodesmata. In this case, sucrose exits the phloem of the seed coat via plasmodesmata, passes symplastically through a layer of cells, and is released into the apoplast surrounding the embryo. The embryo then scavenges the sucrose by active transporters in the plasma membranes of the cotyledons.

Unloading in axial sinks follows either the **symplastic** or **apoplastic** routes, depending on the species, the specific sink, and the stage of development (Ruan 2014). Sugars and other solutes may be released into the **apoplast** or be unloaded through **plasmodesmata**.

Phloem unloading in sink leaves illustrates the need to consider anatomy, physiology, and development to assemble a complete picture of events (Milne et al. 2018). Very young leaves are sinks: they obtain most of their carbohydrate from older leaves. As this photoassimilate enters a young leaf in the phloem it unloads from

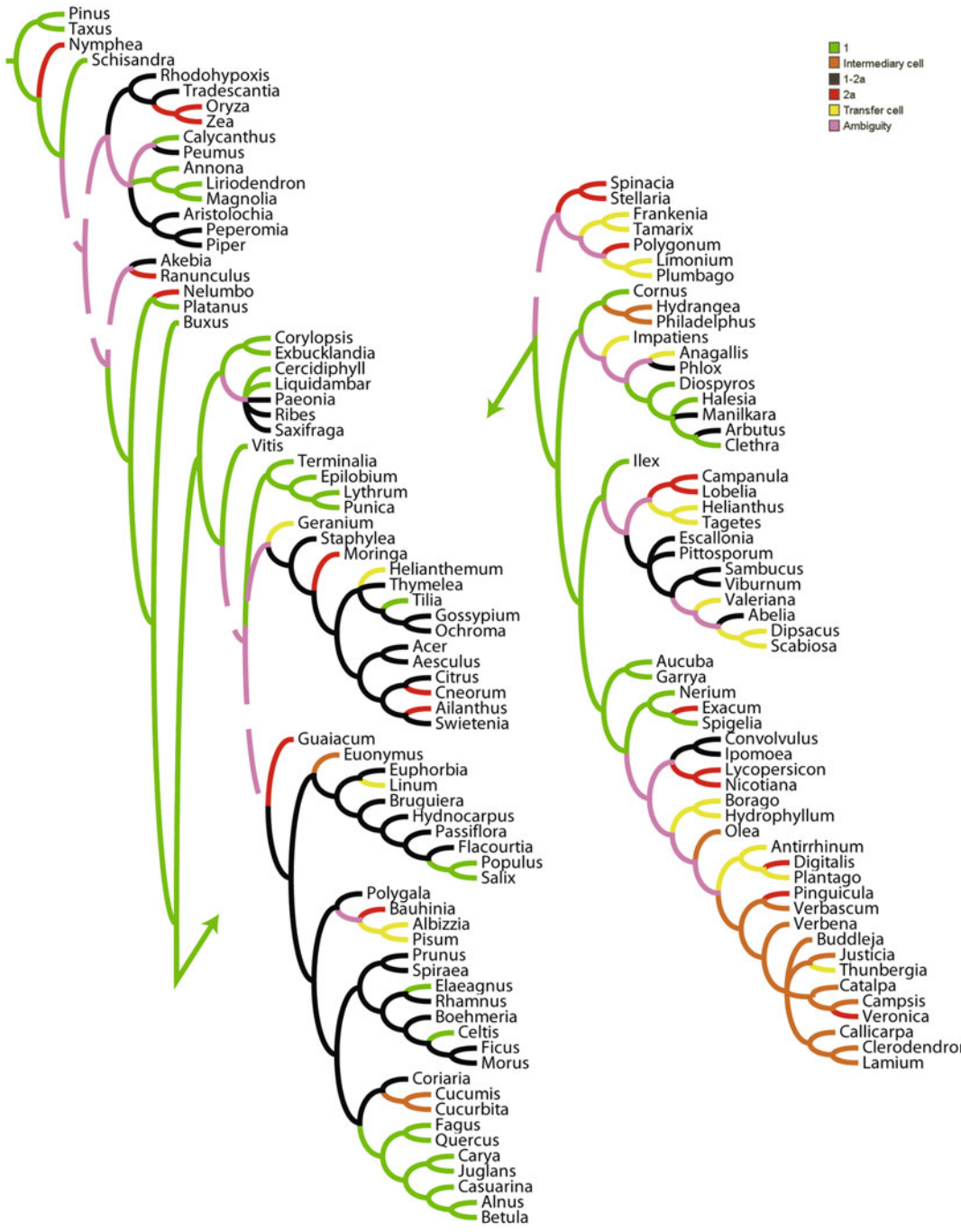

Fig. 4.6 Minor vein companion cell characteristics for 137 taxa mapped onto a phylogenetic tree. Wherever possible, genera for which phloem anatomy is known are coded directly in the matrix, but for some representatives there is no equivalent genus in the molecular matrix. In some of these cases, a closely related confamilial genus is coded for the phloem character. All taxa scored as missing for the phloem loading character are automatically pruned from the consensus tree, producing a tree topology that is a fully congruent subset of the topology with all taxa. The tree has been split at the point indicated by the arrows, with the more ancestral taxa at the left (Turgeon et al. 2001). Copyright The Botanical Society of America.

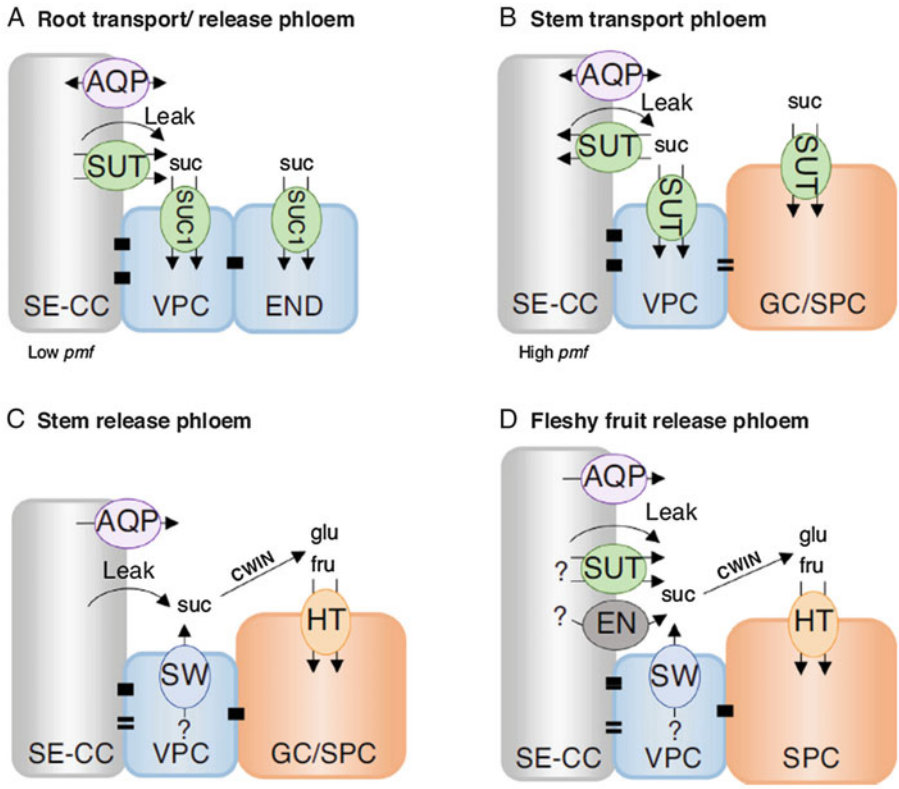

Fig. 4.7 Apoplasmic phloem unloading mechanisms into specified sink types all sharing a passive diffusive leak of sucrose and facilitated water exchange through aquaporins (AQP). (**A**) Apoplastic unloading in roots occurs from release phloem during the de-accelerating phase of cell expansion and from the transport phloem through sucrose symporter (SUT) reversal elicited at low SE-CC proton motive forces (pmf). Sucrose uptake into vascular parenchyma cells (VPC) and endodermis (END) may be mediated by SUC1. (**B**) Apoplasmic unloading from the stem transport phloem may occur solely by a passive leakage with SUTs localized to SE-CCs and VPCs competing for the apoplasmic sucrose along with SUTs located in ground (GC) or specialized storage parenchyma cells (SPCs). (**C**) Apoplasmic unloading from stem release phloem by VPC-localised SWEETs (SW). In monocot stems, unloaded sucrose hydrolysed to hexoses (glu; fru) by cell wall invertases (CWIN) and taken up into GC/SPCs by hexose symporters (HTs). (**D**) Apoplasmic unloading in fleshy fruits may be mediated by SUT reversal, SWs and unidentified energy coupled transporters (EN). CWIN cleaves unloaded sucrose to hexoses which are taken up into SPCs by HTs. indicates conjectured operation of the specified transporter; fru, fructose; glu, glucose; pmf, proton motive force; open plasmodesmata, =; closed plasmodesmata, ■; Copyright Elsevier Science, Ltd.

relatively large veins; the smaller veins are not yet mature (Roberts et al. 1997). As the leaf grows, it reaches a positive carbon balance and then begins to export. Just before it does so, the small veins mature. These **minor veins** are used for photoassimilate **loading**. Therefore, there is a division of labor between veins of different size classes, large ones for **unloading** in young leaves, small ones for loading in mature leaves. Carbohydrate import into **developing seeds** determines seed size, and has been increased through domestication. In *Zea mays* (maize) *ZmSWEET4c* mediates hexose transport across the basal endosperm transfer layer, the entry point of nutrients into the seed. Its activity has increased during domestication (Sosso et al. 2015).

In some organisms structures have evolved to parasitize the phloem-transport system. Rapid phloem unloading occurs when a

phloem-feeding organism (*e.g.*, an aphid) injects its stylet into a sieve tube. The hydrostatic pressure in the sieve pushes the contents of the sieve tube into the aphid. The aphid absorbs predominantly nitrogenous compounds and excretes much of the carbohydrate as '**honeydew**'. The aphids ingest phloem sap without eliciting the sieve tubes' normal response to injury (Sect. 4.3). Another special site where phloem unloading occurs is the **haustoria** of **holoparasites** that depend on their host for their carbon supply. The release of solutes from the phloem of the host is strongly stimulated by the presence of such a parasite (Sect. 15.4). In some species, *e.g.*, *Lupinus albus* (white lupin) the phloem bleeds spontaneously upon cutting (Pate and Hocking 1978). Phloem sap collected in this way or as honeydew has provided valuable information on the composition of phloem sap (Sect. 4.2).

Phloem unloading is affected in a rather special manner by **root nematodes** (*e.g.*, the parasitic nematodes *Meloidogyne incognita* and *Heterodera schachtii*), which can act as major sinks (Dorhout et al. 1993). Unloading from the sieve element companion cell complexes occurs specifically into the 'syncytium', the nematode-induced feeding structure within the vascular cylinder of the root. The infective juvenile nematode selects a procambial or cambial cell as an initial syncytial cell, from which a syncytium develops by integration of neighboring cells. The developing nematode depends entirely on the expanding syncytium, withdrawing nutrients from it through a feeding tube. Unlike in the root tip, the transport of sugars from the phloem to the syncytium in this host-pathogen relationship is apoplastic. The syncytium is not connected via plasmodesmata with the normal root cells. The nematode induces massive leakage from the phloem, thus reducing the transport of phloem solutes to the rest of the roots (Bockenhoff et al. 1996). Feeding of nematodes frequently induces common responses in host cells (*e.g.*, endopolyploidization and cellular hypertrophy). It is thought that these host cell responses are brought about by the interplay of stylet secretions of feeding nematodes (Bockenhoff et al. 1996).

4.6 The Transport Problems of Climbing Plants

Vines can be viewed as 'mechanical parasites' (Ewers et al. 2015). They invest too little in wood to support themselves, and thus depend on other plants for mechanical support. Xylem (wood) tissue has both a transport and a mechanical support function. As discussed in Sect. 5.5.3.5, vines have fewer but longer and wider xylem vessels in their stem per unit stem cross-sectional area. They also have fewer lignified phloem fibers than do trees and shrubs and less phloem tissue per unit of distal area (Ewers and Fisher 1991). How do vines achieve sufficient phloem transport capacity?

Compared with trees and shrubs, vines have **wider sieve tubes** (Fig. 4.8). Since the hydraulic

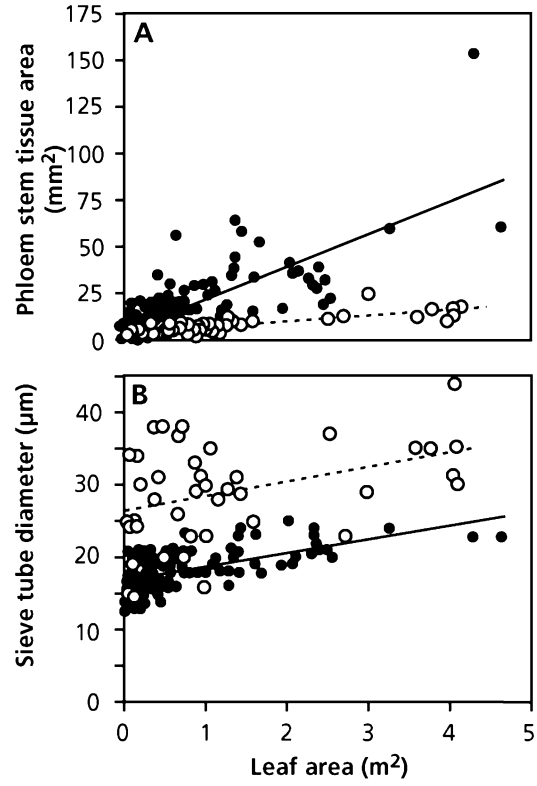

Fig. 4.8 Phloem area (**A**) and maximum diameters of sieve tubes (**B**) of contrasting *Bauhinia* species. Values are plotted as a function of the leaf area distal to the investigated stem section for stems of lianas (dashed line, open symbols) and congeneric trees and shrubs (solid line, closed symbols) (Ewers and Fisher 1991).

conductance, by Hagen-Poiseuille's law for ideal capillaries, is proportional to the fourth power of the conduit radius (Sect. 5.5.3.1), the larger diameter compensates for the smaller total area. The obvious advantage of fewer sieve tubes with a larger diameter is that relatively few resources need to be allocated to producing phloem in the stem, which is therefore light, preventing the supporting plant from toppling over. For a similar investment in stem, the climbing plant will reach a greater height than a nonclimbing plant. If few sieve tubes with large diameters are so advantageous for climbing plants, why do not *all* plants have such wide tubes in their phloem? There is likely a disadvantage in having large-diameter sieve tubes, in that physical damage to a small number of sieve tubes causes a larger proportional loss of transport capacity. Such damage may be mechanical or due to phloem-sucking arthropods or pathogens. As in the xylem of plants with contrasting strategy (Sect. 5.5.3.5), there may be a trade-off between transport **capacity** and **safety**.

4.7 Phloem Transport: Where to Move from Here?

There are three pathways used to load photoassimilates into the phloem, Are there disadvantages and disadvantages associated with each of these pathways? The proton-pumping activity of the transfer cells involved in apoplastic loading requires a substantial amount of metabolic energy. It remains to be demonstrated, however, that this energy requirement is greater than that for the polymerization that occurs in the intermediary cells of plants with symplastic phloem loading. Disadvantages associated with the apoplastic pathway are not immediately obvious.

Phloem unloading can also occur either apoplastically or symplastically, depending on the kind of sink and on species. Phloem unloading in sinks is an important aspect of crop yield, since increases in yield in newer varieties are often determined by the amount of resources transported to harvestable sinks, rather than on the total amount of resources acquired. It is therefore important to develop a good understanding of phloem transport. Unraveling both loading and unloading mechanisms continues to offer major challenges.

References

Batashev DR, Pakhomova MV, Razumovskaya AV, Voitsekhovskaja OV, Gamalei YV. 2013. Cytology of the minor-vein phloem in 320 species from the subclass Asteridae suggests a high diversity of phloem-loading modes. *Front Plant Sci* **4**.

Bockenhoff A, Prior D, Grundler F, Oparka KJ. 1996. Induction of phloem unloading in *Arabidopsis thaliana* roots by the parasitic nematode *Heterodera schachtii*. *Plant Physiol* **112**: 1421–1427.

Chen L-Q, Qu X-Q, Hou B-H, Sosso D, Osorio S, Fernie AR, Frommer WB. 2012. Sucrose efflux mediated by SWEET proteins as a key step for phloem transport. *Science* **335**: 207–211.

Chen Q, Payyavula RS, Chen L, Zhang J, Zhang C, Turgeon R. 2018. *FLOWERING LOCUS T* mRNA is synthesized in specialized companion cells in *Arabidopsis* and Maryland Mammoth tobacco leaf veins. *Proc Natl Acad Sci USA* **115**: 2830–2835.

Dorhout R, Gommers FJ, Kollöffel C. 1993. Phloem transport of carboxyfluorescein through tomato roots infected with *Meloidogyne incognita*. *Physiol Mol Plant Pathol* **43**: 1–10.

Ewers F, Fisher J. 1991. Why vines have narrow stems: histological trends in *Bauhinia* (Fabaceae). *Oecologia* **88**: 233–237.

Ewers FW, Rosell JA, Olson ME 2015. Lianas as structural parasites. In: Hacke U ed. *Functional and Ecological Xylem Anatomy*. Cham: Springer International Publishing, 163–188.

Fu Q, Cheng L, Guo Y, Turgeon R. 2011. Phloem loading strategies and water relations in trees and herbaceous plants. *Plant Physiol* **157**: 1518–1527.

Furch ACU, Hafke JB, Schulz A, van Bel AJE. 2007. Ca^{2+}-mediated remote control of reversible sieve tube occlusion in *Vicia faba*. *J Exp Bot* **58**: 2827–2838.

Gamalei Y. 1989. Structure and function of leaf minor veins in trees and herbs. *Trees* **3**: 96–110.

Gamalei Y. 1991. Phloem loading and its development related to plant evolution from trees to herbs. *Trees* **5**: 50–64.

Garzo E, Fernández-Pascual M, Morcillo C, Fereres A, Gómez-Guillamón ML, Tjallingii WF. 2018. Ultrastructure of compatible and incompatible interactions in phloem sieve elements during the stylet penetration by cotton aphids in melon. *Insect Sci* **25**: 631–642.

Haritatos E, Medville R, Turgeon R. 2000. Minor vein structure and sugar transport in *Arabidopsis thaliana*. *Planta* **211**: 105–111.

Hu H, Penn SG, Lebrilla CB, Brown PH. 1997. Isolation and characterization of soluble boron complexes in higher plants (the mechanism of phloem mobility of boron). *Plant Physiol* **113**: 649–655.

Huang L, Bell RW, Dell B. 2008. Evidence of phloem boron transport in response to interrupted boron supply in white lupin (*Lupinus albus* L. cv. Kiev Mutant) at the reproductive stage. *J Exp Bot* **59**: 575–583.

Juarez MT, Kui JS, Thomas J, Heller BA, Timmermans MCP. 2004. microRNA-mediated repression of rolled leaf1 specifies maize leaf polarity. *Nature* **428**: 84–88.

Lough TJ, Lucas WJ. 2006. Integrative plant biology: role of phloem long-distance molecular trafficking. *Annu Rev Plant Biol* **57**: 203–232.

Milne RJ, Grof CPL, Patrick JW. 2018. Mechanisms of phloem unloading: shaped by cellular pathways, their conductances and sink function. *Curr Opin Plant Biol* **43**: 8–15.

Münch E. 1930. *Die Stoffbewegungen in der Pflanze*. Jena: Gustav Fischer.

Pate JS, Hocking PJ. 1978. Phloem and xylem transport in the supply of minerals to a developing legume (*Lupinus albus* L.) fruit. *Ann Bot* **42**: 911–921.

Patrick JW, Colyvas K. 2014. Crop yield components – photoassimilate supply- or utilisation limited-organ development? *Funct Plant Biol* **41**: 893–913.

Reidel EJ, Rennie EA, Amiard V, Cheng L, Turgeon R. 2009. Phloem loading strategies in three plant species that transport sugar alcohols. *Plant Physiol* **149**: 1601–1608.

Rennie EA, Turgeon R. 2009. A comprehensive picture of phloem loading strategies. *Proc Natl Acad Sci USA* **106**: 14162–14167.

Roberts AG, Cruz SS, Roberts IM, Prior D, Turgeon R, Oparka KJ. 1997. Phloem unloading in sink leaves of *Nicotiana benthamiana*: comparison of a fluorescent solute with a fluorescent virus. *Plant Cell* **9**: 1381–1396.

Ruan Y-L. 2014. Sucrose metabolism: gateway to diverse carbon use and sugar signaling. *Annu Rev Plant Biol* **65**: 33–67.

Savage JA, Beecher SD, Clerx L, Gersony JT, Knoblauch J, Losada JM, Jensen KH, Knoblauch M, Holbrook NM. 2017. Maintenance of carbohydrate transport in tall trees. *Nat Plants* **3**: 965–972.

Schrier AA, Hoffmann-Thoma G, van Bel AJE. 2000. Temperature effects on symplasmic and apoplasmic phloem loading and loading-associated carbohydrate processing. *Funct Plant Biol* **27**: 769–778.

Sosso D, Luo D, Li QB, Sasse J, Yang J, Gendrot G, Suzuki M, Koch KE, McCarty DR, Chourey PS, Rogowsky PM, Ross-Ibarra J, Yang B, Frommer WB. 2015. Seed filling in domesticated maize and rice depends on SWEET-mediated hexose transport. *Nat Gen* **47**: 1489–1493.

Suzuki Y 2015. Polyol metabolism and stress tolerance in horticultural plants. In: Kanayama Y, Kochetov A eds. *Abiotic Stress Biology in Horticultural Plants*. Tokyo: Springer Japan, 59–73.

Turgeon R. 2010. The puzzle of phloem pressure. *Plant Physiol* **154**: 578–581.

Turgeon R, Medville R. 1998. The absence of phloem loading in willow leaves. *Proc Natl Acad Sci USA* **95**: 12055–12060.

Turgeon R, Medville R, Nixon KC. 2001. The evolution of minor vein phloem and phloem loading. *Am J Bot* **88**: 1331–1339.

Turgeon R, Wolf S. 2009. Phloem transport: cellular pathways and molecular trafficking. *Annu Rev Plant Biol* **60**: 207–221.

Van Bel AJE. 2003. The phloem, a miracle of ingenuity. *Plant Cell Environ* **26**: 125–149.

Van Bel AJE 2018. Plasmodesmata: a history of conceptual surprises. In: Sahi VP, Baluška F eds. *Concepts in Cell Biology - History and Evolution.* Cham: Springer International Publishing, 221–270.

Volk GM, Turgeon R, Beebe DU. 1996. Secondary plasmodesmata formation in the minor-vein phloem of *Cucumis melo* L. and *Cucurbita pepo* L. *Planta* **199**: 425–432.

Wang N, Nobel PS. 1998. Phloem transport of fructans in the crassulacean acid metabolism species *Agave deserti*. *Plant Physiol* **116**: 709–714.

White PJ 2012. Long-distance transport in the xylem and phloem. In: Marschner P ed. *Marschner's Mineral Nutrition of Higher Plants (Third Edition)* London: Academic Press, 49–70.

Will T, Tjallingii WF, Thonnessen A, van Bel AJE. 2007. Molecular sabotage of plant defense by aphid saliva. *Proc Natl Acad Sci USA* **104**: 10536–10541.

Zhang C, Turgeon R. 2018. Mechanisms of phloem loading. *Curr Opin Plant Biol* **43**: 71–75.

Zhou Y, Setz N, Niemietz C, Qu H, Offler CE, Tyerman SD, Patrick JW. 2007. Aquaporins and unloading of phloem-imported water in coats of developing bean seeds. *Plant Cell Environ* **30**: 1566–1577.

Plant Water Relations

5

5.1 Introduction

Although water is the most abundant molecule on the Earth's surface, the availability of water is the factor that most strongly restricts terrestrial plant production on a global scale. Low water availability limits the productivity of many natural ecosystems at different time scales (Fig. 5.1). In addition, losses in crop yield due to water stress exceed losses due to all other biotic and environmental factors combined (Boyer 1985). Water availability is also a major determinant of plant and biome distribution. Regions where rainfall is abundant and fairly evenly distributed over the growing season, such as in the wet tropics, have lush vegetation. Where seasonal droughts are frequent and severe, forests are replaced by grasslands or savannas, as in the Asian steppes, North American prairies and tropical savannas (Hirota et al. 2011). Further decrease in rainfall results in semideserts, with scattered shrubs, and finally deserts. Even the effects of temperature are partly exerted through water relations, because rates of evaporation and transpiration are correlated with temperature. Thus, if we want to explain natural patterns of productivity or to increase crop productivity, it is crucial that we understand the controls over plant water relations and the consequences for plant growth of an inadequate water supply. Understanding plant water relations is also important to improve our ability to predict the effects of more frequent extreme climatic events such as droughts and floods on the future distribution and functioning of natural ecosystems.

5.1.1 The Role of Water in Plant Functioning

Water is important to the physiology of plants because of its crucial role in all physiological processes and because of the large quantities that are required. Water typically comprises 70–95% of the biomass of nonwoody tissues such as leaves and roots. At the cellular level, water is the major medium for transporting metabolites through the cell. Because of its highly polar structure, water readily dissolves large quantities of ions and polar organic metabolites like sugars, amino acids, and proteins that are critical to metabolism and life. At the whole-plant level, water is the medium that transports the raw materials (carbohydrates and nutrients) as well as the phytohormones that are required for growth and development from one plant organ to another. Unlike most animals, plants lack a well-developed skeletal system; especially herbaceous plants depend largely on water for their overall structure and support. Due to their high concentrations of solutes, plant cells exert a positive pressure (**turgor**) against their cell walls which is the basic support mechanism in herbaceous plants. Turgor pressures are typically of the order of 1.0–5.0 MPa, similar to the pressure in nuclear steam turbines. Large plants gain

H. Lambers, R. S. Oliveira, *Plant Physiological Ecology*, https://doi.org/10.1007/978-3-030-29639-1_5

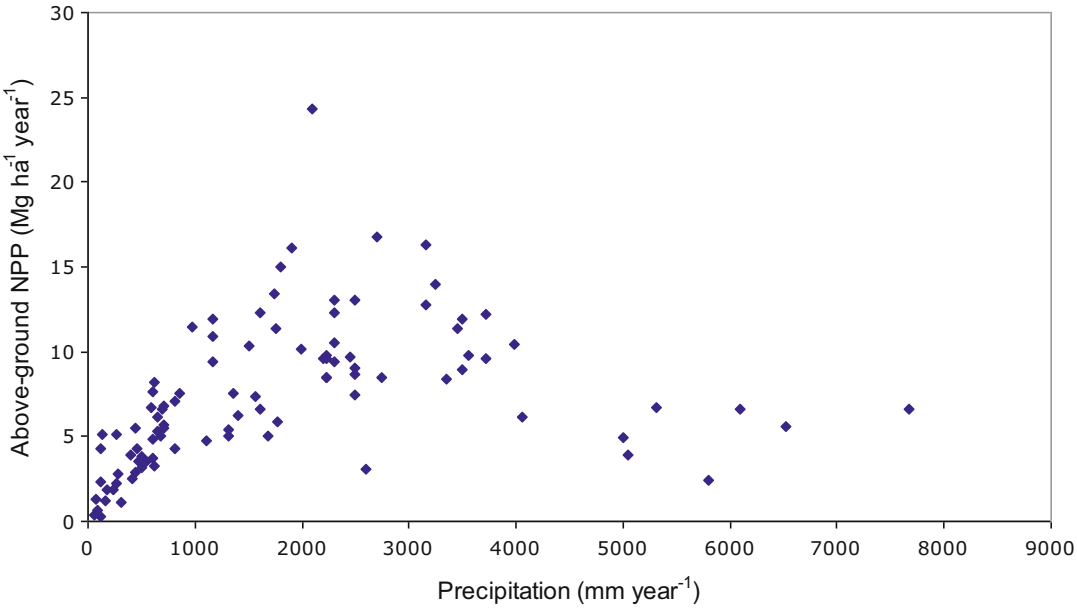

Fig. 5.1 Correlation of aboveground net primary production (NPP, in units of biomass) with precipitation. NPP declines at extremely high precipitation (>3 m year^{-1}) due to indirect effects of excess moisture, such as low soil oxygen and nutrient loss by leaching (Schuur 2003). Copyright Ecological Society of America.

Table 5.1 Concentration of major constituents in a hypothetical herbaceous plant and the amount of each constituent that must be absorbed to produce a gram of dry biomass. The values only give a rough approximation and vary widely among species and with growing conditions, indicated in Sect. 9.4.3 for nutrients, and in Sect. 5.6 for water.

Resource	Concentration (% of fresh mass)	Quantity required (mg g^{-1})
Water	90	2500
Carbon	4	40
Nitrogen	0.3	3
Potassium	0.2	2
Phosphorus	0.02	0.2

additional structural support from fibers and the lignified cell walls of woody tissues. When plants lose turgor (**wilt**), they no longer carry out certain physiological functions, in particular cell expansion and to a lesser extent photosynthesis. Prolonged periods of wilting usually kill the plant.

A second general reason for the importance of water relations to the physiological ecology of plants is that plants require vast quantities of water. Whereas plants incorporate more than 90% of absorbed nitrogen (N), phosphorus (P), and potassium (K), and about 10–70% of photosynthetically fixed carbon (C) into new tissues (depending on respiratory demands for carbon), less than 1% of the water absorbed by plants is retained in biomass (Table 5.1). The remainder is lost by **transpiration**, which is the evaporation of water from plant leaves. The inefficient use of water by terrestrial plants is an unavoidable consequence of photosynthesis. The stomata, which allow CO_2 to enter the leaf, also provide a pathway for water loss. CO_2 that enters the leaf must first dissolve in water on the wet walls of the mesophyll cells before diffusing to the site of carboxylation. This moist surface area of mesophyll cells exposed to the internal air spaces of the leaf is about 7–80 times the external leaf area, depending on species and plant growth conditions (Table 5.2). This causes the air inside the leaf to

Table 5.2 The ratio of the surface area of mesophyll cells and that of the leaf (A_{mes}/A) as dependent on species and growing conditions*.

Leaf morphology/habitat	A_{mes}/A
Shade leaves	7
Mesomorphic leaves	12–19
Xeromorphic sun leaves	17–31
Low altitude (600 m)	37
High altitude (3000 m)	47
Species	A_{mes}/A
Plectranthus parviflorus	
High light	39
Low light	11
Alternanthera philoxeroides	
High light	78
Low light	50

*The data on leaves of species with different morphologies are from Turrell (1936), those on low-altitude and high-altitude species from Körner et al. (1989), those on *Plectranthus parviflorus* from Nobel et al. (1975), and those on *Alternanthera philoxeroides* (alligator weed) from Longstreth et al. (1985)

be saturated with water vapor (almost 100% relative humidity) which usually creates a strong gradient in water vapor concentration from the inside to the outside of the leaf.

5.1.2 Transpiration as an Inevitable Consequence of Photosynthesis

Transpiration is an inevitable consequence of photosynthesis; however, it also has important direct effects on the plant, because it is a major component of the leaf's energy balance. As water evaporates from mesophyll cell surfaces, it cools the leaf. In the absence of transpiration, the temperature of large leaves can rapidly rise to lethal levels. We further discuss this effect of transpiration in Chap. 6. The transpiration stream also allows transport of nutrients from the bulk soil to the root surface and of solutes, such as inorganic nutrients, amino acids, and phytohormones, from the root to transpiring organs. As will be discussed later, however, such transport in the xylem also occurs in the absence of transpiration, so that the movement of materials in the transpiration stream is not strongly affected by transpiration rate.

In this chapter, we describe the environmental factors that govern water availability and loss, the movement of water into and through the plant, and the physiological adjustments that plants make to variation in water supply over diverse time scales. We emphasize the mechanisms by which individual plants adjust water relations in response to variation in water supply and demand and the adaptations that have evolved in environments subjected to water scarcity).

5.2 Water Potential

The status of water in soils, plants, and the atmosphere is commonly described in terms of **water potential** (ψ_w) [*i.e.* the chemical potential of water in a specified part of the system, compared with the chemical potential of pure water at the same temperature and atmospheric pressure; it is measured in units of pressure (MPa)]. The water potential of pure, free water at atmospheric pressure and at a temperature of 298 K is 0 MPa (by definition) (Box 5.1).

Box 5.1: The Water Potential of Osmotic Solutes and the Air

We are quite familiar with the fact that water can have a potential: we know that the water at the top of a falls or in a tap has a higher potential than that at the bottom of the falls or outside the tap. Transport of water, however, occurs not invariably as a result of differences in hydrostatic pressure, but also due to differences in vapor pressure (Sect. 2.2.2.2) or to differences in the amount of dissolved osmotic solutes in two compartments separated by a semipermeable membrane. In fact, in all these cases there is a difference in water potential, which drives the transport of water. For a full appreciation of many aspects of plant water relations, we first introduce the concept of the chemical potential of water, for which we use the symbol μ_w.

(continued)

Box 5.1 (continued)

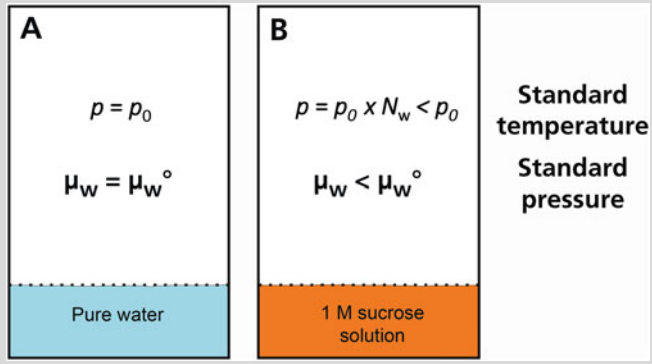

Box Fig. 5.1 The difference in water potential between two systems. The system at the left is a sealed container with pure water at standard temperature and pressure; the partial water vapor pressure in this container is p_o and the chemical potential of water in this system is μ_w^o. The system at the right is a container with a solution of 1 M sucrose at the same temperature and pressure; the water vapor pressure can be calculated according to Raoult's law ($p = p_o.N_w$) and the chemical potential of water in this system is μ_w. The difference in chemical potential between the two systems can be calculated as explained in the text.

By definition, the chemical potential of pure water under standard conditions (298 K and standard pressure), for which the symbol μ_w^o is used, is zero. We can also calculate the chemical potential of water under pressure, water that contains osmotic solutes, or water in air. This can best be explained using a simple example, comparing the chemical potential of water in two sealed containers of similar size (Box Fig. 5.1). One of these containers (A) contains pure water under standard conditions: $\mu_w = \mu_w^o = 0$. Of course the gas phase is in equilibrium with the liquid pure water, and the vapor pressure is p_o. The second container (B) contains a 1 M sucrose solution in water. The gas phase will again be in equilibrium with the liquid phase; the vapor pressure is p. The vapor pressure, however, will be less than p_o, because the sucrose molecules interact with the water molecules via hydrogen bonds, so that the water molecules cannot move into the gas phase as readily as in the situation of pure water. How large is the difference between p and p_o?

To answer this question we use Raoult's law, which states:

$$p/p_0 = N_w \tag{5.1}$$

where N_w is the mol fraction [*i.e.* the number of moles of water divided by the total number of moles in container B; in the case of 1 mole of sucrose in 1 L water (= 55.6 moles of water], N_w equals 55.6/56.6 = 0.982); p_o is the vapor pressure (in Pa) above pure water, at standard pressure and temperature. We can calculate the difference in potential between the two containers ($\mu_w - \mu_w^o$) by considering the amount of work needed to obtain the same (higher) pressure in container B as in container A. To achieve this, we need to compress the gas in container B until the pressure equals p_o:

$$\mu_w - \mu_w^0 = \int_{p_0}^{p} V\,dp = RT \ln\left(\frac{p}{p_0}\right) \tag{5.2}$$

where V is the volume (m^3) of container B, which is compressed until p_o is reached, R is the gas constant (J mol^{-1} K^{-1}), and T is the absolute temperature (K).

Combination of Eqs 5.1 and 5.2 yields:

$$\mu_w - \mu_w^o = RT \ln (1 - N_w) \tag{5.3}$$

(continued)

Box 5.1 (continued)

Because N_w is the mole fraction of water and N_s is the mole fraction of the solute (in our example, 1/56.6 = 0.018), we can write Eq. 5.3 as:

$$\mu_w - \mu_w{}^o = RT \ln (1 - N_s) \quad (5.4)$$

As long as we consider solutions in a physiologically relevant range (*i.e.* not exceeding a few molar) Eq. 5.4 approximates:

$$\mu_w - \mu_w{}^o = RT N_s \quad (5.5)$$

[as can readily be calculated for our example of a 1 M solution of sucrose, N_s is 0.018 and ln $(1 - N_s) = -0.018$].

Dividing N_s by the molar volume of pure water (V_w^o, m^3 mol^{-1}) we arrive at the concentration of the solute, c_s (in mol m^{-3}):

$$N_s / V_w^o = c_s \quad (5.6)$$

We make one further change, by introducing the molar volume of pure water (m^3 mol^{-1}; at 273 K) in Eq. 5.5:

$$\frac{\mu_w - \mu_w^o}{V_w^o} = -RTc_s = \Psi \quad (5.7)$$

Ψ is the water potential. Because we are dealing with the water potential of a solution in this example, we refer to this potential as the osmotic potential of water(Ψ_π). The dimension is Pascal (Pa). It is often more convenient, however, to use megapascal (MPa = 10^6 Pa) instead (1 MPa equals 10 bars, a unit used in the literature, or 10 atmospheres, a unit that is no longer used).

We can therefore calculate that our 1 M sucrose solution has an osmotic potential of −2.4 MPa, which approximates a pressure of a water column of about 250 m!!! In equilibrium, the water potential of the gas phase above the 1 M sucrose solution also equals −2.4 MPa. In the case of electrolytes, the calculation is slightly more complicated in that the dissociation of the solute has to be taken into account.

By modifying Eq. 5.7 we can also calculate the water potential of air that is not in equilibrium with pure water [*i.e.* with a relative humidity (RH) of less than 100%]:

$$\frac{\mu_w - \mu_w^o}{V_w^o} = \frac{RT}{V_w^o} \ln\left(\frac{p}{p_o}\right) \quad (5.8)$$

For air of 293 K and a RH of 75% Ψ equals −39 MPa [to calculate this you need to know that the molar volume of water (molecular mass = 18) at 293 K is 18.10^{-6} m^3 mol^{-1}]. Values for Ψ of air of different RH are presented in Box Table 5.1. Note that even when the water vapor pressure is only marginally lower than the saturated water vapor pressure RH = 100%), the water potential is rather negative.

Box Table 5.1 The water potential (MPa) of air at a range of relative humidities and temperatures*.

	−Ψ (MPa) at different temperatures (°C)				
Relative humidity	10	15	20	25	30
100	0	0	0	0	0
99.5	0.65	0.67	0.68	0.69	0.70
99	1.31	1.33	1.36	1.38	1.40
98	2.64	2.68	2.73	2.77	2.81
95	6.69	6.81	6.92	7.04	7.14
90	13.75	13.99	14.22	14.45	14.66
80	29.13	29.63	30.11	30.61	31.06
70	46.56	47.36	48.14	48.94	49.65
50	90.50	92.04	93.55	95.11	96.50
30	157.2	159.9	162.5	165.2	167.6
10	300.6	305.8	310.8	316.0	320.6
RT/V_w	130.6	132.8	135.0	137.3	139.2

Note: The values were calculated using the formula: $\Psi = -RT/V_w{}^0$ ln(% relative humidity/100)

*Note that all values for Ψ are *negative* and that the effect of temperature is exclusively due to the appearance of temperature in the equation given in the last line of this table, rather than to any effect of temperature on p_o

In an isothermal two-compartment system, in which the two compartments are separated by a **semipermeable membrane**, water will move from a high to a low water potential. If we know the water potential in the two compartments, then we can predict the direction of water movement. It is certainly *not* true, however, that water invariably moves down a gradient in water potential. For example, in the **phloem** of a source leaf the water potential is typically more negative than it is in the phloem of the sink. In this case water transport is driven by a difference in hydrostatic pressure, and water moves up a gradient in water potential. Similarly, when dealing with a nonisothermal system, such as a warm atmosphere and a cold leaf, water vapor may condense on the leaf even though the water potential of the air is more negative than that of the leaf.

Water potential in any part of the system is the sum of the **osmotic potential**, ψ_π, and the **hydrostatic pressure**, ψ_p (the component of the water potential determined by gravity is mostly ignored, but can be relevant for tall trees):

$$\psi_w = \psi_\pi + \psi_p \tag{5.9}$$

where water potential is the overall pressure on water in the system. The **osmotic potential** is the chemical potential of water in a solution due to the presence of dissolved materials. The osmotic potential always has a negative value because water tends to move across a semipermeable membrane from pure water (the standard against which water potential is defined) into water containing solutes (Box 5.1). The higher the concentration of solutes, the lower (more negative) is the osmotic potential. The **hydrostatic pressure**, which can be positive or negative, refers to the physical pressure exerted on water in the system. For example, water in the turgid root cortical cells or leaf mesophyll cells is under positive **turgor pressure** exerted against the cell walls, whereas water in the dead xylem vessels of a rapidly transpiring plant is typically under **suction tension** (negative pressure). Large negative hydrostatic pressures arise because of capillary effects, *i.e.* the attraction between water and hydrophilic surfaces at an air/water interface (Box 5.2). Total

Box 5.2: Positive and Negative Hydrostatic Pressures

Positive values of hydrostatic pressure in plants are typically found in living cells and are accounted for by high concentrations of osmotic solutes. Large negative values arise because of capillary effects (*i.e.* the attraction between water and hydrophilic surfaces at an air–water interface). It is this attraction that explains the negative matric potential in soil and the negative hydrostatic pressure in the xylem of a transpiring plant.

The impact of the attraction between water and hydrophilic surfaces on the pressure in the adjacent water can be understood by imagining a glass capillary tube, with radius a (m), placed vertically with one end immersed in water. Water will rise in the tube, against the gravitational force, until the mass of the water in the tube equals the force of attraction between the water and the glass wall. A fully developed meniscus will exist (*i.e.* one with a radius of curvature equal to that of the tube). The meniscus of the water in the glass tube is curved, because it supports the mass of the water.

The upward acting force in the water column equals the perimeter of contact between water and glass ($2\pi a$) multiplied by the surface tension, $\gamma(\mathrm{Nm}^{-1})$, of water; namely, $2\pi a\gamma$ (provided the glass is perfectly hydrophilic, when the contact angle between the glass and the water is zero; otherwise, this expression has to be multiplied by the cosine of the angle of contact). When in equilibrium, there must be a difference in pressure, ΔP (Pa) across the meniscus, equal to the force of attraction between the water and the capillary wall (*i.e.* the pressure in the water is less than that of the air). The downward acting force (N) on the meniscus is the difference in pressure multiplied by the cross-sectional area of the capillary tube (*i.e.* $\pi a^2 \gamma P$).

(continued)

Box 5.2 (continued)

Thus, because these forces are equal in equilibrium, we have:

$$\pi x\, a^2 \times \Delta P = 2\pi x\, a \times \gamma \qquad (5.10)$$

and:

$$\Delta P = 2\pi a \times \gamma / \pi a^2 = 2\gamma / a \qquad (5.11)$$

The surface tension of water is 0.075 N m^{-1} at about 20 °C, so $\Delta P = 0.15/a$ (Pa). Thus a fully developed meniscus in a cylindrical pore of radius, say 1.5 μm, would have a pressure drop across it of 1.0 MPa; the pressure, P, in the water would therefore be −0.1 MPa if referenced to normal atmospheric pressure, or − 0.9 MPa absolute pressure (given that standard atmospheric pressure is approximately 0.1 MPa).

This reasoning also pertains to pores that are not cylindrical. It is the radius of curvature of the meniscus that determines the pressure difference across the meniscus, and this curvature is uniform over a meniscus that occupies a pore of any arbitrary shape. It is such capillary action that generates the large negative pressures (large suction tension) in the cell walls of leaves that drive the long-distance transport of water from the soil through a plant to sites of evaporation. The pores in cell walls are especially small (approximately 5 nm) and are therefore able to develop very large suction tensions, as they do in severely water-stressed plants.

water potential can have a positive or negative value, depending on the algebraic sum of its components. When dealing with the water potential in soils, an additional term is used: the **matric potential**, ψ_m. The matric potential refers to the force with which water is adsorbed onto surfaces such as cell walls, soil particles, or colloids, similar to the forces in xylem vessels. As such it is actually a convenient *alternative* to hydrostatic pressure for characterizing the water status of a porous solid. The hydrostatic pressure and the matric potential should therefore never be added! The matric potential always has a negative value, because the forces tend to hold water in place, relative to pure water in the absence of adsorptive surfaces. The matric potential becomes more negative as the water film becomes thinner (smaller cells or thinner water film in soil).

Now that we have defined the components of water potential, we show how these components vary along the gradient from soil to plant to atmosphere.

5.3 Water Availability in Soil

The availability of soil water to plants depends primarily on the quantity of water stored in the soil, its relationship to soil water potential, and the spatial geometry of root systems. Clay and organic soils, which have small soil particles, have more small soil pores; these small capillaries generate very negative pressures (large suction tensions) (Box 5.2). Pores larger than 30 μm hold the water only rather loosely, so the water drains out following a rain. Pores smaller than 0.2 μm hold water so tightly to surrounding soil particles that the drainage rate often becomes very small once the large pores have been drained. As a result, most plants cannot extract water from these pores at sufficiently high rates to meet their water needs. It is thus the intermediate-sized pores (0.2–30 μm diameter) that hold most of the water that is tapped by plants.

In friable soil, roots can explore a large fraction of the soil volume; hence, the volume of water that is available to the roots is relatively large. Upon

soil compaction, roots are unable to explore as large a fraction of the soil volume; the roots then tend to be clumped into sparse pores and water uptake is restricted. Compacted soils, however, are not uniformly hard and usually contain structural cracks and biopores (*i.e.* continuous large pores formed by soil fauna and roots). Roots grow best in soil with an intermediate density, which is soft enough to allow good root growth but sufficiently compact to give good root-soil contact (Stirzaker et al. 1996). Root tip geometry affects root elongation rates in soils with contrasting bulk densities, and smaller root tip radius-to-length ratio improves the ability of roots to elongate in hard soils (Colombi et al. 2017). Water stored in bedrock, also termed rock moisture, can also be a significant source of moisture for vegetation growing over rocky substrates (Schwinning 2010; Rempe and Dietrich 2018). However, the root adaptations to take up water from rock moisture and the global importance of water stored in bedrock to meet vegetation transpiration demands still need to be quantified.

Water movement between root and soil can be limited by incomplete root-soil contact, such as that caused by air gaps due to root shrinkage during drought. It can also be influenced by a **rhizosheath** (*i.e.* the soil particles bound together by root exudates and root hairs of sand-binding roots) (McCully and Canny 1988; Shane et al. 2010). Rhizosheaths are limited to distal root regions, which generally have a higher water content than do the more proximal regions, in part due to the immaturity of the xylem in the distal region. The rhizosheath virtually eliminates root-soil air gaps, thus facilitating water uptake in moist soil. On the other hand, bare roots restrict water loss from roots to a drier soil (North and Nobel 1997).

5.3.1 The Field Capacity of Different Soils

Field capacity is defined as the water content after the soil becomes saturated, followed by complete gravitational drainage. The water potential of non-saline soils at field capacity is close to zero (−0.01 to −0.03 MPa). There is a higher soil water content at field capacity in fine-textured soils with a high clay or organic matter content (Fig. 5.2). The lowest water potential at which a plant can access water from soil is the **permanent wilting point**. Although species differ in the extent to which they can draw down soil water (*e.g.*, from −1.0 to −8.0 MPa), as discussed later, a permanent wilting point of −1.5 MPa is common for many herbaceous species (especially crops). The **available water** is the difference in the amount of soil water between field capacity and permanent wilting point, −1.5 MPa (by definition). The amount of available water is higher in clay than it is in sandy soils (Fig. 5.2, Table 5.3). Because species differ in the extent to which they can draw down soil water, for many plants soil water below a soil water potential of –1.5 MPa is available.

In a moist soil, the smallest soil pores are completely filled with water and only the largest

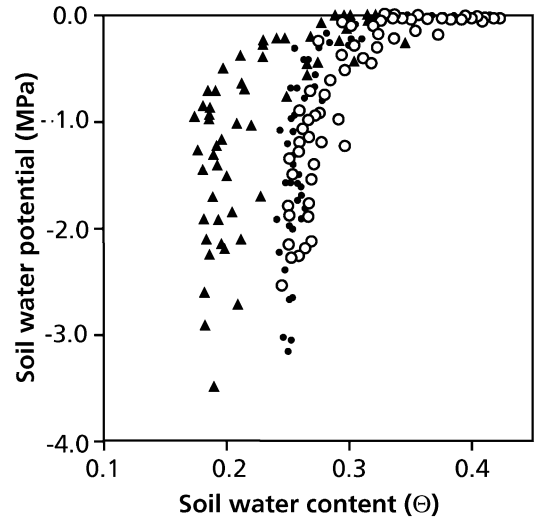

Fig. 5.2 Relationship between soil water potential and volumetric soil water content (ratio of volume taken up by water and total soil volume, θ) at different soil depths: 25 cm, solid triangles; 50–80 cm, open circles; 110–140 cm, filled circles. The top horizon was a silty clay loam, the middle layer was enriched with clay and in the deepest soil layer the clay content decreased again. Soil water potential was measured with tensiometers and micropsychrometers, and soil water content with a neutron probe. Data were obtained over 1 year while water content fell during drought (Bréda et al. 1995). Copyright Springer-Nature.

Table 5.3 Typical pore-size distribution and soil water contents of different soil types.

	Soil type		
	Sand	Loam	Clay
Parameter			
Pore space (% of total)			
>30 μm particles	75	18	6
0.2–30 μm	22	48	40
<0.2 μm	3	34	53
Water content (% of volume)			
Field capacity	10	20	40
Permanent wilting point	5	10	20

pores have air spaces. As soil moisture declines, the thickness of the water film surrounding soil particles declines, and the remaining water is held more tightly to soil particles, giving a low (negative) matric potential. Finally, the gravitational component of the water potential (reflecting the mass of the water column) is generally negligible in soils. In nonsaline soils, the matric potential is the most important component of soil water potential.

In **saline soils**, the osmotic potential adds an additional important component. If plants are well watered with a saline solution of 100 mM NaCl, then the soil water potential is −0.48 MPa. As the soil dries out, the salts become more concentrated and further add to the negative value of the soil water potential. When half of the water available at field capacity has been absorbed, the osmotic component of the soil water potential will have dropped to almost −1 MPa. Under such situations we clearly cannot ignore the osmotic component of the soil water potential.

Soil **organic matter** affects water **retention** because of its hydrophilic character and its influence on soil structure. Increasing the organic matter content from 0.2% to 5.4% more than doubles the water-holding capacity of a sandy soil; from 0.05 to 0.12 (v/v). In silty soils, which have a larger water-holding capacity, the absolute effect of organic matter is similar, but less dramatic when expressed as a percentage; it increases from about 0.20 to less than 0.30 (v/v). Effects on plant-available water content are smaller because the water content at field capacity as well as that at the permanent wilting point is enhanced (Kern 1995). Roots, especially mycorrhizal roots (Sect. 12.2.5), may promote the development of soil aggregates, through the release of organic matter, and thus affect soil hydraulic properties. **Organic matter** may also have the effect of **repelling** water, if it is highly hydrophobic (Chenu and Cosentino 2011). Such situations may arise when plant-derived waxy compounds accumulate on the soil surface. These reduce the rate at which water penetrates the soil so that much of the precipitation from a small shower may be lost through run-off or evaporation rather than becoming available for the plant. Soil **water repellency** may generate soil water-vegetation feedbacks and affect ecosystem dynamics (Siteur et al. 2016). Water repellency is caused by hydrophobic skins of a very stable humic fraction of soil organic matter and plant-derived substances on sand grains (Roberts and Carbon 1972; Doerr et al. 2000). Some roots release surfactants, which may counteract the effect of water-repelling compounds in soil (Read et al. 2003).

5.3.2 Water Movement Toward the Roots

Water moves through soil to the roots of a transpiring plant by flowing down a gradient in hydrostatic pressure. If the soil is especially dry (with a water potential less than −1.5 MPa), then there may be significant movement as water vapor. Under those conditions, however, transpiration rates are very low. Gradients in osmotic potential move little water, because the transport coefficients for diffusion are typically orders of magnitude smaller than for flow down a hydrostatic gradient. Movement across the interface between root and soil is more complicated. There may be a mucilaginous layer that contains pores so small that the flow of water across it is greatly hindered. There may also be a lack of hydraulic continuity between root and soil if the root is growing in a pore wider than itself or if the root has shrunk. As the soil dries and the matric forces holding water to soil particles increases, movement of liquid water through soils declines (Fig. 5.3).

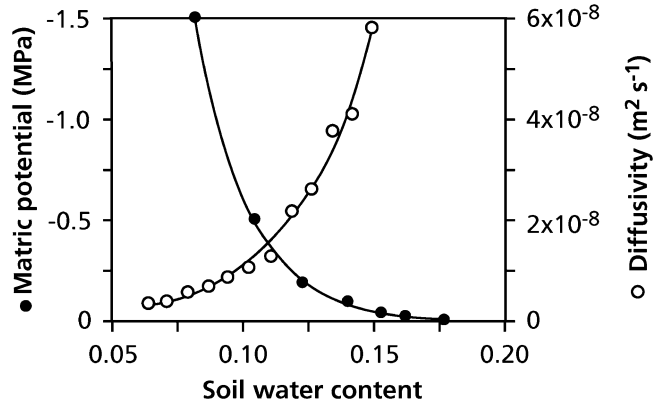

Fig. 5.3 The matric potential and diffusivity of soil water as a function of the volumetric water content (ratio of volume taken up by water and total soil volume) of a sandy loam soil (55% coarse sand, 19% fine sand, 12% silt, and 14% clay) (after Stirzaker and Passioura 1996). © John Wiley & Sons Ltd.

In a situation where the soil is relatively dry and the flow of water through it limits water uptake by the roots, the following equation approximates water uptake by the roots:

$$\mathrm{d}\theta'/\mathrm{d}t = D(\theta' - \theta_\mathrm{a})/2b^2 \qquad (5.12)$$

where $\mathrm{d}\theta'/\mathrm{d}t$ is the rate of fall of mean soil water content, θ', with time, t; D is the diffusivity of soil water, which is approximately constant with a value of 2.10^{-4} m^2 day^{-1} ($0.2.10^{-8}$ m^2 s^{-1}), during the extraction of about the last third of the available water in the soil (Fig. 5.3), when the flow is likely limiting the rate of water uptake; θ_a is the soil water content at the surface of the root; and b is the radius of a putative cylinder of soil surrounding the root, to which that root effectively has sole access, and can be calculated as $b = (\pi L)^{-1/2}$, where L (m m^{-3}), the rooting density, is the length of root per unit volume of soil (m^3) (Passioura 1991).

Under the reasonable assumption that θ_a is constant, as it would be if the root were maintaining a constant water potential of, say, −1.5 MPa at its surface (Fig. 5.3), the equation can be integrated to give:

$$\begin{aligned}(\theta' - \theta_\mathrm{a})_\mathrm{d} &= (\theta' - \theta_\mathrm{a})_0 \exp\left(-Dt/2\mathrm{b}^2\right) \\ &= \theta_{\mathrm{d}0} \exp\left(-t/t^*\right)\end{aligned} \qquad (5.13)$$

where $(\theta' - \theta_\mathrm{a})_0$ is $(\theta' - \theta_\mathrm{a})$ when $t = 0$, and t^* (equal to $2b^2/D$) is the time constant for the system: the time taken for the mean soil water content to fall to 1/e (*i.e.* 0.37) of its initial value. If D is 2.10^{-4} m^2 day^{-1}, then t^* is simply $b^2.10^{-4}$ days. If the roots are evenly distributed in the soil, then, even at a low rooting density, L, of 0.1 m.m^{-3}, t^* (calculated from $b^2 = 1/[\pi L)]$) is only about 3 days. Roots, therefore, should readily be able to extract all the available water from the soil. When the soil is compacted, roots are not distributed so evenly through the soil (Sect. 10.5.5), and Eqs 5.12 and 5.13 no longer apply. Under those conditions t^* could become of the order of weeks. The parameter t^* changes with soil type, soil depth, and also with the osmotic adjustment capacity of the plant extracting the water (Passioura 1991).

If a plant does not absorb all the ions arriving at the surface of its roots, the osmotic potential will drop locally, either only in the apoplast of the roots or possibly in the rhizosphere as well. This is more pronounced in fertilized or saline soils than in nutrient-poor, nonsaline soils. The effect is that plants have greater difficulty in extracting water from soil than expected from the average soil water potential (Stirzaker et al. 1996).

5.3.3 Rooting Profiles as Dependent on Soil Moisture Content

As long as the upper soil is moist, plants tend to absorb most of their water from shallower soil regions, where roots are concentrated. As the soil dries out, relatively more water is absorbed from deeper layers. Water from the deepest layers, even from those where no roots penetrate, may become available through capillary rise

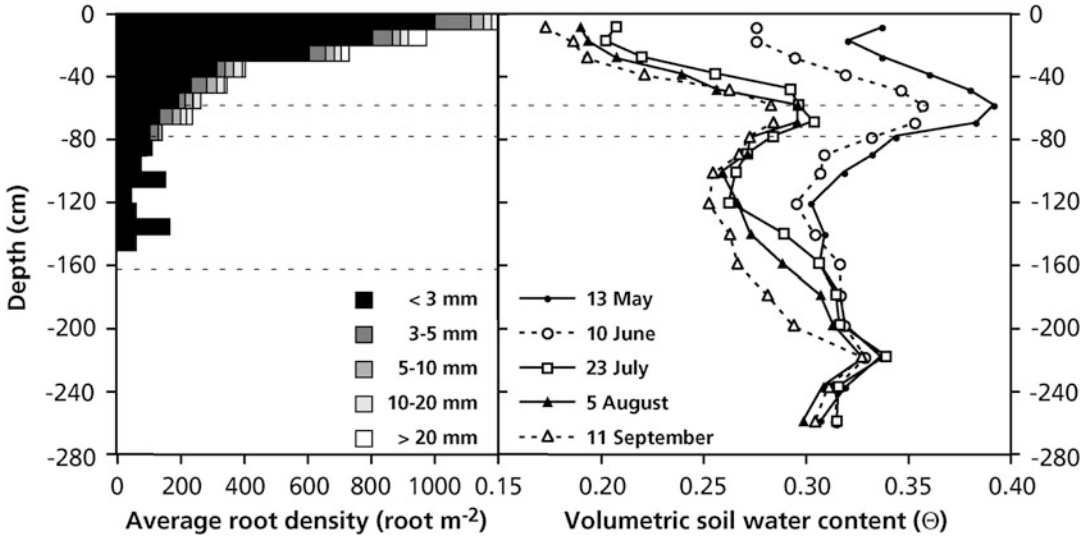

Fig. 5.4 (Left) Rooting profile of *Quercus petraea* (sessile oak) as dependent on soil depth. Roots are divided in different diameter classes. (Right) Volumetric water content of the soil in which the oak tree was growing, as dependent on depth and time of the year. A clay-enriched horizon at around 50 cm depth is indicated by the two broken lines. The third broken line at 160 cm depth indicates the depth of the trench that was dug to make the measurements (Bréda et al. 1995). Copyright Springer-Nature.

(Fig. 5.4; Bréda et al. 1995). The actual **rooting depth** varies greatly among species, with understory trees growing in a seasonal Amazonian forest in Brazil [*Rinorea pubiflora* (Violaceae) and *Coussarea albescens* (Rubiaceae)] tapping water from superficial soils (less than 1 m depth) and canopy trees (*e.g.*, *Manilkara elata*) reaching depths below 8 meters in the soil (Brum et al. 2019), indicating that differences in rooting depth are strongly related to tree size. Maximum rooting depths are found in deserts and tropical grasslands and savannas (Canadell et al. 1996). On the Edwards Plateau of central Texas, United States, rooting depths of a range of species were determined using DNA sequence variation to identify roots from caves 5–65 m deep. At least six tree species in the system produce roots deeper than 5 m, but only the evergreen oak, *Quercus fusiformis*, occurs below 10 m. The maximum rooting depth for the ecosystem is approximately 25 m (Jackson et al. 1999). In the Kalahari Desert, well drillers must bore to great depths in very dry sand to reach water, and drillers reported some of the deepest roots thus far recorded in the world at 68 m (McElrone et al. 2013). A potential mechanism that would facilitate this growth in very dry sand is through hydraulic redistribution (Sect. 5.5.2; Schulze et al. 1998). Even evergreen tropical forests may rely on deep rooting to supply water for their high transpiration demands. Fine roots occur to depths of about 18 m in eastern Amazonian forests, and about half of these forests are estimated to rely on water absorbed from deep soil (below 8 m depth) to maintain transpiration during the dry season (Nepstad et al. 1994).

A global synthesis of 2200 root observations and inverse hydrological modeling suggest water table depth as a key determinant of vegetation rooting depth (Fig. 5.5; Fan et al. 2017). Shallow-rooted vegetation is expected in waterlogged lowland areas to minimize hypoxia conditions below the water table, while rooting depth in uplands should follow infiltration depth. In slopes, seasonal drought should favor roots to grow deeper and reach the groundwater capillary fringe (Fig. 5.6).

The root-trench method, in combination with measurements of volumetric soil water content (Fig. 5.4), is a laborious and expensive method to obtain information on where most of the water comes from that a tree transpires. If the **isotope**

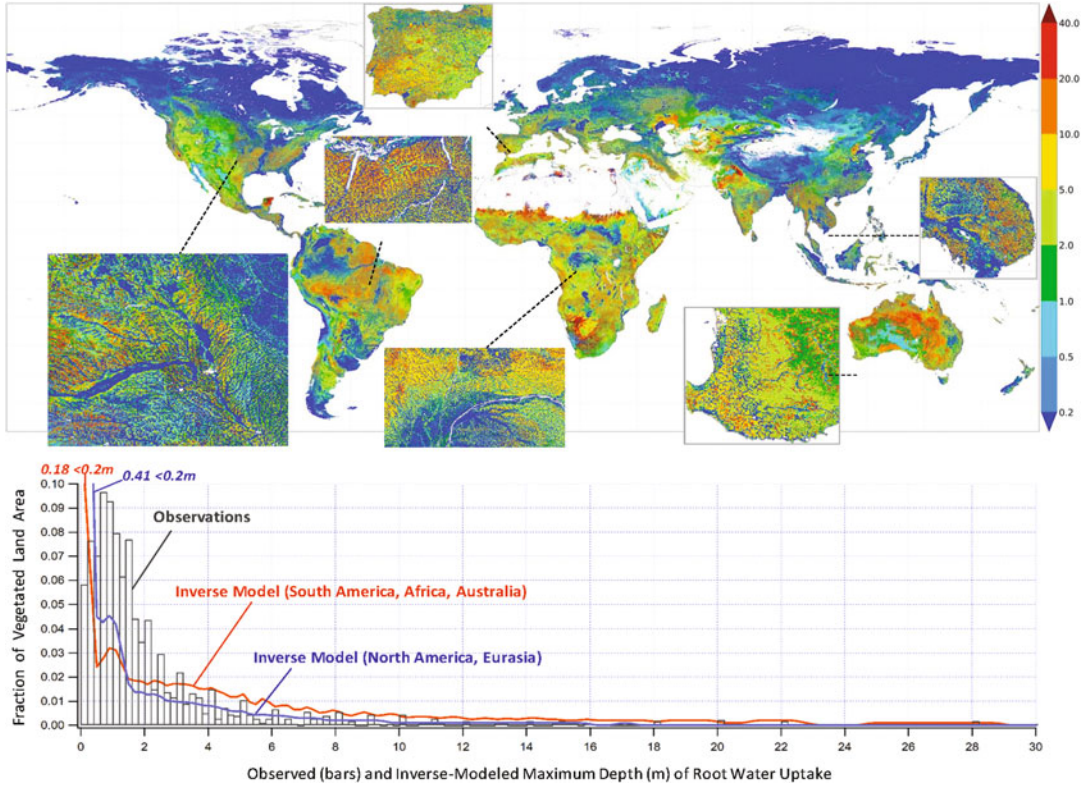

Fig. 5.5 (Upper) Results of an inverse-model of 10-year mean maximum rooting depth (in meters) of root water uptake. Insets in the map reveal strong local topographic influence. (Lower) The frequency distribution over vegetated surface only suggests large model-observation discrepancy, which may imply observation bias (undersampling of very shallow and very deep roots). The oscillations in the model distribution are due to soil water uptake crossing discreet soil layers. Fan Y, Miguez-Macho G, Jobbágy EG, Jackson RB, Otero-Casal C. 2017. Hydrologic regulation of plant rooting depth. Proc Natl Acad Sci USA **114**: 10572–10577.

signature of water differs among soil layers, then this value can be used to obtain information on which soil layers and associated roots provide the water that is transpired (Box 5.3). This technique has shown that perennial groundwater sources can be important (Thorburn and Ehleringer 1995; Boutton et al. 1999). For example, in a Utah desert scrub community, most plants use a water source derived from winter storm recharge for their early spring growth (Ehleringer et al. 1991). As this water source is depleted, however, only the deep-rooted woody perennials continue to tap this source, and more shallow-rooted species such as annuals, herbaceous perennials, and succulent perennials depend on summer rains (Fig. 5.7). Plants that have an isotopic composition of their xylem water that is representative of deep water are less water-stressed, less embolism resistant (Brum et al. 2019), have less negative leaf turgor loss point (Brum et al. 2017), faster transpiration rates and lower **water-use efficiency** (Sect. 5.6) than do species with a shallow-water isotopic signature.

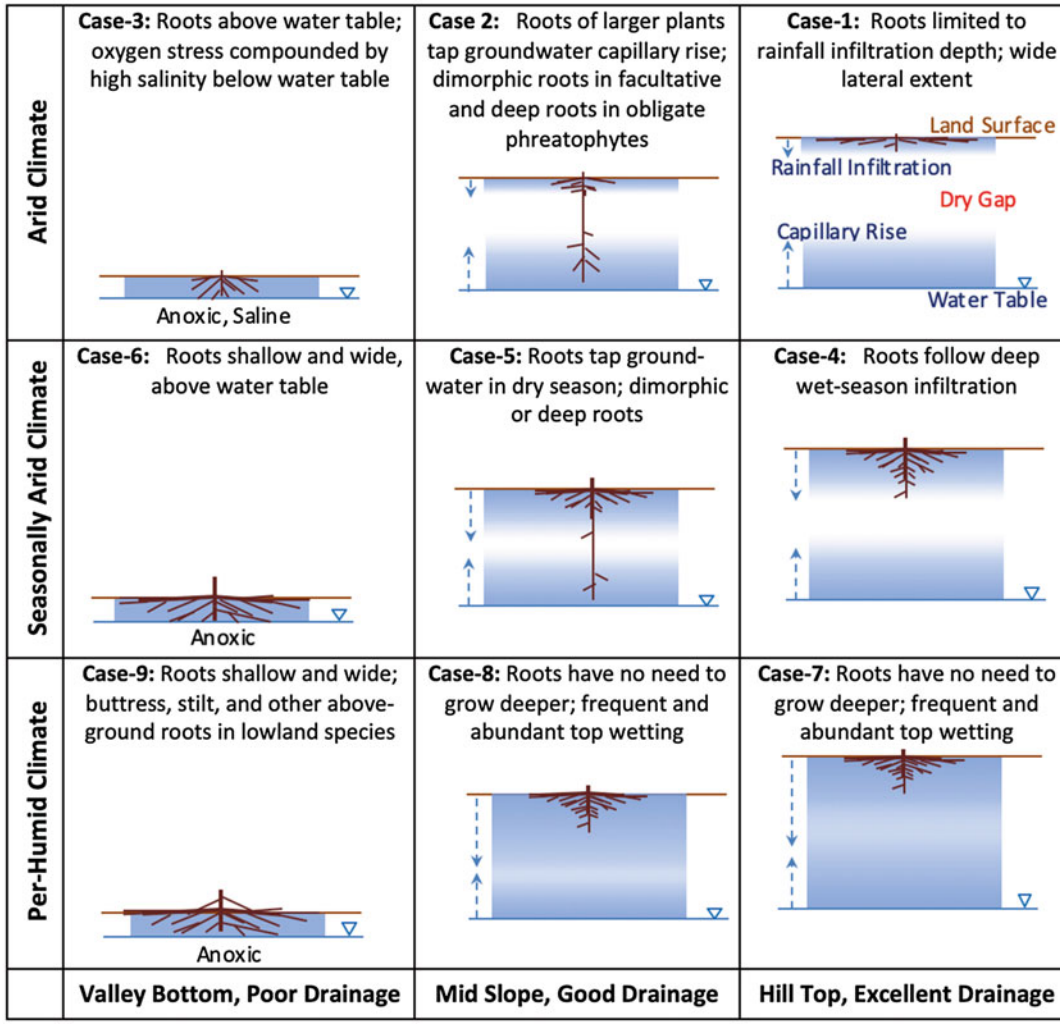

Fig. 5.6 A hydrologic framework for interpreting plant rooting depth along the climate gradient (vertical axis) defining regional patterns in infiltration depth and frequency, and the land drainage gradient (horizontal axis) defining local patterns in groundwater accessibility and oxygen stress. Fan Y, Miguez-Macho G, Jobbágy EG, Jackson RB, Otero-Casal C. 2017. Hydrologic regulation of plant rooting depth. Proc Natl Acad Sci USA **114**: 10572–10577.

Box 5.3: Oxygen and Hydrogen Stable Isotopes

Small fractions of the elements H and O occur as their heavy stable isotopes ^{2}H (also called deuterium; D) and ^{18}O (0.156 and 1.2‰, respectively). Their abundances in water (and CO_2) in the immediate environment of the plant, and in water, metabolites, and macromolecules in the plant itself vary as a result of fractionation processes operating in these two compartments. Isotopic composition, which can be measured with high precision, provides information about environmental and physiological parameters that is otherwise difficult to obtain. Isotopes in xylem water, for

(continued)

Box 5.3 (continued)

instance, can yield information on the source of water tapped by a plant, and isotopes in leaf water are influenced by stomatal conductance and humidity. Isotopes in plant dry matter can give a time-integrated and time-resolved historical record of environmental and physiological processes, as in tree rings (Dawson et al. 2002). A problem, however, with interpreting isotopic composition of plant dry matter or of specific compounds (*e.g.*, cellulose) in field studies is that it is simultaneously influenced by many factors. Models have been developed to resolve these problems as much as possible (Farquhar et al. 1998; Roden et al. 2000; Gessler et al. 2007).

Isotopes are measured as atomic ratios (R = rare isotope/common isotope) using mass spectrometers and are expressed relative to a standard (Standard Mean Ocean Water; SMOW; see also Boxes 2.2 and 3.1):

$$\delta^2\mathrm{H} \text{ or } \delta^{18}\mathrm{O}\ (‰) = \left(R_{\mathrm{sample}}/R_{\mathrm{standard}} - 1\right) \times 1000 \quad (5.14)$$

The δ^2H and δ^{18}O of precipitation water and other water bodies that are regularly involved in the global water cycle (meteoric waters) vary as a result of fractionation during evaporation and condensation in a temperature-dependent manner. Tropical regions are characterized by δ-values close to ocean water, and these values decrease toward the poles, particularly in winter. Values depleted in the heavy isotopes are also found at higher altitudes and further inland on continents. Fractionation processes in meteoric water operates similarly for ^{2}H and ^{18}O, and the δ-values are linearly related. This is known as the global meteoric water line [$\delta^{18}\mathrm{O} = (\delta^2\mathrm{H} - 10)/8$]. Fractionation processes in more closed compartments result in deviations from this line.

Soil moisture in surface layers is typically enriched in the heavier isotopes as a result of evaporation (Box Fig. 5.2). Different isotopic compositions of precipitation events can further add to a profile of δ^2H and δ^{18}O in the soil (Midwood et al. 1998). Since fractionation does not normally occur during uptake of water, the δ-value of xylem water may contain information about the depth of water uptake or source of water (*e.g.*, ground or stream water). Once in the leaf, the water is isotopically enriched as a result of transpiration. The ultimate δ^2H and δ^{18}O of leaf water is influenced by stomatal and boundary layer conductances, vapor pressure difference, transpiration rate and the δ-values of water vapor around the leaf.

The H in photoassimilates stems from water and carries its isotopic composition during assimilation. That is also the case with O, although in an indirect manner. Assimilated O is derived from CO_2, but its O is exchanged with H_2O in the reaction $CO_2 \leftrightarrow HCO_3^-$ catalyzed by carbonic anhydrase. Assimilates thus carry the isotopic signal of leaf water. During CO_2 assimilation, substantial fractionation occurs for ^{2}H (−117‰), whereas fractionation during further metabolism works in the opposite direction (+158‰). There is also isotopic enrichment of ^{18}O during assimilation and metabolism (+27‰). However, the environmental effect on these fractionation processes is limited. During synthesis of macromolecules from assimilates exchange of H and O with water occurs (Box Fig. 5.2). This applies only for part of the atoms. The fraction of exchange during cellulose synthesis in tree rings was estimated at 0.36 for H and 0.42 for O (Roden et al. 2000). Intramolecular positions have different degrees of exchange (Sternberg et al. 2006) which can be used for specific purposes.

The above qualitatively described reactions have been formalized in quantitative models that give good predictions of measured values. When information is available about sufficient environmental variables, unknowns can be calculated on the basis of δ-values.

(continued)

Box 5.3 (continued)

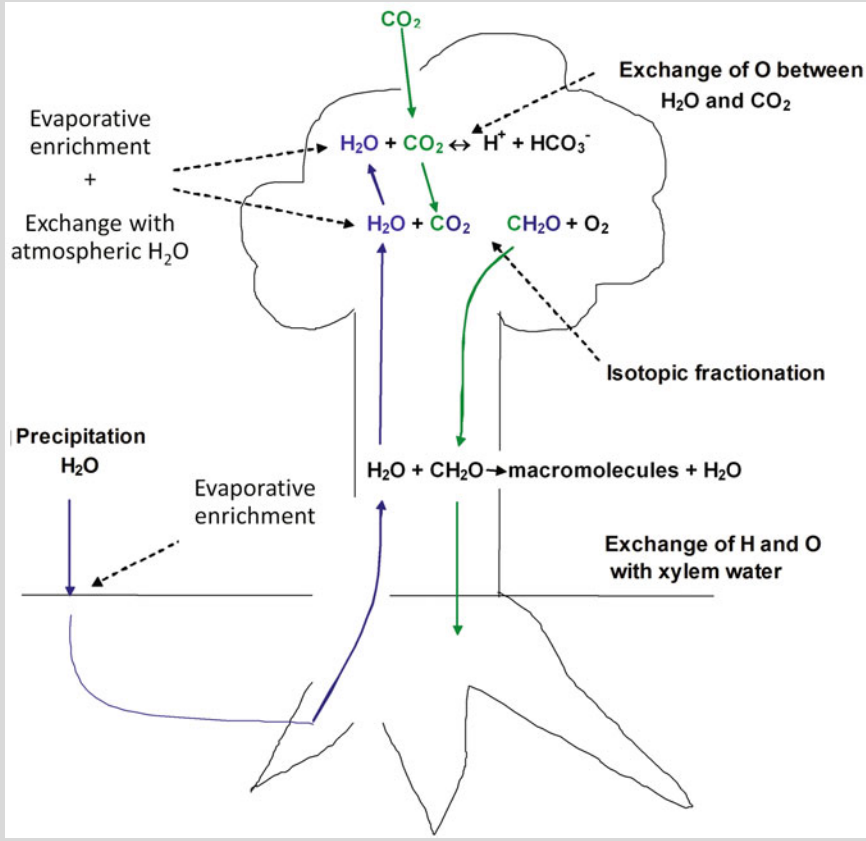

Box Fig. 5.2 Isotopic fractionation and exchange processes of H and O in a tree and its environment.

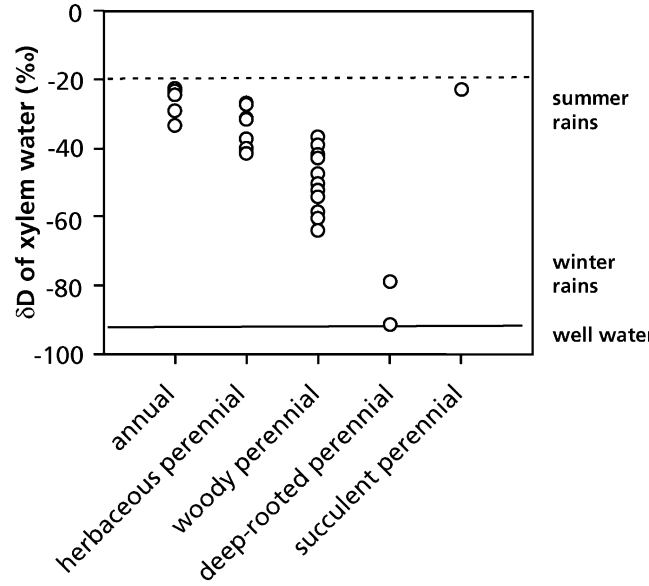

Fig. 5.7 Hydrogen isotope ratios (δD) of xylem water during the summer from plants of different growth forms in a Utah desert scrub community. The mean winter precipitation δD was −88‰, whereas summer precipitation δD ranged from −22% to −80% (Ehleringer et al. 1991). Copyright Springer-Nature.

5.3.4 Roots Sense Moisture Gradients and Grow Toward Moist Patches

As with so many other fascinating phenomena in plants, Darwin (1880) already noticed that roots have the amazing ability to grow away from dry sites and toward wetter pockets in the soil: they are **hydrotropic**. Positive hydrotropism occurs due to inhibition of root cell elongation at the humid side of the root. The elongation at the dry side is either unaffected or slightly stimulated, resulting in a curvature of the root and growth toward a moist patch. The root cap is the site of **hydrosensing**, but the exact mechanism of **hydrotropism** is not known (Cassab et al. 2013). It involves an increase in cell-wall extensibility of the root cells that face the dry side (Sect. 10.2.2). The hydrotropic response is stronger in roots of *Zea mays* (corn), which is a species that tolerates relatively dry soils, than it is in those of *Pisum sativum* (pea), and it shows a strong interaction with the root's gravitropic response (Fig. 5.8).

5.4 Water Relations of Cells

There are major constraints that limit the mechanisms by which plants can adjust cellular water potential. Adjustment of the water potential must come through variation in hydrostatic pressure or osmotic potential. Live cells must maintain a positive hydrostatic pressure (*i.e.* remain turgid) to be physiologically active; in most plants, osmotic potential of the cell or apoplast is the only component that live cells can adjust to modify water potential within hours (Korolev et al. 2000). In the long term, plants can also adjust by changing the elasticity of their cell walls (Wu and Cosgrove 2000). In contrast with living cells, dead xylem cells have very dilute solutes, so their water potential can change only through changes in hydrostatic pressure.

Within a tissue, the water relations of individual cells may differ widely. This accounts for phenomena such as stomatal opening and closure (Sect. 5.5.4.2), leaf rolling and movements (Sect. 5.6.2), and **tissue tension**. Tissue tension plays a role in herbaceous stems (*e.g.*, of Asteraceae), where the

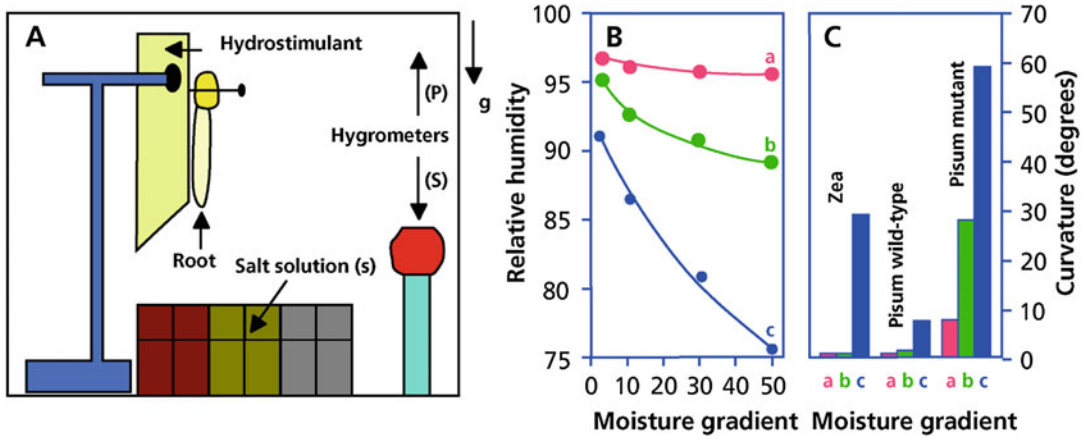

Fig. 5.8 Hydrotropism in roots of *Zea mays* (corn) and of the wild-type and the ageotropic mutant (*ageotropum*) of *Pisum sativum* (pea). (**A**) Diagram showing the humidity-controlled chamber. Roots were placed 2 to 3 mm from the 'hydrostimulant' (wet cheesecloth). Saturated solutions of salts create the humidity gradient. Different salts (KCl, K_2CO_3) give different gradients. The relative humidity and temperature was measured with a thermohygrometer (P). A stationary hygrometer (S) measured the relative humidity in the chamber. The arrow and letter g indicate the direction of gravitational force. (**B**) Moisture gradients, between 0 and 50 mm from the hydrostimulant, created by using no salt (*a*), KCl (*b*), or K_2CO_3 (*c*). (**C**) Root curvature 10 h after the beginning of hydrostimulation by the three moisture gradients shown in (**B**) (after Takahashi and Scott 1993).

outer layers of the stem tissue are held in a state of longitudinal tension by more internal tissues that are held in a reciprocal state of compression (Niklas and Paolillo 1998). We can readily demonstrate this by cutting a stem of *Apium graveolens* (celery) parallel to its axis. Upon cutting, the stem halves curl outwards, illustrating that the inner cells were restrained by outer cells and unable to reach their fully expanded size before the cut. Tissue tension plays a major role in the closing mechanism of the carnivorous plant *Dionaea muscipula* (Venus' flytrap) (Sect. 17.3.1).

5.4.1 Osmotic Adjustment

As the soil dries, causing soil water potential to decline, live cells may adjust their water potential by accumulating osmotically active compounds which reduces the osmotic potential (ψ_π), and, therefore, their water potential (ψ_w). Because of an increased concentration of osmotic solutes, cells have a higher turgor (ψ_p) when fully hydrated, provided the cell walls maintain their original rigidity (Sects 5.4.2 and 5.4.3). In addition, they lose their turgor at a more negative water potential compared with the turgor-loss point of nonacclimated plants (Munns and Gilliham 2015), thereby enabling the plant to continue to acquire water from soil at low soil water potentials. The osmotic solutes in the vacuole, which constitutes most of the volume of the plant cell, are often inorganic ions and organic acids. Such compounds reduce the activity of cytoplasmic enzymes, and plants tend to synthesize other **compatible solutes** in the cytoplasm (*i.e.* solutes that do not have a negative effect on cell metabolism). Such compatible solutes include glycinebetaine, sorbitol, and proline. These compounds are not highly charged, and they are polar, highly soluble, and have a larger hydration shell (the layer of water molecules surrounding each molecule) than denaturing molecules, like NaCl. Compatible solutes do not interfere with the activity of enzymes at a concentration where NaCl strongly inhibits them. Some compatible solutes (*e.g.*, sorbitol, mannitol, and proline) are effective as hydroxyl radical scavengers *in vitro*, but this is not the case for glycinebetaine (Smirnoff and Cumbes 1989). A role as radical scavenger *in vivo* has been established for mannitol, using transgenic *Nicotiana tabaccum* (tobacco) plants that accumulate mannitol in their chloroplasts (Shen et al. 1997). Polyols likely have dual functions: facilitating osmotic adjustment and supporting redox control (Slama et al. 2015).

5.4.2 Cell-Wall Elasticity

When cells lose water, they decrease in volume until the turgor is completely lost. The extent to which the cells can decrease in volume and hence the extent to which their water potential can decrease until the turgor-loss point is reached depends on the **elasticity** of their cell walls. Cells with highly elastic walls contain more water at full turgor; hence, their volume can decrease more before the turgor-loss point is reached. The elasticity of the cell walls depends on chemical interactions between the various cell-wall components. Cells with elastic walls can therefore store water that they accumulate during the night and gradually lose again during the day due to the leaf's transpiration. In this way they can afford to lose more water temporarily than is imported from the root environment.

A greater elasticity of cell walls is expressed as a smaller **elastic modulus,** ε (MPa), which describes the amount by which a small change in volume (ΔV, m^3) brings about a change in turgor, $\Delta\psi_p$ (MPa) at a certain initial cell volume:

$$\Delta\psi_p = \varepsilon\, \Delta V/V, \text{or}\, \varepsilon = d\psi_p/dV.V \qquad (5.15)$$

The **bulk elastic modulus** (ε) can be derived from **Höfler diagrams** (Fig. 5.9); they refer to an entire leaf, rather than individual cells. More commonly, ε is calculated from plots of $-1/\Psi$ *versus* the relative water content (Schulte and Hinckley 1985). [Relative water content (RWC) is defined as the water content of the tissue, relative to that at full hydration.] At full turgor (RWC = 100%), the change in turgor for a change in volume is much greater for *Laurus nobilis* (sweet bay) than for

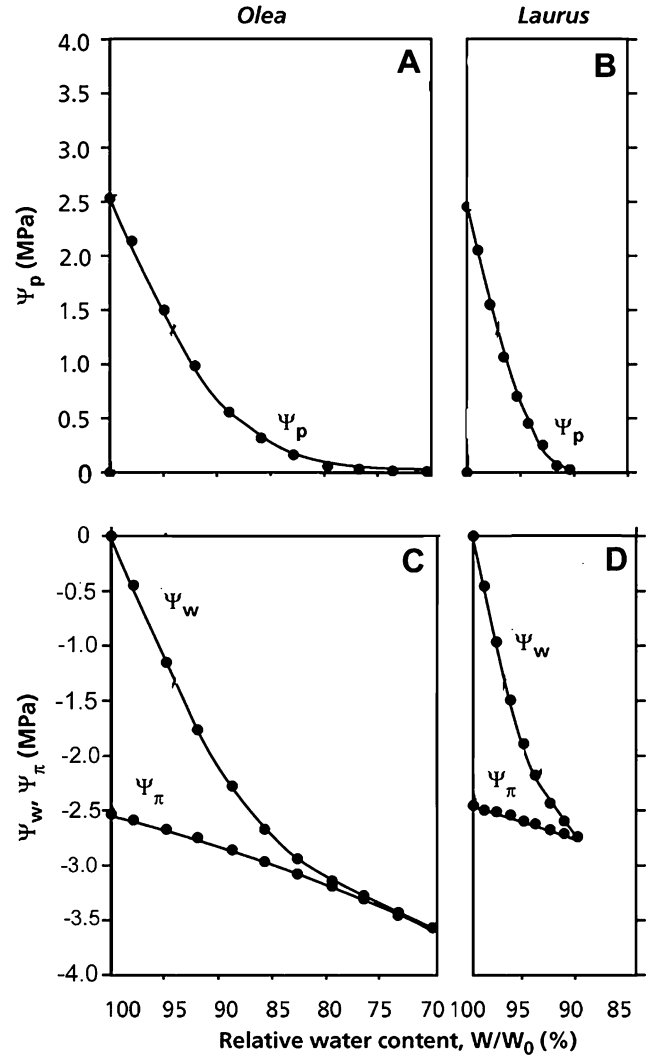

Fig. 5.9 Höfler diagrams, relating turgor pressure (Ψ_p), osmotic potential (Ψ_π), and water potential (Ψ_w), to relative water content for leaves of two Mediterranean tree species. (**A, C**) *Olea oleaster* (olive) and (**B, D**) *Laurus nobilis* (laurel). The bulk elastic modulus, ε, is the initial slope of Ψ_p with relative water content (Lo Gullo and Salleo 1988). Copyright Trustees of The New Phytologist.

Table 5.4 The elastic modulus of 1-year old leaves of three Mediterranean evergreen, sclerophyllous trees, growing in the same Mediterranean environment, but at locations differing in water availability*.

	Elastic modulus, ε at full turgor (MPa)	
Species	Wet season	Dry season
Olea oleaster	19.5	19.3
Ceratonia siliqua	20.5	24.5
Laurus nobilis	28.1	40.7

Source: Lo Gullo and Salleo (1988)

**Olea oleaster* (olive) is the most desiccation-tolerant, followed by *Ceratonia siliqua* (carob); *Laurus nobilis* (laurel) grows at somewhat wetter locations, near river banks. The elastic modulus was determined at full turgor, in both May (wet season) and September (dry season). Additional information about these trees is included in Figs 5.9 and 5.29

Olea oleaster (olive) (*i.e.* ε is greater for *Laurus nobilis*) (Table 5.4). The greater elasticity of the leaf cell walls of *Olea oleaster* from drier sites, in comparison with species from moister sites, implies that its cells can lose more water before they reach the **turgor-loss point** (Table 5.4); they

have cells that can shrink more during periods of water shortage without damage to the cytoplasm. In other words, they have a greater capacity to store water. A meta-analysis of 317 species shows that turgor-loss point strongly correlates with water availability in the species' habitat (Fig. 5.10; Bartlett et al. 2012). Species differences in turgor-loss point are mostly driven

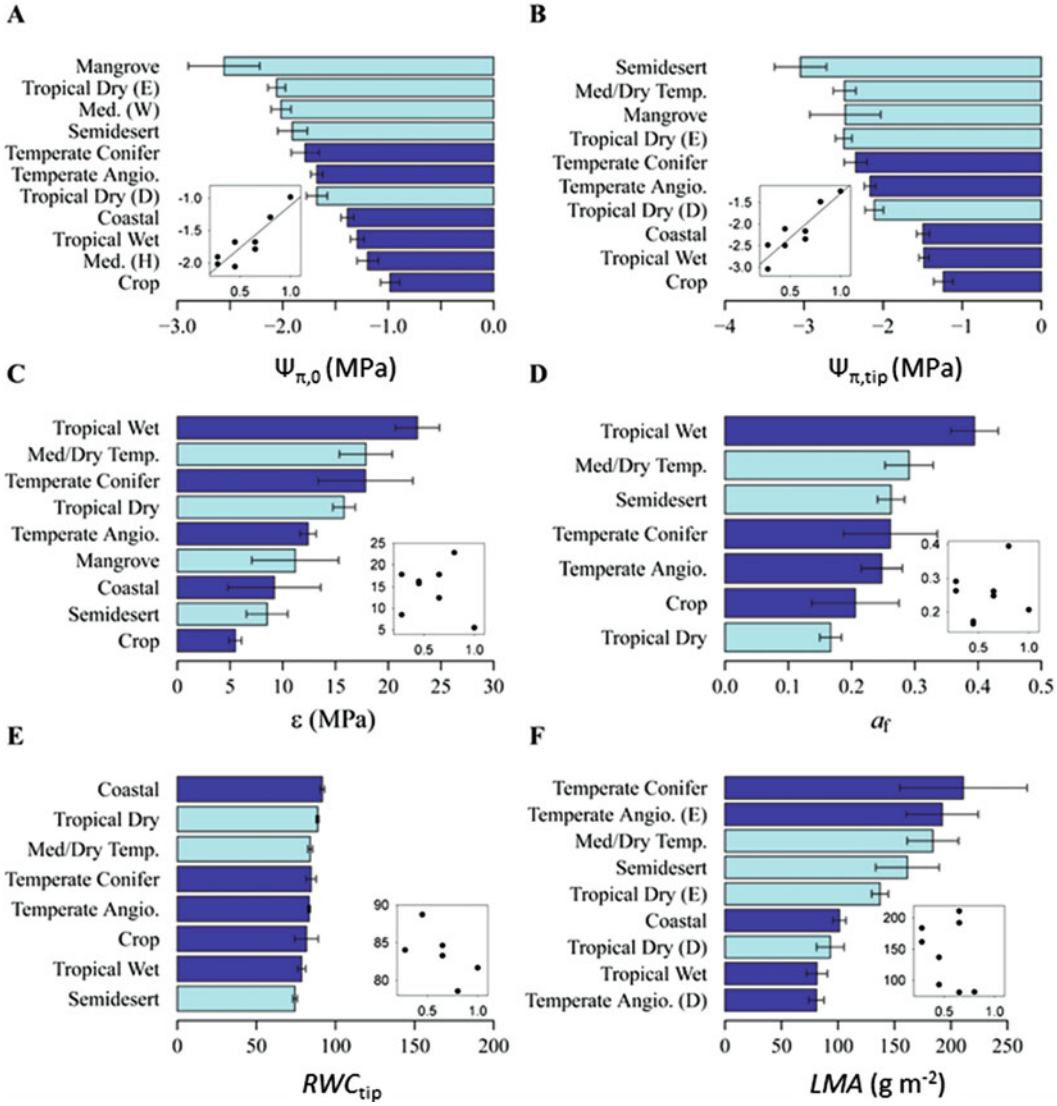

Fig. 5.10 Global data for pressure-volume parameters and leaf mass per area (*LMA*), with mean ± standard error across biome categories, with inset plots of biome category means against the Priestley-Taylor coefficient of annual moisture availability. Biome categories: semi-desert, Mediterranean-type vegetation/ dry temperate woodland, tropical dry and wet forest, temperate forest angiosperm and conifer, coastal vegetation, mangrove and crop herb. (**A**) Osmotic potential at full rehydration; (**B**) turgor loss point; (**C**) modulus of elasticity; (**D**) apoplastic water fraction; (**E**) relative water content at turgor loss point; (**F**) relative water content. Data within biomes were separated into herb (H) vs woody (W), or evergreen (E) vs. deciduous (D) when significantly different. Only $\Psi_{\pi,0}$ and $\Psi_{\pi,tip}$ showed separation of moist and dry biomes (light and dark blue bars respectively), and correlated with Priestley-Taylor coefficient of annual moisture availability across biomes (Bartlett et al. 2012). Reprinted with permission from John Wiley & Sons, Inc.).

by differences in osmotic potential at full turgor, rather than by the bulk elastic module.

The elastic modulus can also be determined for individual cells, by using a **pressure probe** (Tomos and Leigh 1999). It involves the insertion in a cell of a small glass microcapillary. The turgor pressure will then push the fluid back into the capillary. The force to push back the meniscus of the fluid to its position before insertion is then measured, using a sensitive pressure transducer. In this way, we can be measure the pressure in individual cells such as stomatal guard cells very accurately (Sect. 5.5.4.2).

5.4.3 Osmotic and Elastic Adjustment as Alternative Strategies

Osmotic and **elastic adjustment** are alternative strategies for a species to acclimate to water stress. Osmotic adjustment and simultaneous increases in elasticity are not an option, because accumulation of solutes would cause cells to swell, and not lead to the same decrease in water potential (Ngugi et al. 2003; Mitchell et al. 2008; Fig. 5.11). An increase in elasticity (a lower elastic modulus) thus contributes to turgor maintenance in much the same way as a decrease in osmotic potential (greater osmotic adjustment).

In nonadapted species, leaves lose turgor ($\psi_p = 0$) at higher relative water content and higher leaf water potential (Fig. 5.9). The protoplasm of the leaf cells of species from arid environments [*e.g.*, *Olea oleaster* (olive), *Eucalyptus wandoo* (wandoo)] must have the capacity to tolerate more negative water potentials to survive the greater loss of water from their cells with more elastic cell walls (Lo Gullo and Salleo 1988; Mitchell et al. 2008).

Comparing hemiepiphytic *Ficus* (fig) species, which start their life as epiphyte and subsequently establish root connections with the ground, leaf cells have a less negative osmotic potential at full turgor (less osmotic adjustment) and lower bulk elastic modulus (more elastic cells) in the epiphytic stage than they do as terrestrial trees. Lower osmotic potentials (in the tree stage) should allow leaves to withstand greater evaporative demand without wilting, in order to mobilize water from deeper and/or drier soil layers. This strategy, however, requires that there be some substrate moisture in the first place. Given the substrate of the epiphyte which dries rapidly, frequently, and uniformly, a more favorable strategy is to gather water from the aerial rooting medium when it is readily available for storage in highly elastic leaf cells (Holbrook and Putz 1996). In the semiarid woodlands of Central

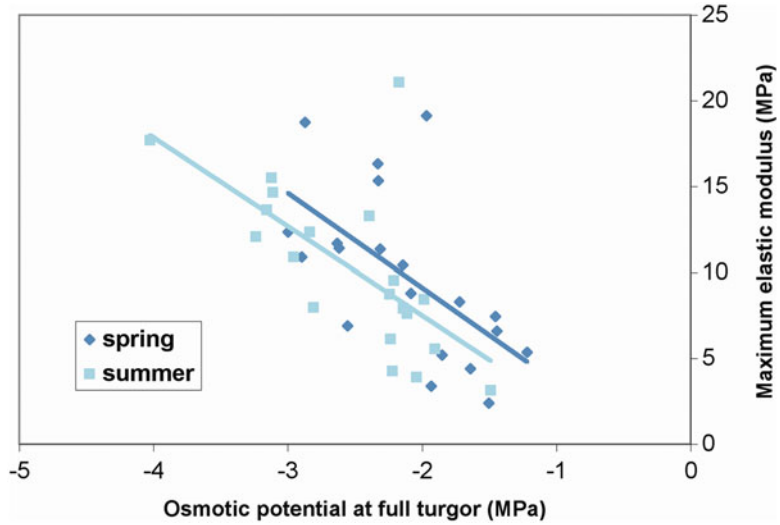

Fig. 5.11 Osmotic potential at full turgor ($\Psi_{\pi 100}$, MPa) *versus* maximum bulk tissue elasticity (ε_{max}, MPa) for spring and summer for 20 species in their natural habitat, in the southwest of Australia, which is characterized by a Mediterranean climate (after Mitchell et al. 2008). (Reprinted with permission from John Wiley & Sons, Inc.).

Texas, United States, species that experience wider fluctuations in leaf water potential have greater plasticity in the leaf hydraulic properties, and adjust their leaf turgor-loss points in response to drying soils in summer, and to wet conditions in winter (Johnson et al. 2018). Leaves of tropical rainforest trees also adjust their hydraulic properties in response to long-term experimental through-fall exclusion in the Amazon (Binks et al. 2016).

5.4.4 Evolutionary Aspects

The capacity to adjust the concentration of **osmotic solutes** and the **elasticity** of the leaves' cell walls are both under genetic control. There is a wide range of species of the genus *Dubautia* (Asteraceae), some of which are restricted to dry habitats and others to moister sites. They are, therefore, ideally suited to an analysis of the survival value of specific traits related to plant water relations. Individuals of the species *Dubautia scabra*, which is restricted to a relatively moist 1935 lava flow in Hawaii, have less negative water potentials, lower turgor, and a higher elastic modulus (less elastic cells) than those of *Dubautia ciliolata*, which is restricted to an older drier lava flow (Robichaux 1984). These differences in tissue elastic properties have a marked influence on diurnal turgor maintenance. Diurnal water potentials of *Dubautia ciliolata* from drier sites are more negative than those of *Dubautia scabra*, but the turgor pressures are very similar throughout the entire day. Cell-wall elasticity obviously allows maintenance of turgor without a major adjustment in osmotic potential. Although these leaf-level hydraulic traits influence species ability to tolerate drought, they have low predictive value of drought-induced cross-species mortality risk in a global meta-analysis (Anderegg et al. 2016).

Fructan accumulation confers stress tolerance (Van den Ende 2013). Some prominent fructan-accumulating families include Poaceae [*Triticum aestivum* (wheat), *Hordeum vulgare* (barley)], Liliaceae [*Allium cepa* (onion)], and Asteraceae [(several species from the Brazilian cerrado; Appezzato-da-Glória et al. 2008), *Cichorium intybus* (chicory)]. Fructan-accumulating taxa increased some 30 to 15 million years ago, when the climate shifted toward seasonal droughts. The distribution of present-day fructan-accumulating species corresponds with regions of seasonal droughts. The appearance of the genes coding for fructan-synthesizing enzymes probably allowed the fructan flora to cope with seasonal droughts (Van den Ende 2013). The deduced amino acid sequence of key enzymes in the formation of fructans shows a high homology with plant **invertases**, which are ubiquitous enzymes that hydrolyze sucrose, producing glucose and fructose. Therefore, the genes in fructan-producing taxa may have emerged because of duplication of the invertase gene, followed by slight modification.

5.5 Water Movement Through Plants

5.5.1 The Soil-Plant-Atmosphere Continuum

Water transport from the soil, through the plant, to the atmosphere, takes place in a soil-plant-air continuum that is interconnected by a continuous film of liquid water (Fig. 5.12). Water moves through the plant along a **gradient**, from high to low **water potential** (if transport occurs across a selectively permeable membrane). Alternatively, it may flow from high to low **hydrostatic pressure** (if no such membrane is involved, as in the transport from source to sink in the phloem; Sect. 4.3). It may also move from a high to a low **water vapor concentration** (but that concentration can be expressed in terms of water potential; Box 5.1). The low concentration of water vapor in the air, compared with that inside the leaves, is the major driving force for water loss from leaves. This, in turn, drives water transport along the gradient in hydrostatic pressure between the xylem in roots and leaves, and down a gradient in water potential between the soil and the cells in the roots (Fig. 5.12). As soils dry out, there are parallel decreases in soil water potential and plant

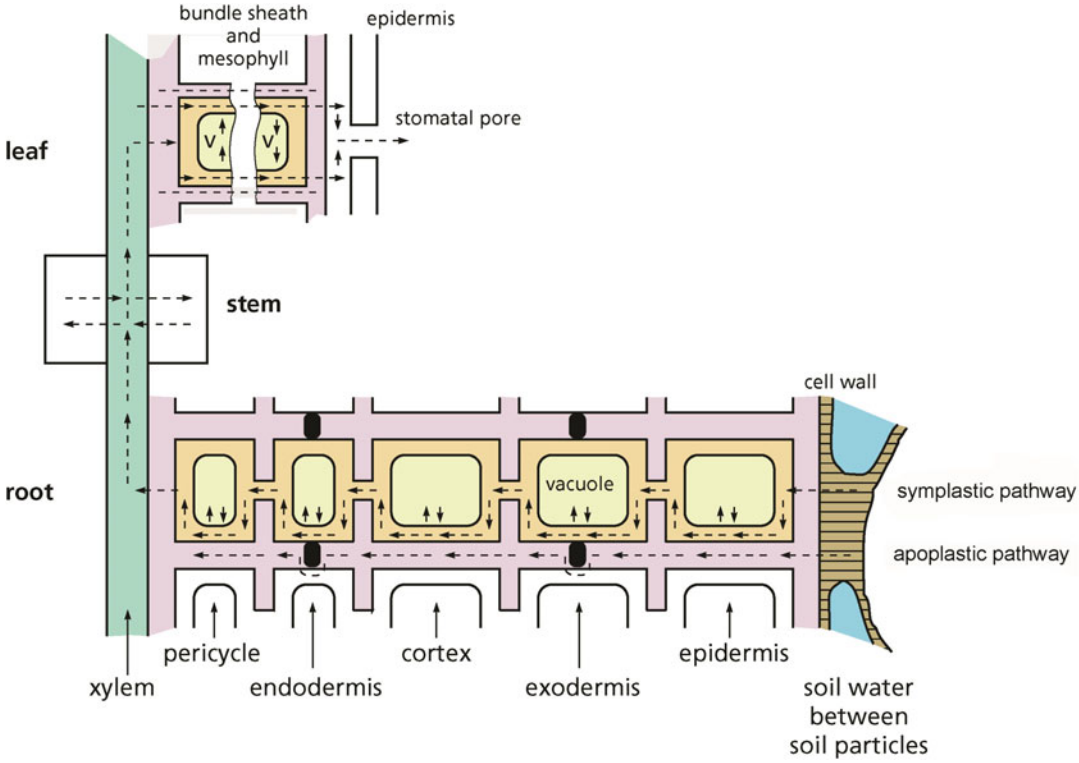

Fig. 5.12 Water transport in the soil-plant-air continuum. Water can move through the cell walls (apoplast), or cross the plasma membrane and move through the cytoplasm and plasmodesmata (symplast). Water cannot move through the suberized Casparian bands in the wall of all endodermal and exodermal cells, including passage cells. Note that the exodermis is absent in some species, in which case water can move from the soil through the apoplast as far as the endodermis.

water potential, both immediately before dawn (when water stress is minimal, and the water potentials of soil and plant are thought to be in equilibrium) and at midday (when water stress is maximal) (Fig. 5.13). The passive movement of water along a gradient differs strikingly from plant acquisition of carbon and nutrients which occurs through the expenditure of metabolic energy. The steepest gradient in the soil-plant-atmosphere continuum occurs at the leaf surface which indicates that the stomata are the major control point for plant water relations. There are substantial resistances to water movement in soil, roots, and stems, however, so short-term stomatal controls are constrained by supply from the soil and resistances to transfer through the plant. An appreciation of these controls that operate at different time scales is essential to a solid understanding of plant water relations.

Water flux, J ($mm^3\ s^{-1}$) (*i.e.* the rate of water movement) between two points in the soil-plant-atmosphere system, is determined by both the gradient between two points and the resistance to flow between these points. The **conductance**, L_p ($mm^3\ s^{-1}\ MPa^{-1}$) (*i.e.* the inverse of resistance), is often a more convenient property to measure. As pointed out earlier, the gradient along which water moves is *not* invariably a gradient in water potential ($\Delta\psi_w$, MPa). It may also be a gradient in hydrostatic pressure ($\Delta\psi_p$, MPa), or in water vapor concentration (Δw, the difference in mole or volume fraction of water vapor in air in the intercellular spaces and in air; Eq. 2.2). In the case of a gradient in water potential, we can write:

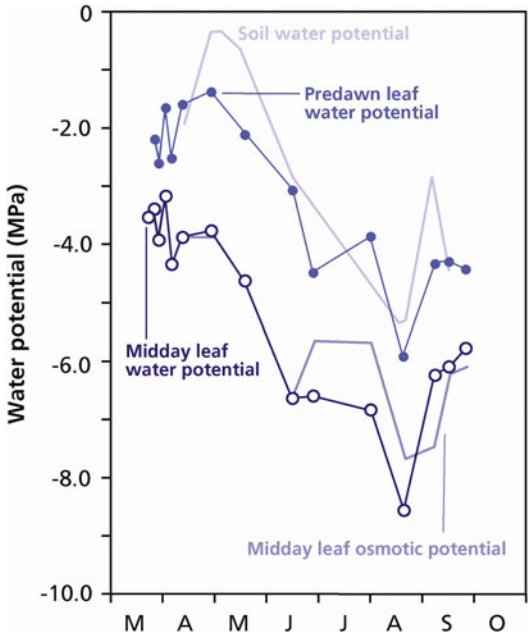

Fig. 5.13 Seasonal changes in soil water potential (dotted line), predawn leaf water potential, midday leaf water potential, and midday leaf osmotic potential (dashed line) in the C_4 plant *Hammada scoparia* (after Schulze 1991).

$$J = L_p \Delta \psi_w \tag{5.16}$$

During the day, the water potential of leaves often declines, when the conductance of the roots or stems is too low to supply sufficient water to the leaves to meet their transpirational water loss. This is not invariably found, however, because roots in drying soil send signals to the leaves which reduce the stomatal conductance and hence water loss (Sect. 5.5.4.1).

5.5.2 Water in Roots

When plants are growing in moist soils, cell membranes are the major resistance to water flow through the roots. Water travels along three pathways from the outside to the inside of the root. If there is no **exodermis** (an outermost layer of root cortical cells adjacent to the epidermis with suberin-coated cell walls; Fig. 5.14A), then water may move through the **apoplast** (*i.e.* the cell walls and other water-filled spaces outside of living cells). Or it may move through the **symplast** (*i.e.* the space comprising all the cells of a plant's tissues connected by plasmodesmata and surrounded by a plasma membrane) (Fig. 5.12), or through the cells by crossing the walls, cytoplasms, and vacuoles (and plasma membranes and tonoplasts). The latter is termed the **transcellular path** and, under normal conditions, is the main pathway used by water. Water must eventually enter the **symplast** at the **endodermis**, which is the innermost cortical layer of cells and has **Casparian bands**. The radial and transverse walls of the endodermal and exodermal cells are rich in cell-wall proteins, and impregnated with lignin, suberin, and wax (Ranathunge et al. 2011), which forms a **Casparian band** (Fig. 5.14A). These hydrophobic bands completely encircle each endodermal cell and prevent further transport of water through the apoplast. Even when the neighboring cortical and pericycle cells plasmolyze, the plasma membrane of the endodermal cells remains attached to the Casparian band. **Plasmodesmata**, which connect the endodermis with the central cortex and pericycle, remain intact and functional during the deposition of suberin lamellae. More importantly for the passage of water, the Casparian bands do not occur in the tangential walls of the endodermal cells, so water may pass through the plasma membranes lining these walls. **Passage cells** frequently occur in both the endodermis and the exodermis; in the endodermis, they are typically located in close proximity to the xylem (Fig. 5.14B). Passage cells have Casparian bands, but the suberin lamellae and thick cellulosic (often lignified) walls that characterize other endodermal and exodermal cells in some species are either absent or are formed at a much later stage of development. The passage cells become the only cells that present a plasma membrane surface to the soil solution once the epidermal and cortical cells die which occurs naturally in some herbaceous and woody species. Passage cells then provide areas of low resistance to water flow (Peterson and Enstone 1996) and play a major role in nutrient uptake (Andersen et al. 2018).

In most plants, water entry into the symplast must occur at the **exodermis**, which has cell

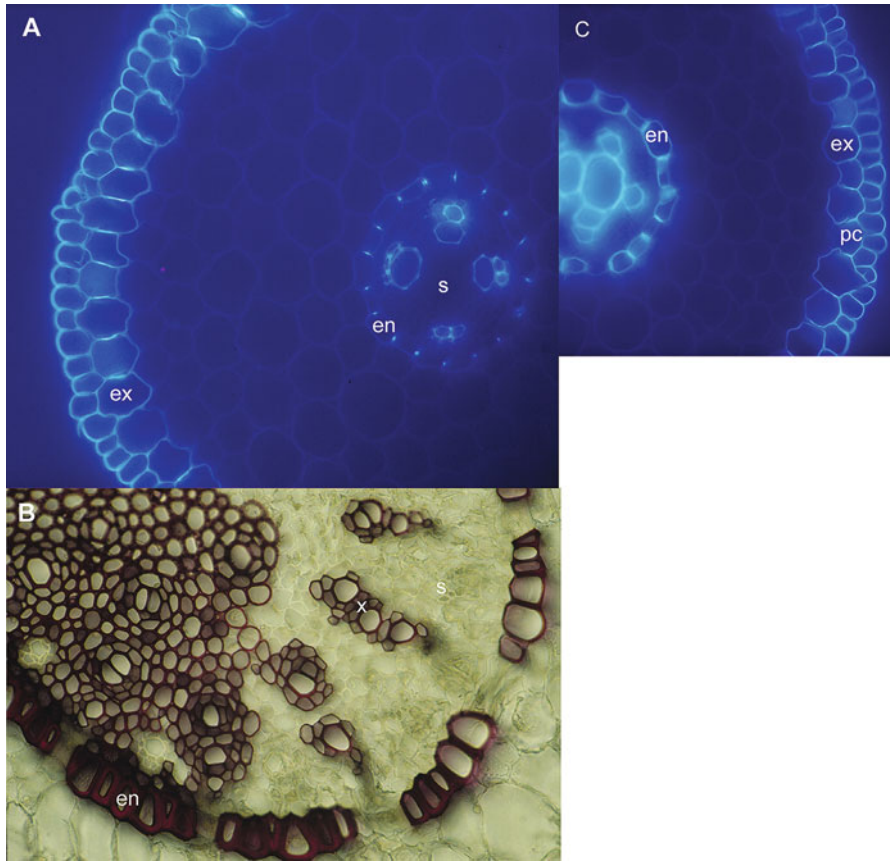

Fig. 5.14 (**A**) Transverse section of an adventitious root of *Allium cepa* (onion). The endodermis (en) and exodermis (ex) both have a Casparian band. The cells of the exodermis also have suberin lamellae. The section has been stained with berberine-aniline blue and viewed with UV light. (**B**) Cross-section of an orchid (*Phalenopsis* sp.) aerial root showing the endodermis (en), one passage cell (pc), and the xylem (x) within the stele (s). Except for the passage cells, the endodermal cells have thick, lignified, tertiary walls. Application of phloroglucinol-HCl has stained lignified walls red. (**C**) Cross-section of an onion root (*Allium cepa*), stained with berberine-aniline blue and viewed with UV light, to show the walls of the epidermis and exodermis. Note the passage cell (pc) in the exodermis; it lacks fluorescence on its inner tangential wall. (Courtesy D.E. Enstone, Biology Department, University of Waterloo, Canada).

properties similar to the endodermis. Only 9% of all investigated species have either no exodermis or have an exodermis without Casparian bands and suberin lamellae (Enstone et al. 2003). At the endodermis or exodermis, water must enter the cells, passing at least the plasma membrane, before it can arrive in the xylem tracheary elements (vessels or tracheids). Like other organisms, plants have a family of **water-channel proteins**, usually called '**aquaporins'**, which are inserted into membranes and allow passage of water in a single file. Water-channel proteins in the plasma membrane play a vital role in water uptake by plants by reducing the resistance to water flow along the transcellular path (Maurel et al. 2016). The number of water-channel proteins decreases during the night and starts to increase again just before dawn which suggests rapid turnover. Water-channel proteins are also 'gated', and affected by phosphorylation, cytosolic pH, Ca^{2+}, pressure, solute gradients, and temperature (Chaumont and Tyerman 2014).

Environmental factors that affect the roots' hydraulic conductance affect either the number or the status of the water channels.

At **low temperature**, when membrane lipids are less fluid and membrane proteins are somewhat immobilized, the resistance of the plasma membrane to water flow is high. Adaptation and acclimation to low temperature generally involves a shift to more unsaturated fatty acids which increases the fluidity of these membranes at low temperature. The resistance to water flow is also high in plants exposed to soil **flooding**, which results in a low oxygen concentration in the soil, followed by inhibition of the normal aerobic respiration and cytosol acidosis. This decreased pH reduces the activity of the water-channel proteins and hence the roots' hydraulic conductance (Sect. 10.5.6; Zhang and Tyerman 1999). An excess of water in the soil may, paradoxically, cause symptoms that also occur in water-stressed plants: wilting, accumulation of ABA, and stomatal closure (Sect. 10.5.6.2).

As the soil dries, roots and soils shrink which reduces the contact between roots and the soil water films, as well as the conductance of water flow into the root. In dry environments, the contact between roots and soil is the greatest resistance to water flux from soil to leaves. Plants increase root conductance primarily by increasing allocation to production of new roots. Root hairs may be important in that they maintain contact between roots and soil. We discuss the role of mycorrhizal associations in water transport in Sect. 12.2.7. A high root mass ratio (RMR, root mass as a fraction of total plant mass) is typical of any plant grown under dry conditions, and drought-adapted C_3 species typically have higher root mass ratios than do nonadapted C_3 species. Despite growing faster than C_3 species, C_4 plants allocate 54% more biomass to roots, with root mass ratios (Sect. 10.2.1.1) averaging 0.46 in C_4 and 0.29 in C_3 plants (Atkinson et al. 2016). When these adaptations and acclimations to low temperature or low water supply are combined in natural vegetation patterns, aboveground biomass declines dramatically along a gradient of increasing aridity, but root biomass often remains relatively constant (Table 5.5), as a result of an increased root mass ratio. Root:shoot ratio also increases significantly with decreases in annual precipitation in terrestrial biomes (Mokany et al. 2006).

In extremely dry soils, where the soil water potential is lower than that of plants, and roots can no longer extract water from soil, it may be advantageous to increase root resistance. For example, cacti shed fine roots in summer and so prevent water loss to soil. The Sonoran Desert plant *Agave deserti* quickly produces new roots (**rain roots**) within 24 h after a shower to exploit new sources of soil moisture (Nobel et al. 1990). Some plants have **contractile roots**. These decrease in length and increase in width, and so maintain hydraulic contact with the surrounding

Table 5.5 Above-ground and below-ground biomass and the root mass ratio in various forest ecosystems, partly grouped by climate, climatic forest type, and species*.

	Above-ground biomass g m^{-2}	Below-ground biomass g m^{-2}	Root mass ratio g g^{-1}
Boreal			
Broadleaf deciduous	50	25	0.32
Needle-leaf evergreen	30–140	7–33	0.20–0.30
Cold-temperate			
Broadleaf deciduous	175–220	25–50	0.13–0.19
Needle-leaf deciduous	170	40	0.18
Needle-leaf evergreen	210–550	50–110	0.14–0.28
Warm-temperate			
Broadleaf deciduous	140–200	40	0.21
Needle-leaf evergreen	60–230	30–35	0.15

Source: Vogt et al. (1995)
**RMR* ratio of root mass and total plant mass

soil. During root contraction in *Hyacinthus orientalis* (hyacinth), mature cortical cells increase in diameter while decreasing in length, suggesting a change in wall extensibility in one or more directions (Sect. 10.2.2; Pritchard 1994).

Many dominant woody species in arid, semi-arid or seasonally dry conditions have **dual** or **dimorphic root systems**. Shallow, superficial roots operate during the wet season, and the deep-penetrating part of the root, which is usually located in relatively unweathered bedrock or deep sands, operates during the dry season. Because most of the nutrients tend to be in the superficial soil layers, they will be taken up by shallow roots. Plants that grow on shallow soil or even bare rock in the Israeli maquis continue to transpire during the entire summer by growing roots in rock fissures. On such sites with shallow soil in semi-arid climate conditions, roots of some plants [*e.g.*, *Arctostaphyllos viscida* (whiteleaf manzanita) and *Arbutus menziesii* (Pacific madrone)] of the Pacific Northwest in the United States, can utilize water from the bedrock. Roots of such plants occupy rock fissures as small as 100 µm. The cortex of such roots may become flat, with wing-like structures on the sides of the stele (Zwieniecki and Newton 1995).

Water in the xylem vessels of the roots is normally under tension (negative hydrostatic pressure). At night under moist conditions and low transpiration, however, the hydrostatic pressure may become positive. A widely held view is that under these conditions the loading of solutes into the xylem is sufficiently rapid to produce a very negative osmotic potential in the xylem. Water may then move osmotically into the xylem vessels and create a positive hydrostatic pressure, forcing water up through the xylem into the stem (**root pressure**). However, measurements, using cryo-analytical microscopy *in situ*, have shown that solute concentrations in the xylem sap of primary roots of *Zea mays* (corn) are fairly low, also when the hydrostatic pressure in the xylem is high (Enns et al. 1998). This suggests that the simple explanation for root pressure outlined above might not be correct. As an alternative, a mechanism similar to the putative mechanism for stem pressure (Sect. 5.5.3.4) has been suggested (Wegner 2014).

Whatever the exact mechanism that accounts for root pressure is, it can push xylem sap out through the leaf tips of short-statured plants: **guttation**, which is a phenomenon that contributes to the formation of 'dew' on leaves. Root pressure is important in reestablishing continuous water columns in stems, after these columns break (Sect. 5.5.3.3). Using Eq. 5.7 in Box 5.1, we can calculate that xylem sap containing 10–100 mM solutes can be 'pushed' up the stem as high as 2.6–26 m. The liquid exuding from tree stumps and wounds in stems may also result from root pressure [*e.g.*, in *Vitis vinifera* (grapevine) and *Betula nigra* (river birch)]. The xylem sap exuded by palms and several maples [*e.g.*, *Acer saccharum* (sugar maple) and *Acer nigrum* (black sugar maple)] which is often tapped commercially to make sugar or syrup, results from stem pressure, and *not* from root pressure (Kramer 1969).

Hydraulic lift is the movement of water from deep moist soils to drier surface soils through the root system (Richards and Caldwell 1987). In C_3 and C_4 species, this occurs primarily at night, when stomata are closed, so that the plant is at equilibrium with root water potential. In the CAM plant *Yucca schidigera* in the Mojave Desert, however, hydraulic lift occurs during the day (Yoder and Nowak 1999). This agrees with maximum stomatal conductance at night in CAM plants (Sect. 2.10.2). Under these circumstances, water will move from deep moist soils with a high water potential into the root and out into dry surface soils of low water potential. Although hydraulic lift was first observed in dry grasslands, it also occurs during dry periods in temperate forests, when high leaf area and rapid transpiration rates deplete water from upper soil horizons. For example, adult sugar maples (*Acer saccharum*) derive all transpirational water from deep roots. Between 3% and 60% of water transpired by shallow-rooted species without direct access to deep water, however, comes from water that is hydraulically lifted by sugar maple (Dawson 1993). Deep groundwater often has a different isotopic signature than does surface water, making it possible to determine the original source of water transpired by plants (Sect. 5.3.3).

Because water in soil can be redistributed via the roots from moist regions in either deep or shallow soil layers, the term **hydraulic redistribution** is now widely used. Hydraulic redistribution can be measured using sap-flow sensors (Box 5.4). In large trees, this redistribution may also involve the stem, where, at night, water can flow upward in one sector of the stem, and downward in another (Burgess and Bleby 2006). This is due to the much greater axial conductance compared with the radial conductance for water movement in the stem.

Box 5.4: Methods to Measure Sap Flow in Intact Plants

Xylem sap-flow rates of whole plants, individual branches, or roots can be measured using a technique that uses heat as a tracer (Box Fig. 5.3). The stem, branch, or root is heated electrically, and the heat balance is solved for the amount of heat taken up by the moving sap stream which is then used to calculate the mass flow of sap in the stem. In the heat-pulse method, rather than using continuous heating, short pulses of heat are applied, and the mass flow of sap is determined from the velocity of the heat pulses moving along the stem. Alternatively, rates of sap flow can be determined from the temperature of sapwood near a continuously powered heater implanted in the stem (Smith and Allen 1996). Heat-based sap-flow techniques play a leading role in the study of transpiration and water relations of woody plants (*e.g.*, Wullschleger et al. 1998; Nadezhdina and Čermák 2003).

Two of the techniques currently available to researchers are the compensation heat-pulse method and the heat-ratio method. Both use the heat-pulse principle, where the mass flow of sap is determined from the velocity of a short pulse of heat moving along xylem tissue through conduction and convection. The heat-ratio method was developed recently by Burgess et al. (2001), whereas the compensation heat-pulse method has a long history. The theory of the compensation heat-pulse method is described in detail by Marshall (1958), Swanson and Whitfield (1981), and Smith and Allen (1996). Briefly, two temperature sensors are inserted to equal depths into the sapwood, and positioned above and below a similarly inserted line heater probe. The temperature probes are spaced asymmetrically from the heater such that the mid-point of the two probes is located at a fixed distance downstream (*i.e.* towards the crown) from the heater and all probes are in line with the axis of the

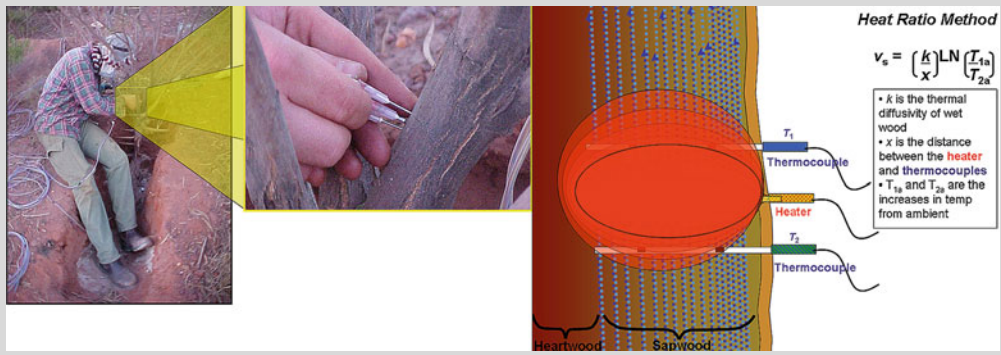

Box Fig. 5.3 Sap-flow measurements using the heat-ratio method require insertion of probes in a stem, root, or branch (left). The middle probe is a heater, the other ones are thermocouples. If sap moves upward, then the heat pulse will reach the upper thermocouple before it reaches the lower one. The equation given in the figure (right) is used to calculate flow rates. Courtesy A. Grigg, University of Western Australia, Crawley, Australia.

(continued)

Box 5.4 (continued)

plant stem. Following the release of a pulse of heat into the sap stream, heat moves toward the downstream temperature probe. Movement of the heat pulse to the mid-point between the temperature probes is indicated when both temperature sensors have warmed to the same degree. The time taken for the heat pulse to move this distance is used to calculate heat-pulse velocity:

$$v_h = \frac{x_d + x_u}{2t_0} 3600, \qquad (5.17)$$

where v_h is heat-pulse velocity (cm h^{-1}), t_0 is the time to thermal equilibrium of the downstream and upstream temperature of the downstream and upstream temperature sensors, x_d and x_u are the distances (cm) from the heater probe of the downstream and upstream temperature sensors, respectively. A negative value is assigned to x_u because it is located on the opposite side of the heater from x_d (Bleby et al. 2004).

The theory of the heat-ratio method is described in detail by Burgess et al. (2001). Briefly, temperature and heater probes are inserted into the sapwood in a similar manner to the compensation heat-pulse method, except that the heater probe is located at a point equidistant from the upstream and downstream temperature sensors (Box Fig. 5.3). Instead of a 'distance-traveled-over time' approach to measuring v_h, the heat-ratio method measures the ratio of the increase in temperature at points equidistant upstream and downstream from a line heater, following the release of a heat pulse. Heat-pulse velocity is calculated as (Marshall 1958):

$$v_h = \frac{k \ln (v_1/v_2)}{x} 3600, \qquad (5.18)$$

where k is thermal diffusivity of wet (fresh) wood, x is the distance from the heater probe of either temperature probe, and v_1 and v_2 are increases in temperature at equidistant points (x cm) downstream and upstream, respectively (in relation to initial temperatures). Thermal diffusivity (k) is assigned a nominal value during measurements and is resolved empirically at a later stage using estimates of thermal conductivity, density and specific heat capacity of fresh sapwood; variables are derived from simple measurements of the water content and density of sapwood (Bleby et al. 2004).

Heat-pulse methods can be used for accurate measurements of sap flow, provided a reliable calibration procedure is used to relate the measured heat-pulse velocity to the actual sap flow. Correction factors are based on comparisons of heat-pulse measurements against actual rates of transpiration determined from measured weight loss of the trees growing in large lysimeters. The compensation heat-pulse method accurately measures flows down to a few cm h^{-1} (Green et al. 2003), but this method is unable to measure low rates of sap flow, due to its inability to distinguish heat-pulse velocities below a threshold velocity of 0.1 kg h^{-1} (3–4 cm h^{-1}). On the other hand, the heat-ratio method accurately describes sap flow at night when rates of flow are low (< 0.1 kg h^{-1}) or near zero (Bleby et al. 2004).

Hydraulic redistribution occurs in Amazonian trees, and has a major impact on climate over the Amazon. Model results show that hydraulic redistribution enhances photosynthesis and evapotranspiration significantly during the dry season. The water subsidy from hydraulic redistribution sustains transpiration at rates that deep roots alone cannot accomplish. The water used for dry-season transpiration is from the deep storage layers in the soil, recharged during the previous wet season. Hydraulic redistribution in the Amazon may increase dry season transpiration by 40%. Such an increase in transpiration over drought-stressed regions affects the seasonal

cycles of temperature through changes in latent heat, thereby establishing a direct link between root functioning and climate (Lee et al. 2005).

Hydraulic redistribution can modify competitive interactions among plants in unexpected ways by resupplying water to shallow-rooted species during dry periods, thereby modifying both water supply and the conditions for nitrogen mineralization and diffusion in dry soils. For example, a substantial amount of the water used by shallow-rooted grass and shrub species comes from water that is hydraulically lifted by neighboring *Protea* species in the Cape Floristic Region, South Africa (Hawkins et al. 2009). We discuss hydraulic lift in this context in Sect. 16.5.2. Water flow into deeper soil layers via **hydraulic redistribution** has been demonstrated for several perennial grass species in the Kalahari Desert. Deuterium labeling shows that water acquired by roots from moist sand in the upper profile can be transported through the root system to roots deeper in the profile, and there released into the dry sand at these depths. This may serve as an important mechanism to facilitate root growth through the dry soil layers below the upper profile where precipitation penetrates, and allow roots to reach deep sources of moisture in water-limited ecosystems (Schulze et al. 1998). The same mechanism accounts for hydraulic redistribution, when water can be transported through roots at the break of the dry season (Burgess et al. 1998).

5.5.3 Water in Stems

Ever since the phenomenon of atmospheric pressure was recognized, it has been evident that even a perfect vacuum pump cannot lift water any higher than 10 m. In addition, even a relatively small xylem vessel with a radius of 20 mm only accounts for about 0.75 m of sap ascent by capillary action; however, plants can pull water well beyond this limit. Some of them, like the giant redwood (*Sequoia gigantea*) in California or karri (*Eucalyptus diversicolor*) in Western Australia, lift substantial quantities of water close to 100 m daily. If a vacuum pump cannot lift water higher than 10 m, then the pressure in the xylem must be lower than that delivered by such a pump (*i.e.* it must be negative!).

Water in the xylem of the stem, in contrast to that in the live cells of the roots and stem, is under **tension** (negative hydrostatic pressure) in transpiring plants. As explained in Box 5.2, these suction tensions are due to interactions of water molecules with the capillaries in the cell walls of transport vessels. In fact, the water column in a 100 m tall tree is held in place by the enormous **capillary forces** in the xylem at the top of the tree. Due to the **cohesion** among water molecules from hydrogen bonding, the water column in the stem is 'sucked upward' to replace water that is transpired from leaves. [This **cohesion theory** of water movement is generally ascribed to Böhm (1893) and Dixon and Joly (1894), but the elements of this theory were already described in 1727 by the English clergyman Stephen Hales (1727).] What is our evidence for such **suction tensions** or negative hydrostatic pressures and what exactly do they mean?

5.5.3.1 Can We Measure Negative Xylem Pressures?

Evidence for negative pressure in the xylem has been obtained using the **pressure chamber** (Scholander et al. 1965). A cut stem is placed in the chamber and sealed from the atmosphere, with the cut stem extending out (Fig. 5.15). A pressure is then applied just high enough to make the xylem sap in the stem appear at the cut surface. The positive pressure applied ('balancing pressure') is equal to the negative pressure in the xylem when the plant was still intact. Although there are problems using this technique when using plants with a low relative water content, the pressure chamber is widely used to assess the water potential in plants.

For a full appreciation of the ascent of sap in plants, we need to consider carefully the exact site the water is coming from that is pushed back into the xylem when pressure is applied to the pressure chamber (Box 5.2). This water is pushed out of the many capillaries in the **walls** of the xylem vessels and adjacent cells, where it was held in

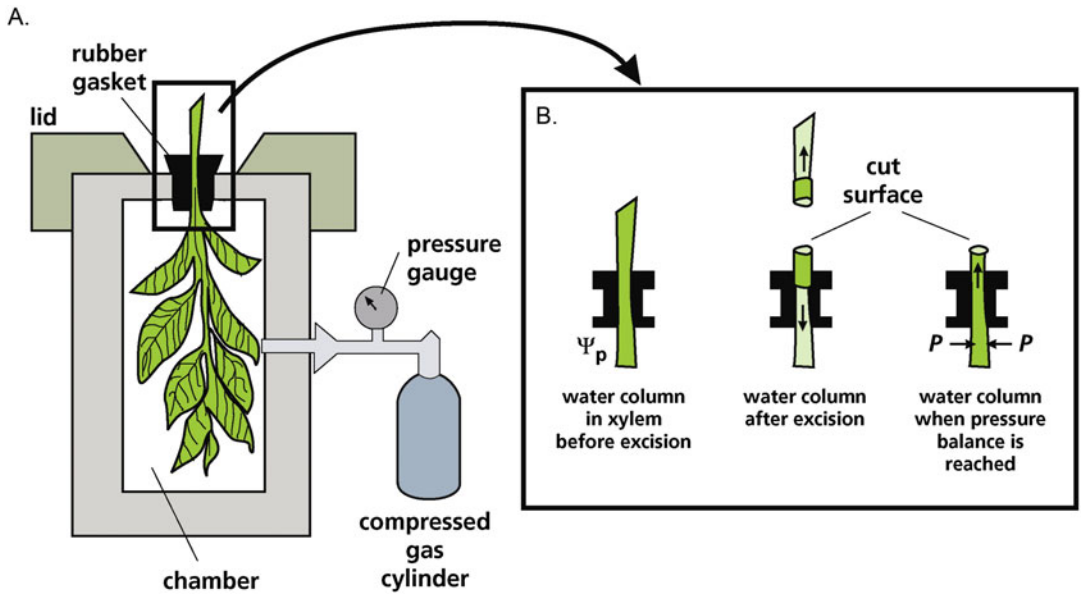

Fig. 5.15 (**A**) Schematic representation of the Scholander pressure chamber that is used for the measurement of negative hydrostatic pressures in the xylem (Ψ_p). A cut shoot, twig, root, or leaf is excised, and the negative Ψ_p in the xylem causes the water column to be drawn into, *e.g.*, the leaf. (**B**) A leaf (or other plant part) is mounted in a gasket and placed in the pressure chamber with the cut end protruding through the lid. The pressure in the chamber is increased, causing the xylem water column to be pushed upward in the xylem until it protrudes at the cut surface. At that point, the pressure inside the chamber (P) equals $-\Psi_p$. The osmotic potential of the xylem fluid is usually ignored, but can be determined by collecting sufficient xylem sap, avoiding contamination from surrounding cells.

place by strong **capillary forces** between the water molecules and the cell walls (Fig. 5.16). In a transpiring plant, water continuously moves from these capillaries to the intercellular spaces in leaves where the water potential is more negative, as long as the water vapor pressure is not saturated (Box 5.1). Due to the strong capillary forces, this water is replaced by water in the lumen of the xylem vessels. These strong capillary forces keep the entire water column in the xylem vessels in place and prevent it from retreating, such as happens when the stem is cut. At physiological temperatures, the **cohesive forces** between the water molecules are so strong that the water column in the xylem will not break (but see Sect. 5.5.3.3).

The most compelling evidence in favor of the cohesion theory for the ascent of sap comes from measurements using a device that involves spinning a length of branch about its center to create a known tension based on centrifugal forces. Results of such experiments agree perfectly with those obtained with the pressure chamber (Holbrook et al. 1995). Tensions can, therefore, be created in xylem vessels and measured accurately by the pressure chamber; but what do these tensions really represent? When stating that the xylem is under tension, we do not actually mean the xylem conduit itself. Rather, the suction tension, or negative hydrostatic pressure, refers to the **adhesive forces** that tightly hold the water in the small **capillaries** in the wall of the xylem conduits (Zwieniecki and Holbrook 2009).

5.5.3.2 The Flow of Water in the Xylem

Hydraulic resistance in the shoot xylem accounts for 20–60% of the total pressure difference between the soil and the air in transpiring trees and crop plants (Sperry 1995). In woody plants, most of this pressure difference occurs in small twigs and branches, where the cross-sectional

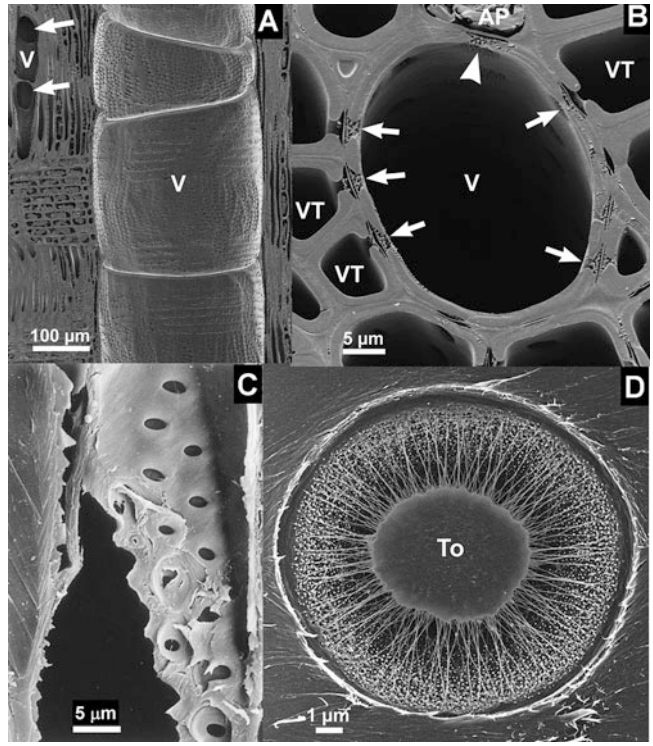

Fig. 5.16 Field-emission scanning electron micrographs showing details of the xylem. (**A**) Radial section of the xylem of *Quercus crispula* (Mongolian oak), showing a wide vessel with numerous pits, and narrow vessel elements that are connected with simple perforations. (**B**) Transverse section of the xylem of *Eucalyptus camaldulensis* (river red gum), showing several vessel-to-vasicentric tracheid pits and vessel-to-axial parenchyma pits. (**C**) A scanning electron micrograph of the sap-wood of *Populus nigra* (Lombardy poplar) hand-sectioned tangentially and slightly oblique. Bordered pits are shown between two adjacent vessels. Ray parenchyma cells are cut transversely in a vertical row to the right and left. Several pit apertures are seen (top central) in face view, with pit membranes visible through them. Lower down, the blade has removed the top borders of four pits, showing the interiors of the lower bordered pit chambers without any pit membranes. A pit can be seen centrally, half-closed by a torn pit membrane: The blade has folded the upper chamber above it revealing the inner cavity (indicated by arrow). The delicate pit membrane capillaries are sufficiently fine to filter fine carbon suspensions from indian ink. They are normally supported from mechanical disruption by the borders if subjected to powerful pressure flow from liquids or gases. Gases can pass when the membranes are physically torn; alternatively, the suctions may be so great that air bubbles are pulled through the capillaries in the membranes initiating embolism in the conduits in which the air bubble enters. (**D**) Intertracheary pit membrane of *Abies sachalinensis* (Sakhalin fir), a typical torus-baring pit membrane of a gymnosperm. *V* vessels, *VT* vasicentric tracheids, *AP* axial parenchyma, *To* torus; arrows in A point to simple perforations; arrows in B point to vessel-to-vasicentric tracheid pits; the arrow head in B points to vessel-to-axial parenchyma pits (A, B, and D: courtesy Y. Sano, Hokkaido University, Sapporo, Japan; C: courtesy J.A. Milburn, University of New England, Australia).

area of xylem is small (Gartner 1995). The water flow (J_v, $mm^3\ mm^{-2}\ s^{-1} = mm\ s^{-1}$) in xylem vessels is approximated by the **Hagen-Poiseuille equation**, which describes transport of fluids in ideal capillaries:

$$J_v = \left(\pi R^4 \Delta\psi\right)/8\eta L \qquad (5.19)$$

where $\Delta\psi_p$ (MPa) is the difference in hydrostatic pressure, R (mm) is the radius of the single element with length L (mm) through which transport

Table 5.6 Hydraulic conductance of xylem conduits, maximum velocity of water transport through the conduits and xylem diameter for stems of different types of plants.

	Hydraulic conductance of xylem lumina ($m^2\ s^{-1}\ MPa^{-1}$)	Maximum velocity ($mm\ s^{-1}$)	Vessel diameter diameter μm
Evergreen conifers	5–10	0.3–0.6	<30
Mediterranean sclerophylls	2–10	0.1–0.4	5–70
Deciduous diffuse porous	5–50	0.2–1.7	5–60
Deciduous ring porous	50–300	1.1–12.1	5–150
Herbs	30–60	3–17	
Lianas	300–500	42	200–300

Source: Milburn (1979), Zimmermann and Milburn (1982)

takes place, and η (mm^2 MPa s) is the viscosity constant. This equation shows that the **hydraulic conductance** is proportional to the fourth power of the vessel diameter. The hydraulic conductance of a stem with only a few xylem vessels with a large diameter is, therefore, much higher than that of a stem with many more vessels with a small diameter, but the same total xylem area. In addition, the **pits** in the connecting walls of the tracheids impose a substantial resistance to water flow (Choat et al. 2008). Pits are narrow channels through the thick secondary walls of vessel elements (Fig. 5.16).

Plants differ widely with respect to the diameter and length of their xylem vessels (Table 5.6). Vessel length in trees varies from less than 0.1 m to well over 10 m or as long as the whole stem. Longer vessels imply less intervessel transfer of water per unit length, and (all else be equal) reduce hydraulic resistance associated with the pit and pit membrane component (Choat et al. 2008). Small vessels may be hydraulically safer and less prone to drought and/or freezing-induced **embolism**, the breakage of the water column in a transport vessel (Sect. 5.5.3.3). Vessel length tends to correlate with vessel diameter. Across a water-availability gradient in Australia, mean vessel diameter of *Eucalyptus* species declines with increasing aridity (Pfautsch et al. 2016). In winter-deciduous trees, xylem vessels produced early in the season tend to be longer and wider than the ones produced later in the year. The difference in xylem diameter between early and late wood shows up as '**annual tree rings**' of the trunk of these '**ring-porous**' trees. '**Diffuse-porous**' trees, on the other hand, with a random distribution of wide and narrow vessels throughout the year, such occur as in many tropical trees, do not always show distinct annual rings (Zimmermann 1983).

Vines, which have relatively narrow stems, have long vessels with a large diameter, compared with related species or with the species in which they climb (Sect. 5.5.3.6). Because the hydraulic conductance is proportional to the fourth power of the vessel diameter (Eq. 5.19), the larger diameter compensates for the smaller total area. For example, the stem of the liana *Bauhinia fassoglensis* (creeping bauhinia) has a conductance equal to the tree *Thuja occidentalis* (white cedar) with a tenfold greater sapwood area (Ewers and Fisher 1991). Xylem vessels with a narrow diameter have the disadvantage of a low **hydraulic conductance**. Because the xylem walls take up more of the total xylem area, they provide greater **mechanical strength**. The narrow xylem vessels are also less vulnerable to freezing-induced embolism (Sect. 5.5.3.6).

5.5.3.3 Cavitation and Embolism: The Interruption of the Xylem Water Flow

Water in the xylem is usually under tension, and this tension increases under severe water stress conditions, *i.e.*, low water supply in the soil and high transpiration rates. When the tension of water within the xylem becomes too high, cavitation (sudden phase change from liquid to vapor) occurs and leads to the formation of gas bubles (embolism), filling the xylem with water vapor and/or air, rather than water. A conduit in this air-filled state is **embolized** and can not transport

water. Under water stress, when the tensions in the xylem become very high, embolism is nucleated by the **entry of air** through the largest pores in the walls of the transport vessels (a mechanism known as 'air-seeding'), located in primary walls of the inter-conduit pits, the **pit membrane** of angiosperms (Figs 5.16C, D and 5.17). Water then begins to evaporate explosively into the air nanobubble, because it is in a metastable state under high tensions. Short acoustic pulses are registered during embolism induced by water stress, allowing sound recordings to document

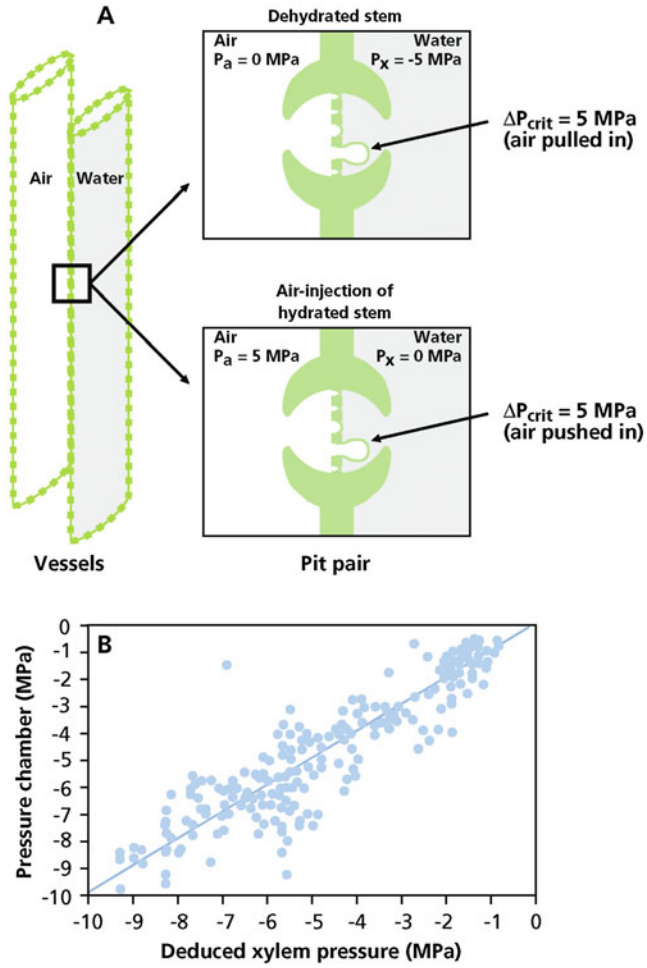

Fig. 5.17 (**A**) Embolism in dehydrating stems as affected by 'air seeding'. Two adjacent xylem vessels are shown. The one on the right is filled with xylem fluid; the one on the left has embolized and is therefore filled with water vapor at a very low pressure, near vacuum: 0 MPa. Pits between the vessels allow water flow and prevent passage of an air-water meniscus in the event that one vessel becomes air-filled. The top part of the illustration shows how a small air bubble is pulled in through the pit membrane pores when the pressure difference between the two vessels exceeds a critical threshold. In the example shown, this occurs at a xylem pressure of −5 MPa. In the experimental design shown in the lower part of the illustration, the critical pressure difference is exceeded by pressurizing the air in the embolized vessel, while the fluid in the other vessel is at atmospheric pressure. Now an air bubble is pushed in. The top part illustrates what is happening in a real plant. (**B**) There is a very close agreement between pressure differences at which embolism occurs in real plants, using the pressure chamber to determine the negative pressure in the xylem, and those achieved as illustrated in the bottom part of the top figure. This confirms that negative pressures occur in the xylem (after Sperry et al. 1996).

embolism rate. The bubble expands and interrupts the water column. Entry of air into the xylem conduit depends on the size of the pores in the pit membrane (Fig. 5.16C, D) and inter-vessel pit membrane thickness (Li et al. 2016). The thin, porous areas in conduit walls allow passage of water between conduits, but not a gas-water meniscus. This minimizes the spread of air bubbles into neighboring conduits. The tension required to cause embolism is a function of the permeability of the inter-conduit pits to an air-water interface, which depends on pore diameters (Pockman et al. 1995; Sperry 1995). Pore diameters range from less than 0.05 to more than 0.4 μm (as opposed to <0.01 μm in the cell wall proper), depending on species and location in the plant. Embolism reduces the ability to conduct water, and, if severe enough, will limit growth and cause mortality.

Xylem vulnerability to embolism formation for different species can be assessed through a vulnerability curve, which describes the percentage loss of conductivity in relation to the xylem water pressure. The curve can be estimated by gradually inducing a decrease of xylem water potential and, then, measuring the respective percentage loss of conductivity. It is possible to induce embolism by just cutting a long branch and let it dry (bench dehydration method (Sperry et al. 1988). Alternatively, air-pressurization can induce embolism in a branch segment by using a pressure sleeve (Cochard et al. 1992), or spinning this segment in a particular centrifuge rotor, and thus creating a negative pressure in the xylem (Alder et al. 1997). A hydraulic apparatus is used to measure the water flow through the segment (Sperry et al. 1988), or can even be measured while spinning (Cochard 2002). Airflow can also be measured directly using a pneumatic apparatus that sucks air from the branch segment (Pereira et al. 2016).

Since manipulations can induce artifacts during measurements, non-destructive methods to detect embolism are desirable, such as acoustic (Milburn 1973) or imaging methods. These include high-resolution x-ray computed tomography (Brodersen et al. 2010) and magnetic resonance imaging (Choat et al. 2010), but it is also possible to detect embolism by taking serial photos of leaves or even stems in a stereoscope or scanner (Brodribb et al. 2016).

Species differ considerably in their vulnerability to embolism, with the less vulnerable species tending to be more common in areas with high precipitation (Fig. 5.18; Choat et al. 2012). Embolism resistance is commonly represented

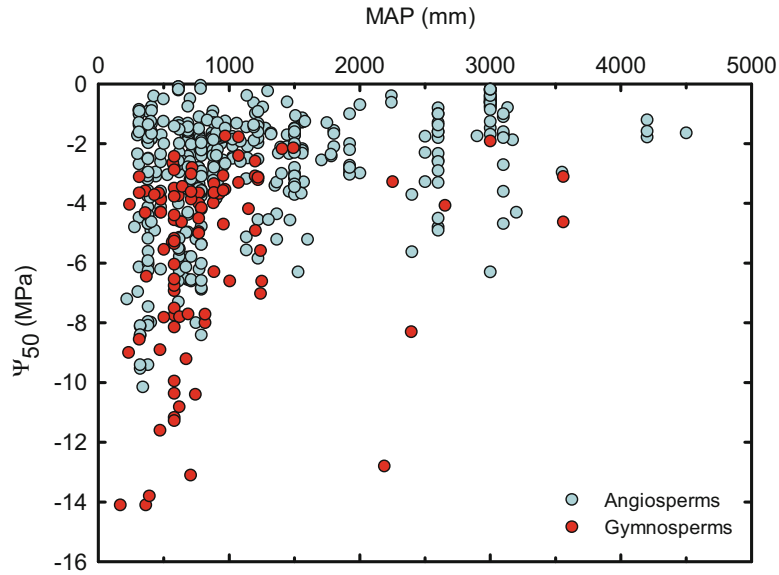

Fig. 5.18 Embolism resistance as a function of mean annual precipitation for 384 angiosperm and 96 gymnosperm species. Each point represents one species. A generalized model indicates that embolism resistance (Ψ_{50}) is related to mean annual precipitation (MAP) for angiosperms and gymnosperms), with decreasing resistance to embolism corresponding to increasing rainfall (Choat et al. 2012). Copyright Springer-Nature.

by an index called P50, *i.e.* the water potential corresponding to 50% loss of hydraulic conductivity. Across biomes, P50 varies from −0.91 MPa for branches of the angiosperms *Salix amygdaloides* (peachleaf willow) in temperate woodlands in Idaho, United States to −14.1 MPa for branches of the gymnosperm *Actinostrobus acuminatus* (dwarf cypress) in the dry shrublands of Western Australia (Fig. 5.18; Choat et al. 2012). There are also phenotypic differences in vulnerability to embolism. For example, root xylem in *Acer grandidentatum* (bigtooth maple) is more vulnerable when plants grow in wetter sites (Alder et al. 1996). Sun-exposed branches of *Fagus sylvatica* (beech) are less vulnerable than branches of the same tree that grow in the shade (Cochard et al. 1999). Because xylem conduits can only acclimate to new environmental conditions over prolonged periods, beech trees that are suddenly exposed to full light (*e.g.*, after forest thinning) may experience xylem embolism if transpiration rates are not efficiently controlled.

The diameter of pores in pit membranes (Fig. 5.16A, B) determines the vulnerability of species to embolism in response to water stress by determining the xylem tension at which an air bubble is sucked into the xylem lumen. It is not known whether pore diameter of the pit membrane also determines phenotypic differences in xylem vulnerability, but this is plausible. Across different *Acer* (maple) species, embolism resistance is associated with pit membrane porosity and thickness (Lens et al. 2011). A recent comparison across a broad range of angiosperm species from temperate and Mediterranean climates suggests that intervessel pit membrane thickness represents a stronger predictor for embolism resistance (Li et al. 2016; Fig. 5.19).

Embolism may also be caused by **freezing and thawing** of the xylem sap when it is under tension (Fig. 5.20). In this case, embolism occurs at much lower tension and is induced by a different mechanism: dissolved gases in the sap are insoluble in ice and freeze out as bubbles. If these bubbles are large enough when tension develops during thawing, then they will grow and cause embolism. When embolism is caused by freeze-thaw cycles, we can predict that wide and long vessels will be more vulnerable than small ones. Differences in conduit diameter are the main factors that account for species differences in vulnerability to embolism from freeze-thaw events (Fig. 5.20). If the air freezes out as one large bubble, rather than a number of smaller ones, then the greater dissolved air content in larger conduits will give rise to larger bubbles that cause embolism at lower tensions (Sperry and Sullivan 1992). Most embolisms in temperate woody plants occur in response to freeze-thaw events during winter and during the growing season rather than in response to drought. Embolism correlates more closely with the number of freeze-thaw episodes than it does with degree of frost (Sperry 1995).

The capacity of xylem to withstand freeze-thaw embolisms has important consequences for the evolution and distribution of woody plants (Zanne et al. 2013). Evergreen trees from cold climates are more likely to be actively transpiring (and therefore developing negative xylem potentials) when freeze-thaw events occur. It is probable for this reason that they have small tracheids that are less likely to embolize and easier to refill (Sect. 5.5.3.5). The disadvantage of narrow conduits is a low conductance. Among deciduous woody plants, there are ring-porous trees that produce large vessels during rapid growth in early spring and diffuse-porous species that have smaller diameter conduits. Ring-porous species cannot refill overwintering xylem, so their transpiration is entirely supported by current year's xylem, which therefore requires large-diameter vessels with high conductance. These species leaf out at least 2 weeks later than co-occurring diffuse-porous species, presumably because of their greater vulnerability to spring frosts (Sperry 1995). Some diffuse-porous species can refill embolized, over-winter conduits and are particularly successful in cold climates, whereas other diffuse-porous species cannot.

Pathogens can also induce embolism. Although we have known for quite some time that vascular diseases induce water stress in their host by reducing the hydraulic conductivity of the xylem, embolism as a cause for this has received

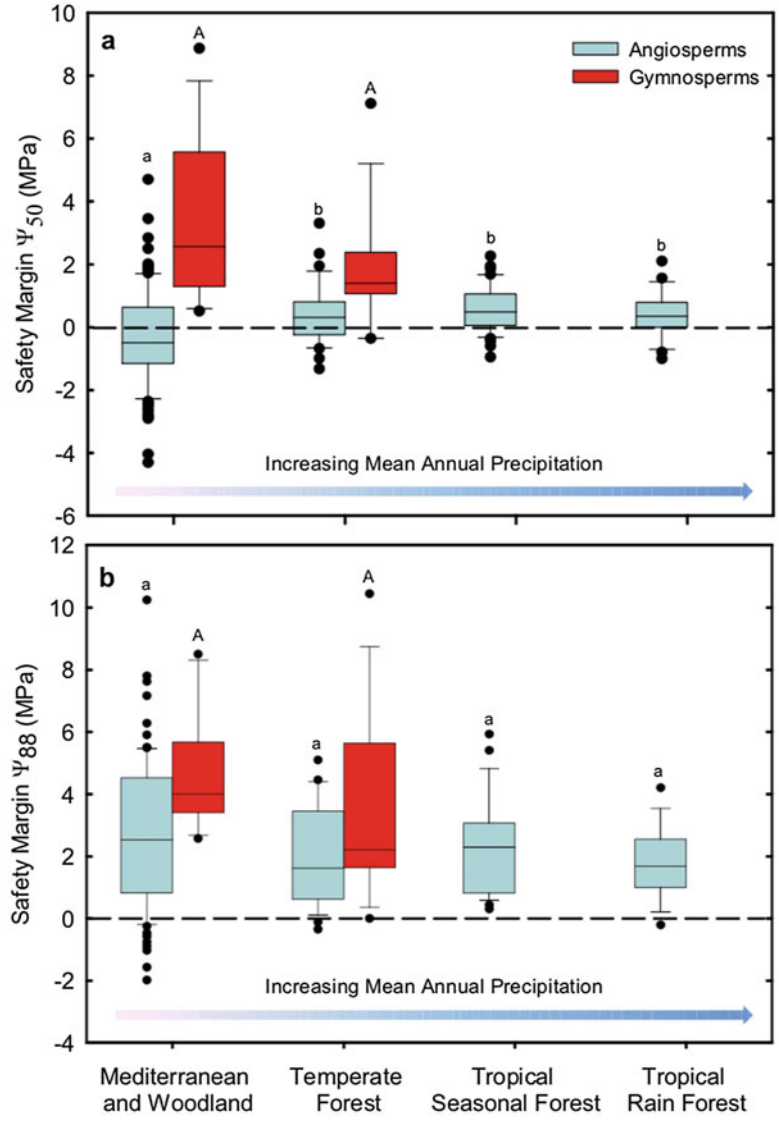

Fig. 5.19 Box plot of hydraulic safety margins for angiosperm and gymnosperm species across forest biomes. The Ψ_{50} ($\Psi min - \Psi_{50}$) safety margin is shown in A (n = 223), and the Ψ_{88} ($\Psi_{min} - \Psi_{88}$) safety margin is shown in B (n = 222). Boxes show the median, 25th and 75th percentiles, error bars show 10th and 90th percentiles, and filled symbols show outliers. Gymnosperm species are not represented in tropical forests. Significant differences ($P < 0.05$) between biome means are indicated by letters above boxes with angiosperms (lower case a, b) and gymnosperms (upper case A) considered separately (Choat et al. 2012). Copyright Springer-Nature.

very little attention. In the case of Dutch elm disease, however, embolism precedes any occlusion of vessels by other means. The exact cause of embolism remains unclear. It might be due to a pathogen-induced increase in stomatal conductance or decrease of water uptake by the roots. Pathogens might also change the xylem sap chemistry. For example, millimolar concentrations of oxalic acid, which is produced by many pathogenic fungi, lower the surface tension of the xylem sap. In *Acer saccharum* (sugar maple) and *Abies balsamea* (balsam fir), **oxalic acid** reduces the tension at which air can enter the xylem (Tyree and Sperry 1989). Xylem conductivity can also change in response to the concentration of **cations** in the xylem fluid (Van Ieperen 2007).

Can embolism also be brought about by xylem-feeding **spittlebug nymphs** (*Philaenus spumarius*)? Frothy white 'spittle' deposits of feeding spittlebug nymphs are familiar to all who have walked through fields and gardens in late spring and early summer. The water of the spittle comes from the xylem sap that is sucked up

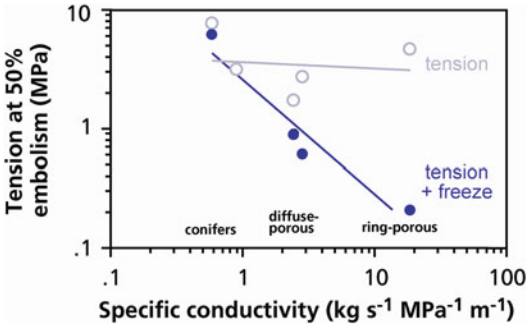

Fig. 5.20 Tension at the time of 50% embolism as dependent on the size of the tracheids or vessels. The experiment was carried out with trees exposed to water stress (tension, open circles) and with trees exposed to a freeze-thaw cycle (tension + freeze, solid circles) (after Sperry and Sullivan 1992). Copyright American Society of Plant Biologists.

through the insect's stylet that is inserted into a single xylem conduit. Because the concentration of nutrients in the xylem sap is very low, these tiny insects pump huge quantities of liquid against a strong pressure gradient, and excrete up to 280 times their body mass in 24 h. How does the spittlebug avoid inducing embolism? Saliva secreted by the insect forms a hardened lining between the stylet bundle and the plant tissues. This **salivary sheath** is continuous through the hole made by the stylet as it enters a vessel, and it extends into the vessel along the periphery beyond the breach. It allows the insects to feed from functioning vessels, without embolizing them. Embolized vessels, which are basically filled with water vapor, would be of no use for the spittlebug nymphs (Crews et al. 1998).

5.5.3.4 Can Embolized Conduits Resume Their Function?

Embolized conduits can potentially refill by **dissolution** of the bubble which can occur at moderately negative xylem pressures, but unequivocal evidence for such process is still very scarce (Brodersen et al. 2010). Dissolution of bubbles under tension may require narrow conduits (Sperry 1995) which perhaps explains the tendency of desert plants and plants from cold environments to have narrow conduits (Sect. 5.5.3.5). When such a moderately negative water potential cannot be reached, the xylem remains filled with water vapor and the conduit no longer functions in water transport (Yang and Tyree 1992). Failure to refill embolized vessels can sometimes be advantageous. For example, conduits of cactus xylem embolize when soil gets extremely dry, preventing water from being lost from the body of the plant to the soil.

Recent work with non-invasive imaging suggests that embolism repair is much rarer than first thought, and it may be restricted to species that produce a lot of **root pressure** such as in *Vitis vinifera* (grapevine) (Choat et al. 2018). This can occur at night under moist conditions, when **root pressure** builds up a positive xylem pressure. In more extreme cases this may not occur until it rains (Fig. 5.21). When roots grow in wet soil, a solute concentration in the xylem sap of 100 mM

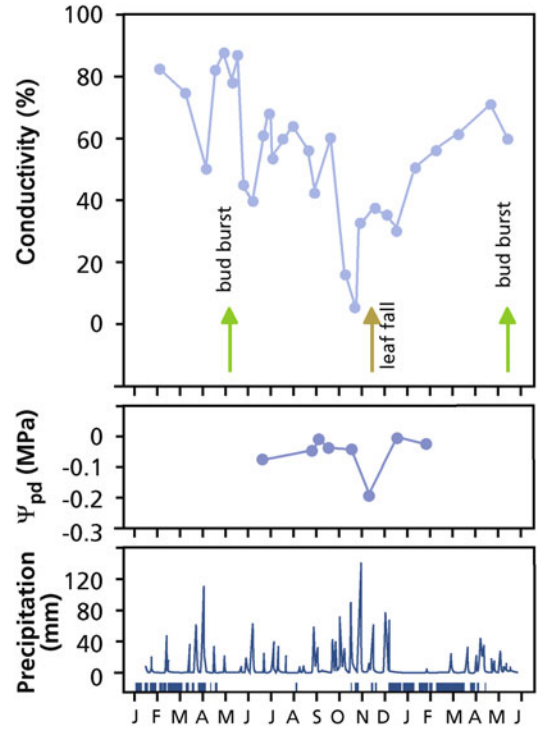

Fig. 5.21 Seasonal changes of xylem embolism in apical twigs, expressed as percentage of hydraulic conductivity (top); predawn water potential (middle); precipitation at the site of the studied tree *Fagus sylvatica* (beech). The occurrence of subzero temperatures is marked by bars at the bottom of the lower graph. Arrows in the top figure indicate bud burst and leaf fall (after Magnani and Borghetti 1995).

exerts just enough positive pressure to balance a water column of about 35 m (0.25 MPa plus 0.1 MPa of ambient pressure; Sect. 5.5.2); therefore, it is unlikely that embolized conduits in the top of a tall tree are ever refilled by root pressure.

Refilling of embolized conduits requires hydraulic isolation from tension (Brodersen et al. 2010) and that water enter the vessel lumen while pressurizing the gas phase until it is forced back into solution (Holbrook and Zwieniecki 1999). This requires a local input of energy that may come from the activities of living cells adjacent to the xylem. Water is possibly released into the vessel lumen from these adjacent living cells in a manner similar to the process that leads to root exudation (Sect. 5.5.2). Water will move from living cells to the embolized vessel if an adequate driving gradient is present, *e.g.*, involving active secretion of solutes by the living cells. Measurements of the osmotic concentration within repairing vessels, however, suggest that osmotic forces may not be adequate to explain the observed exudation (Canny 1997; Tyree et al. 1999). Further studies of water exudation from living cells and the potential involvement of aquaporins are needed to understand exactly how water enters embolized conduits (Wegner 2015). Additional observations are also needed across a wider range of species to better understand this process, but current evidence suggest that refilling after drought is uncommon and that hydraulic recovery is usually facilitated by growth of new xylem tissue.

5.5.3.5 Trade-Off Between Conductance and Safety

Species differences in xylem anatomy and function is thought to reflect the **trade-off** between a large xylem diameter, which maximizes **conductance**, and a small diameter, which increases the **strength** of the wood and minimizes the chances of **embolism** due to drought or freeze-thaw events. Indeed, in a comparison of 335 angiosperm and 89 gymnosperm species no species show both high efficiency and high safety; however, many species have low efficiency as well as low safety (Gleason et al. 2015), This indicates that other functions such as mechanical resistance and storage may be prioritized instead of increasing vessel area for a higher conductance (Bittencourt et al. 2016). **Vines**, which have a small stem diameter, have large vessels with a high conductance and rapid water movement through the vessels, compared with other species (Table 5.6). Their stem does not have the strength of that of a tree with similar leaf area, however. Many plants, including herbs and crop plants, function close to the water potential where embolism occurs (P50). This suggests that the investment in transport conduits is such that it is only just sufficient to allow the required rate of water transport during the growing season (Tyree and Zimmermann 2013).

Some woody species function close to the theoretical limit of the hydraulic conductance of their xylem conduits and loss of xylem conductance due to embolism is a regular event. Species differ enormously in their vulnerability with respect to water-stress induced embolism (Fig. 5.22). In general, embolism resistance, represented by **P50** of species correlates significantly with the mean annual precipitation in their natural habitat, with increasing vulnerability to embolism in high precipitation regions (Fig. 5.18). P50 is also related to the hydrological niche of species in tropical forests, *i.e.* embolism-resistant species (with low P50) tend to occur preferentially in high and well-drained uplands with little access to the water table (Fig. 5.22; Oliveira et al. 2019). The risk of embolism plays a major role in the differentiation between drought-adapted and mesic species. On the one hand, smaller inter-conduit pores confer resistance to embolism. On the other hand, they may reduce the hydraulic conductivity of the xylem. The **safer** the xylem, the **less efficient** it is in water conduction (Gleason et al. 2015). Interestingly, despite the wide range in P50 across natural communities, most of the species from different forest biomes show convergence in their hydraulic safety margins (*i.e.* the difference between the minimum water potential measured during field conditions and P50), suggesting that both dry and mesic biomes are equally vulnerable to droughts (Fig. 5.19; Choat et al. 2012). Additionally, P50 is linearly related to tree maximum growth rates

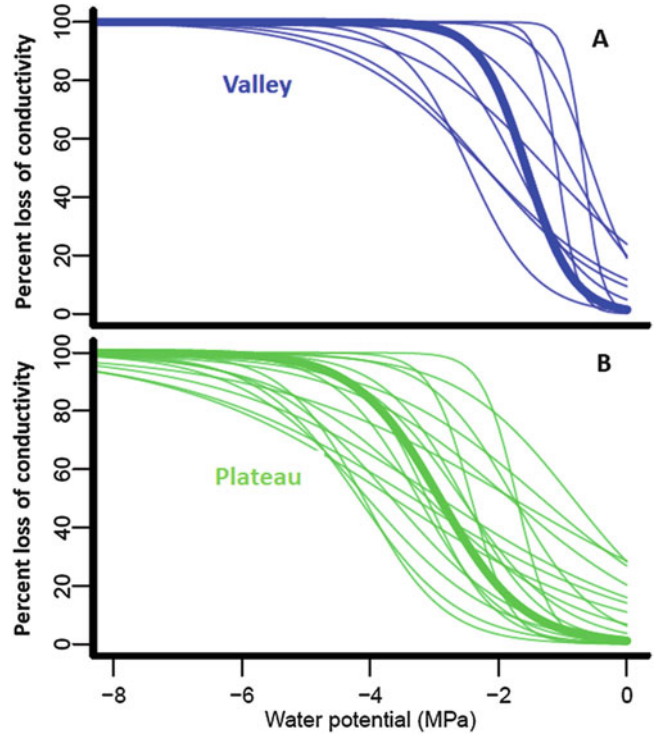

Fig. 5.22 Hydraulic vulnerability curves for 29 Valley (**A**) and Plateau species (**B**) in the Amazon. Increasing loss of conductivity represents the level of embolism when the plants are exposed to increasing levels of water stress. The thicker line in (**A**) and (**B**) is the abundance-weighted mean vulnerability curve at each location. Embolism resistance in this community is very diverse (covering as much as 44% of the global angiosperm variation in P50), and is higher for trees in valleys than for trees on the plateaus (Oliveira et al. 2019). Copyright Trustees of The New Phytologist.

in tropical forests (Eller et al. 2018). This relationship corroborates the existence of a fast-slow economic spectrum (Reich 2014), where xylem hydraulic safety is balanced with the rates of wood production. The generality of this finding remains to be tested in other ecosystems.

Embolism induced by freezing stress occurs at less negative water potential in wide and long xylem conduits than it does in shorter and narrower ones (Fig. 5.20). This may explain why xylem diameters are less in species from high latitude or altitude (Baas 1986). It may also account for the rarity of woody vines at high altitude (Ewers et al. 1990); however, if, as discussed above, the breaking of the water column in the xylem at moderate temperatures is *not* related to conduit size (Fig. 5.20), then why do **desert plants** tend to have narrow vessels? Conduits with a small diameter likely have smaller pit membrane pores than do wide ones, and this probably explains why desert plants have small xylem diameters. That is, the correlation does *not* reflect a direct causal relation. Pits may differ widely in different species, however, and the correlation between pit membrane pore size and xylem diameter is not very strict which accounts for the generally poor correlation between xylem diameter and vulnerability to embolism in different taxa (Sperry 1995). The length of the xylem conduit is also important, and this often correlates with conduit diameter. Many short and narrow xylem conduits (such as those concentrated in the nodes or junctions of a stem segment) may be of ecological significance in that they prevent emboli from spreading from one internode to the next or from a young twig to an older one, thus acting as 'safety zones' (Lo Gullo et al. 1995).

5.5.3.6 Transport Capacity of the Xylem and Leaf Area

In a given stand of trees, there is a strong linear relationship between the cross-sectional area of **sapwood** (A_s), that part of the xylem that functions in water transport, and the foliage area (A_f) supported by that xylem. Given that

Table 5.7 Typical ratios of foliage area (A_f) to sapwood area (A_s) of conifers.

Species	Common name	A_f:A_s (m^2 m^{-2})
Mesic environments		
Abies balsamea	Balsam fir	6700–7100
A. amabilis	Pacific silver fir	6300
A. grandis	Grand fir	5100
A. lasiocarpa	Subalpine fir	7500
Larix occidentalis	Western larch	5000
Picea abies	Norway spruce	4600
P. engelmanni	Engelmann spruce	2900–3400
P. sitchensis	Sitka spruce	4500
Pseudotsuga menziesii	Douglas fir	3800–7000
Tsuga heterophylla	Western hemlock	4600
T. mertensiana	Mountain hemlock	1600
Average		**5000 ± 500**
Xeric environments		
Juniperus monosperma	One-seeded juniper	800
J. occidentalis	Western juniper	1800
Pinus contorta	Lodgepole pine	1100–3000
P. edulis	Pinyon pine	2500
P. nigra	Austrian pine	1500
P. ponderosa	Ponderosa pine	1900
P. sylvestris	Scotch pine	1400
P. taeda	Loblolly pine	1300–3000
Average		**1800 ± 200**

Source: Margolis et al. (1995)

hydraulic conductance of stems differs among species and environments, however, it is not surprising that the ratio of foliage area to sapwood area (A_f:A_s) differs substantially among species and environments (Table 5.7). Desiccation-resistant species generally support much less leaf area per unit of sapwood than desiccation-sensitive species (Table 5.7). This is logical, because vessels are narrower in evergreen species from dry habitats; hence more sapwood is needed for a similar transport capacity (Tyree and Zimmermann 2013). Any factor that speeds the growth of a stand (*i.e.* higher 'site quality') generally increases A_f:A_s because it increases vessel diameter (Fig. 5.23A). For example, nutrient addition and favorable moisture status enhance A_f:A_s, and dominant trees have greater A_f:A_s than do subdominants (Margolis et al. 1995). When conductance per unit sapwood is also considered, there is a much more consistent relationship between foliage area and sapwood area (Fig. 5.23B).

Vines have less xylem tissue area per unit of distal leaf area (*i.e.* per unit leaf area for which they provide water). Their stems are thin relative to the distal leaf area, when compared with plants that support themselves. Vines compensate for this by having vessels with a large diameter (Fig. 5.24). It is interesting that the correlation between sapwood area and distal leaf area also holds when the leaf area is that of a **mistletoe** tapping the xylem, even when there is no host foliage on the branch (Sect. 15.2.3). Because there are no phloem connections between the xylem-tapping mistletoe and its host tree, the correlation cannot be accounted for by signals leaving the leaves and traveling through the phloem. This raises the intriguing question on how leaf area controls sapwood area (or *vice versa*).

5.5.3.7 Storage of Water in Stems

Plants store some water in stems, which can temporarily supply the water for transpiration. For

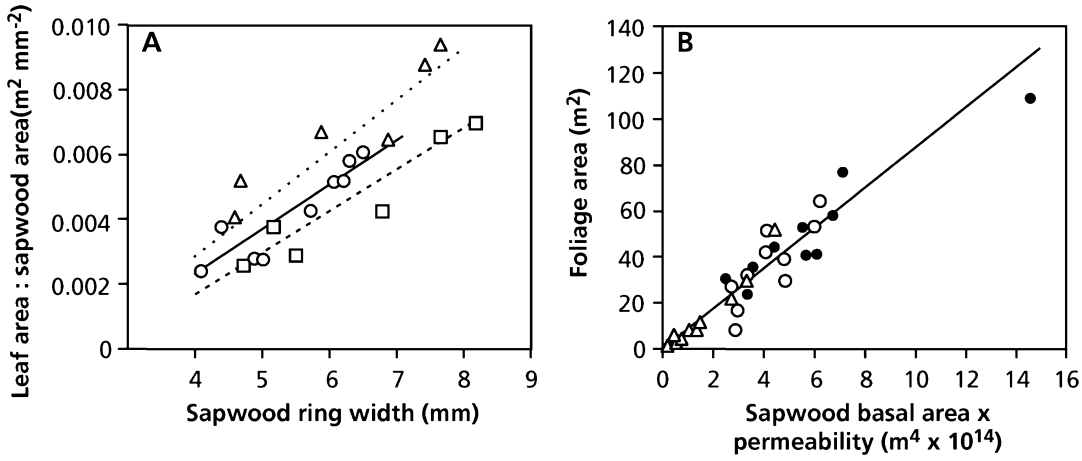

Fig. 5.23 (**A**) Leaf area:sapwood area ratio (A_f:A_s) in relation to sapwood ring width (a measure of growth rate) in Douglas fir (*Pseudotsuga menziesii*) growing in plantations of slow (squares), medium (circles), and fast (triangles) growth rate. (**B**) Relationship of foliage area to sapwood area adjusted for permeability (unit area conductance) in fertilized (solid circles) and control (open circles) trees of *Picea sitchensis* (Sitka spruce) and control trees of *Pinus contorta* (lodgepole pine) (open triangles) (after Margolis et al. 1995).

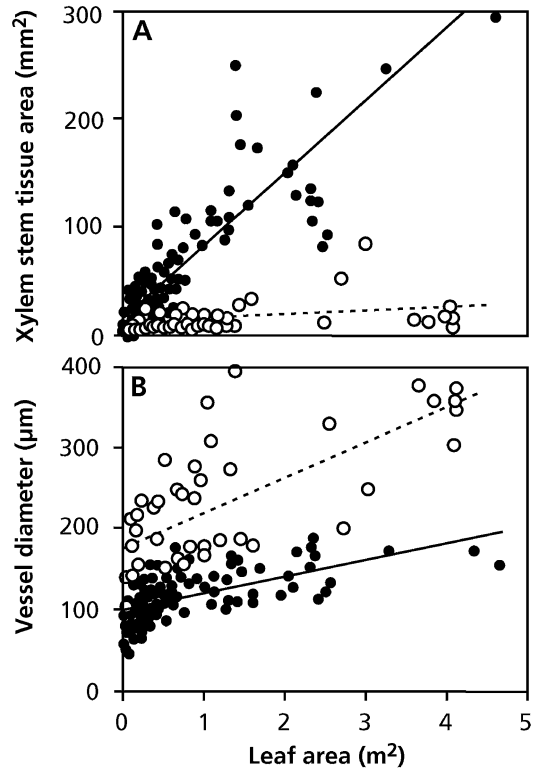

Fig. 5.24 Xylem area (**A**) and maximum diameters of vessels (**B**) of contrasting *Bauhinia* species. Values are plotted as a function of the leaf area distal to the investigated stem section for stems of lianas (dashed line, open symbols) and congeneric trees and shrubs (solid line, closed symbols) (Ewers and Fisher 1991). Copyright Springer-Nature.

example, water uptake and stem flow in many trees lags behind transpirational water loss by about 2 h because the water initially supplied to leaves comes from parenchyma cells in the stem. [Stem flow can be measured using sap-flow equipment (Box 5.4).] Withdrawal of stem water during the day causes stem diameter to fluctuate diurnally, being greatest in the early morning and smallest in late afternoon. Most **stem shrinkage** occurs in living tissues external to the xylem, mainly in the phloem, where cells have more elastic walls and cells decrease in volume when water is withdrawn. Water stored in the phloem can be transferred to the xylem via the symplast of horizontal ray parenchyma cells on a daily basis (Pfautsch et al. 2015). In trees, the stem water provides less than 10–20% of the daily water transpired in most plants, so it forms an extremely small buffer. In addition, if this water becomes available because of embolism, which stops the functioning of the embolized conduit, then the benefit of such a store is questionable.

Under some circumstances, however, stem water storage is clearly important. For example, in tropical dry forests, the loss of leaves in the dry season by drought-deciduous trees eliminates transpirational water loss. Stem water storage makes an important contribution to the water

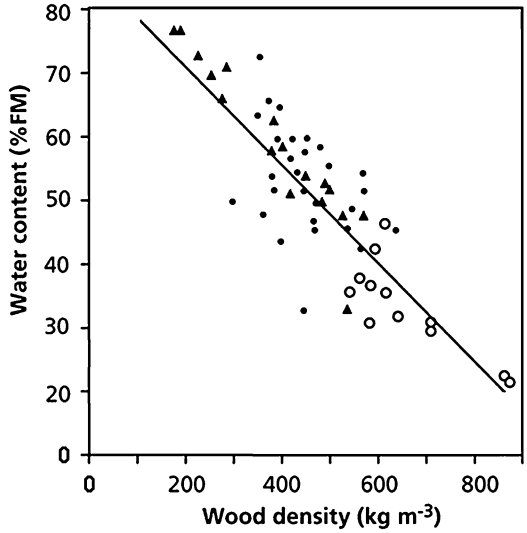

Fig. 5.25 Relationship between stem water content and wood density in 32 species of deciduous trees from a dry tropical forest in Costa Rica (after Borchert 1994). Copyright Ecological Society of America.

required for flowering and leaf flushing by these species during the dry season (Borchert 1994). Water storage in these trees is inversely related to wood density (Fig. 5.25). Early-successional, shade-intolerant species grow rapidly, have low wood density, and, therefore, high water storage that enables them to flower during the dry season and to reflush leaves late in the dry season. By contrast, slow-growing deciduous trees with high wood density and low water storage remain bare to the end of the dry season (Borchert 1994). Storage of water in stems is also important in reducing winter desiccation [*e.g.*, of the needles of *Picea engelmannii* (Engelmann spruce) that grow at the timberline]. Water in the stem may become available when the soil is frozen and air temperatures are above −4 °C (Sowell et al. 1996).

In herbaceous plants and succulents, which have more elastic cell walls than those of the sapwood in trees, storage in the stem is more important. Small herbaceous plants also transpire water made available by embolism of some of the conduits in the stem. They refill the xylem by root pressure during the following night. *Hylocereus undatus* (red pitaya), a hemiepiphytic cactus, has fleshy stems whose water storage is crucial for surviving drought. Under wet conditions, the turgor pressure is 0·45 MPa in its **chlorenchyma**, but only 0·10 MPa in its water-storage parenchyma. During 6 weeks of drought, the stems lose one-third of their water content, predominantly from cells in the **water-storage parenchyma** (**hydrenchyma**), which decrease by 44% in length and volume, whereas cells in the adjacent chlorenchyma decrease by only 6%; the osmotic pressure concomitantly increases by only 10% in the chlorenchyma, but by 75% in the water-storage parenchyma (Nobel 2006).

5.5.3.8 Foliar Water Uptake – The Atmosphere-Plant-Root Continuum

Plants from most ecosystems around the world spend a considerable amount of time with wet canopies due to a variety of climatic phenomena, including snow, dew, fog, and rainfall (Dawson and Goldsmith 2018). One of the consequences of wet canopies on the plant's physiology is triggering the entry of water through plant aerial tissues (Burgess and Dawson 2004; Eller et al. 2013) This pathway of water acquisition has been known for several decades (Stone 1957), but the ubiquity and relevance of this phenomenon have only been noted recently (Goldsmith 2013; Berry et al. 2019).

Plants are capable of absorbing a substantial amount of water directly through their leaves during canopy wetting events, reaching up to 0.39 mmol H_2O m^{-2} s^{-1} (Berry et al. 2019). Other aerial tissues such as twigs can also contribute to direct water uptake (Mason Earles et al. 2016). Aerial water uptake can increase plant survival during drought (Eller et al. 2013), possibly due to its effect increasing plant leaf water potential (Breshears et al. 2008) and contributing to embolism repair (Mayr et al. 2014). Aerial water absorption has been associated with xylem sap flux reversal in plant branches, stems, and roots (Burgess and Dawson 2004; Eller et al.

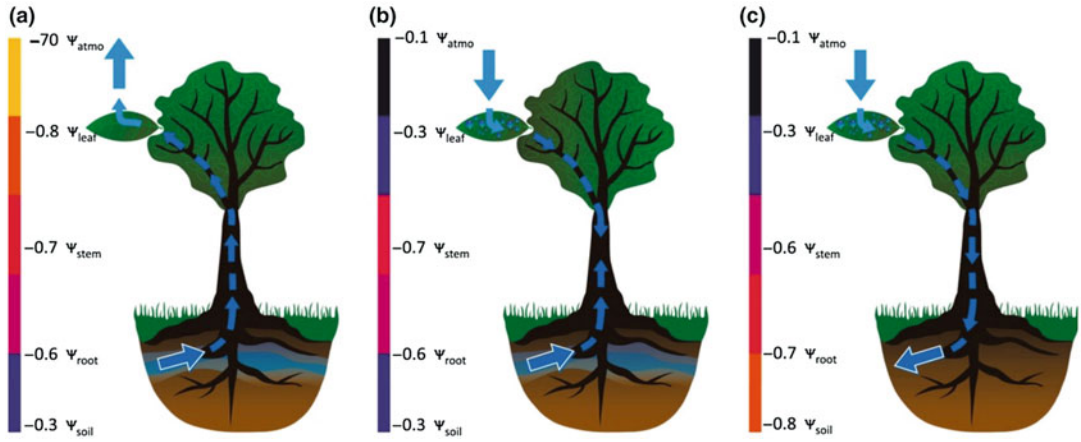

Fig. 5.26 Three potential scenarios for the movement of water through plants based on gradients in water potential (ψ in MPa). In scenario (**A**), water moves from higher ψ_{soil} to lower ψ_{atm} by transpiration. In scenario (**B**), water moves from higher ψ_{atm} (during a leaf wetting event) to lower ψ_{stem} by foliar water uptake, while also simultaneously moving from higher ψ_{soil} to lower ψ_{stem}, thus refilling the plant from two directions. In scenario (**C**), water moves from higher ψ_{atm} (during a leaf wetting event) to lower ψ_{soil} by foliar water uptake. Note that additional scenarios, such as the hydraulic redistribution of water from one soil layer to another by roots, are not included. Hypothetical values of ψ based on Nobel (2009). Illustration courtesy of F. van Osch (Goldsmith 2013); copyright Trustees of The New Phytologist.

2013). This water transport has been interpreted as a type of **hydraulic redistribution** (Sect. 5.5.2; Nadezhdina et al. 2010), caused by the inversion of the water potential gradient along the soil-plant continuum due to water entry and leaf hydration (Fig. 5.26; Goldsmith 2013). The hydraulic redistribution of water absorbed by aerial organs may extend the physiological benefits of aerial water uptake to underground plant organs, increasing the ecological relevance of this process.

The exact pathway of water entry into the leaf is still under debate, but multiple pathways are likely involved. Liquid water uptake may occur via stomata, mediated by salt ions in water that reduce surface tension (Burkhardt et al. 2012). Direct diffusion across the cuticule is another potential pathway for foliar water uptake. For instance, the contrasting foliar water uptake capacities through the cuticule of species from outcrops in central Brazilian mountains are associated with the chemical composition of their epidermal cell walls (Boanares et al. 2018). *Trembleya laniflora* and *Tibouchina heteromalla* (Melastomataceae) have more cellulose in their epidermal cell walls and absorb more water, but more slowly, while *Heteroptery campestris* (Malpighiaceae) and *Ocotea pulchella* (Lauraceae) have higher abundance of pectins, and absorb water at faster rates. Foliar trichomes also play an important role in foliar water uptake, in tropical montane cloud forest species (Eller et al. 2016) and Mediterranean plants (Fernández et al. 2014). Specialized structures such as **hydathodes** on the leaf epidermis are probably involved in foliar water uptake in *Crassula* species in the Namib Desert in Southern Africa (Martin and von Willert 2000).

5.5.3.9 Water Storage in Leaves

Many **succulents** store water in their leaves, often in specialized cells. For example, in the epiphytic *Peperomia magnoliaefolia* (desert privet), water storage occurs in a multiple epidermis (**hydrenchyma**), just under the upper epidermis which may account for 60% of the leaf volume (Fig. 5.37). The water-storage tissue of the epiphytic Bromeliad, *Guzmania monostachia* (strap-leaved guzmania), may amount to as much as 67% of the total leaf volume on exposed sites

(Maxwell et al. 1992). The hydrenchyma in *Peperomia magnoliaefolia* consists of large cells with large vacuoles, but lacking chloroplasts. Their radial walls are thin and 'collapse' when the cells lose water. Beneath the hydrenchyma is a layer of smaller cells that contain many chloroplasts: the **chlorenchyma**. Like in the stems of the hemiepiphytic cactus discussed in Sect. 5.5.3.7, when the leaves lose water, the dehydration of the chlorenchyma is much less than that of the hydrenchyma. The hydrenchyma functions as a reservoir for water lost through transpiration. This allows the chlorenchyma to remain photosynthetically active. During water loss, both solutes and water move from the hydrenchyma to the chlorenchyma. The total amount of water in the hydrenchyma of *Peperomia magnoliaefolia* exceeds 1 kg m^{-2} leaves. At an average transpiration rate of 0.2 mmol H_2O m^{-2} s^{-1} during 12 h of the day, this stored water allows the plant to continue to transpire at the same rate for about 1 week. The stored water allows the plant to maintain a positive carbon balance in the absence of water uptake from the environment for several days.

Microscopical analysis of the hydrenchyma cell walls leaf-succulent Aloe (Asphodelaceae) species shows highly regular folding patterns, indicative of predetermined cell-wall mechanics in the remobilization of stored water (Ahl et al. 2019). The *in situ* distribution of mannans in distinct intracellular compartments during drought, for storage, and apparent upregulation of pectins, imparting flexibility to the cell wall, facilitate elaborate cell wall folding during drought stress.

5.5.4 Water in Leaves and Water Loss from Leaves

The earliest known measurements of stomata were made in 1660 by Mariotte, a French mathematician and physicist who earned his living as a clergyman in Dijon. Fifteen years later, Malpighi, who was a professor of medicine at Bologna and Pisa, mentioned porelike structures on leaf surfaces (Meidner 1987). It is now an established fact that leaves inevitably lose water through their stomatal pores, as a consequence of the photosynthetic activity of the mesophyll leaf cells. Stomata exert the greatest short-term control over plant water relations because of the steep gradient in water potential between leaf and air. There are two major interacting determinants of plant water potential: soil moisture, which governs water supply, and transpiration, which governs water loss. Both of these factors exert their control primarily by regulating stomatal conductance. Stomatal conductance depends both on the availability of moisture in the soil and on vapor pressure in the air, as will be outlined shortly.

5.5.4.1 Effects of Soil Drying on Leaf Conductance

Leaves of '**isohydric**' species, which control gas exchange in such a way that daytime leaf water status is unaffected by soil water deficits, must control stomatal conductance by messages arriving from the root. This is an example of **feedforward control**. That is, stomatal conductance declines before any adverse effects of water shortage arise in the leaves. Isohydric species include *Zea mays* (corn) and *Vigna sinensis* (cowpea). The phytohormone abscisic acid (**ABA**) is the predominant chemical message arriving from roots in contact with drying soil (Schurr et al. 1992; Dodd 2005). Soil drying enhances the concentration of this hormone in the xylem sap as well as in the leaves (Tardieu et al. 1992; Correia et al. 1995). For woody species, leaf endogenous ABA production (McAdam et al. 2016) and changes in leaf turgor play a major role on controlling stomatal responses to soil drought (Rodriguez-Dominguez et al. 2016). Another chemical change related to soil drying is an increase in the pH of the xylem sap flowing from the roots (Gollan et al. 1992; Wilkinson et al. 1998). Injection of ABA in the stem of corn plants has similar effects on the ABA concentration in the xylem sap and on stomatal conductance as exposure to a drying soil. The stomata of desiccated plants become more 'sensitized' to the ABA signal, however, possibly by a combination of other chemical signals (*e.g.*, pH) transported in the xylem and the low water

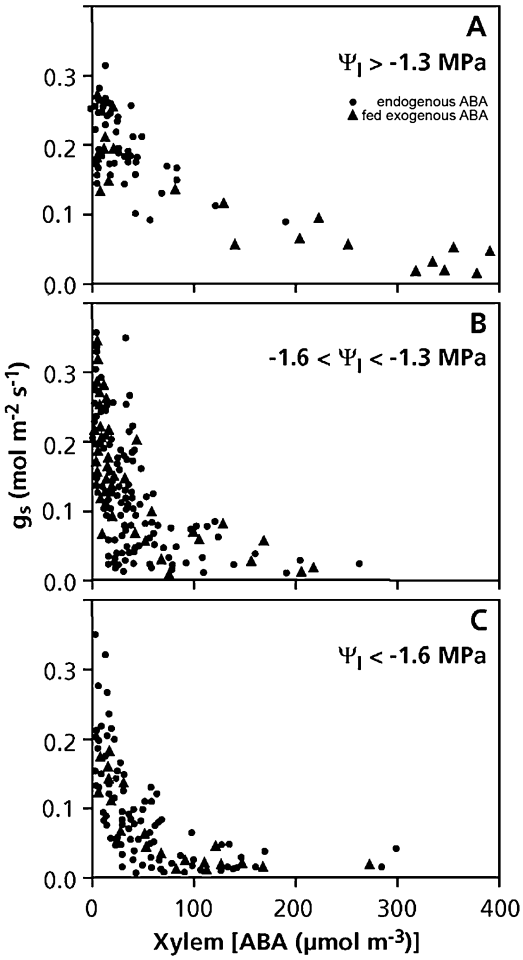

Fig. 5.27 Leaf conductance (g_s) as a function of the concentration of ABA in the xylem sap of field-grown *Zea mays* (corn) plants. Measurements were made over three ranges of leaf water potential (ψ_l) (A, B, C). ABA concentrations varied either due to variation in plants producing different amounts of ABA, or because ABA was injected into the stem (after Davies et al. 1994). Copyright American Society of Plant Biologists.

potential of the leaf itself (Fig. 5.27). The mechanism by which a high pH in the xylem sap affects the stomata is that the mesophyll and epidermal cells have a greatly reduced ability to sequester ABA away from the apoplast when the pH in that compartment is increased by the incoming xylem sap. This follows from the fact that weak acids such as ABA accumulate in compartments that are more alkaline (Wilkinson and Davies 1997; Jia and Davies 2007). Among trees, isohydric species are those that generally occur in mesic habitats and operate at water potentials extremely close to potentials causing complete embolism (Sect. 5.5.3.3; Sperry 1995). The degree of isohydry/anisohydry is linearly related to xylem hydraulic safety margin in biodiverse plant community from South Africa's Cape Floristic Region (Skelton et al. 2015).

In '**anisohydric**' species, such as *Helianthus annuus* (sunflower), both the leaf water potential and stomatal conductance decline with decreasing soil water potential. In these species, both root-derived ABA and leaf water status regulate stomatal conductance. A controlling influence of leaf water status on stomatal conductance need not be invoked. Rather, leaf water status is likely to vary because of water flux through the plant which is controlled by stomatal conductance. Correlations between stomatal conductance and leaf water status are only observed in plants where leaf water status has no controlling action on the stomata (Tardieu et al. 1996).

The spectrum in stomatal 'strategy' between isohydric and anisohydric plants is determined by the degree of influence of leaf water status on stomatal control for a given concentration of ABA in the xylem. There are also effects that are not triggered by ABA arriving from the roots, mediated via ABA produced in the leaf. In addition, both electrical and hydraulic signals control stomatal conductance in response to soil moisture availability (Sect. 2.5.1).

The mechanism by which roots sense dry soil is not clear. ABA, like any other acid, crosses membranes in its undissociated form. It therefore accumulates in soil, especially when the rhizosphere is alkaline. Because the concentration of ABA in soil increases when water is limiting for plant growth, it has been speculated that roots may sense drying soils through ABA released into the soil. Because the presence of NaCl inhibits the microbial degradation of ABA, the concentration of ABA also tends to be higher in saline soils. This might offer a mechanism for the roots to sense a low osmotic potential in the soil (Hartung et al. 1996). On the other hand, roots might also sense a decrease in turgor using **osmosensors** that measure the change in concentration of osmotic solutes; such osmosensors have been extensitvely studied in yeasts (Shinozaki

and Yamaguchi-Shinozaki 1997). More recently, it has been discovered that the activity of a specific plant response to cytokinin is also regulated by changes in turgor pressure (Reiser et al. 2003; Bartels and Sunkar 2005). The topic of sensing dry soil is further discussed in Sect. 10.5.3.1.

The relationship between stomatal conductance (and hence transpiration) and leaf water potential differs strikingly among growth forms. Because the difference in leaf water potential and soil water potential is the driving force for water transport in the plant, the relationship between leaf water potential and transpiration gives the conductance for water transport of the entire system (Schulze et al. 1991). This conductance is greatest in herbaceous annuals and smallest in evergreen conifers. Herbaceous species like *Helianthus annuus* (sunflower) change stomatal conductance and transpiration dramatically in response to small changes in leaf water potential. By contrast, stomatal conductance and transpiration are insensitive to progressively larger changes in water potential as we go from herbaceous annuals to woody shrubs to deciduous trees to conifers. There is a corresponding decrease in conduit diameter and increase in the margin of safety against embolism (Sect. 5.5.3.3). These patterns demonstrate the close integration of various parameters that determine plant 'strategies' of water relations.

Among woody plants, anisohydric species maintain a smaller safety margin against embolism, but they also experience more embolism (up to 50% loss of conductance), compared with isohydric species (Skelton et al. 2015). In anisohydric species, the closure of stomata in response to declines in leaf water potential is essential; otherwise, effects of declines in soil water potential would be augmented by those of embolism which would cause further declines in leaf water potential, and lead to runaway embolism (Sperry 1995).

How do we know that signals from the roots in contact with drying soil, rather than the low water potential in the leaf itself, really account for the decreased stomatal conductance? To address this question, Passioura (1988) used a pressure chamber placed around the roots of a *Triticum aestivum* (wheat) seedling growing in drying soil. As the soil dried out, the hydrostatic pressure on the roots was increased to maintain shoot water potential similar to that of well-watered plants. Despite having the same leaf water status as the control plants, the treated wheat plants showed reductions in stomatal conductance similar to those of plants in drying soil outside a pressure chamber. Additional evidence has come from experiments with small apple trees (*Malus*×*domestica*) growing in two containers (split-root design). Soil drying in one container, while keeping water availability high in the other, restricts leaf expansion and initiation, with no obvious effect on shoot water relations. We must therefore attribute these effects on leaves of wheat seedlings and apple trees to effects of soil drying that do not require a change in shoot water status (Davies et al. 1994). They are a clear example of **feedforward** control. In other species [*e.g.*, *Pseudotsuga menziesii* (Douglas fir) and *Alnus rubra* (red alder)], however, stomata do not respond to soil drying according to a feedforward model. When their leaf water status is manipulated in a pressure chamber, stomatal conductance responds to turgor in the leaves within minutes. In these species, stomatal control is hydraulic and no chemical signal from the roots appears to be involved (Fuchs and Livingston 1996).

Despite being widely used in the literature, classifying plant water use strategies using the iso × anisohydry framework is not a trivial task. Several metrics of iso/anisohydry have been proposed but they can characterize the same species differently (Martínez-Vilalta and Garcia-Forner 2017). Additionally, species can change their stomatal behavior depending on how hydrated the leaves are (Hochberg et al. 2018). Therefore, more comprehensive ecological classifications of plant water-use strategies are needed.

5.5.4.2 The Control of Stomatal Movements and Stomatal Conductance

How do signals discussed in Sect. 2.5.1 affect stomatal conductance? To answer this question we first need to explore the mechanism of opening and closing of the stomata.

Although the anatomy of stomata differs among species, there are a number of traits in common. First, there are two **guard cells** above a **stomatal cavity** (Fig. 5.28A, 1–3). Because the cell walls of these adjacent cells are only linked at their distal end, they form a pore whose aperture can vary because of the swelling or shrinking of the guard cells (Fig. 5.28A, B). Next to the guard cells, there are often a number of lateral and distal **subsidiary cells** (Outlaw 2003; Franks and Farquhar 2007). Stomatal closure occurs when solutes are transported from the guard cells, via the apoplast, to the subsidiary cells, followed by water movement along an osmotic gradient. Stomatal opening occurs by the transport of solutes and water in the opposite direction, from subsidiary cells, via the apoplast, to the guard cells (Fig. 5.28C).

The stomatal pore becomes wider when the guard cells take up solutes and water due to the special structure of the cells, which are attached at their distal ends, and the ultrastructure of their cell walls. The **ultrastructural features** include the radial orientation of rigid microfibrils in the walls which allow the cells to increase in volume only in a longitudinal direction. In addition, the guard cells of some species show some thickening of the cell wall bordering the pore. This may help to explain the movement of the guard cells, but the radial orientation of the microfibrils is the most important feature. The combination of the structural and ultrastructural characteristics forces the stomata to open when the guard cells increase in volume. This can happen in minutes and requires rapid and massive transport of solutes across the plasma membrane of the guard cells (Nilson and Assmann 2007).

Which solutes are transported and how is such transport brought about? The major ion that is transported is K^+, which is accompanied, immediately or with some delay, by Cl^-. On a cell volume basis KCl transport represents a change which is equivalent to 300 mM in osmotically active solutes. As an alternative to the transport of Cl^-, the charge may be (temporarily) balanced by negative charges that are produced inside the guard cells, the major one being malate produced from carbohydrate inside the guard cell (Blatt 2000). Guard cells also accumulate sucrose during stomatal opening (Nilson and Assmann 2007). An **H^+-ATPase** and several **ion-selective channels** play a role in the transport of both K^+ and Cl^-, in the opening as well as the closing reaction. The channels responsible for the entry of K^+ are open only when the membrane potential is very negative (Fig. 5.28C). A very negative membrane potential results from the activation of the H^+-pumping ATPase in the plasma membrane of the guard cells. Activation may be due to **light**, involving a blue-light receptor (Sect. 5.5.4.4). The ion-selective channels responsible for the release of K^+ open when the membrane potential becomes less negative (Hedrich and Schroeder 1989).

ABA affects some of the K^+- and Cl^--selective channels, either directly or indirectly, via the cytosolic Ca^{2+} concentration or pH; the decrease in stomatal conductance as affected by ABA involves both an inhibition of the opening response and a stimulation of the closing reaction. Stomatal closure is a consequence of the stimulation, possibly by ABA directly, of the channel that allows the release of Cl^-, which depolarizes the membrane and generates a driving force for K^+ efflux. ABA inactivates the channel that normally mediates K^+ entry and activates the channel that determines K^+ release. This picture of events pertains to the plasma membrane; however, since much of the solute lost during stomatal closing originates from the vacuole, equivalent events must occur at the tonoplast. Ca^{2+} plays a role as 'second messenger' in the inhibition of the inward-directed K^+-channel and stimulation of the outward-directed Cl^- channel. ABA enhances the Ca^{2+} concentration in the cytosol which in its turn inhibits the inward K^+-selective channel and stimulates the outward Cl^--selective channel. The outward K^+-selective channel is unaffected by $[Ca^{2+}]$. The Ca^{2+}

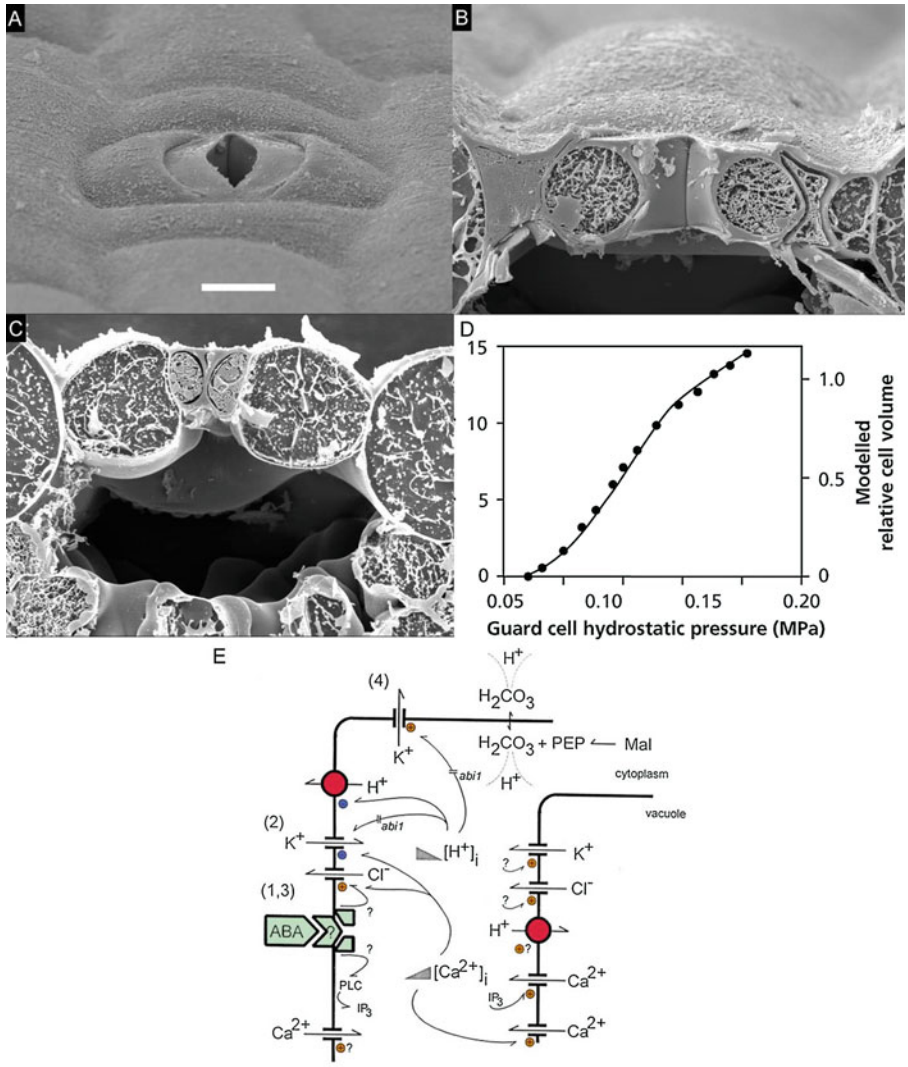

Fig. 5.28 (**A–C**) Stomata of *Tradescantia virginiana* (Virginia spiderwort) sampled by snap freezing an intact leaf. (**A**) View of an open stoma from the top, showing the stomatal pore, two guard cells, and two adjacent subsidiary cells. (**B**) Cross section showing an open stoma, large guard cells, small subsidiary cells, a stomatal pore, and a substomatal cavity. (**C**) Cross section showing a closed stoma, small guard cells, large subsidiary cells, no stomatal pore, and a substomatal cavity (courtesy P.J. Franks, James Cook University, Australia). (**D**) Stomatal aperture and cell volume as a function of the guard cell hydrostatic pressure. The pressure in the cells of *Tradescantia virginiana* was controlled with a pressure probe after the guard cells had been filled with silicon oil (after Franks et al. 1995). (**E**) Effects of ABA on ion fluxes in guard cells. ABA leads to a concerted modulation [(+) = increase or activation, (−) = decrease or inactivation] of at least three subsets of plasma-membrane ion channels. ABA first binds to a plasma-membrane receptor, possibly both from the outside and from the inside (not shown). This triggers the formation of inositol 1,4,5-triphosphate (IP_3), catalyzed by phospholipase C (PLC). IP_3 facilitates the release of Ca^{2+} from intracellular stores, and the consequent rise in cytosolic $[Ca^{2+}]$ affects a number of channels and, possibly, the plasma-membrane H^+-ATPase. ABA also triggers a rise in pH, which affects a number of channels and depletes the substrate for the H^+-ATPase. (Modified after Blatt and Grabov 1997).

that accumulates in the cytosol arrives there via Ca^{2+}-selective channels in the tonoplast and, probably, the plasma membrane (Fig. 5.28C; Mansfield and McAinsh 1995; Blatt 2000).

Irradiance, the **CO_2 concentration** and **humidity** of the air as well as **water stress** affect stomatal aperture. There are **photoreceptors** in stomatal cells that perceive certain wavelengths, thus affecting stomatal movements. We know little about the exact mechanisms and the transduction pathways between perception of the environmental signal and the ultimate effect: stomatal opening and closing, and diurnal variation in stomatal conductance. Expression of a gene encoding a carotenoid cleavage enzyme (9-*cis*-epoxycarotenoid dioxygenase, NCED) in the ABA biosynthetic pathway occurs after a 20 min exposure to high *VPD* for three angiosperms (McAdam et al. 2016). Even within a single species, there can be drastically different diurnal courses of stomatal conductance at different times of year (associated with very different relative water contents and leaf water potentials). In addition, the leaf water potential at which leaf cells start to lose turgor can change through a season (Fig. 5.29). Such a change in **turgor-loss point** must be associated with changes in elastic modulus (Table 5.4; Fig. 5.9; Sect. 5.5.4.6).

5.5.4.3 Effects of Vapor Pressure Difference or Transpiration Rate on Stomatal Conductance

Exposure of a single leaf or a whole plant to dry air is expected to increase transpiration because of the greater vapor pressure difference between the leaf and the air. Such a treatment, however, may also decrease stomatal conductance and hence affect transpiration. These effects on transpiration are readily appreciated when considering the Equation introduced in Sect. 2.2.2.2:

$$E = g_w(w_i - w_a) \qquad (5.20)$$

where g_w is the leaf conductance for water vapor transport, and w_i and w_a are the mole or volume fractions of water vapor in the leaf and air, respectively. Which environmental factors affect Δw, the difference in water vapor concentration between leaf and air and how can stomata respond to humidity?

The water vapor concentration inside the leaf changes with leaf temperature. As temperature rises, the air can contain more water vapor, and evaporation from the wet surfaces of the leaf cells raises the water vapor concentration to saturation. This is true for leaves of both well-watered and water-stressed plants. The air that surrounds the plant can also contain more humidity with rising temperature, but water vapor content of the air typically rises less rapidly than that of the leaf. If the water vapor concentration outside the leaf remains the same, then Δw increases. This enhances the leaves' transpiration in proportion to the increased Δw, because of increasing vapor pressure deficit (*VPD*), unless stomatal conductance declines. However, as *VPD* increases, stomata generally respond by partial closure (Lange et al. 1971). The stomatal closure response to increasing *VPD* generally results in a nonlinear increase in transpiration rate to a plateau and in some cases a decrease at high *VPD*. By avoiding high transpiration rates that would otherwise be caused by increasing Δw, stomatal closure avoids the corresponding decline in plant water potential. The closure response presumably evolved to prevent excessive dehydration and physiological damage. Responses of stomatal conductance to increasing *VPD* generally follow an exponential decrease, but the magnitude of the decrease, the **stomatal sensitivity**, varies considerably both within and among species. Stomatal sensitivity at low *VPD* ($\leq$ 1 kPa) is proportional to the magnitude of stomatal conductance (Fig. 5.30). Individuals, species, and stands with high stomatal conductance at low *VPD* show a greater sensitivity to *VPD*, as required by the role of stomata in regulating leaf water potential (Oren et al. 1999).

Note that as in Sect. 2.2.3 we use absolute values of water vapor in the air, rather than relative humidity or water potential. The relative humidity of the air is the absolute amount of water vapor (partial pressure is p) in the air as a

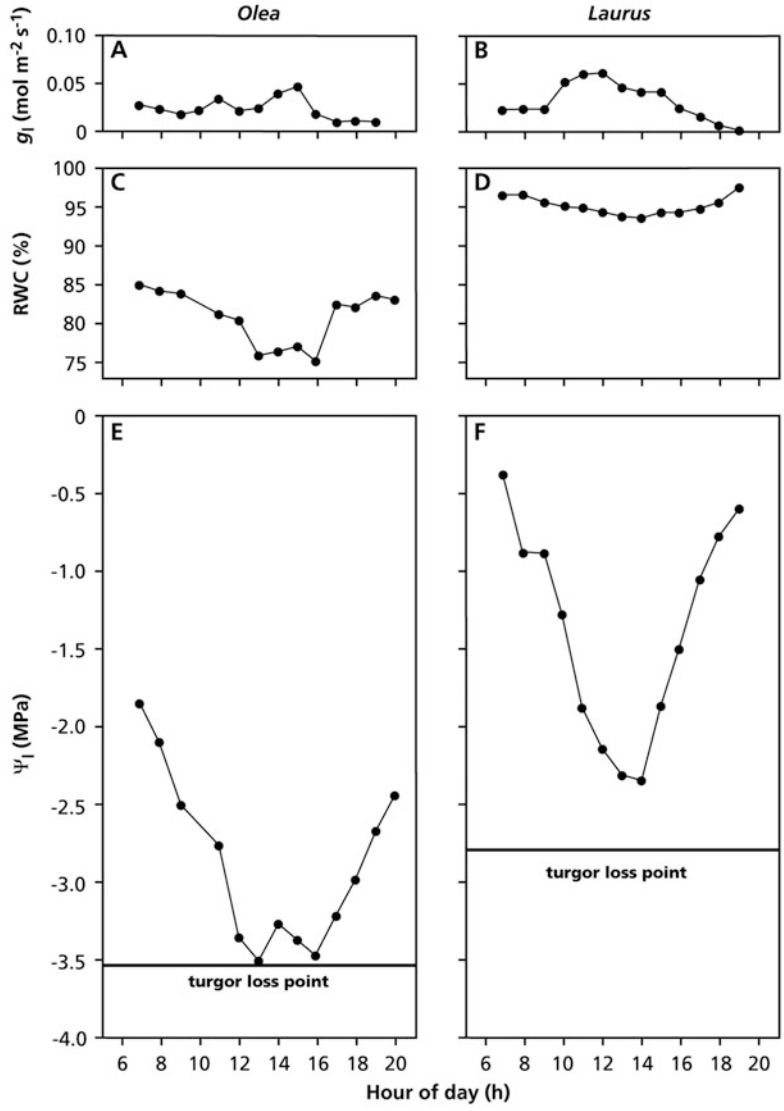

Fig. 5.29 Time course of the leaf conductance to water vapor (**A**, **B**), the relative water content (RWC) of the leaves (**C**, **D**), and the leaf water potential (**E**, **F**) for two Mediterranean tree species, the relatively drought-tolerant *Olea oleaster* (olive) and the less tolerant *Laurus nobilis* (laurel). RWC is defined as the amount of water per unit plant mass relative to the amount when the tissue is fully hydrated. Measurements were made in September (dry season) (after Lo Gullo and Salleo 1988). Additional information about these trees is presented in Table 5.4 and Fig. 5.9. Copyright Trustees of The New Phytologist.

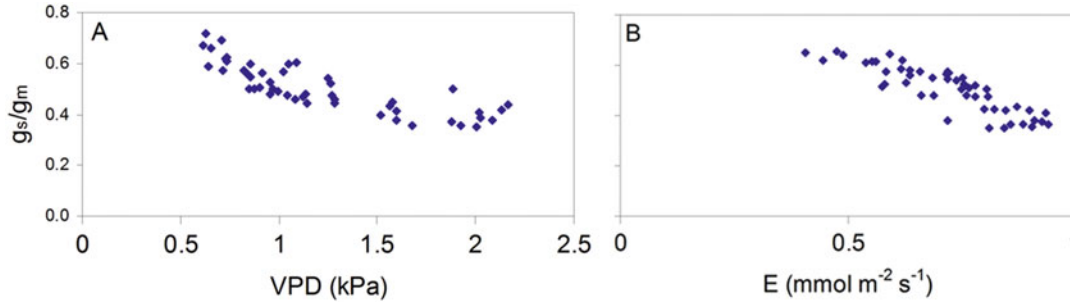

Fig. 5.30 Average canopy stomatal conductance relative to the maximum value in relation to (**A**) vapor pressure deficit (*VPD*) and (**B**) canopy transpiration per unit of leaf area (after Oren et al. 1999).

proportion of the maximum amount of water vapor that can be held at that temperature (partial pressure is p_o). The water potential of the air relates to the relative humidity as (Box 5.1):

$$\psi_{air} = RT/V_w{}^o . \ln\, p/p_o \qquad (5.21)$$

where $V_w{}^o$ is the molar volume of water. For air with a temperature of 293 K and a relative humidity of 75%, the water potential $\psi_{air} = -39$ MPa (using the value for the molar volume of water at 293 K of 18.10^{-6} m^3 mol^{-1}). Air with a lower RH has an even more negative water potential. This shows that water potentials of air that contains less water vapor than the maximum amount are extremely negative (Box 5.1). This negative water potential of the air is the driving force for transpiration. When describing the transport of water in different parts of the soil-plant-atmosphere continuum, it is essential to use the concept of water potential. For an analysis of leaf gas exchange, however, it tends to be more convenient to express the driving force for transpiration in terms of Δw, the difference in water vapor concentration between leaf and air, as is done for the diffusion of CO_2 from air to the intercellular spaces inside the leaf (Sect. 2.2.2.2).

To further elucidate the mechanism that accounts for stomatal responses to humidity, transpiration was measured in several species using normal air and a helium:oxygen mixture (79:21 v/v, with CO_2 and water vapor added) (Mott and Parkhurst 1991). Because water vapor diffuses 2.33 times faster in the helium/oxygen mixture than it does in air, Δw between the leaf and the air at the leaf surface can be varied independently of the transpiration rate, and *vice versa*. The results of these experiments are consistent with a mechanism for stomatal responses to humidity that is based on the rate of water loss from the leaf. It suggests that stomata do not directly sense and respond to either the water vapor concentration at the leaf surface or Δw.

The mechanism that accounts for the stomatal **response to humidity** of the air or **transpiration rate** is unknown (Eamus and Shanahan 2002). It most likely does not involve ABA, because both ABA-deficient and ABA-insensitive mutants of *Arabidopsis thaliana* (thale cress) respond the same as wild-type plants (Assmann et al. 2000). It can even be demonstrated in epidermal strips, isolated from the mesophyll. It is not universal, however, and it may even vary for one plant throughout a day (Franks et al. 1997). The consequence of this phenomenon is that a decrease in water vapor concentration of the air has less effect on the leaf's water potential and relative water content than expected from the increase in Δw. Stomatal response to humidity therefore allows an apparent **feedforward response** (Cowan 1977; Franks et al. 1997). It enables a plant to restrict excessive water loss before it develops severe water deficits and may enhance the ability of plants to use soil water supplies efficiently. The stomatal response to humidity inevitably reduces the intercellular CO_2 pressure in the leaf, C_i, in response to low humidity, and hence the rate of CO_2 assimilation. A compromise, somehow, has to be reached, as discussed in Sect. 5.5.4.7.

5.5.4.4 Effects of Irradiance and CO_2 on Stomatal Conductance

About a century ago, Francis Darwin (1898) already noted that the surface of a leaf facing a bright window had open stomata, whereas the stomata on surface away from the window were closed. When he turned the leaf around, the stomata that were closed before, opened. The ones that were open, then closed. Since Darwin's observation an overwhelming amount of evidence accumulated showing that stomata respond to light (Assmann and Shimazaki 1999). In Sect. 2.4.2, we discussed the rapid response of stomata in plants exposed to sun flecks. The response to light ensures that stomata are only open when there is the possibility to assimilate CO_2. In this way, water loss through transpiration is minimized.

How do stomata perceive the light and how is this subsequently translated into a change in stomatal aperture? There are basically two mechanisms by which stomata respond to light. The *direct* response involves specific pigments in the guard cells. In addition, guard cells respond to C_i, which will be reduced by an increased rate of photosynthesis. This is the *indirect* response.

The light response of guard cells is largely to **blue light** (with a peak at 436 nm) mediated by **phototropin** (Shimazaki et al. 2007). Stomata also open in response to **red light** (with a peak at 681 nm). Since *Paphiopedilum harrisianum*, an orchid species that lacks chlorophyll, has guard cell sensitive only to blue light, the red-light response is most likely mediated by chlorophyll (Kinoshita and Shimazaki 1999). The blue-light receptor (phototropin) affects biochemical events, such as an enhancement of PEP carboxylase, which catalyzes malate formation. Blue light also affects K^+ channels in the plasma membrane of the guard cells, allowing massive and rapid entry of K^+ into the guard cells which is the first step in the train of events that lead to stomatal opening (Blatt and Grabov 1997; Blatt 2000).

Stomata can respond to CO_2, even when isolated or in epidermal peels, but the sensitivity varies greatly among species and depends on environmental conditions. If stomata do respond, then they do so in both light and dark conditions. Mott (1988) used leaves of amphistomatous species (*i.e.* with stomata on both the upper and lower leaf surface) in a gas-exchange system that allows manipulation of C_i, while keeping the CO_2 concentration at one surface of the leaf constant (Sect. 5.5.4.3). In this way, it was shown that stomata sense the **intercellular CO_2 concentration** (C_i), rather than that at the leaf surface. Although the mechanism that accounts for the stomatal response remains unclear, it does play a major role in plant response to elevated atmospheric CO_2 concentrations (Assmann 1999). Under these conditions stomatal conductance is less than it is under present atmospheric conditions, enhancing the plant's photosynthetic water-use efficiency (Sect. 2.10.2).

5.5.4.5 The Cuticular Conductance and the Boundary Layer Conductance

In this chapter, we have so far mainly dealt with stomatal conductance (Sect. 2.2.2.2). The **cuticular conductance** for CO_2 and water vapor is so low that we can ignore it in most cases, except when the stomatal conductance is extremely low. It is widely believed that thick cuticles are better water barriers than thin ones, but all the experimental evidence shows this to be wrong. Cuticles are formed of three main constituents: waxes, polysaccharide microfibrils, and cutin, which is a three-dimensional polymer network of esterified fatty acids. The main barrier for diffusion is located within a waxy band, called the 'skin', whose thickness is much less than 1 μm (Kerstiens 1996).

In the continuum from the cell walls in the leaf, where evaporation takes place, to the atmosphere, there is one more step that cannot be ignored under many conditions. This is the leaf **boundary layer conductance**. We have already dealt with this in Sect. 2.2.2 and will come back to it in Chap. 6. A special case where boundary layer conductance is expected to be very low is that of **sunken stomata**, where stomata are concealed in a **stomatal crypt**, rather than be exposed at the leaf surface (Fig. 5.31). Sunken stomata are relatively common in thick scleromorphic leaves of plants on nutrient-poor soils in (semi-)arid climates (Grieve and Hellmuth 1970; Sobrado and Medina 1980). Because of their effect on boundary layer conductance, sunken stomata will reduce transpiration, but they will have a similar effect on photosynthesis, and hence water-use efficiency can be expected to be the same as that of plants with stomata on the leaf surface, instead of in stomatal crypts (Roth-Nebelsick et al. 2009). The depth of stomatal crypts in the genus *Banksia* correlates with leaf thickness (Lambers et al. 2014). Sunken stomata increase internal ventilation and this allow faster rates of photosynthesis than can be expected of leaves of similar thickness without stomata (Hassiotou et al. 2009; Lambers et al. 2012).

5.5.4.6 Stomatal Control: A Compromise Between Carbon Gain and Water Loss

As first discussed in Sect. 2.5, leaves face the problem of a compromise between maximizing photosynthesis (A) while avoiding excessive water loss through transpiration (E). At a relatively high leaf conductance (g_l; note that leaf conductance includes stomatal conductance,

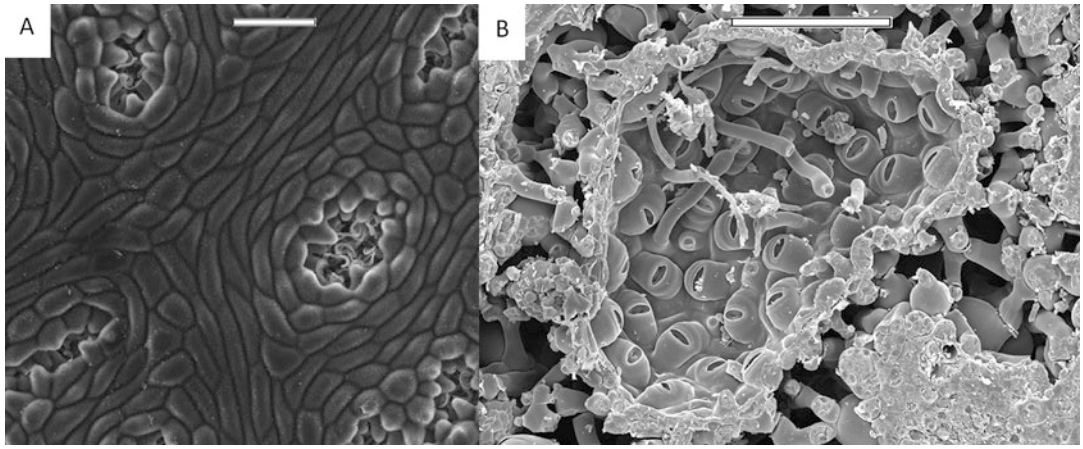

Fig. 5.31 Sunken stomata and stomatal crypts in leaves of *Banksia* species. (**A**) Abaxial leaf surface of *Banksia quercifolia* (oak-leaved banksia) showing stomatal crypts with trichomes. Scanning electron micrograph; scale bar 100 μm (courtesy F. Hassiotou, University of Western Australia, Australia). (**B**) Paradermal section of abaxial leaf surface of *Banksia elderiana* (swordfish banksia) showing a stomatal crypt with a few trichomes and many stomata. Stomata are restricted to the stomatal crypt. Cryoscanning electron micrograph; scale bar 100 μm. (courtesy F. Hassiotou, University of Western Australia, Australia, and C. Huang, Australian National University, Australia).

mesophyll conductance as well as boundary layer and cuticular conductance), A no longer increases linearly with C_i, mostly due to Rubisco activity becoming limiting (Figs 2.6 and 2.28; Sects 2.2.2.1 and 2.4.1). On the other hand, E continues to increase with increasing g_l, because it depends on the gradient in water vapor, and not on the biochemical machinery of photosynthesis (Fig. 2.29, Sect. 2.5.1). As explained, the intrinsic water-use efficiency (A/g_l) declines with increasing g_l. Cowan (1977) shows that the stomatal regulation that maximizes carbon gain per unit water lost over a given time interval maintains a constant ratio of changes between E and A (termed λ), as shown in Fig. 5.32.

Figure 5.32 gives the rate of transpiration as a function of the rate of assimilation and the time of the day, assuming different values for g_l or for λ. If we assume that stomata are regulated only to *maximize* carbon gain, then this produces a transpiration curve with one diurnal peak on the contour of the surface. The peak is due to the high difference in water vapor concentration between the leaf and the atmosphere when the radiation level is high during the middle of the day. Assuming **optimization** of stomatal regulation (*i.e.* carbon assimilation is balanced with water loss through a constant λ) gives a curve with two peaks, when λ is small (*i.e.* when carbon assimilation is an important criterion for optimization). When rates of transpiration change a lot, relative to changes in assimilation rates, *i.e.* λ is large (greater than in the two examples in Fig. 5.32, but stomatal conductance is regulated to optimize carbon gain and water loss), a curve with only one diurnal peak is found. In summary, the optimization model predicts that plants in a water-limited environment should show morning and late-afternoon peaks in transpiration rate and **midday stomatal closure**, whereas plants well supplied with water would perform optimally with a single **midday peak in transpiration**. The two-peak curve may be achieved by (partial) closure of the stomata during that time of the day when the evaporative demand is highest, due to a large difference in water vapor concentration between the leaf and the air.

How should stomata be regulated so as to maximize the fixation of CO_2 with a minimum loss of water? The optimization theory for stomatal action is based on the following assumption: stomatal action is such that for each amount of CO_2 absorbed, the smallest possible amount of

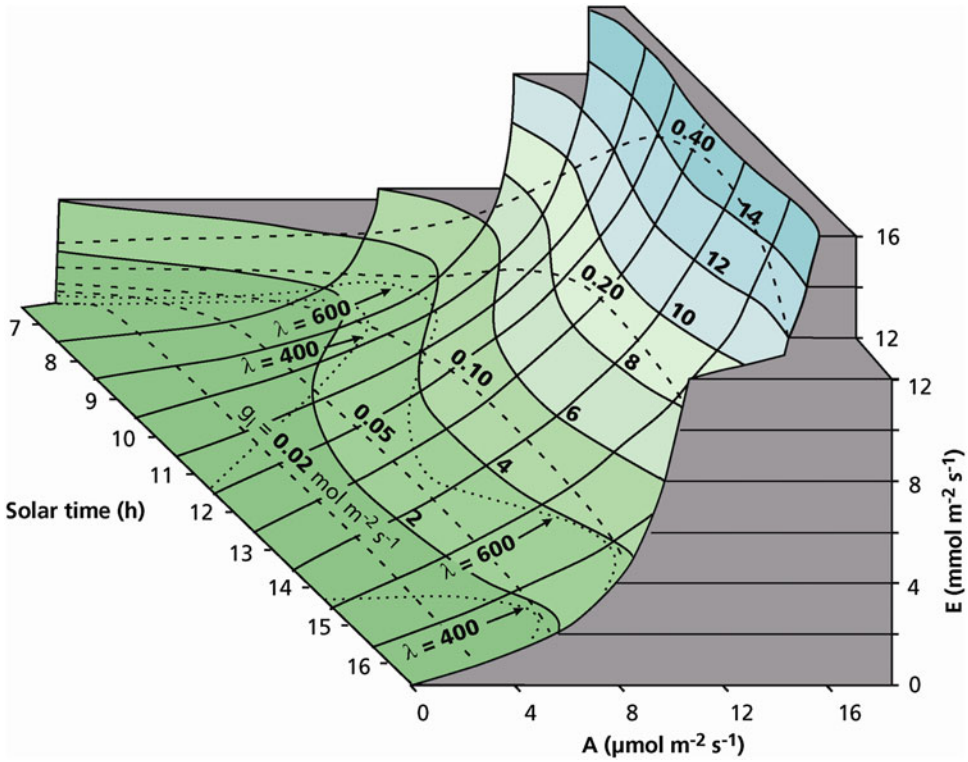

Fig. 5.32 Calculated rates of transpiration (E), as a function of the rate of photosynthesis (A), and time of the day, assuming certain characteristics of leaf metabolism and environment. The magnitudes for E are given on the contours of the surface. The broken lines are diurnal trajectories on the surface giving the diurnal variation in E and A for particular constant magnitudes of leaf conductance (g_l; 0.02, 0.05, 0.10, 0.20, or 0.40 mol m^{-2} s^{-1}). The broken lines are diurnal trajectories for which λ is constant (400 or 600) (Cowan 1977). Copyright Australian Academy of Science.

water is lost. The solution for this constrained optimization problem was originally obtained using numerical techniques (*i.e.* the lagrangian multiplier approach from Cowan (1977), but analytical approximations for the theory have also been developed (Medlyn et al. 2011). The solution, however, can be presented conceptually very briefly: for each infinitesimally small change of E at a certain E, the change in A is constant, λ (Fig. 5.32).

The theoretical curves of Fig. 5.32 agree with observations on both C_3 and C_4 plants in dry environments, where curves with two peaks are quite common. When the water supply is favorable and *VPD* is moderate, however, curves with only one peak are found (*i.e.* there is no partial midday stomatal closure) (Fig. 5.33). This has led to the conclusion that stomatal conductance is regulated so as to optimize carbon gain and water loss. It should be kept in mind, however, that this optimization approach, while very attractive for explanation of stomatal behavior, is teleological in nature; it has no mechanistic basis and is not easily used for predictive purposes (see Sect. 5.5.4.7).

Constancy of λ does not have to be the result of the action of stomata, but it may also be achieved by a specific leaf orientation. For example, vertical leaves absorb least radiation during the middle of the day as opposed to horizontal ones. A vertical orientation of leaves is typically associated with hot and dry places close to the equator. A

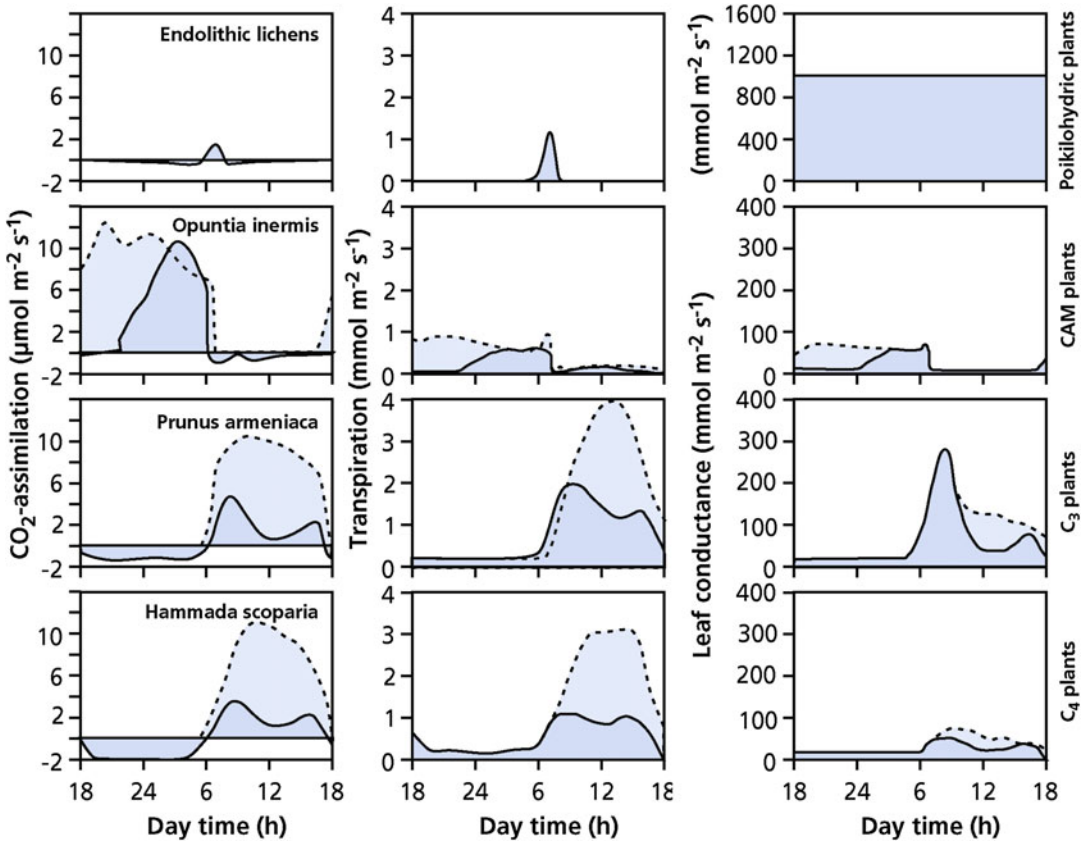

Fig. 5.33 Diurnal variation in the rate of CO_2 assimilation (left), transpiration (middle), and leaf conductance (right) for four different plant types. Light shading (dashed line) shows wet season; dark shading (solid line) shows dry season (Schulze and Hall 1982). Copyright Springer-Nature.

horizontal leaf orientation is common in temperate regions, further away from the equator. Some leaves have the ability to orientate their leaves in response to environmental factors, including the angle of the incident radiation and leaf temperature. Such **heliotropic leaf movements** may also lead to the constancy of λ (Sect. 6.2.2).

5.5.4.7 Stomatal Models and Xylem Hydraulics

The seminal optimization model of Cowan (1977) predicts correct plant stomatal responses to changes in humidity and temperature (Farquhar et al. 1980; Hall and Schulze 1980), but the theory cannot produce stomatal responses to longer-term changes on soil moisture with a constant λ (Cowan 1986). Another limitation with this theory is that it fails to reproduce the observed stomatal closure in response to increased atmospheric CO_2 (Mott 1988). Finally, a practical limitation of the Cowan (1977) model is the unspecified nature of the λ parameter, which cannot be related to a measurable biophysical quantity in plants. Recent studies (Prentice et al. 2014; Wolf et al. 2016; Sperry et al. 2017), proposed an alternative perspective to the stomatal optimization theory that employs plant hydraulics to overcome the limitations of the Cowan (1977) model. This new paradigm proposes that carbon assimilation should be constrained by the instantaneous losses in the plant capacity to transport water (*i.e.* hydraulic conductance) instead of water losses *per se* as in Cowan (1977). This new theory of stomatal optimization circumvents the need for

specifying λ, using instead widely available plant xylem hydraulic traits to predict plant stomatal responses to environmental conditions, including the correct responses to soil moisture and CO_2 (Sperry et al. 2017; Anderegg et al. 2018; Eller et al. 2018). Such theory provides a useful non-empirical basis to model vegetation interactions with climate in earth system models.

5.5.5 Aquatic Angiosperms

Aquatic angiosperms are perhaps comparable to whales: they returned to the water, taking with them some features of terrestrial organisms. In perennially submerged angiosperms, where the pressure in the xylem is never negative, the xylem is somewhat 'reduced'. The structure is like that of resin ducts. The xylem ducts in submerged aquatics often have thin walls, whereas 'conventionally' thick-walled xylem cells are found in aquatics whose tops are able to emerge from the water.

It is well established that water transport from roots to leaves is possible in submerged aquatic angiosperms, and that it is important in the transport of nutrients and root-produced phytohormones to the stem and leaves. The roots of most aquatics serve the same role as those of terrestrial plants as the major site of nutrient uptake and in the synthesis of some phytohormones. In submerged angiosperms, the driving force for xylem transport cannot be the transpiration, and root pressure is the most likely mechanism (Pedersen and Sand-Jensen 1997).

5.6 Water-Use Efficiency

Water-use efficiency (*WUE*) refers to the amount of water lost during the production of biomass or the fixation of CO_2 in photosynthesis. It is defined in two ways. First, the **water-use efficiency of productivity** is the ratio between (above-ground) gain in biomass and loss of water during the production of that biomass; the water loss may refer to total transpiration only, or include soil evaporation. Second, as explained in Sect. 2.5.2, the **photosynthetic water-use efficiency** is the ratio between carbon gain in photosynthesis and water loss in transpiration, *A*/*E*. Instead of the ratio of the rates of photosynthesis and transpiration, the ratio of photosynthesis (*A*) and leaf conductance for water vapor A/g_w can be used (**intrinsic water-use efficiency**) (Comstock and Ehleringer 1992). As expected, there is generally a good correlation between the *WUE* of productivity and the photosynthetic *WUE*. Variation in intrinsic *WUE* is due the way stomata are controlled, as discussed in Sect. 5.5.4.6.

5.6.1 Water-Use Efficiency and Carbon-Isotope Discrimination

As explained in Box 2.2, the carbon-isotope composition of plant biomass is largely determined by the biochemical fractionation of Rubisco and the fractionation during diffusion of CO_2 from the atmosphere to the intercellular spaces. The higher the stomatal conductance, relative to the activity of Rubisco, the less $^{13}CO_2$ ends up in the photosynthates and hence in plant biomass. This is the basis of the generally observed correlation between $\delta^{13}C$-values and both the intercellular CO_2 concentration (C_i) and photosynthetic *WUE* (Fig. 2.30). As a result, **$\delta^{13}C$-values** can be used to assess a plant's *WUE*; however, differences in *WUE* determined at the leaf level may be reduced substantially at the canopy level, as further explained in Sect. 8.4.

A plant's *WUE* depends both on stomatal conductance and on the difference in water vapor pressure in the leaf's intercellular air spaces and that in the air. Because temperature affects the water vapor concentration in the leaf, temperature also has a pronounced effect on plant *WUE*, *A*/*E*. Therefore, the intrinsic water-use efficiency, A/g_w, is a better indicator for a plant's physiological *WUE* (Comstock and Ehleringer 1992).

There are major differences in photosynthetic *WUE* (A/g_w) between C_3, C_4, and CAM plants, as well as smaller differences among species of

Table 5.8 The photosynthetic water-use efficiency* of plants with different photosynthetic pathway** and belonging to different functional groups***.

Functional group	Water-use efficiency (mmol mol^{-1})
CAM-plants	4–20
C_4 plants	4–12
Woody C_3 plants	2–11
Herbaceous C_3 plants	2–5
Hemiparasitic C_3 plants	0.3–2.5

Source: Kluge and Ting (1978), Osmond et al. (1982), Morison (1987), Shah et al. (1987), Ehleringer and Cooper (1988), Marshall and Zhang (1994), Yu et al. (2005)

*Because A/g_w (intrinsic water-use efficiency) is difficult to compare between CAM plants and other plants, A/E (photosynthetic water-use efficiency) was used instead

**C_3, C_4, and CAM; for CAM-plants the high values refer to gas exchange during the night and the low values to the light period

***All species are nonparasitic, unless stated otherwise, grown at an ambient CO_2 concentration of around 350 μmol mol^{-1} and not exposed to severe water stress

the same photosynthetic pathway (Sect. 2.5.2). Xylem-tapping hemiparasitic plants have the lowest *WUE*, as discussed in Chap. 14 (Table 5.8).

5.6.2 Leaf Traits That Affect Leaf Temperature and Leaf Water Loss

As discussed in Sect. 5.5.4.3, leaf temperature affects the water vapor concentration inside the leaf; therefore, it is expected to affect transpiration. At increasing irradiance, leaf temperatures may rise and enhance transpiration enormously. Plants have mechanisms to minimize these effects, however. For example, water stress may cause **wilting** in large-leafed dicots even in moist soils (Chiariello et al. 1987) or **leaf rolling** in many Gramineae (Arber 1923). The latter is associated with the presence of **bulliform** or **hygroscopic** cells in grasses and sedges which are large epidermal cells with thin anticlinal walls (Beal 1886). A decline in relative water content reduces the volume of these cells to a greater extent than that of the surrounding cells, so that the leaves roll up. As a result, less radiation is absorbed, the boundary layer conductance of the adaxial surface is decreased, and further development of water stress symptoms is reduced (Sect. 6.2). Leaf rolling is probably a consequence of the relatively large elasticity of the cell walls and associated water relations of the bulliform cells compared with other epidermal leaf cells.

Leaf movements (heliotropisms) may also reduce the radiation load, as discussed in Sect. 6.2.2. Such leaf movements require a leaf joint, or **pulvinus** at the base of the petiole or leaf sheath (Satter and Galston 1981). Solutes, especially K^+, are actively transported from one side of the pulvinus to the other (Fig. 5.34). Water follows passively, through **aquaporins** (Uehlein and Kaldenhoff 2008), and the turgor is increased which causes movement of the petiole or leaf sheath.

Leaf movements have been studied in detail in *Glycine max* (soybean) (Oosterhuis et al. 1985) and in *Melilotus indicus* (annual yellow sweetclover) (Schwartz et al. 1987). In these plants, as in some other Fabaceae and in *Mimosa* species, the (blue) light stimulus that gives rise to leaf movement is perceived in the pulvinus itself (Vogelmann 1984). In *Crotalaria pallida* (smooth rattlebox) (Schmalstig 1997) and in species belonging to the Malvaceae (Schwartz et al. 1987), perception occurs in the leaf lamina. In *Crotalaria pallida* the signal is transported to the pulvinus at a rate of 30–120 mm h^{-1}. Both the adaxial (upper) and the abaxial (lower) side of the pulvinus of *Melilotus indicus* perceive the light stimulus. Light perception at the adaxial side causes the pulvinus to move upward, whereas perception of light at the abaxial side induces the pulvinus to cause a downward movement (Fig. 5.35).

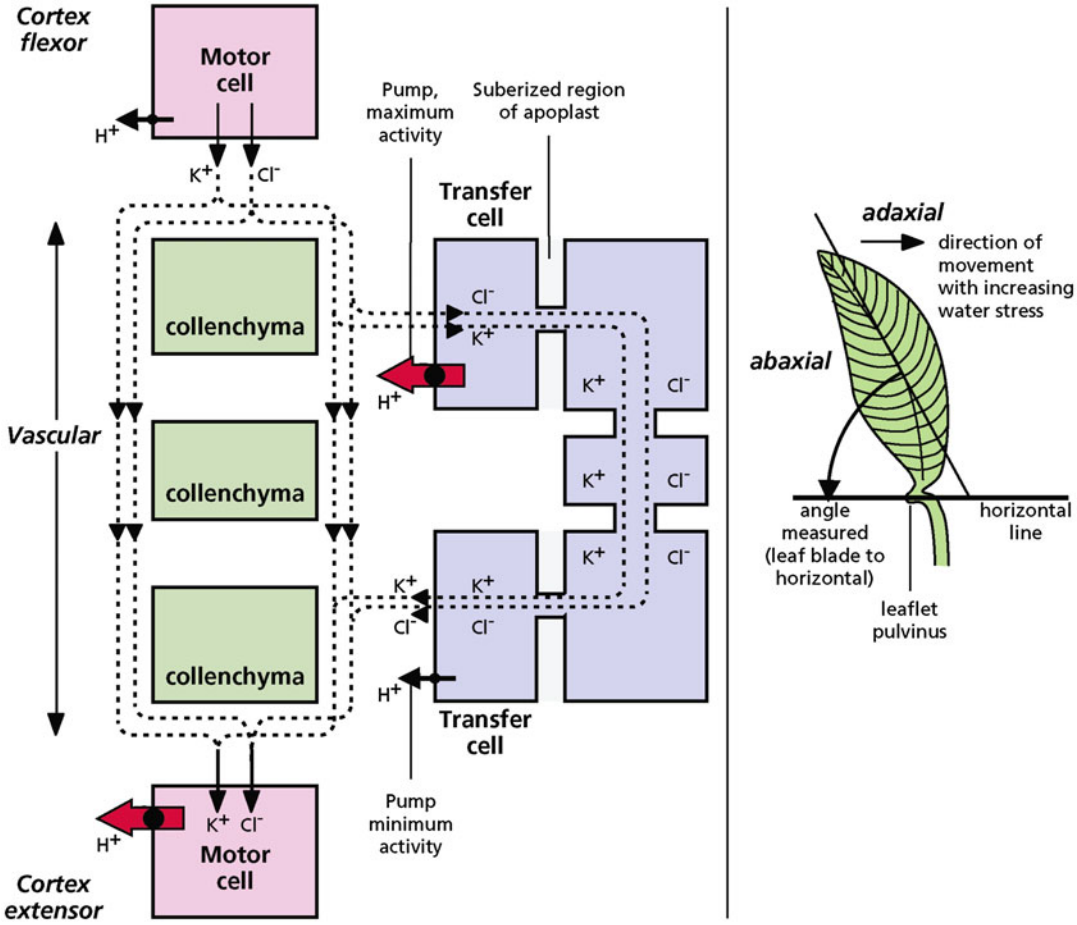

Fig. 5.34 A flow diagram of the direction and pathways of net K^+, Cl^-, and H^+ movements in a pulvinus during leaflet opening (after Satter and Galston 1981; Oosterhuis et al. 1985).

Leaf movements of *Phaseolus vulgaris* (common bean) depend on air temperature (Fu and Ehleringer 1989). The effect of these leaf movements is that at a low air temperature the leaf is oriented in such a way as to enhance the incident radiation, whereas the opposite occurs at a high air temperature. As a result, the leaf temperature is closer to the optimum for photosynthesis (Fig. 5.36). The air temperature that induces the leaf movements in bean is perceived in the pulvinus, rather than in the leaf itself.

Other acclimations and adaptations that affect plant transpiration are discussed in Sect. 6.2.2; Fig. 5.37.

5.7 Water Availability and Growth

During incipient water-stress, specific genes are induced. Some water-stress-induced gene products protect cellular structures from the effects of water loss, whereas others are involved in the regulation of genes for signal transduction in the water-stress response. The protective proteins include **water-channel** proteins (**aquaporins**) (Sect. 5.5.2), enzymes required for the biosynthesis of various **compatible solutes** (Sect. 5.4.1), proteins that may **protect** macromolecules and membranes, **proteases** for protein turnover, **detoxification enzymes**

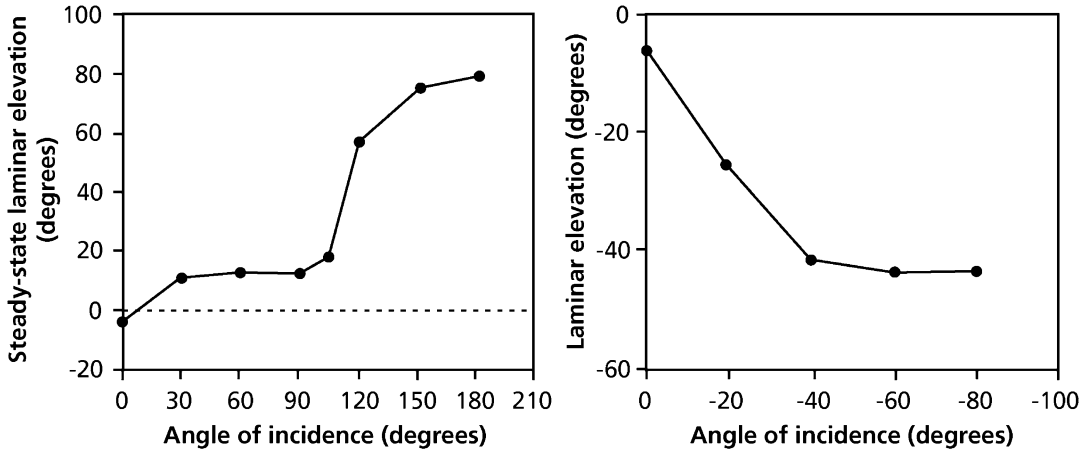

Fig. 5.35 The orientation of the terminal leaf of a composite leaf of *Melilotus indicus* (annual yellow sweetclover), as dependent on the angle of the incident radiation. An angle of 0° and + 180° of the light refers to light in the horizontal plane, from the tip to the base of the leaf, and from the base to the tip, respectively. An angle of +90° and −90° refers to light in the vertical plane, coming from above and below, respectively. For the leaf orientation the same terminology is followed. (Left) the pulvinus is irradiated from above. (Right) the pulvinus is irradiated from below (after Schwartz et al. 1987). Copyright American Society of Plant Biologists.

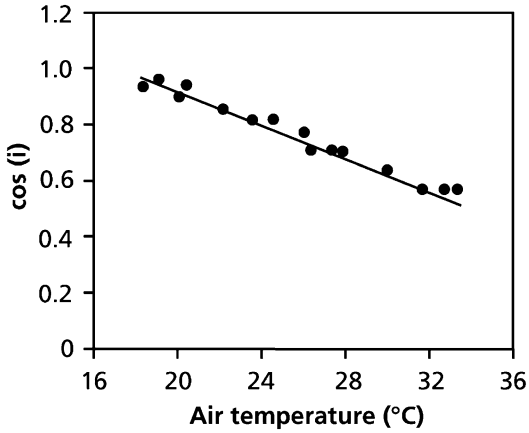

Fig. 5.36 The correlation between the cosine of the angle between the incident light beam and the vector normal to the leaf lamina of *Phaseolus vulgaris* (common bean) as dependent on air temperature. Irradiance, atmospheric CO_2 concentration, and vapor pressure deficit were constant (after Fu and Ehleringer 1989). Copyright American Society of Plant Biologists.

(*e.g.*, catalase and superoxide dismutase) (Zhu 2002; Bray 2004). Aquaporin-encoding genes are also expressed in needles of *Picea glauca* (white spruce) after exposure to high air humidity (Fig. 5.38). This suggests that these proteins also facilitate radial water movement from the needle epidermis toward the vascular tissue, providing a water source from melting snow for embolism repair, before the beginning of the growing season (Laur and Hacke 2014). The protective proteins are predominantly hydrophilic and they are probably located in the cytoplasm where they are involved in the sequestration of ions, which become concentrated during cellular dehydration. They are amphiphilic α-helices (*i.e.* they contain both hydrophilic and hydrophobic parts). The hydrophilic part binds ions, thus preventing damage, whereas the hydrophobic part is associated with membranes. Other proteins have many charged amino acids and possibly have a large water-binding capacity. Some of the proteins may protect other proteins, by replacing water, be involved in renaturation of unfolded proteins, or have a chaperon function (*i.e.* allow the transport of proteins across a membrane, on their way to a target organelle) (Bray 1993).

At a low soil water potential, the rate of photosynthesis decreases, largely due to a decline in stomatal conductance (Sect. 2.5.1). As pointed out in Sect. 10.5.3, however, effects of water stress on growth are largely accounted for by physiological processes other than photosynthesis. Many processes in the plant are far more

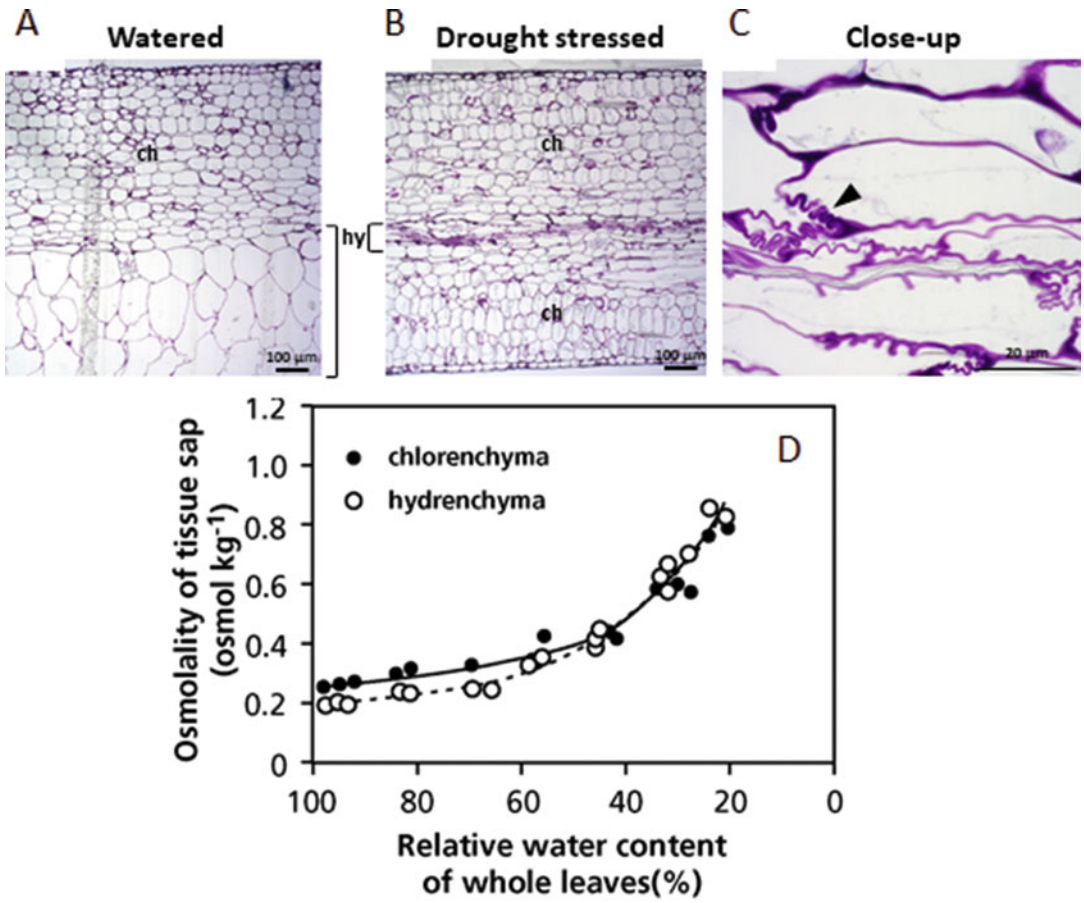

Fig. 5.37 (Top) Comparative morphology and anatomy of *Aloe helenae* (Asphodelaceae). (**A**, **B**) Transverse sections (marked by dashed squares) of hydrenchyma tissue stained with toluidine blue showing typical leaf tissue arrangement in *Aloe* species with hydrenchyma (hy), surrounded by an outer photosynthetic chlorenchyma (ch), epidermis and cuticle. (**C**) Convoluted folding of hydrenchyma cell walls in drought-stressed plants indicated by arrow (Ahl et al. 2019). Copyright John Wiley and Sons. (**D**) The osmolality of the hydrenchyma and chlorenchyma sap of *Peperomia magnoliaefolia* (desert privet) as dependent on the relative water content of whole leaves. The data in A and B refer to results obtained with detached and attached leaves, respectively; the broken line gives the relative water content if both tissues would lose water at the same rate (after Schmidt and Kaiser 1987). Copyright American Society of Plant Biologists.

sensitive to a low water potential than are stomatal conductance and photosynthesis. The growth reduction at a low soil water potential is therefore more likely due to inhibition of more sensitive processes such as **cell elongation** and **protein synthesis**; these processes are, at least partly, also controlled by **ABA** (Box 10.1).

Above-ground plant parts respond more strongly to a decreased soil water potential than do roots. Is this perhaps due to a much greater effect of the low water potential on growth of leaves, as compared with that of the roots, simply because they are closer to the source of water? Do roots and leaves, on the other hand, have a

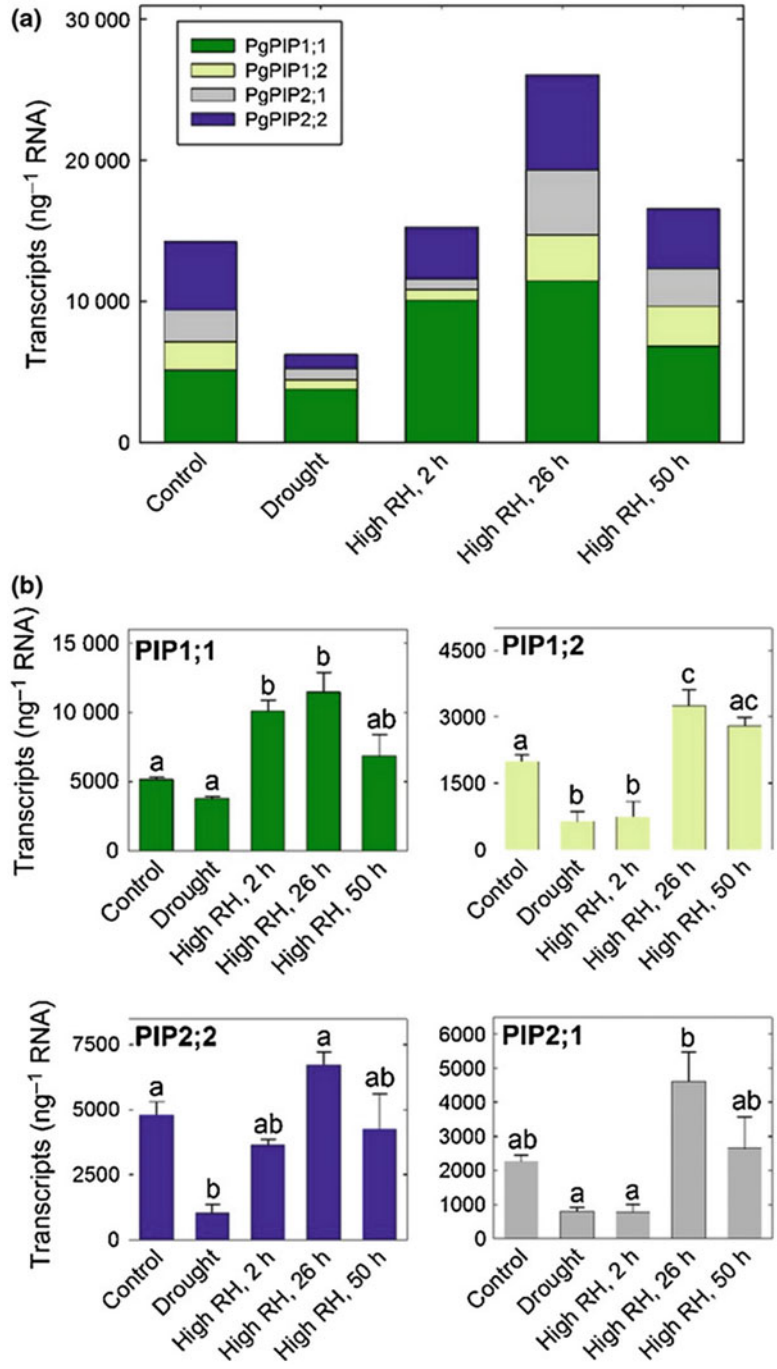

Fig. 5.38 Aquaporin transcript amounts in needles of well-watered (Control) and drought-stressed (Drought) white spruce (*Picea glauca*) plants. Transcript amounts were also measured 2, 26 and 50 h after drought-stressed plants had been transferred to a high-humidity environment. (**A**) Cumulative aquaporin transcript amounts in needles. Individual genes are labeled with different colors. Among the different transcripts, *PgPIP1;1* ranked first in terms of its proportion to the total number of mRNA molecules. (**B**) Transcript abundance of *PgPIP1;1*, *PgPIP1;2*, *PgPIP2;1* and *PgPIP2;2*. Values are means ± SE from three biological samples which were tested in triplicate. Significant differences are indicated by unique letters ($P \leq 0.05$). (Laur and Hacke 2014). Copyright Trustees of The New Phytologist.

different sensitivity for the water potential? In *Zea mays* (corn), the soil water potential causing growth reduction is indeed lower (more negative) for roots than it is for leaves, but this does not provide a conclusive answer to our question. In Sect. 10.5.3, we address this problem more elaborately. Lowering the water potential enhances the transport of assimilates to the roots which is

probably due to the growth reduction of the leaves. Because photosynthesis is less affected than leaf growth is, sugar import as well as root growth may be enhanced, with the overall effect that the leaf area ratio decreases in response to a decrease in soil water potential. That is, the evaporative surface is reduced, relative to the water-absorbing surface.

5.8 Adaptations to Drought

Plants have adapted to a lack of water in the environment either by avoiding drought or by tolerating it. **Desert annuals** and drought-deciduous species **avoid** drought by remaining dormant until water arrives. Other plants in dry or seasonally dry environments avoid drought by producing roots with access to deep groundwater (**phraetophytes**). The alternative strategy is to **tolerate** drought. Tolerance mechanisms are found in evergreen shrubs and in plants that can dry out in the absence of water and 'resurrect' upon exposure to water. Many plants in dry habitats exhibit intermediate strategies. For example, succulents, especially those with the CAM pathway (Sect. 2.10), minimize effects of drought by opening their stomata at night and concentrating their activity in wet seasons, but they also have many characteristics typical of drought-tolerant species.

5.8.1 Desiccation-Avoidance: Annuals and Drought-Deciduous Species

A large proportion of the plants in deserts are annuals with no specific physiological tolerance of desiccation. As is further discussed in Sect. 11.2.2, seeds of these species may germinate only after heavy rain. These species grow very fast following germination, often completing their life cycle in 6 weeks or less. These plants typically have rapid rates of photosynthesis and transpiration as well as a high leaf area ratio to support their rapid growth (Mooney et al. 1976).

The most obvious mechanism of acclimation to drought is perhaps a decrease in canopy leaf area. This can be rapid, through **leaf shedding**, or more slowly, through adjustments in allocation pattern (Sect. 10.5.3). In general, drought-deciduous species in seasonally-dry tropical forests have high stomatal conductance and high rates of photosynthesis and transpiration when water is available, but tend to be more vulnerable to embolim, and lose their leaves and enter **dormancy** under conditions of low water potential. As with desert annuals, their leaves exhibit no physiological adaptations for drought tolerance or water conservation. The advantages of a drought-deciduous strategy (fast rates of photosynthesis and growth under favorable conditions) are offset by the cost of producing new leaves in each new growth period. Therefore, this strategy can only increase in abundance in fertile habitats. Some species [*e.g.*, *Fouqueria splendens* (ocotillo) in the deserts of North America] produce and lose leaves as many as six times per year. There is typically a 2–4 week lag between onset of rains and full canopy development of drought-deciduous species. It is, therefore, not surprising that drought-tolerant evergreens displace drought-deciduous species as rains become more frequent and water availability increases (Fig. 5.39).

Some desert plants, known as **phreatophytes**, produce extremely deep roots that tap the water table. Like the desert annuals and drought-deciduous shrubs, these plants generally have high rates of photosynthesis and transpiration with little capacity to restrict water loss or withstand drought. For example, honey mesquite (*Prosopis glandulosa*) commonly occupies desert washes in the southeastern United States, where there is little surface water but where groundwater is close enough to the surface that seedlings can occasionally produce deep enough roots to reach this groundwater in wet years. In the same area, *Tamarix chinensis* (saltcedar), which is an exotic phreatophyte, has lowered the water table sufficiently through its high transpiration rate that other species of intermediate rooting depth are being eliminated (Van Hylckama 1974). Deep-rooted plants can also be found in evergreen

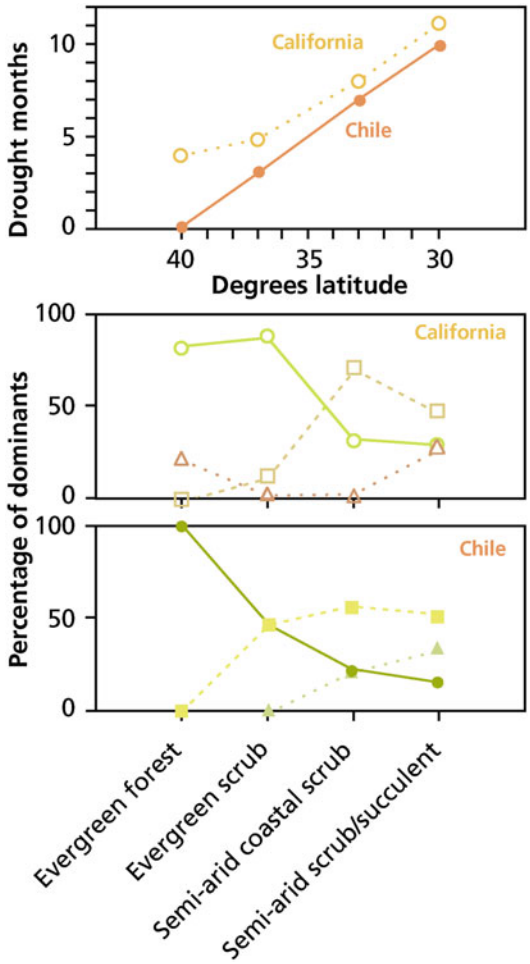

Fig. 5.39 Leaf types of the dominant plants in major vegetation types along a latitudinal drought gradient in California and Chile. Leaf types are evergreen (circles), deciduous (squares), and succulent (triangles) (after Mooney and Dunn 1970).

tropical rainforests that experience a seasonal drought (Nepstad et al. 1994).

5.8.2 Dessication-Tolerance: Evergreen Shrubs

Most evergreen shrubs are exposed to water stress during part of the year, whether during the summer in a Mediterranean climate, or in winter in cooler climates or in neotropical savannas.

Relatively drought-tolerant species [*e.g.*, *Olea oleaster* (olive) in Fig. 5.29] withstand lower water potentials before stomatal closure and before loss of turgor, because they have relatively elastic cell walls (low elastic modulus, ε) and a high resistance to embolism of xylem. Natural selection leading to scleromorphic and evergreen growth habits is complex. Low P availability is a major environmental factor driving the evolution of evergreen, scleromorphic leaves (Loveless 1961, 1962). Low P availability also selects for communities with higher embolism resistance in tropical forests (Oliveira et al. 2019).

Mediterranean shrubs, and rainforest and savanna trees are also characterized by **dual** or **dimorphic root systems**, having both deep taproots and shallow feeder roots. This architecture allows access to semi-permanent groundwater supplies as well as to surface precipitation (Rundel 1995). A large number of woody shrub and tree species [*e.g.*, *Banksia prionotes* (acorn banksia), and *Banksia ilicifolia* (holly-leafed banksia)] of the nutrient-impoverished sandplains of southwest Australia possess dimorphic root systems. Superficial lateral roots exploit nutrient-enriched surface layers during the wet winter season (Sect. 9.2.2.5.2), and a deeply penetrating sinker taps underground sources of water throughout the year, and especially during the prolonged dry summer. Sinkers may reach the water table at 2.5–2.9 m depth. They have xylem vessels with diameters ranging from 55 to 120 μm, as opposed to 30–70 μm for lateral roots. As a result, the hydraulic conductance (on the basis of organ transectional area) of sinker roots ranges from 30 to 780.10^{-3} m^2 MPa^{-1} s^{-1}, which is consistently greater than that of associated laterals ($2–50.10^{-3}$ m^2 MPa^{-1} s^{-1}) or trunks ($0.5–9.10^{-3}$ m^2 MPa^{-1} s^{-1}) (Pate et al. 1995).

5.8.3 'Resurrection Plants'

An extreme case of desiccation tolerance of whole plants is that of **resurrection plants** or '**poikilohydric**' plants. Even after their protoplasm has dried out to the extent that the water potential of the cells is in equilibrium with dry air (with a relative humidity of 20–40%), they can

almost fully restore their physiological activity (Gaff 1981). Their dry, shriveled, and seemingly dead leaves regain turgor in less than 24 h after a shower which makes the term 'resurrection' most appropriate. Many mosses and ferns and some angiosperms, including woody species [*e.g.*, *Myrothamnus flabellifolius* (resurrection bush)] are characterized as resurrection plants. They are mostly found in Southern Africa, North America, Brazil, and Australia in environments where droughts occur regularly (*e.g.*, on rocky substrates). Rock outcrops in the tropics are considered centers of diversity of vascular resurrection plants, and Velloziaceae is the most abundant and species-rich angiosperm family of resurrection plants (Porembski and Barthlott 2000); there are only two European genera of angiosperm resurrection plants, *Ramonda* and *Haberla* (Gesneriaceae).

There are two strategies among resurrection angiosperms:

1. Those that lose chlorophyll and break down their chloroplasts upon drying (**poikilochlorophyllous**);
2. Those that retain some or all of their chlorophyll and chloroplast ultrastructure (**homoiochlorophyllous**).

The poikilochlorophyllous species tend to take longer to recover than do the homoiochlorophyllous ones, because they must reconstitute their chloroplasts (Sherwin and Farrant 1996). All poikilochlorophyllous species are monocots, but some of the grasses are homoiochlorophyllous. The two strategies may have evolved in response to light stress, which is exacerbated during dehydration and rehydration. While the leaf tissue is dehydrating, dry, or rehydrating, light absorption should be minimal and the energy that is absorbed must be dissipated. The leaves of homoiochlorophyllous plants tend to roll or curl and produce protective pigments (*e.g.*, anthocyanins), that act as screens. The poikilochlorophyllous plants tend to have elongate leaves that can only fold, thus leaving a greater surface exposed to light (Sherwin and Farrant 1998).

The exact nature of the reactivation of the physiological processes is not yet fully understood. The following must generally hold:

1. Any damage incurred during the drying phase is not lethal;
2. Some of the metabolic functions are maintained in the dry state, to an extent that they can be deployed upon rewetting;
3. Any damage incurred is repaired during or after rehydration.

Even though the dehydrated homoiochlorophyllous resurrection plants may have lost most of their green color, their thylakoid membranes, chlorophyll complexes, mitochondria, and other membrane systems remain intact. Elements of the protein-synthesizing machinery, including mRNA, tRNA, and ribosomes, also remain functional. Using inhibitors of transcription and translation shows that membrane protection and repair does not require transcription of new gene products or translation of existing transcripts. Full recovery of the photosynthetic apparatus in the homoiochlorophyllous *Craterostigma wilmsii* requires protein synthesis, but not gene transcription. On the other hand, for the poikilochlorophyllous *Xerophyta humilis* both transcription and translation are required for full recovery (Dace et al. 1998). *Myrothamnus flabellifolius* (resurrection bush) is a South African resurrection plant with a woody stem. Transpiration rates in well-watered plants are moderate, generating xylem water potentials of -1 to -2 MPa. Acoustic emissions indicate extensive embolism events at xylem water potentials of -2 to -3 MPa. On re-watering, the root pressures are low (0.0024 MPa), but capillary forces are adequate to account for the refilling of xylem vessels and re-establishment of hydraulic continuity even when water was under a mild tension of -0.008 MPa (Sherwin et al. 1998). *Vellozia flavicans* in the cerrado in central Brazil takes up water via its shoot, as evidenced by sap-flow measurements (Oliveira et al. 2005).

A large number of enzymes associated with carbon metabolism remain intact in the dry state, as found for *Selaginella lepidophylla* (resurrection plant) from the Chihuahua Desert in Texas

Table 5.9 The activity of three enzymes associated with photosynthesis and three involved in respiration*.

Enzyme	Enzyme activity enzyme units g^{-1} DM		Conservation
	Desiccated	Hydrated	%
Photosynthetic enzymes:			
Ribose-5-phosphate isomerase	7.56	9.24	82
Rubisco	0.60	0.96	62
(NADPH)Triose-phosphate dehydrogenase	0.48	1.80	27
Respiratory enzymes:			
Citrate synthase	1.76	2.05	86
Malate dehydrogenase	2.89	2.97	97
(NADH)Triose-phosphate dehydrogenase	1.13	1.40	81

Source: Harten and Eickmeier (1986)

*They were isolated from the resurrection plant *Selaginella lepidophylla*, both from dehydrated plants and 24 h after rehydration

(Table 5.9; Harten and Eickmeier 1986). About 24 h after rewetting, the plants have regained their green appearance, and rates of photosynthesis and respiration are again close to those of normal wet plants. At that time, the activity of many enzymes has increased, compared with that in dehydrated plants. On average, 74% of the enzyme activity remains in the dry phase; however, this value is only 27% for the NADPH-dependent triose phosphate dehydrogenase in *Selaginella lepidophylla*. In addition, in a bryophyte, *Acrocladium cuspidatum*, the activity of this photosynthetic enzyme is reduced more than that of all other enzymes tested. It appears that enzymes involved in respiratory metabolism are conserved better than are those associated with photosynthesis. The increase in activity of the enzymes that are not fully conserved in the dry phase may involve *de novo* protein synthesis (NADP-dependent triose phosphate dehydrogenase, Rubisco). Rapid *de novo* synthesis, in addition to the maintenance of functional enzymes, is clearly important in the reactivation phase after rewetting. Maintenance of the protein-synthesizing machinery, therefore, appears to be of vital importance.

During dehydration of the resurrection plants, as in 'ordinary' plants, the phytohormone **ABA** accumulates. In resurrection plants, ABA induces the **transcription** of a number of genes, which code for proteins that are closely related to those that are abundantly induced during embryo maturation in the seeds of many higher plants or to some extent in water-stressed seedlings (Bartels and Salamini 2001). In the small, herbaceous, homoiochlorophyllous *Craterostigma plantagineum*, **sucrose** accumulates to high concentrations (up to 40% of the dry mass), while the concentration of the C8-sugar octulose declines; upon rehydration, sucrose is converted back into octulose (Bartels and Salamini 2001). In the European *Ramonda* and *Haberlea* species (Gesneriaceae), sucrose is also the predominant sugar that accumulates upon desiccation (Müller et al. 1997). Sucrose and other solutes play a major role in stabilizing subcellular components, including membranes and proteins. The sugars ensure that the small amount of water left in the tissue occurs in a 'glassy' state, like the glass in our windows, which is actually a fluid. Some of the gene products are proteins with both hydrophobic and hydrophilic zones; they may bind ions and be membrane-associated (Bartels and Salamini 2001). These probably have an 'osmoprotective' function, reducing potential damage by high solute concentrations. Other gene products are likely involved in carotenoid biosynthesis (Alamillo and Bartels 1996).

The genes expressed upon dehydration of resurrection plants are similar to those expressed at the end of the ripening of the embryo in **ripening seeds**, described as **late embryogenesis abundant** genes, or *lea* genes. The proteins involved in the survival of dehydrated embryos in dry seeds are similar to those that protect resurrection

plants in their dehydrated state (**LEA proteins** or **dehydrins**). Dehydrins are rich in polar and charged amino acids; their expression is induced by environmental stresses or the application of ABA (Bartels and Salamini 2001). Some of the genes that are expressed in resurrection plants during dehydration are also expressed in water-stressed leaves, and more so in the more desiccation-resistant *Populus popularis* (poplar) than in the less resistant *Populus tomentosa* (Chinese white poplar) (Pelah et al. 1997).

5.9 Winter Water Relations and Freezing Tolerance

As discussed in Sect. 5.5.3.2, subzero temperatures may lead to the formation of air bubbles in xylem conduits, hence to **embolism**. The water in the xylem generally freezes between 0 and −2 °C. Some water transport may still continue after embolism has occurred, although at a very low rate (around 3% of normal rates). This slow movement probably occurs either through late-wood tracheids or through cell-wall cavities (Tranquillini 1982).

Frost damage is also associated with the formation of extracellular **ice crystals** that cause severe dehydration of the cytoplasm and the formation of crystals inside the cells, both being associated with damage to membranes and organelles. The cells become leaky and their water potential declines sharply. Resistance mechanisms predominantly involve the prevention of the formation of intracellular ice crystals, by restricting freezing to the extracellular compartment or by biochemical mechanisms to withstand dehydration (Thomashow 1999; Shinozaki et al. 2003). During cold acclimation, leaves of *Secale cereale* (rye) produce '**antifreeze proteins**' in their apoplast. These proteins interact directly with ice *in planta* and reduce freezing injury by slowing the growth and recrystallization of ice, but have no specific cryoprotective activity (Griffith et al. 2005). At a molecular level, the responses to low temperature share major elements with plant responses to dehydration (Yamaguchi-Shinozaki and Shinozaki 2006).

Changes in the composition of cell walls play a major role in preventing ice formation. For example, deposition of **pectin** in the cell wall reduces the size of the microcapillaries in the walls, allowing a more negative water potential. Pectin formation in the pits between xylem and xylem-parenchyma cells (Fig. 5.16) closes these pores, so that water remains in the cells (Fig. 5.40). In spring, pectin is enzymatically removed again, coinciding with the loss of the capacity to tolerate deep supercooling (Wisniewski et al. 1991). Deep supercooling is only possible to temperatures around −40 °C; below that temperature ice formation occurs in the absence of crystallization nuclei.

In subarctic trees, which tolerate temperatures below −40 °C, supercooling does not play a role. Ice formation starts around −2 to −5 °C, but only in the cell wall. The cold acclimation that occurs in autumn is triggered by photoperiod and exposure to cool temperatures. It involves synthesis of membrane lipids with less saturated fatty acids, so they remain flexible at low temperatures, and the production of osmotically active solutes. Cells that would freeze at −3 to −5 °C in summer remain unfrozen to −40 °C in winter. At subfreezing temperatures, ice forms first in cell walls, reducing the concentration of extracellular liquid water. Water moves out of cells along this water-potential gradient, increasing the intracellular solute concentration, which prevents intracellular freezing. The biochemical mechanisms to withstand this winter desiccation are identical to those caused by lack of water in deserts. It is therefore not surprising that species that tolerate extremely low temperatures are also highly desiccation-tolerant.

5.10 Salt Tolerance

Halophytes are species that typically grow in soils with high levels of NaCl and, hence, a low water potential. They accumulate NaCl in their

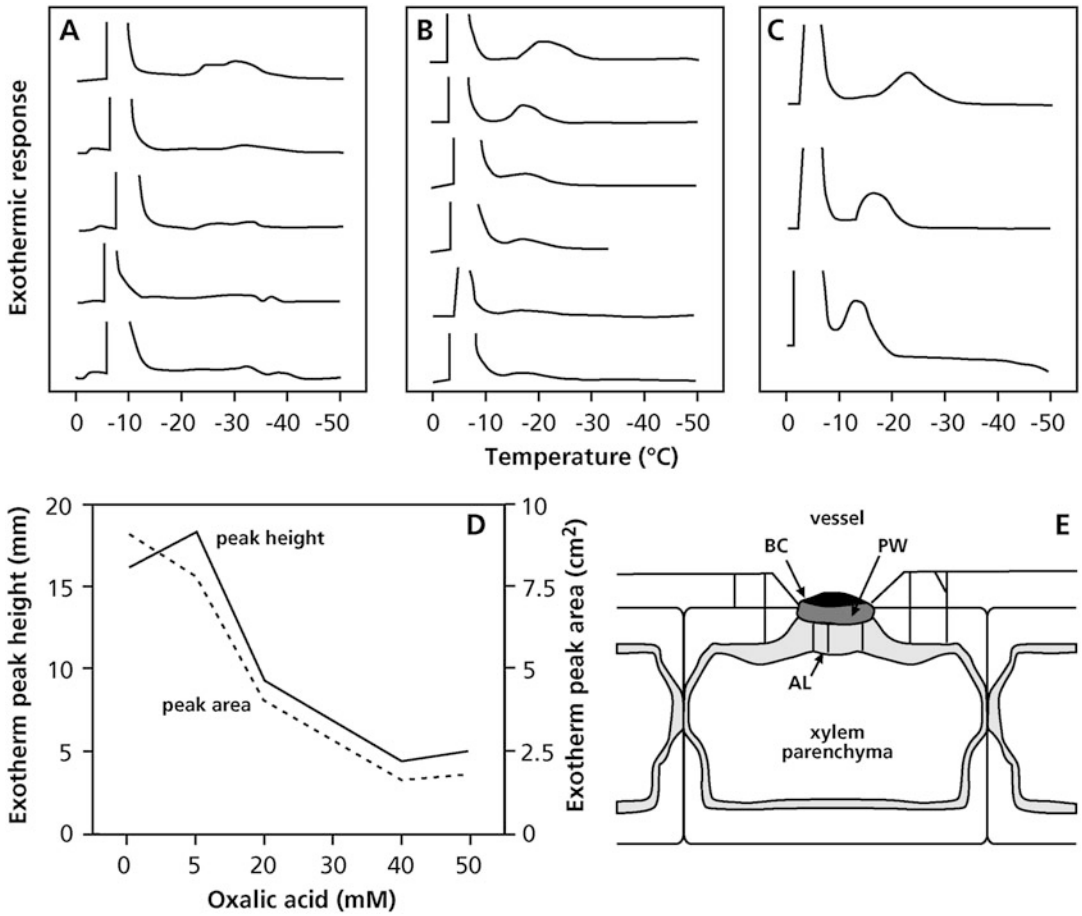

Fig. 5.40 (**A**–**C**) The effect of macerase (an enzyme that hydrolyzes pectin), oxalic acid, and EGTA (both bind Ca^{2+}, responsible for 'cross-linking' in pectin) on the exothermal response. The left peak (which is not relevant in the present context) is due to freezing of extracellular water. The peak to the right decreases, or shifts to lower temperatures, upon removal of pectin. The data in (**B**) have been replotted in (**D**), both as peak height and as peak area *versus* the concentration of oxalic acid. (**E**) The structure of a pit between the xylem and a xylem-ray parenchyma cell of *Prunus persica* (peach). The pit membrane consists of three layers: an outermost black cap (BC) or toruslike layer, a primary wall (PM), and an amorphous layer (AL). The channels are meant to diagrammatically illustrate how pore size or continuity would affect the ability of a cell to exhibit deep supercooling (after Wisniewski et al. 1991). Copyright American Society of Plant Biologists.

vacuoles. By contrast, **glycophytes** have a limited capacity to transport NaCl into their vacuoles and are unable to tolerate high salinity levels. Cytoplasmic enzymes of glycophytes and halophytes are very similar with respect to their sensitivity to high concentrations of inorganic solutes (Fig. 5.8). We discuss tolerance mechanisms of halophytes in Sect. 9.3.4.

5.11 Final Remarks: The Message That Transpires

What have we finally learned from this chapter on water relations? First, that water is a major factor limiting plant growth in many ecosystems, and also that in different species fascinating mechanisms have evolved to cope with this limiting factor, ranging from **avoidance** to **tolerance**.

Table 5.10 Summary of characteristics of drought-sensitive and drought-tolerant evergreen species.

Characteristic	Drought-sensitive species	Drought-tolerant species
Maximum transpiration rate	High	Low
Maximum photosynthetic rate	High	Low
Maximum stomatal conductance	High	Low
Specific leaf area	High	Low
Leaf size	Large	Small
Leaf longevity	Low	High
Potential growth rate	High	Low
Root mass ratio	Low	High
Leaf compatible solute concentration	Low	High
Water potential at turgor loss	High	Low
Stomatal regulation	Iso/anisohydric	Anisohydric
Safety margin for embolism	Small	Large

Tolerance at one level (*e.g.*, of the roots) may allow drought avoidance at another (*e.g.*, of the leaves). Plants have adapted to a limiting supply of water in their environment, but all plants, to varying degrees, can also acclimate to an environment where water is scarce.

The characteristics that enable plants to acquire water from different sources and tolerate drought are strongly interdependent (Table 5.10). To appreciate these mechanisms, a full understanding of the biophysical, physiological, and molecular aspects of plant water relations is essential. Such an appreciation is pivotal, if we aim to improve the performance of crops in dry environments. This is not to say that other ecophysiological aspects are not of equal, or even greater, importance. In fact, vigorous early growth and early flowering may also greatly contribute to a greater water-use efficiency over the entire season, when evaporative demands are considerably less.

Resurrection plants offer one of the most remarkable examples of how plants cope with a shortage of water in their environment. At one stage, it may have been considered esoteric to study these peculiar plants, which would seem useless from an economic point of view. It now becomes increasingly clear, however, that resurrection plants show many similarities to ripening seeds and leaves that are able to cope with water stress. As such, resurrection plants offer a model system to study water-stress resistance, and they may be a source of genes to use to improve the performance of new crop varieties in dry environments. As so often in science, possibilities for applications emerge that are based on fascinating discoveries on fundamental aspects of plant biology.

References

Ahl LI, Mravec J, Jørgensen B, Rudall PJ, Rønsted N, Grace OM. 2019. Polysaccharide composition of folded cell walls in drought-stressed succulent Aloe species. *Plant Cell Environ* **42**: 2458–2471.

Alamillo JM, Bartels D. 1996. Light and stage of development influence the expression of desiccation-induced genes in the resurrection plant *Craterostigma plantagineum*. *Plant Cell Environ* **19**: 300–310.

Alder NN, Sperry JS, Pockman WT. 1996. Root and stem xylem embolism, stomatal conductance, and leaf turgor in Acer grandidentatum populations along a soil moisture gradient. *Oecologia* **105**: 293–301.

Alder NN, Pockman WT, Sperry JS, Nuismer S. 1997. Use of centrifugal force in the study of xylem cavitation. *J Exp Bot* **48**: 665-674.

Anderegg WRL, Klein T, Bartlett M, Sack L, Pellegrini AFA, Choat B, Jansen S. 2016. Meta-analysis reveals that hydraulic traits explain cross-species patterns of drought-induced tree mortality across the globe. *Proc Natl Acad Sci USA* **113**: 5024–5029.

Anderegg WRL, Wolf A, Arango-Velez A, Choat B, Chmura DJ, Jansen S, Kolb T, Li S, Meinzer FC, Pita P, Resco de Dios V, Sperry JS, Wolfe BT, Pacala S. 2018. Woody plants optimise stomatal behaviour relative to hydraulic risk. *Ecol Lett* **21**: 968–977.

Andersen TG, Naseer S, Ursache R, Wybouw B, Smet W, De Rybel B, Vermeer JEM, Geldner N. 2018. Diffusible repression of cytokinin signalling produces endodermal symmetry and passage cells. *Nature* **555**: 529.

Appezzato-da-Glória B, Cury G, Soares MKM, Rocha R, Hayashi AH. 2008. Underground systems of Asteraceae species from the Brazilian Cerrado. *J Torrey Bot Soc* **135**: 103–113.

Arber A. 1923. Leaves of the Gramineae. *Bot Gaz* **76**: 374–388.

Assmann SM. 1999. The cellular basis of guard cell sensing of rising CO_2. *Plant Cell Environ* **22**: 629–637.

Assmann SM, Shimazaki K-i. 1999. The multisensory guard cell. Stomatal responses to blue light and abscisic acid. *Plant Physiol* **119**: 809–816.

Assmann SM, Snyder JA, Lee Y-RJ. 2000. ABA-deficient (*aba1*) and ABA-insensitive (*abi1-1*, *abi2-1*) mutants of *Arabidopsis* have a wild-type stomatal response to humidity. *Plant Cell Environ* **23**: 387–395.

Atkinson RRL, Mockford EJ, Bennett C, Christin P-A, Spriggs EL, Freckleton RP, Thompson K, Rees M, Osborne CP. 2016. C4 photosynthesis boosts growth by altering physiology, allocation and size. *Nat Plants*: 16038.

Baas P 1986. Ecological patterns in xylem anatomy. In: Givnish TJ ed. *On the Economy of Plant Form and Function*. Cambridge Cambridge University Press, 327–352.

Bartels D, Salamini F. 2001. Desiccation tolerance in the resurrection plant *Craterostigma plantagineum*. A contribution to the study f drought tolerance at the molecular level. *Plant Physiol* **127**: 1346–1353.

Bartels D, Sunkar R. 2005. Drought and salt tolerance in plants. *Crit Rev Plant Sci* **24**: 23–58.

Bartlett MK, Scoffoni C, Sack L. 2012. The determinants of leaf turgor loss point and prediction of drought tolerance of species and biomes: a global meta-analysis. *Ecol Lett* **15**: 393–405.

Beal WJ. 1886. The bulliform or hygroscopic cells of grasses and sedges compared. *Bot Gaz* **11**: 321–326.

Berry ZC, Emery NC, Gotsch SG, Goldsmith GR. 2019. Foliar water uptake: processes, pathways, and integration into plant water budgets. *Plant Cell Environ* **42**: 410–423.

Binks O, Meir P, Rowland L, da Costa ACL, Vasconcelos SS, de Oliveira AAR, Ferreira L, Christoffersen B, Nardini A, Mencuccini M. 2016. Plasticity in leaf-level water relations of tropical rainforest trees in response to experimental drought. *New Phytol* **211**: 477–488.

Bittencourt PRL, Pereira L, Oliveira RS. 2016. On xylem hydraulic efficiencies, wood space-use and the safety–efficiency tradeoff. *New Phytol* **211**: 1152–1155.

Blatt MR. 2000. Cellular signaling and volume control in stomatal movements in plants. *Annu Rev Cell Develop Biol* **16**: 221–241.

Blatt MR, Grabov A. 1997. Signalling gates in abscisic acid-mediated control of guard cell ion channels. *Physiol Plant* **100**: 481–490.

Bleby TM, Burgess SSO, Adams MA. 2004. A validation, comparison and error analysis of two heat-pulse methods for measuring sap flow in *Eucalyptus marginata* saplings. *Funct Plant Biol* **31**: 645–658

Boanares D, Ferreira BG, Kozovits AR, Sousa HC, Isaias RMS, França MGC. 2018. Pectin and cellulose cell wall composition enables different strategies to leaf water uptake in plants from tropical fog mountain. *Plant Physiol Bochem* **122**: 57–64.

Böhm J. 1893. Capillarität und Saftsteigen. *Ber Dtsch Bot Ges* **11**: 203–212.

Borchert R. 1994. Soil and stem water storage determine phenology and distribution of tropical dry forest trees. *Ecology* **75**: 1437–1449.

Boutton TW, Archer SR, Midwood AJ. 1999. Stable isotopes in ecosystem science: structure, function and dynamics of a subtropical savanna. *Rap Comm Mass Spectrom* **13**: 1263–1277.

Boyer JS. 1985. Water transport. *Annu Rev Plant Physiol* **36**: 473–516.

Bray EA. 1993. Responses to water deficit. *Plant Physiol* **103**: 1035–1040.

Bray EA. 2004. Genes commonly regulated by water-deficit stress in *Arabidopsis thaliana*. *J Exp Bot* **55**: 2331–2341.

Bréda N, Granier A, Barataud F, Moyne C. 1995. Soil water dynamics in an oak stand. *Plant Soil* **172**: 17–27.

Breshears DD, McDowell NG, Goddard KL, Dayem KE, Martens SN, Meyer CW, Brown KM. 2008. Foliar absorption of intercepted rainfall improves woody plant water status most during drought. *Ecology* **89**: 41–47.

Brodersen CR, McElrone AJ, Choat B, Matthews MA, Shackel KA. 2010. The dynamics of embolism repair in xylem: *in vivo* visualizations using high-resolution computed tomography. *Plant Physiol* **154**: 1088–1095.

Brum M, Teodoro GS, Abrahão A, Oliveira RS. 2017. Coordination of rooting depth and leaf hydraulic traits defines drought-related strategies in the campos rupestres, a tropical montane biodiversity hotspot. *Plant Soil* **420**: 467–480.

Brum M, Vadeboncoeur MA, Ivanov V, Asbjornsen H, Saleska S, Alves LF, Penha D, Dias JD, Aragão LEOC, Barros F, Bittencourt P, Pereira L, Oliveira RS. 2019. Hydrological niche segregation defines forest structure and drought tolerance strategies in a seasonal Amazon forest. *J Ecol* **107**: 318–333.

Burgess SSO, Adams MA, Turner NC, Beverly CR, Ong CK, Khan AAH, Bleby TM. 2001. An improved

heat pulse method to measure low and reverse rates of sap flow in woody plants†. *Tree Physiol* **21**: 589–598.

Burgess SSO, Adams MA, Turner NC, Ong CK. 1998. The redistribution of soil water by tree root systems. *Oecologia* **115**: 306–311.

Burgess SSO, Bleby TM. 2006. Redistribution of soil water by lateral roots mediated by stem tissues. *J Exp Bot* **57**: 3283–3291.

Burgess SSO, Dawson TE. 2004. The contribution of fog to the water relations of *Sequoia sempervirens* (D. Don): foliar uptake and prevention of dehydration. *Plant Cell Environ* **27**: 1023–1034.

Burkhardt J, Basi S, Pariyar S, Hunsche M. 2012. Stomatal penetration by aqueous solutions – an update involving leaf surface particles. *New Phytol* **196**: 774–787.

Brodribb TJ, Skelton RP, McAdam SAM, Bienaimé D, Lucani CJ, Marmottant P. 2016. Visual quantification of embolism reveals leaf vulnerability to hydraulic failure. *New Phytol* **209**: 1403-1409.

Canadell J, Jackson RB, Ehleringer JB, Mooney HA, Sala OE, Schulze E-D. 1996. Maximum rooting depth of vegetation types at the global scale. *Oecologia* **108**: 583–595.

Canny MJ. 1997. Vessel contents during transpiration – embolisms and refilling. *Am J Bot* **84**: 1223.

Cassab GI, Eapen D, Campos ME. 2013. Root hydrotropism: an update. *Am J Bot* **100**: 14–24.

Chaumont F, Tyerman SD. 2014. Aquaporins: highly regulated channels controlling plant water relations. *Plant Physiol* **164**: 1600–1618.

Chenu C, Cosentino D 2011. Microbial regulation of soil structural dynamics. In: Ritz K, Young I eds. *The Architecture and Biology of Soils: Life in Inner Space*. Wallingford, Oxfordshire, UK: CABI, 37–70.

Chiariello NR, Field CB, Mooney HA. 1987. Midday wilting in a tropical pioneer tree. *Funct Ecol* **1**: 3–11.

Choat B, Brodribb TJ, Brodersen CR, Duursma RA, López R, Medlyn BE. 2018. Triggers of tree mortality under drought. *Nature* **558**: 531–539.

Choat B, Cobb AR, Jansen S. 2008. Structure and function of bordered pits: new discoveries and impacts on whole-plant hydraulic function. *New Phytol* **177**: 608–626.

Choat B, Drayton WM, Brodersen C, Matthews M, Shackel KA, Wada H, McElrone A. 2010. Measurement of vulnerability to water stress-induced cavitation in grapevine: a comparison of four techniques applied to a long-vesseled species. *Plant, Cell and Environment* **33**: 1502–1512.

Choat B, Jansen S, Brodribb TJ, Cochard H, Delzon S, Bhaskar R, Bucci SJ, Feild TS, Gleason SM, Hacke UG, Jacobsen AL, Lens F, Maherali H, Martinez-Vilalta J, Mayr S, Mencuccini M, Mitchell PJ, Nardini A, Pittermann J, Pratt RB, Sperry JS, Westoby M, Wright IJ, Zanne AE. 2012. Global convergence in the vulnerability of forests to drought. *Nature* **491**: 752–755.

Cochard H, Cruiziat P, Tyree MT. 1992. Use of positive pressures to establish vulnerability curves. Futher support for the air-seeding hypothesis and implications for pressure-volume analysis. *Plant Physiol* **100**: 205-209.

Cochard H, Lemoine D, Dreyer E. 1999. The effects of acclimation to sunlight on the xylem vulnerability to embolism in Fagus sylvatica L. *Plant Cell Environ* **22**: 101–108.

Colombi T, Kirchgessner N, Walter A, Keller T. 2017. Root tip shape governs root elongation rate under increased soil strength. *Plant Physiol* **174**: 2289–2301.

Comstock JP, Ehleringer JR. 1992. Correlating genetic variation in carbon isotopic composition with complex climatic gradients. *Proc Natl Acad Sci USA* **89**: 7747–7751.

Correia MJ, Pereira JS, Chaves MM, Rodrigues ML, Pacheo CA. 1995. ABA xylem concentrations determine maximum daily leaf conductance of field-grown *Vitis vinifera* L. plants. *Plant Cell Environ* **18**: 511–521.

Cowan I 1986. Economics of carbon fixation in higher plants. In: Givnish TJ ed. *On the Economy of Plant Form and Function*. Cambridge: Cambridge University Press, 133–170.

Cowan IR 1977. Water use in higher plants. In: McIntyre AK ed. *Water Planets, Plants and People*. Canberra: Australian Academy of Science, 71–107.

Crews LJ, McCully ME, Canny MJ, Huang CX, Ling LEC. 1998. Xylem feeding by spittlebug nymphs: some observations by optical and cryo-scanning electron microscopy. *Am J Bot* **85**: 449–460.

Dace H, Sherwin HW, Illing N, Farrant JM. 1998. Use of metabolic inhibitors to elucidate mechanisms of recovery from desiccation stress in the resurrection plant *Xerophyta humilis*. *Plant Growth Regul* **24**: 171–177.

Darwin CR. 1880. *The Power of Movement in Plants*. London: John Murray.

Darwin F. 1898. Observations on stomata. *Phil Trans R Soc Lond B* **190**: 531–621.

Davies WJ, Tardieu F, Trejo CL. 1994. How do chemical signals work in plants that grow in drying soil? *Plant Physiol* **104**: 309–314.

Dawson TE. 1993. Hydraulic lift and water use by plants: implications for water balance, performance and plant-plant interactions. *Oecologia* **95**: 565–574.

Dawson TE, Goldsmith GR. 2018. The value of wet leaves. *New Phytol* **0**.

Dawson TE, Mambelli S, Plamboeck AH, Templer PH, Tu KP. 2002. Stable isotopes in plant ecology. *Annu Rev Ecol Syst* **33**: 507–559.

Dixon HH, Joly J. 1894. On the ascent of sap. *Ann Bot* **8**: 468–470.

Dodd IC. 2005. Root-to-shoot signalling: assessing the roles of "up" in the up and down world of long-distance signalling in planta. *Plant Soil* **274**: 251–270.

Doerr SH, Shakesby RA, Walsh RPD. 2000. Soil water repellency: its causes, characteristics and hydro-geomorphological significance. *Earth-Sci Rev* **51**: 33–65.

Eamus D, Shanahan ST. 2002. A rate equation model of stomatal responses to vapour pressure deficit and drought. *BMC Ecology* **2**: 8.

Ehleringer JR, Cooper TA. 1988. Correlations between carbon isotope ratio and microhabitat in desert plants. *Oecologia* **76**: 562–566.

Ehleringer JR, Phillips SL, Schuster WSF, Sandquist DR. 1991. Differential utilization of summer rains by desert plants. *Oecologia* **88**: 430–434.

Eller CB, Lima AL, Oliveira RS. 2013. Foliar uptake of fog water and transport belowground alleviates drought effects in the cloud forest tree species, *Drimys brasiliensis* (Winteraceae). *New Phytol* **199**: 151–162.

Eller CB, Lima AL, Oliveira RS. 2016. Cloud forest trees with higher foliar water uptake capacity and anisohydric behavior are more vulnerable to drought and climate change. *New Phytol*: n/a-n/a.

Eller CB, Rowland L, Oliveira RS, Bittencourt PRL, Barros FV, da Costa ACL, Meir P, Friend AD, Mencuccini M, Sitch S, Cox P. 2018. Modelling tropical forest responses to drought and El Niño with a stomatal optimization model based on xylem hydraulics. *Phil Trans R Soc Lond B* **373**.

Enns LC, McCully ME, Canny MJ. 1998. Solute concentrations in xylem sap along vessels of maize primary roots at high root pressure. *J Exp Bot* **49**: 1539–1544.

Enstone DE, Peterson CA, Ma F. 2003. Root endodermis and exodermis: structure, function, and responses to the environment. *J Plant Growth Regul* **21**: 335–351.

Ewers F, Fisher J. 1991. Why vines have narrow stems: histological trends in *Bauhinia* (Fabaceae). *Oecologia* **88**: 233–237.

Ewers FW, Fisher JB, Chiu S-T. 1990. A survey of vessel dimensions in stems of tropical lianas and other growth forms. *Oecologia* **84**: 544–552.

Fan Y, Miguez-Macho G, Jobbágy EG, Jackson RB, Otero-Casal C. 2017. Hydrologic regulation of plant rooting depth. *Proc Natl Acad Sci USA* **114**: 10572–10577.

Farquhar GD, Barbour MM, Henry BK 1998. Interpretation of oxygen isotope composition of leaf materia. In: Griffiths H ed. *Stable Isotopes*. Milford Park, Oxfordshire: Bios Scientific Publishers, 27–62.

Farquhar GD, von Caemmerer S, Berry JA. 1980. A biochemical model of photosynthetic CO_2 assimilation in leaves of C_3 species. *Planta* **149**: 78–90.

Fernández V, Sancho-Knapik D, Guzmán P, Peguero-Pina JJ, Gil L, Karabourniotis G, Khayet M, Fasseas C, Heredia-Guerrero JA, Heredia A, Gil-Pelegrín E. 2014. Wettability, polarity, and water absorption of holm oak leaves: effect of leaf side and age. *Plant Physiol* **166**: 168–180.

Franks PJ, Cowan IR, Farquhar GD. 1997. The apparent feedforward response of stomata to air vapour pressure deficit: information revealed by different experimental procedures with two rainforest trees. *Plant Cell Environ* **20**: 142–145.

Franks PJ, Cowan IR, Tyerman SD, Cleary AL, Lloyd J, Farquhar GD. 1995. Guard cell pressure/aperture characteristics measured with the pressure probe. *Plant Cell Environ* **18**: 795–800.

Franks PJ, Farquhar GD. 2007. The mechanical diversity of stomata and its significance in gas-exchange control. *Plant Physiol* **143**: 78–87.

Fu QA, Ehleringer JR. 1989. Heliotropic leaf movements in common beans controlled by air temperature. *Plant Physiol* **91**: 1162–1167.

Fuchs EE, Livingston NJ. 1996. Hydraulic control of stomatal conductance in Douglas fir [*Pseudotsuga menziesii* (Mirb.) Franco] and alder [*Alnus rubra* (Bong)] seedlings. *Plant Cell Environ* **19**: 1091–1098.

Gaff DF 1981. The biology of resurrection plants. In: Pate JS, McComb AJ eds. *The Biology of Australian Plants*. Nedlands: University of Western Australia Press, 115–146.

Gartner BL 1995. Patterns of xylem variation within a tree and their hydraulic and mechanical consequences. In: Gartner BL ed. *Plant Stems*. Sand Diego: Academic Press, 125–149.

Gessler A, Peuke AD, Keitel C, Farquhar GD. 2007. Oxygen isotope enrichment of organic matter in *Ricinus communis* during the diel course and as affected by assimilate transport. *New Phytol* **174**: 600–613.

Gleason SM, Westoby M, Jansen S, Choat B, Hacke UG, Pratt RB, Bhaskar R, Brodribb TJ, Bucci SJ, Cao K-F, Cochard H, Delzon S, Domec J-C, Fan Z-X, Feild TS, Jacobsen AL, Johnson DM, Lens F, Maherali H, Martínez-Vilalta J, Mayr S, McCulloh KA, Mencuccini M, Mitchell PJ, Morris H, Nardini A, Pittermann J, Plavcová L, Schreiber SG, Sperry JS, Wright IJ, Zanne AE. 2015. Weak tradeoff between xylem safety and xylem-specific hydraulic efficiency across the world's woody plant species. *New Phytol*: n/a-n/a.

Goldsmith GR. 2013. Changing directions: the atmosphere–plant–soil continuum. *New Phytol* **199**: 4–6.

Gollan T, Schurr U, Schulze E-D. 1992. Stomatal response to drying soil in relation to changes in the xylem sap composition of *Helianthus annuus*. I. The concentration of cations, anions, amino acids in, and pH of, the xylem sap. *Plant Cell Environ* **15**: 551–559.

Green S, Clothier B, Jardine B. 2003. Theory and practical application of heat pulse to measure sap flow. *Agron J* **95**: 1371–1379.

Grieve BJ, Hellmuth EO. 1970. Eco-physiology of Western Australian plants. *Oecologia Plantarum* **5**: 33–67.

Griffith M, Lumb C, Wiseman SB, Wisniewski M, Johnson RW, Marangoni AG. 2005. Antifreeze proteins modify the freezing process *in planta*. *Plant Physiol* **138**: 330–340.

Hales S. 1727. *Vegetable Staticks*. London: W. & J. Innys ant T. Woodward.

Hall AE, Schulze E-D. 1980. Stomatal response to environment and a possible interrelation between stomatal

effects on transpiration and CO2 assimilation. *Plant Cell Environ* **3**: 467–474.

Harten JB, Eickmeier WG. 1986. Enzyme dynamics of the resurrection plant *Selaginella lepidophylla* (Hook. & Grev.) spring during rehydration. *Plant Physiol* **82**: 61–64.

Hartung W, Sauter A, Turner NC, Fillery I, Heilmeier H. 1996. Abscisic acid in soils: what is its function and which factors and mechanisms influence its concentration? *Plant Soil* **184**: 105–110.

Hassiotou F, Evans JR, Ludwig M, Veneklaas EJ. 2009. Stomatal crypts may facilitate diffusion of CO_2 to adaxial mesophyll cells in thick sclerophylls. *Plant Cell Environ* **32**: 1596–1611.

Hawkins H-J, Hettasch H, West AG, Cramer MD. 2009. Hydraulic redistribution by *Protea* Sylvia (Proteaceae) facilitates soil water replenishment and water acquisition by an understorey grass and shrub. *Funct Plant Biol* **36**: 752–760.

Hedrich R, Schroeder JI. 1989. The physiology of ion channels and electrogenic pumps in higher plants. *Annu Rev Plant Biol* **40**: 539–569.

Hirota M, Holmgren M, Van Nes EH, Scheffer M. 2011. Global Resilience of Tropical Forest and Savanna to Critical Transitions. *Science* **334**: 232–235.

Hochberg U, Rockwell FE, Holbrook NM, Cochard H. 2018. Iso/anisohydry: a plant-environment interaction rather than a simple hydraulic trait. *Trends Plant Sci* **23**: 112–120.

Holbrook NM, Burns MJ, Field CB. 1995. Negative xylem pressures in plants: a test of the balancing pressure technique. *Science* **270**: 1193–1195.

Holbrook NM, Putz FE. 1996. From epiphyte to tree: differences in leaf structure and leaf water relations associated with the transition in growth form in eight species of hemiepiphytes. *Plant Cell Environ* **19**: 631–642.

Holbrook NM, Zwieniecki MA. 1999. Embolism repair and xylem tension: do we need a miracle? *Plant Physiol* **120**: 7–10.

Jackson RB, Moore LA, Hoffmann WA, Pockman WT, Linder CR. 1999. Ecosystem rooting depth determined with caves and DNA. *Proc Natl Acad Sci USA* **96**: 11387–11392.

Jia W, Davies WJ. 2007. Modification of leaf apoplastic pH in relation to stomatal sensitivity to root-sourced abscisic acid signals. *Plant Physiol* **143**: 68–77.

Johnson DM, Berry ZC, Baker KV, Smith DD, McCulloh KA, Domec J-C. 2018. Leaf hydraulic parameters are more plastic in species that experience a wider range of leaf water potentials. *Funct Ecol* **32**: 894–903.

Kern JS. 1995. Evaluation of soil water retention models based on basic soil physical properties. *Soil Sci Soc Am J* **59**: 1134–1141.

Kerstiens G. 1996. Signalling across the divide: a wider perspective of cuticular structure—function relationships. *Trends Plant Sci* **1**: 125–129.

Kinoshita T, Shimazaki Ki. 1999. Blue light activates the plasma membrane H^+-ATPase by phosphorylation of the C-terminus in stomatal guard cells. *EMBO Journal* **18**: 5548–5558.

Kluge M, Ting IP. 1978. *Crassulacean Acid Metabolism: Analysis of an Ecological Adaptation*. Berlin: Springer-Verlag.

Körner C, Neumayer M, Pelaez Mennendez-Riedl S, Smeets-Scheel A. 1989. Functional morphology of moutain plants. *Flora* **182**: 353–383.

Korolev AV, Tomos AD, Bowtell R, Farrar JF. 2000. Spatial and temporal distribution of solutes in the developing carrot taproot measured at single-cell resolution. *J Exp Bot* **51**: 567–577.

Kramer PJ. 1969. *Plant & Soil Water Relationships*. New York: McGraw-Hill.

Lambers H, Cawthray GR, Giavalisco P, Kuo J, Laliberté E, Pearse SJ, Scheible W-R, Stitt M, Teste F, Turner BL. 2012. Proteaceae from severely phosphorus-impoverished soils extensively replace phospholipids with galactolipids and sulfolipids during leaf development to achieve a high photosynthetic phosphorus-use efficiency. *New Phytol* **196**: 1098–1108.

Lambers H, Colmer TD, Hassiotou F, Mitchell PM, Poot P, Shane MW, Veneklaas EJ 2014. Carbon and water relations. In: Lambers H ed. *Plant Life on the Sandplains in Southwest Australia, a Global Biodiversity Hotspot*. Crawley: UWA Publishing, 129–146.

Lange OL, Lösch R, Schulze E-D, Kappen L. 1971. Responses of stomata to changes in humidity. *Planta* **100**: 76–86.

Laur J, Hacke UG. 2014. Exploring *Picea glauca* aquaporins in the context of needle water uptake and xylem refilling. *New Phytol* **203**: 388–400.

Lee J-E, Oliveira RS, Dawson TE, Fung I. 2005. Root functioning modifies seasonal climate. *Proc Natl Acad Sci USA* **102**: 17576–17581.

Lens F, Sperry JS, Christman MA, Choat B, Rabaey D, Jansen S. 2011. Testing hypotheses that link wood anatomy to cavitation resistance and hydraulic conductivity in the genus *Acer*. *New Phytol* **190**: 709–723.

Li S, Lens F, Espino S, Karimi Z, Klepsch M, Schenk HJ, Schmitt M, Schuldt B, Jansen S. 2016. Intervessel pit membrane thickness as a key determinant of embolism resistance in angiosperm xylem. *IAWA J* **37**: 152.

Lo Gullo MA, Sallea S, Piaceri EC, Rosso R. 1995. Relations between vulnerability to xylem embolism and xylem conduit dimensions in young trees of *Quercus corris*. *Plant Cell Environ* **18**: 661–669.

Lo Gullo MA, Salleo S. 1988. Different strategies of drought resistance in three Mediterranean sclerophyllous trees growing in the same environmental conditions. *New Phytol* **108**: 267–276.

Longstreth DJ, Bolaños JA, Goddard RH. 1985. Photosynthetic rate and mesophyll surface area in expanding leaves of *Alternanthera philoxeroides* grown at two light levels. *Am J Bot* **72**: 14–19.

Loveless AR. 1961. A Nutritional Interpretation of Sclerophylly Based on Differences in the Chemical Composition of Sclerophyllous and Mesophytic Leaves. *Ann Bot* **25**: 168–184.

Loveless AR. 1962. Further evidence to support a nutritional interpretation of sclerophylly. *Ann Bot* **26**: 551–561.

Magnani F, Borghetti M. 1995. Interpretation of seasonal changes of xylem embolism and plant hydraulic resistance in *Fagus sylvatica*. *Plant Cell Environ* **18**: 689–696.

Mansfield TA, McAinsh MR 1995. Hormones as regulators of water balance. In: P.J. D ed. *Plant Hormones*. Dordrecht: Kluwer Academic Publishers.

Margolis H, Oren R, Whitehead D, Kaufmann MR 1995. Leaf area dynamics of conifer forests. In: Smith WK, Hinckley TM eds. *Ecophysiology of Coniferous Forests*. San Diego: Academic Press, 181–223.

Marshall DC. 1958. Measurement of sap flow in conifers by heat transport. *Plant Physiol* **33**: 385–396.

Marshall JD, Zhang J. 1994. Carbon isotope discrimination and water-use efficiency in native plants of the North-Central Rockies. *Ecology* **75**: 1887–1895.

Martin, C.E., von Willert aDJ. 2000. Leaf Epidermal Hydathodes and the Ecophysiological Consequences of Foliar Water Uptake in Species of Crassula from the Namib Desert in Southern Africa. *Plant Biol*: 229–242.

Martínez-Vilalta J, Garcia-Forner N. 2017. Water potential regulation, stomatal behaviour and hydraulic transport under drought: deconstructing the iso/anisohydric concept. *Plant Cell Environ* **40**: 962–976.

Mason Earles J, Sperling O, Silva LCR, McElrone AJ, Brodersen CR, North MP, Zwieniecki MA. 2016. Bark water uptake promotes localized hydraulic recovery in coastal redwood crown. *Plant Cell Environ* **39**: 320–328.

Maurel C, Verdoucq L, Rodrigues O. 2016. Aquaporins and plant transpiration. *Plant Cell Environ* **39**: 2580–2587.

Maxwell C, Griffiths H, Borland AM, Broadmeadow MSJ, McDavid CR. 1992. Photoinhibitory responses of the epiphytic bromeliad *Guzmania monostachia* during the dry season in Trinidad maintain photochemical integrity under adverse conditions. *Plant Cell Environ* **15**: 37–47.

Mayr S, Schmid P, Laur J, Rosner S, Charra-Vaskou-K, Dämon B, Hacke UG. 2014. Uptake of water via branches helps timberline conifers refill embolized xylem in late winter. *Plant Physiol* **164**: 1731–1740.

McAdam SAM, Sussmilch FC, Brodribb TJ. 2016. Stomatal responses to vapour pressure deficit are regulated by high speed gene expression in angiosperms. *Plant Cell Environ* **39**: 485–491.

McCully ME, Canny MJ. 1988. Pathways and processes of water and nutrient movement in roots. *Plant Soil* **111**: 159–170.

McElrone AJ, Choat B, Gambetta GA, Brodersen CR. 2013. Water uptake and transport in vascular plants. *Nature Education Knowledge* **4**.

Medlyn BE, Duursma RA, Eamus D, Ellsworth DS, Prentice IC, Barton CVM, CROUS KY, De Angelis P, Freeman M, Wingate L. 2011. Reconciling the optimal and empirical approaches to modelling stomatal conductance. *Glob Change Biol* **17**: 2134–2144.

Meidner H 1987. Three hundred years of research into stomata. In: Zeiger E, Farquhar GD, Cowan IR eds. *Stomatal Function*. Stanford: Stanford University Press, 7–27.

Midwood AJ, Boutton TW, Archer SR, Watts SE. 1998. Water use by woody plants on contrasting soils in a savanna parkland: assessment with δ^2H and $\delta^{18}O$. *Plant Soil* **205**: 13–24.

Milburn JA. 1979. *Water Flow in Plants*. London: Longman.

Mitchell PJ, Veneklaas EJ, Lambers H, Burgess SSO. 2008. Leaf water relations during summer water deficit: differential responses in turgor maintenance and variation in leaf structure among different plant communities in south-western Australia. *Plant Cell Environ* **31**: 1791–1802.

Mokany K, Raison RJ, Prokushkin AS. 2006. Critical analysis of root : shoot ratios in terrestrial biomes. *Glob Change Biol* **12**: 84–96.

Mooney HA, Dunn EL. 1970. Convergent evolution of mediterranean-climate sclerophyll shrubs. *Evolution* **24**: 292–303.

Mooney HA, Ehleringer J, Berry JA. 1976. High photosynthetic capacity of a winter annual in Death Valley. *Science* **194**: 322–324.

Morison JIL 1987. Intercellular CO_2 concentration and stomatal response to CO_2. In: Zeiger E, Farquhar GD, Cowan IR eds. *Stomatal Function*. Stanford: Stanford University Press, 229–251.

Mott KA. 1988. Do stomata respond to CO_2 concentrations other than intercellular? *Plant Physiol* **86**: 200–203.

Mott KA, Parkhurst DF. 1991. Stomatal responses to humidity in air and helox. *Plant Cell Environ* **14**: 509–515.

Müller J, Sprenger N, Bortlik K, Boller T, Wiemken A. 1997. Desiccation increases sucrose levels in *Ramonda* and *Haberlea*, two genera of resurrection plants in the Gesneriaceae. *Physiol Plant* **100**: 153–158.

Munns R, Gilliham M. 2015. Salinity tolerance of crops – what is the cost? *New Phytol* **208**: 668–673.

Nadezhdina N, Čermák J. 2003. Instrumental methods for studies of structure and function of root systems of large trees. *J Exp Bot* **54**: 1511–1521.

Nadezhdina N, David TS, David JS, Ferreira MI, Dohnal M, Tesař M, Gartner K, Leitgeb E, Nadezhdin V, Cermak J, Jimenez MS, Morales D. 2010. Trees never rest: the multiple facets of hydraulic redistribution. *Ecohydrology* **3**: 431–444.

Nepstad DC, de Carvalho CR, Davidson EA, Jipp PH, Lefebvre PA, Negreiros GH, da Silva ED, Stone TA, Trumbore SE, Vieira S. 1994. The role of deep roots

in the hydrological and carbon cycles of Amazonian forests and pastures. *Nature* **372**: 666–669.

Ngugi MR, Doley D, Hunt MA, Dart P, Ryan P. 2003. Leaf water relations of *Eucalyptus cloeziana* and *Eucalyptus argophloia* in response to water deficit. *Tree Physiol* **23**: 335–343.

Niklas K, Paolillo D. 1998. Preferential states of longitudinal tension in the outer tissues of *Taraxcum officinale* (Asteraceae) peduncles. *Am J Bot* **85**: 1068.

Nilson SE, Assmann SM. 2007. The control of transpiration. Insights from *Arabidopsis*. *Plant Physiol* **143**: 19–27.

Nobel PS. 2006. Parenchyma-chlorenchyma water movement during drought for the hemiepiphytic cactus *Hylocereus undatus*. *Ann Bot* **97**: 469–474.

Nobel PS. 2009. *Physicochemical and Environmental Plant Physiology, 4th edn*. Oxford: Academic Press.

Nobel PS, Schulte PJ, North GB. 1990. Water influx characteristics and hydraulic conductivity for roots of *Agave deserti* Engelm. *J Exp Bot* **41**: 409–415.

Nobel PS, Zaragoza LJ, Smith WK. 1975. Relation between mesophyll surface area, photosynthetic rate, and illumination level during development for leaves of *Plectranthus parviflorus* Henckel. *Plant Physiol* **55**: 1067–1070.

North GB, Nobel PS. 1997. Drought-induced changes in soil contact and hydraulic conductivity for roots of *Opuntia ficus-indica* with and without rhizosheaths. *Plant Soil* **191**: 249–258.

Oliveira RS, Costa FRC, van Baalen E, de Jonge A, Bittencourt PR, Almanza Y, Barros FdV, Cordoba EC, Fagundes MV, Garcia S, Guimaraes Zilza TM, Hertel M, Schietti J, Rodrigues-Souza J, Poorter L. 2019. Embolism resistance drives the distribution of Amazonian rainforest tree species along hydro-topographic gradients. *New Phytol* **221**: 1457–1465.

Oliveira RS, Dawson TE, Burgess SSO. 2005. Evidence for direct water absorption by the shoot of the desiccation-tolerant plant *Vellozia flavicans* in the savannas of central Brazil. *J Trop Ecol* **21**: 585–588.

Oosterhuis DM, Walker S, Eastham J. 1985. Soybean leaflet movements as an indicator of crop water stress. *Crop Sci* **25**: 1101–1106.

Oren R, Sperry JS, Katul GG, Pataki DE, Ewers BE, Phillips N, Schafer KVR. 1999. Survey and synthesis of intra- and interspecific variation in stomatal sensitivity to vapour pressure deficit. *Plant Cell Environ* **22**: 1515–1526.

Osmond CB, Winter K, Ziegler H 1982. Functional significance of different pathways of CO 2 fixation in photosynthesis. In: Lange OL, Nobel PS, Osmond CB, Ziegler H eds. *Physiological Plant Ecology*. Berlin: Springer, 479–547.

Outlaw WH. 2003. Integration of cellular and physiological functions of guard cells. *Crit Rev Plant Sci* **22**: 503–529.

Passioura J. 1988. Root signals control leaf expansion in wheat seedlings growing in drying soil. *Funct Plant Biol* **15**: 687–693.

Passioura J. 1991. Soil structure and plant growth. *Soil Res* **29**: 717–728.

Pate JS, Jeschke WD, Aylward MJ. 1995. Hydraulic architecture and xylem structure of the dimorphic root systems of South-West Australian species of Proteaceae. *J Exp Bot* **46**: 907–915.

Pedersen O, Sand-Jensen K. 1997. Transpiration does not control growth and nutrient supply in the amphibious plant *Mentha aquatica. Plant Cell Environ* **20**: 117–123.

Pelah D, Wang W, Altman A, Shoseyov O, Bartels D. 1997. Differential accumulation of water stress-related proteins, sucrose synthase and soluble sugars in Populus species that differ in their water stress response. *Physiol Plant* **99**: 153–159.

Pereira L, Bittencourt PRL, Oliveira RS, Junior MBM, Barros FV, Ribeiro RV, Mazzafera P. 2016. Plant pneumatics: stem air flow is related to embolism – new perspectives on methods in plant hydraulics. *New Phytol* **211**: 357-370.

Peterson CA, Enstone DE. 1996. Functions of passage cells in the endodermis and exodermis of roots. *Physiol Plant* **97**: 592–598.

Pfautsch S, Harbusch M, Wesolowski A, Smith R, Macfarlane C, Tjoelker MG, Reich PB, Adams MA. 2016. Climate determines vascular traits in the ecologically diverse genus *Eucalyptus*. *Ecol Lett* **19**: 240–248.

Pfautsch S, Renard J, Tjoelker MG, Salih A. 2015. Phloem as capacitor: radial transfer of water into xylem of tree stems occurs via symplastic transport in ray parenchyma. *Plant Physiol* **167**: 963–971.

Pockman WT, Sperry JS, O'leary JW. 1995. Sustained and significant negative water pressure in xylem. *Nature* **378**: 715–716.

Porembski S, Barthlott W. 2000. Granitic and gneissic outcrops (inselbergs) as centers of diversity for desiccation-tolerant vascular plants. *Plant Ecol* **151**: 19–28.

Prentice IC, Dong N, Gleason SM, Maire V, Wright IJ. 2014. Balancing the costs of carbon gain and water transport: testing a new theoretical framework for plant functional ecology. *Ecol Lett* **17**: 82–91.

Pritchard J. 1994. The control of cell expansion in roots. *New Phytol* **127**: 3–26.

Ranathunge K, Schreiber L, Franke R. 2011. Suberin research in the genomics era—New interest for an old polymer. *Plant Sci* **180**: 399–413.

Read DB, Bengough AG, Gregory PJ, Crawford JW, Robinson D, Scrimgeour CM, Young IM, Zhang K, Zhang X. 2003. Plant roots release phospholipid surfactants that modify the physical and chemical properties of soil. *New Phytol* **157**: 315–326.

Reich PB. 2014. The world-wide 'fast–slow' plant economics spectrum: a traits manifesto. *J Ecol* **102**: 275–301.

Reiser V, Raitt DC, Saito H. 2003. Yeast osmosensor Sln1 and plant cytokinin receptor Cre1 respond to changes in turgor pressure. *J Cell Biol* **161**: 1035–1040.

Rempe DM, Dietrich WE. 2018. Direct observations of rock moisture, a hidden component of the hydrologic cycle. *Proceedings of the National Academy of Sciences* **115**: 2664–2669.

Richards JH, Caldwell MM. 1987. Hydraulic lift: substantial nocturnal water transport between soil layers by *Artemisia tridentata* roots. *Oecologia* **73**: 486–489.

Roberts F, Carbon B. 1972. Water repellence in sandy soils of south-western Australia. II. Some chemical characteristics of the hydrophobic skins. *Soil Res* **10**: 35–42.

Robichaux RH. 1984. Variation in the tissue water relations of two sympatric Hawaiian *Dubautia* species and their natural hybrid. *Oecologia* **65**: 75–81.

Roden JS, Lin G, Ehleringer JR. 2000. A mechanistic model for interpretation of hydrogen and oxygen isotope ratios in tree-ring cellulose. *Geochim Cosmochim Acta* **64**: 21–35.

Rodriguez-Dominguez CM, Buckley TN, Egea G, de Cires A, Hernandez-Santana V, Martorell S, Diaz-Espejo A. 2016. Most stomatal closure in woody species under moderate drought can be explained by stomatal responses to leaf turgor. *Plant Cell Environ* **39**: 2014–2026.

Roth-Nebelsick A, Hassiotou F, Veneklaas EJ. 2009. Stomatal crypts have small effects on transpiration: a numerical model analysis. *Plant Physiol* **151**: 2018–2027.

Rundel PW 1995. Adaptive significance of some morphological and physiological characteristics in Mediterranean plants: facts and fallacies. In: Roy J, Aronson J, di Castri F eds. *Time Scales of Biological Responses to Water Constraints The case of Mediterranean Biota* Amsterdam: SPB Academic Publishing, 119–139.

Satter RL, Galston AW. 1981. Mechanisms of control of leaf movements. *Annu Rev Plant Physiol* **32**: 83–110.

Schmalstig JG. 1997. Light perception for sun-tracking is on the lamina in *Crotalaria pallida* (Fabaceae). *Am J Bot* **84**: 308–314.

Schmidt JE, Kaiser WM. 1987. Response of the succulent leaves of *Peperomia magnoliaefolia* to dehydration: water relations and solute movement in chlorenchyma and hydrenchyma. *Plant Physiol* **83**: 190–194.

Scholander PF, Bradstreet ED, Hemmingsen EA. 1965. Sap pressure in vascular plants. *Science* **148**: 339–346.

Schulte PJ, Hinckley TM. 1985. A comparison of pressure-volume curve data analysis techniques. *J Exp Bot* **36**: 1590–1602.

Schulze E-D 1991. Water and nutrient interactions with plant water stress. In: Mooney HA, Winner WE, Pell EJ eds. *Response of Plants to Multiple Stresses*. San Diego: Academic Press, 89–101.

Schulze E-D, Caldwell MM, Canadell J, Mooney HA, Jackson RB, Parson D, Scholes R, Sala OE, Trimborn P. 1998. Downward flux of water through roots (i.e. inverse hydraulic lift) in dry Kalahari sands. *Oecologia* **115**: 460–462.

Schulze E-D, Hall AE 1982. Stomatal responses, water loss and CO2 assimilation rates of plants in contrasting environments. In: Lange OL, Nobel PS, Osmond CB, Ziegler H eds. *Physiological Plant Ecology II: Water Relations and Carbon Assimilation*. Berlin, Heidelberg: Springer Berlin Heidelberg, 181–230.

Schulze E-D, Lange OL, Ziegler H, Gebauer G. 1991. Carbon and nitrogen isotope ratios of mistletoes growing on nitrogen and non-nitrogen fixing hosts and on CAM plants in the Namib desert confirm partial heterotrophy. *Oecologia* **88**: 457–462.

Schurr U, Gollan T, Schulze E-D. 1992. Stomatal response to drying soil in relation to changes in the xylem sap composition of *Helianthus annuus.* II. Stomatal sensitivity to abscisic acid imported from the xylem sap. *Plant Cell Environ* **15**: 561–567.

Schuur EAG. 2003. Productivity and global climate revisited: the sensitivity of tropical forest growth to precipitation. *Ecology* **84**: 1165–1170.

Schwartz A, Gilboa S, Koller D. 1987. Photonastic control of leaflet orientation in *Melilotus indicus* (Fabaceae). *Plant Physiol* **84**: 318–323.

Schwinning S. 2010. The ecohydrology of roots in rocks. *Ecohydrology* **3**: 238–245.

Shah N, Smirnoff N, Stewart GR. 1987. Photosynthesis and stomatal characteristics of *Striga hermonthica* in relation to its parasitic habit. *Physiol Plant* **69**: 699–703.

Shane MW, McCully ME, Canny MJ, Pate JS, Huang C, Ngo H, Lambers H. 2010. Seasonal water relations of *Lyginia barbata* (Southern rush) in relation to root xylem development and summer dormancy of root apices. *New Phytol* **185**: 1025–1037.

Shen B, Jensen RG, Bohnert HJ. 1997. Increased resistance to oxidative stress in transgenic plants by targeting mannitol biosynthesis to chloroplasts. *Plant Physiol* **113**: 1177–1183.

Sherwin HW, Farrant JM. 1996. Differences in rehydration of three desiccation-tolerant angiosperm species. *Ann Bot* **78**: 703–710.

Sherwin HW, Farrant JM. 1998. Protection mechanisms against excess light in the resurrection plants *Craterostigma wilmsii* and *Xerophyta viscosa*. *Plant Growth Regul* **24**: 203–210.

Sherwin HW, Pammenter NW, February E, Vander Willigen C, Farrant JM. 1998. Xylem hydraulic characteristics, water relations and wood anatomy of the resurrection plant *Myrothamnus flabellifolius* Welw. *Ann Bot* **81**: 567–575.

Shimazaki K-I, Doi M, Assmann SM, Kinoshita T. 2007. Light regulation of stomatal movement. *Annu Rev Plant Biol* **58**: 219–247.

Shinozaki K, Yamaguchi-Shinozaki K. 1997. Gene expression and signal transduction in water-stress response. *Plant Physiol* **115**: 327–334.

Shinozaki K, Yamaguchi-Shinozaki K, Seki M. 2003. Regulatory network of gene expression in the drought and cold stress responses. *Curr Opin Plant Biol* **6**: 410–417.

Siteur K, Mao J, Nierop KGJ, Rietkerk M, Dekker SC, Eppinga MB. 2016. Soil water repellency: a potential driver of vegetation dynamics in coastal dunes. *Ecosystems* **19**: 1210–1224.

Skelton RP, West AG, Dawson TE. 2015. Predicting plant vulnerability to drought in biodiverse regions using functional traits. *Proc Natl Acad Sci USA* **112**: 5744–5749.

Slama I, Abdelly C, Bouchereau A, Flowers T, Savouré A. 2015. Diversity, distribution and roles of osmoprotective compounds accumulated in halophytes under abiotic stress. *Ann Bot* **115**: 433–447.

Smirnoff N, Cumbes QJ. 1989. Hydroxyl radical scavenging activity of compatible solutes. *Phytochemistry* **28**: 1057–1060.

Smith DM, Allen SJ. 1996. Measurement of sap flow in plant stems. *J Exp Bot* **47**: 1833–1844.

Sobrado MA, Medina E. 1980. General morphology, anatomical structure, and nutrient content of sclerophyllous leaves of the 'bana' vegetation of amazonas. *Oecologia* **45**: 341–345.

Sowell JB, McNulty SP, Schilling BK. 1996. The role of stem recharge in reducing the winter desiccation of *Picea engelmannii* (Pinaceae) needles at alpine timberline. *Am J Bot* **83**: 1351–1355.

Sperry JS, Donnelly JR, Tyree MT. 1988. A method for measuring hydraulic conductivity and embolism in xylem. *Plant Cell Environ* **11**: 35-40.

Sperry JS 1995. Limitations on Stem Water Transport and Their Consequences. In: Gartner BL ed. *Plant Stems*. San Diego: Academic Press, 105–124.

Sperry JS, Saliendra NZ, Pockman WT, Cochard H, Cuizat P, Davis SD, Ewers FW, Tyree MT. 1996. New evidence for large negative xylem pressures and their measurement by the pressure chamber method. *Plant Cell Environ* **19**: 427–436.

Sperry JS, Sullivan JEM. 1992. Xylem embolism in response to freeze-thaw cycles and water stress in ring-porous, diffuse-porous, and conifer species. *Plant Physiol* **100**: 605–613.

Sperry JS, Venturas MD, Anderegg WRL, Mencuccini M, Mackay DS, Wang Y, Love DM. 2017. Predicting stomatal responses to the environment from the optimization of photosynthetic gain and hydraulic cost. *Plant Cell Environ* **40**: 816–830.

Sternberg L, Pinzon MC, Anderson WT, Jahren AH. 2006. Variation in oxygen isotope fractionation during cellulose synthesis: intramolecular and biosynthetic effects. *Plant Cell Environ* **29**: 1881–1889.

Stirzaker RJ, Passioura JB. 1996. The water relations of the root–soil interface. *Plant Cell Environ* **19**: 201–208.

Stirzaker RJ, Passioura JB, Wilms Y. 1996. Soil structure and plant growth: impact of bulk density and biopores. *Plant Soil* **185**: 151–162.

Stone EC. 1957. Dew as an ecological factor: I. A review of the literature. *Ecology* **38**: 407–413.

Swanson RH, Whitfield DAW. 1981. A numerical analysis of heat pulse velocity theory. *J Exp Bot* **32**: 221–239.

Takahashi H, Scott TK. 1993. Intensity of hydrostimulation for the induction of root hydrotropism and its sensing by the root cap. *Plant Cell Environ* **16**: 99–103.

Tardieu F, Lafarge T, Simonneau T. 1996. Stomatal control by fed or endogenous xylem ABA in sunflower: interpretation of correlations between leaf water potential and stomatal conductance in anisohydric species. *Plant Cell Environ* **19**: 75–84.

Tardieu F, Zhang J, Katerji N, Bethenod O, Palmer S, Davies WJ. 1992. Xylem ABA controls the stomatal conductance of field-grown maize subjected to soil compaction or soil drying. *Plant Cell Environ* **15**: 193–197.

Thomashow MF. 1999. Plant cold acclimation: freezing tolerance genes and regulatory mechanisms. *Annu Rev Plant Physiol Plant Mol Biol* **50**: 571–599.

Thorburn PJ, Ehleringer JR. 1995. Root water uptake of field-growing plants indicated by measurements of natural-abundance deuterium. *Plant Soil* **177**: 225–233.

Tomos AD, Leigh RA. 1999. The pressure probe: A versatile tool in plant cell physiology. *Annu Rev Plant Physiol Plant Mol Biol* **50**: 447–472.

Tranquillini W 1982. Frost-drought and its ecological significance. In: Lange OL, Nobel PS, Osmond CB, Ziegler H eds. *Encyclopedia of Plant Physiology, NS*. Berlin: Springer-Verlag, 379–400.

Turrell FM. 1936. The area of the internal exposed surface of dicotyledon leaves. *Am J Bot* **23**: 255–264.

Tyree MT, Salleo S, Nardini A, Assunta Lo Gullo M, Mosca R. 1999. Refilling of embolized vessels in young stems of laurel. Do we need a new paradigm? *Plant Physiol* **120**: 11–22.

Tyree MT, Sperry JS. 1989. Vulnerability of xylem to cavitation and embolism. *Annu Rev Plant Physiol* **40**: 19–36.

Tyree MT, Zimmermann MH. 2013. *Xylem Structure and the Ascent of Sap*. Berlin: Springer Science & Business Media.

Uehlein N, Kaldenhoff R. 2008. Aquaporins and plant leaf movements. *Ann Bot* **101**: 1–4.

Van den Ende W. 2013. Multifunctional fructans and raffinose family oligosaccharides. *Front Plant Sci* **4**: 247.

Van Hylckama TE. 1974. Water use by saltcedar as measured by the water budget method. *US Geological Survey Papers* **491-E.**

Van Ieperen W. 2007. Ion-mediated changes of xylem hydraulic resistance in planta: fact or fiction? *Trends Plant Sci* **12**: 137–142.

Vogelmann TC. 1984. Site of light perception and motor cells in a sun-tracking lupine (Lupinus succulentus). *Physiol Plant* **62**: 335–340.

Vogt KA, Vogt DJ, Palmiotto PA, Boon P, O'Hara J, Asbjornsen H. 1995. Review of root dynamics in forest ecosystems grouped by climate, climatic forest type and species. *Plant Soil* **187**: 159–219.

Wegner LH. 2014. Root pressure and beyond: energetically uphill water transport into xylem vessels? *J Exp Bot* **65**: 381–393.

Wegner LH. 2015. A thermodynamic analysis of the feasibility of water secretion into xylem vessels against a water potential gradient. *Funct Plant Biol* **42**: 828–835.

Wilkinson S, Corlett JE, Oger L, Davies WJ. 1998. Effects of xylem pH on transpiration from wild-type and *flacca* tomato leaves. A vital role for abscisic acid in preventing excessive water loss even from well-watered plants. *Plant Physiol* **117**: 703–709.

Wilkinson S, Davies WJ. 1997. Xylem sap pH increase: a drought signal received at the apoplastic face of the guard cell that involves the suppression of saturable abscisic acid uptake by the epidermal symplast. *Plant Physiol* **113**: 559–573.

Wisniewski M, Davis G, Arora R. 1991. Effect of macerase, oxalic acid, and EGTA on deep supercooling and pit membrane structure of xylem parenchyma of peach. *Plant Physiol* **96**: 1354–1359.

Wolf A, Anderegg WRL, Pacala SW. 2016. Optimal stomatal behavior with competition for water and risk of hydraulic impairment. *Proc Natl Acad Sci USA* **113**: E7222–E7230.

Wu Y, Cosgrove DJ. 2000. Adaptation of roots to low water potentials by changes in cell wall extensibility and cell wall proteins. *J Exp Bot* **51**: 1543–1553.

Wullschleger SD, Meinzer FC, Vertessy RA. 1998. A review of whole-plant water use studies in tree. *Tree Physiol* **18**: 499–512.

Yamaguchi-Shinozaki K, Shinozaki K. 2006. Transcriptional regulatory networks in cellular responses and tolerance to dehydration and cold stresses. *Annu Rev Plant Biol* **57**: 781–803.

Yang S, Tyree MT. 1992. A theoretical model of hydraulic conductivity recovery from embolism with comparison to experimental data on *Acer saccharum*. *Plant Cell Environ* **15**: 633–643.

Yoder C, Nowak R. 1999. Hydraulic lift among native plant species in the Mojave Desert. *Plant Soil* **215**: 93–102.

Yu M, Xie Y, Zhang X. 2005. Quantification of intrinsic water use efficiency along a moisture gradient in northeastern China. *J Environ Qual* **34**: 1311–1318.

Zanne AE, Tank DC, Cornwell WK, Eastman JM, Smith SA, FitzJohn RG, McGlinn DJ, O'Meara BC, Moles AT, Reich PB, Royer DL, Soltis DE, Stevens PF, Westoby M, Wright IJ, Aarssen L, Bertin RI, Calaminus A, Govaerts R, Hemmings F, Leishman MR, Oleksyn J, Soltis PS, Swenson NG, Warman L, Beaulieu JM. 2013. Three keys to the radiation of angiosperms into freezing environments. *Nature* **506**: 89.

Zhang W-H, Tyerman SD. 1999. Inhibition of water channels by $HgCl_2$ in intact wheat root cells. *Plant Physiol* **120**: 849–858.

Zhu J-K. 2002. Salt and drought stress signal transduction in plants. *Annu Rev Plant Biol* **53**: 247–273.

Zimmermann MH. 1983. *Xylem Structure and the Ascent of Sap*. Berlin: Springer-Verlag.

Zimmermann MH, Milburn JA 1982. Transport and storage of water. In: Lange OL, Nobel PS, Osmond CB, Ziegler H eds. *Physiological Plant Ecology II*: Springer, 135–151.

Zwieniecki MA, Holbrook NM. 2009. Confronting Maxwell's demon: biophysics of xylem embolism repair. *Trends Plant Sci* **14**: 530–534.

Zwieniecki MA, Newton M. 1995. Roots growing in rock fissures: their morphological adaptation. *Plant Soil* **172**: 181–187.

Plant Energy Budgets: The Plant's Energy Balance

6

6.1 Introduction

Temperature is a major environmental factor that determines plant distribution. It affects virtually all plant processes, ranging from enzymatically catalyzed reactions and membrane transport to physical processes such as transpiration and the volatilization of specific compounds. Species differ in the activation energy of particular reactions and, consequently, in the temperature responses of most physiological process (*e.g.*, photosynthesis, respiration, biosynthesis). Given the pivotal role of temperature in the ecophysiology of plants, it is critical to understand the factors that determine plant temperature. Air temperature in the habitat provides a gross approximation of plant temperature. Air temperature in a plant's **microclimate**, however, may differ substantially from air temperature measured by standard meteorological methods. The actual temperature of a plant organ often deviates substantially from that of the surrounding air. We can only understand the temperature regime of plants and, therefore, the physiological responses of plants to their thermal environment through study of microclimate and the plant's energy balance.

6.2 Energy Inputs and Outputs

6.2.1 A Short Overview of a Leaf's Energy Balance

Most leaves effectively absorb the **shortwave radiation** (*SR*) emitted by the sun. A relatively small fraction (less than about 20%) of incident solar radiation is **reflected**, **transmitted**, or utilized for processes other than just heating. In bright sunlight the net absorption of solar radiation (SR_{net}) is the main energy input to a leaf. If such a leaf had no means to dissipate this energy, then its temperature would reach 100 °C in less than a minute. Thus, processes that govern heat loss by a plant are critical for maintaining a suitable temperature for physiological functioning.

Heat loss occurs by several processes (Fig. 6.1). A leaf emits longwave infrared radiation (*LR*). At the same time, however, it absorbs *LR* emitted by surrounding objects and the sky. The net effect of **emission** and **absorption** (LR_{net}) may be negative or positive, depending on whether it constitutes an export or import of energy, respectively. When there is a temperature difference between leaf and air, **convective heat transfer** (*C*) takes place from the higher to the

H. Lambers, R. S. Oliveira, *Plant Physiological Ecology*, https://doi.org/10.1007/978-3-030-29639-1_6

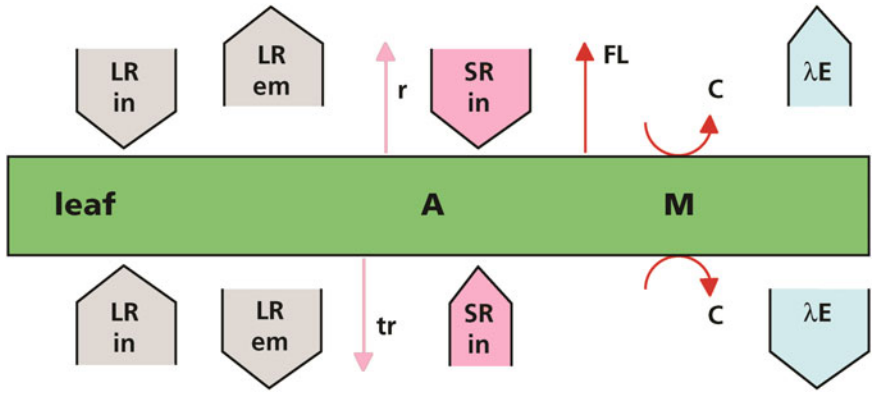

Fig. 6.1 Schematic representation of the components of the energy balance of a leaf consisting of shortwave radiation (*SR*), longwave radiation (*LR*), both incident (in) and emitted (em), convective heat transfer (C), and evaporative heat loss (λ*E*). Reflection (*r*), transmission (*tr*), and fluorescent emission (*FL*) are only given for *SR* incident on the upper side of the leaf. *A* and *M* are CO_2-assimilation and heat-producing metabolic processes, respectively. The arrows are not scaled; in particular LR_{in} from above is often quite small (if skies are clear), and SR_{upward} is shown too large relative to $SR_{downwards}$.

lower temperature. Another major component of the energy balance is cooling caused by **transpiration** (λ*E*; where λ is the energy required to convert liquid water into water vapor, and E is the rate of evaporation. This is called transpiration when it concerns water loss through stomata). In addition, **metabolic processes** are involved in the energy balance. Respiration and other metabolic processes (*M*) generate heat, and energy is consumed when absorbed *SR* is used in photosynthesis (*A*), but these components are typically small compared with other components of the energy balance, and usually ignored. When the temperature rises in response to sunlight, most components of the energy balance that contribute to cooling increase in magnitude until energy gain and loss are in balance. At this point, the leaf has reached an equilibrium temperature (steady state), and the sum of all components of the energy balance must equal zero:

$$SR_{net} + LR_{net} + C + \lambda \times E + M = 0 \qquad (6.1)$$

Any change in the components of the energy balance will alter leaf temperature. For a correct description of the time course of change, a **heat storage** term must be included; however, storage capacity is low in most leaves, and response times of leaf temperature to changing conditions are typically minutes or less. Exceptions are more bulky plant parts such as succulent leaves, stems (particularly the watery stems of cacti), and tree trunks and branches, but these are not dealt with here.

6.2.2 Shortwave Solar Radiation

Absorption of solar radiation normally dominates the input side of the energy balance of sunlit leaves during the light (Jones 2014). About 98% of the radiation emitted by the sun is in the range of 300 to 3000 nm (shortwave radiation, *SR*). Ultraviolet radiation (UV; 300 to 400 nm) has the highest energy content per quantum (shortest wavelength); it constitutes approximately 7% of solar radiation and is potentially damaging to a plant (Sect. 7.2.2). Plants absorb about 97% of incoming UV radiation (Fig. 6.2). About half of the energy content of solar radiation is in the waveband of 400 to 700 nm (photosynthetically active radiation, PAR), which can be used to drive photochemical processes (SR_A); most green leaves absorb around 85% of the incident radiation in this region, depending on the chlorophyll concentration (Fig. 6.2). Shortwave (solar) infrared radiation (IR_s; 700 to 3000 nm) is absorbed to a much lesser extent.

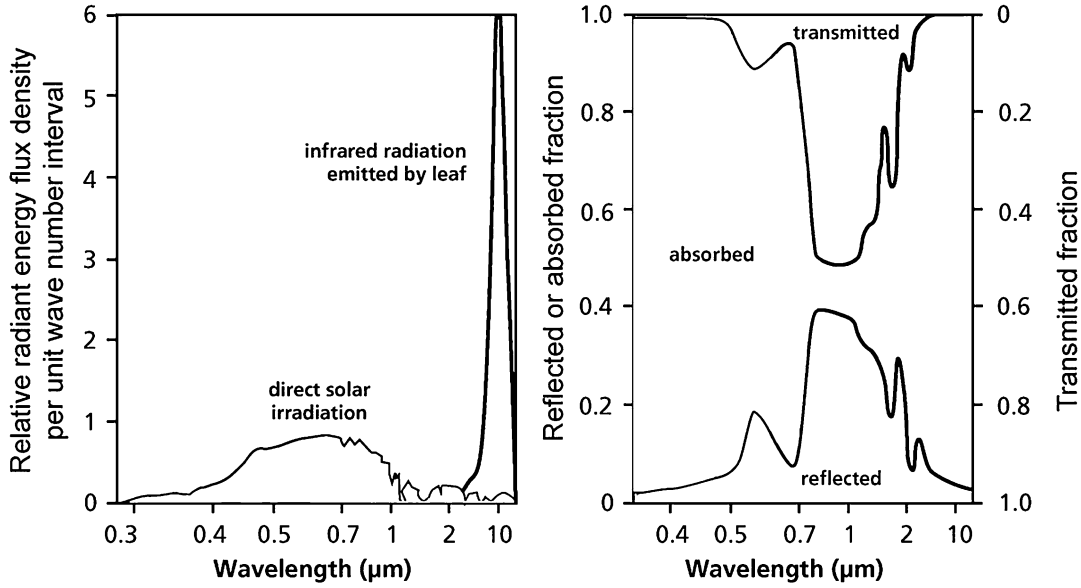

Fig. 6.2 (Left) Wavelength spectrum of skylight (60 W m^{-2}), direct solar radiation (840 W m^{-2}), and infrared radiation emitted by a leaf (900 W m^{-2}) at 25 °C. (Right) Wavelength spectrum of absorbed, transmitted, and reflected radiation (% of total) by a leaf.

This wavelength region can be divided in two parts: 700 to about 1200 nm, which is largely **reflected** or **transmitted** by a leaf and represents the largest part of IR_s in terms of energy content, and 1200 to 3000 nm, which is largely absorbed by water in the leaf (Fig. 6.2). The result is that about 50% of IR_s is absorbed.

Leaves have mechanisms that can modify the magnitude of the components that make up the amount of absorbed solar radiation (SR_{abs}): **incident** (SR_{in}), **reflected** (SR_r) and **transmitted** (SR_{tr}) **radiation.** Changes in SR_{in} can be brought about by changes in leaf orientation with respect to the sun (**heliotropisms** or **solar tracking**) (Sect. 5.5.4.6) (Ehleringer and Forseth 1980). These leaf movements can be active and may orient the leaf perpendicularly to the incident radiation (**diaheliotropism**), thus maximizing SR_{in} under conditions of low temperature and adequate soil moisture (Fig. 6.3); this contrasts with **paraheliotropism** where leaves orient parallel to the incident radiation. A most dramatic example of heliotropic movements is found in flowers of many arctic and alpine plants [*e.g.*, *Dryas octopetala* (mountain avens) and *Ranunculus adoneus* (snow buttercup)] that move diurnally to continually face the sun, thus maximizing radiation gain. The parabolic shape of these heliotropic flowers reflects radiation toward the ovary. Thus, the shape and orientation of flowers maximizes rate of ovule development and attracts pollinators (Sect. 11.3.3.5; (Kjellberg et al. 1982). Floral heliotropic movements are mainly restricted to the Asteraceae, Papaveraceae, Ranunculaceae, and Rosaceae. The mechanism is similar to the more widely studied phenomenon of seedling **phototropism** (Sect. 10.2.2.2), rather than the more common heliotropic leaf movements (Sect. 5.5.4.6) (Sherry and Galen 2002). Another example of a mechanism that increases temperature of a specific part of a plant is that of *Copiapoa* species (barrel cactus) that increase SR_{in} by leaning toward the north in Chile (Ehleringer et al. 1980). The effect of this orientation is that tissue temperatures of the meristematic and floral regions on the tip of the cactus receive high solar radiation loads, which result in high temperatures (30 –40 °C) relative to air temperatures (15 –20) during winter and spring months when adequate soil moisture for growth is

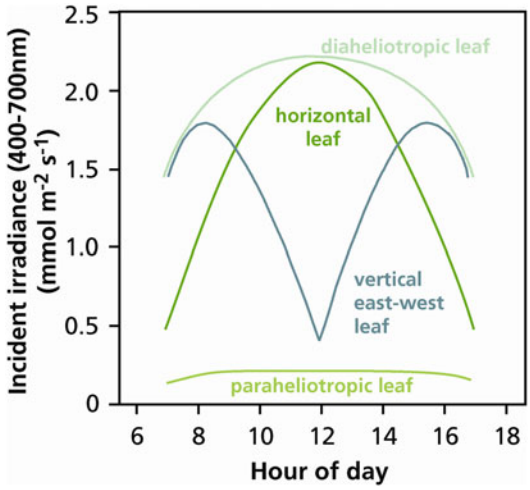

Fig. 6.3 Photosynthetically active radiation incident on four leaf types over the course of a midsummer day: a horizontal leaf, a diaheliotropic leaf (cosine of incidence = 1.0), a vertical east-west facing leaf; a horizontal leaf, and a paraheliotropic leaf (cosine of incidence = 0.1); after Ehleringer and Forseth (1980).

available. Second, absorption of solar radiation by the sides of the cactus is minimized, which reduces the potential detrimental effects of light and heat load on the cactus.

Paraheliotropism has been reported in several species of the Fabaceae family, *e.g.*, *Phaseolus* (bean) species), *Glycine max* (soybean), and *Medicago sativa*. In *Macroptilium atropurpureum* (siratro) these leaf movements coincide with stomatal closure (Ludlow and Björkman 1984). A major stimulus for leaf movement is light, but movements may be modulated by leaf water status and temperature, *i.e.* the leaf orientation is parallel to the incident radiation, thus minimizing SR_{in} (Fig. 6.3) (Kao and Forseth 1992; Foster et al. 2012). Many desert shrubs exhibit steep leaf angles relative to the sun (Smith et al. 1998). This reduces midday SR_{in}, when temperatures are highest, and increases SR_{in} in mornings and afternoons, when radiation is less and temperatures are cooler. Angles can become progressively more horizontal in wetter communities which increases SR_{in} at midday (Ehleringer 1988). This regulation of leaf angle keeps leaf temperatures within limits, thereby reducing transpiration and photoinhibition and maximizing the rate of CO_2 assimilation, *e.g.*, in *Vitis californica* (California wild grape) (Gamon and Pearcy 1989). In three wild *Glycine* (soybean) species, paraheliotropic leaf movements respond in concert with photosynthetic characteristics such that **water-use efficiency** is enhanced and the risk of **photoinhibition** under water deficit is reduced (Kao and Tsai 1998). Wilting and leaf rolling are additional mechanisms by which leaves reduce incident radiation under conditions of water stress.

The **reflection** component (SR_r) of incident radiation in the PAR region is typically small (approximately 5 to 10%; Fig. 6.2) and comprises reflection from the surface which is largely independent of wavelength, and internal reflection, which is wavelength-specific because of absorption by pigments along the internal pathway (Sect. 2.2.1.1). In some plants, surface reflection can be high due to the presence of reflecting **wax** layers, short **white hairs**, or **salt crystals**. Reflection can change seasonally as in the desert shrub *Encelia farinosa* (brittlebush) that produces new leaves during winter with sparse hairs resulting in 80% absorption of incident radiation raising leaf temperature several degrees above ambient (Fig. 6.4). Leaves produced in summer, however, when water is scarce, have dense reflective hairs that reduce absorptance to 30 to 40% of incident radiation, and reduce leaf temperature below ambient. The sympatric *Encelia californica* (bush sunflower) from cooler and more humid coastal habitats has glabrous leaves that increase absorptance and cause leaf temperatures to be 5 °C to 10 °C higher than in the desert species (Fig. 2.2). Because *Encelia farinosa* has an optimum temperature for photosynthesis that is below summer daytime temperature, this reduction in absorptance is critical to leaf carbon balance (Ehleringer and Björkman 1978). Presence of leaf hairs in summer increases carbon gain and reduces water loss by 20–25% through amelioration of leaf temperature (Fig. 6.4). A white layer of salt excreted by salt glands on the leaves of *Atriplex hymenelytra* (desert holly) (Sect. 9.3.4.3), similarly, reduces the absorptance and leaf temperature; it enhances CO_2 assimilation and water-use efficiency, because of a more

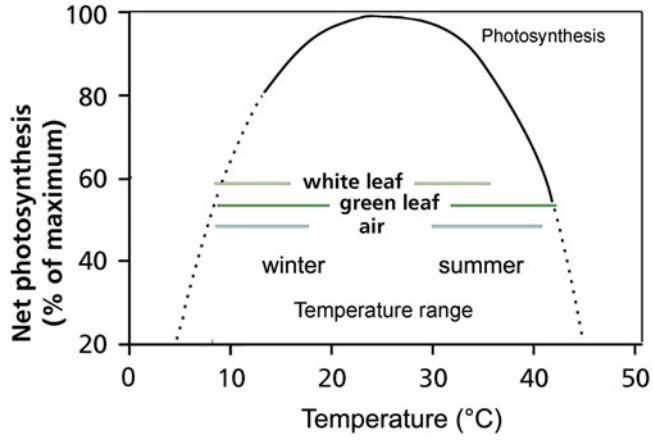

Fig. 6.4 Daily ranges of air temperatures and leaf temperatures of glabrous green winter leaves and pubescent white summer leaves of *Encelia farinosa* (brittlebush). Temperature ranges were measured on a typical winter day for winter leaves and on a summer day for summer leaves; calculated values are shown for the reciprocal conditions. The temperature dependence of photosynthesis is identical in winter and summer (Ehleringer and Mooney 1978).

favorable leaf temperature for photosynthesis (Mooney et al. 1977).

In summary, the components of solar radiation relevant for the energy balance of a leaf are (Jones 2014):

SR shortwave (solar) radiation (300–3000 nm).

SR_{in}	incident radiation ($UV + PAR + IR_s$)
UV	ultraviolet (300–400 nm)
PAR	photosynthetically active radiation (400–700 nm)
IR_s	shortwave infrared radiation (700–3000 nm)

$$\mathrm{SR_{in}} = \mathrm{PAR} + \mathrm{IR_s} + \mathrm{UV} \qquad (6.2)$$

$\mathrm{SR_r}$ reflected
$\mathrm{SR_{tr}}$ transmitted
$\mathrm{SR_{abs}}$ bsorbed

$$\mathrm{SR_{abs}} = \mathrm{R_{in}} - \mathrm{SR_r} - \mathrm{SR_{tr}} \qquad (6.3)$$

$\mathrm{SR_A}$ used in hotosynthesis
$\mathrm{SR_{FL}}$ emitted as fluorescence

SR_{net} equals absorbed radiation minus radiation used in photosynthesis and emitted fluorescence:

$$\mathrm{SR_{net}} = \mathrm{SR_{abs}} - \mathrm{SR_A} - \mathrm{SR_{FL}} \qquad (6.4)$$

Typical values of the energy balance of leaves are given in Fig. 6.5 (and more in Figs 6.8 and 6.10, in Sect. 6.2.4).

A few percent of SR_{abs} is emitted as fluorescence (SR_{FL}) (Box 2.4) and the same is true for the part of SR_{abs} used in photosynthesis (SR_A) in high-light conditions. For simplicity's sake, we generally ignore SR_A and SR_{FL} in energy-balance calculations; however, this may represent a significant error in the case of SR_A under conditions that are favorable for photosynthesis or where light intensity is low.

6.2.3 Longwave Terrestrial Radiation

All objects above 0 K emit energy by radiation. Since we are now dealing with thermal wavelengths, there is no transmission (Jones, 2014). Longwave radiation (LR) is the infrared radiation that objects emit when at temperatures commonly occurring at the earth surface (around 290 K). Its wavelength range (>3000 nm) is much longer than that emitted by the sun (Fig. 6.1). A leaf loses heat by **emission** of LR (LR_{em}). LR_{em} is proportional to the fourth power of the absolute temperature (T) and the **emissivity** of the leaf (ε).

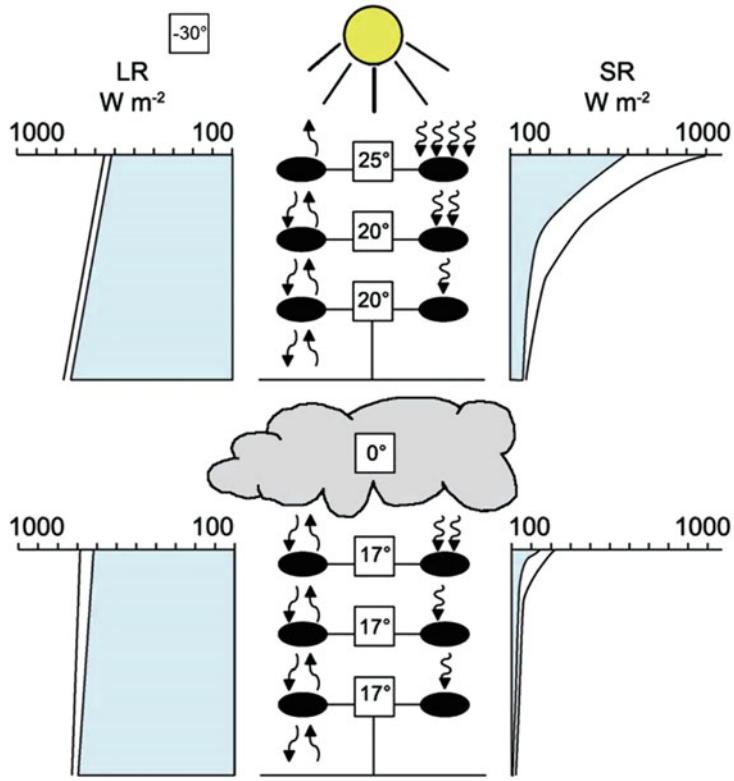

Fig. 6.5 Schematic representation of the longwave radiation (*LR*) and shortwave radiation (*SR*) inputs and outputs for a sunny (left) and cloudy (right) day for leaves at different positions in a canopy. Graphs show the vertical profile of incident radiation (solid line) and net radiation (blue). The lower three are leaf temperatures, and the upper is the effective sky radiation temperature. Assumed is a global incident radiation of 833 W m^{-2}, reflectance by the surroundings of 20%, leaf absorbance of shortwave radiation of 0.6, photosynthetic rate of 8 μmol m^{-2} s^{-1} at the top of the canopy on a sunny day, leaf temperature of 25 °C (top), 20 °C (middle and bottom) on a sunny day, and of 17 °C on a cloudy day. Total incoming radiation (SR_{in}) exceeds the global radiation due to reflectance from surrounding leaves and twigs. Abbreviations as defined in text.

	Cloudless day			Cloudy day		
	Canopy					
Component	Top	Middle	Bottom	Top	Middle	Bottom
SR_{in}	1000	200	40	200	80	10
SR_{abs}	600	100	20	100	40	5
SR_A	7	2	0.4	2	0.8	0.1
SR_{net}	593	198	19.6	98	39.2	4.9
LR_{in}	650	750	833	792	800	802
LR_{abs}	624	720	800	760	768	770
LR_{em}	859	800	800	770	770	770
LR_{net}	-235	-80	0	-10	-2	0
TR_{abs}	1224	820	820	860	808	775
TR_{net}	358	118	19.6	88	37.2	4.9

The proportionality constant (σ, Stefan-Bolzman constant) is 5.57 10^{-8} W m^{-2} K^{-4}):

$$LR_{em} = \varepsilon \times \sigma \times T^4 \qquad (6.5)$$

For a perfect radiator ('black body'), $\varepsilon = 1$; real objects have lower values. Values for ε range from 0 to 1, with leaves having longwave emissivities typically between 0.94 and 0.99. The leaf's emissivity equals 1 minus the reflection coefficient, and is determined by such traits as leaf 'roughness' (*e.g.*, presence of hairs) and leaf color. Heat loss through longwave infrared radiation is a major component of a leaf's energy

balance. This may be balanced, however, by an equally large absorption of *LR* emitted by surrounding objects and the sky. The high ε of leaves causes almost total absorption of incident *LR*. LR_{abs} is low under a clear sky, which may have an effective radiation temperature around −30 °C, but is high when plants grow widely spaced in dry sand or rocks that can reach temperatures of more than 70 °C in full sun. LR_{abs} often accounts for half the total energy gain of a leaf in a canopy exposed to the sun (Fig. 6.5). A negative total radiation (TR) balance of a leaf can occur under a clear sky at night which causes its temperature to drop below air temperature (negative ΔT). Such conditions can also be found during daytime in leaves shaded from the sun, but exposed to a blue sky, as on the north side of objects (rocks, walls, trees) at higher latitudes in the northern hemisphere. Rapidly transpiring plants are often below air temperature, because of high latent heat loss, even in the sun, especially if they have large leaves or high boundary layer resistances (Nobel 1983; Jones 2014).

The components of the longwave radiation balance are summarized below, with values typical of a green leaf exposed to full sun at sea level on a cloudless day presented in Fig. 6.5 (Nobel 1983; Jones 2014):

LR Longwave (terrestrial) radiation (> 3 μm) (6.6)

LR_{in} incidentradiation
LR_r reflected
LR_{abs} absorbed

$$LR_{abs} = LR_{in} - LR_r$$

LR_{em} emitted

$$LR_{net} = LR_{abs} - LR_{em} \quad (6.7)$$

TR Total radiation

$$TR_{abs} = SR_{abs} + LR_{abs} \quad (6.8)$$

$$TR_{net} = SR_{net} + LR_{net} \quad (6.9)$$

The amount of energy gained by a leaf varies greatly through a leaf canopy, and the extent of this change depends on cloud conditions (Fig. 6.5). If we simplify a complex process, and ignore attenuation in the atmosphere and reflection by clouds and leaf angle, in full sun, the shortwave radiation incident on a leaf exceeds that of incoming solar shortwave radiation. This is, because reflection from surrounding leaves and other surfaces, and the total radiation (*TR*) absorbed by a leaf (1224 W m^{-2} in Fig. 6.1) approaches that of the solar constant (1360 W m^{-2}) (*i.e.* the solar energy input above the atmosphere) (Nobel 1983). TR_{abs} declines dramatically in the absence of direct solar radiation, whether this is due to clouds or to canopy shading. Even leaves in full sun absorb more than half their energy as longwave radiation, and leaves in cloudy or shaded conditions receive most energy as longwave radiation emitted by objects in their surroundings. There is a sharp decline in total net radiation gained (and therefore energy that must be dissipated) through the canopy under both sunny and cloudy conditions (Fig. 6.5).

6.2.4 Convective Heat Transfer

Leaf temperature is further determined by **convective** (**sensible**) **heat exchange** (*C*), which is proportional to the temperature difference (Δ*T*) between leaf (T_L) and air (T_a) (Jones 2014). The contribution of *C* to the energy balance of the leaf is negative or positive when leaf temperature is higher or lower than air temperature, respectively; this is typically the case in the light in the sun and at night or in shaded conditions, respectively (Figs. 6.5, 6.8 and 6.10, but see the exception in Fig. 6.4). The magnitude of *C* depends further on the boundary layer conductance for heat transport (g_{ah}), which is proportional to the conductance for diffusion of CO_2 and H_2O (Fig. 6.6):

$$C = g_{ah}(T_a - T_L) \quad (6.10)$$

The **boundary layer** is the layer of air close to a leaf (or any other surface) where air movement is restricted in comparison with that in the free turbulent air. This reduced air flow leads to

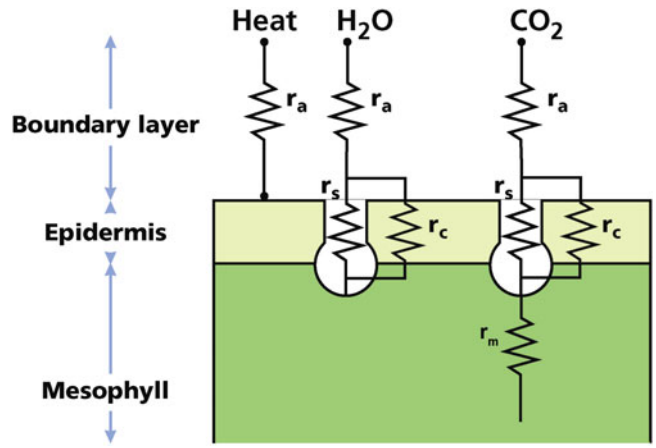

Fig. 6.6 Resistances for the exchange of heat and gas between a leaf and the atmosphere. For CO_2, apart from the cuticular resistance (r_c) three resistances play a role (mesophyll or internal, r_m, stomatal, r_s, boundary layer, r_a), whereas there are only two for H_2O and one for heat exchange. Note that conductance is the inverse of resistance, $g = 1/r$.

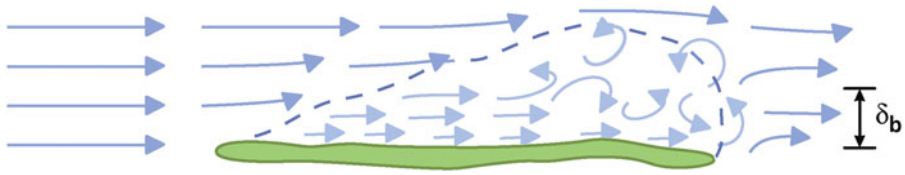

Fig. 6.7 Schematic representation of the flow of nonturbulent air across a leaf. The arrows indicate the relative speed and direction of air movement. As air moves across a leaf, there is a laminar sublayer (short straight arrows), followed by a turbulent region. The effective boundary layer thickness (δ_{bl}) averages across these regions. The exchange of the lower surface of the leaf will be a mirror image of the upper surface (Nobel 1983).

reduced diffusive transfer (and hence a reduced conductance) for heat or gases such as CO_2 and H_2O in this zone as compared with that in the free air stream (Sect. 2.2.2.2) (Fig. 6.7). Boundary layer conductance (g_{ah}) is inversely related to the **boundary layer thickness** (δ), which in turn depends, for flat leaves, on **wind speed** (u) and **leaf dimension** (d; leaf width measured in the direction of the wind):

$$\delta = 4\sqrt{d/u} \qquad (6.11)$$

Equation 6.8 shows that small leaves have higher g_{ah}, and thus tend to have temperatures closer to air temperature, than do large leaves. Compound or highly dissected leaves are functionally similar to small leaves in this respect. Under hot, dry conditions, most plants have small leaves, because they cannot support fast transpiration rates and must rely largely on convective cooling to dissipate absorbed shortwave and longwave radiation. Another mechanism that reduces boundary layer thickness is the increase of effective wind speed across leaves with thin flattened petioles that cause leaves to flutter at low wind speeds, as in some *Populus* species [*Populus tremula* (European aspen) and *Populus tremuloides* (quaking aspen)].

Some plants do not 'obey the rules'. *Welwitschia mirabilis* (two-leafed-cannot-die) is an African long-lived desert plant with extremely large leaves (0.5 to 1.0 m wide, and 1 to 2 m long) (Schulze et al. 1980). Those parts of the leaves not in contact with the ground, however, are often only 4 to 6 °C above air temperature. A high reflectivity of leaves (56%) minimizes SR_{abs}, and relatively cool shaded soils beneath leaves minimize LR_{in} (Fig. 6.8). There is negligible transpiration in summer, so it is primarily through these two mechanisms of minimizing energy

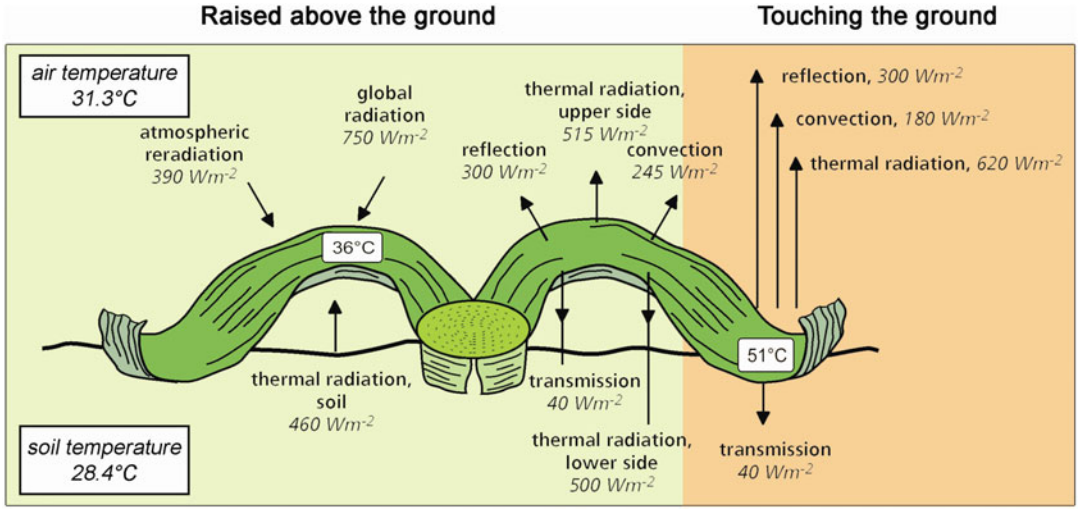

Fig. 6.8 Major components of the energy balance of two parts of leaves of *Welwitschia mirabilis* (two-leafed-cannot-die) in a coastal desert area of Namibia. Leaf tips are in contact with the ground and have a higher temperature (T_L) due to reduced convective transfer (C), and absence of emitted longwave radiation (LR_{em}) at the underside of the leaf. The leaf parts raised above the ground that shades it have lower temperatures as a result the increased C and LR_{net} (Schulze et al. 1980).

gain that this plant avoids serious overheating. Parts of the leaves that touch the ground have substantially higher temperatures, because heat exchange at the lower surface is hampered (Fig. 6.8).

It may be advantageous in cold environments to increase boundary layer thickness in order to raise leaf temperature at high radiation. Some prostrate growth forms such as **cushion plants** in alpine habitats maximize boundary layer thickness by keeping leaves closely packed. They are also close to the ground, where they are in the boundary layer of the ground surface where temperatures are higher during daytime and wind speeds are lower (these aspects are covered in Chap. 7). The plant's sensible heat loss is reduced. Thus, it is possible that some prostrate alpine plants uncouple their microenvironment from ambient to an extent that temperatures of 27 °C, relative humidities of 99%, and calm conditions occur around leaves, while the hiker may experience 10 °C, a relative humidity of 50%, and a wind speed of 4 m s^{-1}. This has been measured under clear sky conditions for *Celmisia longifolia* (snow daisy), *Verbascum thapsus* (common mullein), and other rosette plants with sessile leaves (Körner and Cochrane 1983). The resulting higher plant temperatures are more favorable for many physiological processes. Leaf hairs are another mechanism by which plants in cold environments can increase boundary layer thickness, and, therefore, leaf temperature. Plants from high altitudes, for example a giant Andean paramo rosette plant, *Espeletia timotensis*, has **long hairs** (Meinzer and Goldstein 1985). These increase reflection to a minor extent, but they do reduce the boundary layer conductance considerably so that the leaf temperature becomes substantially higher than that of the air when the incident radiation is high (Fig. 6.9). Hence, depending on their structure, leaf hairs can have different functions with respect to the energy balance. Highly reflective hairs reduce absorption, and thus T_L, and non-reflective hairs reduce boundary layer conductance, and thus increase T_L.

6.2.5 Evaporative Energy Exchange

Heat loss associated with evaporation of water is the result of the energy demand for that process. Its contribution to the energy balance is typically negative during daytime when a leaf transpires,

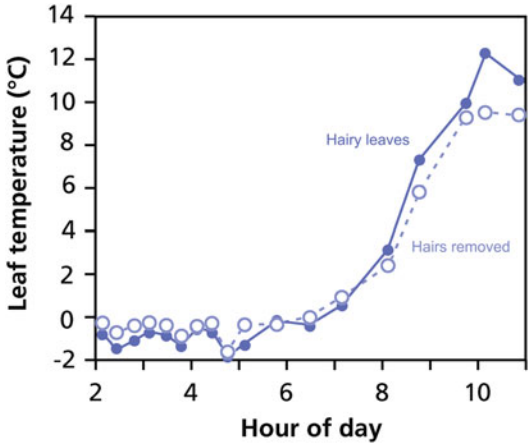

Fig. 6.9 Leaf temperature of *Espeletia timotensis*, a giant rosette plant that occurs in the Venezuelan Andes at elevations up to 4500 m. Measurements were made on plants growing in their natural environment, at different times of the day, both on intact hairy leaves, and on adjacent leaves of which the hairs were partly removed. Sunrise occurred around 6:45 am. The temperature of the intact leaf becomes higher than that of the shaved leaf when global radiation exceeds 300 W m^{-2}; the thick leaf pubescence (up to 30 mm) increases boundary layer thickness and resistance to convective and latent heat transfer; effects of the pubescence on solar radiation absorption are minor. At night, the temperature of the intact leaves is somewhat lower than that of shaved leaves, due to reduced convective heat transfer from air to leaf (Meinzer and Goldstein 1985). © 1985 by the Ecological Society of America.

but it can be positive during nighttime when water condenses on the leaf. The rate of transpiration depends on leaf conductance for diffusion of water vapor (g_w) which consists of the **stomatal conductance** (g_s) and the **boundary layer conductance** (g_a) (Fig. 6.6), and the difference in vapor pressure between leaf (e_i) and air (e_a) ($\Delta w = e_i - e_a$), where e_i is determined by leaf temperature, because it represents the saturated vapor pressure at the leaf temperature (Sect. 2.2.3). Heat loss through transpiration is the product of the rate of transpiration (E) and the latent heat of the vaporization of water (λ, 2450 J g^{-1} or 136 J mol^{-1} at 20 °C); P is the atmospheric pressure:

$$\lambda \times E = \lambda \times g_w(e_i - e_a)/P \qquad (6.12)$$

A popular, but incorrect, idea is that plants control their leaf temperature by regulating transpiration. There is no evidence for such a regulatory mechanism. Leaf cooling through transpiration is only beneficial at high temperatures, but then high transpiration rates may create problems for the plant if water loss is not matched by water uptake; limited water supply often coincides with high temperatures (Chap. 5). Leaf cooling by transpiration also occurs at suboptimal temperatures, because stomata are open during photosynthesis which leads to an even less favorable temperature. Hence, leaf cooling must be considered a *consequence* of transpirational water loss that is inevitably associated with the stomatal opening required to sustain photosynthesis, rather than a mechanism to control leaf temperature, as is the case for some animals.

In many situations, there is an inverse relationship between convective and evaporative heat exchange at any given level of radiation. When stomatal conductance (g_s), and thus evaporative heat loss, decline, leaf temperature increases, which causes an increase in convective heat exchange (by increasing the temperature gradient between leaf and air). Transpiration increases also because of the higher leaf temperature and thus leaf-to-air vapor pressure difference, but that only partly compensates for the effect of the lower g_s (Fig. 6.10).

A negative radiation balance of a leaf under a clear sky at night causes its temperature to drop below air temperature (negative ΔT), causing condensation of water (dew) on the leaf (positive λE); however, not all water on a leaf in early morning is dew; it may also originate from

Fig. 6.10 (continued) energy balance longwave radiation (*LR*), convective heat exchange (*C*), and evaporative heat exchange (*E*) (right Y-axis) are plotted as a function of the leaf dimension (**A**–**C**), stomatal conductance (**D** and **E**), and wind speed (**F**) for conditions pertaining to a clear day in moist conditions (**A**, **D**, and **F**) and in a desert environment (**C**), a clear night (**B**), and an overcast day (**E**). Parameter values used for the calculations are shown below, with letters in brackets referring to the calculated scenarios and the panels in the figure.

	Clear day (a, d, f)	Clear night (b)	Desert (c)	Overcast day (e)
Air temperature, °C	20	10	30	20
Soil temperature, °C	20	20	60	20
Sky temperature, °C	-20	-20	-20	20
Short-wave radiation (SR_{in}), W m^{-2}	800	0	800	100
Leaf dimension, mm	100	-	-	100
Wind speed, m s^{-1}	1	1	1	1
Relative humidity, %	65	100	30	80
Stomatal conductance, mmol m^{-2} s^{-1}	400	0	30	-

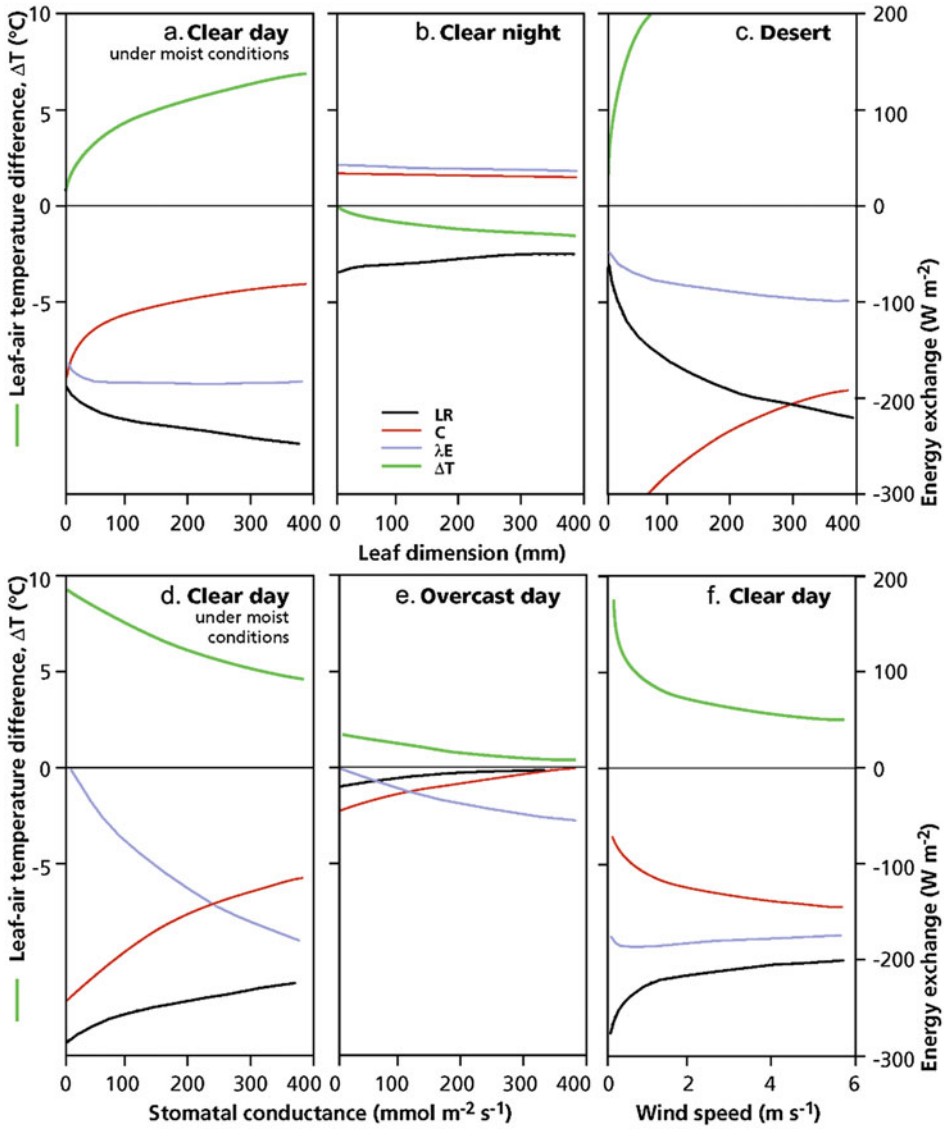

Fig. 6.10 Results of energy-balance model calculations for leaves in different conditions (model provided by F. Schieving, Utrecht University, the Netherlands). The parameter values used for the calculations are shown below the figure. The difference in temperature between leaf and air (ΔT*; left Y-axis) and the components of the*

guttation (Sect. 5.5.2). Guttation water appears as drops on leaf margins (dicots and broad-leafed monocots) or leaf tips (grasses) as opposed to dew that covers the leaf surface.

6.2.6 Metabolic Heat Generation

The metabolic component (M) refers to heat production in **biochemical** reactions. Its contribution in leaves is very small under most circumstances and is generally ignored in calculation of the energy balance. In some plant organs, however, the contribution of metabolism to the energy balance may be substantial. In inflorescences such as the spadix of Araceae and flowers of, *e.g.*, Cycadaceae and Nymphaceae, temperatures may rise several degrees above air temperature, due to their extremely fast **respiration** rates, which largely proceeds through the alternative pathway (Sect. 3.2.6.1).

6.3 Modeling the Effect of Components of the Energy Balance on Leaf Temperature

The analysis of the exact contribution of the different components of the energy balance to leaf temperature is difficult when based on measurements only. The physical relationships as described earlier can be used to calculate leaf temperature from input parameters relevant for the energy balance of a leaf (Jones 2014). By varying parameter values, the influence of a single parameter or combination of parameters on the final leaf temperature and components of the energy balance can be analyzed in a model. Although such a model uses simplifying assumptions, the outcome of the calculations appears to describe the real situation in a satisfactory manner. In Sections 6.2.2 and 6.2.4, we show two examples where energy balance calculations were used (Figs 6.4, 6.5, and 6.8). Here we develop a sensitivity analysis, investigating the effect of changes in one variable on the energy balance, whilst keeping other variables constant.

Figure 6.10 illustrates the result of model calculations on the basis of input parameter values provided. We use realistic values for a clear day under moist conditions, an overcast day, a clear night, and a clear day in a desert. The daytime scenarios have a positive shortwave radiation input (SR_{in}). The other components contribute to the required loss of energy at a stable leaf temperature and are negative. SR_{in} is zero for the nighttime scenario. Components of the energy balance and leaf-to-air temperature difference (ΔT) are calculated in relation to leaf dimension (d), stomatal conductance (g_s), and wind speed (u) for a total of six scenarios (Fig. 6.10).

The calculations show that the difference in leaf-air temperature (ΔT) increases with increasing leaf width, because the boundary layer conductance decreases, which results in a decrease in convective heat exchange (C) in scenarios a, b, and c. On a clear day in cool humid conditions (a), net emission of longwave radiation (LR) increases with leaf width, because of the increasing leaf temperature (T_L). Evaporative cooling (λE) is rather constant, because the high boundary layer conductance (g_{ah}) increases E in small leaves, whereas the higher T_L, and thus larger ($e_i - e_a$), compensates for the lower g_{ah} in larger leaves. At night, (b) leaf temperature (T_L) drops below air temperature (T_a) because of the negative total radiation balance (TR_{net}), causing condensation at the prevailing high humidity. This makes the evaporative heat exchange (λE) positive. C is also positive, because of the lower T_L than T_a, which causes less cooling of the leaf below T_a than would be expected on the basis of the negative radiation balance alone. In a warm dry desert environment (c), with a sparse vegetation cover, the radiation load increases enormously due to the high soil surface temperature. Evaporative cooling is restricted due to stomatal closure (Fig. 6.10). Leaf temperatures only remain within tolerable limits in small leaves that have large convective heat exchange (C). Such conditions occur in deserts as well as on sand dunes in temperate climates on a sunny day.

An increasing stomatal conductance (d) causes a decrease in leaf temperature (T_L), because of increasing evaporative cooling (λE), and LR and C decrease due to the reduced T_L and ΔT, respectively. On a cloudy day (e), the increasing E with increasing g_s compensates for the small influx of

shortwave radiation (SR_{in}), and reduces the leaf temperature to approximately air temperature at higher stomatal conductances (g_s). This reduces LR and C to negligible values at high g_s. Wind (f) reduces T_L due to an increase in convective cooling (C), but transpiration is, again, hardly affected, because the increase in boundary layer conductance (g_{ah}) with increasing wind speed is offset by a decrease in leaf-to-air vapor pressure difference (e_i - e_a) due to the decrease in leaf temperature. The largest effects on leaf temperature occur at the lower ranges of wind speeds which are reflected in the emission of longwave radiation (LR_{em}).

6.4 A Global Perspective of Hot and Cool Topics

We have a sound understanding of the leaf energy budget as affected by leaf traits and environment. What we still need to test experimentally, however, is whether, indeed, some species actually operate at higher leaf temperatures, under field conditions. A recent meta-analysis provides a first global overview of patterns of high temperature tolerance of leaf metabolism (Sect. 3.4.5 and Fig. 3.18). This global analysis shows that both T_{crit} (high temperature where minimal chlorophyll *a* fluorescence rises rapidly, and thus photosystem II is disrupted) and T_{max} (temperature where leaf respiration in darkness is maximal, beyond which respiratory function rapidly declines) increase linearly from polar to equatorial regions. Plants from mid-latitudes (~20–50°) exhibit the narrowest termal safety margins and are at the highest risk of damage due to extreme heat-wave events (O'Sullivan et al. 2017).

References

Ehleringer J, Forseth I. 1980. Solar tracking by plants. *Science* **210**: 1094–1098.

Ehleringer J, Mooney HA, Gulmon SL, Rundel P. 1980. Orientation and its consequences for *Copiapoa* (Cactaceae) in the Atacama Desert. *Oecologia* **46**: 63–67.

Ehleringer JR. 1988. Changes in leaf characteristics of species along elevational gradients in the Wasatch Front, Utah. *Am J Bot* **75**: 680–689.

Ehleringer JR, Björkman O. 1978. Pubescence and leaf spectral characteristics in a desert shrub, *Encelia farinosa*. *Oecologia* **36**: 151–162.

Ehleringer JR, Mooney HA. 1978. Leaf hairs: effects on physiological activity and adaptive value to a desert shrub. *Oecologia* **37**: 183–200.

Foster K, Ryan MH, Real D, Ramankutty P, Lambers H. 2012. Drought resistance at the seedling stage in the promising fodder plant tedera (*Bituminaria bituminosa* var. *albomarginata*). *Crop Past Sci* **63**: 1034–1042.

Gamon JA, Pearcy RW. 1989. Leaf movement, stress avoidance and photosynthesis in Vitis californica. *Oecologia* **79**: 475–481.

Jones HG. 2014. *Plants and Microclimate: A Quantitative Approach to Environmental Plant Physiology*. Cambridge: Cambridge University Press.

Kao W-Y, Forseth IN. 1992. Dirunal leaf movement, chlorophyll fluorescence and carbon assimilation in soybean grown under different nitrogen and water availabilities. *Plant Cell Environ* **15**: 703–710.

Kao WY, Tsai TT. 1998. Tropic leaf movements, photosynthetic gas exchange, leaf $\delta^{13}C$ and chlorophyll a fluorescence of three soybean species in response to water availability. *Plant Cell Environ* **21**: 1055–1062.

Kjellberg B, Karlsson S, Kerstensson I. 1982. Effects of heliotropic movements of flowers of *Dryas octopetala* L. on gynoecium temperature and seed development. *Oecologia* **54**: 10–13.

Körner C, Cochrane P. 1983. Influence of plant physiognomy on leaf temperature on clear midsummer days in the Snowy Mountains, south-eastern Australia. *Acta Oecol/Oecol/ Plant* **4**: 117–124.

Ludlow MM, Björkman O. 1984. Paraheliotropic leaf movement in siratro as a protective mechanism against drought-induced damage to primary photosynthetic reactions: damage by excessive light and heat. *Planta* **161**: 505–518.

Meinzer F, Goldstein G. 1985. Some consequences of leaf pubescence in the Andean giant rosette plant *Espeletia timotensis*. *Ecology* **66**: 512–520.

Mooney HA, Ehleringer J, Björkman O. 1977. The energy balance of leaves of the evergreen desert shrub *Atriplex hymenelytra*. *Oecologia* **29**: 301–310.

Nobel PS. 1983. *Biophysical Plant Physiology and Ecology*. San Francisco, CA: WH Freeman and Company.

O'Sullivan OS, Heskel MA, Reich PB, Tjoelker MG, Weerasinghe LK, Penillard A, Zhu L, Egerton JJG, Bloomfield KJ, Creek D, Bahar

NHA, Griffin KL, Hurry V, Meir P, Turnbull MH, Atkin OK. 2017. Thermal limits of leaf metabolism across biomes. *Glob Change Biol* **23**: 209–223.

Schulze E-D, Eller BM, Thomas DA, Willert DJv, Brinckmann E. 1980. Leaf temperatures and energy balance of*Welwitschia mirabilis* in its natural habitat. *Oecologia* **44**: 258–262.

Sherry RA, Galen C. 2002. The mechanism of floral heliotropism in the snow buttercup, Ranunculus adoneus. *Plant Cell Environ* **21**: 983–993.

Smith WK, Bell DT, Shepherd KA. 1998. Associations between leaf structure, orientation, and sunlight exposure in five Western Australian communities. *Am J Bot* **85**: 56–63.

Plant Energy Budgets: Effects of Radiation and Temperature

7

7.1 Introduction

In Chap. 6, we discussed leaf traits that are related to reflection or avoidance of high radiation loads in high-light environments. Many plants lack these adaptations, and absorb potentially damaging levels of radiation. In this chapter, we discuss some of the negative effects of excess radiation and the physiological mechanisms by which some plants avoid damage (Sect. 7.2.1). Effects of ultraviolet radiation and plant mechanisms to avoid or repair damage are treated in Sect. 7.2.2. Finally, we discuss some effects of both high and low temperatures in Sect. 7.3.

7.2 Radiation

7.2.1 Effects of Excess Irradiance

Species that are adapted to shade often have a restricted capacity to acclimate to a high irradiance. Unacclimated plants have a low capacity to use the products of the light reactions for carbon fixation, and tend to be damaged by high irradiance levels, because the energy absorbed by the photosystems exceeds the energy that can be used by carbon-fixation reactions. The excess energy can give rise to the production of **reactive oxygen species** (**ROS**) (*i.e.* toxic, reactive oxygen-containing molecules that rapidly lose an electron) and **radicals** (molecules with unpaired electrons) that break down membranes and chlorophyll (**photodamage**) (Sect. 2.3.3). Acclimated plants have protective mechanisms that avoid this photodamage. For example, the energy absorbed by the light-harvesting complex may be lost as heat through reactions associated with the **xanthophyll cycle**. When the cycle converts violaxanthin to zeaxanthin or antheraxanthin, nonradiative mechanisms dissipate energy (Sect. 2.3.3.1). When zeaxanthin is present and the thylakoid lumen is acidic, excess light energy is lost as heat. **Chlorophyll fluorescence** analysis can detect this non-photochemical quenching of excess light energy (Box 2.4; Sect. 2.3.1).

7.2.2 Effects of Ultraviolet Radiation

Effects of ultraviolet (UV) radiation on plants have been studied for more than a century. The finding that the stratospheric UV-screening ozone layer has been substantially depleted due to human activities, however, has increased interest in this topic. Ozone in the Earth's atmosphere prevents all of the UV-C (<280 nm) and most of the UV-B (280–320 nm) radiation from reaching the Earth's surface (Fig. 7.1). Due to differences in optical density of the atmosphere, the UV radiation reaching the Earth is least at sea level in polar regions, and greatest at high altitude and low latitude (*e.g.*, the Andes). Cloud cover greatly reduces solar UV irradiance.

H. Lambers, R. S. Oliveira, *Plant Physiological Ecology*, https://doi.org/10.1007/978-3-030-29639-1_7

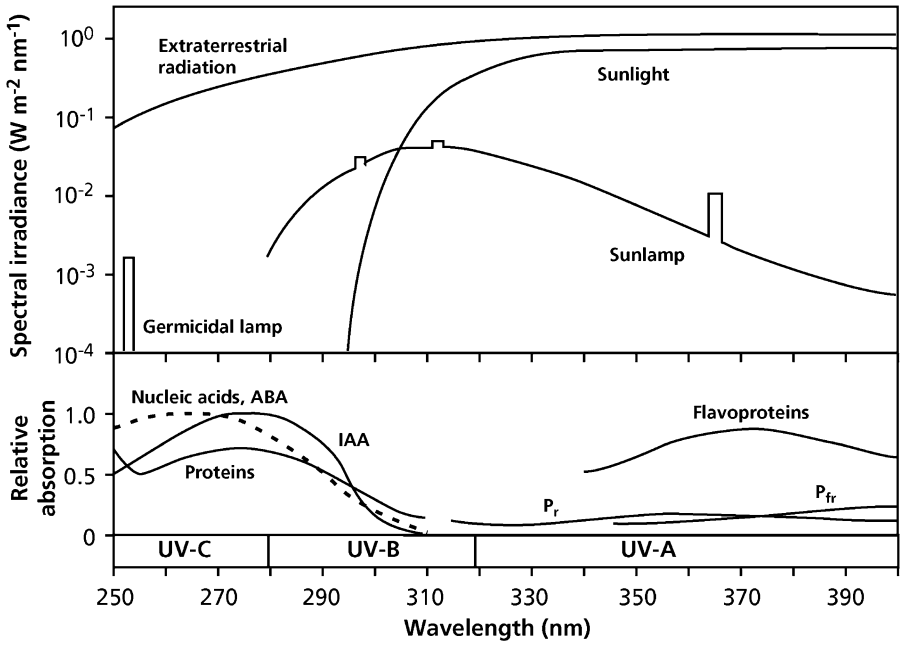

Fig. 7.1 Spectral irradiance at 30 cm from common UV lamps, solar spectral irradiance before attenuation by the Earth's atmosphere (extraterrestrial), and as would be received at sea level at midday in summer at temperate latitudes. The absorption spectra of a number of plant compounds are also shown; ABA (abscisic acid) and nucleic acids are represented by the same curve; IAA (indole acetic acid) and the two forms of phytochrome (P_r and P_{fr}) are represented by the same curve as protein. Major subdivisions of the UV spectrum are indicated at the bottom; UV-B is ultraviolet light in the region 280 to 320 nm (Caldwell 1981).

7.2.2.1 Damage by UV

Many compounds in plant cells absorb photons in the UV region (Fig. 7.1); the most destructive actions of UV include effects on nucleic acids. **DNA** is by far the most sensitive nucleic acid. Upon absorption of UV, polymers of pyrimidine bases, termed **cyclobutane-pyrimidine** dimers, are formed, which leads to loss of biological activity. Although RNA and proteins also absorb UV radiation, much higher doses are required for inactivation to occur, possibly due to their higher concentration in the cell compared with that of DNA. **ROS** play a role in mediating effects of UV-B: membranes are damaged due to lipid peroxidation (Jansen et al. 1998; Verdaguer et al. 2017).

Algae and bacteria are considerably more sensitive to UV-B radiation than are leaves of higher plants, due to less shielding of their DNA. Higher plants that are sensitive to solar UV show a reduction in photosynthetic capacity, leaf expansion, and height; they tend to have thicker leaves, which are often curled, and increased axillary branching. Although part of the reduced leaf expansion may be the result of reduced photosynthesis, it also involves direct effects on cell division (Caldwell 1981), with both effects leading to reductions in plant growth and productivity. There may be additional effects on plant development, *e.g.*, on leaf epidermal cell size and leaf elongation in *Deschampsia antarctica* (Antarctic hair grass) (Ruhland and Day 2000).

7.2.2.2 Protection Against UV: Repair or Prevention

Damage incurred by DNA due to UV absorption can be repaired at the molecular level by splitting the **pyrimidine dimers**, in plants as well as other eukaryotes including humans (Molinier 2017; Elliott et al. 2018). Identification, followed by excision of the lesions from a DNA molecule and replacement by an undamaged patch using

the other strand as a template has also been demonstrated. Plants remove UV photoproducts from their genomic DNA through a dual-incision mechanism that is nearly identical to that in humans and other eukaryotes (Canturk et al. 2016). Scavenging of ROS can also alleviate UV-B stress; levels of key antioxidants (glutathione and ascorbate) and enzymes that detoxify ROS [*e.g.*, superoxide dismutase (SOD) and ascorbate peroxidase] are upregulated in response to UV-B (Fig. 7.2; Janssens et al. 1998).

Plants can minimize UV exposure by having **steeply inclined leaves**, especially at lower latitudes and by **reflecting** or **absorbing UV** in the **epidermis** (Barnes et al. 2015). Epidermal cells may selectively absorb UV, because of the presence of **phenolic compounds** (specific **flavonoids**) (Martz et al. 2007). A UV-B photoreceptor (UVR8) senses UV-B, and this triggers the accumulation of UV-absorbing pigments, but not changes in plant morphology (Coffey et al. 2017). In wild populations of *Betula pubescens* (white birch) in a large climatic transect in Finland, concentrations of quercetin derivatives are positively correlated with latitude (Fig. 7.3). By contrast, the concentrations of apigenin and naringenin derivatives are negatively correlated with latitude. These compound-specific latitudinal gradients compensate each other, resulting in no changes in the concentration of total flavonoids (Stark et al. 2008). Since the antioxidant capacity of quercetin derivatives is greater than that of other flavonoids, the qualitative change reflects acclimation or adaptation to strong light in the north. Along an elevation gradient in Hawaii spanning 2600–3800 m, leaf

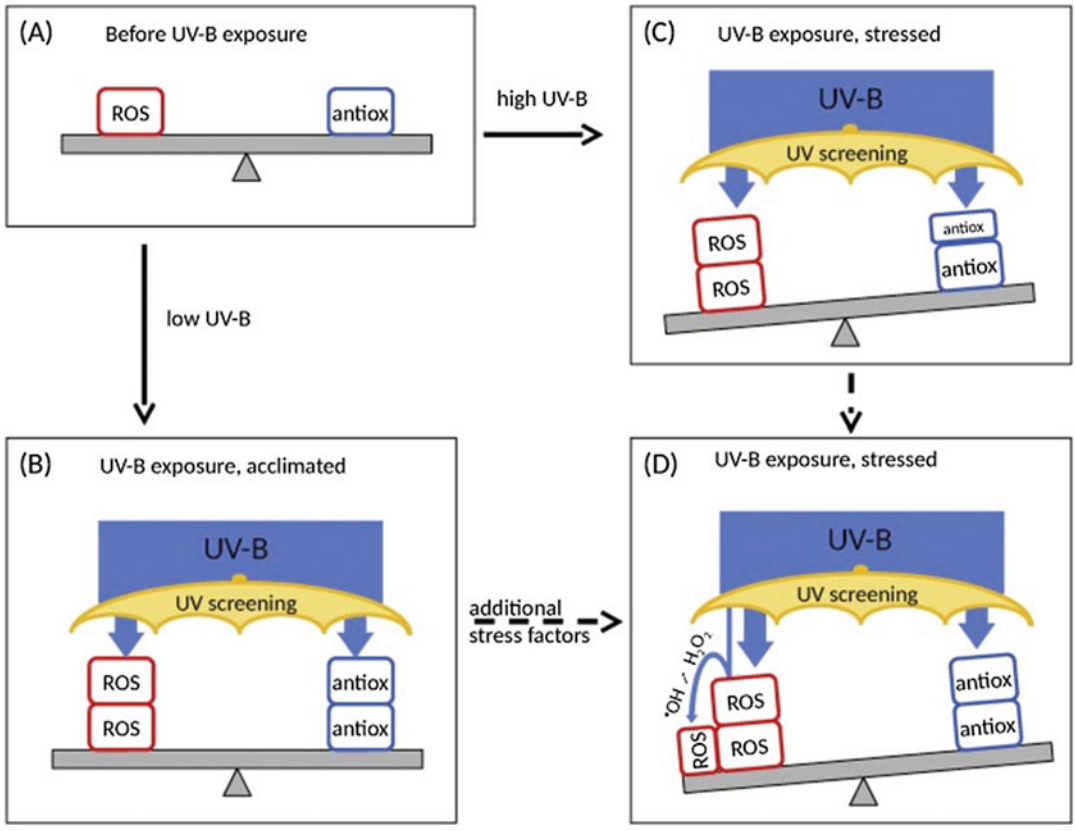

Fig. 7.2 Ultraviolet (UV)-induced changes in the antioxidant-pro-oxidant balance in leaves. Models illustrate the balance between the production of reactive oxygen species (ROS) and activities of antioxidants (antiox) or capacities before (**A**) and during (**B**–**D**) exposure to UV (Czégény et al. 2016); copyright Elsevier Science, Ltd.

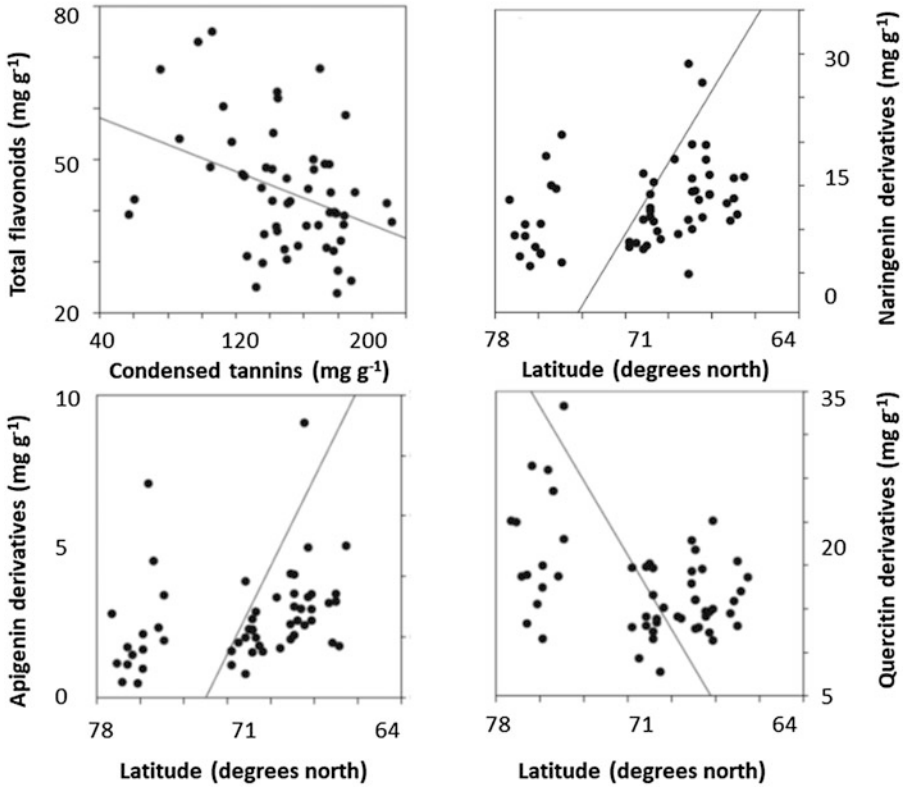

Fig. 7.3 Relationships between the total sum of flavonoids and condensed tannins in the north–south transect and relationships between the concentration of naringenin, apigenin and quercetin derivatives with latitude (degrees north), based on study sites (Stark et al. 2008).

epidermal UV-A transmittance is strongly correlated with elevation and relative biologically effective UV-B in the exotic *Verbascum thapsus* (common mullein); however, transmittance is consistently low, and does not vary with elevation in the native *Vaccinium reticulatum* (ohelo 'ai) (Barnes et al. 2017). UV radiation is the primary factor driving the variation in leaf **phenolics** across Chinese grasslands (Chen et al. 2013). The concentration of UV-protecting compounds can change rapidly, even on a diurnal basis (Barnes et al. 2015).

In addition to flavonoids, sinapate esters of phenolics provide some protection against UV in Brassicaceae [*e.g.*, *Arabidopsis thaliana* (thale cress)] (Sheahan 1996; Dean et al. 2014). The most effective location for compounds to screen UV is in the cell walls of epidermal cells, rather than in their vacuoles, where phenolics may also accumulate. The epidermis of evergreens transmits, on average, approximately 4% of the incident UV, and it does not allow penetration beyond 32 μm, as opposed to, on average, 28% and 75 μm, respectively, for leaves of deciduous plants (Day 1993). Conifer needles screen UV-B far more effectively, because the absorbing compounds are located in the cell walls as well as inside their epidermal cells. The epidermis of herbaceous species is relatively ineffective at UV-B screening, because UV-B may still penetrate through the epidermal cell walls, even if their vacuoles contain large amounts of UV-absorbing phenolics (Day et al. 1994). **Polyamines**, **waxes**, and specific **alkaloids** may also contribute to UV tolerance, either because they absorb UV, or because they act as scavengers of ROS (Frohnmeyer and Staiger 2003).

Exposure of *Phaseolus vulgaris* (common bean) to elevated levels of UV-B enhances nodulation, which is affected by flavonoids (Sect. 12.3.3) (Pinto et al. 2002). Leaf phenolic concentrations in *Eriophorum russeolum* (cotton grass) are increased at high levels of UV-B. At the end of the growing season, the proportion of total soluble phenolics is greater in leaves exposed to enhanced UV-A and UV-B radiation than in control leaves, but the phenolic composition is not affected (Martz et al. 2011). In *Epilobium angustifolium* (willow herb), there is no UV effect. Since both these species are reindeer (*Rangifer tarandus tarandus*) forage plants, there might be a shift in preference in favor of *Epilobium angustifolium*, but there is no information to support this suggestion.

7.3 Effects of Extreme Temperatures

7.3.1 How Do Plants Avoid Damage by Free Radicals at Low Temperature?

Variation in growth potential at different temperatures may reflect the rate of photosynthesis per unit leaf area, as discussed in Sect. 2.7. A common effect of chilling is **photooxidation**, which occurs because the biophysical reactions of photosynthesis are far less temperature-sensitive than are the biochemical ones. Chlorophyll continues to absorb light at low temperatures, but the energy cannot be transferred to the normal electron-accepting components with sufficient speed to avoid **photoinhibition** (Raven, 2011). One mechanism by which cold-acclimated plants avoid photooxidation is to increase the components of the **xanthophyll cycle** (García-Plazaola et al. 2015), just as observed at excess radiation (Sect. 2.3.3.1). This prevents the formation of **ROS**; radicals may form when oxygen is reduced to superoxide (Apel and Hirt 2004; Mittler 2017). The xanthophyll cycle is widespread among plants, however, and other mechanisms also protect the photosynthetic apparatus of cold-adapted species, especially if low temperatures coincide with high levels of irradiance, such as at high altitude.

Once ROS are formed, they must be scavenged to avoid their damaging effect. Upon exposure to oxidative stress, some ROS are produced in nonacclimated plants which induce the expression of genes encoding enzymes involved in the synthesis of phenolic antioxidants (Mittler 2017). High-alpine species contain higher concentrations of a range of **antioxidants**, such as ascorbic acid (vitamin C), α-tocopherol (vitamin E), and the tripeptide glutathione (Wildi and Lütz 1996). Their concentrations increase with increasing altitude (Fig. 7.4). The higher level of

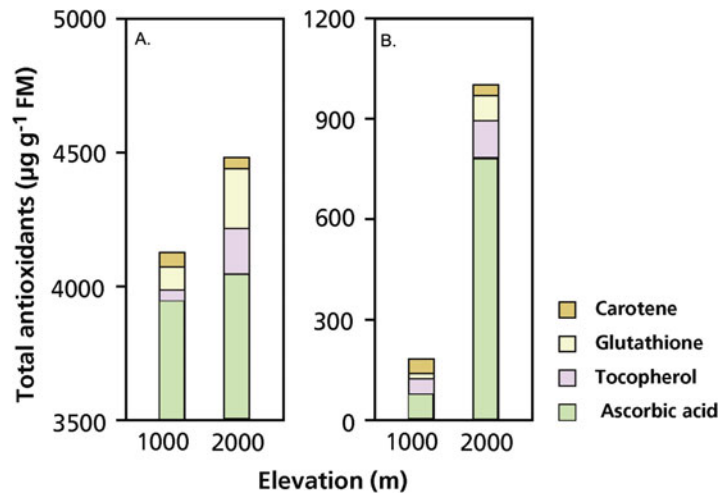

Fig. 7.4 The concentration of various antioxidants in leaves of (**A**) *Homogyne alpina* (alpine coltsfoot) and (**B**) *Soldanella pusilla* (alpine snowbell) measured in plants growing at 1000 m (Wank) and at 2000 m (Obergurgl). Note the different scales on the y-axis (after Wildi and Lütz 1996).

antioxidants in the high-altitude plants enables them to cope with multiple stresses, including lower, early-morning temperature, higher level of irradiance at peak times, or higher levels of UV-B. The concentrations of antioxidants also show a diurnal pattern, with highest values at midday and lower ones at night. **Superoxide dismutase** (SOD) and **catalase** are major enzymes that are involved in avoiding damage by ROS (Mittler 2017). SOD catalyzes the conversion of superoxide to hydrogen peroxide (H_2O_2), and **catalase** converts H_2O_2 to water and oxygen.

7.3.2 Heat-Shock Proteins

A sudden rise in temperature, close to the lethal temperature, induces the formation of mRNAs encoding **heat-shock proteins** (Parcellier et al. 2003). Some of the genes encoding heat-shock proteins are homologous with those from animals; in fact, heat-shock proteins were first discovered in *Drosophila*. Some of these proteins are only produced after exposure to high temperatures; others are also found after exposure to other extreme environmental conditions (*e.g.*, low temperature, water stress, high light, and drought). There is some evidence that an increase in **membrane fluidity** specifically enhances the expression of genes encoding heat-shock proteins (Xiong et al. 2002).

Heat-shock proteins may be involved in the protection of the photosynthetic apparatus and prevent photooxidation. Some act as molecular **chaperones** to prevent irreversible aggregation of stress-labile proteins (Santhanagopalan et al. 2015). Chaperones are involved in arranging the tertiary structure of proteins. Heat-shock proteins are formed both after a sudden increase in temperature, and upon a more gradual and moderate rise in temperature, although not to the same extent. This class of proteins is, therefore, probably also involved in the tolerance of milder degrees of heat stress (Parcellier et al. 2003).

7.3.3 Are Isoprene and Monoterpene Emissions an Adaptation to High Temperatures?

There is increasing evidence that plants, especially some tree species and ferns, can cope with rapidly changing leaf temperatures through the production of the low-molecular-mass hydrocarbon: **isoprene** and **monoterpenes** (Dani et al. 2014). Around Sydney in Australia, these hydrocarbons account for the haze in the Blue Mountains (Nelson 2001). Isoprene (2-methyl-1,3-butadiene) is the single most abundant biogenic, nonmethane hydrocarbon entering the atmosphere due to emission by plants in both temperate and tropical ecosystems, and the reason for these high emission rates have puzzled scientists for a long time (Sharkey et al. 2008). Many isoprene-emitting species lose about 15% of fixed carbon as isoprene, with extreme values up to 50%. Global isoprene emissions from plants to the atmosphere amount to 180–450 10^{12} g carbon per year, more than any other volatile organic carbon lost from plants (Lichtenthaler, 2007). There should be sufficient evolutionary pressure to eliminate this process, if it serves no function. The finding that emissions increase at high temperature and under water stress has stimulated research into a role in coping with high leaf temperatures. The change in **isoprene-emission** capacity through the canopy is similar to the change in **xanthophyll cycle** intermediates which suggests that isoprene and monoterpene emission may be the plant's protection against excess heat, just as the xanthophyll cycle protects against excess light (Loreto and Velikova 2001) (Sect. 2.3.3.1). In the presence of realistic concentrations of isoprene or monoterpenes, leaves are, indeed, protected against high-temperature damage of photosynthesis (Fig. 7.5; Sharkey et al. 2008).

How hot do leaves normally get, if they are not protected in one way or another? Leaves of *Quercus alba* (white oak) at the top of the canopy can reach a temperature of as much as 14 °C above air temperature, and their temperature

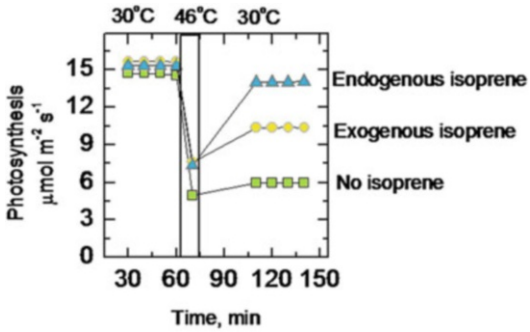

Fig. 7.5 Thermoprotection of photosynthetic capacity by isoprene. Photosynthesis of detached leaves of *Pureria lobata* (kudzu) was measured at the indicated temperatures. One leaf was fed water, and so made isoprene from endogenous sources. Two other leaves were fed 4 µM fosmidomycin, an inhibitor of the pathway leading to isoprene, and isoprene emission was monitored until >90% of the isoprene emission capacity was lost. One of these leaves was then provided with 2 µl l^{-1} isoprene in the air stream (exogenous isoprene treatment). Modified after Sharkey et al. (2008).

may drop by 8 °C within minutes (Singsaas and Sharkey 1998). Using isoprene may be an effective way of changing membrane properties rapidly enough to track leaf temperature. In plants that are not subject to such high temperatures or changes in leaf temperature, slower and less wasteful methods may be more effective.

7.3.4 Chilling Injury and Chilling Tolerance

Many (sub)tropical plants grow poorly at or are damaged by temperatures between 10 and 20 °C. This type of damage is quite different from frost damage, which occurs at subzero temperatures, and is generally described as **chilling injury**. Different parts of the plant may differ in their sensitivity to low temperatures, and this may vary with age. Low-temperature conditioning alleviates *Prunus persica* (peach) fruit chilling injury, resulting in a faster rate of **ethylene** production and a more rapid flesh softening as a result of higher expression of ethylene biosynthetic genes and a series of cell wall hydrolases (Wang et al. 2017). Reduced internal browning of fruit is observed in conditioned plants, with lower transcript levels of **polyphenol oxidase** and **peroxidase**. Conditioned fruits also show increased lipid desaturation. Conditioning is a special case of **cold acclimation**.

The physiological cause of low-temperature damage varies among species and plant organs. The following factors play a role:

1. Changes in membrane fluidity;
2. Changes in the activity of membrane-bound enzymes and processes, such as electron transport in chloroplasts and mitochondria, and in compartmentation;
3. Loss of activity of low-temperature sensitive enzymes;

Chilling tolerance correlates with a high proportion of *cis*-unsaturated fatty acids in the phosphatidyl-glycerol molecules of chloroplast membranes. Evidence for this comes from work with *Nicotiana tabacum* (tobacco) plants transformed with glycerol-3-phosphate acyltransferase from either a cold-tolerant species or a cold-sensitive one. Overexpression of the enzyme from the cold-tolerant species increases cold-tolerance, whereas the tobacco plants become more sensitive to cold stress when overexpressing the enzyme from cold-sensitive plants. Cold sensitivity of the transgenic tobacco plants correlates with the extent of fatty acid unsaturation in phosphatidylglycerol which is due to different selectivities for the saturated and *cis*-unsaturated fatty acids of the enzyme from contrasting sources (Bartels and Nelson 1994).

Heat-shock proteins are expressed at low temperatures (Sabehat et al. 1998), and these probably function in much the same way as discussed in Sect. 7.3.2.

7.3.5 Carbohydrates and Proteins Conferring Frost Tolerance

Plants exposed to sub-zero temperatures face unique challenges that threaten their survival. The growth of ice crystals in the extracellular space can cause cellular dehydration, plasma-membrane rupture, and eventually cell death

(Livingston et al. 2018). Additionally, some **pathogenic bacteria** cause tissue damage by initiating ice crystal growth at high sub-zero temperatures through the use of ice-nucleating proteins, thus providing access to nutrients from lysed cells (Bredow et al. 2018). Frost damage only occurs at subzero temperatures, when the formation of **ice crystals** within cells causes damage to membranes and organelles, and dehydration of cells; ice crystals that form outside of cells (*e.g.*, in cell walls) generally cause little damage. Cold tolerance correlates with the concentration of **soluble carbohydrates** in the cells (Ögren 1997; Shin et al. 2015). These carbohydrates play a role in **cryoprotection** (Pommerrenig et al. 2018). Differences in cold tolerance between *Picea abies* (Norway spruce), *Pinus contorta* (lodgepole pine), and *Pinus sylvestris* (Scots pine), following exposure of hardened needles to 5.5 °C, are closely correlated with their carbohydrate concentration. *Picea abies* maintains high sugar concentrations by having larger reserves to start with and slower rates of respiration, which decline more rapidly when sugars are depleted (Ögren 1997; Ögren et al. 1997).

Many plants that naturally occur in temperate climates go through an annual cycle of frost **hardening** and **dehardening**, with maximum freezing tolerance occurring during winter (Ögren 2001). In many woody plants, short days signal the initiation of cold acclimation, which is mediated by ABA. Freezing tolerance is accompanied by bud dormancy, which is also induced by short days. Despite evidence for gibberellins as negative regulators in growth cessation, and ABA and ethylene in bud formation, understanding of the roles that plant growth regulators play in controlling the activity-dormancy cycle is still very fragmentary (Cooke et al. 2012). In herbaceous plants, frost hardening occurs by exposure to low, nonfreezing temperatures. Antifreeze activity has been detected in more than 60 plant species, and **antifreeze proteins** have been purified from 15 of these, including gymnosperms, dicots, and monocots (Gupta and Deswal 2014). Their main function is inhibition of ice crystal growth, rather than the lowering of freezing temperatures (Fig. 7.6; Bravo and Griffith 2005; Bredow and Walker 2017). Specific antifreeze proteins accumulate in the apoplast of *Secale cereale* (winter rye) and other frost-resistant species. These proteins have the unusual ability to bind to and inhibit the growth of ice crystals (Doxey et al. 2006). Ice-binding surfaces for a diverse range of antifreeze proteins clearly discriminates them from other structures in the Protein Data Bank. Knockdown of ice-binding proteins in *Brachypodium distachyon* (false broom) demonstrates their role in freeze protection (Bredow et al. 2016). Antifreeze proteins that accumulate in several places in the apoplast of rye have no specific cryoprotective activity; rather, they interact directly with ice and reduce freezing injury by slowing the growth and recrystallization of ice (Griffith et al. 2005).

Exposure of *Triticum aestivum* (wheat) to low temperature induces a **dehydrin**; dehydrins are a class of proteins that are related to the products of late embryogenesis abundant genes, which we discussed in Sect. 5.8.3 (Close 1996). In *Picea obovata* (Siberian spruce), two dehydrins first appear late in the acclimation process, and they remain at detectable levels throughout the period of maximum low-temperature tolerance (Kjellsen et al. 2013). Different dehydrins likely have separate but overlapping functions in establishing and maintaining extreme low-temperature tolerance. Upon cold-acclimation, a specific glycoprotein (**cryoprotectin**) accumulates in leaves of *Brassica oleracea* (cabbage) which protects thylakoids from nonacclimated leaves, both of cabbage and of other species such as *Spinacia oleracea* (spinach) (Sieg et al. 1996). Cryoprotectin is a plant **lipid-transfer protein** homologue (Hincha 2002). Plant non-specific lipid-transfer proteins are small, basic proteins present that are involved in key processes such as the stabilization of membranes (Liu et al. 2015). They are also active in plant defense (Sect. 13.2).

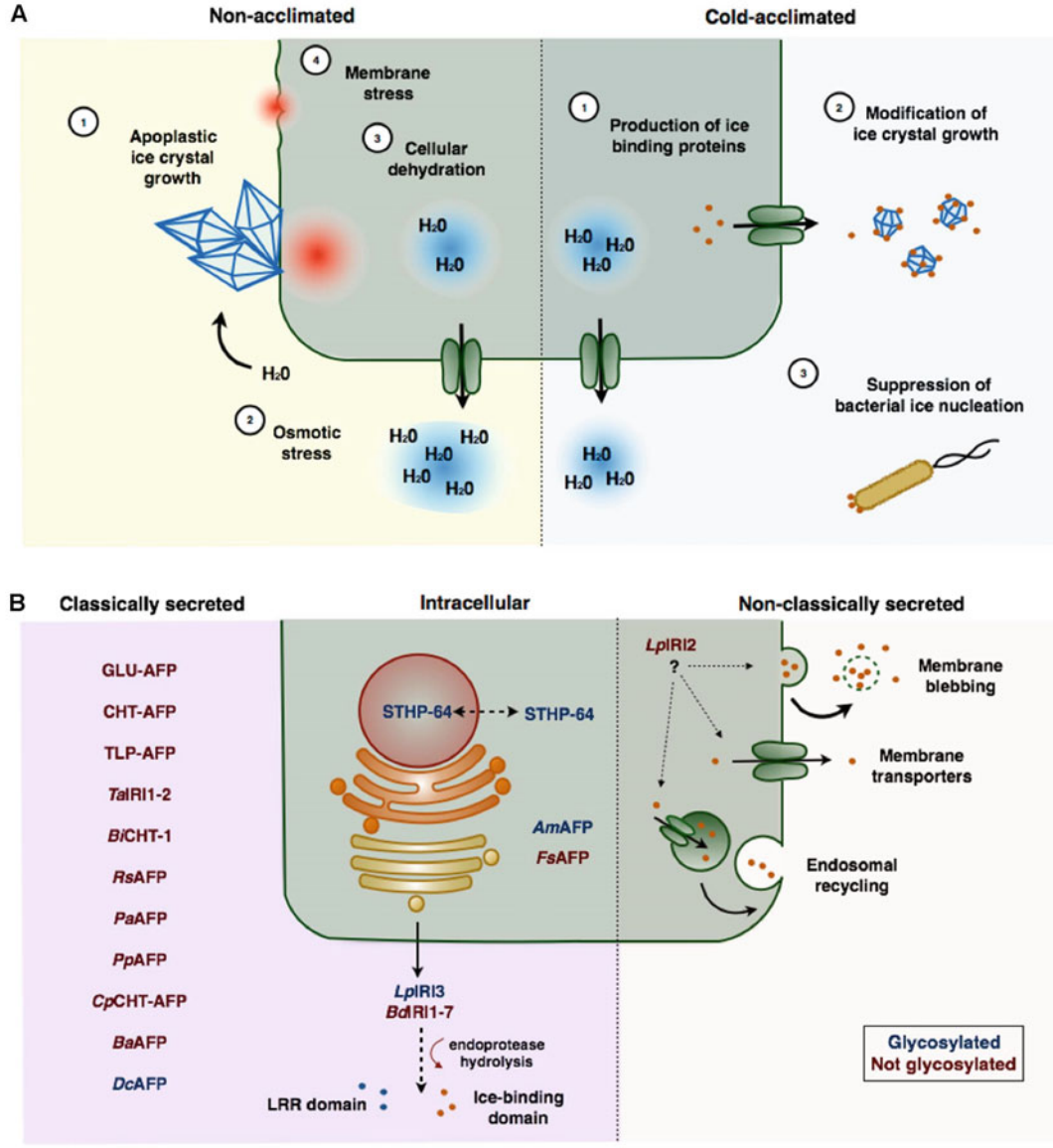

Fig. 7.6 (**A**) Freezing stress and ice-binding proteins (IBP)-induced freeze protection in plants. In the absence of ice-binding proteins, large ice crystals form in the apoplast that can physically damage plasma membranes (*1*). As water molecules join the ice crystal lattice, an osmotic gradient is formed (*2*), resulting in the sequestration of intracellular water, and cellular dehydration (*3*). The loss of cell volume may cause cells to collapse or rupture (*4*). Cold-acclimation-induced expression of ice-binding proteins, which are typically secreted into the apoplast (*1*), adsorb to seed ice crystals preventing their growth (*2*). Ice-binding proteins may also prevent freezing associated with bacterial ice nucleation (*3*). (**B**) Localization and post-translational modification of ice-binding proteins in plants. Most plant ice-binding proteins contain amino-terminal secretion signals and are directed to the apoplast through the endoplasmic reticulum (ER)–Golgi apparatus pathway. Some of these proteins (LpIRI3 and BdIRI1-7), are hydrolyzed following secretion, releasing a leucine-rich repeat (LRR) domain from the ice-binding domain. LpIRI2, which lacks a signal peptide, is secreted, likely through a non-classical secretion pathway. Few ice-binding proteins have been localized to the intracellular space. Glycosylated proteins are indicated in red, proteins that are not glycosylated are indicated in blue (Bredow and Walker 2017).

7.4 Global Change and Future Crops

Plants are frequently exposed to potential harmful radiation and adverse temperatures. Some of the protective mechanisms in plants are universal (*e.g.*, the carotenoids of the xanthophyll cycle that protect against excess radiation). All plants also have mechanisms to avoid effects of UV radiation and repair UV damage. There is a wide variation among species, however, in the extent of the avoidance and probably also in the capacity to repair the damage. The rapid depletion of the stratospheric UV-screening ozone layer, due to human activities, imposes a selective force on plants to cope with UV.

Toxic ROS are produced when the dark reactions of photosynthesis cannot cope with the high activity of the light reactions. This may occur under high-light conditions, in combination with extreme temperatures. The xanthophyll cycle can prevent some of the potential damage. Isoprene production likely provides additional protection of leaves at high temperatures. Specific proteins and carbohydrates offer protection against temperature extremes. Further ecophysiological research on these compounds and on the regulation of genes that encode their production may help us develop crop varieties that have a greater capacity to cope with extreme temperatures. Such plants will be highly desirable for agriculture in those parts of the world where extreme temperatures are a major factor limiting crop productivity.

References

Apel K, Hirt H. 2004. Reactive oxygen species: metabolism, oxidative stress, and signal transduction. *Annu Rev Plant Biol* **55**: 373–399.

Barnes PW, Flint SD, Ryel RJ, Tobler MA, Barkley AE, Wargent JJ. 2015. Rediscovering leaf optical properties: new insights into plant acclimation to solar UV radiation. *Plant Physiol Bochem* **93**: 94–100.

Barnes PW, Ryel RJ, Flint SD. 2017. UV screening in native and non-native plant species in the tropical alpine: implications for climate change-driven migration of species to higher elevations. *Front Plant Sci* **8**: 1451.

Bartels D, Nelson D. 1994. Approaches to improve stress tolerance using molecular genetics. *Plant Cell Environ* **17**: 659–667.

Bravo LA, Griffith M. 2005. Characterization of antifreeze activity in Antarctic plants. *J Exp Bot* **56**: 1189–1196.

Bredow M, Tomalty HE, Smith L, Walker VK. 2018. Ice and anti-nucleating activities of an ice-binding protein from the annual grass, *Brachypodium distachyon*. *Plant Cell Environ* **41**: 983–992.

Bredow M, Vanderbeld B, Walker VK. 2016. Knockdown of ice-binding proteins in *Brachypodium distachyon* demonstrates their role in freeze protection. *PLoS ONE* **11**: e0167941.

Bredow M, Walker VK. 2017. Ice-binding proteins in plants. *Front Plant Sci* **8**: 2153.

Caldwell MM 1981. Plant responses to solar ultraviolet radiation. In: Lange OL, Nobel PS, Osmond CB, Ziegler H eds. *Encyclopedia of Plant Physiology, NS, Vol 12A,*. Berlin: Springer Verlag, 169–197.

Canturk F, Karaman M, Selby CP, Kemp MG, Kulaksiz-Erkmen G, Hu J, Li W, Lindsey-Boltz LA, Sancar A. 2016. Nucleotide excision repair by dual incisions in plants. *Proc Natl Acad Sci USA* **113**: 4706–4710.

Chen L, Niu K, Wu Y, Geng Y, Mi Z, Flynn DFB, He JS. 2013. UV radiation is the primary factor driving the variation in leaf phenolics across Chinese grasslands. *Ecol Evol* **3**: 4696–4710.

Close TJ. 1996. Dehydrins: emergence of a biochemical role of a family of plant dehydration proteins. *Physiol Plant* **97**: 795–803.

Coffey A, Prinsen E, Jansen MAK, Conway J. 2017. The UVB photoreceptor UVR8 mediates accumulation of UV-absorbing pigments, but not changes in plant morphology, under outdoor conditions. *Plant Cell Environ* **40**: 2250–2260.

Cooke JEK, Eriksson ME, Junttila O. 2012. The dynamic nature of bud dormancy in trees: environmental control and molecular mechanisms. *Plant Cell Environ* **35**: 1707–1728.

Czégény G, Mátai A, Hideg É. 2016. UV-B effects on leaves—oxidative stress and acclimation in controlled environments. *Plant Sci* **248**: 57–63.

Dani KGS, Jamie IM, Prentice IC, Atwell BJ. 2014. Evolution of isoprene emission capacity in plants. *Trends Plant Sci* **19**: 439–446.

Day TA. 1993. Relating UV-B radiation screening effectiveness of foliage to absorbing-compound concentration and anatomical characteristics in a diverse group of plants. *Oecologia* **95**: 542–550.

Day TA, Howells BW, Rice WJ. 1994. Ultraviolet absorption and epidermal-transmittance spectra in foliage. *Physiol Plant* **92**: 207–218.

Dean JC, Kusaka R, Walsh PS, Allais F, Zwier TS. 2014. Plant sunscreens in the UV-B: ultraviolet spectroscopy of jet-cooled sinapoyl malate, sinapic acid, and sinapate ester derivatives. *J Am Chem Soc* **136**: 14780–14795.

Doxey AC, Yaish MW, Griffith M, McConkey BJ. 2006. Ordered surface carbons distinguish antifreeze proteins and their ice-binding regions. *Nat Biotech* **24**: 852–855.

Elliott K, Boström M, Filges S, Lindberg M, Van den Eynden J, Ståhlberg A, Clausen AR, Larsson E. 2018. Elevated pyrimidine dimer formation at distinct genomic bases underlies promoter mutation hotspots in UV-exposed cancers. *PLoS Genetics* **14**: e1007849.

Frohnmeyer H, Staiger D. 2003. Ultraviolet-B radiation-mediated responses in plants. Balancing damage and protection. *Plant Physiol* **133**: 1420–1428.

García-Plazaola JI, Rojas R, Christie DA, Coopman RE. 2015. Photosynthetic responses of trees in high-elevation forests: comparing evergreen species along an elevation gradient in the Central Andes. *AoB Plants* **7**: plv058.

Griffith M, Lumb C, Wiseman SB, Wisniewski M, Johnson RW, Marangoni AG. 2005. Antifreeze proteins modify the freezing process *in planta*. *Plant Physiol* **138**: 330–340.

Gupta R, Deswal R. 2014. Antifreeze proteins enable plants to survive in freezing conditions. *J Biosci* **39**: 931–944.

Hincha DK. 2002. Cryoprotectin: a plant lipid–transfer protein homologue that stabilizes membranes during freezing. *Phil Trans R Soc Lond B* **357**: 909–916.

Jansen MAK, Gaba V, Greenberg BM. 1998. Higher plants and UV-B radiation: balancing damage, repair and acclimation. *Trends Plant Sci* **3**: 131–135.

Janssens F, Peeters A, Tallowin JRB, Bakker JP, Bekker RM, Fillat F, Oomes MJM. 1998. Relationship between soil chemical factors and grassland diversity. *Plant Soil* **202**: 69–78.

Kjellsen TD, Yakovlev IA, Fossdal CG, Strimbeck GR. 2013. Dehydrin accumulation and extreme low-temperature tolerance in Siberian spruce (*Picea obovata*). *Tree Physiol* **33**: 1354–1366.

Lichtenthaler H. 2007. Biosynthesis, accumulation and emission of carotenoids, α-tocopherol, plastoquinone, and isoprene in leaves under high photosynthetic irradiance. *Photosyn Res* **92**: 163–179.

Liu F, Zhang X, Lu C, Zeng X, Li Y, Fu D, Wu G. 2015. Non-specific lipid transfer proteins in plants: presenting new advances and an integrated functional analysis. *J Exp Bot* **66**: 5663–5681.

Livingston DP, Tuong TD, Murphy JP, Gusta LV, Willick I, Wisniewski ME. 2018. High-definition infrared thermography of ice nucleation and propagation in wheat under natural frost conditions and controlled freezing. *Planta* **247**: 791–806.

Loreto F, Velikova V. 2001. Isoprene produced by leaves protects the photosynthetic apparatus against ozone damage, quenches ozone products, and reduces lipid peroxidation of cellular membranes. *Plant Physiol* **127**: 1781–1787.

Martz F, Sutinen M-L, Derome K, Wingsle G, Julkunen-TIitto R, Turunen M. 2007. Effects of ultraviolet (UV) exclusion on the seasonal concentration of photosynthetic and UV-screening pigments in Scots pine needles. *Glob Change Biol* **13**: 252–265.

Martz F, Turunen M, Julkunen-Tiitto R, Suokanerva H, Sutinen M-L. 2011. Different response of two reindeer forage plants to enhanced UV-B radiation: modification of the phenolic composition. *Pol Biol* **34**: 411–420.

Mittler R. 2017. ROS are good. *Trends Plant Sci* **22**: 11–19.

Molinier J. 2017. Genome and epigenome surveillance processes underlying UV exposure in plants. *Genes* **8**: 316.

Nelson O. 2001. Polluting eucs. Emissions of organic compounds from eucalypts may add to air pollution. *Trees Nat Res* **43**: 14.

Ögren E. 1997. Relationship between temperature, respiratory loss of sugar and premature dehardening in dormant Scots pine seedlings. *Tree Physiol* **17**: 47–51.

Ögren E. 2001. Effects of climatic warming on cold hardiness of some northern woody plants assessed from simulation experiments. *Physiol Plant* **112**: 71–77.

Ögren E, Nilsson T, Sundblad L-G. 1997. Relationship between respiratory depletion of sugars and loss of cold hardiness in coniferous seedlings over-wintering at raised temperatures: indications of different sensitivities of spruce and pine. *Plant Cell Environ* **20**: 247–253.

Parcellier A, Gurbuxani S, Schmitt E, Solary E, Garrido C. 2003. Heat shock proteins, cellular chaperones that modulate mitochondrial cell death pathways. *Biochem Biophys Res Comm* **304**: 505–512.

Pinto ME, Edwards GE, Riquelme AA, Ku MSB. 2002. Enhancement of nodulation in bean (*Phaseolus vulgaris*) by UV-B irradiation. *Funct Plant Biol* **29**: 1189–1196.

Pommerrenig B, Ludewig F, Cvetkovic J, Trentmann O, Klemens PAW, Neuhaus HE. 2018. In concert: orchestrated changes in carbohydrate homeostasis are critical for plant abiotic stress tolerance. *Plant Cell Physiol* **59**: 1290–1299.

Raven JA. 2011. The cost of photoinhibition. *Physiol Plant* **142**: 87–104.

Ruhland CT, Day TA. 2000. Effects of ultraviolet-B radiation on leaf elongation, production and phenylpropanoid concentrations of *Deschampsia antarctica* and *Colobanthus quitensis* in Antarctica. *Physiol Plant* **109**: 244–251.

Sabehat A, Lurie S, Weiss D. 1998. Expression of small heat-shock proteins at low temperatures. A possible role in protecting against chilling injuries. *Plant Physiol* **117**: 651–658.

Santhanagopalan I, Basha E, Ballard KN, Bopp NE, Vierling E 2015. Model chaperones: small heat shock proteins from plants. In: Tanguay RM, Hightower LE eds. *The Big Book on Small Heat Shock Proteins*. Cham: Springer International Publishing, 119–153.

Sharkey TD, Wiberley AE, Donohue AR. 2008. Isoprene emission from plants: why and how. *Ann Bot* **101**: 5–18.

Sheahan JJ. 1996. Sinapate esters provide greater UV-B attenuation than flavonoids in *Arabidopsis thaliana* (Brassicaceae). *Am J Bot* **83**: 679–686.

Shin H, Oh Y, Kim D. 2015. Differences in cold hardiness, carbohydrates, dehydrins and related gene expressions under an experimental deacclimation and reacclimation in Prunus persica. *Physiol Plant* **154**: 485–499.

Sieg F, Schroder W, Schmitt JM, Hincha DK. 1996. Purification and characterization of a cryoprotective protein (cryoprotectin) from the leaves of cold-acclimated cabbage. *Plant Physiol* **111**: 215–221.

Singsaas EL, Sharkey TD. 1998. The regulation of isoprene emission responses to rapid leaf temperature fluctuations. *Plant Cell Environ* **21**: 1181–1188.

Stark S, Julkunen-Tiitto R, Holappa E, Mikkola K, Nikula A. 2008. Concentrations of foliar quercetin in natural populations of white birch (*Betula pubescens*) increase with latitude. *J Chem Ecol* **34**: 1382–1391.

Verdaguer D, Jansen MAK, Llorens L, Morales LO, Neugart S. 2017. UV-A radiation effects on higher plants: exploring the known unknown. *Plant Sci* **255**: 72–81.

Wang K, Yin XR, Zhang B, Grierson D, Xu CJ, Chen KS. 2017. Transcriptomic and metabolic analyses provide new insights into chilling injury in peach fruit. *Plant Cell Environ* **40**: 1531–1551.

Wildi B, Lütz C. 1996. Antioxidant composition of selected high alpine plant species from different altitudes. *Plant Cell Environ* **19**: 138–146.

Xiong L, Schumaker KS, Zhu J-K. 2002. Cell signaling during cold, drought, and salt stress. *Plant Cell* **14**: S65–183.

8 Scaling-Up Gas Exchange and Energy Balance from the Leaf to the Canopy Level

8.1 Introduction

Having discussed the gas exchange and energy balance of individual leaves in previous chapters, we are now in a position to 'scale up' to the canopy level. In moving between scales, it is important to determine which interactions are strong enough to consider, and which can be ignored. The water relations of plant canopies differ distinctly from what would be predicted from the study of individual leaves, because each leaf modifies the environment of adjacent leaves by reducing irradiance and wind speed, and either decreasing or increasing vapor pressure deficit, depending on transpiration rates. These changes within the canopy reduce transpiration from each leaf more than would be predicted from an individual leaf model, based on the atmospheric conditions above the canopy. For example, **irradiance** declines more or less exponentially with **leaf area index** (leaf area per ground area, ***LAI***) within the canopy, reducing the energy that each leaf absorbs. Friction from the canopy causes **wind speed** to decline close to the canopy, just as it declines close to the ground surface. Wind speed, generally, declines exponentially within the canopy, and individual leaves within a canopy have lower boundary layer conductance than expected from leaf dimensions and the meteorological conditions of the bulk air (Chap. 6). Finally, transpiration by each leaf increases the **water vapor concentration** around adjacent leaves, as does evaporation from a wet soil surface. As stomatal conductance increases, the increasing water vapor concentration within the canopy reduces the driving force for transpiration, so that transpiration increases less than expected from the increase in **stomatal conductance** alone (Jarvis and McNaughton 1986). Because **mesophyll conductance** exhibits similar variation and has similar impact on photosynthesis as stomatal conductance (Sect. 2.5), we also need to consider the role of mesophyll conductance in the economics of photosynthetic resource use (Buckley and Warren 2014).

We can use mathematical functions to describe the effects of variables and their interactions in a model of the system. A good model for scaling will be based on mechanistic processes at a lower scale (Box 8.1). Can we treat the canopy simply as one big leaf to arrive at the gas exchange and energy balance of a canopy? Or do we need to sum up the gas exchange and energy balance of each leaf and its individual microclimate? We will address these questions in the following sections.

H. Lambers, R. S. Oliveira, *Plant Physiological Ecology*, https://doi.org/10.1007/978-3-030-29639-1_8

Box 8.1: Optimization of Nitrogen Allocation to Leaves in Plants Growing in Dense Canopies

Thijs L. Pons
Department Plant Ecophysiology, Institute of Environmental Biology, Utrecht University, Utrecht, The Netherlands

A theoretical optimum distribution of nitrogen (N) over the leaves of a plant that maximizes whole plant photosynthesis per unit leaf N can be calculated (Field 1983; Hirose and Werger 1987; Pons et al. 1989; Evans 1993; Anten et al. 1995). Such an optimum distribution pattern depends on the distribution of light over the leaves of a plant growing in a dense canopy. The approach chosen here is for plant stands consisting of one species of even-sized individuals. Hence, the performance of the stand is identical to the performance of individual plants growing in the stand. The calculations consist of five parts that describe mathematically: (1) the distribution of irradiance in the leaf canopy where the plant is growing, (2) the dependence of photosynthetic rate on irradiance of leaves, (3) the relationships with leaf N of the parameters of the photosynthesis-irradiance relationship, (4) canopy photosynthesis by summation of photosynthetic rates in different canopy layers, and (5) the distribution of leaf N at maximum canopy photosynthesis per unit leaf N.

Following the approach discussed in Box 2.3 on gradients in leaves, we can use the Lambert-Beer law to calculate the light absorption profile in the canopy. An extension of that equation gives the mean irradiance (I_L, μmol m^{-2} s^{-1}) incident on a leaf at a certain depth in the canopy expressed as cumulative leaf area index from the top of the canopy [F, m^2 (leaf area) m^{-2} (ground surface)]:

$$I_L \frac{I_o \times K_L}{1-t} \exp^{(-K_L \times F)} \quad (8.1)$$

where I_o (μmol m^{-2} s^{-1}) is the irradiance above the canopy, and the dimensionless parameters K_L, t, and F are the canopy extinction coefficient, leaf transmission coefficient, and leaf area index, respectively (Hirose and Werger 1987). I_o is multiplied by K_L to account for the deviation of leaf angle from horizontal transmission of light by leaves.

Again following the approach in Box 2.3, we calculate the photosynthetic rate in each canopy layer by using the light-response curve. For this purpose we use the equation introduced in Section 2.3.2.1 on photosynthesis:

$$A = \frac{\Phi \times I + A_{max} - \sqrt{\{\phi \times I + A_{max})^2 - 4\Theta \times I \times \phi \times A_{max}\}}}{2\Theta} - R_{day} \quad (8.2)$$

where A_n (μmol CO_2 m^{-2} s^{-1}) is the actual rate of net photosynthesis, ϕ is the apparent quantum yield at low irradiance [mol CO_2 mol^{-1} (quanta)], I is irradiance (μmol quanta m^{-2} s^{-1}), A_{max} (μmol CO_2 m^{-2} s^{-1}) is the light-saturated rate of (gross) photosynthesis, and Φ (dimensionless) describes the curvature on the A-I relationship.

Parameters of the light-response curve (Eq. 8.2) can be related to leaf N per unit leaf area (N_{LA}). Linear relationships give a satisfactory description of the increase of A_{max} and R_{day} with N_{LA}:

$$A_{max} = a_a \times (N_{LA} - N_b) \quad (8.3)$$

$$R_{day} = a_r \times (N_{LA} - N_b) + R_b \quad (8.4)$$

where a_a and N_b are the slope and intercept of the A_{max}-N_{LA} relation. N_b is the amount of N still present in leaves that have no photosynthetic capacity left. R_b is R_{day} in leaves with $N_{LA} = N_b$. The quantum yield, ϕ, depends on chlorophyll concentration which may also be true for the curvature,

(continued)

Box 8.1 (continued)

Θ. These two parameters may thus also depend on the leaf N concentration, N_{LA}, for which mathematical relationships can be formulated.

Canopy photosynthesis can now be calculated using Eqs. 8.1, 8.2, 8.3 and 8.4 and the leaf N distribution in the canopy. For that purpose distribution functions may be used (Hirose and Werger 1987). Photosynthetic rates are summed over the different canopy layers and over a day or other time interval with varying irradiance. Daily course of irradiance may be described by a sinusoidal curve, or in any other way.

Maximum canopy photosynthesis at constant total leaf N of the plant is reached when at every depth in the canopy a change in leaf N (δN_{LA}) will result in the same change in daily photosynthesis (δA_{day}) (Field 1983):

$$\frac{\delta A_{day}}{\delta N_{LA}} = \lambda \qquad (8.5)$$

The constant λ is called the *Lagrange multiplier*. This is illustrated in Box Fig. 8.1, where the points of contact of the tangents to the lines for daily photosynthesis at different canopy depths as a function of N_{LA} represent the optimal distribution of leaf N. Different total amounts of leaf N will result in different values for λ. In this way optimal leaf N distribution for maximum canopy photosynthesis of a plant per unit leaf N (photosynthetic N-use efficiency, PNUE) can be calculated. Photosynthetic rates at actual distribution of leaf N in plants growing in leaf canopies has been compared with theoretically derived ones as described earlier, and with plants that have a uniform distribution. For instance, in the study of Pons et al. (1989) the performance of *Lysimachia vulgaris* (yellow loosestrife) at uniform and optimal distribution was 73% and 112%, respectively, of that at actual distribution. Hence, plants tend to distribute their leaf N optimally over leaf area.

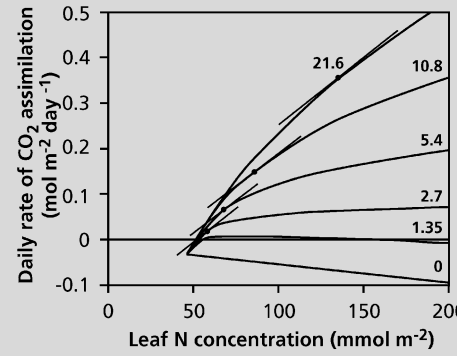

Box Fig 8.1 Calculated daily photosynthesis as a function of leaf N for different depths in a canopy with concomitantly different levels of irradiance (expressed as mol m^{-2} day^{-1}). The points of contact of the parallel tangents to the curves represent the optimal distribution pattern of N at a given total amount of leaf N (after Hirose and Werger 1987).

A submodel of the model developed above is a canopy photosynthesis model. This is a simplified one because both the light distribution and leaf photosynthesis use simplifications that are valid for the purpose of the above calculations, but not when we are interested in the quantitative outcome of canopy photosynthesis itself. The distribution of light as described here gives the average irradiance incident on leaves at a particular depth in a canopy with unidirectional light coming from straight overhead. It provides a reasonable approximation for diffuse light, but not for directional sunlight because spatial variation due to sunflecks and varying angle of incident sunlight are not accounted for. For the leaf photosynthesis module, the Farquhar et al. (1980) model could be used which not only accounts for varying conditions of irradiance, as in this model, but also for variation in temperature and stomatal conductance. This model is described in Box 2.1.

8.2 Canopy Water Loss

In Sect. 2.2.2, we discussed leaf transpiration as measured on a single leaf in a well-ventilated and environmentally controlled gas-exchange cuvette. In such cuvettes, the boundary layer is minimal, and transpiration has little effect on the conditions inside and around the leaf. For leaves in a canopy, however, boundary layers significantly affect the transpiration rate, and the air in the boundary layer contains more water vapor than the bulk ambient air. In a canopy, transpiration is therefore affected by both **stomatal** and **boundary layer conductance**. In effect, the boundary layer provides a **negative feedback** to transpiration. As a result, stomatal conductance has much less effect on canopy water loss than would be expected from study of single leaves (Jarvis and McNaughton 1986).

While we can adequately describe transpiration from individual leaves in a leaf cuvette by the diffusion equation, transpiration from leaves in a canopy requires consideration of both diffusion and the leaf energy balance. The dual processes of **vaporization** and **diffusion** were first considered in an evaporation model by Penman (1948). This work was extended to include evaporation from vegetation by incorporation of a canopy conductance (Monteith 1963, 1965). This line of thinking, which leads to '**single-layer**' models, is to determine the evaporation if the plant canopy were simply a partially wet plane at the lower boundary of the atmosphere. This conceptual plane, which is often referred to as a '**big leaf**', is ascribed a physiological and aerodynamic resistance to water vapor transfer (Fig. 8.1). In an analogy with an individual leaf, a **canopy conductance** is introduced which implicitly

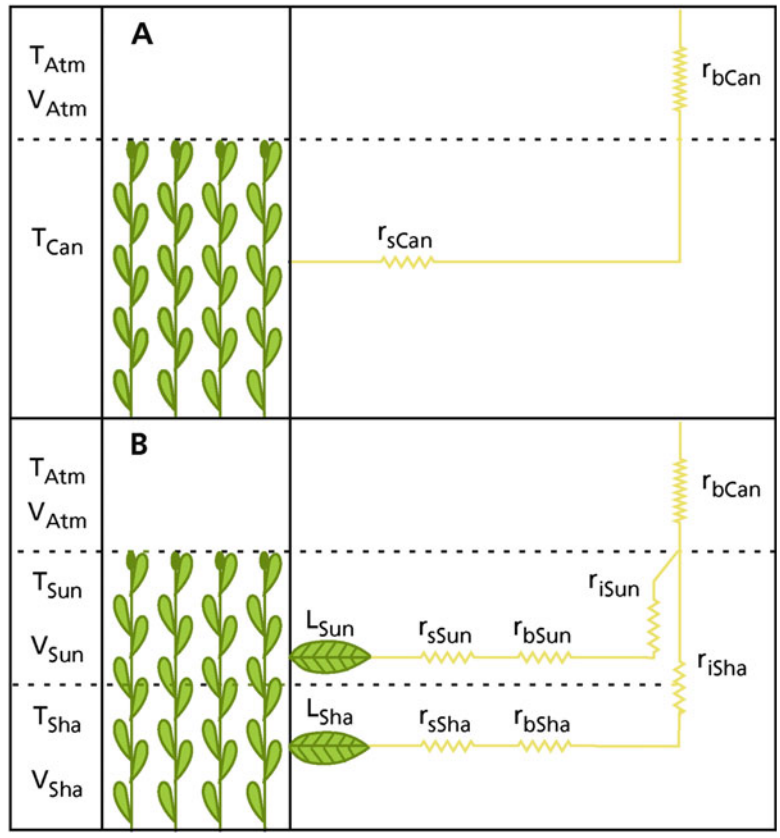

Fig. 8.1 Schematic representation of (**A**) a single-layer ('big-leaf') model and (**B**) a multilayer model used for calculation of canopy evapotranspiration; modified after Raupach and Finnigan (1988). The model includes temperature (T), vapor pressure (V), and resistance (r). Subscripts refer to the canopy (Can), the atmosphere (Atm), sunlit leaves (Sun), and shaded leaves (Sha). Resistances are stomatal (s), boundary layer (b), and in the air within the canopy (i).

assumes that the conductances of individual leaves act in parallel, so that this canopy conductance can be determined by the leaf-area-weighted sum of leaf conductances (Monteith 1973.). This approach ignores details of the canopy profile and simplifies the canopy to one single layer (big leaf), whereas later models differentiate between sunlit and shaded leaves (Dai et al. 2004). The big-leaf models are applicable only in circumstances where the detailed and complete spatial structure of the actual canopy microclimate and difference in light-response curves of individual leaves that make up the canopy are irrelevant (Fig. 8.1).

Whenever details within the canopy (*e.g.*, the interaction between microclimate and physiology) are important to estimate canopy gas exchange, big-leaf models are insufficient. '**Multilayer**' models have therefore been developed (Cowan 1968, 1988). These models describe both the evaporation of the entire canopy and the partitioning of evaporation among various components (*e.g.*, soil, understory, and crown) together with other aspects of the canopy microclimate such as profiles of leaf and air temperature and humidity of the air (Fig. 8.1).

Single-layer models are appropriate when we are concerned with vegetation essentially as a permeable lower boundary of the atmosphere or upper boundary of the soil, in systems with a length scale much larger than that of the vegetation itself. They are useful in hydrological modeling of large-scale or medium-scale catchments (*e.g.*, areas where water is collected for urban use). On the other hand, multilayer models are appropriate when necessary to resolve details within the canopy, either because the detail is important in its own right, or because the height scale is comparable with that of the system under investigation. They are relevant when dealing with interactions between microclimate and plant physiology, or with hydrology in small catchments (Raupach and Finnigan 1988).

Water loss from ecosystems includes both transpiration of leaves and evaporation directly from the soil; infiltration and runoff also play a role. When canopies are sparse, with a projected foliage cover (**leaf area index**, ***LAI***) of less than 1 m^2 of leaf area per m^2 of ground area, as is common for many vegetation types worldwide (Graetz 1991), soil evaporation cannot be ignored, and it should be included in multilayer evaporation models. However, Jasechko et al. (2013) used the distinct isotope effects of transpiration (T) and evaporation (E) to show that transpiration is by far the largest water flux, accounting for 80–90% of terrestrial evapotranspiration (ET). The soil moisture content is affected by the level of radiation that penetrates through the canopy to the soil surface, and hence by the canopy ***LAI***. Evaporation from the soil is also affected by wetness of the soil surface, hydraulic conductivity of the soil, and wind speed beneath the canopy (Vereecken et al. 2016). The rate of soil evaporation is fast, when the surface is wet. As the soil dries out, the point of evaporation moves deeper into the soil, and the surface layer offers a greater impedance, thus dramatically reducing soil evaporation. When the canopy intercepts most of the incident radiation, soil evaporation is probably a minor component of total ET. If rain is infrequent and the soil surface dry, then soil evaporation tends to be insignificant. A compilation of 81 studies that partitioned ET into T and E at the ecosystem scale indicates that T accounts for 61% of ET and returns approximately 39% of incident precipitation to the atmosphere, creating a dominant force in the **global water cycle**. As a proportion of ET, T is highest in tropical rainforests (70%) and lowest in steppes, shrublands and deserts (51%), Changes to transpiration due to increasing atmospheric [CO_2], land-use changes, and global warming will have significant impacts on runoff and groundwater recharge (Schlesinger and Jasechko 2014).

Canopies differ in the extent to which the behavior of individual leaves is 'coupled' to the atmosphere. In **rough canopies**, such as those of forest trees or of small plants in complex terrain, the complex surface structure creates large eddies of air that penetrate the canopies (Bonan 2015). As a result, the air that surrounds each leaf has a temperature and humidity similar to that of bulk air, so that single-leaf models predict the behavior of leaves in canopies. On the other hand,

individual leaves in **smooth canopies** such as in crops or grasslands, are poorly coupled to the atmosphere. Because of the dimensions of their leaves, their higher stomatal conductances, and their tendency to form smooth canopy surfaces, tropical forests are less coupled than boreal forests and the vegetation in the Sahel of North Africa, and considerable vertical gradients of temperature and humidity can develop over just a few meters (Bonan 2015). Leaf resistances are in series with the canopy boundary layer resistance (Fig. 8.1).

8.3 Canopy CO_2 Fluxes

Carbon accumulation in communities involves exchanges of carbon with both the atmosphere and the soil (*i.e.* photosynthesis, plant respiration, and microbial respiration). **Photosynthesis** of the entire canopy can be approached as discussed in Sect. 8.2 for water use, using single-layer or multilayer models. Models of canopy gas exchange based on equations developed for single leaves (**big-leaf** approach) are relatively simple, but can introduce major errors when averaging gradients of light and photosynthetic capacity. We can also model photosynthesis in a 'multilayer' approach (Boxes 2.1 and 8.1). In big-leaf models of canopy photosynthesis, the Rubisco activity and electron-transport capacity per unit ground area are taken as the sums of activities per unit leaf area within the canopy. These models overestimate rates of photosynthesis, unless they adjust the response of photosynthesis to irradiance (Mercado et al. 2007).

Canopy photosynthesis can also be measured using large cuvettes that enclose entire plants or several plants in the canopy, or by **eddy covariance**, which is a micrometeorological approach that compares the concentrations of water vapor, CO_2 and heat in upward-moving *vs.* downward-moving parcels of air. Figure 8.2 shows the rate of canopy CO_2 assimilation and total stomatal conductance of an entire tree of *Macadamia integrifolia* (macadamia). Net CO_2 assimilation and stomatal conductance are related to photon irradiance, but the relationships differ for overcast conditions and clear sky.

The heterogeneity of the canopy complicates model estimates of canopy photosynthesis, because the light environment and leaf physiological properties are highly variable (Sect. 2.3). The resulting variation in photosynthesis and transpiration modify the air within the canopy, creating gradients in humidity, temperature, and CO_2 concentration. We can avoided errors associated with big-leaf models in **multilayer models** that treat the canopy in terms of a number of layers. Thus, by combining a model of **leaf photosynthesis** with a model on **penetration of light** and on transport processes within the canopy, we can estimate the flux from each canopy layer. Such models are essential for analyzing the significance of within-canopy variation in leaf traits. For example, the **allocation of nitrogen** (N) to different leaves within a canopy is determined by the light gradient in a canopy in both single-species and multi-species canopies (Box 8.1), but the gradient in leaf N is always less than that in irradiance (Field 1983; Hirose and Werger 1987); that is why big leaf models do not work. When sunlit and shaded leaf fractions of the canopy are modeled separately, such a **single-layer sun/shade model** is much simpler than a multilayer canopy model (de Pury and Farquhar 1997).

There are important interactions among environmental gradients and physiological processes within a canopy. For example, under moist conditions, the leaves at the top of the canopy, which have the highest N concentrations and experience the highest light availability, account for most of photosynthesis. As the soil dries, particularly for vegetation with tall canopies, the leaves at the top of the canopy may have significantly reduced stomatal conductances compared with those lower down, and the zone of maximum photosynthesis shifts further down in the canopy (Ryan et al. 2006).

It has been consistently more difficult to model **canopy dark respiration** using simple canopy scaling rules, because growth and respiration within the canopy are not a simple function of photosynthesis within the canopy (Sects 3.1 and 3.4). Complications arise, because respiration depends on metabolic activity as well as on carbohydrate status, in a manner that we cannot readily model. Thermal acclimation (Sect. 3.4.5)

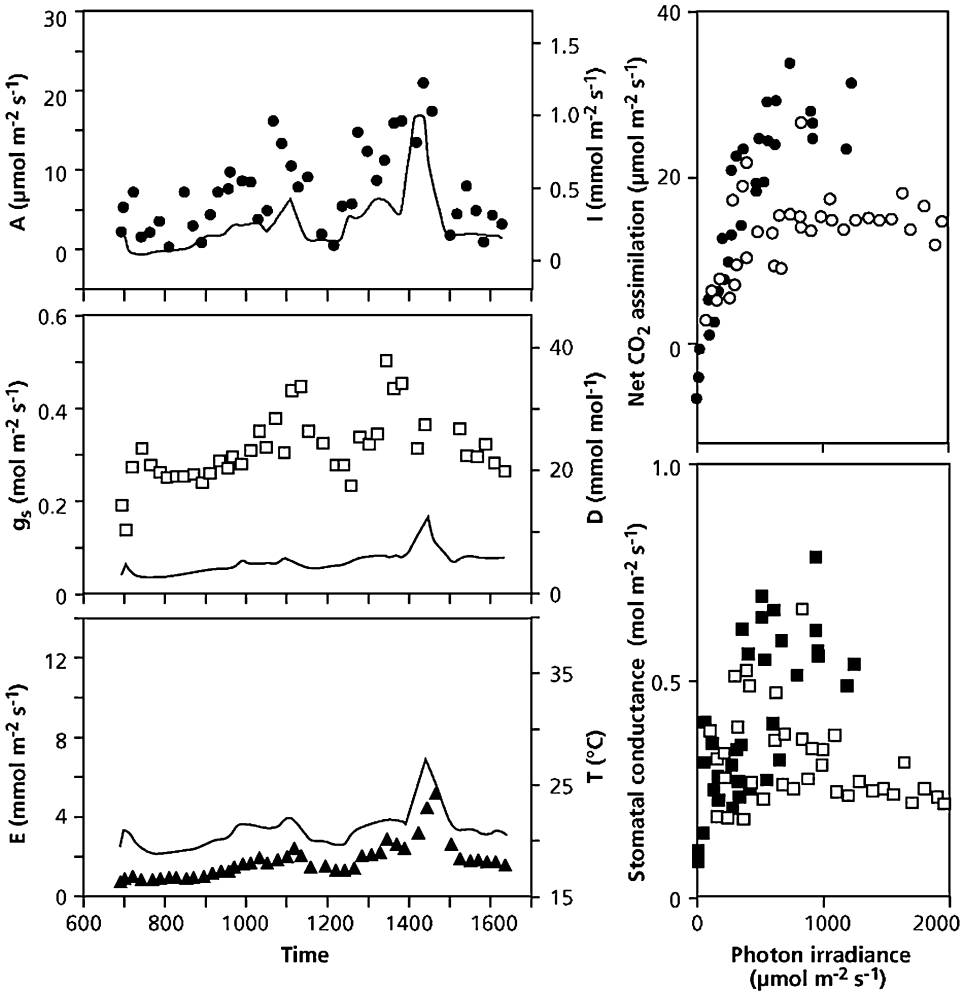

Fig. 8.2 (Left) The rate of CO_2 assimilation, stomatal conductance, and transpiration (all expressed on a ground area basis) of an entire tree of *Macadamia integrifolia* (macadamia), throughout an entire day. Diurnal changes in irradiance (I), leaf-to-air vapor pressure difference (D) and air temperature (T) are also shown (solid lines). (Right) The rate of net CO_2 assimilation and stomatal conductance (expressed on a ground area basis) of an entire tree of *Macadamia integrifolia*, as dependent on photon irradiance. The solid and open symbols refer to overcast and clear-sky conditions, respectively; after Lloyd et al. (1995), *Funct. Plant Biol.* **22**: 987–1000, copyright CSIRO, Australia.

and the extent to which dark respiration continues during photosynthesis (Sect. 3.4.9) (Mercado et al. 2007) represent further uncertainties, with variation among species. This remains an area of plant physiology where we need more information to allow scaling from the leaf's CO_2 flux to that of the canopy, especially if canopy scaling is going to be used to address global issues (Atkin et al. 2015; O'Leary et al. 2019).

8.4 Canopy Water-Use Efficiency

If canopies affect the gas exchange properties of individual leaves, then the water-use efficiency (WUE) of the canopy cannot be deduced simply from that of individual leaves measured under the prevailing bulk air conditions. Does this imply that genotypic differences in WUE at the leaf level (Sect. 5.6) disappear when studied at an

ecological scale (Diefendorf et al., 2010)? When dealing with a **rough canopy** (Sect. 8.2), the differences certainly persist. In a **smooth canopy**, however, such as that of a wheat crop, the differences in conductance are less when scaling from the leaf to the canopy level (Fig. 8.3). For example, a leaf-level difference in photosynthetic water-use efficiency of 24% is only 5% at the canopy level. This decrease in the effect of genotype on WUE, when scaling from a single leaf to the canopy, reflects both the dominance of the **canopy boundary layer conductance** in the total canopy conductance (Sect. 8.2) and the greater leaf area of the cultivar with lower WUE. This greater leaf area reduces the canopy boundary layer conductance which counteracts the greater stomatal conductance. In addition, much of the gain made by decreasing stomatal conductance and transpiration can be offset by greater **soil evaporation**, when the rate of leaf area development decreases simultaneously.

Wheat genotypes with a low WUE tend to develop their leaf area faster and have a higher leaf area ratio (LAR), in comparison with ones that have a higher WUE, with two important consequences. First, genotypes with a lower WUE transpire more of the available water early in the growing season, when the vapor pressure deficit of the air is relatively low due to low temperatures, and, consequently, the WUE is high. Second, transpiration represents a greater fraction of the total crop water use of low-WUE genotypes due to reduced soil evaporation (Condon et al. 1993). A high LAR and vigorous early growth is clearly a major trait determining a crop's water use (Van den Boogaard et al., 1997). This calls for a line of plant breeding that combines a high WUE (low δ^{13}C-value) with vigorous early growth to reduce soil evaporation.

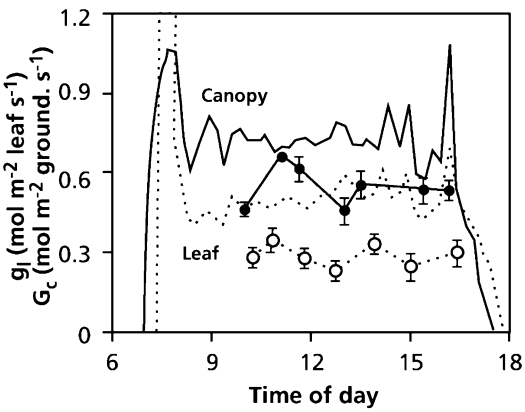

Fig. 8.3 Comparison of the diurnal variation of leaf conductance, g_l (circles connected by lines) and canopy conductance, G_c (lines only) for two cultivars of *Triticum aestivum* (wheat), selected on the basis of their contrasting photosynthetic water-use efficiency at the leaf level (de Pury 1995). (Reproduced with the author's permission).

8.5 Canopy Effects on Microclimate: A Case Study

Individual leaves in smooth canopies, such as in crops or grasslands, are poorly coupled to the atmosphere (Bonan 2015). When stomatal conductance declines, leaves dissipate more heat through convective exchange, warming the air within the canopy. This creates turbulence within the canopy which brings new dry air into the canopy to increase transpiration.

The net loss of radiative energy from a surface exposed to the sky at night is balanced by the flow of heat from the overlying air and the underlying soil. During nights of radiation frost, leaf temperatures of *Eucalyptus pauciflora* (snowgum) exposed to clear skies may be 1 to 3 °C below those of the air (Ball et al. 1997). The resistance to heat transfer between air and grass is less than between air and soil, because of the canopy's greater aerodynamic roughness. Because the thermal resistance of air within the grass sward is high, air temperatures above the grass are lower than those above bare soil, which conducts heat more easily to the surface. As a result, leaf temperatures of seedlings above grass tend to be lower than those above dry soil. This affects the performance of plants growing above a grass canopy, as compared with those above bare patches (Sect. 16.3).

8.6 Aiming for a Higher Level

Scaling of processes from a single leaf to an entire canopy or community is complicated, because of complex environmental and physiological

gradients and interactions within the canopy. Big-leaf models are often a useful simple starting point, especially for estimates of process rates over large areas. However, an understanding of the role of physiology in mediating the exchanges of water, carbon, and heat often benefits from a multilayer approach that uses information about these environmental and physiological gradients to model the gas exchange of the entire canopy.

When dealing with canopies, we often find that differences (*e.g.*, in water-use efficiency) that are relatively large when studied at the leaf level become smaller or disappear at the canopy level. Scaling from single leaves to communities will become increasingly important when ecophysiologists model effects of global change in temperature and atmospheric [CO_2] on primary productivity. Difficulties arise when dealing with the time factor; short-term effects of temperature on rates of processes may differ vastly from those in acclimated plants. Temporal and spatial scaling are, therefore, an important research area for ecophysiologists seeking to develop more effective crops or predict the performance of plants under future conditions.

References

Anten NPR, Schieving F, Werger MJA. 1995. Patterns of light and nitrogen distribution in relation to whole canopy carbon gain in C_3 and C_4 mono- and dicotyledonous species. *Oecologia* **101**: 504–513.

Atkin OK, Bloomfield KJ, Reich PB, Tjoelker MG, Asner GP, Bonal D, Bönisch G, Bradford M, Cernusak LA, Cosio EG, Creek D, Crous KY, Domingues T, Dukes JS, Egerton JJG, Evans JR, Farquhar GD, Fyllas NM, Gauthier PPG, Gloor E, Gimeno TE, Griffin KL, Guerrieri R, Heskel MA, Huntingford C, Ishida FY, Kattge J, Lambers H, Liddell MJ, Lloyd J, Lusk CH, Martin RE, Maksimov AP, Maximov TC, Mahli Y, Medlyn BE, Meir P, Mercado LM, Mirotchnick N, Ng D, Niinemets Ü, O'Sullivan OS, Philips OL, Poorter L, Poot P, Prentice IC, Salinas N, Rowland LM, Ryan MG, Sitch S, Slot M, Smith NG, Turnbull MH, VanderWel MC, Valladares F, Veneklaas EJ, Weerasinghe LK, Wirth C, Wright IJ, Wythers K, Xiang J, Xiang S, Zaragoza-Castells J. 2015. Global variability in leaf respiration in relation to climate, plant functional types and leaf traits. *New Phytol* **206**: 614–636.

Ball MC, Egerton JJG, Leuning R, Cunningham RB, Dunne P. 1997. Microclimate above grass adversely affects spring growth of seedling snow gum (*Eucalyptus pauciflora*). *Plant Cell Environ* **20**: 155–166.

Bonan G 2015. Ecosystems and climate. *Ecological Climatology: Concepts and Applications*. Cambridge: Cambridge University Press, 1–20.

Buckley TN, Warren CR. 2014. The role of mesophyll conductance in the economics of nitrogen and water use in photosynthesis. *Photosyn Res* **119**: 77–88.

Condon A, Richards R, Farquhar G. 1993. Relationships between carbon isotope discrimination, water use efficiency and transpiration efficiency for dryland wheat. *Aust J Agric* **44**: 1693–1711.

Cowan IR. 1968. Mass, heat and momentum exchange between stands of plants and their atmospheric environment. *Q J R Meteorol Soc* **94**: 523–544.

Cowan IR 1988. Stomatal physiology and gas exchange in the field. In: Steffen WL, Denmead OT eds. *Flow and Transport in the Natural Environment: Advances and Applications*. Berlin: Springer-Verlag, 160–172.

Dai Y, Dickinson RE, Wang Y-P. 2004. A two-big-leaf model for canopy temperature, photosynthesis, and stomatal conductance. *J Clim* **17**: 2281–2299.

de Pury DGG. 1995. *Scaling Photosynthesis and Water Use from Leaves to Paddocks.* PhD Thesis thesis, Australian National University, Canberra, Australia.

de Pury DGG, Farquhar GD. 1997. Simple scaling of photosynthesis from leaves to canopies without the errors of big-leaf models. *Plant Cell Environ* **20**: 537–557.

Diefendorf AF, Mueller KE, Wing SL, Koch PL, Freeman KH. 2010. Global patterns in leaf ^{13}C discrimination and implications for studies of past and future climate. *Proc Natl Acad Sci USA* **107**: 5738–5743.

Evans JR. 1993. Photosynthetic acclimation and nitrogen partitioning within a lucerne canopy. II. Stability through time and comparison with a theoretical optimum. *Funct Plant Biol* **20**: 69–82.

Farquhar GD, von Caemmerer S, Berry JA. 1980. A biochemical model of photosynthetic CO_2 assimilation in leaves of C_3 species. *Planta* **149**: 78–90.

Field C. 1983. Allocating leaf nitrogen for the maximization of carbon gain – leaf age as a control on the allocation program. *Oecologia* **56**: 341–347.

Graetz R. 1991. The nature and significance of the feedback of changes in terrestrial vegetation on global atmospheric and climatic change. *Clim Change* **18**: 147–173.

Hirose T, Werger MJA. 1987. Maximizing daily canopy photosynthesis with respect to the leaf nitrogen allocation pattern in the canopy. *Oecologia* **72**: 520–526.

Jarvis PG, McNaughton KG. 1986. Stomatal control of transpiration: scaling up from leaf to region. *Adv Ecol Res* **15**: 1–49.

Jasechko S, Sharp ZD, Gibson JJ, Birks SJ, Yi Y, Fawcett PJ. 2013. Terrestrial water fluxes dominated by transpiration. *Nature* **496**: 347.

Lloyd J, Wong SC, Styles JM, Batten D, Priddle R, Turnbull C, Mcconchie CA. 1995. Measuring and modelling whole-tree gas exchange. *Funct Plant Biol* **22**: 987–1000.

Mercado LM, Huntingford C, Gash JHC, Cox PM, Jogireddy V. 2007. Improving the representation of radiation interception and photosynthesis for climate model applications. *Tellus B* **59**: 553–565.

Monteith JL 1963. Gas exchange in plant communities. In: Evans LT ed. *Environmental Control of Plant Growth*. New York: Academic Press, 95–112.

Monteith JL. 1965. Evaporation and environment. *Symp Soc Exp Biol* **19**: 205–234.

Monteith JL. 1973. *Principles of Environmental Physics*. London: Edward Arnold.

O'Leary BM, Asao S, Millar AH, Atkin OK. 2019. Core principles which explain variation in respiration across biological scales. *New Phytol* **222**: 670–686.

Penman HL. 1948. Natural evaporation from open water, bare soil and grass. *Proc R Soc B Biol Sci* **193**: 120–145.

Pons TL, Schieving F, Hirose T, Werger MJA 1989. Optimization of leaf nitrogen allocation for canopy photosynthesis in *Lysimachia vulgaris*. In: Lambers H, Cambridge ML, Konings H, Pons TL eds. *Causes and Consequences of Variation in Growth Rate and Productivity of Higher Plants*. The Hague: SPB Academic Publishing, 175–186.

Raupach MR, Finnigan JJ. 1988. Single-layer models of evaporation from plant canopies are incorrect but useful, whereas multilayer models are correct but useless: discuss. *Funct Plant Biol* **15**: 705–716.

Ryan MG, Philips N, Bond BJ. 2006. The hydraulic limitation hypothesis revisited. *Plant Cell Environ* **29**: 367–381.

Schlesinger WH, Jasechko S. 2014. Transpiration in the global water cycle. *Agric For Met* **189-190**: 115–117.

Van den Boogaard R, Alewijnse D, Veneklaas EJ, Lambers H. 1997. Growth and water-use efficiency of 10 *Triticum aestivum* cultivars at different water availability in relation to allocation of biomass. *Plant Cell Environ* **20**: 200–210.

Vereecken H, Aitkenhead M, Allison SD, Assouline S, Baveye P, Berli M, Brüggemann N, Finke P, Flury M, Gaiser T, Govers G, Schnepf A, Ghezzehei T, Hallett P, Hendricks Franssen HJ, Heppell J, Horn R, Huisman JA, Jacques D, Jonard F, Kollet S, Lafolie F, Hopmans JW, Lamorski K, Leitner D, McBratney A, Minasny B, Montzka C, Nowak W, Pachepsky Y, Padarian J, Romano N, Roth K, Javaux M, Rothfuss Y, Rowe EC, Schwen A, Šimůnek J, Tiktak A, Van Dam J, van der Zee SEATM, Vogel HJ, Vrugt JA, Wöhling T, Or D, Young IM, Roose T, Vanderborght J, Young MH, Amelung W. 2016. Modeling soil processes: review, key challenges, and new perspectives. *Vadose Zone J* **15**.

Mineral Nutrition

9

9.1 Introduction

Next to water, nutrients are the environmental factor that most strongly constrains terrestrial productivity. The productivity of virtually all natural ecosystems, even arid ecosystems, responds to addition of one or more nutrients, indicating widespread nutrient limitation. Species differ widely in their capacity to acquire nutrients from soil. For example, some plants can take up iron (Fe), phosphorus (P), or other ions from a calcareous soil, from which others cannot take up enough nutrients to persist. In other soils, the concentrations of aluminum (Al), 'heavy metals', or sodium chloride may reach toxic levels, whereas some species have genetic adaptations that enable them to survive in such environments. This does not mean that metallophytes *need* high concentrations of metals or that halophytes *require* high salt concentrations to survive. These species perform well in the absence of these adverse conditions. Their distribution is restricted to these extreme habitats, because, on one hand, these plants resist the adverse conditions, whereas most other plants do not. On the other hand, metallophytes and halophytes generally perform less well than most other plants in habitats without toxic levels of metals or salts. Terms like metallophytes, halophytes, and others that we will encounter in this chapter, therefore, refer to the **ecological amplitude** of the species, rather than to their physiological requirements (Fig. 1.2).

This chapter deals with the acquisition and use of nutrients by plants, focusing on terrestrial plants that take up nutrients predominantly via their roots from soil. Leaves are also capable of acquiring nutrients. For example, volatile nitrogenous and sulfurous compounds, which may occur either naturally or as air pollutants in the atmosphere, can be taken up through the stomata. Nutrients in the water on wet leaves are also available for absorption by leaves. This may be of special importance for aquatic and epiphytic plants as well as for mosses and even *Sequoia sempervirens* (coast redwood) (Burgess and Dawson 2004). Other mechanisms to acquire nutrients include those found in carnivorous plants, which acquire nutrients from their prey (Chap. 17), symbiotic associations with microorganisms (Chap. 12), and parasitic associations with host plants (Chap. 15).

Historically, nitrogen (N) has received most attention, largely because most plant physiologists and ecologists inhabit a part of the world that is characterized by young landscapes, where N is the major nutrient limiting plant productivity (Walker and Syers 1976; Turner and Condron 2013). However, most plant species occur in biodiverse regions in ancient landscapes, in the tropics and subtropics in South and Central America, southeast Asia, and Africa, and in Mediterranean areas in Africa and Australia, where P is the major nutrient limiting plant productivity (Lambers et al. 2010; Oliveira et al. 2015). We are beginning to discover that plant species in these

H. Lambers, R. S. Oliveira, *Plant Physiological Ecology*, https://doi.org/10.1007/978-3-030-29639-1_9

landscapes function fundamentally different from what we know of crop plants and species in young N-limited landscapes, and hence they deserve special attention in this chapter.

9.2 Acquisition of Nutrients

Most terrestrial plants absorb the inorganic nutrients required for growth via their roots from soil. For the uptake into the root cells, plasma membrane-bound transport proteins ('carriers', 'channels', and 'transporters') are used (Sect. 9.2.2.1). Before describing mechanisms associated with transport across the plasma membrane, we first discuss the movement of nutrients in soil.

9.2.1 Nutrients in the Soil

9.2.1.1 Nutrient Availability as Dependent on Soil Age

In relatively young landscapes, following recent volcanic activity or glaciation, P availability is relatively high, and N tends to be the key nutrient that limits plant productivity (Walker and Syers 1976; Turner and Condron 2013). In ancient, highly-weathered soils that characterize much of Africa, Australia, South America, and Southeast Asia, P is the key limiting nutrient for plant productivity (Lambers et al. 2008). **Chronosequences** (gradients of soil age) over various geological time-scales up to four million years constitute natural experiments that allow the study of causes of variation in availability and forms of N and P (Vitousek 2004; Turner et al. 2018a) (Fig. 9.1A) and plant strategies for accessing different forms of nutrients (Zemunik et al. 2015). These strategies broaden the options for acquisition of resources from soils that differ in nutrient availability. Individual strategies such as mycorrhizas, N_2-fixing symbioses (Chap. 12) and P-mobilizing cluster roots (Sect. 9.2.2.5) may augment each other's activities. Together, these strategies allow plants to grow and coexist under a wide range of conditions, including severely nutrient-impoverished soils such as those in ancient landscapes in Australia (Lambers et al. 2018), South Africa (Verboom et al. 2017), and Brazil (Oliveira et al. 2015).

9.2.1.2 Nutrient Supply Rate

Nutrient supply rates in the **soil** ultimately govern the rates of nutrient acquisition by plants. **Parent material**, the rocks or sediments that give rise to soil, determines the proportions of minerals that are potentially available to plants. For example, granite is resistant to weathering and generally has lower concentrations of P and cations required by plants than sandstone (Porder and Ramachandran 2013). Other parent materials such as serpentine rock have high concentrations of metals that are either not required by plants or required in such low concentrations that their high concentrations in serpentine soils can cause toxic accumulation in plants. Various ecological factors (climate, vegetation, topography, and surface age) strongly influence weathering rates and rates of leaching loss, and, therefore, the relationship between parent material and nutrient availability (Jenny 1980).

The **atmosphere** is the major source of N, through both biological N_2 fixation (Sect. 12.2) and deposition of nitrate and ammonium in precipitation. Atmospheric deposition of P is considerably less, but can be important in extremely P-impoverished biomes, such as ocean basins downwind from deserts (Brown et al. 1984) as well as the Amazon, where dust arrives from Chad in Africa (Bristow et al. 2010). There is also substantial input from wet and dry deposition. Some cations [*e.g.*, sodium (Na)] may come primarily from sea salt, particularly in coastal regions, but other nutrients [calcium (Ca), magnesium (Mg), P, and potassium (K)] come predominantly from dust (from deserts, agricultural areas, unpaved roads), and from industrial pollution (Soderberg and Compton 2007). These atmospheric inputs can be substantial. For example, atmospheric inputs of Ca are equivalent to 62%, 42%, and 154% of uptake by forests in the eastern United States, Sweden, and the Netherlands, respectively (Hedin et al. 1994) which is considerably more than annual inputs by weathering. In ecosystems receiving aeolian dust, atmospheric

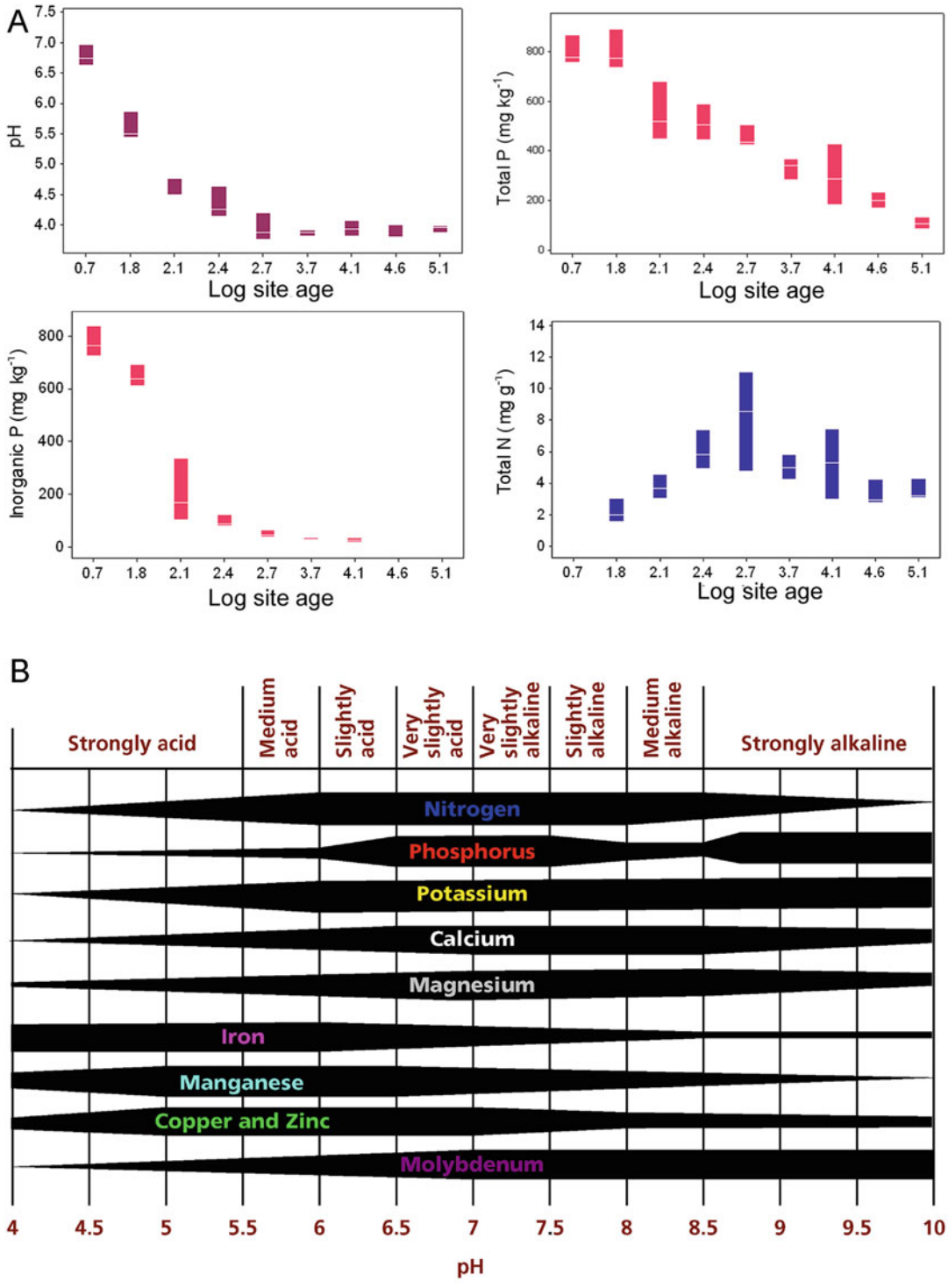

Fig. 9.1 (**A**) Summary of mineral soil properties along the Franz Josef soil chronosequence. Box plot symbols: horizontal lines are the median; shaded bars give 25% and 75% percentiles. Based on Richardson et al. (2004); copyright © 2004, Springer-Verlag. (**B**) The availability of a number of essential nutrients in the soil as dependent on soil pH. Note that the availability for phosphorus (P) reflects that plants take up P as $H_2PO_4^-$, rather than the concentration of inorganic P in solution, which may increase at lower pH (Barrow et al. 2018).

deposition may contribute a substantial proportion of the P requirement of natural vegetation, especially in nutrient-impoverished landscapes (Chadwick et al. 1999; Soderberg and Compton 2007; Eger et al. 2013). Atmospheric inputs may determine external mineral supply to natural ecosystems much more than is generally appreciated (Pett-Ridge 2009; Eger et al. 2013; Yu et al. 2015).

Soil pH is a major factor determining the **availability** of nutrients in soil. High concentrations of hydrogen ions (low pH) cause modest increases in nutrient input by increasing the weathering rate (Johnson et al. 1972), but even greater loss of base cations by leaching (Zhang et al. 2007). Acid rain is a source of soil acidity caused by atmospheric deposition of nitric and sulfuric acids in precipitation; it has increased dramatically because of burning fossil fuel. Protons first displace cations from the exchange complex on clay minerals and soil organic matter. Sulfate anions can then leach below the root zone, carrying with them mobile mineral cations (*e.g.*, K, Ca, and Mg) and leaving behind a predominance of hydrogen and Al ions (Fig. 9.1B) (Driscoll et al. 2001). The availability of other ions is strongly affected by pH, because this affects their oxidation state and solubility (*e.g.*, P, S, and Al), as well as the biological processes that control production and consumption (*e.g.*, N) (Fig. 9.1B).

In the short term, recycling of nutrients from dead organic matter is the major direct source of soluble nutrients to soils (Table 9.1). Soluble cations such as K and Ca are leached from dead organic matter, whereas organically bound nutrients such as N and P must be released by **decomposition**. Plants only take up inorganic phosphate (Pi), predominantly as $H_2PO_4^-$, which is released from organic P by plant or microbial enzymes (**phosphatases**). Nitrogen is released from dead organic matter yielding soluble organic N, which may be further decomposed to NH_4^+ (N **mineralization**). NH_4^+ may then be oxidized, via NO_2^-, to NO_3^- (**nitrification**), and

Table 9.1 Major sources of available nutrients that enter the soil.

Source of nutrient (% of total)			
Nutrient	Atmosphere	Weathering	Recycling
Temperate forest			
N	7	0	93
P	1	<10?	>89
K	2	10	88
Ca	4	31	65
Arctic tundra			
N	4	0	96
P	4	<1	96

Source: Chapin (1991)

NO_3^- may be converted to gaseous N_2 or N_2O (**denitrification**) (Fig. 9.2A). The rates of these steps depend on temperature and soil conditions (*e.g.*, redox potential); however, nitrification is also affected by inhibitors released from roots (Lata et al. 2004; Coskun et al. 2017; Subbarao et al. 2017), as we discuss in Sect. 13.2. At each step, plants or soil microorganisms can take up soluble N, or N can leach from the system, reducing the substrate available for the next N transformation. Therefore, the supply rates of the different forms of 'available N' to plants and microbes must follow this same sequence: dissolved organic N $\geq$ NH_4^+ $\geq$ NO_3^- (Eviner and Chapin 2003).

If N supply rate always follows the same sequence in all soils, why do the quantities and relative concentrations of these soluble forms of N differ among ecosystems? First, microbes generally release Pi or NH_4^+ to the soil solution when their growth is more strongly limited by carbon than by nutrients (Schimel and Bennett 2004). On the other hand, they **immobilize** nutrients when decomposing plant litter with low nutrient concentrations and/or high concentrations of labile carbon (*e.g.*, inputs of straw). Second, environmental conditions further modify rates of specific N transformations. For example, cold anaerobic soils in arctic Alaska limit N mineralization and nitrification (an aerobic process), so

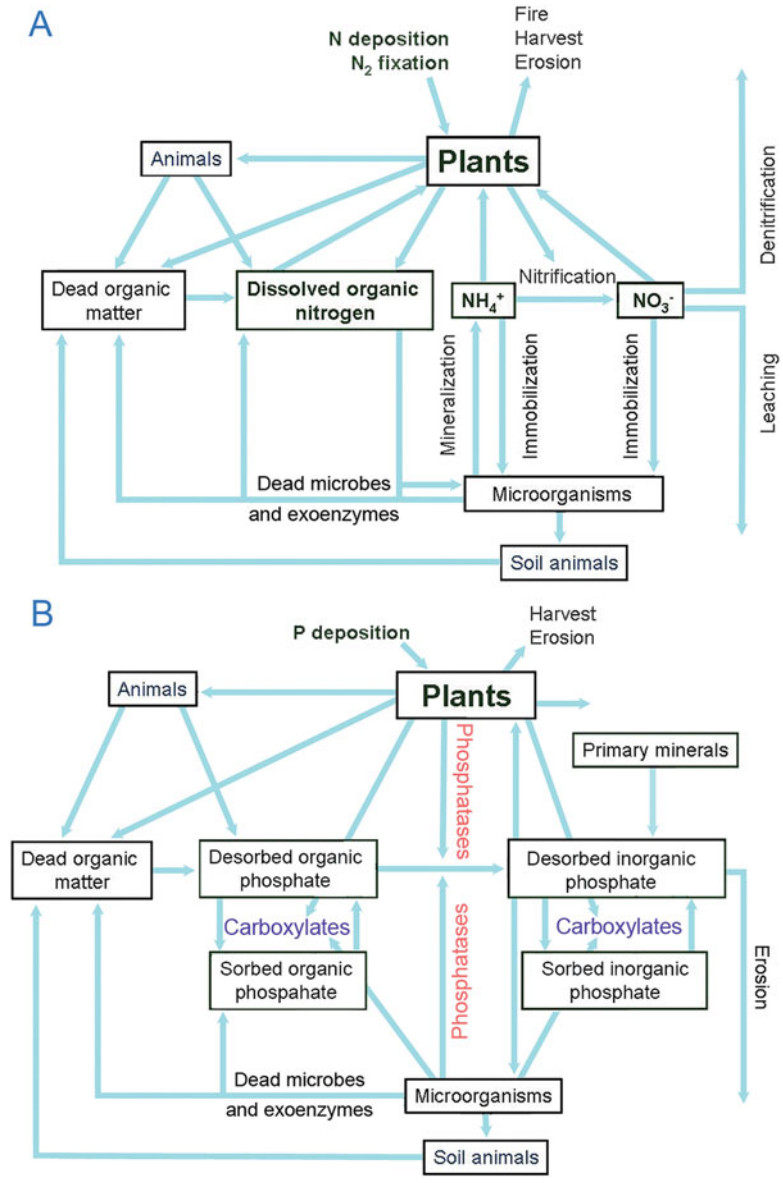

Fig. 9.2 (**A**) A simplified view of the terrestrial nitrogen (N) cycle. All N pools (boxes) and transformations (arrows) are affected by both plants and microorganisms. Dead plants, animals, and microorganisms are decomposed, releasing dead organic matter and then dissolved organic N (*e.g.*, amino acids, urea). Some of the dissolved organic N in soils originates from living organisms. Both plants and microorganisms are capable of using dissolved organic N. Microorganisms use the dissolved organic N as a carbon source, releasing N that is in excess of their requirement as NH_4^+. Both plants and microorganisms can use NH_4^+ as a source of N. Incorporation of NH_4^+ into soil microorganisms leads to N-immobilization; the reverse transformation is mineralization. Immobilization predominates at high availability of a carbon source, whereas mineralization is favored by a shortage of a source of carbon for microorganisms. Under aerobic conditions, some NH_4^+ is transformed into NO_3^-, in a process called nitrification. In alkaline soil, nitrification predominantly results from autotrophic microorganisms, whereas in acid soil heterotrophic microorganisms are probably most important. NO_3^- is available for both plants and microorganisms; as with NH_4^+, some of the NO_3^- may be immobilized, or lost from the system through leaching or denitrification; denitrification can be inhibited by specific compounds released from living roots or litter. (**B**) A simplified representation of the major processes and components of the terrestrial phosphorus (P) cycle in plant-soil systems. Several processes explained for the N cycle (*e.g.*, mineralization, immobilization) play a similar role in the P cycle; however, leaching of P tends to be negligible, due to the low mobility of P in soil. Note that plants have considerably greater control over the P cycle than over the N cycle, *e.g.*, via the release of phosphatases and carboxylates.

amino-acid N concentrations are relatively high and NO_3^- concentrations low (Kielland 1994). However, input of nitrogen oxide has gradually increased soil NO_3^- levels, and NO_3^- now contributes about a third of the bulk N used by tundra plants of northern Alaska (Liu et al. 2018). In many arid and agricultural soils, high temperatures promote rapid mineralization and nitrification, and denitrification (an anaerobic process) occurs slowly, so NO_3^- is the most abundant form of soluble N. Finally, N-uptake rates by plants and microorganisms modify the availability of each N form to other organisms. For example, low concentrations of NO_3^- in acidic conifer forest soils may be caused by rapid microbial NO_3^- uptake (Stark and Hart 1997), and not only by slow nitrification rates (Lodhi and Killingbeck 1980). Plant species in a N-limited, arctic tundra community are differentiated in timing, depth, and chemical form of N uptake, and species dominance is strongly correlated with uptake of the most available soil N forms (McKane et al. 2002).

The activity of **phosphatases** that release Pi from organic P sources (Sect. 9.2.2.5.1) implies that organic P is hydrolyzed independently of the utilization of organic matter by microorganisms (Fig. 9.2B). In addition, root exudates may greatly enhance weathering of primary minerals and mobilize phosphate locked up in rock fragments (Teodoro et al. 2019) or **sorbed** onto soil particles (Sect. 9.2.2.5.2); 'sorption' refers to both adsorption (precipitation) onto soil particles and absorption inside such particles (Barrow 1984). When compared with the N cycle (Fig. 9.2A), the **P cycle**, therefore, depends considerably less on microbial decomposition of organic matter than the **N cycle**, on both biological and geological time scales (Fig. 9.2B) (Porder et al. 2007; Reed et al. 2015).

In summary, each nutrient is returned from dead organic matter to plant-available forms through distinct processes that occur at different rates in response to various environmental controls. Consequently, nutrients in the soil are seldom available in the proportions required by plants.

9.2.1.3 Nutrient Movement to the Root Surface

As roots grow through the soil, they **intercept** some nutrients. This amount, however, is often less than the amount contained in the growing root, and, therefore, cannot serve as a net source of nutrients to the rest of the plant. Thus, roots do not move toward the nutrients; rather the nutrients must move to the roots by mass flow or diffusion (Table 9.2).

Rapid transpiration in plants may result in substantial nutrient transport from the bulk soil to the root surface via **mass flow**. The extent to which mass flow is responsible for ion transport to the roots depends on the concentration of the different ions in the bulk solution relative to the requirement for plant growth (Table 9.2). For N, which is relatively mobile in soil, transpiration-driven mass flow can play a significant role in N acquisition (Matimati et al. 2014). Mass flow is generally considered to be unimportant for P acquisition, but when soils are very sandy and the moisture availability is favorable, it may contribute to P acquisition from severely P-impoverished soils (Huang et al. 2017).

If less nutrients arrive at the root surface than are required to sustain plant growth, the concentration at the root surface drops, due to absorption by the roots. This creates a concentration gradient that drives ion **diffusion** toward the root (*e.g.*, for Pi and K^+) [see Sect. 9.2.3 for the a description of diffusion (**Fick's first law**) and mass flow]. Other ions are delivered more rapidly by mass flow than they are required by the roots (*e.g.*, Ca^{2+}) which causes precipitation on the root surface (often as $CaSO_4$) (Barber and Ozanne 1970). Diffusion from the bulk soil to the root surface depends both on the **concentration gradient**, and on the **diffusion coefficient**. This coefficient, which varies among soil types, differs by three orders of magnitude among common ions. It is large for NO_3^-, which therefore moves quickly to the root surface in moist soils, even when there is little water uptake. The diffusion coefficient is also large for K^+, so that most plants can acquire sufficient K to sustain growth. Diffusion

Table 9.2 The significance of root interception, mass flow and diffusion in supplying *Zea mays* (maize)*.

Nutrient	Amount taken up by the crop	Approximate amounts supplied by:		
		Root interception	Mass flow	Diffusion
***Zea mays*:**				
Nitrogen	190	2	150	38
Phosphorus	40	1	2	37
Potassium	195	4	35	156
Calcium[a]	40	60	165	0
Magnesium[a]	45	15	110	0
Sulfur	22	1	21	0
Copper[a]	0.1	–	0.4	–
Zinc	0.3	–	0.1	–
Boron[a]	0.2	–	0.7	–
Iron	1.9	–	1.0	–
Manganese[a]	0.3	–	0.4	–
Molybdenum[a]	0.01	–	0.02	–

Source: Clarkson (1981); Barber (1995); Jungk and Claassen (1997)
*All data in kg ha^{-1}. The data pertain to a typical fertile silt loam and a maize crop yield of 9500 kg ha^{-1} and the tundra data a wet sedge meadow with a low-nutrient peat soil. The amount supplied by mass flow was calculated from the concentration of the nutrients in the bulk soil solution and the rate of transpiration. The amount supplied by diffusion is calculated by difference; other forms of transport to the root (*e.g.*, mycorrhizas) may also be important but are not included in these estimates. The elements marked [a] are potentially supplied in excess by mass flow; they may accumulate at the soil/root interface and diffuse back into the bulk soil

Table 9.3 Typical values for diffusion coefficients for ions in moist soil*.

Ion	Diffusion coefficient ($m^2\ s^{-1}$)
Cl^-	$2–9 \times 10^{-10}$
NO_3^-	$1–3.3 \times 10^{-10}$
SO_4^{2-}	$1–2 \times 10^{-10}$
$H_2PO_4^-$	$0.3–3.3 \times 10^{-13}$
K^+	$1–28 \times 10^{-12}$
NH_4^+	2.7×10^{-12}
Glycine	9×10^{-12}

Source: Clarkson (1981); Miller and Cramer (2005)
*The range of values represents values for different soil types

coefficients are very low for zinc (Zn^{2+}) and Pi (Table 9.3), due to specific interactions with the clay minerals of the soil cation-exchange complex. Hence, variation in soil clay content is one of the factors that affect the diffusion coefficient. Nitrogen and P, which are the two macronutrients that most frequently limit plant growth, are seldom supplied in sufficient quantities by mass flow to meet the plant requirement; therefore, diffusion generally limits their supply to the plant, particularly in natural ecosystems. When soil solution concentrations are much greater, as they are in agricultural soils, mass flow delivers a major fraction of all N required for plant growth (Table 9.2; Yanai et al. 1998).

Most estimates of the importance of mass flow consider only water movement associated with transpiration. Bulk movement of soil solution, however, also occurs as a 'wetting front' after rain. The wetting front carries ions with it, and replenishes 'diffusion shells' where plant uptake has reduced nutrient concentrations around individual roots. In arctic tundra, where permafrost causes substantial lateral movement of water, bulk water flow accounts for 90% of the nutrient delivery to deep-rooted species (Chapin et al. 1988). Bulk water movement may well have a large influence on nutrient supply in other wet ecosystems. Soil heterogeneity may influence the importance of bulk water flow for nutrient supply to roots. Roots and rainwater both move

preferentially through soil cracks created by small animals or soil drying. These effects of soil heterogeneity may increase the importance of bulk water movement as a mechanism of nutrient supply more than is currently appreciated.

Mass flow and diffusion do not always account for nutrient transport to the root surface. Mass flow usually delivers very little Pi to the roots, and the diffusion coefficient for Pi in soil is too low to allow much Pi to move by diffusion under most circumstances (Table 9.3). Some organic P molecules may diffuse more rapidly and become available for the roots, but generally, diffusion of organic P is also slow (Sect. 9.2.2.5.1). If plants do not have access to this source of P, then special adaptations or acclimations are required to acquire Pi when its concentration in the soil solution is low (Sect. 9.2.2.2). Mycorrhizas are an important additional mechanism of nutrient transport to the root (Sect. 12.2).

Because NO_3^- moves more readily to the roots' surface, it would appear to be available in larger quantities than NH_4^+. Is NO_3^- really the predominant source of N for any plant? That largely depends on environmental conditions. Where both NO_3^- and NH_4^+ are present, NH_4^+ is the preferred source (Garnett and Smethurst 1999; Kronzucker et al. 1999). When amino acids are available, these can also represent a major source of N (Warren 2006). When N mineralization and nitrification are slow, amino acid concentrations are relatively high, and NO_3^- concentrations low (Kielland 1994; Lipson and Näsholm 2001). Under these conditions, amino acids tend to be a major source of N (Henry and Jefferies 2003), but arctic plants also absorb NO_3^- or NH_4^+, and assimilate it, if supplied in sufficient amounts (Liu et al. 2018). Most plants from acid soils, similarly, are capable of absorbing and assimilating NO_3^-, and very few species are incapable of using NO_3^- as a source of N (Atkin 1996). The differences in costs of growth when using either NO_3^- or NH_4^+ are discussed in Sect. 3.5.2.2. The potential to utilize amino acids as N sources is common in most plant communities, regardless of soil fertility (Schmidt and Stewart 1999; Kielland et al. 2006). Some species can also access small peptides and protein, but it is not yet clear how universal this is (Paungfoo-Lonhienne et al. 2008; Soper et al. 2011). The capacity of mycorrhizal fungi to degrade polymeric N compounds is well established, as is their ability to take up amino acids (Näsholm et al. 2009). The carbon cost of assimilating organic N into proteins is lower than that of inorganic N. This makes it more beneficial for plants to take up organic N, rather than inorganic N, even when its availability to the roots is lower. At equal growth rate, the root: shoot ratio may be up to three times greater and N productivity up to 20% higher for organic N than for inorganic N (Franklin et al. 2017).

Low water availability reduces diffusion rates of ions below values in moist soils, because air replaces water in pores of dry soil, greatly lengthening the path from the bulk soil to the root surface (increased 'tortuosity'). Ion mobility in soil can decrease by two orders of magnitude between a soil water potential of −0.01 and −1.0 MPa, which is a range that does not strongly restrict water uptake by most plants (Fig. 9.3). Because diffusion is the rate-limiting step in uptake of the most strongly limiting nutrients

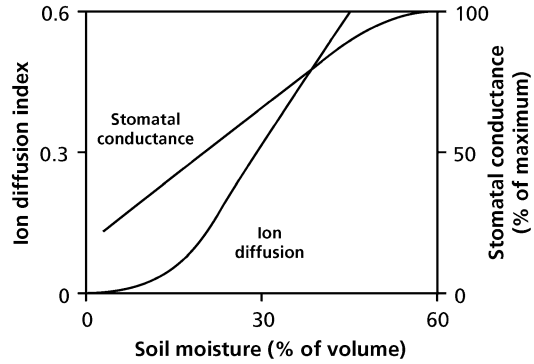

Fig. 9.3 The rate of ion diffusion (deduced from the diffusion impedance factor for Cl^-) and leaf conductance to water vapor as dependent on soil moisture for *Nerium oleander* (oleander) grown in a sandy loam (after Chapin 1991).

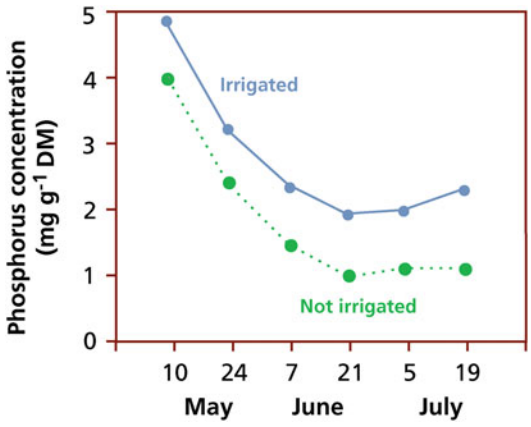

Fig. 9.4 Phosphorus concentration in the shoots of *Hordeum vulgare* (barley) grown with or without irrigation (after Chapin 1991).

(Table 9.2), reduction in water availability can greatly reduce plant growth. Two lines of evidence suggest that this may be a major causal mechanism by which low water supply restricts plant growth (Chapin 1991):

1. Shoot concentrations of growth-limiting nutrients often decline with water stress (Fig. 9.4), whereas one would expect concentrations to increase, if water restricted growth more than nutrient uptake.
2. Nutrient addition enhances growth of some desert annuals more than does water addition (Gutierrez and Whitford 1987).

The implication of this is that, with current predictions of climate change, plant growth in Mediterranean regions will become increasingly limited by P (Sardans et al. 2007).

For soil-mobile ions, such as NO_3^-, leaf concentrations vary with soil moisture availability in exactly the opposite manner as found for immobile ions. That is, in plants of Australian semi-arid woodlands, the leaf NO_3^- concentration tends to be high and the rate of NO_3^- assimilation slow, when the availability of soil moisture is low. After a rain event, the soil NO_3^- concentration rises rapidly, and the rate of NO_3^- assimilation in leaves increases, whereas the leaf NO_3^- concentration declines (Erskine et al. 1996).

9.2.2 Root Traits That Determine Nutrient Acquisition

Rates of nutrient uptake depend on the amount of root surface area and the root uptake properties. Once nutrients arrive at the root surface, they must pass the cell walls and plasma membrane of the root cells. As with carbon uptake by photosynthesis (Sect. 2.2.2), the rate of nutrient uptake depends on both the concentration in the environment and the **demand** by the plant, as well as on the inherent capacity of a plant to take up certain nutrients. The plant's demand is determined by its growth rate and the concentration of the nutrient in the tissues. At a high internal concentration, the capacity for uptake of that nutrient tends to be **downregulated**, and thus cellular nutrient toxicity is avoided. Despite this feedback mechanism, most plants show **luxury consumption** of specific nutrients (*i.e.* absorption at a faster rate than required to sustain growth), leading to the accumulation of that nutrient. Many species from N-rich sites [*e.g.*, *Urtica dioica* (stinging nettle) *Spinacia oleracea* (spinach) and *Lactuca sativa* (lettuce)] show luxury consumption of NO_3^- and accumulate NO_3^- in their vacuoles (Lambers et al. 2015d). Some species from severely P-impoverished habitats [*e.g.*, *Hakea prostrata* (harsh hakea), *Banksia grandis* (bull banksia) and *Protea compacta* (**bot river sugarbush**)] exhibit **P toxicity** when exposed to slightly higher P levels than occur in their natural habitat, because they fail to sufficiently downregulate their P uptake capacity as their leaf P concentration increases (Lambers et al. 2013).

9.2.2.1 Increasing the Roots' Absorptive Surface

Because diffusion is the major process that delivers growth-limiting nutrients to plant roots (Table 9.2), the major way in which plants can augment nutrient acquisition is by increasing the size of the root system. The relative size, expressed as the **root mass ratio** (root mass as a fraction of total plant mass), is enhanced by growth at a low N or P supply (**acclimation**) (Lambers et al. 2006). Similarly, slow-growing

Table 9.4 Phosphorus (P) uptake of seven plant species in relation to morphological root properties (root radius and root hairs).

Species	P_i uptake (10^{-12} mol m^{-1} s^{-1})	Root radius (μm)	Root hairs		
			Number per mm	Average length (mm)	Surface area of root hairs (m^2 m^{-2})
Allium cepa	84	2290	1	0.05	6.5×10^{-3}
Lolium perenne	69	660	45	0.34	1.2
Triticum aestivum	91	770	46	0.33	1.2
Brassica napus	320	730	44	0.31	1.3
Solanum lycopersicum	186	1000	58	0.17	0.6
Spinacia oleracea	485	1070	71	0.62	1.9
Phaseolus vulgaris	60	1450	49	0.20	0.4

Source: Föhse et al. (1991)

dicots **adapted** to low nutrient supply invest relatively more in roots and less in leaves than fast-growing dicots (Poorter and Remkes 1990). Increased biomass allocation to roots is particularly important for those ions that diffuse slowly in soil (*e.g.*, Pi). In a heterogeneous soil, roots tend to proliferate in those zones with highest availability of N or P, rather than in depleted zones, thus maximizing the effectiveness of each unit of root production (but, see Sect. 9.2.2.5).

The effective absorbing root surface can be increased by **root hairs** (Table 9.4), which vary in length from 0.2 to 2 mm, depending on species. Root hair length may increase from 0.1 to 0.8 mm, due to reduced supply of NO_3^- or Pi (Föhse and Jungk 1983; Bates and Lynch 2001). The diameter of most roots involved in ion uptake is between 0.15 and 1.0 mm, so the presence of root hairs allows roots to exploit a considerably larger volume of the soil than could be achieved without root hairs. Root hairs have the greatest effect on absorption of those ions that diffuse slowly in soil; they are probably not important for the uptake of silicon (Si), since mutants of *Oryza sativa* (rice) that lack root hairs take up Si at the same rates as the wild-type, and transporters involved in Si uptake are not expressed in root hairs (Ma et al. 2001a, 2006). In low-P soils, root hairs may be responsible for as much as 90% of total Pi uptake (Föhse et al. 1991). Total root-hair length in cereals may be 20–50 m m^{-1} (of roots from which they emerge); the higher values are typical for P-efficient cultivars (Gahoonia and Nielsen 2004). Species with a high frequency of long root hairs yield relatively more when P is limiting, in comparison with those with less frequent or shorter root hairs which need a high Pi supply for high yields (Brown et al. 2012). Increasing the root mass ratio or production of root hairs must incur costs, in terms of investment of carbon, N and other resources. To achieve an expansion of the root surface by root hairs requires considerably less investment than associated with a similar increase realized by a greater investment in roots (Clarkson 1996). **Mycorrhizal associations** are even more effective in terms of enlarging the Pi-absorbing surface per unit cost, even if we consider that the fungus requires additional plant-derived carbon for its functioning (Sect. 12.2.6).

9.2.2.2 Transport Proteins: Ion Channels and Carriers

Roots transport nutrients across their plasma membrane either by **diffusion** *down* an electrochemical potential gradient or by **active transport** *against* an electrochemical potential gradient. The electrochemical potential gradient is caused by the extrusion of protons by a **proton-pumping ATPase** that pumps H^+ from the cytosol across the plasma membrane. This creates an electrical potential difference of approximately

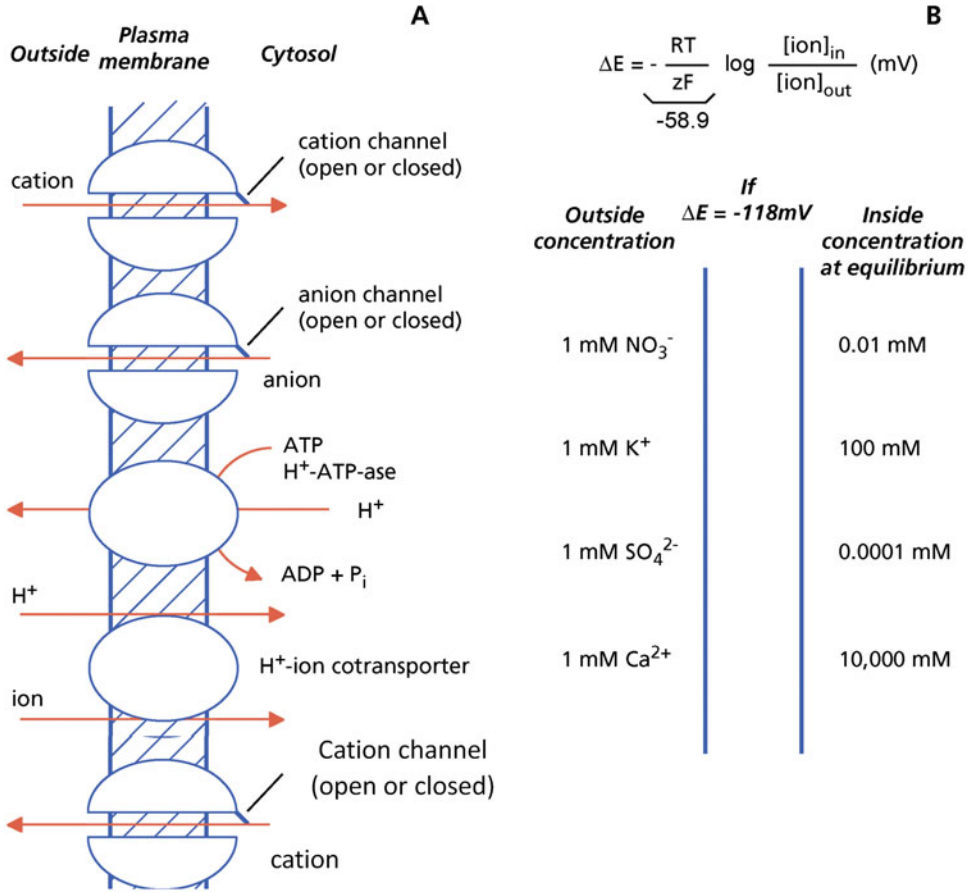

Fig. 9.5 (**A**) Ion transport across the plasma membrane. The membrane potential is negative (*i.e.* there is a negative charge inside and a positive charge outside). Cations can enter via a cation channel, down an electrochemical potential gradient. Anions (*e.g.*, NO_3^-) can only leave the cytosol via an anion channel, down an electrochemical potential gradient. Cations (*e.g.*, K^+) can leave the cytosol via a cation channel when the membrane becomes depolarized. Cations such as Na^+ can also leave via a Na^+/H^+ antiporter. An H^+-ATPase ('proton pump') extrudes protons from the cytosol, thus creating a protonmotive force. Protons are used to drive ion uptake against an electrochemical potential gradient. For further explanation, see text. (**B**) Schematic representation of the concentration of monovalent and divalent anions and cations that is expected if the plasma membrane is perfectly permeable for these ions in the absence of energy-requiring mechanisms at a membrane potential of 118 mV. The Nernst equation gives the relationship between the membrane potential ΔE and the outside and inside ion concentrations. R is the gas constant; T is the absolute temperature; z = the valency of the ion for which the equilibrium concentration is calculated; F is Faraday's number. For further explanation, see text.

80–150 mV (negative inside) across the plasma membrane (Fig. 9.5A). The proton pump functions like the ATPase in the thylakoid membrane of the chloroplast (Sect. 2.2.1.3) and the inner membrane of mitochondria (Sect. 3.2.5.1); however, here the ATPase acts in reverse: it uses ATP and extrudes protons. Cations tend to move inward and anions outward along this electrochemical potential gradient. The **Nernst equation** allows us to calculate that monovalent cations are at electrochemical equilibrium (no driving force for movement) if the concentration of the cation is 40- to 150-fold less outside than inside the cell. For monovalent anions the reverse can be calculated: the concentration of an anion at electrochemical equilibrium is 40- to 150-fold less inside than outside the cell. When concentration gradients are less than this, ions may move in the

direction predicted by the electrochemical gradient; when the concentration gradients exceed these values, ions may move in the opposite direction (Fig. 9.5B).

For most ions, diffusion across the lipid bilayer of the plasma membranes is a very slow process, unless facilitated by special transport proteins. Such transport proteins include **ion-specific channels** (*i.e.* 'pores' in the membrane through which ions can move single file) (Roberts 2006). These channels function in a similar way as the water-channel (aquaporin) proteins discussed in Sect. 5.5.2. The ion channels are either open or closed, depending on the membrane potential or the concentration of specific molecules that affect them (Fig. 9.5A). Ion channels have the advantage that they allow massive transport, albeit only down an electrochemical potential gradient. If such a gradient does not exist, or when the gradient is in the opposite direction, channels cannot be used for net transport. In that case, transport may require, first, the extrusion of protons via an H^+-pumping ATPase (Fig. 9.5A). The proton gradient is then used for uptake of ions, in a proton-cotransport mechanism via **carrier proteins** (Fig. 9.5A). Such carriers are like enzymes: they bind their substrates, followed by a specific reaction (release of the substrate at the other side of a membrane), and may be allosterically regulated. Carriers tend to have a much lower transport capacity than channels. Both types of proteins are subject to turnover so that continuous protein synthesis is required to maintain ion transport.

Although ions can move via a channel down an electrochemical potential gradient across the plasma membrane, ion transport via channels is ultimately an **active process**. This is because charge balance must be accomplished, by the H^+-pumping ATPase, at the expense of ATP; otherwise, membranes subjected to, say, NH_4^+ or Na^+ uniport [that is, transport that is not accompanied with the transport of H^+ in the same (co-transport) or opposite (antiport) direction] would electrically supercharge and 'combust' very quickly (Britto and Kronzucker 2006).

Both channels and carriers are, in principle, ion-specific, but other ions with similar structure might occasionally enter the cell via these transport proteins. This may account for the entry of some Na, metals, and Al in plant roots. Transport proteins are involved in the **influx** of nutrients from the **rhizosphere**, the soil adjacent to the roots and influenced by their presence (Hiltner 1904; Hartmann et al. 2008). Transport proteins also function in the transport of some of the acquired nutrients into the **vacuoles** and their release into the **xylem vessels** (Peuke 2010). Channels and carriers are also involved in ion **efflux**, sometimes spectacularly so, as during stomatal movements (Sect. 5.5.4.2), or they may be responsible for efflux of nutrients, which may occur simultaneously with nutrient influx. Uptake of Na^+ ions from a saline soil occurs down an electrochemical potential gradient, in which case the ions may be extruded with an energy-dependent carrier mechanism (Sect. 9.3.4.1; Britto and Kronzucker 2015). Silicon (as silicic acid) is transported into root cells by a channel, but out of the cells by an active transporter (Ma et al. 2006, 2007).

Transport from the rhizosphere across the plasma membrane into the cytosol (influx) is mostly against an electrochemical potential gradient for all anions and sometimes also for some cations. Such transport must involve an active component (*i.e.* it requires **metabolic energy**); however, transport mediated by channels also requires metabolic energy, although indirectly, to generate the electrochemical potential gradient. This requires respiratory energy: ATP is used to extrude protons, catalyzed by an H^+-ATPase, so that a membrane potential is generated (inside negative). **Efflux** of ions, from the cytosol to the rhizosphere, is mostly down an electrochemical potential gradient for anions; the efflux of NO_3^- may be very slow in some circumstances, but it may also be of similar magnitude as the influx, especially in slow-growing plants grown with a high nutrient supply (Scheurwater et al. 1999). Like the NO_3^--uptake system, the NO_3^--efflux system is NO_3^--inducible, and it strongly increases with increasing internal NO_3^- concentrations. The efflux system requires both RNA and protein synthesis, but has a much slower turnover rate than the uptake system

(Aslam et al. 1996). NO_3^- efflux may contribute significantly to the respiratory costs associated with nutrient acquisition (Sect. 3.5.2.3). NO_3^- efflux may reflect a fine-control of net uptake, compared with the coarse-control of gene expression. Ion efflux from roots is not restricted to Na^+ and NO_3^-, but is quite common for a range of other cations and anions (Demidchik et al. 2002; Roberts 2006), particularly at higher external ion concentrations (Britto and Kronzucker 2006).

9.2.2.3 Acclimation and Adaptation of Uptake Kinetics

9.2.2.3.1 Response to Nutrient Supply

Net nutrient uptake by roots increases in response to increasing nutrient supply up to some maximum uptake rate, where a plateau is reached (Fig. 9.6A) which is very similar to the CO_2 or light-response curves of photosynthesis (Sect. 2.2.2) (Epstein and Hagen 1952). If nutrient uptake is not limited by diffusion of the nutrient to the root surface, then the shape of this curve is also similar to that obtained with enzymes in solution (Michaelis-Menten kinetics). This leads to the suggestion that the **maximum inflow rate** ($\boldsymbol{I_{max}}$) may be determined largely by the abundance or specific activity of transport proteins in the plasma membrane; the $\boldsymbol{K_m}$ describes the **affinity** of the transport protein for its ion. This analogy may not be entirely accurate, however, because the access of ions to carriers and ion channels in plasma membranes of a structurally complex root is probably quite different from the access of substrates to an enzyme in a homogenous stirred solution. Nonetheless, I_{max} is a useful description of the capacity of the root for ion uptake, and K_m describes the capability of the root to utilize low concentrations of substrate (low K_m confers high affinity). Affinities and transporter abundance may be reasonably inferred, provided influx is properly measured, and this can be difficult at high nutrient concentrations (Szczerba et al. 2006). C_{min} is the minimum ion concentration at which net uptake occurs (analogous to the light- and CO_2-compensation points of photosynthesis) (Fig. 9.6A). C_{min} is determined by the balance of influx by ion-transport proteins and efflux down an electrochemical potential gradient. The experimental determination of C_{min} is difficult. For instance, in nonsterile conditions, much of the nutrient remaining in solution is in microorganisms. If these are filtered out, then C_{min} is often spectacularly lower than is usually determined in this critical experiment.

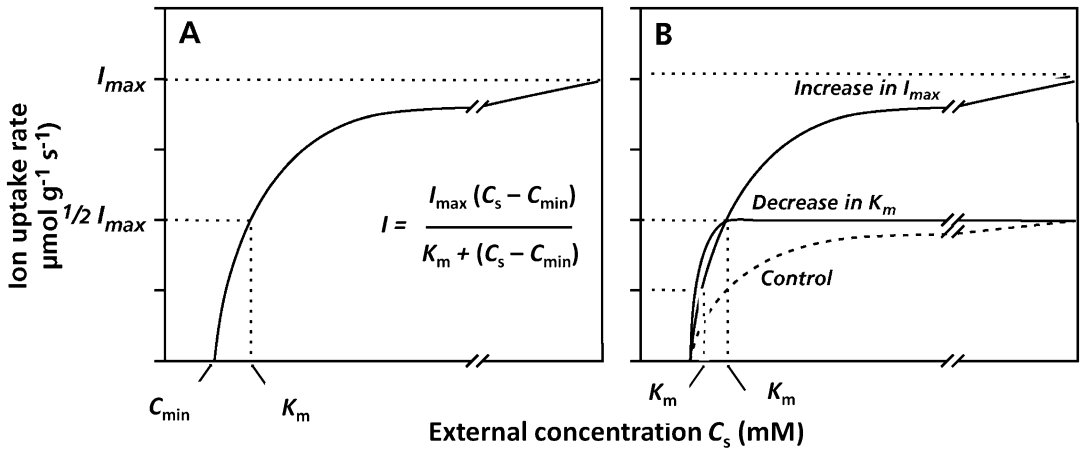

Fig. 9.6 (**A**) The relationships between uptake rates (net inflow = I) of ions and their external concentrations (C_S). At C_{min} the net uptake is zero (influx = efflux). (**B**) Uptake kinetics in control plants and in plants grown with a shortage of nutrients. Note that both induction of a different high-affinity system, and upregulation of the same low-affinity system, can enhance the capacity for nutrient uptake at low external concentration.

For many nutrients, *e.g.*, K, N, and P, roots have both a **high-affinity uptake system**, which functions well at low external nutrient concentration, but has a low I_{max}, and a **low-affinity system**, which is slow at low external concentrations but has a high I_{max} (Wang et al. 1993; Maathuis and Sanders 1996; Bucher 2007; Yong et al. 2010). The high-affinity system is most probably carrier-mediated, whereas the low-affinity system may reflect the activity of a channel, at least for K^+. However, there are also '**dual-affinity transporters**', *e.g.*, for NO_3^- (Liu and Tsay 2003; Morère-Le Paven et al. 2011). Switching between the two modes of action is regulated by **phosphorylation**; when phosphorylated, the transporter functions as a high-affinity NO_3^- transporter, whereas it functions as a low-affinity NO_3^- transporter when dephosphorylated (Liu and Tsay 2003). This regulatory mechanism allows plants to change rapidly between high- and low-affinity NO_3^- uptake. The ecophysiological significance of low-affinity systems for root NO_3^- uptake, which only allow significant uptake at NO_3^- concentrations well above that in most soils, is not yet clear; they likely play a role in NO_3^- efflux (Wang et al. 2012; Krapp et al. 2014; Kiba and Krapp 2016; Wen et al. 2017).

When nutrients are in **short supply**, plants tend to show a **compensatory** response in that the I_{max} is increased and a high-affinity transport system is likely induced. For example, plants exhibit a high capacity (*i.e.* high I_{max}) to absorb Pi when grown at a very low supply of Pi, and a high potential to absorb K^+ or SO_4^{2-} when K or S are limiting (Dunlop et al. 1979; Shinmachi et al. 2010; Cai et al. 2013). For N, the situation is different, however (Sect. 9.2.2.3.2). Information about other macronutrients is sparse, but it suggests that there is little stimulation of the inflow of Ca and Mg (Robinson 1996). The compensatory increase in I_{max} for P and K in response to a shortage of these nutrients occurs over a period of 2–15 days, but can be as fast as hours (Smart et al. 1996; Dong et al. 1999).

Compensatory changes in I_{max} involve synthesis of additional transport proteins for the growth-limiting nutrient, and upregulation of mRNA levels encoding a high-affinity uptake system (Sect. 9.2.2.3.2). A decrease in K_m could be due to induction of such a high-affinity system, or to allosteric effects on, or phosphorylation of, existing transporters (Liu and Tsay 2003). Both an increase in capacity (I_{max}) of a low-affinity system and induction of a high-affinity system may enhance the uptake capacity at a low nutrient supply (Fig. 9.6B).

An increase in I_{max} or a decrease in K_m is functionally important if processes at the root surface limit nutrient uptake, as would be the case for NO_3^-, which is relatively mobile in soil (Table 9.3). The significance of the upregulation of transporters in the uptake system for the plant is that the concentration of the limiting nutrient at the root surface is decreased which increases the concentration gradient and the diffusion of the limiting nutrient from the bulk soil to the root surface. However, the effect of such upregulation for plants growing in soil is small for less mobile ions such as Pi. For less mobile ions, it is the mobility in soil, rather than the I_{max} of the roots, that determines the rate at which roots can acquire this nutrient from the rhizosphere (Sects 9.2.1.2 and 9.2.3). Rather than considering *upregulation* of I_{max} for P uptake at a *low* P availability functionally important, *downregulation* at *higher* P supply is important in avoiding **P toxicity** of plants (Shane et al. 2004b, 2004c).

9.2.2.3.2 Response to Nutrient Demand

Any factor that increases plant **demand** for a specific nutrient tends to increase I_{max} for that nutrient. Upregulation of the transport system for NO_3^- uptake upon an increased demand from the shoot involves the NO_3^- concentration in the root itself as well as **systemic signals** from the shoot, transported via the phloem (King et al. 1993) . The signals that arrive via the phloem probably include a low concentration of amino acids and/or an increased concentration of organic acids (Nazoa et al. 2003). In experiments, effects of the demand for P, K or SO_4^{2-} can be simulated by a period of starvation, as discussed in Sect. 9.2.2.3.1. For example, in *Arabidopsis thaliana* (thale cress), the expression of a gene that encodes a Pi transporter and the capacity to take up Pi increases with decreasing internal P concentration (Dong et al. 1999). The same happens with genes that encode

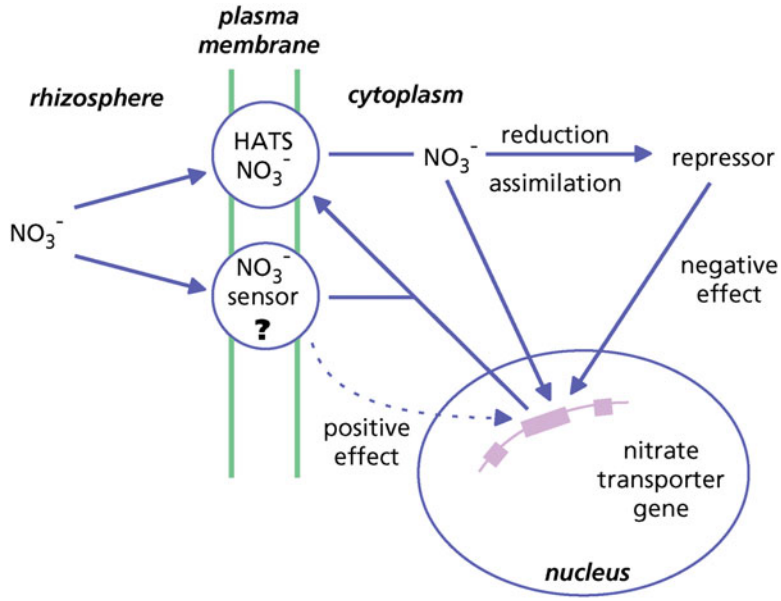

Fig. 9.7 Regulation of the inducible high-affinity NO_3^- uptake system (HATS) by NO_3^-. The HATS is affected both by the external NO_3^- availability and by internal demand. Situation 1: If *no nitrate* is present in the rhizosphere, there is no positive effector. The gene encoding the NO_3^- transporter is repressed and the system cannot respond immediately to the addition of NO_3^-. Situation 2: If there is an *inadequate nitrate* concentration in the rhizosphere, NO_3^- is sensed by the constitutive HATS (cHATS), the gene encoding the NO_3^- transporter is transcribed, and the system responds to the addition of NO_3^-. Products of the reduction and assimilation of NO_3^- (amino acids, organic acids) have a negative effect on the transcription of the gene encoding the HATS.

NH_4^+ transporters and the capacity to take up NH_4^+ when the external NH_4^+ supply increases (Rawat et al. 1999). The influence of demand and starvation on NO_3^- transport, however, is more complex (Fig. 9.7).

For NO_3^-, there are two inducible uptake systems: a **high-affinity transport system** (HATS) and a **low-affinity transport system** (LATS) (Kiba and Krapp 2016). Another gene encoding a **constitutive high-affinity nitrate transport system** (cHATS) is responsible for initial uptake when the availability is low (Kotur and Glass 2015). In the complete absence of external NO_3^-, the NO_3^- uptake capacity is very low. In *Hordeum vulgare* (barley) and *Lotus japonicum* (birdsfoot-trefoil), the mRNA for the HATS is almost absent after 72 h of NO_3^- deprivation. Upon re-exposure of the roots to NO_3^-, this is first taken up by the cHATS. After 30 min, there is a huge rise in mRNA encoding the HATS, and after 2–4 h the inducible HATS is reassembled in the plasma membrane (Trueman et al. 1996), and the rate of NO_3^- uptake increases (Siddiqi et al. 1990). The general experience, however, is that plants receiving NO_3^-, but in amounts inadequate for supporting maximum growth, de-repress their NO_3^--transport activity, so net NO_3^- uptake increases in experimental conditions where the plants are given a sudden dose of NO_3^- (Fig. 9.7).

The cHATS system serves as a **NO_3^--sensing system**, and is associated with a plasma membrane-bound **nitrate reductase**. The concerted action of the constitutive system and its associated nitrate reductase may lead to the production of intermediates that induce both the inducible high-affinity system and cytosolic nitrate reductase. Both the constitutive and the inducible system are carrier-mediated proton-cotransport systems, requiring the entry of two protons for every NO_3^- taken up (Mistrik and Ullrich 1996).

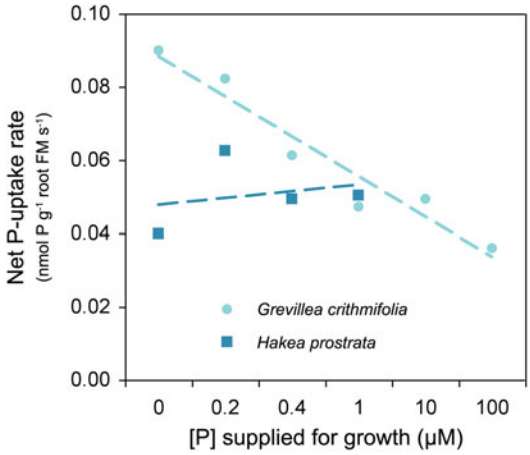

Fig. 9.8 Net uptake rates of inorganic phosphorus (Pi) of intact whole root systems, calculated from Pi-depletion curves. The nutrient solution for the uptake studies contained 5 μM P. Uptake rates are plotted against the external Pi concentration during plant growth, for *Grevillea crithmifolia* and *Hakea prostrata* (harsh hakea). Note downregulation of net P-uptake rates (the common response) in *Grevillea crithmifolia*, and a lack of downregulation of net P-uptake rates in *Hakea prostrata* (which accounts for this species showing signs of P toxicity upon fertilization with P). After Shane et al. (2004c) and Shane and Lambers (2006).

C_{min} for a given ion decreases within minutes to hours in response to decreases in supply of that ion. This is due to decreases in its cytoplasmic concentration, which reduces leakage across the plasma membrane, and, therefore, efflux rates (Kronzucker et al. 1997). The I_{max} increases when plants acclimate to low availability of a given nutrient and increases the plant's capacity to absorb nutrients from solutions with low concentration (Fig. 9.8). This compensation, however, is always incomplete, so plant nutrient concentrations increase under conditions of high nutrient supply (**luxury consumption**), and decrease under conditions of low nutrient supply (high nutrient-use efficiency) (Sect. 9.4). A low capacity to downregulate I_{max} for Pi uptake is typically associated with species occurring on severely P-impoverished soils (Fig. 9.8).

A plant's response to nutrient stress, *e.g.*, a growth-limiting supply of Pi, requires a capacity to sense the internal nutrient status, *e.g.*, leaf [P]. The key **transcriptional activator** in Pi-starvation signaling is the phosphate starvation response 1 gene (*AtPHR1* in *Arabidopsis* and *OsPHR2* in *Orya sativa*, rice) (Ajmera et al. 2018). The active form of the protein encoded by this gene results in the expression of numerous Pi-starvation-induced genes. These genes are involved in making better use of the limited P that is acquired. There is a microRNA, **miR399**, which is the systemic integrator defining Pi demand across the whole plant. Plant miRNAs usually downregulate the abundance of their target mRNAs by post-transcriptional cleavage. For example, miR399 results in downregulation of *UBC24*, a gene involved in **targeted protein degradation**. Plants over-expressing miR399, or defective in the gene involved in targeted protein degradation (*UBC24*), display **P toxicity**, because of increased P uptake, enhanced root-to-shoot translocation, and retention of P in their old leaves. This suggests that the miR399-mediated regulation of *UBC24* expression is critical in the **P-starvation response**. The existence and conservation of miRNAs and their target genes involved in P uptake among many plant species points to the evolutionary importance of these miRNA-mediated nutrient-stress responses (Chiou 2007). Sugars also play a key role in signaling a plant's P status. High levels of sugars induce P-starvation responses, involving **sugar signaling** (Hammond and White 2008; Li and Sheen 2016).

9.2.2.3.3 Response to Other Environmental and Biotic Factors

We can readily predict the responses of nutrient-uptake kinetics to the availability of water, light, and other environmental factors from changes in plant demand for nutrients. **Water stress** may reduce the capacity of roots to absorb nutrients, if it reduces growth, and, therefore, plant demand for nutrients (Fig. 9.9A). The effect of **irradiance** on nutrient-uptake kinetics depends on nutrient supply. With adequate nutrition, low light levels reduce nutrient uptake (Fig. 9.9B). By contrast, light availability has little effect on nutrient uptake in nutrient-limited plants (Chapin 1991).

Low temperature reduces nutrient uptake by plants, as expected for any physiological process that is dependent on respiratory energy (Fig. 9.10A; Macduff et al. 1987). Plants

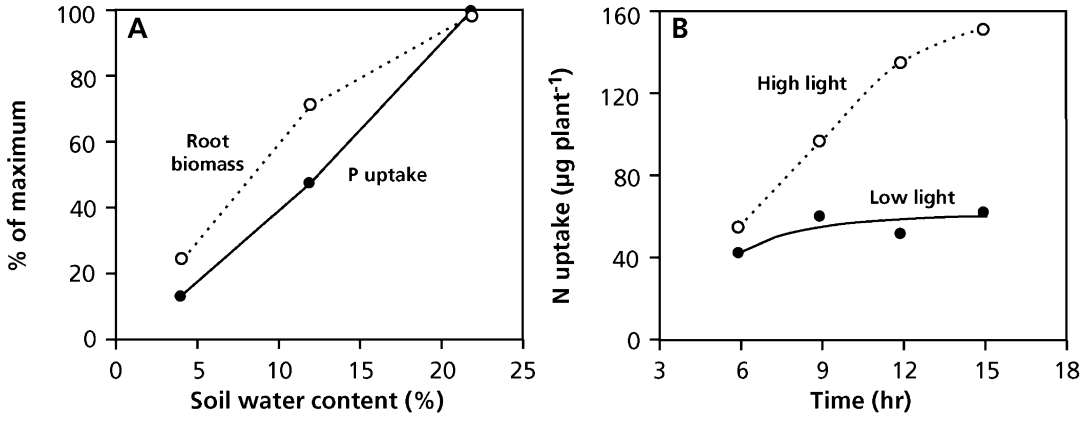

Fig. 9.9 (**A**) Effect of soil water content on root biomass and phosphorus (P) uptake per unit root biomass in *Solanum lycopersicum* (tomato), and (**B**) growth irradiance on ammonium (N) uptake per plant in *Oryza sativa* (rice) (after Chapin 1991).

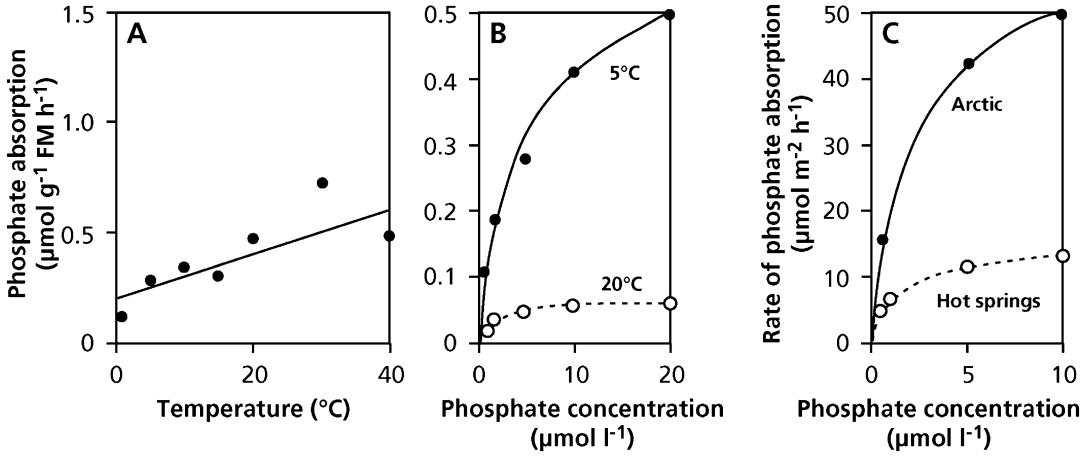

Fig. 9.10 Response of phosphorus (P) uptake by *Carex aquatilis* (a tundra sedge) to temperature at different time scales: (**A**) immediate response, (**B**) response following acclimation, and (**C**) response of adapted genotypes (measured at 5 °C) (after Chapin (1974) and Chapin and Bloom (1976).

compensate through both acclimation and adaptation for this temperature inhibition of uptake by increasing their capacity for nutrient uptake (Fig. 9.10B, C). In contrast to plants from infertile environments, arctic and alpine plants often grow quite rapidly, and so exploit the short growing season; therefore, they have a substantial demand for nutrients.

When plants are grown with an adequate nutrient supply, **grazing** of leaves from those plants reduces plant nutrient demand, and, therefore, their nutrient-uptake capacity (Clement et al. 1978). By contrast, grazing of nutrient-stressed plants can deplete plant nutrient stores, so that plants respond by increasing nutrient uptake capacity (Chapin and Slack 1979). Plants that are adapted to frequent grazing such as grasses from the Serengeti Plains of Africa, similarly increase their capacity to absorb Pi when clipped to simulate grazing (McNaughton and Chapin 1985).

9.2.2.4 Acquisition of Nitrogen

Plants absorb N predominantly in three distinct forms: $\mathbf{NO_3^-}$, $\mathbf{NH_4^+}$, and **amino acids**. Nitrogen assimilation (*i.e.* the conversion of inorganic to organic N) has a substantial carbon cost: NO_3^- is

first reduced to NH_4^+, which is then attached to a carbon skeleton before it can be used in biosynthesis. Thus, the carbon cost of N assimilation which is generally large, changes as follows: NO_3^- >> NH_4^+ > amino acids (Zerihun et al. 1998). Depending on the species, NO_3^- is reduced either in the roots or transported to the leaves, where it is reduced in the light (Xu et al. 2012). The first step in the reduction is catalyzed by **nitrate reductase**, which is an inducible enzyme; the gene encoding nitrate reductase is transcribed in response to NO_3^- availability (Xu et al. 2012). A side reaction of nitrate reductase produces **nitrogen oxide** (NO), a signal molecule that regulates plant development and stress responses (Krapp 2015). Nitrate reductase is controlled by **phosphorylation**, which allows activation/inactivation in response to light/dark transitions or other treatments that regulate the activation state of nitrate reductase (Lillo et al. 2004). A protein phosphatase reactivates the enzyme when irradiance increases (Kaiser and Huber 2001). NO_3^- assimilation is energetically expensive, because of the costs of NO_3^- reduction. NO_2^- and NH_4^+ are toxic to plant cells, and therefore NO_2^- must be further reduced, and NH_4^+ must be rapidly assimilated to produce amino acids. NO_3^- reduction to NH_4^+ requires approximately 15% of plant-available energy when it occurs in the roots (2% in plants that reduce NO_3^- in leaves) with an additional 2–5% of available energy for NH_4^+ assimilation (Bloom 2015). One might think that the lower costs incurred when NH_4^+, rather than NO_3^-, is used as the source of N by the plant, would allow for a faster growth rate. This does not always occur, however, because of adjustments in leaf area ratio (Sect. 10.2.1.1), possibly a lower efficiency of root respiration (Sect. 3.2.6), or simply because carbon is often not the most limiting resource for plant growth. Leaf nitrate reductase activity is typically highest at midday in association with high light intensities. Some plants, particularly Ericaceae, show low levels of nitrate reductase (Smirnoff et al. 1984), presumably because NO_3^- availability is generally low in habitats occupied by these ammonium-adapted species.

Plant species differ in their preferred forms of N absorbed, depending on the forms available in the soil. For example, arctic plants, which experience high amino acid concentrations in soil, preferentially absorb and grow on amino acids, whereas *Picea glauca* (white spruce) preferentially absorbs NH_4^+ (Kronzucker et al. 1997). Much of the early work on NO_3^- and NH_4^+ preference is difficult to interpret, because of inadequate pH control (Sect. 9.2.2.6) or low light intensity. Species from habitats with high NO_3^- availability (*e.g.*, calcareous grasslands), however, often show preference for NO_3^- and have higher nitrate reductase activities than do species from low-NO_3^- habitats. Most plants are capable of absorbing any form of soluble N, however, especially if acclimated to its presence (Atkin 1996; Liu et al. 2018).

Plants can also acquire N from the air. This is an important avenue of N uptake by N-limited forests exposed to rain that has high NO_3^- due to lightning, estimated at 10×10^9 kg per year (Galloway et al. 1995), and fossil fuel combustion, which amounts to 25×10^9 kg per year (Canfield et al. 2010). Natural and agricultural vegetation acts as a major 'sink' for atmospheric pollutants in terrestrial ecosystems. The capacity to assimilate NO_2 from the air varies more than 600-fold among species. Some species [*e.g.*, *Magnolia kobus* (kobus magnolia), *Eucalyptus viminalis* (manna gum), and *Nicotiana tabacum* (tobacco)] may derive more than 10% of their N from NO_2. Information about the species that can assimilate large amounts of NO_x may be useful in choosing street trees in polluted areas (Gawronski et al. 2017).

9.2.2.5 Acquisition of Phosphorus

There are numerous traits involved in acquiring sufficient quantities of Pi from soil. Some of these traits are specific for P (*e.g.*, root phosphatases); other traits (*e.g.*, root hairs and root mass ratio) promote uptake of all ions, but are most critical for Pi, because of the low diffusion coefficient of Pi in soil (Table 9.3), and therefore the small volume of soil that each root can exploit. We discuss the specialized associations with mycorrhizal fungi in Sect. 12.2.3.

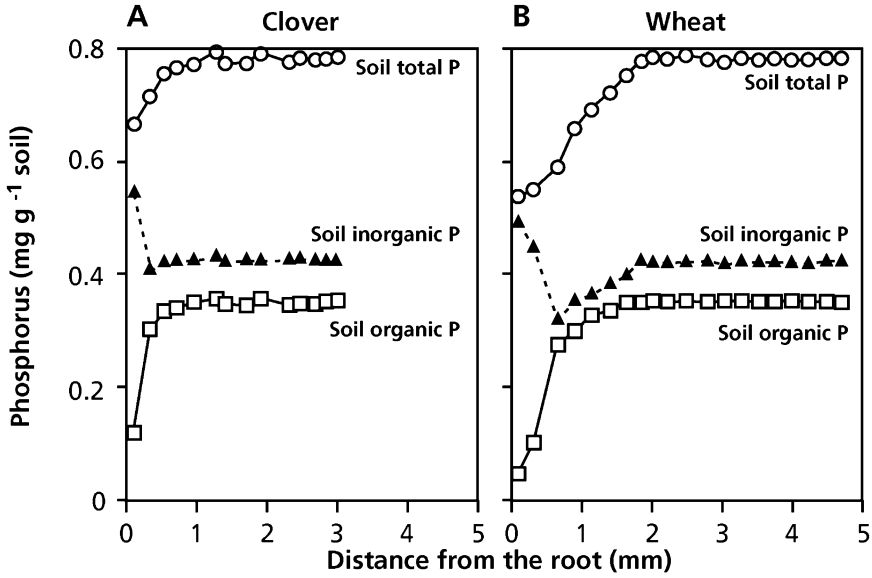

Fig. 9.11 Distribution of total, inorganic and organic phosphorus (P) in the rhizosphere of *Trifolium alexandrinum* (berseem clover, 10 days old) and *Triticum aestivum* (wheat, 15 days old) grown in a silt loam (after Tarafdar and Jungk 1987); copyright © 1987, Springer-Verlag.

9.2.2.5.1 Plants Can Also Use Some Organic Phosphate Compounds

In many soils, 30–70% of all P is present in an **organic** form; in nutrient-poor grasslands, peat soils, and forest soils this may be as much as 80–95% (Macklon et al. 1994; Turner 2006). A major form of soil P is **inositol phosphate**, which consists of esters containing four, five, or six P molecules (Turner and Richardson 2004). Many species [*e.g.*, *Carex acutiformis* (pond sedge) (Pérez Corona et al. 1996), *Trifolium subterraneum* (subclover) (Hayes et al. 2000)] can use nucleic acids, phospholipids, glucose 1-phosphate, and glycerophosphate (all present in soil), in addition to Pi, due to the activity of **phosphatases** in the soil. Production of phosphatases by the roots provides an additional source of Pi; these enzymes hydrolyze organic P-containing compounds, releasing Pi that is absorbed by roots (Richardson et al. 2011). Phosphatase production is enhanced by a low Pi supply to the plants. Most phosphatases cannot hydrolyze **phytate** (the salt of inositol hexakisphosphate), a major fraction of the organic P pool in soil (Turner et al. 2014); **phytase** releases Pi from this source. The nonmycorrhizal tropical montane tree *Roupala montana* (Proteaceae) has the capacity to grow on phytate, unlike its mycorrhizal neighbors (Steidinger et al. 2014). Some plants may release phytase into the rhizosphere (Li et al. 1997; Giles et al. 2017), but for many plants phytate is a poor source of P (George et al. 2006; Secco et al. 2017). Roots may, however, exude organic substances that act as substrates for microorganisms, which produce enzymes that hydrolyze organic phosphate, including phytate (Richardson and Simpson 2011). Whatever the exact mechanism by which organic P is hydrolyzed, the concentration of organic P near the root surface may decrease by as much as 65% in *Trifolium alexandrinum* (berseem clover) and 86% in *Triticum aestivum* (wheat) (Tarafdar and Jungk 1987). This shows that these roots have access to organic forms of P in the soil (Fig. 9.11).

The capacity to use organic P varies among species, and depends on soil conditions. It may range from almost none to a capacity similar to that of the rate of Pi uptake (Hübel and Beck 1993; Steidinger et al. 2014).

9.2.2.5.2 Excretion of Phosphate-Solubilizing Compounds

Some plants that are adapted to low-P soils exude **acidifying** and/or **chelating** compounds (*e.g.*, citric acid and malic acid). Acidification enhances the solubility of Pi in alkaline soils; however, in acid soils, when phosphate is bound to oxides and hydroxides of Al or Fe, a pH decrease in the rhizosphere may not enhance P availability (Fig. 9.1B), even if it increases P solubility (Barrow et al. 2018). Chelating compounds, including citrate and malate, occupy sites that also bind phosphate (ligand exchange), and thus solubilize phosphate **sorbed** to soil particles (Geelhoed et al. 1998). Both acidification (in alkaline soils) and chelation (all soils) processes enhance the concentration gradient for Pi between the bulk soil and the root surface (Lambers et al. 2006). Crop species vary widely in their capacity to access sparingly available P, with cereals generally showing a very low capacity (Rose et al. 2010b; Carvalhais et al. 2011) and many legumes exhibiting a considerably greater capacity (Pearse et al. 2006; Tomasi et al. 2009; Kidd et al. 2018). Such variation offers potential for improving crops for specific soils, intercropping, and crop rotations (Li et al. 2003; Nuruzzaman et al. 2005; Jemo et al. 2006; Rose et al. 2010a; Salehi et al. 2018; Doolette et al. 2019).

The capacity to exude carboxylates is very pronounced in members of the Proteaceae, most of which do not form a mycorrhizal association, but have **proteoid roots** (Fig. 9.12). The term 'proteoid roots' was coined because the structures were first discovered in the Proteaceae (Purnell 1960). Because we can find similar structures in many other families, now the term **cluster roots** is commonly used. Cluster roots comprise a number of determinate extremely hairy rootlets tightly grouped along the parent root; they originate during root development, 1–3 cm from the root tip. One lateral branch may contain one, two or several clusters, centimeters apart from each other. Clusters usually consists of unbranched rootlets [simple cluster roots, as in *Hakea prostrata* (harsh hakea, Proteaceae) and *Lupinus albus* (white lupin, Fabaceae) (Fig. 9.12B, E)]; in some species they are branched rootlets [compound cluster roots, as in *Banksia* species (Proteaceae) (Fig. 9.12A, D) (Shane and Lambers 2005; Shi et al. 2019)]. Cluster roots exude carboxylates, phenolics, and phosphatases, but in most studied species, this process takes place during only a few days after their formation (Lambers et al. 2015d). Many sedges (Cyperaceae) produce **dauciform roots**, carrot-shaped roots with long root hairs (Fig. 9.12C, F), which are functionally similar to the cluster roots in Proteaceae and Fabaceae (Shane et al. 2006a). **Capillaroid roots** are restricted to some species in the Restionaceae, but **sand-binding roots** are common in a wide range of species; their functioning is also similar to that of cluster roots (Lambers et al. 2014; Abrahão et al. 2019). **Vellozioid roots** are typical in rock-dwelling Velloziaceae; they grow inside quartzite rock and mobilize P and other nutrients from these rocks (Teodoro et al. 2019).

Specialized carboxylate-releasing roots are almost universal in the Proteaceae; they also occur in species belonging to the Anarthriaceae, Betulaceae, Cactaceae, Casuarinaceae, Cyperaceae, Elaeagnaceae, Fabaceae, Haemodoraceae, Myricaceae, Restionaceae, and Velloziaceae (Lambers et al. 2015d; Teodoro et al. 2019). Most species that form cluster roots or their functional equivalent are nonmycorrhizal (*e.g.*, Cactaceae, Cyperaceae, some Fabaceae, Proteaceae, Restionaceae) (Shane and Lambers 2005; Shane et al. 2006a; Abrahão et al. 2014), but this is not universal (*e.g.*, Betulaceae, Casuarinaceae, Elaeagnaceae, some Fabaceae) (Reddell et al. 1997; Lambers et al. 2006).

In Australia, Brazil, and South Africa, nonmycorrhizal cluster-bearing species or their functional equivalent occur on the most heavily leached and P-impoverished soils (Shane and Lambers 2005; Lambers et al. 2010; Zemunik et al. 2018). Mycorrhizal species, on the other hand, are found on soil with greater P availability, but they also co-occur with nonmycorrhizal carboxylate-releasing species on severely P-impoverished soils, both in Australia and in Brazil (Zemunik et al. 2015, 2016, 2018). In southern South America, species with cluster

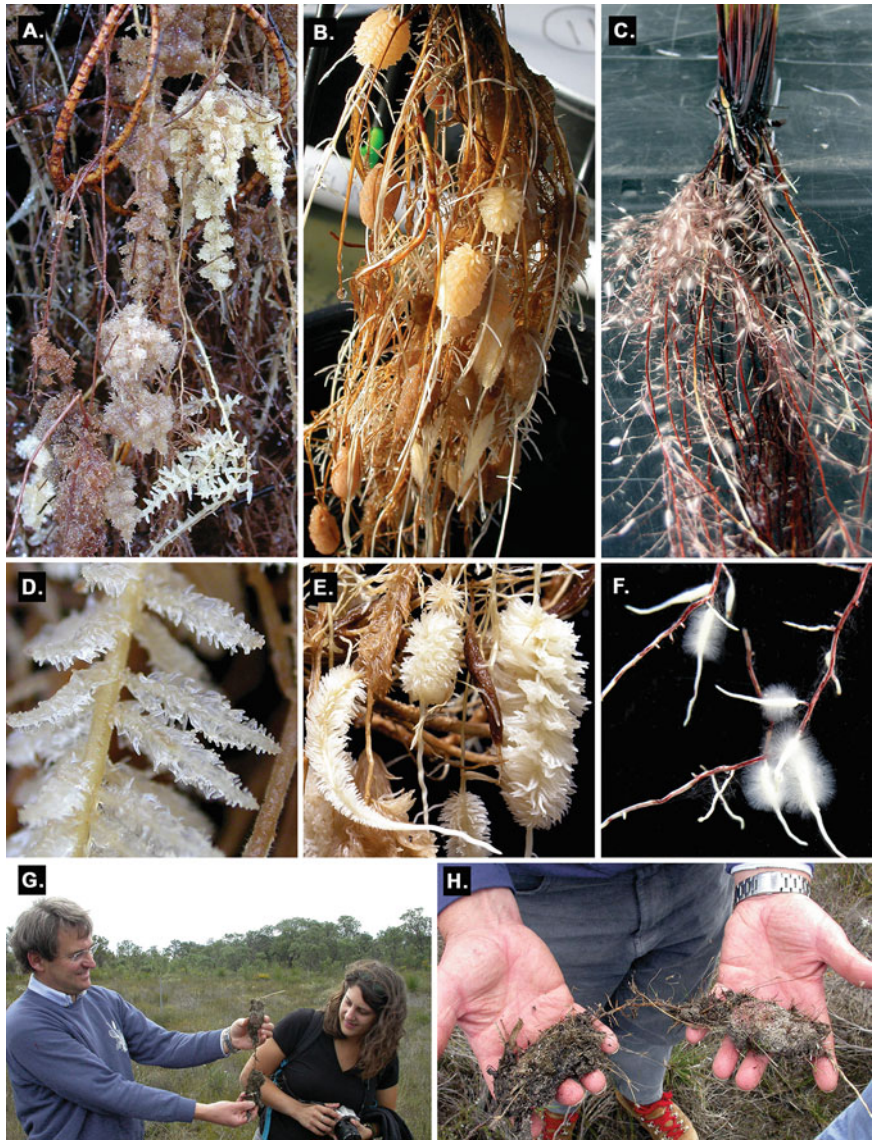

Fig. 9.12 Root morphology of Proteaceae and Cyperaceae species. In A-F plants were grown hydroponically at very low phosphorus (P) supply ($\leq$ 1 μM). (**A**) *Banksia sessilis* (parrot bush) root system with 'compound' 'cluster' roots; bar is 20 mm. (**B**) *Hakea prostrata* (harsh hakea) root system with 'simple' cluster roots; bar is 30 mm. (**C**) *Tetraria* (sedge) species root system with 'dauciform' roots; bar is 20 mm. (**D**) Young, compound cluster roots of *Banksia grandis* (bull banksia) with 3rd order determinate branch rootlets; bar is 3 mm. (**E**) Simple cluster roots of *Hakea sericea* (silky hakea) at various stages of development with 2nd order determinate branch rootlets (white cluster roots are young-mature, whereas brown ones are senescent or dead). (**F**) Higher magnification of dauciform roots of *Tetraria* species in C. Root-hair density is extremely high on individual dauciform roots; bar is 10 mm. (**F**) *Tetraria* species. In **G** and **H**, simple cluster roots of *Hakea ceratophylla* (horned-leaf hakea) that tightly bind the sand excavated at the University of Western Australia's Alison Baird Reserve at Yule Brook (Western Australia) (courtesy M.W. Shane, the University of Western Australia, Perth, Australia). (**A**)–(**F**): copyright Elsevier Science, Ltd.

roots occur on soils with high total P concentrations, but with a low P availability, because the soils are acidic and contain high concentrations of minerals that sorb P (Lambers et al. 2012a; Zúñiga-Feest et al. 2014). These distribution patterns are explained by the fact that cluster roots are very effective at acquiring P from soils in which P is largely **sorbed** to soil particles; they effectively '**mine**' the soil for P (Lambers et al. 2008). Arbuscular mycorrhizal associations, on the other hand, act as '**scavengers**' for Pi that is in the soil solution (Sect. 12.2.2); they are more effective when the Pi concentration in solution is greater than that in soils where Proteaceae are more abundant (Fig. 9.13A; Lambers et al. 2008). The carboxylate-releasing strategy is more costly in terms of carbon requirement when the P availability is in the range where mycorrhizal plants are effective (Raven et al. 2018).

The development of cluster roots and dauciform roots is suppressed at a higher supply of Pi (Fig. 12.9 in Sect. 12.2.3.2) (Reddell et al. 1997; Keerthisinghe et al. 1998; Shane et al. 2006b; Delgado et al. 2014). Because foliar application of Pi inhibits the formation of cluster roots, their induction must be controlled systemically by the internal P concentration, rather than by that in the soil (Marschner et al. 1987; Shane et al. 2003).

Cluster roots of *Lupinus albus* release 40 and 20 times more citric and malic acid, respectively, than lupin roots in which the development of cluster roots is suppressed by P. The massive and rapid release of carboxylates is mediated by anion channels (Zhang et al. 2004). Although the exudation of citrate is fastest close to the root tip, the capacity to absorb P from the medium is equally high close to, and further away from, the tip. *In situ*, however, most of the Pi in the soil will be depleted by root cells close to the tip, leaving little to be absorbed by older zones. The mechanism by which citrate and other chelating substances enhance P uptake is by **solubilizing P** that is **sorbed** to soil particles; a point we made at the start of this section. Both Pi and organic P compounds are solubilized, the latter then becoming available for hydrolysis by **phosphatases** (Fig. 9.13B).

The capacity to exude acidifying and/or chelating compounds is not restricted to species with morphological structures such as cluster roots and dauciform roots. Species in the Fabaceae also exude carboxylates; for example, *Cicer arietinum* (chickpea) releases malonate, and genetic variation in malonate concentrations in the rhizosheath is tightly correlated with the [Mn] in their mature leaves, offering a novel breeding tool (Pang et al. 2018). Some species dissolve poorly soluble phosphate at a faster rate than they take up Pi, leading to accumulation in the rhizosphere (Hinsinger 1998). Neighboring plants may profit from the capacity to release inorganic P from sparingly soluble sources; for example *Triticum aestivum* (wheat) grown with *Lupinus albus* (white lupin) benefits from P mobilized by the cluster roots of white lupin, and this also shows up by elevated levels of Mn in wheat leaves (Gardner and Boundy 1983).

Intercropping, *i.e.* growing at least two crop species on the same plot of land at the same time, often enhances plant productivity. *Zea mays* (maize) yields 43% more and *Vicia faba* (faba bean) yields 26% more when the species are intercropped on a low-P soil, instead of grown as a monoculture on the same soil (Table 9.5). Using permeable and impermeable root barriers, Li et al. (2007) showed that the positive effects on maize yield are accounted for by rhizosphere acidification by faba bean. The positive effect on faba bean is due to exploration of a different rooting depth. Phosphate-solubilizing effects may also benefit the following crop in a rotation (Table 9.5; Li et al. 2007). When *Zea mays* (maize) is grown in rotation with *Glycine max* (soybean) or *Vigna unguiculata* (cowpea) on acid soils of southern Cameroon, maize benefits from the P-solubilizing activity of P-efficient genotypes of soybean and cowpea as the preceding crop (Jemo et al. 2006). Similar effects are common in other cereal-legume rotations (Kamh et al. 2002; Doolette et al. 2019).

9.2.2.6 Changing the Chemistry in the Rhizosphere

Physiological processes in roots greatly affect the availability of several **micronutrients** in the

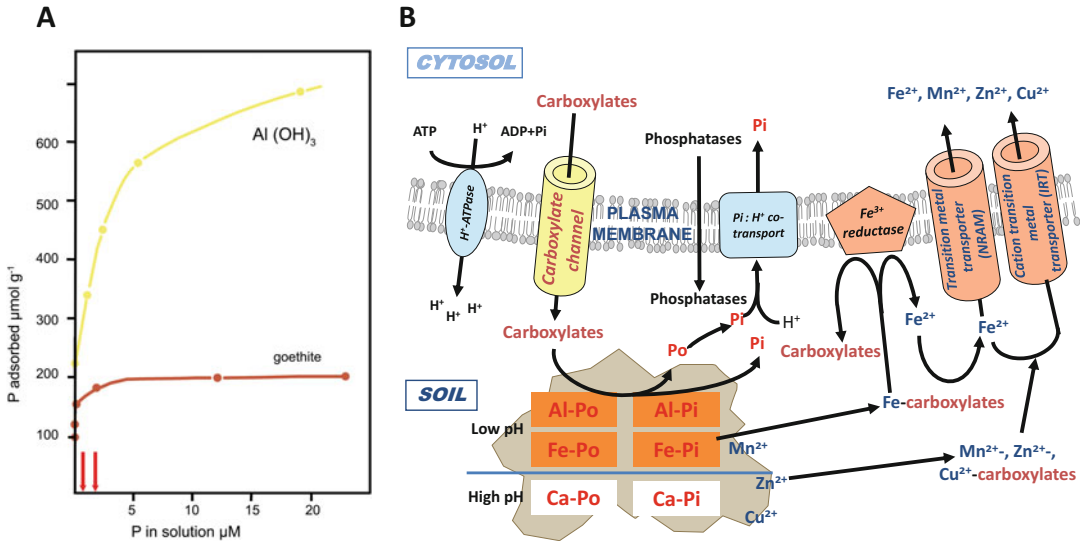

Fig. 9.13 (**A**) Inorganic phosphorus (Pi)-sorption isotherms on goethite (at pH 6.3) and $Al(OH)_3$ (at pH 5.8), using $Ca(H_2PO_4)_2$. Goethite is a common, iron-containing mineral in soil. $Al(OH)_3$ was used for the sake of comparison, since no reduction of the metal was possible. Note that Pi is 'not readily available' for *Lolium perenne* (perennial ryegrass) until about 40% of all the goethite is 'covered'. Pi availability then increases, reaching a maximum at 2 µM in solution, when 75% of the goethite is covered by sorbed Pi. Mycorrhizas increase the availability for ryegrass in the range 0.5–2 µM, marked by the red arrows, when 60–70% of the goethite surface is 'covered by sorbed Pi. Modified after Parfitt (1979). (**B**) Effects of carboxylates (and other exudates) on Pi and organic P (Po) mobilization in soil. Carboxylates are released via an anion channel. The exact way in which phosphatases are released is not known. Carboxylates mobilize Pi as well as Po, which both sorb to soil particles. Phosphatases hydrolyze organic P compounds, once these have been mobilized by carboxylates. Carboxylates will also mobilize some of the cations that bind P. Some of these cations, especially iron (Fe) and manganese (Mn) move to the root surface for uptake by the roots by a transporter that is used for Fe uptake, but also transports Mn (Lambers et al. 2015c).

Table 9.5 Average biomass and grain yield of *Zea mays* (maize) and *Vicia faba* (faba bean) grown in continuous monoculture, in a continuous intercropping system, or in a continuous rotational system for 4 years in a low-phosphorus, high-nitrogen soil in China.

	Crop	Cropping system	Average for 2003–2006 kg ha^{-1}	% Increase
Grain yield	Maize	Continuous monoculture	12,810	–
		Intercropped with faba bean	18,910	49
		Rotated with faba bean	17,360	37
	Faba bean	Monoculture	4290	–
		Intercropped with maize	5240	22
		Rotated with corm	5720	29
Aboveground biomass	Maize	Monoculture	26,920	–
		Intercropped with faba bean	39,990	49
		Rotated with faba bean	36,990	38
	Faba bean	monoculture	10,380	–
		Intercropped with maize	12,660	22
		Rotated with maize	13,000	21

Source: Li et al. (2007)

Table 9.6 The availability of a number of micronutrients, aluminum, and toxic metals for plants when the pH decreases, and the reason for the change in availability.

Microelement	Effect of decreased pH on availability of the microelement	Cause of the effect
Aluminum (Al)	Increase	Increased solubility
Boron (B)	Increase	Desorption
Cadmium Cd)	Increase	Increased solubility
Copper (Cu)	Increase	Desorption, increased solubility
Iron (Fe)	increase	Reduction, increased solubility
Lead (Pb)	Increase	Desorption
Manganese (Mn)	Increase	Increased solubility
Molybdenum (Mo)	Decrease	Decreased solubility
Zinc Zn)	Increase	Desorption, increased solubility

Source: Mengel et al. (2001); He et al. (2005); Kirkham (2006)

rhizosphere (Table 9.6). For example, **proton extrusion** by roots may reduce rhizosphere pH by more than two units from that in the bulk soil (Hinsinger et al. 2003); the capacity to affect the pH is strongest at a soil pH of 5–6. Roots also have the capacity to **reduce** compounds in the rhizosphere or at the plasma membrane which is particularly important for the acquisition of Fe, when available in its less mobile oxidized state in soil (Zanin et al. 2019). On the other hand, roots in flooded soils can **oxidize** compounds in the rhizosphere, largely by the release of oxygen (Sect. 9.3.5). This can reduce the solubility of potentially toxic ions like Fe^{2+} and S^{2-}. Roots often exude compounds that **mobilize** sparingly soluble micronutrients, or stimulate the activity of rhizosphere microorganisms, and therefore the mineralization of N and P.

9.2.2.6.1 Changing the Rhizosphere pH

The **source of N** used by the plant greatly affects the pH in the rhizosphere, because N is the nutrient required in largest quantities by plants and can be absorbed as either a cation (NH_4^+) or an anion (NO_3^-). Roots must remain electrically neutral, so when plants absorb more cations than anions, as when **NH_4^+** is the major N source, more **protons** are extruded (reducing rhizosphere pH) than when **NO_3^-** is the major N source, in which case the pH tends to rise slightly. An additional cause of the decline in rhizosphere pH when NH_4^+ is the source of N is that, for each N that is incorporated into amino acids, one H^+ is produced. Because NH_4^+ is assimilated exclusively in the roots, whereas NO_3^- is assimilated partly in the roots and partly in the leaves, the production of H^+ is greatest with NH_4^+. A somewhat smaller decrease in pH also occurs when atmospheric N_2 is the sole source of N for legumes or other **N_2-fixing** plants (Sect. 12.3). The drop in pH with NH_4^+ as N source is due to exchange of NH_4^+ for H^+ (or uptake of NH_3, leaving H^+ behind). The rise in pH with NO_3^- as the source of N is associated with the generation of hydroxyl ions during its reduction according to the overall equation: $NO_3^- + 8\ e^- + 1.5\ H_2O \rightarrow NH_3 + 3\ OH^-$. A more comprehensive analysis, however, which also accounts for primary transport at the plasma membrane and N metabolism subsequent to NO_3^- reduction shows that NO_3^- entry does not raise the pH intracellularly (Britto and Kronzucker 2005). To compensate for an increase in pH associated with NO_3^- accumulation, protons are taken up; some hydroxyl ions are neutralized by the formation of organic acids (mainly malic acid) from neutral sugars. As a result, plants growing with NO_3^- contain more organic acids (mainly malate) than those using NH_4^+ or N_2.

Application of ammonium or urea as fertilizers can create major agricultural problems, since both the pH in the rhizosphere and that of the bulk soil will decline in the longer term. This may mobilize potentially toxic ions, including Al and Mn, and reduce the availability of required nutrients such as Mo (Fig. 9.1B and Sect. 9.3.1).

Rhizosphere pH affects the availability of both soil micronutrients and potentially toxic elements

that are not required for plant growth (Al) (Table 9.6). The solubility of Fe decreases a thousand-fold for each unit increase in soil pH in the range 4–9; that of Mn, Cu, and Zn decreases a hundred-fold. Manganese and Fe also become more available when they are reduced (to Mn^{2+} and Fe^{2+}, respectively). Although Fe is abundant in the Earth's crust, it predominates as Fe^{3+} precipitates, which are largely unavailable to plants, especially at neutral or alkaline pH (Fig. 9.1B). **Iron-deficiency** symptoms in calcareous soils can be prevented by supplying NH_4^+, which acidifies the rhizosphere, rather than NO_3^-, which tends to further increase the pH around the roots; however, this is only effective in the presence of nitrification inhibitors that prevent the microbial transformation of NH_4^+ to NO_3^-.

The availability of molybdenum (Mo) decreases with decreasing soil pH, whereas that of Fe, Mn (up to a point), and Zn declines (Fig. 9.1B), and that of Cu, which tends to be complexed in the soil, is unaffected by pH. As a result, when grown in soil with $(NH_4)_2SO_4$, the concentrations of Fe, Mn, and Zn are higher in plant biomass than those in plants grown with Ca $(NO_3)_2$ (Table 9.6).

Plants can strongly reduce rhizosphere pH by exuding organic acids (Sect. 9.2.2.6) or by excreting protons, which occurs when the uptake of major cations (*e.g.*, K^+) exceeds that of anions (Hinsinger et al. 2003). In calcareous soils, H^+ excretion occurs to an extent that bulk soil pH is lowered. Some nutrient deficiencies cause plants to reduce the **rhizosphere pH**. When the Fe supply is insufficient, *Helianthus annuus* (sunflower) plants lower the pH of the root solution from approximately 7–4. Similar responses occur in *Zea mays* (maize) and *Glycine max* (soybean) genotypes with a low susceptibility to Fe-deficiency ('lime-induced chlorosis'). Iron deficiency-induced acidification of the rhizosphere is mediated by a proton-pumping ATPase at the plasma membrane, with cations being exchanged for H^+ (Fig. 9.14). Zinc deficiency can also cause a decrease of the rhizosphere pH (Cakmak and Marschner 1990). Organic acid-mediated dissolution of Fe plays a significant role in elevating the concentration of Fe-complexes in the rhizosphere, especially when Fe occurs as $Fe(OH)_3$, but less so when it is present as Fe-oxides (Fe_2O_3 and Fe_3O_4) (Jones et al. 1996).

Lowering the pH in response to Fe deficiency may coincide with an increased capacity to reduce Fe at the root surface, due to the activity of a specific **Fe reductase** in the plasma membrane (Schmidt 2003). Reducing and chelating

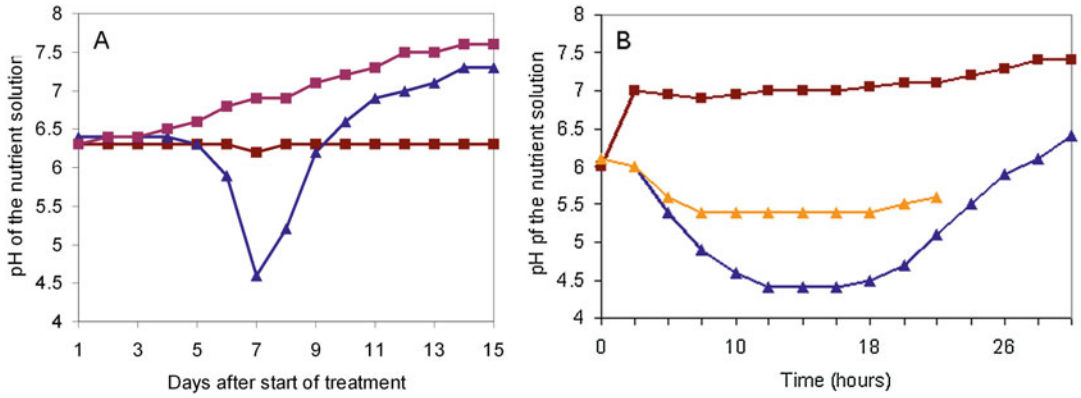

Fig. 9.14 Changes in pH in the root environment of *Cicer arietinum* (chickpea) as affected by iron (Fe) supply. (**A**) Effects of the absence of Fe in the absence (blue triangles) and presence (dark-brown squared) of an organic buffer (MES, 4-morpholineethanesulfonic acid) on the acidification of the nutrient solution. Plants grown with Fe are shown with purple squares. (**B**) Effects of an inhibitor (yellow triangles) of the plasma membrane ATPase (vanadate) on the acidification of the nutrient solution in the absence of Fe. Plants grown with Fe are shown with dark-brown squares (Ohwaki and Sugahara 1997); copyright © 1997, Kluwer Academic Publishers.

compounds (phenolics) may be excreted, solubilizing and reducing Fe^{3+} (Ma 2005). This is the typical response of Fe-efficient dicots and monocots other than grasses ('strategy I' in Fig. 9.16). Exudation of reducing and chelating compounds also enhances the availability and uptake of Mn. In calcareous soils with a low concentration of Fe and a high concentration of Mn, this strategy may lead to Mn toxicity. When the buffering capacity of the soil is large and the pH is high, 'strategy I' is not effective.

Addition of Si, supplied in the form of the bioavailable monosilicic acid, ameliorates Fe-deficiency symptoms in *Cucumis sativus* (cucumber) and suppresses expression of genes that are upregulated in Fe-starved plants (Fig. 9.17). Silicon-treated plants accumulate more root apoplastic Fe, which rapidly decreases when Fe is withheld. Under Fe-deficient conditions, Si also increases the accumulation of Fe-mobilizing compounds in roots, and stimulates root activity of Fe acquisition at the early stage of Fe deficiency stress through regulation of gene expression levels of proteins involved in Fe acquisition (Pavlovic et al. 2013). Silicon is now widely acknowledged as a '**beneficial element**', rather than an essential nutrient (Broadley et al. 2012).

9.2.2.6.2 Exudation of Organic Chelates

Grasses exude very effective chelating compounds, particularly when Fe or Zn are in short supply. These chelators are called **phytosiderophores** ('plant iron carriers', from Greek), because of their role in the acquisition of Fe (Zanin et al. 2017). However, these chelators are also important for the uptake of metals like Zn, when these are in short supply (Cakmak et al. 1996). Phytosiderophores are similar to nicotianamine (Fig. 9.15), which itself is also an effective chelator that plays a role in long-distance Fe-deficiency signaling (Kumar et al. 2017). Phytosiderophores are specific for each species and are more effective in chelating Fe than are many synthetic chelators used in nutrient solutions. They also form stable chelates with Cu, Zn, and, to a lesser extent, Mn, and enhance the availability of these nutrients in calcareous soils. Iron-efficient species belonging to strategy I or II show an enhanced capacity to absorb Fe upon withdrawal of Fe from the nutrient solution (Fig. 9.16).

The release of deoxymugineic acid, the primary phytosiderophore in *Oryza sativa* (rice) and *Hordeum vulgare* (barley), involves phytosiderophore efflux transporters (Nozoye et al. 2011). Under conditions of Fe deficiency, rice and barley roots express high levels of these transporters, and overexpression of the genes encoding them increases tolerance to Fe deficiency. In soil, Fe diffuses in the form of a Fe-phytosiderophore complex to the root surface, and is absorbed as such by root cells ('strategy II'; Fig. 9.16). The system responsible for uptake of the Fe-chelate is induced by **Fe deficiency**. In strategy II plants, Fe reduction takes place after uptake into the root cells, rather than prior to uptake as in strategy I. The amount of phytosiderophore secretion accounts for the level of tolerance of a plant to Fe deficiency; it follows the order: *Hordeum vulgare* (barley)/*Triticum aestivum* (wheat) > *Avena sativa* (oat)/*Secale cereale* (rye) > *Zea mays* (maize)/*Sorghum bicolor* (sorghum) > *Oryza sativa* (rice) (Marschner et al. 1986; Kawai et al. 1988). Genotypes of wheat [*Triticum aestivum* (bread wheat) and *Triticum durum* (durum wheat)] that are more resistant to Zn deficiency exude more phytosiderophores than do more sensitive genotypes (Cakmak et al. 1996).

Phytosiderophores that are exuded by Fe-efficient grasses can also enhance the Fe status of some Fe-inefficient dicotyledonous neighboring plants, both in nutrient solution and in pot experiments. This mechanism offers an explanation for the success of **intercropping** *Arachis hypogaea* (peanut) with *Zea mays* (maize) in northern China (Zuo et al. 2000) and for the re-greening of fruit trees when grown in combination with *Festuca rubra* (red fescue) (Ma et al. 2003). In alkaline soil, the Fe in the Fe-phytosiderophore complex in the rhizosphere of maize is likely acquired by neighboring peanut plants in intercropping systems (Xiong et al. 2013).

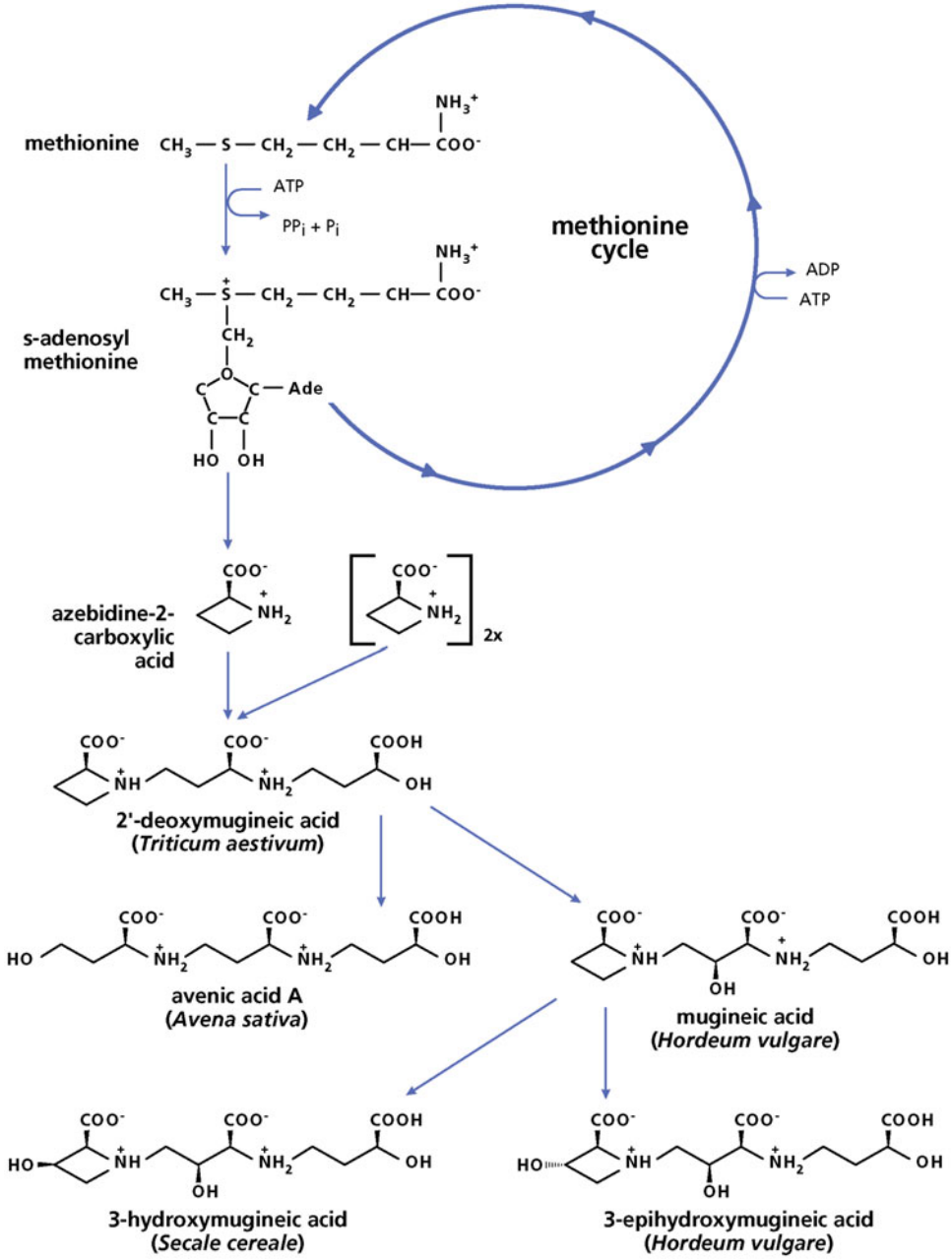

Fig. 9.15 Scheme for the biosynthesis of phytosiderophores, which are hydroxy- and amino-substituted imino-carboxylic acids exuded by graminaceous monocotyledonous plants (Ueno et al. 2007); copyright Trustees of The New Phytologist.

Carboxylates are a common component of root exudates. Roots exude them in response to a shortage of P, Fe, or K (Jones 1998; Vengavasi and Pandey 2018). Depending on the dissociation properties and number of carboxylic groups, carboxylates can carry varying negative charges,

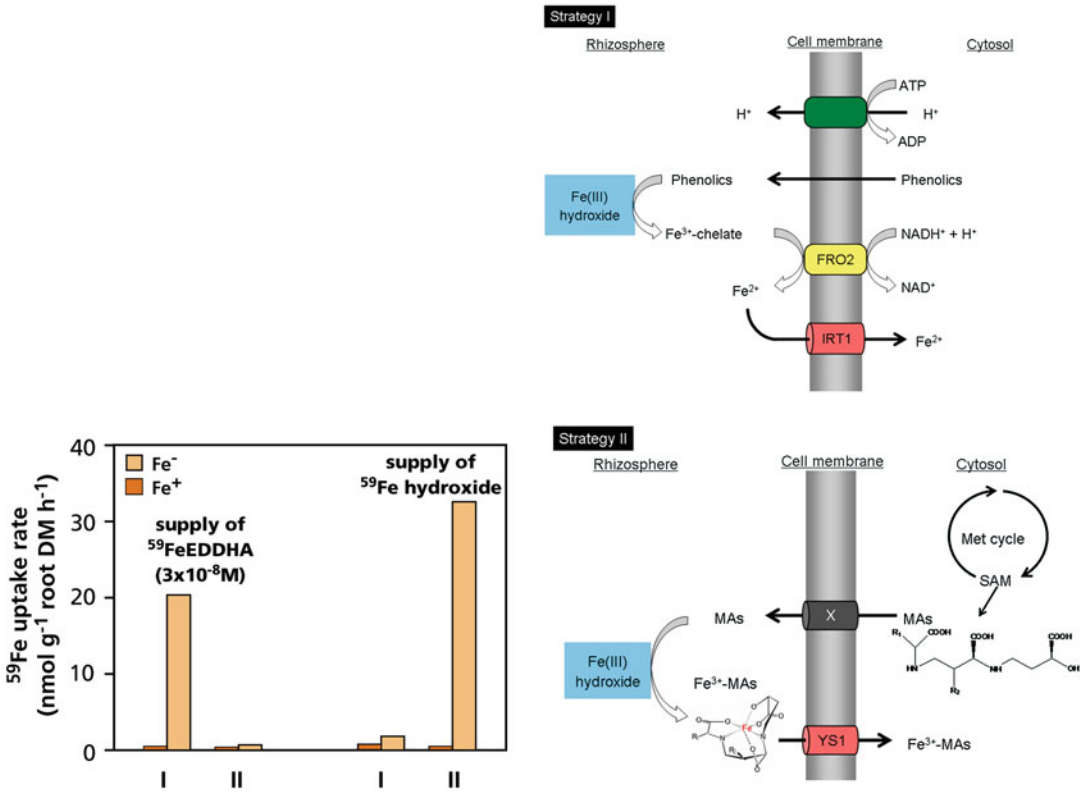

Fig. 9.16 (**A**) The response to iron (Fe) deficiency of species following two contrasting 'strategies'. Strategy II is restricted to grasses. Strategy I is found in dicots and monocots, except grasses. Plants are grown with or without Fe and then supplied with ^{59}FeEDDHA or ^{59}Fe hydroxide (Römheld 1987); © Scandinavian Plant Physiology Society. (**B**) Induction of the capacity to absorb Fe as affected by Fe-deficiency in dicotyledonous and nongraminaceous dicotyledonous species (strategy I) and in grasses (strategy II) (Ma 2005).

thereby allowing the complexation of metal cations in solution and the displacement of anions from the soil matrix. For this reason, carboxylates play a role in many soil processes, including the mobilization and acquisition of nutrients by plants (*e.g.*, Pi and Fe) and the detoxification of metals (*e.g.*, Al, Pb), microbial proliferation in the rhizosphere, and the dissolution of soil minerals, leading to **pedogenesis** (*e.g.*, podzolization) (Fujii et al. 2013). Organic acids transform high-molecular-mass humus compounds into smaller ones (molecular mass less than 10,000). Upon transformation of the humus complex, Ca, Mg, Fe, and Zn are released from the humus complex. In this process, organic acids are more effective than their K^+-salts or inorganic acids; their action is likely a combination of acidification and chelation (Albuzio and Ferrari 1989).

9.2.2.7 Rhizosphere Mineralization

Root exudation of organic acids, carbohydrates, and amino acids, and the sloughing of polysaccharides from growing root tips usually accounts for less than 5% of total carbon assimilation. It may be substantially more when P availability is low (Table 3.1), especially in plants that produce specialized carboxylate-releasing structures (Lambers et al. 2006). Root exudates may have major effects on soil microbial processes, which are often carbon-limited

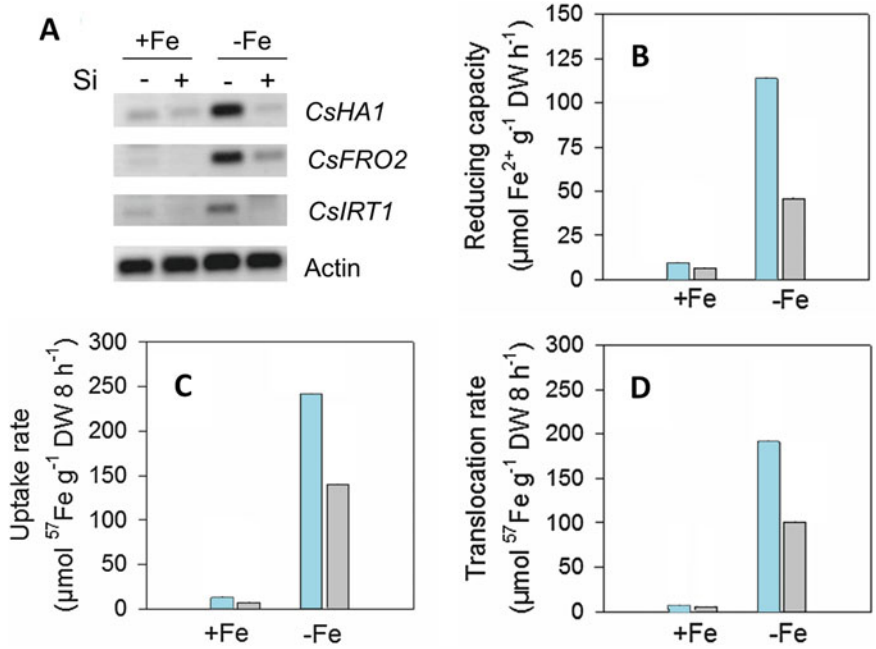

Fig. 9.17 The effect of iron (Fe) and silicon (Si) nutrition on the gene expression of proteins involved in Fe acquisition and the reduction-based uptake and translocation of Fe by *Cucumis sativus* (cucumber). (**A**) Expression of genes involved in Fe acquisition, *HA1*, *FRO2*, and *IRT1*; (**B**); Fe^{III} chelate-reducing capacity; (**C**) uptake and (**D**) root to shoot translocation of ^{57}Fe. Plants were grown in nutrient solution +Fe (50 µM) or -Fe, in the treatments without or with supply of 1.5 mM $Si(OH)_4$ for 7 days. Grey bars, -Si; blue bars, +Si. Amplification of actin is shown (**A**) as a control for equal template loading. Uptake solution contained 10 µM $^{57}Fe^{III}EDTA$ (Pavlovic et al. 2013); copyright Trustees of The New Phytologist.

(Chap. 18). The densities and activity of microorganisms, especially bacteria, and of microbial predators are much greater in the rhizosphere than they are in bulk soil, and they are enhanced by factors, such as elevated atmospheric CO_2 concentrations, that increase root exudation (Pausch and Kuzyakov 2018). The effects of root exudates depend on soil fertility (Sect. 18.3.2). In infertile soils, stimulation of root exudation by elevated atmospheric [CO_2] tends to increase N **immobilization** by rhizosphere microbes, and reduces plant N uptake (Díaz et al. 1993). By contrast, in fertile soils, where microbes are more carbon-limited, the stimulation of root exudation by elevated [CO_2] increases N **mineralization** and plant N uptake (Meier et al. 2017). Annual N uptake by vegetation is often twice the N mineralization estimated from incubation of soils in the absence of roots (Chapin et al. 1988). Much of this discrepancy could involve the more rapid nutrient cycling that occurs in the rhizosphere, as fueled by root exudation.

9.2.2.8 Root Proliferation in Nutrient-Rich Patches: Is It Adaptive?

When N, K, or P are limiting for plant growth and only available in localized root zones, roots tend to **proliferate** in these zones more than they do in microsites with low nutrient availability. Roots experiencing nutrient-rich patches can also enhance their physiological ion-uptake capacities compared with roots of the same plant outside the patch zone (Hodge 2004). Local proliferation,

however, is found only if the **elongating tip** of the axis from which the laterals emerge has experienced these favorable local conditions while elongating. If it has not, or if the plant as a whole does not experience nutrient deficiency, then no laterals emerge in favorable zones (Drew 1975). Local root proliferation occurs similarly in species from nutrient-rich [*Holcus lanatus* (common velvetgrass), *Lolium perenne* (perennial ryegrass)] and nutrient-poor habitats [*Anthoxanthum odoratum* (sweet vernalgrass), *Festuca rubra* (red fescue)] (Fransen et al. 1999).

It would seem that the proliferation of roots in response to a localized nutrient supply is functional, but is it really? When *Triticum aestivum* (wheat) plants are grown with a localized ^{15}N-labeled organic residue in soil, rates of N uptake per unit root length greatly increase during growth through the localized source of N. Plants obtain only 8% of the N that they ultimately absorb during the first 5 days of exploitation of the localized source. Only after this initial absorption do the roots proliferate in the residue; over the next 7 days, they absorb 63% of the total N obtained from the local source. After that time, massive proliferation occurs in the residue, but relatively little further N is captured (Fig. 9.18). This shows that local proliferation is of only limited importance for the capture of the N released from locally decomposing organic matter. When plants are competing for nutrients, however, local proliferation is advantageous. For example when perennial ryegrass grows together with *Poa pratensis* (smooth meadowgrass), perennial ryegrass produces greater root densities in the patch than does smooth meadowgrass, and it also captures more N from the patch (Hodge et al. 1999). Proliferation, triggered by the local source of N, might also be advantageous in the longer term to take up nutrients other than N, especially less mobile nutrients such as P.

The extent of the response to a localized supply depends on the overall nutrient status of the plant. Thus, if one half of the roots receives no nutrients at all, then the response is considerably stronger than if that half is supplied with a moderate amount

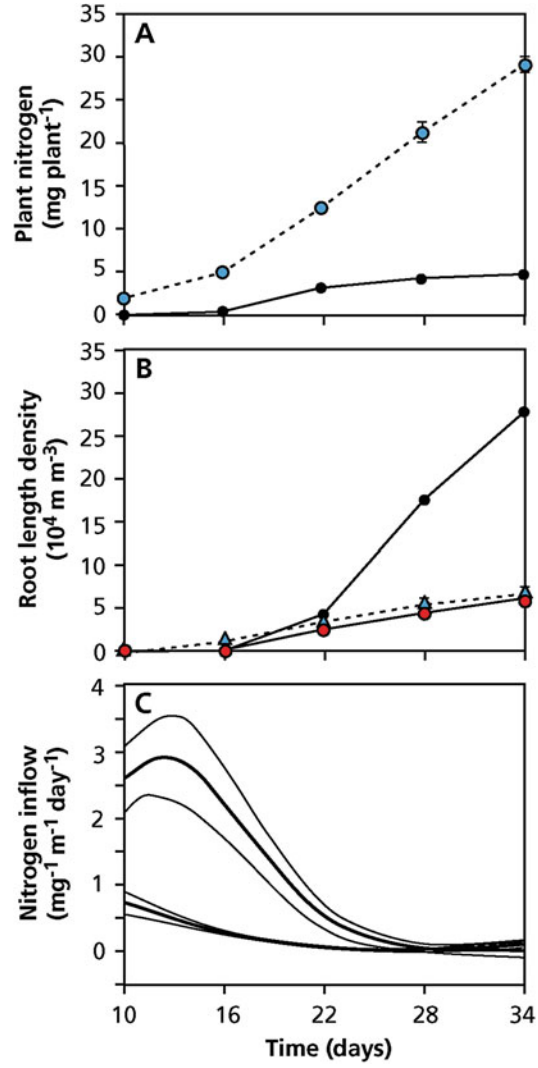

Fig. 9.18 The response of *Triticum aestivum* to a localized organic residue, enriched with a stable isotope of nitrogen (^{15}N). (**A**) Total amount of N in the plant (blue symbols) and N in the plant derived from the organic residue (black symbols); (**B**) Total root length density in the residue (black symbols) and in the soil above (blue triangles) and below (red triangles) the residue; (**C**) N uptake for the whole root system (lower curve) and for the part of the roots that proliferated in the localized residue (upper curve) (Van Vuuren et al. 1996).

(Table 9.7; Robinson 1996). The development of an individual root obviously depends both on the nutrient availability in its own environment and on other roots of the same plant.

Table 9.7 Root development of *Pisum sativum* (garden pea) in a split-root design, in which root halves were grown in different pots and supplied with different nutrient concentrations from the time they were 24 mm long*.

Nutrient strength pot 1–pot 2	Root dry mass (mg)			Ratio pot 1/pot 2	Shoot dry mass (mg)
	pot 1	pot 2	Total		
0–50	51	450	501	0.11	806
1–50	60	427	487	0.14	847
10–50	142	370	512	0.38	874
25–50	194	269	463	0.72	935
50–50	300	283	582	1.05	1032
10–0	225	61	286	3.77	463
25–0	343	52	394	6.76	670

Source: Gersani and Sachs (1992)
*Plants were harvested when they were 3 weeks old

9.2.3 Sensitivity Analysis of Parameters Involved in Pi Acquisition

The contribution of different parameters involved in the uptake of Pi can be assessed using **simulation models**. Such models are valuable to analyze ecophysiological problems. Nye and co-workers (Bhat and Nye 1973; Tinker and Nye 2000) analyzed the significance of root hairs using an experimental and a mathematical approach. They measured the (labeled) Pi concentration at the root surface of a *Brassica napus* (oil seed) root with dense root hairs. In addition, they simulated the Pi concentration under one of the following two assumptions: (1) root hairs are not involved in Pi uptake, and (2) root hairs effectively increase the cylinder intercepted by the root. There was good agreement between the simulated and the experimental data, only when they assumed that **root hairs** are effective (Fig. 9.19A). This work corroborated earlier ideas on the significance of root hairs for the acquisition of immobile ions, including Pi (Table 9.4).

Barber and co-workers (Silberbush and Barber 1983; Barber 1995) analyzed the sensitivity of Pi uptake by pot-grown *Glycine max* (soybean) plants to various soil and root factors (Fig. 9.19B). The simulated uptake agreed well with their experimental results. Their results show that Pi uptake is much more responsive to changes in the rate of **root elongation** (k in Fig. 9.19B) and **root diameter** (r_o) than to changes in **kinetic properties** of the uptake system: K_m, I_{max}, and C_{min}. Soil factors such as **diffusion coefficient** (D_e) and **buffer power** (b) have greater effects if their values are decreased than if they are increased. **Transpiration** (v_o) has no effect at all on the rate of Pi uptake. In infertile soils with a very low P-buffering capacity, transpiration may play a more important role (Huang et al. 2017). The spacing between roots (r_i) was such that there was no inter-root competition; hence, changes in the value for this parameter have no effect. For a relatively immobile nutrient such as Pi, kinetic parameters are considerably less important than are root traits such as the rate of elongation and root diameter. This is consistent with the generalization that diffusion to the root surface, rather than uptake kinetics, is the major factor determining Pi acquisition. For more mobile ions, such as NO_3^-, kinetic properties play a more important role (Kirk and Kronzucker 2005). This example illustrates how simulation models can help to elegantly explore our intuitive ideas, if they are used in combination with experimental approaches.

9.3 Nutrient Acquisition from 'Toxic' or 'Extreme' Soils

The term *toxic* or *extreme* soil is clearly anthropomorphic. For example, a soil of a rather high or low pH may be toxic for some species, but a favorable habitat for others. Similarly, the presence of high concentrations of what we used to

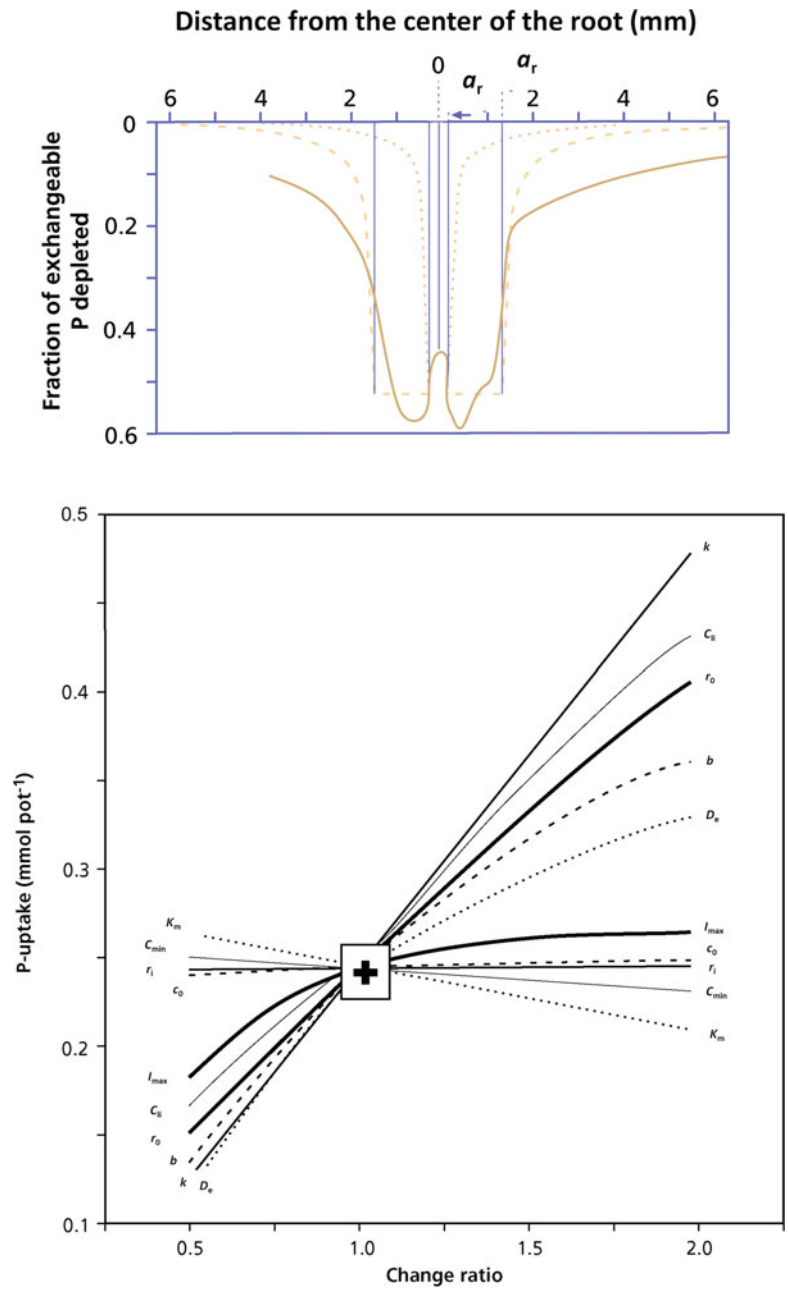

Fig. 9.19 Examples of modeling to gain insight into the significance of specific plant and soil characteristics involved in phosphorus (P) acquisition. (Top) Calculated and measured P-concentration profiles around a *Brassica napus* (oil seed) root. Phosphorus profiles are calculated under the assumption that root hairs do (ii, outer broken lines) or do not (i, inner broken lines) play a role in P uptake. The solid line gives the experimentally determined profile. The radii given are the radius of the root axis only (a_r) and that of the root plus root hairs (a_e) (Bhat and Nye 1973; Nye and Tinker 1977); copyright © 1973, Martinus Nijhoff Publishers. (Bottom) Effects of changing parameter values (from 0.5 to 2.0 times the standard value) on simulated inorganic P (Pi) uptake by roots of *Glycine max* (soybean). k is the rate of root elongation, C_{li} is the initial P concentration in solution, r_o is the root diameter, b is the buffer power of the soil, D_e is the diffusion coefficient of Pi in the soil, I_{max} is the maximum Pi inflow rate, v_o is the rate of transpiration, r_i is the spacing between individual roots, C_{min} is the lowest concentration at which Pi uptake is possible, and K_m is the Pi concentration at which the rate of Pi uptake is half of that of I_{max} (Silberbush and Barber 1983); copyright © 1983, Martinus Nijhoff/Dr W. Junk Publishers.

call 'heavy metals' may prevent the establishment of one species, but allow completion of the life cycle of another. As pointed out in Sect. 9.1, the occurrence of species at sites that we tend to call 'toxic' does not necessarily mean that adapted plants grow better in such sites. We use terms like **halophytes** and **calcicoles** to refer to the **ecological amplitude** of the species. The **physiological amplitude** of a species is usually much broader than its ecological amplitude (Sect. 1.3). The restriction of a species to extreme soils might indicate that adapted plants are the only ones that can survive in these soils, due to their specialized mechanisms, and that they are outcompeted on soils that we consider less extreme (Sect. 1.3).

The following Sections discuss specialized plant traits associated with phenotypic **acclimation** and genotypic **adaptation** to extreme soils and their consequences for species distribution.

9.3.1 Acid Soils

Soils may be acid because of the nature of their **parent material** (Turner et al. 2018b), but they also naturally tend to become acid with increasing age (Richardson et al. 2004; Turner et al. 2018a), because of several processes:

1. **Decomposition of minerals** by weathering, followed by leaching of cations, such as K^+, Ca^{2+}, and Mg^{2+} by rain. This is particularly important in humid regions.
2. **Production of acids** in soils (*e.g.*, due to hydration and dissociation of CO_2, formation of organic acids, oxidation of sulfide to sulfuric acid, and nitrification of ammonia).
3. Plant-induced production of acidity, when plants take up an **excess of cations** over anions (*e.g.*, when they use N_2 or NH_4^+, rather than NO_3^-, as N source).

Soils may also acidify due to human activities such as growing legumes (Bolan et al. 1991), input of nitric and sulfuric acids from 'acid rain' (Driscoll et al. 2001), the use of acidifying fertilizer, such as ammonium sulfate or urea (Schroder et al. 2011), or effects of acidic mine tailings (Johnson and Hallberg 2005).

Soil acidity modifies the availability of many mineral nutrients (Fig. 9.1) as well as the solubility of Al. Although a **low soil pH** *per se* may limit the growth of plants (Kidd and Proctor 2001), **Al toxicity** is a major yield-limiting factor in many acid soils, especially in the tropics and subtropics (Kochian et al. 2015). In acid soils, concentrations of Mn may also increase to toxic levels (Foy et al. 1978), generally at a somewhat higher pH than that which causes Al toxicity. Phosphorus Ca, Mg, K, and Mo availability may decline to an extent that deficiency symptoms arise (Table 9.6 in Sect. 9.2.2.6).

9.3.1.1 Aluminum Toxicity

Aluminum is one of the most abundant metals in the Earth's crust and the third most abundant element. Like all trivalent cations, it is toxic to plants. Aluminum hydrolyzes in solution, such that the trivalent cation dominates at **low pH** (Fig. 9.20). In addition, at low pH Al is released from chelating compounds (Ma et al. 2001b). Many species have a distinct preference for a soil with a particular pH. **Calcifuge** ('chalk-escaping'; also called 'acidophilous', acid-loving) species resist higher levels of soluble Al^{3+} in the root environment. There are several potential sites for injury due to Al (Fig. 9.21; Kopittke 2016):

1. the cell wall
2. the plasma membrane
3. signal-transduction pathways
4. the root cytoskeleton
5. DNA/nuclei

The **root apex** is the most sensitive region for Al toxicity. Inhibition of root elongation is the primary Al-toxicity symptom (Ryan et al. 1993; Kopittke 2016). Inhibition of root elongation in the root tip is due to interference with the formation of **cell walls**, decreasing cell-wall elasticity by cross-linking with pectin (Ma et al. 2005). Root cells become shorter and wider. As a consequence, root elongation is impaired, and the roots have a 'stubby' appearance (Fig. 9.22, top) and a

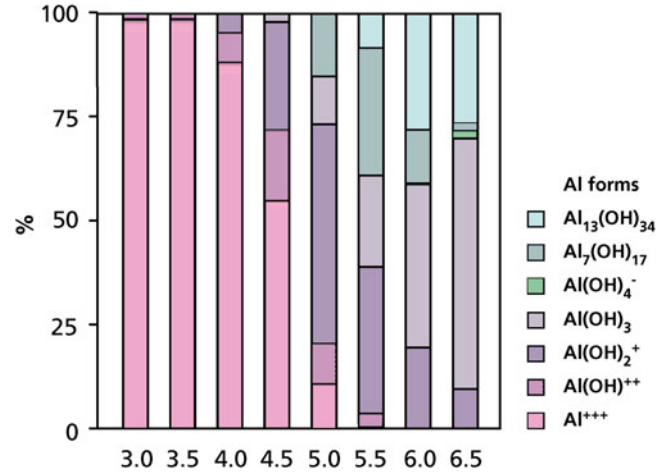

Fig. 9.20 Calculated distribution of total inorganic aluminum (Al) concentration over various monomeric and polymeric forms as a function of pH. Calculations are based on parameters given by Nair and Prenzel (1978).

low specific root length, when grown in the presence of Al (Table 9.8; Delhaize and Ryan 1995).

Important toxic effects of Al occur at the **plasma membrane**. These are partly due to the inhibition of the uptake of Ca and Mg (Table 9.9), due to blockage of ion channels in the plasma membrane (Kochian et al. 2015). Some of the symptoms of Al toxicity are very similar to those of a deficiency of other ions. This may be due to competition for the same site in the cell walls (some cations), precipitation of Al complexes (with Pi), or inhibition of root elongation, which reduces the absorption capacity (Kochian et al. 2005; Kopittke 2016). Inhibition by Al of the uptake of Ca and Mg decreases the concentration of these cations in the cell, causing deficiency symptoms. Calcium is required during cell division for spindle formation and to initiate metaphase/anaphase transition. Hence, the presence of Al prevents cell division and root development (Kochian et al. 2005). Interference with Mg uptake causes Mg-deficiency symptoms (*i.e.* chlorotic leaves with brown spots), and stubby discolored roots (Keltjens and Tan 1993).

Some Al is rapidly taken up in the symplast, possibly via systems whose function is to take up Mg or Fe, or via endocytosis. In the cytosol, with a neutral pH, it is no longer soluble, and the Al^{3+} concentration is less than 10^{-1} M (Kochian et al. 2004), due to the formation of nontoxic forms of Al, *e.g.*, $Al(OH)_3$. Because of the very high affinity of Al for proteins and P-containing compounds, including ATP, phospholipids, and **DNA**, even very low Al concentrations are potentially phytotoxic (Ma 2005). Most of these effects occur *after* the very rapid (1–2 h) inhibition of root elongation. They are, therefore, not the primary cause of inhibition of plant growth.

Leaf disorders (*e.g.*, Fe deficiency symptoms) occur several days after exposure to Al. In *Triticum aestivum*, which exhibits Fe uptake according to strategy II (Sect. 9.2.2.6), Fe deficiency is due to inhibition of the biosynthesis and release of phytosiderophores (Chang et al. 1998).

9.3.1.2 Alleviation of the Toxicity Symptoms by Soil Amendment

Aluminum-toxicity symptoms can be diminished by addition of **Mg** (especially in **monocotyledons**) or **Ca** (especially in **dicotyledons**) (Keltjens and Tan 1993; Silva et al. 2001b). This pattern is consistent with the greater requirement for Ca in dicots (Sect. 9.4). Cation amelioration of Al toxicity is caused by a reduction of Al accumulation (Ryan et al. 1997). In *Glycine max* (soybean), adding 50 μM Mg to a nutrient solution containing toxic levels of Al increases exudation of citrate (which chelates Al) by the tap root tips, several-fold. This

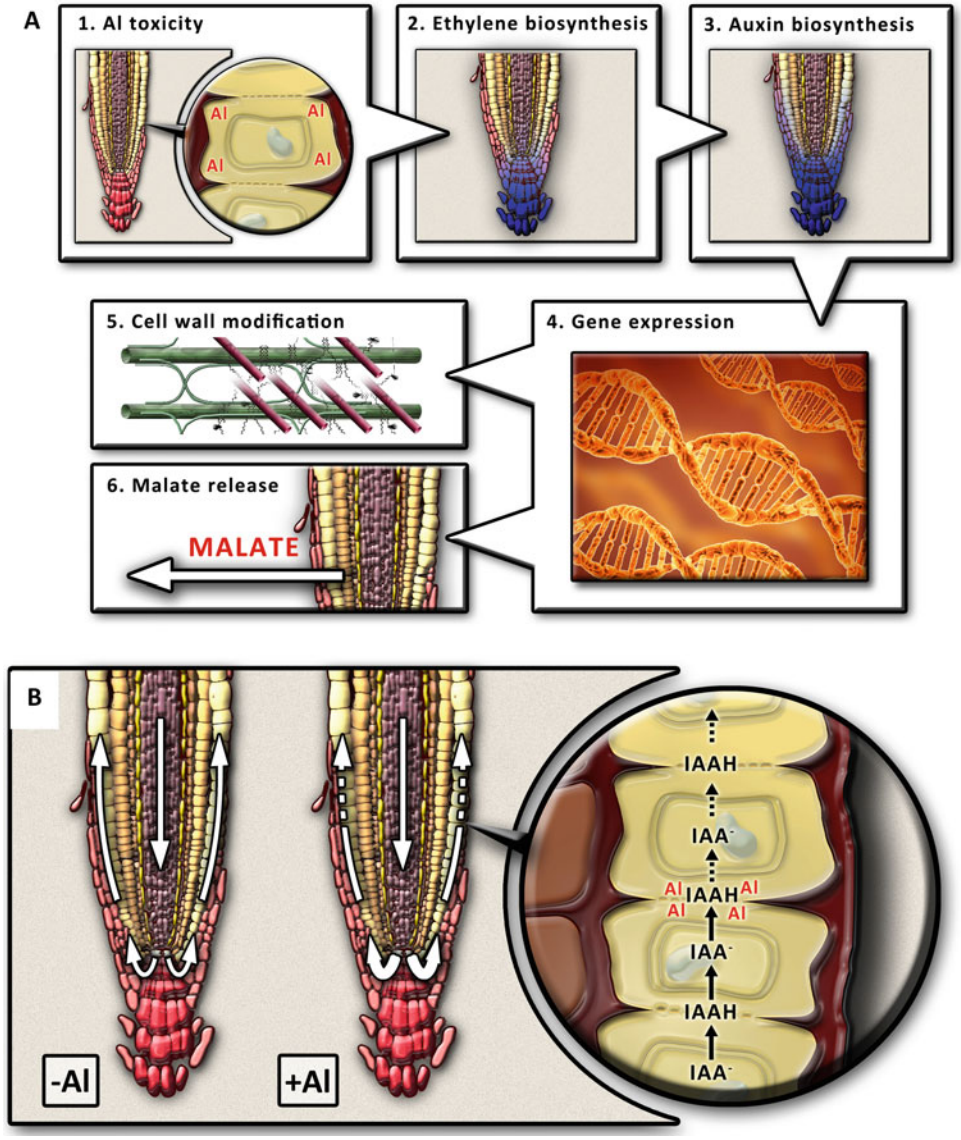

Fig. 9.21 (**A**) Proposed effect of aluminum (Al) on biosynthesis of ethylene and auxin and their subsequent effects. (1) Al is toxic, and rapidly reduces root elongation. (2) In response to the toxic effects of Al, there is a rapid burst of ethylene in the root quiescent center and root cap (indicated in blue). (3) This ethylene burst regulates an increase in auxin in the lateral root cap, rhizodermis, and transition zone (indicated in blue). (4) Increases in auxin biosynthesis influence gene expression, resulting in potential responses including (5) modification of the cell wall, and (6) the release of carboxylates, *e.g.*, malate to chelate and detoxify complexation Al. (**B**) Proposed model showing the inhibitory effect of Al on the basipetal transport of IAA (the main form of auxin) from the transition zone to the elongation zone, resulting in decreased anisotropic cell expansion and reduced root elongation. The white arrows on the left-hand diagram (-Al) indicate the polar and basipetal transport of auxin through the root apical tissues. The middle diagram shows the effects of Al on auxin, with the magnified diagram on the right showing the basipetal transport of auxin through the rhizodermis, with IAAH dominating in the acidic cell wall and IAA^- dominating in the cytoplasm. Note that Al decreases the basipetal transport of IAA (as indicated by the dotted arrows), possibly by binding strongly to the cell wall and decreasing apoplastic flow (Kopittke 2016); reprinted with permission of John Wiley & Sons, Inc.

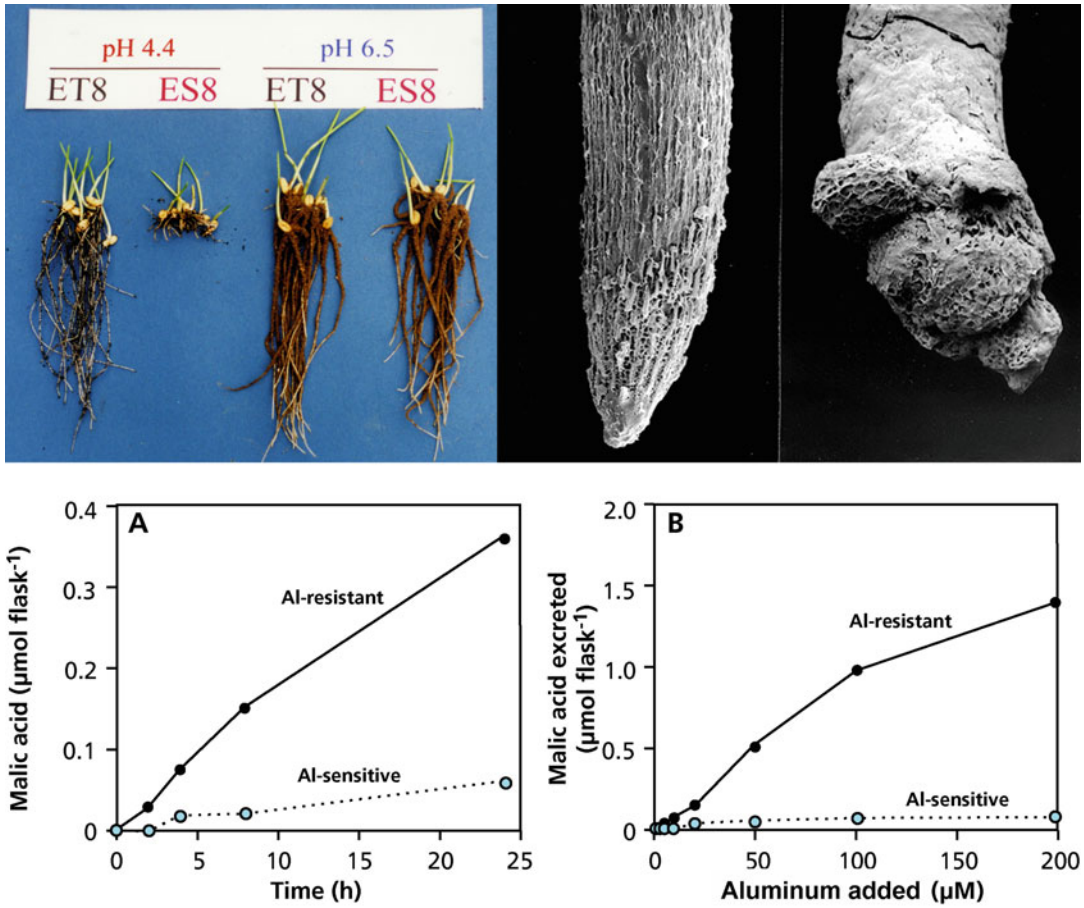

Fig. 9.22 (Top, left) Seedlings of an aluminum (Al)-sensitive (ES8, right) and a near-isogenic Al-resistant (ET8, left) line of *Triticum aestivum* (wheat) grown in soil at pH 6.5, where Al is harmless for roots, and at pH 4.4, where aluminum is toxic if not chelated (Ma 2000); copyright © 2000, Oxford University Press. (Top, right) Scanning electron micrograph of the root tips of the two near-isogenic lines shown in the top panel; the photo on the right shows a root tip of the Al-sensitive line, and the one on the left a root tip of the Al-resistant line. The seedlings were grown for 4 days in a solution containing 5 mM $AlCl_3$ in 200 mM $CaCl_2$ at pH 4.3 (Delhaize and Ryan 1995); copyright American Society of Plant Biologists. (Bottom) (**A**) Malate release from the roots of seedlings of an aluminum (Al)-resistant and an Al-sensitive genotype of *Triticum aestivum* (wheat) incubated in nutrient solution containing 50 mM Al. (**B**) Effect of Al concentration in the nutrient solution on malate release of the same genotypes as shown in (**A**) (after Delhaize et al. 1993); copyright American Society of Plant Biologists.

indicates that Mg alleviates Al toxicity due to increased production and exudation of citrate (Silva et al. 2001a). **Phosphate** addition also has a positive effect, because it precipitates Al, either outside or inside the roots.

The ability of high-molecular mass organic acids, such as **humic acid** and **fulvic acid**, to bind Al is well documented (Harper et al. 1995). These substances form much more stable complexes with Al than do citrate, malate, and oxalate, which are exuded by roots of Al-resistant plants (Sect. 9.3.1.3). Fulvic acid and humic acid are constituents of humus, peat, and leaf litter, which can be added to alleviate toxic effects of Al (Harper et al. 1995). Some of the symptoms of Al toxicity of *Pisum sativum* (pea) are relieved by the addition of B, which interacts with pectins in cell walls (Li et al. 2017).

9.3.1.3 Aluminum Resistance

Recent progress in several laboratories has set the stage for identification and characterization of the genes and associated physiological mechanisms that contribute to Al resistance in important crop species grown on acid soils. This provides the necessary molecular tools to address a major, worldwide agronomic problem (Kochian et al. 2005, 2015). Different mechanisms account for a plant's resistance to potentially toxic levels of Al:

1. Al exclusion from the root apex (avoidance)
2. Al tolerance

There is clear evidence for both **exclusion** mechanisms (Kochian et al. 2005) that confer Al resistance and for **internal detoxification** in species that accumulate Al, such as *Hydrangea macrophylla* (hydrangea), *Camellia sinensis* (tea), *Richeria grandis* (a tropical cloud-forest tree), and *Fagopyrum esculentum* (buckwheat) (Zheng et al. 1998; Ma 2005). Internal detoxification of Al in Al-accumulating species is probably based on binding of Al to **citrate** or **oxalate** in leaf cells (Zheng et al. 1998; Ma et al. 2001b).

Work on the Al-resistant *Fagopyrum esculentum* (buckwheat) and comparisons of resistant and sensitive genotypes of *Phaseolus vulgaris* (common bean), *Triticum aestivum* (bread wheat), and *Holcus lanatus* (common velvetgrass) highlights the importance of release of **carboxylates** (**citrate**, **malate**, and **oxalate**) by roots, especially by root tips (Fig. 9.22, bottom; Zheng et al. 1998; Klug and Horst 2010; Chen et al. 2013). In *Holcus lanatus*, the difference between resistant and sensitive ecotypes is due to the number of *cis*-acting elements for an Al-responsive transcription factor in the promoter region of the gene encoding release of malate (Chen et al. 2013). Some species, *e.g.*, *Lupinus albus* (white lupin) release carboxylates in response to both Al supply and P deficiency, but the response differs in the exact part of the root system from which the carboxylates are released (Wang et al. 2007).

In resistant *Triticum aestivum* (wheat) genotypes, Al activates a channel that allows the

Table 9.8 The effects of aluminum concentration on various root parameters of *Mucuna pruriens* (velvet bean)*.

$[Al^{3+}]$	DM	FM	D	L	SRL
mg L^{-1}	g	g	mm	m	m g^{-1}
0	6.4	126	0.37	1160	175
0.1	6.6	155	0.44	1100	166
0.2	6.6	126	0.46	931	141
0.4	3.3	55	0.51	253	76

Source: Hairiah et al. (1990)
Note: The increase in root dry mass was not statistically significant
**DM* dry mass, *FM* fresh mass, *D* diameter, *L* root length per plant, *SRL* specific root length (root length per gram dry mass of roots)

Table 9.9 Aluminum (Al), phosphorus (P), calcium (Ca), and magnesium (Mg) concentration [mmol (kg dry mass)$^{-1}$] in roots and shoot of *Sorghum bicolor* (sorghum), grown for 35 days at three levels of Al (zero, low: 0.4 mg L^{-1}, high 1.6 mg L^{-1}) and P [low, medium and high: 285, 570 and 1140 mmol plant^{-1} (35 days)$^{-1}$].

P-level	Al-level	Shoot				Root			
		Al	P	Ca	Mg	Al	P	Ca	Mg
Low	Zero	–	26	171	69	–	29	28	22
Medium	Zero	–	30	151	63	–	34	21	20
High	Zero	–	38	139	63	–	39	19	23
Low	Medium	1	27	127	36	7(29)	30	20	16
Medium	Medium	1	29	108	37	5(40)	34	18	16
High	Medium	1	40	85	36	5(40)	46	20	19
Low	High	1	93	61	23	11(36)	70	16	14
Medium	High	1	108	51	21	13(31)	76	15	15
High	High	1	335	65	25	131(45)	263	16	16

Source: Tan and Keltjens (1990)
*Values in brackets indicate the percentage removable with 0.05 M H_2SO_4 (*i.e.* the fraction in the apoplast)

exudation of malate (Delhaize et al. 2007). Transporters responsible for Al-activated release of carboxylates have been identified in several species (Kochian et al. 2015). Faster rates of exudation reflect faster rates of carboxylate synthesis, rather than higher concentrations in the root tips. The exudation of carboxylates is accompanied by K^+ efflux, so the positive effect of the chelator is not negated by lowering the pH. Mucilage exuded by the root cap may allow the malate concentration to remain sufficiently high over extended periods to protect the root tip (Delhaize and Ryan 1995). Microbial degradation of the malate released by the roots of Al-resistant plants could potentially limit the effectiveness of these compounds in sequestering Al, because the half-life of the released organic acids is less than 2 h. For rapidly growing roots (>15 mm day^{-1}), however, the residence time of the malate-releasing root tips in any zone of soil is around 5 h. Because root tips and their carbon release to the rhizosphere move quickly enough, the size of the microbial biomass in the rhizosphere of the root tip does not change much from the time the tip enters a zone. Electron microscopy and physiological studies confirm that there is little microbial proliferation at the root apex. Carboxylate release protects the root tip from the toxic effects of Al, despite some microbial breakdown of malate in the rhizosphere (Jones et al. 1996).

At a high pH, calcifuge species typically show **Fe-deficiency** symptoms (**lime chlorosis**) (Hutchinson 1967), whereas their root growth may be stimulated by low Al concentrations (Pegtel 1987). This growth-enhancing effect of Al is most pronounced at low pH (high H^+ concentration). It is associated with the alleviation of the toxic effects of high H^+ concentrations which is a general effect of cations; trivalent cations have the strongest effect, followed by divalent and then monovalent ones (Kinraide 1993). The growth of Al-sensitive accessions of crop plants, *e.g.*, *Oryza sativa* (rice) and *Triticum aestivum* (wheat) (Foy et al. 1978), and *Betula pendula* (silver birch) (Kidd and Proctor 2000) is also stimulated by Al, but the optimum Al concentration is much lower than that of Al-resistant accessions.

9.3.2 Calcium-Rich Soils

Calcareous soils have a **high pH** and a **high Ca concentrations**, and are rich in (bi)carbonate, and thus have a **high buffering capacity**. However, not all calcium-rich soils are calcareous and alkaline.

Calcifuge ('chalk-escaping') species have a distinct preference for soils with low pH. They tend to have a very low ability to solubilize the **Pi**, **Fe**, and **Zn** in calcareous soil, but resist higher levels of soluble Al^{3+} in the root environment (Sect. 9.3.1); NO_3^- availability will be low, and NH_4^+ will be a more important source of N (Sect. 9.2.1.2). Carbonate-rich soils may contain high levels of Fe, and this may arrive at the root surface, but calcifuge species are unable to acquire sufficient Fe to sustain rapid growth. The lack of a high capacity to utilize the forms of Fe, Zn, and other trace elements that prevail in alkaline soils (Sect. 9.2.2.6) leads to '**lime chlorosis**', and is a major cause of failure of establishment of calcifuge species in such soils. Some calcifuge plants [*e.g.*, *Carex pilulifera* (pill sedge)] are unable to translocate sufficient Fe to their leaves when grown in calcareous soil; Fe may accumulate in or precipitate on their roots. Others [*e.g.*, *Veronica officinalis* (heath speedwell)] may increase the amount of Fe they transport to their leaves, but accumulate this Fe in a form that is not metabolically active (Table 9.10; Zohlen and Tyler 1997, 2000). In addition, calcifuges tend to lack the capacity to access the prevalent poorly soluble P sources in alkaline substrates (Sect. 9.2.2.5). **Calcifuges** have very low leaf **P** concentrations to support physiological functions, and consequently display low biomass production, when grown in calcareous soil (Zohlen and Tyler 2004; Ding et al. 2019).

Some **calcifuge** species are very sensitive to a high supply of Ca, *e.g.*, *Juncus squarrosus* (heath rush) and *Nardus stricta* (matgrass) (Jefferies and Willis 1964), showing that it is not only soil pH that determines the distribution of calcifuge species. A special case is that of **Ca-enhanced P sensitivity** in Proteaceae species whose growth is inhibited at an elevated P availability (Grundon 1972; Hayes et al. 2019b). In such species, Ca

Table 9.10 Total, 'metabolically active', and 'HCl-soluble' iron (Fe) in freshly sampled leaf tissue of two calcifuge species, grown in acid silicate soil, calcareous soil, and calcareous soil amended with calcium phosphate*.

Species	Soil	Total	Metabolically active	HCl soluble
Carex pilulifera	Acid	781	283	691
	Calcareous	491	163	272
	Calcareous + P	360	115	202
Veronica officinalis	Acid	1148	689	818
	Calcareous	1588	399	654
	Calcareous + P	1311	480	593

Source: Zohlen and Tyler (1997)
Note: The 'metabolically active' fraction was extracted with 1,10-phenantroline, an Fe-complexing reagent considered to extract mainly Fe^{2+}; the HCl-soluble fraction is considered the fraction that is important in chlorophyll synthesis
*Expressed as nmol g^{-1} dry mass

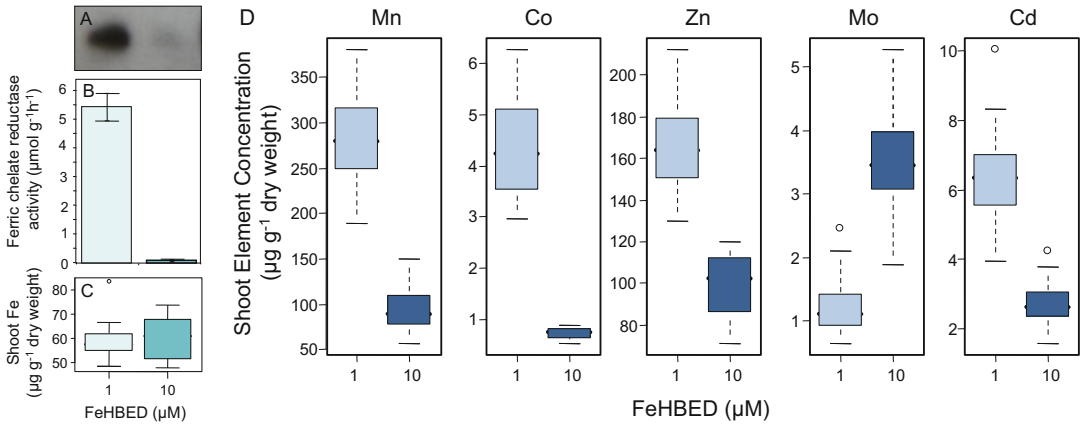

Fig. 9.23 Biochemical assessment of the iron (Fe) response status, Fe accumulation, and effects on metal accumulation in *Arabidopsis thaliana*. (**A**) Immunoblot showing accumulation of a protein involved in Fe uptake, IRT1, in roots; (**B**) ferric chelate reductase activity in roots; (**C**) Fe accumulation in leaves. (**D**) Box plot of the manganese (Mn), cobalt (Co), zinc (Zn), molybdenum (Mo), and cadmium (Cd) concentrations of shoots. Plants were grown under Fe-deficient (1 µM FeHBED, ferric N, N-di-(2-hydroxybenzoyl)-ethylenediamine-N,N-diacetic acid) and Fe-sufficient (10 µM FeHBED) conditions. Box plots represent the interquartile range (IQR); the bisecting line represents the median; the whiskers represent 1.5 times the IQR; the dots represent outlier points. All plants grew in soil. Baxter IR, Vitek O, Lahner B, Muthukumar B, Borghi M, Morrissey J, Guerinot ML, Salt DE. 2008. The leaf ionome as a multivariable system to detect a plant's physiological status. *Proc Natl Acad Sci USA* **105**: 12081–12086; copyright (2008) National Academy of Sciences, U.S.A.

enhances the relative distribution of P to palisade mesophyll, resulting in a greater P concentration in these cells, despite no change in whole leaf P concentration (Hayes et al. 2019a). Calcifuge Proteaceae show a greater palisade mesophyll P concentration than congeneric soil-indifferent ones, corresponding with their greater sensitivity to Ca-enhanced P toxicity (Fig. 9.24; Hayes et al. 2019b).

Calcicole species are associated with calcium-rich soils. High Ca concentrations, which are saturating or inhibitory for calcifuge species, may stimulate their growth, *e.g.*, in *Origanum vulgare* (oregano) (Jefferies and Willis 1964); however, this is not the major factor explaining their distribution. More importantly, calcicole species do not resist high **Al** concentrations in their root environment (Sect. 9.3.1). They have a

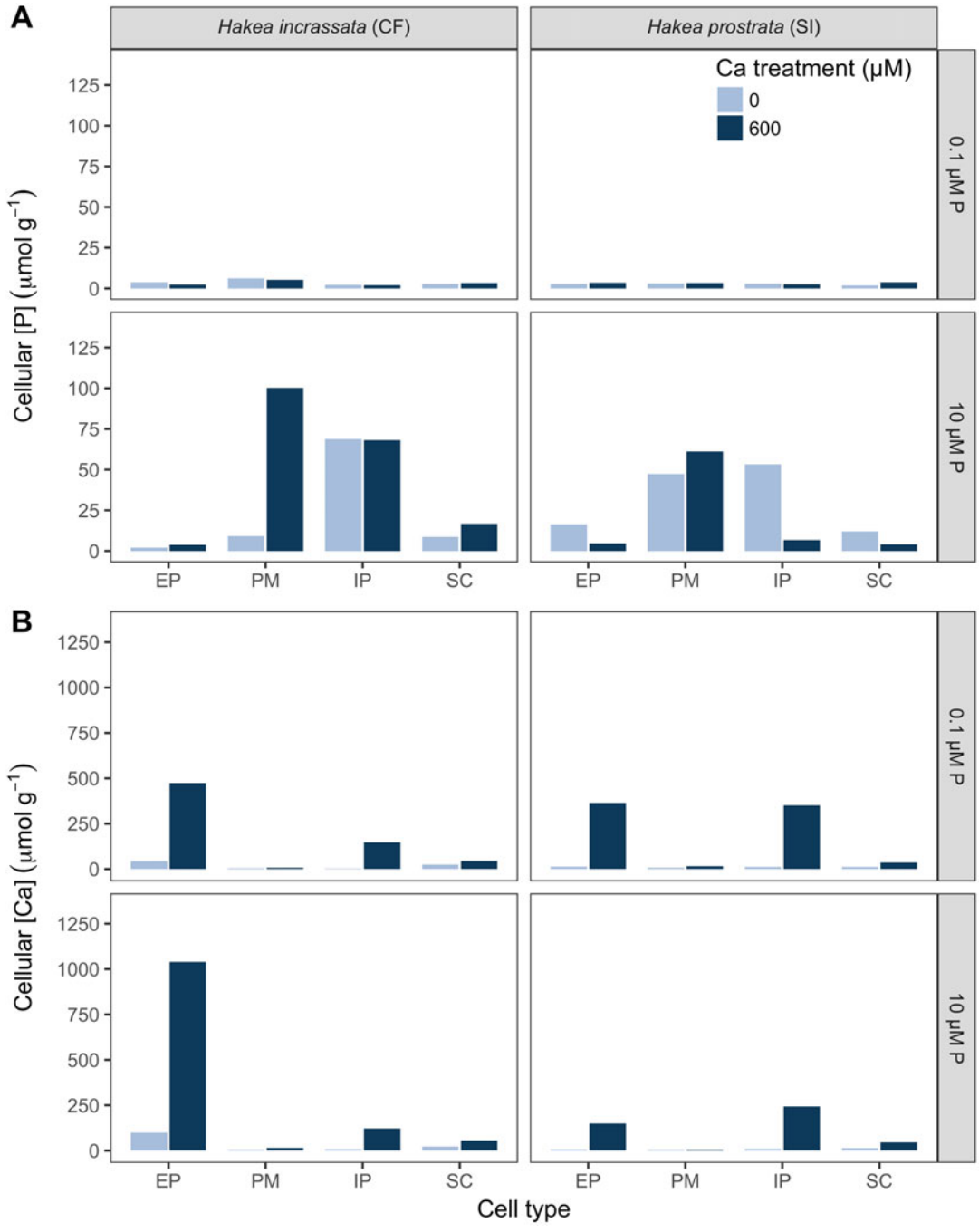

Fig. 9.24 Leaf cell-specific phosphorus (P) and calcium (Ca) concentrations of two *Hakea* species (Proteaceae) grown in nutrient solutions with different P and Ca concentrations. Comparison of a typical calcifuge (*Hakea incrassata*) and a soil-indifferent (*Hakea prostrata*) species. Only plants grown under high P (10 μM)/high Ca (600 μM) showed symptoms of P toxicity. Concentrations are per unit fresh weight, from fully-hydrated cells. 0.1 μM P and 10 μM P, indicate the two P treatments. *EP* epidermis, *PM* palisade mesophyll, *IP* internal parenchyma, *SC* sclerenchyma (after Hayes et al. 2018).

greater capacity to acquire poorly-available nutrients, *e.g.*, Fe, P, and Zn (Sect. 9.2.1.1), from alkaline soils. This involves the release of **organic acids** (Tyler and Ström 1995) or **coumarins**, which mobilize Fe (Tsai and Schmidt 2017).

The solubilization of P and Fe by carboxylate exudation in calcicoles inevitably also enhances the availability of Ca. Indeed, the xylem sap of calcicole species may show high Ca concentrations. Because Ca is an important '**second messenger**' (*e.g.*, in the regulation of stomatal conductance) (Sect. 5.5.4.2), how does a calcicole plant avoid being poisoned by Ca? Calcicoles store excess Ca as crystals (He et al. 2012), sometimes in leaf glands and trichomes, or excrete it via their stomata (Wu et al. 2011). Calcifuge herbs are unable to avoid excessive uptake of **calcium** from calcium-rich soil (Zohlen and Tyler 2004).

9.3.3 Soils with High Levels of Metals

The metals discussed here used to be called 'heavy metals', which are characterized by a density greater than 5 g mL^{-1}. 'Heavy metals' is often used as a group name for metals and semimetals (metalloids) that are associated with contamination and potential toxicity, but there is no authoritative definition in the relevant literature (Duffus 2002; Pourret and Bollinger 2018). Their biological activity is due to **ligand properties**. Some metals [copper (Cu), Fe, Mn, Mo, nickel (Ni), and Zn] are essential micronutrients for plants but become toxic at elevated concentrations. They are cofactors or activators of specific enzymes or stabilize organic molecules. Some metals are beneficial elements [cobalt (Co)]. Other metals [*e.g.*, cadmium (Cd), lead (Pb), chromium (Cr), mercury (Hg), silver (Ag), uranium (U), and gold (Au)] are only toxic for plant functioning.

For metals like Mn, Co, Zn, and Cd that are taken up as cations, there is a strong driving force, because of the electrochemical potential gradient (Sect. 9.2.2.2), but they would need a transport system to cross the plasma membrane. Figure 9.24 illustrates that these metals are taken up by a **Fe transporter**; if the plants produce more of this Fe transporter, because the plants are Fe-starved, they maintain the same internal Fe concentrations, but the concentrations of Mn, Co, Zn, and Cd increase sharply (Baxter et al. 2008; He et al. 2017). For Mo, we do not find this (Fig. 9.23), because it is taken up as the anion molybdate.

9.3.3.1 Why Are Concentrations of Metals in Soil High?

High levels of metals in soils may have a geological or anthropogenic origin (Van der Ent et al. 2013). In 1865, the first reference to metal **hyperaccumulation** in plants was made when *Thlaspi caerulescens* (alpine pennycress) growing on Zn-rich soils near the German-Belgium border, was reported to contain 17% of Zn in its ash. However, it was the discovery in 1948 by Minguzzi and Vergnano of extreme Ni accumulation in *Alyssum bertolonii* from serpentine hills in Italy, reaching 10 mg Ni g^{-1} dry mass, that marks the beginning of an increasing interest in this subject (Assunção et al. 2003). Brooks et al. (1977) used the term **hyperaccumulator** to define plants with Ni concentrations >1000 μg g^{-1} dry mass. The hyperaccumulation phenomenon is exhibited by less than 0.2% of all angiosperms, with most of the ~500 hyperaccumulator species known for Ni (Deng et al. 2018). There is increasing evidence that hyperaccumulation confers protection against herbivores and microbial pathogens (Chaps 12 and 13) (Poschenrieder et al. 2006; Fones et al. 2010).

Serpentine or **ultramafic** soils have naturally high levels of Ni, Cr, Co, and Mg, but low concentrations of Ca, N, and P. The flora associated with these soils is rich in specially adapted **endemic species** (Whittaker 1954; Arianoutsou et al. 1993; Anacker 2014; Van der Ent et al. 2015). It has been known for centuries that rock formations in Europe that contain high levels of certain metals (*e.g.*, Cu) are characterized by certain plant species associated with these sites (**metallophytes**). This is also true for southern Africa and Brazil, where only certain

herbaceous species, *e.g.*, *Senecio anomalochrous* (Asteraceae) or an endemic cactus species (*Arthrocereus glaziovii*) establish on metal-rich sites (Mesjasz-Przybylowicz et al. 2001; Skirycz et al. 2014). Such metal-**hyperaccumulating** plants may contain very high levels of metals. Species that hyperaccumulate Cd contain >0.1 mg g^{-1} dry mass; for Co or Cu: >0.3 mg g^{-1} dry mass; for As, Ni, Pb, and Se: >1 mg g^{-1} dry mass; for Zn: >3 mg g^{-1} dry mass; for Mn >10 mg g^{-1} dry mass (Krämer 2010).

In sites close to mines, where the remains of the mining activity have enriched the soil with metals, or under electricity pylons, which cause Zn contamination due to corrosion of their galvanized surfaces, metal-resistant genotypes emerge. Examples include *Agrostis capillaris* (colonial bentgrass), *Agrostis stolonifera* (creeping bentgrass), *Anthoxanthum odoratum* (sweet vernalgrass), and *Festuca ovina* (sheep's fescue) (Al-Hiyaly et al. 1990). The shoots of such plants may contain as much as 1.5 mg Zn g^{-1} dry mass, whereas 0.3 mg Zn g^{-1} dry mass is considered toxic to most crop plants (Broadley et al. 2007). Along roadsides that have become enriched in Pb from automobile exhaust, Pb-resistant genotypes occur, *e.g.*, of *Senecio vulgaris* (groundsel) (Briggs 1976). Resistant genotypes are usually resistant only to one metal, unless more than one metal is present at a high level at such a site (Krämer 2010).

Cadmium pollution has increased dramatically in recent decades, because of combustion of fossil fuel, disposal of pigments and stabilizers for plastics, application of sewage sludge, and the use of phosphate fertilizers (Alloway and Steinnes 1999). This has led to concern about possible health and ecosystem effects. A comparison of several cultivars of *Lupinus albus* (white lupin), and *Lupinus angustifolius* (narrow-leaved lupin) with *Lolium multiflorum* (Italian ryegrass) shows much greater uptake by the grass. Because the lupins release considerably more **carboxylates** (citrate, malate) into the rhizosphere than the grass does, root exudates likely chelate Cd which would reduce its availability for uptake (Römer et al. 2000).

9.3.3.2 Using Plants to Clean or Extract Polluted Water and Soil: Phytoremediation and Phytomining

Some metal-accumulating species have been used to remove metals from polluted water [*e.g.*, *Eichhornia crassipes* (water hyacinth)], which is considered promising for remediation of natural water bodies and/or wastewater polluted with low levels of Zn, Cr, Cu, Cd, Pb, Ag, or Ni (Odjegba and Fasidi 2007; Rezania et al. 2015). Terrestrial metallophytes are also potentially useful to remove metals from polluted sites, a process termed **phytoremediation** (Krämer 2005). It requires plants that show both a high biomass production and metal accumulation to such high levels that extraction is economically viable. Intercropping of *Avena sativa* (oat) with *Lupinus albus* (white lupin), which mobilizes some metals, might be a promising tool for phytoremediation in soil (Wiche et al. 2016). The combination of high biomass production and hyperaccumulation is common in Brassicaceae (cabbage family). After accumulation of metals from the polluted soil, the plants have to be removed and destroyed, taking care that the toxic metal is removed from the environment. Phytoremediation technologies are currently available for only a small subset of pollution problems, such as arsenic (As). Removal of As employs naturally selected hyperaccumulators [*e.g.*, *Pteris vittata* (brake fern)], which accumulate As specifically in aboveground organs (Krämer 2005).

We can also use metal-accumulating plants as a 'green' alternative to environmentally destructive opencast mining practices. Such production of a crop of high-biomass plants that accumulate high metal concentrations is termed **phytomining** (Brooks 1998; Nkrumah et al. 2016). *Eucalyptus* species (gum trees) may translocate Au from mineral deposits, and support the use of vegetation sampling in mineral exploration, particularly where thick sediments dominate. A recent observation conclusively demonstrates active biogeochemical adsorption of Au, and provides insight into its behavior in natural samples (Lintern et al. 2013).

9.3.3.3 Why Are Metals So Toxic to Plants?

The biochemical basis of metal toxicity is not always clear. Most of the metals discussed here are 'Lewis acids', which can accept a pair of electrons from a coordinate covalent bond; that is, they react with naturally occurring 'Lewis bases' in the cell, such as $-S^-$ groups, $-OH^-$ groups, amino groups, and carboxylic acid termini (Appenroth 2010). Cadmium, Pb, and Hg, which are nonessential, affect **sulfhydryl groups** and **N atoms** in proteins and thus inactivate these. For a redox-active metal, an excess supply may result in uncontrolled redox reactions, giving rise to the formation of toxic **free radicals**. For example: $Fe^{2+} + H_2O_2 \rightarrow Fe^{3+} + OH\cdot + OH^-$, followed by: $Fe^{3+} + H_2O_2 \rightarrow Fe^{2+} + OOH\cdot + H^+$. Free radicals may lead to **lipid peroxidation** and membrane leakage (Clemens 2001). **Silicon** (Si) ameliorates the toxic effects of Zn in *Oryza sativa* (rice) which is associated with enhanced activity of **antioxidative systems**: superoxide dismutase, catalase, and ascorbate peroxidase (Song et al. 2011).

Toxic divalent cations of several transition metal elements have similar chemical properties as plant nutrients, and, when present in excess, one metal can **replace** the **activating cation**. Exposure to excess Ni in the Ni-hyperaccumulating *Alyssum inflatum* results in an inhibition of root-to--shoot translocation of Fe, and Fe accumulation in the root pericycle, endodermis, and cortex cells of the differentiation zone. Shoot Fe concentrations, chlorophyll concentrations and Fe-dependent antioxidant enzyme activities are decreased in Ni-exposed plants (Ghasemi et al. 2009). Like Zn, Cd also affects photosynthesis. Similarly, Cd reduces the concentration of Mn, Cu, and chlorophyll in leaves, even at a concentration in solution that has no effect on biomass production in Cd-resistant species such as *Brassica juncea* (Indian mustard) (Salt et al. 1995).

Most primary effects of metals occur in the **roots**, which show reduced elongation upon exposure. We can therefore assess metal sensitivity and resistance quantitatively by determining the effect of the metal on root elongation (Table 9.11; Godbold et al. 1983; Di Salvatore et al. 2008). **Root elongation** is far more sensitive than root dry matter increment, leading to 'stubby' roots (Brune et al. 1994). Zinc inhibition of water uptake and transpiration in *Hordeum vulgare* (barley) are due to a decreased root hydraulic conductance through reductions in expression of genes encoding **aquaporins** (Sect.

Table 9.11 The effect of cadmium (Cd), lead (Pb), nickel (Ni), and copper (Cu) on root elongation of *Lactuca sativa* (lettuce), *Brassica oleracea* (broccoli), *Solanum lycopersicum* (tomato), and *Raphanus raphanistrum* subsp. *sativus* (radish).

Metal	Dose (μM)	Root length			
		Lettuce	Broccoli	Tomato	Radish
None	0	21	18	18	22
Cd	16	21	18	16	21
	256	11	10	7	20
	1024	n.d.	n.d.	n.d.	20
Pb	16	20	18	17	20
	256	12	10	12	21
	1024	5	6	4	19
Ni	16	17	18	18	20
	256	11	12	8	19
	1024	n.d.	n.d.	n.d.	13
Cu	16	20	14	17	21
	256	8	11	15	20
	1024	n.d.	8	n.d.	13

Source: Di Salvatore et al. (2008)
Note: The plants were tested on filter paper; *n.d.* not determined; seedlings with a root length < 3 mm were not measured

5.5.2) (Gitto and Fricke 2018). Manganese toxicity leads to interveinal chlorosis and reduced photosynthesis, especially when plants are exposed to full sunlight, rather than grown in the shade (Fernando and Lynch 2015).

9.3.3.4 Metal–Resistant Plants

Resistance in higher plants has been demonstrated for the following metals: As, Cd, Cr, Co, Cu, Fe, Hg, Mn, Ni, Pb, selenium (Se), thallium (Tl), and Zn (Krämer 2010; Van der Ent et al. 2013; Rodríguez-Alonso et al. 2017; Saaltink et al. 2017). **Metal resistance** is sometimes partly based on **tolerance**. For example, metal-tolerant plants have modified the activity or the metal affinity of enzymes in such a way that a surplus of metal ions is rapidly removed from the plant cell metabolism to prevent physiological damage. These processes are metal-specific (Baker et al. 2010). Examples are the overexpression of a metallothionein gene in Cu-tolerant ecotypes of *Silene vulgaris* (bladder campion) (Van Hoof et al. 2001a), and the overproduction of histidine in Ni-tolerant *Alyssum* species. (Krämer et al. 1996). **Avoidance** mechanisms generally account for resistance in a range of species. At a cellular level, these mechanisms include (Fig. 9.25):

1. **Exclusion** of the metal:
   (a) binding by mycorrhizal fungi;
   (b) binding to root cell walls;
   (c) chelation by root exudates;
   (d) reduced net uptake: decreased influx or increased efflux.
2. Uptake followed by storage, typically occurring in **hyperaccumulators**:
   (a) chelation of metals in the cytosol;
   (b) repair of metal-damaged proteins;
   (c) compartmentation of metals in specific compartments, *e.g.*, vacuoles or trichomes.

In addition, mechanisms that are expressed at the level of whole plants play a role. These include differences in the proportion of absorbed metals that are either retained in the roots or loaded in the xylem for export to the shoot (Assunção et al. 2003; Van der Ent et al. 2013). Mycorrhizal fungi (Sect. 12.2) can retain metals and thus reduce the toxic effects of metals in their host, *Miscanthis* × *giganteus* (giant miscanthus) (Firmin et al. 2015). Although the root cell walls are in direct contact with metals in the soil solution, adsorption onto these is limited and thus of little consequence for resistance.

As with Al (Sect. 9.3.1.3), metals can be chelated by exudates released from roots of resistant plants. For example, Ni-resistant plants of *Thlaspi arvense* (field pennycress) exude **histidine** and **citrate**, which chelate Ni and thus reduce its uptake by roots (Salt et al. 2000). Lead-resistant varieties of *Oryza sativa* (rice) release **oxalate** into the rhizosphere and so detoxify Pb (Yang et al.

Fig. 9.25 (Continued) plasma membrane. 5. Efflux into the apoplast. 6. Chelation in the cytosol by various ligands, including organic acids, phytochelatins (PC), and metallothioneins (MT). 7. Repair and protection of plasma membranes, *e.g.*, by heat-shock proteins (HSP) and metallothioneins. 8. Transport of PC-Cd complex into the vacuole. 9. Transport and accumulation of metals in the vacuole (Hall 2002). (**C**) Molecular mechanisms involved in metal hyperaccumulation. (1) Metal ions are mobilized by secretion of chelators and acidification of the rhizosphere. (2) Uptake of hydrated metal ions or metal-chelate complexes is mediated by various uptake systems in the plasma membrane. Inside the cell, metals are chelated, and excess metals are sequestered by transport into the vacuole. (3) From the roots, transition metals are transported to the shoot via the xylem. Presumably, the larger portion reaches the xylem via the root symplast. Apoplastic passage might occur at the root tip. Inside the xylem, metals are present as hydrated ions or as metal-chelate complexes. (4) After reaching the apoplast of the leaf, metals are differentially captured by different leaf cell types and move cell-to-cell through plasmodesmata. Storage appears to occur preferentially in trichomes. (5) Uptake into the leaf cells again is catalyzed by various transporters [not depicted in (5)]. Intracellular distribution of essential metals (= trafficking) is mediated by specific metallo-chaperones and transporters localized in endomembranes (note that these processes function in every cell). Abbreviations and symbols: *CW* cell wall, *M* metal; filled circles, chelators; filled ovals, transporters; bean-shaped structures, metallo-chaperones (Clemens et al. 2002);

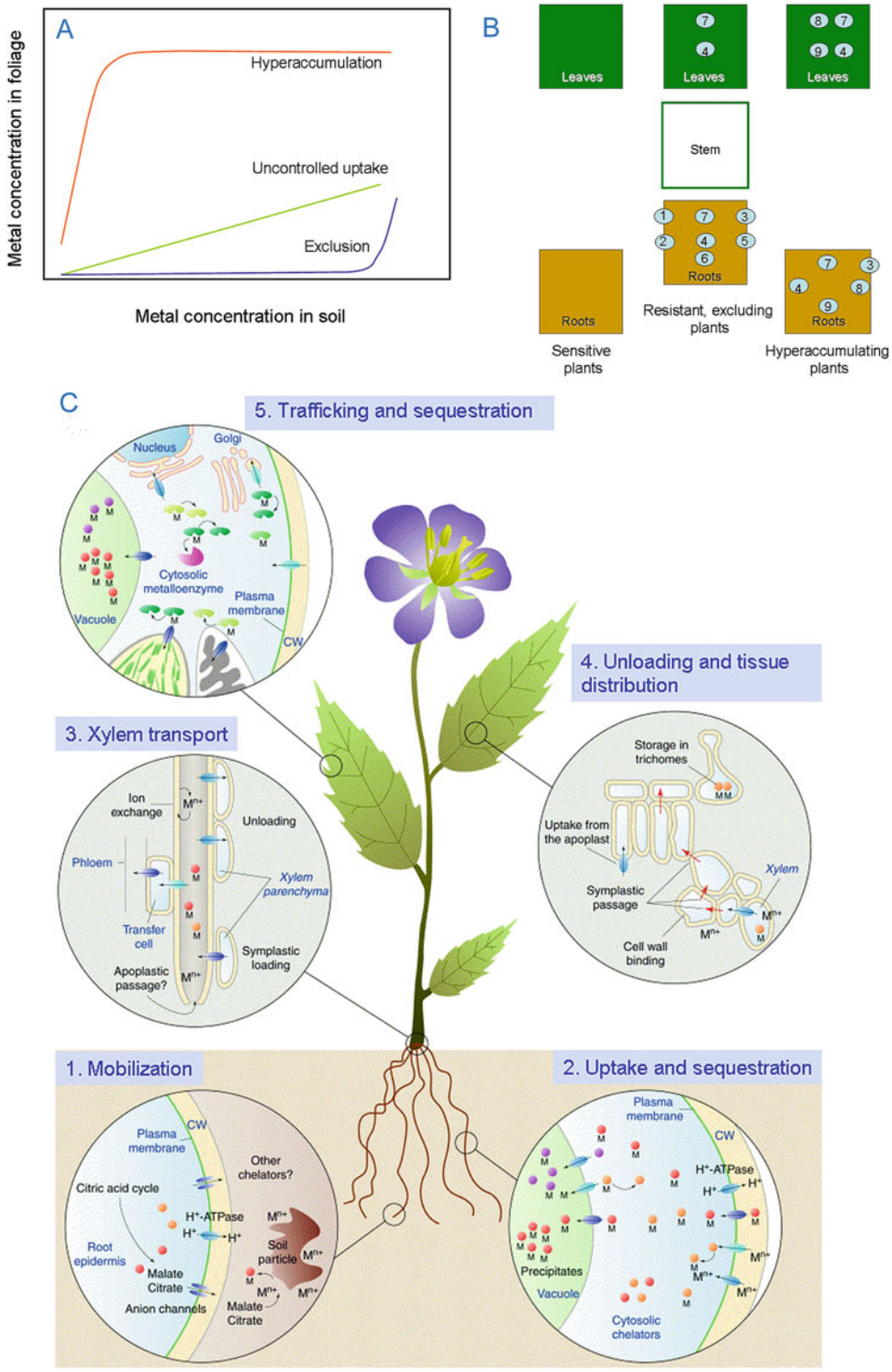

Fig. 9.25 Summary of potential responses of higher plants to metals. (**A**) Typical responses of sensitive plants, bioindicator plants, plants that exclude metals from their foliage, and hyperaccumulating plants (after Van der Ent et al. 2013). (**B**) Mechanisms of metal toxicity and resistance in vascular plants. 1. Restriction of metal movement to roots by mycorrhizal fungi. 2. Binding to cell walls. 3. Chelation by root exudates. 4. Reduced influx across the

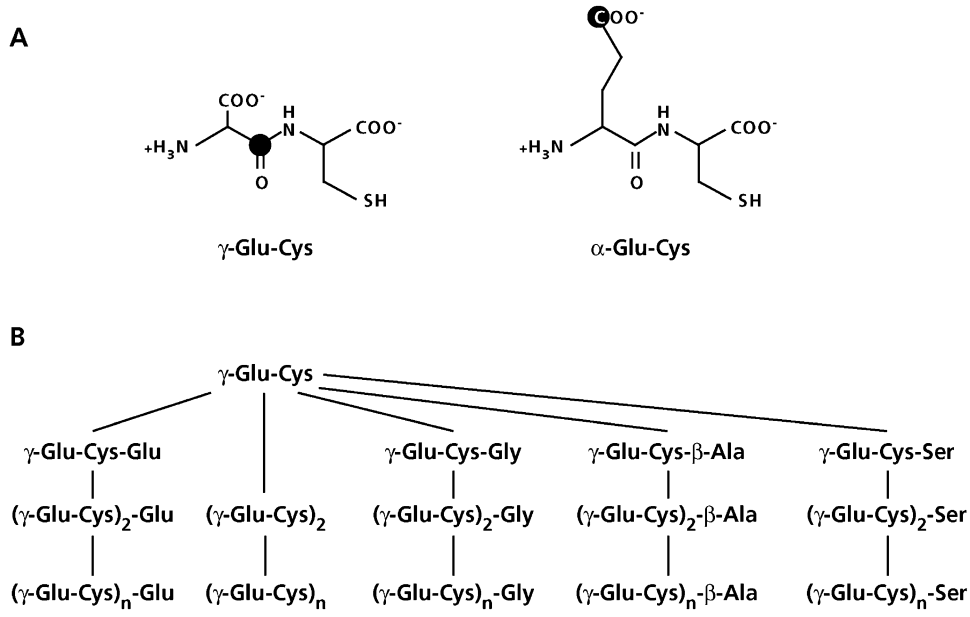

Fig. 9.26 (**A**) The structure of γ(Glu-Cys) peptides. The γ-carboxyl-C of glutamine (Glu) is highlighted to indicate the difference between α- and γ-carboxyamide linkages. (**B**) A model summarizing the five families of γ(Glu-Cys) peptides involved in metal immobilization in plants and yeasts; the lines indicate family relationships and do not necessarily specify biosynthetic sequences (Rauser 1995).

2000). Copper induces release of **malate** and **citrate** from roots of *Triticum aestivum* (wheat) (Nian et al. 2002). Therefore, although not as widely explored as carboxylate release as a mechanism to reduce uptake of Al, a similar mechanism does appear to play a role in preventing entry of some other metals. Reduced uptake of Pb may also be due to the formation of callose between the plasma membrane and walls of root cells providing a mechanical barrier (Fahr et al. 2013).

The clearest example of reduced uptake as a resistance mechanism is for As, first discovered in *Holcus lanatus* (common velvetgrass). Arsenate, which is structurally similar to phosphate, is taken up by the same transport system as Pi, and the As-resistant plants exhibit an absence of the high-affinity Pi-uptake system (Meharg and Macnair 1992).

Chelation of metals following their uptake involves carboxylates as well as several SH-containing compounds. *Gomphrena claussenii* (globe amaranth) sequesters Cd, but not Zn, in vacuolar **oxalate crystals** (Villafort Carvalho et al. 2015). **Cadmium resistance** is also associated with SH-containing **phytochelatins** (PCs) (Fig. 9.26A, B). Phytochelatins are poly(γ-glutamyl-cysteinyl)-glycines, which bind metals. Unlike other peptides, with an α-carboxyl peptide bond, they are not made on ribosomes, but via a specific pathway from **glutathione**. Upon exposure of *Nicotiana rustica* (Aztec tobacco) to Cd in the root environment, Cd-binding peptides [-γ-$(Glu\text{-}Cys)_3$-Gly and γ$(Glu\text{-}Cys)_4$Gly], are produced. Inhibition of PC synthesis leads to loss of the Cd-detoxification mechanism. Together with Cd, some of the PCs are almost exclusively located in the **vacuole** (Sharma and Dietz 2006), and an ATP-dependent mechanism transporting the Cd-PC complex has been identified in tonoplasts of *Avena sativa* (oat) (Salt and Rauser 1995). The formation of PCs, followed by uptake of the Cd-PC complex in the vacuole probably plays a crucial role in Cd resistance. Metallothioneins also have a high affinity for both Cd and Zn. They were first discovered as

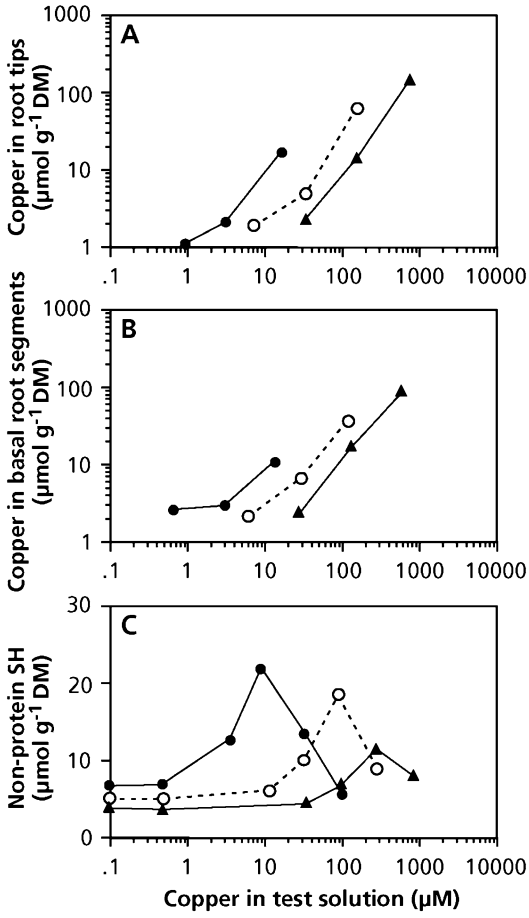

Fig. 9.27 Copper (**A**, **B**) and phytochelatin sulfhydryl concentration (lowest panel) in the roots of one copper (Cu)-sensitive (filled circles) and two Cu-resistant (open circles and filled triangles) ecotypes of *Silene cucubalus* (bladder campion). Copper was measured in the apical 10 mm (**A**) and the adjacent 10 mm (**B**). Phytochelatin was measured for the entire roots (after Schat and Kalff 1992).

the substances that are responsible for Cd accumulation in mammalian kidney. Like other proteins, but unlike phytochelatins, metallothioneins are synthesized on ribosomes (Robinson et al. 1993). Evidence for protection against metal-induced damage comes from enhanced expression of **heat-shock proteins (HSPs).** These proteins characteristically show increased expression in response to exposure of plants to stress, including metals (Savvides et al. 2016) as well as high temperature (Sect. 7.3.2).

Compartmentation of accumulated metals may occur in the vacuole or in the apoplastic space (*e.g.*, for Zn, Cd, Ni, and Cu) (Krämer et al. 2000; Villafort Carvalho et al. 2015). Epidermal cells, with the exception of stomatal cells, may also be used for storage of the metals (Frey et al. 2000). Cadmium, Mn, Zn, and Pb are preferentially accumulated in leaf trichomes [*e.g.*, in *Brassica juncea* (Indian mustard) and *Arabidopsis halleri* (meadow rock-cress) (Salt et al. 1995; Zhao et al. 2000).

Copper resistance in *Silene cucubalus* (bladder campion) is based on **exclusion**, which is at least partly based on ATP-dependent Cu efflux (Van Hoof et al. 2001b). Upon exposure to Cu, both resistant and sensitive *Silene vulgaris* plants accumulate **phytochelatins** (Fig. 9.27). When compared at leaf Cu concentrations that give a similar physiological effect, the phytochelatin concentrations in sensitive and resistant genotypes are similar (Table 9.12). Phytochelatin synthesis is likely essential to bind the toxic Cu, but because phytochelatins are produced in both Cu-resistant and sensitive plants, it is not the basis for Cu resistance in *Silene vulgaris*.

Table 9.12 Phytochelatin sulfhydryl concentration [µmol (g dry mass)$^{-1}$] and molar ratio of phytochelatin to copper (Cu) in the roots of a Cu-sensitive and a Cu-resistant ecotype of *Silene cucubalus* (bladder campion).

	Phytochelatin concentration		Phytochelatin/Cu ratio	
Cu-exposure level	Sensitive	Resistant	Sensitive	Resistant
Highest concentration without any effect	3.7	2.9	3.7	1.6
Concentration giving 50% inhibition of root growth	7.6	7.5	3.7	1.7
Concentration giving 100% inhibition of root growth	19.0	16.0	1.2	0.3

Source: Schat and Kalff (1992)
Note: The same data were used as given in Fig. 9.27 for the apical 10 mm

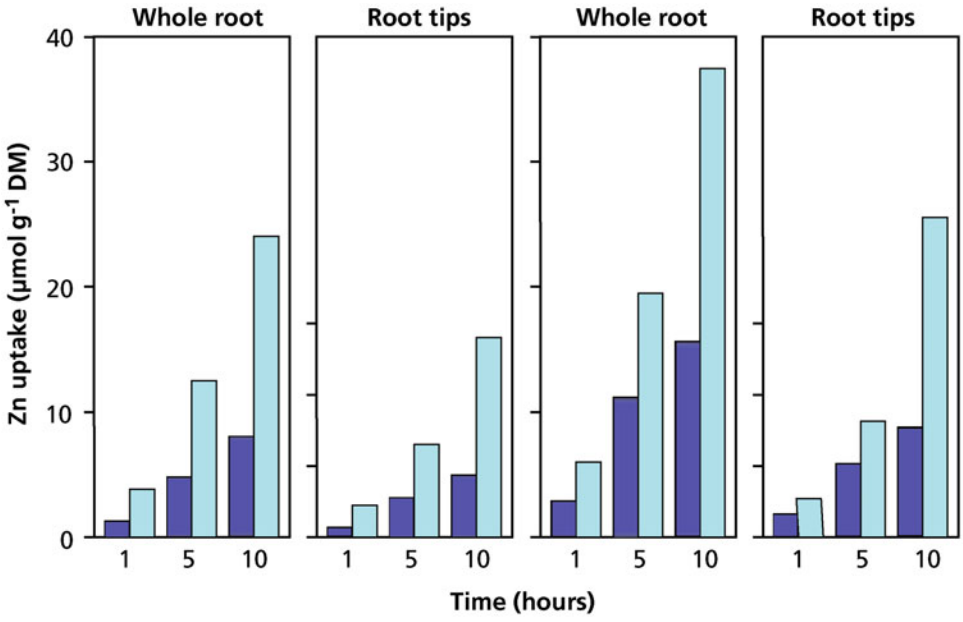

Fig. 9.28 Uptake of radioactive zinc (^{65}Zn) by roots of a Zn-sensitive (dark-blue bars) and a Zn-resistant (light-blue bars) ecotype of *Deschampsia caespitosa*. The plants are compared at low and high external Zn concentrations, which give the same effect on root elongation (Table 9.12). The low Zn concentrations (panels at left) are 25 mM and 250 mM, and the high Zn concentrations (panels at right) are 100 mM and 500 mM for the sensitive and resistant ecotype, respectively. At the end of the experiment, desorption into a nonlabeled Zn solution was allowed for 30 min. The data therefore show uptake into the root cells only, rather than a combination of uptake and binding of labeled Zn to the cell walls (after Godbold et al. 1983).

When compared at the same external Zn concentration (100 µM), a **Zn-resistant** ecotype of *Deschampsia caespitosa* (tufted hair-grass) accumulates less Zn in the apical parts of its roots, but more in the basal parts (further than 50 mm from the apex) (Godbold et al. 1983). At the same external Zn concentration, whole roots of both ecotypes of *Deschampsia caespitosa* absorb Zn at the same rate. When compared at an external Zn concentration that has a similar effect on root growth, the resistant ecotype accumulates more Zn than does the sensitive one (Fig. 9.28). As found for other Zn-resistant genotypes, it also binds a greater fraction of the Zn to its cell walls than does the sensitive one. Inside the cell, Zn is probably stored in the vacuole (as a complex with oxalate or citrate). There is very little transport of Zn to the shoot, especially in the resistant ecotypes. Zinc-resistant ecotypes of *Silene vulgaris* (bladder campion) also accumulate more Zn than sensitive ones. As with Al (Sect. 9.3.1.1), many metals are largely complexed or precipitated at cytosolic pH.

Typical Zn-hyperaccumulating species [*e.g.*, *Thlaspi caerulescens* (alpine pennycress)] accumulate and tolerate up to 40 mg Zn g^{-1} dry mass in their shoots. When exposed to Zn levels that are toxic for most plants, *Thlaspi caerulescens* shows both enhanced Zn influx into the roots and increased transport to the shoots which makes it a promising species to be used for **phytoremediation** (Lasat et al. 1996).

After the discovery of extreme Ni hyperaccumulation in *Alyssum bertolonii* (Brassicaceae) from Italian serpentine soil in 1948, at least 450 species have been identified as Ni hyperaccumulators (Nkrumah et al. 2016). **Nickel resistance** in *Alyssum lesbiacum* (madwort) is associated with the presence of high concentrations of the amino acid **histidine**. Histidine plays a role in the detoxification of absorbed Ni and transport of a Ni-histidine complex in the xylem to the leaves. In some *Alyssum* species Ni

accumulates to 30 mg g^{-1} leaf dry mass (Krämer et al. 1996).

9.3.3.5 Biomass Production of Sensitive and Resistant Plants

The biomass production (Relative Growth Rate; Sect. 10.2.1.1) of Cu- and Pb-resistant genotypes of *Agrostis capillaris* (colonial bentgrass) is less than that of sensitive ones, when compared at a concentration of the metal that is optimal for the plants (Wilson 1988). Biomass production is also less for a Cu-resistant ecotype of *Silene vulgaris* (bladder campion), even when plants are compared at a Cu supply that is optimal, *i.e.* a higher concentration for the resistant plants (Table 9.13; Lolkema et al. 1986). This might be due to the **costs** associated with the resistance mechanism (Faucon et al. 2012), based on higher requirements for Cu (Hego et al. 2014). Alternatively, the low productivity of the resistant plants may be associated with the typically low nutrient availability in their natural environment, which selects for inherently slow-growing plants (Sect. 10.3).

When grown in nontoxic soil, Cu-resistant and Cu-sensitive ecotypes of *Agrostis tenuis* (common bentgrass) have a similar yield in monoculture. In mixtures, the yield of the resistant ecotype is reduced (McNeilly 1968). This explains why we find resistant ecotypes exclusively in environments containing high Cu levels. Since Cu resistance in *Agrostis tenuis* is based on Cu immobilization by the roots (Dahmani-Muller et al. 2000), resistant genotypes have a greater requirement for Cu (Hego et al. 2014), and this would offer an explanation for the poor competition of the resistant ecotype.

Table 9.13 Dry mass (mg per two plants) of roots and shoot of a copper (Cu)-sensitive and a Cu-resistant ecotype of *Silene vulgaris* (bladder campion), after growth in nutrient solution with two Cu concentrations.

Ecotype		0.5 μM	40.5 μM
Sensitive	Roots	64	8
	Shoot	523	169
	Total	587	173
Resistant	Roots	22	33
	Shoot	146	237
	Total	168	270

Source: Lolkema et al. (1986)
Note: The different ecotypes were grown separately

9.3.4 Saline Soils: An Ever-Increasing Problem in Agriculture

The presence of high concentrations of Na^+, Cl^-, Mg^{2+} and SO_4^{2-} ions in saline soils inhibits growth of many plants. On a global scale, salinity affects plant production on more than 800 million hectares, which amount to 6% of the world's land area (Munns and Tester 2008). Most of this salt-affected land has arisen from natural causes, from the accumulation of salts over a long time in arid and semiarid zones. Weathering of parental rocks releases soluble salts of various types, mainly chlorides of sodium, calcium, and magnesium, and to a lesser extent, sulfates and carbonates. The problem of saline soils is ever-increasing, due to poor irrigation and drainage practices, expansion of irrigated agriculture into arid zones with high evapotranspiration rates, or clearing land which leads to rising saline water tables ('dryland salinity') (Munns and Tester 2008; Munns and Gilliham 2015).

9.3.4.1 Glycophytes and Halophytes

Most crop species are relatively salt-sensitive (**glycophytes**). A notable exception is sugar beet (*Beta vulgaris*) (Blumwald and Poole 1987). In saline areas, such as salt marshes, species occur with a high resistance to salt in their root environment (**halophytes**). The problems associated with high salinity are threefold:

1. A high salinity is associated with a low soil **water potential**, giving rise to symptoms similar to those of water stress;
2. Specific ions, especially Na^+ and Cl^-, may be **toxic**;
3. High levels of NaCl may give rise to an **ion imbalance** (predominantly Ca), and lead to deficiency symptoms.

Plant adaptation and acclimation to salinity involve all these aspects; we discussed

acclimation associated with the low water potential in Sect. 5.3.

Toxicity effects may include competition of Na^+ with K^+ in biochemical processes (Flowers and Colmer 2008), and inhibition of NO_3^- uptake by Cl^-, because in *Zea mays* (maize) both anions are transported across the plasma membrane by the same transport protein, a low-affinity NO_3^- transporter that switches to a high-affinity Cl^- transporter (Wen et al. 2017). The toxic effect of Na^+ far exceeds that of Cl^- (Tester and Davenport 2003). Na^+ may replace Ca^{2+} on root cell membranes which may give rise to leakage of K^+ from the root cells. It may also reduce the influx and enhance the efflux of Ca^{2+}. The decreased influx of Ca^{2+} probably results from competition for binding sites in the cell wall which decreases the concentration at the protein in the plasma membrane responsible for Ca^{2+} influx. The toxicity of specific ions may subsequently lead to an ion imbalance and ion deficiency, especially Ca deficiency (Munns 2002). On the other hand, Ca^{2+} reduces the influx of Na^+, due to the inhibition by Ca^{2+} of a voltage-insensitive monovalent channel that allows Na^+ entry into roots (White 1999). However, confirmation of this effect using intact plants is necessary to establish that Ca^{2+} does, indeed, affect influx. Addition of Ca^{2+} is often proposed as a strategy to ameliorate Na^+ toxicity to crops (Cramer 2002).

At a moderate NaCl concentration in the root environment, Na^+ uptake occurs down an electrochemical potential gradient, and we expect higher Na^+ concentrations inside than outside (Table 9.14). Roots of some **glycophytes**, however, maintain a low Na^+ concentration in the presence of 1 mM Na^+ in their medium. This indicates that roots of glycophytes actively excrete Na^+ from their roots.

9.3.4.2 Energy-Dependent Salt Exclusion from Roots

The low Na^+ concentration inside the cells of glycophytes is mostly due to energy-dependent efflux. At an external NaCl concentration of 1 mM, inhibition of the plasma-membrane H^+-ATPase increases net Na^+ uptake in the glycophyte *Plantago media* (hoary plantain), but decreases it in the halophyte *Plantago maritima* (sea plantain). This illustrates that both **ATP-dependent Na^+ excretion** and **uptake** occur in these *Plantago* species (Table 9.15). At higher (10, 50 mM) NaCl concentrations, the roots of the glycophyte continue to excrete Na^+, but not to the extent that accumulation in the plant is avoided. At 10 mM NaCl, there is no evidence for ATPase-mediated uptake in the halophyte, and at 50 mM there is excretion (Table 9.15).

Table 9.15 Net uptake of labeled sodium (Na^+) in a glycophyte, *Plantago media* (hoary plantain), and a halophyte, *Plantago maritima* (sea plantain), in the presence and absence of DES (diethylstilboestrol, an inhibitor of the plasma membrane ATPase)*.

	Plantago media		*Plantago maritima*	
NaCl (mM)	−DES	+DES	−DES	+DES
1	0.5	**2.8**	5.9	**2.7**
10	6.6	**27.7**	21.6	25.5
50	37.3	**121.1**	68.1	**82.5**

Source: De Boer (1985)

*The uptake was measured at three levels of NaCl in the nutrient solution and is expressed as μmol (g root dry mass)$^{-1}$) hour^{-1}. Values printed bold are significantly different from those to their immediate left

Table 9.14 Experimentally determined concentrations of sodium (Na^+) and potassium (K^+) ions in *Avena sativa* (oat) and *Pisum sativum* (pea) roots, compared with values predicted on the basis of the Nernst equation*.

	Oat		Pea	
Ion	Predicted	Experimentally determined	Predicted	Experimentally determined
K^+	27	66	73	75
Na^+	27	3	73	8

Source: Higginbotham et al. (1967)

*The latter values assume that no metabolic energy-dependent mechanism is involved in the transport of these cations. The membrane potential of oat and pea was −84 and −110 mV, respectively

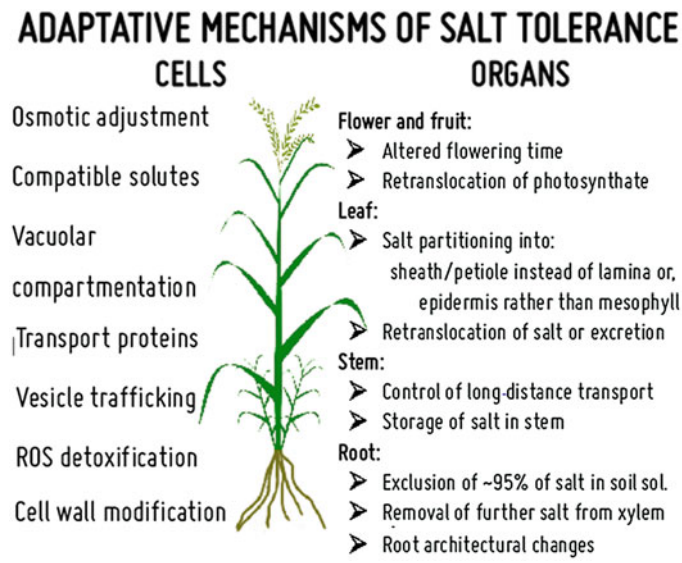

Fig. 9.29 Adaptive mechanisms of salt tolerance in glycophytes. On the left are listed the cellular functions that would apply to all cells within the plant. On the right are the functions of specific tissues or organs. Glycophytes exclude at least 95% of the salt in the soil solution, as plants transpire 20 times more water than they retain (modified after Munns and Gilliham 2015). *ROS* reactive oxygen species, *PGPR* plant growth-promoting rhizobacteria; copyright Trustees of The New Phytologist.

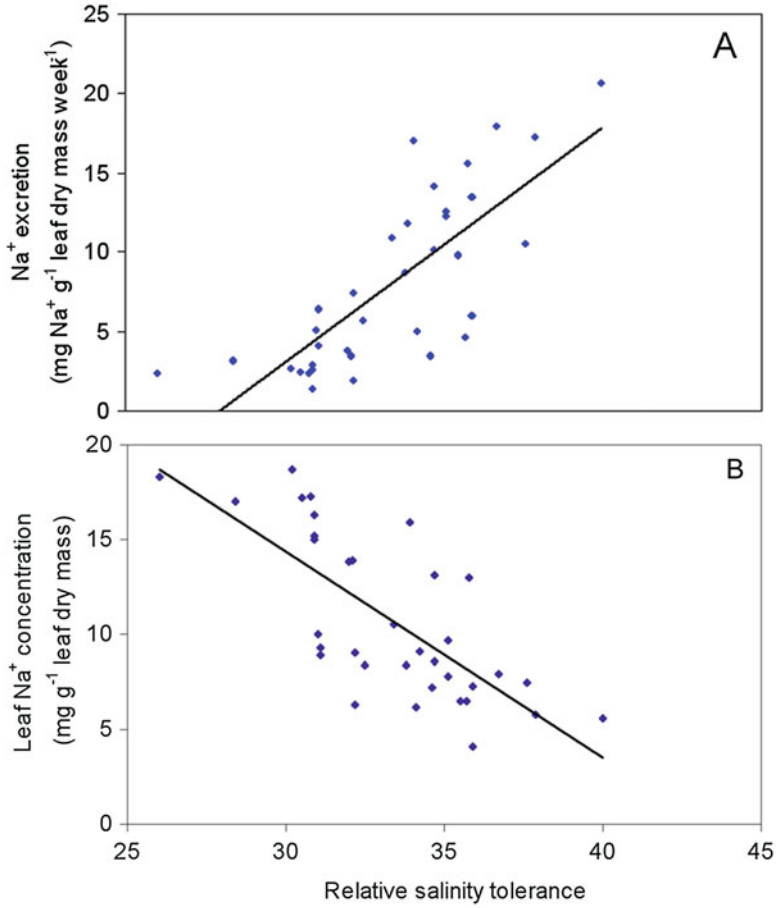

Fig. 9.30 (**A**) Leaf salt gland sodium (Na^+)-excretion rate and (**B**) leaf sap Na^+ concentration plotted against relative salinity tolerance of 35 *Cynodon* (bermudagrass) turfgrass cultivars. Relative salinity tolerance is the salinity level resulting in 50% shoot dry weight relative to that of the control; a broad range in salinity tolerance exists within the *Cynodon* genus (Marcum and Pessarakli 2006); copyright Crop Science Society of America.

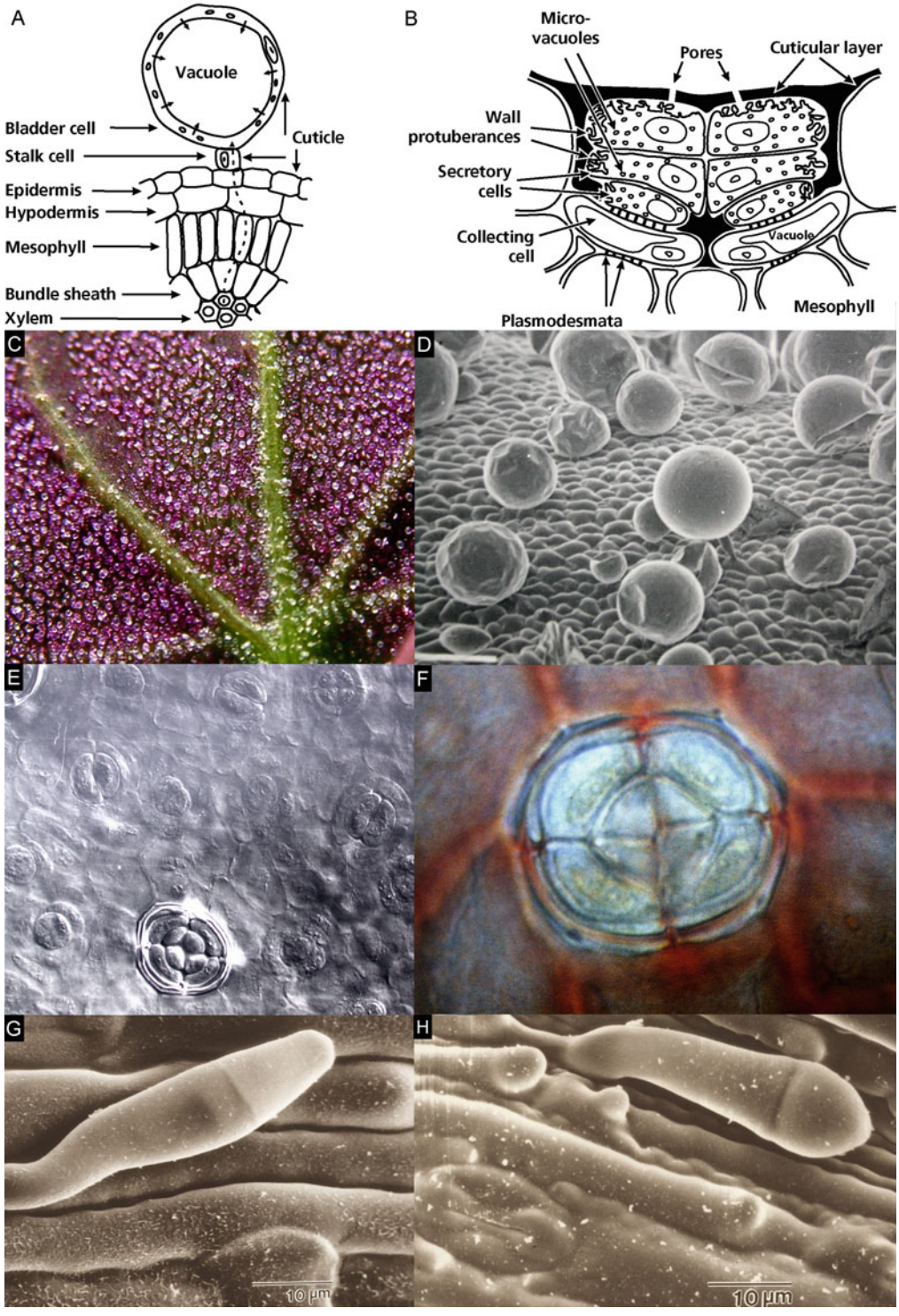

Fig. 9.31 Two schematic diagrams of structures involved in the excretion of salt to the leaf surface. (**A**) Diagram of a trichome of a leaf of an *Atriplex* (saltbush) species. (**B**) Diagram of a salt-excreting gland of *Tamarix aphylla* (athel pine) (after Esau (1977); reprinted with permission of John Wiley & Sons, Inc.). (**C**) Lower leaf surface of

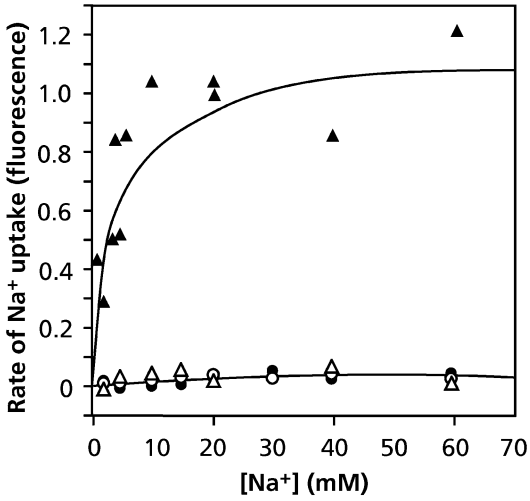

Fig. 9.32 Uptake of sodium (Na^+) in tonoplast vesicles of the glycophyte *Plantago media* (hoary plantain, circles) and the halophyte *Plantago maritima* (sea plantain, triangles). Tonoplast vesicles were isolated from plants grown in the absence (open symbols) or in the presence (filled symbols) of 50 mM NaCl (Staal et al. 1991); © Scandinavian Plant Physiology Society.

9.3.4.3 Energy-Dependent Salt Exclusion from the Xylem

Despite active salt exclusion at the root surface (Sect. 9.3.4.2), glycophytes do take up some NaCl, which is then excluded from the xylem in an oxygen-dependent process, *e.g.*, in the moderately salt-tolerant glycophyte *Lotus tenuis* (narrow-leaf bird's-foot trefoil) (Teakle et al. 2007). In *Arabidopsis thaliana*, Na^+ exclusion from the shoot is based on reabsorption of Na^+ from the xylem by surrounding xylem-parenchyma cells involving a specific Na^+ transporter (Davenport et al. 2007; Kronzucker and Britto 2011). Glycophytes, therefore, maintain a lower Na^+ concentration in their leaves, partly due to excretion by their roots and because of energy-dependent **exclusion from the xylem**.

9.3.4.4 Transport of Na^+ from the Leaves to the Roots and Excretion Via Salt Glands

Salt transported to the shoot via the transpiration stream may be exported again, via the phloem, to the roots. Using $^{22}NaCl$, this was shown for *Capsicum annuum* (sweet pepper) (Blom-Zandstra et al. 1998). For another glycophyte [*Lupinus albus* (white lupin)] this was determined by analyzing phloem sap, which exudes spontaneously from white lupin stems upon cutting (Sect. 4.5). Export of Na^+ to the roots may be followed by excretion, as shown for *Plantago media* (hoary plantain) (Table 9.15). Figure 9.29 summarizes the various traits in glycophytes that express some degree of salt tolerance (Munns and Gilliham 2015).

True halophytes may have **salt glands**, which **excrete** salt from their leaves. These may remove a major part of the salt arriving in the shoot via the transpiration stream, as shown for *Cynodon* (bermudagrass) turf cultivars (Fig. 9.30). We can estimate **salt exclusion** in the roots from the difference in net Cl^- uptake and the product of the transpiration rate and the Cl^- concentration in the root environment. It is substantial in *Avicennia marina* (gray mangrove), increasing from 90% at the lowest salinity level to 97% at 500 mM NaCl (Ball 1988). Exclusion involves active excretion from the roots, as in *Plantago* species (Table 9.15). Active excretion must incur respiratory costs, as discussed in Sect. 3.4.2.

Fig. 9.31 (continued) fresh leaves of *Atriplex pratovii* (Chenopodiaceae) with dense cover of salt bladders. Courtesy M. Wennemann & S.-W. Breckle, Department of Ecology, University of Bielefeld, Bielefeld, Germany. (**D**) Scanning electron micrograph showing salt bladders on a leaf of *Atriplex hortensis* (garden orache). Courtesy U. Schirmer & S.-W. Breckle, University of Bielefeld, Bielefeld, Germany. (**E**) Stages of development of salt glands on a leaf of *Limonium ramosissimum* (Algerian sea lavender). Courtesy W. Wiehe & S.-W. Breckle, University of Bielefeld, Bielefeld, Germany. (**F**) Salt gland on upper leaf surface *Acantholimon ulicinum* var. *creticum* (Plumbaginaceae), stained with Sudan red. Courtesy W. Wiehe & S.-W. Breckle, University of Bielefeld, Bielefeld, Germany. (**G**) Scanning electron micrograph showing a salt hair on a leaf of *Bouteloua eriopoda* (black grama). (**H**) Scanning electron micrograph showing a salt hair on a leaf of *Buchloe dactyloides* (buffalograss). G and H: courtesy K.B. Marcum, Arizona State University, Mesa, USA.

Salt removal from leaves involves special structures, specialized **trichomes** (**salt bladders**) or **salt glands** (Shabala et al. 2014). In *Atriplex* species (Chenopodiaceae), salt that arrives in the transpiration stream is transported via plasmodesmata to the cytosol of epidermal cells, and then to bladderlike cells on stalks (special trichomes) on the epidermal surface (Fig. 9.31A). The salt is pumped into the large vacuole of this bladder cell. In the end, the bladder may collapse and the salt is deposited on the leaf surface, where it gives the leaves a white appearance until washed away by rain. Leaves may also **excrete** salt in such a way that concentrated droplets fall from the leaves, as in *Tamarix usneoides* (South African salt cedar) (Wilson et al. 2017). True salt glands, as opposed to the trichomes of *Atriplex*, are found in *Tamarix usneoides* and *Tamarix aphylla* (athel pine) (Fig. 9.31B; Esau 1977). Salt is transported from mesophyll cells via plasmodesmata to two basal collecting cells that transport it to the secreting cells of the gland. These secreting cells are surrounded by a lipophilic layer, except where they are connected to the basal cells via plasmodesmata. In these secreting cells, salt is pumped into microvacuoles, which merge with the plasma membrane, and the salt is then exported to the apoplast. The invaginations in these cells suggest that active membrane transport is involved as well. The salt diffuses via the apoplast to a pore in the cuticle, where it is deposited on the leaf surface. The waxy layer that surrounds the secreting cells prevents back-diffusion to the mesophyll cells.

What might be the advantage of salt excretion from the leaves over salt excretion from the roots? If roots excluded all the salt that arrives via mass flow at their surface, then the salt concentration in the rhizosphere would rapidly rise to very high levels. In the absence of a substantial removal from the rhizosphere by bulk flow of less saline water, the local accumulation of salt would continue to reduce water potential and aggravate the problems associated with water uptake (Passioura et al. 1992). A high water-use efficiency in combination with salt exclusion, therefore, has advantages over exclusion only. Mangrove species with the highest water-use efficiency are also the most salt-resistant ones (Ball 1988).

9.3.4.5 Compartmentation of Salt Within the Cell and Accumulation of Compatible Solutes

Salt resistance also involves the **compartmentation** of the potentially toxic ions in the vacuole and the capacity to produce nontoxic, **compatible solutes** in the cytoplasm (Sect. 5.3). Compartmentation in the **vacuole** is achieved by an active mechanism that is induced in halophytes such as *Plantago maritima* (sea plantain) (Fig. 9.32) and *Mesembryanthemum crystallinum* (common iceplant) (Barkla et al. 1995), but not in glycophytes, such as *Plantago media* (hoary plantain), in the presence of NaCl in the root medium. A specific vacuolar ATPase is involved in compartmentalizing Na^+ in the vacuole in *Salicornia europaea* (Lv et al. 2017).

Some moderately salt-resistant glycophytes, for example *Hordeum vulgare* (barley) cultivars, also accumulate some salt in their leaves (Fig. 9.29; Munns and Gilliham 2015). Using X-ray diffraction, it can be shown that Cl^- predominantly accumulates in the vacuoles of the epidermis cells of leaf blades and sheaths. To a smaller extent Cl^- is also found in the mesophyll cells of the leaf sheath, whereas the concentration remains low in the mesophyll cells of the leaf blade, even after exposure to 50 mM NaCl in the root environment for 4 days (Huang and Van Steveninck 1989).

9.3.5 Flooded Soils

The absence of oxygen in the soil causes a drop in redox potential, due to microbial activity. At a low redox potential, NO_3^- rapidly disappears due to its use as an electron acceptor by **denitrifying bacteria**, and $\mathbf{NH_4^+}$ is the main source of inorganic N for the plant (Kirk et al. 2014). Iron and Mn are also reduced. These reduced forms are much more soluble and potentially toxic to the plant. Sulfate (SO_4^{2-}) is also used as an alternative electron acceptor by specialized bacteria,

leading to the formation of S^{2-}, which is an inhibitor of cytochrome oxidase (Sect. 3.3.6; Kirk et al. 2014). Thus, the availability of many ions is affected by the redox potential which leads to shortage of some nutrients and potentially toxic levels of others. Toxicity is largely prevented by oxidation, possibly followed by precipitation of these ions in the oxygenated rhizosphere (Bravin et al. 2008). **Oxygenation of the rhizosphere** of flooding-resistant species is due to the presence of an **aerenchyma** (Voesenek and Bailey-Serres 2015), which allows root respiration to continue and leads to detoxification of potentially toxic ions in the rhizosphere (Sects 3.4.1.4 and 10.2.3; Kirk and Kronzucker 2005).

9.4 Plant Nutrient-Use Efficiency

Plants differ both in their capacity to acquire nutrients from the soil (Sect. 9.3) and in the amount of nutrients they need per unit growth or photosynthesis, the nutrient concentrations in their organs, and the time and extent to which they withdraw nutrients during leaf senescence before leaf abscission. In this Section, we discuss several approaches for analyzing the efficiency with which plants utilize nutrients to produce new biomass. Whole-plant nutrient-use efficiency (*NUE*) addresses processes related to carbon gain and loss, whereas photosynthetic nitrogen-use efficiency (Sect. 2.6) addresses only the instantaneous use of N for photosynthetic carbon gain. Historically, N has received most attention, as explained in Sect. 9.1, but most plant species occur in biodiverse regions where P is the major nutrient limiting plant productivity. Because many plant species in P-impoverished biodiverse landscapes function fundamentally different from what we know of species in landscapes where N limits plant productivity (Prodhan et al. 2019), they deserve special attention in this Section.

9.4.1 Variation in Nutrient Concentration

9.4.1.1 Leaf Nutrient Concentration

Plants differ in the concentration of mineral nutrients in their tissue, depending on environment, allocation to woody and herbaceous tissues, developmental stage, and species (Fig. 9.33).

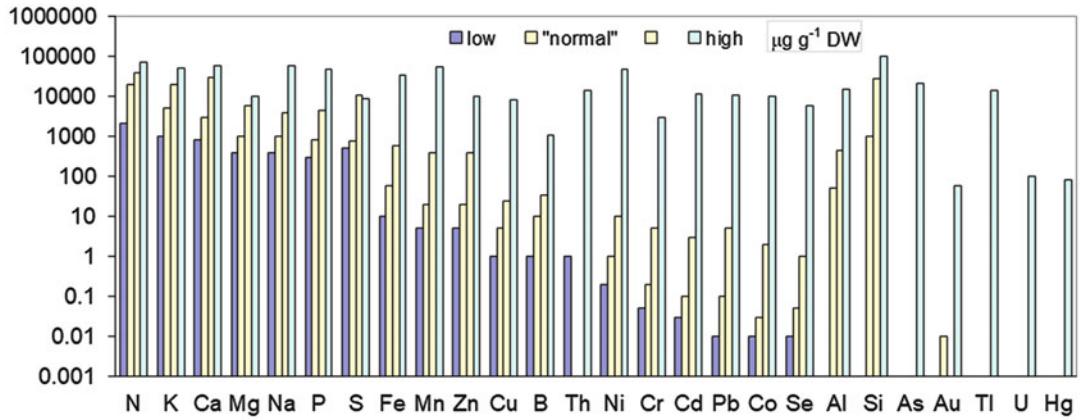

Fig. 9.33 The range of concentrations of minerals as determined in plant dry matter. The two middle bars refer to concentrations commonly observed in healthy plants; the bar at the left refers to plants that are either very efficient at using a specific nutrient, plants that exhibit a low concentration because their leaves are severely deficient or senescent, or because the plants exclude certain elements; the bar at the right refers to plants exhibiting exceptionally high concentrations of an element, *e.g.*, in halophytes or metallophytes. Based on numerous references, including Bell (1997); Anderson et al. (1998); Broadley et al. (2003, 2004); Baxter et al. (2008); Salt et al. (2008); White et al. (2012); Hayes et al. (2014); Neugebauer et al. (2018).

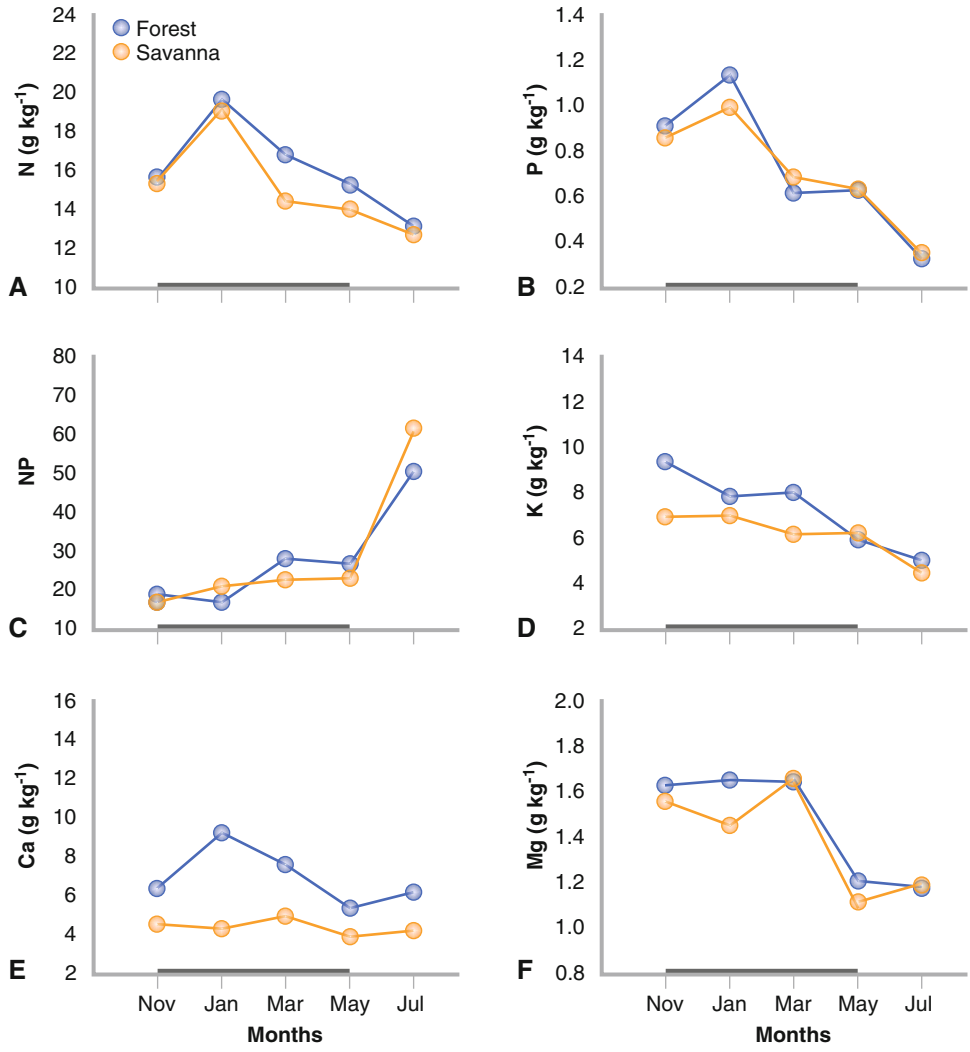

Fig. 9.34 Seasonal variation in leaf nitrogen (N), phosphorus (P), potassium (K), calcium (Ca), and magnesium (Mg) of congeneric species in two habitats in Central Brazil. The increase in N:P indicates that P is remobilized more efficiently than N is, because plant productivity is limited by P, rather than N. Savanna and forest species do not differ in their seasonal behavior. Horizontal solid bar indicates the wet period (Rossatto et al. 2013); copyright © 2013, Springer-Verlag Berlin Heidelberg.

Nitrogen, P, and K are the nutrients that most frequently limit plant growth. However, as explained in Sect. 9.2.1.1 and Fig. 9.1A, N tends to limit plant productivity on young soils, whereas P becomes increasingly limiting as soils age. The presence of a specific mineral in plant tissues does not imply that the plant needs this mineral for growth. For example, we find Cd in leaves of plants growing on Cd-polluted soil, but it is *not* a nutrient for any plant (Sect. 9.3.3). Similarly, high Na concentrations are not required for growth (Sect. 9.3.4).

Nutrient concentrations change predictably with plant development. Especially in woody plants, the whole plant **C:N ratio** increases with increase in plant age, as the ratio of woody mass to physiologically active leaf and root mass increases. Nutrients associated with **metabolism** (*e.g.*, N, P,

and K) have highest concentrations when a leaf or other organ is first produced; then concentrations decline, first as the concentration becomes diluted by increasing quantities of cell-wall material during leaf expansion, then by resorption of nutrients during senescence (Fig. 9.34). **Calcium**, which is largely associated with cell walls and is phloem-immobile (Sect. 5.2) and therefore not resorbed (Sect. 9.4.3), increases continuously throughout leaf development.

Plant organs differ predictably in nutrient concentrations: leaves have higher concentrations of nutrients associated with **metabolism** (N, P, and K) and lower concentrations of Ca than do **woody stems**; roots have intermediate concentrations. Whole-plant nutrient concentrations, therefore, differ among species and environments, depending on relative allocation to these organs. Environment strongly affects plant nutrient concentration by changing both allocation among organs and the composition of individual tissues. The major environmental effect on nutrient composition is to alter the concentration of nutrients associated with **metabolism**. Plants have high concentrations of N, P and K when conditions are favorable for growth (*e.g.*, with adequate water and nutrients) (Niklas and Cobb 2005). The balance of available nutrients in the environment then alters the proportions of these nutrients. Whole-plant biomass **N:P ratios** [g N (g P)$^{-1}$] may vary up to 50-fold, due to differences in root allocation, nutrient uptake, biomass turnover, and reproductive output (Güsewell 2004). At the vegetation level, N:P ratios <10:1 and >20:1 tend to correspond with N- and P-limited biomass production, respectively, as evidenced by short-term fertilization experiments. N:P ratios are, on average, higher in graminoids than in forbs and higher in stress-tolerant species than in ruderals; they correlate negatively with the maximum relative growth rates of species and with their N-indicator values (Sect. 10.3). At the vegetation level, N:P ratios tend to correlate negatively with biomass production; high N:P ratios promote graminoids and stress-tolerating species, relative to other species (Güsewell 2004). The N:P ratios provide useful information when used in a comparative context, but there are unlikely to be universal cut-off values that determine the type of nutrient limitation. Determining a cut-off value to indicate N or P limitation should be a site-specific endeavor (Ostertag and DiManno 2016). Trends persist across taxonomic groups, and presumably reflect both acclimation and adaptation to low soil P availability. Higher leaf N and P concentrations compensate for slow metabolic rates at low temperatures, and older soils tend to exhibit lower P availability, and hence differences in N:P ratio between tropical and temperate regions reflect major differences in soils, rather than climate (Hedin 2004; Vitousek et al. 2010).

There are striking differences in biochemical allocation of P among species from young and old landscapes. For example, Proteaceae from severely P-impoverished environments in southwestern Australia replace most of their phospholipids by lipids that do not contain P during leaf development (Lambers et al. 2012b; Kuppusamy et al. 2014). Since phospholipids comprise about 20% of all P in leaves (Veneklaas et al. 2012), this is a major saving. More importantly, these plants function at much lower levels of ribosomal RNA (rRNA) than *Arabidopsis thaliana* (Sulpice et al. 2014); rRNA is the largest organic P fraction in leaves (Box 9.1; Veneklaas et al. 2012). These species also preferentially allocate P to their mesophyll cells (Hayes et al. 2018), where it is needed to sustain photosynthesis (Sects 2.2.1.3, 2.2.1.4 and 2.4.2). This is not a family trait, because Proteaceae species from South America that naturally occur on soils with much higher P concentrations do not show such preferential allocation of P to mesophyll cells. Conversely, species in other families in southwestern Australia, Borneo, and southeastern Brazil that occur on severely P-impoverished soils also exhibit preferential allocation of P to mesophyll cells (Tsujii et al. 2017a; Guilherme Pereira et al. 2018).

Box 9.1: Phosphorus Fractions in Leaves and Photosynthetic Phosphorus-Use Efficiency

When phosphorus (P) is available to plants in excess of what they need for their immediate growth, the excess is stored as inorganic P (Pi) in vacuoles (luxury consumption). Whereas plants need Pi for their metabolism, most of the Pi in leaves of plants with an excess of P is metabolically inactive. As a result, the Pi fraction changes the most as dependent on P supply. The other fractions comprise three organic P pool, nucleic acid P [mainly ribosomal RNA (rRNA)], phospholipids, and small metabolites, *e.g.*, intermediates of the Calvin-Benson cycle and glycolysis, ATP and NADH (ester P; Box Fig. 9.1). When isolating these fractions, there often is a residual fraction, which is less well-defined, but would include phosphorylated proteins.

Proteaceae from severely P-impoverished habitats show relatively fast rates of photosynthesis at very low eaf P concentrations, and thus exhibit an exceptionally high photosynthetic P-use efficiency (PPUE) (Denton et al. 2007; Lambers et al. 2012b). Plants that achieve a very high PPUE must have economized their P-allocation pattern. So, which of the four fractions shown in Box Fig. 9.1 is/are there in smaller amounts compared with plants with a lower PPUE? In their natural environment, these Proteaceae never accumulate Pi to a major extent, but even when supplied with abundant P, they preferentially allocate this to their mesophyll cells (Shane et al. 2004b; Hayes et al. 2018). In this way, they invest P where it can be used towards photosynthetic carbon assimilation, rather than store it in metabolically-inactive epidermal cells (Hayes et al. 2018). This is not a common family trait, because Proteaceae that occur on soils with more P in South America do not show preferential P allocation (Box Fig. 9.2).

Proteaceae from P-impoverished soils also replace most of their phospholipids by

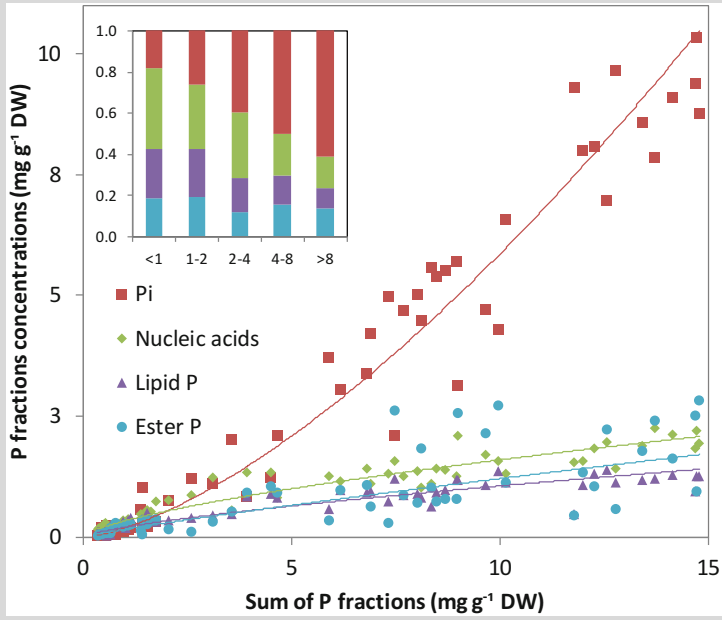

Box Fig. 9.1 Phosphorus (P) pools in photosynthetic tissues of a wide range of plants grown at different P supply. The inset summarizes relative proportions of different P pools as the total P concentration increases; the colors of the bars correspond with the colors in the main figure (Veneklaas et al. 2012); copyright Trustees of The New Phytologist.

(continued)

Box 9.1 (continued)

lipids that do not contain P, *i.e.* sulfolipids and galactolipids (Lambers et al. 2012b). Other species may also replace their phospholipids, but they do so as part of a P-starvation response, rather than a P-economizing strategy (Lambers et al. 2015b). Proteaceae from severely P-impoverished habitats function at very low levels of rRNA (Sulpice et al. 2014), and hence they exhibit major savings in the nucleotide pool, which is the largest organic P fraction (Box Fig. 9.1). The fourth fraction, ester P, is one that shows no difference comparing Proteaceae from severely P-impoverished habitats and other plants.

Maintaining normal levels of intermediates of carbon metabolism (P esters) makes perfect sense, given that these metabolites are substrates for a range of enzymes. Lowering the metabolite concentrations would curtail the activity of the enzymes that use these substrates. This might be compensated by functioning at higher levels of enzymes, but this would require more protein synthesis, and hence incur costs in terms of rRNA, and thus P (Lambers et al. 2015b; Box Fig. 9.3).

The biochemical traits underpinning an extremely high PPUE have been studied in detail in Proteaceae (Lambers et al. 2015a). However, there is evidence that co-occurring species in several other families (*e.g.*, Guilherme Pereira et al. 2018) and species that occupy other P-impoverished habitats such as tropical rainforests in Borneo (*e.g.*, Tsujii et al. 2017b) share at least some of the traits portrayed here.

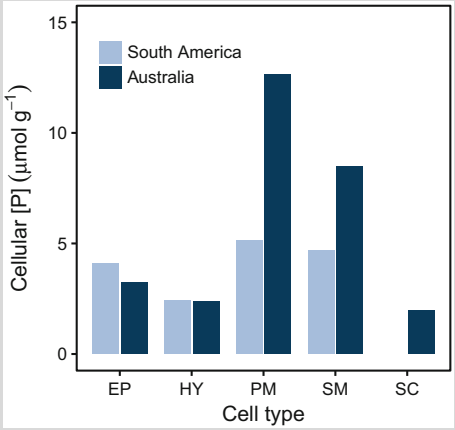

Box Fig. 9.2 Leaf cell-specific phosphorus (P) concentrations; comparing Proteaceae from P-impoverished habitats in Australia with those from P-rich habitats in South America. (**A**) Mean cell-specific P concentrations of Australian and South American species, illustrating differences among cell types within each region. Different sets of cell types are shown, because of differences in leaf anatomy. (**B**) Mean cell P concentration of the common cell types between Australian and South American species, illustrating differences between regions. Common cell types are those found across three or more species in both regions. The hypodermis (HY) is not shown, because it is only found in one South American species. *EP* epidermis, *IP* internal parenchyma, *PM* palisade mesophyll, *SC* sclerenchyma, *SM* spongy mesophyll (after Hayes et al. 2018); © John Wiley & Sons Ltd.

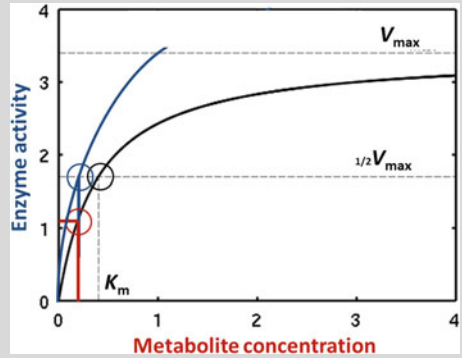

Box Fig. 9.3 Effects of metabolite concentrations and amount of enzyme to illustrate the effect of changes in the concentration of phosphate esters on photosynthetic phosphorus (P)-use efficiency (PPUE). The black circle denotes the activity of an enzyme converting a phosphate ester, assuming the metabolite concentration is close to the K_m value of the enzyme for the phosphate ester, which is commonly the case. Reducing the metabolite concentration would 'economize' on P, but inevitably reduce the rate of conversion catalyzed by the enzyme, as illustrated by the red circle. To maintain the original rate of conversion (blue circle) would require more enzyme protein (blue line), which would require greater investment in ribosomal RNA (rRNA). In most leaves, rRNA is a much greater proportion of total leaf P than the P ester pool, and hence reducing the P ester pool does not lead to a greater PPUE, but has the exact opposite effect. Reducing the P ester pool is a common P-starvation response in plants, but is not what occurs in highly P-efficient Proteaceae (Lambers et al. 2015a); copyright © 2015, Springer Nature.

The P-allocation traits of Proteaceae, and co-occurring species in other families (Yan et al. 2019), allow them to photosynthesize at rates that are similar to species with much higher leaf P concentrations, and to exhibit extremely high photosynthetic P-use efficiencies (*PPUE*) (Denton et al. 2007; Sulpice et al. 2014; Guilherme Pereira et al. 2019). The low rRNA levels in leaves of Proteaceae from severely P-impoverished landscapes, as expected, are associated with low leaf protein and N concentrations, yet the proteins required for photosynthesis are found in similar abundance as in *Arabidopsis thaliana* (Sulpice et al. 2014). Interestingly, when one of these P-efficient species, *Hakea prostrata* (harsh hakea), is provided with abundant N or S in nutrient solution, it does not take up any of this, instead maintaining steady N and P concentrations in all its organs (Prodhan et al. 2016, 2017). This is unlike what we typically know for species that evolved in landscapes where N is limiting plant productivity, but is likely common for species in other P-impoverished habitats, *e.g.*, tropical forests in China (Mo et al. 2015). A picture is beginning to emerge showing that the control of mineral nutrition of plants that evolved in P-impoverished landscapes differs fundamentally from that of plants that occur in habitats where N tends to limit plant productivity (Lambers et al. 2015b; Prodhan et al. 2019).

Differences among plants in terms of nutrient allocation may relate to accumulation of certain compounds in the cytoplasm for osmotic functions (N-containing **compatible solutes**) and in vacuoles for storage functions (*e.g.*, Pi, NO_3^-, and **vegetative storage proteins**; Sect. 10.4.3). Specific strategies of chemical defense (*e.g.*, N-containing alkaloids, nonprotein amino acids, cyanogenic glycosides, and S-containing glucosinolates; Sect. 13.3) also affect nutrient-allocation patterns.

When N or P supply declines relative to plant demand, most plants show the following sequence of events:

1. Decrease in vacuolar reserves of nitrate (Andrews et al. 2013) or Pi (Yang et al. 2017), with little or no effect on growth.
2. Continued reduction in tissue nutrient concentrations, especially in older leaves and stems, reduced rates of leaf growth, increased nonstructural carbohydrate concentrations, reduced rates of photosynthesis, senescence of older leaves, and reallocation of reserves to compensate for reduced nutrient uptake (increased root mass ratio and increased root absorption capacity) (Vos and Van Der Putten 1998; Dissanayaka et al. 2018).
3. Greatly reduced rates of photosynthesis and nutrient absorption, dormancy or death of meristems (Chapin 1980).

9.4.1.2 Leaf Nutrient Requirement

Species differ in their nutrient requirement for maximum growth. For example, the leaf **Ca concentration** at which 90% of the maximum yield is achieved is about twice as high for **dicots** as for **monocots** (Table 9.16; Loneragan 1968). In accordance, when comparing graminoids and forbs at similar sites, the forbs invariably have higher concentrations of both Ca and Mg (Meerts 1997). The root cation-exchange capacity for monocotyledons species is significantly smaller than for dicotyledonous species (Woodward et al. 1984). The Ca requirement of monocotyledons is relatively low, because of their low concentration of **cell wall pectate** (Sect. 10.2.2.2) (White and Broadley 2003).

The leaf **P concentration** at which 90% of the maximum yield occurs, is greater for many **crop legumes** than for **nonlegumes** (Fig. 12.5). A high P requirement is partly accounted for by

Table 9.16 Effect of the calcium concentration in the nutrient solution on the growth and the calcium concentration in the shoots of a monocotyledonous [*Lolium perenne* (perennial ryegrass)] and a dicotyledonous [*Solanum lycopersicum* (tomato)] species.

	Calcium supply (μM)				
Species	0.8	2.5	10	100	1000
Growth rate (% of maximum value)					
Lolium perenne	42	100	94	94	93
Solanum lycopersicum	3	19	52	100	80
Calcium concentration (μmol g^{-1} dry mass)					
Lolium perenne	15	18	37	92	270
Solanum lycopersicum	50	32	75	322	621

Source: Loneragan (1968); Loneragan and Snowball (1969)

the use of P for rRNA to synthesize nitrogenase and other proteins in nodules as well as with the high energetic requirement and use of phosphorylated intermediates to fix N_2 in legume nodules (Sect. 12.3.4; Raven 2012). It is likely also associated with the fast-growing strategy of many legumes (Sect. 10.6; Sprent 1999) and with a leaf P-allocation pattern that is relatively inefficient compared with that of Proteaceae (Yan et al. 2019).

From a biochemical point of view, we expect all plants to require similar amounts of N, P, S, and so on, to make a unit of growth, because they are constructed in a similar manner. However, there are distinct differences between species, depending on their ecological strategy and evolutionary background. For example, some slow-growing species from severely P-impoverished soils maintain relatively fast rates of photosynthesis at extremely low leaf P concentrations, because of the way they invest and allocate P (Sect. 9.4.1.1). There are also differences, because specific enzymes require a specific ion. For instance, **Ni** is an essential element for **urease**, which hydrolyzes urea to CO_2 and H_2O. Urease is required in all plants, but in greater amounts in those legumes that produce ureides when grown symbiotically with rhizobia (Sect. 12.3.4; de Macedo et al. 2016). Thus, there are quantitatively different metabolic requirements. Apart from these differences, variation in nutrient requirement and nutrient productivity (Sect. 9.4.2.1) depend much more on the balance between requirements for protein synthesis for new growth and N storage (Sect. 10.4).

9.4.2 Nutrient Productivity and Mean Residence Time

9.4.2.1 Nutrient Productivity

A measure of the efficiency of nutrient use to produce new biomass is **nutrient productivity** (*NP*) (Ingestad and Ågren 1995), the ratio of relative growth rate (*RGR*, mg g^{-1} day^{-1}) to whole plant nutrient concentration in the plant tissue (*PNC*, mol g^{-1}). For example, N productivity (*NP*, mg mol^{-1} N day^{-1}) is:

$$NP = RGR/PNC \tag{9.1}$$

where *PNC* is the plant N concentration (*i.e.* total plant N per total plant mass). When grown at an optimum nutrient supply, plants differ widely in their *NP* (Fig. 9.35; Poorter et al. 1990). A higher *NP* is associated with rapid growth, a relatively large investment of N in photosynthesizing tissue, an efficient use of the N invested in the leaves for the process of photosynthesis, and a relatively small use of carbon in respiration (Fig. 9.35). C_4 species have a higher *NP* than C_3 species under optimal N supply which reflects their lower N requirement for photosynthesis (high *PNUE*) (Sect. 2.6.1).

Nitrogen productivity shows saturation and sometimes an optimum curve, when plotted as a function of the N supply to the plant (Van der Werf et al. 1993). The decrease in *NP* above the maximum value is due to a decrease in the rate of photosynthesis per unit of leaf N at high leaf N which reflects increased allocation of N to storage (Sect. 10.4). The decrease when the N supply is

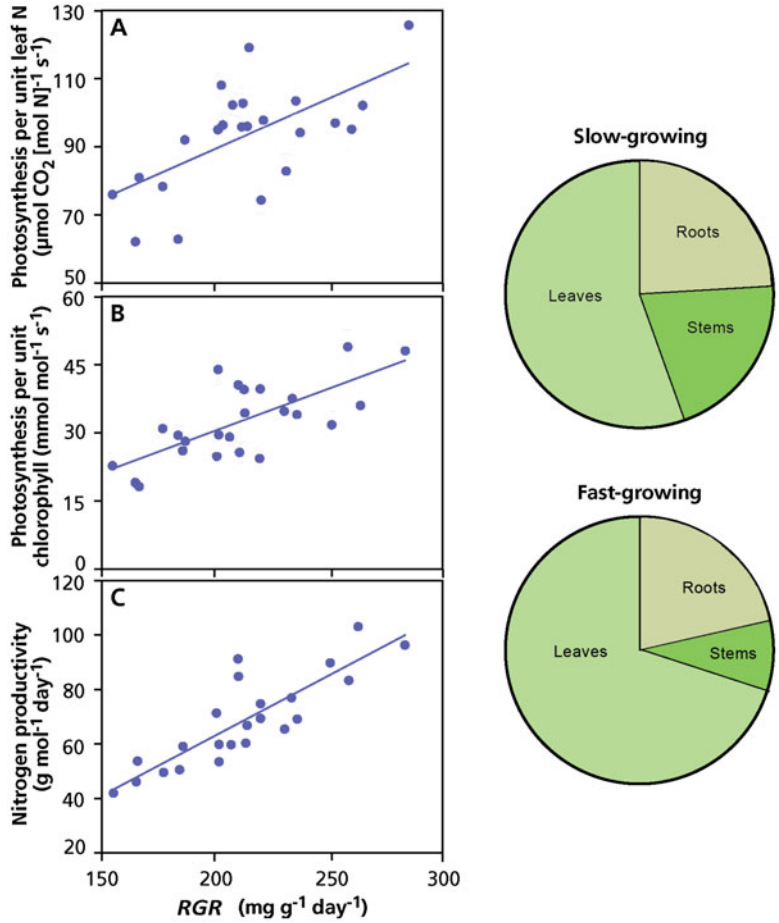

Fig. 9.35 (A) Photosynthetic nitrogen (N)-use efficiency, (**B**) photosynthesis per unit chlorophyll, and (**C**) N productivity of herbaceous plant species differing in their inherent relative growth rate (*RGR*), grown with free access to nutrients in a growth room. The physiological background of the higher N productivity of fast-growing species is their greater investment of N in leaves, as opposed to roots and stems (circles at the right), and their faster rate of photosynthesis per unit N in the leaves (photosynthetic N-use efficiency (after Poorter et al. 1990); copyright American Society of Plant Biologists.

less than that at the maximum value for *NP* is largely due to greater investment of N in nonphotosynthetic tissue (Sect. 10.5.4).

9.4.2.2 The Mean Residence Time of Nutrients in the Plant

Although the nutrient productivity gives a good indication of a plant's **instantaneous nutrient-use efficiency** (*NUE*), it does not provide insight into a plant's **long-term performance** in a natural habitat. To develop such insight, we expand the concept of nutrient-use efficiency to consider the time during which nutrients remain in the plant to support productivity. Plant **nitrogen-use efficiency** (g g^{-1} N), which is the product of the **nitrogen productivity** (g g^{-1} N $year^{-1}$) (as defined in Sect. 9.4.2.1, but is now determined over much longer periods; say one year), and the **mean residence time** (MRT; year) of that nutrient in the plant (Berendse and Aerts 1987):

$$NUE = NP \times MRT$$

The mean residence time is the average time the nutrient remains in the plants, before it is lost due to leaf shedding, herbivory, root death, and so on.

The N-use efficiencies of evergreen heathland shrub species and that of a co-occurring deciduous grass species are remarkably similar, but the underlying components differ (Table 9.17; Aerts 1990). **Evergreen** species achieve their *NUE* with a low N productivity and a high mean residence time, whereas **deciduous** species have a

Table 9.17 The long-term nitrogen productivity (*NP*), the mean residence time of nitrogen (*MRT*) and the nitrogen-use efficiency (*NUE*) of an evergreen heath-land shrub species [*Erica tetralix* (crossleaf heath)] and a co-occurring deciduous grass species [*Molinia caerulea* (purple moorgrass)].

	Erica tetralix	*Molinia caerulea*
Nitrogen productivity (g g^{-1} N $year^{-1}$)	77	110
Mean residence time (year)	1.2	0.8
Nitrogen-use efficiency (g g^{-1} N)	90	89

Source: Aerts (1990)

considerably higher N productivity, but a lower mean residence time. In competition experiments with the species from Table 9.17, the grass wins at a relatively high N supply, because of its higher N productivity. At a low N supply, the competitive ability of the evergreen shrub is greater, because of its long mean residence time of N in the plant. A high mean residence time is the most important mechanism for nutrient conservation in infertile sites (Miatto et al. 2016). Both adaptation and acclimation contribute to the greater mean residence time in infertile sites. Such sites are typically dominated by evergreen shrubs and trees, and both grasses and evergreen trees and shrubs adapt to low nutrient supply through increases in leaf longevity (Westoby et al. 2002).

It is interesting that the plant features that favor a slow rate of nutrient loss (high mean residence time) also decrease the rate of **decomposition** of leaf litter. This tends to aggravate the low availability of nutrients in the already nutrient-poor environments (Sect. 18.3.2). As we discuss in Sects 12.2.4 and 18.2.4, however, some species can make use of nutrients in leaf litter even before it is fully decomposed.

9.4.3 Nutrient Loss from Plants

Nutrient loss is just as important as nutrient uptake in determining the **nutrient budgets** of perennial plants; however, we know much less about the controls over nutrient loss.

9.4.3.1 Leaching Loss

Leaching accounts for about 15% of the N and P and half the K returned from aboveground plant parts to soil (Table 9.18; Chapin 1991), with the remainder coming from senesced leaves and stems. **Leaching** losses can be an even larger proportion (25–55% of nutrient loss from leaves), especially when there are high concentrations of soluble nutrients in the cell walls of leaves, for example, during rapid leaf production or senescence and when plants grow under conditions of high **nutrient availability**. Leaching rate is greatest when rain first hits a leaf, then declines exponentially with continued exposure to rain (Tukey 1970). The frequency of rainfall is, therefore, more important than its intensity in determining leaching loss. **Deciduous** leaves have a greater leaching loss than do **evergreens**, because of their higher nutrient concentrations. This is compensated, however, by the greater time of exposure to leaching in evergreen plants, so that leaching constitutes a similar proportion of aboveground nutrient loss by evergreen and deciduous forests (Table 9.18).

Table 9.18 Nutrients leached from the canopy (throughfall) as a percentage of the total aboveground nutrient return from plants to the soil for 12 deciduous and 12 evergreen forests.

	Throughfall (% of annual return)	
Nutrient	Evergreen forests	Deciduous forests
N	1	15
P	15	15
K	59	48
Ca	27	24
Mg	33	38

Source: Chapin (1991)

The magnitude of nutrient loss by leaching decreases in the order K > Ca > N = P which reflects the greater mobility of monovalent than divalent cations, and the greater susceptibility to loss of inorganic than of organically bound nutrients. It was initially thought that one explanation for the scleromorphic leaves with thick

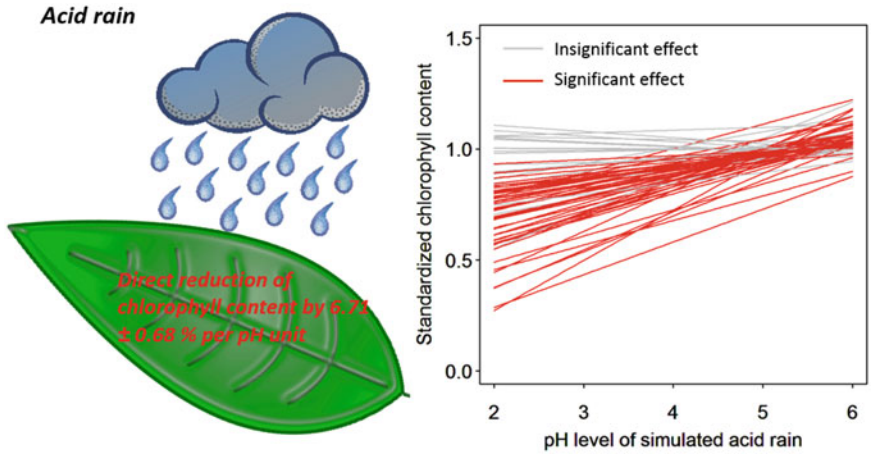

Fig. 9.36 The effect of acid rain on standardized leaf chlorophyll content per unit biomass. Linear regression between pH levels of simulated acid rain and standardized chlorophyll content for each species. Red lines indicate a significant relationship and grey lines indicate an insignificant relationship (Du et al. 2017); © 2017 Elsevier B.V. All rights reserved.

cuticles in nutrient-poor sites was prevention of leaching loss (Loveless 1961); however, there is no relationship between cuticle thickness or scleromorphy and the susceptibility of leaves to leaching loss (Sects 5.5.4.5 and 5.8.2). These leaf traits are more likely selected for their importance in withstanding unfavorable conditions during the nongrowing season, and reducing leaf loss to herbivores and pathogens (Sect. 13.3.2; Read et al. 2006).

Acid rain increases leaching of cations, particularly of Ca (Chapin 1991), because hydrogen ions in the rain exchange with cations held on the cuticular exchange surface and because acidity alters the chemical nature of the cuticle (Barker and Ashenden 1992). Anthropogenic emissions in China have resulted in widespread acid rain since the 1980s. Data on experiments of simulated acid rain, by directly exposing plants to acid solutions with varying pH levels, to assess the direct effect of acid rain on leaf chlorophyll concentrations indicate that acid rain substantially reduces leaf chlorophyll concentration by 6.7% per pH unit across 67 terrestrial plants in China (Fig. 9.36; Du et al. 2017). The effects of acid rain on leaf chlorophyll concentrations are similar for trees, shrubs, and herbs, but they vary across functional groups. Deciduous species are more sensitive to acid rain than evergreens. If the decrease in leaf chlorophyll concentration is indicative for leaf damage and loss of productivity, these findings imply a production loss due to foliage damage by acid rain.

9.4.3.2 Nutrient Loss by Senescence

On average, 62% of the N content and 65% of the P content of **leaves** is resorbed during senescence and used to support further plant growth (Vergutz et al. 2012). For the leaf K and Mg content, these values are 70% and 29%, respectively. By contrast, Ca, which is immobile in the phloem (Sect. 4.2), is barely resorbed (Table 9.19; Vergutz et al. 2012). N : P resorption ratios vary at the global scale, increasing with latitude and decreasing with mean annual temperature and precipitation. In general, tropical sites have N : P resorption ratios of < 1, and plants growing on highly weathered soils maintain the lowest N : P resorption ratios (Reed et al. 2012; Hayes et al. 2014). These correlations with climatic variables likely reflect that soils in the tropics tend to be more P impoverished, and, therefore, plant productivity is limited by P, rather than N. Nutrient-remobilization efficiency strongly depends on nutrient

Table 9.19 Nitrogen (N), phosphorus (P), potassium (K), calcium (Ca), and magnesium (Mg)-resorption efficiency of different growth forms.

Resorption efficiency	Climate classification	Conifers	Ferns	Forbs	Graminoids	Deciduous angiosperms	Evergreen angiosperms
N	A		53	61	68	44	50
	B			69	70	62	61
	C	56	48	70	75	58	55
	D	68	67	73	73	64	62
	E			70	73	68	70
P	A		63	77	79	55	59
	B				82	65	
	C	68	64	64	79	51	52
	D	72	75	77	83	58	71
	E			76	80	66	71
K	A			62		45	52
	B				67		
	C	31			85	61	41
	D	79		92		77	87
	E			74	77	49	58
Ca	A			31		11	1
	B				42		
	C				51	5	0
	D	0					
	E			18	−32	−9.1	−65
Mg	A			31		14	15
	B				42		
	C					32	−7
	D	39		34			
	E			34	32	13	44

Source: Vergutz et al. (2012)

Note: Climate classifications follow Köppen (1931): A, tropical/megathermal; B, dry (arid and semiarid, including desert and steppe climates, where precipitation is less than the potential evapotranspiration); C, temperate/mesothermal (including Mediterranean, oceanic, humid subtropical, and subpolar oceanic climates); D, continental/microthermal; and E, polar. Empty cells mean that no data are available

availability, more so for P than for N (Fig. 9.37; Hayes et al. 2014).

Similar variation as for nutrient-resorption efficiency occurs with respect to the terminal nutrient concentration in senesced leaves (**resorption proficiency**). Concentrations of 0.5 mg N g^{-1} dry mass and 0.03 mg P g^{-1} dry mass in senesced leaves are considered the ultimate potential resorption of these nutrients in woody perennials (Table 9.20). Resorption efficiency of both N and P is highest in graminoids (Vergutz et al. 2012); N-resorption efficiency is higher in deciduous shrubs and trees than it is in evergreens, although the difference is small compared with differences in mean residence time (Table 9.19). Evergreen species have a greater ability to reduce the mass-based P concentration in senescing leaves than do deciduous species (greater P-resorption proficiency) (Table 9.20). On nutrient-rich sites, larger *quantities* of nutrients are generally withdrawn from the leaves and larger *quantities* remain in senesced leaves, compared with leaves of plants growing in infertile sites (Richardson et al. 2005; Hayes et al. 2014; Tsujii et al. 2017b). The proportion of P resorbed is much greater on infertile sites, whereas for N that pattern is less clear (Hayes et al. 2014). Thus, the nutrient concentrations of litter are greater on more fertile sites which has important consequences for microbial decomposition (Chap. 18).

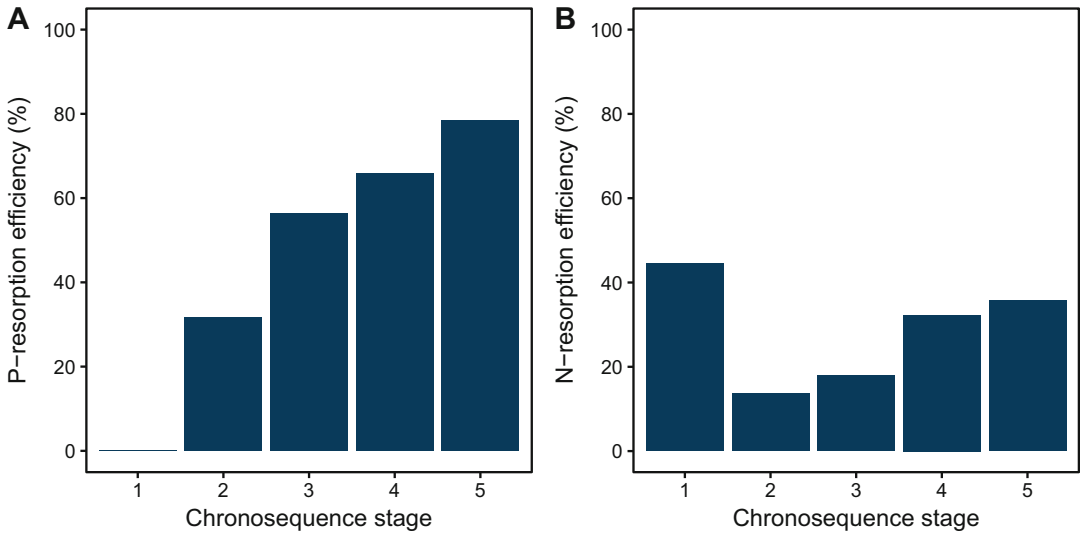

Fig. 9.37 Changes in community-level, cover-weighted (**A**) leaf phosphorus (P)-resorption efficiency, and (**B**) leaf nitrogen (N)-resorption efficiency with decreasing total soil P availability along a >2-million year dune chronosequence (after Hayes et al. 2014).

Table 9.20 Ranges of nitrogen (N), phosphorus (P), and potassium (K) concentrations representing complete and incomplete resorption, which are synonymous with high and low resorption proficiency, respectively.

Resorption proficiency	
Based on nutrient concentrations per unit mass in senesced leaves	
Complete resorption	Incomplete resorption
<7 mg N g^{-1} dry weight	>10 mg N g^{-1} dry weight
<0.5 mg P g^{-1} dry weight (deciduous species)	>0.8 mg P g^{-1} dry weight (deciduous species)
<0.03 mg P g^{-1} dry weight (evergreen species)	>0.5 mg P g^{-1} dry weight (evergreen species)
<1 mg K g^{-1} dry weight (evergreen species)	>1.51 mg K g^{-1} dry weight (evergreen species)
Based on nutrient concentrations per unit area in senesced leaves	
<500 mg N m^{-2} leaf area	>750 mg N m^{-2} leaf area
<30 mg P m^{-2} leaf area	>80 mg P m^{-2} leaf area

Source: Killingbeck (1996); Denton et al. (2007); Hayes et al. (2014); Suriyagoda et al. (2018)
Note: We segregated mass-based P concentrations of deciduous and evergreen species, because of the large difference between these life forms in ability to reduce P concentrations in senescing leaves

Nutrient resorption from senescing leaves is the net result of several processes: enzymatic breakdown of N- and P-containing compounds in the leaves, phloem loading and transport, and the formation of an abscission layer that cuts off the transport path, and causes the leaf to fall. Comparing remobilization of different leaf P fractions (Box 9.1), P resorption of the residual fraction is relatively large and similar in magnitude to that of labile fractions in more efficient trees on P-poor sites in tropical rainforest in Borneo. This suggests that tree species inhabiting P-poor environments increase their P-remobilization efficiency by improving the degradation of recalcitrant compounds (Tsujii et al. 2017b).

Anthocyanins, which typically accumulate during leaf senescence, give rise to autumn colors, protect foliar nutrient resorption by shielding photosynthetic tissues from excess

light. This becomes evident using wild-type and anthocyanin-deficient mutants of three deciduous woody species, *Cornus sericea* (redosier dogwood), *Vaccinium elliottii* (Elliott's blueberry), and *Viburnum sargentii* (Sargent viburnum), and wild-type *Betula papyrifera* (paper birch), a species that does not produce anthocyanins in autumn (Hoch et al. 2003). The appearance of anthocyanins in senescing leaves of wild-type plants coincides with the development of **photoinhibition** (Sect. 2.3.3.1) in mutants of all three anthocyanin-producing species. In a high-light environment, wild-type plants maintain higher photochemical efficiencies than mutants, and are able to recover, whereas mutant leaves drop while still green and display signs of irreversible **photooxidative damage**. Nitrogen-resorption efficiencies and proficiencies (Sect. 9.4.4) of all mutants in stressful treatments are significantly lower than those in wild-type plants. *Betula papyrifera* displays photochemical efficiencies and N-resorption performance similar to those of the anthocyanin-producing species, indicating a photoprotective strategy that differs from that of the other species studied (Fig. 9.38; Hoch et al. 2003).

There is very little information on nutrient resorption from senescing **stems** and **roots**. Freschet et al. (2010) found for a subarctic flora average N-resorption efficiencies of 66%, 48%, and 27% for leaves, fine stems, and fine roots, respectively; the equivalent P-resorption efficiencies are 63%, 56%, and 57%. *Hakea prostrata* (harsh hakea) from a severely P-impoverished habitat efficiently mobilizes P from its cluster roots, with peak concentrations of 2500 μg P g^{-1} root dry mass down to 96 μg P g^{-1} root dry mass, *i.e.* 96% remobilization (Shane et al. 2004a).

9.4.4 Ecosystem Nutrient-Use Efficiency

We have based our definitions of **nutrient-use efficiency** (*NUE*) so far on individual plants. The same concept has been applied to ecosystems that are approximately in steady state [*i.e.* where aboveground production is approximately equal to litter-fall (leaves, twigs, small branches, and reproductive parts)]. Ecosystem *NUE* is the ratio of litter-fall mass to litter-fall nutrient content (*i.e.* the inverse of the nutrient concentration of litter-fall) (Vitousek 1982). This is equivalent to the biomass produced per unit of nutrient gained or lost. Defined in this way, ecosystem *NUE* is generally greater at sites with low availability of nutrients (particularly for N, which is the element that most strongly limits productivity in most terrestrial ecosystems in young landscapes). The data for ecosystem *NUE*, however, must be interpreted with care: *NUE* and nutrient concentration in the litter are inversely and negatively correlated, and are not independent. All else being equal, a high nutrient concentration of the litter (*i.e.* a low dry mass:N ratio) is associated with a high N loss in litter-fall.

The three processes that cause differences in ecosystem *NUE* are:

1. Photosynthesis per unit nutrient (*PNUE* or *PPUE*);
2. Mean residence time (*MRT*) during which the nutrient contributed to production;
3. Proportion of nutrients resorbed prior to senescence.

PPUE is often very high in slow-growing species from severely P-impoverished habitats (Sect. 9.4.1.1), but *PNUE* is low in low-N environments (Fig. 9.34 and Sect. 2.6). This low *PNUE* is offset to an unknown extent by greater mean residence time of N in infertile sites (Westoby et al. 2002). Resorption is similar across sites or slightly greater at infertile sites (Sect. 9.4.3). These patterns are well documented at the scale of individual plants or leaves and communities (Fig. 9.37; Hayes et al. 2014), but we have insufficient information to quantify their net effect on *NUE* at the ecosystem scale. It is, therefore, currently impossible to provide an independent confirmation from physiological measurements of Vitousek's (1982) conclusion that *NUE* is greatest in infertile sites. Current uncertainties include:

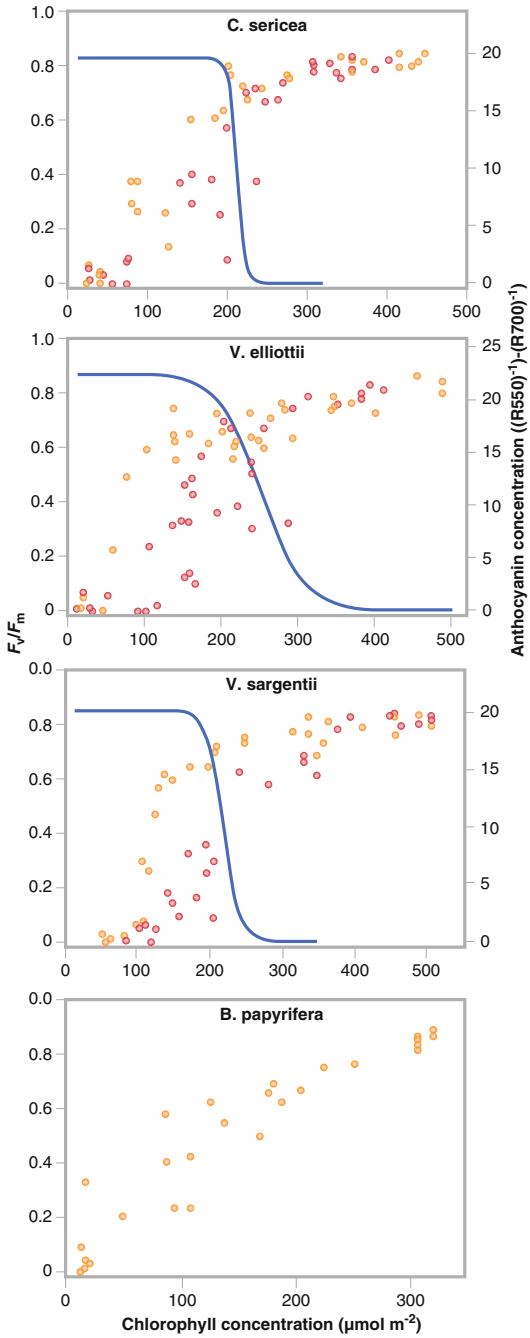

Fig. 9.38 Progression during senescence of the relationship between F_v/F_m and leaf chlorophyll concentrations for mutant (filled circles) and wild-type (open circles) plants of anthocyanin-producing *Cornus sericea* (redosier dogwood), *Vaccinium elliottii* (Elliott's blueberry), and *Viburnum sargentii* (Sargent viburnum), and nonanthocyanin-producing *Betula papyrifera* (paper birch) in an outdoor treatments. The development of anthocyanins in senescing leaves of wild-type plants is indicated on the graphs of the anthocyanin-producing species by a three-parameter sigmoid line (Hoch et al., 2003); copyright American Society of Plant Biologists.

1. The effect of herbivory on nutrient loss (which is greater in fertile sites and removes nutrient-rich tissues, leading to an over-estimate of *NUE* in fertile sites);
2. Leaching losses (which are generally similar between fertile and infertile sites);
3. The omission of belowground dynamics, for which few data are available.

In summary, plants vary in their capacity for nutrient uptake and efficiency of nutrient use. Genetic adaptation and acclimation, however, vary in their relative importance to different processes. Acclimation is probably the major factor that accounts for the high root mass ratio at infertile sites. Due to low availability, rates of nutrient acquisition are low for plants at infertile sites. These plants generally have low leaf P and N concentrations, a high photosynthetic P-use efficiency, but a low photosynthetic N-use efficiency, due primarily to effects of environment on leaf nutrient concentrations and to both genetic and phenotypic differences in photosynthetic nutrient-use efficiency. Plants on infertile sites generally keep their nutrients for a longer period; for example, the *MRT* of nutrients is longer for evergreens than for deciduous leaves, and any given species retains its leaves longer on infertile sites. Plants also differ in the extent to which they withdraw nutrients from senescing leaves, but the variation in the extent to which nutrients are withdrawn shows a less consistent difference between fertile and infertile sites for N than it does for P (Fig. 9.37). The high ecosystem *NUE* at infertile sites reflects low leaf N concentrations and high *MRT*.

9.5 Mineral Nutrition: A Vast Array of Adaptations and Acclimations

Nutrients move in the soil to root surfaces by mass flow and diffusion, but plants then use selective nutrient-transport systems to transport them into the symplast. Because anion transport mostly occurs up an electrochemical potential gradient, metabolic energy is required to import these nutrients from the rhizosphere. Although cation transport may occur down an electrochemical potential gradient, metabolic energy is also required to import these nutrients from the rhizosphere, because the maintenance of the electrochemical potential gradient requires ATP. When essential nutrients move too slowly to the root surface, adaptive mechanisms are required, especially for the acquisition of P, Fe, and Zn.

Species have adapted to adverse or favorable soil conditions, and individual plants have some capacity to acclimate to a range of soil conditions. Some of these acclimations are physiological (*e.g.*, excretion of Fe-chelating molecules). Others are anatomical (*e.g.*, the formation of more or longer root hairs when Pi is in short supply), or morphological (*e.g.*, the increase in root mass ratio when N or P are limiting for growth). These anatomical and morphological acclimations also have a physiological basis, however, and often require induction of specific genes, after they have sensed a shortage of nutrients.

Plants need many macronutrients and micronutrients, but the concentration of the various elements in plant tissues does not necessarily give us a correct estimate of a plant's requirements. Rather, elements may accumulate, because the plant lacks mechanisms to keep these out, and stores these elements in compartments where they are least harmful. In this chapter, we have encountered numerous species that occupy sites that are practically inaccessible to others. These adapted plants include halophytes, metallophytes, calcifuges, and calcicoles. Halophytes and metallophytes do not need high concentrations of NaCl and metals, respectively, for maximum growth, but they are among the few species that can cope with such adverse soil conditions; that is, their **ecological amplitude** is much narrower than their **physiological amplitude** (Sect. 1.3). Calcifuges are largely restricted to acid soils, because they lack the capacity to acquire some nutrients from alkaline soils. On the other hand, calcicoles are restricted to calcium-rich and often alkaline soils, because they are adversely affected by toxic compounds in acid soils (Al, Mn). Understanding plant distribution as dependent on soil type clearly requires an appreciation of a breadth of physiological mechanisms.

Plants differ in the mechanisms employed to acquire nutrients from various soils, as well as in the requirement for these nutrients and in their long-term nutrient-use efficiency. Plants from nutrient-rich sites tend to produce more biomass per unit nutrient in the plant, whereas plants from nutrient-poor sites tend to keep the nutrients they have acquired for a longer time. There is substantial variation among species in the extent to which they resorb nutrients, especially P, from senescing leaves, and some species from severely P-impoverished habitats show remarkable P-resorption proficiency. Variation in P availability influences resorption (*i.e.* a smaller proportion of the P invested in leaf mass is remobilized on P-rich sites than on P-poor sites).

Knowledge of a plant's mineral nutrition is pivotal to understanding the distribution of plant species and the high diversity of plant species in nutrient-impoverished soils. It is also essential for modern agriculture and forestry (*e.g.*, to avoid nutrient deficiency disorders or to breed for plants that can acquire nutrients from soils of low nutrient availability, or use these nutrients more efficiently). It is also important to resolve environmental problems (*e.g.*, through phytoremediation). Mixed cultures and crop rotations can be highly beneficial in cropping situations. Intercrop species (*i.e.* plants that are used because of their favorable effect on the actual crop that is of agronomic

interest), can be selected on the basis of ecophysiological information presented in this chapter. For example, if the intercrop plant solubilizes Fe or P that becomes available to the crop, then it may prevent chlorosis or reduce the need for P fertilization, respectively. This chapter should inspire us to think of traits that we might exploit in future agriculture.

One of the most exciting developments in plant mineral nutrition is our understanding of the pivotal differences between relatively poorly-studied species that evolved in severely P-impoverished landscapes and those plant scientists have focused on most, naturally occurring in young landscapes where N limits productivity. Proteaceae from severely P-impoverished Mediterranean environments have received detailed attention (Lambers et al. 2015a). However, it is becoming increasingly evident that species in other families that inhabit the same or similarly P-impoverished habitats have much in common when it comes to their mineral nutrition.

References

Abrahão A, de Britto Costa P, Lambers H, Andrade SAL, Sawaya ACHF, Ryan MH, Oliveira RS. 2019. Soil types select for plants with matching nutrient-acquisition and -use traits in hyperdiverse and severely nutrient-impoverished *campos rupestres* and *cerrado* in Central Brazil. *J Ecol* **107**: 1302–1316.

Abrahão A, Lambers H, Sawaya ACHF, Mazzafera P, Oliveira RS. 2014. Convergence of a specialized root trait in plants from nutrient-impoverished soils: phosphorus-acquisition strategy in a nonmycorrhizal cactus. *Oecologia* **176**: 345–355.

Aerts R. 1990. Nutrient use efficiency in evergreen and deciduous species from heathlands. *Oecologia* **84**: 391–397.

Ajmera I, Shi J, Giri J, Wu P, Stekel DJ, Lu C, Hodgman TC. 2018. Regulatory feedback response mechanisms to phosphate starvation in rice. *Syst Biol Applic* **4**: 4.

Al-Hiyaly SAK, McNeilly T, Bradshaw AD. 1990. The effect of zinc contamination from electricity pylons. Contrasting patterns of evolution in five grass species. *New Phytol* **114**: 183–190.

Albuzio A, Ferrari G. 1989. Modulation of the molecular size of humic substances by organic acids of the root exudates. *Plant Soil* **113**: 237–241.

Alloway BJ, Steinnes E 1999. Anthropogenic additions of cadmium to soils. In: McLaughlin MJ, Singh BR eds. *Cadmium in Soils and Plants*. Dordrecht: Springer Netherlands, 97–123.

Anacker BL. 2014. The nature of serpentine endemism. *Am J Bot* **101**: 219–224.

Anderson CW, Brooks RR, Stewart RB, Simcock R. 1998. Harvesting a crop of gold in plants. *Nature* **395**: 553–554.

Andrews M, Raven JA, Lea PJ. 2013. Do plants need nitrate? The mechanisms by which nitrogen form affects plants. *Ann Appl Biol* **163**: 174–199.

Appenroth K-J 2010. Definition of "heavy metals" and their role in biological systems. *Soil Heavy Metals Soil Biology*. Berlin: Springer, 19–29.

Arianoutsou M, Rundel PW, Berry WL 1993. Serpentine endemics as biological indicators of soil elemental concentrations. In: Markert B ed. *Plants as Biomonitors Indicators for Heavy Metals in the Terrestrial Environment*. New York: VCH Weinheim, 179–189.

Aslam M, Travis RL, Rains DW. 1996. Evidence for substrate induction of a nitrate efflux system in barley roots. *Plant Physiol* **112**: 1167–1175.

Assunção AGL, Schat H, Aarts MGM. 2003. *Thlaspi caerulescens*, an attractive model species to study heavy metal hyperaccumulation in plants. *New Phytol* **159**: 351–360.

Atkin OK. 1996. Reassessing the nitrogen relations of Arctic plants: a mini-review. *Plant Cell Environ* **19**: 695–704.

Baker AJ, Ernst WH, van der Ent A, Malaisse F, Ginocchio R 2010. Metallophytes: the unique biological resource, its ecology and conservational status in Europe, central Africa and Latin America. In: Batty LC, Hallberg KB eds. *Ecology of Iindustrial Pollution*. Cambridge: Cambridge University Press, 7–39.

Ball M. 1988. Salinity tolerance in the mangroves *Aegiceras corniculatum* and *Avicennia marina*. I. Water use in relation to growth, carbon partitioning, and salt balance. *Funct Plant Biol* **15**: 447–464.

Barber SA. 1995. *Soil nutrient bioavailability, 2nd edition*. New York: Wiley.

Barber SA, Ozanne PG. 1970. Autoradiographic evidence for the differential effect of four plant species in altering the calcium content of the rhizosphere soil. *Soil Sci Soc Am J* **34**: 635–637.

Barker MG, Ashenden TW. 1992. Effects of acid fog on cuticular permeability and cation leaching in holly (*Ilex aquifolium*). *Agric Ecosyst Environ* **42**: 291–306.

Barkla BJ, Zingarelli L, Blumwald E, Smith J. 1995. Tonoplast Na^+/H^+ antiport activity and its energization by the vacuolar H^+-ATPase in the halophytic plant *Mesembryanthemum crystallinum* L. *Plant Physiol* **109**: 549–556.

Barrow NJ. 1984. Modelling the effects of pH on phosphate sorption by soils. *J Soil Sci* **35**: 283–297.

Barrow NJ, Debnath A, Sen A. 2018. Mechanisms by which citric acid increases phosphate availability. *Plant Soil* **423**: 193–204.

Bates TR, Lynch JP. 2001. Root hairs confer a competitive advantage under low phosphorus availability. *Plant Soil* **236**: 243–250.

Baxter IR, Vitek O, Lahner B, Muthukumar B, Borghi M, Morrissey J, Guerinot ML, Salt DE. 2008. The leaf ionome as a multivariable system to detect a plant's physiological status. *Proc Natl Acad Sci USA* **105**: 12081–12086.

Bell RW. 1997. Diagnosis and prediction of boron deficiency for plant production. *Plant Soil* **193**: 149–168.

Berendse F, Aerts R. 1987. Nitrogen-use-efficiency: a biologically meaningful definition? *Funct Ecol* **1**: 293–296.

Bhat KKS, Nye PH. 1973. Diffusion of phosphate to plant roots in soil. *Plant Soil* **38**: 161–175.

Blom-Zandstra M, Vogelzang SA, Veen BW. 1998. Sodium fluxes in sweet pepper exposed to varying sodium concentrations. *J Exp Bot* **49**: 1863–1868.

Bloom AJ. 2015. The increasing importance of distinguishing among plant nitrogen sources. *Curr Opin Plant Biol* **25**: 10–16.

Blumwald E, Poole RJ. 1987. Salt tolerance in suspension cultures of sugar beet. *Environ Stress Physiol* **83**: 884–887.

Bolan NS, Hedley MJ, White RE. 1991. Processes of soil acidification during nitrogen cycling with emphasis on legume based pastures. *Plant Soil* **134**: 53–63.

Bravin MN, Travassac F, Le Floch M, Hinsinger P, Garnier J-M. 2008. Oxygen input controls the spatial and temporal dynamics of arsenic at the surface of a flooded paddy soil and in the rhizosphere of lowland rice (*Oryza sativa* L.): a microcosm study. *Plant Soil* **312**: 207–218.

Briggs D. 1976. Genecological studies of lead tolerance in groundsel (*Senecio vulgaris* L.). *New Phytol* **77**: 173–186.

Bristow CS, Hudson-Edwards KA, Chappell A. 2010. Fertilizing the Amazon and equatorial Atlantic with West African dust. *Geophys Res Lett* **37**: L14807.

Britto DT, Kronzucker HJ. 2005. Nitrogen acquisition, PEP carboxylase, and cellular pH homeostasis: new views on old paradigms. *Plant Cell Environ* **28**: 1396–1409.

Britto DT, Kronzucker HJ. 2006. Futile cycling at the plasma membrane: a hallmark of low-affinity nutrient transport. *Trends Plant Sci* **11**: 529–534.

Britto DT, Kronzucker HJ. 2015. Sodium efflux in plant roots: what do we really know? *J Plant Physiol* **186–187**: 1–12.

Broadley M, Brown P, Cakmak I, Ma JF, Rengel Z, Zhao F 2012. Beneficial elements. In: Marschner P ed. *Marschner's Mineral Nutrition of Higher Plants (Third Edition)*. London: Academic Press, 249–269.

Broadley MR, Bowen HC, Cotterill HL, Hammond JP, Meacham MC, Mead A, White PJ. 2003. Variation in the shoot calcium content of angiosperms. *J Exp Bot* **54**: 1431–1446.

Broadley MR, Bowen HC, Cotterill HL, Hammond JP, Meacham MC, Mead A, White PJ. 2004. Phylogenetic variation in the shoot mineral concentration of angiosperms. *J Exp Bot* **55**: 321–336.

Broadley MR, White PJ, Hammond JP, Zelko I, Lux A. 2007. Zinc in plants. *New Phytol* **173**: 677–702.

Brooks RR, ed. 1998. *Plants that Hyperaccumulate Heavy Metals. Their Role in Phytoremediation, Microbiology, Archaeology, Mineral Exploitation and Phytomining*. Wallingford: CAB International.

Brooks RR, Lee J, Reeves RD, Jaffre T. 1977. Detection of nickeliferous rocks by analysis of herbarium specimens of indicator plants. *J Geochem Explor* **7**: 49–57.

Brown G, Mitchell D, Stock W. 1984. Atmospheric deposition of phosphorus in a coastal fynbos ecosystem of the south-western Cape, South Africa. *J Ecol*: 547–551.

Brown LK, George TS, Thompson JA, Wright G, Lyon J, Dupuy L, Hubbard SF, White PJ. 2012. What are the implications of variation in root hair length on tolerance to phosphorus deficiency in combination with water stress in barley (*Hordeum vulgare*)? *Ann Bot* **110**: 319–328.

Brune A, Urbach W, Dietz KJ. 1994. Compartmentation and transport of zinc in barley primary leaves as basic mechanisms involved in zinc tolerance. *Plant Cell Environ* **17**: 153–162.

Bucher M. 2007. Functional biology of plant phosphate uptake at root and mycorrhiza interfaces. *New Phytol* **173**: 11–26.

Burgess SSO, Dawson TE. 2004. The contribution of fog to the water relations of *Sequoia sempervirens* (D. Don): foliar uptake and prevention of dehydration. *Plant Cell Environ* **27**: 1023–1034.

Cai H, Xie W, Lian X. 2013. Comparative analysis of differentially expressed genes in rice under nitrogen and phosphorus starvation stress conditions. *Plant Mol Biol Rep* **31**: 160–173.

Cakmak I, Marschner H. 1990. Decrease in nitrate uptake and increase in proton release in zinc deficient cotton, sunflower and buckwheat plants. *Plant Soil* **129**: 261–268.

Cakmak I, Sari N, Marschner H, Ekiz H, Kalayci M, Yilmaz A, Braun HJ. 1996. Phytosiderophore release in bread and durum wheat genotypes differing in zinc efficiency. *Plant Soil* **180**: 183–189.

Canfield DE, Glazer AN, Falkowski PG. 2010. The evolution and future of Earth's nitrogen cycle. *Science* **330**: 192–196.

Carvalhais LC, Dennis PG, Fedoseyenko D, Hajirezaei M-R, Borriss R, von Wirén N. 2011. Root exudation of sugars, amino acids, and organic acids by maize as affected by nitrogen, phosphorus, potassium, and iron deficiency. *J Plant Nutr Soil Sci* **174**: 3–11.

Chadwick OA, Derry LA, Vitousek PM, Huebert BJ, Hedin LO. 1999. Changing sources of nutrients during

four million years of ecosystem development. *Nature* **397**: 491–497.

Chang Y-C, Ma JF, Matsumoto H. 1998. Mechanisms of Al-induced iron chlorosis in wheat (*Triticum aestivum*). Al-inhibited biosynthesis and secretion of phytosiderophore. *Physiol Plant* **102**: 9–15.

Chapin FS. 1974. Morphological and physiological mechanisms of temperature compensation in phosphate absorption along a latitudinal gradient. *Ecology*: 1180–1198.

Chapin FS. 1980. The mineral nutrition of wild plants. *Annu Rev Ecol Syst* **11**: 233–260.

Chapin FS 1991. Effects of multiple environmental stresses on nutrient availability and use. In: Mooney HA, Winner WE, Pell EJ eds. *Response of Plants to Multiple Stresses*. San Diego: Academic Press, 67–88.

Chapin FS, Bloom A. 1976. Phosphate absorption: adaptation of tundra graminoids to a low temperature, low phosphorus environment. *Oikos*: 111–121.

Chapin FS, Fetcher N, Kielland K, Everett KR, Linkins AE. 1988. Productivity and nutrient cycling of Alaskan tundra: enhancement by flowing soil water. *Ecology* **69**: 693–702.

Chapin FS, Slack M. 1979. Effect of defoliation upon root growth, phosphate absorption and respiration in nutrient-limited tundra graminoids. *Oecologia* **42**: 67–79.

Chen L-S, Yang L-T, Lin Z-H, Tang N. 2013. Roles of organic acid metabolism in plant tolerance to phosphorus-deficiency. *Progr Bot* **74**: 213–237.

Chiou T-J. 2007. The role of microRNAs in sensing nutrient stress. *Plant Cell Environ* **30**: 323–332.

Clarkson DT 1981. Nutrient interception and transport by root systems. In: Johnson CB ed. *Physiological Processes Limiting Plant Productivity*. London: Butterworths, 307–314.

Clarkson DT 1996. Root structure and sites of ion uptake. In: Waisel Y, Eshel A, Kafkaki U eds. *Plant Roots: The Hidden Half*. New York: Marcel Dekker Inc., 483–510.

Clemens S. 2001. Molecular mechanisms of plant metal tolerance and homeostasis. *Planta* **212**: 475–486.

Clemens S, Palmgren MG, Krämer U. 2002. A long way ahead: understanding and engineering plant metal accumulation. *Trends Plant Sci* **7**: 309–315.

Clement CR, Hopper MJ, Jones LHP, Leafe EL. 1978. The uptake of nitrate by *Lolium perenne* from flowing nutrient solution: II. Effects of light, defoliation, and relationship to CO_2 flux. *J Exp Bot* **29**: 1173–1183.

Coskun D, Britto DT, Shi W, Kronzucker HJ. 2017. Nitrogen transformations in modern agriculture and the role of biological nitrification inhibition. *Nat Plants* **3**: 17074.

Cramer GR 2002. Sodium-calcium interactions under salinity stress. In: Läuchli A, Lüttge U eds. *Salinity: Environment-Plants-Molecules*. Dordrecht: Kluwer, 205–227.

Dahmani-Muller H, van Oort F, Gélie B, Balabane M. 2000. Strategies of heavy metal uptake by three plant species growing near a metal smelter. *Environ Poll* **109**: 231–238.

Davenport RJ, Munoz-Mayor A, Jha D, Essah PA, Rus A, Tester M. 2007. The Na^+ transporter AtHKT1;1 controls retrieval of Na^+ from the xylem in *Arabidopsis*. *Plant Cell Environ* **30**: 497–507.

De Boer AH. 1985. *Xylem/Smplast Ion Exchange: Mechanism and Function in Salt-Tolerance and Growth.* PhD thesis, University of Groningen, Groningen, the Netherlands.

de Macedo FG, Bresolin JD, Santos EF, Furlan F, Lopes da Silva WT, Polacco JC, Lavres J. 2016. Nickel availability in soil as influenced by liming and its role in soybean nitrogen metabolism. *Front Plant Sci* **7**: 1358.

Delgado M, Zúñiga-Feest A, Borie F, Suriyagoda L, Lambers H. 2014. Divergent functioning of Proteaceae species: the South American *Embothrium coccineum* displays a combination of adaptive traits to survive in high-phosphorus soils. *Funct Ecol* **28**: 1356–1366.

Delhaize E, Gruber BD, Ryan PR. 2007. The roles of organic anion permeases in aluminium resistance and mineral nutrition. *FEBS Lett* **581**: 2255.

Delhaize E, Ryan PR. 1995. Aluminium toxicity and tolerance in plants. *Plant Physiol* **107**: 315–321.

Delhaize E, Ryan PR, Randall PJ. 1993. Aluminum tolerance in wheat (*Triticum aestivum* L.) (II. Aluminum-stimulated excretion of malic acid from root apices). *Plant Physiol* **103**: 695–702.

Demidchik V, Davenport RJ, Tester M. 2002. Nonselective cation channels in plants. *Annu Rev Plant Biol* **53**: 67–107.

Deng T-H-B, van der Ent A, Tang Y-T, Sterckeman T, Echevarria G, Morel J-L, Qiu R-L. 2018. Nickel hyperaccumulation mechanisms: a review on the current state of knowledge. *Plant Soil* **423**: 1–11.

Denton MD, Veneklaas EJ, Freimoser FM, Lambers H. 2007. *Banksia* species (Proteaceae) from severely phosphorus-impoverished soils exhibit extreme efficiency in the use and re-mobilization of phosphorus. *Plant Cell Environ* **30**: 1557–1565.

Di Salvatore M, Carafa AM, Carratù G. 2008. Assessment of heavy metals phytotoxicity using seed germination and root elongation tests: A comparison of two growth substrates. *Chemosphere* **73**: 1461–1464.

Díaz S, Grime JP, Harris J, McPherson E. 1993. Evidence of a feedback mechanism limiting plant response to elevated carbon dioxide. *Nature* **364**: 616–617.

Ding W, Clode PL, Lambers H. 2019. Is pH the key reason why some *Lupinus* species are sensitive to calcareous soil? *Plant Soil* **434**: 185–201.

Dissanayaka DMSB, Plaxton WC, Lambers H, Siebers M, Marambe B, Wasaki J. 2018. Molecular mechanisms underpinning phosphorus-use efficiency in rice. *Plant Cell Environ* **41**: 1512–1523.

Dong B, Ryan PR, Rengel Z, Delhaize E. 1999. Phosphate uptake in *Arabidopsis thaliana*: dependence of uptake on the expression of transporter genes and

internal phosphate concentrations. *Plant Cell Environ* **22**: 1455–1461.

Doolette A, Armstrong R, Tang C, Guppy C, Mason S, McNeill A. 2019. Phosphorus uptake benefit for wheat following legume break crops in semi-arid Australian farming systems. *Nutr Cycl Agroecos* **113**: 247–266.

Drew MC. 1975. Comparison of the effects of a localized supply of phosphate, nitrate, ammonium and potassium on the growth of the seminal root system, and the shoot, in barley. *New Phytol* **75**: 479–490.

Driscoll CT, Lawrence GB, Bulger AJ, Butler TJ, Cronan CS, Eagar C, Lambert KF, Likens GE, Stoddard JL, Weathers KC. 2001. Acidic deposition in the northeastern United States: sources and inputs, ecosystem effects, and management strategies. *BioSci* **51**: 180–198.

Du E, Dong D, Zeng X, Sun Z, Jiang X, de Vries W. 2017. Direct effect of acid rain on leaf chlorophyll content of terrestrial plants in China. *Sci Tot Environ* **605–606**: 764–769.

Duffus JH. 2002. Heavy metals-a meaningless term. *Pure Appl Chem* **74**: 793–807.

Dunlop J, Glass ADM, Tomkins BD. 1979. The regulation of K^+ uptake by ryegrass and white clover roots in relation to their competition for potassium. *New Phytol* **83**: 365–370.

Eger A, Almond P, Wells A, Condron L. 2013. Quantifying ecosystem rejuvenation: foliar nutrient concentrations and vegetation communities across a dust gradient and a chronosequence. *Plant Soil* **367**: 93–109.

Epstein E, Hagen CE. 1952. A kinetic study of the absorption of alkali cations by barley roots. *Plant Physiol* **27**: 457.

Erskine PD, Stewart GR, Schmidt S, Turnbull MH, Unkovich M, Pate JS. 1996. Water availability – a physiological constraint on nitrate utilization in plants of Australian semi-arid muiga woodlands. *Plant Cell Environ* **19**: 1149–1159.

Esau K. 1977. *Anatomy of Seed Plants. 2nd edition*. New York: John Wiley and Sons Inc.

Eviner VT, Chapin FS. 2003. Functional matrix: a conceptual framework for predicting multiple plant effects on ecosystem processes. *Annu Rev Ecol Evol Syst* **34**: 455–485.

Fahr M, Laplaze L, Bendaou N, Hocher V, El Mzibri M, Bogusz D, Smouni A. 2013. Effect of lead on root growth. *Front Plant Sci* **4**.

Faucon M-P, Chipeng F, Verbruggen N, Mahy G, Colinet G, Shutcha M, Pourret O, Meerts P. 2012. Copper tolerance and accumulation in two cuprophytes of South Central Africa: *Crepidorhopalon perennis* and *C. tenuis* (Linderniaceae). *Env Exp Bot* **84**: 11∗16.

Fernando DR, Lynch JP. 2015. Manganese phytotoxicity: new light on an old problem. *Ann Bot* **116**: 313–319.

Firmin S, Labidi S, Fontaine J, Laruelle F, Tisserant B, Nsanganwimana F, Pourrut B, Dalpé Y, Grandmougin A, Douay F, Shirali P, Verdin A, Lounès-Hadj Sahraoui A. 2015. Arbuscular mycorrhizal fungal inoculation protects *Miscanthus*×*giganteus* against trace element toxicity in a highly metal-contaminated site. *Sci Tot Environ* **527–528**: 91–99.

Flowers TJ, Colmer TD. 2008. Salinity tolerance in halophytes. *New Phytol* **179**: 945–963.

Föhse D, Claassen N, Jungk A. 1991. Phosphorus efficiency of plants. II. Significance of root radius, root hairs and cation-anion balance for phosphorus influx in seven plant species. *Plant Soil* **132**: 261–272.

Föhse D, Jungk A. 1983. Influence of phosphate and nitrate supply on root hair formation of rape, spinach and tomato plants. *Plant Soil* **74**: 359–368.

Fones H, Davis CAR, Rico A, Fang F, Smith JAC, Preston GM. 2010. Metal hyperaccumulation armors plants against disease. *PLoS Pathog* **6**: e1001093.

Foy CD, Chaney RL, White MC. 1978. The physiology of metal toxicity in plants. *Annu Rev Plant Physiol* **29**: 511–566.

Franklin O, Cambui CA, Gruffman L, Palmroth S, Oren R, Näsholm T. 2017. The carbon bonus of organic nitrogen enhances nitrogen use efficiency of plants. *Plant Cell Environ* **40**: 25–35.

Fransen B, Blijjenberg J, de Kroon H. 1999. Root morphological and physiological plasticity of perennial grass species and the exploitation of spatial and temporal heterogeneous nutrient patches. *Plant Soil* **211**: 179–189.

Freschet GT, Cornelissen JHC, van Logtestijn RSP, Aerts R. 2010. Substantial nutrient resorption from leaves, stems and roots in a subarctic flora: what is the link with other resource economics traits? *New Phytol* **186**: 879–889.

Frey B, Keller C, Zierold K. 2000. Distribution of Zn in functionally different leaf epidermal cells of the hyperaccumulator *Thlaspi caerulescens*. *Plant Cell Environ* **23**: 675–687.

Fujii K, Aoki M, Kitayama K. 2013. Biodegradation of low molecular weight organic acids in rhizosphere soils from a tropical montane rain forest. *Soil Biol Biochem* **56**: 3–9.

Gahoonia TS, Nielsen NE. 2004. Barley genotypes with long root hairs sustain high grain yields in low-P field. *Plant Soil* **262**: 55–62.

Galloway JN, Schlesinger WH, Levy H, II, Michaels A, Schnoor JL. 1995. Nitrogen fixation: anthropogenic enhancement-environmental response. *Glob Biogeochem Cycl* **9**: 235–252.

Gardner WK, Boundy KA. 1983. The acquisition of phosphorus by *Lupinus albus* L. IV. The effect of interplanting wheat and white lupin on the growth and mineral composition of the two species. *Plant Soil* **70**: 391–402.

Garnett TP, Smethurst PJ. 1999. Ammonium and nitrate uptake by *Eucalyptus nitens*: effects of pH and temperature. *Plant Soil* **214**: 133–140.

Gawronski SW, Gawronska H, Lomnicki S, Sæbo A, Vangronsveld J. 2017. Plants in air phytoremediation. *Adv Bot Res* **83**: 319–346.

Geelhoed JS, Hiemstra T, Van Riemsdijk WH. 1998. Competitive interaction between phosphate and citrate on goethite. *Environ Sci Technol* **32**: 2119–2123.

George TS, Quiquampoix H, Simpson RJ, Richardson AE 2006. Interactions between phytases and soil constituents: implications for the hydrolysis of inositol phosphates. In: Turner BL, Richardson AE eds. *Inositol Phosphates: Linking Agriculture and the Environment*: CAB International, 222–242.

Gersani M, Sachs T. 1992. Development correlations between roots in heterogeneous environments. *Plant Cell Environ* **15**: 463–469.

Ghasemi R, Ghaderian SM, Krämer U. 2009. Interference of nickel with copper and iron homeostasis contributes to metal toxicity symptoms in the nickel hyperaccumulator plant *Alyssum inflatum*. *New Phytol* **184**: 566–580.

Giles CD, Brown LK, Adu MO, Mezeli MM, Sandral GA, Simpson RJ, Wendler R, Shand CA, Menezes-Blackburn D, Darch T, Stutter MI, Lumsdon DG, Zhang H, Blackwell MSA, Wearing C, Cooper P, Haygarth PM, George TS. 2017. Response-based selection of barley cultivars and legume species for complementarity: root morphology and exudation in relation to nutrient source. *Plant Sci* **255**: 12–28.

Gitto A, Fricke W. 2018. Zinc treatment of hydroponically-grown barley (*H. vulgare*) plants causes a reduction in root and cell hydraulic conductivity and isoform-dependent decrease in aquaporin gene expression. *Physiol Plant* **164**: 176–190.

Godbold DL, Horst WJ, Marschner H, Collins JC 1983. Effect of high zinc concentrations on root growth and zinc uptake in two ecotypes of *Deschampsia caespitosa* differing in zinc tolerance. In: Böhm W, Kutschera, L., Lichtentegger, E. ed. *Root Ecology and its Practical Application*. Gumpenstein: Bundesanstalt für alpenländische Landwirtscaft, 65–172.

Grundon NJ. 1972. Mineral nutrition of some Queensland heath plants. *J Ecol* **60**: 171–181.

Guilherme Pereira C, Clode PL, Oliveira RS, Lambers H. 2018. Eudicots from severely phosphorus-impoverished environments preferentially allocate phosphorus to their mesophyll. *New Phytol* **218**: 959–973.

Guilherme Pereira C, Hayes PE, O'Sullivan O, Weerasinghe L, Clode PL, Atkin OK, Lambers H. 2019. Trait convergence in photosynthetic nutrient-use efficiency along a 2-million year dune chronosequence in a global biodiversity hotspot. *J Ecol* **107**:2006–2023

Güsewell S. 2004. N : P ratios in terrestrial plants: variation and functional significance. *New Phytol* **164**: 243–266.

Gutierrez JR, Whitford WG. 1987. Chihuahuan desert annuals: importance of water and nitrogen. *Ecology* **68**: 2032–2045.

Hairiah K, Stulen I, Kuiper PJC 1990. Aluminium tolerance of the velvet beans *Mucuna pruriens* var. *utilis* and *Mucuna deeringiana.* I. Effects of aluminium on growth and mineral composition. In: Van Beusichem ML ed. *Plant Nutrition—Physiology and Applications*. Dordrecht: Kluwer Academic Publishing, 365–374.

Hall JL. 2002. Cellular mechanisms for heavy metal detoxification and tolerance. *J Exp Bot* **53**: 1–11.

Hammond JP, White PJ. 2008. Sucrose transport in the phloem: integrating root responses to phosphorus starvation. *J Exp Bot* **59**: 93–109.

Harper SM, Edwards DG, Kerven GL, Asher CJ. 1995. Effects of organic acid fractions extracted from *Eucalyptus camaldulensis* leaves on root elongation of maize (*Zea mays*) in the presence and absence of aluminium. *Plant Soil* **171**: 189–192.

Hartmann A, Rothballer M, Schmid M. 2008. Lorenz Hiltner, a pioneer in rhizosphere microbial ecology and soil bacteriology research. *Plant Soil* **312**: 7–14.

Hayes JE, Simpson RJ, Richardson AE. 2000. The growth and phosphorus utilisation of plants in sterile media when supplied with inositol hexaphosphate, glucose 1-phosphate or inorganic phosphate. *Plant Soil* **220**: 165–174.

Hayes P, Turner BL, Lambers H, Laliberté E. 2014. Foliar nutrient concentrations and resorption efficiency in plants of contrasting nutrient-acquisition strategies along a 2-million-year dune chronosequence. *J Ecol* **102**: 396–410.

Hayes PE, Clode PL, Guilherme Pereira C, Lambers H. 2019a. Calcium modulates leaf cell-specific phosphorus allocation in Proteaceae from south-western Australia. *J Exp Bot*.

Hayes PE, Clode PL, Oliveira RS, Lambers H. 2018. Proteaceae from phosphorus-impoverished habitats preferentially allocate phosphorus to photosynthetic cells: an adaptation improving phosphorus-use efficiency. *Plant Cell Environ* **41**: 605–619.

Hayes PE, Guilherme Pereira C, Clode PL, Lambers H. 2019b. Calcium-enhanced phosphorus-toxicity in calcifuge and soil-indifferent Proteaceae along the Jurien Bay chronosequence. *New Phytol* **221**: 764–777.

He H, Bleby TM, Veneklaas EJ, Lambers H, Kuo J. 2012. Morphologies and elemental compositions of calcium crystals in phyllodes and branchlets of *Acacia robeorum* (Leguminosae: Mimosoideae). *Ann Bot* **109**: 887–896.

He XL, Fan SK, Zhu J, Guan MY, Liu XX, Zhang YS, Jin CW. 2017. Iron supply prevents Cd uptake in *Arabidopsis* by inhibiting *IRT1* expression and favoring competition between Fe and Cd uptake. *Plant Soil* **416**: 453–462.

He ZL, Yang XE, Stoffella PJ. 2005. Trace elements in agroecosystems and impacts on the environment. *J Trace Elem Med Biol* **19**: 125–140.

Hedin LO. 2004. Global organization of terrestrial plant-nutrient interactions. *Proc Natl Acad Sci USA* **101**: 10849–10850.

Hedin LO, Granat L, Likens GE, Adri Buishand T, Galloway JN, Butler TJ, Rodhe H. 1994. Steep declines in atmospheric base cations in regions of Europe and North America. *Nature* **367**: 351–354.

Hego E, Bes CM, Bedon F, Palagi PM, Chaumeil P, Barré A, Claverol S, Dupuy J-W, Bonneu M, Lalanne C, Plomion C, Mench M. 2014. Differential accumulation of soluble proteins in roots of metallicolous and nonmetallicolous populations of *Agrostis capillaris* L. exposed to Cu. *Proteomics* **14**: 1746–1758.

Henry HAL, Jefferies RL. 2003. Plant amino acid uptake, soluble N turnover and microbial N capture in soils of a grazed Arctic salt marsh. *J Ecol* **91**: 627–636.

Higginbotham N, Etherton B, Foster RJ. 1967. Mineral ion contents and cell transmembrane electropotentials of pea and oat seedling tissue. *Plant Physiol* **42**: 37–46.

Hiltner L. 1904. Über neuere Erfahrungen und Probleme auf dem Gebiete der Bodenbakteriologie unter besonderer Berücksichtigung der Gründüngung und Brache. *Arb Dtsch Landwirt Ges* **98**: 59–78.

Hinsinger P. 1998. How do plant roots acquire mineral nutrients? Chemical processes involved in the rhizosphere. *Adv Agron* **64**: 225–265.

Hinsinger P, Plassard C, Tang C, Jaillard B. 2003. Origins of root-mediated pH changes in the rhizosphere and their responses to environmental constraints: a review. *Plant Soil* **248**: 43–59.

Hoch WA, Singsaas EL, McCown BH. 2003. Resorption protection. Anthocyanins facilitate nutrient recovery in autumn by shielding leaves from potentially damaging light levels. *Plant Physiol* **133**: 1296–1305.

Hodge A. 2004. The plastic plant: root responses to heterogeneous supplies of nutrients. *New Phytol* **162**: 9–24.

Hodge A, Robinson D, Griffiths BS, Fitter AH. 1999. Why plants bother: root proliferation results in increased nitrogen capture from an organic patch when two grasses compete. *Plant Cell Environ* **22**: 811–820.

Huang CX, Van Steveninck RFM. 1989. Maintenance of low Cl^- concentrations in mesophyll cells of leaf blades of barley seedlings exposed to salt stress. *Plant Physiol* **90**: 1440–1443.

Huang G, Hayes PE, Ryan MH, Pang J, Lambers H. 2017. Peppermint trees shift their phosphorus-acquisition strategy along a strong gradient of plant-available phosphorus by increasing their transpiration. *Oecologia* **185**: 487–400.

Hübel F, Beck E. 1993. In-situ determination of the P-relations around the primary root of maize with respect to inorganic and phytate-P. *Plant Soil* **157**: 1–9.

Hutchinson TC. 1967. Lime-chlorosis as a factor in seedling establishment on calcareous soils. I. A comparative study of species from acidic and calcareous soils in their susceptibility to lime-chlorosis. *New Phytol* **66**: 697–705.

Ingestad T, Ågren GI. 1995. Plant nutrition and growth: basic principles. *Plant Soil* **168/169**: 15–20.

Jefferies RL, Willis AJ. 1964. Studies on the calcicole-calcifuge habit: II. The Influence of calcium on the growth and establishment of four species in soil and sand cultures. *J Ecol* **52**: 691–707.

Jemo M, Abaidoo R, Nolte C, Tchienkoua M, Sanginga N, Horst W. 2006. Phosphorus benefits from grain-legume crops to subsequent maize grown on acid soils of southern Cameroon. *Plant Soil* **284**: 385–397.

Jenny H. 1980. *The Soil Resource, Origin and Behaviour*. New York: Springer-Verlag.

Johnson DB, Hallberg KB. 2005. Acid mine drainage remediation options: a review. *Sci Tot Environ* **338**: 3–14.

Johnson NM, Reynolds RC, Likens GE. 1972. Atmospheric sulfur: its effect on the chemical weathering of New England. *Science* **177**: 514–516.

Jones DL. 1998. Organic acids in the rhizosphere—a critical review. *Plant Soil* **205**: 25–44.

Jones DL, Darah PR, Kochian LV. 1996. Critical evaluation of organic acid mediated iron dissolution in the rhizosphere and its potential role in root iron uptake. *Plant Soil* **180**: 57–66.

Jungk A, Claassen N. 1997. Ion diffusion in the soil-root system. *Adv Agron* **61**: 53–110.

Kaiser WM, Huber SC. 2001. Post-translational regulation of nitrate reductase: mechanism, physiological relevance and environmental triggers. *J Exp Bot* **52**: 1981–1989.

Kamh M, Abdou M, Chude V, Wiesler F, Horst WJ. 2002. Mobilization of phosphorus contributes to positive rotational effects of leguminous cover crops on maize grown on soils from northern Nigeria. *J Plant Nutr Soil Sci* **165**: 566–572.

Kawai S, Takagi Si, Sato Y. 1988. Mugineic acid-family phytosiderophores in root-secretions of barley, corn and sorghum varieties. *J Plant Nutr* **11**: 633–642.

Keerthisinghe G, Hocking PJ, Ryan PR, Delhaize E. 1998. Effect of phosphorus supply on the formation and function of proteoid roots of white lupin (*Lupinus albus* L.). *Plant Cell Environ* **21**: 467–478.

Keltjens WG, Tan K. 1993. Interactions between aluminium, magnesium and calcium with different monocotyledonous and dicotyledonous plant species. *Plant Soil* **155–156**: 485–488.

Kiba T, Krapp A. 2016. Plant nitrogen acquisition under low availability: regulation of uptake and root architecture. *Plant Cell Physiol* **57**: 707–714.

Kidd DR, Ryan MH, Hahne D, Haling RE, Lambers H, Sandral GA, Simpson RJ, Cawthray GR. 2018. The carboxylate composition of rhizosheath and root exudates from twelve species of grassland and crop legumes with special reference to the occurrence of citramalate. *Plant Soil* **424**: 389–403.

Kidd PS, Proctor J. 2000. Effects of aluminium on the growth and mineral composition of *Betula pendula* Roth. *J Exp Bot* **51**: 1057–1066.

Kidd PS, Proctor J. 2001. Why plants grow poorly on very acid soils: are ecologists missing the obvious? *J Exp Bot* **52**: 791–799.

Kielland K. 1994. Amino acid absorption by arctic plants: implications for plant nutrition and nitrogen cycling. *Ecology* **75**: 2373–2383.

Kielland K, McFarland J, Olson K. 2006. Amino acid uptake in deciduous and coniferous taiga ecosystems. *Plant Soil* **288**: 297–307.

Killingbeck KT. 1996. Nutrients in senesced leaves: keys to the search for potential resorption and resorption proficiency. *Ecology* **77**: 1716–1727.

King BJ, Siddiqi MY, Ruth TJ, Warner RL, Glass A. 1993. Feedback regulation of nitrate influx in barley roots by nitrate, nitrite, and ammonium. *Plant Physiol* **102**: 1279–1286.

Kinraide TB. 1993. Aluminum enhancement of plant growth in acid rooting media. A case of reciprocal alleviation of toxicity by two toxic cations. *Physiol Plant* **88**: 619–625.

Kirk GJD, Greenway H, Atwell BJ, Ismail AM, Colmer TD 2014. Adaptation of rice to flooded soils. In: Lüttge U, Beyschlag W, Cushman J eds. *Progress in Botany: Vol 75*. Berlin: Springer, 215–253.

Kirk GJD, Kronzucker HJ. 2005. The potential for nitrification and nitrate uptake in the rhizosphere of wetland plants: a modelling study. *Ann Bot* **96**: 639–646.

Kirkham MB. 2006. Cadmium in plants on polluted soils: Effects of soil factors, hyperaccumulation, and amendments. *Geoderma* **137**: 19–32.

Klug B, Horst WJ. 2010. Oxalate exudation into the root-tip water free space confers protection from aluminum toxicity and allows aluminum accumulation in the symplast in buckwheat (*Fagopyrum esculentum*). *New Phytol* **187**: 380–391.

Kochian LV, Hoekenga OA, Piñeros MA. 2004. How do crop plants tolerate acid soils? Mechanisms of aluminum tolerance and phosphorous efficiency. *Annu Rev Plant Biol* **55**: 459–493.

Kochian LV, Piñeros MA, Hoekenga OA. 2005. The physiology, genetics and molecular biology of plant aluminum resistance and toxicity. *Plant Soil* **274**: 175–195.

Kochian LV, Piñeros MA, Liu J, Magalhaes JV. 2015. Plant adaptation to acid soils: the molecular basis for crop aluminum resistance. *Annu Rev Plant Biol* **66**: 571–598.

Kopittke PM. 2016. Role of phytohormones in aluminium rhizotoxicity. *Plant Cell Environ* **39**: 2319–2328.

Köppen WP. 1931. *Grundriss der Klimakunde*. Berlin: Walter de Gruyter.

Kotur Z, Glass ADM. 2015. A 150 kDa plasma membrane complex of AtNRT2.5 and AtNAR2.1 is the major contributor to constitutive high-affinity nitrate influx in *Arabidopsis thaliana*. *Plant Cell Environ* **38**: 1490–1502.

Krämer U. 2005. Phytoremediation: novel approaches to cleaning up polluted soils. *Curr Opin Biotechnol* **16**: 133–141.

Krämer U. 2010. Metal hyperaccumulation in plants. *Annu Rev Plant Biol* **61**: 517–534.

Krämer U, Cotter-Howells JD, Charnock JM, Baker AJM, Smith JAC. 1996. Free histidine as a metal chelator in plants that accumulate nickel. *Nature* **379**: 635–638.

Krämer U, Pickering IJ, Prince RC, Raskin I, Salt DE. 2000. Subcellular localization and speciation of nickel in hyperaccumulator and non-accumulator *Thlaspi* species. *Plant Physiol* **122**: 1343–1354.

Krapp A. 2015. Plant nitrogen assimilation and its regulation: a complex puzzle with missing pieces. *Curr Opin Plant Biol* **25**: 115–122.

Krapp A, David LC, Chardin C, Girin T, Marmagne A, Leprince A-S, Chaillou S, Ferrario-Méry S, Meyer C, Daniel-Vedele F. 2014. Nitrate transport and signalling in *Arabidopsis*. *J Exp Bot* **65**: 789–798.

Kronzucker HJ, Britto DT. 2011. Sodium transport in plants: a critical review. *New Phytol* **189**: 54–81.

Kronzucker HJ, Siddiqi MY, Glass AD. 1997. Conifer root discrimination against soil nitrate and the ecology of forest succession. *Nature* **385**: 59–61.

Kronzucker HJ, Siddiqi MY, Glass ADM, Kirk GJD. 1999. Nitrate-ammonium synergism in rice. A subcellular flux analysis. *Plant Physiol* **119**: 1041–1046.

Kumar RK, Chu H-H, Abundis C, Vasques K, Rodriguez DC, Chia J-C, Huang R, Vatamaniuk OK, Walker EL. 2017. Iron-nicotianamine transporters are required for proper long distance iron signaling. *Plant Physiol* **175**: 1254–1268.

Kuppusamy T, Giavalisco P, Arvidsson S, Sulpice R, Stitt M, Finnegan PM, Scheible W-R, Lambers H, Jost R. 2014. Phospholipids are replaced during leaf development, but protein and mature leaf metabolism respond to phosphate in highly phosphorus-efficient harsh hakea. *Plant Physiol* **166**: 1891–1911.

Lambers H, Ahmedi I, Berkowitz O, Dunne C, Finnegan PM, Hardy GESJ, Jost R, Laliberté E, Pearse SJ, Teste FP. 2013. Phosphorus nutrition of phosphorus-sensitive Australian native plants: threats to plant communities in a global biodiversity hotspot. *Cons Physiol* **1**: https://doi.org/10.1093/conphys/cot1010.

Lambers H, Albornoz F, Kotula L, Laliberté E, Ranathunge K, Teste FP, Zemunik G. 2018. How belowground interactions contribute to the coexistence of mycorrhizal and non-mycorrhizal species in severely phosphorus-impoverished hyperdiverse ecosystems. *Plant Soil* **424**: 11–34.

Lambers H, Bishop JG, Hopper SD, Laliberté E, Zúñiga-Feest A. 2012a. Phosphorus-mobilization ecosystem engineering: the roles of cluster roots and carboxylate exudation in young P-limited ecosystems. *Ann Bot* **110**: 329–348.

Lambers H, Brundrett MC, Raven JA, Hopper SD. 2010. Plant mineral nutrition in ancient

landscapes: high plant species diversity on infertile soils is linked to functional diversity for nutritional strategies. *Plant Soil* **334**: 11–31.

Lambers H, Cawthray GR, Giavalisco P, Kuo J, Laliberté E, Pearse SJ, Scheible W-R, Stitt M, Teste F, Turner BL. 2012b. Proteaceae from severely phosphorus-impoverished soils extensively replace phospholipids with galactolipids and sulfolipids during leaf development to achieve a high photosynthetic phosphorus-use efficiency. *New Phytol* **196**: 1098–1108.

Lambers H, Clode PL, Hawkins H-J, Laliberté E, Oliveira RS, Reddell P, Shane MW, Stitt M, Weston P 2015a. Metabolic adaptations of the non-mycotrophic Proteaceae to soil with a low phosphorus availability. In: Plaxton WC, Lambers H eds. *Annual Plant Reviews, Volume 48, Phosphorus Metabolism in Plants*. Chicester: John Wiley & Sons, 289–336.

Lambers H, Finnegan PM, Jost R, Plaxton WC, Shane MW, Stitt M. 2015b. Phosphorus nutrition in Proteaceae and beyond. *Nat Plants* **1**.

Lambers H, Hayes PE, Laliberté E, Oliveira RS, Turner BL. 2015c. Leaf manganese accumulation and phosphorus-acquisition efficiency. *Trends Plant Sci* **20**: 83–90.

Lambers H, Martinoia E, Renton M. 2015d. Plant adaptations to severely phosphorus-impoverished soils. *Curr Opin Plant Biol* **25**: 23–31.

Lambers H, Raven JA, Shaver GR, Smith SE. 2008. Plant nutrient-acquisition strategies change with soil age. *Trends Ecol Evol* **23**: 95–103.

Lambers H, Shane MW, Cramer MD, Pearse SJ, Veneklaas EJ. 2006. Root structure and functioning for efficient acquisition of phosphorus: matching morphological and physiological traits. *Ann Bot* **98**: 693–713.

Lambers H, Shane MW, Laliberté E, Swarts ND, Teste FP, Zemunik G 2014. Plant mineral nutrition. In: Lambers H ed. *Plant Life on the Sandplains in Southwest Australia, a Global Biodiversity Hotspot*. Crawley: UWA Publishing, 101–127.

Lasat MM, Baker AJM, Kochian LV. 1996. Physiological characterization of root Zn^{2+} absorption and translocation to shoots in Zn hyperaccumulator and nonaccumulator species of *Thlaspi*. *Plant Physiol* **112**: 1715–1722.

Lata J-C, Degrange V, Raynaud X, Maron P-A, Lensir R, Abbadie L. 2004. Grass populations control nitrification in savanna soils. *Funct Ecol* **18**: 605–611.

Li L, Li S-M, Sun J-H, Zhou L-L, Bao X-G, Zhang H-G, Zhang F-S. 2007. Diversity enhances agricultural productivity via rhizosphere phosphorus facilitation on phosphorus-deficient soils. *Proc Natl Acad Sci USA* **104**: 11192–11196.

Li L, Sheen J. 2016. Dynamic and diverse sugar signaling. *Curr Opin Plant Biol* **33**: 116–125.

Li L, Tang C, Rengel Z, Zhang F. 2003. Chickpea facilitates phosphorus uptake by intercropped wheat from an organic phosphorus source. *Plant Soil* **248**: 297–303.

Li M, Osaki M, Rao IM, Tadano T. 1997. Secretion of phytase from the roots of several plant species under phosphorus-deficient conditions. *Plant Soil* **195**: 161–169.

Li XW, Liu JY, Fang J, Tao L, Shen RF, Li YL, Xiao HD, Feng YM, Wen HX, Guan JH, Wu LS, He YM, Goldbach HE, Yu M. 2017. Boron supply enhances aluminum tolerance in root border cells of pea (*Pisum sativum*) by interacting with cell wall pectins. *Front Plant Sci* **8**: 742.

Lillo C, Meyer C, Lea US, Provan F, Oltedal S. 2004. Mechanism and importance of post-translational regulation of nitrate reductase. *J Exp Bot* **55**: 1275–1282.

Lintern M, Anand R, Ryan C, Paterson D. 2013. Natural gold particles in *Eucalyptus* leaves and their relevance to exploration for buried gold deposits. *Nat Comm* **4**: 2614.

Lipson D, Näsholm T. 2001. The unexpected versatility of plants: organic nitrogen use and availability in terrestrial ecosystems. *Oecologia* **128**: 305–316.

Liu K-H, Tsay Y-F. 2003. Switching between the two action modes of the dual-affinity nitrate transporter CHL1 by phosphorylation. *EMBO Journal* **22**: 1005–1013.

Liu X-Y, Koba K, Koyama LA, Hobbie SE, Weiss MS, Inagaki Y, Shaver GR, Giblin AE, Hobara S, Nadelhoffer KJ, Sommerkorn M, Rastetter EB, Kling GW, Laundre JA, Yano Y, Makabe A, Yano M, Liu C-Q. 2018. Nitrate is an important nitrogen source for Arctic tundra plants. *Proceedings of the National Academy of Sciences* **115**: 3398–3403.

Lodhi MAK, Killingbeck KT. 1980. Allelopathic inhibition of nitrification and nitrifying bacteria in a ponderosa pine (*Pinus ponderosa* Dougl.) community. *Am J Bot* **67**: 1423–1429.

Lolkema PC, Doornhof M, Ernst WHO. 1986. Interaction between a copper-tolerant and a copper-sensitive population of *Silene cucubalus*. *Physiol Plant* **67**: 654–658.

Loneragan JF. 1968. Nutrient requirements of plants. *Nature* **220**: 1307–1308.

Loneragan JF, Snowball K. 1969. Rate of calcium absorption by plant roots and its relation to growth. *Aust J Agric* **20**: 479–490.

Loveless AR. 1961. A Nutritional Interpretation of Sclerophylly Based on Differences in the Chemical Composition of Sclerophyllous and Mesophytic Leaves. *Ann Bot* **25**: 168–184.

Lv S, Jiang P, Tai F, Wang D, Feng J, Fan P, Bao H, Li Y. 2017. The V-ATPase subunit A is essential for salt tolerance through participating in vacuolar Na^+ compartmentalization in *Salicornia europaea*. *Planta* **246**: 1177–1187.

Ma JF. 2000. Role of organic acids in detoxification of aluminum in higher plants. *Plant Cell Physiol* **41**: 383–390.

Ma JF. 2005. Plant root responses to three abundant soil minerals: silicon, aluminum and iron. *Crit Rev Plant Sci* **24**: 267–281.

Ma JF, Goto S, Tamai K, Ichii M. 2001a. Role of root hairs and lateral roots in silicon uptake by rice. *Plant Physiol* **127**: 1773–1780.

Ma JF, Nagao S, Huang CF, Nishimura M. 2005. Isolation and characterization of a rice mutant hypersensitive to Al. *Plant Cell Physiol* **46**: 1054–1061.

Ma JF, Ryan PR, Delhaize E. 2001b. Aluminium tolerance in plants and the complexing role of organic acids. *Trends Plant Sci* **6**: 273–278.

Ma JF, Tamai K, Yamaji N, Mitani N, Konishi S, Katsuhara M, Ishiguro M, Murata Y, Yano M. 2006. A silicon transporter in rice. *Nature* **440**: 688–691.

Ma JF, Ueno H, Ueno D, Rombolà AD, Iwashita T. 2003. Characterization of phytosiderophore secretion under Fe deficiency stress in *Festuca rubra*. *Plant Soil* **256**: 131–137.

Ma JF, Yamaji N, Mitani N, Tamai K, Konishi S, Fujiwara T, Katsuhara M, Yano M. 2007. An efflux transporter of silicon in rice. *Nature* **448**: 209–212.

Maathuis FJM, Sanders D. 1996. Mechanisms of potassium absorption by higher plant roots. *Physiol Plant* **96**: 158–168.

Macduff JH, Hopper MJ, Wild A. 1987. The effect of root temperature on growth and uptake of ammonium and nitrate by *Brassica napus* L. cv. bien venu in flowing solution culture: II. uptake from solutions containing NH_4NO_3. *J Exp Bot* **38**: 53–66.

Macklon AES, Mackie-Dawson LA, Sim A, Shand CA, Lilly A. 1994. Soil P resources, plant growth and rooting characteristics in nutrient poor upland grasslands. *Plant Soil* **163**: 257–266.

Marcum KB, Pessarakli M. 2006. Salinity tolerance and salt gland excretion efficiency of bermudagrass turf cultivars. *Crop Sci* **46**: 2571–2574.

Marschner H, Römheld V, Cakmak I. 1987. Root-induced changes of nutrient availability in the rhizosphere. *J Plant Nutr* **10**: 1175–1184.

Marschner H, Römheld V, Kissel M. 1986. Different strategies in higher plants in mobilization and uptake of iron. *J Plant Nutr* **9**: 695–713.

Matimati I, Verboom GA, Cramer MD. 2014. Nitrogen regulation of transpiration controls mass-flow acquisition of nutrients. *J Exp Bot* **65**: 159–168.

McKane RB, Johnson LC, Shaver GR, Nadelhoffer KJ, Rastetter EB, Fry B, Giblin AE, Kielland K, Kwiatkowski BL, Laundre JA, Murray G. 2002. Resource-based niches provide a basis for plant species diversity and dominance in arctic tundra. *Nature* **415**: 68–71.

McNaughton SJ, Chapin FS. 1985. Effects of phosphorus nutrition and defoliation on C_4 graminoids from the Serengeti Plains. *Ecology* **66**: 1617–1629.

McNeilly T. 1968. Evolution in closely adjacent plant populations III. *Agrostis tenuis* on a small copper mine. *Heredity* **23**: 99–108.

Meerts P. 1997. Foliar macronutrient concentrations of forest understorey species in relation to Ellenberg's indices and potential relative growth rate. *Plant Soil* **189**: 257–265.

Meharg AA, Macnair MR. 1992. Suppression of the high affinity phosphate uptake system: a mechanism of arsenate tolerance in *Holcus lanatus* L. *J Exp Bot* **43**: 519–524.

Meier IC, Finzi AC, Phillips RP. 2017. Root exudates increase N availability by stimulating microbial turnover of fast-cycling N pools. *Soil Biol Biochem* **106**: 119–128.

Mengel K, Kirkby EA, Kosegarten H, Appel T 2001. Boron. *Principles of plant nutrition*: Springer, 621–638.

Mesjasz-Przybylowicz J, Przybylowicz W, Rama D, Pineda C. 2001. Elemental distribution in *Senecio anomalochrous*, a Ni hyperaccumulator from South Africa. *S Afr J Sci* **97**: 593–595.

Miatto RC, Wright IJ, Batalha MA. 2016. Relationships between soil nutrient status and nutrient-related leaf traits in Brazilian cerrado and seasonal forest communities. *Plant Soil* **404**: 13–33.

Miller AJ, Cramer MD. 2005. Root nitrogen acquisition and assimilation. *Plant Soil* **274**: 1–36.

Mistrik I, Ullrich CI. 1996. Mechanism of anion uptake in plant roots: quantitative evaluation of H^+/NO_3^- and $H^+/H_2PO_4^-$ stoichiometries. *Plant Physiol Bochem* **34**: 629–636.

Mo Q, Zou B, Li Y, Chen Y, Zhang W, Mao R, Ding Y, Wang J, Lu X, Li X, Tang J, Li Z, Wang F. 2015. Response of plant nutrient stoichiometry to fertilization varied with plant tissues in a tropical forest. *Sci Rep* **5**: 14605.

Morère-Le Paven M-C, Viau L, Hamon A, Vandecasteele C, Pellizzaro A, Bourdin C, Laffont C, Lapied B, Lepetit M, Frugier F, Legros C, Limami AM. 2011. Characterization of a dual-affinity nitrate transporter MtNRT1.3 in the model legume *Medicago truncatula*. *J Exp Bot* **62**: 5595–5605.

Munns R. 2002. Comparative physiology of salt and water stress. *Plant Cell Environ* **25**: 239–250.

Munns R, Gilliham M. 2015. Salinity tolerance of crops – what is the cost? *New Phytol* **208**: 668–673.

Munns R, Tester M. 2008. Mechanisms of salinity tolerance. *Annu Rev Plant Biol* **59**: 651–681.

Nair VD, Prenzel J. 1978. Calculations of equilibrium concentration of mono- and polynuclear hydroxyaluminium species at different pH and total aluminium concentrations. *Z Pflanzenernähr Bodenkd* **141**: 741–751.

Näsholm T, Kieland K, Ganeteg U. 2009. Uptake of organic nitrogen by plants. *New Phytol* **182**: 31–48.

Nazoa P, Vidmar JJ, Tranbarger T, Mouline K, Damiani I, Tillard P, Zhuo D, Glass AM, Touraine B. 2003. Regulation of the nitrate transporter gene *AtNRT2.1* in *Arabidopsis thaliana*: responses to

nitrate, amino acids and developmental stage. *Plant Mol Biol* **52**: 689–703.

Neugebauer K, Broadley MR, El-Serehy HA, George TS, McNicol JW, de Moraes MF, White PJ. 2018. Variation in the Angiosperm ionome. *Physiol Plant* **163**: 306–322.

Nian H, Yang ZM, Ahn SJ, Cheng ZJ, Matsumoto H. 2002. A comparative study on the aluminium-and copper-induced organic acid exudation from wheat roots. *Physiol Plant* **116**: 328–335.

Niklas KJ, Cobb ED. 2005. N, P, and C stoichiometry of *Eranthis hyemalis* (Ranunculaceae) and the allometry of plant growth. *Am J Bot* **92**: 1256–1263.

Nkrumah PN, Baker AJM, Chaney RL, Erskine PD, Echevarria G, Morel JL, van der Ent A. 2016. Current status and challenges in developing nickel phytomining: an agronomic perspective. *Plant Soil* **406**: 55–69.

Nozoye T, Nagasaka S, Kobayashi T, Takahashi M, Sato Y, Sato Y, Uozumi N, Nakanishi H, Nishizawa NK. 2011. Phytosiderophore efflux transporters are crucial for iron acquisition in graminaceous plants. *J Biol Chem* **286**: 5446–5454.

Nuruzzaman M, Lambers H, Bolland MDA, Veneklaas EJ. 2005. Phosphorus benefits of different legume crops to subsequent wheat grown in different soils of Western Australia. *Plant Soil* **271**: 175–187.

Nye PH, Tinker PB. 1977. *Solute Mmovement in the Soil-Root System*. Oxford: Blackwell.

Odjegba VJ, Fasidi IO. 2007. Phytoremediation of heavy metals by *Eichhornia crassipes*. *Environmentalist* **27**: 349–355.

Ohwaki Y, Sugahara K. 1997. Active extrusion of protons and exudation of carboxylic acids in response to iron deficiency by roots of chickpea (*Cicer arietinum* L.). *Plant Soil* **189**: 49–55.

Oliveira RS, Galvão HC, de Campos MCR, Eller CB, Pearse SJ, Lambers H. 2015. Mineral nutrition of *campos rupestres* plant species on contrasting nutrient-impoverished soil types. *New Phytol* **205**: 1183–1194.

Ostertag R, DiManno NM. 2016. Detecting terrestrial nutrient limitation: a global meta-analysis of foliar nutrient concentrations after fertilization. *Front Earth Sci* **4**: 23.

Pang J, Ruchi B, Zhao H, Bansal R, Bohuon E, Lambers H, Ryan MH, Ranathunge K, Siddique KMH. 2018. The carboxylate-releasing phosphorus-mobilising strategy could be proxied by foliar manganese concentration in a large set of chickpea germplasm under low phosphorus supply. *New Phytol* **219**: 518–529.

Parfitt RL. 1979. The availability of P from phosphate-goethite bridging complexes. Desorption and uptake by ryegrass. *Plant Soil* **53**: 55–65.

Passioura J, Ball M, Knight J. 1992. Mangroves may salinize the soil and in so doing limit their transpiration rate. *Funct Ecol* **6**: 476–481.

Paungfoo-Lonhienne C, Lonhienne TGA, Rentsch D, Robinson N, Christie M, Webb RI, Gamage HK, Carroll BJ, Schenk PM, Schmidt S. 2008. Plants can use protein as a nitrogen source without assistance from other organisms. *Proc Natl Acad Sci USA* **105**: 4524–4529.

Pausch J, Kuzyakov Y. 2018. Carbon input by roots into the soil: quantification of rhizodeposition from root to ecosystem scale. *Glob Change Biol* **24**: 1–12.

Pavlovic J, Samardzic J, Maksimović V, Timotijevic G, Stevic N, Laursen KH, Hansen TH, Husted S, Schjoerring JK, Liang Y, Nikolic M. 2013. Silicon alleviates iron deficiency in cucumber by promoting mobilization of iron in the root apoplast. *New Phytol* **198**: 1096–1107.

Pearse SJ, Veneklaas EJ, Cawthray GR, Bolland MDA, Lambers H. 2006. Carboxylate release of wheat, canola and 11 grain legume species as affected by phosphorus status. *Plant Soil* **288**: 127–139.

Pegtel DM. 1987. Effect of ionic Al in culture solutions on the growth of *Arnica montana* L. and *Deschampsia flexuosa* (L.) Trin. *Plant Soil* **102**: 85–92.

Pérez Corona ME, Van Der Klundert I, Verhoeven JTA. 1996. Availability of organic and inorganic phosphorus compounds as phosphorus sources for *Carex* species. *New Phytol* **133**: 225–231.

Pett-Ridge JC. 2009. Contributions of dust to phosphorus cycling in tropical forests of the Luquillo Mountains, Puerto Rico. *Biogeochemistry* **94**: 63–80.

Peuke AD. 2010. Correlations in concentrations, xylem and phloem flows, and partitioning of elements and ions in intact plants. A summary and statistical re-evaluation of modelling experiments in Ricinus communis. *J Exp Bot* **61**: 635–655.

Poorter H, Remkes C. 1990. Leaf area ratio and net assimilation rate of 24 wild species differing in relative growth rate. *Oecologia* **83**: 553–559.

Poorter H, Remkes C, Lambers H. 1990. Carbon and nitrogen economy of 24 wild species differing in relative growth rate. *Plant Physiol* **94**: 621–627.

Porder S, Ramachandran S. 2013. The phosphorus concentration of common rocks—a potential driver of ecosystem P status. *Plant Soil* **367**: 41–55.

Porder S, Vitousek P, Chadwick O, Chamberlain C, Hilley G. 2007. Uplift, erosion, and phosphorus limitation in terrestrial ecosystems. *Ecosystems* **10**: 159–171.

Poschenrieder C, Tolrà R, Barceló J. 2006. Can metals defend plants against biotic stress? *Trends Plant Sci* **11**: 288–295.

Pourret O, Bollinger J-C. 2018. "Heavy metal"—What to do now: to use or not to use? *Sci Tot Environ* **610–611**: 419–420.

Prodhan MA, Finnegan PM, Lambers H. 2019. How does evolution in phosphorus-impoverished landscapes impact plant nitrogen and sulfur assimilation? *Trends Plant Sci* **24**: 69–82.

Prodhan MA, Jost R, Watanabe M, Hoefgen R, Lambers H, Finnegan PM. 2016. Tight control of nitrate acquisition in a plant species that evolved in an extremely phosphorus-impoverished environment. *Plant Cell Environ* **39**: 2754–2761.

Prodhan MA, Jost R, Watanabe M, Hoefgen R, Lambers H, Finnegan PM. 2017. Tight control of

sulfur assimilation: an adaptive mechanism for a plant from a severely phosphorus-impoverished habitat. *New Phytol* **215**: 1068–1079.

Purnell H. 1960. Studies of the family Proteaceae. I. Anatomy and morphology of the roots of some Victorian species. *Aust J Bot* **8**: 38–50.

Rauser WE. 1995. Phytochelatins and related peptides (structure, biosynthesis, and function). *Plant Physiol* **109**: 1141–1149.

Raven JA. 2012. Protein turnover and plant RNA and phosphorus requirements in relation to nitrogen fixation. *Plant Sci* **188–189**: 25–35.

Raven JA, Lambers H, Smith SE, Westoby M. 2018. Costs of acquiring phosphorus by vascular land plants: patterns and implications for plant coexistence. *New Phytol* **217**: 1420–1427.

Rawat SR, Silim SN, Kronzucker HJ, Siddiqi MY, Glass ADM. 1999. AtAMT1 gene expression and NH_4^+ uptake in roots of *Arabidopsis thaliana*: evidence for regulation by root glutamine levels. *Plant J* **19**: 143–152.

Read J, Sanson GD, Garine-Wichatitsky Md, Jaffré T. 2006. Sclerophylly in two contrasting tropical environments: low nutrients vs. low rainfall. *Am J Bot* **93**: 1601–1614.

Reddell P, Yun Y, Shipton WA. 1997. Cluster roots and mycorrhizae in *Casuarina cunninghamiana:* their occurrence and formation in relation to phosphorus supply. *Aust J Bot* **45**: 41–51.

Reed SC, Townsend AR, Davidson EA, Cleveland CC. 2012. Stoichiometric patterns in foliar nutrient resorption across multiple scales. *New Phytol* **196**: 173–180.

Reed SC, Yang X, Thornton PE. 2015. Incorporating phosphorus cycling into global modeling efforts: a worthwhile, tractable endeavor. *New Phytol* **208**: 324–329.

Rezania S, Ponraj M, Talaiekhozani A, Mohamad SE, Md Din MF, Taib SM, Sabbagh F, Sairan FM. 2015. Perspectives of phytoremediation using water hyacinth for removal of heavy metals, organic and inorganic pollutants in wastewater. *J Environ Manage* **163**: 125–133.

Richardson AE, Lynch JP, Ryan PR, Delhaize E, Smith FA, Smith SE, Harvey PR, Ryan MH, Veneklaas EJ, Lambers H, Oberson A, Culvenor RA, Simpson RJ. 2011. Plant and microbial strategies to improve the phosphorus efficiency of agriculture. *Plant Soil* **349**: 121–156.

Richardson AE, Simpson RJ. 2011. Soil microorganisms mediating phosphorus availability update on microbial phosphorus. *Plant Physiol* **156**: 989–996.

Richardson S, Peltzer D, Allen R, McGlone M, Parfitt R. 2004. Rapid development of phosphorus limitation in temperate rainforest along the Franz Josef soil chronosequence. *Oecologia* **139**: 267–276.

Richardson SJ, Peltzer DA, Allen RB, McGlone MS. 2005. Resorption proficiency along a chronosequence: responses among communities and within species. *Ecology* **86**: 20–25.

Roberts SK. 2006. Plasma membrane anion channels in higher plants and their putative functions in roots. *New Phytol* **169**: 647–666.

Robinson D. 1996. Variation, co-ordination and compensation in root systems in relation to soil variability. *Plant Soil* **187**: 57–66.

Robinson NJ, Tommey AM, Kuske C, Jackson PJ. 1993. Plant metallothioneins. *Biochem J* **295**: 1–10.

Rodríguez-Alonso J, Sierra MJ, Lominchar MA, Millán R. 2017. Mercury tolerance study in holm oak populations from the Almadén mining district (Spain). *Env Exp Bot* **133**: 98–107.

Römer W, Kang D-K, Egle K, Gerke J, Keller H. 2000. The acquisition of cadmium by *Lupinus albus* L., *Lupinus angustifolius* L., and *Lolium multiflorum* Lam. *J Plant Nutr Soil Sci* **163**: 623–628.

Römheld V. 1987. Different strategies for iron acquisition in higher plants. *Physiol Plant* **70**: 231–234.

Rose TJ, Damon P, Rengel Z. 2010a. Phosphorus-efficient faba bean (*Vicia faba* L.) genotypes enhance subsequent wheat crop growth in an acid and an alkaline soil. *Crop Past Sci* **61**: 1009–1016.

Rose TJ, Hardiputra B, Rengel Z. 2010b. Wheat, canola and grain legume access to soil phosphorus fractions differs in soils with contrasting phosphorus dynamics. *Plant Soil* **326**: 159–170.

Rossatto DR, Hoffmann WA, de Carvalho Ramos Silva L, Haridasan M, Sternberg LSL, Franco AC. 2013. Seasonal variation in leaf traits between congeneric savanna and forest trees in Central Brazil: implications for forest expansion into savanna. *Trees* **27**: 1139–1150.

Ryan PR, Kinraide TB, Kochian LV. 1993. Al^{3+}-Ca^{2+} interactions in aluminum rhizotoxicity. I. Inhibition of root growth is not caused by reduction of calcium uptake. *Planta* **192**: 98–103.

Ryan PR, Reid RJ, Smith FA. 1997. Direct evaluation of the Ca^{2+}-displacement hypothesis for Al toxicity. *Plant Physiol* **113**: 1351–1357.

Saaltink RM, Dekker SC, Eppinga MB, Griffioen J, Wassen MJ. 2017. Plant-specific effects of iron-toxicity in wetlands. *Plant Soil* **416**: 83–96.

Salehi A, Mehdi B, Fallah S, Kaul H-P, Neugschwandtner RW. 2018. Productivity and nutrient use efficiency with integrated fertilization of buckwheat–fenugreek intercrops. *Nutr Cycl Agroecos* **110**: 407–425.

Salt DE, Baxter I, Lahner B. 2008. Ionomics and the study of the plant ionome. *Annu Rev Plant Biol* **59**: 709–733.

Salt DE, Kato N, Krämer U, Smith RD, Raskin I 2000. The role of root exudates in nickel hyperaccumulation and tolerance in accumulator and nonaccumulator species of *Thlaspi*. In: Terry N, Bañuelos GS eds. *Phytoremediation of Contaminated Soil and Water*. Boca Raton, FL, USA: CRC Press, 191–202.

Salt DE, Prince RC, Pickering IJ, Raskin I. 1995. Mechanisms of cadmium mobility and accumulation in Indian mustard. *Plant Physiol* **109**: 1427–1433.

Salt DE, Rauser WE. 1995. MgATP-dependent transport of phytochelatins across the tonoplast of oat roots. *Plant Physiol* **107**: 1293–1301.

Sardans J, Peñuelas J, Estiarte M. 2007. Seasonal patterns of root-surface phosphatase activities in a Mediterranean shrubland. Responses to experimental warming and drought. *Biol Fert Soils* **43**: 779–786.

Savvides A, Ali S, Tester M, Fotopoulos V. 2016. Chemical priming of plants against multiple abiotic stresses: mission possible? *Trends Plant Sci* **21**: 329–340.

Schat H, Kalff MMA. 1992. Are phytochelatins involved in differential metal tolerance or do they merely reflect metal-imposed strain? *Plant Physiol* **99**: 1475–1480.

Scheurwater I, Clarkson DT, Purves JV, Van Rijt G, Saker LR, Welschen R, Lambers H. 1999. Relatively large nitrate efflux can account for the high specific respiratory costs for nitrate transport in slow-growing grass species. *Plant Soil* **215**: 123–134.

Schimel JP, Bennett J. 2004. Nitrogen mineralization: challenges of a changing paradigm. *Ecology* **85**: 591–602.

Schmidt S, Stewart GR. 1999. Glycine metabolism by plant roots and its occurrence in Australian plant communities. *Funct Plant Biol* **26**: 253–264.

Schmidt W. 2003. Iron solutions: acquisition strategies and signaling pathways in plants. *Trends Plant Sci* **8**: 188–193.

Schroder JL, Zhang H, Girma K, Raun WR, Penn CJ, Payton ME. 2011. Soil acidification from long-term use of nitrogen fertilizers on winter wheat. *Soil Sci Soc Am J* **75**: 957–964.

Secco D, Bouain N, Rouached A, Prom-u-thai C, Hanin M, Pandey AK, Rouached H. 2017. Phosphate, phytate and phytases in plants: from fundamental knowledge gained in *Arabidopsis* to potential biotechnological applications in wheat. *Crit Rev Biotechnol* **37**: 898–910.

Shabala S, Bose J, Hedrich R. 2014. Salt bladders: do they matter? *Trends Plant Sci* **19**: 687–691.

Shane MW, Cawthray GR, Cramer MD, Kuo J, Lambers H. 2006a. Specialized 'dauciform' roots of Cyperaceae are structurally distinct, but functionally analogous with 'cluster' roots. *Plant Cell Environ* **29**: 1989–1999.

Shane MW, Cramer MD, Funayama-Noguchi S, Cawthray GR, Millar AH, Day DA, Lambers H. 2004a. Developmental physiology of cluster-root carboxylate synthesis and exudation in harsh hakea. Expression of phospho*enol*pyruvate carboxylase and the alternative oxidase. *Plant Physiol* **135**: 549–560.

Shane MW, De Vos M, De Roock S, Lambers H. 2003. Shoot P status regulates cluster-root growth and citrate exudation in *Lupinus albus* grown with a divided root system. *Plant Cell Environ* **26**: 265–273.

Shane MW, Dixon KW, Lambers H. 2006b. The occurrence of dauciform roots amongst Western Australian reeds, rushes and sedges, and the impact of phosphorus supply on dauciform-root development in *Schoenus unispiculatus* (Cyperaceae). *New Phytol* **165**: 887–898.

Shane MW, Lambers H. 2005. Cluster roots: a curiosity in context. *Plant Soil* **274**: 101–125.

Shane MW, Lambers H. 2006. Systemic suppression of cluster-root formation and net P-uptake rates in *Grevillea crithmifolia* at elevated P supply: a proteacean with resistance for developing symptoms of 'P toxicity'. *J Exp Bot* **57**: 413–423.

Shane MW, McCully ME, Lambers H. 2004b. Tissue and cellular phosphorus storage during development of phosphorus toxicity in *Hakea prostrata* (Proteaceae). *J Exp Bot* **55**: 1033–1044.

Shane MW, Szota C, Lambers H. 2004c. A root trait accounting for the extreme phosphorus sensitivity of *Hakea prostrata* (Proteaceae). *Plant Cell Environ* **27**: 991–1004.

Sharma SS, Dietz K-J. 2006. The significance of amino acids and amino acid-derived molecules in plant responses and adaptation to heavy metal stress. *J Exp Bot* **57**: 711–726.

Shi J, Strack D, Albornoz F, Han Z, Lambers H. 2019. Differences in investment and functioning of cluster roots account for different distributions between *Banksia attenuata* and *B. sessilis,* with contrasting life history. *Plant Soil* **in press**: https://doi.org/10.1007/s11104-11019-03982-11106.

Shinmachi F, Buchner P, Stroud JL, Parmar S, Zhao F-J, McGrath SP, Hawkesford MJ. 2010. Influence of sulfur deficiency on the expression of specific sulfate transporters and the distribution of sulfur, selenium, and molybdenum in wheat. *Plant Physiol* **153**: 327–336.

Siddiqi MY, Glass ADM, Ruth TJ, Rufty TW. 1990. Studies of the uptake of nitrate in barley: I. Kinetics of $^{13}NO_3^-$ influx. *Plant Physiol* **93**: 1426–1432.

Silberbush M, Barber SA. 1983. Sensitivity of simulated phosphorus uptake to parameters used by a mechanistic-mathematical model. *Plant Soil* **74**: 93–100.

Silva IR, Smyth TJ, Israel DW, Raper CD, Rufty TW. 2001a. Magnesium ameliorates aluminum rhizotoxicity in soybean by increasing citric acid production and exudation by roots. *Plant Cell Physiol* **42**: 546–554.

Silva IR, Smyth TJ, Israel DW, Rufty TW. 2001b. Altered aluminum inhibition of soybean root elongation in the presence of magnesium. *Plant Soil* **230**: 223–230.

Skirycz A, Castilho A, Chaparro C, Carvalho N, Tzotzos G, Siqueira JO. 2014. Canga biodiversity, a matter of mining. *Front Plant Sci* **5**.

Smart C, Garvin D, Prince J, Lucas W, Kochian L. 1996. The molecular basis of potassium nutrition in plants. *Plant Soil* **187**: 81–89.

Smirnoff N, Todd P, Stewart GR. 1984. The occurrence of nitrate reduction in the leaves of woody plants. *Ann Bot* **54**: 363–374.

Soderberg K, Compton J. 2007. Dust as a nutrient source for fynbos ecosystems, South Africa. *Ecosystems* **10**: 550–561.

Song A, Li P, Li Z, Fan F, Nikolic M, Liang Y. 2011. The alleviation of zinc toxicity by silicon is related to zinc transport and antioxidative reactions in rice. *Plant Soil* **344**: 319–333.

Soper FM, Paungfoo-Lonhienne C, Brackin R, Rentsch D, Schmidt S, Robinson N. 2011. *Arabidopsis* and *Lobelia anceps* access small peptides as a nitrogen source for growth. *Funct Plant Biol* **38**: 788–796.

Sprent JI. 1999. Nitrogen fixation and growth of non-crop legume species in diverse environments. *Perspect Plant Ecol Evol Syst* **2**: 149–162.

Staal M, Maathuis FJM, Elzenga JTM, Overbeek JHM, Prins HBA. 1991. Na^{+}/H^{+} antiport activity in tonoplast vesicles from roots of the salt-tolerant *Plantago maritima* and the salt-sensitive *Plantago media*. *Physiol Plant* **82**: 179–184.

Stark JM, Hart SC. 1997. High rates of nitrification and nitrate turnover in undisturbed coniferous forests. *Nature* **385**: 61–64.

Steidinger BS, Turner BL, Corrales A, Dalling JW. 2014. Variability in potential to exploit different soil organic phosphorus compounds among tropical montane tree species. *Funct Ecol* **29**: 121–130.

Subbarao G, Arango J, Masahiro K, Hooper A, Yoshihashi T, Ando Y, Nakahara K, Deshpande S, Ortiz-Monasterio I, Ishitani M. 2017. Genetic mitigation strategies to tackle agricultural GHG emissions: The case for biological nitrification inhibition technology. *Plant Sci* **262**: 165–168.

Sulpice R, Ishihara H, Schlereth A, Cawthray GR, Encke B, Giavalisco P, Ivakov A, Arrivault S, Jost R, Krohn N, Kuo J, Laliberté E, Pearse SJ, Raven JA, Scheible WR, Teste F, Veneklaas EJ, Stitt M, Lambers H. 2014. Low levels of ribosomal RNA partly account for the very high photosynthetic phosphorus-use efficiency of Proteaceae species. *Plant Cell Environ* **37**: 1276–1298.

Suriyagoda LDB, Rajapaksha R, Pushpakumara G, Lambers H. 2018. Nutrient resorption from senescing leaves of epiphytes, hemiparasites and their hosts in tropical forests of Sri Lanka. *J Plant Ecol* **11**: 815–826.

Szczerba MW, Britto DT, Kronzucker HJ. 2006. The face value of ion fluxes: the challenge of determining influx in the low-affinity transport range. *J Exp Bot* **57**: 3293–3300.

Tan K, Keltjens WG. 1990. Interaction between aluminium and phosphorus in sorghum plants. II. Studies with the aluminium tolerant sorghum genotype SC0283. *Plant Soil* **124**: 25–32.

Tarafdar JC, Jungk A. 1987. Phosphatase activity in the rhizosphere and its relation to the depletion of soil organic phosphorus. *Biol Fert Soils* **3**: 199–204.

Teakle N, Flowers T, Real D, Colmer T. 2007. *Lotus tenuis* tolerates the interactive effects of salinity and waterlogging by 'excluding' Na^{+} and Cl^{-} from the xylem. *J Exp Bot* **58**: 2169–2180.

Teodoro GS, Lambers H, Nascimento DL, de Britto Costa P, Flores-Borges DNA, Abrahão A, Mayer JLS, Sawaya ACHF, Ladeira FSB, Abdala DB, Pérez CA, Oliveira RS. 2019. Specialized roots of Velloziaceae weather quartzite rock while mobilizing phosphorus using carboxylates. *Funct Ecol* **33**: 762–773.

Tester M, Davenport R. 2003. Na^{+} tolerance and Na^{+} transport in higher plants. *Ann Bot* **91**: 503–527.

Tinker PB, Nye PH. 2000. *Solute Movement in the Rhizosphere*. New York, USA: Oxford University Press.

Tomasi N, Kretzschmar T, Espen L, Weisskopf L, Fuglsang AT, Palmgren MG, Neumann G, Varanini Z, Pinton R, Martinoia E, Cesco S. 2009. Plasma membrane H^{+}-ATPase-dependent citrate exudation from cluster roots of phosphate-deficient white lupin. *Plant Cell Environ* **32**: 465–475.

Trueman LJ, Richardson A, Forde BG. 1996. Molecular cloning of higher plant homologues of the high-affinity nitrate transporters of *Chlamydomonas reinhardtii* and *Aspergillus nidulans*. *Gene* **175**: 223–231.

Tsai HH, Schmidt W. 2017. Mobilization of iron by plant-borne coumarins. *Trends Plant Sci* **22**: 538–548.

Tsujii Y, Oikawa M, Kitayama K. 2017a. Significance of the localization of phosphorus among tissues on a cross-section of leaf lamina of Bornean tree species for phosphorus-use efficiency. *J Trop Ecol* **33**: 237–240.

Tsujii Y, Onoda Y, Kitayama K. 2017b. Phosphorus and nitrogen resorption from different chemical fractions in senescing leaves of tropical tree species on Mount Kinabalu, Borneo. *Oecologia* **185**: 171–180.

Tukey HB. 1970. The leaching of substances from plants. *Annu Rev Plant Physiol* **21**: 305–324.

Turner BL. 2006. Organic phosphorus in Madagascan rice soils. *Geoderma* **136**: 279–288.

Turner BL, Condron LM. 2013. Pedogenesis, nutrient dynamics, and ecosystem development: the legacy of T.W. Walker and J.K. Syers. *Plant Soil* **367**: 1–10.

Turner BL, Laliberté E, Hayes PE. 2018a. A climosequence of chronosequences in southwestern Australia. *Eur J Soil Sci* **69**: 69–85.

Turner BL, Richardson AE. 2004. Identification of-inositol phosphates in soil by solution phosphorus-31 nuclear magnetic resonance spectroscopy. *Soil Sci Soc Am J* **68**: 802–808.

Turner BL, Wells A, Andersen KM, Condron LM. 2018b. Consequences of the physical nature of the parent material for pedogenesis, nutrient availability, and succession in temperate rainforests. *Plant Soil* **423**: 533–548.

Turner BL, Wells A, Condron LM. 2014. Soil organic phosphorus transformations along a coastal dune chronosequence under New Zealand temperate rain forest. *Biogeochemistry* **121**: 595–611.

Tyler G, Ström L. 1995. Differing organic acid exudation pattern explains calcifuge and acidifuge behaviour of plants. *Ann Bot* **75**: 75–78.

Ueno D, Rombolà AD, Iwashita T, Nomoto K, Ma JF. 2007. Identification of two novel phytosiderophores secreted by perennial grasses. *New Phytol* **174**: 304–310.

Van der Ent A, Baker AJM, Reeves RD, Pollard AJ, Schat H. 2013. Hyperaccumulators of metal and

metalloid trace elements: facts and fiction. *Plant Soil* **362**: 319–334.

Van der Ent A, Jaffré T, L'Huillier L, Gibson N, Reeves RD. 2015. The flora of ultramafic soils in the Australia–Pacific Region: state of knowledge and research priorities. *Aust J Bot* **63**: 173–190.

Van der Werf A, Visser A, Schieving F, Lambers H. 1993. Evidence for optimal partitioning of biomass and nitrogen at a range of nitrogen availabilities for a fast-and slow-growing species. *Funct Ecol* **7**: 63–74.

Van Hoof NALM, Hassinen VH, Hakvoort HWJ, Ballintijn KF, Schat H, Verkleij JAC, Ernst WHO, Karenlampi SO, Tervahauta AI. 2001a. Enhanced copper tolerance in *Silene vulgaris* (Moench) Garcke populations from copper mines Is associated with increased transcript levels of a 2b-type metallothionein gene. *Plant Physiol* **126**: 1519–1526.

Van Hoof NALM, Koevoets PLM, Hakvoort HWJ, Ten Bookum WM, Schat H, Verkleij JAC, Ernst WHO. 2001b. Enhanced ATP-dependent copper efflux across the root cell plasma membrane in copper-tolerant *Silene vulgaris*. *Physiol Plant* **113**: 225–232.

Van Vuuren MMI, Robinson D, Griffiths BS. 1996. Nutrient inflow and root proliferation during the exploitation of a temporally and spatially discrete source of nitrogen in soil. *Plant Soil* **178**: 185–192.

Veneklaas EJ, Lambers H, Bragg J, Finnegan PM, Lovelock CE, Plaxton WC, Price C, Scheible W-R, Shane MW, White PJ, Raven JA. 2012. Opportunities for improving phosphorus-use efficiency in crop plants. *New Phytol* **195**: 306–320.

Vengavasi K, Pandey R. 2018. Root exudation potential in contrasting soybean genotypes in response to low soil phosphorus availability is determined by photobiochemical processes. *Plant Physiol Bochem* **124**: 1–9.

Verboom GA, Stock WD, Cramer MD. 2017. Specialization to extremely low-nutrient soils limits the nutritional adaptability of plant lineages. *Amer Nat* **189**: 684–699.

Vergutz L, Manzoni S, Porporato A, Novais RF, Jackson RB. 2012. Global resorption efficiencies and concentrations of carbon and nutrients in leaves of terrestrial plants. *Ecol Monogr* **82**: 205–220.

Villafort Carvalho MT, Pongrac P, Mumm R, van Arkel J, van Aelst A, Jeromel L, Vavpetič P, Pelicon P, Aarts MGM. 2015. *Gomphrena claussenii,* a novel metal-hypertolerant bioindicator species, sequesters cadmium, but not zinc, in vacuolar oxalate crystals. *New Phytol* **208**: 763–775.

Vitousek P. 1982. Nutrient cycling and nutrient use efficiency. *Amer Nat* **119**: 553–572.

Vitousek PM. 2004. *Nutrient Cycling and Limitation: Hawaii as a Model System*. Princeton: Princeton University Press.

Vitousek PM, Porder S, Houlton BZ, Chadwick OA. 2010. Terrestrial phosphorus limitation: mechanisms, implications, and nitrogen-phosphorus interactions. *Ecol Appl* **20**: 5–15.

Voesenek LACJ, Bailey-Serres J. 2015. Flood adaptive traits and processes: an overview. *New Phytol* **206**: 57–73.

Vos J, Van Der Putten PEL. 1998. Effect of nitrogen supply on leaf growth, leaf nitrogen economy and photosynthetic capacity in potato. *Field Crops Res* **59**: 63–72.

Walker TW, Syers JK. 1976. The fate of phosphorus during pedogenesis. *Geoderma* **15**: 1–9.

Wang BL, Shen JB, Zhang WH, Zhang FS, Neumann G. 2007. Citrate exudation from white lupin induced by phosphorus deficiency differs from that induced by aluminum. *New Phytol* **176**: 581–589.

Wang MY, Siddiqi MY, Ruth TJ, Glass AD. 1993. Ammonium uptake by rice roots (II. Kinetics of $^{13}NH_4^+$ influx across the plasmalemma). *Plant Physiol* **103**: 1259–1267.

Wang Y-Y, Hsu P-K, Tsay Y-F. 2012. Uptake, allocation and signaling of nitrate. *Trends Plant Sci* **17**: 458–467.

Warren CR. 2006. Potential organic and inorganic N uptake by six *Eucalyptus* species. *Funct Plant Biol* **33**: 653–660.

Wen Z, Tyerman SD, Dechorgnat J, Ovchinnikova E, Dhugga KS, Kaiser BN. 2017. Maize NPF6 proteins are homologs of *Arabidopsis* CHL1 that are selective for both nitrate and chloride. *Plant Cell* **29**: 2581–2596.

Westoby M, Falster DS, Moles AT, Vesk PA, Wright IJ. 2002. Plant ecological strategies: some leading dimensions of variation between species. *Annu Rev Ecol Syst* **33**: 125–159.

White PJ. 1999. The molecular mechanism of sodium influx to root cells. *Trends Plant Sci* **4**: 245–246.

White PJ, Broadley MR. 2003. Calcium in plants. *Ann Bot* **92**: 487–511.

White PJ, Broadley MR, Thompson JA, McNicol JW, Crawley MJ, Poulton PR, Johnston AE. 2012. Testing the distinctness of shoot ionomes of angiosperm families using the Rothamsted Park Grass Continuous Hay Experiment. *New Phytol* **196**: 101–109.

Whittaker RH. 1954. The ecology of serpentine soils. I. Introduction. *Ecology* **35**: 258–259.

Wiche O, Székely B, Kummer N-A, Moschner C, Heilmeier H. 2016. Effects of intercropping of oat (*Avena sativa* L.) with white lupin (*Lupinus albus* L.) on the mobility of target elements for phytoremediation and phytomining in soil solution. *Int J Phytorem* **18**: 900–907.

Wilson H, Mycock D, Weiersbye IM. 2017. The salt glands of *Tamarix usneoides* E. Mey. ex Bunge (South African salt cedar). *Int J Phytorem* **19**: 587–595.

Wilson JB. 1988. The cost of heavy-metal tolerance: an example. *Evolution* **42**: 408–413.

Woodward RA, Harper KT, Tiedemann AR. 1984. An ecological consideration of the significance of cation-exchange capacity of roots of some Utah range plants. *Plant Soil* **79**: 169–180.

Wu G, Li M, Zhong F, Fu C, Sun J, Yu L. 2011. *Lonicera confusa* has an anatomical mechanism to respond to calcium-rich environment. *Plant Soil* **338**: 343–353.

Xiong H, Kakei Y, Kobayashi T, Guo X, Nakazono M, Takahashi H, Nakanishi H, Shen H, Zhang F, Nishizawa NK, Zuo Y. 2013. Molecular evidence for phytosiderophore-induced improvement of iron nutrition of peanut intercropped with maize in calcareous soil. *Plant Cell Environ* **36**: 1888–1902.

Xu G, Fan X, Miller AJ. 2012. Plant nitrogen assimilation and use efficiency. *Annu Rev Plant Biol* **63**: 153–182.

Yan L, Zhang X, Han Z, Lambers H, Finnegan PM. 2019. Leaf phosphorus fractions in species with contrasting strategies as dependent on soil phosphorus concentrations along the Jurien Bay chronosequence. *New Phytol* **223**: 1621–1633.

Yanai J, Robinson D, Young IM, Kyuma K, Kosaki T. 1998. Effects of the chemical form of inorganic nitrogen fertilizers on the dynamics of the soil solution composition and on nutrient uptake by wheat. *Plant Soil* **202**: 263–270.

Yang S-Y, Huang T-K, Kuo H-F, Chiou T-J. 2017. Role of vacuoles in phosphorus storage and remobilization. *J Exp Bot* **68**: 3045–3055.

Yang Y-Y, Jung J-Y, Song W-Y, Suh H-S, Lee Y. 2000. Identification of rice varieties with high tolerance or sensitivity to lead and characterization of the mechanism of tolerance. *Plant Physiol* **124**: 1019–1026.

Yong Z, Kotur Z, Glass ADM. 2010. Characterization of an intact two-component high-affinity nitrate transporter from *Arabidopsis* roots. *Plant J* **63**: 739–748.

Yu H, Chin M, Yuan T, Bian H, Remer LA, Prospero JM, Omar A, Winker D, Yang Y, Zhang Y, Zhang Z, Zhao C. 2015. The fertilizing role of African dust in the Amazon rainforest: a first multiyear assessment based on CALIPSO lidar observations. *Geophys Res Lett*: 2015GL063040.

Zanin L, Tomasi N, Cesco S, Varanini Z, Pinton R. 2019. Humic substances contribute to plant iron nutrition acting as chelators and biostimulants. *Front Plant Sci* **10**.

Zanin L, Venuti S, Zamboni A, Varanini Z, Tomasi N, Pinton R. 2017. Transcriptional and physiological analyses of Fe deficiency response in maize reveal the presence of Strategy I components and Fe/P interactions. *BMC Genomics* **18**: 154.

Zemunik G, Lambers H, Turner BL, Laliberté E, Oliveira RS. 2018. High abundance of non-mycorrhizal plant species in severely phosphorus-impoverished Brazilian campos rupestres. *Plant Soil* **424**: 255–271.

Zemunik G, Turner BL, Lambers H, Laliberté E. 2015. Diversity of plant nutrient-acquisition strategies increases during long-term ecosystem development. *Nat Plants* **1**: https://doi.org/10.1038/nplants.2015.1050.

Zemunik G, Turner BL, Lambers H, Laliberté E. 2016. Increasing plant species diversity and extreme species turnover accompany declining soil fertility along a long-term chronosequence in a biodiversity hotspot. *J Ecol* **104**: 792–805.

Zerihun A, McKenzie BA, Morton JD. 1998. Photosynthate costs associated with the utilization of different nitrogen–forms: influence on the carbon balance of plants and shoot–root biomass partitioning. *New Phytol* **138**: 1–11.

Zhang J-E, Ouyang Y, Ling D-J. 2007. Impacts of simulated acid rain on cation leaching from the Latosol in south China. *Chemosphere* **67**: 2131–2137.

Zhang W-H, Ryan PR, Tyerman SD. 2004. Citrate-permeable channels in the plasma membrane of cluster roots from white lupin. *Plant Physiol* **136**: 3771–3783.

Zhao FJ, Lombi E, Breedon T, M SP. 2000. Zinc hyperaccumulation and cellular distribution in *Arabidopsis halleri*. *Plant Cell Environ* **23**: 507–514.

Zheng SJ, Ma JF, Matsumoto H. 1998. High aluminum resistance in buckwheat I. Al-induced specific secretion of oxalic acid from root tips. *Plant Physiol* **117**: 745–751.

Zohlen A, Tyler G. 1997. Differences in iron nutrition strategies of two calcifuges, *Carex pilulifera* L. and *Veronica officinalis* L. *Ann Bot* **80**: 553–559.

Zohlen A, Tyler G. 2000. Immobilization of tissue iron on calcareous soil: differences between calcicole and calcifuge plants. *Oikos* **89**: 95–106.

Zohlen A, Tyler G. 2004. Soluble inorganic tissue phosphorus and calcicole–calcifuge behaviour of plants. *Ann Bot* **94**: 427–432.

Zúñiga-Feest A, Delgado M, Bustos Á 2014. Cluster roots. In: Morte A, Varma A eds. *Root Engineering*. Berlin Springer, 353–367.

Zuo Y, Zhang F, Li X, Cao Y. 2000. Studies on the improvement in iron nutrition of peanut by intercropping with maize on a calcareous soil. *Plant Soil* **220**: 13–25.

Growth and Allocation

10

10.1 Introduction: What Is Growth?

Plant growth results from interactions among all the processes discussed in Chapters 2, 3, 4, 5, and 9. On the other hand, growth rate may control these physiological processes through its effect on plant demands for carbon, water, and nutrients, as discussed in the preceding chapters. What exactly do we mean by plant growth? **Growth** is the increment in dry mass, volume, length, or area that results from the **division**, **expansion**, and **differentiation** of cells. Increment in dry mass may not coincide with changes in each of these components of growth. For example, leaves often expand and roots elongate at night, when the entire plant is decreasing in dry mass, because of carbon use in respiration. On the other hand, a tuber may gain dry mass without concomitant change in volume, as starch accumulates. Discussion of 'growth', therefore, requires careful attention to context and the role of different processes at different times. For example, cell divisions often initiate growth, but cell division by itself is insufficient to cause growth. In addition, growth requires cell elongation and the deposition of mass in the cytoplasm and cell walls, which determines the increment in volume or mass. To appreciate ecophysiological aspects of plant growth, we must understand its cellular basis. Although this is a fascinating and rapidly moving field, many questions remain unanswered, as we will reveal in this chapter.

This chapter also deals with the question of why some plants grow faster than others do. A plant's growth rate is the result of both its genetic background and the environment in which it grows. Plants are the product of natural selection, resulting in genotypes with different **suites of traits** that allow them to perform in specific habitats. Such a suite of traits constitutes a '**strategy**'. We use the term to indicate the capacity of a plant to perform effectively in a specific ecological and evolutionary context (Box 16.1). In this chapter, we discuss how genetic and environmental factors affect the growth of plants.

10.2 Growth of Whole Plants and Individual Organs

We can analyze plant growth in terms of an increase in total plant dry mass and its distribution (**allocation**) among organs involved in acquisition of aboveground or belowground resources. In such an approach, the pattern of biomass allocation plays a pivotal role in determining a plant's access to resource, and therefore its growth rate. We can also study plant growth at the level of individual organs or cells. Using this approach, we can ask why the leaves of one plant grow faster or bigger than those of another. The two approaches are complementary, and we should integrate them to highlight traits that determine a plant's growth potential.

H. Lambers, R. S. Oliveira, *Plant Physiological Ecology*, https://doi.org/10.1007/978-3-030-29639-1_10

10.2.1 Growth of Whole Plants

Growth analysis provides considerable insight into the functioning of a plant as dependent on genotype or environment. Different growth analyses can be carried out, depending on what is considered a key factor for growth (Lambers and Poorter 1992). Leaf area and net assimilation rate are often considered 'driving variables'. As discussed in Sect. 9.4.2, however, we can also consider the plant's nutrient concentration and nutrient productivity as driving variables. In either case, 'driving variables' represent aspects of a plant's suite of traits (Sect. 10.3.7), rather than offering a mechanistic explanation for differences in growth rate.

10.2.1.1 A High Leaf Area Ratio Enables Plants to Grow Fast

We first focus on the plant's leaf area as the driving variable for the **relative growth rate** (***RGR***, the rate of increase in plant mass per unit of plant mass already present). According to this approach, *RGR* is factored into two components. First, the **leaf area ratio** (***LAR***), which is the amount of leaf area per unit total plant mass; second, the **net assimilation rate** (***NAR***), which is the net rate of increase in plant mass per unit leaf area (see Table 10.1 for a list of abbreviations and the units in which they are expressed):

$$RGR = LAR\,x\,NAR \tag{10.1}$$

The *LAR* is the product of the **specific leaf area** (***SLA***), which is the amount of leaf area per unit leaf mass, and the **leaf mass ratio** (***LMR***), which is the fraction of the total plant biomass allocated to leaves:

$$LAR = SLA\ x\ LMR \tag{10.2}$$

The *NAR*, which is the rate of dry mass gain per unit leaf area, is largely the net result of the rate of carbon gain in **photosynthesis** per unit leaf area (*A*) and that of carbon use in **respiration** of leaves, stems, and roots (*LR*, *SR*, and *RR*, respectively) which, in this case, is also expressed per unit leaf area. If these physiological processes are expressed in moles of carbon, the net balance of photosynthesis and respiration has to be divided by the carbon concentration of the newly formed material, [*C*], to obtain the increase in dry mass. The balance can be completed by subtracting losses due to volatilization and exudation per unit time, again expressed on a leaf area basis. For simplicity's sake, we will ignore

Table 10.1 Abbreviations use in plant growth analysis and their units used in the main text and legends.

Abbreviation	Meaning	Preferred units
A_a	Rate of CO_2 assimilation per unit leaf area	μmol CO_2 m^{-2} s^{-1}
[C]	Carbon concentration	mmol C g^{-1}
LAR	Leaf area ratio	m^2 kg^{-1}
LMA	Leaf mass per unit leaf area	kg m^{-2}
LMR	Leaf mass ratio	g g^{-1}
LR_a (LR_m)	Rate of leaf respiration	μmol CO_2 m^{-2} (leaf area) s^{-1}
	per unit leaf area (or mass)	[nmol CO_2 g^{-1} (leaf mass) s^{-1}]
NAR	Net assimilation rate	g m^{-2} day^{-1}
NP	Nutrient productivity	g (plant mass) mol^{-1} (plant nutrient) day^{-1}
PNC	Plant nutrient concentration	mol (nutrient) g^{-1} (plant mass)
RGR	Relative growth rate	mg g^{-1} day^{-1}
RMR	Root mass ratio	g g^{-1}
RR	Rate of root respiration	nmol CO_2 g^{-1} (root mass) s^{-1}
SLA	Specific leaf area	m^2 kg^{-1}
SR	Rate of stem respiration	nmol CO_2 g^{-1} (stem mass) s^{-1}
SRL	Specific root length	m g^{-1}
SMR	Stem mass ratio	g g^{-1}

volatilization and exudation here, although these processes can be ecologically important to the plant's carbon budget under some circumstances. We discussed volatile losses (Sect. 6.3.3), and discuss this further in Sect. 10.5.2; the process of exudation has been treated in Sects 9.2.2.5, 9.2.2.6, 9.3.1.3, and 9.3.2. The simplified equation for *NAR* is:

$$NAR = \frac{[A_a - LR_a - (SR\,x\,SMR)/LAR) - (RR\,x\,RMR)/LAR)]}{[C]} \tag{10.3}$$

The subscript a indicates that the rates are expressed on a leaf area basis. This is a common way to express rates of CO_2 assimilation (Chap. 2). Of course, stem and root respiration are not directly related to leaf area, but rather to the biomass of the different organs. This has been resolved by multiplying the rate of stem respiration (*SR*) and root respiration (*RR*) by *SMR*/*LAR* and *RMR*/*LAR*, respectively; *SMR* and *RMR* are the stem mass ratio and the root mass ratio, *i.e.* the fraction of plant biomass allocated to stems and roots, respectively (Table 10.1). Although *NAR* is relatively easy to estimate from harvest data, it is not really an appropriate parameter to gain insight into the relation between physiology and growth. Rather, we should concentrate on the underlying processes: **photosynthesis**, **respiration**, and **allocation**.

For *RGR*, we can now derive the following equation:

$$RGR = \frac{A_a\,x\,SLA\,x\,LMR - LR_m - SR\,x\,SMR - RR\,x\,RMR}{[C]} \tag{10.4}$$

This equation has been widely used to identify traits that are associated with genetic variation in a plant's *RGR* at an optimum nutrient supply as well as variation due to environmental factors such as light intensity, temperature, or nutrient supply.

10.2.1.2 Plants with High Nutrient Concentrations Can Grow Faster

In an alternative approach, the plant's nutrient concentration (mostly **plant N concentration**, ***PNC***) is assumed to be a driving variable, as discussed in Sect. 9.4. *PNC*, in combination with the nutrient productivity (commonly **N productivity**, ***NP***) determines plant growth. Thus, we arrive at:

$$RGR = NP\,x\,PNC \tag{10.5}$$

As pointed out in Sect. 9.4.2, plants differ widely in their N productivity, when grown with free access to nutrients. A high N productivity is associated with a relatively large investment of N in photosynthesizing tissue, efficient use of N invested in leaves for the process of photosynthesis, and a relatively low carbon use in respiration (Poorter et al. 1990; Garnier et al. 1995).

10.2.2 Growth of Cells

Insights into the cellular basis of growth analysis come from studying the actual processes of growth (cell division, cell expansion, mass deposition) in detail.

10.2.2.1 Cell Division and Cell Expansion: The Lockhart Equation

Growth of leaves and roots, like that of other organs, is determined by **cell division**, **cell expansion,** and **deposition** of cell material. Cell division cannot cause an increase in volume, however, and therefore does not drive growth by itself. Rather, it provides the structural framework for subsequent cell expansion (Green 1976).

The processes of cell division and cell expansion are interdependent. Cells divide when they reach a certain size (*i.e.* they elongate after division and then divide again, before they have elongated substantially). This limits the developmental phase at which cell division can occur, and implies that any process that slows down cell expansion inevitably leads to fewer cells per leaf or root, and hence smaller leaves or roots. For example, consider a newly formed meristematic leaf cell that differentiates to produce epidermal leaf cells. Suppose this cell divides only after it doubles in cell volume, and that it has 240 h left to undergo repeated mitoses at the point of

determination. If the cell doubled in volume every 10 h, then cell divisions will occur 24 times, which produces 2^{24} cells. If an environmental factor slows the rate of cell expansion such that the cells now take 12 h to double in volume, however, then only 20 division cycles will occur which gives rise to 2^{20} cells. Such a reduction in cell number could substantially reduce leaf surface area (Van Volkenburgh 1994).

Once a cell has divided, it can elongate and expand, provided the turgor pressure (Ψ_p, MPa) exceeds a certain **yield threshold** (Y, MPa). In cells capable of expansion, this threshold value is around 15 to 50% of the turgor pressure under normal conditions (no stress) (Pritchard, 1994). The proportional growth rate (r, s^{-1}) is measured as the rate of increase in volume (dV, m^3) per unit volume (V, m^3); r is proportional to the difference between **turgor** and **yield threshold**. The proportional rate of expansion ($dV/V\ x\ dt$, s^{-1}) is described by the simplified **Lockhart equation** (Lockhart 1965; Braidwood et al. 2014):

$$R = dV/(V\,x\,dt) = \phi\left(\Psi_p - Y\right) \qquad (10.6)$$

where ϕ is the cell-wall **yield coefficient** ($MPa^{-1}\ s^{-1}$), which is a proportionality constant that depends on biochemical and biophysical properties of the cell wall. Plant cell expansion is, therefore, a **turgor-driven** process, controlled, both in extent and in direction, by the physical properties of the primary (growing) cell wall. If cells expand more in one direction than in another, the cell walls are more **extensible** (looser) in the direction in which they expand most. This simple analysis using the Lockhart equation assumes that neither water flow nor solute influx is limiting. This assumption appears to be met when plants are growing under favorable conditions. In later Sections of this chapter, we discuss whether this assumption still applies under conditions of environmental stress.

Because cell expansion and cell division are closely linked, the increase in length or volume of entire leaves and other organs can be analyzed with a similar equation (Braidwood et al. 2014). Both the cell-wall yield coefficient, ϕ, and the yield threshold, Y, reflect the **extensibility** of the cell walls, as determined by their biochemical and biophysical properties. The turgor pressure, Ψ_p, or, more precisely, the difference between Ψ_p and Y, allows cell expansion. Uptake of ions into the cell maintains the turgor pressure, which tends to drop as the cell volume increases.

Turgor tends to be **tightly regulated**, particularly in growing cells (Pritchard 1994). This tight regulation of cell turgor is most likely due to modification of the activity ('gating') of **aquaporins** in the plasma membrane and tonoplast which are highly expressed in zones of rapid division and expansion (Tyerman et al. 2002; Siefritz et al. 2004). There are several examples, however, where a step-change in turgor does *not* lead to (full) readjustment to the original turgor pressure (Zhu and Boyer 1992; Passioura 1994). This probably reflects differences in original water status (Hsiao et al. 1998) or between-species and/or tissue-specific behavior. These results also point out that growth is not really controlled by turgor in the simple manner suggested by the Lockhart equation. Above the turgor threshold, the rate of cell enlargement is controlled by metabolic reactions, which cause synthesis and/or extension of wall polymers. Inside the cell, sufficient solutes must be generated to maintain turgor above the threshold.

10.2.2.2 Cell-Wall Acidification and Removal of Calcium Reduce Cell-Wall Rigidity

The fundamental structure of the primary (growing) cell wall is very similar in all vascular plants: cellulose microfibrils are embedded in a hydrated matrix composed mostly of neutral and acidic polysaccharides and a small amount of structural proteins (Cosgrove 2016). The polysaccharides include the negatively charged cation-binding **polygalacturonic acids**. **Cellulose microfibrils**, which consist of bundles of around 50 cellulose molecules, provide the tensile strength of the cell wall. In expanding cells, the microfibrils tend to be arranged transversely, which favors expansion in a longitudinal, rather than in a radial direction. **Glycoproteins** add further strength to the cell walls. **Hemicelluloses** (*i.e.* polysaccharides with

a glucan or similar backbone) bind to cellulose microfibrils and to each other by means of hydrogen bonds. Because there are many hemicellulose molecules per cellulose microfibril, the microfibrils are completely coated, making a three-dimensional net. Finally, there are several enzymes that cleave covalent bonds that link the sugar residues of the noncellulosic polymers in the walls, and other enzymes that can join loose ends of similar polymers (Wu et al. 2018). The growing wall possesses a remarkable combination of strength and pliancy, enabling it to withstand the large mechanical forces that arise from cell turgor pressure, while at the same time permitting a controlled polymer 'creep' that distends the wall and creates space for the enlarging protoplast. Cellulose microfibrils themselves are effectively inextensible; wall expansion occurs by slippage or rearrangement of the matrix polymers that coat the microfibrils and hold them in place **Expansins** are proteins that induce extensibility and stress relaxation of plant cell walls in a pH-dependent manner (McQueen-Mason et al. 1992). Their discovery as enzymes involved in loosening of cell walls has uncovered a major mechanism of wall enlargement (Cosgrove 2000, 2016).

Hormonal and environmental stimuli promote growth of plant cells by inducing polymer rearrangement and loosening of the primary (growing) cell wall. Expansins are small extracellular proteins that enhance polymer creep, and thereby wall extensibility, by disrupting non-covalent interactions between wall polysaccharides (Braidwood et al. 2014). Normally, expansins are a minor component of the cell wall; both binding to the cell wall and expansin activity reach a maximum at an expansin-protein-to-wall ratio of about 1:1000. Expansins weaken the noncovalent binding (hydrogen bonding) between wall polysaccharides, thereby allowing turgor-driven polymer creep (Cosgrove 2016).

Expansins are encoded by a gene family (Kende et al. 2004); expression of individual genes may be differentially regulated at various developmental stages and by diverse environmental stimuli (Sects 10.5.3 and 10.5.6.1). Loosening of primary and secondary walls can be modulated in various ways (*e.g.*, by changes in wall pH, secretion of molecules that affect the activity of wall enzymes, and secretion of substrates). Additionally, the wall can be modified by other enzymes that change the structure in such a way that they can no longer be affected by the wall-loosening agents: **wall stiffening** (Braidwood et al. 2014).

Calcium enhances cell-wall stiffening by binding to pectin components, forming **Ca-pectate complexes**; the more Ca^{2+}-pectate present, the more inextensible the cell wall (Höfte et al. 2012). For example, shade enhances stem elongation because of the removal of Ca^{2+} from the cell walls. Protons also play an important role in the breaking of cross-linkages. For example, extrusion of protons from the cytosol into the cell wall precedes the light-induced growth of leaves (phototropism). A low pH in the cell wall, through activation of **expansins**, induces disruption of hydrogen bonding between cellulose microfibrils and matrix polymers (Fig. 10.1).

The **light-induced enhancement of leaf growth** which is preceded by the perception of light by both a red-light receptor (phytochrome) and a blue-light receptor (cryptochrome), is due to **cell-wall acidification**, which enhances expansin activity (Fig. 10.1) and increases the extensibility of the cell walls (Sect. 10.5.1.1). Cells of stems may also respond to light, perceived by **phytochrome**, *i.e.* red light suppresses stem elongation and far-red light enhances it. Gibberellins enhance cell elongation, but through a different mechanism. In *Lactuca sativa* (lettuce) hypocotyls, this effect of gibberellin is associated with the removal of **Ca^{2+}** from the cell walls, rather than with cell-wall acidification. **Cytokinins** promote and **abscisic acid** (ABA) reduces the rate of **leaf expansion**, but, as with gibberellins, this is unlikely to be due to cell-wall acidification. Cytokinins and ABA have either no effect or the opposite effect on **root elongation** (*i.e.* cytokinins tend to inhibit and ABA tends to promote root growth); in the case of ABA, that may depend on the level of water stress (Sect. 10.5.3.2).

Phototropic reactions, which allow coleoptiles to grow toward the light (Goyal et al.

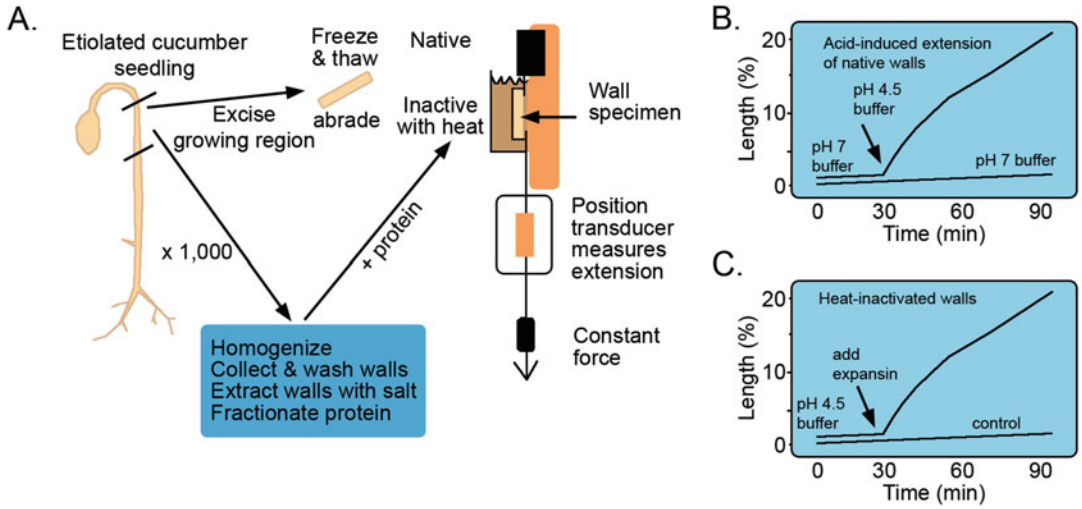

Fig. 10.1 Diagram of extensometer assays. (**A**) The growing hypocotyl of a seedling is cut and frozen to kill the cells. The wall specimen is either directly clamped in a constant-force extensometer ('native walls') or first inactivated with a brief heat treatment, before being clamped in the extensometer ('heat-inactivated walls'). Expansin protein is prepared by extraction from native walls, followed by fractionation and addition to the wall. (**B**) Native walls extend very little at neutral pH, but rapidly extend in acidic pH. (**C**) Heat-inactivated walls lack acid-induced extension, which can be restored by addition of expansin to the walls (Modified after Cosgrove, 2000); copyright © 2000, Springer Nature.

2013), are based on greater **acidification** of the walls of cells furthest away from the light source as compared with the more proximal cells. Such a difference in acidification is based on a difference in **auxin activity** in the distal and proximal cells (Box 10.1). These examples show that cells respond to light and hormones, sometimes in interaction, by changes in cell-wall properties that, in turn, affect growth of leaf, stem, or root cells. Genetic or environmental factors that affect the cell-wall cross-linkages, and hence ϕ or Y, affect the rate of cell expansion and the extent to which an organ will grow. Environmental factors such as hypoxia, water stress, and light affect leaf or stem growth exactly in this manner (Sect. 10.5).

Box 10.1: Phytohormones

Many aspects of plant growth and development are controlled by internal messengers; phytohormones. In the animal literature, the term hormone refers to a molecule that is produced in cells of a specific organ (gland) and that has specific effects on other cells (target cells). Phytohormones are not produced in specific glands, but in organs and tissues that serve other functions as well. The effect of phytohormones is also less specific than that of their animal counterparts. They may mediate among several environmental factors and lead to several plant responses.

Phytohormones are characterized as:

1. organic molecules produced by the plant itself;
2. compounds that affect growth and development (either positively or negatively) at very low concentrations;
3. compounds that act primarily in a part of the plant that differs from the site they are produced;
4. compounds whose action depends on their chemical structure, rather than the elements they contain.

There are at least seven groups of phytohormones (Box Fig. 1). The first

(continued)

Box 10.1 (continued)

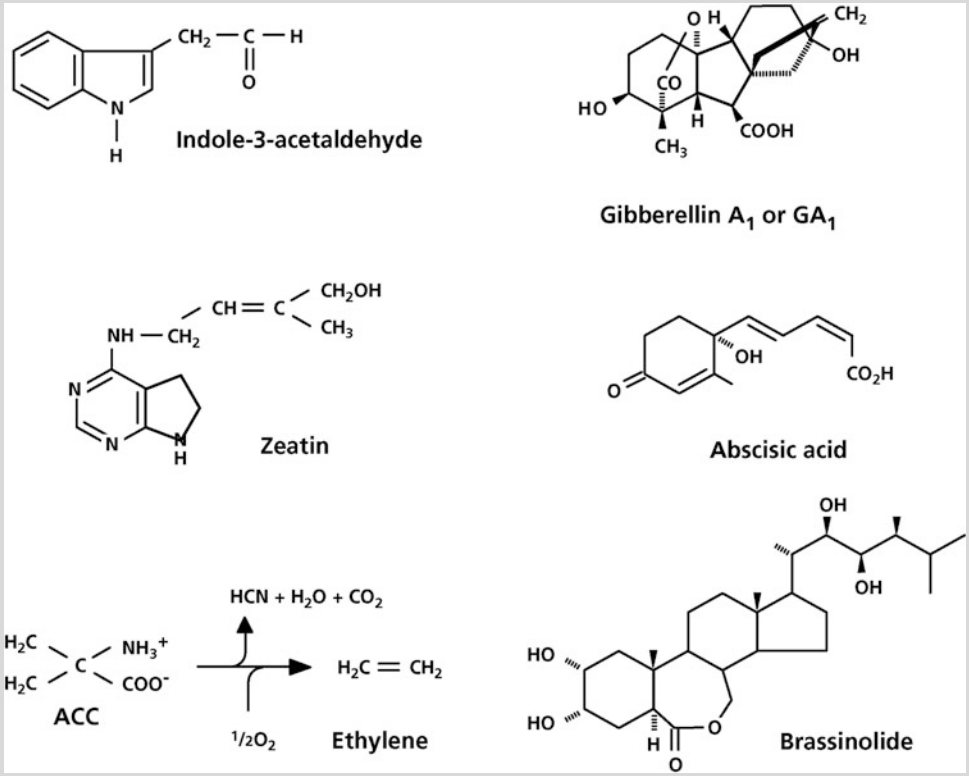

Box Fig. 1 The chemical structure of a representative of the six groups of phytohormones: indole-3-acetyaldehyde (IAA, an auxin), gibberellin A_1 (GA_1, one of many gibberellins, of which only a small number is physiologically active; GA_1 is the gibberellin that usually induces stem elongation), zeatin [a common bioactive cytokinin first identified in *Zea mays* (corn)], abscisic acid (ABA), ethylene (the only gaseous phytohormone) and its water-soluble precursor: 1-amino-cyclopropane-1-carboxylic acid (ACC), and brassinolide, which is the most biologically active brassinosteroid.

phytohormone was discovered in the 1920s by F.W. Went (1926), who was doing a PhD with his father, F.A.F.C. Went, at Utrecht University, where they identified the structure of **auxin**. It is indoleacetic acid (IAA), termed auxin, because of its involvement in the growth of *Avena sativa* (oat) coleoptiles toward the light (auxin comes from the Greek verb to grow). It is involved in the promotion of cell growth, differentiation in the root and shoot meristem, and apical dominance. Auxin is produced in leaves and transported to the site of action through specific carrier proteins located in the plasma membrane. Localized effects, such as tropisms and tissue polarity, depend on this highly regulated transport.

The **gibberellins** or gibberellic acids (GAs) derived their name from the fungus *Gibberella fujikori*, which turns dwarf rice cultivars into tall ones. It is a complex class of phytohormones of which the active compounds strongly stimulate elongation growth through an effect on both cell division and cell elongation. GA has also a key role in the first steps leading to germination of seeds.

(continued)

Box 10.1 (continued)

Cytokinins were discovered in a search for a medium suitable for tissue culture, where they stimulate cell division. The bioactive members of this family of phytohormones are also involved in chloroplast maturation, the delay of senescence, leaf expansion, and several other morphogenetic processes. Root tips are a major site of cytokinin production, and the primary transport path to the site of action is in the transpiration stream.

Abscisic acid (ABA) derives its name from its stimulation of leaf abscission. This phytohormone is, however, involved in a wide range of regulatory process. ABA plays a key role in stress responses (*e.g.*, desiccation, salinity). ABA causes stomatal closure, inhibits extension growth, and induces senescence. ABA also induces dormancy of buds and seeds**.**

Ethylene is the only gaseous hormone. It is produced from the water-soluble precursor 1-amino-cyclopropane-1-carboxylic acid (ACC) in an oxygen-requiring step, catalyzed by ACC oxidase. It induces senescence and inhibits cell growth at higher concentrations in most plants, but it stimulates growth in flooding-resistant plants (Sect. 10.7.5.7).

The hormonal status of **brassinosteroids** has been established more recently (Yokota 1997). They were first isolated in 1974 from *Brassica napus* (oilseed rape) pollen, and have since been found in many species. This group of hormones stimulates growth, as evidenced by mutants with defects in brassinosteroid biosynthesis or sensitivity which are all dwarfs. They stimulate senescence, stress tolerance, and germination of seeds.

The latest group of phytohormone are **small peptides**, which play major roles in many processes, including gravitropism (Whitford et al. 2012), nodulation (Djordjevic et al. 2015), expansion of lateral roots (Araya et al. 2014), plant responses to macronutrient availability (de Bang et al. 2017), and cluster-root formation (Zhou et al. 2019).

Hormonal status is also claimed for other compounds such as jasmonate, salicylic acid, and several small peptides, but this is not generally accepted (Reski 2006). These compounds play, among others, a role in plant defense against pathogens and herbivores (Chap. 13).

Phytohormones are important both to internally coordinate the growth and development of different organs and as chemical messengers whose synthesis may be affected when plants are exposed to certain environmental factors. Many, if not all, developmental processes in plants depend on a coordinated action of several hormones. External or internal factors need to be sensed first, which is the first step in a signal-transduction pathway, ultimately leading to the plant's response. The plant's response is not necessarily due to an effect on the rate of production of the phytohormone, but it may involve its rate of breakdown or the sensitivity of the target cells to the hormone. At a molecular level, a plant's response may involve up-regulation or down-regulation of genes coding for enzymes involved in synthesis or breakdown of the phytohormone, or genes encoding a receptor of the phytohormone. Most of these receptor proteins have recently been identified in *Arabidopsis thaliana* (thale cress).

Cell-wall extensibility declines with age of the cells, so that the walls of older cells no longer respond to cell-wall acidification. This is associated with changes in chemical composition (*e.g.*, incorporation of more galactose). Formation of **phenolic cross-links** between wall components might also play a role, as do **extensins**, which are rigid cell-wall glycoproteins that are particularly abundant in secondary cell

walls. A wide range of environmental factors, including water-stress, flooding, and soil compaction, affect leaf growth through their effect on cell-wall extensibility, as discussed later in this chapter.

10.2.2.3 Cell Expansion in Meristems Is Controlled by Cell-Wall Extensibility and Not by Turgor

The growth rate of individual cells along a growing root tip varies considerably. A pressure probe that measures the **turgor pressure** in individual growing root cells shows that the turgor varies little along the growing root. Changes in **cell-wall mechanical properties**, rather than in turgor, must therefore be responsible for the immediate control of the expansion rate of roots (Pritchard 1994).

Removal of minute quantities of sap from expanding cells shows that the **osmotic component of the water potential** becomes less negative by approximately 15% during cell expansion. This change is small, compared with that in cell volume during expansion, and it results from the drop in K^+ concentration by about 50%. The concentration of other solutes is constant, showing that solute uptake into the expanding cells occurs at about the same rate as that of water.

As the cells expand, mechanical forces facilitate the insertion of wall components, in particular **pectins**, so that the cell-wall thickness remains approximately the same during the expansion phase (Ali and Traas 2016). Further **deposition of cell-wall material** may occur after the cells have reached their final size which causes the cell walls to become thicker.

10.2.2.4 The Physical and Biochemical Basis of Yield Threshold and Cell-Wall Yield Coefficient

From a physical point of view, the parameters ϕ, the cell-wall yield-coefficient, and Y, the yield threshold, in the Lockhart equation make intuitive sense. We can also demonstrate this experimentally, by using a pressure probe to determine turgor (Ψ_P) in the growing zone. The Lockhart 'parameters' often behave as 'variables', however (*i.e.* the relationship between r and P is often nonlinear) (Passioura 1994). What exactly do these 'parameters' mean?

In hypocotyl segments of *Vigna unguiculata* (cowpea), the cell-wall mechanical properties are affected by auxin and gibberellin (Box 10.1). In segments that are deficient in endogenous gibberellin, **auxin** only affects the **yield threshold**, but not the yield coefficient. As a result, the effect of auxin is only half that in segments with normal gibberellin levels. After pretreatment with **gibberellin**, auxin does affect the **yield coefficient**. These results suggest that auxin decreases the yield threshold independently of gibberellin, but that it increases the yield coefficient only in the presence of gibberellin (Okamoto et al. 1995). In the same tissue, both the yield coefficient and the yield threshold are affected by the **pH** in the cell wall. Both parameters are also affected by exposure to high temperature and proteinase, but not in the same manner. That is, a brief exposure to 80 °C affects the yield threshold, but not the yield coefficient. Exposure to proteinase affects the yield coefficient, but not the yield threshold. The two cell-wall mechanical properties are controlled by different proteins, both of which are activated by low pH (Okamoto and Okamoto 1995).

10.2.2.5 The Importance of Meristem Size

As discussed in previous Sections, cell elongation depends on an increase in cell-wall extensibility. A more rapid rate of cell elongation may lead to a faster rate of leaf expansion or root elongation. A faster rate of leaf expansion or root elongation, however, is not invariably due to greater cell-wall extensibility. If more cells in the meristem divide and elongate at the same rate, this also results in faster rates of expansion. Indeed, variation in growth can be associated with variation in **meristem size** (*i.e.* the number of cells that divide and elongate at the same time). In a comparison of the growth of *Festuca arundinacea* (tall fescue) at high and low N supply, the major factor contributing to variation in leaf elongation is the size of the meristem (Fig. 10.2A). Likewise, two *Festuca arundinacea* genotypes that differ in their rate of leaf elongation by 50% when grown

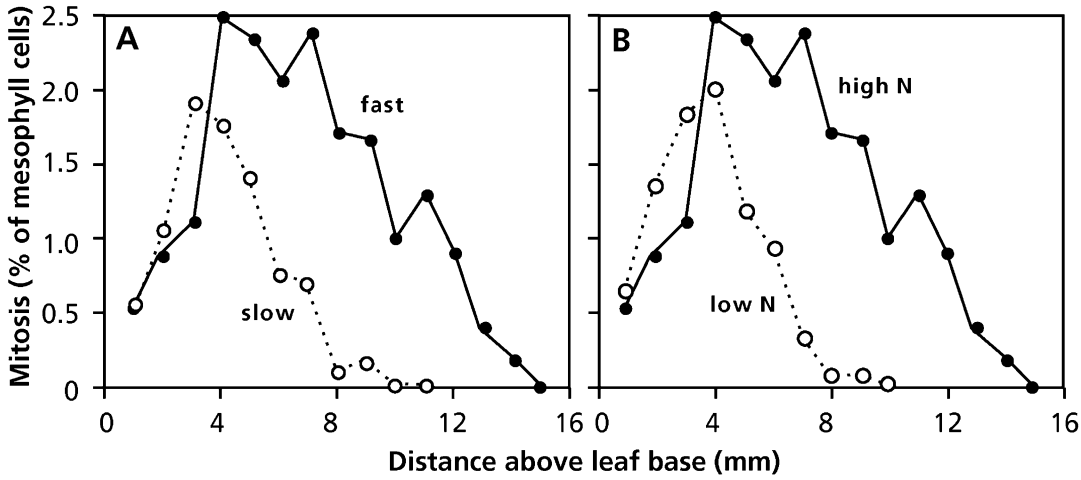

Fig. 10.2 Percentage of mesophyll cells that are in mitosis as observed in longitudinal sections from the basal 40 mm of elongating leaf blades of *Festuca arundinacea* (tall fescue). A greater area under the curves indicates a larger meristem. (**A**) A comparison of meristem size of a fast-elongating and a slow-elongating genotype. (**B**) Effects of nitrogen (N) supply on leaf meristem size in the fast-elongating genotype (After MacAdam et al. 1989); copyright American Society of Plant Biologists.

at high nutrient supply differ in the number of cells that elongate at the same time, whereas the rate of elongation of the expanding cells is similar (Fig. 10.2B). Similarly, the number of meristems can be an important determinant of whole-plant growth rate.

10.3 The Physiological Basis of Variation in *RGR*—Plants Grown with Free Access to Nutrients

Plant species characteristic of **favorable environments** often have inherently faster maximum relative growth rates ($\boldsymbol{RGR_{max}}$) than do species from less favorable environments (Grime and Hunt 1975; Lambers and Poorter 1992). For example, inherently slow growth is common in species characteristic of nutrient-poor (Grime and Hunt 1975), saline (Ball and Pidsley 1995) and alpine (Atkin et al. 1996) environments. It is clear from Eqs. 10.1 and 10.2 that a high *RGR* might be associated with a high *NAR* (reflecting rapid rates of photosynthesis and/or slow whole-plant respiration rates), a high *SLA* (*i.e.* high leaf area per unit leaf mass), and/or a high *LMR* (high allocation to leaf mass). Which of these traits is most strongly correlated with a high *RGR*?

10.3.1 SLA Is a Major Factor Associated with Variation in *RGR*

The main trait associated with inherently **slow growth** in temperate herbaceous lowland species from nutrient-poor habitats is their **low SLA**, in seedlings of both monocots and dicots (Lambers and Poorter 1992). The same conclusion holds for a wide range of both deciduous and evergreen tree species (Antúnez et al. 2001; Ruiz-Robleto and Villar 2005). A meta-analysis based on 103 studies shows that *SLA* is correlated with *RGR* in seedlings, but not in adult plants (Gibert et al. 2016; Falster et al. 2018). Low SLA values decrease the amount of leaf area available for light interception and hence photosynthetic carbon gain, therefore reducing *RGR*. Although this conclusion follows logically from Eq. (10.4), it does not provide insight into the exact **mechanisms** that account for slow growth. A further understanding of these mechanisms

requires a thorough analysis of the processes discussed in Sect. 10.2.2.

Herbaceous C_3 species show significant positive correlations of *RGR* with *LAR*, *LMR*, and *SLA*, but not *with NAR* (Fig. 10.3). For example, in a broad comparison using 80 woody species from the British Isles and Northern Spain, ranging widely in leaf habit and life-form, *RGR* is tightly correlated with *LAR* (Cornelissen 1996). When comparing more productive cultivars of tree species with less productive ones, *SLA*, rather than photosynthesis, is the main factor that accounts for variation in *RGR* (Ceulemans 1989). Surprisingly, faster growth of C_4 grasses in a very broad comparison with C_3 grasses from similar ecological habitats and evolutionary history reveals that, *LAR*, rather than *NAR* drives faster growth (Atkinson et al. 2016).

LMR does not correlate with *RGR* in monocotyledons, but it may account for some of the variation in *RGR* among dicotyledonous species. This reflects the phylogenetic constraints on a plant: a change in *LMR* may require a greater genetic change than that allowed by the genetic variation within a species, genus, or perhaps even family (Marañón and Grubb 1993). Fast-growing species allocate relatively less to their stems, in terms of both biomass and N, when compared with slower-growing ones. Similarly, high-yielding crop varieties generally have a low allocation to stems (Sinclair 1998; Berger et al. 2012). A high allocation to stems reflects a diversion of resources from growth to storage in slower-growing species or lower-yielding crop varieties (Sect. 10.4).

In broad comparisons, ***NAR*** is often not correlated with *RGR* in dicots, whereas it is in monocots. Comparing five tree and six herb C_3 species grown under optimal conditions, Osone et al. (2008) found correlation between *RGR* and both *SLA* and *NAR*. The effect of variation in *SLA* on the *RGR* of monocots is invariably stronger

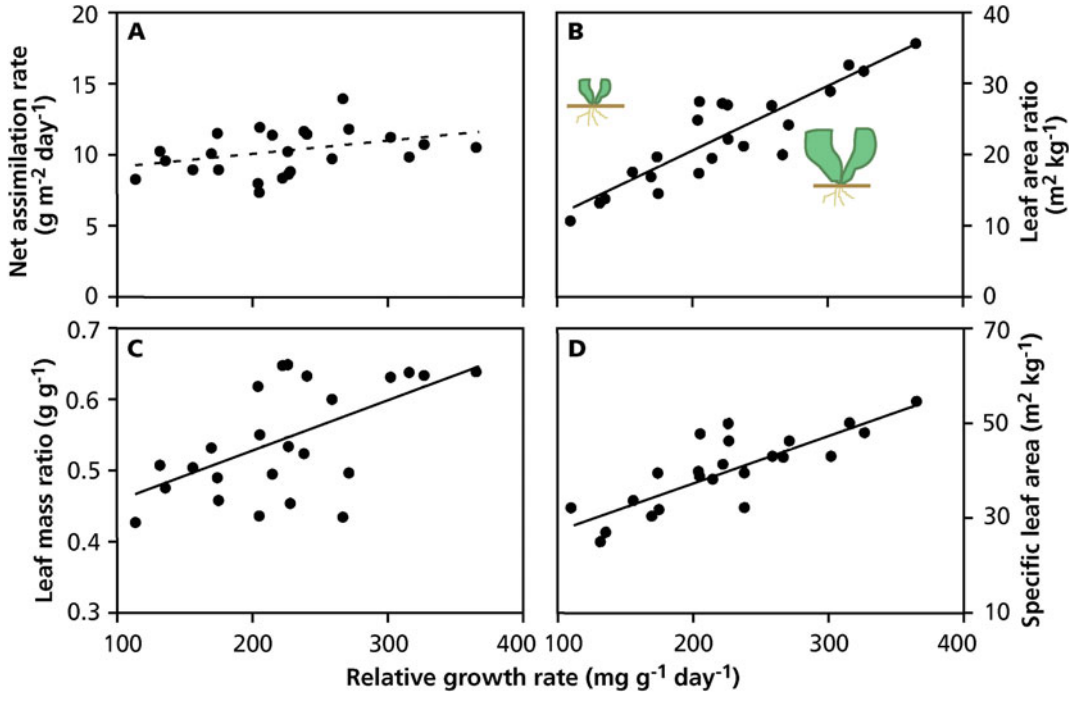

Fig. 10.3 A comparison of the *NAR*, *LAR*, *LMR*, and *SLA* of 24 herbaceous C_3 species that differ in their *RGR* as determined on plants grown with free access to nutrients. The broken line indicates a nonsignificant regression; solid lines indicate significant regressions. For explanation of abbreviations, see Table 10.1 (Poorter and Remkes 1990);

than that of variation in *NAR*. When we compare pairs of annual and perennial grass species that belong to the same genus, the faster *RGR* is invariably associated with the **annual life form**. Because annuals likely descended from perennial ancestors, the same morphological changes that enhance a genotype's *RGR* probably occurred repeatedly in different genera (**convergent evolution**) and a high *RGR* is the more recent development (Garnier and Vancaeyzeele 1994).

10.3.2 Leaf Thickness and Leaf Mass Density

Variation in ***SLA***, or its inverse [leaf mass per unit leaf area (***LMA***, kg m^{-2})] must be due to variation in **leaf thickness** (m) or in **leaf mass density** (kg m^{-3}) (Witkowski and Lamont 1991).

$$LMA = (\text{leaf thickness}) x (\text{leaf mass density}) \tag{10.7}$$

LMA varies more than 100-fold among species (Poorter et al. 2009). When we compare **shade leaves** and **sun leaves**, leaf thickness is a major parameter in determining variation in *LMA*, and it reflects greater **thickness of palisade parenchyma** in sun leaves (Sect. 2.3.2.2). In addition, comparing alpine species, which are characteristically exposed to high light, and congeneric lowland species, variation in *LMA* is associated with that in leaf thickness. Likewise, variation in *LMA* between congeneric evergreen and deciduous species is mainly explained by a greater leaf thickness of evergreens, and not by a greater leaf mass density (Villar et al. 2013). However, leaf mass density also accounts for a part of the variation in *LMA* between shade leaves and sun leaves, between widely contrasting woody species (Cornelissen et al. 1996), and especially when comparing congeneric lowland and alpine species (Atkin et al. 1996).

In comparisons of closely related species from nutrient-poor and nutrient-rich habitats, variation in *LMA* is due to differences in leaf mass density (Garnier and Laurent 1994). Comparing 53 European woody species yields a strong, positive correlation of *LMA* with leaf mass density, but no correlation with leaf thickness; in fact leaf mass density and leaf thickness are negatively correlated (Fig. 10.4; Castro-Díez et al. 2000). A comparison of Mediterranean woody species (20 evergreen and 14 deciduous) growing in the field along a water availability gradient, variation in *LMA* is associated with both leaf mass density and leaf thickness (de la Riva et al. 2016a).

In summary, differences in leaf mass density are generally the primary factor explaining differences in *LMA* (and its inverse: *SLA*), except in sun-shade and evergreen-deciduous comparisons, where number of cell layers (leaf thickness) is also important.

Fast-growing herbaceous species tend to have a lower tissue density in their roots as well as in their leaves (Wahl and Ryser 2000), but this pattern does not appear in 80 Mediterranean woody species (de la Riva et al. 2018a). In general, there are many strong correlations among many root morphological traits, supporting the concept of a 'root economics spectrum' (Fig. 10.4). Root diameter does not completely align, suggesting a multidimensional spectrum of root traits (Weemstra et al. 2016). Soil nutrient and water availability are the main drivers of root trait variation (de la Riva et al. 2018b).

10.3.3 Anatomical and Chemical Differences Associated with Leaf Mass Density

The inherent variation in *LMA* and **leaf mass density** (Fig. 10.4) is associated with differences in both leaf **anatomy** and **chemical composition** (Villar et al. 2006; Poorter et al. 2009). Fast-growing species with a low *LMA* have relatively **large epidermal leaf cells**. Because these cells lack chloroplasts, which are a major component of the mass in the cytoplasm of mesophyll cells, they have a low density. Slow-growing plants with a high *LMA* have **thicker cell walls** and contain more **sclerenchymatic cells** (Villar et al. 2013; Onoda et al. 2017). These cells are small and characterized by very thick cell walls; they have a high density. In a comparison of 11 broad-

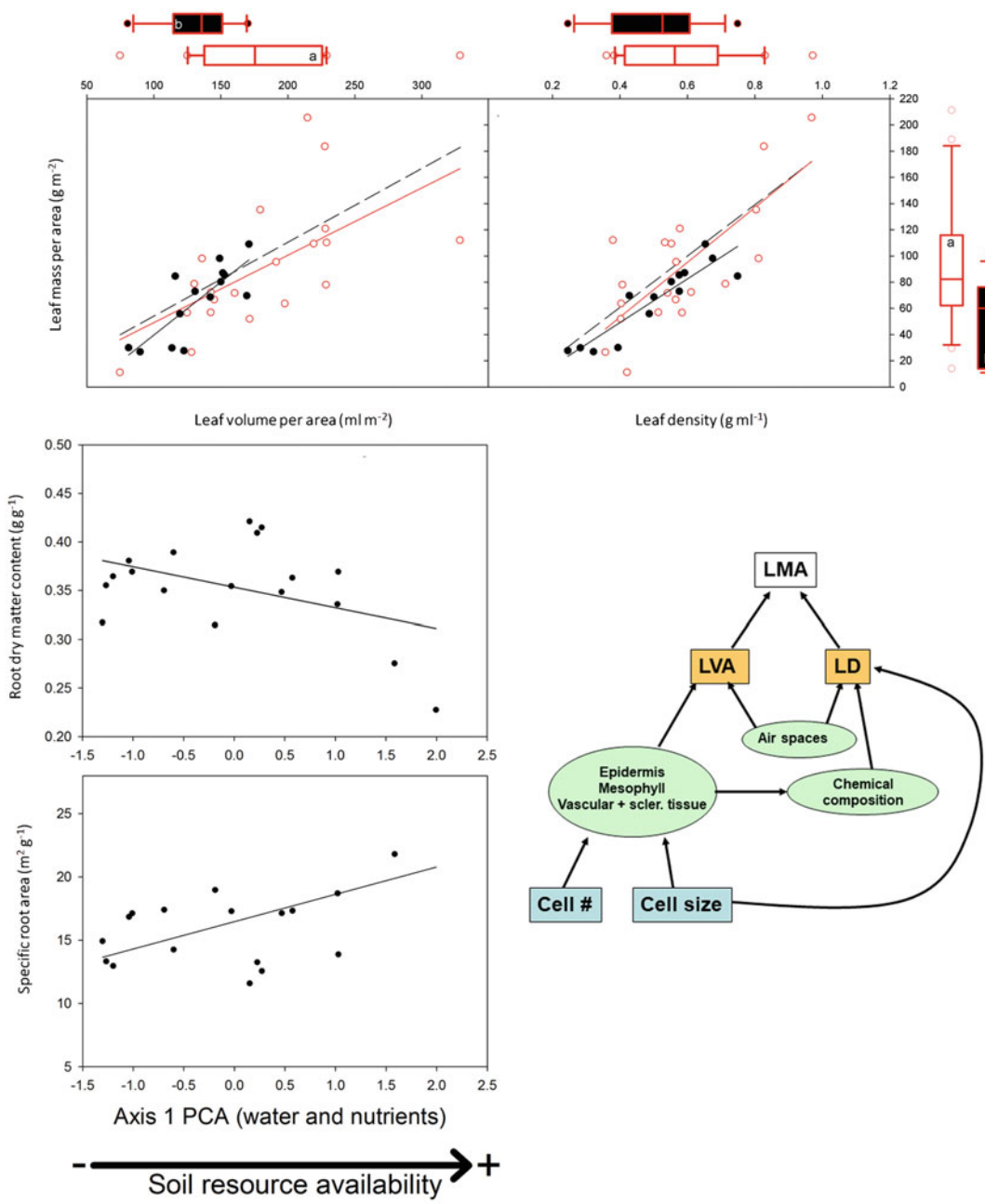

Fig. 10.4 (Top) Linear regressions of leaf dry mass per area with leaf volume to area and leaf density for deciduous species (dark line and circles), evergreens (red line and empty red circles) and all the species (dashed line). Box plots (median and 1st and 3rd quartiles) of deciduous *vs.* evergreen species are included along the top margins. Whiskers show the minimum and maximum values that fall within 1.5× the length of the box away from the interquartile range; data further away are shown as outliers (de la Riva et al. 2016a). (Bottom left) Correlations between two root community-weighted traits, specific root area and root dry matter content, and the first axis that represents soil resource availability in a principal component analysis (PCA) (de la Riva et al. 2018a); copyright © 2017, Springer International Publishing AG. (Bottom right) Conceptual diagram of the anatomical characteristics at three integration levels (leaf, tissue, and cell) (marked with different colors) to show variation in *LMA* in this study. Vascular + scler. tissue = vascular tissue plus sclerenchymatic tissue (Villar et al. 2013); copyright John Wiley and Sons.

leaved woody angiosperm species, ranging in *LMA* from 33 to 262 g m^{-2}, high *LMA* results from greater major vein allocation, greater numbers of mesophyll cell layers, and higher cell mass densities (Fig. 10.4; John et al. 2017).

10.3.4 Net Assimilation Rate, Photosynthesis, and Respiration

As explained in Sect. 10.2.1.1, the **net assimilation rate** (*NAR*) relates to the balance of carbon gain in **photosynthesis** and carbon use in whole-plant **respiration**. Variation in *NAR* may, therefore, be due to variation in photosynthesis, respiration, or a combination of the two. In a comparison of 24 herbaceous species (Fig. 10.3), there is no clear trend of *NAR* with RGR. Rate of photosynthesis per unit leaf area also shows no correlation with *RGR* (Fig. 10.5). **Slow-growing species**, however, use relatively more of their carbon for **respiration**, especially in their roots (Fig. 5), whereas **fast-growing** species invest a relatively greater proportion of assimilated carbon in **new growth**, especially **leaf growth**. Next to the variation in *LAR* (*SLA* and *LMR*), this difference in the amount of carbon required for respiration is the second-most important factor that is associated with inherent variation in *RGR*.

If we compare a dataset comprising 1509 species from 288 sites, rates of **photosynthesis** per unit leaf area is virtually unrelated to *LMA* (Maire et al. 2015). *LMA* and allocation, however, differ strikingly among taxa (Onoda et al. 2017). The lack of a correlation between photosynthesis and *RGR* among closely related taxa or among morphologically similar taxa (Fig. 10.3) indicates that these broad differences in photosynthetic rate are not a major driver of differences in *RGR*.

10.3.5 *RGR* and the Rate of Leaf Elongation and Leaf Appearance

The higher *RGR* and *SLA* of fast-growing grass species is associated with a more **rapid leaf elongation** (Fig. 10.6; Groeneveld & Bergkotte, 1996). Does cell-wall acidification or the removal of Ca^{2+} from the cell walls play a role? Are the cells of rapidly elongating leaves more responsive to changes in pH or Ca^{2+}? Does it reflect a difference in meristem size, as shown in Fig. 10.2? Answers to these basic questions provide rich opportunities for research to improve our basic understanding of plant growth. It is also apparent

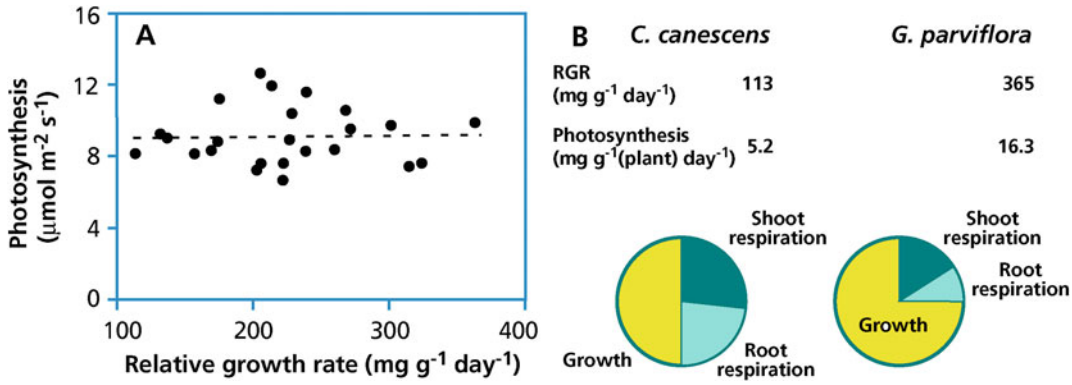

Fig. 10.5 (**A**) The rate of photosynthesis per unit leaf area in fast- and slow-growing herbaceous species (after Poorter et al. 1990); copyright American Society of Plant Biologists). (**B**) The carbon budget of a slow-growing species [*Corynephorus canescens* (grey hair-grass)] and a fast-growing species [*Galinsoga parviflora* (gallant soldier)]. The relative growth rate (*RGR*) and daily gross CO_2 fixation of these species is also shown (Lambers and Poorter 1992); copyright Elsevier Science Ltd.

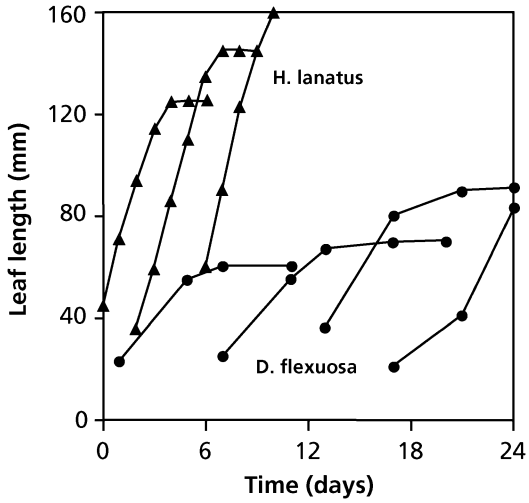

Fig. 10.6 The rate of leaf elongation of a slow-growing grass species [*Deschampsia flexuosa* (tufted hair-grass), circles] and a fast-growing grass [*Holcus lanatus* (common velvet grass) triangles] (After Groeneveld and Bergkotte 1996); copyright John Wiley and Sons.

that in the fast-growing grass *Holcus lanatus* (common velvet grass) the next leaf starts to grow just before the previous one has reached its final size. This typically contrasts with the pattern in slow-growing grasses [*e.g.*, *Deschampsia flexuosa* (tufted hair-grass)], where the next leaf does not start elongating until well after the previous one has stopped (Fig. 10.6).

10.3.6 *RGR* and Activities per Unit Mass

The growth analysis discussed in Sect. 10.3.2 shows that *SLA* 'explains' much more of the variation in *RGR* than do area-based measures of *NAR* and photosynthesis. This area-based measure is the most logical way to describe the environmental controls over capture of light and CO_2. **Economic analyses of plant growth** (the return on a given biomass investment in leaves or roots), however, more logically express resource capture (photosynthesis or nutrient uptake) per unit plant mass. We achieve this by multiplying the area-based measures of carbon gain by *SLA*, for example:

$$NAR_m = NAR_a \, x \, SLA \qquad (10.8)$$

Because of the strong correlation between *SLA* and *RGR*, *RGR* also has a strong positive correlation with NAR_m (Fig. 10.7A). The low NAR_m of slow-growing species in part reflects their high carbon requirement for root respiration (Fig. 10.5; Sect. 3.5.2.3). Both the V_{max} for NO_3^- uptake and the net rate of NO_3^- inflow show a strong correlation with RGR_{max} (Fig. 10.7B, C). This correlation is probably a result, rather than the cause of variation in growth rates (Sect. 9.2.2.3.2; Touraine et al. 1994; Forde 2002). The positive correlations between RGR_{max} and mass-based activity of both roots and leaves hold for monocots and dicots (Figs 10.7A–C). By contrast, there is no correlation of RGR_{max} with biomass allocation to roots and leaves for monocotyledonous species (Fig. 10.7D), whereas RGR_{max} decreases with increasing biomass allocation to roots in dicotyledonous species (Fig. 10.7E).

The correlations discussed above result from **rapidly growing plants** producing leaves and roots with relatively large allocation to metabolically active components, rather than to cell walls and storage (Onoda et al. 2017; de la Riva et al. 2018a). As a result, they have leaves with a high mass-based photosynthetic capacity and roots with a high mass-based capacity for N inflow. The balance of net mass-based carbon gain (leaf photosynthesis minus total plant respiration, NAR_m) and mass-based maximum rate of NO_3^- inflow (NIR_m) in combination with the pattern of root:leaf allocation (Fig. 10.4E, F) accounts for differences in RGR_{max}. The limited data available suggest that NIR_m has a stronger correlation with RGR_{max} than does NAR_m. This is evident from the positive correlation between RGR_{max} and the ratio of mass-based specific ion uptake rate and mass based net assimilation rate (Fig. 10.7D).

10.3.7 *RGR* and Suites of Plant Traits

Our analysis of the correlations of RGR_{max} with plant traits suggests that *SLA* is the key trait, because it enables the plant to expose a large

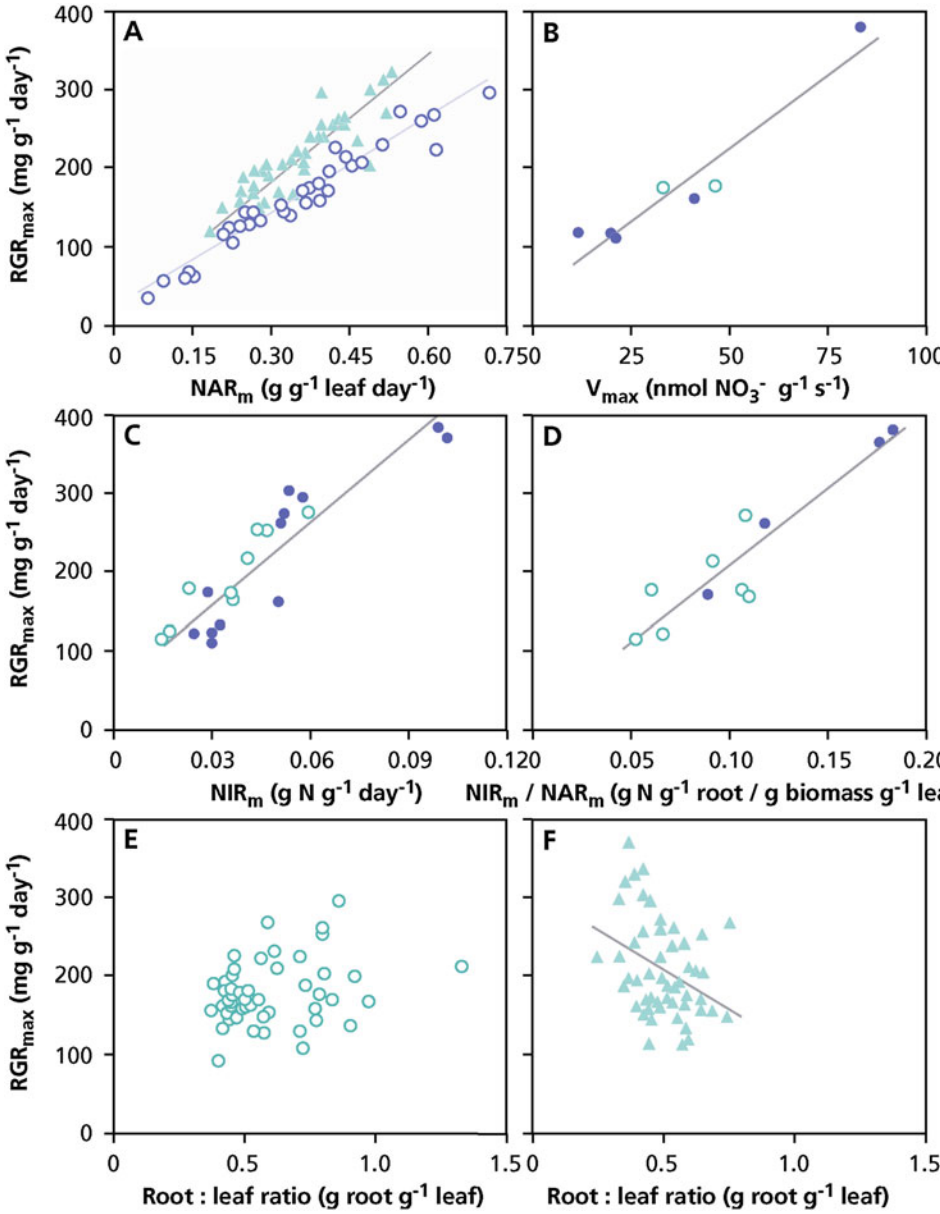

Fig. 10.7 Correlation between maximum relative growth rate (RGR_{max}) and (**A**) mass-based net assimilation rate (NAR_m), (**B**) mass-based maximum rate of NO_3^- uptake (V_{max}), (**C**) mass-based specific NO_3^- inflow rate (NIR_m), (**D**) the ratio of NIR_m/NAR_m, and (**E** and **F**) the ratio of biomass allocation to roots and leaves for 51 monocotyledonous (**E**) and 53 dicotyledonous (**F**) species. Each point represents a separate species of monocot (open symbols) or dicot (closed symbols) grown with free access to nutrients (redrawn after data synthesized by Garnier 1991).

leaf area to light and CO_2 per given biomass invested in leaves. Certain other traits, however, also correlate positively with RGR_{max}, for example, mass-based measures of photosynthesis and nutrient uptake, and hydraulic traits (Eller et al. 2018). Some traits are negatively associated with RGR_{max}, for example, leaf mass density due to support tissues and root respiration. These

observations suggest that there is a **suite of plant traits** associated with rapid growth (high *SLA*, high mass-based rates of photosynthesis, and nutrient uptake), whereas other traits are typically associated with slow growth (greater investment in cell walls and fiber) (Lambers and Poorter 1992). These dichotomies suggest a **trade-off** between traits that promote rapid growth and those that promote persistence, a **plant economics spectrum** (Díaz et al. 2016).

Due to their greater investment in carbon-rich compounds, such as lignin, and less accumulation of minerals, the carbon concentration of slow-growing species is greater than that of fast-growing ones. This additional, albeit minor, factor contributes to their low growth potential. There may well be differences in exudation and volatilization, but their quantitative significance in explaining variation in *RGR* is generally small, except for species with cluster roots (Sect. 9.2.2.5.2).

10.4 Allocation to Storage

Up to now in this chapter, we have only dealt with allocation of resources to structural components of the plant, during vegetative growth. Plants, however, also channel some resources to storage compartments, where the stored resources are available for future growth. Plants store both carbon and nutrients, but there is a wide variation in the amount and kind of resources that are stored, and in the organ where the storage predominantly takes place: leaves, stems, roots, or specialized storage organs. We will first discuss the concept of storage and its chemical nature, and then describe differences in the role of storage in annuals, biennials, and perennials.

10.4.1 The Concept of Storage

We define **storage** as resources that build up in the plant and can be mobilized in the future to support biosynthesis. There are three general categories of storage:

1. **Accumulation** is the increase in compounds that do not directly promote growth. Accumulation occurs when **acquisition** of **nitrate** (Blom-Zandstra 1989) or **phosphate** (Hawkins et al. 2008) exceeds **demands** for growth.
2. **Reserve formation** involves the metabolically regulated synthesis of storage compounds that might otherwise promote growth. Reserve formation may compete for resources with growth and defense (Liu et al. 2018). Trade-offs between investment in carbohydrate reserves and growth occur among deciduous woody savanna species (Tomlinson et al. 2014).
3. **Recycling** is the reutilization of compounds whose immediate physiological function contributes to growth (Dissanayaka et al. 2018) or defense (Gleadow and Møller 2014), but which can subsequently be broken down to support future growth.

Accumulation accounts for much of the short-term fluctuations in chemical composition of plants [*e.g.*, the daily fluctuation of starch in chloroplasts (Sect. 2.2.1.4) or of NO_3^- in vacuoles (Sect. 9.2.2)]. Accumulation allows a relatively constant export rate of carbohydrates from source leaves throughout the 24-h cycle, despite the obvious diurnal pattern of photosynthetic carbon gain (Fondy and Geiger 1982). Nitrate or phosphate accumulation, also termed 'luxury consumption', occur after pulses of N or P availability or when N or P supply exceed the capacity of the plant to utilize N or P in growth (Cogliatti and Clarkson 1983; Li et al. 2017). In a Mediterranean climate, nutrient uptake predominantly occurs in the wet season, whereas growth occurs later in the year (Mooney and Rundel 1979; Pate and Jeschke 1993); this obviously requires nutrients to be stored. Although accumulation may explain many of the short-term changes in storage, it is less important over time scales of weeks to years. Over these longer time scales, capacities for photosynthesis and nutrient uptake adjust to plant demand, thus minimizing large long-term imbalance between carbon and nutrient stores.

Reserve formation diverts newly acquired carbon and nutrients from growth or respiration into storage. This can occur when rates of acquisition are fast and vegetative growth is slow, and during periods of rapid vegetative growth, often in competition with it. Grafting experiments clearly demonstrate this competition between storage and growth. For example, roots of sugar beet (*Beta vulgaris*), which allocate strongly to storage in a taproot, decrease shoot growth when grafted to shoots of a leafy variety of the same species (chard). On the other hand, chard roots, which have a small capacity for storage, cause grafted sugar beet shoots to grow larger than normal (Rapoport and Loomis 1985). Stored reserves make a plant less dependent on current photosynthesis or nutrient uptake from the soil, and provide resources at times when growth demands are large, but when there are few leaves or roots present to acquire these resources, such as in early spring in cold climates. Stored reserves also enable plants to recover following catastrophic loss of leaves or roots to fire, herbivores, or other disturbances. Finally, stored reserves enable plants to shift rapidly from a vegetative to a reproductive mode, even at times of year when conditions are not favorable for resource acquisition.

Recycling of nutrients following **leaf senescence** allows reutilization of about half of the N and P originally contained in the leaf (Sect. 9.4), but it is a relatively unimportant source of carbon for growth. These stored nutrients are then a nutrient source for developing leaves. For example, in arctic and alpine plants, 30 to 60% of the N and P requirement for new growth comes from retranslocated nutrients. Reserve formation and recycling allow plants to achieve rapid growth following snowmelt, despite low soil temperatures that may limit nutrient uptake from the soil (Chapin et al. 1986; Atkin 1996).

10.4.2 Chemical Forms of Stores

In Sect. 10.4.1, we demonstrated that there are several types of controls over carbon and nutrient stores (accumulation, reserve formation, and recycling). The chemistry and location of stored reserves, however, may be similar for each of these processes.

Carbohydrates are stored as **soluble sugars** (predominantly sucrose), **starch**, or **fructans**, depending on the species; fructans (polyfructosylsucrose) are only found in some taxa: Asterales, Poales, and Liliales (Van den Ende 2013). Storage of carbohydrates as sucrose [*e.g.*, in the taproot of *Beta vulgaris* (sugar beet)] coincides with the accumulation of KCl in the apoplast, so that cell turgor is maintained, despite the accumulation of vast amounts of osmotic solutes inside the storage cells (Leigh and Tomos 1983). Stored carbohydrates in roots of *Lolium perenne* (perennial ryegrass) are predominantly used to support root respiration, rather than export to the shoot (Schnyder and de Visser 1999).

The capacity for storage depends on the presence of a specific organ, such as a stem, rhizome, tuber, bulb, or taproot. Thus, an important cost of storage is production of the storage structure, in addition to the stores themselves. In a comparison of 92 species (15 genera) of Ericaceae in a fire-dominated Australian habitat, species that regenerate from seeds (**obligate seeders**) have low starch levels in their roots (2 mg g^{-1} dry mass) when compared with **resprouters** (14 mg g^{-1} dry mass), without differences in their shoots (Bell et al. 1996). Nutrient addition to woody shrubs reduces allocation to root mass, and resprouters consistently allocate more than congeneric obligate seeders to root mass (Knox and Morrison 2005). The rate of root respiration in *Daucus carota* (carrot) decreases greatly when the capacity to store carbohydrates in the taproot increases with increasing plant age (Steingröver 1981). Thus, storage of carbohydrates does not invariably occur at the expense of vegetative growth, but may involve a decline in carbon expenditure in respiration.

Nitrogen is stored as $\mathbf{NO_3^-}$ (especially in petioles and shoot axes of fast-growing species), when plants are supplied with excessive levels of NO_3^-. At a moderate or low N availability, N is stored as **amino acids** (often of a kind not found in proteins), **amides** (asparagine and glutamine),

or **protein** (including **Rubisco** and **vegetative storage proteins**) (Meuriot et al. 2004). Storage as protein involves the additional costs of protein synthesis, but has no effects on the cell's osmotic potential. In addition, proteins may serve a catalytic or structural function as well as being a store of N. Leaves contain vast amounts of Rubisco, of which some may be inactivated and not contribute to photosynthesis (Sect. 9.4.2). Rubisco is not a storage protein in a strict sense, but it is nonetheless available as a source of amino acids that are exported to other parts of the plant (Girondé et al. 2015). Storage of nitrogenous compounds is sometimes considered an indication of 'luxury consumption', but N-deficient plants also store some N, which they later use to support reproductive growth (Millard 1988; Liu et al. 2018).

Phosphorus is stored as **inorganic phosphate** (orthophosphate) as well as in **organic phosphate-containing compounds** (*e.g.*, inositol phosphate) (Sect. 9.2.2.5.1) (Hübel and Beck 1996). *In vivo* NMR (Sects 2.2.5.2 and 2.4.1.3) has been used to determine the Pi concentration in the cytoplasm and vacuoles of the root tips of *Pinus serotina* (pond pine). In P-starved plants, the Pi concentration is 0.75 mM, as compared with 1.5 mM in plants that are grown with abundant P. In the vacuoles of the root tips, on the other hand, the concentration drops from 3.4 mM to a level that is too low to determine (Ayling and Topa 2002). This shows that the vacuoles are the major storage site for Pi, and that the concentration of Pi in the cytoplasm is relatively constant over a wide range of Pi concentrations in the root environment.

10.4.3 Storage and Remobilization in Annuals

Annuals allocate relatively little of their acquired resources (carbon and nutrients) to storage which contributes to their fast growth rate. Annuals are generally short-lived, and the rapid formation of a large seed biomass ensures survival of the population and avoids periods of low resource supply.

During seed filling, carbohydrate reserves in stems are depleted, and the N and P invested in the N- and P-containing molecules is exported, after hydrolysis of the proteins to amino acids and nucleic acids to Pi, which are exported via the phloem. The gradual breakdown and export of resources invested in leaves occurs during leaf **senescence**. This is a **controlled process** in plants, and it is rather different from the uncontrolled collapse with increase in age of animal cells (Woo et al. 2018). It ensures remobilization of resources previously invested in vegetative structures to developing reproductive structures. Roots and some parts of the reproductive structures also show a net loss of N and a decrease in nutrient uptake during some stages of seed filling (Table 10.2).

Table 10.2 Net export of nitrogen (N, mainly as amino acids and amides after protein hydrolysis) from senescing glumes, leaves, stem, and roots, and accumulation of the same amount in the grains of *Triticum aestivum* (wheat), between 9 and 15 days after flowering.

Plant part	Change in nitrogen content μg (plant part)$^{-1}$ day^{-1}
Glumes	–192
Leaves	–335
Stem	–193
Roots	–132
Total	–852
Grains	+850

Source: Simpson et al. (1983)

In addition to the use of proteins that first function in the plant's primary metabolism during vegetative growth, plants also have specific **vegetative storage proteins**. These glycoproteins accumulate abundantly in leaves or stolons (Staswick 1990; Goulas et al. 2007). Wounding, water deficit, blockage of export via the phloem, and exposure to jasmonic acid (a molecule signaling stress in plants; Sect. 13.4.3) all enhance the accumulation of vegetative storage proteins in leaves of soybean (Staswick et al. 1991) and *Arabidopsis thaliana* (thale cress) (Berger et al. 1995).

10.4.4 The Storage Strategy of Biennials

Biennials represent a specialized life history that enables them to exploit habitats where resources

are available intermittently. And where a small change in these environmental conditions may tip the balance toward either annuals or perennials (Hart 1977). In their first year, biennials develop a storage organ, as do perennials. In their second year, they invest all available resources into reproduction, in a manner similar to that in annuals.

The storage organs of biennials contain both **carbohydrates** and **N**. Do the stored reserves of C or N add significantly to seed yield? In the biannual thistle, *Arctium tomentosum* (woolly burdock), the carbohydrates stored in the taproot are important to sustaining **root respiration**, but they contribute less than 0.5% to the formation of new leaves (Heilmeier et al. 1986). Carbohydrate storage only primes the growth of the first leaves, after which the next leaves grow independently of stored carbon. Of all the N invested into growth of new leaves, however, about half originates from the N that is remobilized from the storage root. The N stored in roots contributes 20% to the total N requirement during the second season. Under shaded conditions, this fraction is as high as 30%. Seed yield significantly correlates with total plant N content early in the second year. In shaded plants, the amount of N in the seeds is very similar to the amount stored after the first year, whereas in plants grown at normal levels of irradiance, the amount of N in the seeds is about twice that which was stored (Fig. 10.8; Heilmeier et al. 1986).

10.4.5 Storage in Perennials

Perennials have a large capacity for storage of both nutrients and carbohydrates which is frequently associated with a reduced growth potential in the early vegetative stage (Rosnitschek-Schimmel 1983; Karlsson and Méndez 2005). Storage of resources, however, enables these plants to start growth early in a seasonal climate, and to survive conditions that are unfavorable for CO_2 assimilation or nutrient acquisition. The stored resources allow rapid leaf development, whereas annuals depend on recently acquired carbon and nutrients (Bausenwein et al. 2001).

In the tundra sedge *Eriophorum vaginatum* (cotton grass), amino-acid N and organic P reserves vary nearly fourfold during the growing season and provide all the nutrients required to support leaf growth in early summer, when the arctic soil is largely frozen (Chapin et al. 1986).

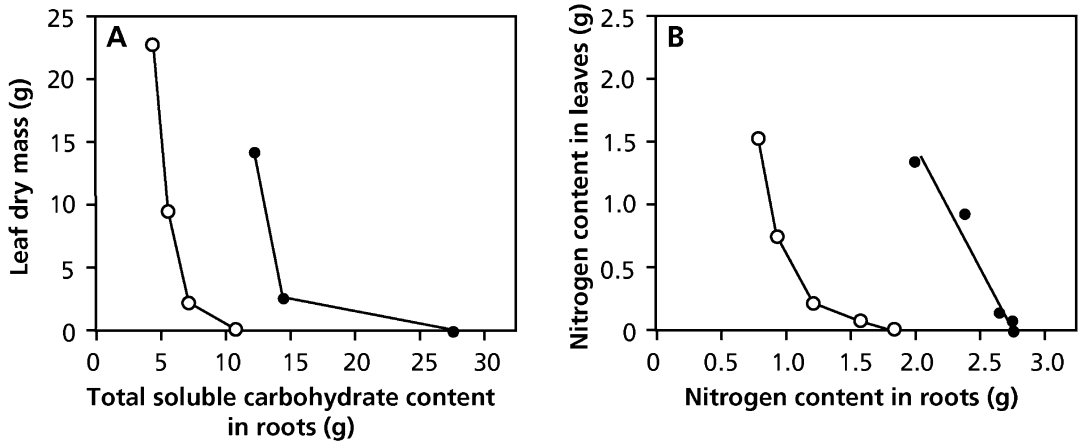

Fig. 10.8 The relation between (**A**) the decrease with time of the content of total soluble carbohydrates in the taproot and the increase with time of leaf dry mass, and (**B**) the decrease with time of the nitrogen (N) content of the taproot and the increase with time of the N content of the leaves, at the beginning of the second season in an biennial herbaceous thistle, *Arctium tomentosum* (woolly burdock). Filled circles refer to control plants, grown under natural light in the field, and open circles to plants grown in shade, 20% of the irradiance of control plants (Heilmeier et al. 1986); copyright © 1986, Springer-Verlag.

As in the annual *Glycine max* (soybean) (Sect. 10.4.1), some perennial herbaceous species also accumulate specific **storage proteins** [*e.g.*, in the taproots of *Taraxacum officinale* (dandelion) and *Cichorium intybus* (chicory) (Cyr and Derek Bewley 1990). Accumulation of vegetative storage proteins in stolons of *Trifolium repens* (white clover) during autumn and winter is encoded by a cold-induced gene (Goulas et al. 2007). Storage proteins have the advantage over amino acids and amides as storage products in that they allow storage at a lower cellular water content and thereby reduce the danger of freezing damage. Upon defoliation, the storage proteins are remobilized during regrowth of the foliage [*e.g.*, in the taproot of *Medicago sativa* (alfalfa)] where they constitute approximately 28% of the soluble protein pool. Several weeks after defoliation, the storage proteins may again comprise more than 30% of the soluble protein pool (Avice et al. 1996).

Storage proteins also occur in woody plants, especially in structural roots, bark, and wood tissue of trees, where they may constitute 25 to 30% of the total extractable proteins (Babst and Coleman 2018). In *Populus canadensis* (Canada poplar), **storage glycoproteins** accumulate in protein bodies in ray parenchyma cells of the wood in autumn and disappear again in spring (Sauter and van Cleve 1991). In *Populus* (poplar) the synthesis of storage proteins is induced by exposure to short days and low temperature (Fig. 10.9), under the control of **phytochrome** (Coleman et al. 1992; Babst and Coleman 2018).

The persistence of grassland species such as *Lolium perenne* (perennial ryegrass) greatly depends on their capacity to grow after cutting or grazing. After defoliation, the carbohydrate reserves in the stubble (mainly fructans) are rapidly depleted during regrowth. The carbohydrate content of the roots also declines after defoliation, but the roots remain a net sink for carbon, even immediately after defoliation. Morvan-Bertrand et al. (1999) showed that after a regrowth period of 28 days, 45% of all carbon fixed before defoliation is still present in the roots and leaves, and only 1% is incorporated in entirely new tissue, demonstrating the importance of recently fixed carbon for regrowth.

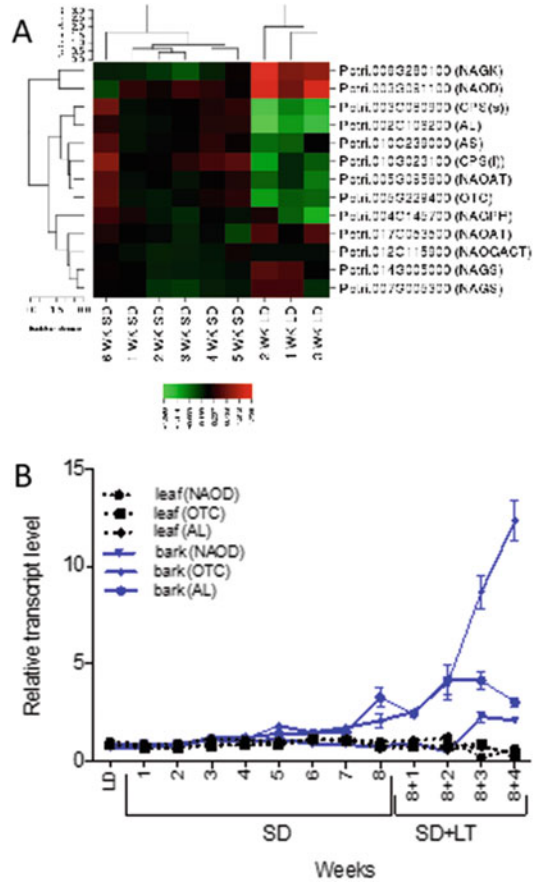

Fig. 10.9 Bark and leaf expression of *Populus* (poplar) genes in the arginine biosynthesis pathway during short-day-induced accumulation of bark storage proteins. (**A**) Relative bark transcript abundance for genes in the arginine biosynthetic pathway based on DNA microarray analysis. (**B**) Relative transcript levels based on qRT-PCR for N-acetylornithinedeacetylase (NAOD), ornithine transcarbamoylase (OTC) and argininosuccinate lyase (AL) in bark (blue lines) and leaves (black lines) during leaf senescence of plants treated with short days (SD) or short days combined with low-temperature (SD+LT) (Babst and Coleman 2018).

10.4.6 Costs of Growth and Storage: Optimization

Costs of storage include **direct costs** for **translocation** of storage compounds to and from storage sites, **chemical conversions** to specific storage compounds, and **construction of special cells**, **tissues**, or **organs** for storage as well as their protection. There are also **opportunity costs** (*i.e.* diminished growth because of diverting

metabolites from resources that might have been used for structural growth) (Bloom et al. 1985). The construction of storage cells and tissue does not necessarily occur at the same time as the accumulation of the stored products which makes it difficult to assess whether vegetative growth and storage are competing processes. If the storage compounds are derived from recycling of leaf proteins (*e.g.*, Rubisco), which functioned in metabolism during the growing season, then storage does not compete with vegetative growth. Use of accumulated stores similarly does not compete with growth and has negligible opportunity cost. If carbohydrates accumulate during the period of most vigorous vegetative growth, particularly when plants are light-limited, then there is no competition between storage and vegetative growth (Heilmeier and Monson 1994).

10.5 Environmental Influences

In earlier Sections, we discussed the causes of inherent differences among species in growth rate under favorable conditions. Natural conditions, however, are seldom optimal for plant growth, so it is critical to understand the patterns and mechanisms by which growth responds to variation in environmental factors, including water and nutrient supply, irradiance, O_2 availability, and temperature. Plants may acclimate to different environmental conditions, or they may differ genetically in their programmed response to the environment. In this Section, we discuss aspects of both acclimation and adaptation.

Plants generally respond to suboptimal conditions through reductions in growth rate and changes in allocation to minimize the limitation of growth by any single factor. Arguments based on economic analogies suggest that plants can minimize the cost of growth (and therefore maximize growth rate) if allocation is adjusted such that all resources are equally limiting to growth (Bloom et al. 1985). Thus, we might expect greater allocation to leaves when light strongly limits growth, and greater allocation to roots in response to water or nutrient limitation (Brouwer 1963). The net result of these adjustments, through both adaptation and acclimation, should be a functional balance between the activity of roots and shoots in which belowground resources are acquired in approximate balance with aboveground resources (Garnier 1991):

$$(\text{root mass})\, x NIR_{\text{m}} = k\, x\, (\text{leaf mass})\, x NAR_{\text{m}} \tag{10.9}$$

where NIR_{m} is the net inflow of N per unit root mass, NAR_{m} is the net assimilation rate, which is now expressed per unit leaf mass, rather than leaf area, and k is the concentration of N; instead of N, the net inflow and concentration of other nutrients can be used in this equation. The accumulation of nutrients under conditions of carbon limitation and of carbohydrates under conditions of nutrient or water limitation (Sect. 10.4) shows that plants never achieve perfect functional balance.

Growth is arguably the most important process to understand in predicting plant **responses to environment**, and we therefore need to understand the **basic mechanisms** by which growth responds to environment. Does growth decline in direct response to reductions in resource supply and acquisition, or does the plant anticipate and respond to specific signals before any single resource becomes overwhelmingly limiting to all physiological processes? In other words, is growth **source-controlled** or do specific signals modulate sink activity (growth), which then governs rates of resource acquisition (**feedforward control**)? For example, if growth responds directly to reduced source strength, low availability of light or CO_2 would act primarily on photosynthesis, which would reduce the carbon supply for growth; similarly, water or N shortage would restrict acquisition of these resources such that water potential or N supply would directly determine growth rate. On the other hand, if plants sense unfavorable environmental conditions and trigger signals that reduce growth rate directly, this would lead to a feedforward response that would reduce rates of acquisition of nonlimiting resources before the plant experiences severe resource imbalance.

Unfavorable environmental conditions tend to reduce growth. For example, unfavorable soil conditions often trigger changes in the balance among abscisic acid, cytokinins, and gibberellins which leads to changes in growth rate that precede any direct detrimental effects of these changes in environment. This **feedforward response** minimizes the physiological impact of the unfavorable environment on plant growth. In the following Sections, we describe the evidence for the relative importance of direct environmental effects on resource acquisition (source control) *versus* those mediated by feedforward responses. Current simulation models of plant growth in agriculture and ecology assume that source control is the major mechanism of plant response to environment. If this is incorrect, it is important to know whether the feedforward responses of plants lead to qualitatively different predictions of how plants respond to their environment.

10.5.1 Growth as Affected by Irradiance

Light is one of the most important environmental factors, providing plants with both a source of energy and **informational signals** that control their growth and development. Plants contain an array of **photoreceptors** that track almost all parameters of incoming light signals, including presence, absence, colors, intensity, direction, and duration. These effects of light are the topics of this Section, whereas we discussed effects of UV radiation in Sect. 7.2.2, and effects of day-length (photoperiod) on flowering in Sect. 11.3.3.1. Allocation of N to different leaves, as dependent on incident irradiance is covered in Sect. 10.5.4.6, after discussing the involvement of cytokinins in N allocation (Sect. 10.5.4.4).

10.5.1.1 Growth in Shade

Shade caused by a leaf canopy reduces the irradiance predominantly in the photosynthetically active region of the spectrum (400–700 nm), causing a shift in both the quantity and the spectral composition of light (Box 10.2).

Box 10.2: Phytochrome

Thijs L. Pons
Department Plant Ecophysiology, Institute of Environmental Biology, Utrecht University, Utrecht, The Netherlands

Plants monitor various aspects of the light climate, and they use this information to adjust their growth and reproduction to environmental conditions. Phytochrome is one of the photoreceptors in plants that allow them to gain information about their light environment. Butler et al. (1959) discovered phytochrome as the photoreceptor involved in red to far-red reversible reactions. *In vivo*, the phytochrome chromophore exists in two photoconvertible forms (Box Fig. 2): the red (R)-light-absorbing form (P_r) and the far-red (FR)-light-absorbing form (P_{fr}). Absorption of R and FR causes transformations between the two forms. Other processes affecting the fraction of phytochrome in the P_{fr} form (P_{fr}/P_{tot}) are its synthesis as P_r and its degradation as P_{fr}. Conversion of P_{fr} to P_r can also take place independent of light, in the process of dark reversion (Box Fig. 2). The active form of phytochrome is P_{fr}, which migrates to the nucleus to bind to a phytochrome-interacting factor (PIF), which is involved in gene expression. Phytochrome plays a key role throughout the life cycle of plants, from seed maturation and germination, to seedling development, vegetative growth, and in the control of flowering and senescence. The main function of phytochrome is the detection of the presence of competing neighbors and

(continued)

Box 10.2 (continued)

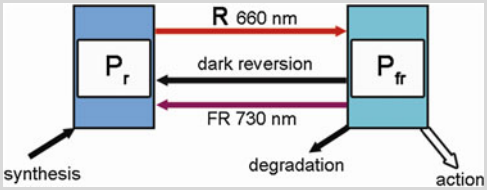

Box Fig. 2 Conversion of phytochrome between the red (R)- and far-red (FR)-absorbing forms of phytochrome (P_r and P_{fr}, respectively). Phytochromes are synthesized in the P_r form and broken down in the P_{fr} form. Absorption of R (peak sensitivity 660 nm) and FR (peak sensitivity 730 nm) generate photoconversions of the chromophore. P_{fr} can also be converted to P_r independently of light (dark reversion). P_{fr} is the biologically active form that migrates to the nucleus where it regulates transcription.

mediation of a response known as shade avoidance (Sect. 10.5.1.1). This is achieved by the perception of light *per se*, its spectral composition, its irradiance level and its direction (Ballaré 1999). Phytochrome is also involved in the perception of day-length.

In *Arabidopsis thaliana*, five genes encoding different apoproteins of phytochrome have been identified: *PHYA-PHYE*. They have different and partly overlapping functions during various developmental stages. PhyA is labile and easily degrades to the P_{fr} form, whereas phyB is more stable, and can be subject to repeated photoconversions. The use of mutants lacking one or more phytochromes has provided a powerful tool in unraveling their functions. *Arabidopsis thaliana* has an extreme shade-avoiding phenotype when all phytochrome is absent due to a mutation in the synthesis of the chromophore, even to the extent that the plant no longer has a rosette habit. The presence of phytochromes in the P_{fr} form appears necessary for attaining a normal light-grown phenotype (Smith 2000).

The more abundant phyB is the principal regulator of the classical R-FR reversibility of seed germination in the so-called low fluence response (LFR; Sect. 11.2.5). A similar role has been identified for phyE. Buried seeds can detect extremely low quantities of light in the so-called very low fluence response (VLFR) where phyA is the actor. Exposure to a light dose of 0.1 μmol photons m^{-2} is effective in these sensitized seeds, whereas the LFR operates in the 100 to 1000 μmol m^{-2} range (Sect. 10.11.2.5). Phytochrome A is also important for the high-irradiance response (HIR) that inhibits germination under prolonged exposure to light of high irradiance (Box Fig. 3A; Franklin and Whitelam 2004).

After germination, the etiolated seedling is highly sensitive to light due to the accumulation of phyA. De-etiolation starts after exposure to light, even before the seedling breaks through the soil surface. Subsequent hypocotyl extension is under control of the R:FR ratio (and thus canopy density), where phyB is the principal actor in inhibition of hypocotyl extension in normal daylight together with phyD, and possibly phyC.

Further development, particularly of light-demanding herbaceous species such as *Arabidopsis thaliana*, is strongly influenced by the degree of canopy shade, which comprises both reduced irradiance (Poorter et al. 2019) and a low R:FR ratio. Particularly a low R:FR ratio is involved in the shade-avoidance syndrome (SAS) in which phytochrome plays an important role (Ballaré and Pierik 2017). The SAS is essentially the priority of erect growth that optimizes placement of leaf blades in more favorable light conditions in canopies composed of similar-sized plants. This is achieved by internode and petiole extension, and hyponasty (vertical orientation of petioles and/or leaf blades) (Sect. 10.5.1.1). Mutants lacking phyB have a constitutive shade-avoiding phenotype, indicating that this phytochrome plays a major role in that response (Box Fig. 3B). However, the fact that these mutants

(continued)

Box 10.2 (continued)

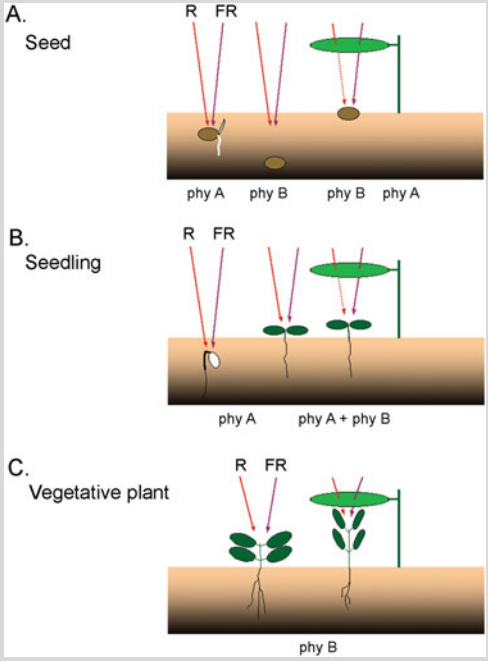

Box Fig. 3 Simplified scheme to show the role of phytochromes at two developmental stages. (**A**) Seed and emerging seedling. Darkness keeps light-sensitive seeds in an inhibited state. In addition, canopy-filtered light with a low R:FR ratio inhibits germination *via* the high-irradiance response (HIR; phyA) and the low fluence response (LFR; phyB). Unmodified daylight may stimulate germination *via* the low- (LFR; phyB), or the very-low fluence response (VLFR; phyA) when shallowly buried, stimulating germination when conditions are suitable. Seedling are highly light sensitive due to accumulation of phyA in the P_r form. Their de-etiolation is initiated even before the surface is reached, irrespective of canopy shade. (**B**) Vegetative plant. Under a canopy, plants develop a shade-avoiding phenotype, *i.e.* extension of petioles and internodes, and a vertical orientation of petioles and/or leaves (hyponasty). This is regulated mainly by phyB, which responds to the reduced R:FR ratio in canopy shade.

still show a shade-avoidance response in low R:FR indicates that other phytochromes are also involved. These appear to be phyD and phyE, whereas phyA and phyC modulate the effects of the other photoreceptors (Franklin and Whitelam 2004).

10.5.1.1.1 Effects on Growth Rate, Net Assimilation Rate, and Specific Leaf Area

Plants that grow in a shady environment invest relatively more of the products of photosynthesis and other resources in leaf area: they have a **high *LAR***. Their leaves are relatively thin: they have a **high *SLA*** (Sect. 2.3.2.2) and **low leaf mass density**. This is associated with relatively few, small **palisade mesophyll** cells per unit area. The leaves have a high **chlorophyll concentration** per unit fresh mass which results in a rather similar chlorophyll concentration per unit leaf area as that in sun leaves, but relatively **less protein** per unit chlorophyll (Sect. 2.3.2.3).

Trees, *e.g.*, ecotypes of *Fagus crenata* (Japanese beech), produce sun leaves with thick palisade tissue comprising two cell layers. The number of cell layers in the palisade tissue is determined in the **winter buds**, by early winter of the year prior to leaf unfolding. When sun-exposed branches with young expanding leaves are shaded, the resultant leaves show intermediate characteristics: they have palisade tissue with two cell layers, but the height of the palisade tissue is less than that in the fully exposed sun leaves (Terashima et al. 2006). This suggests that several different signals are used for the determination of characteristics of sun leaves. When plants of the annual herb *Chenopodium album* (lambsquarters) are shaded in various ways, the developing leaves, irrespective of their own light environments, form palisade tissue with two cell layers if mature leaves are exposed to high light. On the other hand, when mature leaves are shaded, palisade tissue with one cell layer is formed. These results show that the light environment of mature leaves determines the number of cell layers in the palisade tissue of new leaves, and suggest a signal-transduction system that conveys a signal from the mature leaves to the developing leaves (Yano and Terashima 2001). The signal from the mature leaves regulates the direction of cell division. In the future sun leaves; the signal probably induces periclinal division in addition to anticlinal division, while the signal from the shaded mature leaves only allows the cells to divide anticlinally (Yano and Terashima

Table 10.3 Effects of the irradiance level on growth parameters of a sun-adapted species, *Dactylis glomerata* (cocksfoot), and a shade-adapted species *Dactylis polygama* (slender cocksfoot). Daily irradiances (100% values) were full sunlight for both species.

	Relative irradiance level			
Growth parameter	100	30	20	5.5
Relative growth rate (mg g^{-1} day^{-1})				
Dactylis glomerata	98	88	88	56
Dactylis polygama	98	88	100	29
Net assimilation rate (g m^{-2} day^{-1})				
Dactylis glomerata	13.2	7.5	6.9	1.5
Dactylis polygama	8.8	5.9	5.9	0.7
Leaf area ratio (m^2 kg^{-1} dry mass)				
Dactylis glomerata	7.4	11.7	12.7	38.0
Dactylis polygama	11.2	15.0	17.0	38.5
Specific leaf area (m^2 kg^{-1} dry mass)				
Dactylis glomerata	28.5	36.4	33.7	66.6
Dactylis polygama	31.7	36.4	40.4	74.9
Leaf mass ratio (g g^{-1})				
Dactylis glomerata	0.26	0.34	0.37	0.57
Dactylis polygama	0.36	0.41	0.42	0.52
Leaf mass density (kg dry mass m^{-3})				
Dactylis glomerata	217	217	217	142
Dactylis polygama	247	248	244	155
Root length ratio (m g^{-1} dry mass)				
Dactylis glomerata	141	105	102	59
Dactylis polygama	110	92	88	96
Specific root length (m g^{-1} dry mass)				
Dactylis glomerata	287	282	303	416
Dactylis polygama	278	277	279	407

Source: Ryser and Eek (2000)

2004). This signal might be the abundance of photosynthates (Terashima et al. 2006).

Table 10.3 summarizes the results of morphological acclimation and adaptation to low irradiance. The *RGR* of the **shade-avoiding** *Dactylis glomerata* (cocksfoot) is reduced less by growth in shade as compared with full sun, than that of *Dactylis polygama* (slender cocksfoot), which is a **shade-tolerant** species. This is due to a stronger increase of *LAR* in the shade in *Dactylis polygama*, which is due to a large increase in *SLA* and a small increase in *LMR* (the various abbreviations used in growth analysis are explained in Table 10.1 and Sect. 10.2.1). The regulation of the increase in *LAR* may involve signaling, as discussed in this Section for *Chenopodium album*; it serves to capture more of the growth-limiting resource in the shade. Table 10.3 also shows trade-offs between resource allocation to leaves and roots. The overall patterns indicate that changes in allocation and leaf morphology in response to shade maximize capture of the growth-limiting resource (light), and that this shade acclimation is more extreme in shade-adapted species.

At a very low irradiance, such as under a dense canopy, many shade-avoiding plants do not survive, even though they may exhibit a positive *RGR* in short-term growth experiments (Table 10.3). Thus, there must be additional factors that account for the distribution of sun-adapted and shade-adapted species. First, **leaf longevity** is important. Shade-tolerant species tend to keep their leaves for a longer time, and so increase the potential photosynthetic return (Reich et al. 1991, 1992). When grown in shade, fast-growing tropical trees show a higher *LAR* and lower *RMR*, as well as a greater mortality than do slower-growing ones (Kitajima 1994). Shade-tolerant plants also minimize leaf loss through their greater allocation to chemical defenses against pathogens and herbivores than in shade-avoiding species (Chap. 13). In addition, the enhanced rate of stem elongation (Sect. 10.5.1.1.3) may weaken the shade-avoiding plants.

10.5.1.1.2 Adaptations to Shade

In addition to **acclimation** to a specific light environment, there are also specific **adaptations**. That is, there are species with a genetic constitution that restricts their distribution to an environment with a specific light climate. To put it simply, there are three plant strategies:

1. Plants avoiding shade, or obligate sun plants
2. Plants tolerating shade, or facultative sun or shade plants
3. Plants requiring shade, or obligate shade plants

Many weedy species and most crop species are **obligate sun species**. **Obligate shade plants** include some mosses, ferns, club mosses and a

few vascular plant species in tropical rainforests (*e.g.*, young individuals of *Monstera* and *Philodendron* species). Among vascular plants, obligate shade species are rare in temperate regions and we will not discuss them here. Most understory species are **facultative**, rather than obligate shade plants.

10.5.1.1.3 Stem and Petiole Elongation: The Search for Light

Stem and petiole elongation of **shade-avoiding** plants growing in the shade are greatly enhanced, branching is reduced (increased apical dominance), total leaf area and **leaf thickness** are less, and ***SLA*** is increased. The effects of leaf canopy shade can be separated into those due to **reduced irradiance** and those affected by the **red/far-red ratio**.

Plants that tolerate shade do not respond with increased stem elongation; instead, they increase their leaf area. Their leaf thickness is reduced to a smaller extent than it is in shade-avoiding species, and their chlorophyll concentration per unit leaf area often increases. The increased chlorophyll concentration gives these plants [*e.g.*, *Hedera* spp. (ivy) and species from the understory of tropical rain forests] their dark-green color. Less extreme shade-tolerant species also enhance their chlorophyll concentration per unit fresh mass. Because their *SLA* is increased at the same time, however, the chlorophyll concentration per unit area does not increase, and they do not appear dark-green.

The **red/far-red ratio** (R/FR) is the ratio of the irradiance at 655–665 nm and that at 725–735 nm. Comparison of a number of species from open habitats and from closed habitats (shade in forest understory) shows that the stem elongation of sun-adapted species responds much more strongly to R/FR than that of shade species does. The effect of a change in R/FR on stem elongation can be recorded within 10 to 15 min, *e.g.*, in *Sinapis alba* (white mustard) (Fig. 10.10).

10.5.1.1.4 The Role of Phytochrome

Perception of R/FR involves the **phytochrome** system (Box 9.2 and Sect. 10.2.2.2). In *Vigna sinensis* (cowpea) the response of **stem elongation** to R/FR is similar to that of **gibberellins** (GAs). In fact, inhibition of stem elongation by light is associated with a decrease in tissue responsiveness to GAs (Sun and Gubler 2004). Using *Arabidopsis thaliana* that has mutations affecting GA- and/or phytochrome-action shows that a fully functional GA system is necessary for full expression of the phytochrome response (Peng and Harberd 1997). The phytochrome responses clearly demonstrate that many of the light responses of shade plants are hormonally mediated, rather than direct responses to irradiance level.

10.5.1.1.5 Phytochrome and Cryptochrome: Effects on Cell-Wall Elasticity Parameters

Both red light and **blue light** inhibit stem elongation. The photoreceptor **cryptochrome** is involved in the perception of blue light. Both red and blue light affect cell-wall properties, rather than the osmotic or turgor potential of the cells (Table 10.4). As explained in Sect. 10.2.2, stem elongation is the result of cell expansion ($dV/V\ x\ t$), which is related to the cell-wall yield coefficient, the turgor pressure, and the yield threshold. Red light inhibits elongation mainly by lowering the **cell-wall yield coefficient** (ϕ), whereas blue light predominantly acts by enhancing the **yield threshold** (Y) (Table 10.4). This indicates that shade affects growth through **feedforward responses**, rather than through direct supply of photosynthates.

10.5.1.1.6 Effects of Total Level of Irradiance

The total level of irradiance is the major factor that determines the *LAR* and *SLA* of shade-avoiding species, but the spectral composition of the irradiance also has an effect in some species. Shade-avoiding species respond to the spectral composition in the shade primarily with enhanced stem elongation, at the expense of their leaf mass ratio.

Annighöfer et al. (2017) compared three shade-tolerant temperate forest tree species (*Acer pseudoplatanus* (sycamore maple), *Fagus*

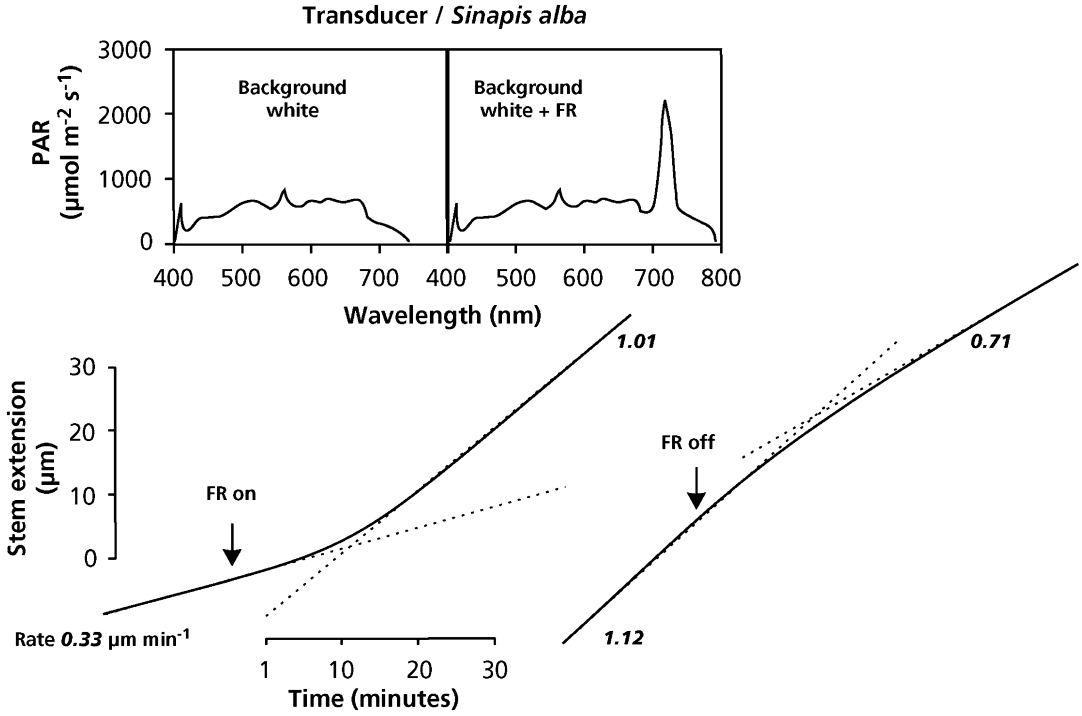

Fig. 10.10 Continuous measurements of stem extension rate by a position-sensitive transducer. A seedling attached to the transducer and exposed to background white fluorescent light was given far-red (FR) light via a fiber-optic probe. The FR source was switched on and off as indicated. Solid lines show the observed stem extension, and the dotted lines show the best fit initial and final extension rates, the values of which are presented next to the lines. The insets show the spectral composition of the irradiance of the background white light with and without FR (Data of D.C. Morgan, as presented in Smith 1981).

Table 10.4 Effects of darkness, red light and blue light on *in vivo* cell-wall properties of stems of etiolated *Pisum sativum* (pea) seedlings*.

	Dark	Red light	Blue light
Elongation rate, µm m^{-1} s^{-1}	9.2	3.3	3.0
Turgor potential, MPa	0.53	0.59	0.58
Osmotic potential, MPa	0.84	0.82	0.83
Yield threshold (Y), MPa	0.05	0.16	0.33
Yield coefficient (ϕ), Pa^{-1} s^{-1}	19.1	7.8	15.6

Source: Kigel and Cosgrove (1991)
*In darkness, the P_{fr} configuration of phytochrome reverts to the P_r configuration

sylvatica (European beech), and *Fraxinus excelsior* (European ash) responding to a light gradient. *Fagus sylvatica* allocated more biomass to its branches and less to its stem, in comparison with the other two species. The *RGR* and *LMA* of all species increased with increasing light gradient, whereas the *LAR* decreased. *NAR* also increased with light availability. This study shows varying reactions of the three species to light, and allows a quantitative distinction among the species regarding their shade tolerance (ash < maple < beech).

The responses to the level of irradiance are most likely mediated through **sugar-sensing systems** (Sects 2.4.3 and 2.12.1, and Sect. 3.4.4).

10.5.1.2 Effects of the Photoperiod

The length of the photoperiod affects the flowering response of long-day and short-day

plants, and tuber formation [*e.g.*, in *Solanum tuberosum* (potato)] (Sect. 11.3.3.1) as well as aspects of vegetative plant development that are not directly related to reproduction. These effects are mediated by the **phytochrome** system and differ from those that result from changes in the total level of irradiance received by the plants. It is interesting that a leaf from a tobacco plant (*Nicotiana tabacum*) that is induced to flower induces a potato plant (*Solanum tuberosum*) to tuberize when the tobacco leaf is grafted onto the potato plant. Antisense phytochrome B potato plants provide evidence for the role of phytochrome B (Box 10.2) in tuberization (Jackson et al. 1998).

Day length is sensed by the leaves, which produce a mobile signal transported to the shoot apex or underground stems to induce flowering or tuberization, respectively. A mobile *FLOWERING LOCUS T* (*FT*) protein is a main component of the long-range 'florigen', or flowering hormone (Sect. 11.3.3.1). Expression of the *Hd3a* gene, an *FT* orthologue, in *Solanum tuberosum* (potato) induces strict short-day potato types to tuberize in long days. Tuber induction is graft-transmissible (Fig. 10.11) and the protein is detected in the stolons of grafted plants, showing that transport of the protein correlates with tuber formation. The potato floral and tuberization transitions are controlled by two different *FT*-like paralogues (*StSP3D* and *StSP6A*) that respond to independent environmental cues, and show that an autorelay mechanism involving CONSTANS modulates expression of the tuberization-control *StSP6A* gene (Navarro et al. 2011).

10.5.2 Growth as Affected by Temperature

Temperature affects a range of enzymatically-catalyzed and membrane-associated processes in a plant, and is a major factor affecting plant distribution. The **activation energy** of different reactions differs widely. Growth, development, and allocation are affected in different ways in different species. Effects of temperature on plant development are commonly related to **degree days**, computed as the integral of a function of time that varies with temperature. The number of degree days accumulated over a period is often related to the phenological development of plants. Degree days are used to predict the date a flower will bloom or a crop reach maturity (Leon et al. 2001). Analyses of datasets throughout the temperate mid-latitude regions show a widespread tendency for species to advance their springtime phenology, consistent with warming trends over the past 20–50 years. Within these general trends toward earlier spring, however, are species that either have insignificant trends or have delayed their timing (Cook et al. 2012). An analysis of long-term data on phenology and seasonal temperatures from 490 species on two continents shows:

1. apparent nonresponding species are actually responding to warming, but their responses to fall/winter and spring warming are opposite in sign and of similar magnitude;
2. trends in first flowering date depend strongly on the magnitude of a given species' response to fall/winter *vs.* spring warming;
3. inclusion of fall/winter temperature cues strongly improves hindcast model predictions of long-term flowering trends compared with models with spring warming only.

Some studies report root growth lagging shoot growth by several weeks, and attribute this to air temperature warming faster than soil temperature in the spring (Steinaker and Wilson 2008). Others report root growth preceding shoot growth by several weeks to months, and these differences are clearly related to environment (Fig. 10.12). In a common garden study in Pennsylvania, United States, some species such as *Acer negundo* (boxelder maple) and *Pinus strobus* (white pine) show large inter-annual variability in root phenology, while others such as *Liriodendron tulipfera* (tulip tree) do not (McCormack et al. 2014). This suggests that some trees may be environmentally cued, while others are inflexible in their timing (Abramoff and Finzi 2015).

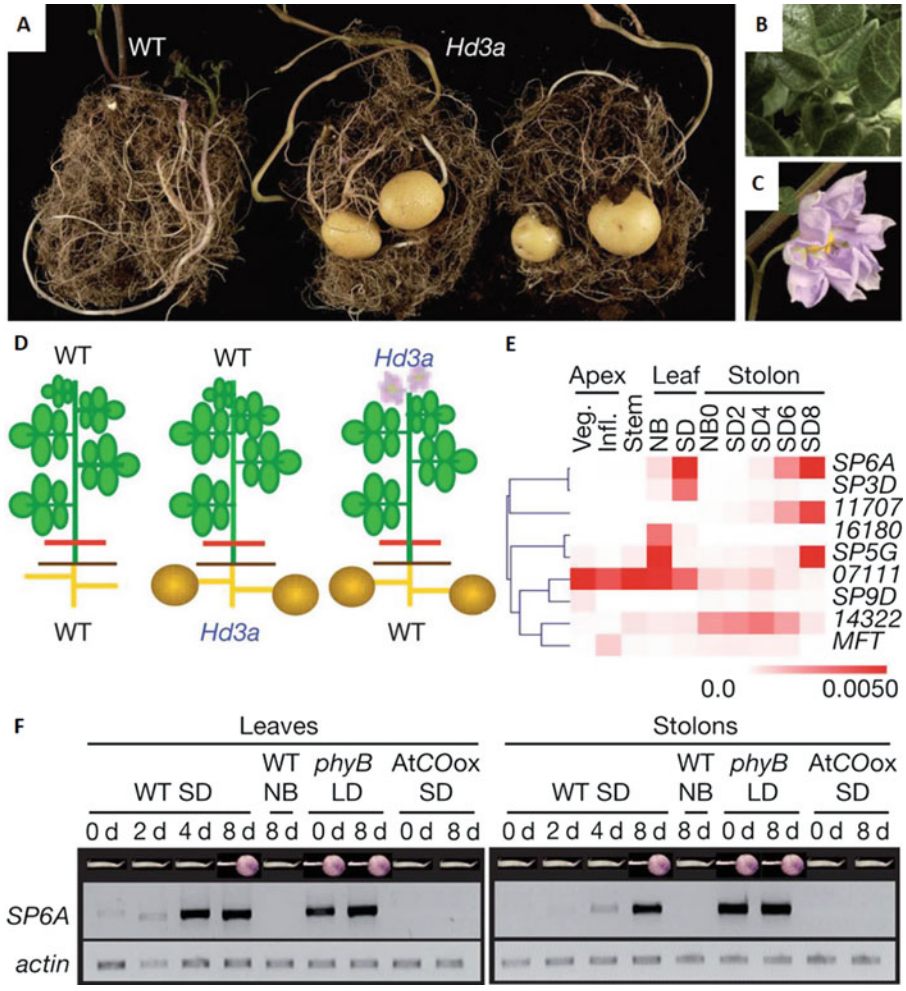

Fig. 10.11 Tuberization in *Solanum tuberosum* (potato). (**A**) Hd3a lines (center and right) tuberize under long-day conditions, unlike the wild-type control (left). (**B** and **C**) Early-flowering Hd3a plants relative to wild-type. (**D**) Tuber induction in long days of wild-type plants grafted with Hd3a donors (right) or stocks (center). Wild-type control grafts do not tuberize (left). Red lines indicate the graft junction. (**E**) Relative levels of expression of the *FT*- and *TFL1*-like genes, *11707*, *PGSC0003DMG400011707*; *16180*, PGSC0003DMG400016180; 07111, *PGSC0003 DMG400007111*; *14322*, *PGSC0003DMG400014322*; Veg., vegetative apex; Inf., inflorescence apex; NB, night break; SD, short day. (**F**) Semi-quantitative RT–PCR analysis of *StSP6A* expression in leaves and stolons of plants with different tuberization states (indicated on top). The pictures show noninduced stolons or tubers. LD, long day (Navarro et al. 2011). Reprinted by permission from Springer Nature Customer Service Centre GmbH: *Nature* **478**: 119. Control of flowering and storage organ formation in potato by FLOWERING LOCUS T. Navarro C, Abelenda JA, Cruz-Oró E, Cuéllar CA, Tamaki S, Silva J, Shimamoto K, Prat S; copyright 2011.

Fig. 10.12 (Continued) growth, and light green to shoot growth. The blue dotted line is mean monthly precipitation (mm, right-hand side y-axis). The color bar across the top is a heat map showing seasonal temperatures ranging from −10 °C (purple) to +25 °C (red), with 0 °C as bright blue. Panels (**E**)–(**H**) plot the proportion of maximum monthly root *vs.* shoot growth. In these panels, black lines join consecutive months, and the direction of the arrowheads indicates time from January to December. This approach assumes that shoot growth is a suitable proxy for the initiation of photosynthesis. Calculating the proportion of peak root or shoot growth, rather than absolute growth rates, allows plotting the different types of data on the same y-axis (Abramoff and Finzi 2015); copyright Trustees of The New Phytologist.

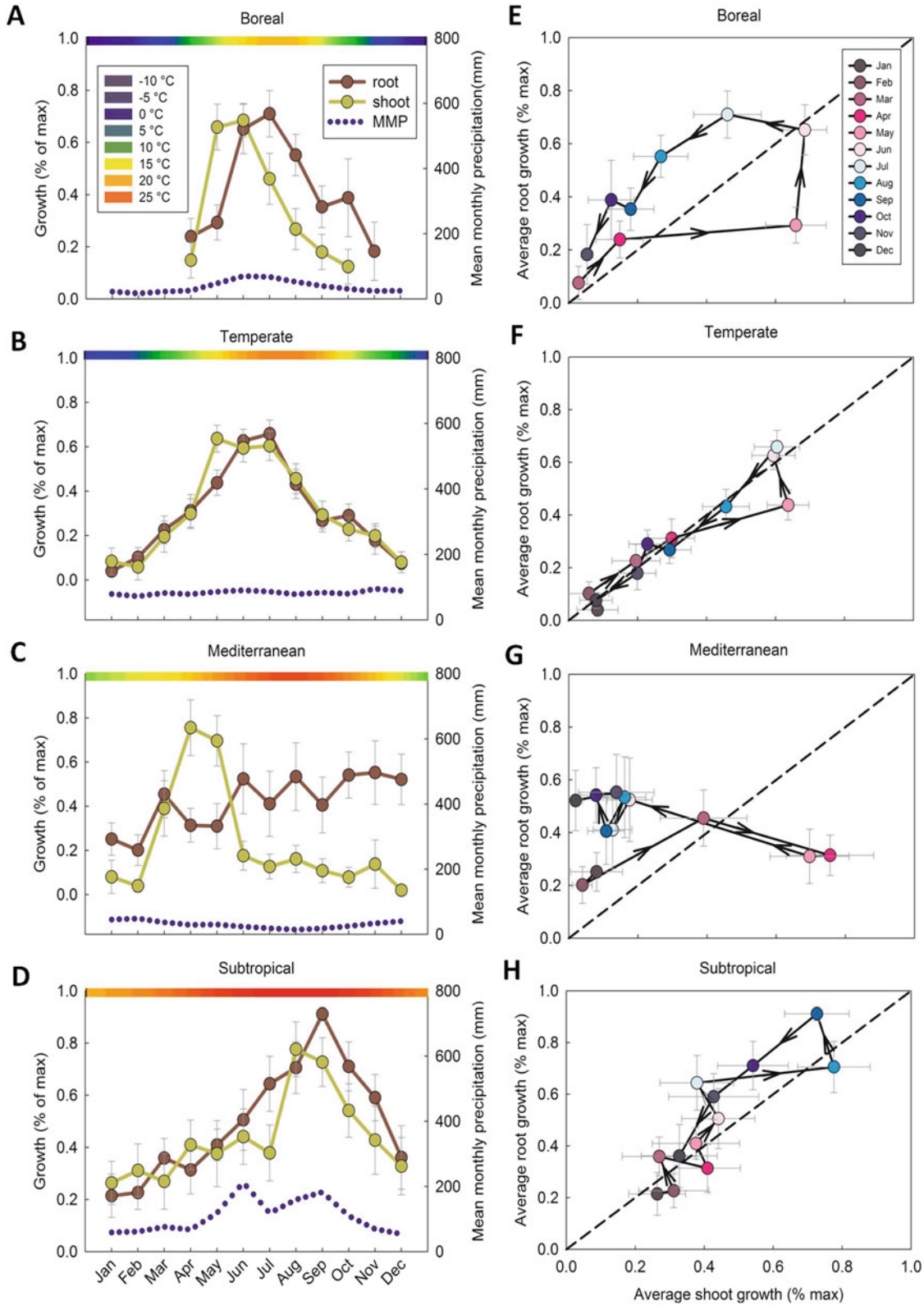

Fig. 10.12 The proportion of maximum monthly root and shoot growth for each month in: (**A**) boreal, (**B**) temperate, (**C**) Mediterranean, and (**D**) subtropical biomes. In panels (**A**)–(**D**), dark brown corresponds to root

10.5.2.1 Effects of Low Temperature on Root Functioning

Exposure to a low temperature reduces **root elongation**, without an effect on turgor in the elongation zone. In *Zea mays* (maize) the reduction in elongation rate is associated with a decrease in cell-wall extensibility, more specifically in the **cell-wall yield coefficient**. Reduced elongation may lead to an increased number of rather small cells, immediately behind the root tip. These resume expansion upon exposure of the roots to a more favorable temperature (Pritchard 1994).

For a proper functioning of roots at low temperature, their membranes must remain fluid and semipermeable. The **lipid composition** of the membranes in the roots affects membrane fluidity and interactions with membrane-bound proteins, and, therefore, the transport of both ions and water. Freezing-tolerant acclimated plants, *e.g.*, *Secale cereale* (rye) contain greater proportions of sterols, sphingolipids, and saturated phospholipids than less tolerant plants such as *Avena sativa* (oat) (Takahashi et al. 2016).

The major resistances for **water flow** in the roots are in the **exodermis**, if present, and the **endodermis**. At the exodermis or endodermis, water must enter the **symplast** before it can arrive in the xylem vessels. Water passes the membranes in a single file through specific water-channel proteins (**aquaporins**) (Sect. 5.5.2). The effect of temperature on the rate of water uptake by roots, therefore, reflects direct effects on these water-channel proteins and indirect effects on membrane fluidity (Chaumont and Tyerman 2014).

The effects of temperature on the roots' capacity to absorb water largely account for temperature effects on plant growth. Increasing the root temperature of *Glycine max* (soybean) in the range that is suboptimal for growth, while maintaining a constant shoot temperature, increases the water potential of the whole plant (Kuo and Boersma 1971). The effects of temperature on the relative investment of biomass in roots and leaves likely reflect the roots' capacity to take up water, at least in the range of temperatures around the optimum. The capacity to take up water is, in turn, influenced by plant hormones (Sect. 10.5.3). Does this imply that effects of temperature on the allocation pattern are accounted for by an effect of root temperature on the roots' capacity to transport water, and that temperature effects on nutrient uptake are not a cause for changes in the allocation pattern? Current evidence does indeed support this contention. Whereas growth at a low root temperature does affect the rate of absorption of both NO_3^- and NH_4^+, this appears to be a response to a decline in growth rate (Clarkson et al. 1992). That is, the decline in the rate of nutrient absorption at low root temperatures is, in part, a response to the decreased nutrient demand of the plant (Sect. 9.2.2.3.2).

10.5.2.2 Changes in the Allocation Pattern

Variation in growth rate with temperature is associated with changes in plant carbon balance. A positive carbon balance can be maintained at adverse temperatures by changes in the pattern of resource allocation to leaves and nonphotosynthetic plant parts. Acclimation to different temperatures, therefore, may affect the rate of photosynthesis per unit leaf area (Fig. 2.25) or the plant's allocation pattern. In very general terms, the effect of temperature on biomass allocation in the vegetative stage is that the relative investment of biomass in roots is lowest at a certain optimum temperature, and that it increases at both higher and lower temperatures. This is found both when the temperature of the entire plant is varied and when only root temperature is changed (constant shoot temperature) (Bowen 1991).

An increase in root temperature in the suboptimal range may increase the demand for respiratory substrate in roots which results in lower carbohydrate concentrations in the whole plant or in the shoots. These effects of root temperature on root respiration are often only transient, however, with values returning to control rates within a day (Sect. 3.4.5).

Temperature strongly affects the uptake of both nutrients and water by the roots. Although **nutrient uptake** depends on root temperature, at

least in short-term experiments, it is unlikely that long-term temperature effects on biomass partitioning are due to effects on nutrient uptake. Upon prolonged exposure to low root temperature, the uptake system acclimates (Sect. 9.2.2.3.3); there is compelling evidence that, at a low root temperature, **growth controls the rate of nutrient uptake**, rather than being controlled by it (Clarkson et al. 1992). Effects of root temperature, through the plant's water relations, are probably mediated by **ABA** (Sect. 10.5.3), but we need further evidence to support this contention.

There are also indirect effects of temperature on nutrient availability, in that rates of mineralization are slow at low temperatures (*e.g.*, in arctic and alpine environments).

10.5.3 Growth as Affected by Soil Water Potential and Salinity

Many processes in a plant are far more sensitive to a low water potential than stomatal conductance and photosynthesis are (Sect. 2.5.2). The growth reduction at a low soil water potential is largely due to inhibition of more sensitive processes, such as **leaf cell elongation** and **protein synthesis**. At a low soil water potential, the rate of leaf expansion decreases, whereas the rate of **root elongation** is much less affected (Fig. 10.13). In glycophytes [*e.g.*, *Zea mays* (maize)], root elongation is inhibited by exposure to high concentrations of NaCl. This inhibition is not associated with a loss of turgor of the growing tip, but with an **increased yield threshold pressure** (Neumann et al. 1994). Maintenance of root elongation at a low soil water potential may occur despite a (transient) decline in turgor of the root cells. This suggests that the yielding capacity of the elongating cells has increased due to an increase in the **amount** and **activity** of **expansins** in the root tip of plants grown at low soil water potential and an increase in the sensitivity of the cell wall to expansins (Le Gall et al. 2015).

Although it is tempting to think that the reduction in leaf expansion is due to a loss in turgor of the leaf cells, such a turgor loss usually does not occur, and the reduction in leaf growth is due primarily to leaf cell-wall stiffening (Van Volkenburgh and Boyer 1985). In *Zea mays* (maize), salt stress impairs epidermal wall-loosening in leaves (Zörb et al. 2015). The shoot responses occur in response to (**chemical**) **signals** arriving from the roots in contact with drying soil (Davies and Zhang 1991). How do we know that chemical signals play a role? We explore this in the next Section.

10.5.3.1 Do Roots Sense Dry Soil and Then Send Signals to the Leaves?

To answer the question about root signals, Passioura (1988) used a pressure vessel placed around the roots of a *Triticum aestivum* (wheat) seedling growing in drying soil. As the soil dries, the hydrostatic pressure in the vessel is increased to maintain shoot water relations similar to those of well-watered plants. The treated wheat plants show reductions in leaf growth similar to those of plants in drying soil without a pressure chamber. Additional evidence comes from experiments with small apple trees (*Malus* x *domestica*) with their roots growing in two separate containers, one with moist and one with dry soil. Soil drying in one container restricts leaf expansion and initiation, but the roots in the moist soil continue to maintain shoot water relations similar to those of control plants. Leaf growth recovers upon severing the roots in contact with the drying soil (Gowing et al. 1990). We must therefore attribute these effects on leaves of wheat seedlings and apple trees to effects of soil drying that do not require a change in shoot water status.

As with effects of soil drying on stomatal conductance (Sect. 2.5.1 and Sect. 5.5.4.1), **hydraulic** and **electric signals**, in addition to **chemical messengers** from the roots, possibly play a role in effects of drying soils on leaf growth (Dodd 2005). Thus, there are multiple signal-transduction pathways by which water shortage reduces plant growth.

10.5.3.2 ABA and Leaf Cell-Wall Stiffening

The effect of water stress on leaf elongation is mediated by the phytohormone abscisic acid

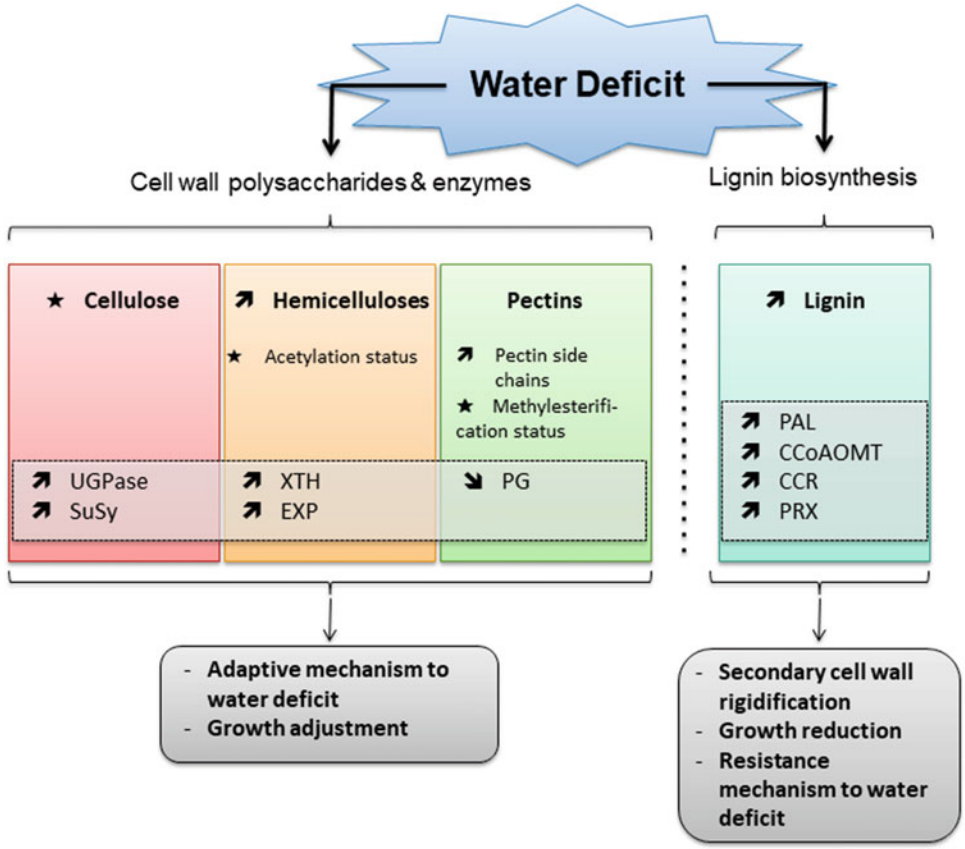

Fig. 10.13 Diagram summarizing the plant cell wall response to water deficit. Upward arrow means increased abundance and downward arrow means decreased abundance of the molecules. Star means contrasting data on the gene/protein or the molecule studied according to the literature. Cell wall (CW); xyloglucan endo-β-transglucosylases/hydrolases (XET/XTH); expansin (EXP); sucrose synthase (SuSy); UDP-glucose pyrophosphorylase (UGPase); polygalacturonase (PG); pectin methylesterase (PME); phenylalanine ammonia-lyase (PAL); caffeoyl-CoA 3-O-methyl-transferase (CCoAOMT); cinnamoyl-CoA reductase (CCR); cell wall peroxidases (PRX) (Le Gall et al. 2015).

(**ABA**) (Dodd 2005). Soil drying and salinity enhance the concentration of this hormone in the leaves (Tardieu et al. 1992). The **pH of the xylem sap** also affects leaf elongation, and this effect is, again, mediated via ABA (Bacon et al. 1998). Species differ considerably in the dynamics of pH changes in xylem in drying soil. Changes in xylem sap pH during drying may be affected by sap flow rate (Gloser et al. 2016).

Aboveground plant parts respond more strongly to a decreased soil water potential than do roots. This is due to a greater **inhibition by ABA of leaf growth** than that of the roots (Saab et al. 1990), at least during the initial phase of imposed water stress. At a later stage, ABA acts to maintain leaf growth, albeit at a slower rate than in well-watered plants (Sharp 2002). When plants are exposed to water stress, leaves show higher endogenous ABA concentrations and reduced leaf growth. ABA most likely affects the growth of roots and leaves through its inhibitory effect on **ethylene** biosynthesis (Dodd 2005).

Salt-sensitive species respond more strongly, in terms of both increases in ABA level and decreases in leaf expansion, than do resistant species (He and Cramer 1996). ABA triggers

hardening of the leaf cell walls by increasing the yield threshold, *Y*, and decreasing wall extensibility, ϕ. In a salt-tolerant *Zea mays* (maize) hybrid, which maintains leaf growth under salinity, the epidermal cell wall is more extensible under salt stress. This is associated with a shift of the epidermal apoplastic pH to a range favorable for 'acid growth'. A more sensitive hybrid that displays reduced leaf growth has stiffer epidermal cell walls under salinity stress. This may be attributable to the reduced abundance of cell wall-loosening β-expansin proteins following a high salinity-treatment (Zörb et al. 2015). Salt stress impairs epidermal wall loosening in sensitive maize leaves which constrains their expansion. We discuss toxic effects of NaCl in Sect. 9.3.4.1.

10.5.3.3 Effects on Root Elongation

Roots that experience a moderate water stress may loosen their walls and increase their extension rate. **Wall loosening** is probably due to an increase in activity of **expansins** (Sect. 10.2.2.4; Cosgrove 2000, 2015). An increase in expansin proteins and wall-loosening capacity in the root apex in response to water stress is widespread, and, presumably, an adaptation to growth in drying soils that allows exploitation of a falling water table. The size of the root meristem is also reduced under water stress, so fewer root cells contribute to the elongation process (Sharp et al. 2004). As in leaves, osmotic stress has no effect on the **turgor** of *Zea mays* (maize) root cells; however, it increases the **concentration of osmotic solutes** to the extent that the difference in cell water potential and that of the root environment is restored (Pritchard et al. 1996).

Lowering the water potential around the roots also enhances sugar transport to the roots, probably due to the growth reduction of the leaves. Because water deficit affects photosynthesis less affected than it affects leaf growth, it may enhance sugar transport as well as root growth in both a relative and an absolute sense, at least in the early stages of water deficit stress. How does an increased concentration of sugars affect the growth of roots? This probably requires a sugar-sensing mechanism similar to that discussed for leaves where a specific system senses hexose levels and affects the repression of genes that encode photosynthetic enzymes (Sect. 2.4.3). Gene transcription in roots is indeed affected by sugar levels, as discussed for respiratory enzymes (Sect. 3.4.4), but the search continues for genes that affect root elongation. We are still far from understanding the entire signal-transduction pathway from elevated sugar levels in root cells to stimulation of root elongation. This is clearly a major challenge for molecular ecophysiologists.

10.5.3.4 A Model That Accounts for Effects of Water Stress on Biomass Allocation

Figure 10.14 summarizes effects of water stress on phytohormone production in the roots, leaf expansion, and root growth. Whatever the exact signal-transduction pathway, the overall effect of inhibition of leaf area expansion while root elongation is inhibited less, or even stimulated, is that the *LAR* decreases, and that the *RMR* increases in response to a decrease in soil water potential. The increased respiratory costs of such an increase in *RMR* may contribute to reduced growth of water-stressed plants; they also reduce the dry mass gain per unit of water lost in transpiration (Van den Boogaard et al. 1996).

10.5.4 Growth at a Limiting Nutrient Supply

Plants allocate relatively less biomass to leaves and more to their roots when N or P is in short supply (*e.g.*, Brouwer 1963). Like the response to water stress (Sect. 10.5.3), the response to nutrient shortage is also functional. In both situations, the investment in plant parts that acquire the limiting resource is favored, at the expense of allocation to plant parts that have a high requirement for the limiting resource. We find the opposite, and equally functional, response when plants are growing at a low irradiance (Sect. 10.5.1).

In this Section, we focus on the response to N shortage, because the effect of N shortage on biomass allocation is stronger than that of other nutrients, but P has similar effects. Leaves of

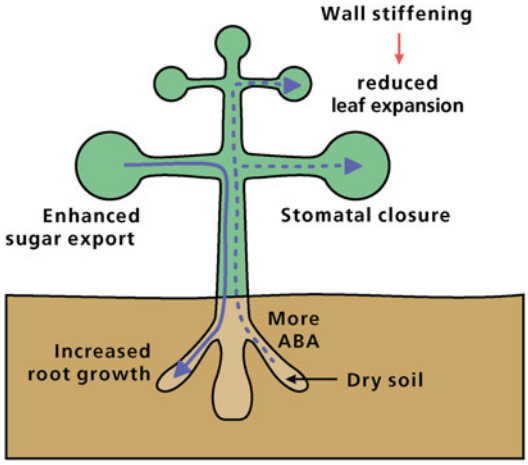

Fig. 10.14 Hypothetical model to account for the effects of water stress on plant growth and biomass allocation. Roots sensing dry soil enhance the production of abscisic acid (ABA), which they export to the xylem, and then ABA moves to the leaves. Here, it reduces stomatal conductance and wall extensibility of growing cells. The effects are a reduction in the rate of transpiration and photosynthesis as well as in leaf expansion. As long as photosynthesis is affected less than leaf expansion is, the export of assimilates to the roots is enhanced. The increased import of assimilates, in combination with ABA-enhanced wall loosening of growing root cell, enhances the rate of root growth.

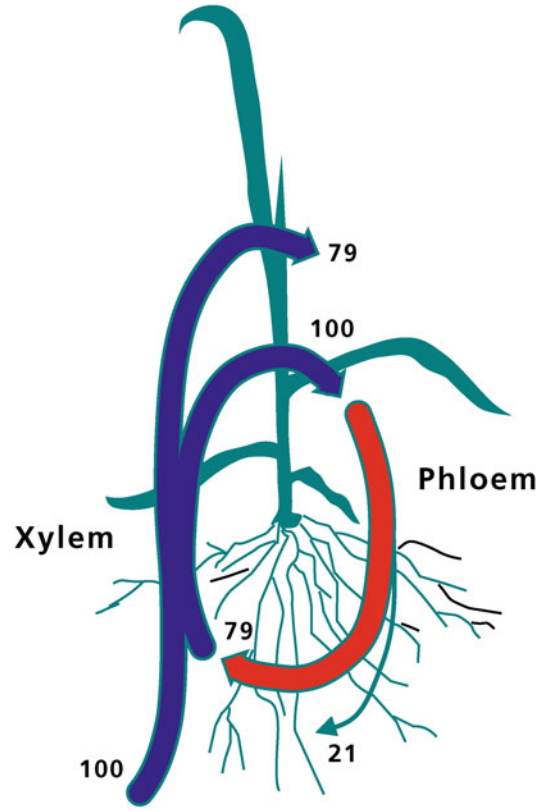

Fig. 10.15 'Cycling' of nitrogen (N) in a vegetative wheat plant (*Triticum aestivum*). Much of the N (NO_3^-, amino acids, and amides) that arrives in the leaves via the xylem is exported again in the phloem (amino acids and amides). Upon arrival in the roots, some of the N is used for root growth, whereas the remainder cycles back to the shoot (Simpson et al. 1982b); copyright Physiologia Plantarum.

plants grown with a limiting N supply are smaller, compared with those of plants grown with an optimum nutrient supply, predominantly due to an effect on **meristem size** and **cell number** (Fig. 10.2B; Terry 1970). How are the changes in biomass allocation pattern brought about?

10.5.4.1 Cycling of Nitrogen Between Roots and Leaves

NO_3^- can act as a signaling molecule that affects local root proliferation (Sect. 9.2.2.8), and also plays a signaling role in the control of biomass partitioning between roots and leaves (Scheible et al. 1997). Since plants respond to NH_4^+ supply in a similar way as they do to NO_3^-, additional signals must be involved. In vegetative plants, whether grown with an optimum or a limiting N supply, much of the N transported from the roots via the xylem to the leaves is exported back to the roots, as amino acids and amides, via the phloem (Fig. 10.15; Simpson et al. 1982b). Such a process of continuous **N cycling** between roots and leaves makes it highly unlikely that the transport of N to the leaves itself is a controlling factor. Rather, we should search for signals, in addition to NO_3^-, that change concomitantly with the N supply.

10.5.4.2 Hormonal Signals That Travel via the Xylem to the Leaves

The response of plants to a low N or P supply is akin to that to a limiting supply of water: reduced leaf growth, while root growth is maintained or enhanced. This response is generally described in terms of a **functional equilibrium** between

leaves and roots (Brouwer 1962, 1963). That is, when resources that are acquired by the roots are in short supply, the growth of the roots is favored over that of the leaves so that the *RMR* is increased. Transgenics that have a very low nitrate reductase activity (1–5% of wild-type levels) also exhibit an increased *RMR* when NO_3^- is in short supply which shows that **NO_3^-** itself, rather than a product of its assimilation, is the primary signal that induces this response (Scheible et al. 1997). We have encountered a similar **signaling role of NO_3^-** in the proliferation of roots in response to a local NO_3^- supply (Sect. 9.2.2.8), but know less about the signaling pathways in plants from environments with low nitrification potential. It is interesting that N deficiency reduces the roots' **hydraulic conductivity**; it is very likely that this is controlled by a decreased expression or activity of **aquaporins**, water-channel proteins involved in water uptake by the roots (Sect. 5.5.2; Clarkson et al. 2000). The rapid decline (within hours) in leaf growth of *Zea mays* (maize) upon transfer to a low-nutrient solution is associated with a decreased extensibility of the cell walls of expanding leaf cells. Transfer to high-nutrient conditions enhances this extensibility.

Contrary to what we discussed for plants exposed to water stress, there is no evidence that ABA plays a role as a signal between roots and leaves of plants exposed to a nutrient supply that is limiting to plant growth. Rather, a reduced nutrient supply to the roots reduces the synthesis of **cytokinins** in the root tips and their subsequent export to the leaves (Fetene and Beck 1993). Due to the lower cytokinin import into leaves of plants grown with a limiting N supply, growth of the leaves is reduced (Simpson et al. 1982a). Cytokinins affect the growth of leaves and roots in an opposite manner (Sect. 10.2.2.2); root growth is either stimulated or unaffected by a low N supply (Kudo et al. 2010).

In plants grown with a limiting supply of nutrients, the level of cytokinins can be maintained by the addition of benzyladenine, a synthetic **cytokinin**, to the roots (Table 10.5). This maintains the *RGR* of the leaves of plants transferred to a low nutrient supply at a rate close to that in plants grown with a full nutrient supply; this effect can only last for a few days, after which the plants run out of N. On the other hand, addition of benzyladenine reduces the root growth to the level of plants well supplied with nutrients.

What kind of effects do cytokinins have on leaf metabolism? First, cytokinins promote the synthesis of several proteins that are involved in photosynthesis. **Cytokinins** also have a specific effect on a gene encoding a protein involved in the cell cycle, and promote cell division and cell expansion (Sect. 10.2.2.2). To put it simply, cytokinins promote **leaf cell division** and **leaf cell expansion**, increase the **photosynthetic capacity**, **delay leaf senescence**, and enhance **leaf expansion**. Thus, as with water and temperature, nutrient supply governs growth through hormonal signals (**feedforward control**), rather than through a direct effect on the availability of substrates for protein synthesis (source control). The hormonal signals that regulate growth in response to nutrient shortage (cytokinins), however, differ from those associated with water and salinity stress (ABA) and light shortage (phytochrome-induced changes in gibberellins).

Table 10.5 Cytokinin (zeatin) concentrations (pmol g^{-1} FM) and the relative growth rate (*RGR*, mg g^{-1} day^{-1}) of *Plantago major* (common plantain) plants, exposed to a full-strength nutrient solution, or transferred to a diluted solution, plus or minus 10^{-8} M benzyladenine (BA), a synthetic cytokinin.

	Cytokinin concentration		Growth (*RGR*)	
Treatment	Shoot	Roots	Shoot	Roots
Full nutrients	110	160	220	160
Diluted solution				
without BA	25	23	150	180
with BA	100	140	190	160

Source: Kuiper and Staal (1987) and Kuiper et al. (1989)

10.5.4.3 Signals That Travel from the Leaves to the Roots

Leaves that experience a low import of nutrients probably send signals back to the roots, which accounts for their enhanced growth. These signals are associated with the amount of **carbohydrates** exported via the phloem. When the low nutrient supply reduces leaf growth, products of photosynthesis accumulate. These affect **sugar-sensing** (Sect. 2.4.3). The increased level of carbohydrates in the leaves implies that more photosynthates are available for translocation to the roots. There, sugars affect sugar-sensing mechanisms. Rather than suppressing genes, as in leaves, sugars derepress genes encoding respiratory enzymes (Sect. 3.4.4) and others (Yan et al. 2011).

10.5.4.4 Integrating Signals from the Leaves and the Roots

The results presented in Sect. 10.5.4.2 lead to the model depicted in Fig. 10.16. An early response to a decline in N supply is a decrease in synthesis and export of **cytokinins**. This reduces the rate of protein synthesis, cell division, and expansion in the growing leaves. Carbohydrates accumulate, leading to downregulation of photosynthesis, but plenty of carbohydrates are available for export to the roots. In the roots, they derepress genes that encode respiratory and possibly other enzymes. The roots either grow at the same rate as those of control plants, or their growth may be increased.

The relative increase in biomass allocation to roots with N shortage is largely accounted for by a decrease in production of **cytokinins** in the roots. This phytohormone then sets the change in biomass partitioning in motion which leads to a new **functional equilibrium** between roots and leaves. Roots appear to have very little *direct* control over the rate of carbon import from the leaves. They do exert *indirect* control, however, via their effect on leaf growth, which depends on the supply of cytokinins from the roots.

10.5.4.5 Effects of Nitrogen Supply on Leaf Anatomy and Chemistry

In a comparison of four congeneric grass species [*Poa annua* (annua meadow-grass), *Poa trivialis* (rough bluegrass), *Poa compressa* (Canada bluegrass) and *Poa pratensis* (Kentucky blue grass)]

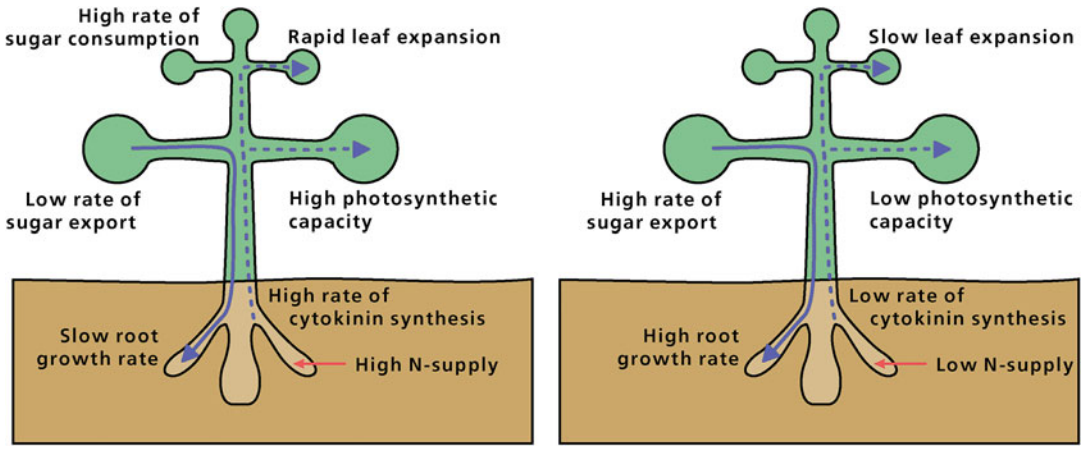

Fig. 10.16 A model to account for the effects of nitrogen (N) supply on plant growth and biomass allocation. (Left) Roots sensing a high N availability produce large amounts of cytokinins, which they export via the xylem to the leaves. Here the cytokinins enhance the photosynthetic capacity and leaf expansion. Hence, a large fraction of the photosynthates is consumed in the leaves, and a relatively small fraction is available for export to the roots. (Right) Roots sensing a low N availability produce only small amounts of cytokinins. The import of cytokinins into leaves is small, so that their photosynthetic capacity and rate of leaf expansion is reduced. Only a small fraction of the photosynthates is consumed in the leaves, so that the concentration of sugars in the leaves is high, and a relatively large fraction is available for export to the roots. The high level of sugars in leaves suppresses genes encoding photosynthetic enzymes. In roots, high sugar levels induce genes encoding respiratory and other enzymes.

grown at both an optimum and a limiting N supply, *RGR* and N concentrations decrease at low N supply (Van Arendonk et al. 1997). The decrease in *RGR* is accounted for by a decrease in ***LAR***, especially in the fastest-growing *Poa annua*. Nitrogen shortage invariably enhances the proportion of leaf biomass that is occupied by **sclerenchymatic cells**, from about 0.5 to 6%, predominantly due to an increase in number of these cells. The area occupied by **vein tissue** doubles, from approximately 4.5 to 9%, whereas that occupied by epidermal cells is constant (25%), despite a substantial decrease in **size of the epidermal cells**, especially in *Poa annua*. Mesophyll + intercellular spaces occupy a variable area of about 60% in all species and treatments. Nitrogen stress decreases the concentration of protein and enhances that of (hemi) cellulose and lignin. The anatomical changes are probably ecologically important, in that the increase in sclerenchymatic and vein tissue give better protection of leaves from herbivores and desiccation (Lambers and Poorter 1992).

Nitrogen shortage also has a major effect on allocation to nonstructural secondary metabolites such as **lignin and tannins** (Sect. 13.4.1). Because these compounds slow down the rate of litter decomposition, this response aggravates the N shortage in the environment (Sects 18.2 and 18.3).

10.5.4.6 Nitrogen Allocation to Different Leaves, as Dependent on Incident Irradiance

Different leaves of a plant may differ widely with respect to their N concentration, partly due to **N withdrawal** from older, senescing leaves (Sect. 10.4). Leaves also adjust their N concentration to the **level of incident irradiance**; leaves at the top of the canopy that are exposed to full sunlight have higher N concentrations per unit leaf area than leaves near the ground surface, where they are shaded by leaves higher in the canopy (Hirose and Werger 1987a).

Most of the leaf N is associated with the photosynthetic apparatus (Sect. 2.3.2.3). Because light intensity is higher for the top leaves than for the bottom ones, the observed **gradient in leaf N concentration** enables plants to optimize their use of N to fix carbon (Hirose and Werger 1987b; Field 1991; Pons 2016). Models assess the significance of a gradient in leaf N concentration, as opposed to a uniform distribution (Box 8.1).

What might be the physiological mechanism to achieve a N gradient that tends to follow the gradient of irradiance in the canopy? Leaves exposed to higher levels of irradiance, high in the canopy, will have faster rates of transpiration than shaded ones lower in the canopy. This occurs partly because stomata respond to the level of irradiance (Sect. 5.5.4.4), partly because of the greater vapor pressure difference between leaf and air higher in the canopy, and possibly also because the temperature of the top leaves is higher which increases the partial pressure of water vapor inside the leaf. The faster rate of transpiration causes a greater influx of solutes imported via the xylem, including amino acids and root-produced phytohormones. The greater N influx is probably not the immediate cause of enhanced incorporation of N into the photosynthetic apparatus, because far more N is imported via the xylem into leaves than is required for biosynthesis (Fig. 10.15). Other xylem-transported compounds likely control the differential incorporation of N into the leaves. **Cytokinins** are transported in greater amounts to rapidly transpiring leaves that are exposed to high levels of irradiance, compared with slowly transpiring leaves that are lower in the canopy. In the top leaves, the greater inflow of cytokinins enhances the net incorporation of N into the photosynthetic apparatus (Sect. 10.5.4.4, Fig. 10.17; Pons 2016). Other factors may play an additional role, especially in trees where leaves in the outer canopy may have an extra layer of palisade parenchyma (Sect. 2.3.2.2), which may be programmed well before the leaf has developed and begins to transpire (Sect. 10.5.1.1.1).

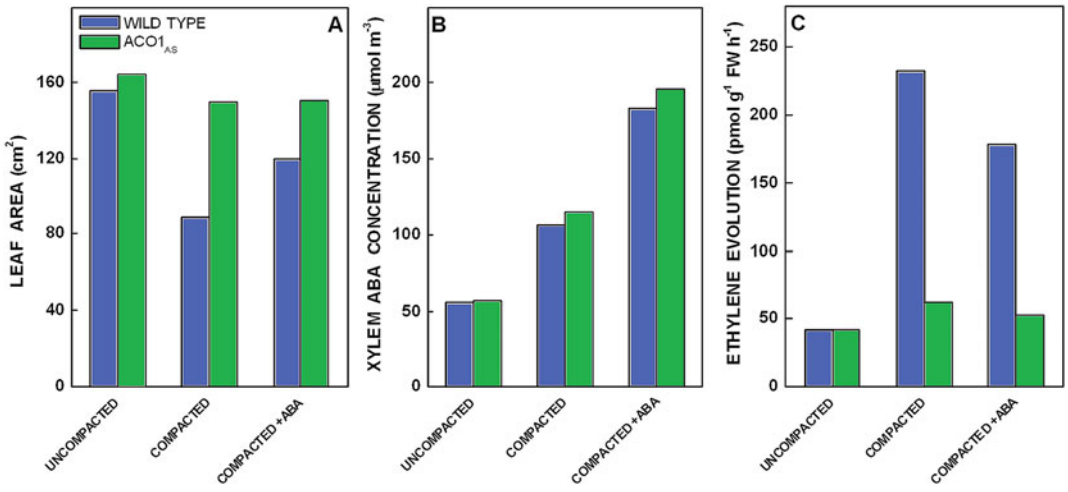

Fig. 10.17 Effects of soil compaction on leaf growth, xylem abscisic acid (ABA) concentration, and ethylene production in wild-type and a transgenic with a low capacity to produce ethylene of *Solanum lycopersicum* (tomato). (**A**) Total leaf area; (**B**) xylem sap ABA concentration; (**C**) leaf ethylene evolution at 21 days after emergence. Plants were well watered and grown in a split-pot system in which either both compartments contained uncompacted soil or one compartment contained uncompacted soil and the other compacted soil. The compartment containing compacted soil was supplied either with water or with 100 nM ABA (compacted +ABA) twice daily from day 5 (after Hussain et al. 2000). © John Wiley & Sons Ltd.

The mechanism depicted in Fig. 10.17 leads us to the following question: to what extent does the plant achieve its N allocation to different leaves so as to maximize its rate of photosynthesis? To answer this question, ecophysiological experiments have to be combined with a modeling approach. To assess whether plants optimize the allocation of N to the different leaves, we need to know (1) the gradient of light within the canopy, (2) the relationship between photosynthesis and the level of irradiance, and (3) the relationship between photosynthesis and leaf N concentration. The optimal pattern of N distribution is the one that maximizes the rate of photosynthesis of the entire plant (Box 8.1). We can summarize the outcome as follows. Plants may not quite achieve the pattern of N allocation to their leaves that would yield the fastest possible rate of canopy photosynthesis, but monocotyledons and dicotyledons, and both C_3 and C_4 plants, have an N allocation pattern that approaches the optimal pattern. In this way, the plants have a faster rate of canopy photosynthesis than could have been achieved with a uniform N allocation pattern (Anten et al. 1995; Anten and Poorter 2009).

10.5.5 Plant Growth as Affected by Soil Compaction

Soil structure affects plant performance in many ways, both reducing leaf growth and changing root morphology. Roots are smooth and cylindrical in friable soil, but they become **stubby** and **gnarled** with soil compaction and explore less soil, with potentially deleterious effects on the supply of water and nutrients (Bengough et al. 2006).

10.5.5.1 Effects on Biomass Allocation: Is ABA Involved?

Plants that grow in compacted soil have a **reduced *LMR***, even in the presence of adequate nutrients and water. Soil compaction tends to enhance the concentration of ABA in the xylem sap (Sharp 2002). ABA is probably responsible for a reduced stomatal conductance, but is it also the cause of the reduction in leaf growth, as it is under water stress? This is unlikely, because ABA-deficient mutants of both *Solanum lycopersicum* (tomato) and *Zea mays* (maize) show exactly the same response to soil

Table 10.6 Effects of root confinement on yield and physiology of 14-day-old *Helianthus annuus* (sunflower) plants*.

	Fresh mass (mg)						
Treatment	Shoot	Root	*RMR*	Transpiration (mm day^{-1})	K^+ transport (pmol g^{-1} s^{-1}	Plant water potential (MPa)	[ABA] in xylem (nM)
Control	163	9.5	0.055	0.054	97	−0.51	10
Confined	112	7.3	0.061	0.053	136	−0.51	70

Source: Ternesi et al. (1994)

*The root mass ratio (*RMR*) is the root fresh mass as a fraction of total plant mass; K^+ transport (expressed per unit root fresh mass) was calculated from the concentration of K^+ in the xylem exudate and the rate of exudation). Plants were grown in such a way as to ensure that water and nutrients were supplied at an optimum level

compaction as the wild-type plants (Munns and Cramer 1996).

Hussain et al. (2000) compared a wild-type tomato (*Solanum lycopersicum*), an ABA-deficient mutant, and a transgenic genotype with a reduced capacity to produce **ethylene**. They grew their plants in pots with soil that was noncompacted, compacted, or layered in such a way that the plants first encountered noncompacted and then compacted soil. The wild-type and the transgenic with a low capacity to produce ethylene show a similar increase in ABA concentration in the xylem sap. Because the leaf area expansion of the wild-type tomatoes is reduced more than that of the transgenics, ABA can be dismissed as the root-produced signal that affects leaf growth in compacted soil. Leaf expansion is invariably less in the ABA-deficient mutant. Reductions in leaf area expansion in wild-type and ABA-deficient mutants are associated with increased ethylene production. Application of ABA enhances the leaf expansion of the ABA-deficient mutant, and to a lesser extent that in the wild-type. These results suggest that antagonistic interactions between ABA and ethylene regulate leaf expansion in tomato when the roots simultaneously encounter uncompacted and compacted soil (Fig. 10.17).

The responses of plants that grow in compacted soil are similar to those of plants that are **pot-bound** (*i.e.* grown in pots that are too small for their roots). The roots somehow sense the walls of the pots to be 'impenetrable soil'. Leaf area expansion is reduced, even when sufficient water and nutrients are provided. The xylem sap of pot-bound sunflower (*Helianthus annuus*) plants contains far more ABA than does the sap of control plants (Table 10.6), but in bean (*Phaseolus vulgaris*) no such effect is observed (Munns and Cramer 1996). We might also expect these responses in plants that encounter rocks or a hardpan, but root growth of *Hakea* species adapted to ironstone habitats and a Mediterranean climate in Western Australia, typically do not show inhibition of root growth when reaching the hard surface. Instead, they continue growth and thus maximize chances to reach cracks in the rocks which is essential for survival in their natural habitat (Poot and Lambers 2003, 2008).

10.5.5.2 Changes in Root Length and Diameter: A Modification of the Lockhart Equation

Mechanical resistance (impedance) of the soil can be an important factor that limits root growth in cropping as well as natural systems (Hamza and Anderson 2005). The resulting increase in the rate of **ethylene** production is the most likely cause for the observed reduction in root elongation and an increase in root diameter and (sometimes) number of cortical cells (Harpham et al. 1991). There is also a change in the branching pattern. When ethylene production is inhibited, however, soil compaction still induces the same root morphology. The effects of soil compaction on root morphology may therefore also be accounted for by physical effects.

For roots to be able to elongate, the mechanical impedance of the soil matrix acting against the cross-section of the root tip must be less than the pressure exerted by the root itself. To expand on

Eq. 10.10 (Sect. 10.2.2), the proportional root elongation (r) is the result of cell expansion, which is related to the cell-wall yield coefficient (ϕ, $MPa^{-1}\ s^{-1}$), the turgor pressure (Ψ_p, Pa), the **yield threshold of the root** (Ψ_r, MPa), and the **yield threshold of the soil** (Ψ_s, MPa) (Pritchard, 1994):

$$r = \phi(\Psi_P\text{-}Y_r - Y_s) \qquad (10.10)$$

Maximum axial and radial root growth pressures range from 0.24 to 1.45 and from 0.51 to 0.90 MPa, respectively, and vary with plant species. Because it is impractical to measure the mechanical impedance of the soil directly by using actively growing roots, we use a **penetrometer** that measures the pressure required to force a steel probe, with a 60 or 30° conical tip (*i.e.* 30 or 15° semiangle), into the soil (Fig. 10.18).

Root elongation is primarily determined by the rate at which files of cells are produced and by the cell-elongation rate in the apex. Root elongation and total root length are reduced by mechanical impedance, due to inhibition of cell elongation. Root **exudates** ease soil compression and improve the mechanical resilience of compacted soils, possibly having a large positive impact on rhizosphere physical conditions (Fig. 10.19; Oleghe et al. 2017). Future research with model root exudates that vary in chemistry, and plants with contrasting exudation properties may identify favorable exudate characteristics that improve the capacity of roots to restructure degraded soils. Such understanding would benefit practical applications in crop breeding to improve the capacity of roots to grow through and restructure soils (Oleghe et al. 2017).

The root diameter of plants growing in compacted soil commonly increases, because of radial cell expansion of cortical cells (Fig. 10.20; Alameda and Villar 2012) and the solute concentration of the root cells is enhanced (Atwell 1989). Thicker and more rigid roots, which result from radial root expansion, are thought to exert higher pressure on the surrounding soil and deform the soil ahead of the root which facilitates subsequent penetration (Pritchard 1994). Turgor measurements show **turgor pressures** of 0.78 MPa in impeded root tips of *Pisum sativum*

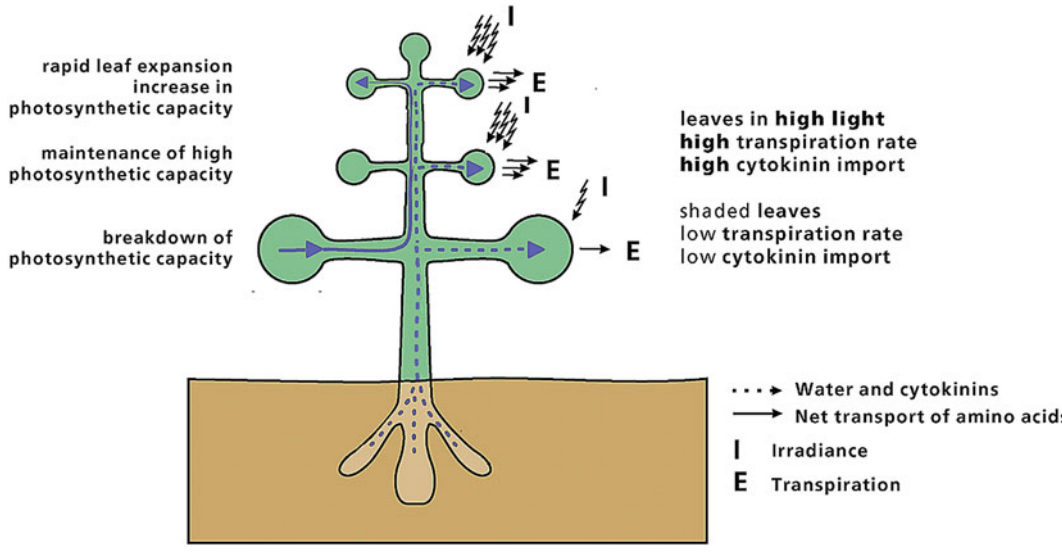

Fig. 10.18 A hypothetical model to account for the differential allocation of nitrogen (N) to leaves exposed to high or low levels of irradiance. Cytokinins are imported in greater amounts by rapidly transpiring leaves high in the canopy than by leaves lower in the canopy which have slower rates of transpiration. Cytokinins then promote N incorporation into the photosynthetic apparatus. In the absence of a large inflow of cytokinins, much of the nitrogenous compounds imported via the xylem are exported again via the phloem. Based on information in Pons and Bergkotte (1996).

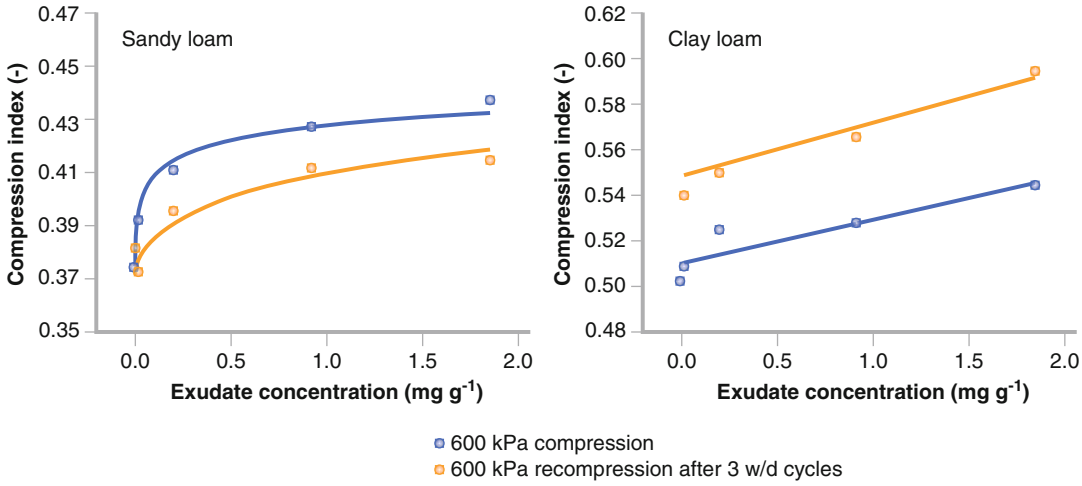

Fig. 10.19 Compression index at −50 kPa matric potential plotted as a function of exudate concentration for sandy loam and clay loam soils for (i) 200 kPa loading, (ii) 600 kPa loading and (iii) 600 kPa loading with wetting and drying (w/d) cycles. The compression index measures soil mechanical resistance to compression, with larger values indicating less resistance of soil to compression (Oleghe et al. 2017). © The Authors 2017.

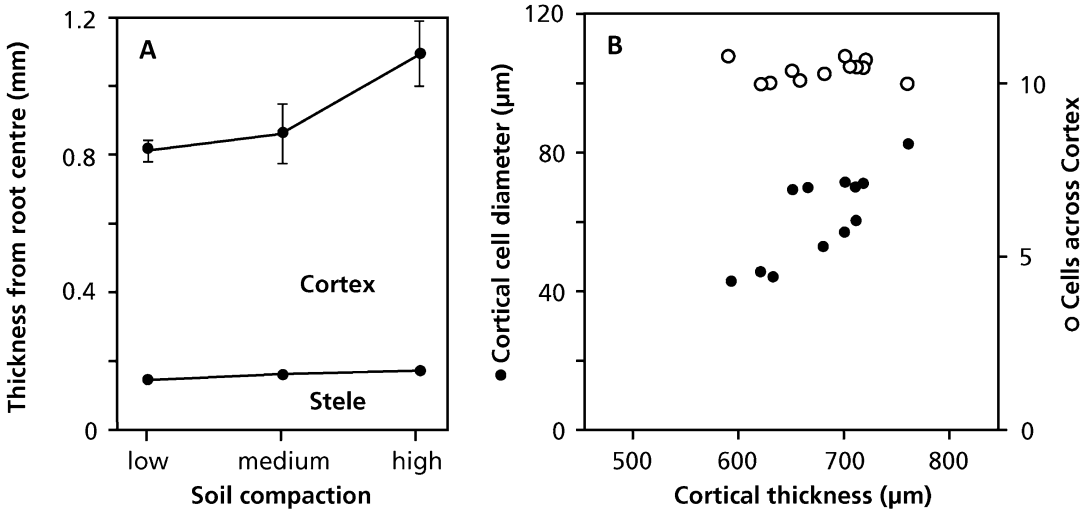

Fig. 10.20 The radius of the stele and cortex in roots of *Lupinus angustifolius* (narrow-leaved lupin), (**A**) grown at three levels of soil compaction, and (**B**) the diameter and number of cortical cells and mean cortical cell diameter of the same plants. Increasing cortical thickness on the abscissa in the right-hand figure is the result of increased soil compaction, as illustrated in the left-hand figure (Atwell 1989).

(pea), as compared with 0.55 MPa in unimpeded root tip cells (Clark et al. 1996).

A smaller root system under conditions of soil compaction will be detrimental for the uptake of nutrients and water, and hence reduce the plant's growth rate and productivity. There are also effects on leaf expansion, however, that are not accounted for by the plant's water or nutrient status. Roots perceive soil compaction as such, and they send inhibitory signals to the leaves which cause a **feedforward response** (Stirzaker et al. 1996). Species may differ in their capacity to

grow in compacted soil, depending on the type of exudates they release (Oleghe et al. 2017). They may also differ in their capacity to find less compacted sites in the same soil (Sect. 10.5.5.1) or in the size of their root system and hence in the extent to which they explore the soil, including the compacted part (Materechera et al. 1993).

10.5.6 Growth as Affected by Soil Flooding

Flooding or inundation of the soil leads to filling with water of the soil pores that are normally filled with air. This reduces the supply of soil O_2 and restricts aerobic respiration (Sect. 3.4.1). Flooding also affects the roots' hormone metabolism. Concentrations of **ethylene** in the roots increase, largely because this gas diffuses more slowly in a flooded soil than it does in a well-aerated soil, so that it gets trapped in the roots, and partly because of an enhanced production of this hormone (Colmer 2003).

10.5.6.1 The Pivotal Role of Ethylene

Ethylene inhibits root elongation and induces the formation of **aerenchyma** in roots (Fig. 10.21). **Lysigenous aerenchyma** formation, which involves death and dissolution of cortical cells, is preceded by enhanced transcription of a gene that encodes a **xyloglucan endotransglycosylase**, an enzyme involved in the **lysis** of some **cortical cells** (Saab and Sachs 1996; Leite et al. 2017): **programmed cell death**. The ethylene-induced aerenchyma facilitates **gas diffusion** between roots and aerial parts (Sect. 3.4.1.4), because the large cross-sectional area of gas space reduces the physical resistance to gas movement. Many hydrophytes such as *Oryza sativa* (rice) possess extensive aerenchyma even when growing in well-drained conditions (Colmer et al. 2014). In mesophytes such as *Zea mays* (maize) and *Helianthus annuus* (sunflower), however, cortical aerenchyma formation by cell

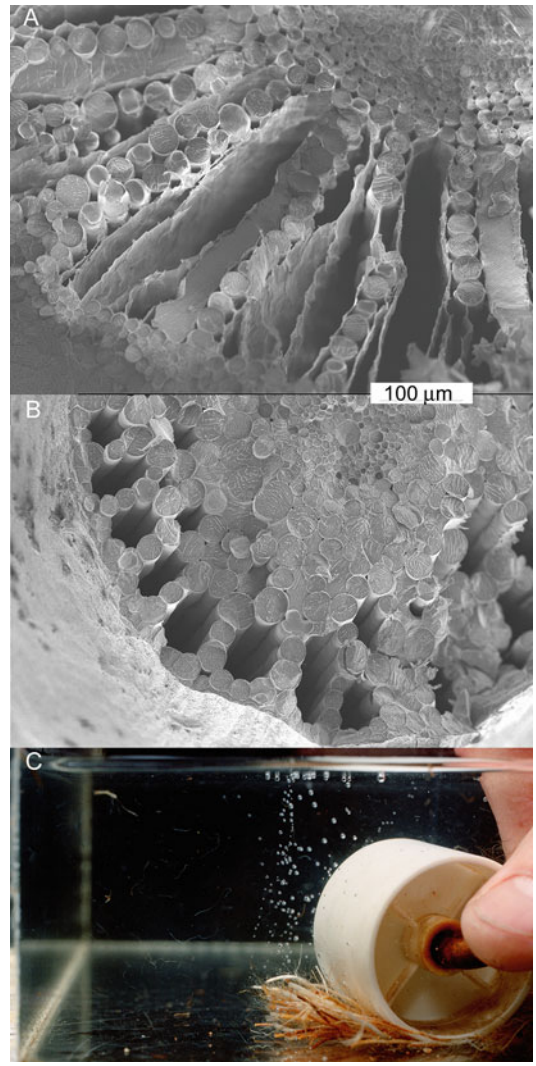

Fig. 10.21 Aerenchyma in roots. Scanning electron micrograph of (**A**) constitutive, lysigenous aerenchyma of *Juncus effusus* (soft rush), and (**B**) constitutive, schyzogenous aerenchyma of *Rumex palustris* (marsh dock). The horizontal bars indicate a length of 100 µm (courtesy L. Mommer, Radboud University Nijmegen, the Netherlands). (**C**) Bubbles coming from cut ends of roots squeezed gently with a roller under water provide evidence of air-filled aerenchyma in roots of *Oryza sativa* (rice). The rice plants were grown in waterlogged soil (courtesy T. L. Setter, Department of Primary Industries and Regional Development Western Australia, Perth, Australia; Setter, T.L. & Belford, B. (1990). Waterlogging: how it reduces plant growth and how plants can overcome its effects. *W. A. J. Agric.* **31**: 51–55).

breakdown is minimal in well-aerated conditions, and promoted by poor aeration (Colmer 2003). In maize, **phosphorus deficiency** also induces **cortical lysis** (Konings and Verschuren 1980; Postma and Lynch 2011).

Ethylene increases the **elongation of the coleoptile** in seedlings of *Oryza sativa* (rice), and, at later growth stages, stem internodes, so that shoots reach the surface of the water more rapidly. In the flood plains of Bangladesh, internodal growth rates of *Orya sativa* (rice) ecotypes of ('deepwater rice') may be up to 25 cm day^{-1}. Submergence induces accumulation of mRNA that encodes **expansins**, before the rate of growth starts to increase (Cho and Kende 1997b; Colmer et al. 2014). The 'snorkeling' response is characteristic of most flood-tolerant species in environments with prolonged flooding. A similar response occurs in petioles and lamina in the flood-tolerant *Rumex palustris* (marsh dock) during submergence of entire plants. The flood-sensitive *Rumex acetosa* (sorrel), on the other hand, responds to flooding with enhanced ethylene concentrations in the shoot, but not with enhanced elongation rates (Peeters et al. 2002). This indicates that it is the greater **responsiveness to ethylene**, and not the enhanced ethylene production, that increases petiole elongation in the flood-tolerant *Rumex* species. The interaction of three hormones (ethylene, ABA, and GA) determines the growth rate of the shoot. In the case of 'deepwater rice', ethylene renders the internode more responsive to GA by lowering the level of endogenous ABA. GA is the immediate growth-promoting hormone, and acts by enhancing cell elongation, and, probably indirectly, by increasing cell-division activity in the intercalary meristem. internodes of deepwater rice, which contain two **expansins** that may mediate acid-induced wall extension (Cho and Kende 1997a).

Transient complete submergence reduces survival and yield on more than 20 million ha of rice in rainfed lowlands and flood-prone areas in Asia. Some *Oryza sativa* (rice) landraces can withstand over two weeks of complete submergence (Ismail et al. 2013). The gene *SUB1* controls most of the tolerance phenotype, and this gene has been transferred into numerous varieties, recently released for commercial use in Asia. Varieties carrying the *SUB1* gene have the same agronomic, yield and quality traits as their nonSub1 counterparts when grown under non-flooded conditions, but show significant yield advantages after complete submergence in flooded fields. Sub1 varieties have been spreading fast in several countries, and are currently grown by more than four million farmers in Asia (Ismail et al. 2013). This success is attributed to several factors, including the choice of varieties that are popular among rainfed lowland farmers for deploying *SUB1* and its consistent effectiveness in different genetic backgrounds and environments (Dar et al. 2018).

10.5.6.2 Effects on Ion and Water Uptake and on Leaf Growth

Oxygen deficiency during soil waterlogging inhibits respiration in roots, resulting in severe energy deficits (Sect. 3.4.11). Decreased root-to-shoot ratio and suboptimal functioning of the roots result in nutrient deficiencies in the shoots. Stelar hypoxia–anoxia can develop, so that the activity of H^+-ATPases in the xylem parenchyma declines; diminished H^+ gradients and depolarized membranes reduce secondary energy-dependent ion transport (Greenway and Colmer 2010).

The responses of leaf growth and metabolism to soil inundation are similar to those of water-stressed plants. Flooding delays the normal daily increase in root **hydraulic conductance** in flooding-sensitive *Solanum lycopersicum* (tomato) plants (Else et al. 1995). This is probably due to **cytosolic acidosis** and the inhibitory effect of a low pH on **aquaporins** (Sect. 5.5.2). **Stomatal conductance** declines, and the rate of **leaf elongation** is reduced (Fig. 10.22). If the lower hydraulic conductance is compensated by pressurizing the roots (Sect. 10.5.3), however, both the stomatal conductance and the rate of leaf expansion remain low. As in plants exposed to water shortage (Sect. 10.5.3.1), **chemical signals** are responsible for the early responses to flooding in sensitive plants. **ABA** is one of the chemical signals arriving from the roots that

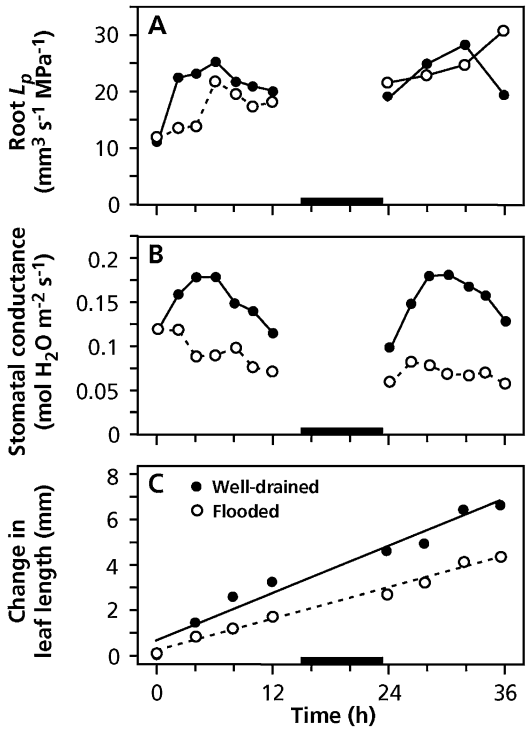

Fig. 10.22 Effects of soil flooding for 24 to 36 h on (**A**) root hydraulic conductance, (**B**) stomatal conductance, and (**C**) leaf elongation of *Solanum lycopersicum* (tomato) (After Else et al. 1995); copyright American Society of Plant Biologists.

cause stomatal closure (Else et al. 1995). Exposure of roots to hypoxia also reduces leaf **cell-wall extensibility**, and it is paralleled by a decreased capacity to **acidify leaf cell walls** (Van Volkenburgh 1994).

10.5.6.3 Effects on Adventitious Root Formation

When the effects of soil flooding become too severe, plants with some degree of flooding tolerance make new, aerenchymatous adventitious roots with air channels to the shoot that permit O_2 diffusion to the new roots (Colmer 2003). Endogenous **auxin** is the phytohormone that is generally responsible for adventitious root formation, even in flooding-sensitive plants. Auxin accumulates at the base of the shoot, possibly due to inhibition of the energy-dependent transport of auxin to the roots. In the flood-tolerant

Table 10.7 The effect of exposure to hypoxia and treatment with auxin, ethylene or a combination of ethylene and an inhibitor of auxin transport on the formation of adventitious roots in the flooding-tolerant *Rumex palustris* (marsh dock).

Treatment	Number of adventitious roots
Aerobic control	4
Anaerobic control	43
Auxin	45
Ethylene	44
Ethylene + inhibitor	8

Source: Visser et al. (1996)

Rumex palustris (marsh dock) both **ethylene** and **auxin** enhance the formation of new adventitious roots (Table 10.7).

10.5.6.4 Effects on Radial Oxygen loss

Aerenchyma provides a low-resistance internal pathway for the exchange of gases between the atmosphere and the submerged plant parts. Respiration of tissues along the pathway in aerenchymatous roots decreases the amount of O_2 that is available for the growing root apex, eventually restricting the maximum length of these roots in an O_2-free environment. A potentially greater sink for O_2 along the pathway is the **radial loss of O_2** to the soil. Many wetland species prevent excessive O_2 loss from the basal root zones by forming a complete or partial **barrier to radial O_2 loss** (Armstrong 1971; Colmer et al. 2014). Radial O_2 loss tends to be less in species that are adapted to waterlogging than in waterlogging-sensitive species. The barrier for radial O_2 loss may be constitutive [*e.g.*, in *Carex acuta* (slender tufted sedge), and *Juncus effusus* (common rush)] or inducible [*e.g.*, in *Caltha palustris* (marsh marigold), and *Oryza sativa* (rice)] (Visser et al. 2000).

10.5.7 Growth as Affected by Submergence

Flooding of terrestrial plants may also submerge aerial parts, restricting gas exchange not only of the roots, but also of the leaves. There are two alternative responses under different flooding regimes: (1) dormancy, characterized by

tolerance of the stress and reduced metabolic activity; (2) escape, due to shoot elongation, which establishes aerial contact. The **elongation response** requires energy expenditure, which is only 'paid back' when aerial contact is established. Under conditions of deep or short-lasting floods tolerance of **hypoxia** and reduced metabolic activity are favored (Voesenek and Bailey-Serres 2015).

Plants that escape **submergence** occur in habitats that experience prolonged submergence (*e.g.*, more than a few weeks), and where the water table rises gradually, but to a level that can be 'reached' by the growing shoots. This is the type of environment where Sub1 rice is ideally suited (Bailey-Serres et al. 2010). Plants with a rosette habit typically show hyponastic growth (upward curving) of petioles and leaves and increased extension of petioles (Fig. 10.23). When a stem is present, internodes elongate strongly upon submergence. The increased growth towards the surface re-establishes or maintains aerial contact that facilitates gas exchange and increases survival (Voesenek and Bailey-Serres 2015). Tolerance of the conditions after the water level drops is part of the **suite of traits** that allow survival in occasionally flooded areas. Protection against desiccation and damage, because of the sudden exposure to O_2 after a prolonged period of hypoxia, is an important aspect.

10.5.7.1 Gas Exchange

Net photosynthetic CO_2 uptake essentially stops upon submergence of terrestrial plants at the low ambient CO_2 concentrations in water. Only higher CO_2 concentrations allow net CO_2 assimilation (and thus net O_2 production). Terrestrial wetland plants generally lack the numerous beneficial leaf traits possessed by aquatic plants (Sect. 2.11), so submergence markedly reduces net

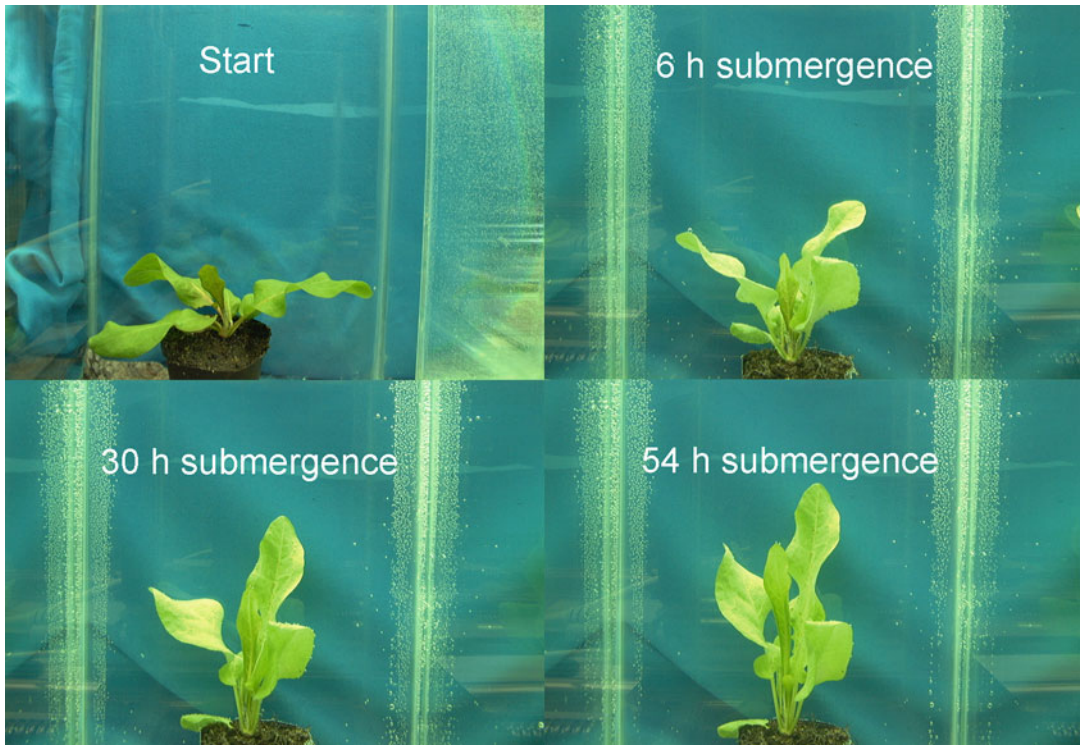

Fig. 10.23 Submergence-induced hyponastic growth and petiole elongation in *Rumex palustris* (marsh dock). At the start of the submergence treatment, plants were 28 days old. Plants were submerged up to 54 h (Voesenek et al. 2003). Courtesy M.C.H. Cox & L.A.C.J. Voesenek, Utrecht University, Utrecht, the Netherlands.

photosynthesis. Some terrestrial species, however, produce new leaves with a thinner cuticle and higher specific leaf area, whereas others have leaves with hydrophobic surfaces so that gas films are retained when submerged; both improve CO_2 entry (Colmer et al. 2011). Underwater photosynthesis provides both sugars and O_2 to submerged plants.

Although photosynthetic O_2 evolution may be restricted under low ambient CO_2 conditions, it can be substantial at elevated CO_2 concentrations in floodwater. Moreover, O_2 can diffuse into the leaf at sufficiently high concentrations (Mommer et al. 2004). Hence, provided the water is clear and gas concentrations are suitable, the internal O_2 allows aerobic respiration. Internal diffusion through aerenchyma to belowground parts can further improve O_2 conditions and contribute to long-term survival of submergence-tolerant plants.

10.5.7.2 Perception of Submergence and Regulation of Shoot Elongation

Ethylene accumulates under submergence conditions (Sect. 10.5.6). Normal internal concentrations are in the range of 0.02–0.05 μmol mol^{-1}, but they can increase to 1 μmol mol^{-1} within an hour after submergence (Bailey-Serres et al. 2012), and enhance further by increased ethylene production (Kende et al. 1998). Exposure of a responsive plant to a high ethylene concentration without submergence is sufficient to initiate shoot elongation. Reduced internal O_2 levels further promote the submergence-avoidance response and increased CO_2 concentrations contribute to the signal in deepwater rice (*Oryza sativa*). Ethylene also accumulates upon submergence in *Rumex acetosa* (sorrel), but this flood-intolerant species does not respond to submergence or high ethylene concentration with enhanced shoot elongation.

The first reaction of *Rumex palustris* (marsh dock) upon submergence is **hyponastic growth**, *i.e.* a more vertical orientation of the petiole and leaf blade (Fig. 10.23) which is a condition for further petiole extension. Ethylene-stimulated petiole and internode elongation in *Rumex palustris* and *Oryza sativa* (rice) depends on a reduced level of the inhibitor ABA relative to the stimulator of extension growth GA (Voesenek et al. 2006). The ABA:GA ratio quickly changes upon submergence by increased breakdown of ABA and *de novo* synthesis of GA. A further essential step is that cell-wall extensibility is enhanced by increased expression of specific **expansins** and **acidification** of the cell wall. These events downstream of the signal perception allow the rapid (within a few hours) onset of extension growth towards the water surface.

10.5.8 Growth as Affected by Touch and Wind

Some plants can 'move' when touched. Unless *Mimosa pudica* (touch-me-not) has just been assaulted by a classroom of schoolchildren, its petioles and pinnate leaves will respond to touch, due to the movement of ions in the pulvinus (Sect. 5.5.4.6). These movements in response to touch are *not* related to growth. The growth of some plant organs, however, does respond to touch (*e.g.*, the **tendrils** of climbing plants like *Clematis* or *Lathyrus*). Upon contact, these tendrils enhance their growth at the side away from the point of contact, sometimes in combination with a growth reduction at the side where contact occurred. Another response of tendrils to contact may be a strong reduction in the rate of elongation, as in *Cucumis sativus* (cucumber) (Ballaré et al. 1995). Susceptibility of plants to contact was already recognized by Theophrastus, around 300 BC, and by Darwin (1880), who described this phenomenon for the apex of the radicle of *Vicia faba* (broad bean). Since then, it has been shown that wind, vibrations, rain, and turbulent water flow affect a plant's physiology and morphology which is a phenomenon termed **thigmomorphogenesis** (Chehab et al. 2012). Wind exposure may make plants less susceptible to other forms of stress. Mechanical stimulation of young internodes of *Bryonia dioica* (red bryony) reduces their elongation and increases their radial expansion. This is associated with an acceleration of lignification and a transient increase in

ethylene production, preceded by a redistribution of Ca^{2+} within the cell and expression of specific proteins (Thonat et al. 1997). An extreme form of thigmomorphogenesis occurs in trees at high altitude, which show the typical '**Krumholz**' sculpture (*i.e.* a wind-induced deformation). Trees at the edge of a plantation or forest tend to be hardened by wind, and have thicker and shorter trunks. Upon removal of these trees, the weaker, slender trees are easily knocked over (Jaffe and Forbes 1993; Chehab et al. 2012).

Plant growth may decline in response to careful touching or stroking of leaves, much to the disappointment of some students who have tried to carry out a **nondestructive growth analysis**. Although not all species or genotypes of a species show thigmomorphogenesis to the same extent, it is a common and often underestimated phenomenon, generally associated with a reduction in plant growth. Canopy effects on stem growth are usually ascribed to shading, but reduced mechanical stress also plays a role. This canopy effect on *Nicotiana tabacum* (tobacco) is that plants produce shorter, thicker and more flexible stems (Table 10.8). Touching the leaves may also affect leaf respiration, transpiration, and chemical composition, even in plants whose growth may not be reduced by such a treatment (Kraus et al. 1994). Roots show thigmotropic reactions when encountering obstacles in soil and grow around these (Braam and Chehab 2017).

Plants sense and respond to many of the same **mechanical stimuli** as animals, including **touch** and **gravity** (Hamilton et al. 2015). In many cases, applying a mechanical stimulus leads to a rapid burst of ion flux, and it has long been speculated that this correlation may be attributed to the action of specific ion channels in the stimulated cells, in part because of the speed of the response. The flux of **Ca^{2+}** is involved in various mechanosensory pathways, including touch stimulus signaling, consistent with the action of a mechanically gated **calcium channel** in these processes. After influx, Ca^{2+} serves as a **second messenger** in downstream events such as the activation of **calmodulin** and calmodulin-like proteins, which are also implicated in thigmomorphogenesis (Chehab et al. 2009).

The phytohormone jasmonate (JA) is both required for and promotes the characteristics of thigmomorphogenesis in *Arabidopsis thaliana*, including a touch-induced delay in flowering and rosette diameter reduction. Repetitive **mechanostimulation** enhances pest resistance in a JA-dependent manner. These results highlight an important role for JA in mediating touch-induced plant developmental responses and resultant cross-protection against biotic stress (Chehab et al. 2012).

Japanese farmers have used mechanical stress treatment of plants for centuries, purposefully stepping on wheat and barley seedlings to strengthen roots, shorten stem height, and

Table 10.8 Stem characteristics measured on control and flexed *Nicotiana tobacco* (tobacco) plants grown either in isolation or in a mixed stand*.

	Isolated plants		Mixed stand	
	Control	Flexed	Control	Flexed
Mechanical properties:				
Height (cm)	84	67	61	27
Diameter	13.3	14.8	8.4	7.1
σ_b	10.7	9.3	10.1	4.3
E	1.6	0.9	1.1	0.1
Growth data:				
Leaf mass ratio	0.47	0.49	0.49	0.54
Stem mass ratio	0.38	0.35	0.38	0.34
Root mass ratio	0.15	0.16	0.13	0.11

Source: Anten et al. (2005)

*In the mixed stand, flexed and control plants were mixed. The properties σ_b and E are the breaking stress and Young's modulus (a measure for stiffness) of the stem, respectively; both σ_b and E are expressed in N m^{-2}

improve yield. Another practice involves the release of ducks onto rice fields, not only to fertilize the plants, but also to pad them down, resulting in thicker and stronger stems. Such methods highlight the benefits of capitalizing on plant touch sensitivity to promote crop yield and stress tolerance (Braam and Chehab 2017).

10.5.9 Growth as Affected by Elevated Atmospheric CO_2 Concentrations

On average, the final mass of C_3 plants, grown at high nutrient supply (without shading by neighboring plants, increases by 47% when the atmospheric CO_2 concentration is increased to 700 μmol mol^{-1} (70 Pa) (Poorter et al. 1996). About two-thirds of all studies show enhanced biomass production at elevated [CO_2] (Luo et al. 2006). In free-air CO_2 enrichments (FACE) studies, biomass and yield of all C_3 crops species, but not C_4 species, except when water is limiting, is greater. Yields of C_3 grain crops, on average, are 19% greater (Kimball 2016). When plants have **numerous sinks**, such as tillers or side shoots, this stimulation can be much greater, but the average enhancement is much less than the stimulation of the rate of **photosynthesis** in short-term experiments (Fig. 10.6; Sect. 2.2.2.1).

To explain why growth is less sensitive to [CO_2] than is photosynthesis, it is helpful to examine the impact of elevated [CO_2] on each growth parameter (Sect. 10.2.1.1):

$$RGR = \frac{(A_a\,x\,SLA\,x\,LMR - LR_m\,x\,LMR - SR_m\,x\,SMR - RR_m\,x\,RMR)}{[C]} \tag{10.11}$$

(for an explanation of all parameters, see Table 10.1). If the *RGR* and final mass of the plants increase less than expected from the increase in A_a, one or more of the parameters in Eq. 10.11 must have been affected by elevated atmospheric [CO_2], compensating for the faster rate of photosynthesis as found in A versus C_c curves. We address photosynthetic **acclimation** to high [CO_2] in Sect. 2.12.1. Here we discuss some additional changes that counteract the initial stimulation of photosynthesis. There are numerous examples where exposure of plants to a high atmospheric [CO_2] transiently enhances the plant's *RGR*, followed by a return to the *RGR* in control plants (*e.g.*, Fonseca et al. 1996). The **transient increase in *RGR*** may account entirely for the increase in final mass of the plants grown at elevated [CO_2] (Fig. 10.24). Some species show a sustained enhancement of *RGR*, but some degree of acclimation is common. Which component of the growth equation accounts for such acclimation? A **decrease in *SLA*** is the major adjustment upon prolonged exposure to elevated [CO_2], partly due to accumulation of nonstructural carbohydrates (Sect. 4.3.4). *LMR*, *SMR*, and *RMR* are not or only marginally affected (Stulen and den Hertog 1993). If they

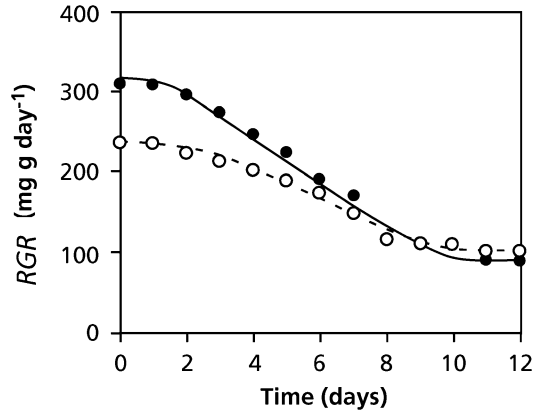

Fig. 10.24 The relative growth rate (*RGR*, expressed on a fresh mass basis) of *Plantago major* (common plantain) grown at 350 μmol mol^{-1} CO_2 (open symbols) or at 700 μmol mol^{-1} CO_2 from day zero onward, when the plants were four weeks old (Fonseca et al. 1996); copyright Trustees of The New Phytologist.

are affected, then this is due to depletion of nutrients in the soil of the faster-growing plants exposed to elevated [CO_2]. **Leaf respiration** increases upon long-term exposure to high [CO_2] (Sect. 3.4.7). The carbon concentration varies with atmospheric [CO_2], but without a distinct trend (Poorter et al. 1992). We cannot simply extrapolate results from short-term measurements of photosynthesis on single leaves to the long-term effects on growth of whole plants.

Different functional plant types may respond to varying degrees to elevated [CO_2]. For example, **C_4 plants**, whose rate of photosynthesis is virtually saturated at 400 μmol mol^{-1} CO_2, respond to a smaller extent (Poorter et al. 1996). Elevated [CO_2] does not consistently affect the **competitive balance between C_3 and C_4 plants** (Sect. 16.5.4). Plant species that associate with **ectomycorrhizal** fungi show a 30% biomass increase in response to elevated [CO_2], regardless of N availability, whereas low N availability limits CO_2 fertilization in plants that associate with arbuscular mycorrhizal fungi (Terrer et al. 2016). However, the additional growth in ectomycorrhizal plants may not greatly enhance soil carbon accumulation, because it is partly offset by decreases in soil carbon pools via **priming** (Terrer et al. 2018).

10.6 Adaptations Associated with Inherent Variation in Growth Rate

10.6.1 Fast-Growing and Slow-Growing Species

In **unpredictable but productive environments**, where 'catastrophes' like fire, inundation, or other forms of disturbance occur, **fast-growing short-lived species** are common. In more **predictable environments**, with a low incidence of disturbance, **longer-lived slow-growing species** predominate. Apart from their life span, these short- and long-lived species differ in many other traits, and, broadly generalizing, have been termed **r-species** and **K-species**, where r and K are constants in a logistic growth curve (McArthur and Wilson 1967). Such a classification, once proposed for both plants and animals, has been questioned, but it provides a useful context in which to understand the ecological performance of vastly different species (Table 10.9). Grime (2006) extended this concept, proposing that there are two major categories of selective factors: **stress**, which is an environmental factor that reduces the growth rate of plants, and **disturbance**, which is a factor that destroys plant biomass. High-stress environments include those with low availability of water, nutrients, or light, or where other conditions are unfavorable for

Table 10.9 Some of the characteristics of r- and K-species and the habitats in which they occur.

	r selection	K selection
Climate	Variable and/or unpredictable; uncertain	Fairly constant and/or predictable; more certain
Mortality	Often catastrophic; density-independent	Density-dependent
Population size	Variable; usually well below carrying capacity; frequent recolonization	Fairly constant; at or near carrying capacity; no recolonization required
Intra- and interspecific competition	Variable; often minor	Usually severe
Traits favored by selection	Rapid development	Slower development
	High growth rate	
	Early reproduction	Competitive ability
	Single reproduction	Delayed reproduction
		Repeated reproductions
Life span	Relatively short	Longer

growth (extreme temperatures, high salinity, low oxygen, extreme pH, high metal concentrations). Disturbance can result from herbivory or from environmental factors like fire or wind.

Grime describes three extreme types of plant strategies: **competitors**, which exist under conditions of low stress and low disturbance, **stress-tolerant** species, which occupy habitats with high stress and low disturbance, and **ruderals**, which occur in highly disturbed nonstressful environments. There is no viable plant strategy that can deal with the combination of high stress and high disturbance. Most plants actually fall at intermediate points along these continua of stress and disturbance, so it is most useful to use the scheme in a comparative sense, with some species being more stress-tolerant than others, some species more tolerant of disturbance than others. Although this classification has been questioned, it has led to the recognition that plants characteristic of low-resource and stressful environments consistently have a lower *RGR* than do plants from more favorable environments (Box 16.1). The extent to which plant species fit into the major categories may change when seedlings grow up to become adults (Dayrell et al. 2018).

The close association between a species' growth potential and the quality of its natural habitat (Fig. 10.25) raises two questions. First, how are the differences in growth rate between species brought about? Second, what ecological advantage does a plant's growth potential confer? These two questions are in fact closely related. Before evaluating the **ecological significance** of the inherent *RGR* of a species, it is important to analyze the **physiological basis** of inherent variation in *RGR* (Lambers and Poorter 1992). Numerous plant traits contribute to a plant's absolute growth rate in its natural habitat (*e.g.*, seed size, germination time, or plant size after overwintering). In view of the close correlation between a plant's inherent *RGR* and environmental parameters (Fig. 10.25), we restrict the present discussion to traits that contribute to variation in *RGR*. Finally, we discuss the ecological implications of inherent differences in the various traits and in the growth rate itself.

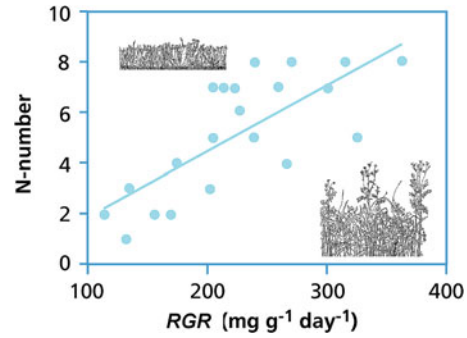

Fig. 10.25 The relationship between the relative growth rate (*RGR*) of 24 herbaceous C_3 species and the 'N number' of the species' habitat (high values correspond to nutrient-rich habitats). The *RGR* was determined under identical conditions for all species: free access to nutrients and an irradiance of 320 μmol m^{-2} s^{-1} (Poorter and Remkes 1990); copyright © 1990, Springer-Verlag.

10.6.2 Growth of Inherently Fast- and Slow-Growing Species under Resource-Limited Conditions

In Sect. 10.2.1, we compared plants under conditions favorable for growth. How do fast- and slow-growing species perform at a low nutrient concentration?

10.6.2.1 Growth at a Limiting Nutrient Supply

Although the *RGR* of potentially fast-growing species is reduced more than that of slow-growing ones, when nutrients are in short supply, the inherently fast-growing species still tend to grow fastest (Fig. 10.26). We find similar results in a situation where a fast-growing species competes with a slow-growing one under nutrient stress, at least when the duration of the experiment is short, relative to the plant's life span. The higher *RGR* of inherently fast-growing species at a low nutrient supply, in comparison with slow-growing ones, is largely 'explained' by differences in *LAR* (*SLA*) which is similar to the situation with free access to nutrients (Table 10.10). (Note that we use 'explained' here in a statistical sense, and that it does not refer to physiological mechanisms.)

10.6.2.2 Growth in Shade

In a comparison of tropical tree species, fast-growing species with a high LAR and low *RMR* maintain a higher *RGR* when grown in the shade; however, they also show greater mortality (Kitajima 1994). This trend can be accounted for by greater investment in defense against herbivores and pathogens (dense and tough leaves) in the slower-growing trees, which have a large root system and a high wood density (Kitajima 1996).

10.6.3 Are There Ecological Advantages Associated with a High or Low *RGR*?

The ecological advantage of a high *RGR* seems straightforward: fast growth results in the rapid occupation of space, which is advantageous in a situation of competition for limiting resources. A high *RGR* may also maximize the reproductive output in plants with a short life span, which is particularly important for ruderals.

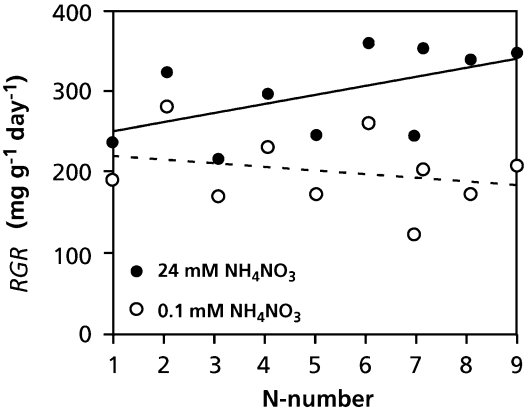

Fig. 10.26 The *RGR* of 10 annual herbaceous C_3 species grown at a high and a low nitrogen (N) supply. The 10 species were from habitats differing in 'N-number' (higher values indicating a higher nutrient availability as well as an inherently higher RGR_{max}) (Fichtner and Schulze 1992); copyright © 1992, Springer-Verlag.

10.6.3.1 Various Hypotheses

What is the possible survival value of slow growth? Slow-growing species make modest demands and are therefore less likely to exhaust the available nutrients, but this is not a stable evolutionary strategy, because a neighboring individual with a faster nutrient uptake could absorb most nutrients. In addition, these modest demands cannot explain slow growth as an adaptation to saline environments or other situations where conditions are stressful for reasons other than low resource supply.

Slow-growing species were thought to incorporate less photosynthates and nutrients into structural biomass. This might allow them to form reserves for later growth, thereby enabling them to maintain physiological integrity during periods of low nutrient availability. As we discuss in Sects. 10.5.3.3 and 10.5.4.3, however, under such adverse conditions, growth is restricted before photosynthesis is, and sugars tend to accumulate. Hence, it is unlikely that survival during periods of nutrient shortage depends on storage of photosynthates. There is also no evidence that slow-growing species have a greater capacity to accumulate nutrients, perhaps with the exception of P. Finally, it has been suggested that a rapid growth rate cannot be realized in a low-resource environment; therefore, a high potential *RGR* is a selectively neutral trait. As discussed in Sect. 10.6.2, however, potentially fast-growing species

Table 10.10 The effect of a nutrient solution with a high or a low NO_3^- concentration on some growth parameters of an inherently slow-growing species [*Deschampsia flexuosa* (tufted hair-grass)] and a fast-growing one [*Holcus lanatus* (common velvet grass)].

	High [NO_3]		Low [NO_3]	
Parameter	*Deschampsia*	*Holcus*	*Deschampsia*	*Holcus*
RGR	97	172	47	66
NAR	6.9	8.5	5.2	4.6
LAR	13	20	9	14
SLA	28	51	24	44

Source: Poorter et al. (1995)

still grow faster than potentially slow-growing ones, even in low-resource environments. This indicates that the potential *RGR* is not a selectively neutral trait. Even in low-resource environments, fast-growing species attain a larger size more rapidly which has advantages in terms of their competitive ability and fitness. Although a very high *RGR* is not attainable, a slightly higher *RGR* might, therefore, still be advantageous.

10.6.3.2 Selection on RGR_{max} Itself, or on Traits That Are Associated with RGR_{max}?

Having scrutinized some hypotheses accounting for variation in growth potential, we conclude that a low potential growth rate *per se* does not confer ecological advantage. Why, then, do slow-growing species occur more frequently in unfavorable habitats than do fast-growing ones (Grime and Hunt 1975)? An alternative explanation for the observed differences in potential growth rate is that one of the **components linked with *RGR***, and not *RGR* itself, has been the target of natural selection (Lambers and Poorter 1992).

The most likely traits selected for are those that protect plant organs (**quantitative defense**; Sect. 13.3.2). In leaves, this is associated with a **low *SLA***, which is accounted for by variation in **leaf mass density** (*i.e.* the amount of dry mass per unit fresh mass). Variation in leaf mass density is largely accounted for by variation in cell-wall thickness, number of sclerenchymatic cells, and the concentration of quantitatively important secondary plant compounds (Sects. 10.3.2 and 10.3.3; Onoda et al. 2017). Variation in these traits closely correlates with that in *RGR* (Figs 10.3 and 10.4). When nutrients are limiting, conservation of the scarce resource is at least as important as its capture (Sect. 9.4). Hence, we expect plants growing under severe nutrient limitation to **conserve their nutrients**. Indeed, low-productivity species are more successful due to slow leaf turnover; therefore, nutrient losses are restricted (Sects. 9.4.3 and 9.4.4). Comparing tree seedlings, a close negative correlation exists between *RGR* and leaf life-span (Reich et al. 1992).

How can **leaf longevity** be increased? This depends on the environmental factor that affects leaf longevity. Herbivory can be reduced by increasing leaf toughness and accumulating palatability-reducing compounds (Sect. 13.3; Wright et al. 2005). The abrasive effects of high wind speeds can be reduced by investment in fiber and sclerenchyma (Sect. 10.3.3). Trampling resistance may be the result of a large amount of cell-wall material per cell. Transpiration can be decreased and water-use efficiency can be increased by the construction of leaf hairs or epicuticular waxes (Sect. 6.2). Epicuticular waxes may also confer disease resistance and diminish deleterious effects of salt spray (Lambers and Poorter 1992). Each of these additional investments increases the leaf's longevity, but also decreases *SLA*, and therefore diminishes the plant's growth potential, but positively influences its fitness under adverse conditions.

There is considerably less information on root turnover than on leaf turnover. Root turnover decreases from tropical to high-latitude systems for all plant functional groups (Gill and Jackson 2000), but there are not enough data to generalize about inherent differences associated with a plant's growth potential (McCormack and Guo 2014). We do know, however, that the **root mass density** tends to be greater in roots of slow-growing species, when compared with that in fast-growing ones which is similar to what has been found for leaves (Ryser and Lambers 1995; de la Riva et al. 2018a); this higher root mass density is associated with thicker cell walls. The high mass density might be associated with slow root turnover, but this remains speculative. Fast root turnover increases the uptake of poorly mobile nutrients such as P (Steingrobe 2005), and hence the correlation between root and leaf mass density is unlikely to be a general one (Lambers et al. 2018).

Is there any indication that plants without the types of leaf and root adjustment discussed in this Section could not survive in unfavorable habitats? This would require introduction of plants that only differ in one specific trait in different environments. Such isogenic genotypes are rarely available, however, and we may expect variation

in one trait to affect related traits. The best ecological information available does support the contention that a decrease in *SLA* enhances the capacity to survive in more stressful environments, and that there is a coordination of traits, involving leaves, stems, and roots (Lambers and Poorter 1992; de la Riva et al. 2016b).

10.6.3.3 An Appraisal of Plant Distribution Requires Information on Ecophysiology

A plant's growth potential is part of a strategy that explains the distribution of a species (Sect. 10.3). Various hypotheses have been proposed to account for the ecological advantage of a high or low RGR_{max}. As we learned before, however, when discussing the ecology and physiology of C_4 and CAM plants (Sects. 2.9 and 2.10), and of cluster-root-producing species (Sect. 9.2.2.5.2), detailed information on biochemistry and physiology is essential to fully appreciate a plant's functioning in different environments as well as a species' distribution.

In the present context, we conclude that a thorough **ecophysiological analysis** of inherent variation in *RGR* has led to greater insight in the **ecological significance** of this trait. Rather than *RGR per se*, one or more underlying components has been the target of natural selection. This natural selection has inevitably led to variation in maximum *RGR* and an associated **suite of traits** (Table 10.11). This analysis also serves to

Table 10.11 Typical characteristics of inherently fast-growing and slow-growing herbaceous C_3 species, summarizing information presented in the text.

Characteristic	Fast-growing species	Slow-growing species
Habitat:		
nutrient supply	high	low
potential productivity	high	low
Morphology and allocation:		
leaf area ratio	high	low
specific leaf area	high	low
leaf mass ratio	higher	lower
root mass ratio	lower	higher
Physiology:		
photosynthesis		
(per unit leaf area)	equal	equal
(per unit leaf mass)	high	low
carbon use in respiration		
(% of total C fixed)	low	high
ion uptake rate		
(per unit root mass)	high	low
Chemical composition:		
concentration of quantitative		
secondary compounds	low	high
concentration of qualitative		
secondary compounds	variable	variable
Other aspects:		
leaf mass density	low	high
root mass density	low	high
leaf turnover	high	low
root turnover	high?	low?
leaf longevity	low	high
root longevity	low?	low?

Note: Unless stated otherwise, the differences refer to plants grown with free access to nutrients. A ? indicates that further study is needed

illustrate that a thorough ecophysiological analysis is essential for a full appreciation of a species' strategy.

10.7 Growth and Allocation: The Messages About Plant Messages

The numerous examples in this chapter provide a wealth of information on how plants cope with their environment. Plant responses to mild stress are not merely the direct effect of resource deprivation on growth rate. Intricate physiological adjustments that minimize major disturbances in plant metabolism take place. Upon sensing water or nutrient shortage in the root environment, roots send signals to the leaves, which respond in such a way as to minimize deleterious effects. This is a **feedforward response**: an anticipating response in which the rate of a process is affected before large deleterious effects of that process have occurred. Low levels of irradiance are similarly detected, in both developing and mature leaves, and the signals leads to a feedforward response that minimizes the effect of growth in the shade.

What do all these examples have in common? They demonstrate that a plant is continuously **sensing** its changing **environment** and using this information to control its physiology and allocation pattern. They indicate that, in general, environment affects growth via chemical or hydraulic messages (**sink control**). We assume that all plants have this capacity to sense their environment. What makes species different from one another is the manner in which they are able to **respond**, rather than the variation in their capacity to sense the environment. The typical response of a ruderal species upon sensing nutrient shortage is to slow down leaf expansion and allocate more resources to root growth; it will promote leaf senescence, and so withdraw nutrients from older leaves and use these for its newly developing organs. A species naturally occurring on nutrient-poor sandplains will use the same signal to slow down the production of new leaves, with less dramatic effects on leaf senescence and allocation pattern. Upon sensing water shortage, some plants may similarly respond by severely reducing leaf expansion, and others by shedding some leaves, whereas facultative CAM plants switch from the C_3 or C_4 pathway to the CAM mode. Shade is perceived by shade-avoiding and shade-tolerant plants, but the response to promote stem elongation is typical only for shade-avoiding species.

It is the **variation in responses**, rather than the actual sensing mechanism itself, that must be of paramount importance accounting for a species' **ecological amplitude** as well as in such ecological processes as **succession** and **competition**. Ignoring the capacity of plants to process and respond to environmental information (and assuming that plants grow until they run out of resources) leads to a distorted view of the process of competition. As neighbors interact, how do the continuous changes in plant form and function, elicited by information-sensing systems, contribute to competitive success? To what extent does the capacity of an individual to adjust its allocation and development contribute to the outcome of competition? It is not our aim to promote the 'Panglossian' view, which we refer to in Chap. 1, that just because a species exhibits certain traits in a particular environment, these traits must be beneficial and have resulted from natural selection in that environment. We do wish to stress, however, that plants are **information-acquiring systems**, rather than passively responding organisms, and that we must not ignore this capability, as we discuss in Chap. 16.

If we aim to understand plant functioning in different environments, information at the cellular and molecular level is of vital importance. Perception of the environment by specific molecules (*e.g.*, phytochrome), followed by transduction of the information and effects on cell growth (*e.g.*, through cell-wall acidification), allow the plant to acclimate to its environment (*e.g.*, shade). In the past decade, our understanding of numerous intricate processes has increased enormously. We can expect that fascinating progress will be made in the next decade that will allow us both to deepen our understanding of plant performance in an ecological context and to apply this information in modeling plant performance as dependent on global change and in breeding new varieties for adverse conditions.

References

Abramoff RZ, Finzi AC. 2015. Are above- and below-ground phenology in sync? *New Phytol* **205**: 1054–1061.

Alameda D, Villar R. 2012. Linking root traits to plant physiology and growth in *Fraxinus angustifolia* Vahl. seedlings under soil compaction conditions. *Env Exp Bot* **79**: 49–57.

Ali O, Traas J. 2016. Force-driven polymerization and turgor-induced wall expansion. *Trends Plant Sci* **21**: 398–409.

Annighöfer P, Petritan AM, Petritan IC, Ammer C. 2017. Disentangling juvenile growth strategies of three shade-tolerant temperate forest tree species responding to a light gradient. *For Ecol Manag* **391**: 115–126.

Anten NP, Poorter H. 2009. Carbon balance of the oldest and most-shaded leaves in a vegetation: a litmus test for canopy models. *New Phytol* **183**: 1–3.

Anten Niels PR, Raquel CG, Nagashima H. 2005. Effects of mechanical stress and plant density on mechanical characteristics, growth, and lifetime reproduction of tobacco plants. *Amer Nat* **166**: 650–660.

Anten NPR, Schieving F, Werger MJA. 1995. Patterns of light and nitrogen distribution in relation to whole canopy carbon gain in C_3 and C_4 mono- and dicotyledonous species. *Oecologia* **101**: 504–513.

Antúnez I, Retamosa EC, Villar R. 2001. Relative growth rate in phylogenetically related deciduous and evergreen woody species. *Oecologia* **128**: 172–180.

Araya T, Miyamoto M, Wibowo J, Suzuki A, Kojima S, Tsuchiya YN, Sawa S, Fukuda H, von Wirén N, Takahashi H. 2014. CLE-CLAVATA1 peptide-receptor signaling module regulates the expansion of plant root systems in a nitrogen-dependent manner. *Proc Natl Acad Sci USA* **111**: 2029–2034.

Armstrong W. 1971. Radial oxygen losses from intact rice roots as affected by distance from the apex, respiration and waterlogging. *Physiol Plant* **25**: 192–197.

Atkin OK. 1996. Reassessing the nitrogen relations of Arctic plants: a mini-review. *Plant Cell Environ* **19**: 695–704.

Atkin OK, Botman B, Lambers H. 1996. The relationship between the relative growth rate and nitrogen economy of alpine and lowland *Poa* species. *Plant Cell Environ* **19**: 1324–1330.

Atkinson RRL, Mockford EJ, Bennett C, Christin P-A, Spriggs EL, Freckleton RP, Thompson K, Rees M, Osborne CP. 2016. C_4 photosynthesis boosts growth by altering physiology, allocation and size. *Nat Plants*: 16038.

Atwell BJ 1989. Physiological responses of lupin roots to soil compaction. In: Loughman BC, Gasparikova O, Kolek J eds. *Structural and Functional Aspects of Transport in Roots*. Dordrecht: Kluwer Academic Publishers, 251–255.

Avice JC, Ourry A, Volenec JJ, Lemaire G, Boucaud J. 1996. Defoliation-induced changes in abundance and immuno-localization of vegetative storage proteins in taproots of *Medicago sativa*. *Plant Physiol Bochem* **34**: 561–570.

Ayling SM, Topa MA. 2002. Phosphorus compartmentation in *Pinus serotina* Michx. (pond pine); observations from in vivo nuclear magnetic resonance spectroscopy. *Plant Cell Environ* **21**: 723–730.

Babst BA, Coleman GD. 2018. Seasonal nitrogen cycling in temperate trees: transport and regulatory mechanisms are key missing links. *Plant Sci* **270**: 268–277.

Bacon MA, Wilkinson S, Davies WJ. 1998. pH-regulated leaf cell expansion in droughted plants is abscisic acid dependent. *Plant Physiol* **118**: 1507–1515.

Bailey-Serres J, Fukao T, Gibbs DJ, Holdsworth MJ, Lee SC, Licausi F, Perata P, Voesenek LACJ, van Dongen JT. 2012. Making sense of low oxygen sensing. *Trends Plant Sci* **17**: 129–138.

Bailey-Serres J, Fukao T, Ronald P, Ismail A, Heuer S, Mackill D. 2010. Submergence tolerant rice: *SUB1*'s journey from landrace to modern cultivar. *Rice* **3**: 138–147.

Ball MC, Pidsley SM. 1995. Growth responses to salinity in relation to distribution of two mangrove species, *Sonneratia alba* and *S. lanceolata*, in Northern Australia. *Funct Ecol* **9**: 77–85.

Ballaré CL. 1999. Keeping up with the neighbours: phytochrome sensing and other signalling mechanisms. *Trends Plant Sci* **4**: 97–102.

Ballaré CL, Pierik R. 2017. The shade-avoidance syndrome: multiple signals and ecological consequences. *Plant Cell Environ* **40**: 2530–2543.

Ballaré CL, Scopel AL, Roush ML, Radosevich SR. 1995. How plants find light in patchy canopies. a comparison between wild-type and phytochrome-B-deficient mutant plants of cucumber. *Funct Ecol* **9**: 859–868.

Bausenwein U, Millard P, Thornton B, Raven JA. 2001. Seasonal nitrogen storage and remobilization in the forb *Rumex acetosa*. *Funct Ecol* **15**: 370–377.

Bell TL, Pate JS, Dixon KW. 1996. Relationships between fire response, morphology, root anatomy and starch distribution in south-west Australian Epacridaceae. *Ann Bot* **77**: 357–364.

Bengough AG, Bransby MF, Hans J, McKenna SJ, Roberts TJ, Valentine TA. 2006. Root responses to soil physical conditions; growth dynamics from field to cell. *J Exp Bot* **57**: 437–447.

Berger JD, Buirchell BJ, Luckett DJ, Palta JA, Ludwig C, Liu DL. 2012. How has narrow-leafed lupin changed in its 1st 40 years as an industrial, broad-acre crop? A G×E-based characterization of yield-related traits in Australian cultivars. *Field Crops Res* **126**: 152–164.

Berger S, Bell E, Sadka A, Mullet JE. 1995. *Arabidopsis thaliana Atvsp* is homologous to soybean *VspA* and *VspB*, genes encoding vegetative storage protein acid

phosphatases, and is regulated similarly by methyl jasmonate, wounding, sugars, light and phosphate. *Plant Mol Biol* **27**: 933–942.

Blom-Zandstra M. 1989. Nitrate accumulation in vegetables and its relationship to quality. *Ann Appl Biol* **115**: 553–561.

Bloom AJ, Chapin FS, Mooney HA. 1985. Resource limitation in plants-an economic analogy. *Annu Rev Ecol Syst* **16**: 363–392.

Bowen GD 1991. Soil temperature, root growth, and plant function. In: Waisel Y, Eshel A, Kafkaki U eds. *Plant Roots: The Hidden Half, 1st edn*. New York: Marcel Dekker, 309–330.

Braam J, Chehab EW. 2017. Thigmomorphogenesis. *Curr Biol* **27**: R863–R864.

Braidwood L, Breuer C, Sugimoto K. 2014. My body is a cage: mechanisms and modulation of plant cell growth. *New Phytol* **201**: 388–402.

Brouwer R. 1962. Nutritive influences on the distribution of dry matter in the plant. *Neth J Agric Sci* **10**: 399–408.

Brouwer R. 1963. Some aspects of the equilibrium between overground and underground plant parts. *Meded Inst Biol Scheikd Onderz Landbouwgew* **1963**: 31–39.

Butler W, Norris K, Seigelman H, Hendricks S. 1959. Detection, assay, and preliminary purification of the pigment controlling photoresponsive development of plants. *Proc Natl Acad Sci USA* **45**: 1703.

Castro-Díez P, Puyravaud JP, Cornelissen JHC. 2000. Leaf structure and anatomy as related to leaf mass per area variation in seedlings of a wide range of woody plant species and types. *Oecologia* **124**: 476–486.

Ceulemans R 1989. Genetic variation in functional and structural productivity components in populus. In: Lambers H, Cambridge ML, Konings H, Pons TL eds. *Causes and Consequences of Variation in Growth Rate and Productivity of Higher Plants*. The Hague: SPB Academic Publishing, 69–85.

Chapin FS, Shaver GR, Kedrowski RA. 1986. Environmental controls over carbon, nitrogen and phosphorus fractions in *Eriophorum vaginatum* in Alaskan tussock tundra. *J Ecol* **74**: 167–195.

Chaumont F, Tyerman SD. 2014. Aquaporins: highly regulated channels controlling plant water relations. *Plant Physiol* **164**: 1600–1618.

Chehab EW, Eich E, Braam J. 2009. Thigmomorphogenesis: a complex plant response to mechano-stimulation. *J Exp Bot* **60**: 43–56.

Chehab EW, Yao C, Henderson Z, Kim S, Braam J. 2012. *Arabidopsis* touch-induced morphogenesis is jasmonate mediated and protects against pests. *Curr Biol* **22**: 701–706.

Cho HT, Kende H. 1997a. Expansins in deepwater rice internodes. *Plant Physiol* **113**: 1137–1143.

Cho HT, Kende H. 1997b. Expression of expansin genes is correlated with growth in deepwater rice. *Plant Cell* **9**: 1661–1671.

Clark LJ, Whalley WR, Dexter AR, Barraclough PB, Leigh RA. 1996. Complete mechanical impedance increases the turgor of cells in the apex of pea roots. *Plant Cell Environ* **19**: 1099–1102.

Clarkson DT, Carvajal M, Henzler T, Waterhouse RN, Smyth AJ, Cooke DT, Steudle E. 2000. Root hydraulic conductance: diurnal aquaporin expression and the effects of nutrient stress. *J Exp Bot* **51**: 61–70.

Clarkson DT, Jones LHP, Purves JV. 1992. Absorption of nitrate and ammonium ions by *Lolium perenne* from flowing solution cultures at low root temperatures. *Plant Cell Environ* **15**: 99–106.

Cogliatti DH, Clarkson DT. 1983. Physiological changes in, and phosphate uptake by potato plants during development of, and recovery from phosphate deficiency. *Physiol Plant* **58**: 287–294.

Coleman GD, Chen THH, Fuchigami LH. 1992. Complementary DNA cloning of poplar bark storage protein and control of its expression by photoperiod. *Plant Physiol* **98**: 687–693.

Colmer TD. 2003. Long-distance transport of gases in plants: a perspective on internal aeration and radial oxygen loss from roots. *Plant Cell Environ* **26**: 17–36.

Colmer TD, Armstrong W, Greenway H, Ismail AM, Kirk GJD, Atwell BJ. 2014. Physiological mechanisms of flooding tolerance in rice: transient complete submergence and prolonged standing water. *Progr Bot* **75**: 255–307.

Colmer TD, Winkel A, Pedersen O. 2011. A perspective on underwater photosynthesis in submerged terrestrial wetland plants. *AoB PLANTS* **2011**.

Cook BI, Wolkovich EM, Parmesan C. 2012. Divergent responses to spring and winter warming drive community level flowering trends. *Proc Natl Acad Sci USA* **109**: 9000–9005.

Cornelissen JHC. 1996. An experimental comparison of leaf decomposition rates in a wide range of temperate plant species and types. *J Ecol* **84**: 573–582.

Cornelissen JHC, Diez PC, Hunt R. 1996. Seedling growth, allocation and leaf attributes in a wide range of woody plant species and types. *J Ecol* **84**: 755–765.

Cosgrove DJ. 2000. Loosening of plant cell walls by expansins. *Nature* **407**: 321–326.

Cosgrove DJ. 2015. Plant expansins: diversity and interactions with plant cell walls. *Curr Opin Plant Biol* **25**: 162–172.

Cosgrove DJ. 2016. Plant cell wall extensibility: connecting plant cell growth with cell wall structure, mechanics, and the action of wall-modifying enzymes. *J Exp Bot* **67**: 463–476.

Cyr DR, Derek Bewley J. 1990. Proteins in the roots of the perennial weeds chicory (*Cichorium intybus* L.) and dandelion (*Taraxacum officinale* Weber) are associated with overwintering. *Planta* **182**: 370–374.

Dar MH, Zaidi NW, Waza SA, Verulkar SB, Ahmed T, Singh PK, Roy SKB, Chaudhary B, Yadav R, Islam MM, Iftekharuddaula KM, Roy JK, Kathiresan RM, Singh BN, Singh US, Ismail AM. 2018. No

yield penalty under favorable conditions paving the way for successful adoption of flood tolerant rice. *Sci Rep* **8**: 9245.

Darwin CR. 1880. *The Power of Movement in Plants*. London: John Murray.

Davies WJ, Zhang J. 1991. Root signals and the regulation of growth and development of plants in drying soil. *Annu Rev Plant Biol* **42**: 55–76.

Dayrell RLC, Arruda AJ, Pierce S, Negreiros D, Meyer PB, Lambers H, Silveira FAO. 2018. Ontogenetic shifts in plant ecological strategies. *Funct Ecol* **32**: 2730–2741.

de Bang TC, Lay KS, Scheible W-R, Takahashi H. 2017. Small peptide signaling pathways modulating macronutrient utilization in plants. *Curr Opin Plant Biol* **39**: 31–39.

de la Riva EG, Marañón T, Pérez-Ramos IM, Navarro-Fernández CM, Olmo M, Villar R. 2018a. Root traits across environmental gradients in Mediterranean woody communities: are they aligned along the root economics spectrum? *Plant Soil* **424**: 35–48.

de la Riva EG, Olmo M, Poorter H, Ubera JL, Villar R. 2016a. Leaf mass per area (LMA) and its relationship with leaf structure and anatomy in 34 Mediterranean woody species along a water availability gradient. *PLoS ONE* **11**: e0148788.

de la Riva EG, Tosto A, Pérez-Ramos IM, Navarro-Fernández CM, Olmo M, Anten NPR, Marañón T, Villar R. 2016b. A plant economics spectrum in Mediterranean forests along environmental gradients: is there coordination among leaf, stem and root traits? *J Veg Sci* **27**: 187–199.

de la Riva EG, Villar R, Pérez-Ramos IM, Quero JL, Matías L, Poorter L, Marañón T. 2018b. Relationships between leaf mass per area and nutrient concentrations in 98 Mediterranean woody species are determined by phylogeny, habitat and leaf habit. *Trees* **32**: 497–510.

Díaz S, Kattge J, Cornelissen JHC, Wright IJ, Lavorel S, Dray S, Reu B, Kleyer M, Wirth C, Colin Prentice I, Garnier E, Bönisch G, Westoby M, Poorter H, Reich PB, Moles AT, Dickie J, Gillison AN, Zanne AE, Chave J, Joseph Wright S, Sheremet'ev SN, Jactel H, Baraloto C, Cerabolini B, Pierce S, Shipley B, Kirkup D, Casanoves F, Joswig JS, Günther A, Falczuk V, Rüger N, Mahecha MD, Gorné LD. 2016. The global spectrum of plant form and function. *Nature* **529**: 167–171.

Dissanayaka DMSB, Plaxton WC, Lambers H, Siebers M, Marambe B, Wasaki J. 2018. Molecular mechanisms underpinning phosphorus-use efficiency in rice. *Plant Cell Environ* **41**: 1512–1523.

Djordjevic MA, Mohd-Radzman NA, Imin N. 2015. Small-peptide signals that control root nodule number, development, and symbiosis. *J Exp Bot* **66**: 5171–5181.

Dodd IC. 2005. Root-to-shoot signalling: assessing the roles of "up" in the up and down world of long-distance signalling in planta. *Plant Soil* **274**: 251-270.

Eller CB, de V. Barros F, Bittencourt PRL, Rowland L, Mencuccini M, Oliveira R. 2018. Xylem hydraulic safety and construction costs determine tropical tree growth. *Plant Cell Environ* **41**: 548-562.

Else MA, Davies WJ, Malone M, Jackson MB. 1995. A negative hydraulic message from oxygen-deficient roots of tomato plants? (Influence of soil flooding on leaf water potential, leaf expansion, and synchrony between stomatal conductance and root hydraulic conductivity). *Plant Physiol* **109**: 1017-1024.

Falster DS, Duursma RA, FitzJohn RG. 2018. How functional traits influence plant growth and shade tolerance across the life cycle. *Proc Natl Acad Sci USA* **115**: E6789-E6798.

Fetene M, Beck E. 1993. Reversal of the direction of photosynthate allocation in *Urtica dioica* L. plants by increasing cytokinin import into the shoot. *Bot Acta* **106**: 235-240.

Fichtner K, Schulze E-D. 1992. The effect of nitrogen nutrition on growth and biomass partitioning of annual plants originating from habitats of different nitrogen availability. *Oecologia* **92**: 236-241.

Field CB 1991. Ecological scaling of carbon gain to stress and resource availability. In: Mooney HA, Winner WE, Pell EJ eds. *Integrated Responses of Plants to Stress*. San Diego: Academic Press, 35-65.

Fondy BR, Geiger DR. 1982. Diurnal pattern of translocation and carbohydrate metabolism in source ;eaves of *Beta vulgaris* L. *Plant Physiol* **70**: 671-676.

Fonseca F, Den Hertog J, Stulen I. 1996. The response of *Plantago major* ssp. *pleiosperma* to elevated CO_2 is modulated by the formation of secondary shoots. *New Phytol* **133**: 627-635.

Forde BG. 2002. Local and long-range signaling pathways regulating plant responses to nitrate. *Annu Rev Plant Biol* **53**: 203-224.

Franklin KA, Whitelam GC. 2004. Light signals, phytochromes and cross-talk with other environmental cues. *J Exp Bot* **55**: 271-276.

Garnier E. 1991. Resource capture, biomass allocation and growth in herbaceous plants. *Trends Ecol Evol* **6**: 126-131.

Garnier E, Gobin O, Poorter H. 1995. Nitrogen productivity depends on photosynthetic nitrogen use efficiency and on nitrogen allocation within the plant. *Ann Bot* **76**: 667-672.

Garnier E, Laurent G. 1994. Leaf anatomy, specific mass and water content in congeneric annual and perennial grass species. *New Phytol* **128**: 725-736.

Garnier E, Vancaeyzeele S. 1994. Carbon and nitrogen content of congeneric annual and perennial grass species: relationships with growth. *Plant Cell Environ* **17**: 399-407.

Gibert A, Gray EF, Westoby M, Wright IJ, Falster DS. 2016. On the link between functional traits and growth rate: meta-analysis shows effects change with plant size, as predicted. *J Ecol* **104**: 1488-1503.

Gill RA, Jackson RB. 2000. Global patterns of root turnover for terrestrial ecosystems. *New Phytol* **147**: 13-31.

Girondé A, Etienne P, Trouverie J, Bouchereau A, Le Cahérec F, Leport L, Orsel M, Niogret M-F, Nesi N, Carole D, Soulay F, Masclaux-Daubresse C, Avice J-C. 2015. The contrasting N management of two oilseed rape genotypes reveals the mechanisms of proteolysis associated with leaf N remobilization and the respective contributions of leaves and stems to N storage and remobilization during seed filling. *BMC Plant Biol* **15**: 59.

Gleadow RM, Møller BL. 2014. Cyanogenic glycosides: synthesis, physiology, and phenotypic plasticity. *Annu Rev Plant Biol* **65**: 155-185.

Gloser V, Korovetska H, Martín-Vertedor AI, Hájíčková M, Prokop Z, Wilkinson S, Davies W. 2016. The dynamics of xylem sap pH under drought: a universal response in herbs? *Plant Soil* **409**: 259-272.

Goulas E, Richard-Molard C, Le Dily F, Le Dantec C, Ozouf J, Ourry A. 2007. A cytosolic vegetative storage protein (TrVSP) from white clover is encoded by a cold-inducible gene. *Physiol Plant* **129**: 567-577.

Gowing DJG, Davies WJ, Jones HG. 1990. A positive root-sourced signal as an indicator of soil drying in apple, *Malus* x *domestica* Borkh. *J Exp Bot* **41**: 1535-1540.

Goyal A, Szarzynska B, Fankhauser C. 2013. Phototropism: at the crossroads of light-signaling pathways. *Trends Plant Sci* **18**: 393-401.

Green PB. 1976. Growth and cell pattern formation on an axis: critique of concepts, terminology, and modes of study. *Bot Gaz* **137**: 187-202.

Greenway H, Colmer TD. 2010. Ion transport in seminal and adventitious roots of cereals during O_2 deficiency. *J Exp Bot* **62**: 39-57.

Grime JP. 2006. *Plant Strategies and Vegetation Processes*. Chichester: Wiley.

Grime JP, Hunt R. 1975. Relative growth-rate: its range and adaptive significance in a local flora. *J Ecol* **63**: 393-422.

Groeneveld HW, Bergkotte M. 1996. Cell wall composition of leaves of an inherently fast- and an inherently slow-growing grass species. *Plant Cell Environ* **19**: 1389-1398.

Hamilton ES, Schlegel AM, Haswell ES. 2015. United in diversity: mechanosensitive ion channels in plants. *Annu Rev Plant Biol* **66**: 113-137.

Hamza MA, Anderson WK. 2005. Soil compaction in cropping systems: A review of the nature, causes and possible solutions. *Soil and Tillage Research* **82**: 121-145.

Harpham NVJ, Berry AW, Knee EM, Roveda-Hoyos-G, Raskin I, Sanders IO, Smith AR, Wood CK, Hall MA. 1991. The effect of ethylene on the growth and development of wild-type and mutant *Arabidopsis thaliana* (L.) Heynh. *Ann Bot* **68**: 55-61.

Hart R. 1977. Why are biennials so few? *Amer Nat* **111**: 792-799.

Hawkins H-J, Hettasch H, Mesjasz-Przybylowicz J, Przybylowicz W, Cramer MD. 2008. Phosphorus toxicity in the Proteaceae: a problem in post-agricultural lands. *Scientia Horticulturae* **117**: 357-365.

He T, Cramer GR. 1996. Abscisic acid concentrations are correlated with leaf area reductions in two salt-stressed rapid-cycling Brassica species. *Plant Soil* **179**: 25-33.

Heilmeier H, Monson RK 1994. Carbon and nitrogen storage in herbaceous plants. In: Roy J, Garnier E eds. *A Whole Plant Perspective on Carbon-itrogen Interactions*. The Hague: SPB Academic Publishing, 149-171.

Heilmeier H, Schulze E-D, Whale DM. 1986. Carbon and nitrogen partitioning in the biennial monocarp *Arctium tomentosum* Mill. *Oecologia* **70**: 466-474.

Hirose T, Werger MJA. 1987a. Maximizing daily canopy photosynthesis with respect to the leaf nitrogen allocation pattern in the canopy. *Oecologia* **72**: 520-526.

Hirose T, Werger MJA. 1987b. Nitrogen use efficiency in instantaneous and daily photosynthesis of leaves in the canopy of a *Solidago altissima* stand. *Physiol Plant* **70**: 215-222.

Höfte H, Peaucelle A, Braybrook S. 2012. Cell wall mechanics and growth control in plants: the role of pectins revisited. *Front Plant Sci* **3**: 121.

Hsiao TC, Frensch J, Rojas-Lara BA. 1998. The pressure-jump technique shows maize leaf growth to be enhanced by increases in turgor only when water status is not too high. *Plant Cell Environ* **21**: 33-42.

Hübel F, Beck E. 1996. Maize root phytase (purification, characterization, and localization of enzyme activity andiIts putative substrate). *Plant Physiol* **112**: 1429-1436.

Hussain A, Black CR, Taylor IB, Roberts JA. 2000. Does an antagonistic relationship between ABA and ethylene mediate shoot growth when tomato (*Lycopersicon esculentum* Mill.) plants encounter compacted soil? *Plant Cell Environ* **23**: 1217-1226.

Ismail AM, Singh US, Singh S, Dar MH, Mackill DJ. 2013. The contribution of submergence-tolerant (Sub1) rice varieties to food security in flood-prone rainfed lowland areas in Asia. *Field Crops Res* **152**: 83-93.

Jackson SD, James P, Prat S, Thomas B. 1998. Phytochrome B affects the levels of a graft-transmissible signal involved in tuberization. *Plant Physiol* **117**: 29-32.

Jaffe MJ, Forbes S. 1993. Thigmomorphogenesis: the effect of mechanical perturbation on plants. *Plant Growth Regul* **12**: 313-324.

John GP, Scoffoni C, Buckley TN, Villar R, Poorter H, Sack L. 2017. The anatomical and compositional basis of leaf mass per area. *Ecol Lett* **20**: 412-425.

Karlsson PS, Méndez M 2005. 1 – The resource economy of plant reproduction. In: Reekie EG, Bazzaz FA eds. *Reproductive Allocation in Plants*. Burlington: Academic Press, 1-49.

Kende H, Bradford K, Brummell D, Cho H-T, Cosgrove D, Fleming A, Gehring C, Lee Y, McQueen-Mason S, Rose J. 2004. Nomenclature for members of the expansin superfamily of genes and proteins. *Plant Mol Biol* **55**: 311-314.

Kende H, van der Knaap E, Cho H-T. 1998. Deepwater rice: a model plant to study stem elongation. *Plant Physiol* **118**: 1105-1110.

Kigel J, Cosgrove DJ. 1991. Photoinhibition of stem elongation by blue and red light. Effects on hydraulic and cell wall properties. *Plant Physiol* **95**: 1049-1056.

Kimball BA. 2016. Crop responses to elevated CO_2 and interactions with H_2O, N, and temperature. *Curr Opin Plant Biol* **31**: 36-43.

Kitajima K. 1994. Relative importance of photosynthetic traits and allocation patterns as correlates of seedling shade tolerance of 13 tropical trees. *Oecologia* **98**: 419-428.

Kitajima K 1996. Ecophysiology of tropical tree seedling. In: Mulkey SS, Chazdon RL, Smith AP eds. *Tropical Forest Plant Ecophysiology*. New York: Chapman & Hall, 559-596.

Knox KJE, Morrison DA. 2005. Effects of inter-fire intervals on the reproductive output of resprouters and obligate seeders in the Proteaceae. *Austr Ecol* **30**: 407-413.

Konings H, Verschuren GER. 1980. Formation of aerenchyma in roots of Zea mays in aerated solutions, and its relation to nutrient supply. *Physiol Plant* **49**: 265-270.

Kraus E, Kollöffel C, Lambers H. 1994. The effect of handling on photosynthesis, transpiration, respiration, and nitrogen and carbohydrate content of populations of *Lolium perenne*. *Physiol Plant* **91**: 631-638.

Kudo T, Kiba T, Sakakibara H. 2010. Metabolism and long-distance translocation of cytokinins. *J Integr Plant Biol* **52**: 53-60.

Kuiper D, Kuiper PJC, Lambers H, Schuit J, Staal M. 1989. Cytokinin concentration in relation to mineral nutrition and benzyladenine treatment in *Plantago major* ssp. *pleiosperma*. *Physiol Plant* **75**: 511-517.

Kuiper D, Staal M. 1987. The effects of exogenously applied plant growth substances on the physiological plasticity in *Plantago major* ssp. *pleiosperma*: responses of growth, shoot to root ratio and respiration. *Physiol Plant* **69**: 651-658.

Kuo T, Boersma L. 1971. Soil water suction and root temperature effects on nitrogen fixation in soybeans. *Agron J* **63**: 901-904.

Lambers H, Albornoz F, Kotula L, Laliberté E, Ranathunge K, Teste FP, Zemunik G. 2018. How belowground interactions contribute to the coexistence of mycorrhizal and non-mycorrhizal species in severely phosphorus-impoverished hyperdiverse ecosystems. *Plant Soil* **424**: 11-34.

Lambers H, Poorter H. 1992. Inherent variation in growth rate between higher plants: a search for physiological causes and ecological consequences. *Adv Ecol Res* **22**: 187-261.

Le Gall H, Philippe F, Domon J-M, Gillet F, Pelloux J, Rayon C. 2015. Cell wall metabolism in response to abiotic stress. *Plants* **4**: 112.

Leigh RA, Tomos AD. 1983. An attempt to use isolated vacuoles to determine the distribution of sodium and potassium in cells of storage roots of red beet (*Beta vulgaris* L.). *Planta* **159**: 469-475.

Leite DCC, Grandis A, Tavares EQP, Piovezani AR, Pattathil S, Avci U, Rossini A, Cambler A, De Souza AP, Hahn MG, Buckeridge MS. 2017. Cell wall changes during the formation of aerenchyma in sugarcane roots. *Ann Bot* **120**: 693-708.

Leon AJ, Lee M, Andrade FH. 2001. Quantitative trait loci for growing degree days to flowering and photoperiod response in sunflower (*Helianthus annuus* L.). *Theor Appl Gen* **102**: 497-503.

Li X, Gao Y, Wei H, Xia H, Chen Q. 2017. Growth, biomass accumulation and foliar nutrient status in fragrant rosewood (*Dalbergia odorifera* T.C. Chen) seedlings cultured with conventional and exponential fertilizations under different photoperiod regimes. *Soil Sci Plant Nutr* **63**: 153–162.

Liu T, Ren T, White PJ, Cong R, Lu J. 2018. Storage nitrogen co-ordinates leaf expansion and photosynthetic capacity in winter oilseed rape. *J Exp Bot*: ery134-ery134.

Lockhart JA. 1965. An analysis of irreversible plant cell elongation. *J Theor Biol* **8**: 264-275.

Luo Y, Hui D, Zhang D. 2006. Elevated CO_2 stimulates net accumulations of carbon and nitrogen in land ecosystems: a meta-analysi. *Ecology* **87**: 53-63.

MacAdam JW, Volenec JJ, Nelson CJ. 1989. Effects of nitrogen on mesophyll cell division and epidermal cell elongation in tall fescue leaf blades. *Plant Physiol* **89**: 549-556.

Maire V, Wright IJ, Prentice IC, Batjes NH, Bhaskar R, van Bodegom PM, Cornwell WK, Ellsworth D, Niinemets Ü, Ordonez A, Reich PB, Santiago LS. 2015. Global effects of soil and climate on leaf photosynthetic traits and rates. *Glob Ecol Biogeogr* **25**: 706-717.

Marañón T, Grubb PJ. 1993. Physiological basis and ecological significance of the seed size and relative growth rate relationship in Mediterranean annuals. *Funct Ecol* **7**: 591-599.

Materechera SA, Alston AM, Kirby JM, Dexter AR. 1993. Field evaluation of laboratory techniques for predicting the ability of roots to penetrate strong

soil and of the influence of roots on water sorptivity. *Plant Soil* **149**: 149-158.

McArthur RH, Wilson EO. 1967. *The Theory of Island Biogeography*. Princeton: Princeton University Press.

McCormack ML, Adams TS, Smithwick EAH, Eissenstat DM. 2014. Variability in root production, phenology, and turnover rate among 12 temperate tree species. *Ecology* **95**: 2224-2235.

McCormack ML, Guo D. 2014. Impacts of environmental factors on fine root lifespan. *Front Plant Sci* **5**: 205.

McQueen-Mason S, Durachko DM, Cosgrove DJ. 1992. Two endogenous proteins that induce cell wall extension in plants. *Plant Cell* **4**: 1425-1433.

Meuriot F, Noquet C, Avice J-C, Volenec JJ, Cunningham SM, Sors TG, Caillot S, Ourry A. 2004. Methyl jasmonate alters N partitioning, N reserves accumulation and induces gene expression of a 32-kDa vegetative storage protein that possesses chitinase activity in *Medicago sativa* taproots. *Physiol Plant* **120**: 113-123.

Millard P. 1988. The accumulation and storage of nitrogen by herbaceous plants. *Plant Cell Environ* **11**: 1-8.

Mommer L, Pedersen O, Visser EJW. 2004. Acclimation of a terrestrial plant to submergence facilitates gas exchange under water. *Plant Cell Environ* **27**: 1281-1287.

Mooney H, Rundel P. 1979. Nutrient relations of the evergreen shrub, *Adenostoma fasciculatum*, in the California chaparral. *Bot Gaz* **140**: 109-113.

Morvan-Bertrand A, Pavis N, Boucaud J, Prud'Homme MP. 1999. Partitioning of reserve and newly assimilated carbon in roots and leaf tissues of *Lolium perenne* during regrowth after defoliation: assessment by ^{13}C steady-state labelling and carbohydrate analysis. *Plant Cell Environ* **22**: 1097-1108.

Munns R, Cramer GR. 1996. Is coordination of leaf and root growth mediated by abscisic acid? Opinion. *Plant Soil* **185**: 33-49.

Navarro C, Abelenda JA, Cruz-Oró E, Cuéllar CA, Tamaki S, Silva J, Shimamoto K, Prat S. 2011. Control of flowering and storage organ formation in potato by FLOWERING LOCUS T. *Nature* **478**: 119.

Neumann PM, Azaizeh H, Leon D. 1994. Hardening of root cell walls: a growth inhibitory response to salinity stress. *Plant Cell Environ* **17**: 303-309.

Okamoto A, Katsumi M, Okamoto H. 1995. The effects of auxin on the mechanical properties *in vivo* of cell wall in hypocotyl segments from gibberellin-deficient cowpea seedlings. *Plant Cell Physiol* **36**: 645-651.

Okamoto A, Okamoto H. 1995. Two proteins regulate the cell wall extensibility and the yield threshold in glycerinated hollow cylinders of cowpea hypocotyl. *Plant Cell Environ* **18**: 827-830.

Oleghe E, Naveed M, Baggs EM, Hallett PD. 2017. Plant exudates improve the mechanical conditions for root penetration through compacted soils. *Plant Soil* **421**: 19-30.

Onoda Y, Wright IJ, Evans JR, Hikosaka K, Kitajima K, Niinemets Ü, Poorter H, Tosens T, Westoby M. 2017. Physiological and structural tradeoffs underlying the leaf economics spectrum. *New Phytol* **214**: 1447–1463.

Osone Y, Ishida A, Tateno M. 2008. Correlation between relative growth rate and specific leaf area requires associations of specific leaf area with nitrogen absorption rate of roots. *New Phytol* **179**: 417-427.

Passioura J. 1988. Root signals control leaf expansion in wheat seedlings growing in drying soil. *Funct Plant Biol* **15**: 687-693.

Passioura JB. 1994. The physical chemistry of the primary cell wall: implications for the control of expansion rate. *J Exp Bot* **45**: 1675-1682.

Pate JS, Jeschke WD. 1993. Mineral uptake and transport in xylem and phloem of the proteaceous tree, *Banksia prionotes*. *Plant Soil* **155–156**: 273–276.

Peeters AJM, Cox MCH, Benschop JJ, Vreeburg RAM, Bou J, Voesenek LACJ. 2002. Submergence research using *Rumex palustris* as a model; looking back and going forward. *J Exp Bot* **53**: 391–398.

Peng J, Harberd NP. 1997. Gibberellin deficiency and response mutations suppress the stem elongation phenotype of phytochrome-deficient mutants of *Arabidopsis*. *Plant Physiol* **113**: 1051–1058.

Pons TL 2016. Regulation of leaf traits in canopy gradients. In: Hikosaka K, Niinemets Ü, Anten NPR eds. *Canopy Photosynthesis: From Basics to Applications*. Dordrecht: Springer Netherlands, 143–168.

Pons TL, Bergkotte M. 1996. Nitrogen allocation in response to partial shading of a plant: possible mechanisms. *Physiol Plant* **98**: 571–577.

Poorter H, Gifford R, M, Kriedemann P, E, Wong S, C. 1992. A quantitative-analysis of dark respiration and carbon content as factors in the growth-response of plants to elevated CO_2. *Aust J Bot* **40**: 501–513.

Poorter H, Niinemets Ü, Ntagkas N, Siebenkäs A, Mäenpää M, Matsubara S, Pons T. 2019. A meta-analysis of plant responses to light intensity for 70 traits ranging from molecules to whole plant performance. *New Phytol* **0**.

Poorter H, Niinemets Ü, Poorter L, Wright I, J**, Villar R. 2009.** Causes and consequences of variation in leaf mass per area (LMA): a meta-analysis. *New Phytol* **182**: 565–588.

Poorter H, Remkes C. 1990. Leaf area ratio and net assimilation rate of 24 wild species differing in relative growth rate. *Oecologia* **83**: 553–559.

Poorter H, Remkes C, Lambers H. 1990. Carbon and nitrogen economy of 24 wild species differing in relative growth rate. *Plant Physiol* **94**: 621–627.

Poorter H, Roumet C, Campbell BD 1996. Interspecific variation in the growth response of plants to elevated CO_2: a search for functional types. In: Körner C, Bazzaz FA eds. *Biological Diversity in a CO_2 Rich World Physiological Ecology Series*. San Diego: Academic Press, 375–412.

Poorter H, Van de Vijver C, Boot R, Lambers H. 1995. Growth and carbon economy of a fast-growing and a

slow-growing grass species as dependent on nitrate supply. *Plant Soil* **171**: 217–227.

Poot P, Lambers H. 2003. Are trade-offs in allocation pattern and root morphology related to species abundance? A congeneric comparison between rare and common species in the south-western Australian flora. *J Ecol* **91**: 58–67.

Poot P, Lambers H. 2008. Shallow-soil endemics: adaptive advantages and constraints of a specialized root-system morphology. *New Phytol* **178**: 371–381.

Postma JA, Lynch JP. 2011. Theoretical evidence for the functional benefit of root cortical aerenchyma in soils with low phosphorus availability. *Ann Bot* **107**: 829–841.

Pritchard J. 1994. The control of cell expansion in roots. *New Phytol* **127**: 3–26.

Pritchard J, Fricke W, Tomos D. 1996. Turgor-regulation during extension growth and osmotic stress of maize roots. An example of single-cell mapping. *Plant Soil* **187**: 11–21.

Rapoport HF, Loomis RS. 1985. Interaction of storage root and shoot in grafted sugarbeet and chard. *Crop Sci* **25**: 1079–1084.

Reich PB, Uhl C, Walters MB, Ellsworth DS. 1991. Leaf lifespan as a determinant of leaf structure and function among 23 amazonian tree species. *Oecologia* **86**: 16–24.

Reich PB, Walters MB, Ellsworth DS. 1992. Leaf lifespan in relation to leaf, plant, and stand characteristics among diverse ecosystems. *Ecol Monogr* **62**: 365–392.

Reski R. 2006. Small molecules on the move: homeostasis, crosstalk, and molecular action of phytohormones. *Plant Biol* **8**: 277–280.

Rosnitschek-Schimmel I. 1983. Biomass and nitrogen partitioning in a perennial and an annual nitrophilic species of *Urtica*. *Zeitschrift für Pflanzenphysiologie* **109**: 215–225.

Ruiz-Robleto J, Villar R. 2005. Relative growth rate and biomass allocation in ten woody species with different leaf longevity using phylogenetic independent contrasts (PICs). *Plant Biol* **7**: 484–494.

Ryser P, Eek L. 2000. Consequences of phenotypic plasticity vs. interspecific differences in leaf and root traits for acquisition of aboveground and belowground resources. *Am J Bot* **87**: 402–411.

Ryser P, Lambers H. 1995. Root and leaf attributes accounting for the performance of fast- and slow-growing grasses at different nutrient supply. *Plant Soil* **170**: 251–265.

Saab IN, Sachs MM. 1996. A flooding-Induced xyloglucan endo-transglycosylase homolog in maize is responsive to ethylene and associated with aerenchyma. *Plant Physiol* **112**: 385–391.

Saab IN, Sharp RE, Pritchard J, Voetberg GS. 1990. Increased endogenous abscisic acid maintains primary root growth and inhibits shoot growth of maize seedlings at low water potentials. *Plant Physiol* **93**: 1329–1336.

Sauter JJ, van Cleve B. 1991. Biochemical, immunochemical, and ultrastructural studies of protein storage in poplar(*Populus* × *canadensis* 'robusta') wood. *Planta* **183**: 92–100.

Scheible W-R, Lauerer M, Schulze E-D, Caboche M, Stitt M. 1997. Accumulation of nitrate in the shoot acts as a signal to regulate shoot-root allocation in tobacco. *Plant J* **11**: 671–691.

Schnyder H, de Visser R. 1999. Fluxes of reserve-derived and currently assimilated carbon and nitrogen in perennial ryegrass recovering from defoliation. The regrowing tiller and its component functionally distinct zones. *Plant Physiol* **119**: 1423–1436.

Sharp RE. 2002. Interaction with ethylene: changing views on the role of abscisic acid in root and shoot growth responses to water stress. *Plant Cell Environ* **25**: 211–222.

Sharp RE, Poroyko V, Hejlek LG, Spollen WG, Springer GK, Bohnert HJ, Nguyen HT. 2004. Root growth maintenance during water deficits: physiology to functional genomics. *J Exp Bot* **55**: 2343–2351.

Siefritz F, Otto B, Bienert GP, Van Der Krol A, Kaldenhoff R. 2004. The plasma membrane aquaporin NtAQP1 is a key component of the leaf unfolding mechanism in tobacco. *Plant J* **37**: 147–155.

Simpson RJ, Lambers H, Dalling MJ. 1982a. Kinetin application to roots and its effect on uptake, translocation and distribution of nitrogen in wheat (*Triticum aestivum*) grown with a split root system. *Physiol Plant* **56**: 430–435.

Simpson RJ, Lambers H, Dalling MJ. 1982b. Translocation of nitrogen in a vegetative wheat plant (*Triticum aestivum*). *Physiol Plant* **56**: 11–17.

Simpson RJ, Lambers H, Dalling MJ. 1983. Nitrogen redistribution during grain growth in wheat (*Triticum aestivum* L.): IV. Development of a quantitative model of the translocation of nitrogen to the grain. *Plant Physiol* **71**: 7–14.

Sinclair TR. 1998. Historical changes in harvest index and crop nitrogen accumulation. *Crop Sci* **38**: 638–643.

Smith H 1981. Adaptation to shade. In: Johnson CB ed. *Physiological Processes Limiting Plant Productivity*. London: Butterworths, 159–173.

Smith H. 2000. Phytochromes and light signal perception by plants—an emerging synthesis. *Nature* **407**: 585.

Staswick PE. 1990. Novel regulation of vegetative storage protein genes. *Plant cell* **2**: 1–6.

Staswick PE, Huang J-F, Rhee Y. 1991. Nitrogen and methyl jasmonate induction of soybean vegetative storage protein genes. *Plant Physiol* **96**: 130–136.

Steinaker DF, Wilson SD. 2008. Phenology of fine roots and leaves in forest and grassland. *J Ecol* **96**: 1222–1229.

Steingrobe B. 2005. A sensitivity analysis for assessing the relevance of fine-root turnover for P and K uptake. *J Plant Nutr Soil Sci* **168**: 496–502.

Steingröver E. 1981. The relationship between cyanide-resistant root respiration and the storage of sugars in the taproot in *Daucus carota* L. *J Exp Bot* **32**: 911–919.

Stirzaker RJ, Passioura JB, Wilms Y. 1996. Soil structure and plant growth: impact of bulk density and biopores. *Plant Soil* **185**: 151–162.

Stulen I, den Hertog J. 1993. Root growth and functioning under atmospheric CO_2 enrichment. *Vegetatio* **104**: 99–115.

Sun T-P, Gubler F. 2004. Molecular mechanism of gibberellin signaling in plants. *Annu Rev Plant Biol* **55**: 197–223.

Takahashi D, Imai H, Kawamura Y, Uemura M. 2016. Lipid profiles of detergent resistant fractions of the plasma membrane in oat and rye in association with cold acclimation and freezing tolerance. *Cryobiology* **72**: 123–134.

Tardieu F, Zhang J, Katerji N, Bethenod O, Palmer S, Davies WJ. 1992. Xylem ABA controls the stomatal conductance of field-grown maize subjected to soil compaction or soil drying. *Plant Cell Environ* **15**: 193–197.

Terashima I, Hanba YT, Tazoe Y, Vyas P, Yano S. 2006. Irradiance and phenotype: comparative eco-development of sun and shade leaves in relation to photosynthetic CO_2 diffusion. *J Exp Bot* **57**: 343–354.

Ternesi M, Andrade AP, Jorrin J, Benlloch M. 1994. Root-shoot signalling in sunflower plants with confined root systems. *Plant Soil* **166**: 31–36.

Terrer C, Vicca S, Hungate BA, Phillips RP, Prentice IC. 2016. Mycorrhizal association as a primary control of the CO_2 fertilization effect. *Science* **353**: 72–74.

Terrer C, Vicca S, Stocker BD, Hungate BA, Phillips RP, Reich PB, Finzi AC, Prentice IC. 2018. Ecosystem responses to elevated CO_2 governed by plant–soil interactions and the cost of nitrogen acquisition. *New Phytol* **217**: 507–522.

Terry N. 1970. Devlopmental physiology of sugar-Beet: II. Effects of temperature and nitrogen supply on the growth, soluble carbohydrate content and nitrogen content of leaves and roots. *J Exp Bot* **21**: 477–496.

Thonat C, Mathieu C, Crevecoeur M, Penel C, Gaspar T, Boyer N. 1997. Effects of a mechanical stimulation on localization of annexin-like proteins in *Bryonia dioica* internodes. *Plant Physiol* **114**: 981–988.

Tomlinson KW, Poorter L, Bongers F, Borghetti F, Jacobs L, van Langevelde F. 2014. Relative growth rate variation of evergreen and deciduous savanna tree species is driven by different traits. *Ann Bot* **114**: 315–324.

Touraine B, Clarkson DT, Muller B 1994. Regulation of nitrate uptake at the whole plant level. In: Roy J, Garnier E eds. *A Whole Plant Perspective on Carbon-Nitrogen Interactions*. The Hague: SPB Academic Publishing, 11–30.

Tyerman SD, Niemietz CM, Bramley H. 2002. Plant aquaporins: multifunctional water and solute channels with expanding roles. *Plant Cell Environ* **25**: 173–194.

Van Arendonk JJCM, Niemann GJ, Boon JJ, Lambers H. 1997. Effects of nitrogen supply on the anatomy and chemical composition of leaves of four grass species belonging to the genus *Poa*, as determined by image-processing analysis and pyrolysis-mass spectrometry. *Plant Cell Environ* **20**: 881–897.

Van den Boogaard R**, Goubitz S, Veneklaas EJ, Lambers H. 1996.** Carbon and nitrogen economy of four Triticum aestivum cultivars differing in relative growth rate and water use efficiency. *Plant Cell Environ* **19**: 998–1004.

Van den Ende W. 2013. Multifunctional fructans and raffinose family oligosaccharides. *Front Plant Sci* **4**: 247.

Van Volkenburgh E 1994. Leaf and shoot growth In: Boote KJ, Bennet JM, Sinclair TR, Paulsen GM eds. *Physiology and determination of crop yield*. Madison: American Society of Agronomy, Crop Science Society of America, Soil Science Society of America, 101–120.

Van Volkenburgh E, Boyer JS. 1985. Inhibitory effects of water deficit on maize leaf elongation. *Plant Physiol* **77**: 190–194.

Villar R, Ruíz-Robleto J, De Jong Y, Poorter H. 2006. Differences in construction costs and chemical composition between deciduous and evergreen woody species are small as compared to differences among families. *Plant Cell Environ* **29**: 1629–1643.

Villar R, Ruiz-Robleto J, Ubera JL, Poorter H. 2013. Exploring variation in leaf mass per area (LMA) from leaf to cell: an anatomical analysis of 26 woody species. *Am J Bot* **100**: 1969–1980.

Visser E, Cohen JD, Barendse G, Blom C, Voesenek L. 1996. An ethylene-mediated increase in sensitivity to auxin induces adventitious root formation in flooded *Rumex palustris* Sm. *Plant Physiol* **112**: 1687–1692.

Visser EJW, Colmer TD, Blom CWPM, Voesenek LACJ. 2000. Changes in growth, porosity, and radial oxygen loss from adventitious roots of selected mono- and dicotyledonous wetland species with contrasting types of aerenchyma. *Plant Cell Environ* **23**: 1237–1245.

Voesenek LACJ, Bailey-Serres J. 2015. Flood adaptive traits and processes: an overview. *New Phytol* **206**: 57–73.

Voesenek LACJ, Benschop JJ, Bou J, Cox MCH, W. GH, Millenaar FF, Vreeburg RAM, Peeters AJM. 2003. Interactions between plant hormones regulate submergence-induced shoot elongation in the flooding-tolerant dicot *Rumex palustris*. *Ann Bot* **91**: 205–211.

Voesenek LACJ, Colmer TD, Pierik R, Millenaar FF, Peeters AJM. 2006. How plants cope with complete submergence. *New Phytol* **170**: 213–226.

Wahl S, Ryser P. 2000. Root tissue structure is linked to ecological strategies of grasses. *New Phytol* **148**: 459–471.

Weemstra M, Mommer L, Visser EJW, van Ruijven J, Kuyper TW, Mohren GMJ, Sterck FJ. 2016. Towards a multidimensional root trait framework: a tree root review. *New Phytol* **211**: 1159–1169.

Went FW. 1926. On growth-accelerating substances in the coleoptile of *Avena sativa*. *Proceedings of the Koninklijke Nederlandse Academie van Wetenschappen Series C* **30**: 10–19.

Whitford R, Fernandez A, Tejos R, Pérez Amparo C, Kleine-Vehn J, Vanneste S, Drozdzecki A, Leitner J, Abas L, Aerts M, Hoogewijs K, Baster P, De Groodt R, Lin Y-C, Storme V, Van de Peer Y, Beeckman T, Madder A, Devreese B, Luschnig C, Friml J, Hilson P. 2012. GOLVEN secretory peptides regulate auxin carrier turnover during plant gravitropic responses. *Developmental Cell* **22**: 678–685.

Witkowski ETF, Lamont BB. 1991. Leaf specific mass confounds leaf density and thickness. *Oecologia* **88**: 486–493.

Woo HR, Masclaux-Daubresse C, Lim PO. 2018. Plant senescence: how plants know when and how to die. *J Exp Bot* **69**: 715–718.

Wright IJ, Reich PB, Cornelissen JHC, Falster DS, Groom PK, Hikosaka K, Lee W, Lusk CH, Niinemets Ü, Oleksyn J, Osada N, Poorter H, Warton DI, Westoby M. 2005. Modulation of leaf economic traits and trait relationships by climate. *Glob Ecol Biogeogr* **14**: 411–421.

Wu H-C, Bulgakov VP, Jinn T-L. 2018. Pectin methylesterases: cell wall remodeling proteins are required for plant response to heat stress. *Front Plant Sci* **9**: 1612–1612.

Yan Y-S, Chen X-Y, Yang K, Sun Z-X, Fu Y-P, Zhang Y-M, Fang R-X. 2011. Overexpression of an F-box protein gene reduces abiotic stress tolerance and promotes root growth in rice. *Mol Plant* **4**: 190–197.

Yano M, Terashima I. 2004. Developmental process of sun and shade leaves in *Chenopodium album* L. *Plant Cell Environ* **27**: 781–793.

Yano S, Terashima I. 2001. Separate localization of light signal perception for sun or shade type chloroplast and palisade tissue differentiation in *Chenopodium album*. *Plant Cell Physiol* **42**: 1303–1310.

Yokota T. 1997. The structure, biosynthesis and function of brassinosteroids. *Trends Plant Sci* **2**: 137–143.

Zhou Y, Sarker U, Neumann G, Ludewig U. 2019. The LaCEP1 peptide modulates cluster root morphology in *Lupinus albus*. *Physiol Plant* **166**: 525–537.

Zhu GL, Boyer JS. 1992. Enlargement in *Chara* studied with a turgor clamp. Growth rate is not determined by turgor. *Plant Physiol* **100**: 2071–2080.

Zörb C, Mühling KH, Kutschera U, Geilfus C-M. 2015. Salinity stiffens the epidermal cell walls of salt-stressed maize leaves: is the epidermis growth-restricting? *PLoS ONE* **10**: e0118406.

Life Cycles: Environmental Influences and Adaptations

11

11.1 Introduction

Previous chapters have emphasized the physiological responses of mature plants to their environment. The environmental stresses encountered and optimal physiological solutions, however, can change dramatically as plants develop from the seedling to vegetative and reproductive phases. Following germination, most species pass through several distinctive life phases: **seedling** (loosely defined as the stage during which cotyledons are still present), **vegetative** (sometimes with a juvenile phase preceding the adult phase), and **reproductive**. This chapter addresses the major ecophysiological changes that occur in the life cycles of plants. These involve changes in **development** (*i.e.* the initiation and occurrence of organs), **phenology** (*i.e.* the progress of plants through identifiable stages of development), and **allocation of resources** to different plant parts. We discuss the pattern and duration of developmental phases as dependent on environmental conditions and pattern of acclimation to specific conditions. The developmental pattern also varies genetically which may reflect adaptations to specific abiotic or biotic environments. This chapter discusses plant development and processes associated with transition between developmental stages.

11.2 Seed Dormancy, Quiescence, and Germination

Germination includes those events that commence with **imbibition** of water by the quiescent usually dry seed, and terminate with the elongation of the embryonic axis which usually can be determined upon radicle protrusion. Germination marks the transition between two developmental stages of a plant: **seed** and **seedling**. The seed has a package of food reserves that makes it largely independent of environmental resources for its survival. This changes dramatically in the photoautotrophic seedling, which depends on a supply of light, CO_2, water, and inorganic nutrients from its surroundings for autotrophic growth, *i.e.* the phase when the seedling has become independent of maternal reserves. In this section, we discuss the mechanisms by which some seeds sense the suitability of the future seedling's environment. For example, how does a seed acquire information about the expected light, nutrient, and water availabilities?

Germination is the process when part of the embryo, usually the radicle, penetrates the seed coat and may proceed with adequate water and O_2, and at a suitable temperature. **Dormancy** is defined as the incapacity of an intact viable seed to complete germination under favorable conditions (Née et al. 2017). Dormancy thus

H. Lambers, R. S. Oliveira, *Plant Physiological Ecology*, https://doi.org/10.1007/978-3-030-29639-1_11

effectively spreads germination in both time and space. Conditions required to break dormancy and allow subsequent germination are often quite different from those that are favorable for growth or survival of the autotrophic life stage of a plant. Nondormant seeds are common in wet tropical forests, whereas dormancy should be evolutionarily stable in temperate lineages with small seeds. When the favorable season is fleeting, seed dormancy is the only adaptive strategy (Rubio de Casas et al. 2017).

Timing of seed germination can be critical for the survival of natural plant populations, and dormancy mechanisms play a major role in such timing (Donohue 2005). These mechanisms are pronounced in many **ruderals** and other species from habitats that are subject to disturbance. Many trees, particularly temperate and tropical species from undisturbed forest, lack dormancy, and their large seeds often do not tolerate desiccation. The germination of these **recalcitrant** seeds typically occurs quickly after dispersal. Recalcitrant seeds rapidly lose viability when dried and storage of such seeds is notoriously difficult (Berjak and Pammenter 2008). Some seeds are **viviparous**; they germinate prior to, or coincident with, abscission from the maternal plant (*e.g.*, seeds of many mangroves, seagrasses, and coastal cacti) (Farnsworth and Farrant 1998; Cota-Sánchez et al. 2007).

In a dormant seed, the chain of events that leads to germination of the seed is blocked. This block, and hence dormancy itself, can be relieved by a specific factor (*e.g.*, temperature); once dormancy has been relieved, germination can be stimulated by specific factors (*e.g.*, light, smoke) (Thompson and Ooi 2010). In some cases, environmental factors, such as the absence of light, NO_3^-, and/or a diurnally fluctuating temperature, may prevent seeds from germinating (**enforced dormancy** or **quiescence**) (Baskin and Baskin 2014). The term dormancy is used here, because these environmental factors function as an environmental signal that removes a block leading to germination, rather than being involved in metabolism, as is the case for environmental factors such as water, O_2, and temperature (Finch-Savage and Leubner-Metzger 2006). This form of dormancy is relieved as soon as the signal is present. Quiescence is not considered a form of dormancy, but a mechanism that prevents germination (Baskin and Baskin 2004). We consider seeds to be in a dormant state when they do not germinate, even if given favorable conditions for germination. Breaking of this type of dormancy occurs gradually, over weeks, months, or even longer. Seeds may be dormant upon release from the mother plant (**primary** or **innate dormancy**), and dormancy can also be induced in seeds after they have become nondormant (**secondary** or **induced dormancy**), if conditions become unfavorable for germination. Transitions among the various forms of dormancy are illustrated in Fig. 11.1. Various regulators like plant hormones and dormancy proteins control the induction and release of dormancy. The relative strengths of these regulators are influenced by environmental factors during seed maturation and storage (Née et al. 2017).

Baskin and Baskin (2014) distinguish five classes of primary dormancy. **Physiological dormancy** (PD) refers to physiological mechanisms in the embryo and/or its surrounding structures (endosperm, seed coat) that prevent radicle emergence. **Morphological dormancy** (MD) is considered the ancestral state (Willis et al. 2014). Seeds with morphological dormancy have small underdeveloped or even undifferentiated embryos; germination will only occur until growth and development have proceeded until a predefined stage. Seeds with hard coats that are impermeable to water have **physical dormancy** (PY). Separate classes are reserved for combinations of physiological with morphological dormancy [**morphophysiological dormancy** (MPD)] and physiological with physical dormancy [**combinational dormancy** (PD + PY). Physiological dormancy at a nondeep level is the most common kind of dormancy in seed banks in temperate climates, and occurs in gymnosperms and in all major clades of angiosperms (Willis et al. 2014).

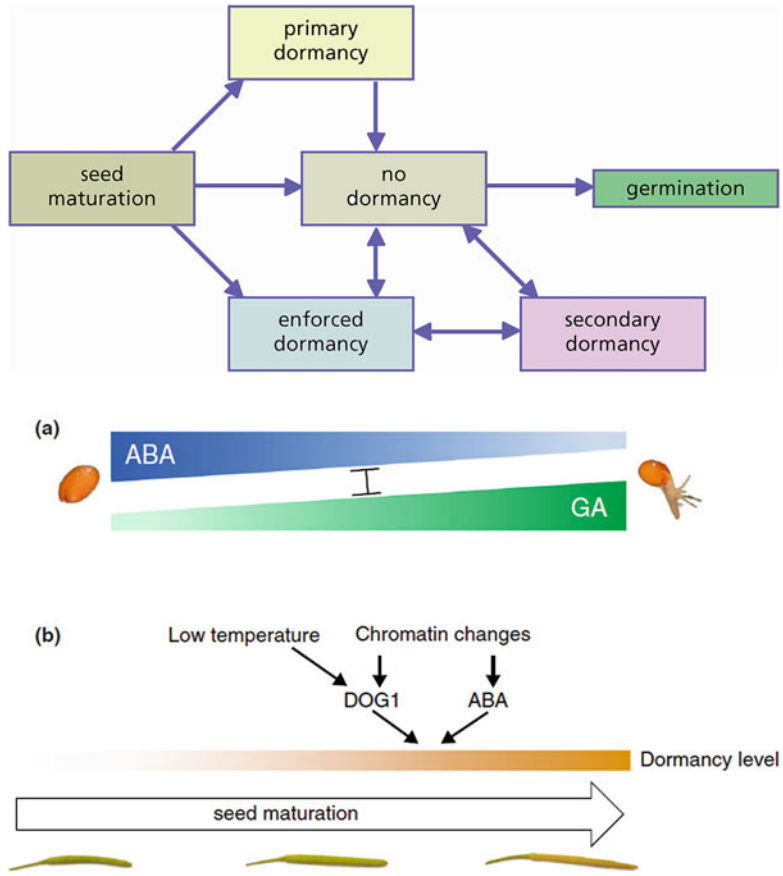

Fig. 11.1 (Top) Schematic representation of changes in dormancy after seed maturation. (Bottom) The roles of environmental and endogenous factors in seed dormancy. (**A**) Dormancy and germination are regulated by the balance between abscisic acid (ABA) and gibberellic acid (GA). (**B**) Factors controlling the induction of dormancy during seed maturation. Both environmental (temperature) and developmental (chromatin changes) factors regulate the dormancy protein DOG1 and the hormone ABA. Representative siliques of *Arabidopsis thaliana* (thale cress) are shown below the seed maturation arrow. The intensity of the colors in the bars indicates the strength of the indicated processes and factors. Arrows indicate positive and stop bars negative effects (Née et al. 2017; copyright Elsevier Science, Ltd.).

11.2.1 Hard Seed Coats

The hard **seed coat** of many species (*e.g.*, Fabaceae, Malvaceae, and Geraniaceae) can prevent germination because it is largely impermeable to water (physical dormancy) (Baskin and Baskin 2014). Water uptake occurs only when the seed coat is sufficiently deteriorated; imbibition increases with the degree of damage to the seed coat, *e.g.*, in *Coronilla varia* (purple crown vetch) seeds (Fig. 11.2). In *Pelargonium* species with hard seed coats, palisade cells effectively close the site where water will ultimately enter the seed, whereas soft seeds form a wide opening at this site (Meisert et al. 1999).

Hard seed coats that are permeable to water do not represent a real mechanical barrier for outgrowth of the embryo in nondormant seeds (Baskin and Baskin 2014), but merely protect it. In other seeds, the seed coat is not hard, but the outer layers such as the endosperm and seed coat can represent a mechanical barrier in combination with the force exerted by the embryo (coat-imposed dormancy). The balance in strength of the two opposing forces determines whether the radicle will break through. This balance is subject

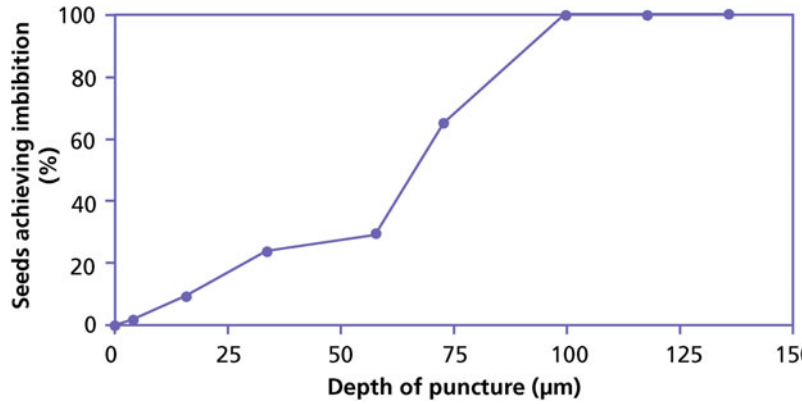

Fig. 11.2 Impermeability of the seed coat of *Coronilla varia* (purple crown vetch). The seed coat was pierced to varying depths by a 0.4 mm diameter indentor, after which the seeds were left to imbibe on moist filter paper. (After McKee et al. 1977).

to regulation and an important mechanism involved in physiological dormancy (Sect. 11.2.7).

Deterioration of the seed coat may be due to microbial breakdown, when seeds are buried in soil. It may also be due to physical processes, such as exposure to strong temperature fluctuations at the soil surface, as occurs in tropical forest gaps, with seed persistence in the soil seed bank allowing trees to recruit even decades after dispersal (Zalamea et al. 2015). In both conditions, the breakdown of the seed coat is gradual, and, consequently, germination is spread in time. Exposure to short periods of high temperatures, such as during a fire (approximately 100 °C) may lead to synchronous breaking of dormancy. However, temperature can easily become lethal in intense fires or when seeds are at the soil surface. Another mechanism that stimulates germination after fire is related to specific chemicals in smoke (Sect. 11.2.4).

In the seed coat, there is a preformed 'weak site', *e.g.*, the **strophiole** in Fabaceae, where tissue degradation first occurs and through which water uptake starts. Dormancy associated with constraining tissues often complicates germination for plant cultivation purposes. It can be relieved artificially in hard-coated seeds by boiling, mechanical (sanding or breaking the seed coat), or chemical (concentrated sulfuric acid) treatments.

11.2.2 Germination Inhibitors in the Seed

Arid climates are characterized by little precipitation, often concentrated in just a few unpredictable showers. After such a shower, massive seed germination of short-lived plants may occur. How can the seeds perceive that the environment has become more favorable for germination and growth? A common trait of many species germinating under such conditions is the presence of **water-soluble inhibitors** in the pericarp (*i.e.* the matured ovulary wall, including seed coat and attached parts of the fruit). Light rain may not fully remove these inhibitors, so germination cannot take place (Fig. 11.3). Germination occurs only after a major rainfall event or prolonged rain that elutes the inhibitor; in this case the emerged seedling has access to sufficient water to enhance its chances to survive and complete its life cycle (Koller and Negbi 1959). Following moderate rains, those seeds that fail to germinate synthesize additional inhibitors; therefore, subsequent rains must still be substantial to trigger germination.

Germination inhibitors also play an important role in preventing germination of seeds in fleshy fruits. These inhibitors can be general (*e.g.*, high solute concentration of many fruits) or highly specific such as lipids, glycoalkaloids, coumarin, abscisic acid (ABA), HCN (Samuels and Levey

2005). For example, ABA inhibits the germination of the seeds of *Solanum lycopersicum* (tomato) in combination with osmotic strength, as illustrated by seed germination inside the fruit of ABA-deficient mutants (Hilhorst and Karssen 1992). Passage through an animal's gut may remove the inhibitors (Samuels and Levey 2005). ABA levels are consistently lower in embryos of **viviparous** mangrove species than in related nonviviparous nonmangrove species (Farnsworth and Farrant 1998).

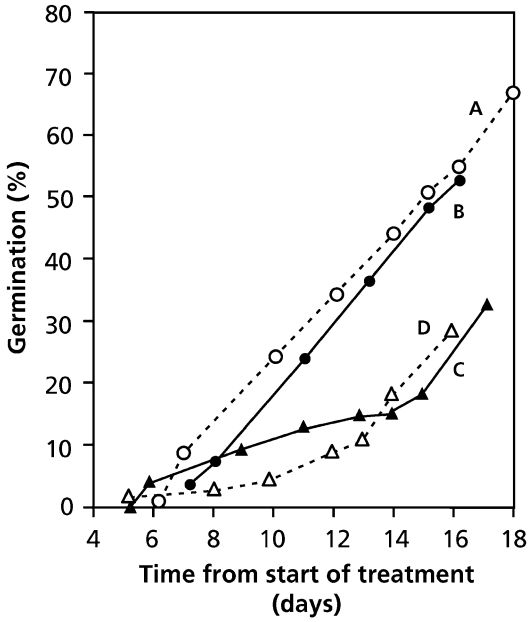

Fig. 11.3 Time course of germination of *Oryzopsis miliacea* (smilograss) as affected by duration of a drip treatment. The origin of the x-axis represents the start of the drip treatment. Curves A, B, C, and D refer to a duration of the treatment of 93, 72, 48, and 24 h, respectively. Control seeds did not germinate (Koller and Negbi 1959. Copyright Ecological Society of America.

11.2.3 Effects of Nitrate

Nitrate stimulates germination of many seeds of **ruderal** species (Hesse 1924; He et al. 2016). This role of NO_3^- as an environmental trigger is not associated with a need for NO_3^- for protein synthesis, because mutants lacking nitrate reductase activity also exhibit such stimulation (Fig. 11.4). A specific protein is essential for NO_3^--promoted seed germination in *Arabidopsis thaliana* (thale cress). Seed germination in mutants that lack this protein does not respond to NO_3^-. The protein is responsible for a decrease in **ABA** levels in a NO_3^--dependent manner and directly binds to a promoter, encoding an enzyme that breaks down ABA. The protein localizes to nuclei and it appears that seeds have a unique mechanism for **NO_3^- signaling** (Yan et al. 2016).

Why would weedy and ruderal species use NO_3^- as an environmental cue? A **NO_3^- requirement** may function as a mechanism to

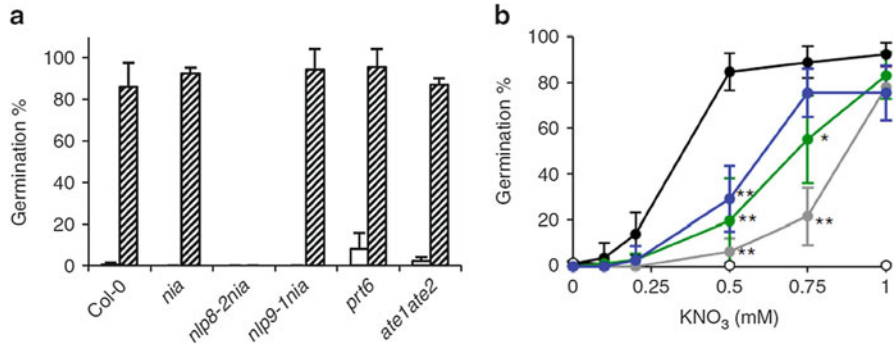

Fig. 11.4 (**A**) Germination of *nia1nia2* nitrate reductase mutant (*nia*), *nlp8–2nia1nia2* (*nlp8–2nia*) and *nlp9-1nia1nia2* (*nlp9-1nia*) triple mutants, NO-insensitive *ate1ate2* and *prt6* mutants with or without nitrate. Percentage of germination is shown. A white and blue bar indicates percentage of germination in water with 1 mM KCl and KNO_3, respectively. (**B**) Nitrate dose responses of nitrate transceptor mutant lines, *chl1–5*, *T101A/chl1–5* and *T101D/chl1–5*, and the *nlp8–2* mutant during seed germination. Percentage of germination is shown. Wild-type, black; *chl1–5,* gray; *T101A/chl1–5*, green; *T101D/chl1–5*, blue; *nlp8–2*, red (after Yan et al. 2016).

detect a **gap in the vegetation**, just like the perception of other environmental variables, *e.g.*, light and diurnal temperature fluctuation, which are involved in release from quiescence. Seeds in soil where a large plant biomass depletes soil NO_3^- experience a low-NO_3^- environment, which enforces quiescence. When the above-ground vegetation is destroyed, mineralization and nitrification continue, but absorption by plants declines. This increases soil NO_3^- concentrations to levels that can stimulate germination as shown for seeds of *Plantago lanceolata* (snake plantain) buried in grassland in open patches and between the grass (Pons 1989).

11.2.4 Other External Chemical Signals

Various compounds in the natural environment of seeds may have stimulating or inhibiting effects on seed germination (Finkelstein et al. 2008). We often cannot explain inhibition of germination of buried seeds by the absence of light or alternating temperatures alone. The gaseous environment may play a role (low O_2 and high CO_2 concentrations), and in some cases specific organic compounds such as leachates from living or decaying plant material contain **allelochemicals** (Sect. 13.2) inhibit seed germination, *e.g.*, in *Nicotiana attenuata* (Indian tobacco) in response to *Artemisia tridentata* (sagebush), which releases methyl jasmonate (Preston et al. 2002).

Germination can be stimulated by **smoke** derived from the combustion of plant material; this stimulates seed germination of *Audouinia capitata*, a fire-dependent South African fynbos species (De Lange and Boucher 1990). Exposure of dormant seeds to cold smoke derived from burnt vegetation also promotes seed germination of many species from the English moorlands, the California chaparral in USA, and Western Australian sandplains (Nelson et al. 2012). The main compound that triggers germination in most smoke-sensitive seeds is **karrikinolide** (Flematti et al. 2004). Some smoke-sensitive species that are unresponsive to karrikinolide respond to another minor component of smoke, cyanohydrins, which release cyanide (Nelson et al. 2012). Triggering of germination by karrikinolide is not restricted to plants in fire-dominated ecosystems, but also includes several crop and weed species that have evolved in ecosystems where fire is not an ecological trigger. Karrikinolides mimic an endogenous compound that has roles in seed germination and early plant development (Flematti et al. 2015). The endogenous signaling compound is presumably not only similar to karrikinolides, but also to the related **strigolactones** (Fig. 11.5). Commercial 'smoke'

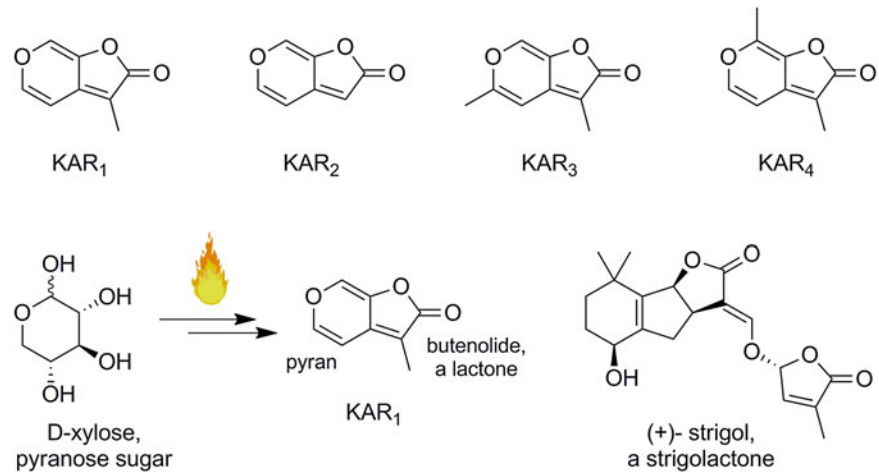

Fig. 11.5 The karrikin family. The first karrikin discovered was KAR1, known as karrikinolide. Since karrikins can be produced by burning sugars such as xylose, the pyran ring of karrikins is probably derived from such pyranose sugars. Both karrikins and strigolactones such as strigol have a butenolide ring (Flematti et al. 2015).

products are available to enhance the germination of seeds that are difficult to germinate (Roche et al. 1997).

11.2.5 Effects of Light

Light is an important factor stimulating seed germination (Footitt et al. 2013). A wide variety of light responses have been described. These depend strongly on other environmental conditions, such as temperature, water potential, and nitrate, and on prior conditions, such as temperature regime, and include conditions to which the parent plant was exposed.

The light climate under natural conditions has many components, some of which affect seed germination. We can distinguish three major types of light responses.

1. A **light requirement** prevents germination of seeds that are buried too deeply in soil. Such seeds germinate only when exposed to **light**, and thus do not germinate below a soil depth where no light penetrates. This prevents 'fatal germination' of the predominantly small seeds in which this mechanism is most common (Milberg et al. 2000). Germination occurs only when the seeds reach the soil surface where they are exposed to light. This often coincides with damage or the complete disappearance of the established vegetation. The emergent seedlings thus have a more favorable position with respect to established plants than they would have otherwise.
2. **Light intensity and duration of exposure** (photon dose, integrated over a period of time) determine if seeds will germinate. A steep light gradient exists near the soil surface. Seeds of some species [*e.g.*, *Digitalis pupurea* (foxglove)] germinate at the extremely low intensity prevailing at 10 mm depth in sand (0.026 μmol m^{-2} s^{-1}), whereas others [*e.g.*, *Chenopodium album* (lambsquarters)] do not germinate below 2 mm (Bliss and Smith 1985). The very low photon dose required by buried weed seeds is also illustrated by their emergence after soil cultivation in light, but not in darkness, with an estimated exposure time of about 0.2 s (Scopel et al. 1994). Other species, *e.g.*, *Plantago major* (common plantain) require much longer or repeated exposures (Pons 1991b). A high light sensitivity may provide more certainty of germination after a disturbance event, but increases the probability of fatal germination after reburial.
3. The **spectral composition** of daylight as modified by a leaf canopy also influences the **timing of germination after disturbance** of vegetation. Light under a leaf canopy is depleted in red compared with that above the canopy (Fig. 11.6), resulting in a low red:far-red ratio. This inhibits germination in many species (Fig. 11.7). This is particularly important shortly after seed shedding, when conditions might otherwise be suitable for germination. The seeds may subsequently get mixed into the soil, where a light-requirement further enforces dormancy, and where the risks of predation are smaller than at the soil surface. Litter, especially dry litter, also decreases the red/far-red ratio, which further reduces the probability of germination (Vazquez-Yanes et al. 1990).

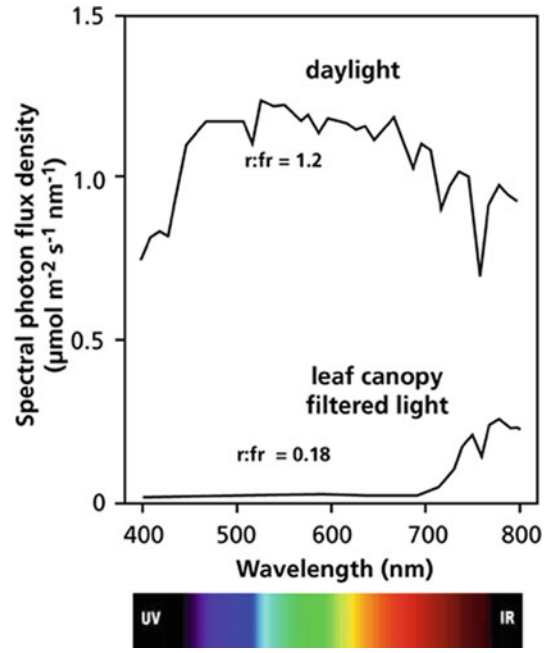

Fig. 11.6 The spectral energy distribution of sunlight and light filtered through a leaf canopy. Red/far-red ratios (660/730) are also shown) (after Pons 2000).

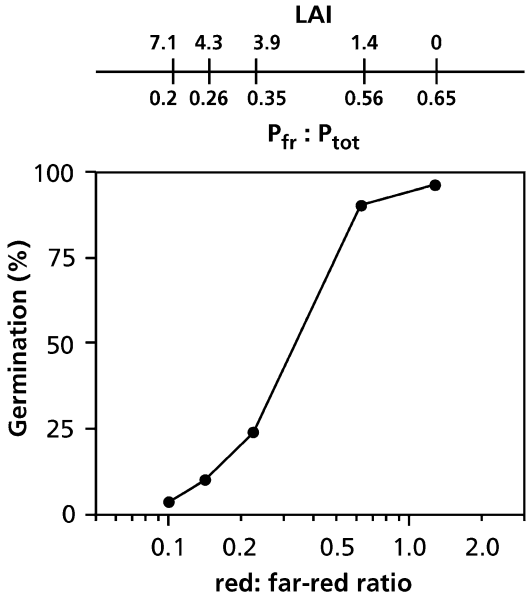

Fig. 11.7 Germination of *Plantago major* (common plantain) in daylight under stands of *Sinapis alba* (white mustard) of different densities resulting in different red/far-red photon ratios of the transmitted light. Corresponding leaf area index (LAI) and phytochrome photoequilibria (P_{fr}:P_{total} ratios) are shown (after Pons 2000).

Perception of light *per se* as well as the response to the spectral composition of the light involves the **phytochrome** system (Box 10.2). Seeds with a dormancy mechanism involving phytochrome require a minimum amount of the far-red-absorbing form of phytochrome (P_{fr}) to break dormancy (Footitt et al. 2013). Light with a high red:far-red ratio enhances the formation of P_{fr}. When the seeds are exposed to light with a low red:far-red ratio, less P_{fr} is formed. The amount of P_{fr} is also determined by photon dose in the nonsaturating region. The amount of P_{fr} required for germination depends on environmental conditions and differs among species. Hence, a low red:far-red ratio does not inhibit germination in all light-requiring species and not under all conditions.

If, after exposure to light of appropriate spectral composition, germination is subsequently impaired by some other environmental factor, then a new exposure to light is required to stimulate germination. This is due to the decay of P_{fr} in the dark. This mechanism also explains why seeds that are initially not light-requiring upon ripening become so after burial in the soil (Pons 1991b). A requirement for light to stimulate germination is clearly not a fixed characteristic of a species. Seeds that are not obviously light-requiring may still have a mechanism that is regulated by phytochrome. This is because the seeds that retain chlorophyll for longer would have most of the phytochrome that accumulates during the ripening period in seeds, in the P_r form (Batlla and Benech-Arnold 2014).

Many light responses of seeds are typically referred to as the **low fluence response** (LFR). That is, a rather low photon dose is required to give the response. Some seeds under certain conditions germinate following much lower light doses (three to four orders of magnitude). Such a response is called the **very low fluence response** (VLFR) (Batlla and Benech-Arnold 2014). The two responses can be found in the same seeds, depending on pretreatment, *e.g.*, in *Lactuca sativa* (lettuce) (Fig. 11.8). Transition between LFR and VLFR also varies seasonally during burial of seeds in soil (Batlla and Benech-Arnold 2014). The VLFR under natural conditions is probably involved in the response to the short exposures to light that occur during soil disturbance, as mentioned above (Scopel et al. 1994).

Studies with mutants of *Arabidopsis thaliana* have shown that different forms of phytochrome trigger VLFR and LFR responses. Phytochrome A is required for the VLFR and phytochrome B for the LFR (Casal and Sánchez 1998) that acts together with phytochrome in the far-red reversible stimulation of germination by red light (Batlla and Benech-Arnold 2014).

Germination of many species (but not of *Arabidopsis thaliana*) can also be inhibited by exposure to light when exposure times are long. The inhibition increases with increasing irradiance (Fig. 11.8), and the maximum effective wavelength region is 710–720 nm. This response is called the **high-irradiance response** (HIR). The cycling between P_r and P_{fr} and their intermediates is somehow involved in the HIR, but the mechanism is not fully understood. Seeds

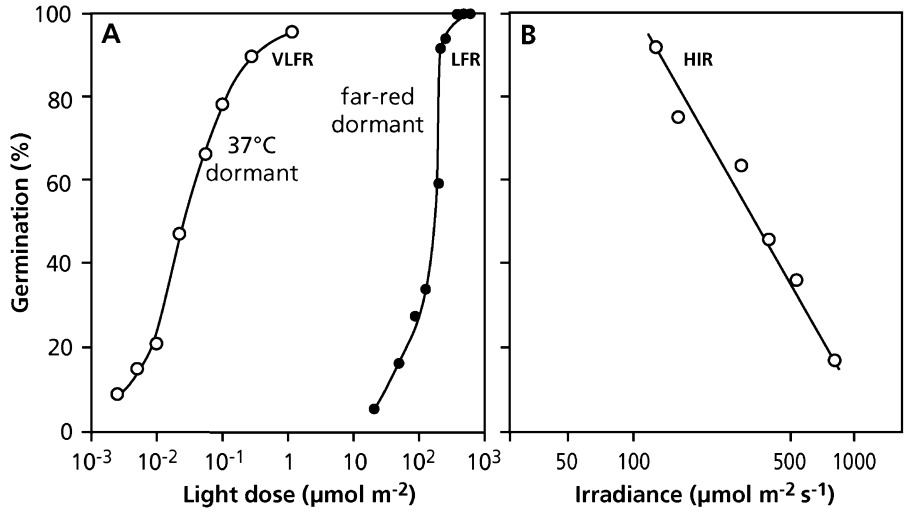

Fig. 11.8 The three light responses of seed germination demonstrated in one species *Lactuca sativa* (lettuce). (**A**) Fluence response to red light of seeds pretreated at 37 °C and with far-red showing the very low fluence response (VLFR) and the low fluence response (LFR), respectively (after Blaauw-Jansen and Blaauw 1975). (**B**) Irradiance response to daylight showing the high-irradiance response (HIR) (Górski and Górska 1979).

that are negatively **photoblastic**, *i.e.* whose germination is prevented by light, have a strongly developed HIR. Short exposures and low irradiances are not inhibitory, and they sometimes even stimulate germination in such seeds. Experiments with mutants of *Solanum lycopersicum* (tomato) that are deficient in different forms of phytochrome show that phytochrome A is the principal form involved in the HIR (Appenroth et al. 2006).

Light responses of seeds have been extensively studied with short exposures to light (LFR and VLFR). Seeds, however, mostly experience long exposure times under natural conditions. For seeds under a leaf canopy, both the photoequilibrium of phytochrome and the HIR are important, because seeds experience many hours of exposure to wavelengths that are effective. Hence, the inhibiting effect of a leaf canopy can be stronger than expected from the spectral composition alone.

Seeds on the surface of bare soil may be inhibited by the HIR due to the prevailing high irradiances. In light-requiring seeds, this may restrict germination to the upper few millimeters of the soil profile where light penetrates, but does not reach a high intensity, and where both light and moisture are available.

11.2.6 Effects of Temperature

Temperature influences seed dormancy and germination in several ways:

1. **Diurnal fluctuation** in temperature controls quiescence of many seeds. The response is independent of the absolute temperature which illustrates that it is the amplitude that causes the response (Fig. 11.9). This mechanism prevents germination of seeds **buried deep** in the soil, where temperature fluctuations are damped. In neotropical trees, diel fluctuations in soil temperature effectively discriminate both understory sites and small gaps (25 m^2) from **larger gaps** (Pearson et al. 2002). Hence, the capacity to perceive temperature fluctuations allows the detection of soil depth and of gaps in the vegetation. Most small-seeded marsh plants also germinate in response to diurnally fluctuating temperature which indicates the absence of deep water over the seed. Hence, in these plants temperature fluctuation functions as a mechanism to detect **water depth** (Fig. 11.9).
2. The **temperature range** over which germination can occur is an indication of the degree of dormancy of the seed. If this range is narrow,

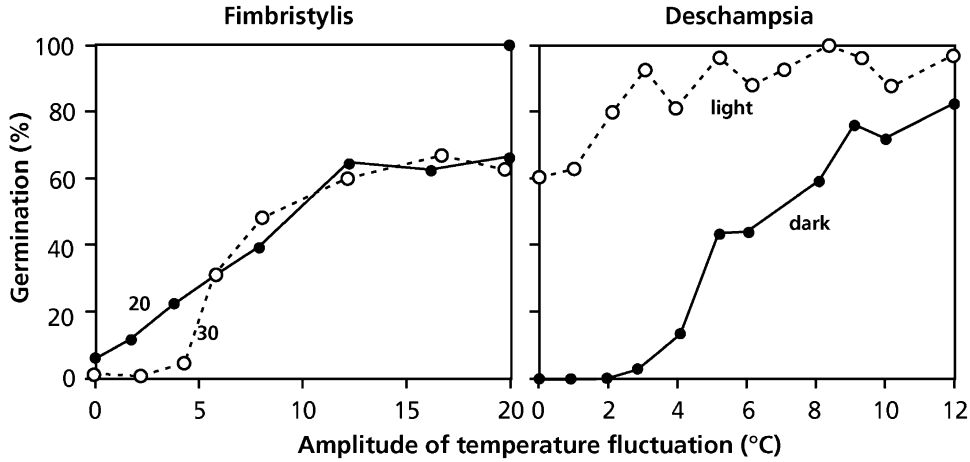

Fig. 11.9 Germination responses to various amplitudes of diurnal temperature fluctuations. (Left) The light-requiring rice-field weed *Fimbristylis littoralis* (grasslike fimbry) at mean temperatures of 20 °C and 30 °C (Pons and Schröder 1986). (Right): The grass species *Deschampsia caespitosa* (tufted hairgrass) in light and darkness (Thompson et al. 1977. Copyright © 1977, Springer Nature.

then the seed is conditionally dormant. If it is wider, then the seed is less dormant or nondormant. Variation in this temperature range may occur as a result of a shift in the upper and/or lower critical temperature limits for germination (Baskin and Baskin 2014).

3. The **temperature** to which the seed is exposed when no germination takes place is a major factor in determining release and induction of physiological dormancy, mostly at a nondeep level (Baskin and Baskin 2014). Two main types of responses are discerned in climates with seasonally changing temperatures:
   (a) **Summer annuals** and other species that produce seeds in autumn and germinate in the spring. A long exposure (1–4 months) of imbibed seeds to low temperature (approximately 4 °C; **stratification** or chilling) relieves dormancy by gradually decreasing the minimum temperature for germination (Fig. 11.11). In many species with a persistent seed bank, secondary dormancy is subsequently induced by exposure to higher summer temperatures (*e.g.*, 20 °C), which causes large seasonal changes in the degree of dormancy (Fig. 11.10). This seasonal change in dormancy restricts germination to spring, the beginning of the most suitable season for growth in temperate climates (Fig. 11.11).
   (b) **Winter annuals** set seed in spring and early summer; they generally germinate in autumn. Exposure to relatively high summer temperatures gradually relieves the dormancy by increasing the maximum temperature that allows germination. This occurs even without imbibition. In this case, low temperatures induce dormancy (Fig. 11.10). This seasonal dormancy pattern causes the seeds to germinate in autumn (Fig. 11.11), which is the beginning of the most suitable season for many species from Mediterranean climates.

Seeds may go through several cycles of induction and release of dormancy if quiescence prevents germination (*e.g.*, by the light-requirement of seeds buried in the soil) (Fig. 11.1).

Water supply is the factor that makes winter the most favorable season for growth of winter annuals, and, thus, autumn the best period for germination; however, seed dormancy is controlled by **temperature**. In many seasonal

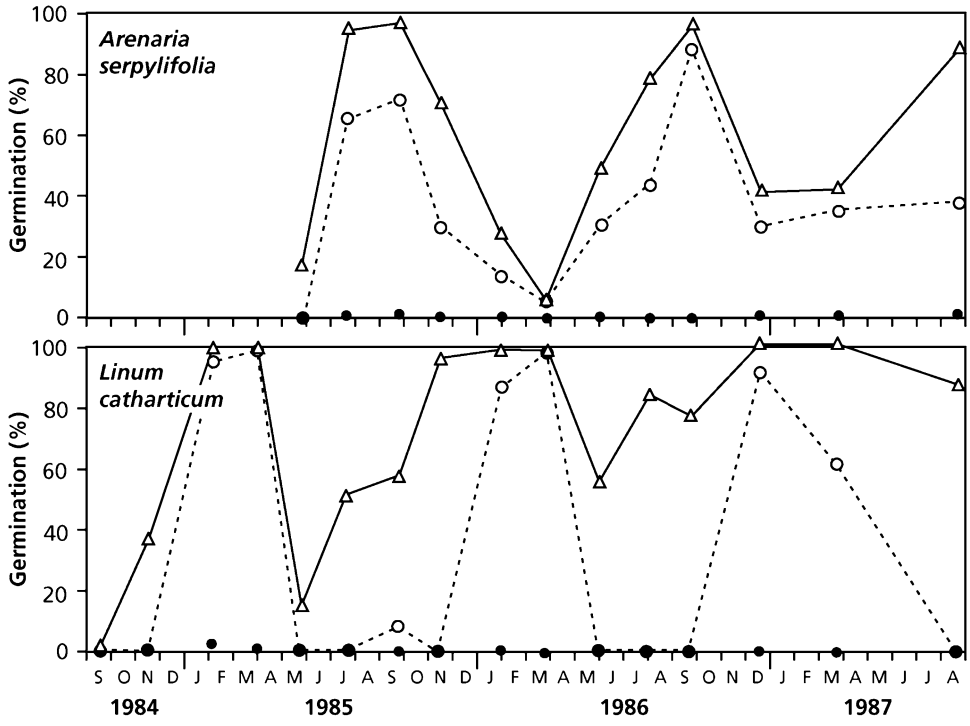

Fig. 11.10 Germination of exhumed seeds under laboratory conditions after different burial times in a chalk grassland in South Limburg, the Netherlands. *Arenaria serpylifolia* (thyme-leaved sandwort), which is a winter annual, and *Linum catharticum* (fairy flax), which is a biennial that emerges in spring. Germination in darkness (closed symbols) and in light (open symbols), solid line final germination percentage, dashed line, germination after 1 week at 22/12 °C (after Pons 1991a).

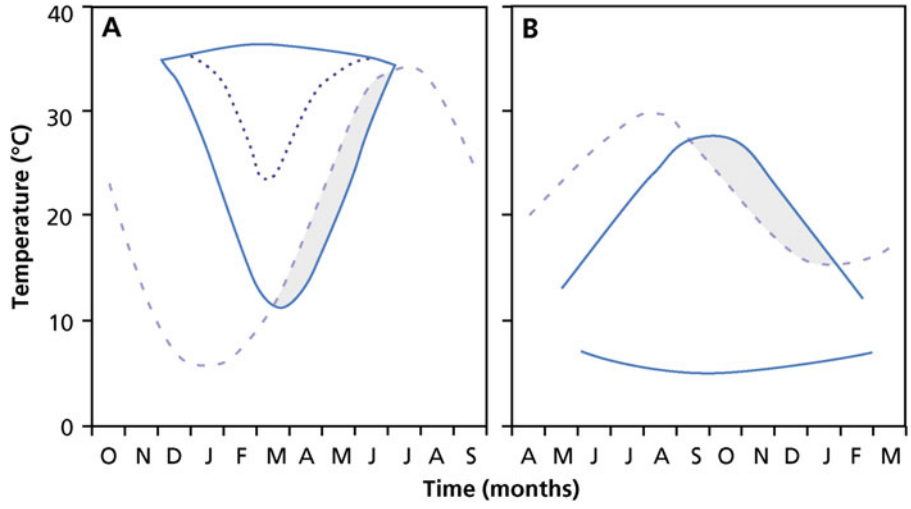

Fig. 11.11 Widening and narrowing of the temperature range of germination in relation to the temperature in the natural habitat during the season. The broken line gives the mean daily maximum temperature in the field; the continuous line gives the temperature range for germination in light; the dotted line represents the minimum temperature for germination in darkness. In the hatched area, the actual and the required temperatures in light overlap. (**A**) summer annual; (**B**) winter annual (after Karssen 1982).

climates, such as the Mediterranean climate, temperature and water supply are closely correlated, but temperature is a better predictor of the beginning of the wet season than is moisture itself. In summer annuals, it is the low temperature in winter that releases dormancy in the seeds, and seeds use this as a signal; however, the subsequently occurring high temperatures in summer form the suitable conditions for growth of the autotrophic plant.

11.2.7 Physiological Aspects of Dormancy

Many studies have examined the mechanisms of physiological dormancy, particularly the role of **phytohormones** (Box 10.2). Molecular work using the large variation in accessions of *Arabidopsis thaliana* has greatly contributed to the understanding of the complex nature of this form of dormancy. On the basis of these studies, a fascinating view has emerged that probably applies to many species where the structures surrounding the embryo restrict radicle outgrowth (Née et al. 2017).

During seed development on the mother plant, there is an increase in **ABA** in the embryo (Fig. 11.1b). This phytohormone is involved in prevention of precocious germination, synthesis of reserve proteins, development of desiccation tolerance, and induction of primary dormancy. Induction of and release from primary dormancy involves changes in both the concentration of ABA and the sensitivity to this phytohormone. **Gibberellic acid** (GA) has an effect opposite to that of ABA, and the ABA:GA ratio resulting from synthesis and catabolism and the sensitivities to these hormones regulate the release and induction of physiological dormancy (Fig. 11.1b). an increase in sensitivity to GA typically accompanies release from dormancy (Fig. 11.12). On the other hand, with release from quiescence, GA is synthesized *de novo*. Abscisic acid reduces the growth potential of the embryo, whereas GA can stimulate it. GA is further involved in the induction of enzymatic hydrolysis of carbohydrates, especially of

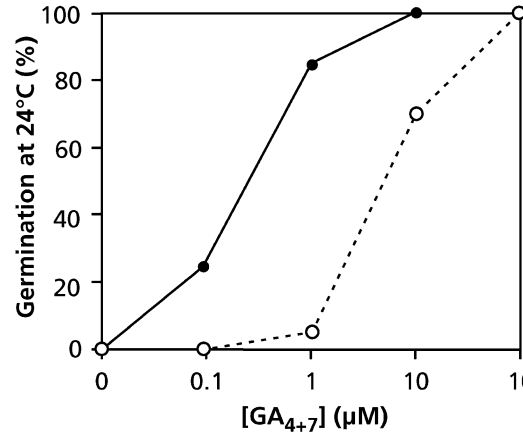

Fig. 11.12 The effect of gibberellin (GA) concentration on the germination of a GA-deficient mutant of *Arabidopsis thaliana* (thale cress) in darkness at 24 °C. Seeds directly sown (open symbols), or preincubated at 2 °C for seven days (filled symbols) (after Hilhorst and Karssen 1992).

galactomannan-rich endosperm cell walls (Tuan et al. 2018). Cell-wall hydrolysis weakens the endosperm layer, so that the radicle of the embryo can penetrate the seed coat, when its growth potential is sufficiently large, leading to germination.

Induction of secondary dormancy, as occurs in buried seeds, is accompanied by a decrease in the sensitivity to GA. Phytohormone receptors in the plasma membrane may be affected by the temperature-dependent state of membranes, thus at least partly explaining the effect of temperature on dormancy. The change in sensitivity to GA is reflected in sensitivity for environmental stimuli that break quiescence, such as light that stimulates GA synthesis, causing the above-mentioned endosperm weakening.

11.2.8 Summary of Ecological Aspects of Seed Germination and Dormancy

Section 11.2 discussed how environmental factors control dormancy and affect quiescence. These environmental cues lead to a **timing** of germination that maximizes the chances of seedling survival and subsequent reproductive

Table 11.1 A summary of the possible ecological significance of environmental factors involved in releasing seed quiescence.

Environmental factor	Ecological role
Light	Gap detection
	Sensing depth in soil
Diurnal temperature fluctuation	Increasing longevity in seed bank
	Gap detection
	Sensing depth in soil and water
Nitrate	Gap detection
	Nutrient availability
Rain event in desert	Detection of water availability
Smoke	Response to fire
High temperature	Response to fire
Seasonal temperature regime	Detection of suitable season
	Increasing longevity in soil
Time	Avoidance of unsuitable season
	Spreading risks in time

success. Table 11.1 summarizes these germination cues. The cues that indicate presence of disturbance (light, diurnal temperature fluctuation, nitrate, and other chemicals) are typically best developed in early-successional species. In the absence of these cues, these species enter long-lasting 'seed banks' in the soil, where they can remain for tens or even hundreds of years until the next disturbance occurs. By contrast, late-successional species produce short-lived seeds regularly and have poorly developed seed dormancy mechanisms. As a result, these species are poorly represented in the seed bank. The viability of seeds in the seed bank declines with time, but it is quite common for the seed bank to be a major source of germinants, even when disturbance occurs more than a century after the previous disturbance that gave rise to the seed bank.

11.3 Developmental Phases

Most species pass through several distinct life phases after germination. Plants grow most rapidly, but are most vulnerable to environmental stress and to the effects of competition, during the seedling phase. There is then a gradual transition from the seedling to the juvenile phase, where many species allocate significant resources to defense and storage. Finally, there is an abrupt hormonally-triggered shift to the reproductive phase, where some shoot meristems produce reproductive, rather than vegetative organs. The response of plants to the environment often differs among these developmental phases, and species differ substantially in the timing and triggers for phase shifts. For example, **annuals** rapidly switch to their reproductive phase, whereas **perennials** may remain vegetative for a longer time, sometimes many years or decades. **Biennials** are programmed to complete their life cycle within 2 years, but this may take longer if environmental conditions are less favorable. What are the physiological differences between plants with these contrasting strategies, and how is the program in biennials modified by the environment?

11.3.1 Seedling Phase

Seedlings are susceptible to many abiotic and biotic stresses after germination (Leck et al. 2008). During germination of a dicotyledonous plant, such as *Pisum sativum* (pea), the shoot emerges from the seed with a hook-shaped structure that protects the apical meristem and first leaves, while the seedling pushes through the soil. When the seedling reaches the light as perceived by **phytochrome**, the leaves expand, and the photosynthetic apparatus differentiates, a process called **de-etiolation**. Until that time the apical hook is maintained by an inhibition of cell elongation of the inner portion of the hook which is mediated by **ethylene** (Peck et al. 1998). In darkness in dicot seedlings, gibberellins act via a specific pathway, and ethylene acts via another pathway to control the asymmetric accumulation of auxin required for apical hook formation and maintenance. These core pathways form a network with multiple points of connection. Light perception by phytochromes and cryptochromes lowers the levels of gibberellins, and triggers

hook opening as a component of the switch between heterotrophic and photoautotrophic development (Mazzella et al. 2014).

Due to their small root systems, seedlings are vulnerable to desiccation from minor soil drying events, so there is strong selection for rapid root extension. Where seedling densities are high, there is also strong competition for light, and even 1 or 2 days advantage in time of germination is a strong determinant of competitive success (Harper 1977). Most plant mortality occurs in the seedling phase through the interactive effects of environmental stress, competition, pathogens, and herbivory, so there is strong selection for rapid growth at this vulnerable phase to acquire resources (leaves and roots) and to grow above neighbors (stem). Most species achieve this only through minimal allocation to storage or defense.

Seed size is a major determinant of initial size and absolute growth rate of seedlings (Leishman et al. 1995; Fig. 11.13). Species that colonize disturbed open sites with minimal competition typically produce abundant, small seeds which maximizes the probability of a seed encountering a disturbed patch, but minimizes the reserves available to support initial growth and survivorship (Leishman and Westoby 1994; Fig. 11.14). Trees, shrubs, and woodland herbs, which are exposed to stronger competition at the seedling stage, however, often produce a few large seeds (Shipley and Dion 1992). Thus, for a given reproductive allocation, there is a clear **trade-off** between seed size and seed number, with seed size generally favored in species that establish in closed vegetation. *Banksia* species that are killed by fire produce more, but smaller seeds with a lower P content than congeneric species that re-sprout after a fire (Denton et al. 2007). There is a trade-off between physical (fibre) and chemical defenses (phenolics) in seeds, but this relationship is much stronger among small seeds than among large seeds (Wang et al. 2017).

Many tropical trees and some temperate trees produce extremely large nondormant seeds that germinate, grow to a small seedling, and then cease growth until a branch or tree-fall opens a gap in the canopy. This **seedling bank** is analogous to the seed bank of ruderal species in that it allows new recruits to persist in the environment until disturbance creates an environment favorable for seedling establishment. Large seed reserves to support maintenance respiration are essential to species that form a seedling bank. There is a strong negative relationship between

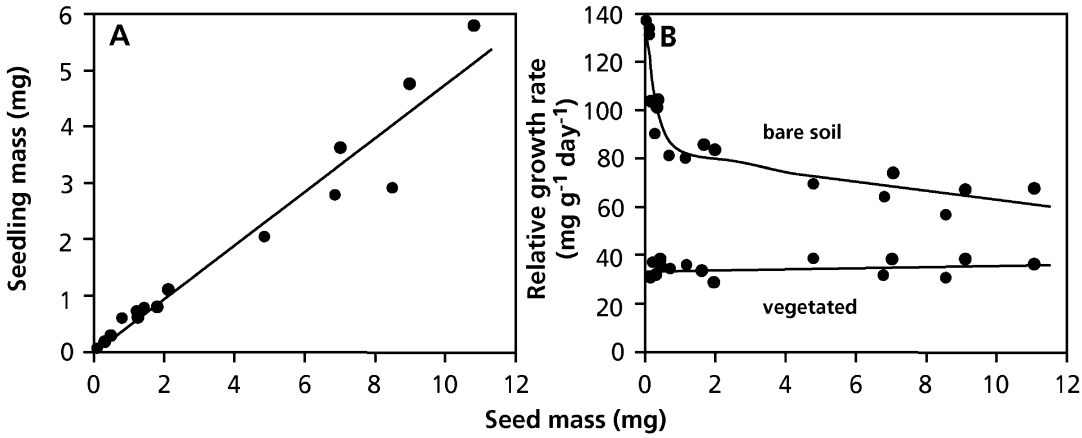

Fig. 11.13 Relationship between seed mass of prairie perennials and (**A**) mass of newly emerged seedlings (<12 h) or (**B**) relative growth rate of seedlings on bare soil and in a mat of *Poa pratensis* (Kentucky bluegrasss) in the glasshouse. Absolute plant size increases with increasing seed mass. Relative growth rate decreases with increasing seed size in absence of competition, but it increases with increasing seed size in presence of competition. Species are *Verbascus thapsus* (mullein), *Oenothera biennis* (evening primrose), *Daucus carota* (carrot), *Dipsacus sylvestris* (common teasel), *Tragopogon dubius* (yellow salsify), and *Arctium minus* (lesser burdock) (after Gross 1984).

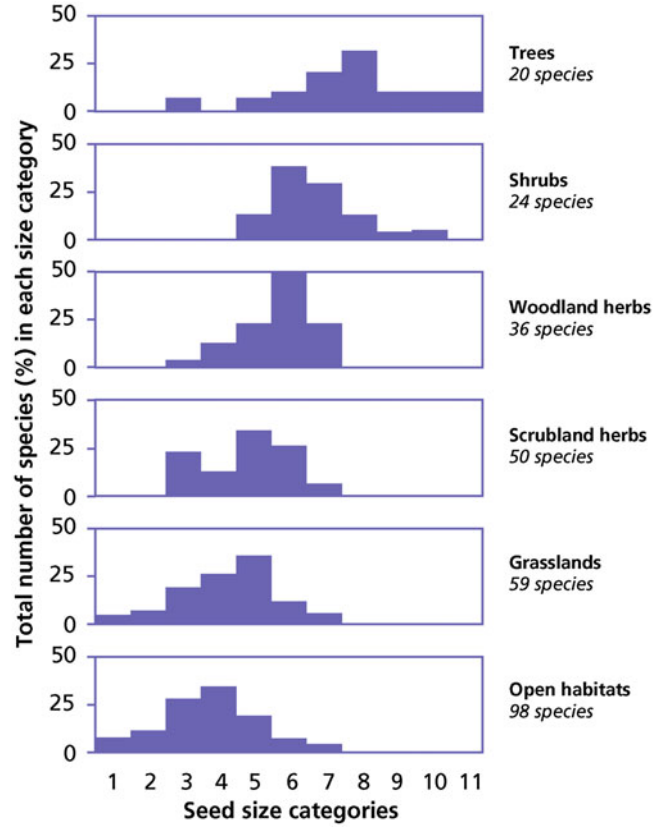

Fig. 11.14 Frequency distribution of seed size in different ecological groups of plants (after Salisbury 1942). Species that establish in closed habitats tend to have larger seeds than open-habitat plants.

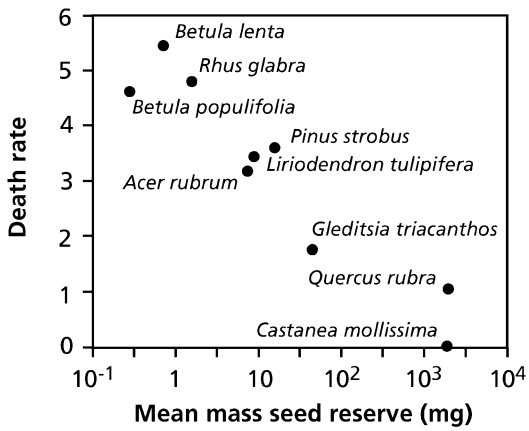

Fig. 11.15 Relationship between death rate (mean number of fatalities per container in 12 weeks in shade) and log mean mass of seed reserve in nine North American tree species (after Grime and Jeffrey 1965).

seed size and death rate in shade (Fig. 11.15). In contrast to the situation in fast-growing seedlings, the leaves of seedlings in the seedling bank are very well defended against herbivores and pathogens. These seedlings quickly resume growth following disturbance and have a strong initial competitive advantage over species that persist as a seedbank in the soil (Grime and Jeffrey 1965).

11.3.2 Juvenile Phase

There is a gradual transition from a seedling phase with minimal storage reserves to a juvenile phase with accumulation of some reserves to buffer the plant against unfavorable environmental conditions. There are striking differences among plants in the length of the juvenile phase and the extent of reserve accumulation, however. At one extreme, *Chenopodium rubrum* (red goosefoot) can be induced to flower at the cotyledon stage immediately after germination (Seidlová and Štichová 1968), whereas *Fagus*

grandifolia (American beech) takes 40–60 year before switching to significant reproduction (Tubbs and Houston 1990). The switch to reproduction is typically hormonally mediated.

Annuals allocate relatively little of their acquired resources (carbon and nutrients) to storage, whereas perennials store both nutrients and carbohydrates. The greater resource allocation to storage, rather than to leaf area, partly accounts for the slower growth rate of perennials. The stored reserves, however, allow perennials to start growth early in a seasonal climate, and to survive conditions that are unfavorable for photosynthesis or nutrient acquisition.

11.3.2.1 Delayed Flowering in Biennials

Biennial species typically grow as vegetative rosettes until the storage pools are sufficiently filled to allow a switch to the reproductive phase; this transition commonly requires **vernalization** (Sect. 11.3.3.3; Kim et al. 2009). Compared with an annual, biennials are able to grow and accumulate nutrients throughout a larger part of the year, and are therefore able to produce more seeds (de Jong et al. 1987). Biennials may grow longer than 2 years at a low irradiance (Pons and During 1987) or low nutrient supply if their stores are not filled sufficiently to induce a switch to flowering (Table 11.2). In general, shifts from one developmental phase to another correlate more closely with plant size than with plant age. Hence, the term **biennial** is less appropriate than **monocarpic perennial,** which indicates that the plant terminates its life cycle once the transition to the reproductive stage has been made. *Musa acuminata* (East African highland banana) plants flower when they reach a threshold total dry mass of 1.5 kg per plant (Taulya et al. 2014). Physiological age at flowering is delayed by 739 °C day at Kawanda (central Uganda) compared with that at Ntungamo (southwest Uganda), whose chronological age at flowering is 51 days older. Vegetative growth in some monocarpic perennials can be very long; *e.g.*, plants of *Agave palmeri* (Palmer's agave) grow for up to 35 years before flowering, and then die after producing a single 3–5 m tall inflorescence (Pavliscak et al. 2015).

Table 11.2 Probability of flowering in *Cirsium vulgare* (spear thistle) of small rosettes after transfer from the field to a long-day regime in a growth room in February.

Treatment	Probability of flowering (%)	Average time before bolting (days)
Without nutrients	25	45
With nutrients	80	40

Source: Klinkhamer et al. (1987)
Note: A control group in the field showed 13% flowering

11.3.2.2 Juvenile and Adult Traits

In woody plants, there is a distinctive suite of morphological and chemical traits that disappear when the plant becomes reproductively mature. Juvenile plants are typically more strongly defended against herbivores, either by producing spines (*e.g.*, apple or orange trees) or a variety of chemical defenses (Herms and Mattson 1992). Many woody species exhibit a difference in morphology between their **juvenile** and **adult foliage**. For example, the young foliage of many *Acacia* (wattle) species in Australia is characterized by bipinnate leaves, whereas older individuals produce 'phyllodes' (*i.e.* compressed petioles) (Ullmann 1989).

Acacia melanoxylon (blackwood) is an Australian forest species with a mosaic of leaves, like the Hawaiian shade-intolerant *Acacia koa* (koa) that grows at sites characterized by unpredictable drought periods. Leaves have faster mass-based gas exchange rates, while the water storage tissue in phyllodes contributes to greater capacitance per area (Pasquet-Kok et al. 2010). Phyllodes also show stronger stomatal closure at high vapor pressure deficit, and greater maximum hydraulic conductance per area, with stronger decline during desiccation and recovery with rehydration.

11.3.2.3 Vegetative Reproduction

Many plants such as grasses or root-sprouting trees have a modular structure composed of units, each of which has a shoot and root system. This 'vegetative reproduction' can be viewed simply as a form of growth, as described in Chap. 10, or as a mechanism of producing

physiologically independent individuals without going through the bottleneck of reproduction and establishment (Jónsdóttir et al. 1996).

Vegetative reproduction is best developed in environments where flowering is infrequent and seedling establishment is a rare event. For example, *Larrea tridentata* (creosote bush) specimens across the Chihuahuan, Sonoran, and Mohave Deserts of western North America are thousands of years old (McAuliffe et al. 2007). In this situation, the carbon cost of producing a new tiller by sexual reproduction is estimated to be 10,000-fold greater than the cost of a new tiller by vegetative reproduction, because of very slow rates of seedling establishment. *Populus tremuloides* (trembling aspen) clones in the Rocky Mountains of the central United States are similarly estimated to be of Pleistocene age as a result of root sprouting (Jelinski and Cheliak 1992). The maintenance of diversity in the absence of frequent recruitment, and resistance to further geographic differentiation in this spatially heterogeneous environment probably reflect occasional seedling establishment through 'windows of opportunity'. The phalanx growth form and concomitant physiological integration between ramets combine to spread the risk of death and buffer the effects of selection over time and space.

Clonal growth is one mechanism by which plants can explore **patchy habitats**. For example, daughter ramets (*i.e.* a unit composed of a shoot and root) of *Fragaria chiloensis* (beach strawberry) draw on reserves of the parental ramet to grow vegetatively. If the daughter ramet encounters a resource-rich patch, it produces additional ramets, whereas ramets that move into resource-poor patches fail to reproduce vegetatively. Resource translocation can also occur between established ramets of clonal plants, supporting damaged or stressed ramets growing under relatively unfavorable conditions (Jónsdóttir et al. 1996). When the roots of one ramet of *Trifolium repens* (white clover) are in a dry patch, whereas those of another are well supplied with water, relatively more roots are produced in the wet patch (Stueffer et al. 1996). Similarly, when leaves of one ramet are exposed to high irradiance, whereas those of another are in the shade, the ramet exposed to high irradiance produces relatively more leaf mass (Fig. 11.16). Note that these environmental responses are opposite to the changes in allocation that occur when an entire plant is exposed to these conditions (Sect. 10.5.1).

The developmental process by which vegetative reproduction occurs differs among taxonomic groups (Vallejo-Marín et al. 2010). These

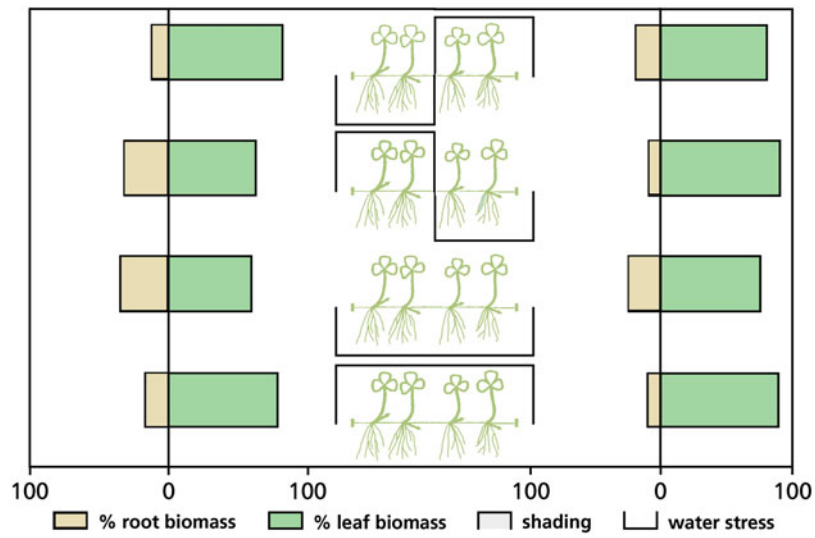

Fig. 11.16 Percentage biomass allocation to leaves and roots of two interconnected ramets of *Trifolium repens* (white clover) (afterStueffer et al. 1996).

mechanisms include production of new tillers (a new shoot and associated roots) in grasses and sedges, initiation of new shoots from the root system (root suckering) in some shrubs and trees, production of new shoots at the base of the parental shoot (stump sprouting) in other shrubs and trees, initiation of new shoots from below-ground stems or burls, as in many Mediterranean shrubs, and rooting of lower limbs of trees that become covered by soil organic matter (layering) in many conifers. Reproductive output (*i.e.* the product of seed output and seed size) is lower in clonal than in nonclonal plants; within nonclonal species, it is high in annuals and monocarpic plants relative to nonclonal perennials (Herben et al. 2015).

11.3.2.4 Delayed Greening During Leaf Development

Many tropical, shade-tolerant rainforest species initiate leaves that are white, red, blue, or light-green, during leaf expansion which indicates their low chlorophyll concentration (Woodall and Stewart 1998; Coley et al. 2018). This pattern of **delayed greening** is typical of shade-tolerant species and is less common in gap specialists (Table 11.3). It is also common in savanna trees in southern Africa (Ludlow 1991) and in P-impoverished Mediterranean ecosystems (Lambers et al. 2015). It has been suggested to be a strategy to deter herbivores (Numata et al. 2004) and it is also a P-saving strategy (Sulpice et al. 2014).

Table 11.3 The color of young leaves of 175 species, common in a tropical rain forest in Panama.

	Gap-specialist	Shade-tolerant
Leaf color	%	%
White	0	8
Red	3	33
Light-green	3	41
Delayed greening	7	82
Green	93	18

Source: Kursar and Coley (1992c)
Note: Values are the number of species and families in each category. Percentages are calculated for gap-specialist and shade-tolerant species separately

The pattern of delayed greening is distinctly different from the shift from juvenile to adult foliage, because it is typical of all young leaves, even those on mature plants. Leaves that show delayed greening function below the light-compensation point for photosynthesis at saturating light until fully expanded. After full expansion, their rate of dark respiration is very fast, presumably due to fast rates of metabolism associated with the development of chloroplasts. The completion of this development may take as long as 30 days after the leaves have fully expanded. In contrast, normally greening leaves achieve maximum photosynthetic capacity at the end of leaf expansion (Kursar and Coley 1992b; Woodall et al. 1998).

There is obviously a cost involved in delayed greening: during leaf expansion species showing this pattern exhibit only 18–25% of the maximum possible photosynthetic rate, compared with 80% for leaves that show a normal developmental pattern. At the irradiance level that is typical of the forest understory, the quantum yield of photosynthesis is also less than half that of green leaves, largely due to their low photon absorption (Kursar and Coley 1992a).

What might be the advantages of delayed greening? Delayed greening may be a strategy to reduce herbivory of young leaves or play a role in photoprotection (Queenborough et al. 2013). All young leaves lack toughness, which is provided by cell-wall thickening and lignification, which are processes that tend to be incompatible with cell expansion and leaf growth. Because toughness provides protection against both biotic and abiotic factors, young leaves are poorly protected (Table 11.4). The accumulation of proteins and other nutrients associated with chloroplast development in species without delayed greening presumably makes young unprotected leaves even more attractive to herbivores. Hence, although delayed greening may represent a loss of potential carbon gain, it also reduces carbon losses associated with **herbivory**. In a high-irradiance environment, losses incurred by delayed greening could be substantial. In the low-light environment of shade-adapted species, where the irradiance is only

Table 11.4 Rates of herbivory of young leaves, measured during the three days prior to full expansion (when they lack toughness) and four to six days after full expansion (when their toughness has increased substantially).*

Species	Number of leaves	During expansion	After expansion
Ouratea lucens	274	3.08	1.63
Connarus panamensis	179	0.22	0.03
Xylopia micrantha	90	0.57	0.01
Desmopsis panamensis	262	0.75	0.27
Annona spragueii	204	0.37	0.08

Source: Kursar and Coley (1992c)
*Values are expressed as the percentage of the leaves that was eaten per day

about 1% of full sunlight, losses by herbivory could be relatively more important.

We have so far discussed the delayed greening in terms of lack of chlorophyll; however, the red or blue appearance also reflects the presence of specific pigments: **anthocyanins**. These anthocyanins may protect against damage by ultraviolet light (Sect. 7.2.2.2). Bioassays using leaf-cutter ants suggest that these anthocyanins may protect the leaves because of their **antifungal** properties. These leaf-cutter ants collect leaves, and store them underground as substrate for fungi, which are consumed by ants. Leaves that contain anthocyanins, either naturally or experimentally added, are collected to a lesser extent than leaves with lower anthocyanin concentrations (Coley and Aide 1989).

Delayed greening is also a strategy to save P, *e.g.*, in Proteaceae from severely P-impoverished habitats in southwest Australia (Sulpice et al. 2014). These plants first invest P in cytosolic ribosomal RNA (rRNA), the largest organic P pool in leaves (Veneklaas et al. 2012). Once they have toughened up, most of the cytosolic rRNA is recycled, and the leaves accumulate rRNA in the chloroplasts, and develop their photosynthetic capacity (Fig. 11.17).

11.3.3 Reproductive Phase

We know that some plants **flower** in spring, when days are getting warmer and longer, whereas others flower in autumn, when temperatures are getting lower and days are shortening. Similarly, **tuber formation** typically occurs also either in spring or in autumn. How do plants sense that it is spring or autumn? Depending on the species, plants may use either the **day-length** or the **temperature** as environmental cues. Many plants from temperate regions use a combination of both cues and are thus able to distinguish between spring and autumn (Garner and Allard 1920; Samach and Coupland 2000). Our understanding of the timing mechanisms of plants has led to greater insight in how plants time their switch from the vegetative to the reproductive phase, as well as to important applications in the glasshouse industry.

11.3.3.1 Timing by Sensing Day-Length: Long-Day and Short-Day Plants

In Sect. 10.5.1.2, we discuss how vegetative growth can be affected by day-length. This environmental cue is pivotal in triggering **flowering** (Mouradov et al. 2002; Teotia and Tang 2015) and **tuberization** (Martinez-Garcia et al. 2002; Morris et al. 2014) in many species. Day-length does not play a role in so-called **day-neutral plants**, like *Cucumis sativus* (cucumber), *Ilex aquifolium* (sparked holly), *Solanum lycopersicum* (tomato), *Impatiens balsamina* (touch-me-not), and *Poa annua* (annual meadow-grass). It is most important, however, in plants whose flowering is triggered by the short days in autumn (**short-day plants**, which require a photoperiod less than about 10–12 h) or the long days in spring (**long-day plants**, which require a photoperiod longer than about 12–14 h).

Examples of short-day plants include *Chrysanthemum* species, *Eupatorium rugosa* (snakeroot), *Euphorbia pulcherrima* (poinsettia), some *Fragaria* species (strawberry), *Glycine max* (soybean), *Nicotiana tabacum* (tobacco), *Oryza sativa* (rice), and *Xanthium strumarium* (cocklebur),

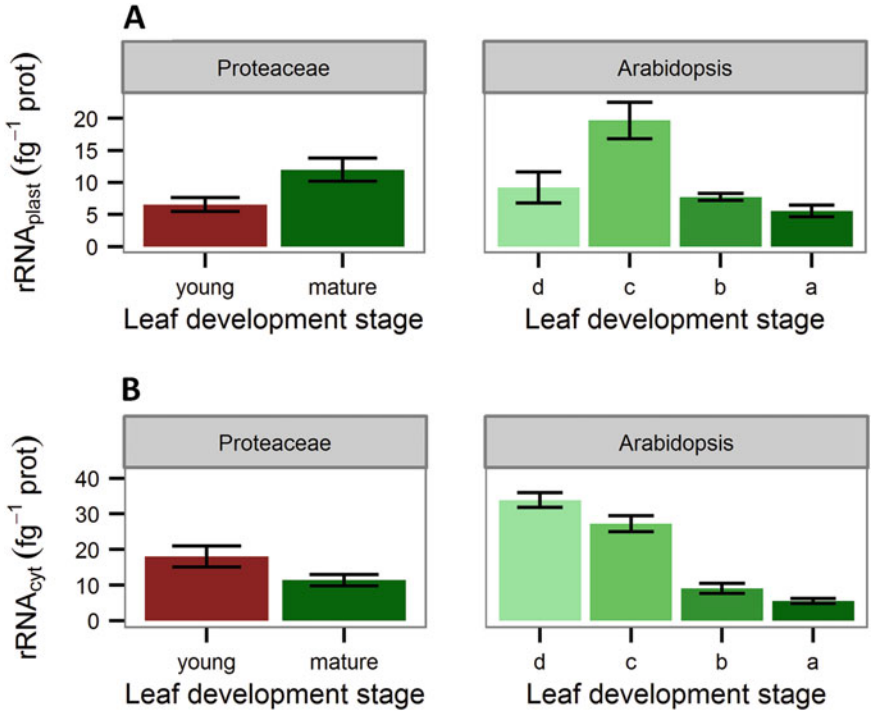

Fig. 11.17 Average biochemical characteristics of young expanding and mature fully expanded leaves of three *Banksia* and three *Hakea* species (Proteaceae) in comparison with *Arabidopsis thaliana.* (**A**) Plastidic ribosomal RNA expressed on a leaf protein basis; (**B**) cytosolic ribosomal RNA expressed on a leaf protein basis (after Sulpice et al. 2014).

which is one of the best-studied short-day species (Fig. 11.18). Long-day plants include *Arabidopsis thaliana*, *Avena sativa* (oat), *Coreopsis verticillata* (tickseed), *Hordeum vulgare* (barley), *Lolium perenne* (perennial ryegrass), *Rudbeckia fulgida* (black-eyed Susan), *Trifolium pratense* (strawberry clover), *Triticum aestivum* (wheat), and *Hyoscyamus niger* (black henbane), which is a much-researched long-day species (Fig. 11.19). Some species [*e.g.*, *Bouteloua curtipendula* (side-oats grama)] have short-day ecotypes at the southern end of their distribution, and long-day ecotypes at the northern end (Olmsted 1944). The requirement for a certain day-length may be **qualitative** [*e.g.*, in *Perilla nankinensis* (shiso)] meaning that plants will not flower at all without exposure to at least 1 day of the appropriate photoperiod. It may also be **quantitative** or **facultative** (*e.g.*, in *Arabidopsis thaliana*), which means that flowering will occur more quickly when exposed to the appropriate photoperiod.

Do plants really sense the day-length, or do they perceive the duration of the night period? The answer to this question has come from experiments in which the night was interrupted with either **white** or **red light**. A short interruption of the dark period prevents or delays flowering in a short-day plant, whereas the same treatment promotes flowering in long-day plants. Interrupting the light period has no effect on either short-day or long-day plants. The period between two light periods, normally the **night**, clearly must be the **critical time** that plants sense.

How do plants perceive the duration of the night? The answer again, has come from experiments in which the night was interrupted, now using light of a specific wavelength: **red** (660 nm) or **far-red** (730 nm). A short flash is generally sufficient to obtain the effect: red light

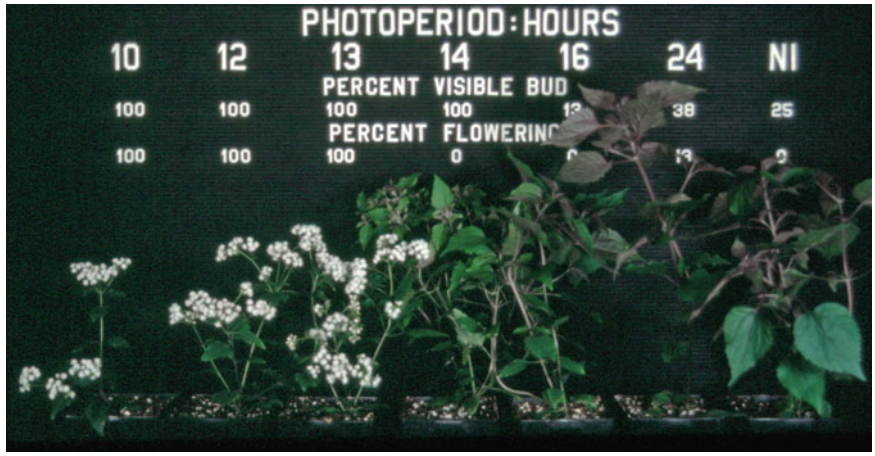

Fig. 11.18 Induction of flowering by exposure to short days (= long nights) in *Eupatorium rugosa* (snakeroot). No flowering is observed above a critical day-length of 16 h (Courtesy B. Fausey and A. Cameron, Department of Horticulture, Michigan State University, USA.

Fig. 11.19 Induction of flowering by exposure to long days (= short nights) in *Rudbeckia fulgida* (black-eyed Susan). No flowering is observed below a critical day-length of 14 h (Courtesy E. Runkle, Royal Heins, and A. Cameron, Department of Horticulture, Michigan State University, USA.

has the same effect as white light, and this effect is reversed by exposure to far-red light. This points to **phytochrome** as the photoreceptor involved in perception of the photoperiod (Box 10.2). In fact, phytochrome was discovered in the first place through these sorts of experiments (Garner and Allard 1920; Amasino and Michaels 2010).

Classic grafting experiments have shown that day-length is detected in the leaves that have just matured and that a signal is transmitted from there to the shoot apex where flowering is induced (Piñeiro and Coupland 1998). Exposure of just one leaf to the inducing photoperiod may be enough. Experiments with the short-day plant *Zea mays* (corn) have shown that four to six leaves are required for the shoot meristem to become committed to form flowers. The day-length signal is transmitted to the shoot apical meristem, both in the long-day plant *Arabidopsis thaliana* (Corbesier et al. 2007) and in the short-day plant *Oryza sativa* (rice) (Tamaki et al. 2007).

In many plant species, the timing of flowering depends largely on seasonal changes in the expression of the gene *FLOWERING LOCUS T* (***FT***), which encodes a systemic signaling molecule that is a key component of the long-sought **florigen** (Zeevaart 2008; Song et al. 2015). It is synthesized in the leaves, but moves to the shoot apex to induce flowering. The photoperiodic flowering mechanism induced by *FT* expression has been best characterized in the long-day plant *Arabidopsis thaliana*. In long-day plants, long-day conditions induce high levels of expression of ***FT*** which consequently accelerates flowering, whereas short-day conditions lead to very low levels of *FT* expression. The day-length-dependent induction of *FT* is governed mainly by a transcriptional activator CONSTANS (CO) (Song et al. 2013). The **circadian clock** and light signaling tightly control CO protein activity throughout the day in the companion cells of the leaf phloem (Imaizumi 2010). CYCLING DOF FACTOR (CDF) proteins play major roles in regulating daily *CO* expression profiles (Fig. 11.20).

A circadian clock also plays a role in plants that fold their leaves at night and in many other processes. The biological clock controls the sensitivity for P_{fr}. If the ability of plants from temperate climates to sense the length of the night is impressive, that of some tropical species is truly astounding. Here the variation in day-length may be very short and a change of 20–30 min may suffice to trigger flowering (Mouradov et al. 2002).

11.3.3.2 Do Plants Sense the Difference Between a Certain Day-Length in Spring and Autumn?

Day-length is a tricky environmental cue, because days of the same length occur in both spring and autumn. How do plants sense the difference between the two seasons? Many long-day and short-day plants from cold climates may never perceive day-length in spring, since there is no appreciable metabolic activity. This would be the case for *Eupatorium rugosum* (white snakeroot) and various *Helianthus* (sunflower) species in Michigan, USA. However, that situation is different in warmer environments.

It was once thought that plants could sense the **lengthening** or the **shortening** of days; however, experiments have not confirmed the existence of such a mechanism. How, then, do they do it? Recent studies show that various factors including photoperiod, **temperature**, plant age, and GA, converge to regulate *FT* expression for flowering (Fig. 11.20). Plants integrate both photoperiod and temperature cues to control seasonal flowering (Song et al. 2013). Studies on the effects of temperature changes on flowering time have mostly focused on **vernalization** responses (Kim et al. 2009). The key regulator of the vernalization response in *Arabidopsis thaliana* is the *FLC* gene, which encodes a transcription repressor of *FT*. Vernalization represses the expression of FLC by regulating the chromatin status of the *FLC* locus; therefore, *FLC* repression is removed in the spring. A combination of photoperiod and temperature is required to induce flowering in *Fragaria ananassa* (strawberry) and *Beta vulgaris* (sugar beet). Flower primordia are induced in autumn, when day-length is reduced to a critical level. Further development of the primordia is stopped by low temperature in winter, and only continues when the temperature increases in spring (Andrés and Coupland 2012).

11.3.3.3 Timing by Sensing Temperature: Vernalization

In temperate climates, changes in day-length coincide with changes in temperature. Many species that flower in spring are not long-day plants; rather, they use **temperature** as an environmental cue (Fig. 11.19). Exposure of the entire plant or of the moist seed induces flowering. We owe much of the information on effects of temperature on flower induction to the Russian botanist **Lysenko**. He showed that exposure of moist seeds of winter wheat (*Triticum aestivum*) to low temperatures allowed the plants to flower, without exposure of the seedlings to the harsh Russian winter. The physiological changes triggered by exposure to low temperature are called **vernalization** (from the Latin word for spring, *ver*) (Kim et al. 2009).

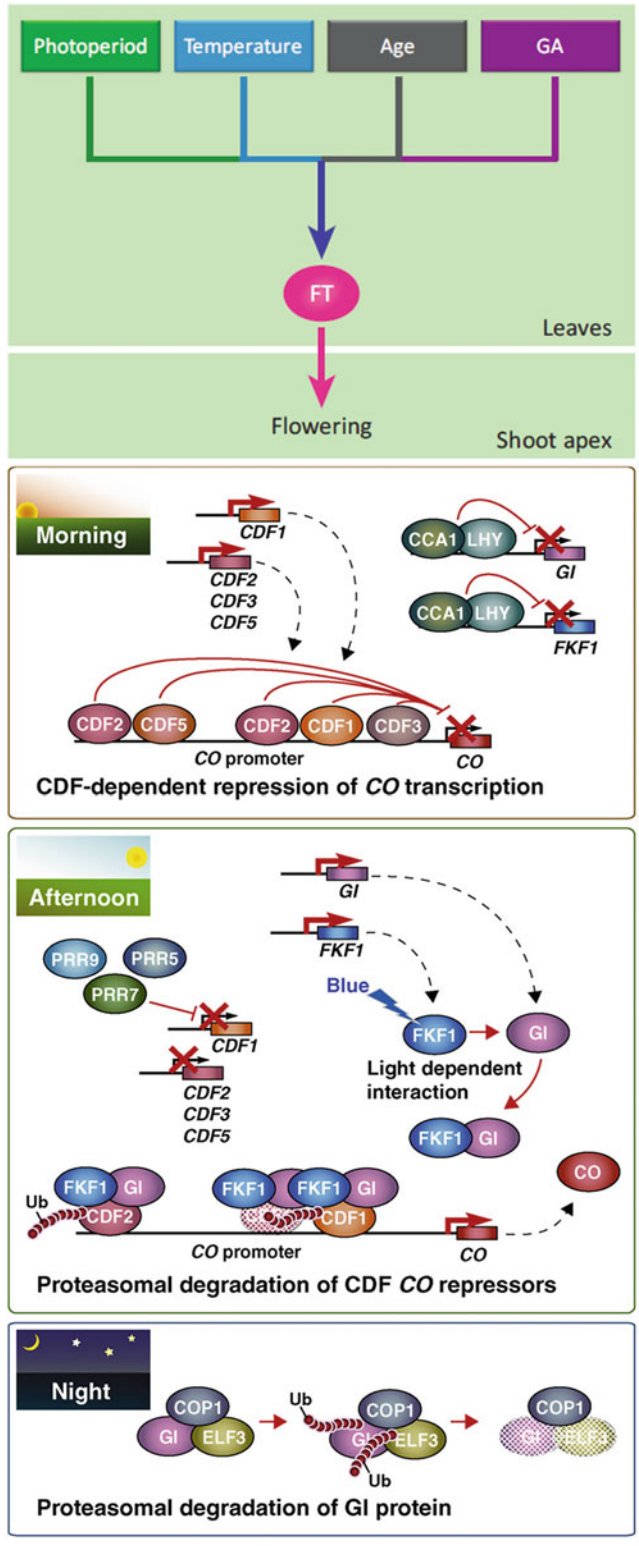

Fig. 11.20 (**A**) Integration of external and internal signals for flowering. External stimuli (photoperiod and temperature) and internal conditions [plant age and amount of gibberellic acid (GA)] converge in the regulation of FLOWERING LOCUS T (FT) gene expression and they all affect FT protein output from the leaves. FT

Lysenko unfortunately did not place his important findings in the right scientific perspective. Rather than concluding that phenotypic changes in the seeds exposed to low temperature accounted for the flowering of the mature wheat plants, he insisted that the changes were genetic. Inspired and supported by the political flavor of the 1930s in his country, he stuck to his genetic explanation, much to the detriment of genetics and geneticists in the Soviet Union (Roll-Hansen 1985).

Vernalization is essential, both for crop species such as *Triticum aestivum* (winter wheat) and for winter annuals in general which survive during winter as seedlings. Vernalization also triggers flowering in biennials that overwinter as a rosette, such as *Digitalis purpurea* (fox glove), *Lunaria annua* (honesty), *Daucus carota* (carrot) and *Beta vulgaris* (beet), and in perennials such as *Primula* (primrose) and *Aster* species, and plants that overwinter as a bulb, tuber, or rhizome. Figure 11.21 shows the effect of exposure to low temperature for 3–12 weeks on flowering of *Campanula* (harebell).

Vernalization is the process by which a prolonged exposure to the cold of winter results in competence to flower during the following spring (Ream et al. 2014). Although originally defined as prolonged cold treatment of seeds, vernalization also accelerates flowering when applied to plants during the vegetative growth phase (Gott 1957). In *Triticum aestivum* (wheat) the difference between winter wheat and spring wheat is controlled by a single gene, *VRN1* (Yan et al. 2003). After cold treatment, the transcripts of *VRN1* are down-regulated, and remain so for the remainder of the plant's life (Amasino and Michaels 2010). Cold treatment induces the breakdown of a compound that accumulated during exposure to short days in autumn, and which inhibits flower induction. At the same time, a chemical compound is produced that promotes flower induction, most likely GA (Mouradov et al. 2002).

The practical applications of our ecophysiological knowledge on environmental cues that trigger flowering are enormous. We can now produce many flowers that used to be available during specific seasons only all year round. Building on fundamental ecophysiological experiments, in the Netherlands the flower industry has become a flourishing branch of horticulture.

11.3.3.4 Effects of Temperature on Plant Development

Low temperature is a **trigger** for flower induction of biennials (Sect. 11.3.3.3) and also affects plant **development**, with strong genotypic components, *e.g.*, in *Triticum aestivum* (wheat) (Kiss et al. 2017). Reaumur (1735) introduced the concept of a **thermal unit** to predict plant development. This concept assumes that plants need a fixed **temperature sum** to fulfill a developmental phase. This assumption implies that the rate of development, expressed as the inverse of the duration in days for a given phase, is a linear

Fig. 11.20 (continued) protein moves to the shoot apex and induces flowering (Song et al. 2013; copyright Elsevier Science, Ltd). (**B**) Schematic representation of the diurnal regulation of CO expression. In the morning, the expression levels of *CDF1*, *CDF2*, *CDF3*, and *CDF5* genes are high. These CYCLING DOF FACTOR (CDF) proteins likely bind to the *CO* promoter and are involved in suppression of *CO* transcription. The transcription of afternoon-phased *GI* and *FKF1* is thought to be directly repressed by CCA1 and LHY. In the afternoon, the expression of these four *CDF* genes declines, and at least PRR5, PRR7, and PRR9 participate in the downregulation of *CDF1* expression. Decreasing levels of CCA1 and LHY release the repression *FKF1* and *GI* and allow them to be expressed at high levels. Once FKF1 observes blue light, FKF1 forms a complex with GI. This complex is involved in the degradation of CDF1 and CDF2, and possibly other CDFs. Removal of *CO* repressors facilitates the expression of *CO*. At night, GI is degraded by a COP1 complex that contains ELF3. COP1 directly interacts with ELF3 to control ELF3 protein turnover. COP1 forms a complex with GI via ELF3 and also regulates GI stability. GI is required for the stabilization of FKF1 protein, although it is not certain whether FKF1 is also degraded by COP1. Ub stands for ubiquitin (Imaizumi 2010; copyright Elsevier Science, Ltd.).

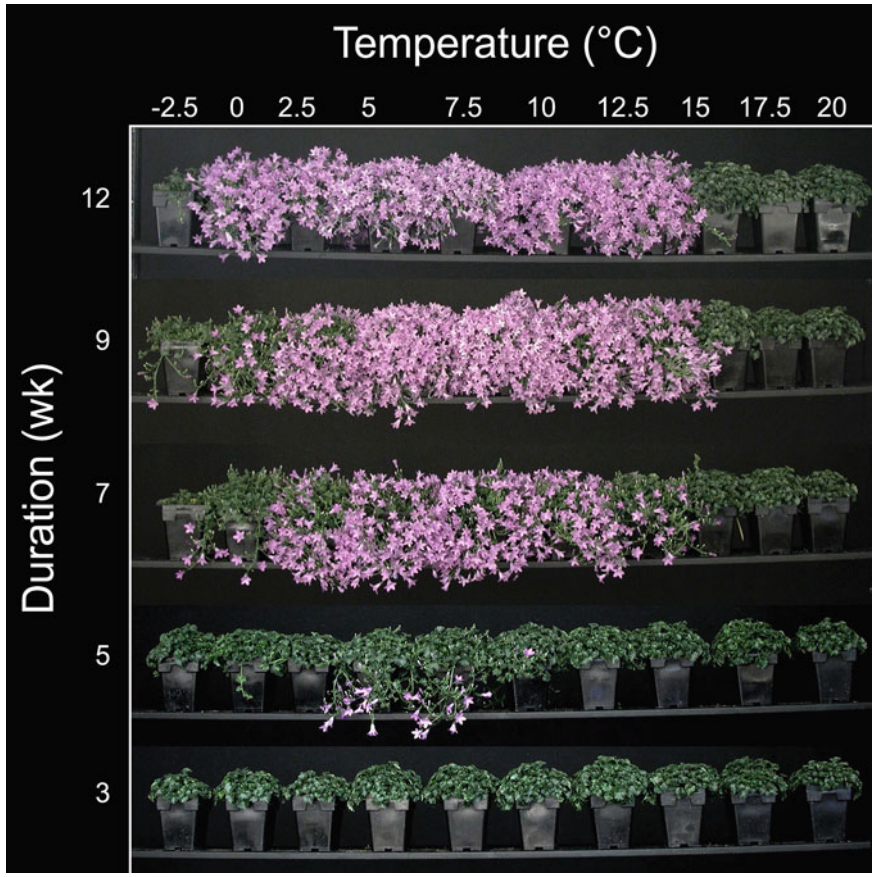

Fig. 11.21 The effect of vernalization temperature and duration of flowering of *Campanula* birch hybrid (harebell). No flowering is observed if the vernalization period is less than 5 weeks. (Courtesy S. Padhye and A. Cameron, Department of Horticulture, Michigan State University, USA).

function of temperature. The concept of thermal unit is applied widely, but it has no physiological basis (Horie 1994).

11.3.3.5 Attracting Pollinators

Pollination of flowers by insects, birds, lizards, small marsupials, or bats requires attraction of pollinators. Attraction may occur through secondary phenolic compounds (flavonoids) in the petals (Shirley 1996). These **UV-absorbing compounds** are invisible to the human eye, but pollinating bees perceive them. Floral color mediates plant–pollinator interactions by often signaling floral resources. In this sense, hummingbird-pollinated flowers are frequently red (Bergamo et al. 2016). Sensory exclusion of bees, rather than a preference of hummingbirds, turns out to be the pressure for red-reflecting flower evolution in *Costus arabicus* (spiral ginger). The floral scent of different neotropical palm species in Ecuador and Puerto Rico is dominated by a variety of compounds, *e.g.*, the fatty-acid derived 3-pentanone and the hydrocarbon series dodecane to pentadecane, the benzenoid compound 1,4-dimethoxybenzene, the isoprenoids (E)-ocimene, myrcene, linalool, and (E)-a-farnesene and the nitrogen-containing compound 2-methoxy-sec-butylpyrazine (Knudsen et al. 2001). Specific scent compounds, as found in these beetle-pollinated species, appear to have evolved as a response to pollinator preferences. The scents released by flowers may be faint smells or an olfactory delight for humans, *e.g.*, terpenoids released by **thermogenic** cones of

Macrozamia (cycad) species (Terry et al. 2004). On the other hand, *Helicodiceros muscivorus* (dead horse arum) produces an inflorescence that resembles the anal area of a dead mammal and produces a fetid scent during a few hours after sunrise (Seymour et al. 2003). Flies enter the floral chamber, pollinate the female florets and become trapped until the next morning, when pollen is shed from the male florets, and the flies are released. Some orchids attract their pollinators by releasing sex pheromones (Bohman et al. 2014).

The flowers of many species change color with pollination, thus guiding potential pollinators to those flowers that are still unpollinated, and provide a nectar reward (Weiss 1991). The change in color may be due to a change of the pH in the vacuole, in which the phenolics compounds are located. For example, the reddish-purple buds of *Ipomoea nil* (Japanese morning glory) change into blue when the flowers open, and the shift in the flower coloration correlates with an increase in the vacuolar pH of the flower epidermal cells (Ohnishi et al. 2005). Following pollination, most flowers cease nectar production. Pollinators quickly learn which colors provide a nectar reward. Pheromone-releasing orchids provide no nectar reward (Phillips et al. 2014), thereby 'cheating' on pollinators.

The quantity of nectar provided by a flower depends on the number of flowers in an inflorescence (the floral display) and the type of pollinator that a flower attracts. For example, long-tubed red flowers pollinated by hummingbirds typically produce more nectar than short-tubed flowers pollinated by small insects; this makes sense in view of the 140-fold greater energy requirement of hummingbirds (Heinrich and Raven 1972). Species that produce many flowers in an inflorescence typically produce less nectar per flower than do species that produce a single flower.

In **thermogenic** flowers, the cyanide-resistant **alternative path** increases in activity prior to heat production and is partly responsible for it (Sect. 3.3.1). Although this is not the only reason for thermogenesis (rapid respiration rates *per se* are also important), it definitely contributes to **heat production** because the lack of proton extrusion coupled to electron flow allows release of a large fraction of the energy in the substrate as heat. The temperature of the flower, compared with that of the ambient air, can also be enhanced by **solar tracking**, which is a common phenomenon in alpine and arctic Asteraceae, Papaveraceae, Ranunculaceae, and Rosaceae, and involves the perception of **blue light** (Stanton and Galen 1993). This may raise flower temperature by several degrees above the ambient temperature, as long as the wind speed is not too high (Sect. 6.2.2). When solar tracking is prevented in *Dryas octopetala* (mountain avens), by tethering the plants, lighter seeds are produced, but the seed set is not affected (Kjellberg et al. 1982). The flowers of the solar-tracking Norwegian alpine buttercup (*Ranunculus acris*) traverse an arc of about 50 degrees, with speed of movement and solar tracking accuracy being highest between 11 am and 5 pm. This solar tracking enhances flower temperature by about 3.5 °C (Totland 1996). Solar tracking decreases with flower aging and stops completely as the petals wither, so that it cannot have effects on post-anthesis events. Tethering the flowers does not affect the attractiveness to pollinating insects, seed:ovule ratio, seed mass, or seed abortion rate (Totland 1996). If solar tracking has any selective advantage in this species, then it is probably only under special weather conditions (*e.g.*, when pollinator activity is limited by low temperatures).

Orchids, more than any other plant family. Have engaged in complex pollination systems, with species adopting the full spectrum of pollination syndromes from autogamy (a means of self-pollinating), food rewarding, food deception, nest-site deception, to sexual deception (Cozzolino and Widmer 2005). Whereas food-deceptive systems are the most common in orchids, it is sexual-deceptive systems that have attracted most interest; orchid flowers produce insectiform flowers and pheromones (known as **allomones**) that match the calling hormones of female insects, usually wasps and bees. The most extreme cases of sexual deception occur in Australian orchids, where hammer orchids (*Drakaea* and *Chiloglottis*) have almost exclusive one-to-one relationships between male wasps and

orchid species (Phillips et al. 2010, 2014). In the case of *Chiloglottis*, the hormone has been characterised and is known as chiloglottine (Schiestl et al. 2003; Schiestl 2005); it precisely matches the pheromone chemistry produced by the female wasp. Such levels of evolutionary specialisation present important consequences for conservation management, where managing the orchid requires careful consideration of the wasp.

11.3.3.6 The Cost of Flowering

Some of the most important tropical-subtropical fruit trees produce extremely large numbers of flowers, increasing the floral display. Their respiratory demands are high (Sect. 3.5.1.2) and the overall daily demand for carbohydrates during bloom may exceed the daily photosynthate production. Flowering in *Citrus paradisi* (grapefruit) for a tree that bears 20,000–50,000 flowers requires 166–400 mol C $tree^{-1}$ (Bustan and Goldschmidt 1998). In comparison, the amount of carbon required for the growth of the ovaries, the only floral organs that persist after flowering, is only 33–38 mol C $tree^{-1}$. Together with the abscission of fruitlets, the amount of carbon that is lost at early stages of the reproductive cycle is about 27% of the annual photosynthate production.

From an evolutionary perspective, the advantages that are associated with the production of large numbers of reproductive units must justify the apparent waste of resources. Uncertainties concerning pollination and improvement of fruit/seed quality by selective fruit abscission may be factors influencing the excessive production of reproductive units. From the grower's point of view, the heavy bloom of *Citrus* may seem to be a waste of resources; preventing it might lead to an increase in yield or fruit quality.

11.3.4 Fruiting

Allocation to reproduction varies substantially among plants and with environmental conditions, ranging from 1% to 30% of net primary production, with median values of perhaps 10%. This modest allocation to reproduction (the process that most directly governs plant fitness) is less than typical allocation to root exudation under nutrient stress or nutrient uptake under favorable conditions (Table 3.1) which suggests that the processes of resource acquisition under conditions of environmental stress and competition with neighboring plants often leave relatively few resources for reproduction.

Wild plants generally produce fewer fruits than flowers. Low allocation to reproduction sometimes reflects poor pollination, when weather conditions are bad for pollinators or for appropriate pollen-producing plants. Even when the flowers are artificially pollinated, however, the ratio between fruits and flowers, commonly referred to as **fruit set**, may still be well below 1. In addition, increased pollination may have more seeds setting, but at the expense of seed size, which indicates that seed production may be both 'pollen-limited' and 'resource-limited' (Stanton et al. 1987).

The identification of patterns in life-history strategies across the tree of life is essential to our prediction of population persistence, extinction, and diversification. Plants exhibit a wide range of patterns of longevity, growth, and reproduction. Demographic data from plant species in the wild, from annual herbs to supercentennial trees, can be used to examine how growth form, habitat, and phylogenetic relationships structure plant life histories and to develop a framework to predict population performance (Salguero-Gómez et al. 2016). More than half of the variation in plant life-history strategies is adequately characterized using two independent axes First, the fast–slow continuum, including fast-growing, short-lived plant species at one end and slow-growing, long-lived species at the other. Second, a reproductive strategy axis, with highly reproductive species characterized by a single reproductive episode before death (iteroparous) at one extreme, and species characterized by multiple reproductive cycles over the course of their lifetime (semelparous) at the other. Across major habitats, plant growth forms and phylogenetic ancestry, the findings are consistent, suggesting

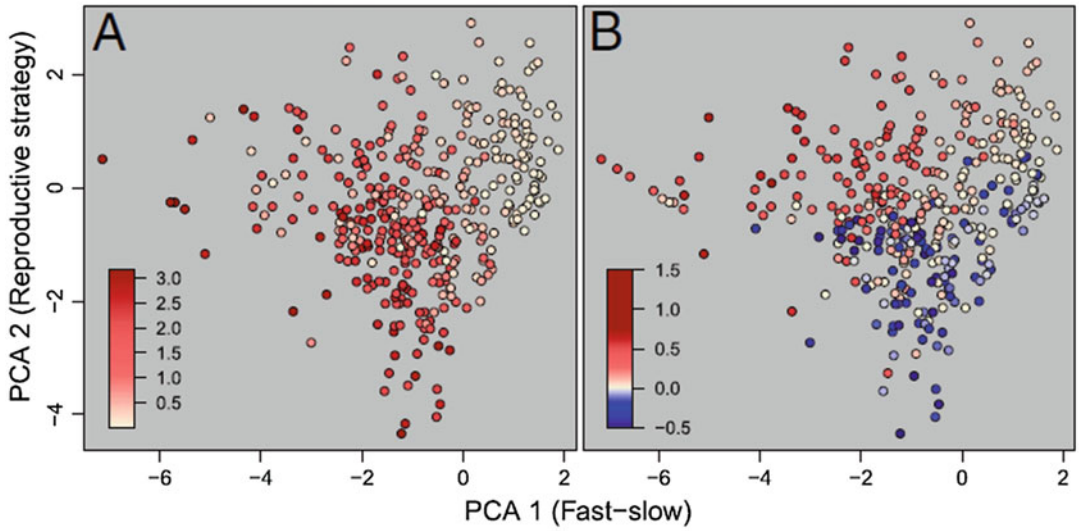

Fig. 11.22 Scores of species on the fast-slow continuum and its reproduction strategy predict population performance including damping ratio (*i.e.* the rate at which a population returns to equilibrium after disturbance) (**A**) And the population growth rate (r, *i.e.* the rate of population size change through time) (**B**). Redder tones indicate a higher value of these metrics. Bluer colors of r reflect population decline. The damping ratio was quantified for 389 species (Salguero-Gómez et al. 2016).

that the relative independence of the fast–slow and reproduction strategy axes is general in the plant kingdom (Fig. 11.22). This life-history framework may complement trait-based frameworks on leaf and wood economics (Salguero-Gómez et al. 2016).

Allocation to reproduction is difficult to quantify, because the inflorescence can often meet much of its own carbon requirement and because some structures serve both reproductive and non-reproductive roles. In cereals, the reproductive organ (ear) accounts for up to 75% of the photosynthate required for grain production, and the inflorescence plus the closest leaf (the flag leaf) provide all of the photosynthate required for reproduction (Evans and Rawson 1970). When vegetative leaves are removed by herbivores, an increased proportion of flag-leaf photosynthate goes to vegetative organs, whereas damage to the flag leaf increases carbon transport from other leaves to the inflorescence. Thus, the role of each leaf in supporting reproduction depends on the integrated carbon supply and demand of the entire plant. Stem growth often increases during reproduction of herbaceous plants which increases the probability of pollen exchange and the dispersal distance of wind-dispersed fruits. The greatest gains in yield of crops (*e.g.*, cereals, peanuts, sugar beet) have come from breeding for a higher **harvest index** [*i.e.* the ratio between harvestable biomass and total (aboveground) biomass]. In cereals, this has been achieved by selection for varieties with reduced allocation to the stem which is due to a low production of or sensitivity to GA. There has been no increase in photosynthetic capacity during crop breeding for higher grain yield (Gifford et al. 1984). Over 84 years of breeding of *Glycine max* (soybean), seed biomass increased at a rate greater than that of total aboveground biomass, resulting in an increased harvest index (Koester et al. 2014). A better understanding of the physiological basis for yield gains will help to identify targets for crop improvement in the future.

11.3.5 Senescence

After flowering, phloem-mobile nutrients are exported from the senescing leaves and roots to

the developing fruits (Sect. 9.4.3.2). Unlike 'getting old and wearing out', senescence in plants is a carefully programmed, hormonally-controlled developmental process: **programmed cell death** (Coll et al. 2011). It is an integral part of plant development that is affected by environmental factors (*e.g.*, irradiance, photoperiod, and nutrient supply). It is promoted by **ethylene** and **ABA**, and slowed down or reversed by **cytokinins** and/or **GA**. Plant senescence is regarded as a complex process in which various environmental signals are integrated into developmental, age-dependent pathways. Mechanisms exist that sense the age of cells, organs, and the whole plant, as well as environmental signals. They integrate these signals, transduce them, select the appropriate pathways and execute the degeneration process (Woo et al. 2018). Nitrogenous and P-containing compounds are remobilized, as are most other compounds that can move in the phloem. Unlike phloem-mobile elements, calcium (Ca) concentrations in phloem sap are very low, and very little Ca is remobilized during senescence (Sect. 4.2).

Considering the driving force for phloem transport (*i.e.* a gradient in hydrostatic pressure between source and sink; Sect. 4.3), it is not surprising that some of the compounds remobilized from senescing leaves are transported to roots, even though these may show a net export of nutrients (Simpson et al. 1983). The rather indirect manner in which N moves from senescing leaves to developing kernels probably reflects the way the systems for long-distance transport (*i.e.* xylem and phloem) operate. That is, phloem sap will move in the sieve tubes from a site where the phloem is loaded, thus creating a high pressure, to a site where phloem unloading takes place, thus decreasing the pressure. Xylem sap will move in the xylem conduits, down a gradient in hydrostatic pressure. There is some exchange between the transport pathways, especially in the stem (Pate and Herridge 1978), but this is not sufficient to stop the need for a continuous cycling process in plants (Simpson et al. 1983).

11.4 Seed Dispersal

Seeds are often well protected, either physically, by a hard seed coat (Sect. 11.2.1), or chemically, due to toxic compounds, *e.g.*, cyanogenic glycosides or specific inhibitors of digestive enzymes (Sects. 13.3.1 and 13.3.2).

Numerous plant traits are associated with seed dispersal (Murray 1986). These include floating designs in aquatics (Gurnell et al. 2008), sticky seed parts in mistletoes that ensure deposition on a host branch (Mitich 1991; Amico and Aizen 2000), hooks that facilitate attachment to animal furs (Albert et al. 2015), structures that attract animals (Hall and Walter 2013), 'ballistic' structures in dwarf mistletoes (*Arceuthobium* sp.) (Hawksworth 1959), and plumes and wings that allow transfer through air (Casseau et al. 2015). Some of these mechanisms involve aspects of the plant's physiology, of which we present a few examples in this section.

11.4.1 Dispersal Mechanisms

Explosive or **ballistic** seed dispersal occurs in many plant species (Sakes et al. 2016), and may involve heat production associated with the alternative oxidase (Sect. 3.3.1). Such dispersal mechanisms are highly undesirable in crop plants because they cause 'shattering' and loss of seed during harvest [*e.g.*, in *Brassica napus* (canola)] (Raman et al. 2014). In *Tetrabelinia moreliana*, a tropical rainforest legume tree, such a mechanism allows seeds to be launched and transferred over as much as 50 m (Van Der Burgt 1997). It is a consequence of drying of the pod walls which creates tension that builds up between the two valves of the pod. Once the tension exceeds a threshold value, the pod explodes and the seed is launched (Fig. 11.23).

Tension in the tissue may also occur without drying of the reproductive structure [*e.g.*, in *Impatiens* (touch-me-not)] (Deegan 2012). In this case the tissue tension reflects an aspect of tissue water relations, which we alluded to in

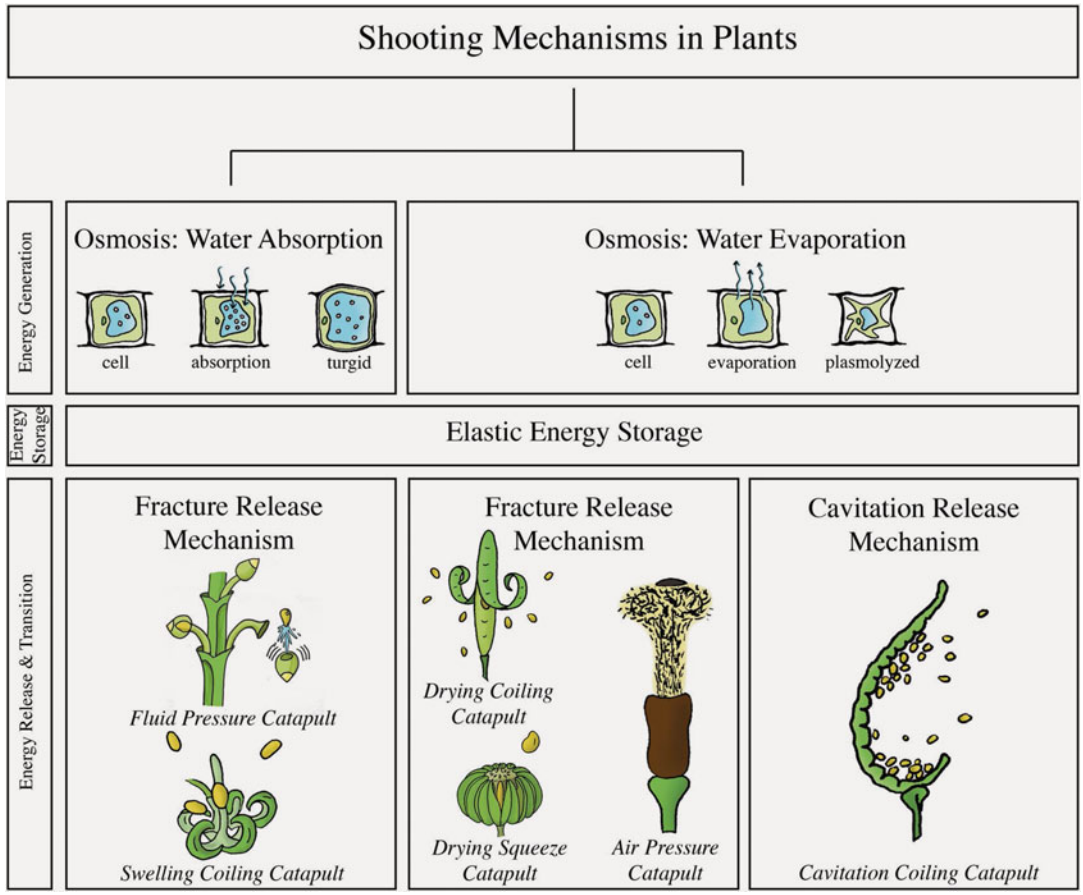

Fig. 11.23 The structural categorization of shooting mechanisms in plants, based on their energy management criteria. Fluid pressure catapult, in the genus *Arceuthobium* (dwarf mistletoe). Swelling coiling catapult, in *Cornus canadensis* (bunchberry) and *Morus alba* (white mulberry), and the genus *Impatiens*; schematic illustration of *Impatiens capensis* (orange jewelweed). Drying coiling catapult, in the genus *Cardamine* and in Fabaceae. Schematic illustration of *Cardamine parviflora* (sand bittercress). Drying squeeze catapult, in Euphorbiaceae and Rutaceae, the genus *Illicium*, *Oxalis acetosella* (common wood sorrel), and the Viola family. Schematic illustration of *Hura crepitans* (sandbox tree). Air pressure catapult, in the genus *Sphagnum*. Cavitation coiling catapult, in Polypdiaceae and *Selaginella*; schematic illustration of *Polypodium aureum* (an epiphytic fern) (Sakes et al. 2016).

Sect. 5.4. That is, within the reproductive tissue, the water relations of individual cells must differ widely, creating **tissue tension**. Touch or wind may cause a threshold be exceeded which causes rupture in the reproductive structure and launching of the seeds.

11.4.2 Life-History Correlates

Plants have an ancient and uneasy relationship with vertebrate animals that eat their fruits, and either digest or disperse their seeds. As early as 300 million years ago, Carboniferous progenitors of modern cycads bore fleshy fruits, which were apparently adapted for consumption by primitive reptiles that then dispersed the seeds (Howe 1986). Passage through an animal's gut may be crucial for seed germination and establishment of the seedling, *e.g.*, for a southern South American mistletoe (*Tristerix corymbosus*) dispersed by a marsupial, *Dromiciops australis* (Amico and Aizen 2000). Very few seeds germinate and even less connect with the host without passage

through this animal. The same is true for another mistletoe, *Amyema quandong*, that is dispersed by the mistletoe bird *Dicaeum hirundinaceum* (Murphy et al. 1993).

Many species [*e.g.*, *Calathea* species in tropical rainforest in Mexico] produce a lipid-rich morphological structure, termed **aril** or **elaiosome**. Such a structure allows dispersal via ants (Horvitz and Beattie 1980), which transport the seeds to their nest. *Cabralea canjerana* (cancharana), on the other hand, is a typical bird-dispersed tree in Atlantic forests in southeast Brazil. Ants treat their seeds in different ways, depending on the species. Some remove the arillate seeds to their nest, thus reducing seed predation by insects and rodents. Other ants remove the aril on the spot, or cover the seeds before removing the aril. Aril removal greatly facilitates seed germination in some species (Pizo and Oliveira 1998).

11.5 The Message to Disperse: Perception, Transduction, and Response

Plants continuously **sense** their environment, both as adults and as seeds, before germination has started. Seeds acquire information about the suitability of their environment for seedling growth, and they use this information to germinate or to remain dormant. There are numerous environmental cues, with plants from different environments using different cues. At a later stage, plants similarly sense their environment to change from the vegetative to the reproductive stage and to time their flowering. Day-length and low temperature are major cues, with irradiance level and nutrient supply occasionally playing an additional role in the transition to the reproductive phase in biennials.

There are also changes during development that are programmed, with environmental factors playing at most a moderating role. For example, leaf senescence is part of a scenario of programmed cell death that can be hastened by low irradiance and limiting N or P supply. The switch from juvenile to adult foliage is also programmed, but it can be affected by irradiance, nutrient availability, and plant water status.

Once flowering has started, the plant may require pollinating animals to produce seeds. Plants produce olfactory and visual cues to attract these pollinators. The seeds that are subsequently produced may end up close to the mother plant which is common in ancient, nutrient-impoverished landscapes. However, there are also numerous mechanisms that ensure dispersal of seeds over relatively great distances. One of the mechanisms of ecophysiological interest is that of plants that 'launch' their seeds. Other dispersal mechanisms require allocation of reserves to reward animals that disperse them.

Plants sense their environment during their entire life, and the acquired information determines what is going to happen in several steps of the plant's life cycle. We now have a good understanding of important environmental cues and plant responses. Right now, our knowledge of signal-transduction pathways that connect the environmental cue and the plant's response is expanding rapidly.

References

Albert A, Auffret AG, Cosyns E, Cousins SAO, D'hondt B, Eichberg C, Eycott AE, Heinken T, Hoffmann M, Jaroszewicz B, Malo JE, Mårell A, Mouissie M, Pakeman RJ, Picard M, Plue J, Poschlod P, Provoost S, Schulze KA, Baltzinger C. 2015. Seed dispersal by ungulates as an ecological filter: a trait-based meta-analysis. *Oikos* **124**: 1109–1120.

Amasino RM, Michaels SD. 2010. The timing of flowering. *Plant Physiol* **154**: 516–520.

Amico G, Aizen MA. 2000. Mistletoe seed dispersal by a marsupial. *Nature* **408**: 929–930.

Andrés F, Coupland G. 2012. The genetic basis of flowering responses to seasonal cues. *Nat Rev Gen* **13**: 627.

Appenroth KJ, Lenk G, Goldau L, Sharma R. 2006. Tomato seed germination: regulation of different response modes by phytochrome B2 and phytochrome A. *Plant Cell Environ* **29**: 701–709.

Baskin CC, Baskin JM. 2014. *Seeds: Ecology, Biogeography and Evolution of Dormancy and Germination, 2nd edn.* San Diego, CA, USA: Elsevier/Academic Press.

Baskin JM, Baskin CC. 2004. A classification system for seed dormancy. *Seed Sci Res* **14**: 1–16.

Batlla D, Benech-Arnold RL. 2014. Weed seed germination and the light environment: implications for weed management. *Weed Biol Manage* **14**: 77–87.

Bergamo PJ, Rech AR, Brito VLG, Sazima M. 2016. Flower colour and visitation rates of *Costus arabicus* support the 'bee avoidance' hypothesis for red-reflecting hummingbird-pollinated flowers. *Funct Ecol* **30**: 710–720.

Berjak P, Pammenter NW. 2008. From *Avicennia* to *Zizania*: seed recalcitrance in perspective. *Ann Bot* **101**: 213–228.

Blaauw-Jansen G, Blaauw OH. 1975. A shift of the response thershold to red irradiation in dormant lettuce seeds. *Acta Bot Neerl* **24**: 199–202.

Bliss D, Smith H. 1985. Penetration of light into soil and its role in the control of seed germination. *Plant Cell Environ* **8**: 475–483.

Bohman B, Phillips RD, Menz MHM, Berntsson BW, Flematti GR, Barrow RA, Dixon KW, Peakall R. 2014. Discovery of pyrazines as pollinator sex pheromones and orchid semiochemicals: implications for the evolution of sexual deception. *New Phytol* **203**: 939–952.

Bustan A, Goldschmidt EE. 1998. Estimating the cost of flowering in a grapefruit tree. *Plant Cell Environ* **21**: 217–224.

Casal JJ, Sánchez RA. 1998. Phytochromes and seed germination. *Seed Sci Res* **8**: 317–329.

Casseau V, De Croon G, Izzo D, Pandolfi C. 2015. Morphologic and aerodynamic considerations regarding the plumed seeds of *Tragopogon pratensis* and their implications for seed dispersal. *PLoS ONE* **10**: e0125040.

Coley PD, Aide TM. 1989. Red coloration of tropical young leaves: a possible antifungal defence? *J Trop Ecol* **5**: 293–300.

Coley PD, Endara M-J, Kursar TA. 2018. Consequences of interspecific variation in defenses and herbivore host choice for the ecology and evolution of Inga, a speciose rainforest tree. *Oecologia* **187**: 361–376.

Coll NS, Epple P, Dangl JL. 2011. Programmed cell death in the plant immune system. *Cell Death Different* **18**: 1247.

Corbesier L, Vincent C, Jang S, Fornara F, Fan Q, Searle I, Giakountis A, Farrona S, Gissot L, Turnbull C, Coupland G. 2007. FT protein movement contributes to long-distance signaling in floral induction of *Arabidopsis*. *Science* **316**: 1030–1033.

Cota-Sánchez JH, Reyes-Olivas Á, Sánchez-Soto B. 2007. Vivipary in coastal cacti: a potential reproductive strategy in halophytic environments. *Am J Bot* **94**: 1577–1581.

Cozzolino S, Widmer A. 2005. Orchid diversity: an evolutionary consequence of deception? *Trends Ecol Evol* **20**: 487–494.

de Jong TJ, Klinkhamer P, G. L. , Nell HW, Troelstra SR. 1987. Growth and nutrient accumulation of the biennials *Cirsium vulgare* and *Cynoglossum officinale* under nutrient-rich conditions. *Oikos* **48**: 62–72.

De Lange J, Boucher C. 1990. Autecological studies on *Audouinia capitata* (Bruniaceae). I. Plant-derived smoke as a seed germination cue. *S Afric J Bot* **56**: 700–703.

Deegan RD. 2012. Finessing the fracture energy barrier in ballistic seed dispersal. *Proc Natl Acad Sci USA* **109**: 5166–5169.

Denton MD, Veneklaas EJ, Freimoser FM, Lambers H. 2007. *Banksia* species (Proteaceae) from severely phosphorus-impoverished soils exhibit extreme efficiency in the use and re-mobilization of phosphorus. *Plant Cell Environ* **30**: 1557–1565.

Donohue K. 2005. Seeds and seasons: interpreting germination timing in the field. *Seed Sci Res* **15**: 175–187.

Evans L, Rawson H. 1970. Photosynthesis and respiration by the flag leaf and components of the ear during grain development in wheat. *Aust J Biol Sci* **23**: 245–254.

Farnsworth EJ, Farrant JM. 1998. Reductions in abscisic acid are linked with viviparous reproduction in mangroves. *Am J Bot* **85**: 760–769.

Finch-Savage WE, Leubner-Metzger G. 2006. Seed dormancy and the control of germination. *New Phytol* **171**: 501–523.

Finkelstein R, Reeves W, Ariizumi T, Steber C. 2008. Molecular aspects of seed dormancy. *Annu Rev Plant Biol* **59**: 387–415.

Flematti GR, Dixon KW, Smith SM. 2015. What are karrikins and how were they 'discovered' by plants? *BMC Biol* **13**: 108.

Flematti GR, Ghisalberti EL, Dixon KW, Trengove RD. 2004. A compound from smoke that promotes seed germination. *Science* **305**: 977.

Footitt S, Huang Z, Clay HA, Mead A, Finch-Savage WE. 2013. Temperature, light and nitrate sensing coordinate *Arabidopsis* seed dormancy cycling, resulting in winter and summer annual phenotypes. *Plant J* **74**: 1003–1015.

Garner WW, Allard HA. 1920. Effects of the relative length of night and day and other factors of the environment on growth and reproduction in plants. *J Agric Res* **18**: 553–606.

Gifford RM, Thorne JH, Hitz WD, Giaquinta RT. 1984. Crop productivity and photoassimilate partitioning. *Science* **225**: 801–808.

Górski T, Górska K. 1979. Inhibitory effects of full daylight on the germination of *Lactuca sativa* L. *Planta* **144**: 121–124.

Gott MB. 1957. Vernalization of green plants of a winter wheat. *Nature* **180**: 714–715.

Grime JP, Jeffrey DW. 1965. Seedling establishment in vertical gradients of sunlight. *J Ecol* **53**: 621–642.

Gross KL. 1984. Effects of seed size and growth form on seedling establishment of six monocarpic perennial plants. *J Ecol* **72**: 369–387.

Gurnell A, Thompson K, Goodson J, Moggridge H. 2008. Propagule deposition along river margins: linking hydrology and ecology. *J Ecol* **96**: 553–565.

Hall JA, Walter GH. 2013. Seed dispersal of the Australian cycad *Macrozamia miquelii* (Zamiaceae):

are cycads megafauna-dispersed 'grove forming' plants? *Am J Bot* **100**: 1127–1136.

Harper JL. 1977. *Population Biology of Plants*. LondoN: Academic Press.

Hawksworth FG. 1959. Ballistics of dwarf mistletoe seeds. *Science* **130**: 504–504.

He H, Willems LAJ, Batushansky A, Fait A, Hanson J, Nijveen H, Hilhorst HWM, Bentsink L. 2016. Effects of parental temperature and nitrate on seed performance are reflected by partly overlapping genetic and metabolic pathways. *Plant Cell Physiol* **57**: 473–487.

Heinrich B, Raven PH. 1972. Energetics and pollination ecology. *Science* **176**: 597–602.

Herben T, Šerá B, Klimešová J. 2015. Clonal growth and sexual reproduction: tradeoffs and environmental constraints. *Oikos* **124**: 469–476.

Herms DA, Mattson WJ. 1992. The dilemma of plants: to grow or defend. *Q Rev Biol* **67**: 283–335.

Hesse O. 1924. Untersuchungen über die Einwirkung chemischer Stoffe auf die Keimung lichtempfindlicher Samen. *Bot Arch* **5**: 133–171.

Hilhorst HWM, Karssen CM. 1992. Seed dormancy and germination: the role of abscisic acid and gibberellins and the importance of hormone mutants. *Plant Growth Regul* **11**: 225–238.

Horie T 1994. Crop ontogeny and development. In: Boote KJ, Bennet JM, Sinclair TR, Paulsen GM eds. *Physiology and Determination of Crop Yield, (eds)*. Madison: American Society of Agronomy, Crop Science Society of America, Soil Science Society of America, 153–180.

Horvitz CC, Beattie AJ. 1980. Ant dispersal of Calathea (Marantaceae) seeds by carnivorous ponerines (Formicidae) in a tropical rain forest. *Am J Bot* **67**: 321–326.

Howe HF 1986. Seed dispersal by fruit-eating birds and mammals. In: Murray DR ed. *Seed Dispersal*. Sydney: Academic Press, 189.

Imaizumi T. 2010. *Arabidopsis* circadian clock and photoperiodism: time to think about location. *Curr Opin Plant Biol* **13**: 83–89.

Jelinski DE, Cheliak WM. 1992. Genetic diversity and spatial subdivision of *Populus tremuloides* (Salicaceae) in a heterogeneous landscape. *Am J Bot* **79**: 728–736.

Jónsdóttir IS, Callaghan TV, Headly AD. 1996. Resource dynamics within arctic clonal plants. *Ecol Bull*: 53–64.

Karssen CM 1982. Seasonal patterns of dormancy in weed seeds. In: Kahn AA ed. *The Physiology and Biochemistry of Seed Development, Dormancy and Germination*. Amsterdam: Elsevier, 243–270.

Kim D-H, Doyle MR, Sung S, Amasino RM. 2009. Vernalization: winter and the timing of flowering in plants. *Annu Rev Cell Develop Biol* **25**: 277–299.

Kiss T, Dixon LE, Soltész A, Bányai J, Mayer M, Balla K, Allard V, Galiba G, Slafer GA, Griffiths S, Veisz O, Karsai I. 2017. Effects of ambient temperature in association with photoperiod on phenology and on the expressions of major plant developmental genes in wheat (*Triticum aestivum* L.). *Plant Cell Environ* **40**: 1629–1642.

Kjellberg B, Karlsson S, Kerstensson I. 1982. Effects of heliotropic movements of flowers of *Dryas octopetala* L. on gynoecium temperature and seed development. *Oecologia* **54**: 10–13.

Klinkhamer PGL, de Jong TJ, Meelis E. 1987. Delay of flowering in the 'biennial' *Cirsium vulgare*: size effects and devernalization. *Oikos* **49**: 303–308.

Knudsen JT, Tollsten L, Ervik F. 2001. Flower scent and pollination in selected neotropical palms. *Plant Biol* **3**: 642–653.

Koester RP, Skoneczka JA, Cary TR, Diers BW, Ainsworth EA. 2014. Historical gains in soybean (*Glycine max* Merr.) seed yield are driven by linear increases in light interception, energy conversion, and partitioning efficiencies. *J Exp Bot* **65**: 3311–3321.

Koller D, Negbi M. 1959. The regulation of germination in *Oryzopsis miliacea*. *Ecology* **40**: 20–36.

Kursar TA, Coley PD. 1992a. The consequences of delayed greening during leaf development for light absorption and light use efficiency. *Plant Cell Environ* **15**: 901–909.

Kursar TA, Coley PD. 1992b. Delayed development of the photosynthetic apparatus in tropical rain forest species. *Funct Ecol* **6**: 411–422.

Kursar TA, Coley PD. 1992c. Delayed greening in tropical leaves: an antiherbivore defense? *Biotropica* **24**: 256–262

Lambers H, Clode PL, Hawkins H-J, Laliberté E, Oliveira RS, Reddell P, Shane MW, Stitt M, Weston P 2015. Metabolic adaptations of the non-mycotrophic Proteaceae to soil with a low phosphorus availability. In: Plaxton WC, Lambers H eds. *Annual Plant Reviews, Volume 48, Phosphorus Metabolism in Plants*. Chicester: John Wiley & Sons, 289–336.

Leck MA, Parker VT, Simpson RL. 2008. *Seedling Ecology and Evolution*. Cambridge: Cambridge University Press.

Leishman MR, Westoby M. 1994. The role of large seed size in shaded conditions: experimental evidence. *Funct Ecol* **8**: 205–214.

Leishman MR, Westoby M, Jurado E. 1995. Correlates of seed size variation: a comparison among five temperate floras. *J Ecol* **83**: 517–529.

Ludlow AE. 1991. *Ochna pulchra* Hook: leaf growth and development related to photosynthetic activity. *Ann Bot* **68**: 527–540.

Martinez-Garcia JF, Virgos-Soler A, Prat S. 2002. Control of photoperiod-regulated tuberization in potato by the Arabidopsis flowering-time gene CONSTANS. *Proc Natl Acad Sci USA* **99**: 15211–15216.

Mazzella M, Casal J, Muschietti J, Fox A. 2014. Hormonal networks involved in apical hook development in darkness and their response to light. *Front Plant Sci* **5**: 52.

McAuliffe JR, Hamerlynck EP, Eppes MC. 2007. Landscape dynamics fostering the development and persistence of long-lived creosotebush (*Larrea tridentata*) clones in the Mojave Desert. *J Arid Environ* **69**: 96–126.

McKee GW, Peiffer RA, Mohsenin NN. 1977. Seedcoat structure in *Coronilla varia* and its relations to hard seed. *Agron J* **69**: 53–58.

Meisert A, Schulz D, Lehmann H. 1999. Structural features underlying hardseededness in Geraniaceae. *Plant Biol* **1**: 311–314.

Milberg P, Andersson L, Thompson K. 2000. Large-seeded spices are less dependent on light for germination than small-seeded ones. *Seed Sci Res* **10**: 99–104.

Mitich LW. 1991. Mistletoe: the Christmas weed. *Weed Technol*: 692–694.

Morris WL, Hancock RD, Ducreux LJM, Morris JA, Usman M, Verrall SR, Sharma SK, Bryan G, McNicol JW, Hedley PE, Taylor MA. 2014. Day length dependent restructuring of the leaf transcriptome and metabolome in potato genotypes with contrasting tuberization phenotypes. *Plant Cell Environ* **37**: 1351–1363.

Mouradov A, Cremer F, Coupland G. 2002. Control of flowering time. *Interacting Pathways as a Basis for Diversity* **14**: S111–S130.

Murphy SR, Reid N, Yan Z, Venables WN. 1993. Differential passage time of mistletoe fruits through the gut of honeyeaters and flowerpeckers: effects on seedling establishment. *Oecologia* **93**: 171–176.

Murray DR, ed. 1986. *Seed Dispersal*. Sydney: Academic Press.

Née G, Xiang Y, Soppe WJJ. 2017. The release of dormancy, a wake-up call for seeds to germinate. *Curr Opin Plant Biol* **35**: 8–14.

Nelson DC, Flematti GR, Ghisalberti EL, Dixon KW, Smith SM. 2012. Regulation of seed germination and seedling growth by chemical signals from burning vegetation. *Annu Rev Plant Biol* **63**: 107–130.

Numata S, Kachi N, Okuda T, Manokaran N. 2004. Delayed greening, leaf expansion, and damage to sympatric *Shorea* species in a lowland rain forest. *J Plant Res* **117**: 19–25.

Ohnishi M, Fukada-Tanaka S, Hoshino A, Takada J, Inagaki Y, Iida S. 2005. Characterization of a novel Na^+/H^+ antiporter gene *InNHX2* and comparison of *InNHX2* with *InNHX1*, which is responsible for blue flower coloration by increasing the vacuolar pH in the Japanese morning glory. *Plant Cell Physiol* **46**: 259–267.

Olmsted CE. 1944. Growth and development in range grasses. IV. Photoperiodic responses in twelve geographic strains of side-oats grama. *Bot Gaz* **106**: 46–74.

Pasquet-Kok J, Creese C, Sack L. 2010. Turning over a new 'leaf': multiple functional significances of leaves versus phyllodes in Hawaiian *Acacia koa*. *Plant Cell Environ* **33**: 2084–2100.

Pate JS, Herridge DF. 1978. Partitioning and utilization of net photosynthate in a nodulated annual legume. *J Exp Bot* **29**: 401–412.

Pavliscak LL, Fehmi JS, Smith SE. 2015. Assessing emergence of a long-lived monocarpic succulent in disturbed, arid environments: evaluating abiotic factors in effective *Agave* restoration by seed. *Arid Land Research and Management* **29**: 98–109.

Pearson TRH, Burslem DFRP, Mullins CE, Dalling JW. 2002. Germination ecology of neotropical pioneers: interacting effects of environmental conditions and seed size. *Ecology* **83**: 2798–2807.

Peck SC, Pawlowski K, Kende H. 1998. Asymmetric responsiveness to ethylene mediates cell elongation in the apical hook of peas. *Plant Cell* **10**: 713–719.

Phillips RD, Hopper SD, Dixon KW. 2010. Pollination ecology and the possible impacts of environmental change in the Southwest Australian Biodiversity Hotspot. *Phil Trans R Soc Lond B* **365**: 517–528.

Phillips RD, Peakall R, Dixon KW 2014. The beguiling and the warty – pollination of kwongan orchids. In: Lambers H ed. *Plant Life on the Sandplains in Southwest Australia, a Global Biodiversity Hotspot*. Crawley: UWA Publishing, 181–193.

Piñeiro M, Coupland G. 1998. The control of flowering time and floral identity in *Arabidopsis*. *Plant Physiol* **117**: 1–8.

Pizo MA, Oliveira PS. 1998. Interaction between ants and seeds of a nonmyrmecochorous neotropical tree, *Cabralea canjerana* (Meliaceae), in the Atlantic forest of southeast Brazil. *Am J Bot* **85**: 669–674.

Pons TL. 1989. Breaking of seed dormancy by nitrate as a gap detection mechanism. *Ann Bot* **63**: 139–143.

Pons TL. 1991a. Dormancy, germination and mortality of seeds in a chalk-grassland flora. *J Ecol* **79**: 765–780.

Pons TL. 1991b. Induction of dark dormancy in seeds: its importance for the seed bank in the soil. *Funct Ecol* **5**: 669–675.

Pons TL 2000. Seed responses to light. In: Fenner M ed. *Seeds, the Ecology of Regeneration in Plant Communities, 2nd edition*. Wallingford: C.A.B. International, 237–260.

Pons TL, During HJ. 1987. Biennal behaviour of *Cirsium palustre* in ash coppice. *Ecography* **10**: 40–44.

Pons TL, Schröder HFJM. 1986. Significance of temperature fluctuation and oxygen concentration for germination of the rice field weeds *Fimbristylis littoralis* and *Scirpus juncoides*. *Oecologia* **68**: 315–319.

Preston CA, Betts H, Baldwin IT. 2002. Methyl jasmonate as an allelopathic agent: sagebrush inhibits germination of a neighboring tobacco, *Nicotiana attenuata*. *J Chem Ecol* **28**: 2343–2369.

Queenborough SA, Metz MR, Valencia R, Wright SJ. 2013. Demographic consequences of chromatic leaf defence in tropical tree communities: do red young leaves increase growth and survival? *Ann Bot* **112**: 677–684.

Raman H, Raman R, Kilian A, Detering F, Carling J, Coombes N, Diffey S, Kadkol G, Edwards D, McCully M, Ruperao P, Parkin IAP, Batley J, Luckett DJ, Wratten N. 2014. Genome-wide delineation of natural variation for pod shatter resistance in *Brassica napus*. *PLoS ONE* **9**: e101673.

Ream TS, Woods DP, Schwartz CJ, Sanabria CP, Mahoy JA, Walters EM, Kaeppler HF, Amasino RM. 2014. Interaction of photoperiod and vernalization determines flowering time of *Brachypodium distachyon*. *Plant Physiol* **164**: 694–709.

Reaumur RAF 1735. Observations du thermomètre faites à Paris pendant l'anneé 1735, comparées avec celles qui ont été faites sous la Ligne, à l'Isle de France, à Algeres, & en quelquesunes de nos Isles de l'Amerique. *Histoire de l'Academie Royale des Sciences, avec les Mémoires de Mathematique & de Physique pour la même année*. Paris, 545–580.

Roche S, Koch JM, Dixon KW. 1997. Smoke enhanced seed germination for mine rehabilitation in the south-west of Western Australia. *Rest Ecol* **5**: 191–203.

Roll-Hansen N. 1985. A new perspective on Lysenko? *Annals of Science* **42**: 261–278.

Rubio de Casas R, Willis CG, Pearse WD, Baskin CC, Baskin JM, Cavender-Bares J. 2017. Global biogeography of seed dormancy is determined by seasonality and seed size: a case study in the legumes. *New Phytol* **214**: 1527–1536.

Sakes A, van der Wiel M, Henselmans PWJ, van Leeuwen JL, Dodou D, Breedveld P. 2016. Shooting mechanisms in nature: a systematic review. *PLoS ONE* **11**: e0158277.

Salguero-Gómez R, Jones OR, Jongejans E, Blomberg SP, Hodgson DJ, Mbeau-Ache C, Zuidema PA, de Kroon H, Buckley YM. 2016. Fast–slow continuum and reproductive strategies structure plant life-history variation worldwide. *Proc Natl Acad Sci USA* **113**: 230–235.

Salisbury EJ. 1942. *The Reproductive Capacity of Plants*. London: Bell.

Samach A, Coupland G. 2000. Time measurement and the control of flowering in plants. *BioEssays* **22**: 38–47.

Samuels IA, Levey DJ. 2005. Effects of gut passage on seed germination: do experiments answer the questions they ask? *Funct Ecol* **19**: 365–368.

Schiestl FP. 2005. On the success of a swindle: pollination by deception in orchids. *Naturwissenschaften* **92**: 255–264.

Schiestl FP, Peakall R, Mant JG, Ibarra F, Schulz C, Franke S, Francke W. 2003. The chemistry of sexual deception in an orchid-wasp pollination system. *Science* **302**: 437–438.

Scopel AL, Ballaré CL, Radosevich SR. 1994. Photostimulation of seed germination during soil tillage. *New Phytol* **126**: 145–152.

Seidlová F, Štichová J. 1968. Development of the shoot apex of *Chenopodium rubrum* L. after photoperiodic induction in the cotyledon stage. *Biol Plant* **10**: 131.

Seymour RS, Gibernau M, Ito K. 2003. Thermogenesis and respiration of inflorescences of the dead horse arum *Helicodiceros muscivorus*, a pseudo-thermoregulatory aroid associated with fly pollination. *Funct Ecol* **17**: 886–894.

Shipley B, Dion J. 1992. The allometry of seed production in herbaceous angiosperms. *Amer Nat* **139**: 467–483.

Shirley BW. 1996. Flavonoid biosynthesis: 'new' functions for an 'old' pathway. *Trends Plant Sci* **1**: 377–382.

Simpson RJ, Lambers H, Dalling MJ. 1983. Nitrogen redistribution during grain growth in wheat (*Triticum aestivum* L.): IV. Development of a quantitative model of the translocation of nitrogen to the grain. *Plant Physiol* **71**: 7–14.

Song YH, Ito S, Imaizumi T. 2013. Flowering time regulation: photoperiod- and temperature-sensing in leaves. *Trends Plant Sci* **18**: 575–583.

Song YH, Shim JS, Kinmonth-Schultz HA, Imaizumi T. 2015. Photoperiodic flowering: time measurement mechanisms in leaves. *Annu Rev Plant Biol* **66**: 441–464.

Stanton M, Galen C. 1993. Blue light controls solar tracking by flowers of an alpine plant. *Plant Cell Environ* **16**: 983–989.

Stanton ML, Bereczky JK, Hasbrouck HD. 1987. Pollination thoroughness and maternal yield regulation in wild radish, *Raphanus raphanistrum* (Brassicaceae). *Oecologia* **74**: 68–76.

Stueffer JF, De Kroon H, During HJ. 1996. Exploitation of environmental hetergeneity by spatial division of labor in a clonal plant. *Funct Ecol* **10**: 328–334.

Sulpice R, Ishihara H, Schlereth A, Cawthray GR, Encke B, Giavalisco P, Ivakov A, Arrivault S, Jost R, Krohn N, Kuo J, Laliberté E, Pearse SJ, Raven JA, Scheible WR, Teste F, Veneklaas EJ, Stitt M, Lambers H. 2014. Low levels of ribosomal RNA partly account for the very high photosynthetic phosphorus-use efficiency of Proteaceae species. *Plant Cell Environ* **37**: 1276–1298.

Tamaki S, Matsuo S, Wong HL, Yokoi S, Shimamoto K. 2007. Hd3a protein Is a mobile flowering signal in rice. *Science* **316**: 1033–1036.

Taulya G, van Asten PJA, Leffelaar PA, Giller KE. 2014. Phenological development of East African highland banana involves trade-offs between physiological age and chronological age. *Eur J Agron* **60**: 41–53.

Teotia S, Tang G. 2015. To bloom or not to bloom: role of microRNAs in plant flowering. *Mol Plant* **8**: 359–377.

Terry I, Moore CJ, Walter GH, Forster PI, Roemer RB, Donaldson JD, Machin PJ. 2004. Association of cone thermogenesis and volatiles with pollinator specificity in *Macrozamia* cycads. *Plant Syst Evol* **243**: 233–247.

Thompson K, Grime JP, Mason G. 1977. Seed germination in response to diurnal fluctuations of temperature. *Nature* **267**: 147–149.

Thompson K, Ooi MKJ. 2010. To germinate or not to germinate: more than just a question of dormancy. *Seed Sci Res* **20**: 209–211.

Totland O. 1996. Flower heliotropism in an alpine population of *Ranunculus acris* (Ranunculaceae): effects on flower temperature, insect visitation, and seed production. *Am J Bot* **83**: 452–458.

Tuan PA, Kumar R, Rehal PK, Toora PK, Ayele BT. 2018. Molecular mechanisms underlying abscisic acid/gibberellin balance in the control of seed dormancy and germination in cereals. *Front Plant Sci* **9**: 668.

Tubbs CH, Houston DR 1990. *Fagus grandifolia* Ehrh. American beech. *Silvics of North America,*

Volume 2, Hardwoods. Washington, DC: Forest Service, United States of Department of Agriculture, 325–332.

Ullmann I. 1989. Stomatal conductance and transpiration of *Acacia* under field conditions: similarities and differences between leaves and phyllodes. *Trees* **3**: 45–56.

Vallejo-Marín M, Dorken ME, Barrett SCH. 2010. The ecological and evolutionary consequences of clonality for plant mating. *Annu Rev Ecol Evol Syst* **41**: 193–213.

Van Der Burgt XM. 1997. Explosive seed dispersal of the rainforest tree *Tetraberlinia moreliana* (Leguminosae - Caesalpinioideae) in Gabon. *J Trop Ecol* **13**: 145–151.

Vazquez-Yanes C, Orozco-Segovia A, Rincon E, Sanchez-Coronado ME, Huante P, Toledo JR, Barradas VL. 1990. Light beneath the litter in a tropical forest: effect on seed germination. *Ecology* **71**: 1952–1958.

Veneklaas EJ, Lambers H, Bragg J, Finnegan PM, Lovelock CE, Plaxton WC, Price C, Scheible W-R, Shane MW, White PJ, Raven JA. 2012. Opportunities for improving phosphorus-use efficiency in crop plants. *New Phytol* **195**: 306–320.

Wang B, Phillips JS, Tomlinson KW. 2017. Tradeoff between physical and chemical defense in plant seeds is mediated by seed mass. *Oikos* **127**: 440–447.

Weiss MR. 1991. Floral colour changes as cues for pollinators. *Nature* **354**: 227–229.

Willis CG, Baskin CC, Baskin JM, Auld JR, Venable DL, Cavender-Bares J, Donohue K, Rubio de Casas R. 2014. The evolution of seed dormancy: environmental cues, evolutionary hubs, and diversification of the seed plants. *New Phytol* **203**: 300–309.

Woo HR, Masclaux-Daubresse C, Lim PO. 2018. Plant senescence: how plants know when and how to die. *J Exp Bot* **69**: 715–718.

Woodall GS, Dodd IC, Stewart GR. 1998. Contrasting leaf development within the genus *Syzygium*. *J Exp Bot* **49**: 79–87.

Woodall GS, Stewart GR. 1998. Do anthocyanins play a role in UV protection of the red juvenile leaves of *Syzygium*? *J Exp Bot* **49**: 1447–1450.

Yan D, Easwaran V, Chau V, Okamoto M, Ierullo M, Kimura M, Endo A, Yano R, Pasha A, Gong Y, Bi Y-M, Provart N, Guttman D, Krapp A, Rothstein SJ, Nambara E. 2016. NIN-like protein 8 is a master regulator of nitrate-promoted seed germination in *Arabidopsis*. *Nat Comm* **7**: 13179.

Yan L, Loukoianov A, Tranquilli G, Helguera M, Fahima T, Dubcovsky J. 2003. Positional cloning of the wheat vernalization gene *VRN1*. *Proc Natl Acad Sci USA* **100**: 6263–6268.

Zalamea P-C, Sarmiento C, Arnold AE, Davis A, Dalling JW. 2015. Do soil microbes and abrasion by soil particles influence persistence and loss of physical dormancy in seeds of tropical pioneers? *Front Plant Sci* **5**: 799.

Zeevaart JAD. 2008. Leaf-produced floral signals. *Curr Opin Plant Biol* **11**: 541–547.

Biotic Influences: Symbiotic Associations 12

12.1 Introduction

Symbiosis is the 'living together' of two or more organisms, often involving specialized structures. In its broadest sense, symbiotic associations include parasitic and commensal as well as mutually beneficial partnerships. It is common in the ecophysiological literature, however, to use the term **symbiosis** in a narrow sense to refer to **mutually beneficial associations** between plants and microorganisms. Mutual benefits may not always be easy to determine, particularly for the microsymbiont. In this chapter, benefits for the macrosymbiont ('host') are often expressed in terms of amount of accumulated biomass or acquired resources. In an ecological context, benefits in terms of 'fitness' may be more relevant, but these are rarely documented. In the mutually beneficial associations we discuss in this chapter, nutrients or specific products of the partners are shared between two or three partners; the macrosymbiont and the microsymbiont(s). Parasitic associations between plants are dealt with in Chap. 15; parasitic associations between microorganisms and plants are discussed briefly in this chapter, and more elaborately in Chap. 14.

In Chap. 9, we discussed numerous special mechanisms that allow some plants to acquire sparingly soluble nutrients from soil (*e.g.*, exudation of carboxylates and phytosiderophores). We also pointed out (Sects. 9.2.2.5 and 9.2.2.6) that some species are quite capable of growing in soils where phosphorus (P) is sparingly available, without having a large capacity to exude carboxylates. How do these plants manage to grow? It is also obvious that special mechanisms to take up nutrients (*e.g.*, N) are of little use, if the N is simply not there. Such plants must have alternative ways to acquire N.

This chapter discusses associations between plants and microorganisms that are of vital importance for the acquisition of nutrients. Such symbiotic associations play a major role in environments where the supply of P, nitrogen (N), or poorly mobile cations limits plant growth. In the **rhizosphere** (or elsewhere in the plant's immediate surroundings), mycorrhiza-forming fungi and N_2-fixing bacteria (including cyanobacteria and actinobacteria) may form symbiotic associations. For those species that are capable of such symbioses, it tends to be beneficial for both the plant (**macrosymbiont**) and the microorganism (**microsymbiont**). Some plants are associated with more than one microsymbiotic species at the same time.

12.2 Mycorrhizas

The vast majority (85%) of vascular plant species can form symbiotic associations with **mycorrhizal fungi** (Brundrett and Tedersoo 2018). Mycorrhizas are the structures arising from the association of roots and fungi; except for nonmycorrhizal species (Sect. 12.2.2), we should consider roots in soil in conjunction with their

H. Lambers, R. S. Oliveira, *Plant Physiological Ecology*, https://doi.org/10.1007/978-3-030-29639-1_12

mycorrhizal symbionts. The evolution of the plant–mycorrhizal fungus symbiosis was one of the key processes that contributed to the origin of land flora (Wang et al. 2010).

There are four main types of mycorrhizas (Sect. 12.2.1; Smith and Read 2008). The most ancient type dates back to the early Devonian, some 400 million years ago (Selosse et al. 2015; Brundrett and Tedersoo 2018). The first bryophyte-like land plants had endophytic associations resembling **arbuscular mycorrhizas** (**AM**), even before roots evolved (Martin et al. 2017). The symbionts are Glomerocota or Mucoromycota (Brundrett and Tedersoo 2018; Feijen et al. 2018). The **ectomycorrhizal** (**ECM**) symbiosis has evolved repeatedly over the last 130–180 million years; the symbionts are mostly Basidiomycota (Martin et al. 2017). Like root hairs (Sects. 9.2.2.1 and 9.2.2.5), mycorrhizal associations enhance the symbiotic plant's belowground absorbing surface. For some mycorrhizas (Table 12.1), this is the primary mechanism of AM plants to acquire scarcely available, poorly mobile nutrients, especially inorganic P (Pi) (Sect. 12.2.1). For other mycorrhizas, additional mechanisms such as release of hydrolytic enzymes and carboxylates also plays a role (Sect. 12.2.1).

The mycorrhizal associations may enhance plant growth, especially when Pi or other poorly mobile nutrients limit plant growth; they may also be beneficial when water is in short supply and suppress infection by parasitic plants (Sect. 15.2.1). Mycorrhizas also enhance plant defense against soil-borne pathogens (Jacott et al. 2017). As such, mycorrhizas are of great ecological and agronomic significance. When the nutrient supply is high, however, they are a potential carbon drain on the plant, providing less nutritional benefits in return. Plants, however, have mechanisms to suppress the symbiotic association at a high supply of Pi (Sect. 12.2.3.1).

Some species never form a mycorrhizal association, even when P is in short supply. Some of these (*e.g.*, Proteaceae, Cyperaceae; Sect. 9.2.2.5.2), perform well when Pi is severely limiting; other nonmycorrhizal plants may even be harmed by mycorrhizal fungi (Sect. 16.7 of Chap. 16). On the other hand, some nonmycorrhizal plants severely inhibit the growth of mycorrhizal hyphae. Before dealing with these complex interactions (Sect. 12.2.2), we discuss some general aspects of mycorrhizal associations.

12.2.1 Mycorrhizal Structures: Are They Beneficial for Plant Growth?

Mycorrhizas occur in the vast majority of all angiosperm species investigated to date; all

Table 12.1 The length of mycorrhizal hyphae per unit colonized root length for a number of plant species, colonized by different arbuscular mycorrhiza-forming fungal species.

Fungus	Host	Hyphal length (m cm^{-1} root)
Glomus mosseae	*Allium cepa* (onion)	0.79–2.5
Glomus mosseae	*Allium cepa*	0.71
Glomus macrocarpus var. *geospora*	*Allium cepa*	0.71
Glomus microcarpus	*Allium cepa*	0.71
Glomus sp.	*Trifolium* sp. (clover)	1.29
Glomus sp.	*Lolium* sp. (ryegrass)	1.36
Glomus fasciculatum	*Trifolium* sp.	2.50
Glomus tenue	*Trifolium* sp.	14.20
Gigaspora calospora	*Allium cepa*	0.71
Gigaspora calospora	*Trifolium* sp.	12.30
Acaulospora laevis	*Trifolium* sp.	10.55

Source: Various authors, as cited in Smith and Gianinazzi-Pearson (1988)

gymnosperms are mycorrhizal (Brundrett and Tedersoo 2018). A mycorrhizal association consists of three vital parts:

1. The root;
2. The fungal structures in close association with the root;
3. The external mycelium growing in the soil.

Mycorrhizas are classified in different types, but some are very similar (Smith and Read 2008). **Arbuscular mycorrhizas** (**AM**) are the most widespread. A large fraction of the fungal tissue is within root cortical cells, outside their plasma membrane (Fig. 12.1). They frequently occur on herbaceous plants, but also on trees, especially in tropical forests. **Ericoid mycorrhizas** in the Ericaceae and **orchid mycorrhizas** in the Orchidaceae have somewhat different structures and functions (Fig. 12.2). Some plants that predominantly have ECM associations, such as *Alnus* (alder), *Eucalyptus* (gumtrees), and *Salix* (willow) also have AM, for example as seedlings, or when growing in extreme habitats (Fig. 12.3; Brundrett and Tedersoo 2018).

Arbuscular mycorrhizas are the most widespread mycorrhizal association, occurring in 72% of all vascular plants, with fungi belonging to Glomeromycota (Brundrett and Tedersoo 2018). These fungi are considered 'primitive', because they have relatively simple spores, and they associate with a wide range of plant species. They are not capable of growing without a plant host. The AMs are named after the **arbuscules** (which are treelike structures that occur inside root cortical cells (Fig. 12.1). Although the arbuscule can fill most of the cell space, it does not compromise the integrity of the plant plasma membrane, because cortical cells envelop the arbuscules in a specialized host membrane, the **periarbuscular membrane** (Javot et al. 2007). The roots of 80% of all surveyed plant species and 92% of all families can be colonized by AM-forming fungi (Wang and Qiu 2006). Even species that are typically ectomycorrhizal may form AM associations in the absence of ectomycorrhizal inoculum.

In ericoid and orchid mycorrhizas, like in AMs, a large fraction of the fungal tissues is within the root cortical cells. Many forest trees worldwide, particularly in temperate and boreal biomes, form ectomycorrhizal symbioses with basidiomycete and, to a lesser extent, ascomycete fungi (Cairney 2011). The oldest fossils of ECM roots of Pinaceae and Dipterocarpaceae are from the Early Eocene, 41 to 56 million years ago (Martin et al. 2017). **Ectomycorrhizas** independently evolved many times through **parallel evolution**. Coevolution between plant and fungal partners in ECM has probably contributed to diversification of both plant hosts and fungal symbionts (Wang and Qiu 2006).

12.2.1.1 The Infection Process

Root exudates from AM host plants enhance, but are not required for spore germination, whereas exudates from nonhost plants, *e.g.*, *Lupinus* (lupine) or *Brassica* (cabbage) species, do not stimulate germination. Roots of host plants also release a signal or signals that stimulate(s) the directional growth of the AM fungus toward them. CO_2 may be one such signal (Becard et al. 2004), but there are others, analogous to the signal molecules (flavonoids) involved in the legume-rhizobium recognition interactions (Sect. 12.3.3; Scervino et al. 2005; Catford et al. 2006). In fact, flavonoids have been implicated in the recognition between AM hosts and fungi (Hause and Fester 2005), but they are not the key components in the AM fungus-host recognition (Schmitz and Harrison 2014).

Fungal signals comprise a mix of sulfated and nonsulfated **lipochitooligosaccharides**, which are structurally related to rhizobial nodulation-factor lipochitooligosaccharides that induce the formation of N_2-fixing root nodules in legumes (Maillet et al. 2011). These signals are transduced via a common symbiotic signaling pathway that activates a group of transcription factors. Gene expression activation by lipochitooligosaccharides requires transcription factors. A central regulator of root colonization by AM fungi controls genes activated by nonsulfated lipochitooligosaccharides during the pre-symbiotic stage that are also upregulated in areas with early physical contact, linking responses to externally applied

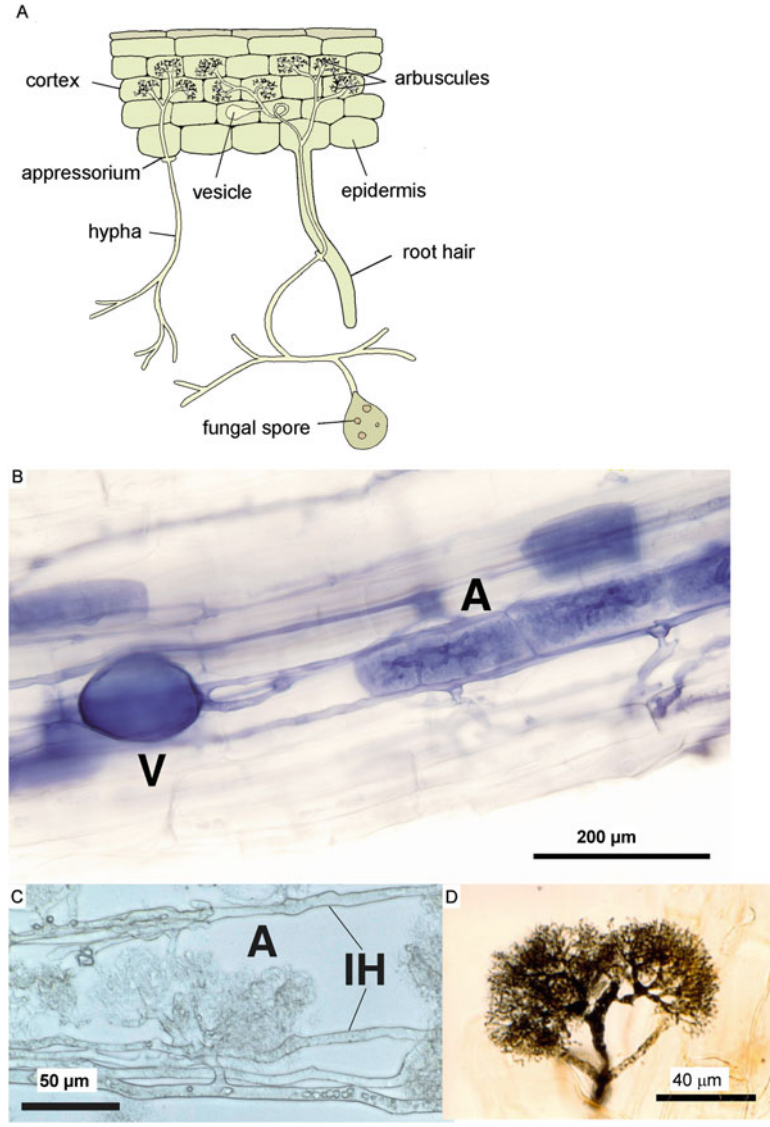

Fig. 12.1
(**A**) Schematic structure of an arbuscular mycorrhiza (AM). (**B**) Arbuscules (A) and a vesicle (V) of *Glomus* sp. colonized on the root of *Tagetes patula* (marigold). (**C**) Arbuscules (A) and intercellular hyphae (IH) of *Glomus etunicatum* isolated from the root of *Tagetes patula* after enzymatic digestion. (**D**) Detail of the intraradical hyphae of *Glomus mosseae* in a root of *Tagetes patula* (marigold), after enzymatic digestion of the root, showing fine branches and trunks of an arbuscule (courtesy T. Ezawa, Nagoya University, Japan; Ezawa et al. 1995).

lipochitooligosaccharides with early root colonization (Hohnjec et al. 2015).

In one of the first stages of AM **host recognition**, the hyphae of AM fungi show extensive branching in the vicinity of host roots in response to signaling molecules (Fig. 12.4). Root exudates contain a **branching factor** identified as a **strigolactone**, 5-deoxy-strigol (Akiyama et al. 2005; Paszkowski 2006). Strigolactones are a group of sesquiterpene lactones (Goulet and Klee 2010), originally isolated as seed-germination stimulants for the **parasitic weeds** *Striga* and *Orobanche* (Sect. 15.2.1). Several phytohormones play a role in the structural responses to Pi deficiency including **strigolactones**, which are primary signals for initiating AM symbiosis and enhance lateral root growth in P-limited plants (Czarnecki et al. 2013). Strigolactones induce extensive **hyphal branching** in germinating spores of the AM fungus *Gigaspora margarita* at very low concentrations (Bouwmeester et al. 2007). Within

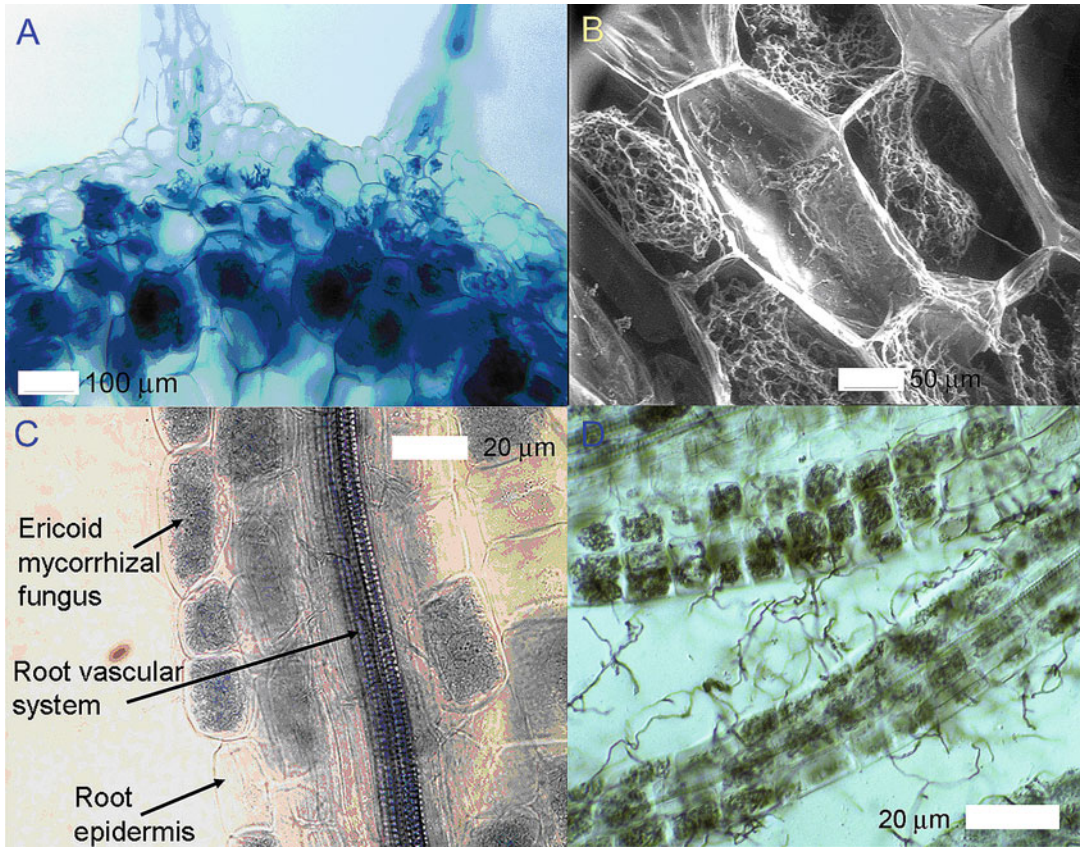

Fig. 12.2 (**A**) Orchidaceous mycorrhizal association in a stem of *Pterostylis sanguinea* (greenhood orchid). (**B**) Transverse section of a stem of *Caladenia arenicola* (carousel spider orchid) showing intracellular fungal coils (courtesy A.L. Batty and M.C. Brundrett, The University of Western Australia, Australia). (**C**) Ericoid mycorrhizal association of *Woollsia pungens* (Ericaceae), showing epidermal cells colonised by coils of an ericoid mycorrhizal fungus (stained blue, arrowed) (courtesy S. Chambers and J.W.G. Cairney, Western Sydney University, Australia). Copyright Elsevier Science, Ltd.). (**D**) Ericoid mycorrhizal association of *Leucopogon verticillatus* (tassel flower, Ericaceae) (courtesy M.C. Brundrett, The University of Western Australia, Australia).

1 h of exposure at concentrations as low as 10^{-13} M, the density of mitochondria in the fungal cells increases, and their shape and movement changes drastically which is associated with a rapid increase of mitochondrial density and respiration (Besserer et al. 2006, 2009). Isolation and identification of plant symbiotic signals has opened up new ways for studying the molecular basis of plant-AM-fungus interactions. This discovery also provides a clear answer to a long-standing question on the evolutionary origin of the release from host roots of molecules that stimulate seed germination in parasitic plants (Sect. 15.2.1; Akiyama and Hayashi 2006). Similar signaling between host and fungus also plays a role in mycorrhizal associations other than AM, but we know much less about this (Martin et al. 2016).

During the establishment of AM, fungal hyphae that grow from spores in the soil or from adjacent plant roots contact the root surface, where they differentiate to form an **appressorium** in response to signals released from the host roots, and initiate the internal colonization phase (Genre and Bonfante 2005). Appressoria form only on epidermal cells, and generally not on the roots of nonhost plants, a further indication of recognition signals (Harrison 2005).

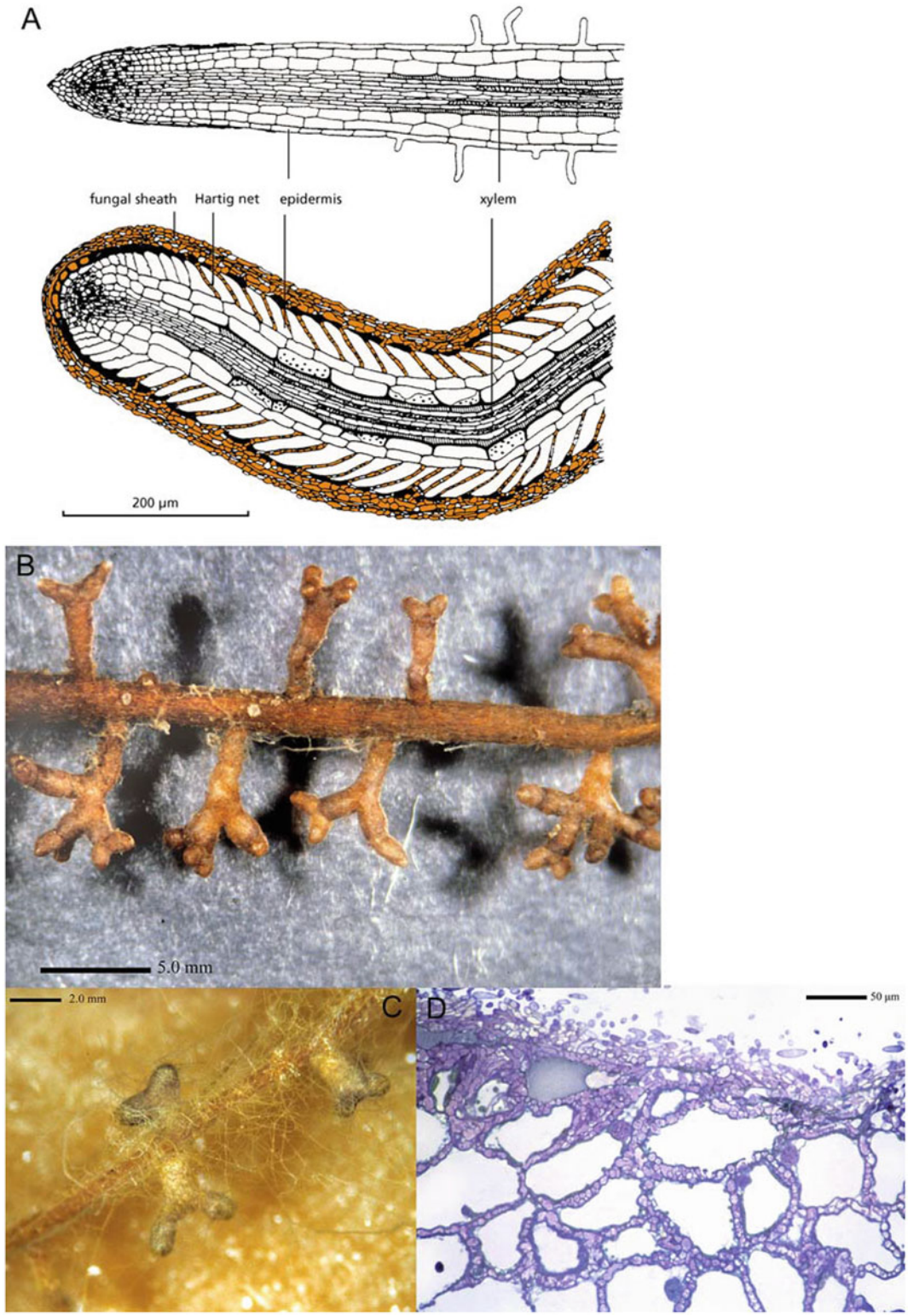

Fig. 12.3 (**A**) Schematic representation of an ectomycorrhiza, showing the fungal mantle around the root and the hyphae in the cortex which form the Hartig net. (**B–D**) Ectomycorrhizal association between *Pinus resinosa*

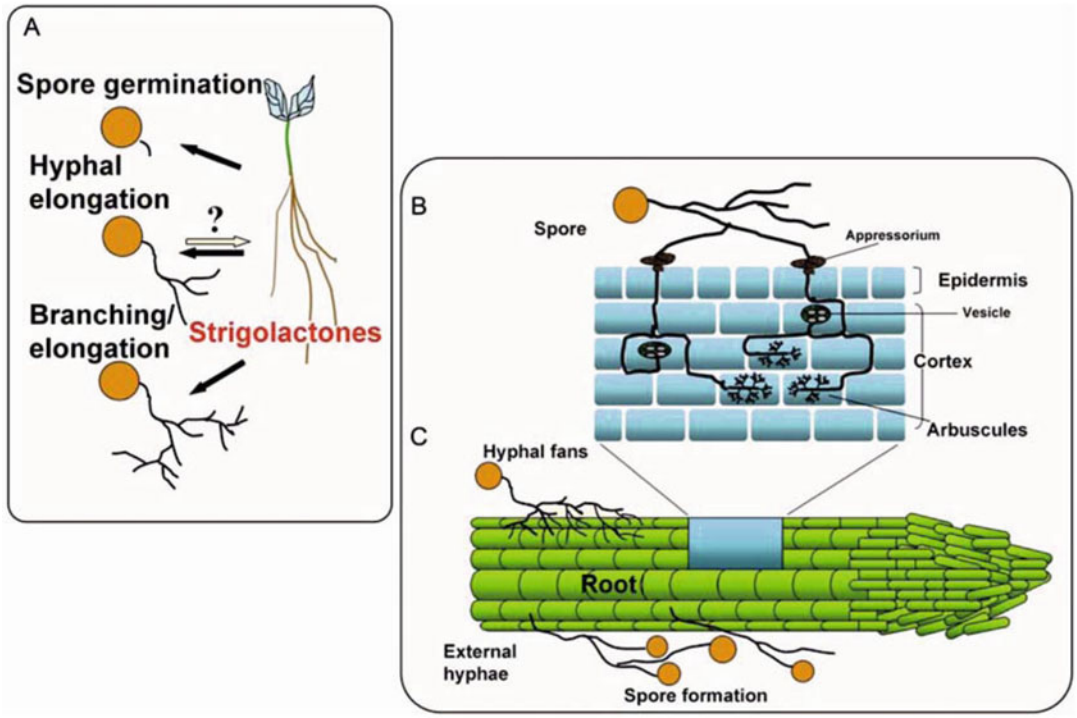

Fig. 12.4 The complete life cycle of arbuscular mycorrhizal fungi, involving recognition, communication, and establishment of symbiosis between fungus and host. The pre-germination stages may be stimulated by plant root exudates, but may also occur in its absence (after Gadkar et al. 2001).

Penetration of the root occurs via the appressoria, and the fungus frequently enters between two epidermal cells. Alternatively, a hypha may penetrate the cell wall of an epidermal or root-hair cell, and grow through the cell as a result of localized production of hydrolytic enzymes by the fungus.

Once inside the root, the fungus produces intercellular hyphae, coils, and **arbuscules** (Wang et al. 2017). The arbuscules increase the surface area of membranes over which exchange of metabolites occurs, and so enhance transport between the plasma membrane of the host and the hyphae of the fungus. Plants provide carbon in the form of sugars (*e.g.*, glucose; Pfeffer et al. 1999) and lipids (Jiang et al. 2017; Luginbuehl et al. 2017). The invaginated membranes of the arbuscules are highly specialized; they contain mycorrhiza-inducible **Pi transporters** (Glassop et al. 2005; Walder et al. 2016) and **H^+-pumping ATPases** (Requena et al. 2003). Arbuscules are short-lived, and usually degenerate within a week or two. Thus, progression of colonization requires continuous arbuscule formation as the fungus spreads in the roots (Gadkar et al. 2001; Luginbuehl et al. 2017). The hyphae proliferate both in the cortex and in the soil. **Vesicles**, in which lipids are stored, are sometimes formed at a later stage, either between or within cells. The AM fungus does not penetrate into the

Fig. 12.3 (continued) (red pine). and an unknown fungal species. A higher magnification of *Pinus resinosa* and *Pisolithus tinctorius* as the mycobiont, showing thickened branched rootlets, covered in a fungal mantle, and external hyphae. The highest magnification is of a longitudinal section of a *Pinus resinosa-Pisolithus tinctorius* mycorrhizal root, showing mantle hyphae on the root surface and Hartig net hyphae surrounding epidermal and cortical cells (courtesy R.L. Peterson, University of Guelph, Canada).

endodermis, stele, or meristems; it usually colonizes roots where the endodermis does not yet have a complete suberin barrier (Smith and Read 2008).

As with AM, orchid mycorrhizas show extensive intracellular growth with fungi forming intracellular **fungal coils**, rather than arbuscules (Fig. 12.2). The fungi forming the mycorrhizas are Basidiomycota, and many belong to the genus *Rhizoctonia*. As soon as they have germinated, the orchid seedlings, which have very few reserves, depend on organic matter in the soil or from other host plants which is supplied via the mycorrhizal fungus. *Rhizoctonia* species may form associations with both orchids and conifers. The orchids are therefore not saprophytic, but **mycoheterotrophic** (*i.e.* parasitic on the fungus) (Leake 2004); the association between host and fungus does not appear to be mutually beneficial. Even orchids that have the ability to photosynthesize may form ECM with forest trees, and their stable N- and C-isotope signatures indicate a dependence on ECM. This would explain the success of orchids in low-light environments (Waterman and Bidartondo 2008). In those orchids that remain nonphotosynthetic during their entire life cycle [*e.g.*, the Western Australian fully subterranean *Rhizanthella gardneri* (Bougoure et al. 2010)], the fungus continues to play this role. In all orchids, including those that are green (photosynthetic) as adults, the fungi also absorb mineral nutrients from soil (like AM, see below) (Cameron et al. 2006).

In ericoid mycorrhizas, a large number of infection points are found; up to 200 per mm root in *Calluna*, as opposed to 2 to 10 per mm in *Festuca ovina* (sheep's fescue), infected by an AM fungus. Up to 80% of the volume of these mycorrhizas may be fungal tissue (not including the external mycelium). The fungi infecting Ericaceae are Ascomycota (*e.g.*, *Hymenoscyphus ericae*) (Cairney and Ashford 2002).

Spores of **ectomycorrhizal** fungi in the rhizosphere may germinate to form a **monokaryotic mycelium**. This fuses with another hypha, forming a **dikaryotic mycelium**, which can then colonize the root, forming a mantle of fungal hyphae that enclose the root. The hyphae usually penetrate intercellularly into the cortex, where they form the **Hartig net** (Fig. 12.3; Brundrett and Tedersoo 2018). The hyphae always remain apoplastic, and can colonize the epidermal (angiosperms) and the cortical (gymnosperms) layers. As hyphae contact the root surface, roots may respond by increasing their diameter and switching from apical growth to precocious branching (Peterson and Bonfante 1994). Fungal biomass constitutes about 40% of ectomycorrhizas. Numerous fungal species have the capacity to form ectomycorrhizas. Most of these belong to the Basidiomycota and Ascomycota, and they are often species that we are familiar with as toadstools. Some of these are edible (*e.g.*, *Boletus*, truffles), whereas others are highly toxic (*e.g.*, *Amanita* species, agarics).

In contrast to infection by pathogenic fungi, colonization with mycorrhizal fungi never causes disease symptoms. In the presence of mycorrhizal fungi in the rhizosphere, flavonoids accumulate in the roots of the host *Medicago sativa* (alfalfa), similar to, but much weaker than the response to pathogenic fungal attack (Sect. 14.3). Arbuscular mycorrhizal fungi initiate a transient **host-defense response** in the early stages of colonization, followed by suppression to levels well below those of noncolonized plants. The production of defense-related gene products is restricted to **arbusculated cells**; intercellular hyphae and vesicles elicit no such defense response (Hause and Fester 2005). The rate and location of fungal growth within the root may be controlled through activation of plant defense mechanisms.

Some mutants of *Pisum sativum* (pea) and other legumes are characterized by aborted mycorrhizal infections, after formation of appressoria. Most mycorrhizal mutants reported in legumes were identified from small populations of nodulation mutants, and consequently genes required for both symbioses were found (Sect. 12.2.3), although some genes have separate functions in each symbiosis (Parniske 2008; Oldroyd 2013). This may point to a tight

control of two carbon-consuming and potentially competing symbioses (Sect. 12.2.6).

12.2.1.2 Mycorrhizal Responsiveness

In soils with low P availability, plants vary widely in the extent to which their growth responds to root colonization by mycorrhizal fungi (Johnson et al. 1997; Smith et al. 2004). **Mycorrhizal dependency** is the ratio of the dry mass of mycorrhizal plants to that of nonmycorrhizal plants; it depends both on functional group and soil fertility (Hoeksema et al. 2010). Species that depend less on AM fungi for their nutrient acquisition are generally colonized to a lesser extent in the field than are more AM-dependent ones. This suggests that species that have root systems with low dependency on mycorrhizas also have mechanisms to suppress mycorrhizal colonization (Sect. 12.2.3.1). Mycorrhizal dependency of a plant species also varies with the AM fungal species involved in the symbiosis. In grassland communities, dominant species tend to have a greater mycorrhizal dependency than subordinate species, so that suppression of the AM symbiosis enhances plant species diversity (Hartnett and Wilson 2002). Mycorrhizal colonization increases linearly with increasing root diameter, both in herbaceous and in woody species (Ma et al. 2018).

Plants that show little responsiveness to AM fungi in terms of growth may, in fact, acquire significant amounts of Pi via the fungus (Smith et al. 2003; Yang et al. 2012). Using a compartmented pot system and ^{33}P-labeled Pi (Fig. 12.5A), the contribution of the mycorrhizal uptake pathway to total plant Pi uptake can be estimated. The hyphal compartment is capped with 25-μm nylon mesh, which allows hyphae to penetrate, but excludes roots. Unlabeled Pi can be absorbed directly by roots or via the mycorrhizal pathway. Compared with noninoculated plants without additional Pi, *Linum usitatissimum* (flax) grows better, but to different extents, depending on the AM fungus tested (*Gigaspora rosea*, *Glomus caledonium*, or *Glomus intraradices*). *Medicago truncatula* (barrel medic) responds positively to the two *Glomus* species in terms of dry weight production, but shows a small growth depression with *Gigaspora rosea*, compared with nonmycorrhizal plants. *Solanum lycopersicum* (tomato) does not respond positively to any of the fungi. Phosphorus uptake also varies among the different plant-fungus combinations, and **mycorrhizal phosphorus dependencies** (Fig. 12.5B, middle) are similar to **mycorrhizal growth dependencies** (Fig. 12.5B, top). By supplying ^{33}Pi in a compartment to which only the fungal hyphae have access (Fig. 12.5A), it is possible to show that the mycorrhizal pathway differs in its contribution to total Pi uptake, depending on fungal and plant species. Phosphorus transfer via the mycorrhizal pathway is very high in five out of the nine individual plant-fungus combinations, but this is not correlated with mycorrhizal P dependency. With *Glomus intraradices* as the fungal partner, all of the Pi is delivered via the mycorrhizal pathway to all tested plants (Fig. 12.5B, bottom). These findings indicate that mycorrhizas may be an important pathway of Pi uptake, even in plants that do not show a positive effect on growth or P status as a result of AM colonization. It would be interesting to learn more about the conditions that cause down-regulation of Pi transporters responsible for Pi uptake from the root environment (Sect. 9.2.2.2) when AM fungi colonize the roots (Karandashov and Bucher 2005; Wang et al. 2017).

Mycorrhizal responsiveness is generally assessed using single species in a pot experiment, which poorly reflects the real world. When paired with a near-isogenic nonmycorrhizal genotype, even *Solanum lycopersicum* (tomato) shows a positive growth response (Cavagnaro et al. 2004), when this is not the case when tested singly (Fig. 12.5B, top). We discuss this aspect further in Sect. 12.2.2.

Crop cultivars, *e.g.*, of *Zea mays* (maize) that have been selected for high-input systems in Europe have not lost their ability to be colonized, and may be more responsive to inoculation by *Glomus intraradices* than those suited for low-input African systems (Wright et al. 2005). However, specific adaptations that allow nonmycorrhizal plants developed for low-input systems to perform well in low-P soils may limit

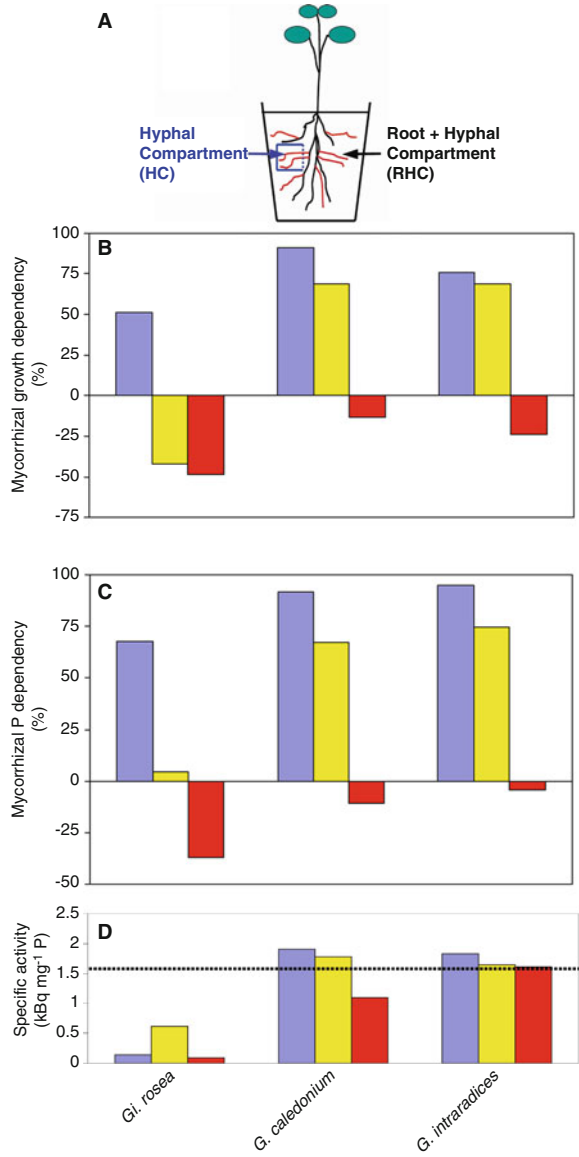

Fig. 12.5 (**A**) Diagrammatic representation (not to scale) of a compartmented pot design to assess phosphorus (P) uptake by mycorrhizas and roots. The main root + hyphae compartment is a nondraining pot containing a mixture of sand and soil. For mycorrhizal treatments, this mixture includes inoculum of three fungi: *Gigaspora rosea*, *Glomus caledonium*, and *Glomus intraradices*. Nonmycorrhizal treatments receive no inoculum. The hyphal compartment is a small plastic tube containing the same soil + sand mixture, but without inoculum; it is capped with 25 μm nylon mesh, which allows hyphae (shown in red), but not roots (shown in black) to grow into the hyphae compartment. The soil in the hyphae compartment is well mixed with ^{33}P-labeled orthophosphate of high specific activity. (**B**–**D**) Mycorrhizal effects on (**A**) growth, (**B**) total P uptake, and (**C**) specific activities of ^{33}P, in *Linum usitatissimum* (flax, blue bars), *Medicago truncatula* (barrel medic, yellow bars), and *Solanum lycopersicum* (tomato, red bars). Mycorrhizal dependencies for growth and P uptake are calculated as: 100 (value for mycorrhizal plant – mean value for nonmycorrhizal plants)/value for mycorrhizal plant. In the bottom panel, the dotted horizontal line indicates the predicted specific activity of ^{33}P in the plants if 100% of P is derived via the mycorrhizal pathway. This percentage is calculated using values for specific activities of ^{33}P in the plants, bicarbonate-extractable P in the hyphae compartment, and the total P available in the pots and in the hyphae compartment. It assumes that the densities of hyphae (meters per gram of soil) are the same in the hyphae compartment and in the hyphae + roots compartment (after Smith et al. 2003). Copyright American Society of Plant Biologists.

their ability to respond to higher nutrient supply rates and mycorrhizal infection. High-input cultivars may have traits that are useful for low-input cropping systems where mycorrhizal symbioses are established (Wright et al. 2005). A high mycorrhizal responsiveness is commonly associated with lack of well-developed root hairs and coarse fibrous roots (Sect. 9.2.2.1; Yang et al. 2015; Wen et al. 2019).

12.2.2 Nonmycorrhizal Species and Their Interactions with Mycorrhizal Species

Although mycorrhizal associations are very common, some species cannot be colonized, or only marginally so (Brundrett and Tedersoo 2018). These **nonmycorrhizal species** can be broadly categorized as either **ruderal** species that inhabit relatively fertile sites or species that occur on severely P-impoverished soils (Lambers and Teste 2013). The nonmycorrhizal ruderals include many that belong to the Brassicaceae, Caryophyllaceae, Chenopodiaceae, and Urticaceae. The species from severely **P-impoverished habitats** include Cyperaceae, Proteaceae, and Restionaceae, as well as carnivorous (Chap. 17) and parasitic species (Chap. 15) (Fig. 12.6; Brundrett and Tedersoo 2018). The 'scavenging' strategy of mycorrhizal species, which access P that is in the soil solution, but too far away from roots or inside soil pores that are too small for roots to enter, does not work on severely P-impoverished soils. The little amount of Pi that is present in these soils is predominantly sorbed to soil particles. Cluster roots, which release large amounts of carboxylates in an exudative burst (Sect. 9.2.2.5.2) effectively 'mine' Pi from these soils (Fig. 12.7). In younger landscapes, nonmycorrhizal species with cluster roots tend to occur on either calcareous soils, where the availability of Pi is low due to precipitation as calcium phosphates, or on acid soils, where Pi is associated with oxides and hydroxides of iron and aluminum (Fig. 9.1 in Sect. 9.2.1; Lambers et al. 2006, 2008). Carboxylate-releasing strategies are considerably more costly in terms of carbon requirements than mycorrhizal strategies (Raven et al. 2018).

Even within typical nonmycorrhizal genera, mycorrhizal colonization has been observed in some species (Boulet and Lambers 2005; Lagrange et al. 2013). It is interesting, as we discussed in Sect. 9.2.2.5.2, that many of the nonmycorrhizal species from severely P-impoverished soils have **cluster roots** or their functional equivalent (*e.g.*, Cactaceae, Cyperaceae, Proteaceae, and Velloziaceae). Other nonmycorrhizal species include **carnivorous** species, *e.g.*, *Drosera* (sundew) and **hemiparasitic** species, *e.g.*, *Nuytsia floribunda* (Western Australian Christmas tree) (Fig. 12.7).

The mechanisms that prevent colonization in nonmycorrhizal species are not fully understood. Nonmycorrhizal plants such as *Lupinus albus* (white lupin) and *Spinacea oleracea* (spinach) do exude strigolactones at low levels, but P deficiency hardly affects their exudation (Xie et al. 2010). In some species, the exudation of fungitoxic compounds, such as **glucosinolates** in Brassicaceae (Schreiner and Koide 1992) or **hevein** in *Urtica dioica* (stinging nettle) (Vierheilig et al. 1996) and *Hevea brasiliensis* (rubber tree) (Sosa-Rodriguez et al. 2013), may prevent or delay colonisation. More importantly, the correct chemical cues necessary for development after spores have germinated (Sect. 12.2.1.1) may be lacking (Schmitz and Harrison 2014).

Mycorrhizal fungi may enhance growth of mycorrhizal plants at a low P supply. In some nonmycorrhizal species, however, we find the exact opposite, i.e. growth inhibition (Sanders and Koide 1994; Veiga et al. 2013). This mechanism may well explain why nonmycorrhizal species show poor growth in a community dominated by mycorrhizal species, unless the P availability is increased (Francis and Read 1994).

12.2.3 Phosphate Relations

Like root hairs, the external mycelium of mycorrhizas increases the roots' absorptive surface. In fact, the effective root length of the

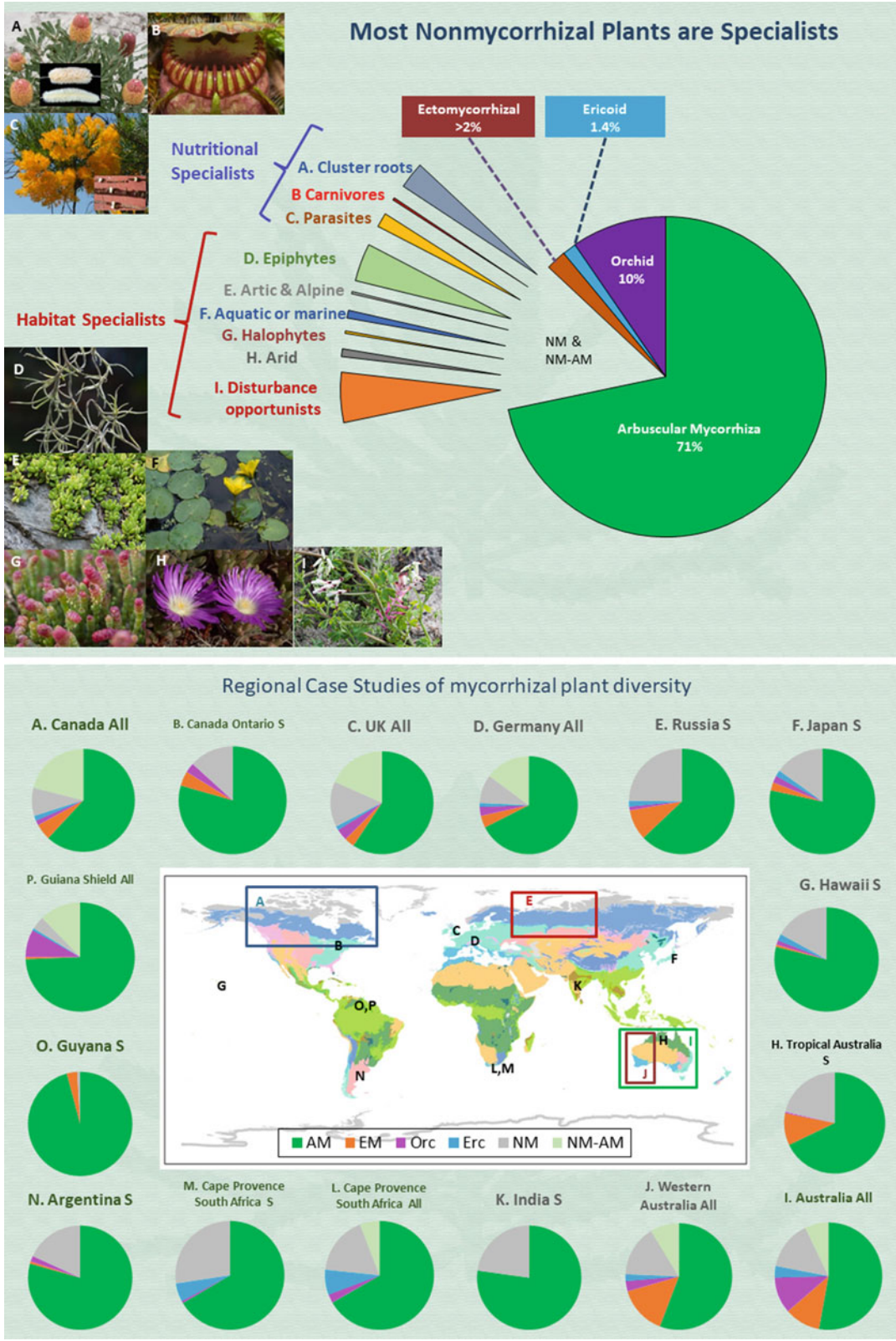

Fig. 12.6 (Top) Pie chart showing the taxonomic diversity of plants with different types of mycorrhizas, nonmycorrhizal (NM) roots, or inconsistent mycorrhizas (arbuscular mycorrhiza (AM–NM)). Exploded pie segments show plants assigned to the categories NM and NM–AM, which are combined and then reallocated to

mycorrhizal associations may increase 100-fold or more per unit root length (Table 12.1).

12.2.3.1 Mechanisms That Account for Enhanced Phosphate Absorption by Mycorrhizal Plants

Arbuscular mycorrhizal associations enhance Pi uptake and growth most strongly when the availability of Pi in the soil is fairly low (Sect. 9.2.2.5.2; Bolan et al. 1987; Thingstrup et al. 1998). In severely P-impoverished soils, however, the biomass of external AM and ECM hyphae is constrained (Abbott et al. 1984; Teste et al. 2016). In such situations, the mycorrhizal associations cannot contribute to Pi acquisition of the host plant, but they may remain important in boosting the host plants' defense against pathogens (Albornoz et al. 2017; Lambers et al. 2018).

Experiments using different soil compartments and different labeled sources of Pi show that AM plants do not have access to different chemical pools of Pi in soil (Fig. 12.8). They are capable, however, of acquiring P outside the depletion zone that surrounds the root, because of the **widely ramified hyphae**. These hyphae allow P transport over as much as 10 cm from the root surface and at rates that far exceed diffusion in soil (Fig. 12.9). In addition, they may access smaller soil pores and compete effectively with other microorganisms (Smith and Read 2008). Ectomycorrhizal hyphae can extend even greater distances than AM hyphae, possibly several meters. Arbuscular mycorrhizas do not access significant amounts of organic P directly (Smith et al. 2015), but microbes should be recognized as a third part of the AM symbiosis, not just soil-borne 'free riders' (Jansa et al. 2013). AM hyphae and free-living phosphate-solubilizing bacteria may interact by providing the carbon or P that the other microorganism requires, depending on Pi availability (Zhang et al. 2016).

Ectomycorrhizas and ericoid mycorrhizas frequently occur in organic soils, whereas AM are more typical of mineral soils. Ectomycorrhizal and ericoid mycorrhizal roots have access to additional chemical pools of P; they may release **phosphatases**, which enhance the availability of organic P or exude **carboxylates**, which increase the availability of sparingly soluble organic P and Pi (Landeweert et al. 2001; Van Hees et al. 2006). *Hymenoscyphus ericae*, which forms mycorrhizas with a number of Ericaceae, also produces extracellular enzymes. This allows ericoid mycorrhizal fungi to decompose components of plant cell walls and access mineral nutrients in these walls (Leake and Read 1989; Adamczyk et al. 2016).

Laccaria bicolor, an ectomycorrhizal fungus, is capable of paralyzing, killing, and digesting **springtails**. A significant portion of the organic N that is subsequently hydrolyzed ends up in its macrosymbiont, *Pinus strobus* (eastern white pine) (Klironomos and Hart 2001). Springtails selectively feed on fungi, including mycorrhizal fungi. Should this phenomenon prove to be widespread, nutrient cycling in forests may turn out to be more complicated than is currently recognized.

The external AM mycelium consists of both large 'runner' hyphae and finer hyphae with a role in nutrient absorption. As in roots, Pi uptake by the fine mycorrhizal hyphae occurs via active transport, against an electrochemical potential gradient, with a proton-cotransport mechanism (Sect. 9.2.2.2). Once absorbed by the external hyphae, Pi is rapidly transported into vacuoles where most of it is polymerized into inorganic **polyphosphate** (poly-P), a linear polymer of three to thousands of Pi molecules, connected by high-energy phosphate bonds (Ezawa et al.

Fig. 12.6 (continued) groups based on mineral nutrition or habitat specializations. These specialized plants are assigned to categories at the family level, based on the most important strategy for each family (families often include several of these strategies). Note that these specialized habitats also include many mycorrhizal plants, but NM and NM–AM plants are much more common than elsewhere. Inset photos show mycorrhizal structures (right) or examples of specialized plants (left). (Bottom) Regional-scale case studies of mycorrhizal diversity shown as pie charts with locations shown on a global vegetation map. These charts were produced by assigning mycorrhizal status to all of the species in a region based on phylogeny (Brundrett and Tedersoo 2018). Copyright Trustees of The New Phytologist.

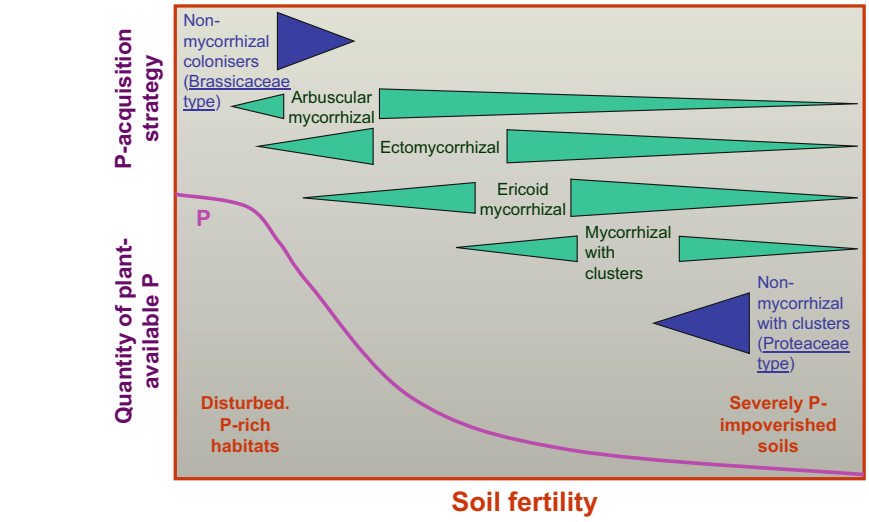

Interactions between mycorrhizal and non-mycorrhizal plant species

Moderately fertile soils; Brassicaceae type of non-mycorrhizal species

- Strongly competitive interactions
- Release of allelochemicals by non-mycorrhizal plants (chemical weapons)
- Pathogenic effects of mycorrhizal hyphae penetrating non-mycorrhizal plants (biological weapons)

Very infertile soils; Proteaceae type of non-mycorrhizal species

- Evidence for facilitative interactions
- Release nutrient-mobilising exudates by non-mycorrhizal species
- Preliminary evidence for adverse effects on mycorrhizal species

Fig. 12.7 (Top) Ecological distribution, along a soil fertility axis, of different functional types with respect to phosphorus (P) acquisition. Note that nonmycorrhizal species occur at two extremes of the axis. At the left are typically species without morphological root adaptations, other than root hairs; some may release some carboxylates. These are referred to as the Brassicaceae type. At the right are non-mycorrhizal species referred to as the Proteaceae type. These typically have morphological adaptations such as cluster roots, dauciform roots, or sand-binding roots. (Bottom) Interactions between mycorrhizal plant species and nonmycorrhizal plants of either the Brassicaceae type or the Proteaceae type. We find adverse effects typically on species of the Brassicaceae type, possibly because the mycorrhizal fungi act as pathogens; competition is fierce. There is little evidence for adverse effects on species of the Proteaceae type; facilitative interactions appear to dominate, based on the nutrient-mobilizing strategy of the non-mycorrhizal species (Lambers and Teste 2013). Copyright John Wiley and Sons.

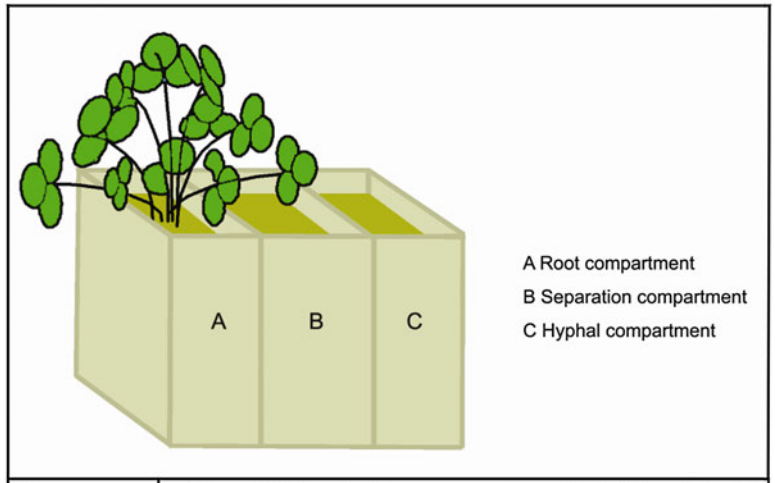

P source	Shoot 32 P content as a percentage of total P uptake (%)	
	Nonmycorrhizal	Mycorrhizal
Ca_2-P	0.2	18.5
Ca_8-P	0.9	13.2
$Ca_{10}P$	0.7	0.8
A1-P	1.2	14.0

Fig. 12.8 Diagram showing the design of the rhizoboxes used to assess which chemical forms of phosphorus (P) can be accessed by arbuscular mycorrhizal hyphae. $Ca_{10}P$ (in red) is a P source that is not readily available to plants, unlike the other sources. The ^{32}P-labeled P source is added to the hyphal compartment only. The ^{32}P content is expressed as a proportion of the total P content of the shoots of *Trifolium pratense* (red clover) (Yao et al. 2001). Copyright © 2001, Kluwer Academic Publishers.

2002). This reaction is catalyzed by **polyphosphate kinase**, which is induced when excess Pi is absorbed (Tani et al. 2009). Poly-P accumulated in the vacuole is translocated from the external hyphae to the hyphae inside the roots, dependent on host transpiration. Transpiration provides a primary driving force for poly-P translocation, and **fungal aquaporins** play a key role in the transport in the hyphae towards the arbuscules (Kikuchi et al. 2016). Transport of poly-P and other poorly-mobile ions through the external hyphae to the plant is relatively rapid, bypassing the very slow diffusion of these ions in soil. Once the poly-P has arrived near the plant cells, it is degraded, releasing Pi is by **vacuolar polyphosphatases**, exported to the cytosol through a vacuolar Pi exporter (Ezawa and Saito 2018).

Transfer of Pi and other nutrients from fungus to plant is a two-step process over the membranes of the two symbionts, probably involving passive efflux from the fungus and active uptake by the plant (Javot et al. 2007). Some of the plant Pi-transporter genes involved in this process are mycorrhiza-specific, and differ genetically from those discussed in Sect. 9.2.2.2 (Karandashov and Bucher 2005). These mycorrhiza-inducible Pi-transporter genes are upregulated in roots that are colonized by AM fungi, and expressed at a very low level in noncolonized parts of the same root system. These findings show that in species that form AM associations with members of the Glomeromycota, Pi transporters have evolved that are involved in scavenging Pi from the apoplast between intracellular AM structures and root cortical cells (Glassop et al. 2005; Walder et al. 2016).

12.2.3.2 Suppression of Colonization at High Phosphate Availability

The AM fungus colonizes roots to a greater extent in low-P soils than in soils that are more fertile (Fig. 12.10; Smith and Read 2008). To some

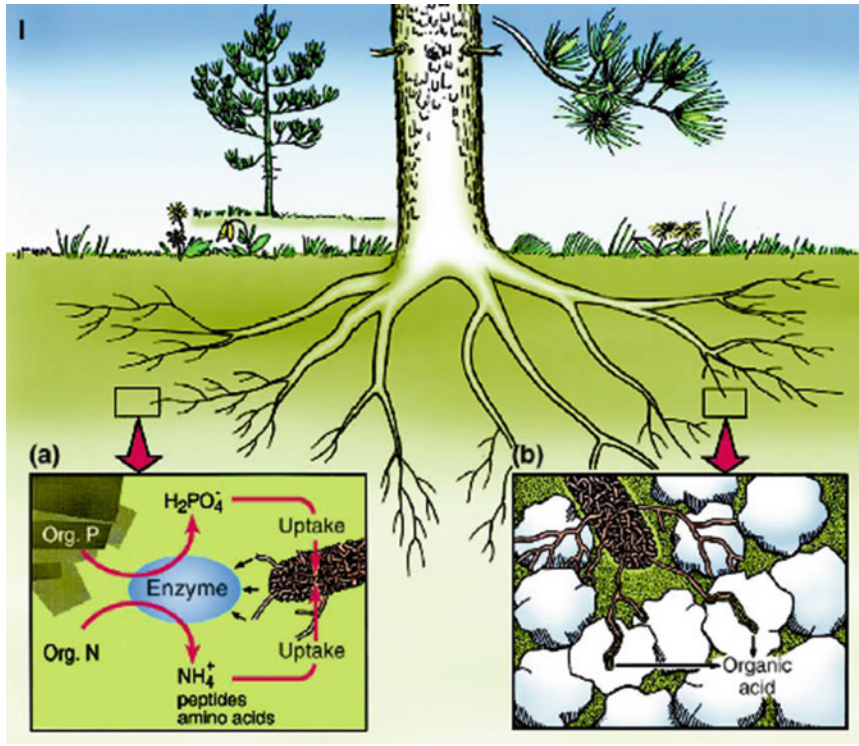

Fig. 12.9 Ectomycorrhizal fungi influence the uptake of plant nutrients in two ways, in addition to increasing plant nutrient uptake by increasing the surface are for uptake and exploiting a greater soil volume. (**A**) Via enzyme production, the ectomycorrhizal fungus can utilize organic nitrogen (N) and phosphorus (P) forms, which would otherwise remain largely unavailable to roots. Nutrients are mobilized from amino acids, peptides, proteins, amino sugars, chitin and nucleic acids, followed by transfer of N and P into the host plant. Direct hyphal absorption of amino acids and simple peptides can also occur. (**B**) The ectomycorrhizal fungus can mobilize P, potassium (K), calcium (Ca) and magnesium (Mg) from solid mineral substrates through organic acid excretion. Essential nutrients become available to the host plant via the ectomycorrhizal mycelium. Analogous to their organic nutrient mobilizing capabilities, the abilities of different ectomycorrhizal fungi to mobilize inorganic nutrients may be species specific (Landeweert et al. 2001).

extent, this may be associated with a decreased rate of root elongation, so that the colonization by the fungus keeps up with the growth of the root. **Systemic effects** of P are also important, however. This can be shown in an analysis of *Solanum tuberosum* (potato) grown with a divided root system of which only one half is inoculated with the AM fungus *Glomus intraradices*. When high Pi levels are applied to the noncolonized part of the root system, the formation of both arbuscules and vesicles is suppressed in the colonized portion of the root, despite the presence of more internal hyphae. Moreover, a high Pi supply may lead to down-regulation of the expression of both the mycorrhiza-inducible and other Pi transporters (Rausch et al. 2001; Glassop et al. 2005).

Once a root is infected by an AM fungus, further infection of the roots tends to be suppressed (Vierheilig et al. 2000); this phenomenon is called **autoregulation**. To explore this, we can use plants of *Hordeum vulgare* (barley) grown with a divided root system, where one half is inoculated with an AM fungus. After extensive root colonization, the other half is inoculated, but colonization is suppressed (Fig. 12.11). In such plants, some of the P acquired by the colonized root part ends up in the roots that are not colonized, as a result of transport via the xylem to the shoot, followed by export via the phloem to

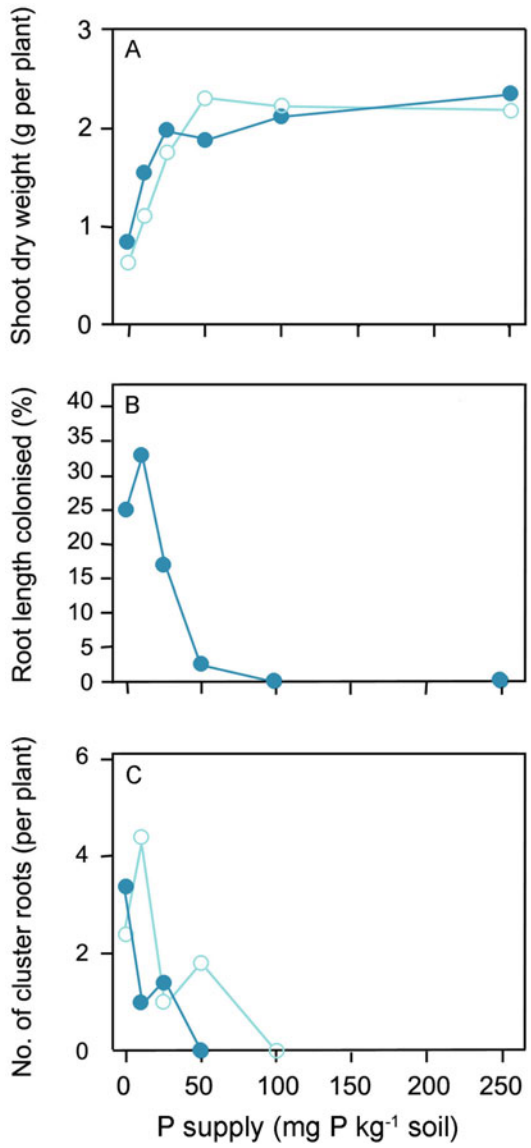

Fig. 12.10 Response of *Casuarina cunninghamiana* (sheoak) seedlings to inoculation with an arbuscular mycorrhizal fungus (*Glomus* sp.) over a range of phosphorus (P) supplies in sand culture. (**A**) Shoot dry weight; (**B**) mycorrhizal colonization of roots; (**C**) occurrence of cluster roots. Filled symbols: inoculated with *Glomus*; open symbols uninoculated. After Reddell et al. (1997), *Austr J Bot* **45**: 41–51. Copyright CSIRO, Australia.

the roots. Because the biomass and the P concentration of both root halves are the same, elevated P concentrations do not explain the suppression (Fig. 12.11). A **systemic suppression**, *i.e.* a response triggered by mycorrhizal colonization followed by signaling to the rest of the plant, is the most likely explanation for the autoregulatory effect of prior mycorrhization on subsequent colonization. This involves signaling molecules such as **strigolactones** (Sect. 12.2.1.1), whose release from roots of plants that are hosts for AM fungi is promoted by Pi deficiency (Yoneyama et al. 2007). By contrast, in roots of nonmycorrhizal species, P deficiency does not affect exudation (Yoneyama et al. 2008). Interestingly, the systemic autoregulatory effect not only suppresses mycorrhization in *Hordeum vulgare* (barley), but also reduces root **infection** by the take-all **disease** caused by the fungus *Gaeumannomyces graminis* var. *tritici*. This effect is found when barley plants show a high degree of mycorrhizal root colonization, whereas a low mycorrhizal root colonization has no effect on take-all (Khaosaad et al. 2007). The mechanism of mycorrhizal autoregulation shares elements with the pathway for autoregulation of nodulation in legumes (Wang et al. 2017) which we discuss in Sect. 12.3.9.

12.2.4 Effects on Nitrogen Nutrition and Water Acquisition

Unlike AM, some **ectomycorrhizas** may utilize **organic N**, including proteins. This has been documented *in situ*, as revealed by a comparison of **^{15}N fractionation** in plants with and without ectomycorrhizas. Ectomycorrhizal plants may have a 1.0 to 2.5‰ more positive $\delta^{15}N$ value than do plants colonized by AM (Table 12.2), suggesting that different N sources are used (either different compounds or different regions in the soil). Fractionation of the heavy N isotope (^{15}N) occurs during **mineralization** and **nitrification**; therefore, the organic N becomes enriched with ^{15}N (Gebauer and Schulze 1991). The data in Table 12.2 provide evidence that the ectomycorrhizal plants use a significant amount of N from a pool that was not decomposed and nitrified, *i.e.* organic N. In boreal forest and arctic tundra, ectomycorrhizal plant species also have distinctive ^{15}N signatures, with ^{15}N concentrations that are higher than those of species with ericoid

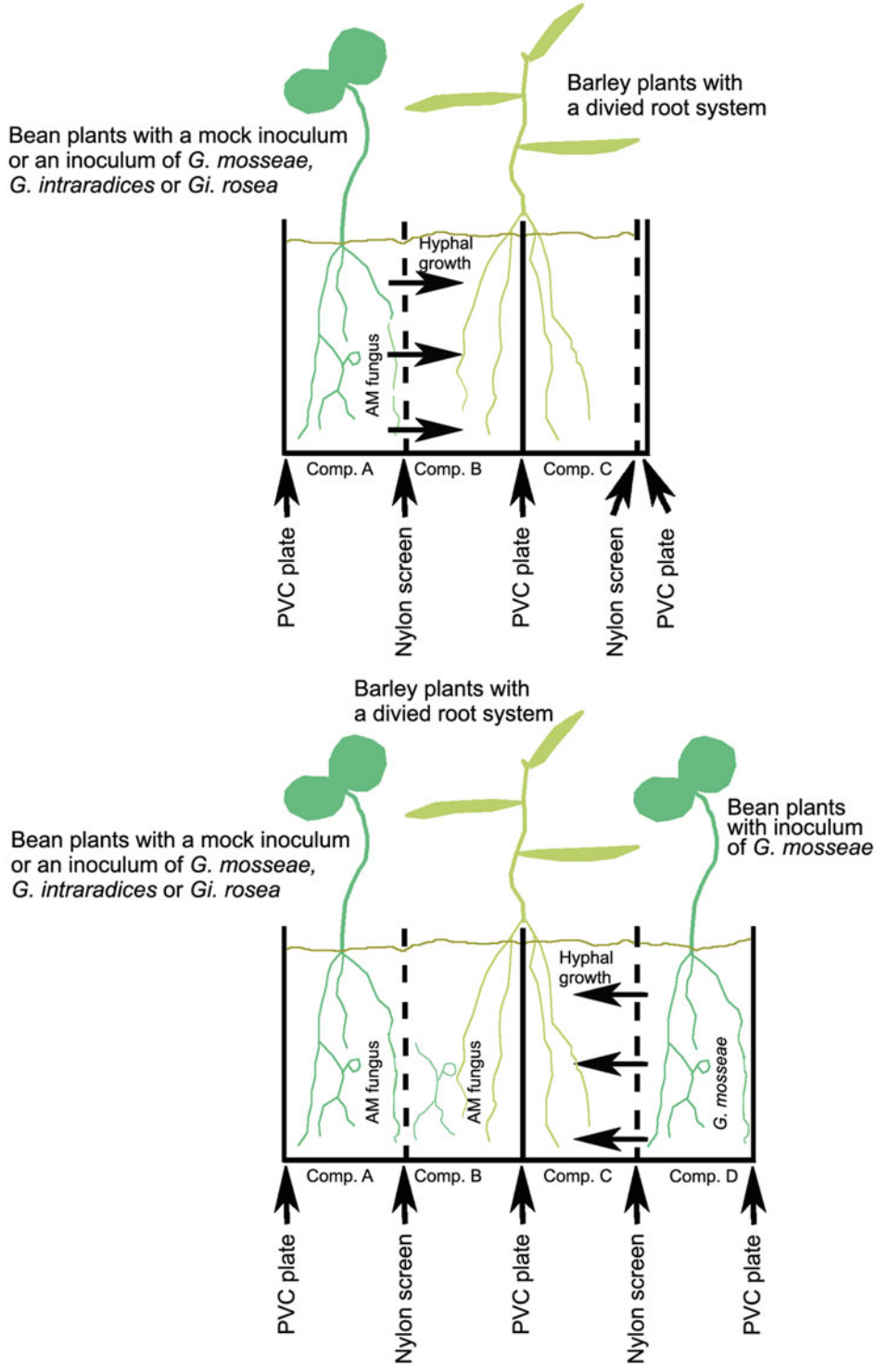

Fig. 12.11 Diagram showing the experimental design of rhizoboxes used to assess the systemic effect of prior infection of *Hordeum vulgare* (barley) by arbuscular mycorrhizal fungi (compartment B) on subsequent infection (in compartment C). Infection takes place from roots of *Phaseolus vulgaris* (common bean) in adjacent compartments (A or D) (after Vierheilig et al. 2000). Copyright © 2000 Elsevier Science Ltd. All rights reserved.

Table 12.2 Nitrogen-isotope signatures (^{15}N abundance) of leaf samples collected in three years in Tanzania.*

Species	Symbiotic status	$\delta^{15}N$		
		1980	1981	1984
Brachystegia boehmii	EC	1.64	1.32	1.23
B. microphylla	EC	1.53	1.51	1.73
Julbernardia globiflora	EC	2.81	1.63	1.60
Pterocarpus angolensis	AM+NO	−0.81	−0.87	−0.93
Diplorynchus condylocarpon	AM	–	−0.36	−0.60
Xeroderris stuhlmannii	AM+NO	–	0.01	0.62
Dichrostachys cinerea	AM+NO	–	0.45	−0.38

Source: Högberg (1990)

*EC = ectomycorrhizal; AM = arbuscular mycorrhizal; NO = nodulated. The experiments summarized here were carried out with the aim to determine the extent of symbiotic N_2 fixation of the nodulated plants. Since nodulated plants have access to dinitrogen from the atmosphere, they are expected to have $\delta^{15}N$ values closer to atmospheric N_2 than do plants that do not fix N_2. The data presented here stress that control plants need to be sampled to allow a proper comparison. This table shows that the choice of the control plants is highly critical (see also Sect. 12.3)

mycorrhizas, but lower than those of AM or nonmycorrhizal species (Nadelhoffer et al. 1996). Rooting depth or the isotope composition of the inorganic N that is utilized may also contribute to different ^{15}N signatures (Gebauer and Schulze 1991). An ectomycorrhizal N economy based on the use of organic N and maintaining very low soil inorganic N concentrations may facilitate monodominance in neotropical forests (Corrales et al. 2016).

Ericoid mycorrhizas, like ectomycorrhizas, can use quite **complex organic sources of N and P** (Fig. 12.9; Read 1996). This ability may contribute to the dominance of Ericaceae on many cold and wet soils, where rates of decomposition and mineralization are slow (Read and Perez-Moreno 2003). Arbuscular mycorrhizas are at the other extreme of the continuum of mycorrhizal associations. They do not access organic P direly (Smith et al. 2015), but may do so together with phosphatase-releasing microorganisms they associate with (Zhang et al. 2016). Their predominant significance lies in the acquisition of sparingly available inorganic nutrients, especially Pi. Arbuscular mycorrhizas are relatively unimportant for acquisition of N, if this is available as NO_3^-, but they may enhance N acquisition when mineral N is present as the less mobile NH_4^+ (Tanaka and Yano 2005). In the extraradical hyphae, NH_4^+ is assimilated into **arginine**, and then transported toward the arbuscules, where arginine is broken down, followed by transfer of NH_4^+ to the host cells (Chalot et al. 2006). Ectomycorrhizas are thought to be intermediate between ericoid and AM in terms of accessing organic N.

Arbuscular mycorrhizal plants may have an enhanced capacity to acquire water from the root environment (Augé 2001). Water transport through AM fungal hyphae has been proposed in many studies, but has ever been demonstrated (Ezawa and Saito 2018). In the ECM *Pseudotsuga menziesii* (Douglas fir), however, isotopically labeled water is transferred via mycorrhizal hyphae (Plamboeck et al. 2007). There may be indirect effects on water uptake, also in AM plants, via the **improved P status** of the plant which may increase the hydraulic conductance of the roots or affect stomatal conductance. *Lactuca sativa* (lettuce) plants colonized by the AM fungi *Glomus coronatum*, *Glomus intraradices*, *Glomus claroideum*, and *Glomus mosseae* deplete soil water to a greater extent than control plants or plants colonized by *Glomus constrictum* or *Glomus geosporum*. The differences in soil-moisture depletion can be ascribed to the activity of AM fungi, but fungi differ in their effectiveness to enhance plant water uptake from soil (Marulanda et al. 2003). The improved plant water status might be an effect of mycorrhizas on **soil structure** (Bearden and Petersen 2000).

12.2.5 Role of Mycorrhizas in Defense

Both AM and ECM play a role in defense against **pathogens** (see also Sect. 13.4.2). We have known this for a long time (Marx 1969), but its ecological implications are only now receiving increasing attention (Maherali and Klironomos 2007; Sikes et al. 2009). Ectomycorrhizas can provide physical barriers around roots against soil-borne pathogens (Marx 1972; Branzanti et al. 1999), whereas AM can induce production of root callose around infected root cells (Pozo et al. 2002). Ectomycorrhizas may also produce a vast number of antifungal compounds (Duchesne et al. 1988) and induce systemic resistance (Martin et al. 2016). AM fungi may modify the microbial community in the rhizosphere, favoring organisms capable of producing antibiotics (Wehner et al. 2010). Mycorrhizas may also neutralize the negative effects of pathogens for seedling survival and growth (Liang et al. 2015). The role of mycorrhizas in defense is not restricted to pathogens (Cameron et al. 2013; Bennett et al. 2017), but also includes protection against nematodes (Vos et al. 2013) and herbivores (Minton et al. 2016).

In *Vitis vinifera* (grapevine), a pathogen defense response is enhanced in plants that are colonized by AM fungi, with an intensity level depending on the defense gene, plant cultivar and the pathogen (Bruisson et al. 2016). In *Triticum aestivum* (wheat), mycorrhizal colonization reduces infection by the foliar biotrophic pathogen *Blumeria graminis* f. sp. *tritici* by 78%. Wheat roots inoculated with the mycorrhizal fungus *Funneliformis mosseae* show a systemic resistance in leaves to the pathogen, associated with a reduction of pathogen haustorium formation on epidermal leaf cells and an accumulation of phenolic compounds and H_2O_2 at pathogen penetration sites (Mustafa et al. 2017). These findings suggest potential trade-offs between AM colonization, ecological and agronomic traits, and disease resistance. They highlight the need for translational research to apply fundamental knowledge to ecological understanding and crop improvement (Jacott et al. 2017).

12.2.6 Carbon Costs of the Mycorrhizal Symbiosis

Mycorrhizas can provide nutritional benefits, which may enhance **resource allocation to leaves** (Baas and Lambers 1988; Grimoldi et al. 2005) and **photosynthetic carbon gain** of the host (Wright et al. 2002; Kaschuk et al. 2009), but they also incur **carbon costs** for the host. Plants provide carbon in the form of sugars and lipids (Sect. 12.2.1.1). The amount of carbon that intact roots exude into the apoplast and normally ends up in the rhizosphere is insufficient to satisfy the demand of the microsymbiont of the mycorrhizal association. Passive efflux of carbon may be increased in mycorrhizal plants; alternatively, the host's active carbon-uptake system may be inhibited. A high-affinity monosaccharide transporter with a broad substrate spectrum functions at several symbiotic root locations (Helber et al. 2011). Expression of the gene that encodes this transporter closely correlates with that of a mycorrhiza-specific Pi transporter. In addition to glucose, cell-wall monosaccharides can provide a source of organic carbon for AM fungi (Roth and Paszkowski 2017).

Costs associated with the AM symbiosis have been estimated in various ways (*e.g.*, by comparing plants with and without the mycorrhizal symbiont growing at the same rate). This can be achieved by providing more P to the nonmycorrhizal plant than to the mycorrhizal plant. We can then use the carbon allocated to growth and respiration by the roots of both types of plants to quantify costs of the mycorrhizal symbiosis (Snellgrove et al. 2006). The problem with this method is that it assumes steady-state rates of P acquisition and carbon consumption, whereas these may vary following active root colonization. A variation of this approach is to grow nonmycorrhizal plants at a range of P supplies, so that a P-response curve can be constructed with which to compare the mycorrhizal plants (Rousseau and Reid 1991). It is also possible to calculate carbon costs of the mycorrhizal symbiosis by measuring the flow of ^{14}C-labeled assimilates into soil and external hyphae

(Jakobsen and Rosendahl 1990). In *Solanum lycopersicum* (tomatao), AM fungus colonization decreases the rate of root respiration and the exudation of citrate and malate, but increases plant growth. In nonmycorrhizal plants, respiration *via* the **alternative oxidase** (Sect. 3.2.3) is associated with exudation of citrate and less biomass production (Del-Saz et al. 2017).

The estimates of the carbon costs of the AM symbiosis vary between 4 and 16% of the carbon fixed in photosynthesis (Kaschuk et al. 2009). Only a minor part (15%) of the increased rate of root respiration is associated with an increased rate of ion uptake by the mycorrhizal roots. The major part (83%) is explained by the respiratory metabolism of the fungus and/or other effects of the fungus on the roots' metabolism (Baas et al. 1989). The costs for the ECM symbiosis are probably greater, but there is little information available (Hobbie 2006).

In addition to a higher carbon expenditure, mycorrhizal plants also tend to have a faster rate of photosynthesis per plant, partly due to faster rates of photosynthesis per unit leaf area (Kaschuk et al. 2009) and partly to their greater leaf area (Wright et al. 2002). When P and water are limiting for growth, benefits outweigh the costs, and mycorrhizal plants usually grow faster, despite the large carbon sink of the symbiotic system. The relatively large costs of the mycorrhizal association, however, may partly explain why mycorrhizal plants sometimes grow less than their nonmycorrhizal counterparts, especially when a second microsymbiont (rhizobium) plays a role (Bethlenfalvay et al. 1982).

Mycorrhizal symbioses are far less costly per unit Pi acquired that plant strategies based on carboxylate exudation (Raven et al. 2018). Yet, even in habitats where the carboxylate-releasing strategy is more effective to acquire Pi than mycorrhizal strategies, plant species with these contrasting strategies coexist (Zemunik et al. 2015, 2018). This is accounted for by a combination of facilitation of Pi acquisition by carboxylate-releasing species of their mycorrhizal neighbors (Sect. 16.6.2) and a better defense against pathogens of the mycorrhizal species (Sect. 12.2.5). Plant species cannot be good at everything, and efficient Pi acquisitions is traded off against defense against pathogens (Lambers et al. 2018).

12.2.7 Agricultural and Ecological Perspectives

From an ecological perspective, information on the mycorrhizal status of plants in a community is important. Intriguingly, AM and ECM can link neighboring plants, forming **common mycelial networks** (**CMNs**) (Molina and Horton 2015; van der Heijden et al. 2015). What are the terms of trade in such CMNs between plants and their shared fungal partners? To address this question, Walder et al. (2012) set up microcosms with a pair of test plants, interlinked by a CMN of *Glomus intraradices* or *Glomus mosseae* (Fig. 12.12). The plants were *Linum usitatissimum* (flax), a C_3 plant, and *Sorghum bicolor* (sorghum), a C_4 plant, which display distinctly different $^{13}C/^{12}C$ isotope compositions (Sect. 2.9.7). This allows differential assessment of the carbon investment of the two plants into the CMN through stable isotope tracing. In parallel, they determined the plants' 'return of investment' (*i.e.* the acquisition of nutrients via CMN) using ^{15}N and ^{33}P as tracers. Depending on the AM species, there is a strong asymmetry in the terms of trade: flax invests little carbon, but gains up to 94% of N and P provided by the CMN, which enhances their growth. The neighboring sorghum invests larger amounts of carbon with little return, but is barely affected in growth (Fig. 12.12). Overall biomass production in the mixed culture surpasses the mean of the two monocultures. Thus, CMNs may contribute to interplant facilitation and the productivity boosts that are often found with intercropping compared with conventional monocropping.

In a mixed community, **nonmycorrhizal species** may profit most from fertilization with Pi, because the mycorrhizal association is often suppressed at a higher Pi supply, and not necessarily because the growth of nonmycorrhizal species is more severely P-limited (Sect. 12.2.3). Suppression of the mycorrhizas might then

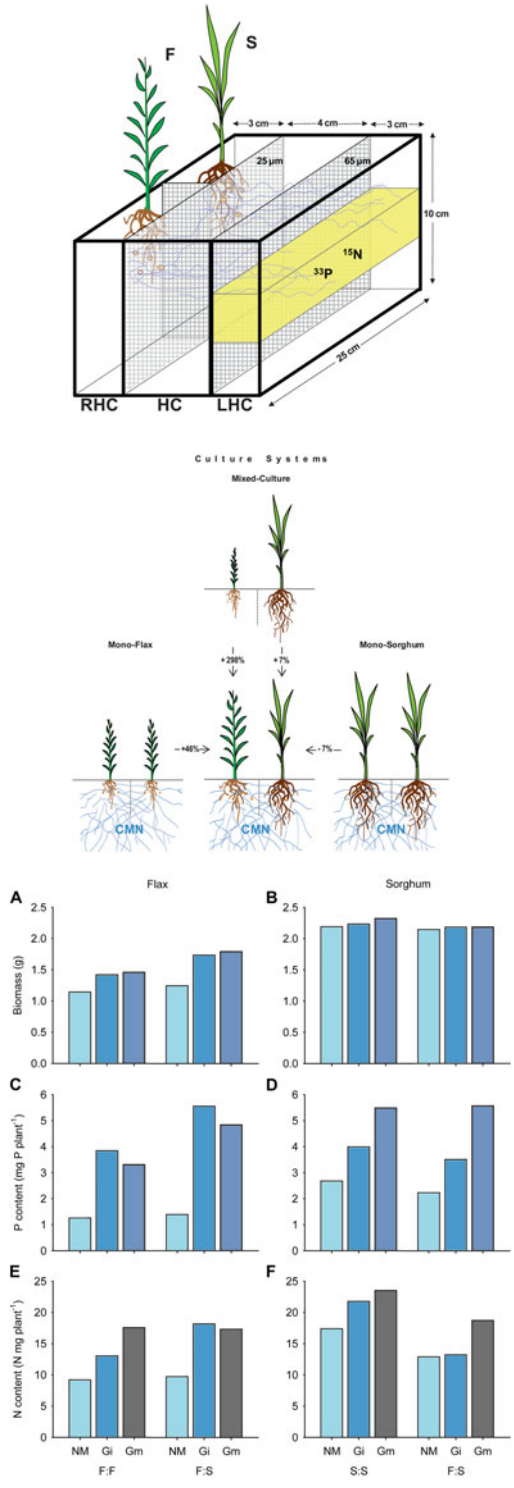

Fig. 12.12 (Top) Compartmented microcosms to study the role of common mycorrhizal networks (CMNs) in monocultures and mixed culture. Microcosms comprise two plant individuals, set up in compartmented containers subdivided by nylon mesh screens (25 and 65 µm, respectively, as indicated). Both types of screens are pervious for

reduce the harmful effect of the mycorrhizal fungus on nonmycorrhizal species (Sect. 12.2.2). We should therefore be cautious when interpreting the effects of P fertilization on the growth of certain plants in a community.

Mycorrhizas can obviously never enhance growth and productivity of crop plants in the absence of any P. Mycorrhizal associations, however, do have potential in improving crop production when Pi or other immobile nutrients are in short supply. They can also be agronomically important by boosting the defense against pathogens (Jacott et al. 2017). Introduction of spores of the best microsymbiont and breeding for genotypes with a more efficient mycorrhizal symbiosis are tools to enhance food production in countries where poorly-mobile nutrients restrict crop production.

Nitrogenous compounds are transported bidirectionally between N_2-fixing *Casuarina cunninghamiana* (sheoak) and *Eucalyptus maculata* (spotted gum) trees, connected via the ectomycorrhizal fungus *Pisolithus* sp., especially in a nodulated ectomycorrhizal treatment. About twice as much N moves from *Eucalyptus maculata* toward *Casuarina cunninghamiana* as in the opposite direction, irrespective of the source of N ($^{15}NH_4^+$ or $^{15}NO_3^-$), resulting in increased growth of *Casuarina cunninghamiana* due to interspecific N transfer. Since there is virtually no N transfer in a nonmycorrhizal treatment, N transfer between the two tree species is mediated by ectomycorrhizal fungi. The much greater N transfer between nodulated mycorrhizal plants indicates that mycorrhizas and *Frankia* together enhance bidirectional N fluxes between N_2-fixing *Casuarina cunninghamiana* and non-N_2-fixing mycorrhizal *Eucalyptus maculata*, contradicting the view that N flows from N_2-fixing to nonfixing plants. However, the fraction of N derived from transfer is similar for both species, because the N concentrations are greater in the N_2-fixing *Casuarina cunninghamiana* (He et al. 2004, 2005).

Benefits of N nutrition to nonfixing plants by neighboring N_2-fixing plants are well documented (Sect. 12.3.6). Differences in net N transfer with different nodulation/mycorrhizal combinations could have important ecological implications, both for nutrient cycling and for the structure and function of natural or agricultural plant communities, particularly with respect to those plants that can potentially construct a CMN to transfer nutrients (He et al. 2005). Mycorrhizal colonization can result in **resource equalization** or sharing, thus reducing dominance of aggressive native species and promoting coexistence and biodiversity (Van Der Heijden and Horton 2009). Changes in ectomycorrhizal fungal community parallel those of the ectomycorrhizal tree communities at a dipterocarp tropical rainforest site (Peay et al. 2010). This suggest a link between the distribution of tropical tree diversity and the distribution of tropical ectomycorrhizal diversity in relation to local-scale edaphic variation.

Exploitation of AM networks may be a mechanism by which some **invasive weeds** outcompete their neighbors (Reinhart and Callaway 2006). Transport of carbon via mycorrhizal hyphae is also important in **mycoheterotrophic** plants, which depend on carbon supplied by a

Fig. 12.12 (continued) fungal hyphae, but not for roots, and allow the separation into compartments for root and hyphal growth (RHC), a compartment for hyphal growth only (HC), and a compartment for supplying nitrogen (^{15}N) and phosphorus (^{33}P) labels (LHC). The plants used were *Linum usitatissimum* (flax, F) and *Sorghum bicolor* (sorghum, S), either as a pair of conspecific plants (F:F, S:S) as a model of monoculture or in combination (F:S) as a model of a mixed culture. (Middle) Impact of a CMN in monocultures and mixed culture. The presence of a CMN of *Glomus intraradices* strongly enhances the biomass production of flax in mixed culture with sorghum. Sorghum is not significantly affected by the presence of a CMN in the mixed culture with flax. The flax plants grow significantly faster in the flax/sorghum mixed cultures than in the flax monocultures. In contrast, the growth of sorghum is only marginally influenced by the culture system. (Bottom) Impact of a CMN on plant growth performance and nutrient uptake in monocultures or mixed culture. A, C, and E, Performance of flax in monoculture (F:F) or mixed culture (F:S). B, D, and F, Performance of sorghum in monoculture (S:S) or mixed culture (F:S). NM, Nonmycorrhizal control; Gi, *Glomus irregulare*; Gm, *Glomus mosseae* (Walder et al. 2012). Copyright American Society of Plant Biologists.

photosynthetic plant to which they are connected via mycorrhizal hyphae (Sect. 12.2.1.1; Selosse et al. 2006). However, putatively autotrophic orchids also receive significant amounts of carbon from their fungal associates (Gebauer and Meyer 2003). Across a natural fertility gradient spanning the isthmus of Panama, and in a long-term nutrient-addition experiment, mycoheterotrophs are absent when readily-available soil P concentrations exceed 2 mg P kg^{-1}. Because P addition reduces the abundance of both AM fungi and AM fungal taxa required by the mycoheterotrophs, the P sensitivity of mycoheterotrophs is likely underpinned by the P sensitivity of their AM fungal hosts (Sheldrake et al. 2017) .

At a global scale, the intensity of colonization by AM mycorrhizal fungi relates to warm-season temperature, frost periods and soil carbon-to-nitrogen ratio. It is highest at sites featuring continental climates with mild summers and a high availability of soil N. In contrast, the intensity of ECM colonization in plant roots is related to soil acidity, soil carbon-to-nitrogen ratio and seasonality of precipitation, and is highest at sites with acidic soils and relatively constant precipitation levels (Soudzilovskaia et al. 2015, 2017). However, these distribution patterns show a strong bias, and ignore the vast number of nonmycorrhizal species in severelely P-impoverished regions in South Africa, south-eastern Brazil, and south-western Australia (Oliveira et al. 2015; Brundrett and Tedersoo 2018). In addition to climate and soil N availabily, the soil P availability as dependent on soil age is a major driver of the colonization by AM and ECM fungi and of the presence of nonmycorrhizal species (Fig. 12.7; Lambers et al. 2008, 2010; Brundrett and Tedersoo 2018).

12.3 Associations with Nitrogen-Fixing Organisms

Nitrogen is a major limiting nutrient for the growth of many plants in many environments in young landscapes (Sect. 9.2.1). Terrestrial N is subject to rapid turnover, and is eventually lost as nitrogen gas to the atmosphere or deposited in marine sediments. Its maintenance, therefore, requires a continuous reduction of atmospheric N_2. Biological reduction of N_2 to ammonia is performed only by some prokaryotes, and is a highly O_2-sensitive process. The most efficient N_2-fixing microorganisms establish a symbiosis with plants, in which the energy for N_2 fixation and the O_2-protection system are provided by the plant partner (Vessey et al. 2005; Franche et al. 2009; Tedersoo et al. 2018).

The evolutionary origin of nodulation is still under debate. Nodulation only occurs in a specific plant clade, the Fabids, but not in all species of that clade (Soltis et al. 1995). Root nodular N_2-fixing symbioses may have evolved multiple times within this clade: two to five times with rhizobia (one to four times in legumes and once in *Parasponia* (Cannabaceae)), and approximately nine times in actinorhizal species associating with *Frankia* (Geurts et al. 2016). Alternatively, the predisposition for nodulation may have evolved once, with multiple subsequent losses, likely in response to changes in atmospheric CO_2 concentration (Van Velzen et al. 2019). It remains unclear exactly what genetic gains or losses were associated with the evolution of nodulation (Griesmann et al. 2018).

Rhizobia are taxonomically heterogeneous and polyphyletic, but the known examples were first confined to the Alphaproteobacteria class ('α-rhizobia') until the identification of nodulating *Burkholderia* and *Cupriavidus* established that there are also 'β-rhizobia' (Bontemps et al. 2010). So far, we know of five nodulating *Burkholderia* species and *Cupriavidus taiwanensis* as β-rhizobium. The core genomes of α-rhizobia and β-rhizobia are highly diverged, genes for the symbiotic interaction such as *nodA* are no more diverged between the α-rhizobia and β-rhizobia than they are within the α-rhizobia (Moulin et al. 2001), suggesting that they have been transferred laterally, rather than evolved separately.

Symbiotic N_2-fixing associations may be of major importance for a symbiotic plant's N acquisition, especially in environments where N is severely limiting to plant growth. As such, the symbiosis is of agronomic and environmental

importance, because it reduces the need for costly fertilizers and greenhouse gas emissions associated with their production. We sometimes find a symbiotic association that does not involve nodule structures, for example, with *Azospirillum* in the rhizosphere of tropical grasses (Cohen et al. 1980; Pereg et al. 2016) or *Gluconacetobacter* in the apoplast of stems of *Saccharum officinarum* (sugarcane) (Boddey et al. 2003; Reis and dos Santos Teixeira 2015). Contrary to the strictly symbiotic systems, no special morphological structures are induced.

Symbiotic N_2-fixing systems require a carbon input from the host that is far greater than the carbon requirements for the acquisition of N as NO_3^-, NH_4^+, or amino acids) (Kaschuk et al. 2009). Are there mechanisms to suppress the symbiosis when there is plenty of combined N around? How does a plant discriminate between a symbiont and a pathogenic microorganism? Finally, what is the significance of symbiotic N_2 fixation without specialized structures for plants? To answer these ecological questions we will first provide a basic understanding of some physiological aspects of this symbiotic association.

12.3.1 Symbiotic N_2 Fixation Is Restricted to a Fairly Limited Number of Plant Species

Because of its overwhelming economic importance, the most widely studied associations between N_2-fixing microorganisms and vascular plants are those that involve **legumes**. The story of symbiotic N_2 fixation in legumes has become more complicated following the discovery that not only rhizobia, Alphaproteobacteria in the family Rhizobiaceae, but also some Betaproteobacteria establish effective nodules on legumes. Both acquired the nodulation genes at approximately the same time as the legumes were evolving (Walker et al. 2015). The microsymbionts are collectively known as **rhizobia**. The macrosymbionts comprise Mimosoideae and Papillionoideae in **Fabaceae**, whereas Caesalpinioideae in that family are less likely to nodulate (Walker et al. 2015). *Parasponia* (Cannabaceae) is the only nonlegume species with a symbiotic association with rhizobium (Vessey et al. 2005). Invariably, **root nodules** are formed (Figs. 12.13 and 12.14), with the exception of *Azorhizobium* and *Bradyrhizobium*, which induce nodules on both stems and roots (of *Sesbania rostrata* and *Aeschynomene* species, respectively). The symbiosis between rhizobia and legume crops is of enormous agronomic importance when N-fertilizer inputs are low.

There are also **nonlegume species** capable of forming a symbiotic association with N_2-fixing organisms. First, there is the **actinorhizal symbiosis** between soil bacteria (*Frankia*, Actinobacteria) and more than 200 species from eight nonlegume families of angiosperms [*e.g.*, *Alnus* (alder), *Hippophae* (sea buckthorn), *Myrica* (myrtle), *Elaeagnus* (silverberry), and *Casuarina* (sheoak)]. In all these symbioses, **root nodules** are formed (Fig. 12.13; Ibáñez et al. 2017; Martin et al. 2017). Second, there are symbioses between **cyanobacteria** (*Nostoc*, *Anabaena*) and plant species of the genera *Azolla, Gunnera*, and *Macrozamia* and other cycads (Chalk et al. 2017). Special morphological structures are sometimes formed on the roots (*e.g.*, the **coralloid roots** in cycads) (Fig. 12.13; Lindblad 2009). The cyanobacteria produce neurotoxins, renderining cycads toxic (Brenner et al. 2003). The microsymbionts only fix N_2, not CO_2, although cyanobacteria are photosynthetically active when free-living. *Nostoc* in the *Gunnera-Nostoc* symbiosis maintains its photosystem II units, but their photochemical efficiency is reduced (Black and Osborne 2004). In the symbiosis between fungi and cyanobacteria (*Nostoc*), the cyanobacteria are photosynthetically active; this symbiosis occurs in **lichens** and may also involve algae (Green et al. 2012).

Table 12.3 gives an overview of major symbiotic associations between plants and microorganisms capable of fixing N_2. It shows that N_2-fixing organisms can be very significant for the input of N into natural and agricultural systems.

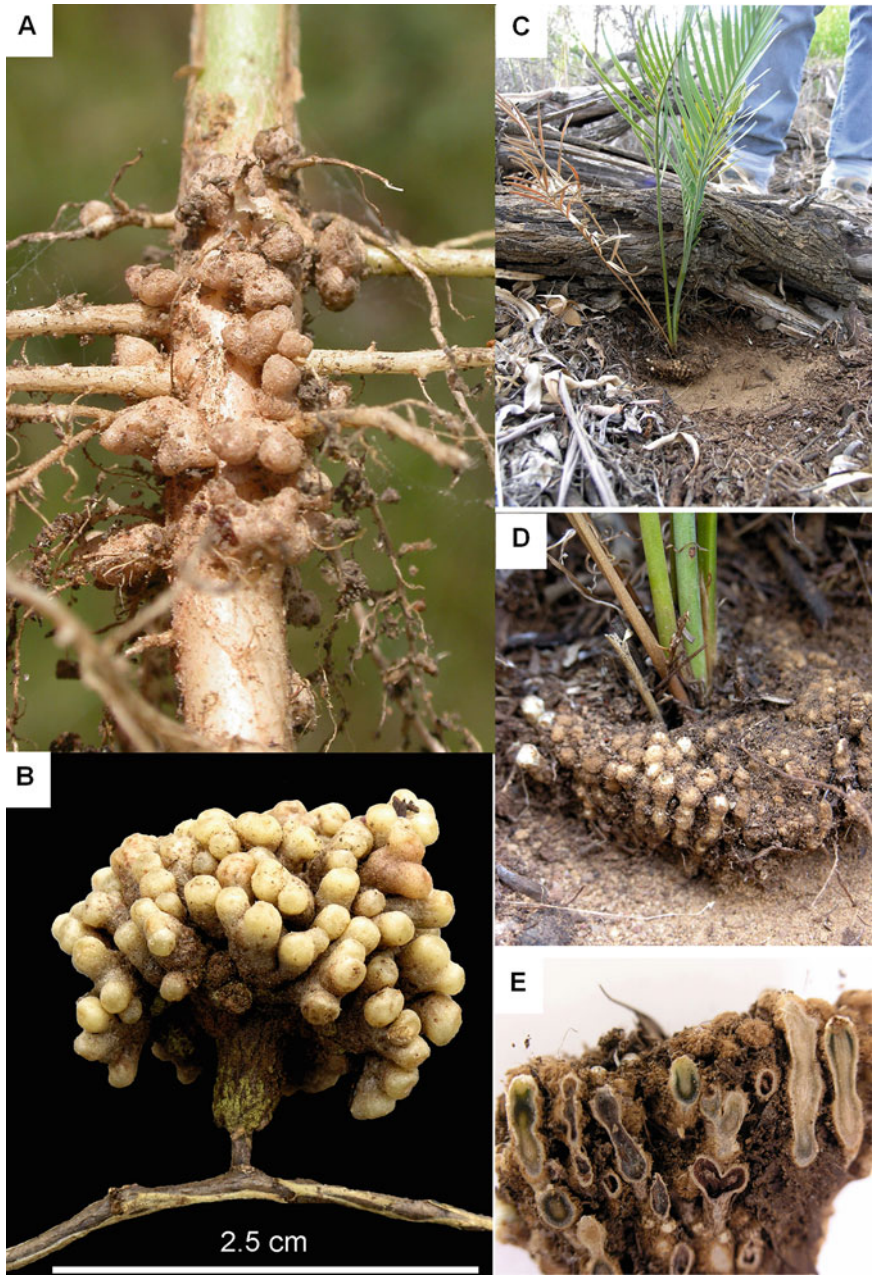

Fig. 12.13 Nitrogen-fixing symbiotic systems. (**A**) Legume-rhizobium symbiosis (nodules) on the South African *Chamaecrista mimosoides* (fishbone dwarf cassia) (photo: H. Lambers). (**B**) Symbiotic structure (rhizothamnia) between the Western Australian *Allocasuarina humilis* (dwarf sheoak) and an actinobacteria (*Frankia*) (photo: M.W. Shane, The University of Western Australia, Australia). (**C**–**E**) Symbiotic structure (coralloid roots) between *Macrozamia riedlii* (zamia) and cyanobacteria (courtesy M.W. Shane, School of Plant Biology, The University of Western Australia, Crawley, Australia).

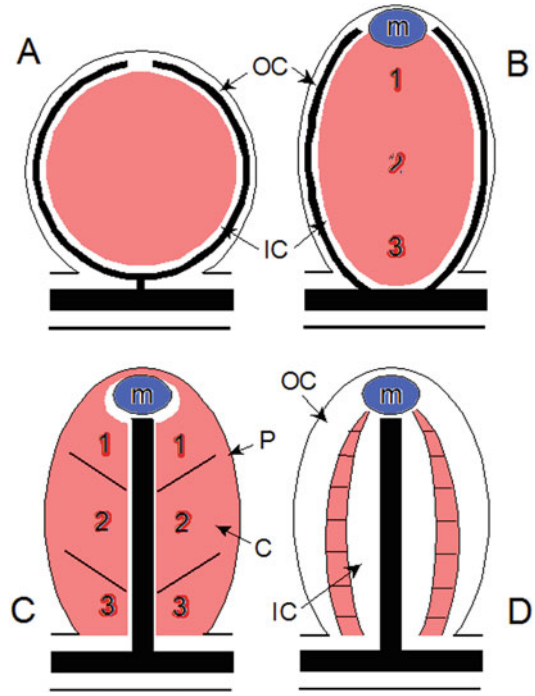

Fig. 12.14 Diagrammatic representation of longitudinal sections through (**A**) an indeterminate legume nodule, (**B**) a determinate legume nodule, (**C**) an actinorhizal nodule, and (**D**) a lobe of a symbiotic coralloid root cluster. The red colored regions represent the infected zones. The dark, thick lines represent vascular tissues. Outer cortical (OC) tissue, inner cortical (IC) tissue, and meristems (m, blue) are indicated. In the indeterminate legume nodule (**B**) and the actinorhizal nodule (**C**), the zones of infection (1), N_2 fixation (2), and senescence (3) are indicated (after Vessey et al. 2005). Copyright © 2004, Kluwer Academic Publishers.

12.3.2 Host–Guest Specificity in the Legume–Rhizobium Symbiosis

Many associations between legumes and rhizobia are highly specific. For example, *Sinorhizobium meliloti* effectively nodulates species of *Medicago truncatula* (barrel medic), *Melilotus alba* (honey clover), and *Trigonella coerulea* (fenugreek), whereas *Rhizobium leguminosarum* bv *viciae* induces N_2-fixing nodules on *Pisum* (pea), *Vicia* (bean), *Lens* (lentil), and *Lathyrus* (pea) species. Closely related to the pea strain is *Rhizobium leguminosarum* bv *trifolii*, which initiates nodules only on *Trifolium* species (clover) (Hirsch et al. 2001). However, not all rhizobia strain-legume associations are this tight. For example, *Rhizobium* strain NGR234 nodulates 232 species of legumes from 112 genera tested and even nodulates the nonlegume *Parasponia andersonii* (Cannabaceae). What determines the specificity and why does this specificity vary among different rhizobia? To answer these questions, we first discuss the infection process in more detail.

12.3.3 The Infection Process in the Legume–Rhizobium Association

Nodule formation in legumes such as *Pisum sativum* (pea) and *Glycine max* (soybean) is preceded by the release of **specific phenolic compounds** (**flavonoids**: flavones, flavanones, or isoflavones) and betaines from the legume roots (Maxwell et al. 1989; Weston and Mathesius 2013). The same or similar flavonoids

Table 12.3 Symbiotic associations between plants and microorganisms capable of fixing atmospheric N_2.*

Plant type	Plant genus	Microorganism	Location	Amount of N_2 fixed (kg N ha^{-1} $season^{-1}$)
Fabaceae	*Pisum*	*Rhizobium*	Root nodules	10–350
	Glycine	*Bradyrhizobium*	Root nodules	15–250
	Medicago	*Sinorhizobium*	Root nodules	440–790
	Sesbania	*Azorhizobium*	Stem and root nodules	7–324
		Mesorhizobium		
Cannabaceae	*Parasponia*	*Bradyrhizobium*	Root nodules	20–70
Betulaceae	*Alnus*	*Frankia*	Root nodules	15–300
Casuarinaceae	*Casuarina*	(Actinobacteria)	Root nodules	9–440
Eleagnaceae	*Eleagnus*	(Actinobacteria)	Root nodules	nd
Rosaceae	*Rubus*	(Actinobacteria)	Root nodules	nd
Pteridophytes	*Azolla*	*Anabaena*	Heterocysts in cavities of dorsal leaf lobes	40–120
Cycads	*Ceratozamia*	*Nostoc*	Coralloid roots	19–60
Lichens	*Collema*	*Nostoc*	Interspersed between fungal hyphae	nd

Source: Kwon and Beevers (1992); Gault et al. (1995); Peoples et al. (1995)
*Only a limited number of species are listed, just to provide an example; nd is not determined

can be induced as antibiotics (phytoalexins) upon infection by pathogenic microorganisms (Sect. 14.3). Subtle differences between host plant species, of which we are only just beginning to understand the details, determine if an interaction between a bacterium and a plant results in symbiosis or pathogenesis (Zipfel and Oldroyd 2017). The flavonoids bind with a bacterial gene product encoding the transcription factor **NodD**, which then interacts with specific promoters in the genome of rhizobium. This promoter is associated with the genes responsible for inducing nodulation (the nodulation, or ***nod* genes**). As detailed in following Sections, the products of these genes, the **Nod factors**, induce **root-hair curling** on the plant and **cortical cell divisions**, which are among the earliest, microscopically observable events in the nodulation of most legume species. Nod factors were previously thought to be essential for the legume-rhizobium symbiosis, but are actually dispensable under particular conditions (Gourion et al. 2015), and not required for symbiosis in some legumes, *e.g.*, *Aeschynomene* species (jointvetches), forming a symbiosis with photosynthetic *Bradyrhizobium* species (Giraud et al. 2007). Rhizobia mostly enter the root through **infection threads** initiated in **root hairs**, but may also enter through **cracks** in the epidermis, associated with lateral-root formation, or wounds; for 25% of all legumes this is the only way of entry (Sprent 2007).

The actinorhizal symbiosis between plant species like *Alnus glutinosa* (black alder) and the actinobacteria *Frankia* also involves the release of specific compounds (flavonols) that enhance the level of nodulation, but their exact role in the process is unknown (Delaux et al. 2015; Ibáñez et al. 2017). Very little is known about the chemical nature of attractants from hosts to cyanobacteria, but these may be sugars (Delaux et al. 2015).

12.2.3.1 The Role of Flavonoids

To some extent, **specificity** between the host and rhizobium is determined by the type of **flavonoids** released by the host and by the sensitivity of the rhizobium NodD protein for a given type of flavonoid. Rhizobium species that form symbioses with a broad range of plant species respond to a wider range of flavonoids than

those that are more specific, but if the flavonoid concentration is increased, a response may occur, even in those more specific rhizobia. In addition, nonlegumes may also exude flavonoids, and several legumes exude flavonoids that also activate the promoter of rhizobium species that are unable to establish a symbiosis. Other factors must, therefore, also contribute to specificity (Hassan and Mathesius 2012). What ultimate effects do the flavonoids have in rhizobium?

To study the effect of flavonoids on rhizobium an appropriate assay is required that is less elaborate than measuring root-hair curling (Maxwell et al. 1989). This assay involves coupling the gene from *Escherichia coli* that encodes β-galactosidase to the promoter of the *nod* genes. The activity of the enzyme β-galactosidase is then measured in a simple spectrophotometric assay. In this way, we can assess the relative effect of various flavonoids by determining the activity of β-galactosidase, rather than the extent of root-hair curling. In the following Section we examine the kind of products produced by the bacterial *nod* genes.

12.3.3.2 *Rhizobial* Nod *Genes*

There are three types of rhizobial ***nod* genes**. First, most rhizobia have a *nod* gene that is transcribed **constitutively**. The product of this gene, NodD, is a **transcription factor** that binds with **flavonoids** produced by the host plant to activate the **common *nod* genes**, which are found in almost all rhizobium species. This leads to the production of a bacterial **lipochitooligosaccharide**. The flavonoids also activate the transcription of **host-specific *nod* genes**, which encode enzymes that 'decorate' this lipochitooligosaccharide. The decorated lipochitooligosaccharides are **Nod factors**. The lipid component of the Nod-factor allows penetration through membranes, but their mobility in the plant is limited. Different side groups are added to the backbone of this molecule, and this confers the **specificity** of a certain rhizobium (Fig. 12.15). Rhizobial species with a broad specificity produce many different Nod factors, as opposed to ones with a narrow host range. That is, the structure of the lipochitooligosaccharide determines if it will be recognized as a symbiont or as a pathogen by a potential host plant. Because the Nod factor is effective at concentrations as low as 10^{-12} M, a plant **receptor** must be involved which has been identified as a LysM-type receptor in different legumes (Radutoiu et al. 2003; Oldroyd et al. 2005). Rhizobial Nod factors trigger *NOD* gene transcription in plant epidermal cells within 1 h of exposure; maximum expression is in the differentiating region of the root between the growing root tip and the zone of root-hair emergence, where the nodulation process is initiated. A periodic increase of the **cytosolic Ca^{2+} concentration**, which originates from intracellular sources and from the apoplast, plays a role in the signal-transduction pathway that starts with the perception of the Nod factor and leads to downstream *NOD* gene expression (Ehrhardt et al. 1996).

Interestingly, certain *Bradyrhizobium* species do not encode any of the *nod* genes common in other rhizobia. Yet, these symbionts nodulate certain host legumes, for example *Aeschynomene* species (jointvetches). These usually enter via **cracks**, rather than trough infection threads. Cytokinin-related signals made by these rhizobia might support nodulation in the absence of Nod factors, but this remains to be tested (Podlešáková et al. 2013). This higlights one of many alternative mechanisms of nodulation in legumes (Masson-Boivin et al. 2009).

The infection processes and the massive colonization of nodule tissues raise the question how the plant host tolerates the rhizobia without eliciting a **defense response** . Indeed, there are clear commonalities between aspects of rhizobial and pathogen infection (Gourion et al. 2015). For example, as with plant pathogens, rhizobia actively suppress the host immune response to allow infection and symbiosis establishment. Likewise, the host has retained mechanisms to control the nutrient supply to the symbionts and the number of nodules, so that they do not become too burdensome. Subsequent to these early infection events, plant immune responses can also be induced inside nodules and likely play a role in nodule senescence. Thus, a balanced regulation of innate immunity is likely required throughout rhizobial infection, symbiotic establishment, and maintenance (Fig. 12.16; Cao et al. 2017; Yu et al. 2019).

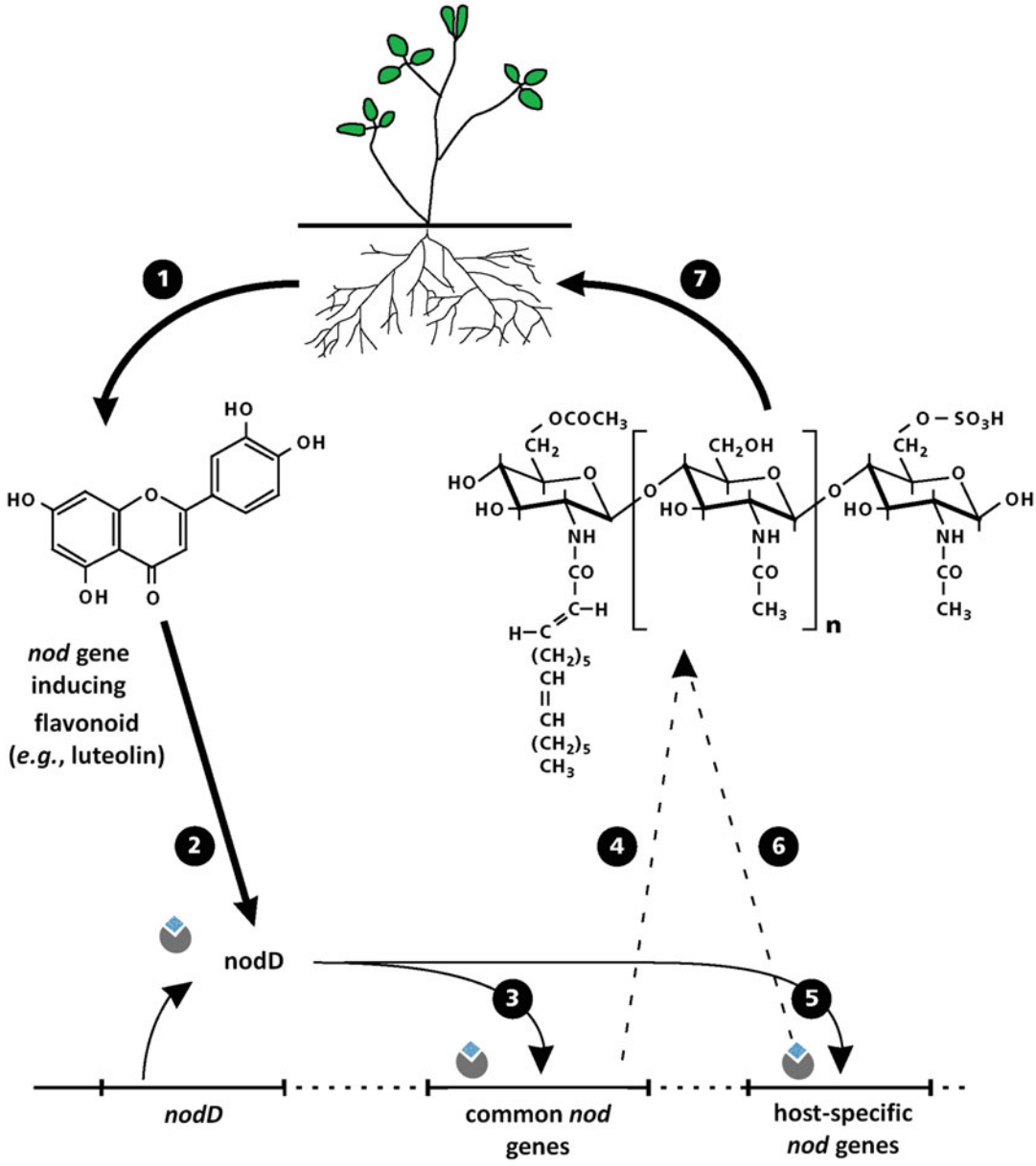

Fig. 12.15 Symbiotic signaling between legume plants and rhizobia. (1) Flavonoids are exuded by the legume roots. (2) The flavonoids bind to the gene product of a constitutively expressed nodulation (*nod*) gene, the transcription factor, NodD. (3) After this binding, NodD becomes activated to enhance expression of common *nod* genes. (4) This leads to the production of lipochitooligosaccharide (5) The flavonoids also activate the transcription of specific *nod* genes. (6) The products of the specific *nod* genes lead to modification of the lipochitooligosaccharides and the formation of nodulation (nod) factors, which confer host specificity. (7) The Nod factors are recognized by receptors on the surface of the legume-host's roots, where they initiate nodule development and infection.

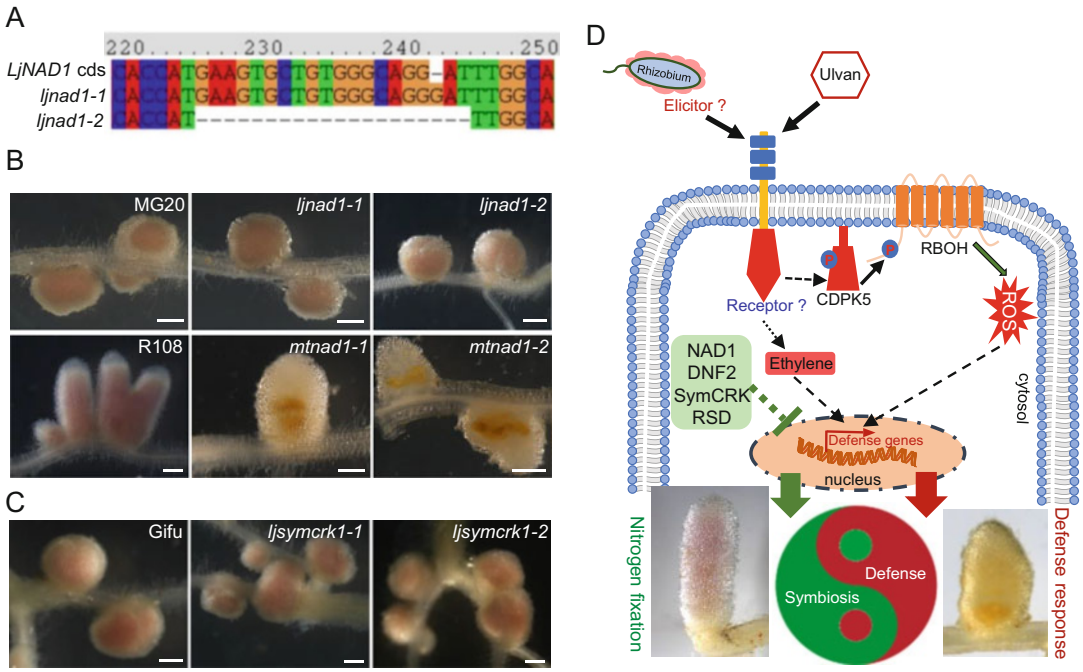

Fig. 12.16 Proposed immune pathway during rhizobial residence in nodules. (**A**) Two loss-of-function mutants of *Lotus japonicus* (birdsfoot trefoil), generated using CRISPR–Cas9 technology. *Ljnad1-1* mutants have one 'G' insertion, while *ljnad1-2* mutants have a 20-nucleotide deletion in the *LjNAD1* gene (Lj1gv3182390). (**B**) Comparison of nodule phenotypes between *ljnad1* and *mtnad1* mutants 21 days after inoculation with *Mesorhizobium loti* and *Sinorhizobium meliloti*, respectively. (**C**) Nodule phenotypes of two *Lotus japonicus* Symbiotic Cysteine-rich Receptor Kinase (*symcrk*) mutants 21 days after inoculation with *Mesorhizobium loti*. (**D**) A proposed immune pathway during terminal bacteroid differentiation in nodules. Ulvan (a compound in regular agar) and other elicitors from rhizobia trigger innate immunity via uncharacterized receptors; CDPK–RBOH-activated production of reactive oxygen species (ROS) and the phytohormone ethylene are proposed as downstream components. *Medicago truncatula* (barrel medic) proteins NAD1, SymCRK, DNF2, and RSD might directly target and suppress the innate immunity pathway to allow bacteroid differentiation in nodules. Bar, 1 mm (Yu et al. 2019). Copyright Elsevier Science, Ltd.

12.3.3.3 Entry of the Bacteria

After the release of flavonoids by the host and the release of the Nod factors by rhizobium, the bacteria multiply rapidly in the rhizosphere. Depending on the host, the bacteria may adhere to root hairs, which they subsequent invade through **infection threads**, or entry may occur through **cracks** in the epidermis or wounds. This is the only way of entry for 25% of all legumes (Sprent 2007; Ibáñez et al. 2017).

During the formation of an infection thread, the cell wall of the affected root hair is partly hydrolyzed at the tip. In this process, the root hairs curl, engulfing some of the bacteria within the curled root hair. On those locations on the root hairs that have become deformed due to the presence of rhizobia, the cell wall is degraded, allowing the bacteria to enter. An **infection thread** is formed by invagination of the cell wall and plasma membrane. This thread consists of cell-wall components similar to those that form the normal root-hair cell wall. The infection thread grows down the root hair, and provides a conduit for bacteria to reach the root cortex. The tip of the transcellular infection thread appears to be open and releases rhizobia in small vesicles into the cortex; sealing of the thread tip results in abortion of the infection thread. The formation of the infection thread may well be analogous to the enlargement of epidermal cell walls, in response to a pathogen's attempted penetration (Sprent et al. 2013).

Table 12.4 Comparison of indeterminate and determinate legume nodules.

Parameter	Indeterminate	Determinate
Nodule initiation	Inner cortex and pericycle	Outer/middle cortex and pericycle
Cell infection through	Infection threads	Infection threads and cell division
Meristem	Persistent (months)	Nonpersistent (days)
Bacteroid size	Larger than bacteria	Variable, although usually not too much larger than bacteria
Peribacteroid membrane	One bacteroid per symbiosome	Several bacteroids per symbiosome
N_2 fixation products transported	Amides usually	Ureides usually
Infected cells	Vacuolate	Nonvacuolate
Geographical origin	Temperate	Tropical to subtropical
Examples of genera	*Medicago*, *Trifolium*, *Pisum*, *Lupinus*	*Glycine*, *Phaseolus*, *Vigna*
nod Gene inducers	Flavones, isoflavones, chalcones	Isoflavones
Ploidy level of bacteroids	Polyploid	Diploid
Viability of bacteroids	Nonviable upon release in soil	Viable upon release in soil

Source: Vance (2002) Vessey et al. (2005); Mergaert et al. (2006); Mortimer et al. (2008)

If the infection is successful, then specific genes are activated in the cortex and pericycle which allows the formation of an infection thread through which the bacteria enter (Sprent 2007). At the same time, but independent of infection-thread formation, cell divisions start in the inner cortex (indeterminate nodules) or outer cortex (determinate nodules), opposite protoxylem poles, so that a new **meristem** is formed due to the presence of the rhizobia. This meristem gives rise to the **root nodule**. The infection thread grows inward, and, finally, the bacteria are taken up into the cytoplasm of the cells of the center of the developing nodule. Inside the infected host plant cell, the bacteria continue to divide for some time, now differentiating into **bacteroids**, which have a diminished ability to grow on laboratory culture media; they may be greatly enlarged with various shapes. In most legumes, bacteroids are enclosed within a **peribacteroid membrane**, to form a **symbiosome** (Udvardi and Poole 2013). Most symbiosomes are of a similar volume, but in some nodules, each symbiosome contains a single, enlarged pleomorphic bacteroid, whereas there may be up to 20 smaller, rod-shaped bacteroids in others. Symbiosomes with a single bacteroid are more typical of elongate, cylindrical nodules of the so-called **indeterminate** class, as on *Trifolium repens* (white clover) or *Pisum sativum* (pea) (Table 12.4). These nodules have a persistent meristem. Bacteroids in indeterminate nodules are polyploid, and have lost their ability to divide; hence they are nonviable when released from nodules (Mergaert et al. 2006). Symbiosomes with several bacteroids are common in spherical, **determinate** nodules (with no meristem), such as those of *Vigna unguiculata* (cowpea) or *Glycine max* (soybean). Bacteroids in determinate nodules are diploid, like free-living rhizobia, and can divide in soil upon release from nodules. The ploidy level of the bacteroids is controlled by the host (Mergaert et al. 2006). A few legumes have nodules in which there are no symbiosomes, the bacteria being retained within multiply branched infection threads. Mature nodules of the determinate and indeterminate type are strikingly different, but their initiation from dividing cortical cells is rather similar (Sprent 2007; Ibáñez et al. 2017).

12.3.3.4 Final Stages of the Establishment of the Symbiosis

Each **infected cell** may contain many hundreds of symbiosomes. The symbiosome membrane (**peribacteroid membrane**) originates from an invagination and endocytosis of the plasma membrane of the infected cortical cells. This

membrane acts as a selective permeability barrier to metabolite exchange between the bacteroids and the cytosol of the infected cells. Interspersed between the infected cells of many nodules are smaller, **uninfected cells**, which occupy about 20% of the total volume of the central zone of the nodules of *Glycine max* (soybean). **Plasmodesmata** connect uninfected with infected cells and with other uninfected cells in the central zone of the nodule. These plasmodesmata allow massive transport of carbon from the uninfected cells to the infected ones, and of nitrogenous compounds in the reverse direction (Brown et al. 1995). Both infected and uninfected cells contain numerous plastids and mitochondria. Uninfected and infected cells in nodules have different metabolic roles in symbiotic N_2 fixation (Day and Copeland 1991). The central tissue of some nodules, however, contains no uninfected cells. Nodules can be infected by a mixture of effective and ineffective rhizobial strains, and the plant has the ability to 'sanction' nodules that are inefficient in N_2 fixation (Denison 2000). In addition to rhizobia, nodules often contain many other species of nonrhizobia that might benefit from the reduced defense responses associated with invasion of rhizobia into legume nodules (Berrabah et al. 2019).

In *Glycine max* (soybean) nodules, an outer layer of cortical cells surrounds an endodermal cell layer, which in turn encloses several layers of subcortical cells. The central zone of the nodules contains several thousand infected cells. The nodule is connected with the **vascular tissue** in the stele, due to the proliferation of cells from the pericycle. Transfer cells in the vascular tissue likely enhance the exchange of carbon and N between partners (Guinel 2009).

The pattern of gene expression in the host cells that are part of the nodules is altered by the presence of the bacteria, resulting in the synthesis of many different proteins, known as **nodulins**. Some of these nodulins have been characterized biochemically, including the O_2 carrier **leghemoglobin** and nodule-specific forms of the enzymes uricase, glutamine synthetase, and sucrose synthase (Gourion et al. 2015).

12.3.4 Nitrogenase Activity and Synthesis of Organic Nitrogen

Biological reduction of N_2 to NH_3 is catalyzed by **nitrogenase**, in a highly **O_2-sensitive process**. This O_2 sensitivity accounts for the pink color of the nodule tissue which is due to the presence of **leghemoglobin** in the cytoplasm of the infected legume cells (Vieweg et al. 2004), or **hemoglobin** in nodules of species living symbiotically with *Frankia* (Gualtieri and Bisseling 2000). This heme-protein may comprise 35% of the total nodule soluble protein. Leghemoglobin is related to myoglobin of mammalian muscle. The genes encoding the synthesis of hemoglobin in legume nodules are in the host genome [*e.g.*, in *Vicia faba* (faba bean)] (Vieweg et al. 2004). Symbiotic leghemoglobins are crucial for N_2 fixation in legume root nodules (Ott et al. 2005) for the **O_2 supply** to the bacteroid. Leghemoglobin has a high affinity for O_2 and a relatively fast O_2-dissociation rate, which ensures sufficiently rapid **O_2 supply** for the highly active respiratory processes in the plant and bacteroid compartment, while maintaining a low concentration of free O_2 (between 3 and 30 nM). The latter is very important, because **nitrogenase**, which is responsible for the fixation of N_2 to NH_3, is rapidly damaged by **free O_2** (Gualtieri and Bisseling 2000; Raven 2012).

To control the O_2 supply and O_2 concentration to and within infected cells, **nodule permeability to O_2 diffusion** varies within seconds to hours in response to changes in carbohydrate supply via the phloem, adenylate demand, and O_2 status. This permeability control is associated with the reversible flow of water into or out of intercellular spaces. When nodulated *Glycine max* (soybean) plants are exposed to treatments that decrease the nodules' O_2 permeability, the K^+ concentration in the nodule cortex increases, relative to that in the central zone of the nodules, whereas treatments that increase O_2 permeability have the opposite effect. The energy-dependent coupled movement of ions and water into and out of infected cells offers a possible mechanism for diffusion barrier control in legume nodules (Wei and Layzell 2006).

The bacteroids contain **nitrogenase**, which is an enzyme complex that consists of two proteins. One, **nitrogenase-reductase**, is an Fe-S-protein that accepts electrons, via an intermediate electron carrier, from NADPH and then binds ATP. At the same time, the other subunit (an **Fe-Mo-protein**) binds N_2. Reduction of N_2 occurs if the two subunits have form an active complex. A minimum of 12, and possibly as many as 16 ATP are required per N_2; therefore the overall equation is:

$$\begin{aligned} &\nearrow N_2 + 8H^+ + 8e^- + 16ATP \\ &\nearrow\nearrow \quad \rightarrow 2NH_3 + H_2 + 16ADP + 16P_i \end{aligned} \tag{12.1}$$

Most of the N_2 fixed by the bacteroids is released as $\mathbf{NH_3}$ to the peribacteroid space, and then as $\mathbf{NH_4^+}$, via a voltage-driven channel across the peribacteroid membrane, to the cytosol of the nodule cells (Fig. 12.17). Alternatively, NH_3 may be converted into alanine, and then exported (Fig. 12.17; White et al. 2007). A nodule-specific glutamine synthetase is expressed in the cytosol of infected cells. Glutamine 2-oxoglutarate aminotransferase (GOGAT) then catalyses the formation of two molecules of glutamate from one molecule of glutamine. The major N-containing products exported via the xylem are the **amides** asparagine and glutamine in species such as *Pisum sativum* (pea), *Medicago sativa* (alfalfa), and *Trifolium repens* (white clover). These products are typical for nodules that are elongate-cylindrical with **indeterminate** apical meristematic activity (Fig. 12.18; Table 12.4). In *Phaseolus vulgaris* (common bean) and *Glycine max* (soybean), the products are predominantly **ureides**: allantoin and allantoic acid (Fig. 12.18; Table 12.4). Nodules exporting these compounds are spherical with **determinate** internal meristematic activity (Vessey et al. 2005).

The ureides released to the xylem of plants with **determinate** nodules are products that are only found when the symbiotic plants are fixing N_2 (Peoples et al. 1996). Hence, the concentration of these compounds in the xylem sap, relative to the total amount of N transported in the xylem, has been used to estimate the proportion of N derived from N_2 fixation, as opposed to the assimilation of combined N. The amides released to the xylem of plants with **indeterminate** nodules are also found when these plants grow nonsymbiotically. In fact, they are not even typical for legumes. Hence, we cannot use them as 'markers' for symbiotic N_2 fixation.

12.3.5 Carbon and Energy Metabolism of the Nodules

Carbohydrates are supplied via the phloem to the nodules, where they are rapidly converted in the plant compartment to **dicarboxylic acids** (malate, succinate), predominantly in the uninfected cells in the nodules (White et al. 2007). Malate and succinate are the major substrates for the bacteroids (Fig. 12.17). How do the infected cells prevent a large part of the organic acids from being oxidized via the nonphosphorylating alternative path in a situation where the demand for organic acids of the bacteroids is very large (Sect. 3.2.3)? Mitochondria from nodules have very little **alternative path** capacity; the little capacity they have is restricted to the uninfected cortical cells, rather than to the infected ones (Table 12.5; Kearns et al. 1992). There is, therefore, no risk of oxidizing the organic acids destined for the bacteroids.

Apart from N_2, H^+ is also reduced by nitrogenase [see Eq. (12.1) in Sect. 12.3.4], leading to the production of H_2. Most rhizobia, however, contain **hydrogenase**, which is an enzyme that recaptures H_2, using it as an electron donor. The characteristic of nitrogenase to reduce acetylene (ethyne) to ethylene (ethene) is frequently used to assay nitrogenase activity *in vivo*. Because the assay itself, however, interferes with the process of N_2 fixation, it should only be considered as a *qualitative* indicator for the occurrence of nitrogenase activity, and not as a *quantitative* measure for its actual activity (Unkovich et al. 2008).

The carbon costs of the legume-rhizobium symbiosis are 4–14% of the total amount of carbon fixed in photosynthesis, but the symbiosis causes an increase in photosynthetic carbon gain

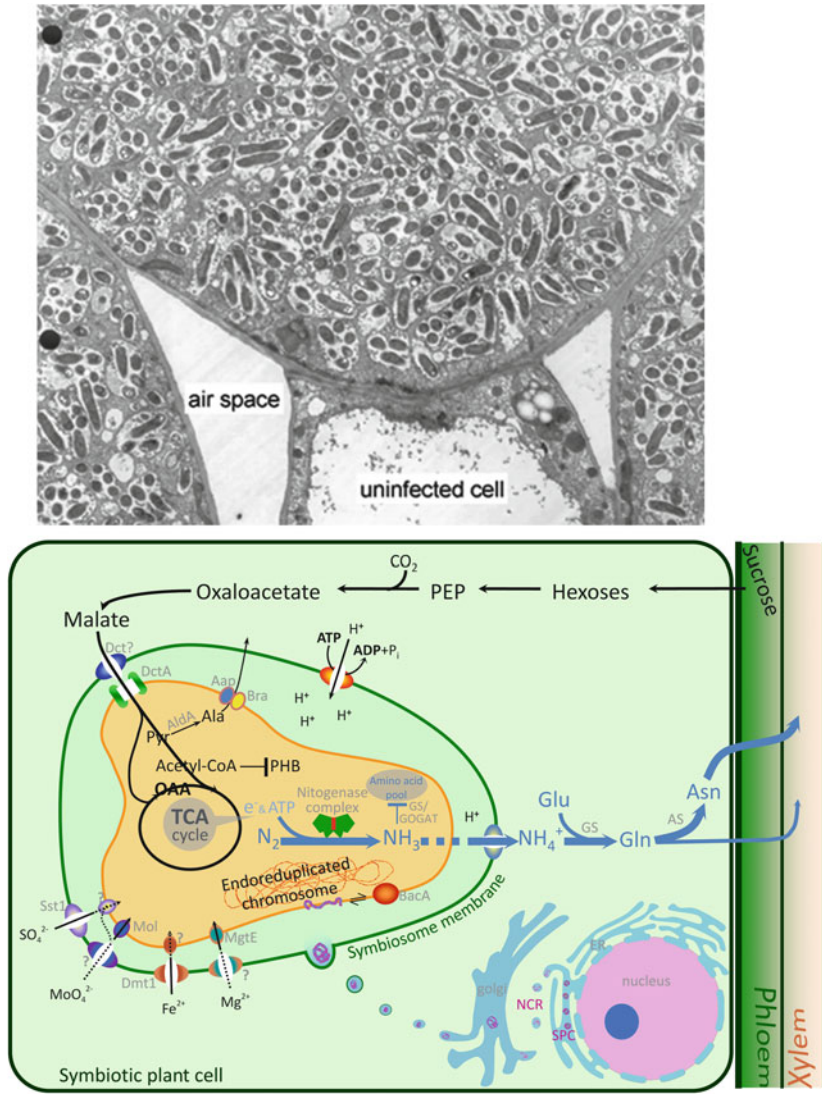

Fig. 12.17 (Top) Electron micrograph of a nodule of *Glycine max* (soybean), infected with *Bradyrhizobium japonicum*. The photo shows three infected cells and one uninfected cell, with two air spaces in between. Note that the uninfected cell is much smaller than the infected ones, and that the bacteroids are grouped as 'symbiosomes', surrounded by a peribacteroid membrane (courtesy D. Price, Australian National University, Canberra, Australia). (Bottom) Transport and metabolism in an infected nodule cell. Sucrose from the shoot is converted to malate in the plant and imported across the symbiosome membrane and into bacteroids, where it fuels nitrogen fixation. The product of the nitrogen fixation is then exported back to the plant, where it is assimilated into asparagine (Asn) for export to the shoot (blue arrows). In determinate nodules, the export products are ureides instead of Asn (modified after Oldroyd et al. 2011; Udvardi and Poole 2013).

that allows legumes to take advantage of the nutrient supply from their microsymbionts, without compromising the total amount of photosynthates available for plant growth (Kaschuk et al. 2009).

12.3.6 Quantification of N_2 Fixation *In Situ*

$^{15}N_2$ is the only direct method for quantifying biological N_2 fixation, and stable isotope probing

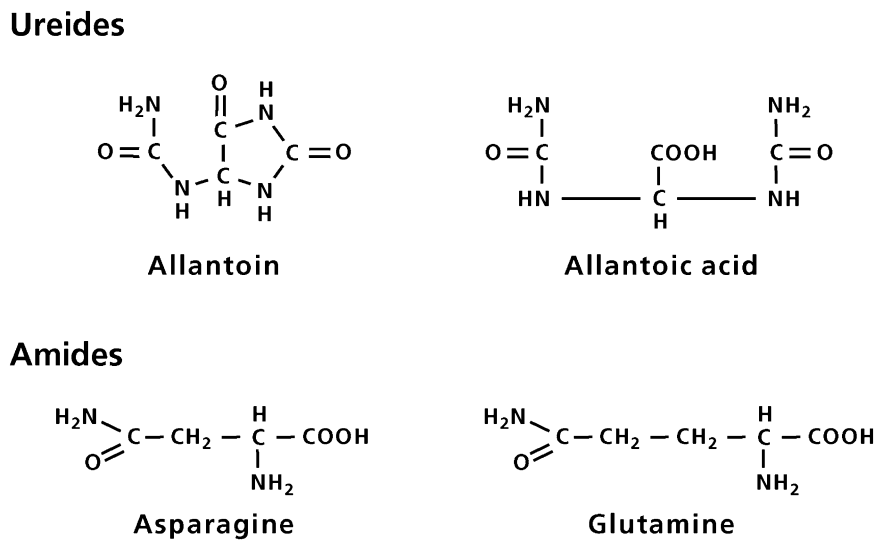

Fig. 12.18 Major nitrogen transport products from legume nodules. The carbon:nitrogen ratio of ureides in determinate nodules is 1:1, whereas that of amides in indeterminate nodules is 2:1 (asparagine) or 2.5:1 (glutamine).

Table 12.5 Cyanide-resistant, SHAM-sensitive respiration in infected and uninfected cells isolated from *Glycine max* (soybean); KCN and SHAM are inhibitors of the cytochrome and apternative pathway, respectively.*

	O_2 consumption [nmol mg^{-1} (protein) min^{-1}]		
Cells from root nodules	Control	KCN-resistant respiration	KCN resistant respiration (%)
Infected	60	0	0
Uninfected	45	22	49

Source: Kearns et al. (1992)

*Measurements were made on isolated mitochondria from different tissues, as well as on infected and uninfected cells from root nodules

with $^{15}N_2$ can identify uncultured diazotrophs (^{15}N is a stable isotope of N) (Chalk et al. 2017). Indirect methods for estimating biological N_2 fixatio should always be verified by the $^{15}N_2$ method.

The contribution of symbiotic N_2 fixation to the total accumulation of N in above-ground biomass of a crop or a plant community can be determined by applying ^{15}N-labeled inorganic N ($^{15}NO_3^-$ or $^{15}NH_4^+$) separately to N_2-fixing plants and reference plants (*i.e.* nonfixing species or mutants). For example, it can be given to a plant community that consists of both N_2-fixing species (*e.g.*, clover) and other species (*e.g.*, grasses). The grasses have a $^{15}N/^{14}N$ ratio that is used as a reference. N_2 fixation in the N_2-fixing clovers will 'dilute' their ^{15}N concentration. The extent of the dilution is used to calculate the contribution of fixation to the total amount of N that accumulates in the clover plants. The contribution of N_2 fixation to the total amount of N in the plant may amount to 75 and 86% in *Trifolium repens* (white clover) and *Trifolium pratense* (strawberry clover). Transfer of N is most likely via release of ammonium and amino acids from legume roots (Paynel et al. 2001). The contribution depends on the amount of inorganic combined N that plants receive from soil and fertilizer, and varies with the developmental stage of the plant and the time of the year. Table 12.6 illustrates the overwhelming importance of symbiotic N_2 fixation in some agricultural systems.

Sometimes the **natural abundance** of ^{15}N in the soil is used to quantify N_2 fixation (Table 12.2 in Sect. 12.2.4; Burchill et al. 2014). Instead of adding ^{15}N-labeled inorganic combined N, the

Table 12.6 Symbiotic nitrogen (N_2) fixation by legume crop and pasture species (Gault et al. 1995; Vance 2002; Herridge et al. 2008; Burchill et al. 2014), native legumes including Mimosoid and Papilionoid legumes in their natural environment in Brazil (Sprent et al. 1996), and native actinorhizal species in their natural habitat (Andrews et al. 2011).*

Species	N_2 fixed (kg ha^{-1} per season)	Plant N absorbed from atmosphere (%)
Legume crop and pasture species		
Arachis hypogaea	88	nd
Cicer arietinum	58	nd
Glycine max	176	68
Lens culinaris	51	nd
Lotus corniculatus	92	55
Lupinus angustifolius	170	65
Medicago sativa	180–780	65–96
Phaseolus vulgaris	23	40
Pisum sativum	86	35
Trifolium pratense	170	59
Trifolium repens	64	71
Vicia faba	107	nd
Vigna angularis	80	70
Native legumes		
Chamaecrista species	nd	66–79
Cratylia mollis	40	nd
Pterocarpus lucens	35	23–29
Mimosoid legumes	nd	42–63
Papilionoid legumes	nd	68–79
Actinorhizal species		
Alnus incana	43	96
Alnus glutinosa	nd	94
Discaria chacaye	nd	91
Ceanothus leucodermis	nd	54
Purshia tridentata	nd	55
Myrica gale	nd	53

*not determined

natural abundance of N in the soil is used (Unkovich 2013). The natural abundance of soil N likely differs from that of N_2 in the atmosphere, due to discrimination against the heavy isotope in various biological processes (*e.g.*, nitrification and denitrification) (Gebauer and Schulze 1991). Nitrogen in the soil is, therefore, 'enriched' with ^{15}N, relative to N_2 in the air. To apply this technique *in situ*, we have to use reliable reference plants. Ideally, reference plants should be located at the same distance to the sampled legume as the closest neighboring legume plant (Carlsson and Huss-Danell 2014). As discussed in Sect. 12.2 (Table 12.2), they should also be of the same mycorrhizal type.

The ^{15}N technique has also been used to demonstrate a significant transfer of N from symbiotic plants to neighboring grasses (up to 52 kg N ha^{-1} $year^{-1}$; on average a value of 17 kg ha^{-1} $year^{-1}$ is found). Conditions favoring N_2 fixation by the legume, such as a high irradiance, a favorable temperature, long days, and a relatively high P supply, enhance the transfer of N from the legume to the nonfixing neighbors. The transfer of N is to some extent the result of the uptake of nitrogenous compounds released after decomposition of parts of the legumes. Some of it is also due, however, to the exudation of nitrogenous compounds by the legumes, followed by absorption by the nonfixing plants. Some transfer

of N may occur through mycorrhizal hyphae (Sect. 12.2.3.1). Neighbors can have a profound effect on N_2 fixation by legumes by lowering the soil N concentrations and relieving inhibition of nodule formation and fixation (Li et al. 2009). *Zea mays* (maize) intercropped with *Vicia faba* (faba bean) promotes N_2 fixation, because the maize roots release **exudates** that promote flavonoid synthesis in faba bean, increase nodulation, and stimulate N_2 fixation after enhanced gene expression. (Fig. 12.19; Li et al. 2016).

The maximum yield of *Lolium rigidum* (annual ryegrass) is reached at a much lower supply of Pi than that of *Trifolium subterraneum* (subclover), when both species are grown in monoculture) (Bolan et al. 1987). This demand for a higher P is fairly common for crop and pasture legumes, but it is not universal (Sandral et al. 2018). The high demand for P of many crop legumes may reflect their adaptation to soils with a high Pi availability (Sect. 9.4.1.1), and points out that we can only expect a benefit from such legumes when these have access to sufficient Pi. Molybdenum (Mo) also has to be available to the legume to allow effective symbiotic N_2 fixation, because Mo is a pivotal cofactor of **nitrogenase** (Sect. 12.3.4; Rubio and Ludden 2008). It may become limiting at low pH (Fig. 9.1B) (Mortvedt 1981; Reed et al. 2013).

What is the role of N_2-fixing species in biodiverse grasslands? To address this question, test plants ('phytometers') can be planted in plots under investigation, to sample their aboveground biomass at a later stage (both N concentration and natural abundance of ^{15}N: $\delta^{15}N$). Phytometers in a particular study belonged to four '**plant functional groups**' (Chap. 16): *Festuca pratensis* (meadow fescue), *Plantago lanceolata* (snake plantain), *Knautia arvensis* (field scabious), and *Trifolium pratense* (strawberry clover) (Temperton et al. 2007). Significantly lower $\delta^{15}N$ values and higher N concentrations and N contents were found in all phytometer species growing with legumes, indicating a **facilitative** role for legumes in these natural grassland ecosystems. The magnitude of the positive interactions depends on the exact phytometer species, but increased N uptake in communities containing legumes is found in all three nonlegume phytometer species. In contrast, the legume phytometer species *Trifolium pratense* is negatively affected when other legumes are present in their host communities across all diversity levels (Temperton et al. 2007).

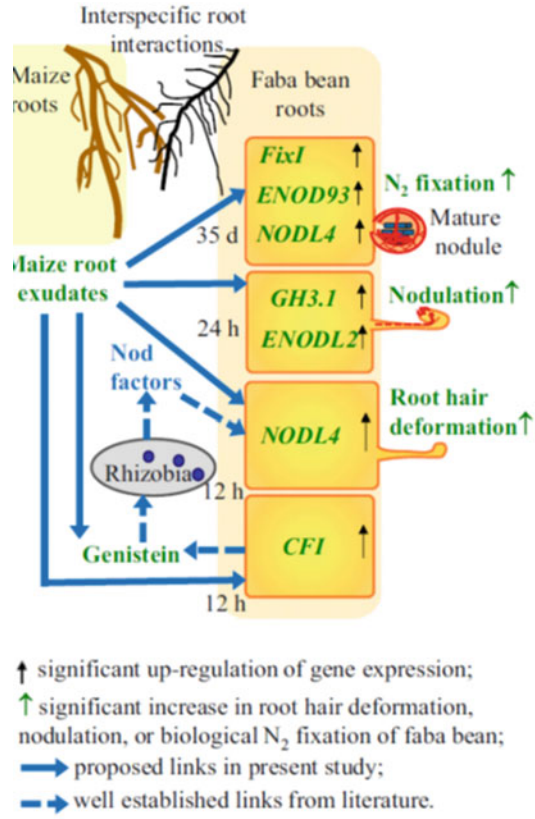

Fig. 12.19 The root-root interactions driven by *Zea mays* (maize) root exudates stimulate nodulation and nitrogen fixation of *Vicia faba* (faba bean) in a maize/faba bean intercropping system. Maize root exudates induce significant upregulation of expression of chalcone-flavanone isomerase (*CFI*), nodulin-like 4 (*NODL4*), an auxin-responsive gene (*GH3.1*), an early nodulin gene (*ENODL2*), a putative N_2 fixation gene (*FixI*), and another early nodulin gene (*ENOD93*) in faba bean roots. This provides an explanation for curling of root hairs, nodulation, and nodule maturation. Upregulation of *CFI* expression enhances genistein synthesis and secretion. Genistein released from maize and faba bean roots promotes rhizobium enrichment and release of Nod factors, which facilitate nodulation. Li B, Li Y-Y, Wu H-M, Zhang F-F, Li C-J, Li X-X, Lambers H, Li L. 2016. Root exudates drive interspecific facilitation by enhancing nodulation and N_2 fixation. *Proc Natl Acad Sci USA* **113**: 6496–6501.

12.3.7 Ecological Aspects of the Symbiotic Association with N_2-Fixing Microorganisms That Do Not Involve Specialized Structures

Next to the truly symbiotic associations involving symbiotic structures that lead to N_2 fixation, as discussed in Sect. 12.3.3, associations with *Azospirillum* have been investigated; these do not involve specialized symbiotic structures. Inoculation of the soil in which *Zea mays* (maize) plants are grown with *Azospirillum* bacteria significantly enhances the yield of maize, especially when the N supply is relatively low (Table 12.7). It is not certain, however, that this is a result of the fixation of N_2 by the *Azospirillum* bacteria. These organisms may also enhance the growth of plants by their production of phytohormones (Pereg et al. 2016). Microorganisms may promote plant growth in many ways, including **suppression of pathogenic organisms**.

In some areas in Brazil, farmers have grown *Saccharum officinarum* (sugarcane) continuously for more than a century without any nitrogenous fertilizer. Although it had long been suspected that substantial N_2 fixation occurs in such systems, none of the N_2-fixing bacteria isolated from the rhizosphere of *Saccharum officinarum* occur in large enough numbers to account for the rapid rates of N_2 fixation in these crops. An acid-tolerant N_2-fixing bacterium (*Gluconacetobacter diazotrophicus*) and a range of others have been identified in the **intercellular spaces** of sugarcane stem parenchyma (James et al. 1994). These spaces are filled with a solution that contains 12% sucrose (pH 5.5). *Gluconacetobacter diazotrophicus* shows optimal growth with 10% sucrose and pH 5.5. It will grow in a medium with 10% sucrose and rapidly acidifies its surroundings by the formation of acetic acid. It has been isolated from sugarcane tissues, but is not found in the soil between rows of sugarcane or in grasses from the same location. The apoplastic fluid occupies approximately 3% of the stem volume, which is equivalent to 3 tons of fluid per hectare of the sugarcane crop. This amount may suffice to make the sugarcane independent of N fertilizers. *Gluconacetobacter diazotrophicus* also promotes plant growth, and increases whole canopy photosynthesis of *Arabidopsis thaliana* which is useful for molecular studies of the mechanisms involved in the interaction between plants and *Gluconacetobacter diazotrophicus* (Rangel de Souza et al. 2016).

Recently, an N_2-fixing symbiosis was described in a landrace of *Zea mays* (maize), which grows well in N-depleted soil in the Sierra Mixe region of Oaxaca, Mexico (Van Deynze et al. 2018). The plants develop extensive aerial roots that secrete carbohydrate-rich mucilage. The mucilage harbors diazotrophic taxa and exhibits **nitrogenase** activity, as assessed by acetylene reduction and $^{15}N_2$ incorporation assays. Field experiments using ^{15}N natural abundance or ^{15}N-enrichment assessments over five years showed that atmospheric N_2 fixation contributes 29–82% of the N nutrition of this landrace. *Enterobacter agglomerans*, *Herbaspirillum seropedicae*, *Klebsiella terrigena*, and *Burkholderia australis* are also believed to be able to fix atmospheric N_2 in the apoplast of plants that have high apoplastic sugar

Table 12.7 The effect of inoculation with *Azospirillum brasiliense* on the production of *Zea mays* (maize) plants as dependent on the nitrogen (N) supply.*

N supply (g l^{-1})	Shoot dry mass (g)		Root dry mass (g)		Relative increment of total plant mass (%)
	Inoculated	Control	Inoculated	Control	
0	0.49	0.32	0.36	0.27	44
0.04	0.97	0.66	0.76	0.53	45
0.08	1.84	1.23	0.97	0.86	34
0.16	2.93	2.52	1.96	1.70	16

Source: Cohen et al. (1980)
*N was supplied as NH_4NO_3

concentrations (Boddey et al. 2003; Paungfoo-Lonhienne et al. 2014).

N_2 fixation in associations of the **feather moss** *Pleurozium schreberi* and cyanobacteria contributes about 2 kg N ha^{-1} $year^{-1}$ to N-limited boreal forests (Gundale et al. 2011). A drying period of three days almost completely eliminates N_2 fixation in the moss, but rates slowly recover within five days after rewetting (Rousk et al. 2013). Atmospheric N deposition inhibits cyanobacterial N_2 fixation, but likely not until it reaches >10 kg N ha^{-1} $year^{-1}$. The cyanobacteria associated with *Pleurozium schreberi* can recover from high N inputs and fix atmospheric N_2 after a period of N deprivation (Rousk et al. 2014).

Molecular techniques have made it easier to elucidate which N_2-fixing bacteria may be responsible for any biological N_2 fixation, and where within plants this N_2 fixation mainly occurs (de Souza et al. 2016). However, in most cases, the initial isolation and identification of these diazotrophs still requires semi-solid media and re-inoculation onto host plants, techniques that were developed a long time ago (Baldani et al. 2014).

12.3.8 Carbon Costs of the Legume-Rhizobium Symbiosis

Because all the organic acids required for symbiotic N_2 fixation by rhizobium and for maintenance of the root nodules come from the plant, there are costs involved in this symbiotic system for the plant. These costs exceed those required for assimilation of NO_3^- or NH_4^+ (Kaschuk et al. 2009), and have been estimated in various ways. For example, for an association of *Trifolium repens* (white clover) and rhizobium, in which the clover plants totally depend on the microsymbiont for their supply of N. In this system, the N_2 fixation is briefly interrupted by decreasing the O_2 concentration that surrounds the plants, but kept sufficiently high to fully maintain aerobic plant metabolism. It is sufficiently low, however, to completely block the respiration and N_2 fixation of the bacteroids. By relating the decrease in respiration upon blocking the N_2 fixation to the activity of N_2 fixation as determined from the N accumulation in the clover plants, **carbon costs** per unit fixed N are calculated. These costs amount to approximately 4–14% of all the carbon fixed in photosynthesis per day (Kaschuk et al. 2009). This proportion is rather high, compared with the figures for N acquisition by nonsymbiotic fast-growing plants given in Table 3.1: 4% when plants grow at an optimum nutrient supply. At a limiting nutrient supply, the percentage is likely greater than that of the costs of N_2 fixation.

Because of the high carbon costs of symbiotic N_2 fixation, it has been suggested that **elevated atmospheric CO_2 concentrations** will stimulate this process. However, a meta-analysis shows that elevated atmospheric [CO_2] stimulates symbiotic N_2 fixation only when sufficient soil nutrients, other than N, are available (Van Groenigen et al. 2006). Short-term experiments frequently show a positive effect of elevated atmospheric [CO_2] on symbiotic N_2 fixation, but in the long run, a reduced availability of Pi or Mo leads to rates of N_2 fixation similar to those under ambient [CO_2] (Hungate et al. 2004).

12.3.9 Suppression of the Legume-Rhizobium Symbiosis at Low pH and in the Presence of a Large Supply of Combined Nitrogen

Once rhizobia have successfully infected legume roots and nodules have formed, further infection is suppressed. This is called **autoregulation** of root nodule formation; a phenomenon we encountered before in the establishment of a mycorrhizal symbiosis (Sect. 12.2.3.1). Using plants grown with a divided root system shows that autoregulation depends on **systemic signals** (Catford et al. 2003; Reid et al. 2011b). For example, infection of one root of *Vicia sativa* (common vetch) with *Rhizobium leguminosarum* inhibits nodulation of a spatially separated root, when this root is inoculated two days later with the same bacteria (Kosslak and Bohlool 1984). The mechanism by which nodulation is

autoregulated is similar to that by which combined N inhibits nodulation, as discussed below.

Split-root experiments show that the signal for **systemic suppression** of nodulation is generated after root-hair curling, but before N_2 fixation and initiation of visible cortical and pericycle cell divisions in *Medicago truncatula* (barrel medic) (Mortier et al. 2012). The mechanism of **autoregulation** involves the synthesis of regulatory **peptides** in the root in response to rhizobia. The peptides are exported to the shoot, where they bind to a receptor that activates the synthesis of an inhibitory signal that is transported back to the roots There the signal inhibits further nodulation (Reid et al. 2011b). Tsikou et al. (2018) identified a **microRNA** produced in the shoots of *Lotus japonicus* (birdsfoot trefoil) that moves to the roots, where it posttranscriptionally regulates a key suppressor of symbiosis. In its presence, this keeps the uninfected root susceptible to productive infection by symbiotic bacteria. Autoregulation mechanisms via the shoot are likely necessary to balance carbon supply from the shoot with N demand in the root.

At **low pH**, nodule formation in legumes tends to be inhibited. Because fixation of N_2 lowers soil pH (Sect. 9.3.1), continued use of legumes in agriculture requires **regular liming**. Why is nodulation impaired at a low soil pH? An assay system as described in Sect. 12.3.3.1 can be used to establish that a relatively acid or alkaline, as opposed to a neutral pH of the soil, leads to less effective root exudates (Richardson et al. 1988). Compounds that stimulate *nod* gene expression are present in exudates of *Trifolium repens* (white clover) and *Trifolium subterraneum* (subterranan clover) seedlings grown between pH 3.0 and pH 8.0. The *nod* gene-induction activity of exudates is reduced when seedlings of both clover species are grown at pH > 7.0, and at pH < 4.0 and pH < 5.0 for white clover and subterranean clover, respectively. This explains the common observation of poor nodulation of many legumes in acid or alkaline soils. Survival of rhizobia is also lower in soils with a low pH, but some degree of adaptation of rhizobia strains has been observed, for example, on acid soils that are used to grow *Glycine max* (soybean) in Ethiopia (Muleta et al. 2017).

N_2 fixation is an energetically more expensive than the assimilation of NO_3^- or NH_4^+. Reminiscent of the effect of Pi on the formation of the mycorrhizal symbiosis, $\mathbf{NO_3^-}$ often inhibits the **infection** of legumes by rhizobia, but this is not invariably found (Sprent 1999). When *Medicago sativa* (alfalfa) plants are grown under N-limiting conditions, the expression of the genes involved in flavonoid biosynthesis and the production of root flavonoids are enhanced. This may account for greater infection by *Rhizobium meliloti* under conditions when N is in short supply, as opposed to suppression of nodulation in the presence of high NO_3^- concentrations (Coronado et al. 1995).

Soil N, in general, and **nitrate** in particular, inhibits **N_2 fixation** (Table 12.8; Schipanski et al.

Table 12.8 Apparent nitrogenase activity and the oxygen (O_2)-limitation coefficient, 2 days after addition of NO_3^- to the root environment of nodulated 21-days-old plants of *Pisum sativum* (pea).*

$[NO_3]$ (mM)	Apparent nitrogenase activity	O_2 limitation coefficient
	[nmol H_2 g^{-1} (nodule dry mass) s^{-1}]	
0	45	0.89
5	38	0.64
10	22	0.45
15	24	0.49

Source: Kaiser et al. (1997)

*The apparent nitrogenase activity was measured as the rate of hydrogen (H_2) evolution. As explained in Sect. 12.3.4, nitrogenase activity leads to the production of H_2. There is normally no net evolution of H_2, because rhizobia have a hydrogenase, an enzyme that recaptures and uses H_2 as an electron donor. In the present experiment, Kaiser et al. (1997) used a rhizobium strain that lacks hydrogenase so that the evolution of H_2 could be measured. The O_2 limitation coefficient is calculated as the ratio between total nitrogenase activity (H_2 evolution in the absence of N_2) and potential nitrogenase activity (H_2 evolution in the absence of N_2 at an optimum concentration of O_2)

Table 12.9 Antiherbivore effects of fungal endophytes that infect grasses.

Animal	Host grass genus	Fungal endophyte genus	Comments
Mammals			
Cattle, horses	*Festuca*	*Neotyphodium*	Reduced mass gain, gangrene, spontaneous abortion
Cattle, sheep, deer	*Lolium*	*Neotyphodium*	Reduced mass gain, tremors, staggers, death
Cattle, goats	*Andropogon*	*Balansia*	Reduced milk production, death
Cattle	*Paspalum*	*Myriogenospora*	Reduced mass gain, tremors gangrene
Insects			
Fall armyworm reduced survival	*Cenchrus*	*Balansia*	Avoidance
	Cyperus	*Balansia*	Reduced growth, increased development time
	Festuca	*Neotyphodium*	
	Lolium	*Neotyphodium*	
	Paspalum	*Myriogenospora*	
	Stipa	*Atkinsonella*	
Aphids	*Festuca*	*Neotyphodium*	Avoidance
Billbugs		*Lolium*	
		Neotyphodium	Reduced feeding and oviposition
Crickets		*Lolium*	
		Neotyphodium	Complete mortality
Cutworms		*Dactylis*	
		Epichloe	Reduced survival and mass gain
Flour beetles	*Lolium*	*Neotyphodium*	Reduced population growth
Sod webworms	*Lolium*	*Neotyphodium*	Reduced feeding and oviposition
Stem weevils	*Lolium*	*Neotyphodium*	Reduced feeding and oviposition

Source: Clay (1988)
Note: The examples are representative, but not exhaustive. *Neotyphodium* was previously known as *Acremonium*

2010). This regulation can be achieved through several mechanisms, including changes in carbon metabolism, O_2 supply, overproduction of reactive oxygen and nitrogen species, and/or cycling of amino acids between the plant and bacteroid fractions (Sulieman and Tran 2013). **Small peptides** that act as phytohormones also play an important role in signaling the N status of the plant and affect nodule activity (de Bang et al. 2017). The peptides controlling N inhibition of nodulation bind to the same receptor as the very similar peptides induced by rhizobia during autoregulation (Reid et al. 2011a).

12.4 Endosymbionts

Many plants are infected by **fungal endophytes** (Ascomycota) that live their entire life cycle within a plant (Mayerhofer et al. 2013). The fungi form nonpathogenic and usually intercellular associations in living plant tissues. The endophytes are often transmitted through the plant seed (Zhang et al. 2017), particularly in grasses and sedges, but seeds may lose their endophytes upon prolonged storage (Tian et al. 2016). Infection through germinating spores is an alternative way to enter the macrosymbiont. The association between plants and endosymbiotic fungi has been well studied in grasses in which the fungi may produce **alkaloids** inside their hosts, many of which have a neurotoxic effect, and hence make the infected plants poisonous to domestic mammals and increase their resistance to insect herbivores (Table 12.9; Bultman et al. 2018).

In some species, plant growth and seed production can be increased by infection with the endophyte. The symbiotic associations between grasses and fungal endophytes may be an

association in which the fungi derive carbohydrates from their host and defend their host against **herbivory**, thereby defending their own resources (Lugtenberg et al. 2016). Similar to the effect that mycorrhizal fungi have on interactions among mycorrhizal and nonmycorrhizal plants (Sect. 12.2.2), fungal endophytes may influence competitive interactions among plants. For example, the fungus *Neotyphodium* (previously *Acremonium*), profits from host plants by receiving nutrients, shelter, and guaranteed transmission to the next host generation. All of these benefits are a direct consequence of the fungus' strictly symbiotic dependence, with the fungus living within the host's body. By contrast, the benefits for the host plant are indirect and more complex. Infection by *Neotyphodium* induces increased aboveground biomass, tiller number, seed production, root growth and stress tolerance in the grass host (Müller and Krauss 2005). The presence or absence of fungal endophytes is not a specific trait of a plant species; rather, it depends on environmental conditions in an as-yet-unclear manner.

Bacteria may also act as endosymbionts. Common endophytic bacteria from healthy tubers of *Solanum tuberosum* (potato) belong to six genera (*Pseudomonas*, *Bacillus*, *Xanthomonas*, *Agrobacterium*, *Actinomyces*, and *Acinetobacter*). As we discuss in Sect. 14.3, many bacterial endophytes boost the host plant's resistance to pathogen attack (**induced resistance**) or they enhance growth. There are also endophytic bacteria, however, that are plant-growth-neutral or plant-growth-retarding (Sturz et al. 2000; Hardoim et al. 2015).

A special group of endophytes that is receiving increasing attention is that of **fine root endophytes** (Fig. 12.20). These are a group with a distinctive microscopic morphology when stained, including thin hyphae (c. 1.5 μm diameter), which branch in a distinctive fan-like pattern. Fine root endophytes also form arbuscule-like structures; this led them to be considered, as *Glomus tenue*, an AM fungus within the Glomeromycotina. However, molecular studies recently suggested that fine root endophytes are related to fungi from the Mucoromycotina (Orchard et al. 2017a); they have since been

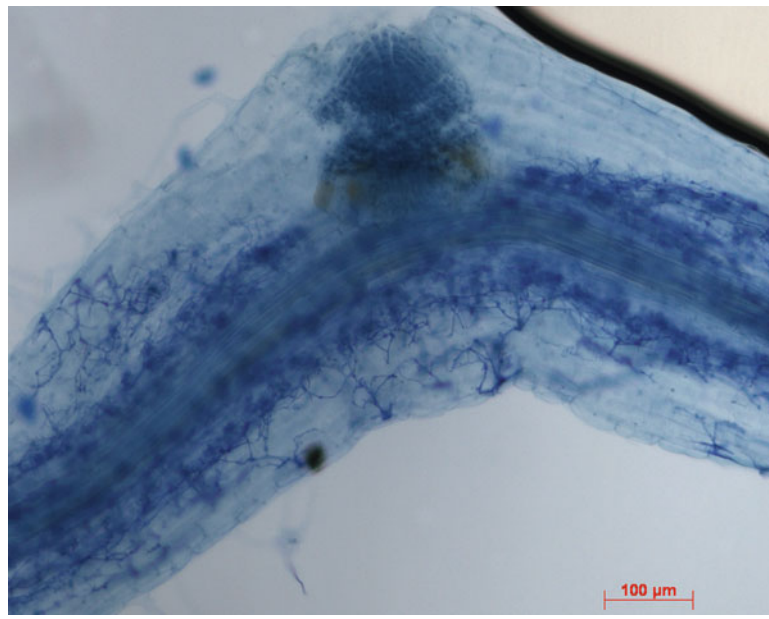

Fig. 12.20 A cleared and stained root of *Lotus subbiflorus* (hairy birdsfoot trefoil) heavily colonized by fine root endophytes. The structure at the top is an emerging lateral root primordium. There are several entry points in the epidermis; these are linked to characteristically branching thin hyphae in the outer cortex and abundant arbusculelike structures in the inner cortex. The small darkly stained swollen segments of hyphae, 'vesicles', that are evident are also characteristic of fine root endophytes (courtesy J.J. Bougoure, M.H. Ryan and S. Orchard, University of Western Australia, Australia).

placed in a new genus, within the Mucoromycotina, as *Planticonsortium tenue* (Walker et al. 2018). Fine root endophytes are globally distributed across many ecosystems and colonize numerous vascular plant families; in some circumstances they colonise roots to a greater extent than AM fungi do (Orchard et al. 2017b). While colonization by fine root endophytes is often intermixed with that of AM fungi (Jeffery et al. 2018), their interactions with host plants and AM fungi are little explored. Like AM fungi, fine root endophyte are present in the fossil record of early land plants (Krings et al. 2017). Thus, the evolution and ecology of AM fungi, fine root endophytes and other Mucoromycotina endophytes are perhaps closely linked (Hoysted et al. 2018). The recent finding on fine root endophytes highlights plant-fungal root symbioses are more complex than AM, and that there is a need for improved techniques to untangle the complex interactions among multiple fungal root endophytes and their hosts.

12.5 Plant Life Among Microsymbionts

At one stage in the history of plant ecophysiology, it may have seemed most to discuss the mineral nutrition and performance of plants devoid of their microsymbionts. If we wish to unravel basic principles of plant mineral nutrition (*e.g.*, the nature of a NO_3^- transporter or the function of a micronutrient), then this remains a valid approach. If the aim is to understand plant functioning in a real environment, whether a natural ecosystem or an agricultural field, however, then we cannot ignore the existence and overwhelming importance of the microsymbionts that interact with plants in an intricate manner. This is certainly true for mycorrhizal fungi, which affect both mycorrhizal and nonmycorrhizal species, although in a very different manner.

Plant-microbe interactions have not always received the attention they deserve. Interactions with N_2-fixing symbionts have been the target of research for a long time. Why buy N if you can grow your own? In recent years, there has been an enormous development in the understanding of signaling between rhizobia and legumes. Similar signaling processes probably exist between other N_2-fixing microsymbionts and their nonlegume hosts, and major progress has been made on signaling between mycorrhizal fungi and their macrosymbiotic partners.

Endophytes other than the 'classic' mycorrhizal fungi and N_2-fixing microorganisms include the fascinating N_2-fixing microorganisms in the apoplast of *Saccharum officinarum* (sugarcane) and in feather mosses in boreal forests as well as toxin-producing endophytes in cycads and grasses, and fine endophytes. We are only just beginning to understand the agronomic and ecological significance of these endophytes. Another question that we are now gradually answering is how symbiotic microorganisms are allowed entry into the plant, when plants have a wide array of defense mechanisms to keep microorganisms at bay.

In this chapter we have showcased one of many areas in plant physiological ecology where 'established' terms like **ecology** and **molecular plant physiology** have become obsolete. We can only further our basic understanding of interactions between plants and their microsymbionts, if we abolish old barriers that hinder the developments in this field. We can expect many applications flowing from a basic understanding of symbiotic associations between plants and microorganisms.

References

Abbott LK, Robson AD, De Boer G. 1984. The effect of phosphorus on the formation of hyphae in soil by the vesicular-arbuscular mycorrhizal fungus *Glomus fasciculatum*. *New Phytol* **97**: 437–446.

Adamczyk B, Ahvenainen A, Sietiö O-M, Kanerva S, Kieloaho A-J, Smolander A, Kitunen V, Saranpää P, Laakso T, Straková P, Heinonsalo J. 2016. The contribution of ericoid plants to soil nitrogen chemistry and organic matter decomposition in boreal forest soil. *Soil Biol Biochem* **103**: 394–404.

Akiyama K, Hayashi H. 2006. Strigolactones: chemical signals for fungal symbionts and parasitic weeds in plant roots. *Ann Bot* **97**: 925–931.

Akiyama K, Matsuzaki K, Hayashi H. 2005. Plant sesquiterpenes induce hyphal branching in arbuscular mycorrhizal fungi. *Nature* **435**: 824–827.

Albornoz FE, Burgess TI, Lambers H, Etchells H, Laliberté E. 2017. Native soil-borne pathogens equalise differences in competitive ability between plants of contrasting nutrient-acquisition strategies. *J Ecol* **105**: 549–557.

Andrews M, James EK, Sprent JI, Boddey RM, Gross E, dos Reis FB. 2011. Nitrogen fixation in legumes and actinorhizal plants in natural ecosystems: values obtained using ^{15}N natural abundance. *Plant Ecol Divers* **4**: 131–140.

Augé RM. 2001. Water relations, drought and vesicular-arbuscular mycorrhizal symbiosis. *Mycorrhiza* **11**: 3–42.

Baas R, Lambers H. 1988. Effects of vesicular-arbuscular mycorrhizal infection and phosphate on *Plantago major* ssp. *pleiosperma* in relation to the internal phosphate concentration. *Physiol Plant* **74**: 701–707.

Baas R, van der Werf A, Lambers H. 1989. Root respiration and growth in *Plantago major* as affected by vesicular-arbuscular mycorrhizal infection. *Plant Physiol* **91**: 227–232.

Baldani JI, Reis VM, Videira SS, Boddey LH, Baldani VLD. 2014. The art of isolating nitrogen-fixing bacteria from non-leguminous plants using N-free semi-solid media: a practical guide for microbiologists. *Plant Soil* **384**: 413–431.

Bearden B, Petersen L. 2000. Influence of arbuscular mycorrhizal fungi on soil structure and aggregate stability of a vertisol. *Plant Soil* **218**: 173–183.

Becard G, Kosuta S, Tamasloukht M, Sejalon-Delmas-N, Roux C. 2004. Partner communication in the arbuscular mycorrhizal interaction. *Can J Bot* **82**: 1186–1197.

Bennett JA, Maherali H, Reinhart KO, Lekberg Y, Hart MM, Klironomos J. 2017. Plant-soil feedbacks and mycorrhizal type influence temperate forest population dynamics. *Science* **355**: 181–184.

Berrabah F, Ratet P, Gourion B. 2019. Legume nodules: massive infection in the absence of defense induction. *Mol Plant-Microbe Interact* **32**: 35–44.

Besserer A, Bécard G, Roux C, Séjalon-Delmas N. 2009. Role of mitochondria in the response of arbuscular mycorrhizal fungi to strigolactones. *Plant Signal Behav* **4**: 75–77.

Besserer A, Puech-Pagès V, Kiefer P, Gomez-Roldan V, Jauneau A, Roy S, Portais J-C, Roux C, Bécard G, Séjalon-Delmas N. 2006. Strigolactones stimulate arbuscular mycorrhizal fungi by activating mitochondria. *PLoS Biol* **4**: e226.

Bethlenfalvay GJ, Pacovsky RS, Bayne HG, Stafford AE. 1982. Interactions between nitrogen fixation, mycorrhizal colonization, and host-plant growth in the *Phaseolus-Rhizobium-Glomus* symbiosis. *Plant Physiol* **70**: 446–450.

Black K, Osborne B. 2004. An assessment of photosynthetic downregulation in cyanobacteria from the *Gunnera–Nostoc* symbiosis. *New Phytol* **162**: 125–132.

Boddey RM, Urquiaga S, Alves BJR, Reis V. 2003. Endophytic nitrogen fixation in sugarcane: present knowledge and future applications. *Plant Soil* **252**: 139–149.

Bolan NS, Robson AD, Barrow NJ. 1987. Effects of vesicular-arbuscular mycorrhiza on the availability of iron phosphates to plants. *Plant Soil* **99**: 401–410.

Bontemps C, Elliott GN, Simon MF, Dos Reis JÚNior FB, Gross E, Lawton RC, Neto NE, De Fátima Loureiro M, De Faria SM, Sprent JI, James EK, Young JPW. 2010. *Burkholderia* species are ancient symbionts of legumes. *Mol Ecol* **19**: 44–52.

Bougoure JJ, Brundrett MC, Grierson PF. 2010. Carbon and nitrogen supply to the underground orchid, *Rhizanthella gardneri*. *New Phytol* **186**: 947–956.

Boulet F, Lambers H. 2005. Characterisation of arbuscular mycorrhizal fungi colonisation in cluster roots of shape *Hakea verrucosa* F. Muell (Proteaceae), and its effect on growth and nutrient acquisition in ultramafic soil. *Plant Soil* **269**: 357–367.

Bouwmeester HJ, Roux C, Lopez-Raez JA, Bécard G. 2007. Rhizosphere communication of plants, parasitic plants and AM fungi. *Trends Plant Sci* **12**: 224–230.

Branzanti MB, Rocca E, Pisi A. 1999. Effect of ectomycorrhizal fungi on chestnut ink disease. *Mycorrhiza* **9**: 103–109.

Brenner ED, Stevenson DW, Twigg RW. 2003. Cycads: evolutionary innovations and the role of plant-derived neurotoxins. *Trends Plant Sci* **8**: 446–452.

Brown SM, Oparka KJ, Sprent JI, Walsh KB. 1995. Symplastic transport in soybean root nodules. *Soil Biol Biochem* **27**: 387–399.

Bruisson S, Maillot P, Schellenbaum P, Walter B, Gindro K, Deglène-Benbrahim L. 2016. Arbuscular mycorrhizal symbiosis stimulates key genes of the phenylpropanoid biosynthesis and stilbenoid production in grapevine leaves in response to downy mildew and grey mould infection. *Phytochemistry* **131**: 92–99.

Brundrett MC, Tedersoo L. 2018. Evolutionary history of mycorrhizal symbioses and global host plant diversity. *New Phytol* **220**: 1108–1115.

Bultman TL, McNeill MR, Krueger K, De Nicolo G, Popay AJ, Hume DE, Mace WJ, Fletcher LR, Koh YM, Sullivan TJ. 2018. Complex interactions among sheep, insects, grass, and fungi in a simple New Zealand grazing system. *J Chem Ecol* **44**: 957–964.

Burchill W, James EK, Li D, Lanigan GJ, Williams M, Iannetta PPM, Humphreys J. 2014. Comparisons of biological nitrogen fixation in association with white clover (*Trifolium repens* L.) under four fertiliser nitrogen inputs as measured using two ^{15}N techniques. *Plant Soil* **385**: 287–302.

Cairney J. 2011. Ectomycorrhizal fungi: the symbiotic route to the root for phosphorus in forest soils. *Plant Soil* **344**: 51–71.

Cairney JW, Ashford AE. 2002. Biology of mycorrhizal associations of epacrids (Ericaceae). *New Phytol* **154**: 305–326.

Cameron DD, Leake JR, Read DJ. 2006. Mutualistic mycorrhiza in orchids: evidence from plant-fungus carbon and nitrogen transfers in the green-leaved terrestrial orchid *Goodyera repens*. *New Phytol* **171**: 405–416.

Cameron DD, Neal AL, van Wees SCM, Ton J. 2013. Mycorrhiza-induced resistance: more than the sum of its parts? *Trends Plant Sci* **18**: 539–545.

Cao Y, Halane MK, Gassmann W, Stacey G. 2017. The role of plant innate immunity in the legume-rhizobium symbiosis. *Annu Rev Plant Biol* **68**: 535–561.

Carlsson G, Huss-Danell K. 2014. Does nitrogen transfer between plants confound ^{15}N-based quantifications of N_2 fixation? *Plant Soil* **374**: 345–358.

Catford J-G, Staehelin C, Lerat S, Piche Y, Vierheilig H. 2003. Suppression of arbuscular mycorrhizal colonization and nodulation in split-root systems of alfalfa after pre-inoculation and treatment with Nod factors. *J Exp Bot* **54**: 1481–1487.

Catford JG, Staehelin C, Larose G, Piché Y, Vierheilig H. 2006. Systemically suppressed isoflavonoids and their stimulating effects on nodulation and mycorrhization in alfalfa split-root systems. *Plant Soil* **285**: 257–266.

Cavagnaro TR, Smith FA, Hay G, Carne-Cavagnaro VL, Smith SE. 2004. Inoculum type does not affect overall resistance of an arbuscular mycorrhiza-defective tomato mutant to colonisation but inoculation does change competitive interactions with wild-type tomato. *New Phytol* **161**: 485–494.

Chalk PM, He J-Z, Peoples MB, Chen D. 2017. $^{15}N_2$ as a tracer of biological N_2 fixation: A 75-year retrospective. *Soil Biol Biochem* **106**: 36–50.

Chalot M, Blaudez D, Brun A. 2006. Ammonia: a candidate for nitrogen transfer at the mycorrhizal interface. *Trends Plant Sci* **11**: 263–266.

Clay K. 1988. Fungal endophytes of grasses: a defensive mutualism between plants and fungi. *Ecology* **69**: 10–16.

Cohen E, Okon Y, Kigel J, Nur I, Henis Y. 1980. Increase in dry weight and total nitrogen content in *Zea mays* and *Setaria italica* associated with nitrogen-fixing *Azospirillum* spp. *Plant Physiol* **66**: 746–749.

Coronado C, Zuanazzi J, Sallaud C, Quirion JC, Esnault R, Husson HP, Kondorosi A, Ratet P. 1995. Alfalfa root flavonoid production Is nitrogen regulated. *Plant Physiol* **108**: 533–542.

Corrales A, Mangan SA, Turner BL, Dalling JW. 2016. An ectomycorrhizal nitrogen economy facilitates monodominance in a neotropical forest. *Ecol Lett* **19**: 383–392.

Czarnecki O, Yang J, Weston DJ, Tuskan GA, Chen J-G. 2013. A dual role of strigolactones in phosphate acquisition and utilization in plants. *Int J Mol Sci* **14**: 7681–7701.

Day DA, Copeland L. 1991. Carbon metabolism and compartmentation in nitrogen fixing legume nodules. *Plant Physiol Bochem* **29**: 185–201.

de Bang TC, Lay KS, Scheible W-R, Takahashi H. 2017. Small peptide signaling pathways modulating macronutrient utilization in plants. *Curr Opin Plant Biol* **39**: 31–39.

de Souza RSC, Okura VK, Armanhi JSL, Jorrín B, Lozano N, da Silva MJ, González-Guerrero M, de Araújo LM, Verza NC, Bagheri HC, Imperial J, Arruda P. 2016. Unlocking the bacterial and fungal communities assemblages of sugarcane microbiome. *Sci Rep* **6**: 28774.

Del-Saz NF, Romero-Munar A, Cawthray GR, Aroca R, Baraza E, Flexas J, Lambers H, Ribas-Carbó M. 2017. Arbuscular mycorrhizal fungus colonization in *Nicotiana tabacum* decreases the rate of both carboxylate exudation and root respiration and increases plant growth under phosphorus limitation. *Plant Soil* **416**: 97–106.

Delaux P-M, Radhakrishnan G, Oldroyd G. 2015. Tracing the evolutionary path to nitrogen-fixing crops. *Curr Opin Plant Biol* **26**: 95–99.

Denison RF. 2000. Legume sanctions and the evolution of symbiotic cooperation by rhizobia. *Amer Nat* **156**: 567–576.

Duchesne LC, Peterson RL, Ellis BE. 1988. Pine root exudate stimulates the synthesis of antifungal compounds by the ectomycorrhizal fungus *Paxillus involutus*. *New Phytol* **108**: 471–476.

Ehrhardt DW, Wais R, Long SR. 1996. Calcium spiking in plant root hairs responding to rhizobium nodulation signals. *Cell* **85**: 673–681.

Ezawa T, Saito K. 2018. How do arbuscular mycorrhizal fungi handle phosphate? New insight into fine-tuning of phosphate metabolism. *New Phytol* **220**: 1116–1121.

Ezawa T, Saito M, Yoshida T. 1995. Comparison of phosphatase localization in the intraradical hyphae of arbuscular mycorrhizal fungi, *Glomus* spp. and *Gigaspora* spp. *Plant Soil* **176**: 57–63.

Ezawa T, Smith SE, Smith FA. 2002. P metabolism and transport in AM fungi. *Plant Soil* **244**: 221–230.

Feijen FAA, Vos RA, Nuytinck J, Merckx VSFT. 2018. Evolutionary dynamics of mycorrhizal symbiosis in land plant diversification. *Sci Rep* **8**: 10698.

Franche C, Lindström K, Elmerich C. 2009. Nitrogen-fixing bacteria associated with leguminous and non-leguminous plants. *Plant Soil* **321**: 35–59.

Francis R, Read DJ. 1994. The contributions of mycorrhizal fungi to the determination of plant community structure. *Plant Soil* **159**: 11–25.

Gadkar V, David-Schwartz R, Kunik T, Kapulnik Y. 2001. Arbuscular mycorrhizal fungal colonization. Factors involved in host recognition. *Plant Physiol* **127**: 1493–1499.

Gault RR, Peoples MB, Turner GL, Lilley DM, Brockwell J, Bergersen FJ. 1995. Nitrogen fixation by irrigated lucerne during the first three years after establishment. *Aust J Agric* **46**: 1401–1425.

Gebauer G, Meyer M. 2003. ^{15}N and ^{13}C natural abundance of autotrophic and myco-heterotrophic orchids provides insight into nitrogen and carbon gain from fungal association. *New Phytol* **160**: 209–223.

Gebauer G, Schulze E-D. 1991. Carbon and nitrogen isotope ratios in different compartments of a healthy and a declining *Picea abies* forest in the Fichtelgebirge, NE Bavaria. *Oecologia* **87**: 198–207.

Genre A, Bonfante P. 2005. Building a mycorrhizal cell: how to reach compatibility between plants and arbuscular mycorrhizal fungi. *J Plant Interact* **1**: 3–13.

Geurts R, Xiao TT, Reinhold-Hurek B. 2016. What does it take to evolve a nitrogen-fixing endosymbiosis? *Trends Plant Sci* **21**: 199–208.

Giraud E, Moulin L, Vallenet D, Barbe V, Cytryn E, Avarre J-C, Jaubert M, Simon D, Cartieaux F, Prin Y, Bena G, Hannibal L, Fardoux J, Kojadinovic M, Vuillet L, Lajus A, Cruveiller S, Rouy Z, Mangenot S, Segurens B, Dossat C, Franck WL, Chang W-S, Saunders E, Bruce D, Richardson P, Normand P, Dreyfus B, Pignol D, Stacey G, Emerich D, Vermeglio A, Medigue C, Sadowsky M. 2007. Legumes symbioses: absence of *Nod* genes in photosynthetic bradyrhizobia. *Science* **316**: 1307–1312.

Glassop D, Smith SE, Smith FW. 2005. Cereal phosphate transporters associated with the mycorrhizal pathway of phosphate uptake into roots. *Planta* **222**: 688–698.

Goulet C, Klee HJ. 2010. Climbing the branches of the strigolactones pathway one discovery at a time. *Plant Physiol* **154**: 493–496.

Gourion B, Berrabah F, Ratet P, Stacey G. 2015. Rhizobium–legume symbioses: the crucial role of plant immunity. *Trends Plant Sci* **20**: 186–194.

Green TGA, Henskens FL, Wilkins A. 2012. Cyanolichens can have both cyanobacteria and green algae in a common layer as major contributors to photosynthesis. *Ann Bot* **110**: 555–563.

Griesmann M, Chang Y, Liu X, Song Y, Haberer G, Crook MB, Billault-Penneteau B, Lauressergues D, Keller J, Imanishi L, Roswanjaya YP, Kohlen W, Pujic P, Battenberg K, Alloisio N, Liang Y, Hilhorst H, Salgado MG, Hocher V, Gherbi H, Svistoonoff S, Doyle JJ, He S, Xu Y, Xu S, Qu J, Gao Q, Fang X, Fu Y, Normand P, Berry AM, Wall LG, Ané J-M, Pawlowski K, Xu X, Yang H, Spannagl M, Mayer KFX, Wong GK-S, Parniske M, Delaux P-M, Cheng S. 2018. Phylogenomics reveals multiple losses of nitrogen-fixing root nodule symbiosis. *Science* **361**.

Grimoldi AA, Kavanová M, Lattanzi FA, Schnyder H. 2005. Phosphorus nutrition-mediated effects of arbuscular mycorrhiza on leaf morphology and carbon allocation in perennial ryegrass. *New Phytol* **168**: 435–444.

Gualtieri G, Bisseling T. 2000. The evolution of nodulation. *Plant Mol Biol* **42**: 181–194.

Guinel FC. 2009. Getting around the legume nodule: I. The structure of the peripheral zone in four nodule types. *Botany* **87**: 1117–1138.

Gundale MJ, Deluca TH., Nordin A. 2011. Bryophytes attenuate anthropogenic nitrogen inputs in boreal forests. *Glob Change Biol* **17**: 2743–2753.

Hardoim PR, van Overbeek LS, Berg G, Pirttilä AM, Compant S, Campisano A, Döring M, Sessitsch A. 2015. The hidden world within plants: ecological and evolutionary considerations for defining functioning of microbial endophytes. *Microbiol Mol Biol Rev* **79**: 293–320.

Harrison MJ. 2005. Signaling in the arbuscular mycorrhizal symbiosis. *Annu Rev Microbiol* **59**: 19–42.

Hartnett DC, Wilson GWT. 2002. The role of mycorrhizas in plant community structure and dynamics: lessons from grasslands. *Plant Soil* **244**: 319–331.

Hassan S, Mathesius U. 2012. The role of flavonoids in root–rhizosphere signalling: opportunities and challenges for improving plant–microbe interactions. *J Exp Bot* **63**: 3429–3444.

Hause B, Fester T. 2005. Molecular and cell biology of arbuscular mycorrhizal symbiosis. *Planta* **221**: 184–196.

He X, Critchley C, Ng H, Bledsoe C. 2004. Reciprocal N ($^{15}NH_4^+$ or $^{15}NO_3^-$) transfer between nonN_2-fixing *Eucalyptus maculata* and N_2-fixing *Casuarina cunninghamiana* linked by the ectomycorrhizal fungus *Pisolithus* sp. *New Phytol* **163**: 629–640.

He X, Critchley C, Ng H, Bledsoe C. 2005. Nodulated N_2-fixing *Casuarina cunninghamiana* is the sink for net N transfer from non-N_2-fixing *Eucalyptus maculata* via an ectomycorrhizal fungus *Pisolithus* sp. using $^{15}NH_4^+$ or $^{15}NO_3^-$ supplied as ammonium nitrate. *New Phytol* **167**: 897–912.

Helber N, Wippel K, Sauer N, Schaarschmidt S, Hause B, Requena N. 2011. A versatile monosaccharide transporter that operates in the arbuscular mycorrhizal fungus *Glomus* sp is crucial for the symbiotic relationship with plants. *Plant Cell* **23**: 3812–3823.

Herridge DF, Peoples MB, Boddey RM. 2008. Global inputs of biological nitrogen fixation in agricultural systems. *Plant Soil* **311**: 1–18.

Hirsch AM, Lum MR, Downie JA. 2001. What makes the rhizobia-legume symbiosis so special? *Plant Physiol* **127**: 1484–1492.

Hobbie EA. 2006. Carbon allocation to ectomycorrhizal fungi correlates with belowground allocation in culture studies. *Ecology* **87**: 563–569.

Hoeksema JD, Chaudhary VB, Gehring CA, Johnson NC, Karst J, Koide RT, Pringle A, Zabinski C, Bever JD, Moore JC, Wilson GWT, Klironomos JN, Umbanhowar J. 2010. A meta-analysis of context-dependency in plant response to inoculation with mycorrhizal fungi. *Ecol Lett* **13**: 394–407.

Högberg P. 1990. ^{15}N natural abundance as a possible marker of the ectomycorrhizal habit of trees in mixed African woodlands. *New Phytol* **115**: 483–486.

Hohnjec N, Czaja-Hasse LF, Hogekamp C, Küster H. 2015. Pre-announcement of symbiotic guests: transcriptional reprogramming by mycorrhizal lipochitooligosaccharides shows a strict co-dependency on the GRAS transcription factors NSP1 and RAM1. *BMC Genomics* **16**: 994.

Hoysted GA, Kowal J, Jacob A, Rimington WR, Duckett JG, Pressel S, Orchard S, Ryan MH,

Field KJ, Bidartondo MI. 2018. A mycorrhizal revolution. *Curr Opin Plant Biol* **44**: 1–6.

Hungate BA, Stiling PD, Dijkstra P, Johnson DW, Ketterer ME, Hymus GJ, Hinkle CR, Drake BG. 2004. CO_2 elicits long-term decline in nitrogen fixation. *Science* **304**: 1291.

Ibáñez F, Wall L, Fabra A. 2017. Starting points in plant-bacteria nitrogen-fixing symbioses: intercellular invasion of the roots. *J Exp Bot* **68**: 1905–1918.

Jacott C, Murray J, Ridout C. 2017. Trade-offs in arbuscular mycorrhizal symbiosis: disease resistance, growth responses and perspectives for crop breeding. *Agronomy* **7**: 75.

Jakobsen I, Rosendahl L. 1990. Carbon flow into soil and external hyphae from roots of mycorrhizal cucumber plants. *New Phytol* **115**: 77–83.

James EK, Reis VM, Olivares FL, Baldani JI, Döbereiner J. 1994. Infection of sugar cane by the nitrogen-fixing bacterium *Acetobacter diazotrophicus*. *J Exp Bot* **45**: 757–766.

Jansa J, Bukovská P, Gryndler M. 2013. Mycorrhizal hyphae as ecological niche for highly specialized hypersymbionts – or just soil free-riders? *Front Plant Sci* **4**.

Javot H, Penmetsa RV, Terzaghi N, Cook DR, Harrison MJ. 2007. A *Medicago truncatula* phosphate transporter indispensable for the arbuscular mycorrhizal symbiosis. *Proc Natl Acad Sci USA* **104**: 1720–1725.

Jeffery RP, Simpson RJ, Lambers H, Orchard S, Kidd DR, Haling RE, Ryan MH. 2018. Contrasting communities of arbuscule-forming root symbionts change external critical phosphorus requirements of some annual pasture legumes. *Appl Soil Ecol* **126**: 88–97.

Jiang Y, Wang W, Xie Q, Liu N, Liu L, Wang D, Zhang X, Yang C, Chen X, Tang D, Wang E. 2017. Plants transfer lipids to sustain colonization by mutualistic mycorrhizal and parasitic fungi. *Science* **356**: 1172–1175.

Johnson NC, Graham JH, Smith FA. 1997. Functioning of mycorrhizal associations along the mutualism–parasitism continuum. *New Phytol* **135**: 575–585.

Kaiser BN, Layzell DB, Shelp BJ. 1997. Role of oxygen limitation and nitrate metabolism in the nitrate inhibition of nitrogen fixation by pea. *Physiol Plant* **101**: 45–50.

Karandashov V, Bucher M. 2005. Symbiotic phosphate transport in arbuscular mycorrhizas. *Trends Plant Sci* **10**: 22–29.

Kaschuk G, Kuyper TW, Leffelaar PA, Hungria M, Giller KE. 2009. Are the rates of photosynthesis stimulated by the carbon sink strength of rhizobial and arbuscular mycorrhizal symbioses? *Soil Biol Biochem* **41**: 1233–1244.

Kearns A, Whelan J, Young S, Elthon T, Day D. 1992. Tissue-specific expression of the alternative oxidase in soybean and siratro. *Plant Physiol* **99**: 712–717.

Khaosaad T, Garcia-Garrido JM, Steinkellner S, Vierheilig H. 2007. Take-all disease is systemically reduced in roots of mycorrhizal barley plants. *Soil Biol Biochem* **39**: 727–734.

Kikuchi Y, Hijikata N, Ohtomo R, Handa Y, Kawaguchi M, Saito K, Masuta C, Ezawa T. 2016. Aquaporin-mediated long-distance polyphosphate translocation directed towards the host in arbuscular mycorrhizal symbiosis: application of virus-induced gene silencing. *New Phytol* **211**: 1202–1208.

Klironomos JN, Hart MM. 2001. Food-web dynamics: animal nitrogen swap for plant carbon. *Nature* **410**: 651–652.

Kosslak RM, Bohlool BB. 1984. Suppression of nodule development of one side of a split-root system of soybeans caused by prior inoculation of the other side. *Plant Physiol* **75**: 125–130.

Krings M, Harper CJ, White JF, Barthel M, Heinrichs J, Taylor EL, Taylor TN. 2017. Fungi in a *Psaronius* root mantle from the Rotliegend (Asselian, Lower Permian/Cisuralian) of Thuringia, Germany. *Rev Palaeobot Palynol* **239**: 14–30.

Kwon DK, Beevers H. 1992. Growth of *Sesbania rostrata* (Brem) with stem nodules under controlled conditions. *Plant Cell Environ* **15**: 939–945.

Lagrange A, L'Huillier L, Amir H. 2013. Mycorrhizal status of Cyperaceae from New Caledonian ultramafic soils: effects of phosphorus availability on arbuscular mycorrhizal colonization of *Costularia comosa* under field conditions. *Mycorrhiza* **23**: 655–661.

Lambers H, Albornoz F, Kotula L, Laliberté E, Ranathunge K, Teste FP, Zemunik G. 2018. How belowground interactions contribute to the coexistence of mycorrhizal and non-mycorrhizal species in severely phosphorus-impoverished hyperdiverse ecosystems. *Plant Soil* **424**: 11–34.

Lambers H, Brundrett MC, Raven JA, Hopper SD. 2010. Plant mineral nutrition in ancient landscapes: high plant species diversity on infertile soils is linked to functional diversity for nutritional strategies. *Plant Soil* **334**: 11–31.

Lambers H, Raven JA, Shaver GR, Smith SE. 2008. Plant nutrient-acquisition strategies change with soil age. *Trends Ecol Evol* **23**: 95–103.

Lambers H, Shane MW, Cramer MD, Pearse SJ, Veneklaas EJ. 2006. Root structure and functioning for efficient acquisition of phosphorus: matching morphological and physiological traits. *Ann Bot* **98**: 693–713.

Lambers H, Teste FP. 2013. Interactions between arbuscular mycorrhizal and non-mycorrhizal plants: do non-mycorrhizal species at both extremes of nutrient-availability play the same game? *Plant Cell Environ* **36**: 1911–1915.

Landeweert R, Hoffland E, Finlay RD, Kuyper TW, van Breemen N. 2001. Linking plants to rocks: ectomycorrhizal fungi mobilize nutrients from minerals. *Trends Ecol Evol* **16**: 248–254.

Leake JR. 2004. Myco-heterotroph/epiparasitic plant interactions with ectomycorrhizal and arbuscular mycorrhizal fungi. *Curr Opin Plant Biol* **7**: 422–428.

Leake JR, Read DJ. 1989. The biology of mycorrhiza in the Ericaceae. *New Phytol* **113**: 535–544.

Li B, Li Y-Y, Wu H-M, Zhang F-F, Li C-J, Li X-X, Lambers H, Li L. 2016. Root exudates drive interspecific facilitation by enhancing nodulation and N_2 fixation. *Proc Natl Acad Sci USA* **113**: 6496–6501.

Li Y-Y, Yu C-B, Cheng X, Li C-J, Sun J-H, Zhang F-S, Lambers H, Li L. 2009. Intercropping alleviates the inhibitory effect of N fertilization on nodulation and symbiotic N_2 fixation of faba bean. *Plant Soil* **323**: 295–308.

Liang M, Liu X, Etienne RS, Huang F, Wang Y, Yu S. 2015. Arbuscular mycorrhizal fungi counteract the Janzen-Connell effect of soil pathogens. *Ecology* **96**: 562–574.

Lindblad P 2009. Cyanobacteria in symbiosis with cycads. In: Pawlowski K ed. *Prokaryotic Symbionts in Plants*. Berlin Springer, 225–233.

Luginbuehl LH, Menard GN, Kurup S, Van Erp H, Radhakrishnan GV, Breakspear A, Oldroyd GED, Eastmond PJ. 2017. Fatty acids in arbuscular mycorrhizal fungi are synthesized by the host plant. *Science* **356**: 1175–1178.

Lugtenberg BJ, Caradus JR, Johnson LJ. 2016. Fungal endophytes for sustainable crop production. *FEMS Microbiol Ecol* **92**: 1–17.

Ma Z, Guo D, Xu X, Lu M, Bardgett RD, Eissenstat DM, McCormack ML, Hedin LO. 2018. Evolutionary history resolves global organization of root functional traits. *Nature*: 94–97.

Maherali H, Klironomos JN. 2007. Influence of phylogeny on fungal community assembly and ecosystem functioning. *Science* **316**: 1746–1748.

Maillet F, Poinsot V, André O, Puech-Pagès V, Haouy A, Gueunier M, Cromer L, Giraudet D, Formey D, Niebel A, Martinez EA, Driguez H, Bécard G, Dénarié J. 2011. Fungal lipochitooligosaccharide symbiotic signals in arbuscular mycorrhiza. *Nature* **469**: 58–64.

Martin F, Kohler A, Murat C, Veneault-Fourrey C, Hibbett DS. 2016. Unearthing the roots of ectomycorrhizal symbioses. *Nat Rev Microbiol* **14**: 760–773.

Martin FM, Uroz S, Barker DG. 2017. Ancestral alliances: plant mutualistic symbioses with fungi and bacteria. *Science* **356**: eaad4501.

Marulanda A, Azcón R, Ruiz-Lozano JM. 2003. Contribution of six arbuscular mycorrhizal fungal isolates to water uptake by *Lactuca sativa* plants under drought stress. *Physiol Plant* **119**: 526–533.

Marx DH. 1969. The influence of ectotrophic mycorrhizal fungi on the resistance of pine roots to pathogenic infections. I. Antagonism of mycorrhizal fungi to root pathogenic fungi and soil bacteria. *Phytopathology* **59**: 153–163.

Marx DH. 1972. Ectomycorrhizae as biological deterrents to pathogenic root infections. *Annu Rev Phytopathol* **10**: 429–454.

Masson-Boivin C, Giraud E, Perret X, Batut J. 2009. Establishing nitrogen-fixing symbiosis with legumes: how many rhizobium recipes? *Trends Microbiol* **17**: 458–466.

Maxwell CA, Hartwig UA, Joseph CM, Phillips DA. 1989. A chalcone and two related flavonoids released from alfalfa roots induce *nod* genes of *Rhizobium meliloti*. *Plant Physiol* **91**: 842–847.

Mayerhofer M, Kernaghan G, Harper K. 2013. The effects of fungal root endophytes on plant growth: a meta-analysis. *Mycorrhiza* **23**: 119–128.

Mergaert P, Uchiumi T, Alunni B, Evanno G, Cheron A, Catrice O, Mausset A-E, Barloy-Hubler F, Galibert F, Kondorosi A, Kondorosi E. 2006. Eukaryotic control on bacterial cell cycle and differentiation in the *Rhizobium*-legume symbiosis. *Proc Natl Acad Sci USA* **103**: 5230–5235.

Minton MM, Barber NA, Gordon LL. 2016. Effects of arbuscular mycorrhizal fungi on herbivory defense in two *Solanum* (Solanaceae) species. *Plant Ecol Evol* **149**: 157–164.

Molina R, Horton TR 2015. Mycorrhiza specificity: its role in the development and function of common mycelial networks. In: Horton TR ed. *Mycorrhizal Networks*. Dordrecht: Springer Netherlands, 1–39.

Mortier V, Holsters M, Goormachtig S. 2012. Never too many? How legumes control nodule numbers. *Plant Cell Environ* **35**: 245–258.

Mortimer PE, Pérez-Fernández MA, Valentine AJ. 2008. The role of arbuscular mycorrhizal colonization in the carbon and nutrient economy of the tripartite symbiosis with nodulated *Phaseolus vulgaris*. *Soil Biol Biochem* **40**: 1019–1027.

Mortvedt JJ. 1981. Nitrogen and molybdenum uptake and dry matter relationships of soybeans and forage legumes in response to applied molybdenum on acid soil. *J Plant Nutr* **3**: 245–256.

Moulin L, Munive A, Dreyfus B, Boivin-Masson C. 2001. Nodulation of legumes by members of the β-subclass of Proteobacteria. *Nature* **411**: 948–950.

Muleta D, Ryder MH, Denton MD. 2017. The potential for rhizobial inoculation to increase soybean grain yields on acid soils in Ethiopia. *Soil Sci Plant Nutr* **63**: 441–451.

Müller CB, Krauss J. 2005. Symbiosis between grasses and asexual fungal endophytes. *Curr Opin Plant Biol* **8**: 450–456.

Mustafa G, Khong NG, Tisserant B, Randoux B, Fontaine J, Magnin-Robert M, Reignault P, Sahraoui AL-H. 2017. Defence mechanisms associated with mycorrhiza-induced resistance in wheat against powdery mildew. *Funct Plant Biol* **44**: 443–454.

Nadelhoffer K, Shaver G, Fry B, Giblin A, Johnson L, McKane R. 1996. ^{15}N natural abundances and N use by tundra plants. *Oecologia* **107**: 386–394.

Oldroyd GED. 2013. Speak, friend, and enter: signalling systems that promote beneficial symbiotic associations in plants. *Nat Rev Microbiol* **11**: 252–263.

Oldroyd GED, Harrison MJ, Udvardi M. 2005. Peace talks and trade deals. Keys to long-term harmony in

legume-microbe symbioses. *Plant Physiol* **137**: 1205–1210.

Oldroyd GED, Murray JD, Poole PS, Downie JA. 2011. The rules of engagement in the legume-rhizobial symbiosis. *Annu Rev Gen* **45**: 119–144.

Oliveira RS, Galvão HC, de Campos MCR, Eller CB, Pearse SJ, Lambers H. 2015. Mineral nutrition of *campos rupestres* plant species on contrasting nutrient-impoverished soil types. *New Phytol* **205**: 1183–1194.

Orchard S, Hilton S, Bending GD, Dickie IA, Standish RJ, Gleeson DB, Jeffery RP, Powell JR, Walker C, Bass D, Monk J, Simonin A, Ryan MH. 2017a. Fine endophytes (*Glomus tenue*) are related to Mucoromycotina, not Glomeromycota. *New Phytol* **213**: 481–486.

Orchard S, Standish RJ, Dickie IA, Renton M, Walker C, Moot D, Ryan MH. 2017b. Fine root endophytes under scrutiny: a review of the literature on arbuscule-producing fungi recently suggested to belong to the Mucoromycotina. *Mycorrhiza* **27**: 619–638.

Ott T, Van Dongen JT, Günther C, Krusell L, Desbrosses G, Vigeolas H, Bock V, Czechowski T, Geigenberger P, Udvardi MK. 2005. Symbiotic leghemoglobins are crucial for nitrogen fixation in legume root nodules but not for general plant growth and development. *Curr Biol* **15**: 531–535.

Parniske M. 2008. Arbuscular mycorrhiza: the mother of plant root endosymbioses. *Nat Rev Microbiol* **6**: 763–775.

Paszkowski U. 2006. Mutualism and parasitism: the yin and yang of plant symbioses. *Curr Opin Plant Biol* **9**: 364–370.

Paungfoo-Lonhienne C, Lonhienne TGA, Yeoh YK, Webb RI, Lakshmanan P, Chan CX, Lim PE, Ragan MA, Schmidt S, Hugenholtz P. 2014. A new species of *Burkholderia* isolated from sugarcane roots promotes plant growth. *Microb Biotechnol* **7**: 142–154.

Paynel F, Murray PJ, Cliquet JB. 2001. Root exudates: a pathway for short-term N transfer from clover and ryegrass. *Plant Soil* **229**: 235–243.

Peay KG, Kennedy PG, Davies SJ, Tan S, Bruns TD. 2010. Potential link between plant and fungal distributions in a dipterocarp rainforest: community and phylogenetic structure of tropical ectomycorrhizal fungi across a plant and soil ecotone. *New Phytol* **185**: 529–542.

Peoples MB, Herridge DF, Ladha JK. 1995. Biological nitrogen fixation: an efficient source of nitrogen for sustainable agricultural production? *Plant Soil* **174**: 3–28.

Peoples MB, Palmer B, Lilley DM, Duc LM, Herridge DF. 1996. Application of ^{15}N and xylem ureide methods for assessing N_2 fixation of three shrub legumes periodically pruned for forage. *Plant Soil* **182**: 125–137.

Pereg L, de-Bashan LE, Bashan Y. 2016. Assessment of affinity and specificity of *Azospirillum* for plants. *Plant Soil* **399**: 389–414.

Peterson R, Bonfante P. 1994. Comparative structure of vesicular-arbuscular mycorrhizas and ectomycorrhizas. *Plant Soil* **159**: 79–88.

Pfeffer PE, Douds DD, Bécard G, Shachar-Hill Y. 1999. Carbon uptake and the metabolism and transport of lipids in an arbuscular mycorrhiza. *Plant Physiol* **120**: 587–598.

Plamboeck AH, Dawson TE, Egerton-Warburton LM, North M, Bruns TD, Querejeta JI. 2007. Water transfer via ectomycorrhizal fungal hyphae to conifer seedlings. *Mycorrhiza* **17**: 439–447.

Podlešáková K, Fardoux J, Patrel D, Bonaldi K, Novák O, Strnad M, Giraud E, Spíchal L, Nouwen N. 2013. Rhizobial synthesized cytokinins contribute to but are not essential for the symbiotic interaction between photosynthetic *Bradyrhizobia* and *Aeschynomene* legumes. *Mol Plant-Microbe Interact* **26**: 1232–1238.

Pozo MJ, Cordier C, Dumas-Gaudot E, Gianinazzi S, Barea JM, Azcón-Aguilar C. 2002. Localized versus systemic effect of arbuscular mycorrhizal fungi on defence responses to *Phytophthora* infection in tomato plants. *J Exp Bot* **53**: 525–534.

Radutoiu S, Madsen LH, Madsen EB, Felle HH, Umehara Y, Gronlund M, Sato S, Nakamura Y, Tabata S, Sandal N, Stougaard J. 2003. Plant recognition of symbiotic bacteria requires two LysM receptor-like kinases. *Nature* **425**: 585–592.

Rangel de Souza ALS, De Souza SA, De Oliveira MVV, Ferraz TM, Figueiredo FAMMA, Da Silva ND, Rangel PL, Panisset CRS, Olivares FL, Campostrini E, De Souza Filho GA. 2016. Endophytic colonization of *Arabidopsis thaliana* by *Gluconacetobacter diazotrophicus* and its effect on plant growth promotion, plant physiology, and activation of plant defense. *Plant Soil* **399**: 257–270.

Rausch C, Daram P, Brunner S, Jansa J, Laloi M. 2001. A phosphate transporter expressed in arbuscule-containing cells in potato. *Nature* **414**: 462–466.

Raven JA. 2012. Protein turnover and plant RNA and phosphorus requirements in relation to nitrogen fixation. *Plant Sci* **188–189**: 25–35.

Raven JA, Lambers H, Smith SE, Westoby M. 2018. Costs of acquiring phosphorus by vascular land plants: patterns and implications for plant coexistence. *New Phytol* **217**: 1420–1427.

Read DJ. 1996. The structure and function of the ericoid mycorrhizal root. *Ann Bot* **77**: 365–374.

Read DJ, Perez-Moreno J. 2003. Mycorrhizas and nutrient cycling in ecosystems - a journey towards relevance? *New Phytol* **157**: 475–492.

Reddell P, Yun Y, Shipton WA. 1997. Do *Casuarina cunninghamiana* seedlings dependent on symbiotic N_2 fixation have higher phosphorus requirements than those supplied with adequate fertilizer nitrogen? *Plant Soil* **189**: 213–219.

Reed S, Cleveland C, Townsend A. 2013. Relationships among phosphorus, molybdenum and free-living nitrogen fixation in tropical rain forests: results from

observational and experimental analyses. *Biogeochemistry* **114**: 135–147.

Reid DE, Ferguson BJ, Gresshoff PM. 2011a. Inoculation- and nitrate-induced CLE peptides of soybean control NARK-dependent nodule formation. *Mol Plant-Microbe Interact* **24**: 606–618.

Reid DE, Ferguson BJ, Hayashi S, Lin Y-H, Gresshoff PM. 2011b. Molecular mechanisms controlling legume autoregulation of nodulation. *Ann Bot* **108**: 789–795.

Reinhart KO, Callaway RM. 2006. Soil biota and invasive plants. *New Phytol* **170**: 445–457.

Reis VM, dos Santos Teixeira KR. 2015. Nitrogen fixing bacteria in the family Acetobacteraceae and their role in agriculture. *J Bas Microbiol* **55**: 931–949.

Requena N, Breuninger M, Franken P, Ocón A. 2003. Symbiotic status, phosphate, and sucrose regulate the expression of two plasma membrane H^+-ATPase genes from the mycorrhizal fungus *Glomus mosseae*. *Plant Physiol* **132**: 1540–1549.

Richardson AE, Djordjevic MA, Rolfe BG, Simpson RJ. 1988. Effects of pH, Ca and Al on the exudation from clover seedlings of compounds that induce the expression of nodulation genes in *Rhizobium trifolii*. *Plant Soil* **109**: 37–47.

Roth R, Paszkowski U. 2017. Plant carbon nourishment of arbuscular mycorrhizal fungi. *Curr Opin Plant Biol* **39**: 50–56.

Rousk K, Jones D, DeLuca T. 2013. The resilience of nitrogen fixation in feather moss (*Pleurozium schreberi*)-cyanobacteria associations after a drying and rewetting cycle. *Plant Soil* **377**: 159–167.

Rousk K, Jones D, DeLuca T. 2014. Exposure to nitrogen does not eliminate N_2 fixation in the feather moss *Pleurozium schreberi* (Brid.) Mitt. *Plant Soil* **374**: 513–521.

Rousseau JV, .D., Reid CP, .P. 1991. Effects of phosphorus fertilization and mycorrhizal development on phosphorus nutrition and carbon balance of loblolly pine. *New Phytol* **117**: 319–326.

Rubio LM, Ludden PW. 2008. Biosynthesis of the iron-molybdenum cofactor of nitrogenase. *Annu Rev Microbiol* **62**: 93–111.

Sanders IR, Koide RT. 1994. Nutrient acquisition and community structure in co-occurring mycotrophic and non-mycotrophic oldfield annuals. *Funct Ecol* **8**: 77–84.

Sandral GA, Haling RE, Ryan MH, Price A, Pitt WM, Hildebrand SM, Fuller CG, Kidd DR, Stefanksi A, Lambers H, Simpson RJ. 2018. Intrinsic capacity for nutrient foraging predicts critical external phosphorus requirement of 12 pasture legumes. *Crop Past Sci* **69**: 174–182.

Scervino JM, Ponce MA, Erra-Bassells R, Vierheilig H, Ocampo JA, Godeas A. 2005. Flavonoids exclusively present in mycorrhizal roots of white clover exhibit a different effect on arbuscular mycorrhizal fungi than flavonoids exclusively present in non-mycorrhizal roots of white clover. *J Plant Interact* **1**: 15–22.

Schipanski ME, Drinkwater LE, Russelle MP. 2010. Understanding the variability in soybean nitrogen fixation across agroecosystems. *Plant Soil* **329**: 379–397.

Schmitz AM, Harrison MJ. 2014. Signaling events during initiation of arbuscular mycorrhizal symbiosis. *J Integr Plant Biol* **56**: 250–261.

Schreiner RP, Koide RT. 1992. Antifungal compounds from the roots of mycotrophic and non-mycotrophic plant species. *New Phytol* **123**: 99–105.

Selosse M-A, Richard F, He X, Simard SW. 2006. Mycorrhizal networks: *des liaisons dangereuses*? *Trends Ecol Evol* **21**: 621–628.

Selosse M-A, Strullu-Derrien C, Martin FM, Kamoun S, Kenrick P. 2015. Plants, fungi and oomycetes: a 400-million year affair that shapes the biosphere. *New Phytol* **206**: 501–506.

Sheldrake M, Rosenstock NP, Revillini D, Olsson PA, Wright SJ, Turner BL. 2017. A phosphorus threshold for mycoheterotrophic plants in tropical forests. *Proc R Soc B Biol Sci* **284**: 20162093.

Sikes BA, Cottenie K, Klironomos JN. 2009. Plant and fungal identity determines pathogen protection of plant roots by arbuscular mycorrhizas. *J Ecol* **97**: 1274–1280.

Smith SE, Anderson IC, Smith FA 2015. Mycorrhizal associations and P acquisition: from cells to ecosystems In: Plaxton WC, Lambers H eds. *Annual Plant Reviews, Volume 48, Phosphorus Metabolism in Plants*. Chicester: John Wiley & Sons, 409–440.

Smith SE, Gianinazzi-Pearson V. 1988. Physiological interactions between symbionts in vesicular-arbuscular mycorrhizal plants. *Annu Rev Plant Physiol Plant Mol Biol* **39**: 221–244.

Smith SE, Read DJ. 2008. *Mycorrhizal Symbiosis*. London: Academic Press and Elsevier.

Smith SE, Smith FA, Jakobsen I. 2003. Mycorrhizal fungi can dominate phosphate supply to plants irrespective of growth responses. *Plant Physiol* **133**: 16–20.

Smith SE, Smith FA, Jakobsen I. 2004. Functional diversity in arbuscular mycorrhizal (AM) symbioses: the contribution of the mycorrhizal P uptake pathway is not correlated with mycorrhizal responses in growth or total P uptake. *New Phytol* **162**: 511–524.

Snellgrove RC, Splittstoesser WE, Stribley DP, Tinker PB. 2006. The distribution of carbon and the demand of the fungal symbiont in leek plants with vesicular arbuscular mycorrhizas. *New Phytol* **92**: 75–87.

Soltis DE, Soltis PS, Morgan DR, Swensen SM, Mullin BC, Dowd JM, Martin PG. 1995. Chloroplast gene sequence data suggest a single origin of the predisposition for symbiotic nitrogen fixation in angiosperms. *Proc Natl Acad Sci USA* **92**: 2647–2651.

Sosa-Rodriguez T, Declerck S, Granet F, Gaurel S, Damme EM, Dupré de Boulois H. 2013. *Hevea brasiliensis* and *Urtica dioica* impact the in vitro mycorrhization of neighbouring *Medicago truncatula* seedlings. *Symbiosis* **60**: 123–132.

Soudzilovskaia NA, Douma JC, Akhmetzhanova AA, van Bodegom PM, Cornwell WK, Moens EJ, Treseder KK, Tibbett M, Wang Y-P, Cornelissen JHC. 2015. Global patterns of plant root colonization intensity by mycorrhizal fungi explained by climate and soil chemistry. *Glob Ecol Biogeogr* **24**: 371–382.

Soudzilovskaia NA, Vaessen S, van't Zelfde M, Raes N 2017. Global patterns of mycorrhizal distribution and their environmental drivers. In: Tedersoo L ed. *Biogeography of Mycorrhizal Symbiosis*. Cham: Springer International Publishing, 223–235.

Sprent JI. 1999. Nitrogen fixation and growth of non-crop legume species in diverse environments. *Perspect Plant Ecol Evol Syst* **2**: 149–162.

Sprent JI. 2007. Evolving ideas of legume evolution and diversity: A taxonomic perspective on the occurrence of nodulation. *New Phytol* **174**: 11–25.

Sprent JI, Ardley JK, James EK. 2013. From North to South: a latitudinal look at legume nodulation processes. *S Afric J Bot* **89**: 31–41.

Sprent JI, Geoghegan IE, Whitty PW, James EK. 1996. Natural abundance of ^{15}N and ^{13}C in nodulated legumes and other plants in the cerrado and neighbouring regions of Brazil. *Oecologia* **105**: 440–446.

Sturz AV, Christie BR, Nowak J. 2000. Bacterial endophytes: potential role in developing sustainable systems of crop production. *Crit Rev Plant Sci* **19**: 1–30.

Sulieman S, Tran L-SP. 2013. Asparagine: an amide of particular distinction in the regulation of symbiotic nitrogen fixation of legumes. *Crit Rev Biotechnol* **33**: 309–327.

Tanaka Y, Yano K. 2005. Nitrogen delivery to maize via mycorrhizal hyphae depends on the form of N supplied. *Plant Cell Environ* **28**: 1247–1254.

Tani C, Ohtomo R, Osaki M, Kuga Y, Ezawa T. 2009. Polyphosphate-synthesizing activity in extraradical hyphae of an arbuscular mycorrhizal fungus: ATP-dependent but proton gradient-independent synthesis. *Applied and Environmental Microbiology* **75**: 7044–7050.

Tedersoo L, Laanisto L, Rahimlou S, Toussaint A, Hallikma T, Pärtel M. 2018. Global database of plants with root-symbiotic nitrogen fixation: NodDB. *J Veg Sci* **29**: 560–568.

Temperton VM, Mwangi PN, Scherer-Lorenzen M, Schmid B, Buchmann N. 2007. Positive interactions between nitrogen-fixing legumes and four different neighbouring species in a biodiversity experiment. *Oecologia* **151**: 190–205.

Teste FP, Laliberté E, Lambers H, Auer Y, Kramer S, Kandeler E. 2016. Mycorrhizal fungal biomass and scavenging declines in phosphorus-impoverished soils during ecosystem retrogression. *Soil Biol Biochem* **92**: 119–132.

Thingstrup I, Rubaek G, Sibbesen E, Jakobsen I. 1998. Flax (*Linum usitatissimum* L.) depends on arbuscular mycorrhizal fungi for growth and P uptake at intermediate but not high soil P levels in the field. *Plant Soil* **203**: 37–46.

Tian P, Le TN, James A, Inch C, Piercy J, Guthridge KM, Forster JW, Spangenberg GC. 2016. Assessment of germination and endophyte viability in perennial ryegrass and tall fescue seeds following accelerated ageing treatment. *Seed Sci Technol* **44**: 531–541.

Tsikou D, Yan Z, Holt DB, Abel NB, Reid DE, Madsen LH, Bhasin H, Sexauer M, Stougaard J, Markmann K. 2018. Systemic control of legume susceptibility to rhizobial infection by a mobile microRNA. *Science* **362**: 233–236.

Udvardi M, Poole PS. 2013. Transport and metabolism in legume-rhizobia symbioses. *Annu Rev Plant Biol* **64**: 781–805.

Unkovich M. 2013. Isotope discrimination provides new insight into biological nitrogen fixation. *New Phytol* **198**: 643–646.

Unkovich M, Herridge D, Peoples M, Cadisch G, Boddey B, Giller K, Alves B, Chalk P. 2008. *Measuring plant-associated nitrogen fixation in agricultural systems*. Canberra: Australian Centre for International Agricultural Research.

Van Der Heijden MGA, Horton TR. 2009. Socialism in soil? The importance of mycorrhizal fungal networks for facilitation in natural ecosystems. *J Ecol* **97**: 1139–1150.

van der Heijden MGA, Martin FM, Selosse M-A, Sanders IR. 2015. Mycorrhizal ecology and evolution: the past, the present, and the future. *New Phytol* **205**: 1406–1423.

Van Deynze A, Zamora P, Delaux P-M, Heitmann C, Jayaraman D, Rajasekar S, Graham D, Maeda J, Gibson D, Schwartz KD, Berry AM, Bhatnagar S, Jospin G, Darling A, Jeannotte R, Lopez J, Weimer BC, Eisen JA, Shapiro H-Y, Ané J-M, Bennett AB. 2018. Nitrogen fixation in a landrace of maize is supported by a mucilage-associated diazotrophic microbiota. *PLoS Biol* **16**: e2006352.

Van Groenigen K-J, Six J, Hungate BA, De Graaff M-A, Van Breemen N, Van Kessel C. 2006. Element interactions limit soil carbon storage. *Proc Natl Acad Sci USA* **103**: 6571–6574.

Van Hees PAW, Rosling A, Essen S, Godbold DL, Jones DL, Finlay RD. 2006. Oxalate and ferricrocin exudation by the extramatrical mycelium of an ectomycorrhizal fungus in symbiosis with *Pinus sylvestris*. *New Phytol* **169**: 367–378.

Van Velzen R, Doyle JJ, Geurts R. 2019. A resurrected scenario: single gain and massive loss of nitrogen-fixing symbioses. *Trends Plant Sci* **24**: 49–57.

Vance CP 2002. Root-bacteria interactions. Symbiotic nitrogen fixation. In: Waisel Y, Eshel A, Kafkaki U eds. *Plant Roots: The Hidden Half, 3rd edition*. New York: Marcel Dekker, 839–868.

Veiga RSL, Faccio A, Genre A, Pieterse CMJ, Bonfante P, van der Heijden MGA. 2013. Arbuscular mycorrhizal fungi reduce growth and infect

roots of the non-host plant *Arabidopsis thaliana*. *Plant Cell Environ* **36**: 1926–1937.

Vessey J, Pawlowski K, Bergman B. 2005. Root-based N_2-fixing symbioses: legumes, actinorhizal plants, *Parasponia* sp. and cycads. *Plant Soil* **266**: 205–230.

Vierheilig H, Garcia-Garrido JM, Wyss U, Piché Y. 2000. Systemic suppression of mycorrhizal colonization of barley roots already colonized by AM fungi. *Soil Biol Biochem* **32**: 589–595.

Vierheilig H, Iseli B, Alt M, Raikhel N, Wiemken A, Boller T. 1996. Resistance of *Urtica dioica* to mycorrhizal colonization: a possible involvement of *Urtica dioica* agglutinin. *Plant Soil* **183**: 131–136.

Vieweg MF, Fruhling M, Quandt HJ, Heim U, Baumlein H. 2004. The promoter of the *Vicia faba* L. leghemoglobin gene *VfLb29* is specifically activated in the infected cells of root nodules and in the arbuscule-containing cells of mycorrhizal roots from different legume and nonlegume plants. *Mol Plant-Microbe Interact* **17**: 62–69.

Vos C, Schouteden N, van Tuinen D, Chatagnier O, Elsen A, De Waele D, Panis B, Gianinazzi-Pearson V. 2013. Mycorrhiza-induced resistance against the root–knot nematode Meloidogyne incognita involves priming of defense gene responses in tomato. *Soil Biol Biochem* **60**: 45–54.

Walder F, Boller T, Wiemken A, Courty P-E. 2016. Regulation of plants' phosphate uptake in common mycorrhizal networks: role of intraradical fungal phosphate transporters. *Plant Signal Behav* **11**: e1131372.

Walder F, Niemann H, Natarajan M, Lehmann MF, Boller T, Wiemken A. 2012. Mycorrhizal networks: common goods of plants shared under unequal terms of trade. *Plant Physiol* **159**: 789–797.

Walker C, Gollotte A, Redecker D. 2018. A new genus, *Planticonsortium* (*Mucoromycotina*), and new combination (*P. tenue*), for the fine root endophyte, *Glomus tenue* (basionym *Rhizophagus tenuis*). *Mycorrhiza* **28**: 213–219.

Walker R, Agapakis CM, Watkin E, Hirsch AM 2015. Symbiotic nitrogen fixation in legumes: perspectives on the diversity and evolution of nodulation by *Rhizobium* and *Burkholderia* species. In: De Bruin FJ ed. *Biological Nitrogen Fixation*: John Wiley & Sons, Inc, 913–923.

Wang B, Qiu Y-L. 2006. Phylogenetic distribution and evolution of mycorrhizas in land plants. *Mycorrhiza* **16**: 299–363.

Wang B, Yeun LH, Xue J-Y, Liu Y, Ané J-M, Qiu Y-L. 2010. Presence of three mycorrhizal genes in the common ancestor of land plants suggests a key role of mycorrhizas in the colonization of land by plants. *New Phytol* **186**: 514–525.

Wang W, Shi J, Xie Q, Jiang Y, Yu N, Wang E. 2017. Nutrient exchange and regulation in arbuscular mycorrhizal symbiosis. *Mol Plant* **10**: 1147–1158.

Waterman RJ, Bidartondo MI. 2008. Deception above, deception below: linking pollination and mycorrhizal biology of orchids. *J Exp Bot* **59**: 1085–1096.

Wehner J, Antunes PM, Powell JR, Mazukatow J, Rillig MC. 2010. Plant pathogen protection by arbuscular mycorrhizas: a role for fungal diversity? *Pedobiologia* **53**: 197–201.

Wei H, Layzell DB. 2006. Adenylate-coupled ion movement. A mechanism for the control of nodule permeability to O_2 diffusion. *Plant Physiol* **141**: 280–287.

Wen Z, Li H, Shen Q, Tang X, Xiong C, Li H, Pang J, Ryan M, Lambers H, Shen J. 2019. Trade-offs among root morphology, exudation and mycorrhizal symbioses for phosphorus-acquisition strategies of 16 crop species. *New Phytol* **in press**.

Weston LA, Mathesius U. 2013. Flavonoids: their structure, biosynthesis and role in the rhizosphere, including allelopathy. *J Chem Ecol* **39**: 283–297.

White J, Prell J, James EK, Poole P. 2007. Nutrient sharing between symbionts. *Plant Physiol* **144**: 604–614.

Wright DP, Scholes JD, Read DJ. 2002. Effects of VA mycorrhizal colonization on photosynthesis and biomass production of *Trifolium repens* L. *Plant Cell Environ* **21**: 209–216.

Wright DP, Scholes JD, Read DJ, Rolfe SA. 2005. European and African maize cultivars differ in their physiological and molecular responses to mycorrhizal infection. *New Phytol* **167**: 881–896.

Xie X, Yoneyama K, Yoneyama K. 2010. The strigolactone story. *Annu Rev Phytopathol* **48**: 93–117.

Yang H, Zhang Q, Dai Y, Liu Q, Tang J, Bian X, Chen X. 2015. Effects of arbuscular mycorrhizal fungi on plant growth depend on root system: a meta-analysis. *Plant Soil* **389**: 361–374.

Yang S-Y, Grønlund M, Jakobsen I, Grotemeyer MS, Rentsch D, Miyao A, Hirochika H, Kumar CS, Sundaresan V, Salamin N, Catausan S, Mattes N, Heuer S, Paszkowski U. 2012. Nonredundant regulation of rice arbuscular mycorrhizal symbiosis by two members of the *PHOSPHATE TRANSPORTER1* gene family. *Plant Cell* **24**: 4236–4251.

Yao Q, Li X, Feng G, Christie P. 2001. Mobilization of sparingly soluble inorganic phosphates by the external mycelium of an abuscular mycorrhizal fungus. *Plant Soil* **230**: 279–285.

Yoneyama K, Xie X, Kusumoto D, Sekimoto H, Sugimoto Y, Takeuchi Y, Yoneyama K. 2007. Nitrogen deficiency as well as phosphorus deficiency in sorghum promotes the production and exudation of 5-deoxystrigol, the host recognition signal for arbuscular mycorrhizal fungi and root parasites. *Planta* **227**: 125–132.

Yoneyama K, Xie, X, Sekimoto, H, Takeuchi, Y, Ogasawara, S, Akiyama, K, Hayashi, H, Yoneyama, K. 2008. Strigolactones, host recognition signals for root parasitic plants and arbuscular mycorrhizal fungi, from Fabaceae plants. *New Phytol* **179**: 484–494.

Yu H, Bao H, Zhang Z, Cao Y. 2019. Immune signaling pathway during terminal bacteroid differentiation in nodules. *Trends Plant Sci* **24**: 299–302.

Zemunik G, Lambers H, Turner BL, Laliberté E, Oliveira RS. 2018. High abundance of non-mycorrhizal plant species in severely phosphorus-impoverished Brazilian campos rupestres. *Plant Soil* **424**: 255–271.

Zemunik G, Turner BL, Lambers H, Laliberté E. 2015. Diversity of plant nutrient-acquisition strategies increases during long-term ecosystem development. *Nat Plants* **1**: https://doi.org/10.1038/nplants.2015.1050.

Zhang L, Xu M, Liu Y, Zhang F, Hodge A, Feng G. 2016. Carbon and phosphorus exchange may enable cooperation between an arbuscular mycorrhizal fungus and a phosphate-solubilizing bacterium. *New Phytol* **210**: 1022–1032.

Zhang W, Card SD, Mace WJ, Christensen MJ, McGill CR, Matthew C. 2017. Defining the pathways of symbiotic *Epichloë* colonization in grass embryos with confocal microscopy. *Mycologia* **109**: 153–161.

Zipfel C, Oldroyd GED. 2017. Plant signalling in symbiosis and immunity. *Nature* **543**: 328–336.

13 Biotic Influences: Ecological Biochemistry: Allelopathy and Defense Against Herbivores

13.1 Introduction

Plants contain a vast array of compounds referred to as **secondary metabolites** that play no role in primary catabolic or biosynthetic pathways. Many of these metabolites influence important ecological interactions (*e.g.*, deterring herbivores, protection against pathogens, allelopathy, symbiotic associations, seed germination of parasites, or interactions with pollinators). Others provide protection against ultraviolet radiation or high temperatures. We have already discussed some of these roles. In this chapter, we discuss the role of secondary compounds in allelopathic and plant-herbivore interactions. As an example of the metabolic versatility of plants, their responses to xenobiotics will be discussed in the context of phytoremediation. Plant-pathogen interactions are discussed in Chap. 14.

13.2 Allelopathy (Interference Competition)

Some plants harm the growth or development of surrounding plants by the release of chemical compounds: **allelopathic compounds** or **allelochemicals**. These **allelopathic** effects are invariably negative, and the compounds may come from living roots or leaves or from decomposing plant remains (Fig. 13.1). Other released compounds may have positive effects, such as the carboxylates that solubilize phosphate in the rhizosphere or chelate toxic metals and avoid their toxicity (Sects. 9.2.2.5 and 9.3.1.2). These positive effects are *not* referred to as **interference competition** or **allelopathy** [the word allelopathy is derived from two Greek words: *allelon* (of each other) and *pathos* (to suffer)]. The chemicals involved in positive interactions, however, may still be referred to as allelochemicals.

Many allegedly allelopathic interactions can be explained in other ways. For example, the absence of seedlings near aromatic shrubs that produce volatile growth inhibitors suggested that allelopathy might be involved (Muller et al. 1964), but closer investigation showed that seed-eating animals prefer to graze in the shelter of the shrub, where they are in less danger from predatory birds (Bartholomew 1970). There is general agreement in the literature, however, that allelopathic interactions do exist and can be ecologically important. Both water-soluble compounds and volatiles can have allelopathic effects (Birkett et al. 2001; Bais et al. 2006; Weston and Mathesius 2013).

Activated carbon, which adsorbs allelochemicals, has been used to assess the significance of allelopathic interactions in natural ecosystems, for example to study the allelopathic potential of an **invasive weed**, *Centaurea maculosa* (spotted knapweed) in western North America (Ridenour and Callaway 2001). Root elongation and biomass production of *Festuca idahoensis* (Idaho fescue) plants that grow

H. Lambers, R. S. Oliveira, *Plant Physiological Ecology*, https://doi.org/10.1007/978-3-030-29639-1_13

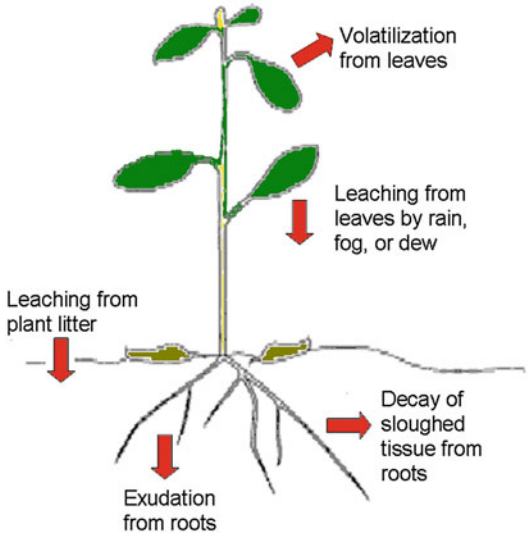

Fig. 13.1 Routes of entry of allelochemicals from plants into the rhizosphere and atmosphere.

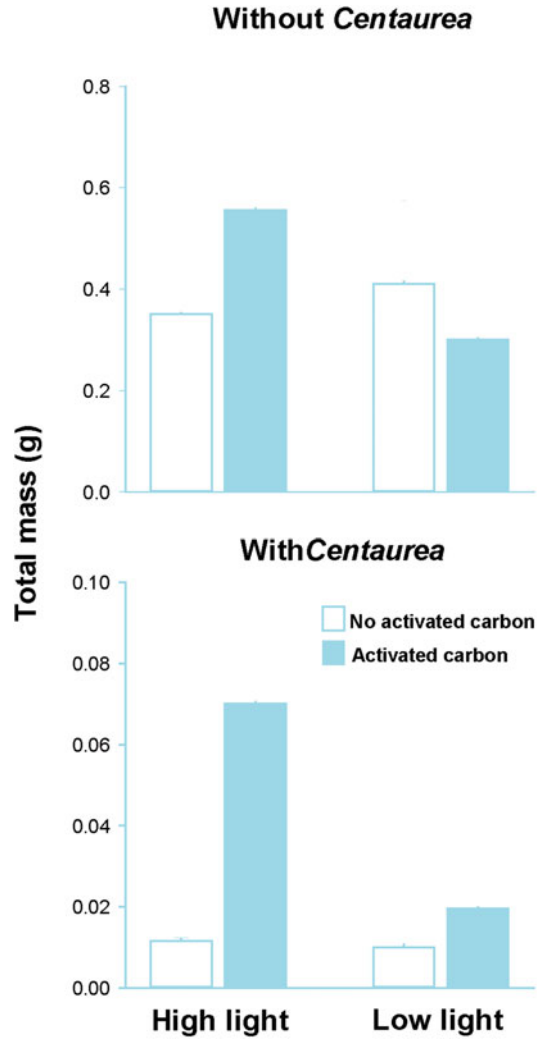

Fig. 13.2 (**A**) The total mass of *Koeleria macrantha* (prairie Junegrass or crested hair-grass) when grown alone at high and low light intensity and with and without activated carbon in the soil. (**B**) The total mass of *Koeleria macrantha* when grown with *Centaurea stoebe* (spotted knapweed) at high and low light intensity and with and without activated carbon in the soil (Chen et al. 2012); rights managed by Taylor & Francis.

together with this invasive weed is enhanced in the presence of activated carbon in the root environment. Using activated carbon, it can be shown that allelopathy accounts for a substantial proportion of the total interference of *Centaurea maculosa* on *Festuca idahoensis*, shifting the balance of competition in favor of the invasive weed. However, *Centaurea maculosa* outperforms *Festuca idahoensis* even in the absence of activated carbon, which shows the combined roles of **resource competition** and allelopathy. Allelopathic effects may depend on other environmental conditions such as **light intensity**. *Centaurea stoebe* (spotted knapweed), an exotic invasive forb in North America, has an allelopathic effect on *Koeleria macrantha* (prairie Junegrass or crested hair-grass), a North American native bunchgrass (Chen et al. 2012). The biomass of *Koeleria macrantha* is the same in low- and high-light treatments when grown alone and is strongly suppressed by *Centaurea stoebe* in both low- and high-light conditions (Fig. 13.2). Activated carbon treatments at high light intensity results in a major increase in the growth of *Koeleria macrantha*, but has a much weaker positive effects in low light. Activated carbon had no effect in the absence of the invasive species. Activated carbon is obviously a great tool to learn more about allelopathic effects, but there may be side effects to be aware of (Lau et al. 2008; Wurst et al. 2010).

Benzoxazinoids (cyclic hydroxamic acids) are common allelochemicals in root exudates from *Triticum aestivum* (wheat), *Zea mays* (corn), and *Secale cereale* (rye) (Understrup et al. 2005). In soil, the exudates may be converted into other

benzoxazinoids, many with a similar phytotoxic effect (Macías et al. 2005). Benzoxazinoids in corn root exudates act as an attractant for a beneficial rhizosphere microorganism, *Pseudomonas putida* strain (Neal et al. 2012). Breeding of rye with high benzoxazinoid contents may allow the use of allelopathic rye varieties in organic cropping systems for weed control (Schulz et al. 2013).

Allelopathic compounds may have originally evolved as compounds that enhance nutrient acquisition (Nishanth et al. 2009) or deter pathogens (Chap. 14) or herbivores (Sect. 13.3) and subsequently have become involved in interactions between higher plants. Secretory glands were well developed in the early gymnosperms and angiosperms of the Paleozoic before there were terrestrial herbivores, but after the evolution of terrestrial fungi which suggests that early defense systems may have been directed at pathogens (Chap. 14; Bais et al. 2004).

The mode of action of many allelopathic compounds is unknown. Gallic acid is one of several allelochemicals that enhances the production of toxic **reactive oxygen species** (**ROS**) in sensitive plants (Gniazdowska et al. 2015). Resistant species such as *Lupinus sericeus* (silky lupine) and *Gaillardia grandiflora* (blanket flower) release increased amounts of **oxalate** in response to catechin exposure. Oxalate blocks generation of reactive oxygen species, reducing oxidative damage generated in response to catechin (Weir et al. 2006). Volatile terpenoids can inhibit respiration (Gniazdowska et al. 2015).

The allelopathic effects of *Juglans nigra* (black walnut) illustrate the ecological and economic effects. In a zone up to 27 m from the tree trunk, many plants [*e.g.*, *Solanum lycopersicum* (tomato), *Medicago sativa* (alfalfa)] die. The toxic effects are due to the leaching from the leaves, stems, branches, and roots of a bound phenolic compound, which undergoes hydrolysis and oxidation in the soil. The bound compound, which is nontoxic itself, is the 4-glucoside of 1,4,5-trihydroxy-naphthalene. It is converted to the toxic compound juglone (5-hydroxynaphtoquinone). Some species are resistant to juglone [*e.g.*, *Poa pratensis* (Kentucky bluegrass)], probably because they detoxify this allelochemical (Sect. 13.5). Juglone severely inhibits the relative growth rate, photosynthesis, stomatal conductance, and respiration of *Zea mays* (corn) and *Glycine max* (soybean), when applied at a concentration of 10 μM or more. This concentration can be found in soil under black walnut when it is used in alley cropping (Jose and Gillespie 1998a, 1998b).

Sorghum species have a reputation for suppressing weed growth, due to the exudation of allelochemicals. One of these is a dihydroxyquinone (sorgoleone), which inhibits mitochondrial respiration (Rasmussen et al. 1992) and electron transport in photosystem II (Nimbal et al. 1996), presumably due to the structural similarity between sorgoleone and both ubiquinone and plastoquinone (Sect. 15.2.1). Similarly, very few weeds occur under trees of *Leucaena leucocephala* (white leadtree) plantations in Taiwan. This has been ascribed to the presence of high concentrations of mimosine (a toxic nonproteinogenic amino acid) as well as a range of phenolic compounds, which originate from the tree leaves and inhibit germination and growth of many forest species (Table 13.1). Allelopathic interactions also appear to play a major role in desert plants [*e.g.*, between *Encelia farinosa*

Table 13.1 The effects of *Leucaena leucocephala* (white leadtree) leaves mixed with 150 g of soil or mulched and spread on the soil surface on survival of seedlings of a number of plant species.*

	Survival (% of control)		
	Leaves mixed with soil		Leaf mulch added
Species	1 g	2 g	5 g
Leucaena leucocephala	100	100	87
Alnus formosana	72	44	37
Acacia confusa	30	19	14
Liquidamber formosana	5	9	31
Casuarina glauca	0	0	0
Mimosa pudica	0	0	0

Source: Chou and Kuo (1986)

*The data are expressed as percent survival relative to that in the soil alone

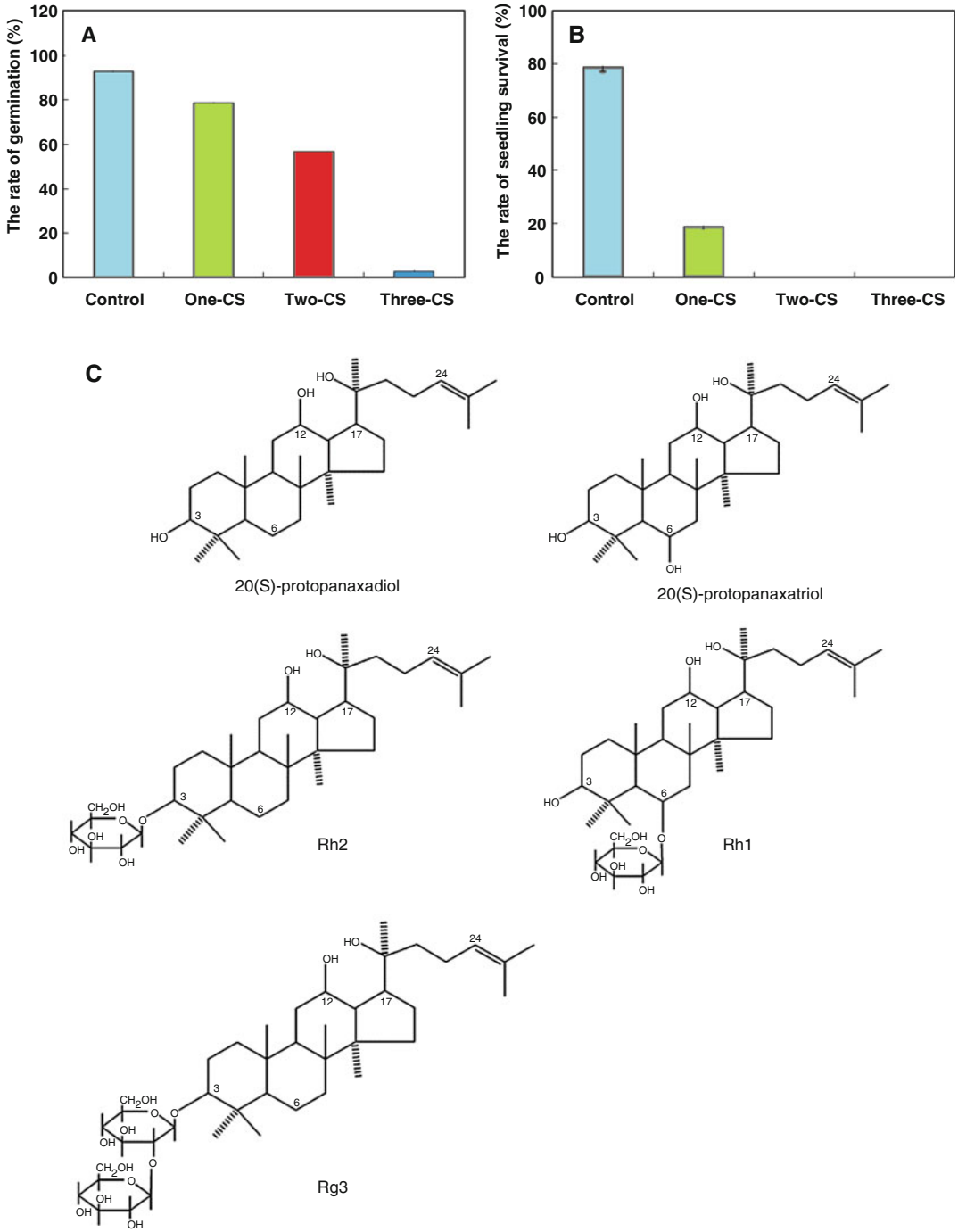

Fig. 13.3 (**A**) Seedling germination rate and (**B**) seedling survival rate in continuously cultivated soil and uncultivated soil. Control represents the uncultivated soil, and One-CS, Two-CS, and Three-CS represent one, two, and three years of continuously cultivated soil. (Yang et al. 2015). (**C**) Structures of some ginsenosides (Popovich and Kitts 2002).

(brittlebush) and its surrounding plants in the Mojave desert in California, USA]. In many of these plants, a simple benzene derivative is produced, primarily in the leaves (Fig. 13.3). It is released when the leaves fall to the ground and decompose.

An example of growth inhibition by a toxin produced in roots is that of ginsenosides released

by *Panax notoginseng* (Sanqi ginseng) (Yang et al. 2015). Ginsenosides inhibit the growth of plants of the same species that produce them (**autotoxicity**). They contribute to 'soil sickness'; that is, a reduction in yield when crops are grown on the same plot without rotation. Autotoxicity results in replant failure of Sanqi ginseng, because some ginsenosides can accumulate in the rhizosphere soil through root exudates or root decomposition, which impedes seedling emergence and growth (Fig. 13.3). Similar examples of autotoxicity have been found for cultivars of *Triticum aestivum* (wheat) in bioassays under laboratory conditions; this suggest that cultivars may have to be selected carefully if wheat is to be used in a continuous cropping system (Wu et al. 2007). In several cucurbit crops [*e.g.*, *Citrullus lanatus* (watermelon), *Cucumis melo* (melon), and *Cucumis sativus* (cucumber)], autotoxicity also contributes to soil sickness (Yu et al. 2000). Cinnamic acid is one of the autotoxic compounds in cucumber; it induces formation of **ROS** (Ding et al. 2007). Autotoxicity can also play a role in **negative plant-soil feedback**. That is plants change the soil they grow in in a manner that inhibits the growth of their offspring. This has been demonstrated in glasshouse studies with *Senecio vulgaris* (groundsel) (Van de Voorde et al. 2012).

Allelopathic and autotoxic effects probably play a role in many environments; however, it is hard to estimate their ecological significance. Some of the released compounds are probably decomposed rather rapidly by microorganisms, thus diminishing their potential effects (Weidenhamer et al. 2013). Other allelopathic compounds decompose rather slowly, including a group of phenolic compounds mostly referred to as tannins (Sect. 13.3.1). We discussed the consequences of this slow decomposition for nutrient cycling in Chap. 18.

Allelochemicals may also affect soil microorganisms, and thus indirectly affect surrounding plants. For example, monoterpenes from *Picea abies* (Norway spruce) inhibit **nitrification**, either directly or indirectly due to immobilization of mineral nitrogen (N) (Sect. 9.2.1.1) (Paavolainen et al. 1998). Allelochemicals released from grass roots may also inhibit **nitrification** (Lata et al. 2004; Subbarao et al. 2006). Since NO_3^- is far more prone to losses by denitrification and leaching, the biological nitrification inhibitors may enhance the efficiency of N use at the ecosystem level, both in natural and in managed systems. This is why their potential is currently being explored in crop species (Subbarao et al. 2017).

Exudates released by some plants, *e.g.*, *Eragrostis curvula* (weeping lovegrass) are antagonistic against plant-parasitic nematodes (Chitwood 2002). *Phyllanthus niruri* (gale of the wind) produces a prenylated flavanone, which is **nematicidal** against *Meloidogyne incognita* and.

Rotylenchulus reniformis (Shakil et al. 2008). *Verbesina encelioides* (golden crownbeard) has potential as a green manure or its extracts can be used as nematicide for the control of root-knot nematodes (Oka 2012). *Ochradenus baccatus* (tauly weed) is a widely distributed shrub in desert regions of the Middle East and North Africa which contains exceptionally high levels of **glucosinolates**. *In vitro* assays with aqueous extracts of this plant completely immobilize juveniles of *Meloidogyne javanica* (Oka et al. 2014). Incorporation of root core or bark into the soil reduces the number of nematodes recovered from the soil by 95–100%. The very poor host status of *Ochradenus baccatus* to *Meloidogyne javanica*, *Meloidogyne incognita*, and *Meloidogyne hapla*, but with root-penetration rates of juveniles similar to those in roots of a suitable host, suggest that this species may be useful as a cover crop or trap plant to reduce nematode populations in the soil.

13.3 Chemical Defense Mechanisms

Many secondary plant compounds play a role in deterring herbivores; however, some herbivores have found ways 'to get around the problem' or even prefer the plants that contain specific secondary compounds: food selection. Both topics will be discussed in this section.

13.3.1 Defense Against Herbivores

Chemical defense is quite obvious in poison ivy (*Toxicodendron radicans*) as well as in the stinging nettle (*Urtica dioica*) and closely related members of the Urticaceae. Touching the nettle, breaks off the tip of the hairs on leaves or stem. The walls of these hairs are thin, and contain **silica**, which gives the cut hair a sharp end to penetrate the skin. The contents of the hair are then released, giving local pain and swelling of the skin. This is a clear example of a **direct defense**. Oxalic acid and tartaric acid are major long-lasting pain-inducing toxins in the stinging hairs of *Urtica thunbergiana* (Fu et al. 2006). A tropical member of the Urticaceae, *Laportea moroides*, accumulates peptides, including a tricyclic octapeptide (moroidin) (Leung et al. 1986). The number of stinging hairs varies widely in *Urtica dioica*; some plants have none at all, and this has a genetic basis. Grazing by large herbivores is negatively correlated with the number of hairs (Pollard and Briggs 1984).

Some secondary compounds inhibit specific steps in mitochondrial respiration. For example, **HCN** (prussic acid or hydrogen cyanide), which blocks cytochrome oxidase, is released from **cyanogenic** compounds that are present in a wide range of species (Gleadow and Møller 2014). **Fluoroacetate** (1080), after conversion to fluorocitrate, blocks aconitase, which is an enzyme in the TCA cycle (Twigg 2014). **Rotenone**, which is an isoflavonoid in roots of *Derris*, *Lonchocarpus*, and *Tephrosia* species (Fabaceae) (de Oliveira et al. 2014), blocks the mitochondrial internal NADH dehydrogenase (Sect. 3.2.3.1). **Platanetin**, which is a flavonoid from the bud scales of *Platanus acerifolia* (plane tree) (Ravanel et al. 1986), inhibits the mitochondrial external NADH dehydrogenase (Sect. 3.2.3.1). Seeds of a wide range of *Phaseolus* (bean), *Vigna radiata* (mungbean), and *Cicer arietinum* (chickpea) species contain specific inhibitors of α-amylase, which is a digestive enzyme that hydrolyzes starch (Pueyo José and Delgado-Salinas 1997; Wisessing et al. 2010), or of proteinases (Green and Ryan 1972; Hartl et al. 2010). Other secondary plant compounds are much less specific; for example, **tannins** precipitate proteins and thus interfere with food digestion. Toxic phenolic glycosides in *Salix* (willow) species deter herbivores. Others [*e.g.*, glucosinolates in Brassicaceae (cabbage family)] probably evolved as secondary metabolites in plants, because they are toxic to most herbivores. The stored glucosinolate **sinigrin** is converted enzymatically to highly toxic allyl isothiocyanate, which gives mustard its distinct sharpness (Fig. 13.4). Some herbivores have evolved mechanisms, however, that defy this chemical defense, and use glucosinolates as **attractants**. In *Brassica oleracea* (cabbage) and other Brassicaceae, sinigrin attracts butterflies of *Pieris brassicae* (cabbage moth) as well as certain aphids (*e.g.*, *Brevicoryne brassicae*) and cabbage-root flies (*Delia radicum*). Cabbage moths normally deposit their eggs only on plants that contain sinigrin, but accept filter paper that contains this compound as a substitute. Their larvae exclusively eat food that contains sinigrin, either naturally or experimentally added (Van Loon et al. 1992).

Cyanogenic glucosides are widespread in the plant kingdom (Gleadow and Møller 2014),

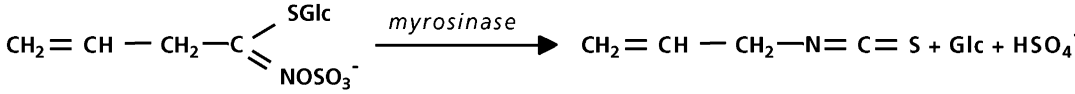

sinigrin allyl isothiocyanate

Fig. 13.4 The chemical structure of sinigrin, which is a glucosinolate in *Brassica* (cabbage) species, and allyl isothiocyanate, into which it can be converted. The reaction is catalyzed by endogenous β-thioglucosidases (myrosinases) that are localized in 'myrosin' cells, scattered throughout most plant tissues. Within these cells the enzyme is stored inside myrosin grains (Rask et al. 2000).

whereas **glucosinolates** are evolutionarily younger and found in Brassicaceae and in the genus *Drypetes* (Euphorbiaceae) and in *Ochradenus baccatus* (Resedaceae) (Halkier and Gershenzon 2006; Oka et al. 2014). Because both groups of natural products are derived from **amino acids** and have aldoximes as intermediates, it has been hypothesized that glucosinolates developed based on a predisposition for making cyanogenic glucosides. Consistent with an evolutionary relationship between the cyanogenic glucoside and glucosinolate pathways, the aldoxime-metabolizing enzymes in both pathways belong to the same gene family. A mutation in the aldoxime-metabolizing enzyme in the cyanogenic pathway may have resulted in the production of toxic compounds, which the plant subsequently had to get rid of, instead of the original hydroxynitrile in the pathway towards cyanogenic glucosides (Halkier and Gershenzon 2006).

Many plants contain defensive phenolics [*e.g.*, tannins in leaves *of Quercus* (oak)]. In the bark of *Picea abies* (Norway spruce) clones that are resistant to *Ceratocystis polonica* (a fungal pathogen that is transmitted through bark beetles) specialized phloem-parenchyma cells contain deposits of polyphenols. These parenchyma cells are enriched in phenylalanine ammonia lyase, which is a key enzyme in the synthesis of phenolics. Susceptible clones have much less of these **polyphenol-containing parenchyma cells**. The phenolics in the resistant clone are mobilized upon fungal attack which indicates that the specialized parenchyma cells are an important site of both **constitutive** and **inducible** defense (Franceschi et al. 1998). In *Picea galuca* (white spruce), laser microdissection shows that the transcriptomes of cortical resin duct cells, phenolic cells and phloem of bark is constitutive and inducible by methyl jasmonate (Celedon et al. 2017). Overall, ~3700 bark transcripts are differentially expressed in response to methyl jasmonate. Approximately 25% of transcripts were expressed in only one cell type, revealing cell specialization at the transcriptome level. Methyl jasmonate causes cell-type-specific transcriptome responses and changes the overall patterns of cell-type-specific transcript accumulation.

Both *Populus* (poplar) and *Salix* (willow) plants contain a wide range of toxic phenolic glycosides, including salicin (Clausen et al. 1989). After ingestion, salicin is hydrolyzed and oxidized, producing **salicylic acid** (Fig. 13.5), which **uncouples oxidative phosphorylation** in mitochondrial preparations. In addition, salicylic acid is associated with stress signaling and systemic acquired resistance (Heil and Baldwin 2002). The structure of phenolic glycosides resembles that of many allelopathic compounds which suggests that the driving force in evolution for the formation of allelopathic compounds may well have been their role in deterring herbivores or pathogens (Bais et al. 2004, 2006). Both the total phenolic glycoside concentration in the leaves and the composition of these compounds varies among *Salix* species (Table 13.2).

The role of phenolic glycosides in the **food-selection** pattern of beetles feeding on willow leaves has been investigated extensively. Leaves of the eight willow species shown in Table 13.2 were used for laboratory feeding experiments with four beetle species. In all cases, the leaves of the *Salix* species that is chemically most related to the preferred species are fed on to the highest degree (Fig. 13.6). Both the total amount and the quality of the phenolic glycosides determine the food-selection pattern of the investigated beetles.

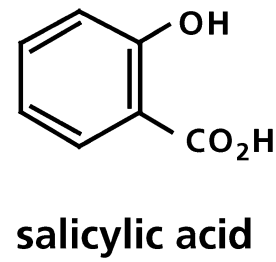

Fig. 13.5 The chemical structure of salicylic acid, which is produced after ingestion from some of the phenolic glycosides that regularly occur in *Populus* and *Salix* species. Salicylic acid is a precursor of acetylsalicylic acid, which is the active ingredient of aspirin.

Table 13.2 Phenolic glycoside concentration [mg g^{-1} (dry mass)] in the leaves of eight *Salix* (willow) species that are native to Finland or have been introduced to this area.*

	Salicortin	Salicilin	Fragilin	Triandrin	Salidroside	Picein	Total
Native willows							
S. nigricans	48	3	0.2				51
S. phylicifolia	0.5	0.1	0.1	0.3	0.1		1.8
S. caprea	0.3	0.2	0.1	0.1			1.2
S. pendandra		0.7	0.7				7.6
Introduced willows							
S. cv. *aquatica*	6.4	1.3	0.1				
S. dascylados	9.9	2.0	0.2				
S. viminalis	0.1		0.1	0.1		0.2	1.5
S. triandra		0.3			7.4		7.8

Source: Tahvanainen et al. (1985)
*Apart from these identified compounds, some others were present, so that the total amount differs from the sum of the identified ones

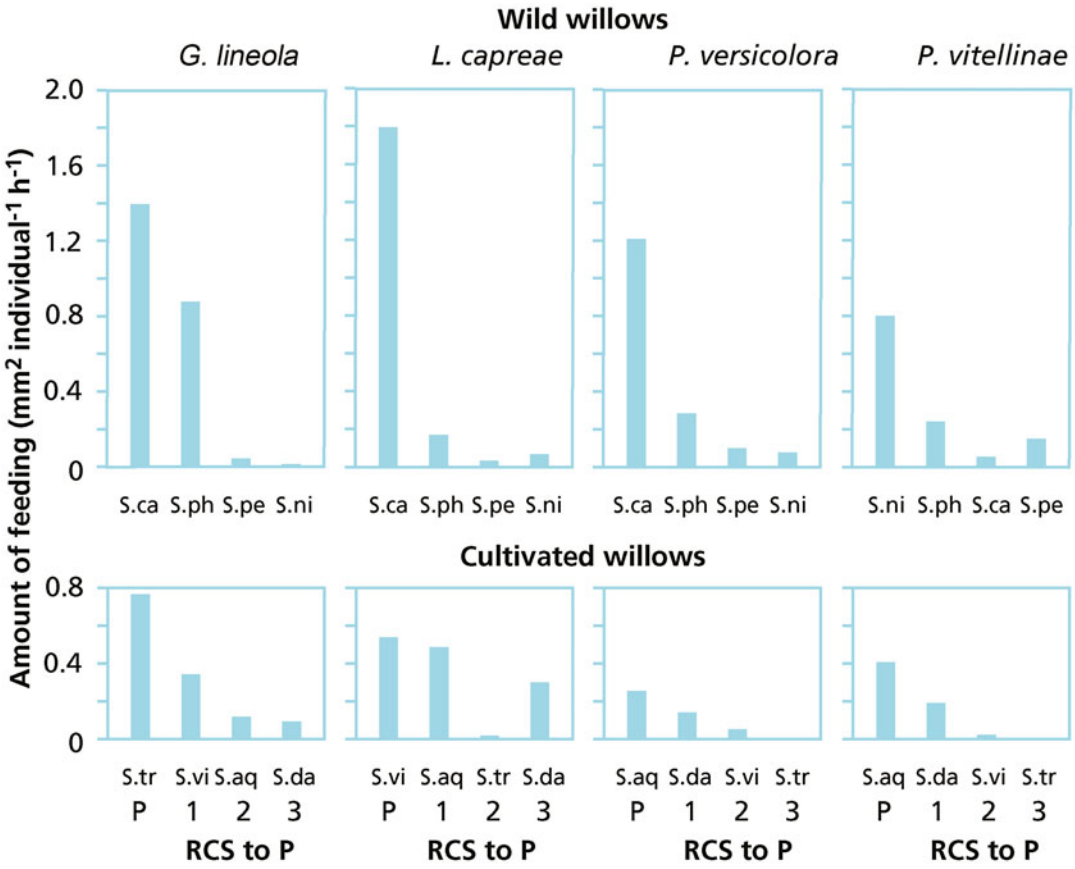

Fig. 13.6 Food-selection pattern by four beetle species (*Galerucella lineola*, *Lochmaea capreae*, *Plagiodera versicolora,* and *Pratora vitellinae*) when leaves of four native and four introduced *Salix* (willow) species are offered in two separate food choice experiments. The preferred species is placed at the left; the others are ranked according to their chemical similarity to the preferred species. The species are the same as those presented in Table 13.2 (Tahvanainen et al. 1985); copyright © 1985, Springer-Verlag.

Mammals have been important selective influences for the patterns of defense in woody plants, which are vulnerable to mammalian herbivory throughout the winter in northern parts of Europe and North America. Mammalian herbivory is a major cause of mortality in woody plants, in part because mammals remain active and often have highest energy demand in winter, when plants cannot grow to compensate for tissues lost to herbivores. Woody plant defenses are better developed in regions with a long history of vertebrate browsing than in regions that were glaciated during the Pleistocene (Bryant et al. 1989). There is strong developmental control over defenses in woody plants, with these being most strongly expressed in juvenile woody plants that grow in a height range where they are vulnerable to mammalian herbivores. After browsing, juvenile shoots are produced that have higher levels of secondary metabolites that deter further browsing. These defenses include ether-soluble terpenes [*e.g.*, papyriferic acid in *Betula resinifera* (paper birch), and pinosylvin in *Alnus viridis* subsp. *fruticosa* (green alder)] that deter feeding below levels required for weight maintenance, and, if consumed, result in a negative N and Na^+ balance (Bryant et al. 1992).

Plants that hyperaccumulate **metals** [*e.g.*, nickel-accumulating Brassicaceae (cabbage family); (Sect. 9.3.3; Boyd 2012) or silicon (Cooke and Leishman 2012) are also better protected against herbivores.

13.3.2 Qualitative and Quantitative Defense Compounds

Secondary metabolites involved in deterring herbivores can be divided into two broad categories:

1. **Qualitatively** important secondary plant compounds. These are **toxins**, which are usually present in low concentrations, but may constitute up to 10% of the fresh weight of some leaves or seeds. Numerous compounds belong to this category, including **alkaloids** (Fig. 13.7), **cyanogenic glycosides**, **nonproteinogenic amino acids**, **cardiac glycosides**, **glucosinolates** (Fig. 13.4), and polypeptides (Mithöfer and Maffei 2017). Their mode of action varies widely.
2. **Quantitatively** important secondary plant compounds. These reduce the **digestibility** and/or **palatability** of the food source and invariably make up a major fraction of the biomass. They are mostly phenolic compounds (phenolic acids, tannins, lignin; Fig. 13.8) or terpenoids resins. Tannins and some other phenolics reduce the digestibility of plant tissues by blocking the action of digestive enzymes, binding to proteins being digested, or interfering with protein activity in the gut wall. Tannins, as well as lignin, also increase the leaf's toughness (Read et al. 2009).

If one considers that relatively few resources are required to acquire protection against herbivores by toxic compounds, one may wonder why the alternative strategy of the digestibility-reducing compounds, which requires far greater investment of carbon resources, has evolved at all. The answer to this question is that there are numerous examples of herbivores in which mechanisms have evolved to cope with the toxic compounds that are effective against most herbivores. These herbivores may metabolize the toxin to an extent that it is used as a food source, they may store the toxin, sometimes after slight modification, and thus gain protection themselves, or they rapidly excrete the toxic compound. Such combinations of toxic plants and animals that cope with the toxin provide examples of **coevolution** of plants and animals in an ever-continuing 'arms race' (Ehrlich and Raven 1964; Coley et al. 2018).

Although the distinction between qualitative and quantitative defenses is a useful starting point, it is not a clear-cut dichotomy. Many phenolic compounds also have toxic effects on herbivores and may be more toxic against some herbivores than others (Mithöfer and Maffei 2017), and some cyanogenic glycosides or alkaloids accumulate to rather high levels in some species [*e.g.*, prunasin in *Eucalyptus*

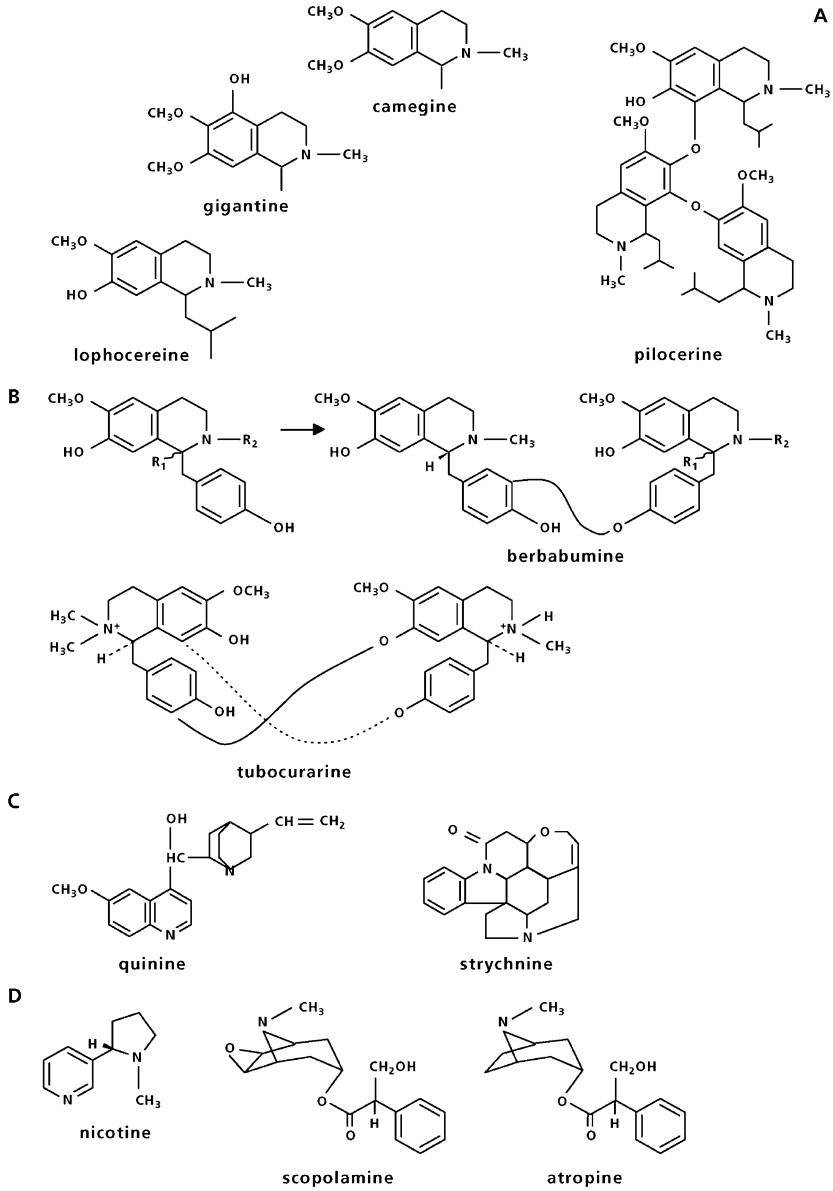

Fig. 13.7 Alkaloid subclasses. (**A**) Isoquinoline alkaloids. These are synthesized (*e.g.*, carnegine and gigantine in a species-specific manner in saguaro (*Carnegia gigantean*) and cardon (*Pachycereus pringlei*) cacti). Sentia cactus (*Lophocereus schottii*) contains as much as 30 to 150 mg g^{-1} (DM) lophocerine and its trimers, pilocereine and piloceredine. (**B**) bisbenzylisoquinoline alkaloids. Examples include berbamunine from barberry (*Berberis stolonifera*) and tubocurarine, an arrow poison, from *Chondrodendron tomentosum*. (**C**) Monoterpene indole alkaloids, including quinine (from *Cinchona officinalis*) and strychnine (from *Strychnos nux-vomica*). (**D**) Nicotine and tropane alkaloids. These are naturally occurring insecticides and feeding deterrents in Solanaceae [*e.g.*, nicotine in *Nicotiana tabacum* (tobacco), scopolamine in *Hyoscyamus niger* (henbane), and atropine in *Atropa belladonna* (deadly nightshade)] (Harborne 1988; Schuler 1996).

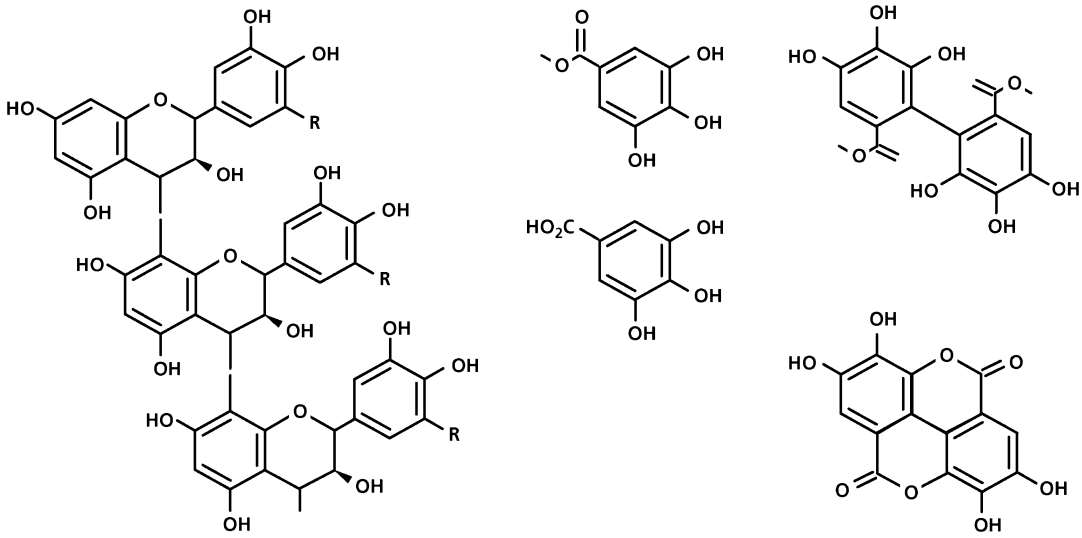

Fig. 13.8 The chemical structure of proanthocyanidin (condensed tannin) (left). Gallotannin (top, middle) and ellagitannin (top, right) are hydrolyzable tannins, releasing gallic acid (bottom, middle) and ellagic acid (bottom, right), respectively, and the esterified sugar(s), mostly glucose, upon hydrolysis.

cladocalyx (sugar gum) (Gleadow and Møller 2014) and nicotine in *Nicotiana attenuata* (wild tobacco) (Baldwin and Preston 1999)].

13.3.3 The Arms Race of Plants and Herbivores

The expression 'arms race' graphically describes the continuous evolution of ever more toxic defense compounds in plants and of more mechanisms to cope with these compounds in herbivores. Numerous examples of such a **coevolution** exist, showing mechanisms in herbivores that store, detoxify, or excrete qualitative defense compounds, with very little evidence for evolutionary escape from quantitative defenses. We will first present a number of striking examples of coevolution of predators coping with qualitative defenses.

Coevolutionary interactions are thought to have spurred the evolution of key innovations and driven the diversification of much of life on Earth. The coevolutionary interactions between plants (Brassicales) and butterflies (Pieridae) show evidence for an escalating evolutionary arms race. Gradual changes in trait complexity appear to have been facilitated by allelic turnover, but key innovations are associated with gene and genome duplications (Edger et al. 2015). The origins of both chemical defenses and of molecular counter-adaptations are associated with shifts in diversification rates during the arms race.

Another example of coevolution that involves defensive secondary plant compounds is that of marsupials and numerous other native animal species in Southwest Australia that are resistant to the very poisonous **fluoroacetate**, which is a potent inhibitor of an enzyme of the TCA cycle (aconitase). Fluoroacetate occurs in *Gastrolobium* species (poison pea, Fabaceae), and is poisonous to introduced cows, sheep, and feral animals (Twigg 2014). Consequently, fluoroacetate (generally known as 1080) can be used to control feral animals, *e.g.*, rabbits, foxes, cats, and pigs, without harming native animals. Another well studied example of coevolution is the combination of *Senecio jacobaea* (tansy ragwort) and *Tyria jacobaea* (cinnabar moth) (Hartmann 1999). The *Senecio jacobaea* plants contain at least six pyrrolizidine **alkaloids** (Fig. 13.9). Alkaloids are characterized by a nitrogen-containing heterocyclic ring and their alkaline reaction. They represent the largest

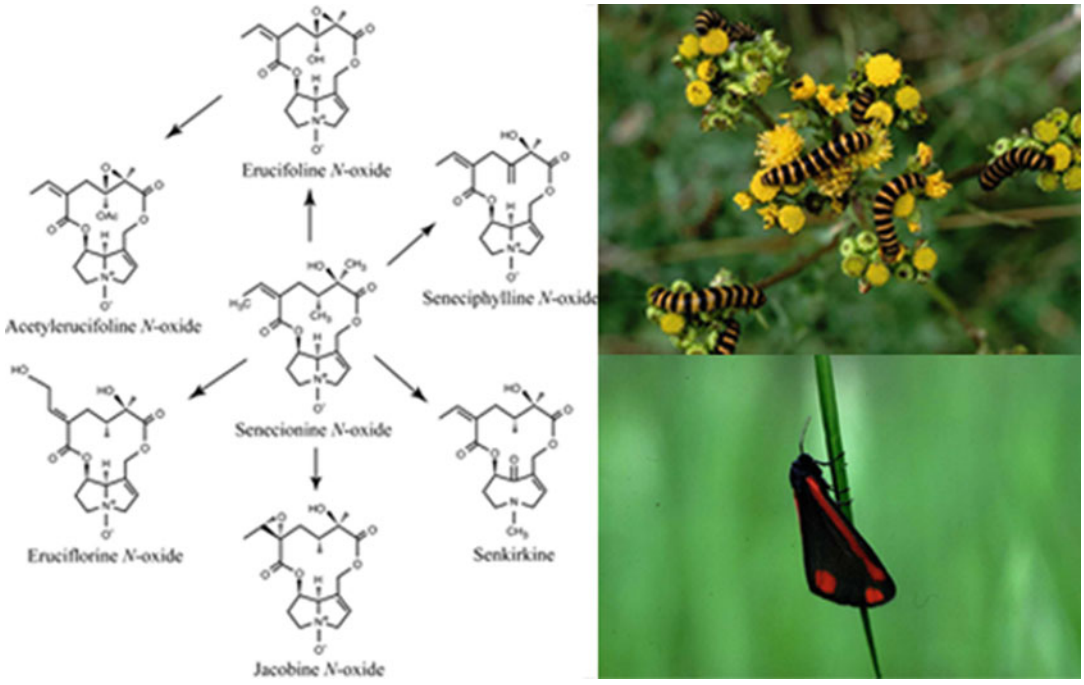

Fig. 13.9 (Left) Examples of pyrrolizidine alkaloids in *Senecio* species. Senecionin N-oxide is the basic structure from which other pyrrolizidine alkaloids are formed. These senecionine type pyrrolizidine alkaloids have an otonecine (senkirkine) or retronecine ester base (*e.g.*, senecionine) and a 12-membered macro-cyclic ring. (Right) (**A**) Larvae of the specialist moth *Tyria jacobaeae* feeding on their host plant *Senecio jacobaea*; (**B**) adult *Tyria jacobaeae*. Both larvae and adults contain pyrrolizidine alkaloids and show aposematic warning coloring (Macel 2011); © The Author 2010.

(>12,000 structures) and one of the most structurally diverse groups of substances that serve as plant defense agents (Poppenga 2010). The highly toxic alkaloids from *Senecio* may cause damage to the liver. The larvae of *Tyria jacobaea* are not harmed by these alkaloids, and use *Senecio jacobaea* as a **preferred food source**. They accumulate the toxins, which end up in the mature butterfly. Both the larvae and the butterflies are poisonous to birds. The toxic nature of these animals coincides with black and bright yellow **warning coloration** (visual advertisement). In addition to the larvae of *Tyria jacobaea*, there are some other animals that cope with the toxic alkaloids in *Senecio* [*e.g.*, the tiger moth (*Arctia caja*) and the flee beetle (*Longitarsus jacobaea*)] (Macel 2011).

The interaction of *Asclepias curassavica* (milkweed) and *Danaus plexippus* (the monarch butterfly) is similar to that of *Senecio jacobaea* and *Tyria jacobaea*; the *Asclepias curassavica-Danaus plexippus* interaction has an interesting additional dimension in that it is exploited by *Limenitis archippus* (the viceroy butterfly). The milk sap of *Asclepias curassavica* plants contains **cardiac glycosides** (calotropine and calactine). Cardiac glycosides (cardenolides) are bitter compounds that stimulate the heart when applied in small doses, but are lethal in slightly higher doses; the structure of some cardiac glycosides is given in Fig. 13.10. The presence of these toxic compounds in the larvae of *Danaus plexippus* is again advertised; moreover, caterpillars of the viceroy butterfly have similar colors, but without containing any cardiac glycosides (**mimicry**) (Brower 1969).

Being able to cope with toxic plants does not invariably lead to accumulation of the toxin. Larvae of the beetle *Caryedes brasiliensis* from Costa Rica largely feed on the seeds of *Dioclea*

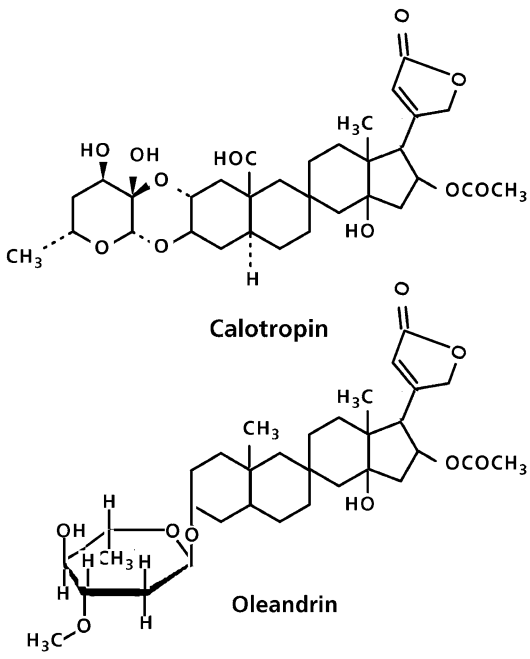

Fig. 13.10 The chemical structure of some cardiac glycosides, including calotropin from *Asclepias curassavica* (milkweed).

megacarpa (Rosenthal et al. 1982). These seeds contain canavanine, a toxic **nonproteinogenic amino acid** that resembles arginine (Fig. 13.11) and may constitute up to 10% of the seed fresh mass. Nonproteinogenic amino acids are toxic because they act as 'antimetabolites'. That is, their structure is recognized as the same as that of the amino acid they resemble which leads to proteins without the same tertiary structure and function of the protein containing the normal amino acid. Resistance of the larvae of *Caryedes brasiliensis* is based on two principles. First, the larvae have a slightly different tRNA synthetase, which recognizes arginine as being different from canavanine. Second, they have high levels of the enzyme urease, which breaks down canavanine. Thus, the toxin is a major N source for the larvae.

These few examples selected from a vast array show that one or more animal species have invariably coevolved with a plant species producing a toxin. Thus, while **qualitative defense** against herbivores requires relatively little investment of resources, it is also a vulnerable strategy. Some animals can cope with large quantities of digestibility-reducing and unpalatable compounds (**quantitative defense**). For example, mule deer (*Odocoileus hemionus*) and black bears (*Ursus americanus*) consuming condensed tannin produce tannin-binding salivary proteins that reduce fecal-nitrogen losses per unit of ingested tannin and reduce tannin metabolism relative to domestic sheep and prairie voles. However, these examples are rare, and hence, the strategy that requires a major investment of carbon is most certainly the safest. A large investment of carbon in protective compounds and structures inevitably goes at the expense of the possibility of investment of carbon in growth. It is therefore most predominant in slow-growing species, especially those with evergreen leaves with a long life-span (Lambers and Poorter 1992; Wright and Cannon 2001). On the other hand, toxins are found in both fast-growing and slow-growing species. In the evergreen *Ilex opaca* (America holly) the toxic saponins are only found in young leaves and in the mesophyll cells of older leaves. Nonmesophyll cells of older leaves contain digestibility-reducing compounds like lignin, crystals, and tannin (Kimmerer and Potter 1987).

13.3.4 How Do Plants Avoid Being Killed by Their Own Poisons?

Most secondary plant compounds that deter herbivores are also toxic to the plants themselves. Prussic acid (HCN) is produced upon ingestion of plant material of approximately 3000 species from some 130 families, including genotypes of *Trifolium* spp. (clover), *Linum usitatissimum* (flax), *Sorghum bicolor* (millet), *Pteridium aquilinum* (bracken fern), and *Manihot esculenta* (cassava) (Gleadow and Møller 2014). If HCN inhibits several enzymes in both animals and plants (*e.g.*, cytochrome oxidase and catalase), and this also holds for plants that contain the cyanogenic compounds, how do cyanogenic plants protect themselves from this toxic HCN?

Cyanogenic plants do not actually store HCN, but contain **cyanogenic glycosides** (*i.e.* cyanide attached to a sugar moiety) or **cyanogenic lipids**

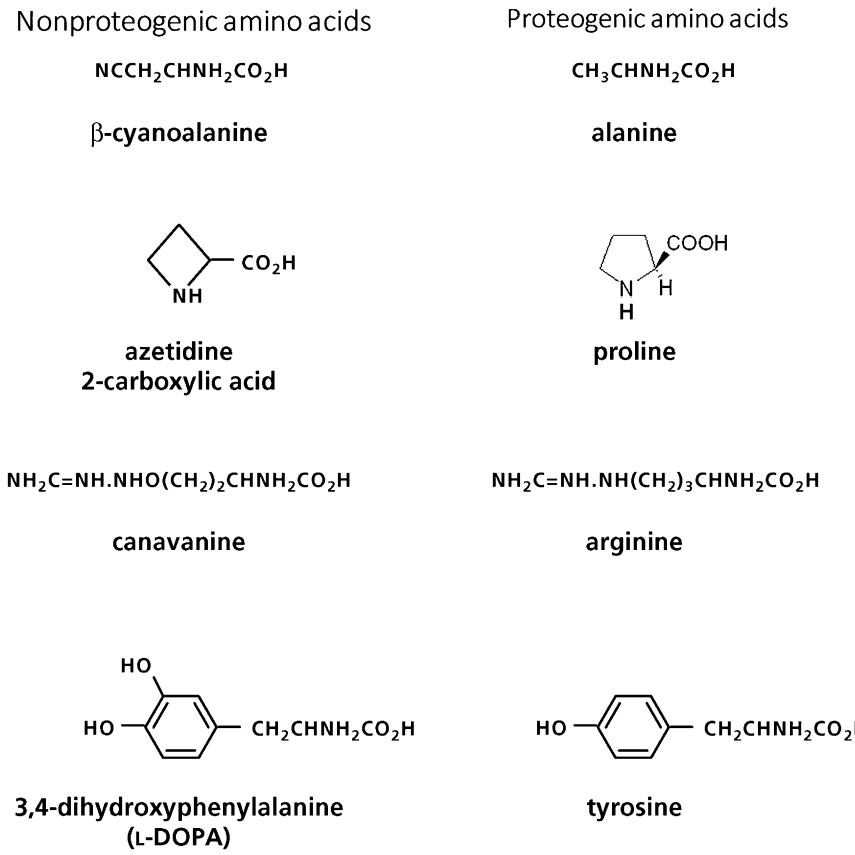

Fig. 13.11 Some examples of nonproteinogenic amino acids from higher plants, including canavanine from *Dioclea megacarpa*. The structure of the corresponding proteinogenic amino acids is also given for comparison (Harborne 1988).

(in Sapindaceae), and these only release HCN upon hydrolysis (Gleadow and Møller 2014). The reaction is catalyzed by specific enzymes (*e.g.*, linamarase, which catalyzes hydrolysis of linamarin in some legumes) (Fig. 13.12). Synthesis of many cyanogenic compounds requires amino acids as precursors, as Fig. 13.12 illustrates for the synthesis of linamarin from valine. The enzymes responsible for the breakdown of the cyanogenic compound and the cyanogenic compounds themselves occur in different cell compartments or tissue types. Upon damage, such as after ingestion, the enzyme and its substrate come into contact. For example, dhurrin, which is a cyanogenic glycoside in *Sorghum* species, occurs exclusively in the vacuole of leaf epidermal cells, whereas the enzyme responsible for its hydrolysis is located in mesophyll cells (Halkier and Moller 1989; Nielsen et al. 2016). Linamarase, hydrolyzing linamarin, occurs in the walls of mesophyll cells, whereas its substrate is stored inside the cell. As long as this strict **compartmentation** between cyanogenic compounds and hydrolyzing enzymes is maintained, no problem arises for the plant itself. The linamarin (monoglucoside of acetone cyanohydrin) that is found in the roots of *Hevea brasiliensis* (rubber tree) and *Manihot esculenta* (cassava), however, is synthesized in the shoot and imported via the phloem. In the rubber tree the transport compound is linustatin, which is a nonhydrolyzable diglucoside of acetone cyanohydrin, rather than the hydrolyzable linamarin itself. Transport as the diglucoside avoids the risk of HCN production during transport from leaf cells, via the phloem, to the roots (Selmar 1993).

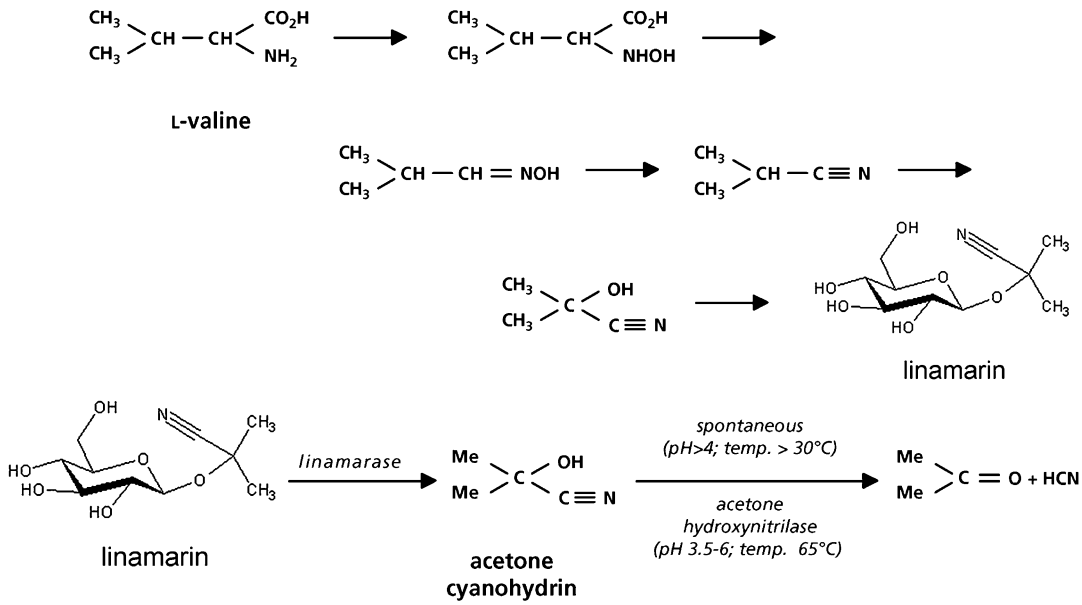

Fig. 13.12 In the synthesis of linamarin (a cyanogenic glucoside) the amino acid valine is used as a precursor. The release of HCN from linamarin is catalyzed by a specific enzyme, linamarase (McMahon et al. 1995).

Although avoidance of damage by compartmentation is the best strategy, some **detoxification mechanisms** may be needed. Detoxification of HCN in plants is possible; it is catalyzed by β-cyano-alanine synthase, transforming L-cysteine + HCN into β-cyano-alanine. The N in cyanogenic compounds that are stored in seeds, can therefore be remobilized and incorporated into primary nitrogenous metabolites (Nielsen et al. 2016). In addition, in vegetative plant organs, cyanogenic compounds are subject to some turnover, without the release of toxic HCN, indicating a role of cyanogenic glucosides as reduced N storage compounds (Pičmanová et al. 2015).

Resistance against cyanogenic glycosides in animals is mainly based on the presence of the enzyme rhodanese (*e.g.*, in sheep and cattle). It catalyzes the transfer of sulfur from a sulfur donor to cyanide to form thiocyanate, which is eliminated via the urine. The limiting factor in cyanide detoxification is the availability of sulfur donors; endogenous stores of sulfur are quickly depleted resulting in a slowing of cyanide inactivation (Poppenga 2010).

Cyanogenesis is a stable, heritable trait. In some species, all individuals are cyanogenic, whereas others are highly polymorphic, with phenotypically acyanogenic individuals (Gleadow and Møller 2014). One locus is responsible for the production of cyanogenic glucosides, which are stored in the vacuole, and the other locus codes for the production of an enzyme that hydrolyses the glycosides. Plants must be homozygous recessive at one of the loci to be acyanogenic. Highly cyanogenic genotypes *Phaseolus lunatus* (lima bean) are better defended against Mexican bean beetle (*Epilachna varivestis*), but they produce less aboveground biomass and seeds when grown in the absence of herbivores (Ballhorn et al. 2014). *Hevea brasiliensis* (rubber tree) releases HCN when it is infected by a pathogenic fungus (*Microcyclus ulei*). HCN then interferes with both the plant host and the fungal pathogen. Because of its inhibition of cytochrome oxidase, this inhibits energy-requiring defense responses, hampering the plant's ability to ward off the fungus (Lieberei et al. 1989).

Like cyanogenic compounds, many alkaloids are also stored in specific compartments (*i.e.* either the vacuole or smaller vesicles in which they are produced). In *Papaver somniferum*

(opium poppy), benzylisoquinoline alkaloids accumulate in the cytoplasm, or latex, of specialized **laticifers** that accompany vascular tissues throughout the plant. However, immunofluorescence labeling shows that three key enzymes involved in the biosynthesis of morphine and the related antimicrobial alkaloid sanguinarine, are restricted to the parietal region of sieve elements adjacent or proximal to laticifers (Bird et al. 2003). In *Berberis wilsoniae* (barberry), *Thalictrum glaucum* (rue), and many other species cells have similar 'alkaloid vesicles', which contain berberine or other alkaloids and some of the enzymes of the pathway that produce them. The 'alkaloid vesicles' may fuse with the central vacuole and thus deposit the alkaloids there (Hashimoto and Yamada 1994).

Ricin is a highly toxic and abundant protein in seeds of *Ricinus communis* (**castor bean**). Like **abrin** from *Abrus precatorius* (jequirity bean), ricin is a **ribosome-inactivating protein** (Bolognesi et al. 2016). Ricin is a heterodimeric protein that consists of an enzymatic polypeptide that destroys ribosomal RNA; it is covalently bound to a galactose-binding **lectin** [lectins are proteins with noncatalytic sugar-binding domains; the first ones were discovered in *Ricinus communis* (castor bean) more than a century ago; numerous other plants were found to contain lectins since then (Peumans and Van Damme 1995); see also Sect. 13.3.3]. This bipartite structure and functional properties allow ricin to bind to galactosides on the cell surface. Upon binding, ricin enters the cell via endocytotic uptake and traverses an intracellular membrane to deliver the enzymatic component to the cytosol. Once it is there, it irreversibly inhibits protein synthesis, followed by death of the cell (Authier et al. 2016). Ricin is one of the most potently toxic compounds known, and entry of a single toxin molecule into the cytosol may be sufficient to kill the cell. *Ricinus* ribosomes that synthesize ricin are also susceptible to the catalytic action of this protein. How, then, does *Ricinus* avoid suicide? The subunits of which the heterodimer is composed are originally synthesized together in the form of a single precursor protein: proricin, which is an active lectin, but it does not bind to ribosomal RNA. It is transported to the vacuole, where acidic endoproteases remove amino acid residues to generate the heterodimer: ricin. None of the ricin appears to escape from the vacuole (Lord and Roberts 1996).

13.3.5 Secondary Metabolites for Medicines and Crop Protection

Secondary metabolites that deter herbivores or inhibit pathogens have been used by humans for a very long time. The bark of willow (*Salix*) has been used as medicine; it contains **salicylic acid** (Fig. 13.5), which is closely related to acetylsalicylic acid (**aspirin**). Quinine, which is an alkaloid from the bark of *Cinchona officinalis* (quinine), has been used for centuries to combat **malaria**. Artemisinins are extracted from *Artemisia annua* (sweet wormwood); they are potent antimalarials, rapidly killing all asexual stages of *Plasmodium falciparum* (Eckstein-Ludwig et al. 2003). Other examples of secondary compounds used as medicine are included in Table 13.3; some of these are still used [*e.g.*, atropine from *Atropa belladonna* (deadly nightshade)]. Others are used because of their antitumor activity [*e.g.*, the diterpene taxol from *Taxus brevifolia* (western yew), and other *Taxus* species] (Heinstein and Chang 1994), and the polypeptides ricin and abrin from *Ricinus communis* (castor bean) and *Abrus precatorius* (jequirity bean), respectively (Bolognesi et al. 2016)]. Many more compounds, as-yet-undiscovered, may well be found to have similar effects, as long as the species that contain them do not become extinct, thus offering a strong argument for plant conservation. About 25% of currently prescribed medicines originate from plant compounds that evolved as defenses against herbivores (Dirzo and Raven 2003).

Humans have also found other uses for secondary metabolites, some of these in ancient history, such as taxine [from *Taxus baccata* (yew)] to make arrowheads poisonous (Wehner and Gawatz 2003), and alkaloids [from *Conium maculatum* (poison hemlock)] to poison Socrates

Table 13.3 Examples of secondary metabolites for which man has found some use.

Chemical compound	Species	Applications
Salicylic acid	*Salix* species, *Populus* species	Pain killer
Aconitine	*Aconitum napellus*	Pain killer
Atropine	*Atropa bella-donna*	Ophthalmology
Cytisine	*Cytisus laburnum*	Migraine
Germerine, protoveratrine	*Veratrum album*	Muscle diseases, pain killer
Cardiac glycosides	*Digitalis* sp., *Asclepias* sp.	Heart diseases
Linarine, linine	*Linaria vulgaris*	Haemorrhoids
Quinine	*Cinchona officinalis*	Malaria
Ricin	*Ricinus communis*	Tumors
Abrin	*Abrus precatorius*	Tumors
Atropine	*Atropa bella-donna*	Poisoning
Taxine	*Taxus baccata*	Poisoning (arrowheads of Celts)
Cicutoxin	*Cicuta virosa*	Poisoning (of Socrates)
Hyoscyamine, scopolamine	*Hyoscyamus niger*	Poisoning (in Shakespeare's 'Hamlet')
Pyrethrins	*Chrysanthemum cinearifolium*	Insecticide
Rotenone	*Derris* sp., *Lonchocarpus* sp.	Rat and fish poisoning, pesticide
Camphor	*Cinnamonum camphora*	Moth balls

(Reynolds 2005). One of the more recent applications includes the now widespread use of pyrethrins from *Tanacetum cinerariifolium* (=*Chrysanthemum cinerariifolium*, Dalmatian chrysanthemum) as an 'environmentally friendly' insecticide (Marongiu et al. 2009). Over 800 compounds have been reported in the Asteraceae, including nematicides [*e.g.*, thiarubrine and terthienyl in the roots of *Calendula officinalis* (marigold)], fungicides, and bactericides (Flores et al. 1999).

The ancestors of our food plants also contain many toxic compounds, including alkaloids in *Solanum lycopersicum* (tomato) and *Solanum tuberosum* (potato) (Fig. 13.13). Breeding has greatly reduced the alkaloid levels in tomato and potato, so that food poisoning by potatoes, which was known until the beginning of the twentieth century, no longer occurs. Whenever wild species are used to make new crosses, however, new cultivars emerge that may produce poisonous solanine. The majority of pyrolizidine alkaloids cause serious diseases in domestic animals and humans through liver bioactivation. Grazing animals, however, usually avoid plants with high levels of pyrolizidine alkaloids, unless there is shortage of other herbaceous food, apparently because of their deterrent taste (Hartmann 1999).

Cyanogenic glycosides (Sect. 13.3.4) in *Manihot esculenta* (cassava), *Sorghum bicolor* (millet), and *Vicia faba* (broad bean) are made harmless during food preparation (Jones 1998). This also holds for many inhibitors of digestive enzymes (proteases, amylases), if the food is properly prepared. Eating raw or insufficiently cooked pulses is an unhealthy affair because they will still contain large amounts of secondary compounds (Campos-Vega et al. 2010). Some compounds in herbs that are commonly used to flavor our food are on the black list of carcinogenic substances. These include **safrole** (in nutmeg, cacao, black pepper) and capsaicin (in red pepper, hot pepper), but taken in small doses they do not cause problems (Jin et al. 2011). There are certainly compounds, however, that should be avoided at all costs (*e.g.*, **aflatoxin**). This is a fungal compound produced by *Aspergillus flavus* growing on *Arachis hypogaea* (peanuts), *Zea mays* (corn), and some other crop plants. This compound may cause severe liver damage or cancer (Wang et al. 2015b).

Some secondary compounds have a distinctly positive effect on our health in that they reduce the risks for certain forms of cancer. These include the **flavonoids** in a so-called fiber-rich diet (Rodgers 2016). These phenolics likely inhibit the production of sex hormones; hence,

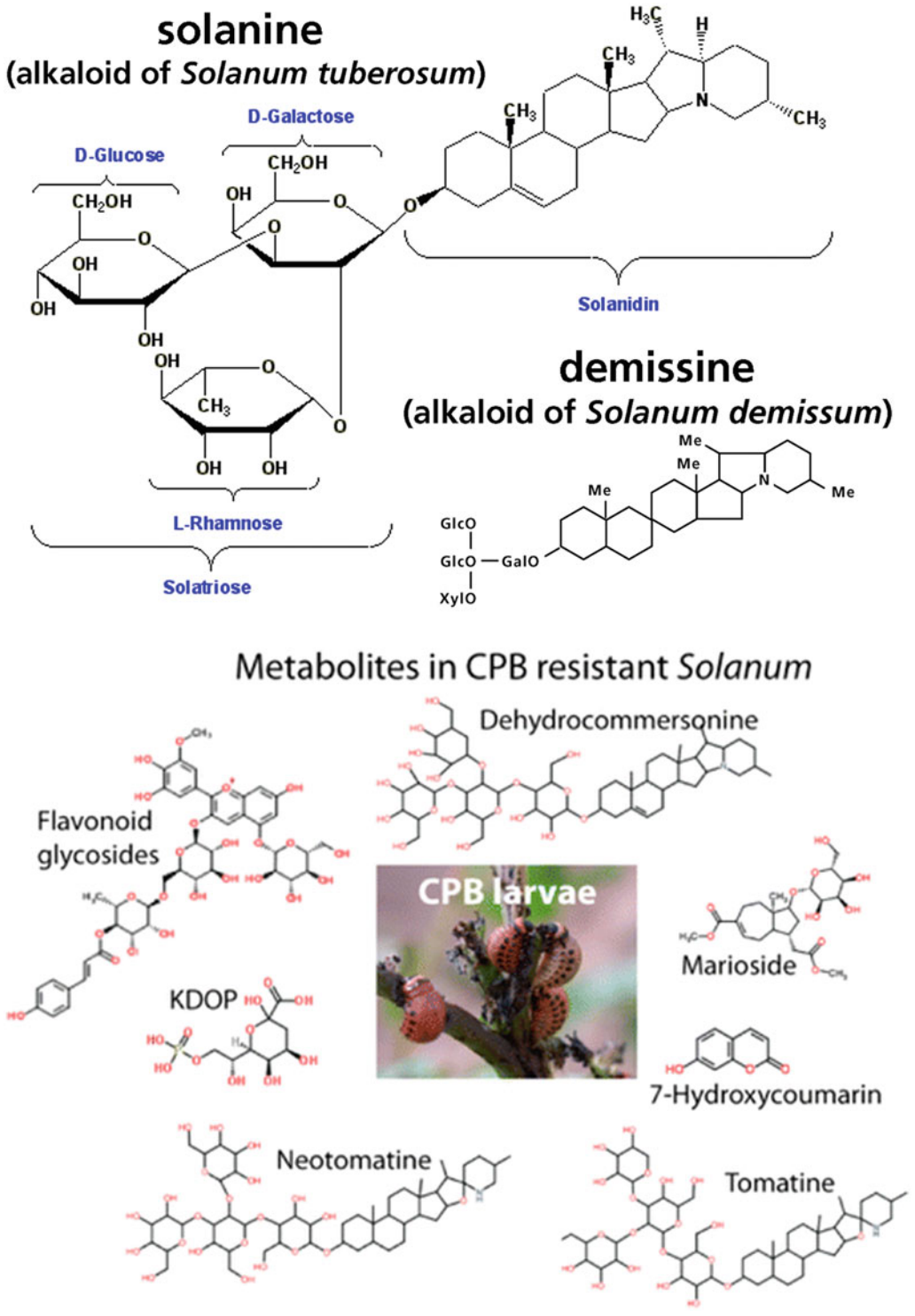

Fig. 13.13 (Top) The chemical structures of two alkaloids: solanine from *Solanum tuberosum* (cultivated potato), and demissine from *Solanum demissum* (wild potato), which is resistant to *Leptinotarsa decemlineata* (Colorado potato beetle, CPB) (Bennett and Wallsgrove 1994). (Bottom) Chemical structures of six resistant wild *Solanum* species. Only *Solanum tuberosum* produces solanine and chaconine. The six wild species produced glycoalkaloids that all have tetrose sugar side chain (Tai et al. 2014).

they appear to reduce the incidence of cancers in which these hormones play a role, including breast cancer and prostate cancer. The alkaloid camptothecin, from the roots of the Chinese medicinal herb *Camptotheca acuminata*, is an anticancer drug (Cragg and Newman 2003). **Isothiocyanates**, which are produced upon degradation of glucosinolates, induce anticarcinogenic enzymes which suggests that high consumption of *Brassica* (cabbage) species could reduce the risk of developing cancer (Vale et al. 2015). The roles of fruit, vegetables, and red wine in disease prevention have been attributed, in part, to the **antioxidant** (radical-scavenging) properties of their constituent phenol compounds (polyphenols; Sect. 13.3.1), some of which are more effective antioxidants *in vitro* than are vitamin C (ascorbic acid) and vitamin E (α-tocopherol) (Rice-Evans et al. 1997; Borochov-Neori et al. 2015).

Breeding or genetically modifying genotypes of crop species that contain antiherbivore compounds is of increasing economic importance and may lead to more environmentally friendly methods in agriculture. The tendency to breed for oilseed varieties with low glucosinolate levels to improve the feeding quality of rape meal is an excellent example how *not* to go about it. Such a breeding approach makes the crop more vulnerable to herbivores and makes agriculture more dependent on pesticides. It would be better instead, to aim for oilseed varieties that have their leaves well protected against herbivores, while having a reduced level of **glucosinolates** only in their seeds (Halkier and Gershenzon 2006). This promising strategy has been taken on board in more recent breeding efforts.

There are increasingly positive developments in breeding resistant cultivars. For example, *Leptinotarsa decemlineata* (Colorado potato beetle) is a well-known herbivore of *Solanum tuberosum* (potato) and may cause severe damage to potato crops in North America and Western Europe. Six resistant wild *Solanum* species all have low levels of glycoalkaloids. Comparative analysis of the metabolite profiles of the foliage shows metabolites shared between the wild species, but not with *Solanum tuberosum* (potato). Only *Solanum tuberosum* produces the triose glycoalkaloids solanine and chaconine, whereas the wild species all produce glycoalkaloids with tetrose sugar side chains. Additionally, there are non-glycoalkaloid metabolites associated with resistance including hydroxycoumarin and a phenylpropanoid, which are produced in all wild species, but not in *Solanum tuberosum* (Fig. 13.13; Tai et al. 2014). One striking example of the application of ecophysiological information on plant-herbivore interactions is the incorporation of a gene from *Phaseolus vulgaris* (common bean), encoding an amylase inhibitor, into *Pisum sativum* (garden pea). The transgenic plants are considerably less affected by pea weevils (*Bruchus pisorum*) than the wild-type is (Schroeder et al. 1995). Similarly, genes encoding a proteinase inhibitor or lectins have been inserted.

Herbivores may acclimate and possibly even adapt to an increased level of a specific proteinase or amylase inhibitor. They do so by producing other proteinases or amylases, whose activity is not inhibited by the plant-produced inhibitor. For example, one type of α-amylase inhibitor protects seeds of *Phaseolus vulgaris* (common bean) against predation by the cowpea weevil (*Callosobruchus maculatus*) and the azuki bean weevil *Callosobruchus chinensis*), but not against predation by the bean weevil (*Acanthoscelides obtectus*) or the Mexican bean weevil (*Zabrotus subfasciatus*). A serine protease in midgut extracts of the larvae of the Mexican bean weevil rapidly digests and inactivates α-amylase from *Phaseolus vulgaris* as well as from *Phaseolus coccineus* (scarlet runner bean), but not the α-amylase from wild accessions of *Phaseolus vulgaris* or *Phaseolus acutifolius* (tepary bean) (Ishimoto and Chrispeels 1996).

Lectins bind carbohydrates (by definition). As such they play a role as defense compounds (Fig. 13.14; Peumans and Van Damme 1995). Lectins occur in many plants, including *Sambucus nigra* (elderberry), *Hevea brasiliensis* (rubber tree), *Galanthus nivalis* (snowdrop), and *Datura stramonium* (thorn apple) (Raikhel et al. 1993). In *Sambucus nigra*, lectin is located in protein bodies in the phloem parenchyma of the

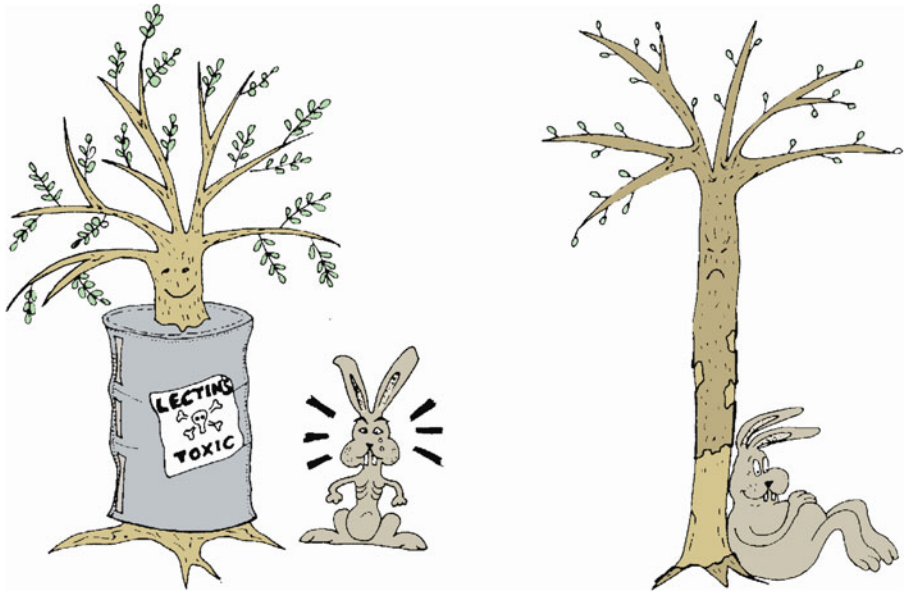

Fig. 13.14 Lectins are carbohydrate-binding proteins. Some of these give plants protection against insects as well as vertebrates. When present in bark [*e.g.*, in *Sambucus nigra* (elderberry)] they offer good protection against rodents and deer (after Peumans and Van Damme 1995).

bark (Greenwood et al. 1986). Some lectins are highly toxic to many animals and also offer good protection against viruses and some fungi (Sect. 14.2). Although some insects appear to tolerate lectins, sucking insects like aphids are highly sensitive.

The gene encoding the lectin from *Galanthus nivalis* (snowdrop) has been linked to a promoter that ensures expression of the gene in the phloem (Hilder et al. 1995). It has been inserted in *Oryza sativa* (rice) in an attempt to develop a plant that contains its own insecticide to enhance its resistance to aphids and brown plant-hoppers (Sudhakar et al. 1998; Wu et al. 2002). Ever-increasing numbers of transgenic plants with a range of different resistance genes inserted are now being produced (Chakravarthy et al. 2014; Lombardo et al. 2016).

13.4 Environmental Effects on the Production of Secondary Plant Metabolites

Although many secondary metabolites tend to be specific for certain species, the concentration of these compounds may vary greatly, depending on environmental conditions.

13.4.1 Abiotic and Biotic Factors

The concentration of secondary plant compounds depends on plant age as well as on abiotic environmental factors (*e.g.*, light intensity, water stress, waterlogging, frost, pollution, and nutrient supply). In *Leucaena retusa* (goldenball leadtree) the production of organic sulfur compounds (COS and CS_2) from crushed roots increases with increasing supply of sulfate, especially in young seedlings (Feng and Hartel 1996). The concentration of L-theanine (a nonproteinogenic amino acid) and caffeine (alkaloid) in the shoot of *Camellia sinensis* (tea) decreases as leaves age (Song et al. 2012). Increased temperatures trigger a **drought stress** in *Pinus sylvestris* (Scots pine) in the Swiss Rhone valley which renders the host trees susceptible to insect attack. They also accelerate insect development. As more frequent drought periods are likely as a result of climate change, even trees only slightly or temporarily weakened will be more prone to attack by

aggressive species such as scolytine *Ips acuminatus* and the buprestid *Phaenops cyanea* (Wermelinger et al. 2008). Exposure of *Toxicodendron radicans* (poison ivy) to elevated atmospheric CO_2 concentrations enhances its growth as well as the production of urushiol, suggesting the rate of spread of poison ivy and its ability to recover from herbivory may be enhanced in a future environment with higher CO_2 concentrations (Ziska et al. 2007). In some plants, stress enhances the production of secondary metabolites, *e.g.*, in *Salix aquatica* (willow) the concentration of tannin and lignin is enhanced when plants are grown under N limitation as compared with an optimum supply (Northup et al. 1995). Spice and medicinal plants grown under water deficiency show much higher concentrations of isoprenoids, phenols or alkaloids compared with identical plants cultivated with sufficient water (Selmar and Kleinwächter 2013). These effects may be mediated via carbohydrate-modulated gene expression (Sect. 2.12.1). Whereas genes that encode photosynthetic enzymes are down-regulated by carbohydrates, evidence is accumulating that a number of defense genes are positively modulated by carbohydrates (Koch 1996; Ruan 2014).

Growth–defense trade-offs are thought to occur in plants due to resource restrictions, which demand prioritization towards either growth or defense, depending on external and internal factors (Huot et al. 2014). These tradeoffs have profound implications in agriculture and natural ecosystems, as both processes are vital for plant survival, reproduction, and, ultimately, plant fitness (Fig. 13.15A). We still have a lot to learn about the molecular mechanisms underlying growth and defense tradeoffs, and hormone crosstalk has emerged as a major player in regulating trade-offs needed to achieve a balance. Understanding the molecular basis of these tradeoffs in plants should provide a foundation for the development of breeding strategies that optimize the growth–defense balance to maximize crop yield to meet rising global food and biofuel demands (Fig. 13.15B).

13.4.2 Induced Defense and Communication Between Neighboring Plants

The production of secondary metabolites depends on abiotic environmental factors as well as on the presence of microbes and herbivores: **induced defense**. Physical damage of leaves often enhances the transcription of genes encoding polyphenol oxidase (Mayer 2006). Transgenic hybrid poplar saplings (*Populus tremula* x *Populus alba*) overexpressing horseradish peroxidase are more resistant to caterpillars (*Lymantria dispar*) than wild-type poplars. Their level of a phenolic substrate increases when leaves had prior feeding damage. Damaged leaves produce greater amounts of hydrogen peroxide, which is used by peroxidases to increase the production of semiquinone radicals in the midguts of the larvae (Barbehenn et al. 2010). Damage also induces the formation of total phenols shortly after simulated browsing, and these may persist for at least a month. Condensed tannins exhibit a delayed induction, but are more persistent, remaining for 2 months after simulated browsing. [*e.g.*, in *Abies balsamea* (balsam fir) (Nosko and Embury 2018)]. The production of proteinase inhibitors may also be enhanced [*e.g.*, in *Solanum nigrum* (black nightshade) (Hartl et al. 2010)].

In both *Fagus sylvatica* (European beech) and *Acer pseudoplatanus* (sycamore maple), **jasmonates** are activated after clipping of buds and leaves. Additional application of saliva roe deer (*Capreolus capreolus*) activates **salicylic acid** in beech leaves and leads to increases in cytokinins in beech buds. **Saliva** application also lead to an increased biosynthesis of several hydrolyzable tannins (mainly ellagitannins) and flavonols in maple leaves. Condensed tannins, the most abundant phenolics in beech buds and leaves, do not change after either clipping or saliva application. However, clipping with additional saliva application decreases levels of phenolic acids (cinnamic acid derivatives) in beech buds (Ohse et al. 2017). These plant responses reduce the quality of both the attacked and other leaves on the same plant as a food source (Sharma

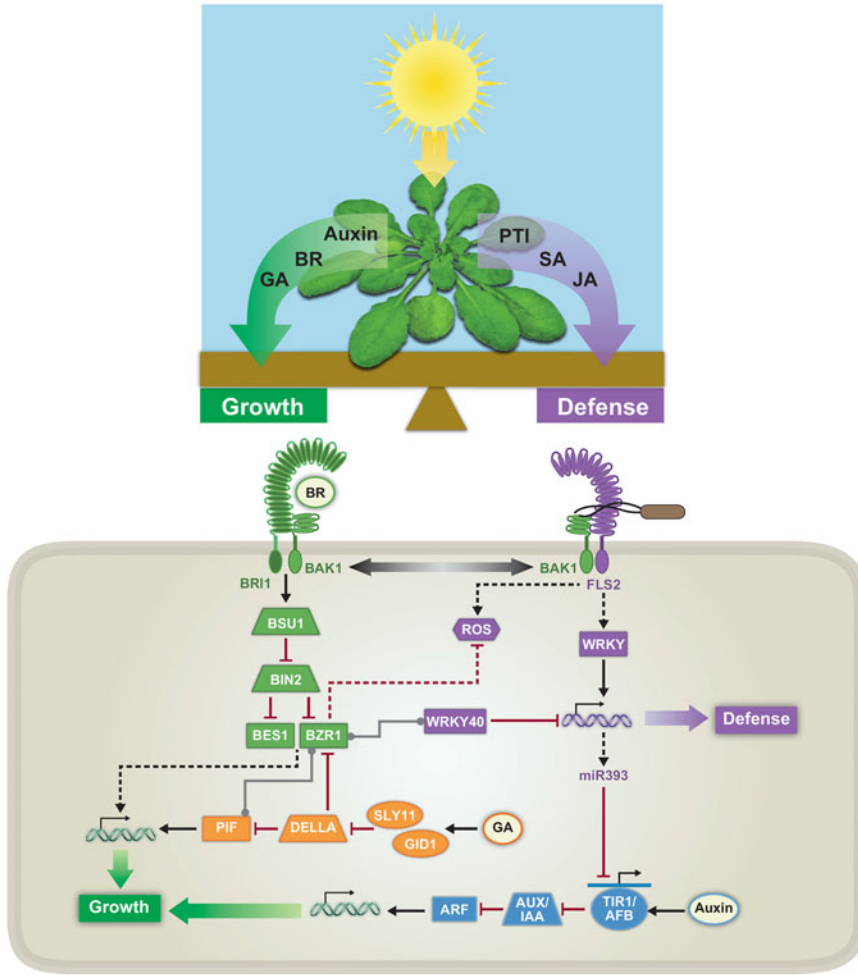

Fig. 13.15 (**A**) A diagram depicting the concept of growth vs. defense trade-offs. Plants use photosynthesis to convert light energy into chemical energy in the form of carbohydrates. These resources are then allocated towards growth or defense, depending on the presence or absence of specific stresses. This process is mediated by hormone cross-talk and is referred to as the growth–defense trade-off. (**B**) Known signaling contributing to growth–defense trade-offs between PTI-mediated defense and auxin-, BR-, and GA-mediated growth. BR, brassinosteroid; GA, gibberellin; PTI, pathogen-associated-molecular-pattern-triggered immunity; SA, salicylic acid; JA, jasmonates. Black arrows and red, blunted lines represent positive and negative regulation, respectively. Double helices with arrows represent global transcriptional reprogramming, and gray lines with dots at both ends indicate protein–protein interactions. Solid lines indicate a known connection between two components, whereas dashed lines indicate unknown connections or missing steps between two components. The solid blue line with an arrow represents expression of TIR1/AFB genes, the transcripts of which are targeted by miR393. FLS2, FLAGELLIN SENSING 2; ROS, reactive oxygen species; WRKY, WRKY DNA-BINDING PROTEIN; miR393, microRNA 393; TIR1, TRANSPORT INHIBITOR RESPONSE 1; AFB, AUXIN SIGNALING F-BOX; AUX/IAA, AUXIN-INDUCIBLE/INDOLE-3-ACETIC ACID INDUCIBLE; ARF, AUXIN RESPONSE FACTOR; BAK1, BRI1-ASSOCIATED RECEPTOR KINASE 1; BRI1, BRASSINOSTEROID INSENSITIVE 1; BSU1, BRI1 SUPPRESSOR 1; BIN2, BRASSINOSTEROID INSENSITIVE 2; BES1, BRI1-EMS-SUPPRESSOR 1; BZR1, BRASSINAZOLE-RESISTANT 1; SLY1, SLEEPY 1; GID1, GA.

et al. 2017). As a result of these induced responses, insects or large herbivores cannot feed continuously on a few leaves. Rather, they must constantly move among leaves which makes them more vulnerable to predators. Short-term induced defenses are effective against those herbivores that cause the initial damage.

There are also **long-term induced defenses** produced by the next cohort of leaves after severe insect outbreaks. These serve to protect plants against catastrophic herbivory by insects with large population outbreaks. Long-term induction is typically associated with increases in phenolics or fiber, less leaf protein and often smaller leaves. Long-term induced defenses are best developed in tree populations with an evolutionary history of outbreaking insects. In some cases they are induced more strongly by insect feeding than they are by comparable amounts of physical damage which suggests a tight evolutionary linkage with insect herbivores (Haukioja and Neuvonen 1985).

Induced responses in *Plantago lanceolata* are modulated by the **arbuscular mycorrhizal** (AM) fungus *Funneliformis mosseae* (Wang et al. 2015a). The AM fungus enhances the concentration of both catalpol and aucubin (Fig. 13.16). These are **iridoid glycosides**, whose levels can constitute more than 10% of leaf dry weight (Bowers et al. 1992). This response illustrates how AM fungi can boost the plant's defense, as further explored in Sect. 12.2.5. The amount of leaf area consumed by later arriving beet armyworms (*Spodoptera exigua*) decreases with time after induction by early herbivores. Mycorrhizal infection reduces the relative growth rate of later arriving herbivores, associated with a reduction in efficiency of conversion of ingested food, rather than a reduction in consumption. In nonmycorrhizal plants, leaf concentrations of catalpol shows a twofold increase during 8 days following early herbivory. By contrast, mycorrhizal plants, which already had elevated levels of leaf catalpol prior to their exposure to early herbivory, and do not show any further increase following herbivory. These results indicate that AM fungi result in a **systemic induction**, rather than priming of these defenses. Plant responses to future herbivores are not only influenced by exposure to prior aboveground and belowground organisms, but also by when these prior organisms arrive and interact (Wang et al. 2015a).

Although many studies show that species can induce defenses, this strategy makes little sense for expanding leaves when herbivore pressure is constantly high, for example in the tropics. In the case of *Inga*, a genus in species-rich rainforests, expanding leaves show little or no induction of quantitative or qualitative defense-related metabolites in response to herbivory; their defense is **constitutive** (Coley et al. 2018).

Neighboring, unattacked plants often respond by increasing the activity of enzymes involved in the synthesis of defense compounds and the concentration of defensive compounds (Fig. 13.17), and become less attractive to herbivores (Baldwin et al. 2006; Paschold et al. 2006). Neighbors may pick up signals as volatiles (Sugimoto et al. 2014; Erb 2018) or via mycorrhizal networks (Song et al. 2015). *Pseudotsuga menziesii* var. *glauca* (Douglas-fir) forests in North America are being damaged by drought and western spruce budworm (*Choristoneura occidentalis*). This damage is resulting from warmer and drier summers associated with climate change. Defoliated ectomycorrhizal fir trees directly transfer resources to *Pinus ponderosa* (ponderosa pine) regenerating nearby. Growing seedlings in pots with a mesh of 35 μm or 0.5 μm, or without a mesh barrier shows 'donor' plants transfer defense-inducing substances to ponderosa pine 'receiver' plants through **mycorrhizal networks**, but not through soil or root pathways (Song et al. 2015). Dolch and Tscharntke (2000) investigated the effects of manual defoliation, to simulate herbivory, of *Alnus glutinosa* (black alder) on subsequent herbivory by the alder leaf beetle (*Agelastica alni*) in northern Germany (Fig. 13.18). Subsequent damage by the leaf beetle is less when the trees are close to the manually defoliated tree. In addition, the extent of leaf consumption in laboratory feeding-preference tests and the number of eggs laid per leaf are positively correlated with distance from the defoliated tree. **Resistance** is therefore **induced**,

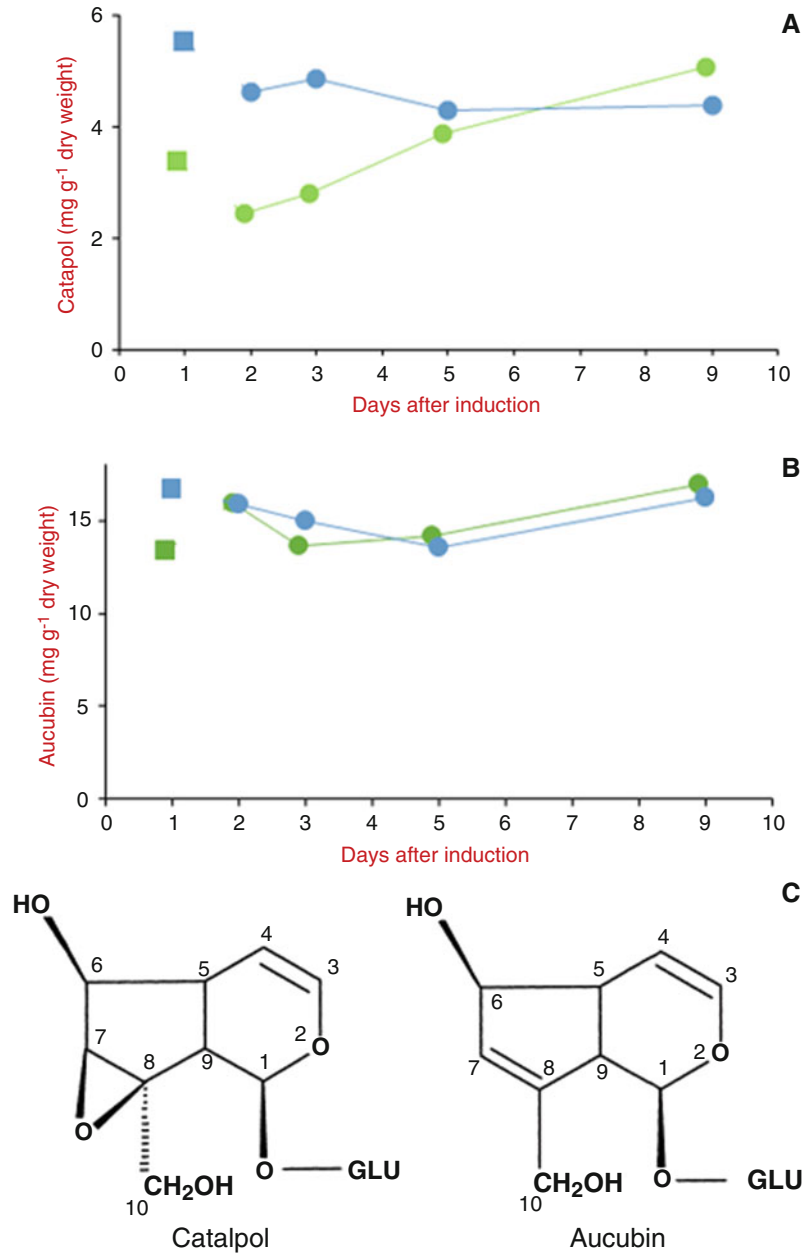

Fig. 13.16 Mean shoot catalpol (**A**) and aucubin (**B**) concentration of mycorrhizal (filled symbols) and nonmycorrhizal (open symbols) *Plantago lanceolata* (ribwort plantain) plants that had experienced no herbivory (squares) or a controlled 24 h period of herbivory 1, 2, 4, or 8 days prior to the bioassay (circles) (Wang et al. 2015a). (**C**) Structures of catalpol (1) and aucubin (2). GLU designates the glycosidic residue (Suomi et al. 2001); copyright Elsevier Science, Ltd.

both in defoliated alders and in their undamaged neighbors, demonstrating that defoliation triggers interplant resistance transfer, and therefore reduces herbivory in whole alder stands. This indicates that plants **communicate** with each other after herbivore attack.

Effects of leaf damage on neighboring trees of *Acer saccharum* (sugar maple) involve volatile signal transfer between leaves, because these effects are also found when plants are grown in separate pots. Volatile compounds play a role in this type of **communication** between plants, including octadecanoid-derived 'green leaf volatiles', volatile terpenoids and phenols (Tscharntke et al. 2001; Turlings and Ton 2006). **Jasmonate** is also involved; it primes

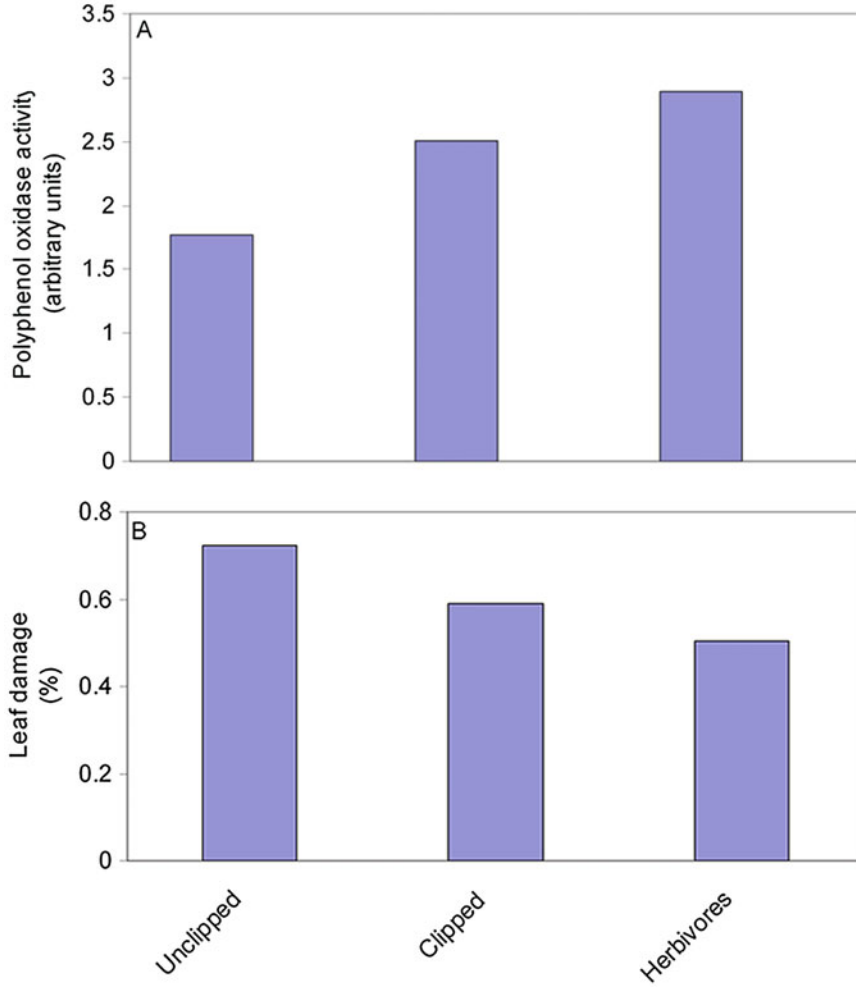

Fig. 13.17 Eavesdropping among plants in nature. (**A**) *Artemisia tridentata* (sagebrush) plants induce increased activity of polyphenol oxidase in neighboring *Nicotiana attenuata* (wild tobacco) plants when the sagebrush neighbors are either clipped manually or damaged by real herbivores. (**B**) Maximum proportion of tobacco leaves that are damaged by herbivores on tobacco plants with sagebrush neighbors that were unclipped, clipped artificially, or clipped by real herbivores (Karban et al. 2003); copyright Blackwell Science Ltd.

defense-related genes for induction upon subsequent defense elicitation (Ton et al. 2007). Plants of different species can also respond to signals released from damaged plants. For example, *Nicotiana attenuata* (wild tobacco) plants next to damaged *Artemisia tridentata* (sagebrush) plants have higher levels of the defensive enzyme polyphenol oxidase and reduced levels of insect damage, compared with control plants next to undamaged sagebrush plants (Karban et al. 2003). In addition to signaling via volatiles released from damaged leaves, plants also communicate via signals released from roots (Turlings et al. 2012). The relative importance of airborne and soil-borne signals as well as unknown effects of intensified nutrient absorption of defoliated trees, possibly reducing foliage quality of undamaged neighbors, remains to be further investigated (Fig. 13.19). This type of communication between plants of the same or different species offers a promising tool for **integrated pest management**, for example in *Gossypium hirsutum*

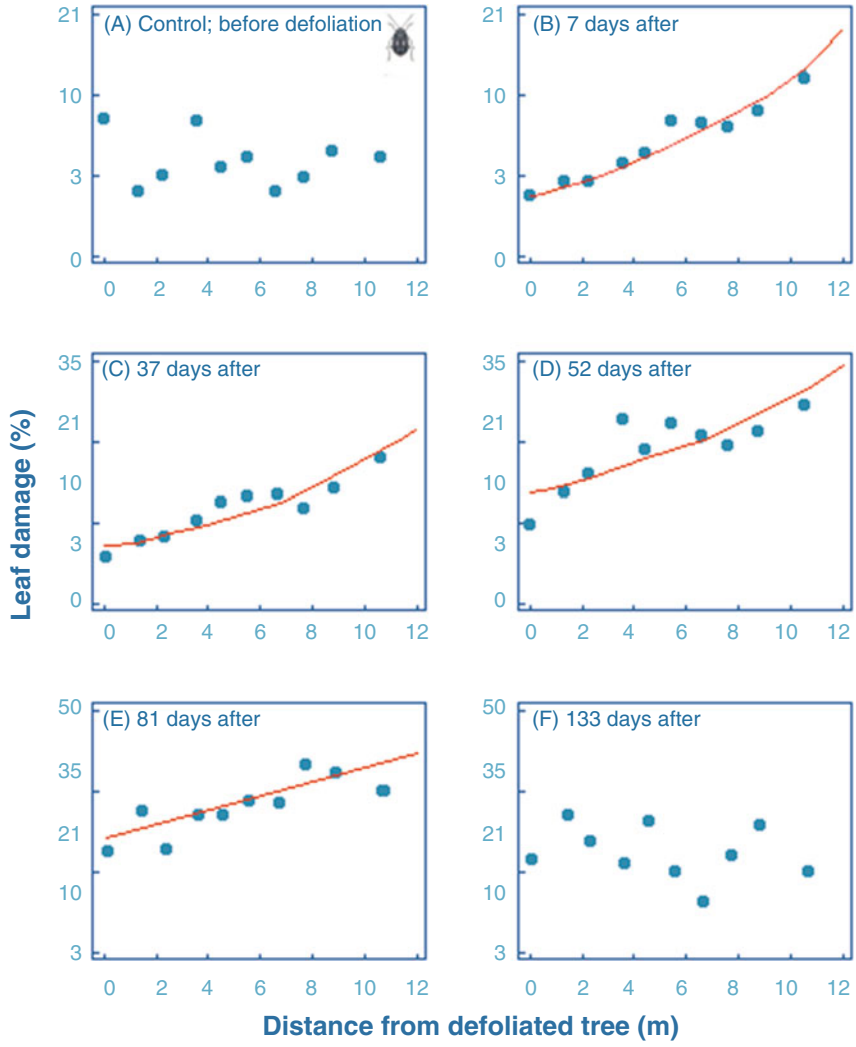

Fig. 13.18 Relationship between leaf damage by *Agelastica alni* (alder leaf beetle) to *Alnus glutinosa* (black alder) and distance from the manually defoliated tree in the field. (**A**) Control: before defoliation, the amount of leaf damage within each plot is randomly distributed. (**B–E**) 7–81 days after defoliation: herbivory by *Agelastica alni* is greater at increasing distance from the manually defoliated tree. (**F**) 133 days after defoliation: the distribution pattern of leaf damage no longer depends on distance from the manually defoliated tree (Dolch and Tscharntke 2000); copyright © 2000, Springer-Verlag.

(cotton) (Llandres et al. 2018). Enhancing cotton pest management using plant natural defenses can improve the management of crop pests, based on an ancient technique called **plant training** or **priming**. Trained plants can be promoted to a state of enhanced defense that causes faster and more robust activation of their defense responses. It can mediate plant interactions with conspecific neighbors plants, pests, and associated natural enemies. Plant training for induced defense involves inducing plant defense by artificial injuries. Experimental evidence from various studies shows that cotton training is a promising technique, particularly for smallholders which can be used to significantly reduce insecticide use and to improve productivity in cotton farming (Llandres et al. 2018).

There is a wide variation in the extent to which plants respond to browsing with an increased concentration of phenolics. Of three

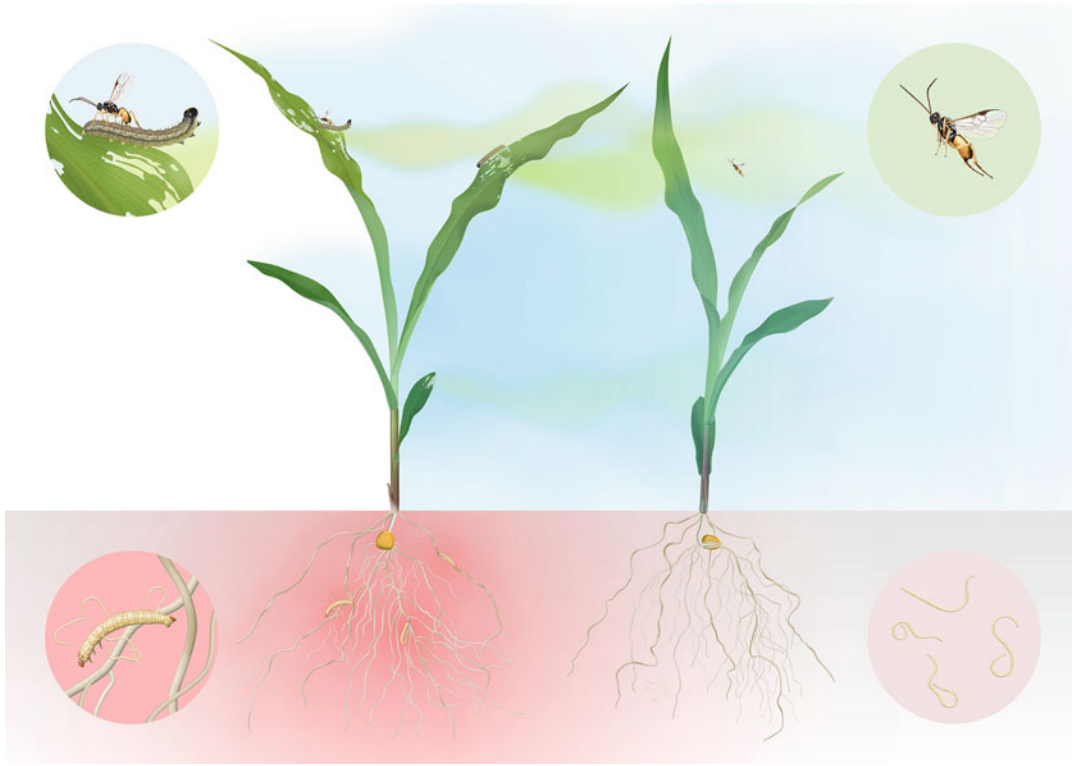

Fig. 13.19 When damaged by caterpillars, young plants of *Zea mays* (corn), immediately release several typical octadecanoid-derived 'green leaf volatiles' from the damaged sites (indicated in green). In addition, elicitors in the caterpillar's oral secretions cause the induction of a systemic release of volatiles that mainly comprise terpenoids but also include some aromatic compounds, such as indole and methyl salicylate (indicated in blue). This blend of herbivore-induced volatiles is highly attractive to various parasitic wasps that lay their eggs in the caterpillars. Belowground beetle larvae might cause the emission of similar signals by damaged roots (indicated in red). Corn roots release one dominating compound, (E)-β-caryophyllene, in response to root feeding. This sesquiterpene is attractive to entomopathogenic nematodes and increases the effectiveness of these nematodes in finding and killing herbivore larvae. In addition, the herbivore-induced volatiles might repel other herbivores and can induce or prime defense responses in neighboring plants. All of these effects might be exploitable for the control of agricultural pests (after Turlings and Ton 2006); copyright Elsevier Science, Ltd.

South African Karoo shrubs, the deciduous species [*Osteospermum sinuatum* (African daisy)] is the most palatable. It contains very few polyphenols, does not enhance this level upon browsing, but has a high **regrowth capacity**. On the other hand, the evergreen succulent species (*Ruschia spinosa*) shows almost no regrowth after browsing, but contains the highest level of constitutive and browser-induced levels of polyphenols, condensed tannins, and protein-precipitating tannins. The evergreen sclerophyllous species [*Pteronia pallens* (scholtz bush)] shows an intermediate response in terms of regrowth capacity and browser-induced phenols. It also contains intermediate levels of phenols before browsing (Stock et al. 1993). This suggests a trade-off between allocation to (induced) defense (**avoidance**) and regrowth capacity (**tolerance**) upon attack by herbivores.

In *Leucaena* (leadtree) species (Feng and Hartel 1996) and several other Fabaceae (Piluk et al. 2001; Musah et al. 2015), damaging the roots or shoots greatly enhances the production of organic sulfur compounds (COS and CS_2). These are foul-smelling compounds, derived from djenkolic acid, a nonproteinogenic amino acid. They are toxic to bacteria, fungi, and animals like nematodes and insects.

13.4.3 Communication Between Plants and Their Bodyguards

Volatile compounds play a role in communication between neighboring plants, when attacked by herbivores (Sect. 13.4.2), as well as between plants and predatory mites or parasitic wasps. These **tritrophic systems** offer another fascinating example of coevolution in the arms race between plants and herbivores, except now there is an ally involved: **indirect defense**, as opposed to the **direct defense** responses that were discussed above in this chapter (Alba et al. 2012). The volatiles that are released by leaves upon attack by herbivorous mites or caterpillars attract predatory mites or parasitic wasps, respectively. These predatory mites and parasitic wasps then act as **bodyguards** (D'Alessandro et al. 2006). The attractants produced by plants upon attack are specific in that they are not produced upon artificially damaging the leaves or are produced in much smaller quantities. Upon attack of *Brassica oleracea* (cabbage) plants by caterpillars of *Pieris brassicae* (cabbage moth) the plant responds to a specific caterpillar enzyme (-β-galactosidase) with the synthesis of a mixture of volatiles, which are highly specific for a parasitic wasp, *Cotesia glomerata* (Vos et al. 2001). Leaves treated with β-galactosidase from almonds respond in a similar manner, which shows that this compound acts as an 'elicitor' (Mattiacci et al. 1995). *Zea mays* plants attacked by larvae of *Spodoptera frugiperda* and *Spodoptera exigua* (armyworms) respond to a specific compound [N-(17-hydroxylinolenoyl)-L-glutamine, or volicitin] (Alborn et al. 1997). Upon attack, they emit terpenoids and indole that attract a parasitic wasp, *Cotesia marginiventris*. Mechanical damage, without application of volicitin, does not trigger the same blend of compounds. When infested by the larvae of *Pseudaletia separata*, the corn plants emit terpenoids, indole, oximes, and nitriles that attract *Cotesia kariyai*. The production of the attractants is **systemic**. In other words, it is not restricted to the damaged parts of the plant, but also occurs in undamaged leaves.

Several crop species infested by the herbivorous two-spotted spider mite, *Tetranychus urticae*, or larvae of *Spodoptera exigua* (beet armyworm) become attractive to a predatory mite, *Phytoseiulus persimilis* and *Cotesia marginiventris*, respectively (Fig. 13.19). Many plant species respond to arthropod attack with the release of a blend of volatiles that attract predators or parasitic wasps. Each species, however, produces its own blend of chemicals that attract their **bodyguards** (Xiao et al. 2012). The bodyguards can learn to distinguish between herbivore-induced volatiles emitted by different species. The attractants produced by *Phaseolus lunatus* are presented in Fig. 13.20. There is substantial genetic variation in the amount of attractants produced upon attack on which natural selection can act (Baldwin et al. 2006; Joo et al. 2018). This provides substantial scope for breeding efforts to exploit this aspect of ecological biochemistry. Tritrophic interactions are not restricted to above-ground plant organs and interacting animals. For example, *Thuja occidentalis* releases chemicals upon attack by larvae of *Otiorhynchus sulcatus* (a weevil) and thus attracts *Heterorhabditis megidis* (a parasitic nematode), which then preys on the weevil larvae (Van Tol et al. 2001). Similar **below-ground tritrophic interactions** occur in *Zea mays* (corn). Upon attack by beetle larvae, their roots release a sesquiterpene, (E)-β-caryophyllene, which attracts entomopathogenic nematodes and increases the effectiveness of these nematodes in finding and killing herbivore larvae (Rasmann et al. 2005). Improved knowledge in this area should provide opportunities for applications in plant management systems, similar to those existing for above-ground tritrophic interactions (Turlings et al. 2012).

A fascinating example of a tritrophic interaction is found in *Nicotiana attenuata* (wild tobacco), which contains high levels of the alkaloid **nicotine** (up to 12% of the dry mass of leaves). Upon attack by most herbivores, **jasmonic acid** is produced, which is transported via the phloem to the roots. Here, it induces the production of more nicotine, which is transported

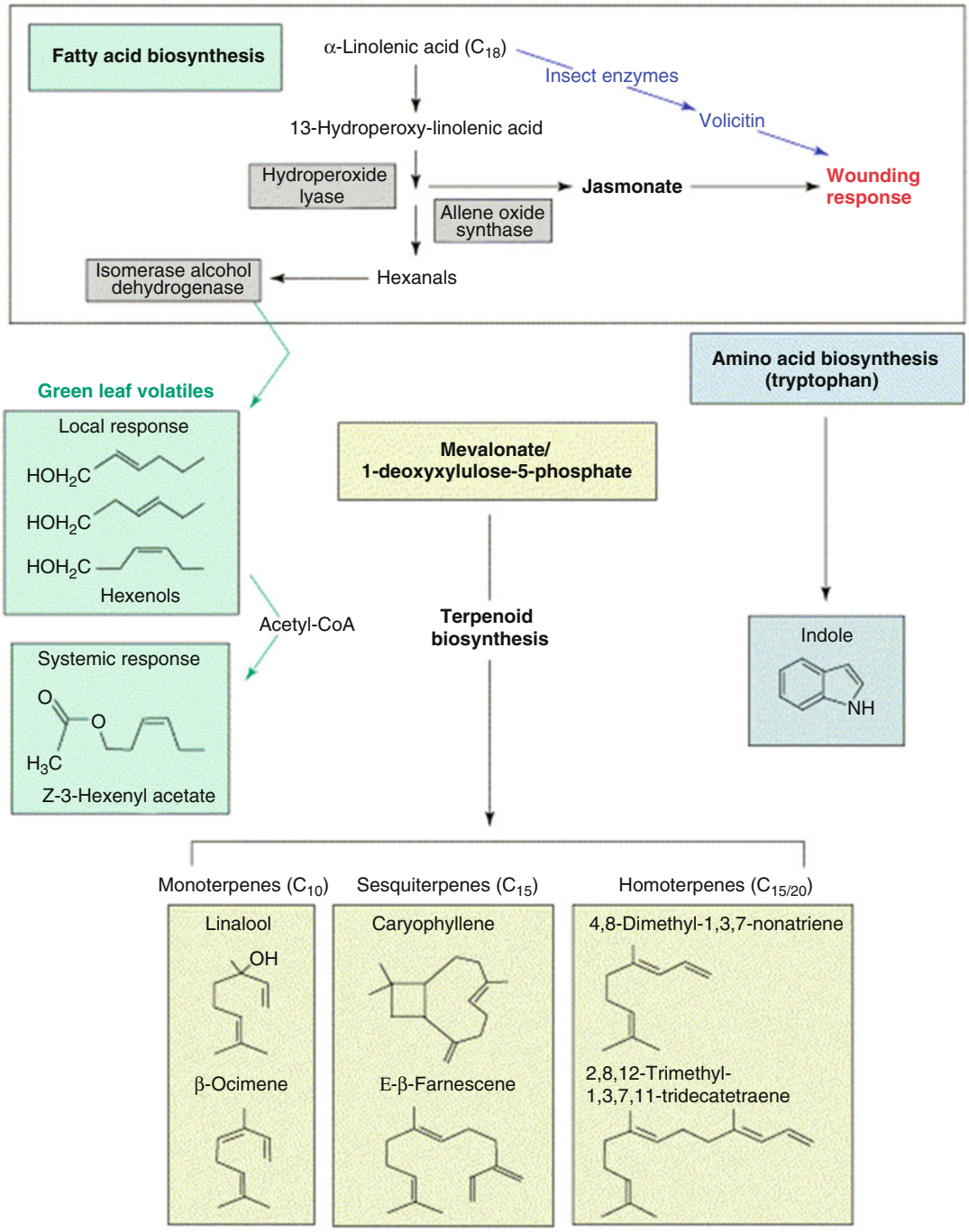

Fig. 13.20 General overview of plant volatiles synthesised in response to insect attack, either locally or systemically (after Ferry et al. 2004); copyright Elsevier Science, Ltd.

to the leaves, via the xylem, where it accumulates to even higher levels than in control plants. When a specialist caterpillar, *Manduca sexta* (tobacco hawkmoth) attacks *Nicotiana attenuata*, however, there is no increased synthesis and accumulation of nicotine. Rather, **bodyguards** are

attracted, involving specific signals, like in the examples given above. The bodyguards can kill the specialist caterpillar, without being affected by increased nicotine levels in the caterpillar. That is, in this case, suppression of the transduction pathway that leads to increased nicotine levels in the leaves is advantageous for the host plant (Kahl et al. 2000).

13.5 The Costs of Chemical Defense

The production of secondary plant compounds requires **investment** of carbon, as well as some other elements. Does this mean that a gram of biomass is more costly to produce if it contains large quantities of secondary plant compounds? This is not so when costs are expressed in terms of grams of glucose required for carbon skeletons and for production of energy to produce the biomass. Approximately equal amounts of glucose are needed to produce 1 g of dry mass in slow-growing herbaceous species (which contain relatively small amounts of phenolic compounds) and fast-growing ones (Sect. 3.5). Per gram of fresh mass or per unit leaf area, the situation is different, but this is due to the lower water content or thicker leaves of the slow-growing species.

13.5.1 Diversion of Resources from Primary Growth

There are **costs** associated with the strategy of accumulating vast quantities of secondary plant compounds. This can best be illustrated by imagining a leaf with a certain amount of protein. If half of this protein were to be replaced by lignin or tannin, then its physiological performance would probably be less. It is quite likely that its photosynthetic capacity would decline by approximately half. The greater costs of well protected leaves, therefore, do not reflect high costs of the production of new leaves. Rather, defense is costly, because it diverts resources from primary growth (an opportunity cost, *i.e.* the cost of resources that would otherwise be gained by an alternative allocation), which reduces the potential growth rate of the plant (Fig. 13.15).

Investment of large quantities of resources in secondary plant compounds that reduce herbivory will lead to greater plant fitness only when the costs of repairing the damage incurred by herbivory exceed those needed for protection. This explains why quantitatively important secondary plant compounds are more pronounced in inherently slow-growing species from low-productivity environments than they are in fast-growing ones from more productive habitats. Costs select against defensive adaptations, whereas herbivore pressure leads to investment in defense. Defensive adaptations may then lead to offensive adaptations in animals (*e.g.*, the coevolution of fluoroacetate-bearing *Gastrolobium* species and Western Australian native animals) (Fig. 13.21).

13.5.2 Strategies of Predators

Two strategies may be discerned among the offensive adaptations of animals (Fig. 13.22). The evolutionary response to communication between plants which leads to the accumulation of protective compounds in neighboring plants may be to **suppress the communication** or to emit **countersignals**. The response to the accumulation of protective compounds in plants upon recognition of a predator may be either to **suppress recognition** of the predator or to **consume** the plant quickly and so prevent protection (surprise). Inducible defenses may be counteracted by **suppression** of the induced defense or by decreasing the defense. Constitutive defense may be counteracted by detoxification or avoidance of the most toxic plant parts (Karban and Agrawal 2002). In addition, prior attack of *Nicotiana attenuata* (wild tobacco) by some insects, *e.g.*, the sap-feeding *Tupiocoris notatus*, results in '**vaccination**' of the tobacco plant against subsequent attacks by chewing hornworms (*Manduca sexta*). This vaccination is mediated by a combination of direct and indirect defenses (Kessler et al. 2006).

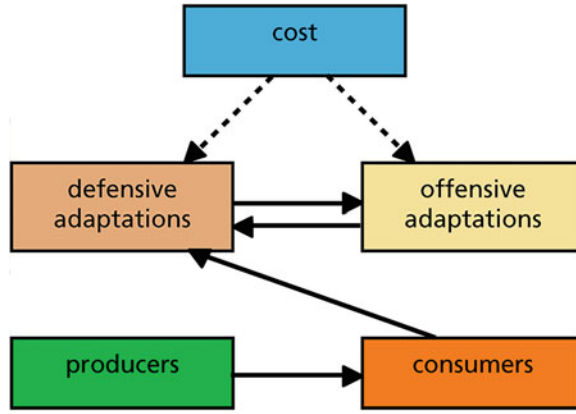

Fig. 13.21 Interactions between higher plants and animals involving secondary plant compounds. Attack by herbivores leads to the evolution of protection with defense compounds (defensive adaptations in producers). At the same time, there is a selection against production of defense compounds because it incurs a cost. Defensive adaptations in plants lead to the evolution of offensive adaptations in consumers. These offensive adaptations are selected against because they incur some costs (after Rhoades 1985).

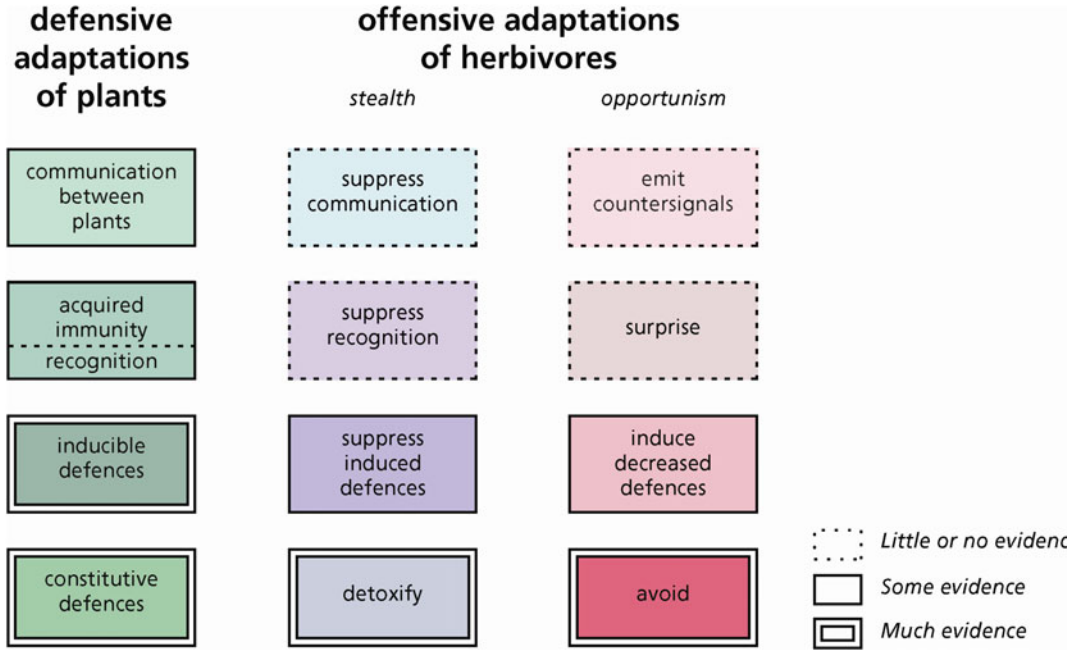

Fig. 13.22 The evolutionary strategy of 'stealthy' and 'opportunistic' animals to cope with the defensive adaptations of plants (after Rhoades 1985).

13.5.2.1 Mutualistic Associations with Ants and Mites

Instead of investing in defense compounds, plants can also form a **mutualistic association** with animals that protect them. Several thousand seed plants have extrafloral nectaries that indicate some level of **ant defense**. *Phaseolus lunatus* (lima bean) plants increase the secretion of

extrafloral nectar after exposure to spider-mite (*Tetranychus urticae*)-induced plant volatiles. Predatory mites (*Phytoseiulus persimilis*), disperse more slowly from an exposed intact plant than from a control plant (plant exposed to volatiles from intact conspecific). The predators also disperse more slowly from those plants that are provided with extra extrafloral nectar than from untreated plants (Choh et al. 2006).

Most mutualistic associations involve a limited coevolved specialization between the partners. A small number of plant species that attract ants for their defense [*e.g.*, species belonging to the genera *Acacia* (wattle), *Cecropia*, and *Macaranga*] have obligate or facultative relationships with a single ant species. *Acacia* species that form an obligate relationship provide their allies with nectar, lipids, and proteins in special structures, and shelter in special plant parts (**domatia**). The resident ants are very aggressive and defend the tree against both invertebrate and vertebrate herbivores. Some of these species have lost their major line of chemical defense against herbivores, and the tree is quickly destroyed if the ants are removed. The costs of ant defense (production of extrafloral nectaries), therefore, are partly compensated for by lower costs of chemical defense (Heil et al. 2001). However, there are additional benefits in that the ants bring in substantial resources, and most of the N that is accumulated in *Cecropia peltata* (trumpet tree) trees is derived from debris deposited by its mutualistic *Azteca* ants (Fig. 13.23; Sagers et al. 2000).

The defending ants form a potential risk, however, because the plants still need a suite of insect

Fig. 13.23 An example of a mutualistic association between an ant plant (*Cecropia peltat*a) and an ant (*Azteca xanthochroa*). (Top left) *Cecropia peltata* growing in the cerrado in Brazil. (Bottom left) Trunk of *Cecropia peltata* showing one of the many entry points for *Azteca xanthochroa* (Aztec ant, an ant species defending the tree). The base of each petiole bears a trichilium, a pad of densely packed trichomes, from which emerge 1–2 mm long glycogen-containing beads called Muellerian bodies. (Top right) An individual of an Aztec ant exiting the special hole in the stem, and another one descending from the stem. (Bottom right) Cross section of the stem of *Cecropia peltata*, showing the hollow stem and perforated internodes, large enough for Aztec ants to move up and down the stem.

pollinators for cross-pollination. Observations on the African *Vachellia* (formerlya *Acacia*) *zanzibarica* reveal that ants quickly abandon first-day flowers when they encounter them, and return after pollinator activity ceases. It is likely that a volatile that triggers alarm behavior in ants is produced by flowers before pollination has occurred, but this has yet to be confirmed (Willmer and Stone 1997).

In addition to ants, predatory mites may also inhabit domatia, *e.g.*, on leaves of *Cupania vernalis* in southeast Brazil. Blocking leaf domatia shows that leaf domatia can benefit plants against herbivory in a natural system (Romero and Benson 2004).

13.6 Detoxification of Xenobiotics by Plants: Phytoremediation

Plants, like any other organisms in any environment, are continually exposed to potentially toxic chemicals that are not naturally synthesized by the plant itself: **xenobiotics**. These xenobiotics may be natural secondary plant chemicals, which we discussed in this chapter, industrial pollutants, or agrochemicals. Many xenobiotics are lipophilic; they are therefore readily absorbed and accumulate to toxic levels within the plant, unless effective means of detoxification are present. If plants have pathways to produce and cope with a vast array of natural secondary chemicals, can they also be put to use to clean up environmental pollutants? In Sect. 9.3.3.2, we discuss the capacity of **metallophytes** to clean up inorganic pollutants. In this section we discuss the capacity of some plants to detoxify **organic pollutants** (Martin et al. 2014; Rezania et al. 2015).

The cellular detoxification systems of plants dispose of the xenobiotics by two sequential processes (Coleman et al. 1997):

1. Chemical modification
2. Compartmentation

The reactions responsible for chemical modification of lipophilic xenobiotics involve hydrolysis or oxidation that makes the chemicals more hydrophilic, and creates reactive sites by the addition or exposure of functional groups (*e.g.*, hydroxyl or carboxyl groups) (step I); the modified chemicals may still be toxic. If the xenobiotic already has a functional group that is suitable for conjugation, then there is no need for step I. The next step is the conjugation of the modified xenobiotic (phase II), followed by export from the cytosol (step III).

Hydrolysis of the xenobiotics in phase I is catalyzed by various esterases and amidases, but the major reactions are oxidations catalyzed by the **cytochrome P-450** system, which involves mono-oxygenases that insert one atom of oxygen into inert hydrophobic molecules to make them more reactive and water-soluble (Siminszky 2006). The rates of chemical transformation and the types of metabolites that are formed depend on plant genotype and accounts for variation in **herbicide resistance** and **tolerance to pollutants**. In phase II, the (modified) xenobiotic is deactivated by covalent linkage to endogenous hydrophilic molecules (*e.g.*, glucose, malonate, or glutathione) which produces a water-soluble nontoxic conjugate. Export of the conjugates from the cytosol to the vacuole or apoplast (phase III) occurs by membrane-located transport proteins. This detoxification pathway shares many features with the pathway used by plants for the vacuolar deposition of secondary metabolites (*e.g.*, anthocyanins).

One important detoxification mechanism is chemical modification of the xenobiotic by covalent linkage to tripeptides like **glutathione**. Conjugation with xenobiotics may take place spontaneously or may require catalysis by glutathione-S-transferase (Komives and Gullner 2005). Glutathione is an important plant metabolite that acts both as a reducing agent that protects the cell against oxidative stress (Sects. 7.2.2.2 and 7.3.1) and guards against chemical toxicity via the modification reactions of phase II. Glutathione conjugates that are deposited in the vacuole can undergo further metabolism. For example, the glycine residue of the glutathione moiety may be removed enzymatically which is sometimes followed by enzymatic removal of the glutamic acid residue (Fig. 13.24).

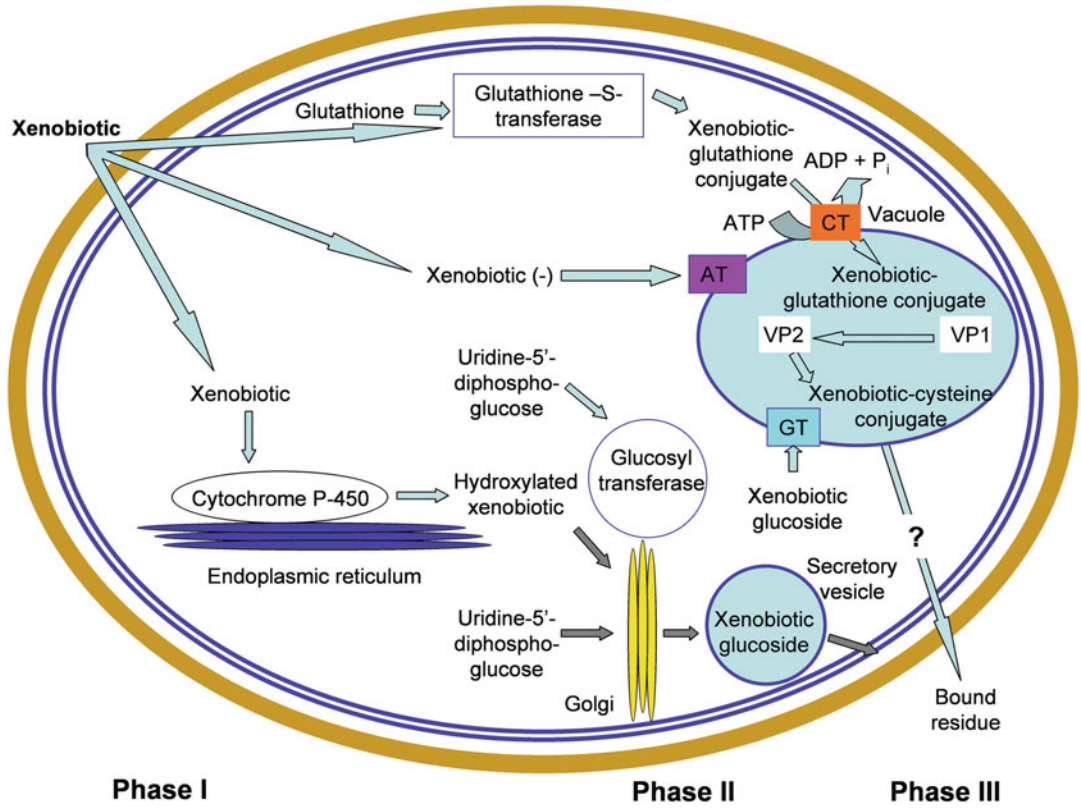

Fig. 13.24 Enzyme-catalyzed reactions that are responsible for the detoxification of xenobiotics in plants are localized in or associated with several organelles and cellular compartments. The grey arrows represent a proposed pathway for the glucosylation of xenobiotics in the Golgi, followed by release of the metabolites via exocytosis. CT, glutathione-conjugate; AT, ATP-dependent xenobiotic anion transporter; GT, ATP-dependent glucoside-conjugate transporter; VP, vacuolar peptidases that catalyze the removal of glycine (VP1) and glutamic acid (VP2) from the glutathione moiety of the conjugate. For further explanation, see text (after Coleman et al. 1997).

The glutathione-mediated and related detoxification systems probably evolved for the metabolism and compartmentation of natural substrates. For example, a glutathione-S-transferase is required for the synthesis of **anthocyanins**; it produces a glutathione-conjugate that can be transported to the vacuole. Cytochrome P-450 is, similarly, involved in anthocyanin biosynthesis. Therefore, the selective mechanisms that led to the catalytic proteins of the pathway that has an apparent specificity for industrial chemicals are probably associated with the metabolism of natural secondary plant products, including allelochemicals and pigments (Komives and Gullner 2005).

Plants, unlike microorganisms and animals, are unable to catabolize xenobiotics; instead, detoxification mechanisms have evolved that lead to the formation of water-soluble conjugates that are compartmented in the vacuole or deposited in the apoplast. The residues may persist in plant tissues for a considerable time, and may affect consumers of the plant tissues. A thorough understanding of the metabolic fate of xenobiotics is therefore important. Genetic engineering of crops with plant or bacterial genes has already produced transgenics that are resistant to herbicides and air pollutants. In time, similar approaches may lead to workable strategies to develop the **phytoremediation** of land and

water polluted by industrial chemicals. For example, *Nicotiana tabacum* (tobacco) plants overexpressing a glutathione transferases have increased tolerance to the diphenyl ether herbicide fluorodifen (Lo Cicero et al. 2015).

13.7 Secondary Chemicals and Messages That Emerge from This Chapter

Plants produce a wealth of secondary plant compounds that play a pivotal role in defense and communication. We are only just beginning to understand how plants communicate with their neighbors, symbionts, pathogens, herbivores, and with their 'bodyguards', both above- and belowground, via chemical signals, which are often very specific. This new area is fascinating from an ecological and evolutionary point of view, and it has tremendous potential for major applications in agriculture, forestry, and horticulture. For example, **intercrops** and **trained plants** can be selected that protect a crop in an environmentally friendly manner (Sect. 16.6.2). For the intercrop to be of maximum benefit, however, intercrops should not compete to any great extent with the crop plant. It is up to ecophysiologists to help define desirable traits of an intercrop, with respect to its secondary chemistry, and also in terms of root traits that minimize competition of the intercrop or, even better, that are beneficial to the crop. Numerous pertinent traits can be found in this and preceding chapters to help identify a desirable intercrop. Plants can also be used for phytoremediation, to remove organic pollutants from the environment.

Knowledge of the chemical compounds that protect plants, preferably with identification of the genes encoding the traits, will allow us to design crop plants that are better protected against herbivores. Such plants will reduce the need for pesticides, and many examples are now available of transgenic plants with enhanced protection. We should be aware, however, that the arms race between plants and herbivores will continue, and that for every new crop genotype resistant herbivores will coevolve. A thorough understanding of the intricate chemical interactions between plants and their herbivores is required to sustainably enhance the production of new crops.

INSENSITIVE DWARF 1A; DELLA, repressor protein; PIF, PHYTOCHROME INTERACTING FACTOR (Huot et al. 2014); copyright Elsevier Science, Ltd.).

References

Alba J, Allmann S, Glas J, Schimmel BJ, Spyropoulou E, Stoops M, Villarroel C, Kant M 2012. Induction and suppression of herbivore-induced indirect defenses. In: Witzany G, Baluška F eds. *Biocommunication of Plants*. Berlin Springer, 197–212.

Alborn HT, Turlings TCJ, Jones TH, Stenhagen G, Loughrin JH, Tumlinson JH. 1997. An elicitor of plant volatiles from beet armyworm oral secretion. *Science* **276**: 945–949.

Authier F, Djavaheri-Mergny M, Lorin S, Frénoy JP, Desbuquois B. 2016. Fate and action of ricin in rat liver in vivo: translocation of endocytosed ricin into cytosol and induction of intrinsic apoptosis by ricin B-chain. *Cell Microbiol* **18**: 1800–1814.

Bais HP, Park S-W, Weir TL, Callaway RM, Vivanco JM. 2004. How plants communicate using the underground information superhighway. *Trends Plant Sci* **9**: 26–32.

Bais HP, Weir TL, Perry LG, Gilroy S, Vivanco JM. 2006. The role of root exudates in rhizosphere interactions with plants and other organisms. *Annu Rev Plant Biol* **57**: 233–266.

Baldwin IT, Halitschke R, Paschold A, von Dahl CC, Preston CA. 2006. Volatile signaling in plant-plant interactions: "talking trees" in the genomics era. *Science* **311**: 812–815.

Baldwin IT, Preston CA. 1999. The eco-physiological complexity of plant responses to insect herbivores. *Planta* **208**: 137–145.

Ballhorn DJ, Godschalx AL, Smart SM, Kautz S, Schädler M. 2014. Chemical defense lowers plant competitiveness. *Oecologia* **176**: 811–824.

Barbehenn R, Dukatz C, Holt C, Reese A, Martiskainen O, Salminen J-P, Yip L, Tran L, Constabel C. 2010. Feeding on poplar leaves by caterpillars potentiates foliar peroxidase action in their guts and increases plant resistance. *Oecologia* **164**: 993–1004.

Bartholomew B. 1970. Bare zone between California shrub and grassland communities: the role of animals. *Science* **170**: 1210–1212.

Bennett RN, Wallsgrove RM. 1994. Secondary metabolites in plant defence mechanisms. *New Phytol* **127**: 617–633.

Bird DA, Franceschi VR, Facchini PJ. 2003. A tale of three cell types: alkaloid biosynthesis is localized to sieve elements in opium poppy. *Plant Cell* **15**: 2626–2635.

Birkett MA, Chamberlain K, Hooper AM, Pickett JA. 2001. Does allelopathy offer real promise for practical weed management and for explaining rhizosphere interactions involving higher plants? *Plant Soil* **232**: 31–39.

Bolognesi A, Bortolotti M, Maiello S, Battelli M, Polito L. 2016. Ribosome-inactivating proteins from plants: a historical overview. *Molecules* **21**: 1627.

Borochov-Neori H, Judeinstein S, Greenberg A, Volkova N, Rosenblat M, Aviram M. 2015. Antioxidant and antiatherogenic properties of phenolic acid and flavonol fractions of fruits of 'Amari' and 'Hallawi' date (*Phoenix dactylifera* L.) varieties. *J Agric Sci Food Chem* **63**: 3189–3195.

Bowers DM, Collinge SK, Gamble SE, Schmitt J. 1992. Effects of genotype, habitat, and seasonal variation on iridoid glycoside content of *Plantago lanceolata* (Plantaginaceae) and the implications for insect herbivores. *Oecologia* **91**: 201–207.

Boyd RS. 2012. Plant defense using toxic inorganic ions: conceptual models of the defensive enhancement and joint effects hypotheses. *Plant Sci* **195**: 88–95.

Brower LP. 1969. Ecological chemistry. *Sci Am* **220**: 22–29.

Bryant JP, Reichardt PB, Clausen TP, Provenza FD, Kuropat P 1992. Woody plant-mammal interactions. In: Rosenthal GA ed. *Herbivores: Their Interactions with Secondary Plant Metabolites*. San Diego: Academic Press, 343–370.

Bryant JP, Tahvanainen J, Sulkinoja M, Julkunen-Tiitto R, Reichardt P, Green T. 1989. Biogeographic evidence for the evolution of chemical defense by boreal birch and willow against mammalian browsing. *Amer Nat* **134**: 20–34.

Campos-Vega R, Loarca-Piña G, Oomah BD. 2010. Minor components of pulses and their potential impact on human health. *Food Res Int* **43**: 461–482.

Celedon JM, Yuen MMS, Chiang A, Henderson H, Reid KE, Bohlmann J. 2017. Cell-type- and tissue-specific transcriptomes of the white spruce (*Picea glauca*) bark unmask fine-scale spatial patterns of constitutive and induced conifer defense. *Plant J* **92**: 710–726.

Chakravarthy VSK, Reddy TP, Reddy VD, Rao KV. 2014. Current status of genetic engineering in cotton (*Gossypium hirsutum* L): an assessment. *Crit Rev Biotechnol* **34**: 144–160.

Chen S, Xiao S, Callaway RM. 2012. Light intensity alters the allelopathic effects of an exotic invader. *Plant Ecol Divers* **5**: 521–526.

Chitwood DJ. 2002. Phytochemical based strategies for nematode control. *Annu Rev Phytopathol* **40**: 221–249.

Choh Y, Kugimiya S, Takabayashi J. 2006. Induced production of extrafloral nectar in intact Lima bean plants in response to volatiles from spider mite-infested conspecific plants as a possible indirect defense against spider mites. *Oecologia* **147**: 455–460.

Chou C-H, Kuo Y-L. 1986. Allelopathic research of subtropical vegetation in Taiwan. *J Chem Ecol* **12**: 1431–1448.

Clausen TP, Reichardt PB, Bryant JP, Werner RA, Post K, Frisby K. 1989. Chemical model for short-term induction in quaking aspen (*Populus tremuloides*) foliage against herbivores. *J Chem Ecol* **15**: 2335–2346.

Coleman J, Blake-Kalff M, Davies E. 1997. Detoxification of xenobiotics by plants: chemical modification and vacuolar compartmentation. *Trends Plant Sci* **2**: 144–151.

Coley PD, Endara M-J, Kursar TA. 2018. Consequences of interspecific variation in defenses and herbivore host choice for the ecology and evolution of Inga, a speciose rainforest tree. *Oecologia* **187**: 361–376.

Cooke J, Leishman MR. 2012. Tradeoffs between foliar silicon and carbon-based defences: evidence from vegetation communities of contrasting soil types. *Oikos* **121**: 2052–2060.

Cragg GM, Newman DJ. 2003. Plants as a source of anti-cancer and anti-HIV agents. *Ann Appl Biol* **143**: 127–133.

D'Alessandro M, Held M, Triponez Y, Turlings T. 2006. The role of indole and other shikimic acid derived maize volatiles in the attraction of two parasitic wasps. *J Chem Ecol* **32**: 2733–2748.

de Oliveira JL, Campos EVR, Bakshi M, Abhilash PC, Fraceto LF. 2014. Application of nanotechnology for the encapsulation of botanical insecticides for sustainable agriculture: prospects and promises. *Biotechnol Adv* **32**: 1550–1561.

Ding J, Sun Y, Xiao CL, Shi K, Zhou YH, Yu JQ. 2007. Physiological basis of different allelopathic reactions of cucumber and figleaf gourd plants to cinnamic acid. *J Exp Bot* **58**: 3765–3773.

Dirzo R, Raven PH. 2003. Global State of Biodiversity and Loss. *Annu Rev Environ Res* **28**: 137–167.

Dolch R, Tscharntke T. 2000. Defoliation of alders (*Alnus glutinosa*) affects herbivory by leaf beetles on undamaged neighbours. *Oecologia* **125**: 504–511.

Eckstein-Ludwig U, Webb RJ, van Goethem IDA, East JM, Lee AG, Kimura M, O'Neill PM, Bray PG, Ward SA, Krishna S. 2003. Artemisinins target the SERCA of Plasmodium falciparum. *Nature* **424**: 957–961.

Edger PP, Heidel-Fischer HM, Bekaert M, Rota J, Glöckner G, Platts AE, Heckel DG, Der JP, Wafula EK, Tang M, Hofberger JA, Smithson A, Hall JC, Blanchette M, Bureau TE, Wright SI, dePamphilis CW, Eric Schranz M, Barker MS, Conant GC, Wahlberg N, Vogel H, Pires JC, Wheat CW. 2015. The butterfly plant arms-race escalated by gene and genome duplications. *Proc Natl Acad Sci USA* **112**: 8362–8366.

Ehrlich PR, Raven PH. 1964. Butterflies and plants: a study in coevolution. *Evolution* **18**: 586–608.

Erb M. 2018. Volatiles as inducers and suppressors of plant defense and immunity—origins, specificity, perception and signaling. *Curr Opin Plant Biol* **44**: 117–121.

Feng Z, Hartel PG. 1996. Factors affecting production of COS and CS2 in *Leucaena* and *Mimosa* species. *Plant Soil* **178**: 215–222.

Ferry N, Edwards MG, Gatehouse JA, Gatehouse AMR. 2004. Plant–insect interactions: molecular approaches to insect resistance. *Curr Opin Biotechnol* **15**: 155–161.

Flores HE, Vivanco JM, Loyola-Vargas VM. 1999. 'Radicle' biochemistry: the biology of root-specific metabolism. *Trends Plant Sci* **4**: 220–226.

Franceschi V, Krekling T, Berryman A, Christiansen E. 1998. Specialized phloem parenchyma cells in Norway spruce (Pinaceae) bark are an important site of defense reactions. *Am J Bot* **85**: 601–601.

Fu HY, Chen SJ, Chen RF, Ding WH, Kuo-Huang LL, Huang RN. 2006. Identification of oxalic acid and tartaric acid as major persistent pain-inducing toxins in the stinging hairs of the nettle, *Urtica thunbergiana*. *Ann Bot* **98**: 57–65.

Gleadow RM, Møller BL. 2014. Cyanogenic glycosides: synthesis, physiology, and phenotypic plasticity. *Annu Rev Plant Biol* **65**: 155–185.

Gniazdowska A, Krasuska U, Andrzejczak O, Soltys D 2015. Allelopathic compounds as oxidative stress agents: Yes or NO. In: Gupta KJ, Igamberdiev AU eds. *Reactive Oxygen and Nitrogen Species Signaling and Communication in Plants*. Cham: Springer International Publishing, 155–176.

Green TR, Ryan CA. 1972. Wound-induced proteinase inhibitor in plant leaves: a possible defense mechanism against insects. *Science* **175**: 776–777.

Greenwood JS, Stinissen HM, Peumans WJ, Chrispeels MJ. 1986. *Sambucus nigra* agglutinin is located in protein bodies in the phloem parenchyma of the bark. *Planta* **167**: 275–278.

Halkier BA, Gershenzon J. 2006. Biology and biochemistry of glucosinolates. *Annu Rev Plant Biol* **57**: 303–333.

Halkier BA, Moller BL. 1989. Biosynthesis of the cyanogenic glucoside dhurrin in seedlings of *Sorghum bicolor* (L.) Moench and partial purification of the enzyme system involved *Plant Physiol* **90**: 1552–1559.

Harborne JB. 1988. *Introduction to Ecological Biochemistry.* New York: Academic Press.

Hartl M, Giri AP, Kaur H, Baldwin IT. 2010. Serine protease inhibitors specifically defend *Solanum nigrum* against generalist herbivores but do not influence plant growth and development. *Plant Cell* **22**: 4158–4175.

Hartmann T. 1999. Chemical ecology of pyrrolizidine alkaloids. *Planta* **207**: 483–495.

Hashimoto T, Yamada Y. 1994. Alkaloid biogenesis: molecular aspects. *Annu Rev Plant Biol* **45**: 257–285.

Haukioja E, Neuvonen S. 1985. Induced long-term resistance of birch foliage against defoliators: defensive or incidental? *Ecology* **66**: 1303–1308.

Heil M, Baldwin IT. 2002. Fitness costs of induced resistance: emerging experimental support for a slippery concept. *Trends Plant Sci* **7**: 61–67.

Heil M, Fiala B, Maschwitz U, Linsenmair KE. 2001. On benefits of indirect defence: short- and long-term studies of antiherbivore protection via mutualistic ants. *Oecologia* **126**: 395–403.

Heinstein P, Chang C. 1994. Taxol. *Annu Rev Plant Biol* **45**: 663–674.

Hilder VA, Powell KS, Gatehouse AMR, Gatehouse JA, Gatehouse LN, Shi Y, Hamilton WDO, Merryweather A, Newell CA, Timans JC, Peumans WJ, van Damme E, Boulter D. 1995. Expression of snowdrop lectin in transgenic tobacco plants results in added protection against aphids. *Transgen Res* **4**: 18–25.

Huot B, Yao J, Montgomery BL, He SY. 2014. Growth–defense tradeoffs in plants: a balancing act to optimize fitness. *Mol Plant* **7**: 1267–1287.

Ishimoto M, Chrispeels MJ. 1996. Protective mechanism of the Mexican bean weevil against high levels of [alpha]-amylase inhibitor in the common bean. *Plant Physiol* **111**: 393–401.

Jin M, Kijima A, Suzuki Y, Hibi D, Inoue T, Ishii Y, Nohmi T, Nishikawa A, Ogawa K, Umemura T. 2011. Comprehensive toxicity study of safrole using a medium-term animal model with gpt delta rats. *Toxicology* **290**: 312–321.

Jones DA. 1998. Why are so many food plants cyanogenic? *Phytochemistry* **47**: 155–162.

Joo Y, Schuman MC, Goldberg JK, Kim SG, Yon F, Brütting C, Baldwin IT. 2018. Herbivore-induced volatile blends with both 'fast' and 'slow' components provide robust indirect defence in nature. *Funct Ecol* **32**: 136–149.

Jose S, Gillespie AR. 1998a. Allelopathy in black walnut (*Juglans nigra* L.) alley cropping. I. Spatio-temporal variation in soil juglone in a black walnut–corn (*Zea mays* L.) alley cropping system in the midwestern USA. *Plant Soil* **203**: 191–197.

Jose S, Gillespie AR. 1998b. Allelopathy in black walnut (*Juglans nigra* L.) alley cropping. II. Effects of juglone on hydroponically grown corn (*Zea mays* L.) and soybean (Glycine maxL. Merr.) growth and physiology. *Plant Soil* **203**: 199–206.

Kahl J, Siemens DH, Aerts RJ, Gäbler R, Kühnemann F, Preston CA, Baldwin IT. 2000. Herbivore-induced ethylene suppresses a direct defense but not a putative indirect defense against an adapted herbivore. *Planta* **210**: 336–342.

Karban R, Agrawal AA. 2002. Herbivore offense. *Annu Rev Ecol Syst* **33**: 641–664.

Karban R, Maron J, Felton GW, Ervin G, Eichenseer H. 2003. Herbivore damage to sagebrush induces resistance in wild tobacco: evidence for eavesdropping between plants. *Oikos* **100**: 325–332.

Kessler A, Halitschke R, Diezel C, Baldwin IT. 2006. Priming of plant defense responses in nature by airborne signaling between *Artemisia tridentata* and *Nicotiana attenuata*. *Oecologia* **148**: 280–292.

Kimmerer TW, Potter DA. 1987. Nutritional quality of specific leaf tissues and selective feeding by a specialist leafminer. *Oecologia* **71**: 548–551.

Koch KE. 1996. Carbohydrate-modulated gene expression in plants. *Annu Rev Plant Physiol Plant Mol Biol* **47**: 509.

Komives T, Gullner G. 2005. Phase I xenobiotic metabolic systems in plants. *Z Naturforsch C* **60**: 179–185.

Lambers H, Poorter H. 1992. Inherent variation in growth rate between higher plants: a search for physiological causes and ecological consequences. *Adv Ecol Res* **22**: 187–261.

Lata J-C, Degrange V, Raynaud X, Maron P-A, Lensir R, Abbadie L. 2004. Grass populations control nitrification in savanna soils. *Funct Ecol* **18**: 605–611.

Lau JA, Puliafico KP, Kopshever JA, Steltzer H, Jarvis EP, Schwarzländer M, Strauss SY, Hufbauer RA. 2008. Inference of allelopathy is complicated by effects of activated carbon on plant growth. *New Phytol* **178**: 412–423.

Leung T-WC, Williams DH, Barna JCJ, Foti S, Oelrichs PB. 1986. Structural studies on the peptide moroidin from *Laportea moroides*. *Tetrahedron* **42**: 3333–3348.

Lieberei R, Biehl B, Giesemann A, Junqueira NTV. 1989. Cyanogenesis inhibits active defense reactions in plants. *Plant Physiol* **90**: 33–36.

Llandres AL, Almohamad R, Brévault T, Renou A, Téréta I, Jean J, Goebel FR. 2018. Plant training for induced defense against insect pests: a promising tool for integrated pest management in cotton. *Pest Manage Sci* **74**: 2004–2012.

Lo Cicero L, Madesis P, Tsaftaris A, Lo Piero AR. 2015. Tobacco plants over-expressing the sweet orange tau glutathione transferases (CsGSTUs) acquire tolerance to the diphenyl ether herbicide fluorodifen and to salt and drought stresses. *Phytochemistry* **116**: 69–77.

Lombardo L, Coppola G, Zelasco S. 2016. New technologies for insect-resistant and herbicide-tolerant plants. *Trends Biotechnol* **34**: 49–57.

Lord J, Roberts L. 1996. The intracellular transport of ricin: why mammalian cells are killed and how *Ricinus* cells survive. *Plant Physiol Bochem* **34**: 253–261.

Macel M. 2011. Attract and deter: a dual role for pyrrolizidine alkaloids in plant–insect interactions. *Phytochem Rev* **10**: 75–82.

Macías FA, Oliveros-Bastidas A, Marin D, Castellano D, Simonet AM, Molinillo JMG. 2005. Degradation studies on benzoxazinoids. Soil degradation dynamics of (2R)-2-O-β-d-glucopyranosyl-4-hydroxy-(2H)- 1,4-benzoxazin-3(4H)-one (DIBOA-Glc) and its degradation products, phytotoxic allelochemicals from gramineae. *J Agric Sci Food Chem* **53**: 554–561.

Marongiu B, Piras A, Porcedda S, Tuveri E, Laconi S, Deidda D, Maxia A. 2009. Chemical and biological comparisons on supercritical extracts of *Tanacetum cinerariifolium* (Trevir) Sch. Bip. with three related species of chrysanthemums of Sardinia (Italy). *Nat Prod Res* **23**: 190–199.

Martin BC, George SJ, Price CA, Ryan MH, Tibbett M. 2014. The role of root exuded low molecular weight organic anions in facilitating petroleum hydrocarbon degradation: Current knowledge and future directions. *Sci Tot Environ* **472**: 642–653.

Mattiacci L, Dicke M, Posthumus MA. 1995. beta-Glucosidase: an elicitor of herbivore-induced plant odor that attracts host-searching parasitic wasps. *Proc Natl Acad Sci USA* **92**: 2036–2040.

Mayer AM. 2006. Polyphenol oxidases in plants and fungi: going places? A review. *Phytochemistry* **67**: 2318–2331.

McMahon JM, White WLB, Sayre RT. 1995. Cyanogenesis in cassava (*Manihot esculenta* Crantz). *J Exp Bot* **46**: 731–741.

Mithöfer A, Maffei ME 2017. General mechanisms of plant defense and plant toxins. In: Gopalakrishnakone P, Carlini CR, Ligabue-Braun R eds. *Plant Toxins*. Dordrecht: Springer, 3–24.

Muller CH, Muller WH, Haines BL. 1964. Volatile growth inhibitors produced by aromatic shrubs. *Science* **143**: 471–473.

Musah RA, Lesiak AD, Maron MJ, Cody RB, Edwards D, Fowble KL, Dane AJ, Long MC. 2015. Mechanosensitivity below ground: touch-sensitive smell-producing roots in the "shy plant," *Mimosa pudica* L. *Plant Physiol* **170**: 1075–1089.

Neal AL, Ahmad S, Gordon-Weeks R, Ton J. 2012. Benzoxazinoids in root exudates of maize attract *Pseudomonas putida* to the rhizosphere. *PLoS ONE* **7**: e35498.

Nielsen LJ, Stuart P, Pičmanová M, Rasmussen S, Olsen CE, Harholt J, Møller BL, Bjarnholt N. 2016. Dhurrin metabolism in the developing grain of *Sorghum bicolor* (L.) Moench investigated by metabolite profiling and novel clustering analyses of time-resolved transcriptomic data. *BMC Genomics* **17**: 1021.

Nimbal CI, Yerkes CN, Weston LA, Weller SC. 1996. Herbicidal activity and site of action of the natural product sorgoleone. *Pestic Biochem Physiol* **54**: 73–83.

Nishanth T, Prasanta B, Peter A, Elsbeth W, Dulasiri A, Baoshan X. 2009. Dual purpose secondary compounds: phytotoxin of *Centaurea diffusa* also facilitates nutrient uptake. *New Phytol* **181**: 424–434.

Northup RR, Yu Z, Dahlgren RA, Vogt KA. 1995. Polyphenol control of nitrogen release from pine litter. *Nature* **377**: 227–229.

Nosko P, Embury K. 2018. Induction and persistence of allelochemicals in the foliage of balsam fir seedlings following simulated browsing. *Plant Ecol* **219**: 611–619.

Ohse B, Hammerbacher A, Seele C, Meldau S, Reichelt M, Ortmann S, Wirth C. 2017. Salivary cues: simulated roe deer browsing induces systemic changes in phytohormones and defence chemistry in wild-grown maple and beech saplings. *Funct Ecol* **31**: 340–349.

Oka Y. 2012. Nematicidal activity of *Verbesina encelioides* against the root-knot nematode *Meloidogyne javanica* and effects on plant growth. *Plant Soil* **355**: 311–322.

Oka Y, Shuker S, Tkachi N, Trabelcy B, Gerchman Y. 2014. Nematicidal activity of *Ochradenus baccatus* against the root-knot nematode *Meloidogyne javanica*. *Plant Pathol* **63**: 221–231.

Paavolainen L, Kitunen V, Smolander A. 1998. Inhibition of nitrification in forest soil by monoterpenes. *Plant Soil* **205**: 147–154.

Paschold A, Halitschke R, Baldwin IT. 2006. Using 'mute' plants to translate volatile signals. *Plant J* **45**: 275–291.

Peumans WJ, Van Damme E. 1995. Lectins as plant defense proteins. *Plant Physiol* **109**: 347–352.

Pičmanová M, Neilson EH, Motawia MS, Olsen CE, Agerbirk N, Gray CJ, Flitsch S, Meier S, Silvestro D, Jørgensen K, Sánchez-Pérez R, Møller BL, Bjarnholt N. 2015. A recycling pathway for cyanogenic glycosides evidenced by the comparative metabolic profiling in three cyanogenic plant species. *Biochem J* **469**: 375–389.

Piluk J, Hartel PG, Haines BL, Giannasi DE. 2001. Association of carbon disulfide with plants, in the family Fabaceae. *J Chem Ecol* **27**: 1525–1534.

Pollard AJ, Briggs D. 1984. Genecological studies of *Urtica dioica* L. III Stinging hairs and plant-herbivore interactions. *New Phytol* **97**: 507–522.

Popovich DG, Kitts DD. 2002. Structure–function relationship exists for ginsenosides in reducing cell proliferation and inducing apoptosis in the human leukemia (THP-1) cell line. *Arch Biochem Biophys* **406**: 1–8.

Poppenga RH 2010. Poisonous plants. . In: Luch A ed. *Molecular, Clinical and Environmental Toxicology*. Basel: Birkhäuser 123–175.

Pueyo José J, Delgado-Salinas A. 1997. Presence of α-amylase inhibitor in some members of the subtribe Phaseolinae (Phaseoleae: Fabaceae). *Am J Bot* **84**: 79–84.

Raikhel NV, Lee HI, Broekaert WF. 1993. Structure and function of chitin-binding proteins. *Annu Rev Plant Biol* **44**: 591–615.

Rask L, Andréasson E, Ekbom B, Eriksson S, Pontoppidan B, Meijer J. 2000. Myrosinase: gene family evolution and herbivore defense in Brassicaceae. *Plant Mol Biol* **42**: 93–114.

Rasmann S, Köllner TG, Degenhardt J, Hiltpold I, Toepfer S, Kuhlmann U, Gershenzon J, Turlings TCJ. 2005. Recruitment of entomopathogenic nematodes by insect-damaged maize roots. *Nature* **434**: 732–737.

Rasmussen JA, Hejl AM, Einhellig FA, Thomas JA. 1992. Sorgoleone from root exudate inhibits mitochondrial functions. *J Chem Ecol* **18**: 197–207.

Ravanel P, Tissut M, Douce R. 1986. Platanetin: a potent natural uncoupler and inhibitor of the exogenous NADH dehydrogenase in intact plant mitochondria. *Plant Physiol* **80**: 500–504.

Read J, Sanson GD, Caldwell E, Clissold FJ, Chatain A, Peeters P, Lamont BB, De Garine-Wichatitsky M, Jaffré T, Kerr S. 2009. Correlations between leaf toughness and phenolics among species in contrasting environments of Australia and New Caledonia. *Ann Bot* **103**: 757–767.

Reynolds T. 2005. Hemlock alkaloids from Socrates to poison aloes. *Phytochemistry* **66**: 1399–1406.

Rezania S, Ponraj M, Talaiekhozani A, Mohamad SE, Md Din MF, Taib SM, Sabbagh F, Sairan FM. 2015. Perspectives of phytoremediation using water hyacinth for removal of heavy metals, organic and inorganic pollutants in wastewater. *J Environ Manage* **163**: 125–133.

Rhoades DF. 1985. Offensive-defensive interactions between herbivores and plants: their relevance in herbivore population dynamics and ecological theory. *Amer Nat* **125**: 205–238.

Rice-Evans C, Miller N, Paganga G. 1997. Antioxidant properties of phenolic compounds. *Trends Plant Sci* **2**: 152–159.

Ridenour WM, Callaway RM. 2001. The relative importance of allelopathy in interference: the effects of an invasive weed on a native bunchgrass. *Oecologia* **126**: 444–450.

Rodgers S. 2016. Minimally processed functional foods: technological and operational pathways. *J Food Sci* **81**: R2309–R2319.

Romero GQ, Benson WW. 2004. Leaf domatia mediate mutualism between mites and a tropical tree. *Oecologia* **140**: 609–616.

Rosenthal GA, Hughes CG, Janzen DH. 1982. L-Canavanine, a dietary nitrogen source for the seed predator *Caryedes brasiliensis* (Bruchidae). *Science* **217**: 353–355.

Ruan Y-L. 2014. Sucrose metabolism: gateway to diverse carbon use and sugar signaling. *Annu Rev Plant Biol* **65**: 33–67.

Sagers CL, Ginger SM, Evans RD. 2000. Carbon and nitrogen isotopes trace nutrient exchange in an ant-plant mutualism. *Oecologia* **123**: 582–586.

Schroeder HE, Gollasch S, Moore A, Tabe LM, Craig S, Hardie DC, Chrispeels MJ, Spencer D, Higgins T. 1995. Bean [alpha]-amylase inhibitor confers resistance to the pea weevil (*Bruchus pisorum*) in transgenic peas (*Pisum sativum* L.). *Plant Physiol* **107**: 1233–1239.

Schuler MA. 1996. The role of cytochrome P450 monooxygenases in plant-insect interactions. *Plant Physiol* **112**: 1411.

Schulz M, Marocco A, Tabaglio V, Macias FA, Molinillo JMG. 2013. Benzoxazinoids in rye allelopathy - from discovery to application in sustainable weed control and organic farming. *J Chem Ecol* **39**: 154–174.

Selmar D. 1993. Transport of cyanogenic glucosides: linustatin uptake by *Hevea* cotyledons. *Planta* **191**: 191–199.

Selmar D, Kleinwächter M. 2013. Stress enhances the synthesis of secondary plant products: the impact of stress-related over-reduction on the accumulation of natural products. *Plant Cell Physiol* **54**: 817–826.

Shakil NA, Kumar J, Pandey RK, Saxena DB. 2008. Nematicidal prenylated flavanones from *Phyllanthus niruri*. *Phytochemistry* **69**: 759–764.

Sharma E, Anand G, Kapoor R. 2017. Terpenoids in plant and arbuscular mycorrhiza-reinforced defence against herbivorous insects. *Ann Bot* **119**: 791–801.

Siminszky B. 2006. Plant cytochrome P450-mediated herbicide metabolism. *Phytochem Rev* **5**: 445–458.

Song R, Kelman D, Johns KL, Wright AD. 2012. Correlation between leaf age, shade levels, and characteristic beneficial natural constituents of tea (*Camellia sinensis*) grown in Hawaii. *Food Chem* **133**: 707–714.

Song YY, Simard SW, Carroll A, Mohn WW, Zeng RS. 2015. Defoliation of interior Douglas-fir elicits carbon transfer and stress signalling to ponderosa pine neighbors through ectomycorrhizal networks. *Sci Rep* **5**: 8495.

Stock WD, Le Roux D, Van der Heyden F. 1993. Regrowth and tannin production in woody and succulent karoo shrubs in response to simulated browsing. *Oecologia* **96**: 562–568.

Subbarao G, Arango J, Masahiro K, Hooper A, Yoshihashi T, Ando Y, Nakahara K, Deshpande S, Ortiz-Monasterio I, Ishitani M. 2017. Genetic mitigation strategies to tackle agricultural GHG emissions: The case for biological nitrification inhibition technology. *Plant Sci* **262**: 165–168.

Subbarao GV, Ishikawa T, Ito O, Nakahara K, Wang HY, Berry WL. 2006. A bioluminescence assay to detect nitrification inhibitors released from plant roots: a case study with *Brachiaria humidicola*. *Plant Soil* **288**: 101–112.

Sudhakar D, Fu X, Stoger E, Williams S, Spence J, Brown DP, Bharathi M, Gatehouse JA, Christou P. 1998. Expression and immunolocalisation of the snowdrop lectin, GNA in transgenic rice plants. *Transgen Res* **7**: 371–378.

Sugimoto K, Matsui K, Iijima Y, Akakabe Y, Muramoto S, Ozawa R, Uefune M, Sasaki R, Alamgir KM, Akitake S, Nobuke T, Galis I, Aoki K, Shibata D, Takabayashi J. 2014. Intake and transformation to a glycoside of (*Z*)-3-hexenol from infested neighbors reveals a mode of plant odor reception and defense. *Proc Natl Acad Sci USA* **111**: 7144–7149.

Suomi J, Sirén H, Wiedmer SK, Riekkola M-L. 2001. Isolation of aucubin and catalpol from *Melitaea cinxia* larvae and quantification by micellar electrokinetic capillary chromatography. *Anal Chim Acta* **429**: 91–99.

Tahvanainen J, Julkunen-Tiitto R, Kettunen J. 1985. Phenolic glycosides govern the food selection pattern of willow feeding leaf beetles. *Oecologia* **67**: 52–56.

Tai HH, Worrall K, Pelletier Y, De Koeyer D, Calhoun LA. 2014. Comparative metabolite profiling of *Solanum tuberosum* against six wild *Solanum* species with Colorado potato beetle resistance. *J Agric Sci Food Chem* **62**: 9043–9055.

Ton J, D'Alessandro M, Jourdie V, Jakab G, Karlen D, Held M, Mauch-Mani B, Turlings TCJ. 2007. Priming by airborne signals boosts direct and indirect resistance in maize. *Plant J* **49**: 16–26.

Tscharntke T, Thiessen S, Dolch R, Boland W. 2001. Herbivory, induced resistance, and interplant signal transfer in *Alnus glutinosa*. *Biochem Syst Ecol* **29**: 1025–1047.

Turlings T, Hiltpold I, Rasmann S. 2012. The importance of root-produced volatiles as foraging cues for entomopathogenic nematodes. *Plant Soil* **358**: 51–60.

Turlings TC, Ton J. 2006. Exploiting scents of distress: the prospect of manipulating herbivore-induced plant odours to enhance the control of agricultural pests. *Curr Opin Plant Biol* **9**: 421–427.

Twigg LE 2014. Fluoroacetate, plants, animals and a biological arms race. In: Lambers H ed. *Plant Life on the Sandplains in Southwest Australia, a Global Biodiversity Hotspot*. Crawley, Australia: UWA Publishing, 225–240.

Understrup AG, Ravnskov S, Hansen HCB, Fomsgaard IS. 2005. Biotransformation of 2-benzoxazolinone to 2-amino-(3H)-phenoxazin-3-one and 2-acetylamino-(3H)-phenoxazin-3-one in soil. *J Chem Ecol* **31**: 1205–1222.

Vale AP, Santos J, Brito NV, Fernandes D, Rosa E, Oliveira MBPP. 2015. Evaluating the impact of sprouting conditions on the glucosinolate content of *Brassica oleracea* sprouts. *Phytochemistry* **115**: 252–260.

Van de Voorde TFJ, Ruijten M, Van der Putten WH, Bezemer TM. 2012. Can the negative plant–soil feedback of *Jacobaea vulgaris* be explained by autotoxicity? *Bas Appl Ecol* **13**: 533–541.

Van Loon JJA, Blaakmeer A, Griepink FC, Van Beek TA, Schoonhoven LM, De Groot A. 1992. Leaf surface compound from *Brassica oleracea* (Cruciferae) induces oviposition by *Pieris brassicae* (Lepidoptera: Pieridae). *Chemoecology* **3**: 39–44.

Van Tol RWHM, Van Der Sommen ATC, Boff MIC, Van Bezooijen J, Sabelis MW, Smits PH. 2001. Plants protect their roots by alerting the enemies of grubs. *Ecol Lett* **4**: 292–294.

Vos M, Berrocal SM, Karamaouna F, Hemerik L, Vet L. 2001. Plant-mediated indirect effects and the persistence of parasitoid–herbivore communities. *Ecol Lett* **4**: 38–45.

Wang M, Bezemer TM, van der Putten WH, Biere A. 2015a. Effects of the timing of herbivory on plant defense induction and insect performance in ribwort plantain (*Plantago lanceolata* L.) depend on plant mycorrhizal status. *J Chem Ecol* **41**: 1006–1017.

Wang T, Li C, Liu Y, Li T, Zhang J, Sun Y. 2015b. Inhibition effects of Chinese cabbage powder on aflatoxin B1-induced liver cancer. *Food Chem* **186**: 13–19.

Wehner F, Gawatz O. 2003. Suicidal yew poisoning–from Caesar to today–or suicide instructions on the internet. *Arch Kriminol* **211**: 19–26.

Weidenhamer JD, Li M, Allman J, Bergosh RG, Posner M. 2013. Evidence does not support a role for gallic acid in *Phragmites australis* ivasion success. *J Chem Ecol* **39**: 323–332.

Weir TL, Bais HP, Stull VJ, Callaway RM, Thelen GC, Ridenour WM, Bhamidi S, Stermitz FR, Vivanco JM. 2006. Oxalate contributes to the resistance of *Gaillardia grandiflora* and *Lupinus sericeus* to a phytotoxin produced by *Centaurea maculosa*. *Planta* **223**: 785–795.

Wermelinger A, Rigling A, Schneider Mathis D, Dobbertin M. 2008. Assessing the role of bark- and wood-boring insects in the decline of Scots pine (*Pinus sylvestris*) in the Swiss Rhone valley. *Ecol Entomol* **33**: 239–249.

Weston LA, Mathesius U. 2013. Flavonoids: their structure, biosynthesis and role in the rhizosphere, including allelopathy. *J Chem Ecol* **39**: 283–297.

Willmer PG, Stone GN. 1997. How aggressive ant-guards assist seed-set in *Acacia* flowers. *Nature* **388**: 165–167.

Wisessing A, Engkagul A, Wongpiyasatid A, Choowongkomon K. 2010. Biochemical characterization of the α-amylase Inhibitor in mungbeans and its application in inhibiting the growth of *Callosobruchus maculatus*. *J Agric Sci Food Chem* **58**: 2131–2137.

Wright IJ, Cannon K. 2001. Relationships between leaf lifespan and structural defences in a low-nutrient, sclerophyll flora. *Funct Ecol* **15**: 351–359.

Wu A, Sun X, Pang Y, Tang K. 2002. Homozygous transgenic rice lines expressing GNA with enhanced resistance to the rice sap-sucking pest *Laodelphax striatellus*. *Plant Breed* **121**: 93–95.

Wu H, Pratley J, Lemerle D, An M, Liu D. 2007. Autotoxicity of wheat (*Triticum aestivum* L.) as determined by laboratory bioassays. *Plant Soil* **296**: 85–93.

Wurst S, Vender V, Rillig M. 2010. Testing for allelopathic effects in plant competition: does activated carbon disrupt plant symbioses? *Plant Ecol* **211**: 19–26.

Xiao Y, Wang Q, Erb M, Turlings TCJ, Ge L, Hu L, Li J, Han X, Zhang T, Lu J, Zhang G, Lou Y. 2012. Specific herbivore-induced volatiles defend plants and determine insect community composition in the field. *Ecol Lett* **15**: 1130–1139.

Yang M, Zhang X, Xu Y, Mei X, Jiang B, Liao J, Yin Z, Zheng J, Zhao Z, Fan L, He X, Zhu Y, Zhu S. 2015. Autotoxic ginsenosides in the rhizosphere contribute to the replant failure of *Panax notoginseng*. *PLoS ONE* **10**: e0118555.

Yu JQ, Shou SY, Qian YR, Zhu ZJ, Hu WH. 2000. Autotoxic potential of cucurbit crops. *Plant Soil* **223**: 149–153.

Ziska LH, Sicher RC, George K, Mohan JE. 2007. Rising atmospheric carbon dioxide and potential impacts on the growth and toxicity of poison ivy (*Toxicodendron radicans*). *Weed Sci* **55**: 288–292.

Biotic Influences: Effects of Microbial Pathogens

14

14.1 Introduction

Plants frequently encounter potentially pathogenic fungi, bacteria, and viruses, yet disease results from relatively few of these exposures. In many cases, there is no obvious trace of its occurrence, and the microorganism fails to establish itself due to a low pathogenicity or highly effective plant defense mechanisms. Other encounters leave evidence of an intense plant-microbe interaction, which results in the arrest of pathogen development after attempted colonization. In these cases, plant tissues often display activated defense functions that produce antimicrobial compounds (phytoalexins), enzymes, and structural reinforcement that may limit pathogen growth (Pedras and Abdoli 2017). Fungal plant pathogens are either **biotrophs** or **necrotrophs** (and there are some hemibiotrophs that start off as biotrophs but become necrotrophs later).

Biotrophs such as rusts, powdery mildews, and downy mildews either directly penetrate the epidermis or they invade leaves through stomata (Spanu and Panstruga 2017). They grow intercellularly, without obvious host response, and may produce intracellular branches, the haustoria, which invaginate the host plasma membrane, forming areas for nutrient exchange. How can these pathogens evade the normal host's responses to damage? **Necrotrophs** are wound invaders. They produce toxins that kill cells in advance of fungal hyphae. Most necrotrophs have wide host ranges, whilst biotrophs are much more host specific. There are some **hemibiotrophs** that start off as biotrophs, and become necrotrophs later.

Plant defense responses against **pathogens** have much in common with responses following **herbivore** attack (Chap. 13), in terms of both signaling and final outcome, as we explore below. Because of the marked differences between their cellular structures and modes of life, one might expect very different strategies for attack, defense, and counterattack to have evolved in plants and animals and their respective pathogens (Pajerowska-Mukhtar et al. 2013). However, plants and animals also share several individual components of host-pathogen interactions, either conceptually or mechanistically.

14.2 Constitutive Antimicrobial Defense Compounds

Host resistance to microbial pathogens may be based on the constitutive accumulation of inorganic compounds, *e.g.*, **silicon** (Si) in *Oryza sativa* (rice) (Swain and Rout 2017), a typical Si-accumulating species (Sect. 9.4.1). Silicon may act as a **physical barrier**, when it is deposited beneath the cuticle to form a cuticle-Si double layer. This layer can mechanically impede penetration by fungi. An alternative mechanism is that soluble Si acts as a **modulator of host resistance** to pathogens. Several studies in both

H. Lambers, R. S. Oliveira, *Plant Physiological Ecology*, https://doi.org/10.1007/978-3-030-29639-1_14

monocots and dicots show that plants supplied with Si produce phenolics and phytoalexins (Sect. 14.3) in response to fungal infection, such as those causing rice blast and powdery mildew. Silicon may also activate some defense mechanisms. For example, in roots of *Cucumis sativus* (cucumber) that are infected and colonized by *Pythium*, Si enhances the activity of chitinases, peroxidases, and polyphenol oxidases. Unlike rice, many plants do not accumulate Si at high enough levels to be beneficial; genetically manipulating the Si uptake capacity of the root might help plants to accumulate more Si, and improve their ability to overcome biotic and abiotic stresses (Ma and Yamaji 2006). Physical barriers are not effective against pathogens such as **viruses** that are transferred by insects, *e.g.*, aphids tapping into the phloem (Sect. 4.5). Chitinases are effective against fungi, but oomycetes (water molds) such as *Phytophthora*, do not have chitin in their cell walls (Badreddine et al. 2008).

Other inorganic compounds that may confer resistance against microbial pathogens include **metals**, which offer an attractive explanation for the existence of **hyperaccumulators** (Sect. 9.3.3). The hypothesis that hyperaccumulation confers resistance against biotic stress was initially formulated based on an observation that fewer insects feed on nickel (Ni) hyperaccumulators. Further investigations have subsequently shown that high levels of Ni, zinc (Zn), cadmium (Cd), or selenium (Se) can provide effective protection against fungi, or viruses (Poschenrieder et al. 2006). Hyperaccumulation might therefore offer **cross-resistance** against microbial pathogens and herbivores (Sect. 12.3.1). The term **hormesis** is used for a stimulatory effect of sub-inhibitory concentrations of any toxic substances on any organism (Poschenrieder et al. 2013). How do those metals boost a plant's resistance? As we discuss in Sect. 9.3.3.3, metals may induce uncontrolled redox reactions, which may lead to the production of **reactive oxygen species** (**ROS**). These general defense reactions can lead to cross-protection against another stressor such as a pathogen (Fig. 14.1).

Organic compounds, rather than inorganic nutrients or metals, are the most common molecules involved in plant defense. Some of these compounds have multiple defense functions, acting against both microbial pathogens and herbivores (**cross-resistance**). For example, aucubin and catalpol, two iridoid glycosides in *Plantago lanceolata* (snake plantain), confer *in vivo* resistance to both the generalist insect herbivore *Spodoptera exigua* (beet armyworm) and the biotrophic fungal pathogen *Diaporthe adunca*. The bitter taste of iridoid glycosides probably deters feeding by *Spodoptera exigua*, whereas the hydrolysis products formed after tissue damage following fungal infection likely mediate pathogen resistance (Biere et al. 2004).

Plants produce a wide range of compounds with an **antimicrobial** effect (**phytoanticipins**) (VanEtten et al. 1995). Some of these have already been discussed in Sect. 13.2.1 (*e.g.*, alkaloids, flavonoids, and lignin). **Saponins** are plant glycosides that derive their name from their soaplike properties. A common species that contains saponins is *Saponaria officinalis* (soapwort), which used to be grown near wool mills; the soapy extracts from its leaves and roots were used for washing wool. Saponins consist of triterpenoid, steroid, or steroidal glyco-alkaloid molecules that bear one or more sugar chains (Fig. 14.2; Osbourn 1996). Saponins have been implicated as preformed determinants of resistance to fungal attack. For example, wounding of *Avena strigosa* (lopsided oat) plant tissue which results from pathogen attack causes a breakdown of compartmentalization which allows an enzyme to contact the saponin avenacoside B, yielding a fungitoxic compound that causes loss of membrane integrity (Osbourn 2003).

Lipid-transfer proteins, which we discussed in Sect. 7.3.5, may also be active in plant defense. Lipid-transfer proteins from *Raphanus sativus* (radish), *Hordeum vulgare* (barley), and *Spinacia oleracea* (spinach) are active against several pathogens, with varying degrees of specificity (Nawrot et al. 2014). The extracellular

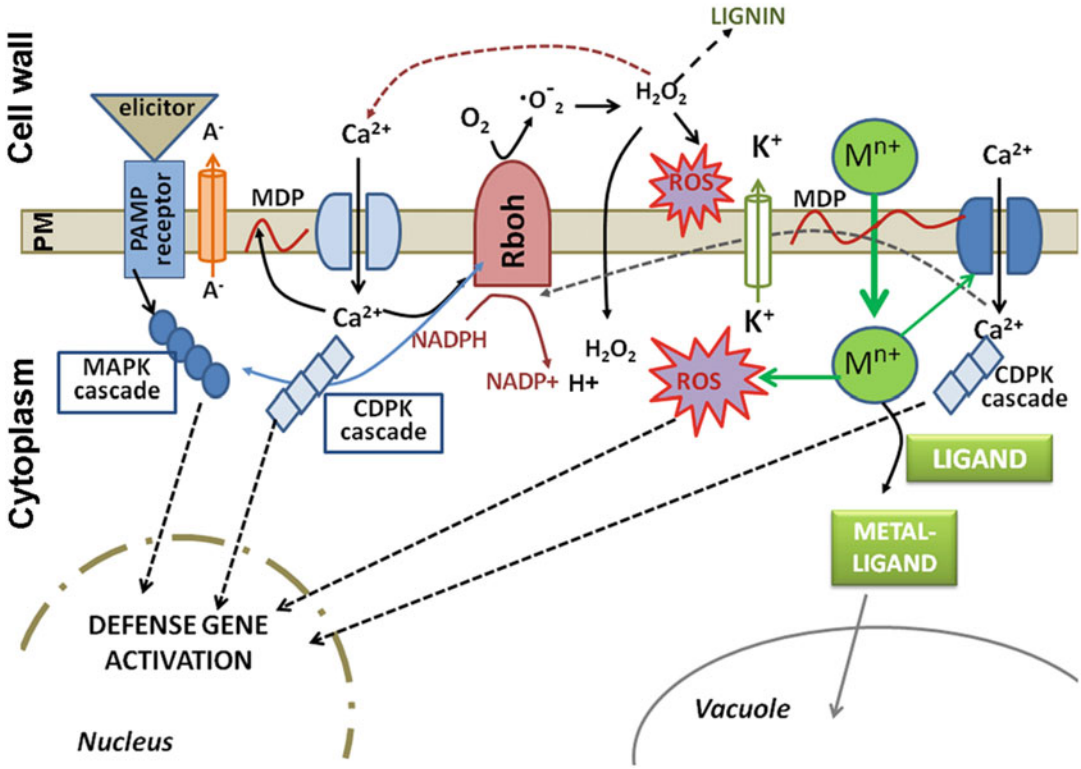

Fig. 14.1 Cross-signaling pathways between toxic metal ions and biotic stress that may lead to metal-induced defense activation and growth stimulation under latent biotic stress. Early mechanisms for sensing pathogen attack and metal ion toxicity: pathogen elicitors are recognized by specific receptors (*e.g.*, recognition of pathogen-associated molecular patterns, PAMPs); both pathogens and metal ions (M^{n+}) cause membrane depolarization (MDP), increased cytoplasmic Ca^{2+}, and reactive oxygen species (ROS) by respiratory burst oxidase homologues (Rbohs). Mitogen-activated protein kinases (MAPK) and Ca-dependent protein kinases (CDPK) have key roles in signal transduction of both stress factors (Poschenrieder et al. 2013); copyright © 2013 Elsevier Ireland Ltd. All rights reserved.

localization of lipid-transfer proteins is thought to contribute to the generation of a defensive shield over plant surfaces, interfering with the membranes of target organisms, leading to a loss in membrane integrity (Liu et al. 2015).

Lectins (defense compounds against herbivores; Sects. 13.3.4 and 13.3.5) are also effective against pathogens. For example, chitin-binding lectins from *Solanum integrifolium* (pumpkin-tree plant) play roles in immune defense against chitin-containing pathogens (*Rhizoctonia solani* and *Colletotrichum gloeosporioide*) (Chen et al. 2018). **Thionins**, which are cysteine-rich proteins, represent another group of antimicrobial proteins that are involved in plant defenses. In *Oryza sativa* (rice) thionin genes are involved in defense against both the root-knot nematode *Meloidogyne graminicola* and the oomycete *Pythium graminicola* (Chen et al. 2018). The constitutive defense against microorganisms obviously incurs **costs** for synthesis and storage. When a range of cultivars of *Raphanus sativus* (radish) that differ widely in their sensitivity to *Fusarium oxysporum* (fungal wilt disease) are compared, the most resistant ones have the slowest relative growth rate and *vice versa* (Fig. 14.3; Hoffland et al. 1996). The exact nature of the constitutive defense is unknown, but it is probably not based solely on the presence of glucosinolates, which tend to be present only in low amounts (Sect. 13.3.1). Slow-growing, resistant radish cultivars contain more

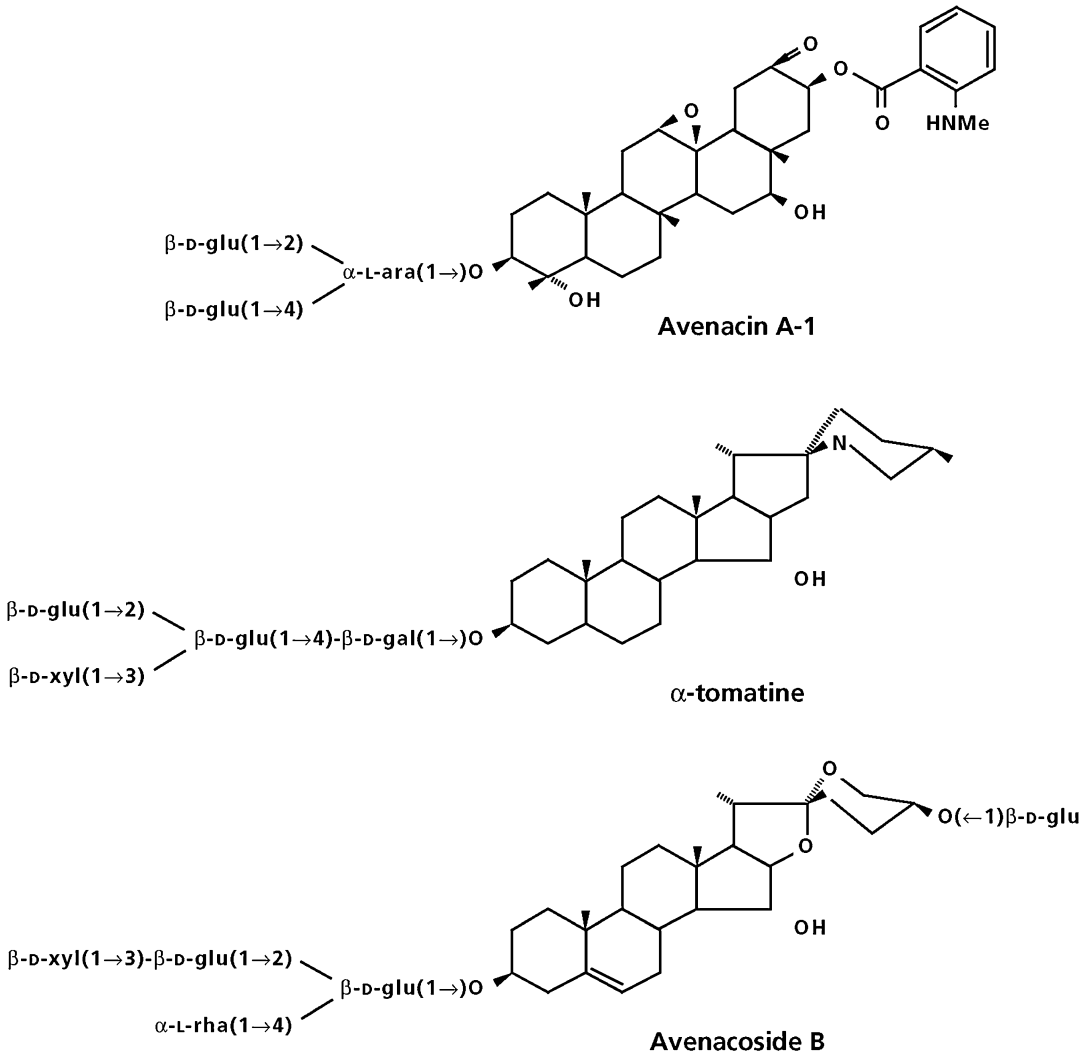

Fig. 14.2 Structures of saponins from *Solanum lycopersicum* (tomato) and *Avena strigosa* (lopsided oat) (Osbourn 1996). Copyright © 1996 Published by Elsevier Ltd.

cell-wall material in leaves, but their roots have a high biomass density due to more cytoplasmic elements (proteins), rather than large amounts of cell-wall material. This higher protein concentration might account for the rapid and adequate resistance reaction, although at the expense of greater construction and turn-over costs (Hoffland et al. 1996).

In some phytopathogenic fungi, **detoxifying enzymes** have evolved that break through the plant's constitutive or induced defense against fungal attack (VanEtten et al. 1995). A number of fungi avoid the toxicity of plant saponins. Some do so by growing only in extracellular plant compartments. Some fungi that infect *Solanum lycopersicum* (tomato) **lower the pH** at the infection sites to levels at which the saponin in tomato (α-tomatin) has no effect on membrane integrity. More important mechanisms involve a change in **membrane composition** of the fungus and the production of **saponin-detoxifying enzymes**. For example, *Fusarium graminearum* (fungal wilt disease) produces a tomatinase-like enzyme that detoxifies saponins produced by

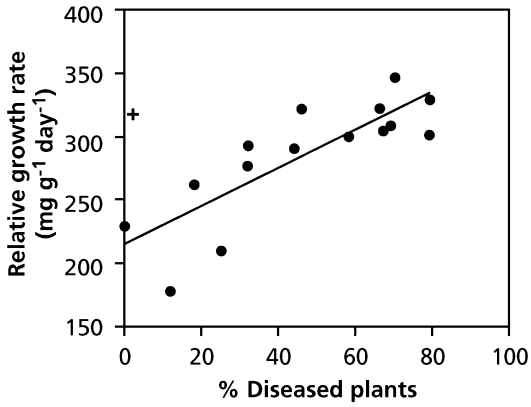

Fig. 14.3 Correlation between the relative growth rate (*RGR*) of *Raphanus sativus* (radish) grown in the absence of pathogens and resistance level to *Fusarium oxysporum* in 15 cultivars. Each symbol refers to a different cultivar (after Hoffland et al. 1996).

Triticum aestivum (wheat) (Carere et al. 2017). Several pathogens can overcome **stomatal defense** (Sect. 14.3) using specific phytotoxins that prevent stomatal closure triggered by **pathogen-associated molecular patterns** (PAMPs) (Melotto et al. 2017).

14.3 The Plant's Response to Attack by Microorganisms

Highly sophisticated defense strategies have evolved in plants to counteract pathogenic microorganisms. Stomata serve as passive ports of bacterial entry during infection, and stomatal closure is part of a plant's innate immune response to restrict bacterial invasion. Stomatal guard cells of *Arabidopsis thaliana* (thale cress) perceive bacterial surface molecules, and this leads to stomatal closure, restriction pathogen entry (**stomatal defense**) (Melotto et al. 2006, 2017). The primary immune response in plants has evolved to recognize common features of the microbial pathogens that are referred to **PAMPs** (Chisholm et al. 2006; Jones and Dangl 2006). PAMP-triggered immunity is part of the first line of induced defense, and results in a basal level of resistance. During the evolutionary '**arms race**', pathogens acquired the ability to suppress this first line of induced defense via the delivery of effector proteins. In turn, plants acquired R proteins that recognize these attacker-specific effector proteins, resulting in a highly effective second line of defense, **effector-triggered immunity** (Chisholm et al. 2006). Effector-triggered immunity is also known as the gene-for-gene relationship, which was first identified in the 1940s in *Linum usitatissimum* (flax) and its fungal pathogen *Melampsora lini* (flax rust) (Flor 1971). Many different plant genes that encode disease resistance occur in clusters, either as single genes with multiple alleles that encode different resistance specificities, or as a series of tightly linked genes forming complex loci (Pryor and Ellis 1993). For example, in *Triticum aestivum* (wheat) and *Triticum turgidum* (emmer wheat), 17 functional *Pm3* alleles confer agronomically important race-specific resistance to *Blumeria graminis* (powdery mildew) (Bourras et al. 2015). Resistance to pathogens involves a specific recognition between a resistant plant and the pathogen. This interaction triggers a set of responses that act to confine the pathogen. If the specific gene is absent in the plant or in the pathogen (or in both), then there is no concerted defense response and disease generally ensues. The first resistance (R) gene to be cloned in *Zea mays* (maize), *Hm1*, was published over 25 years ago, and since then, many R genes have been identified (Kourelis and van der Hoorn 2018). The encoded proteins have provided clues to the diverse molecular mechanisms underlying immunity. The majority of R genes encode cell surface or intracellular receptors, and there are nine molecular mechanisms by which R proteins can elevate or trigger disease resistance. First, there is direct (1) or indirect (2) perception of pathogen-derived molecules on the cell surface by receptor-like proteins and receptor-like kinases (3). Then, direct or indirect (4) intracellular detection of pathogen-derived molecules by nucleotide binding, leucine-rich repeat receptors, or detection through integrated domains (5). In addition, there is perception of transcription activator-like effectors through activation of executor genes (6), and active (7), passive (8), or host reprogramming-mediated (9) loss of

susceptibility. We now understand the molecular mechanisms underlying the functions of R genes for a small proportion of known R genes, and a clear understanding of mechanisms is emerging gradually. Instead of confinement of the pathogen, plants may respond with the abscission of an affected organ, or compartmentalization of the damaged tissue. This is particularly important in woody plants, where the pathogen is still viable, but contained by chemical responses in the ray cells, annual rings, or new periderms in the bark. These responses will only be effective if they are sufficiently rapid and occur in the right tissue.

Plants react to pathogen attack by activating an elaborate defense system that acts both locally and systemically which is in many ways similar to the kind of response we discussed in Sect. 13.3. In many cases, local resistance is manifested as a **hypersensitive response** (Stakman 1915): membrane damage, necrosis, and collapse of cells. This 'suicidal' response is often confined to individual penetrated cells. It is considered a sacrifice of locally-infected tissue (sometimes only one or a few cells) to protect against the spread of the pathogen into healthy tissue. Mutants that spontaneously form patches of dead tissue (necrosis) occur in many plant species. Further analysis of these mutants shows that the hypersensitive response is caused by the production of toxic compounds by the plant or pathogen and also results, partly, from genetically programmed cell death (Coll et al. 2011). The hypersensitive response differs from cell death that spreads beyond the point of infection which follows from the interaction of a susceptible plant and a virulent pathogen.

The hypersensitive response often enhances the production of **ROS** (O_2^-, H_2O_2), which are generated by a signaling pathway similar to that employed by mammalian neutrophils during immune responses (Fig. 14.1). The ROS are involved in cross-linking of cell-wall proteins, rendering these more resistant to attack by enzymes from the pathogen. They are also thought to be toxic for pathogens. In addition ROS may act as 'second messengers' in the induction of defense genes (Coll et al. 2011). These ROS might be the cause of upregulation of the gene encoding the **alternative oxidase**. Upregulation of this gene greatly enhances the capacity for cyanide-resistant respiration of the infected plant tissue (Sect. 3.4.8). Increased activity of the alternative path presumably allows a rapid flux through the oxidative pentose phosphate pathway and NADP-malic enzyme, thus producing carbon skeletons and NADPH that are required in the defense reaction (Fig. 14.4; Simons and Lambers 1998).

Many plants, both in natural and in managed systems, are resistant to multiple diseases. Although much of the plant innate immunity system provides highly specific resistance, some components of plant defense are relatively nonspecific, providing **multiple disease resistance** (Wiesner-Hanks and Nelson 2016). These components include an **oxidative burst**, which can lead to cell death; thus, the pathogen may be 'trapped' in dead cells and be prevented from spreading from the site of infection. The cells surrounding the site of entry modify their cell walls so that they can inhibit penetration by the pathogen. They also produce antimicrobial compounds, such as **phytoalexins** (*i.e.* low-molecular-mass antibiotics that are not found in uninfected plants) (Coll et al. 2011). The chemical nature of phytoalexins is extremely variable (Fig. 14.5); closely related species often have phytoalexins with a similar structure. Microorganisms, or components thereof (**elicitors**), induce the formation of phytoalexins (Boller and Felix 2009). Numerous other compounds in microbial pathogens (*e.g.*, carbohydrates and lipids) may also cause nonspecific production of phytoalexins. In addition, cell-wall components (*e.g.*, glucans or glucomannans) may elicit rapid synthesis of phytoalexins in resistant cultivars.

Now that we have introduced phytoalexins, we stress two points. First, accumulation of a specific compound upon attack does not prove that this compound is involved in resistance. Rather, accumulation may be a side reaction that has nothing to do with the actual resistance mechanism. To prove that a compound is involved in a resistance mechanism may require mutants that are unable to make the putative defense compound. Some

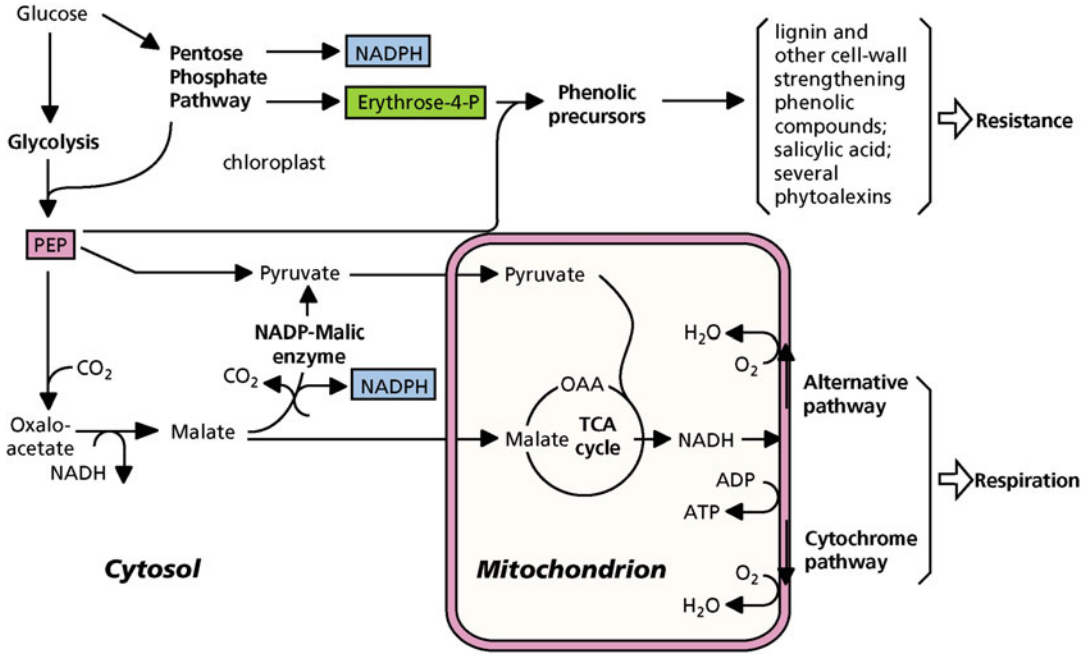

Fig. 14.4 Major metabolic pathways involved in a plant's resistance response to pathogens and its association with respiration. Plant defense requires an increased production of erythrose-4-phosphate for numerous phenolic precursors. Erythrose-4-phosphate is produced in the oxidative pentose pathway, which also generates the NADPH that is required for the biosynthesis of, *e.g.*, lignin and some phytoalexins. Additional NADPH is produced by NADP-malic enzyme, which decarboxylates malate to pyruvate. Increased activity of these reactions enhances the production of pyruvate, which may require an increased activity of the alternative path. Upregulation of the gene encoding the alternative oxidase may be triggered by accumulation of reactive oxygen species (after Simons and Lambers 1998).

50 years ago, Chamberlain and Paxton (1968) demonstrated that the stems of a cultivar of *Glycine max* (soybean), which is susceptible to the fungus *Phytophthora megasperma*, can become resistant upon addition of a phytoalexin isolated from a resistant cultivar. Inhibition of phenylalanine **ammonia lyase**, which is a key enzyme in the synthesis of isoflavanoids, decreases the concentration of phytoalexins and increases the growth of the infecting oomycete. Similar to what we discussed in Sect. 13.3.3, there is also an **arms race** between plants and microbial pathogens, which have evolved to detoxify phytoalexins. For example, fungal pathogens of Brassicaceae (cabbage family) such as *Alternaria brassicicola*, *Botrytis cinerea*), *Leptosphaeria maculans*, *Rhizoctonia solani*, and *Sclerotinia sclerotiorum* detoxify phytoalexins using different reaction types (Pedras and Abdoli 2017). The second point we stress is that synthesis of phytoalexins is only one of a range of mechanisms involved in combating the pathogen. Production of hydrolytic enzymes (*e.g.*, chitinases and glucanases) is also part of the defense response (AbuQamar et al. 2017). The proteins induced upon pathogen attack are referred to as **pathogenesis-related proteins** (**PRs**); they accumulate either in intercellular spaces or intracellularly in the vacuole (Van Loon et al. 2006). Some of these PRs confer disease resistance and inhibit fungal growth *in vitro* as well as *in vivo* (Boller and Felix 2009). Whilst phytoalexins typically accumulate at the site of attack, PR proteins also accumulate **systemically** (Van Loon et al. 2006).

After attack of a resistant host by an avirulent pathogen, the enzymes required for the synthesis of phytoalexins are first produced *de novo*, and

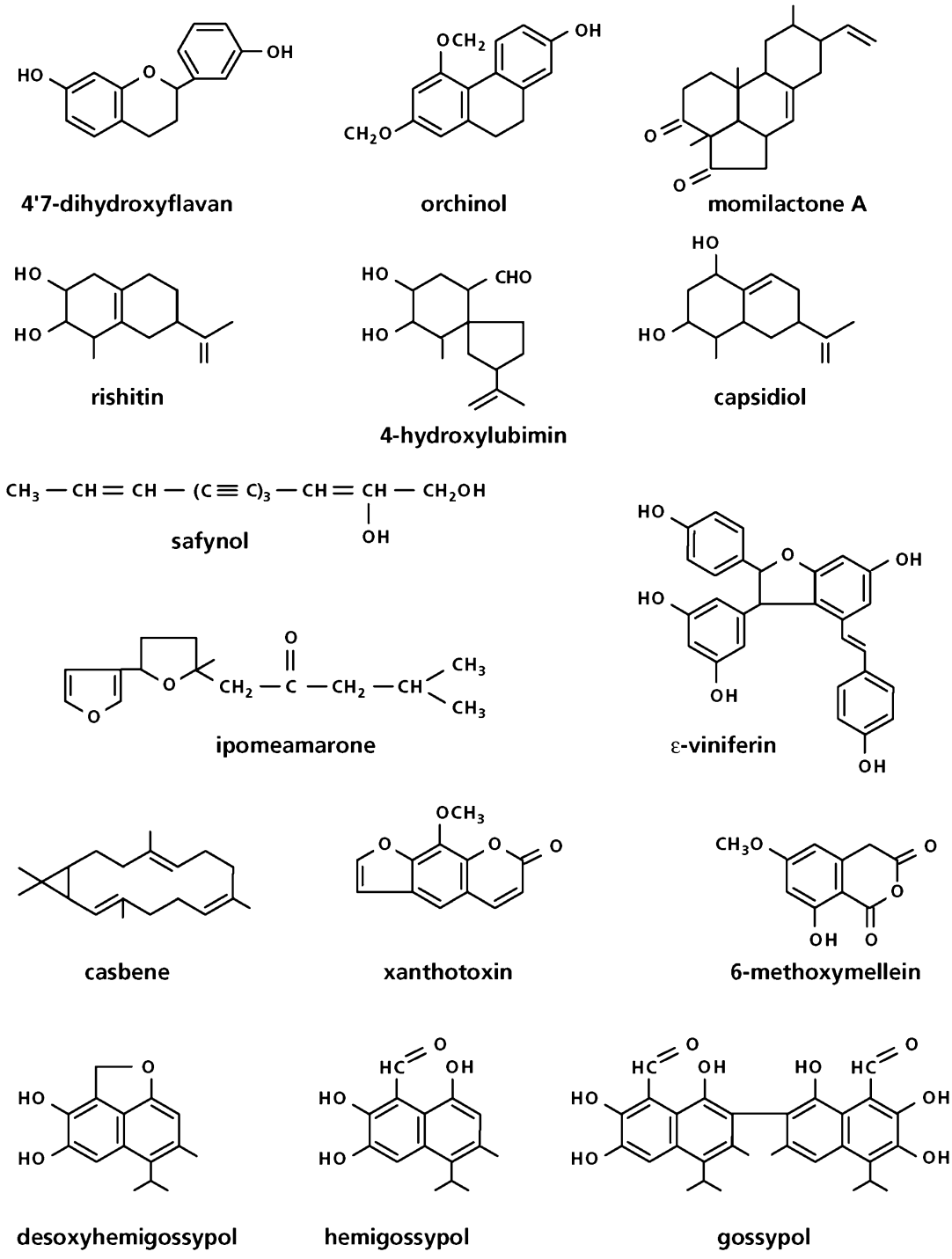

Fig. 14.5 Some examples of phytoalexins in different plant species (Bell 1981).

then the phytoalexins accumulate. The chemicals are produced in living plant cells, and may well lead to the death of these cells, due to their toxicity for the host plant as well as for the pathogenic microorganism. Some phytoalexins [*e.g.*, glyceollin from *Glycine max* (soybean)] are

specific inhibitors of complex I of the mitochondrial electron-transport chain (Sect. 3.2.2.1). Glyceollin can be found in soybean roots as soon as two hours after inoculation with the oomycete pathogen *Phytophthora megasperma* (Hahn et al. 1985).

In several pathosystems, the hypersensitive response to an avirulent pathogen (incompatible interaction) as well as the response to a virulent pathogen (compatible interaction) are accompanied by an **induced systemic resistance** to infection by other pathogens (Pieterse et al. 2014). It involves **salicylate-** and **jasmonate**-dependent defense pathways (Gkizi et al. 2016) and activation of **PR genes** (Kourelis and van der Hoorn 2018). **Methyl salicylate**, which is a volatile liquid known as oil of wintergreen, is produced from salicylic acid by a number of plant species. It is a major volatile compound released by *Nicotiana tabacum* (tobacco) inoculated with tobacco mosaic virus. Methyl salicylate may act as an airborne signal that activates disease resistance and the expression of defense-related genes in neighboring plants and in the healthy tissues of infected plants (Park et al. 2007). Plants treated with salicylic acid or acetylsalicylic acid (aspirin) for 12 to 24 hours are primed to respond much faster to pathogen-derived signals with the production of phytoalexins and their biosynthetic enzymes, PRs, and the production of ROS. Humans are obviously not the only organisms that benefit from aspirin.

Resistance genes are also activated by exposure to ethylene or the vapor of methyl jasmonic acid (Pieterse et al. 2014), *e.g.*, in *Solanum lycopersicum* (tomato), *Medicago sativa* (alfalfa), or *Nicotiana tabacum* (tobacco). Methyl jasmonic acid is a cyclopentanone that it synthesized from linolenic acid; it is well known as a fragrant constituent of the essential oil of *Jasminum grandiflorum* (Spanish jasmine) (Demole et al. 1962), but is universal in plants. Jasmonic acid or methyl jasmonic acid from either a synthetic solution or from undamaged twigs of *Artemisia tridentata* (sagebrush) are equally effective. They are common secondary metabolites that often occur in higher levels in damaged plants. Plants like *Artemisia tridentata* are promising for use as an '**intercrop**' (*i.e.* plants used in combination with a crop plant to protect the crop against pests in an environmentally friendly way (Kessler et al. 2006). Intercropping has been proposed as a method to contribute to **pest control** (Brooker et al. 2015). Plants can also become resistant by exposure to nonpathogenic root-colonizing bacteria, *e.g.*, to fluorescent *Pseudomonas* sp. in *Dianthus caryophyllus* (carnation). In this **induced systemic resistance**, however, salicylic acid does not play a role (Pieterse et al. 2014).

14.4 Cross-Talk Between Induced Systemic Resistance and Defense Against Herbivores

The responses to microbial pathogens (Sect. 14.3) have much in common with responses to herbivory (Sect. 13.3). For example, the expression of resistance to **pathogens** as well as to **insect herbivores** involves two signaling pathways, one involving **salicylic acid**, and another involving **jasmonic acid**. Stimulation of induced systemic resistance in field-grown *Solanum lycopersicum* (tomato) plants with benzothiadiazole (a salicylate mimic) (1) attenuates the jasmonate-induced expression of the antiherbivore defense-related enzyme **polyphenol oxidase**, and (2) compromises host-plant resistance to larvae of the beet armyworm, *Spodoptera exigua.* On the other hand, treatment of plants with jasmonic acid at concentrations that induce resistance to insects reduces **pathogenesis-related protein** gene expression induced by benzothiadiazole; this partially reverses the protective effect of benzothiadiazole against bacterial speck disease, which is caused by *Pseudomonas syringae*. This suggests that the sharing of elements of the two defense pathways may involve **trade-offs** (Fig. 14.6; Pieterse et al. 2014). Therefore, effective utilization of induced systemic resistance to multiple pests typically encountered in agriculture requires understanding potential signaling conflicts in plant defense responses.

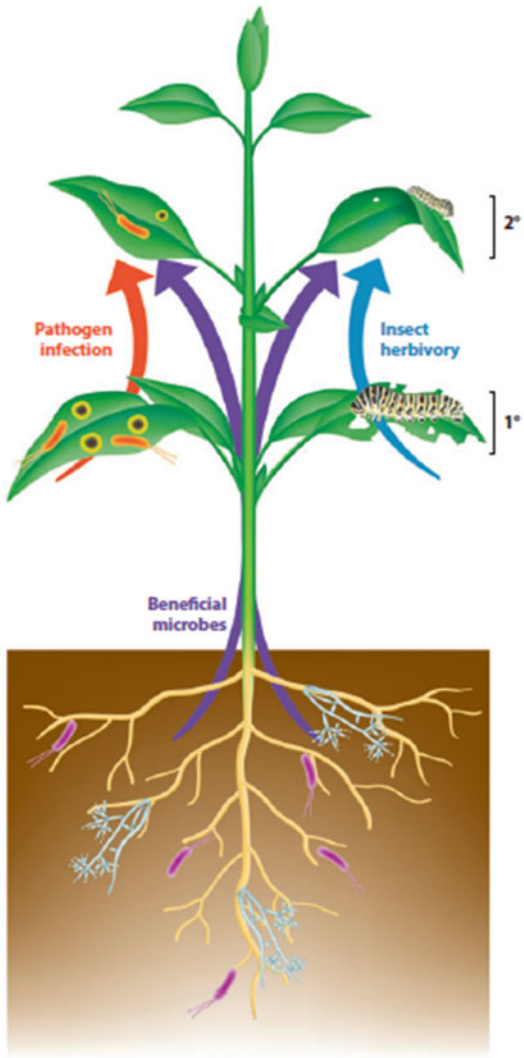

Fig. 14.6 Schematic representation of biologically induced resistance triggered by pathogen infection (orange arrow), insect herbivory (blue arrow), and colonization of the roots by beneficial microbes (purple arrows). Induced resistance involves long-distance signals that are transported through the vasculature or as airborne signals, and systemically propagate an enhanced defensive capacity against a broad spectrum of attackers in still healthy plant parts. Consequently, secondary (2°) pathogen infections or herbivore infestations of induced plant tissues cause significantly less damage than those in primary (1°) infected or infested tissues (modified after Pieterse et al. 2014).

Considering the case study of *Solanum lycopersicum* (tomato) discussed above, variable outcomes can be expected when plants are exposed to microbial pathogens, because there can be **cross-talk** between signaling pathways, leading to induced defense as well as induced resistance against herbivores. On one hand, resistance elicited by one group of enemies and active (also) against another is called **cross-resistance** (*e.g.*, resistance against pathogens induced by herbivores, and *vice versa*). Cross-resistance has been found in different systems. For example, feeding by thrips and aphids reduces infection of *Cucurbita citrullus* (watermelon) by the fungus *Colletotrichum orbiculare*. Defoliation of *Glycine max* (soybean) by *Pseudoplusia includens* (soybean looper moth) reduces the severity of two different fungal infections. Beetle grazing can induce resistance against fungal infections in *Rumex obtusifolius* (bitter dock). *Helicoverpa zea* (corn earworm) feeding can increase resistance of *Solanum lycopersicum* (tomato) plants to an aphid species (*Macrosiphum euphorbiae*), a mite species (*Tetranychus urticae*), corn earworm (*Spodoptera exigua*), and to a bacterial phytopathogen, *Pseudomonas* (Bostock 2005). In *Arabidopsis thaliana*, feeding by caterpillars of the cabbage white butterfly (*Pieris rapae*) results in enhanced resistance against the bacterial pathogens *Pseudomonas syringae* and *Xanthomonas campestris*, and turnip crinkle virus (De Vos et al. 2006).

Instead of cross-talk, there may be **trade-offs**, *i.e.* compromised resistance against one group of enemies when the plant is in the induced stage against the other group. For example, chemical induction of induced systemic resistance decreases a plant's ability to express wound-inducible proteinase inhibitors. Similarly, salicylic-acid treatment inhibits wound- and jasmonic-acid-induced responses in the same plant, and application of jasmonic acid partially reduces the efficacy of chemically-induced systemic resistance elicitors. Results available so far show that salicylic acid can inhibit the signaling cascade at different steps that are located both upstream and downstream of jasmonic acid (Spoel et al. 2003).

In summary, there are three steps in the induction pathway leading to defense: (1) **elicitation**, (2) **signaling**, and (3) **production**, *i.e.* gene

expression and synthesis of enzymes and other proteins involved in the establishment of the resistant phenotype. Interactions may occur independently on all three levels.

1. **Elicitation:** salicylic acid is synthesized in response to mechanical damage, necrosis and oxidative stress. Compounds resulting from the degradation of cells or cell walls might be involved in eliciting the systemic signal, and induced systemic resistance can thereby be induced by different types of enemies. Correspondingly, jasmonic acid can be induced in response to cell-wall degradation. Further elicitors in the context of both wound response and induced systemic response include the development of ROS. Therefore, events at the elicitation level will mainly lead to the expression of a rather nonspecific cross-resistance.
2. **Signaling:** further interactions can occur at the signaling level. Different activities of the various intermediates leading to jasmonic acid may lead to a diversity of potential outcomes. Similar regulatory properties might characterize the salicylic-acid-dependent signaling. An inhibition of the jasmonic acid pathway by salicylic acid has been described in different plant species. While herbivores can induce both an induced systemic response and induced resistance to herbivores, an induction by pathogens leads to synthesis of high concentrations of salicylic acid, and thus blocks later steps in signaling involving the jasmonic acid pathway. Phenotypically, pathogen attack thus induces mainly (or only) induced systemic response compounds.
3. **Production:** The trade-offs might, in contrast, occur mainly at the production level (*i.e.* signal-response coupling). Production of defensive compounds can be limited by the supply of available precursors such as amino acids, ATP, and other biosynthetic cofactors, and so does not depend only on the outcome of events at the signaling level. Induction of salicylic-acid-responsive and of jasmonic-acid-responsive genes appear to occur each at the cost of the other group, presumably since plants are compromised in the total amount of defensive compounds that can be produced during a limited time span.

14.5 Messages from One Organism to Another

Plants continually receive messages from their environment, including chemical messages (elicitors) released by pathogenic and nonpathogenic microorganisms. Resistant plants respond to these messages by defending themselves. This involves sacrificing a small number of cells in a programmed manner, and trapping the pathogen inside dead cells; it also involves both a physical and chemical defense of the surviving cells. Upon attack by pathogens, both resistant and surviving sensitive plants acquire greater resistance to subsequent attack, be it by the same or by a different pathogen. In recent years, remarkable surveillance mechanisms have been discovered that have evolved in plants to recognize microbial factors and combat pathogenic microbes. The discovery of resistance that is induced by nonpathogenic rhizobacteria which is a process of plant **immunization** to diseases, is receiving increased attention. It may help us protect our crops against pathogens in an environmentally friendly manner.

Many plants may be damaged by herbivores at the same time as being attacked by microbial pathogens. The subsequent defense responses may either induce **cross-resistance** or involve a **trade-off**, depending on the plant species and the attacking organism. If nonpathogenic rhizobacteria induce cross-resistance, this offers potential for applications in intensive agricultural systems.

References

AbuQamar S, Moustafa K, Tran LS. 2017. Mechanisms and strategies of plant defense against Botrytis cinerea. *Crit Rev Biotechnol* **37**: 262-274.

Badreddine I, Lafitte C, Heux L, Skandalis N, Spanou Z, Martinez Y, Esquerré-Tugayé M-T, Bulone V, Dumas B, Bottin A. 2008. Cell wall chitosaccharides are essential components and exposed patterns of the phytopathogenic oomycete *Aphanomyces euteiches*. *Eukaryot Cell* **7**: 1980-1993.

Bell AA. 1981. Biochemical mechanisms of disease resistance. *Annu Rev Plant Physiol* **32**: 21-81.

Biere A, Marak HB, van Damme JMM. 2004. Plant chemical defense against herbivores and pathogens: generalized defense or trade-offs? *Oecologia* **140**: 430-441.

Boller T, Felix G. 2009. A renaissance of elicitors: perception of microbe-associated molecular patterns and danger signals by pattern-recognition receptors. *Annu Rev Plant Biol* **60**: 379-406.

Bostock RM. 2005. Signal crosstalk and induced resistance: straddling the line between cost and benefit. *Annu Rev Phytopathol* **43**: 545-580.

Bourras S, McNally KE, Ben-David R, Parlange F, Roffler S, Praz CR, Oberhaensli S, Menardo F, Stirnweis D, Frenkel Z, Schaefer LK, Flückiger S, Treier G, Herren G, Korol AB, Wicker T, Keller B. 2015. Multiple avirulence loci and allele-specific effector recognition control the *Pm3* race-specific resistance of wheat to powdery mildew. *Plant Cell* **27**: 2991-3012.

Brooker RW, Bennett AE, Cong W-F, Daniell TJ, George TS, Hallett PD, Hawes C, Iannetta PPM, Jones HG, Karley AJ, Li L, McKenzie BM, Pakeman RJ, Paterson E, Schöb C, Shen J, Squire G, Watson CA, Zhang C, Zhang F, Zhang J, White PJ. 2015. Improving intercropping: a synthesis of research in agronomy, plant physiology and ecology. *New Phytol* **206**: 107-117.

Carere J, Benfield AH, Ollivier M, Liu CJ, Kazan K, Gardiner DM. 2017. A tomatinase-like enzyme acts as a virulence factor in the wheat pathogen saponin-detoxifying enzymes *Fung Gen Biol* **100**: 33-41.

Chamberlain DW, Paxton JD. 1968. Protection of soybean plants by phytoalexins. *Phytopathology* **58**: 1349 1350.

Chen C-S, Chen C-Y, Ravinath DM, Bungahot A, Cheng C-P, You R-I. 2018. Functional characterization of chitin-binding lectin from *Solanum integrifolium* containing anti-fungal and insecticidal activities. *BMC Plant Biol* **18**: 3.

Chisholm ST, Coaker G, Day B, Staskawicz BJ. 2006. Host-microbe interactions: shaping the evolution of the plant immune response. *Cell* **124**: 803-814.

Coll NS, Epple P, Dangl JL. 2011. Programmed cell death in the plant immune system. *Cell Death Different* **18**: 1247.

De Vos M, Van Zaanen W, Koornneef A, Korzelius JP, Dicke M, Van Loon LC, Pieterse CMJ. 2006. Herbivore-induced resistance against microbial pathogens in *Arabidopsis*. *Plant Physiol* **142**: 352-363.

Demole E, Lederer E, Mercier D. 1962. Isolement et détermination de la structure du jasmonate de méthyle, constituant odorant caractéristique de l'essence de jasmin. *Helv Chim Acta* **45**: 675-685.

Flor HH. 1971. Current status of the gene-for-gene concept. *Annu Rev Phytopathol* **9**: 275-296.

Gkizi D, Lehmann S, L'Haridon F, Serrano M, Paplomatas EJ, Métraux J-P, Tjamos SE. 2016. The innate immune signaling system as a regulator of disease resistance and induced systemic resistance activity against *Verticillium dahliae*. *Mol Plant-Microbe Interact* **29**: 313-323.

Hahn MG, Bonhoff A, Grisebach H. 1985. Quantitative localization of the phytoalexin glyceollin I in relation to fungal hyphae in soybean roots Infected with *Phytophthora megasperma* f. sp. *glycinea*. *Plant Physiol* **77**: 591-601.

Hoffland E, Niemann GJ, Van Pelt JA, Pureveen JBM, Eijkel GB, Boon JJ, Lambers H. 1996. Relative growth rate correlates negatively with pathogen resistance in radish: the role of plant chemistry. *Plant Cell Environ* **19**: 1281-1290.

Jones JDG, Dangl JL. 2006. The plant immune system. *Nature* **444**: 323-329.

Kessler A, Halitschke R, Diezel C, Baldwin IT. 2006. Priming of plant defense responses in nature by airborne signaling between *Artemisia tridentata* and *Nicotiana attenuata*. *Oecologia* **148**: 280-292.

Kourelis J, van der Hoorn RAL. 2018. Defended to the nines: 25 Years of resistance gene cloning Identifies nine mechanisms for R protein function. *Plant Cell* **30**: 285-299.

Liu F, Zhang X, Lu C, Zeng X, Li Y, Fu D, Wu G. 2015. Non-specific lipid transfer proteins in plants: presenting new advances and an integrated functional analysis. *J Exp Bot* **66**: 5663-5681.

Ma JF, Yamaji N. 2006. Silicon uptake and accumulation in higher plants. *Trends Plant Sci* **11**: 392-397.

Melotto M, Underwood W, Koczan J, Nomura K, He SY. 2006. Plant stomata function in innate immunity against bacterial invasion. *Cell* **126**: 969-980.

Melotto M, Zhang L, Oblessuc PR, He SY. 2017. Stomatal defense a decade later. *Plant Physiol* **174**: 561-571.

Nawrot R, Barylski J, Nowicki G, Broniarczyk J, Buchwald W, Goździcka-Józefiak A. 2014. Plant antimicrobial peptides. *Folia Microbiologica* **59**: 181-196.

Osbourn A. 1996. Saponins and plant defence — a soap story. *Trends Plant Sci* **1**: 4-9.

Osbourn AE. 2003. Saponins in cereals. *Phytochemistry* **62**: 1-4.

Pajerowska-Mukhtar KM, Emerine DK, Mukhtar MS. 2013. Tell me more: roles of NPRs in plant immunity. *Trends Plant Sci* **18**: 402-411.

Park S-W, Kaimoyo E, Kumar D, Mosher S, Klessig DF. 2007. Methyl salicylate Is a critical mobile signal for plant systemic acquired resistance. *Science* **318**: 113-116.

Pedras MSC, Abdoli A. 2017. Pathogen inactivation of cruciferous phytoalexins: detoxification reactions, enzymes and inhibitors. *RSC Advances* **7**: 23633-23646.

Pieterse CMJ, Zamioudis C, Berendsen RL, Weller DM, Van Wees SCM, Bakker PAHM. 2014. Induced

systemic resistance by beneficial microbes. *Annu Rev Phytopathol* **52**: 347-375.

Poschenrieder C, Cabot C, Martos S, Gallego B, Barceló J. 2013. Do toxic ions induce hormesis in plants? *Plant Sci* **212**: 15-25.

Poschenrieder C, Tolrà R, Barceló J. 2006. Can metals defend plants against biotic stress? *Trends Plant Sci* **11**: 288-295.

Pryor T, Ellis J. 1993. Genetic complexity of fungal resistance genes in plants. *Adv Plant Pathol* **10**: 281-305.

Simons BH, Lambers H 1998. The alternative oxidase: is it a respiratory pathway allowing a plant to cope with stress? In: Lerner HR ed. *Plant Responses to Environmental Stresses: from Phytohormones to Genome Reorganization*. New York: Marcel Dekker, 265-286.

Spanu PD, Panstruga R. 2017. Biotrophic plant-microbe interactions. *Front Plant Sci* **8**: 192.

Spoel SH, Koornneef A, Claessens SMC, Korzelius JP. 2003. NPR1 modulates cross-talk between salicylate-and jasmonate-dependent defense pathways through a novel function in the cytosol. *Plant Cell* **15**: 760-770.

Stakman EC. 1915. Relation between *Puccinia graminis* and plants highly resistant to its attack. *J Agric Res* **4**: 193-200.

Swain R, Rout GR 2017. Silicon in agriculture. In: Lichtfouse E ed. *Sustainable Agriculture Reviews*. Cham: Springer International Publishing, 233-260.

Van Loon LC, Rep M, Pieterse CMJ. 2006. Significance of inducible defense-related proteins in infected plants. *Annu Rev Phytopathol* **44**: 135-162.

VanEtten HD, Sandrock RW, Wasmann CC, Soby SD, McCluskey K, Wang P. 1995. Detoxification of phytoanticipins and phytoalexins by phytopathogenic fungi. *Can J Bot* **73**: 518-525.

Wiesner-Hanks T, Nelson R. 2016. Multiple disease resistance in plants. *Annu Rev Phytopathol* **54**: 229-252.

Biotic Influences: Parasitic Associations 15

15.1 Introduction

We have so far mainly dealt with **autotrophic** plants that assimilate CO_2 from the atmosphere into complex organic molecules and acquire nutrients and water from the rhizosphere. There are also fascinating plant species that lack the capacity to assimilate sufficient CO_2 to sustain their growth and that cannot absorb nutrients and water from the rhizosphere in sufficient quantities to reproduce successfully. These plants comprise approximately 1% of all flowering plant species; they are parasitic and rely on a host plant to provide them with the materials they cannot acquire from their abiotic environment (Nickrent et al. 1998; Westwood et al. 2010). About 4000 plant species within 270 genera in over 20 families [predominantly angiosperms; we only have firm evidence for one gymnosperm parasite: *Parasitaxus ustus* (conifer coral tree) (Feild and Brodribb 2005)] rely on a parasitic association with a host plant for their mineral nutrition, water uptake, and/or carbon supply (Fig. 15.1). Molecular analysis of nuclear, chloroplast, and mitochondrial DNA suggests at least 12 or 13 origins of parasitism in angiosperms (Nickrent et al. 1998; Barkman et al. 2007; Westwood et al. 2010). They inhabit ecosystems ranging from the high Arctic to the tropics (Press and Phoenix 2005). Some of these species [*e.g.*, *Striga* spp. (witchweed), *Orobanche* spp. (broomrape), *Cuscuta* spp. (dodder laurel), and *Arceuthobium douglasii* (Douglas-fir dwarf mistletoe)] are economically important pests that cause large yield losses of crop or forest plants, especially in Africa and Mediterranean countries (Estabrook and Yoder 1998; Runyon et al. 2010). Other parasitic species (*Cistanche* spp.) are grown commercially to extract traditional medicines in China (Li et al. 2016), or for their fragrant wood [*Santalum album* and *Santalum spicatum* (sandalwood)] (Jones et al. 1995). Ecologically, parasitic plants fill a fascinating niche in their exploitation of other plants to acquire sparingly available resources.

Parasitic angiosperms are generally divided into **holoparasites** and **hemiparasites** (Fig. 15.1). Holoparasites are **obligate** parasites; they depend entirely on their host for the completion of their life cycle. Although they do have chloroplasts (Song et al. 2017), they contain very little chlorophyll and lack the capacity to photosynthesize at rapid rates. *Cuscuta pentagona* (dodder) even exchanges large amount of mRNA with its hosts, *Arabidopsis thaliana* and *Solanum lycopersicum* (tomato); nearly half the expressed transcriptome of *Arabidopsis thaliana* can be found in the parasite (Kim et al. 2014). *Cuscuta campestris* (field dodder) haustoria accumulate high levels of many novel microRNAs (miRNAs) while parasitizing *Arabidopsis thaliana*. The same miRNAs that are expressed and active when *Cuscuta campestris* parasitizes *Arabidopsis thaliana* are also expressed and active when it infects *Nicotiana benthamiana* (Australian tobacco). These

H. Lambers, R. S. Oliveira, *Plant Physiological Ecology*, https://doi.org/10.1007/978-3-030-29639-1_15

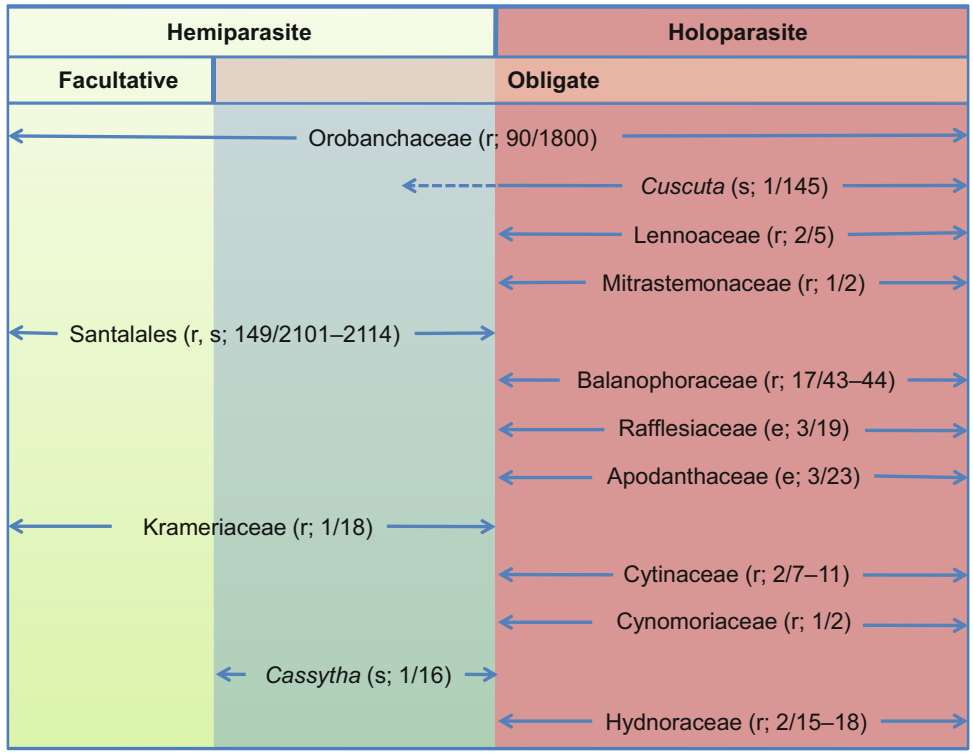

Fig. 15.1 The diversity of parasitism in flowering plants, reflecting a likely 12 or 13 surviving origins of parasitism in angiosperm evolutionary history. Several studies suggest that Balanophoraceae, a family of holoparasitic root parasites, could be closely related to Santalales; however, it is not yet clear if Balanophoraceae represents a derived holoparasitic lineage within the parasitic Santalales, or a basal lineage that has independently evolved parasitism. Thirteen lineages are indicated, with mode of feeding (r, root; s, stem; e, plant is principally an internal endophyte), whether individual species are facultative (optional) or obligate parasites, if species are hemiparasitic or holoparasitic, and the estimated number of genera and species. Only parasites that directly invade the tissue of a photosynthetic host plant via a haustorium are included; parasitism of mycorrhizal interactions has also evolved on numerous occasions. Most of the lineages are fully holoparasitic (8 of 13), although three contain only facultative and/or obligate hemiparasites. Orobanchaceae has the full trophic range of parasitic plants from facultative hemiparasites through obligate hemiparasites and completely heterotrophic holoparasites. Within Orobanchaceae, hemiparasitism has progressed to holoparasitism on at least five, and possibly more, occasions. Most *Cuscuta* (dodder) species produce chlorophyll and perform photosynthesis, but photosynthesis in at least some *Cuscuta* species serves to recycle host-derived carbon rather than fix carbon from the atmosphere. Members of traditional Santalales (mistletoe) families range from free-living non-parasitic trees to species that maintain only minimal photosynthesis at narrow points in the life cycle (Westwood et al. 2010); copyright Elsevier Science, Ltd.

miRNAs act as regulators of host-gene expression, and may act as virulence factors during parasitism (Shahid et al. 2018). Glucosinolates (Sect.13.3.2) also move from *Arabidopsis thaliana* towards *Cuscuta gronovii* (common dodder); hosts with high levels of glucosinolates reduce both the growth of the dodder and survival on dodder vines by pea aphids (*Acyrthosiphon pisum*) (Smith et al. 2016). Large molecules can be exchanged, because there is unselective symplasmic transfer between host and parasite (Birschwilks et al. 2006).

Hemiparasites may be either **facultative** or **obligate** parasites. They contain chlorophyll and have some photosynthetic capacity, but they depend on their host for the supply of water and nutrients. The distinction between holoparasites and hemiparasites is not sharp. For example,

Striga species are considered hemiparasites, but they have very little chlorophyll and show only a limited photosynthetic capacity (Table 15.1).

Parasitic angiosperms are further subdivided into **stem parasites**, such as the holoparasitic *Cuscuta* and *Cassytha* (dodder and dodder laurel) and the hemiparasitic *Viscum* and *Amyema* (mistletoes), and **root parasites**, such as the holoparasitic *Orobanche* (broomrape) and the hemiparasitic *Striga* (witchweed) (Stewart and Press 1990).

Parasites may be entirely endophytic, living embedded in the stem of their legume host during their vegetative stage, *e.g.*, *Pilostylis* species (Fay et al. 2010). More often, they are small herbaceous species [*e.g.*, *Rhinantus sclerotinus* (yellow rattle) and *Melampyrum pratense* (cow-wheat), shrubs [*e.g.*, *Santalum acuminatum* (quandong), or large trees [*e.g.*, *Nuytsia floribunda* (Western Australian Christmas tree) and *Exocarpus cupressiformis* (cherry ballart)]. The largest parasitic plant is the west African rainforest tree, *Okoubaka aubrevillei* that can be 40 m tall (Veenendaal et al. 1996). Many parasitic plants have a broad host range. For example, *Castilleja* (paintbrush) species parasitize over a hundred different hosts from a variety of families (Press 1998), and *Rhinanthus minor* (yellow rattle) has approximately 50 different host species from 18 families within European grasslands; a single *Rhinanthus minor* plant may parasitize up to seven different host species simultaneously. In contrast, *Santalum acuminatum* (quandong) has a strong preference for some nitrogen-fixing Fabaceae and Casuarinaceae which strongly restricts its distribution in Australia (Nge et al. 2019). Shoot parasites tend to have a much smaller host range than do root parasites, but broad host ranges still occur, such as with *Cuscuta* (dodder) and *Cassytha* (dodder laurel) species with hosts that number in the hundreds. Also, the tropical rainforest mistletoe *Dendrophthoe falcata* has nearly 400 known host species. Parasitic plants that can only utilize one or few host species are the exception; one of the most notable is the root parasite *Epifagus virginiana* (beech-drops), which only parasitizes *Fagus grandifolia* (American beech). Among shoot parasites, mistletoes provide examples of narrow host range, including the dwarf mistletoe *Arceuthobium minutissimum* (Himalayan dwarf mistletoe), which only parasitizes the pine species *Pinus griffithii* (Himalayan blue pine), and the Mexican mistletoe *Phoradendron scabberimum*, which only grow on other mistletoes (Press and Phoenix 2005).

Table 15.1 Some characteristics of *Striga hermonthica* (purple witchweed), which is an obligate root hemiparasite, in comparison with *Antirrhinum majus* (snapdragon), which is a related nonparasitic species.

Trait	*Striga hermonthica*	*Antirrhinum majus*
Stomatal frequency (mm^{-2})		
adaxial leaf surface	114	36
abaxial leaf surface	192	132
stem	24	28
Transpiration (mmol m^{-2} s^{-1})	8.5	5.7
Chlorophyll a + b content (g m^{-2})	2.6	7.2
Soluble protein content (g m^{-2})	12	23
Photosynthesis		
per m^2 leaf area (μmol s^{-1})	2.5	15.0
per g chlorophyll (μmol s^{-1})	1.0	2.6
Water-use efficiency [(mmol CO_2 mol^{-1} (H_2O)]	0.3	2.9

Source: Shah et al. (1987)

15.2 Growth and Development

15.2.1 Seed Germination

Many parasitic angiosperms have small seeds with a hard seed coat and remain viable for many years. The seeds have very small reserves so that the seedlings run the risk of dying if they do not quickly find a host to attach to. **Germination** of the seeds of the holoparasitic stem parasite *Cuscuta* (dodder) is completely independent of its host (Dawson et al. 1994), but many species [*e.g.*, *Alectra* (witchweed),

Orobanche (broomrape), and *Striga* (witchweed)] require a **chemical signal** from their host to trigger germination which increases their chances to survive (Bouwmeester et al. 2007). The first naturally occurring stimulant, **strigol**, was identified from *Gossypium hirsutum* (cotton, a nonhost); it stimulates germination of *Striga* (Cook et al. 1966). Strigol has also been found in root exudates from plants that do act as a host for *Striga* (Siame et al. 1993). It is a sesquiterpene, active in concentrations as low as 10^{-12} M in the soil solution. A second compound has been isolated from the root exudate of *Vigna unguiculata* (cowpea), which is a host for both *Striga* and *Alectra*. A range of other germination-stimulating compounds have since been isolated from roots of a range of species. These stimulants have somewhat differing structures; they are collectively known as **strigolactones** (Fig. 15.2). When seeds of *Striga asiatica* are placed in agar at a distance of about 5 mm from the root surface of *Sorghum bicolor* (millet), germination takes place. No germination occurs at a distance of 10 mm or more. Germination only occurs after a minimum of 5 h exposure to 1 mM hydroquinone. Root exudates of the host *Avena strigosa* (black oat) contain at least six different germination stimulants for root parasitic plants, **avenaol**, but no known strigolactones (Kim et al. 2014). Avenaol contains an additional carbon compared with known strigolactones. It is a potent germination stimulant of *Phelipanche ramosa* seeds, but only a weak stimulant for seeds of *Striga hermonthica* and *Orobanche minor*.

The stimulant from *Sorghum bicolor* (millet) enhances the synthesis of the phytohormone **ethylene**, which is a requirement for the germination of *Striga* (witchweed) seeds. Inhibition of the action or synthesis of ethylene prevents the effect of the germination stimulant, whereas its action

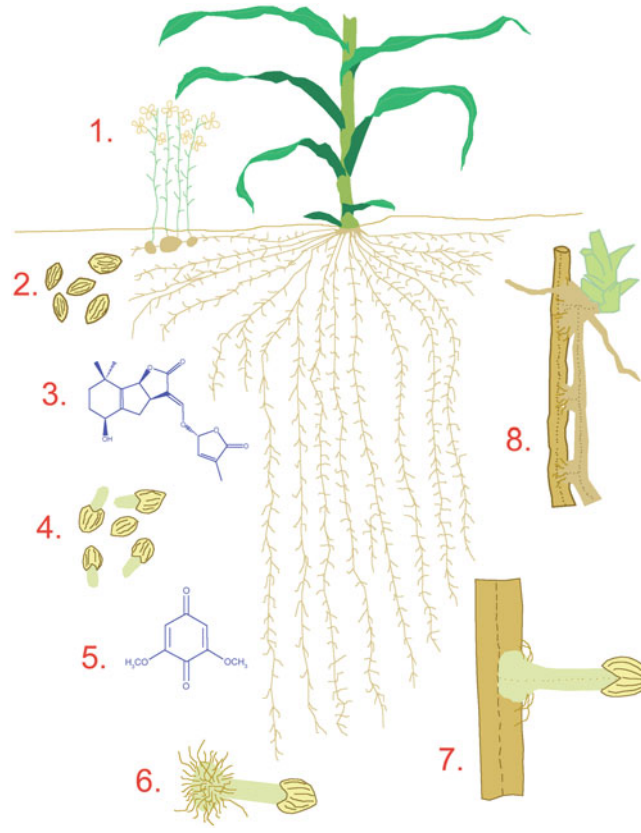

Fig. 15.2 Life cycle of *Striga* (witchweed), an obligate root hemiparasite that can only complete its life cycle when attached to a host (1). Germination of the very small seeds (2) is stimulated by signal molecules (strigolactones) released from the roots of a host plant (3). Attachment via a haustorium (4) requires an additional signal molecule (5). Upon penetration of the root via its haustorium, inorganic nutrients are imported from the host's xylem (7). Once the parasite starts growing, more haustoria are produced (8).

can be substituted by ethylene (Logan and Stewart 1991; Babiker et al. 1993).

The release of germination stimulants by roots of *Triticum aestivum* (wheat), which is not a host, has encouraged the use of this species as a 'trap crop' for *Orobanche minor* (broomrape) (Lins et al. 2006). A '**trap crop**' is a '**false host**' that is used to stimulate the germination of as many seeds as possible, without attachment, so that the problems for the next crop, which can act as a host, are minimized. **Intercrops** of *Desmodium uncinatum* silverleaf) that inhibit the growth of *Striga hermonthica* are use in *Zea mays* (maize) cropping in Kenya (Khan et al. 2002; Sect. 16.6.3). *Glycine max* (soybean) shows promising genetic variation in inducing germination of *Striga hermonthica* with little attachment (Odhiambo et al. 2011). The relative germination induction by soybean varieties ranged from 8% to 66% compared with 70% for a synthetic stimulant. Intercropping *Zea mays* (maize) with soybeans in the field leads to a low *Striga hermonthica* count and high maize yield.

If strigol is abundant in the soil during seed ripening, then it does not stimulate germination in the normal concentration range. A much higher concentration of strigol is then required to allow germination. This may be a mechanism avoiding germination at the end of the season, when the concentration of root exudates may be high. **Analogues of strigol** and numerous other, unrelated compounds have been synthesized and tested for their capacity to stimulate germination (Zwanenburg et al. 2009). Such compounds are potentially useful to reduce the economic problems that parasites cause to crops.

Genetic control is the most feasible means of crop protection from *Striga*. Recently, a gene regulating *Striga* resistance in *Sorghum bicolor* (sorghum) and the associated change in strigolactone chemistry were identified (Gobena et al. 2017). Knowing this gene and its various natural alleles, sorghum breeders can design markers within it to facilitate its transfer into improved varieties providing farmers effective control of *Striga* in infested fields. The gene could also be used to potentially improve *Striga* resistance through genome editing in crops that have few *Striga* resistance genes such as *Zea mays* (maize) (Yoneyama et al. 2015), which evolved away from *Striga*. The most economical and environmentally friendly control option is the use of resistant crop varieties; however, breeding for resistance is a difficult task considering the scarce and complex nature of resistance in most crops (Rubiales and Fernández-Aparicio 2012).

What might be the evolutionary advantage, if any, of the release of compounds that promote the growth and development of parasitic plants, and thus endanger their own existence? Some of the chemicals that act as triggers for germination or haustorium formation are **allelochemicals** or related to **phytoalexins**. For example, the stimulant from *Sorghum bicolor* (millet) readily oxidizes to a more stable quinone (sorgoleone) that strongly inhibits the growth of neighboring weeds (Sect. 13.2; Einhellig and Souza 1992). More importantly, plant-derived **strigolactones**, which are well known as germination stimulants for root parasitic plants, are 'branching factors', involved in a critical step in host recognition by **arbuscular mycorrhizal fungi** (Sect. 12.2; Akiyama et al. 2005; Bouwmeester et al. 2007). In *Trifolium pratense* (red clover), which is a host for arbuscular mycorrhizal fungi as well as for the root holoparasitic plant *Orobanche minor* (broomrape), a reduced phosphorus (P) supply promotes the release of orobanchol (a strigolactone), by clover roots. The level of orobanchol exudation is controlled by P availability and correlates with germination stimulation activity of the root exudates. Therefore, under **P deficiency**, roots attract not only symbiotic fungi, but may also promote root parasitic plants through the release of strigolactones (Yoneyama et al. 2007b). It is, therefore, not surprising that root exudates from **arbuscular mycorrhizal** plants of *Sorghum bicolor* (millet) induce lower germination of *Striga hermonthica* (purple witchweed) seeds than do exudates from nonmycorrhizal sorghum plants (Lendzemo et al. 2007). Field inoculation with arbuscular mycorrhizal fungi reduces the impact of *Striga hermonthica* on cereal crops, and has the potential to contribute to integrated *Striga* management (Lendzemo et al. 2005).

Nitrogen (N) **deficiency** in *Sorghum bicolor* (millet) also promotes the production and exudation of 5-deoxystrigol, the host recognition signal for arbuscular mycorrhizal fungi, (Yoneyama et al. 2007a). This would explain why germination of *Striga hermonthica* (purple witchweed) decreases with increasing root N concentrations (Ayongwa et al. 2006). Root parasitic plants have long been associated with nutrient-poor soils. This may in part be explained by their low competitive ability, but the recent findings that increased N and P availability reduce the release of strigolactones now offers an additional explanation.

15.2.2 Haustoria Formation

All parasitic plant species, with the exception of members of the endophytic Apodanthaceae, have a **haustorium**, which is a specialized multifunctional organ that functions in attachment, penetration, and transfer of water and solutes (Yoshida et al. 2016). Most parasitic plants will only develop a functional haustorium in the presence of a **chemical signal** from the host which differs from the signal that triggers germination. For example, haustorium formation in *Striga* (witchweed) species proceeds only when a signal molecule is released from host roots. An example of such a signal molecule is 2,6-dimethoxy-*p*-benzoquinone, which is produced by the host roots, in response to an enzyme from the parasite (Smith et al. 1990). Seeds of *Zea mays* (corn) are a rich source of a range of anthocyanins, other flavonoids, and simple phenolics that induce haustoria formation in *Triphysaria versicolor* (yellow owl's clover) (Albrecht et al. 1999). The chemical signals are often bound tightly to cell walls and are not released into the root environment. They are classified in four groups: flavonoids, *p*-hydroxy acids, quinones, and cytokinins; they are biologically active in the concentration range of 10^{-5}–10^{-7} M (Estabrook and Yoder 1998). The holoparasitic stem parasite *Cuscuta pentagona* (dodder) uses volatile cues from *Solanum lycopersicum* (tomato), *Impatiens walerana* (patient Lucy), and *Triticum aestivum* (wheat) to direct its growth toward nearby plants. Seedlings of the parasite can distinguish volatiles from different hosts and preferentially grow toward *Solanum lycopersicum* plants. Several individual compounds from *Solanum lycopersicum* and *Triticum aestivum* elicit directed growth by *Cuscuta pentagona*, whereas one compound from *Triticum aestivum* is repellent (Runyon et al. 2006).

Signals that are involved in preventing haustoria formation and subsequent attachment of the parasite to its host may explain **resistance** of some species to parasites (Rispail et al. 2007; Sect. 15.2.1). In *Vigna unguiculata* (cowpea) a typical nucleotide-binding site–leucine-rich repeat immune sensor protein confers resistance against *Striga gesnerioides* (cowpea witchweed) (Li and Timko 2009). This suggests that *Striga gesnerioides* secretes a corresponding effector that is recognized by the sensor protein in a resistant host, but suppresses the immune system in hosts that lack this sensor protein. Complete resistance to *Striga hermonthica* (purple witchweed) infection has not been identified in *Zea mays* (corn). A valuable source of resistance may be present in the genetic potential of wild germplasm, especially a wild relative of corn, *Tripsacum dactyloides* (gamma grass). *Striga hermonthica* development is arrested after attachment to *Tripsacum dactyloides*. Vascular continuity is established between parasite and host, but there is poor primary haustorial tissue differentiation on *Tripsacum dactyloides* compared with that on *Zea mays*. Partial resistance is inherited in a hybrid between the two species. *Tripsacum dactyloides* produces a signal that inhibits haustorial development; this signal may be mobile within the parasite haustorial root system (Gurney et al. 2003). Two distinct defense responses against *Rhinanthus minor* (yellow rattle) occur in the nonhost forbs *Leucanthemum vulgare* (field daisy) and *Plantago lanceolata* (snake plantain). *Leucanthemum vulgare* encapsulates the parasite's invading structures, thus preventing it from gaining access to the stele. In *Plantago lanceolata*, host cell fragmentation occurs at the interface between the parasite and host. Grasses and a legume that are good hosts for *Rhinanthus*

minor show no evidence of defense at the host/parasite interface (Cameron et al. 2006).

Elaborate work has been done on the ultrastructure of haustoria formation in a range of root parasites [*e.g.*, in the Australian root hemiparasite *Olax phyllanthi* (Kuo et al. 1989)]. Walls of parasitic cells that contact host xylem are thickened with polysaccharides rather than with lignin. Host xylem pits are a major pathway for water and solute transport from the host to the haustorium, whereas direct connections between xylem conducting elements of host and parasite are extremely rare. Symplasmic connections between the two partners are absent. Cells of the parasite that are adjacent to host cells often have an appearance similar to that of **transfer cells**.

The completely encircling haustorium of the root hemiparasite *Nuytsia floribunda* (Western Australian Christmas tree) is unique in cutting the host root transversely by means of a sclerenchymatic sickle-like cutting device (Fig. 15.3). Electron micrographs suggest that the developing haustorium acts as 'scissors', which effectively cut off the distal part of the host from the rest of the plant. Parenchymatic tissue of the parasite then develops tubelike apical extensions into the cut host xylem vessels, thereby facilitating absorption of xylem solutes from host xylem sap. Conducting xylem tissue in the haustorium terminates some distance from the interface, so absorbed substances must traverse several layers of parenchyma before gaining access to the xylem stream of the parasite. When grown in pots with a range of hosts, as well as in the field, *Nuytsia floribunda* has a more negative water potential than its host, causing water movement to the parasite (Calladine and Pate 2000).

After germination in the soil, the seedlings of the obligate stem parasite *Cuscuta* (dodder) start to grow up and circumnutate. *Cuscuta pentagona* uses volatile cues to locate its hosts (Mescher et al. 2006). Under favorable conditions many stems may grow from a twined seedling after attachment to the host. Enzymes from the parasite soften the surface tissue of the host, and the haustorium penetrates the host tissue. Vascular cells of the parasite contact vascular cells of the host, and the contents of the host's sieve tubes

Fig. 15.3 (**A**, **B**) Haustoria of root hemiparasites on host roots. (**A**) *Santalum acuminatum* (quandong) and (**B**) *Nuytsia floribunda* (Western Australian Christmas tree) (courtesy M.W. Shane, University of Western Australia, Perth, Australia). (**C**) Haustoria of the stem holoparasite *Cassytha* sp. (dodder laurel) parasitizing on a leaf of *Banksia elderiana* (swordfish banksia) (photo H. Lambers).

and xylem conduits are diverted into the parasite. As the dodder continues to grow, it maintains its support by continually reattaching to host plants (Mescher et al. 2006). A few plants exhibit **resistance** against infestation by *Cuscuta* spp. For example, cultivated *Solanum lycopersicum* (tomato) fends off *Cuscuta reflexa* (giant dodder) by means of a hypersensitive-type response occurring in the early penetration phase (Kaiser et al. 2015). This plant–plant dialog between *Cuscuta* spp. and its host plants involves an incompatible interaction as we discussed for plant pathogen interactions in Sect. 14.3 (Fig. 15.4).

Transfer of solutes via the haustorium may be partly passive, via the apoplast. The presence of

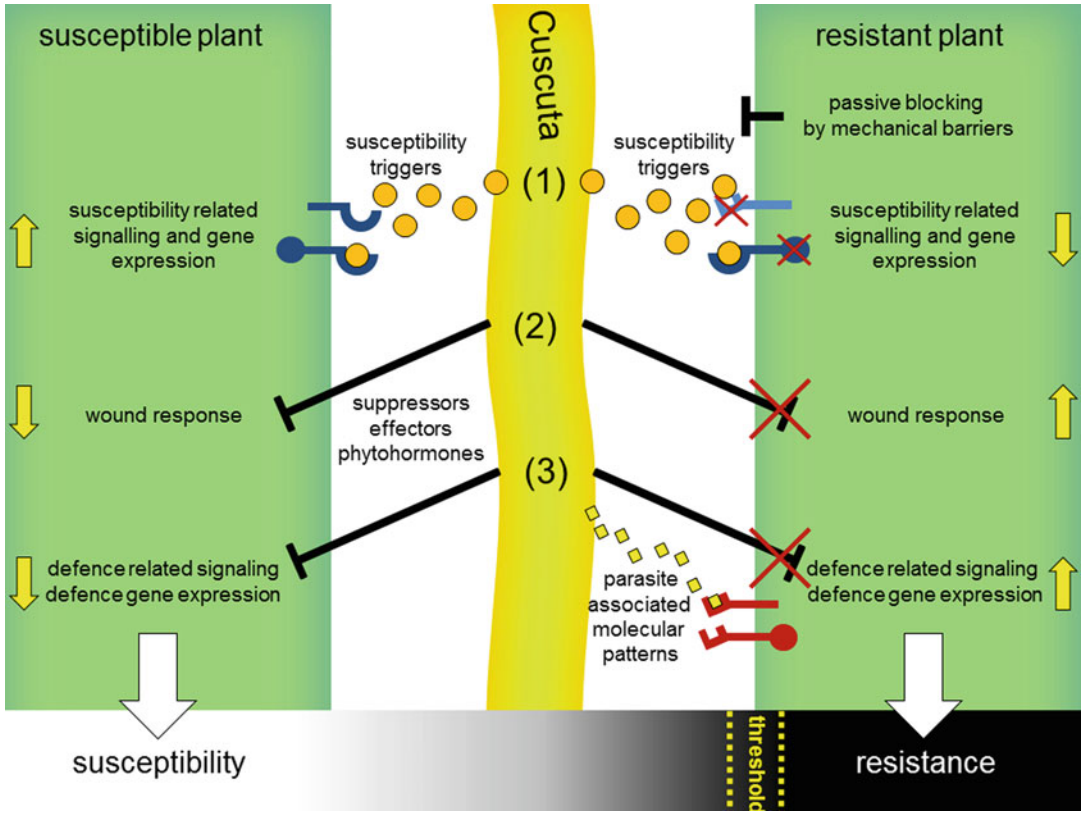

Fig. 15.4 Hypothetical model for interaction mechanisms of parasitic *Cuscuta* (dodder) with susceptible and resistant host plants. *Cuscuta* (middle, light green) attacking susceptible plants (left) release susceptibility triggers (orange dots) including common phytohormones and yet unknown signals, which get perceived by host plant receptors (blue) and consequently manipulate hosts to set on susceptibility-related responses and gene expression (1). In parallel, wound-related (2) and defense-related responses (3) that occur in the context of host penetration might get blocked by yet unknown suppressors. Resistant plants (right) might prevent a parasitic attack passively, *e.g.*, by reinforced cell walls as mechanical barriers or by nonresponsiveness to susceptibility triggers (1). Incompatibility could also result from a deficient blocking of the host wound (2) or defense response (3). In analogy to the perception of microbial pathogens, defense reactions might be actively triggered by host immunoreceptors (PRRs, red) that detect specific parasite-associated molecular patterns (3) (yellow diamonds) or secondary generated (*e.g.*, by parasitic hydrolytic enzymes) damage-associated molecular patterns (DAMPs). Susceptibility or resistance of host plants might be a sum of these interaction processes and, rather than black and white, appears to be a gradual process occurring in many plants. Thus, a certain threshold for the strength of defense reactions might be passed by host plants for a successful resistance against dodder (Kaiser et al. 2015).

parenchyma cells with many mitochondria, dictyosomes, ribosomes, and a well-developed ER, however, suggests that active processes play a role as well. Indeed, compounds absorbed by the haustoria may be processed before entering the shoot. As a result, the carbohydrates, amino acids, and organic acids in the xylem sap of *Striga hermonthica* (purple witchweed) and *Olax phyllanthi* differ from those in their hosts. The major compound in *Striga hermonthica* is mannitol, which does not occur in the host *Sorghum bicolor* (millet). Similarly, in xylem sap of *Sorghum bicolor* asparagine predominates as a nitrogenous compound, and malate and citrate as organic acids, whereas the major nitrogenous compound of *Striga hermonthica* is citrulline, and shikimic acid is the main organic acid. The carbohydrate concentrations in the parasite xylem sap may be five times greater than those in the xylem of the host (Pate 2001).

15.2.3 Effects of the Parasite on Host Development

Although some hemiparasitic plants can grow in the absence of a host, their productivity is greatly enhanced when they are attached to a host (Klaren 1975). At the same time, the growth of the host is reduced when a parasite is attached to it. The reduction in growth and grain yield of *Sorghum bicolor* (millet) infected by the parasitic *Striga hermonthica* (purple witchweed) is strongest at low N supply and may disappear completely at optimum N supply (Cechin and Press 1993). The parasite is also affected by the low N supply, with considerably reduced seed germination, reduced attachment, and poor growth of *Striga hermonthica* plants (Fig. 15.5).

Even though the root growth of *Ricinus communis* (castor bean) is inhibited when parasitized by *Cuscuta reflexa* (giant dodder), which is an obligate stem holoparasite, the rate of **NO_3^- uptake** per unit root mass is stimulated (Jeschke and Hilpert 1997). The rate of NO_3^- uptake in the host plant obviously increases with increasing N demand of the parasite-host association (Sect. 9.2.2.3). When parasitized by holoparasites, host plants may transiently show a faster rate of **photosynthesis**, greater stomatal conductance, and faster rates of transpiration, despite their smaller root system (Watling and Press 2001). Enhanced photosynthesis may be due to a higher N concentration in the leaves (Sect. 2.6.1), a higher sink demand (Sect. 2.4.2), or delayed leaf senescence (Jeschke and Hilpert 1997; Hibberd et al. 1999). Hemiparasites tend to have a negative effect on host photosynthesis (Watling and Press 2001). Likewise, *Cuscuta campestris* (field dodder) inhibits both growth and photosynthesis of *Mikania micrantha* (mile-a-minute). Therefore, in addition to utilizing the host's resources, the holoparasite also reduces growth of the infected hosts because of its must also be due to the negative effect on host photosynthesis (Shen et al. 2007).

Xylem-tapping stem hemiparasites (mistletoes), such as *Phoradendron juniperinum* (juniper mistletoe) and *Amyema preissii* (wire-leaf mistletoe), have no phloem connection with their host, and they tend to kill the host shoot beyond the point of infection. In this way, the mistletoe is the only green tissue to be supplied via the xylem by a particular branch. Despite the absence of phloem connections, the growth of the mistletoe and that of xylem of the host are closely correlated. Just like the correlation between leaf area and sapwood area in trees (Sect. 5.5.3.5), there is also a close correlation between the leaf area of the mistletoe and the sapwood area of the

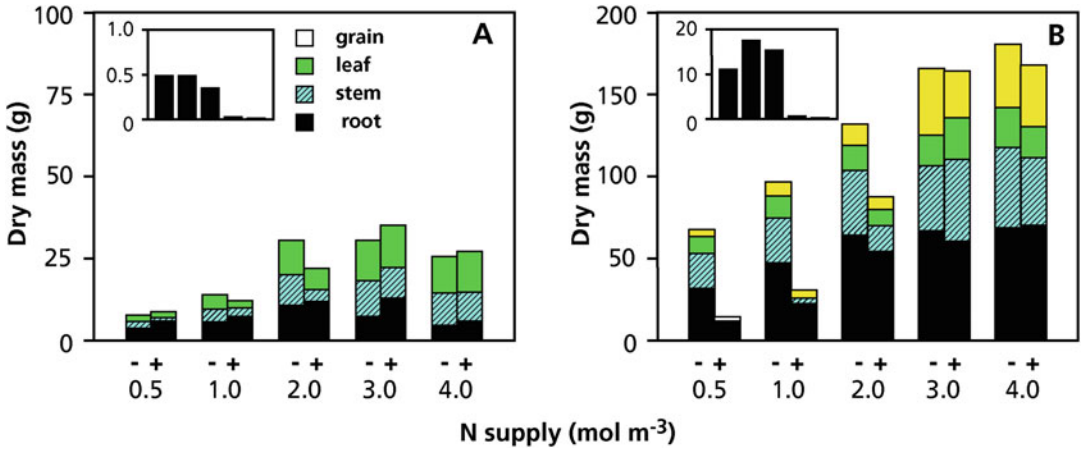

Fig. 15.5 Partitioning of dry mass in *Sorghum bicolor* (millet) grown at a range of N-supply rates in the absence (-) and presence (+) of *Striga hermonthica* (purple witchweed). Dry masses of the parasite are shown in the insets; (**A**) and (**B**) refer to 50 and 140 days after planting. Different shades in the columns, from bottom to top, refer to roots, stems, leaves, and seeds (after Cechin and Press 1993).

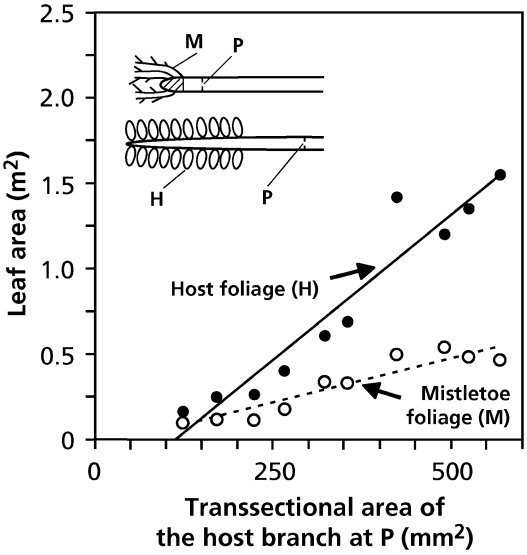

Fig. 15.6 Correlations between the area of the foliage of a nonparasitized branch of *Acacia acuminata* (raspberry jam) or the foliage of the xylem-tapping stem hemiparasite *Amyema preissii* (mistletoe), parasitizing on *Acacia acuminata*, and the transectional area of the branch of the host. Note that a similar transectional branch area supports substantially more foliage of the host than of the parasite (after Tennakoon and Pate 1996).

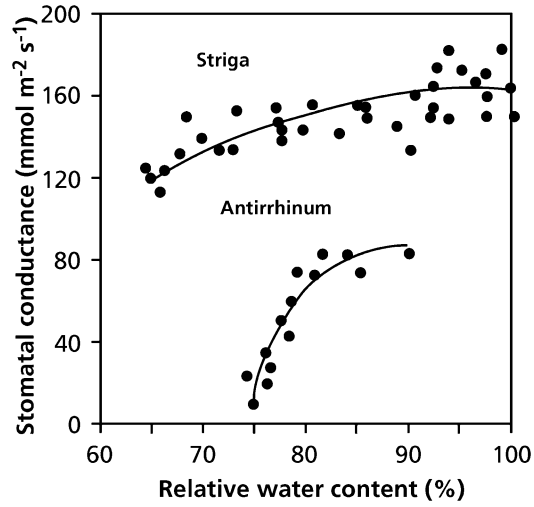

Fig. 15.7 The relationship between stomatal conductance and the relative water content of the leaves for the hemiparasite *Striga hermonthica* (purple witchweed) and the closely related nonparasitic plant *Antirrhinum majus* (snapdragon) (Shah et al. 1987). Copyright Physiologia Plantarum.

host branch proximal to the point of attachment (Fig. 15.6). This indicates that enlargement of the host stem must proceed, despite the impossibility of transport of any signals from the parasites' leaves via the phloem. For a similar area of foliage, the mistletoe appears to require a substantially greater sapwood area than does the host plant itself. This is correlated with a relatively faster rate of transpiration of the hemiparasite (Sect. 15.4).

15.3 Water Relations and Mineral Nutrition

Most herbaceous root and stem hemiparasites have high **stomatal frequencies**, rapid rates of **transpiration** and low **water-use efficiency** compared with their host (Schulze and Ehleringer 1984). The stomata of the herbaceous hemiparasites do respond to water stress, but stomatal closure is induced at much lower relative water contents (Fig. 15.7). Thus, the gradient in **water potential** between leaves and roots is steeper for the parasite than it is for its host, facilitating the flux of solutes imported *via* the xylem. This reflects a lower sensitivity of the stomata to ABA, the hormone associated with stomatal closure during water stress (Sect. 5.5.4.2), in the parasitic species [*Striga hermonthica* (purple witchweed)] than in related nonparasites (*Antirrhinum majus*) (Shah et al. 1987). Leaves of *Zea mays* (corn) plants that are parasitized by *Striga hermonthica* have higher levels of ABA than leaves of control plants, and the concentration of this phytohormone is an order of magnitude greater again in the leaves of the parasite (Taylor et al. 1996). The stomates of *Striga hermonthica* do not close, however, even when the relative water content of its leaves declines to 70% or less.

Rapid rates of transpiration are one of the reasons for a more negative **water potential** of the shoots of the hemiparasites compared with that of their hosts. This low shoot water potential of hemiparasites requires accumulation of solutes to maintain turgor. In *Santalum acuminatum* (quandong) a significant proportion of the

osmotic potential is accounted for by mannitol, Na^+, K^+, and Cl^-. A water potential difference of 1–2 MPa is maintained between this hemiparasitic shrub and its host. Xylem sap and leaves of *Santalum acuminatum* contain considerable concentrations (0.1–0.4 mol kg^{-1} tissue water) of mannitol (Loveys et al. 2001a). A favorable water-potential gradient toward *Striga hermonthica* (purple witchweed) is maintained, even when rates of transpiration are severely reduced. This is due to the haustorial resistance to water flow, which is 1.5–4.5 times greater than that offered by the parasite shoot (Ackroyd and Graves 1997). Both the fast rate of transpiration and the high resistance across the haustoria facilitate the diversion of host resources to the parasite. These host resources may also include **secondary metabolites** (naturally occurring insecticides) that increase the parasite's resistance against insects, *e.g.*, in *Santalum acuminatum* (quandong) attached to *Melia azedarach* (Cape lilac) (Loveys et al. 2001b).

The fast rates of transpiration of hemiparasitic plants have major consequences for the **leaf temperature** of the parasitic plants. The leaf temperature of *Striga hermonthica* (purple witchweed) may be as much as 7 °C below air temperature (Sect. 6.2.1). The use of **antitranspirants**, which reduce transpirational water loss, may enhance the leaf temperature of parasites to an extent that the leaves blacken and die. These compounds have been suggested as tools to control parasitic pests (Press et al. 1989).

The high stomatal conductance and fast rate of transpiration of parasites allow rapid import of solutes via the xylem. As expected, the C_i of hemiparasites is relatively high and the **carbon-isotope fractionation** is stronger in mistletoes than it is in their host, because of the high stomatal conductance of the parasite (Sect. 5.6). It is interesting that the difference in fractionation between host and parasite is less when the host is an N_2-fixing tree than when it is a nonfixing one (Table 15.2; Schulze and Ehleringer 1984). This is because more nitrogenous carbon compounds are imported when the host is fixing N_2, making the carbon-isotope composition more similar to that of the host. A substantial part of the carbon in mistletoes originates from the host via the xylem as organic acids and amino acids (Sect. 15.4).

Table 15.2 Carbon-isotope fractionation values for mistletoe-host pairs (number of pairs in brackets) from different continents; mean values and standard errors in brackets.

	Carbon-isotope composition (‰)		Difference between host and mistletoe (‰)
Region	Host	Mistletoe	
	Nitrogen-fixing hosts		
United States (7)	−26.3 (0.5)	−26.5 (0.2)	0.2
Australia (28)	−26.9 (0.2)	−28.3 (0.3)	1.4
South Africa (4)	−24.7 (0.3)	−25.7 (1.0)	1.1
	Non-fixing hosts		
United States (8)	−23.4 (0.1)	−26.6 (0.1)	3.2
Australia (19)	−26.5 (0.3)	−28.8 (0.2)	2.3
South Africa (11)	−24.7 (0.4)	−26.9 (0.6)	2.2

Source: Ehleringer et al. (1985)

Holoparasites, which predominantly import compounds from the sieve tubes of the host, have distinctly lower calcium to potassium (**Ca:K**) ratios than do parasites that only tap the xylem (Ziegler 1975). This is due to the fact that Ca is only present in very low concentrations in phloem sap, whereas most other minerals occur in higher concentrations in phloem sap than in xylem fluid (Sect. 4.2). To acquire sufficient Ca for their growth, some additional xylem connections are required. Whereas *Cuscuta reflexa* (giant dodder) acquires 94% of its N and 74% of its K from the phloem of the host *Lupinus albus* (white lupin), virtually none of its Ca arrives via the phloem (Jeschke et al. 1995).

Because most xylem-tapping hemiparasites have no mechanism to selectively import specific ions that arrive *via* the xylem or to export ions that have arrived in excess of their requirement, mistletoes often accumulate vast amounts of inorganic ions. Increased succulence with increasing leaf age and sequestration of sodium (Na) in older

leaves appear to be mechanisms to maintain inorganic solute concentrations at a tolerable level (Popp et al. 1995). A consequence of the accumulation of vast amounts of inorganic ions is the need for compatible solutes in the cytoplasm (Sect. 5.4.1). This would account for the high concentrations of polyols in xylem-tapping mistletoes (Popp et al. 1995). Some of the accumulated ions may be excreted via leaf glands [*e.g.*, in *Odontites verna* (red bartsia) and *Rhinanthus serotinus* (late-flowering yellow rattle) (Govier et al. 1968; Klaren and Van de Dijk 1976)].

Rapid import of N may lead to higher concentrations of organic N in the leaves of the parasite than in those of the host. This often coincides with a similarity in leaf shape and appearance: **cryptic mimicry** (Barlow and Wiens 1977; Bannister 1989). The N concentration of the parasite's leaves, however, is sometimes lower than that of the host, which may coincide with differences in leaf shape and appearance between host and parasite: **visual advertisement**. Because many herbivores prefer leaves with a high organic N concentration, it has been suggested that both 'cryptic mimicry' and 'visual advertisement' **reduce herbivory** (Ehleringer et al. 1986).

High leaf nutrient concentrations in combination with a low nutrient-resorption proficiency (Sect. 9.4.3) in hemiparasitic plants give rise to litter with high nutrient concentrations (Quested et al. 2002; Scalon and Wright 2017). Since most hemiparasites also produce less **quantitative secondary metabolites** (Sect. 13.3.2) than their hosts, their leaf litter tends to decompose readily. As a consequence, hemiparasites can accelerate nutrient cycling in nutrient-poor communities, as found for *Bartsia alpina* (velvetbells) in a European subarctic community (Bardgett et al. 2006), and *Amyema miquelii* in southern Australia (Watson 2009). In the nutrient-impoverished environment of Western Australia, introduced weeds often thrive under hemiparasitic trees and shrubs, when they show very poor growth away from these plants.

15.4 Carbon Relations

Hemiparasites are assumed to rely on their hosts only for water and mineral nutrients, but to fix their own CO_2. Their photosynthetic capacity, however, is often very low (0.5–5.0 μmol m^{-2} s^{-1}), and in many species there is substantial carbon import from the host. *Striga gesnerioides* (witchweed), which is an obligate root hemiparasite, has a very low photosynthetic capacity coupled with a very fast rate of respiration. There is no net CO_2 fixation even at light saturation (Graves et al. 1992), so it imports carbon from its host. In *Striga hermonthica* (purple witchweed) approximately 27% of the carbon is derived from its host [*Sorghum bicolor* (millet)] at a low N supply; this value declines to approximately 6% at a high N supply and faster rates of host photosynthesis (Cechin and Press 1993). Xylem-tapping mistletoes also import a large fraction of all their carbon from the host (Schulze et al. 1991) [*e.g.*, 23–43% in *Viscum album* (European mistletoe) (Richter and Popp 1992)]. Two methods have been used to assess heterotrophic carbon gain in the African xylem-tapping mistletoe, *Tapinanthus oleifolius* (lighting match). One method is based on an analysis of xylem sap and transpiration rate (Sect. 11.3.4; Pate et al. 1991); the other is based on an analysis of carbon-isotope composition and gas exchange (Sect. 2.5.3; Box 2.2; Marshall and Ehleringer 1990). Both methods agree and yield values in the range of 55–80%, with the higher values pertaining to older leaves that have fast transpiration rates (Table 15.3).

The presence of a parasite like *Cuscuta europaea* (dodder) on the stem of a host plant greatly enhances the release of amino acids and other solutes from the **phloem** of the host (Fig. 15.8). In *Cuscuta* parasitizing on *Genista acantholada*, *Lupinus albus* (white lupin), or *Digitalis* sp. (foxglove) alkaloids and glycosides synthesized in the host are transported to the parasite (Rothe et al. 1999). These results suggest an open symplastic connection between the phloem of host and parasite. This is confirmed

Table 15.3 Heterotrophic carbon gain of the xylem-tapping mistletoe *Tapinanthus oleifolius* (lighting match) on *Euphorbia virosa* (milkbush) and *Acacia nebrownii* (water acacia).*

	Tapinanthus oleifolius on *Euphorbia virosa*		*Tapinanthus oleifolius* on *Acacia nebrownii*
	Young leaves	Old leaves	
Carbon-budget method			
Carbon concentration of xylem sap (mmol C l^{-1} xylem sap)	121	121	116
Transpiration [l H_2O m^{-2} $(10\ h)^{-1}$]	1.3	3.9	1.6
Carbon import via the xylem (C_x) [mmol C m^{-2} $(10\ h)^{-1}$]	157	470	188
CO_2 assimilation in photosynthesis [mmol CO_2 m^{-2} $(10\ h)^{-1}$]	126	108	144
Total carbon gain [mmol C m^{-2} $(10\ h)^{-1}$]	283	578	332
Heterotrophic carbon gain (%)	55	81	57
δ^{13}C-difference method			
δ^{13}C xylem sap (‰)	−16.92	−16.92	−21.05
δ^{13}C parasite leaves (‰, measured)	−23.73	−18.99	−26.81
δ^{13}C parasite leaves (‰, predicted from measured C_i/C_a)	−29.60	−33.20	−32.88
Heterotrophic carbon gain (%)	46	87	51

Source: Richter et al. (1995)

*The host-derived part of the mistletoe's carbon was calculated from the carbon flux from the host xylem sap (*i.e.* carbon concentration in the xylem sap multiplied by the transpiration rate; 'carbon-budget method') or from the difference between the predicted and the actual carbon isotope ratios of the parasite ('δ^{13}C-difference method')

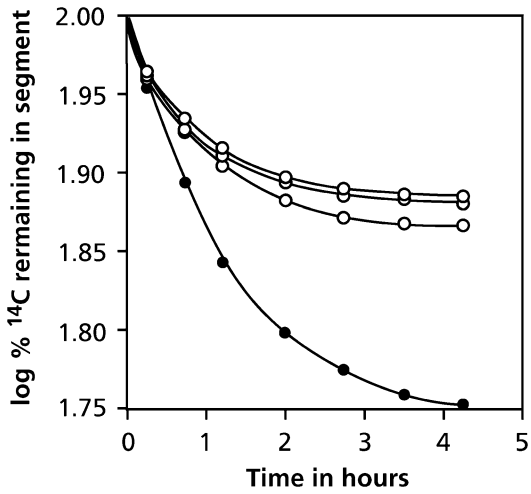

Fig. 15.8 The effect of *Cuscuta europaea* (dodder), a stem parasite, on the release of ^{14}C-labeled valine from the sieve tubes in the stem of its host, *Vicia faba* (broad bean). The values represent the fraction of the labeled amino acid originally present in the stem segment that was not released from the sieve tubes to the apoplast. Open symbols refer to nonparasitized segments of the stem; filled symbols refer to the release in the apoplast of the segment where the parasite had formed a haustorium (after Wolswinkel et al. 1984). Copyright American Society of Plant Biologists.

by translocation experiments using fluorescent dyes, which are translocated together with assimilates in the phloem and unloaded symplastically into the sinks. In all investigated host-parasite systems with *Cuscuta* species the dyes are detectable in the parasite 3 h after application. In both the host and the parasite the fluorescence is restricted to the phloem (Birschwilks et al. 2006).

A parasite like *Striga gesnerioides* (witchweed) may use up to 70% of all the imported carbohydrates for its respiration; the use of carbon from the host may be even more important for the yield reduction of its host, *Vigna unguiculata* (cowpea), than the reduction in host photosynthesis (Graves et al. 1992). It is not clear why such a large fraction of imported carbon is used in respiration; in the holoparasite *Cuscuta reflexa* (giant dodder), when it grows on the stem of *Lupinus albus* (white lupin), only 29% of all the incorporated carbon is respired (Jeschke et al. 1994). This value is in the same range as that of heterotrophic plant parts of nonparasitic plants (Sect. 3.5).

Cassytha pubescens (dodder laurel) significantly reduces the maximum electron transport rates and total biomass of *Ulex europaeus* (gorse) but not those of *Acacia paradoxa* (kangaroo thorn), regardless of N supply. Infection significantly decreases the root biomass of *Acacia paradoxa* only at low N supply, while the significant negative effect of infection on roots of *Ulex europaeus* is less severe at low N supply. Infection has a significant negative impact on host nodule biomass. *Ulex europaeus* supports significantly greater parasite biomass (also per unit host biomass) than *Acacia paradoxa*, regardless of N supply (Cirocco et al. 2017).

15.5 What Can We Extract from This Chapter?

The 4000 or so species of parasitic angiosperms of the world flora collectively represent an extraordinarily broad assemblage of taxa from distantly related families of predominantly angiosperm species and an equally profuse range of woody forms, morphologies, and life strategies. **Hemiparasites** tend to have fast rates of transpiration, and a low shoot water potential, which ensures rapid intake **of xylem solutes**. Hemiparasites also import carbon (amino acids, organic acids) via the transpiration stream which supports their carbon requirement to a varying extent: from almost none to virtually completely.

Holoparasites tap the host's phloem and depend entirely on their host for their carbon requirements. Because the phloem contains very little Ca, holoparasites have distinctly lower Ca:K ratios than do hemiparasites.

Some parasitic plants are notorious **pests**, reducing crop yield in many areas of the world. A thorough understanding of host factors that affect seed germination of some parasitic plants may help to control these pests, either by employing trap crops or intercrops, or by using analogues that stimulate seed germination of the parasite.

References

Ackroyd RD, Graves JD. 1997. The regulation of the water potential gradient in the host and parasite relationship between *Sorghum bicolor* and *Striga hermonthica*. *Ann Bot* **80**: 649–656.

Akiyama K, Matsuzaki K, Hayashi H. 2005. Plant sesquiterpenes induce hyphal branching in arbuscular mycorrhizal fungi. *Nature* **435**: 824–827.

Albrecht H, Yoder JI, Phillips DA. 1999. Flavonoids promote haustoria formation in the root parasite *Triphysaria versicolor*. *Plant Physiol* **119**: 585–592.

Ayongwa GC, Stomph TJ, Emechebe AM, Kuyper TW. 2006. Root nitrogen concentration of sorghum above 2% produces least *Striga hermonthica* seed stimulation. *Ann Appl Biol* **149**: 255–262.

Babiker AGT, Ejeta G, Butler LG, Woodson WR. 1993. Ethylene biosynthesis and strigol-induced germination of *Striga asiatica*. *Physiol Plant* **88**: 359–365.

Bannister P. 1989. Nitrogen concentration and mimicry in some New Zealand mistletoes. *Oecologia* **79**: 128–132.

Bardgett RD, Smith RS, Shiel RS, Peacock S, Simkin JM, Quirk H, Hobbs PJ. 2006. Parasitic plants indirectly regulate below-ground properties in grassland ecosystems. *Nature* **439**: 969–972.

Barkman TJ, McNeal JR, Lim S-H, Coat G, Croom HB, Young ND, DePamphilis CW. 2007. Mitochondrial DNA suggests at least 11 origins of parasitism in angiosperms and reveals genomic chimerism in parasitic plants. *BMC Evol Biol* **7**: 248.

Barlow BA, Wiens D. 1977. Host-parasite resemblance in Australian mistletoes: the case for cryptic mimicry. *Evolution* **31**: 69–84.

Birschwilks M, Haupt S, Hofius D, Neumann S. 2006. Transfer of phloem-mobile substances from the host plants to the holoparasite *Cuscuta* sp. *J Exp Bot* **57**: 911–921.

Bouwmeester HJ, Roux C, Lopez-Raez JA, Bécard G. 2007. Rhizosphere communication of plants, parasitic plants and AM fungi. *Trends Plant Sci* **12**: 224–230.

Calladine A, Pate JS. 2000. Haustorial structure and functioning of the root hemiparastic tree *Nuytsia floribunda* (Labill.) R.Br. and water relationships with its hosts. *Ann Bot* **85**: 723–731.

Cameron DD, Coats AM, Seel WE. 2006. Differential resistance among host and non-host species underlies the variable success of the hemi-parasitic plant *Rhinanthus minor*. *Ann Bot* **98**: 1289–1299.

Cechin I, Press MC. 1993. Nitrogen relations of the sorghum-*Sfriga hermonthica* hostparasite association: growth and photosynthesis. *Plant Cell Environ* **16**: 237–247.

Cirocco RM, Facelli JM, Watling JR. 2017. Does nitrogen affect the interaction between a native hemiparasite and its native or introduced leguminous hosts? *New Phytol* **213**: 812–821.

Cook CE, Whichard LP, Turner B, Wall ME, Egley GH. 1966. Germination of witchweed (*Striga lutea* Lour.): isolation and properties of a potent stimulant. *Science* **154**: 1189–1190.

Dawson JH, Musselman LJ, Wolswinkel P, Dörr I 1994. Biology and control of *Cuscuta*. In: Duke SO ed. *Reviews of Weed Science*. Champaign: Imperial Printing Company, 265–317.

Ehleringer JR, Schulze, E.-D., Ziegler, H., Lange, O.L., Farquhar, G.D., Cowan, I.R. 1985. Xylem-tapping mistletoes: water or nutrient parasites? *Science* **227**: 1479–1481.

Ehleringer JR, Ullmann I, Lange OL, Farquhar GD, Cowan IR, Schulze ED, Ziegler H. 1986. Mistletoes: a hypothesis concerning morphological and chemical avoidance of herbivory. *Oecologia* **70**: 234–237.

Einhellig F, Souza I. 1992. Phytotoxicity of sorgoleone found in grain Sorghum root exudates. *J Chem Ecol* **18**: 1–11.

Estabrook EM, Yoder JI. 1998. Plant-plant communications: rhizosphere signaling between parasitic angiosperms and their hosts. *Plant Physiol* **116**: 1–7.

Fay MF, Bennett JR, Dixon KW, Christenhusz MJM. 2010. Parasites, their relationships and the disintegration of Scrophulariaceae *sensu lato*. *Curtis Bot Mag* **26**: 286–313.

Feild TS, Brodribb TJ. 2005. A unique mode of parasitism in the conifer coral tree *Parasitaxus ustus* (Podocarpaceae). *Plant Cell Environ* **28**: 1316–1325.

Gobena D, Shimels M, Rich PJ, Ruyter-Spira C, Bouwmeester H, Kanuganti S, Mengiste T, Ejeta G. 2017. Mutation in sorghum *LOW GERMINATION STIMULANT 1* alters strigolactones and causes *Striga* resistance. *Proc Natl Acad Sci USA* **114**: 4471–4476.

Govier RN, Brown JGS, Pate JS. 1968. Hemiparasitic nutrition in angiosperms. II. Root haustoria and leaf glands of *Odontites verna* (Bell.) Dum. and their relevance to the abstraction of solutes from the host. *New Phytol* **67**: 963–972.

Graves JD, Press MC, Smith S, Stewart GR. 1992. The carbon canopy economy of the association between cowpea and the parasitic angiosperm *Striga gesnerioides*. *Plant Cell Environ* **15**: 283–288.

Gurney AL, Grimanelli D, Kanampiu F, Hoisington D, Scholes JD, Press MC. 2003. Novel sources of resistance to *Striga hermonthica* in *Tripsacum dactyloides*, a wild relative of maize. *New Phytol* **160**: 557–568.

Hibberd JM, Quick WP, Press MC, Scholes JD, Jeschke WD. 1999. Solute fluxes from tobacco to the parasitic angiosperm *Orobanche cernua* and the influence of infection on host carbon and nitrogen relations. *Plant Cell Environ* **22**: 937–947.

Jeschke WD, Bäumel P, Räth N. 1995. Partitioning of nutrients in the system *Cuscuta reflexa-Lupinus albus*. *Asp Appl Biol* **42**: 71–79.

Jeschke WD, Bäumel P, Räth N, Czygan F-C, Proksch P. 1994. Modelling of the flows and partitioning of carbon and nitrogen in the holoparasite *Cuscuta reflexa* Roxb. and its host *Lupinus albus* L.: II. Flows between host and parasite and within the parasitized host. *J Exp Bot* **45**: 801–812.

Jeschke WD, Hilpert A. 1997. Sink-stimulated photosynthesis and sink-dependent increase in nitrate uptake: nitrogen and carbon relations of the parasitic association *Cuscuta reflexa–Ricinus communis*. *Plant Cell Environ* **20**: 47–56.

Jones GP, Rao KS, Tucker DJ, Richardson B, Barnes A, Rivett DE. 1995. Antimicrobial activity of santalbic acid from the oil of *Santalum acuminatum* (quandong). *Intern J Pharmacogn* **33**: 120–123.

Kaiser B, Vogg G, Fürst UB, Albert M. 2015. Parasitic plants of the genus *Cuscuta* and their interaction with susceptible and resistant host plants. *Front Plant Sci* **6**: 45.

Khan ZR, Hassanali A, Overholt W, Khamis TM, Hooper AM, Pickett JA, Wadhams LJ, Woodcock CM. 2002. Control of witchweed *Striga hermonthica* by intercropping with *Desmodium* spp., and the mechanism defined as allelopathic. *J Chem Ecol* **28**: 1871–1885.

Kim G, LeBlanc ML, Wafula EK, dePamphilis CW, Westwood JH. 2014. Genomic-scale exchange of mRNA between a parasitic plant and its hosts. *Science* **345**: 808–811.

Klaren CH. 1975. *Physiological aspects of the hemiparasite Rhinanthus serotinus.* University of Groningen, the Netherlands.

Klaren CH, Van de Dijk SJ. 1976. Water relations of the hemiparasite *Rhinanthus serotinus* before and after attachment. *Physiol Plant* **38**: 121–125.

Kuo J, Pate JS, Davidson NJ. 1989. Ultrastructure of the haustorial interface and apoplastic continuum between host and the root hemiparasite *Olax phyllanthi* (Labill.) R. Br. (Olacaceae). *Protoplasma* **150**: 27–39.

Lendzemo VW, Kuyper TW, Kropff MJ, Van Ast A. 2005. Field inoculation with arbuscular mycorrhizal fungi reduces *Striga hermonthica* performance on cereal crops and has the potential to contribute to integrated *Striga* management. *Field Crops Res* **91**: 51–61.

Lendzemo VW, Kuyper TW, Matusova R, Bouwmeester HJ, Van Ast A. 2007. Colonization by arbuscular mycorrhizal fungi of sorghum leads to reduced germination and subsequent attachment and emergence of *Striga hermonthica*. *Plant Signal Behav* **2**.

Li J, Timko MP. 2009. Gene-for-gene resistance in *Striga*-cowpea associations. *Science* **325**: 1094–1094.

Li Z, Lin H, Gu L, Gao J, Tzeng C-M. 2016. Herba *Cistanche* (rou cong-rong): one of the best

pharmaceutical gifts of traditional Chinese medicine. *Front Pharmacol* **7**: 41.

Lins RD, Colquhoun JB, Mallory-Smith CA. 2006. Investigation of wheat as a trap crop for control of *Orobanche minor*. *Weed Res* **46**: 313–318.

Logan DC, Stewart GR. 1991. Role of ethylene in the germination of the hemiparasite *Striga hermonthica*. *Plant Physiol* **97**: 1435–1438.

Loveys BR, Loveys BR, Tyerman SD. 2001a. Water relations and gas exchange of the root hemiparasite *Santalum acuminatum* (quandong). *Aust J Bot* **49**: 479–486.

Loveys BR, Tyerman SD, Loveys BR. 2001b. Transfer of photosynthate and naturally occurring insecticidal compounds from host plants to the root hemiparasite *Santalum acuminatum* (Santalaceae). *Aust J Bot* **49**: 9–16.

Marshall JD, Ehleringer JR. 1990. Are xylem-tapping mistletoes partially heterotrophic? *Oecologia* **84**: 244–248.

Mescher MC, Runyon J, De Moraes CM. 2006. Plant host finding by parasitic plants. *Plant Signal Behav* **1**: 284–286.

Nge FJ, Ranathunge K, Kotula L, Lambers H. 2019. Strong host preference of a root hemiparasite (*Santalum acuminatum*) limits its distribution: beggars can be choosers. *Plant Soil* **437**: 159–177.

Nickrent DL, Duff RJ, Colwell AE, Wolfe AD, Young ND, Steiner KE, dePamphilis CW 1998. Molecular phylogenetic and evolutionary studies of parasitic plants. In: Soltis DE, Soltis PS, Doyle JJ eds. *Molecular Systematics of Plants II: DNA Sequencing*. Boston, MA: Springer US, 211–241.

Odhiambo JA, Vanlauwe B, Tabu IM, Kanampiu F, Khan Z. 2011. Effect of intercropping maize and soybeans on Striga hermonthica parasitism and yield of maize. *Arch Phytopathol Plant Protect* **44**: 158–167.

Pate JS. 2001. Haustoria in action: case studies of nitrogen acquisition by woody xylem-tapping hemiparasites from their hosts. *Protoplasma* **215**: 204–217.

Pate JS, True KC, Rasins E. 1991. Xylem transport and storage of amino acids by S.W. Australian mistletoes and their hosts. *J Exp Bot* **42**: 441–451.

Popp M, Mensen R, Richter A, Buschmann H, von Willert DJ. 1995. Solutes and succulence in southern African mistletoes. *Trees* **9**: 303–310.

Press MC. 1998. Dracula or Robin Hood? A functional role for root hemiparasites in nutrient poor ecosystems. *Oikos* **82**: 609–611.

Press MC, Nour JJ, Bebawi FF, Stewart GR. 1989. Antitranspirant-induced heat stress in the parasitic plant *Striga hermonthica* - a novel method of control. *J Exp Bot* **40**: 585–591.

Press MC, Phoenix GK. 2005. Impacts of parasitic plants on natural communities. *New Phytol* **166**: 737–751.

Quested HM, Press MC, Callaghan TV, Cornelissen HJ. 2002. The hemiparasitic angiosperm *Bartsia alpina* has the potential to accelerate decomposition in sub-arctic communities. *Oecologia* **130**: 88–95.

Richter A, Popp M. 1992. The physiological importance of accumulation of cyclitols in *Viscum album* L. *New Phytol* **121**: 431–438.

Richter A, Popp M, Mensen R, Stewart G, Willert D. 1995. Heterotrophic carbon gain of the parasitic angiosperm *Tapinanthus oleifolius*. *Funct Plant Biol* **22**: 537–544.

Rispail N, Dita M-A, Gonzalez-Verdejo C, Perez-de-Luque A, Castillejo M-A, Prats E, Roman B, Jorrin J, Rubiales D. 2007. Plant resistance to parasitic plants: molecular approaches to an old foe. *New Phytol* **173**: 703–712.

Rothe K, Diettrich B, Rahfeld B, Luckner M. 1999. Uptake of phloem-specific cardenolides by *Cuscuta* sp. growing on *Digitalis lanata* and *Digitalis purpurea*. *Phytochemistry* **51**: 357–361.

Rubiales D, Fernández-Aparicio M. 2012. Innovations in parasitic weeds management in legume crops. A review. *Agron Sustain Develop* **32**: 433–449.

Runyon JB, Mescher MC, De Moraes CM. 2006. Volatile chemical cues guide host location and host selection by parasitic plants. *Science* **313**: 1964.

Runyon JB, Tooker JF, Mescher MC, Moraes CM 2010. Parasitic plants in agriculture: chemical ecology of germination and host-plant location as targets for sustainable control: a review. In: Lichtfouse E ed. *Organic Farming, Pest Control and Remediation of Soil Pollutants*: Springer Netherlands, 123–136.

Scalon MC, Wright IJ. 2017. Leaf trait adaptations of xylem-tapping mistletoes and their hosts in sites of contrasting aridity. *Plant Soil* **415**: 117–130.

Schulze E-D, Ehleringer JR. 1984. The effect of nitrogen supply on growth and water-use efficiency of xylem-tapping mistletoes. *Planta* **162**: 268–275.

Schulze E-D, Lange OL, Ziegler H, Gebauer G. 1991. Carbon and nitrogen isotope ratios of mistletoes growing on nitrogen and non-nitrogen fixing hosts and on CAM plants in the Namib desert confirm partial heterotrophy. *Oecologia* **88**: 457–462.

Shah N, Smirnoff N, Stewart GR. 1987. Photosynthesis and stomatal characteristics of *Striga hermonthica* in relation to its parasitic habit. *Physiol Plant* **69**: 699–703.

Shahid S, Kim G, Johnson NR, Wafula E, Wang F, Coruh C, Bernal-Galeano V, Phifer T, dePamphilis CW, Westwood JH, Axtell MJ. 2018. MicroRNAs from the parasitic plant *Cuscuta campestris* target host messenger RNAs. *Nature* **553**: 82–85.

Shen H, Hong L, Ye W, Cao H, Wang Z. 2007. The influence of the holoparasitic plant *Cuscuta campestris* on the growth and photosynthesis of its host *Mikania micrantha*. *J Exp Bot* **58**: 2929–2937.

Siame BA, Weerasuriya Y, Wood K, Ejeta G, Butler LG. 1993. Isolation of strigol, a germination stimulant for *Striga asiatica*, from host plants. *J Agric Sci Food Chem* **41**: 1486–1491.

Smith CE, Dudley MW, Lynn DG. 1990. Vegetative/parasitic transition: control and plasticity in *Striga* development. *Plant Physiol* **93**: 208–215.

Smith JD, Woldemariam MG, Mescher MC, Jander G, De Moraes CM. 2016. Glucosinolates from host plants influence growth of the parasitic plant *Cuscuta gronovii* and its susceptibility to aphid feeding. *Plant Physiol* **172**: 181–197.

Song Y, Yu W-B, Tan Y, Liu B, Yao X, Jin J, Padmanaba M, Yang J-B, Corlett RT. 2017. Evolutionary comparisons of the chloroplast genome in Lauraceae and insights into loss events in the magnoliids. *Genome Biol Evol* **9**: 2354–2364.

Stewart GR, Press MC. 1990. The physiology and biochemistry of parasitic angiosperms. *Annu Rev Plant Biol* **41**: 127–151.

Taylor A, Martin J, Seel WE. 1996. Physiology of the parasitic association between maize and witchweed (*Striga hermonthica*): is ABA involved? *J Exp Bot* **47**: 1057–1065.

Tennakoon KU, Pate JS. 1996. Effects of parasitism by a mistletoe on the structure and functioning of branches of its host. *Plant Cell Environ* **19**: 517–528.

Veenendaal EM, Abebrese IK, Walsh MF, Swaine MD. 1996. Root hemiparasitism in a West African rainforest tree *Okoubaka aubrevillei* (Santalaceae). *New Phytol* **134**: 487–493.

Watling JR, Press MC. 2001. Impacts of infection by parasitic angiosperms on host photosynthesis. *Plant Biol* **3**: 244–250.

Watson DM. 2009. Parasitic plants as facilitators: more Dryad than Dracula? *J Ecol* **97**: 1151–1159.

Westwood JH, Yoder JI, Timko MP, dePamphilis CW. 2010. The evolution of parasitism in plants. *Trends Plant Sci* **15**: 227–235.

Wolswinkel P, Ammerlaan A, Peters HFC. 1984. Phloem unloading of amino acids at the site of attachment of *Cuscuta europaea*. *Plant Physiol* **75**: 13–20.

Yoneyama K, Arakawa R, Ishimoto K, Kim HI, Kisugi T, Xie X, Nomura T, Kanampiu F, Yokota T, Ezawa T, Yoneyama K. 2015. Difference in *Striga*-susceptibility is reflected in strigolactone secretion profile, but not in compatibility and host preference in arbuscular mycorrhizal symbiosis in two maize cultivars. *New Phytol* **206**: 983–989.

Yoneyama K, Xie X, Kusumoto D, Sekimoto H, Sugimoto Y, Takeuchi Y, Yoneyama K. 2007a. Nitrogen deficiency as well as phosphorus deficiency in sorghum promotes the production and exudation of 5-deoxystrigol, the host recognition signal for arbuscular mycorrhizal fungi and root parasites. *Planta* **227**: 125–132.

Yoneyama K, Yoneyama K, Takeuchi Y, Sekimoto H. 2007b. Phosphorus deficiency in red clover promotes exudation of orobanchol, the signal for mycorrhizal symbionts and germination stimulant for root parasites. *Planta* **225**: 1031–1038.

Yoshida S, Cui S, Ichihashi Y, Shirasu K. 2016. The haustorium, a specialized invasive organ in parasitic plants. *Annu Rev Plant Biol* **67**: 643–667.

Ziegler H 1975. Nature of transported substances. In: Zimmermann MH, Milburn JA eds. *Encyclopedia of Plant Physiology, New Series*. Berlin: Springer Verlag, 59–100.

Zwanenburg B, Mwakaboko AS, Reizelman A, Anilkumar G, Sethumadhavan D. 2009. Structure and function of natural and synthetic signalling molecules in parasitic weed germination. *Pest Manage Sci* **65**: 478–491.

16 Biotic Influences: Interactions Among Plants

16.1 Introduction

In previous chapters, we dealt with many physical and chemical environmental factors that affect a plant's performance, and with effects of microsymbionts, herbivores, pathogens, and parasitic plants. For many plants, however, the most important factor shaping their environment is neighboring plants. One of the most active debates in both ecology and agriculture focuses on the question of the mechanisms by which plants interact with one another. Plant-plant interactions range from positive (**facilitation**) to neutral to negative (**competition**) effects on the performance of neighbors (Callaway 2007; Wright et al. 2017). Competition occurs most commonly when plants utilize the same pool of growth-limiting resources (**resource competition**). Competition may also occur when one individual produces chemicals that negatively affect their neighbors (**interference competition** or **allelopathy**). Competition between two individuals is often highly asymmetric, with one individual having much greater negative impact than the other does. We define plant competition as "the ability of individuals to usurp resources or otherwise suppress their neighbor's fitness and include both resource and interference competition" (Aschehoug et al. 2016). Facilitation leads to "species-specific **overyielding**, which is the case where a species grows more in mixture than it does in monoculture, after accounting for differences in proportion of seed planted" (Wright et al. 2017). What we show in this chapter is that the outcome of plant interactions simultaneously involves competition and facilitation happening at the same time.

The question of which species wins in competition also depends strongly on the time scale of the study (Koffel et al. 2018). Short-term outcomes of competition often depend on rates of resource acquisition and growth, whereas equilibrium persistence of a species in a community is affected by rates of resource acquisition, tolerance of ambient resource availability, efficiency of converting acquired resources into biomass, and retention of acquired resources. Rare extreme events, *e.g.*, a severe drought, flood, fire, or frost, once in a decade, may be more important for the outcome of competition than mean conditions. Plant ecologists have discovered much about competition, but the mechanisms of competition and how competition affects the organization of communities in nature still require further exploration (Aschehoug et al. 2016).

The **competitive ability** of a species depends on environment. There are no 'super species' that are competitively superior in all environments; rather, there are **trade-offs** among traits that are beneficial in some environments, but which reduce competitive ability in others. For a plant to compete successfully in a particular environment, it must have specific ecophysiological traits that allow effective growth in that environment (the **physiological filter** discussed in Sect. 1.3). An extreme cold temperature represents an

H. Lambers, R. S. Oliveira, *Plant Physiological Ecology*, https://doi.org/10.1007/978-3-030-29639-1_16

absolute boundary for survival of some *Rhododendron* species in a common garden experiment, whereas warm temperatures do not. These *Rhododendron* species may therefore survive **global warming** *in situ*, because of high temperature tolerance, but temperature effects on reproduction are uncertain. There may also be a significant time lag between change in climate and transient species distribution which makes the effect of global warming on species distribution difficult to predict (Vetaas 2002).

We have provided many examples of physiological traits necessary for ecological success in dry, cold, hot, saline, flooded, nutrient-impoverished, or other harsh environments. Only those species that are adapted, or can acclimate to such environmental conditions can survive, compete, and reproduce successfully in these environments. As the saying goes: "when the going gets tough, the tough get going". Other plants typically grow in more favorable conditions where abiotic stresses are moderate. Most species can survive in these conditions, but only a small proportion compete effectively (Sect. 1.3). We have already discussed many of the traits that enable plants to grow rapidly under these conditions. Although this brief introduction of 'plant strategies' provides a context for the present discussion of ecophysiological traits that are important in competitive interactions, the situation is far more complicated (Box 16.1). Traits that are important for **competitive success** at an early stage of succession may differ greatly from those that are pertinent in later stages. Similarly, plant characteristics that determine the outcome of competition in short-term experiments often differ from those that give a species a competitive edge in the long run (Sect. 16.4).

Box 16.1: Plant Ecological Strategies

Fernando A.O. Silveira
Department of Plant Biology
Federal University of Minas Gerais
Belo Horizonte
Brazil

Plant ecological strategy schemes arrange species in categories or along spectra, according to their functional traits. Major aims of studying plant ecological strategies include the examination of the major selective pressures shaping species traits (including life-history, architecture, and allocation), and the understanding of trait-environment relationships across different scales. Historically, plant functional classifications date back to Teophrastos's (c.371–c.287 BC) *Historia Plantarum* (Egerton 2001), which was the first to group plants into different growth forms (*i.e.* trees, shrubs, and herbs; Weiher et al. 1999). There have been numerous propositions and attempts to classify plant ecological strategies (Westoby et al. 2002). For example, the widely known Raunkiaer's life-form scheme is based on the location of the buds where regrowth arises after the unfavorable season of the year (Box Fig. 16.1). Although based on a single trait, this scheme has proved useful in many natural communities worldwide.

A key element underpinning plant ecological strategies is the evolution of correlated traits. Traits can be negatively correlated, positively correlated, or can be uncorrelated (Box Fig. 16.2). Trade-offs represent a balance between two incompatible traits, and are represented by a negative correlation between a pair of traits, due to physiological or genetic constraints (Lambers and Poorter 1992; Grime 2006). The relationships between a given set of traits defines the possible viable trait combinations and the functional spectrum occupied by individuals, species or communities (Díaz et al. 2016).

Trait Dimensions

All modern functional classifications are based on quantitative, rather than qualitative traits. Shifting from qualitative to

(continued)

Box 16.1 (continued)

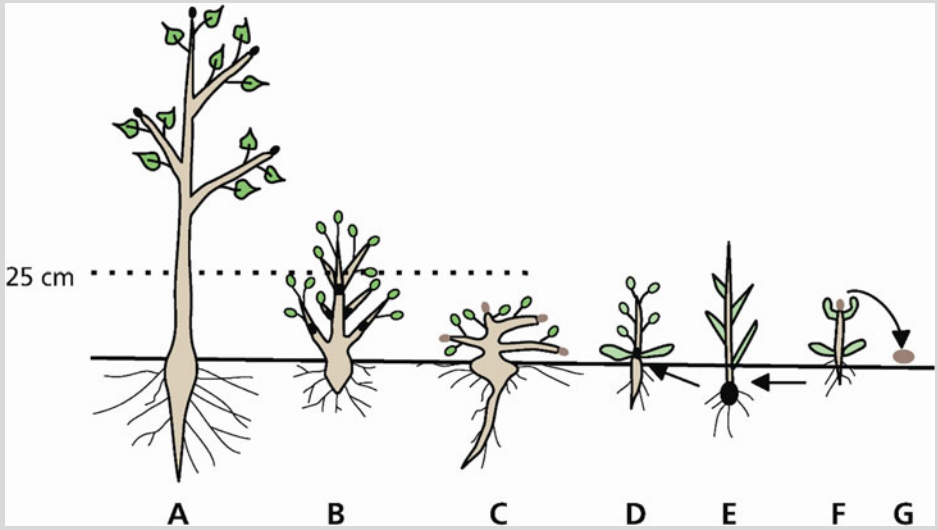

Box Fig. 16.1 Plant life-forms of Raunkiaer (1907, English translation 1934). Perennating organs are shown in black, woody organs in brown, and deciduous organs green. (**A**) Phanerophyte (tree or tall shrub), with buds more than 25 cm above the ground. (**B**) Chamaephyte, shrub, with buds both above and less than 25 cm above the ground. (**C**) Chamaephyte, semishrub, with buds less than 25 cm above the ground. (**D**) Hemicryptophyte, perennial herb with its bud at ground surface. (**E**) Geophyte, perennial herb with a bulb or other perennating organ below the ground surface. (**F**) Therophyte, annual plant surviving unfavorable periods only as seed. Barkman (1988) reviewed the wide range of life form and growth form systems. Other life-forms not shown here include epiphytes, hemi-epiphytes, aerophytes, among others (Galán de Mera et al. 1999).

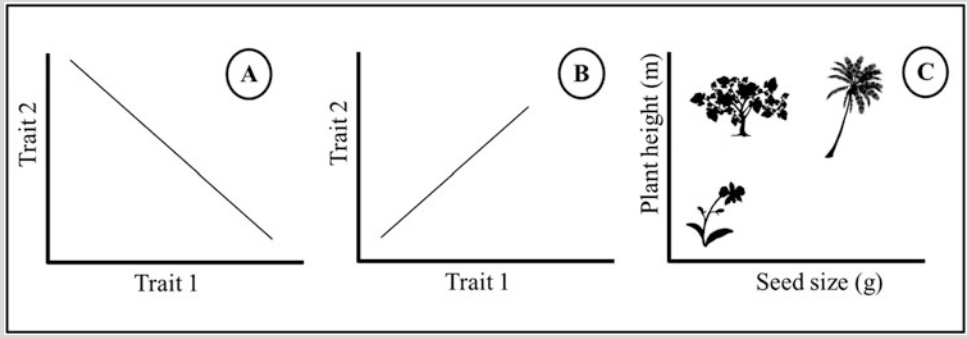

Box Fig. 16.2 Bivariate trait-trait relationships showing negative (trade-off) (**A**), and positive (coordinated) correlation between Trait 1 and Trait 2 (**B**). (**C**) shows the relationships between seed size and plant height. Only three combinations are possible. Plants can be either small and produce small seeds (the orchid), can be tall and produce large seeds (the palm), or can be tall and produce small seeds (the fig tree). However, due to biophysical constraints, small plants can never produce large seeds, creating a gap in the functional space.

quantitative traits allows us to position individuals, species or communities along functional spectra, rather than in artificial, arbitrary categories. A key advantage of using functional traits to build on plant ecological strategies is to overcome the problems of comparing communities with different taxonomic compositions: by considering functional traits,

(continued)

Box 16.1 (continued)

rather than species identity, we can compare communities across geo-climatic gradients, regardless of taxonomic issues, and gain ecological insights at biogeographic scales (Weiher et al. 1999).

Trait-dimensions, that is, spectra of variation with respect to measurable quantitative traits, have gained momentum with the construction of global plant trait databases (Westoby et al. 2002; McGill et al. 2006; Westoby and Wright 2006; Kattge et al. 2011; Díaz et al. 2016). Here, I first summarize two dimensions that are well characterized and understood, and then comment on the value of Grime's 'CSR classification'.

Leaf Economics Spectrum

Five traits that are coordinated across species are leaf mass per area (LMA), leaf life-span, leaf N concentration, and photosynthesis and dark respiration on a mass basis. In the five-trait space, 79% of all variation worldwide lies along a single main axis (Fig. 2.33; Wright et al. 2004). Species with a low LMA tend to have short leaf life-spans, high leaf nutrient concentrations, and high rates of mass-based photosynthesis. These species occur at the 'quick-return' end of the leaf economics spectrum (Reich 2014). The fast turnover of plant organs permits a more flexible response to the spatial patchiness of light and soil resources (Grime 1994). At the 'slow-return' end of the spectrum are species with long leaf life-span, expensive leaf construction (high LMA), low nutrient concentrations, and slower photosynthetic rates.

Seed-Size-Seed-Output Trade-Off

The seed size : seed number trade-off is one of the best-established trait-trait relationships. Species with small seeds produce more seeds within a given mass devoted to reproduction. Present-day species have seed masses ranging over 11.5 orders of magnitude, from the dust-like seeds of orchids (some of which weigh just 0.0001 mg) to the 20-kg seeds of the double coconut (Moles et al. 2005). Seed output strongly varies across species. Seed mass is also a good indicator of the likelihood of seed predation, dispersal distance and a seedling's ability to survive herbivory and different kinds of disturbances (Westoby et al. 2002; Saatkamp et al. 2019). Seed mass is also positively correlated with leaf area and maximum plant height (Díaz et al. 2016), suggesting coordinated evolution of these traits.

Grime's CSR Theory

A combination of low and high levels of stress (conditions that restrict productivity) and disturbance (conditions that partially or totally destroy biomass) results in the well-known Grime's CSR triangle (Box Fig. 16.3) (see also Sects 10.6.1 and 10.6.3). In this scheme, only three combinations are possible, because in highly disturbed habitats, severe stress prevents recovery or reestablishment of the vegetation (Grime 1977). According to this CSR theory, sets of functional traits define plant ecological strategies, representing trade-offs between the capacity to compete with neighbors (strategy C), tolerate stress (strategy S), or survive biomass destruction (strategy R). Therefore, this two-dimensional scheme consists of a C-S axis, which reflects adaptation to favorable *vs.* unfavorable sites for plant growth, and an R-axis, which reflects adaptation to disturbance.

As originally proposed, CSR classification had several limitations. First, it relied on artificial categories reflecting the combination of each of three strategies. Second, species positioning on the triangle depended

(continued)

Box 16.1 (continued)

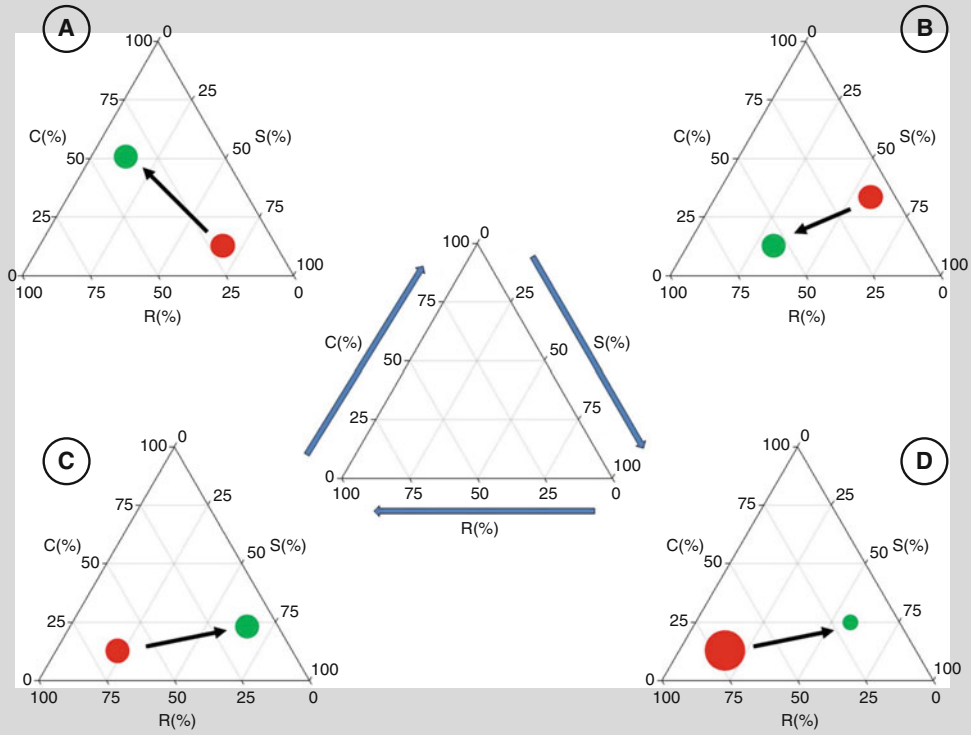

Box Fig. 16.3 The CSR triangle model (Grime 1977) depicting the spectrum of ecological strategies at the three corners: C, competitor; S, stress-tolerators; R, ruderals. The blue arrows in the central triangle show the trade-offs in ecological strategies. Particular species can engage in any mixture of these three primary strategies, and the mixture is described by their position within the triangle. Examples include: changes in average community strategies along forest successional gradients (**A**) or along disturbances gradients (**B**), ontogenetic changes in ecological strategies (**C**), and assessments of intraspecific changes (**D**). Circle sizes represent the variation in CSR strategies.

on sampling numerous hard-to-sample traits. Third, analyses were available only for herbaceous species. In recent years, however, we have seen significant advances in the CSR theory which have overcome such limitations. Modern tools are more quantitative, and easy-to-sample traits are used for functional classifications (Pierce et al. 2013). There is now experimental evidence supporting the two primary axes of Grime's CSR triangle (Li and Shipley 2017). CSR schemes have been validated and calibrated to the world flora, including woody species (Pierce et al. 2017). The scope of the CSR theory has also expanded, and with the available tools, analyses can readily be implemented to examine how CSR strategies change across ecological scales including ontogenetic stages and intraspecific variation (Dayrell et al. 2018), communities (Caccianiga et al. 2006) and biomes (Pierce et al. 2017). Using CSR theory to examine plant functional strategies has proven useful to a myriad of purposes across ecological scales (Box Fig. 16.3).

(continued)

Box 16.1 (continued)

The Future

Despite recent progress in trait standardization, development of robust statistical tools to inform plant ecological strategies, and construction of global trait databases, functional plant ecology has typically focused on aboveground traits, and particularly leaf traits. Databases of plant functional traits are also strongly biased towards temperate ecosystems (Kattge et al. 2011). Nevertheless, there is now evidence to support the idea of trade-offs and coordinated evolution of traits in stems (Chave et al. 2009), roots (Laliberté 2017), and seeds (Saatkamp et al. 2019). Therefore, attempting to examine functional spectra and dimensions at the whole-plant level would represent the next frontier in plant ecological strategies schemes. Ideally, future research should also be able to fill in knowledge gaps in tropical ecosystems.

In this text on physiological ecology we emphasize the physiological mechanisms, rather than the community consequences of competition. An ecophysiologist attempts to explain competitive and facilitative interactions in terms of the performance of individual plants that make up a community (McIntire and Fajardo 2014; Wright et al. 2017). The challenge then is to scale up from the knowledge that is available at the cell, organ, and whole-plant level, to the processes that occur in natural and managed communities.

An important aspect of the functioning of a plant among surrounding competitors may well be to *avoid* potentially negative effects. That is, rather than producing leaves that are acclimated to shade, or roots that can access sparingly available nutrients, a plant might grow away from its neighbors and make leaves that are acclimated to a high level of irradiance and roots that can exploit a favorable nutrient patch. This requires sensing mechanisms, however, that allow a plant to detect the proximity of its neighbors (Sect. 16.3).

16.2 Theories of Competitive Mechanisms

Several theoretical frameworks have been developed to predict the outcome of plant competition. Grime (1977) suggested that species with fast **relative growth rates** are effective competitors because rapid growth enables them to dominate available space and to acquire the most resources (Sect. 10.6.1). If correct, then traits that promote rapid resource acquisition and growth should be favored. On the other hand, Tilman (1988) suggested that the species that can draw a resource down to the lowest level is the best competitor for that resource. These perspectives are not incompatible (Grace 1990). We expect that, in short-term growth experiments, especially in high-resource environments, traits that contribute to rapid growth contribute to competitive success. In the long term, however, especially in low-resource environments, when species effects on resource availability should be greatest, the potential of a species to extract scarce resources may be more important than maximum rates of resource acquisition, and facilitation may be more important (McIntire and Fajardo 2014; Wright et al. 2017; Lambers et al. 2018). In addition, it also matters what neighbors are competing for, because competition for light, nutrients, or water involve fundamentally different mechanisms, as explored in this chapter.

Two major **physiological trade-offs** have been discussed as the basis of broad patterns of competitive ability in different environments. First, there is a trade-off between rapid growth to occupy space and maximize resource acquisition *vs.* resource conservation through reductions in tissue turnover (Sect. 16.4; Grime 1977). Second, there is a trade-off between allocation to roots to acquire water and nutrients *vs.* allocation to shoots to capture light and CO_2 (Sect. 16.7; Brouwer 1963; Pierik et al. 2013). Because of these trade-offs, no species can be a superior competitor in all environments, but instead will specialize to grow and compete effectively in a certain restricted set of environments.

In low-resource environments, however, where growth rates are slow, competitive exclusion may take a very long time. Before there is any winner, environmental conditions (*e.g.*, frost, drought, or fire) may change. This might account, in part, for the enormous richness of plant species on severely nutrient-impoverished sandplains in South Africa, Brazil and southwestern Australia (Oliveira et al. 2015; Verboom et al. 2017). On the other hand, the distribution of Proteaceae in southwestern Australia appears to be driven by plant adaptations to function on severely phosphorus (P)-impoverished soils (Lambers et al. 2018). Facilitation, rather than competitive exclusion, appears to be very important in these habitats. As resource availability increases, facilitation becomes less important and competitive interactions become dominant, consistent with the stress gradient hypothesis (Wright et al. 2017).

Competition is least likely in recently disturbed habitats where low plant biomass and/or high resource supply minimize resource limitation. In other cases, coexisting species may be limited by different factors, as when species have radically different phenology, height, or rooting depth. In order for plants to minimize competition, they must adjust growth to tap resources that are not utilized by neighbors.

16.3 How Do Plants Perceive the Presence of Neighbors?

Plants can perceive the proximity of neighbors, as described when discussing plant growth in shady conditions. First, a reduction in the level of photosynthetically active radiation reduces the concentration of soluble sugars, which can be sensed by plant cells (Sect. 2.6.3). Second, special pigments, **cryptochrome** and **phytochrome**, perceive both the level and the red/far-red ratio of radiation (Sect. 10.5.1.1). In *Populus* (poplar), for example, linear relationships exist between stem growth rate, plant spacing, and P_{fr}/P_t calculated from radiation that is propagated vertically within the canopy. The dynamics of developing or regenerating canopies is partly based on phytochrome-mediated perception of the proximity of neighboring plants (Ballaré et al. 2013; Gommers et al. 2013). Through the phytochrome system, plants clearly sense cues that indicate current or future shading. Shade-avoiding species typically respond with enhanced stem elongation, whereas no such response is found for species naturally occurring under a dense canopy (Sect. 10.5.1.1; Fig. 16.1).

Plants are also capable of 'smelling' the presence of neighbors that release above-ground **chemical signals**, such as jasmonate or other volatiles (Sects. 13.2 and 14.3). Contrary to common expectation, plants have highly sensitive **chemoperception** systems that play a central role in communication with surrounding organisms (Chaps. 12, 13, 14 and 15). Physically touching surrounding plants is an additional way in which neighbors can be perceived (Sect. 10.5.7; Elhakeem et al. 2018).

Plants can also sense the presence of neighbors below ground, especially when impacted by herbivory. In a greenhouse experiment, **volatile emission** by *Trifolium pratense* (strawberry clover) growing alone, with a conspecific, or with an individual of the naturally co-occurring *Dactylis glomerata* (orchard grass), show that conspecifics suppress volatile release, especially in the presence of caterpillar larvae (*Spodoptera littoralis*) (Fig. 16.2). When *Trifolium pratense* grows together with a conspecific, both total and herbivore-induced emission of volatiles is reduced as compared with *Trifolium pratense* growing with *Dactylis glomerata* or growing alone. This reduction in emission occurs despite the fact that there is a significant reduction in *Trifolium pratense* biomass due to competition with *Dactylis glomerata.* The suppression of *Trifolium pratense* volatile emission growing next to a conspecific is a general pattern observed for all major herbivore-induced volatiles and independent of whether plants are in contact aboveground, **belowground**, or both. The reduction in volatile emission from plants growing with conspecifics may serve to reduce attack by specialist herbivores and minimize exploitation of herbivore attack information by neighbors (Kigathi et al. 2013).

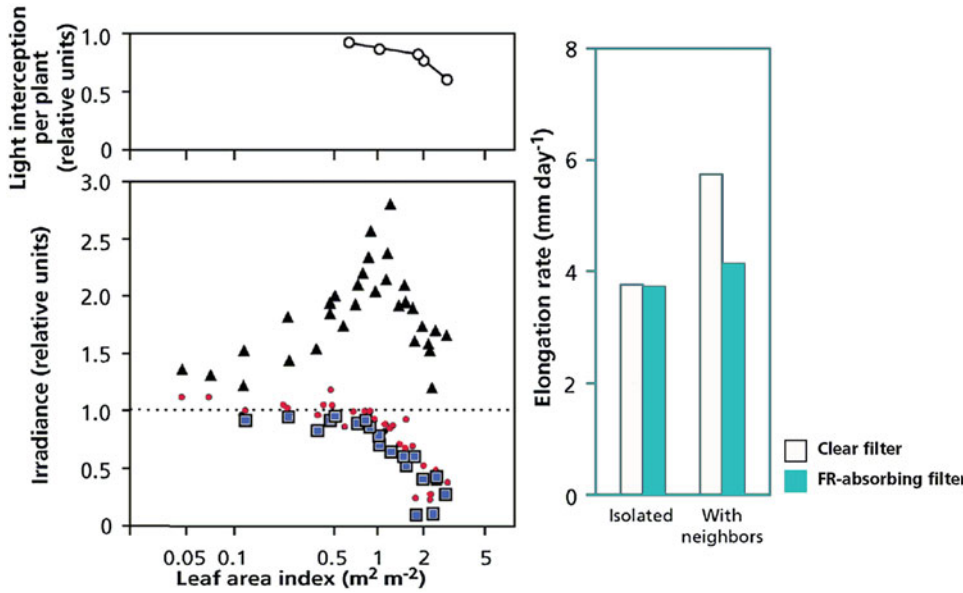

Fig. 16.1 (Left) Effects of increasing the leaf area index [LAI, m^2 (leaf area) per m^2 (soil surface)] in even-height canopies of dicotyledonous seedlings on (top) light interception and (bottom) the light climate of the stem. Seedling stands of *Sinapis alba* (mustard) and *Datura ferox* (thorn apple) of differing densities and plant sizes were used to obtain a range for the leaf area index. The values are given relative to the measurements obtained for isolated plants (horizontal line). Triangles: far-red light; circles, red light; squares, blue light. (Right) Elongation response of the first internode of *Datura ferox* (thorn apple) seedlings to the proximity of neighboring plants. The seedlings were placed at the center of an even-height canopy with a leaf area index of approximately 0.9. During the 3-day experiment the seedlings are surrounded by cuvettes containing distilled water (clear filter) or a $CuSO_4$ solution (far-red-absorbing filter) that maintain the red/far-red radiation near 1.0 (Ballaré et al. 1995); reproduced with the author's permission from *HortSci.* **30**: 1172–1182.

A chemical root interaction (*i.e.* the accumulation of **allelochemicals**) is a likely explanation for many of the distribution patterns observed in the field (Sect. 13.2). When the roots of *Ambrosia dumosa* (white bursage), whose growth is normally inhibited by the presence of the roots of *Larrea divaricata* (creosote bush), are treated with activated carbon that adsorbs allelochemicals, the inhibition is reduced (Mahall and Callaway 1992). This is consistent with inhibition by an allelochemical that is released by the roots of *Larrea divaricata*, and may account for the dispersed distribution of *Larrea divaricata* in the Mojave Desert in California, USA.

Intraspecific inhibition of root growth of *Ambrosia dumosa* (white bursage) is not affected by activated carbon, suggesting that it depends on **physical contact** (Mahall and Callaway 1992), based on **thigmomorphogenetic** processes (Sect. 10.5.8). **Identity recognition** among the roots of different accessions of *Pseudoroegneria spicata* (bluebunch wheatgrass) contribute to **over-yielding** in plots with high intraspecific richness of this species relative to monocultures. When plants from different populations are planted together in pots, the total biomass yield is 30% more than in pots with two plants from the same population. Second, the elongation rates of roots of *Pseudoroegneria spicata* decreases more after contact with roots from another plant from the same population than after contact with roots from a plant from a different population. If decreased growth after contact results in reduced root overlap, and reduced root overlap corresponds with reduced growth and productivity, then variation in detection and avoidance among related and unrelated accessions may contribute to how ecotypic diversity in *Pseudoroegneria spicata* increases productivity (Yang et al. 2015). Climbing plants, which

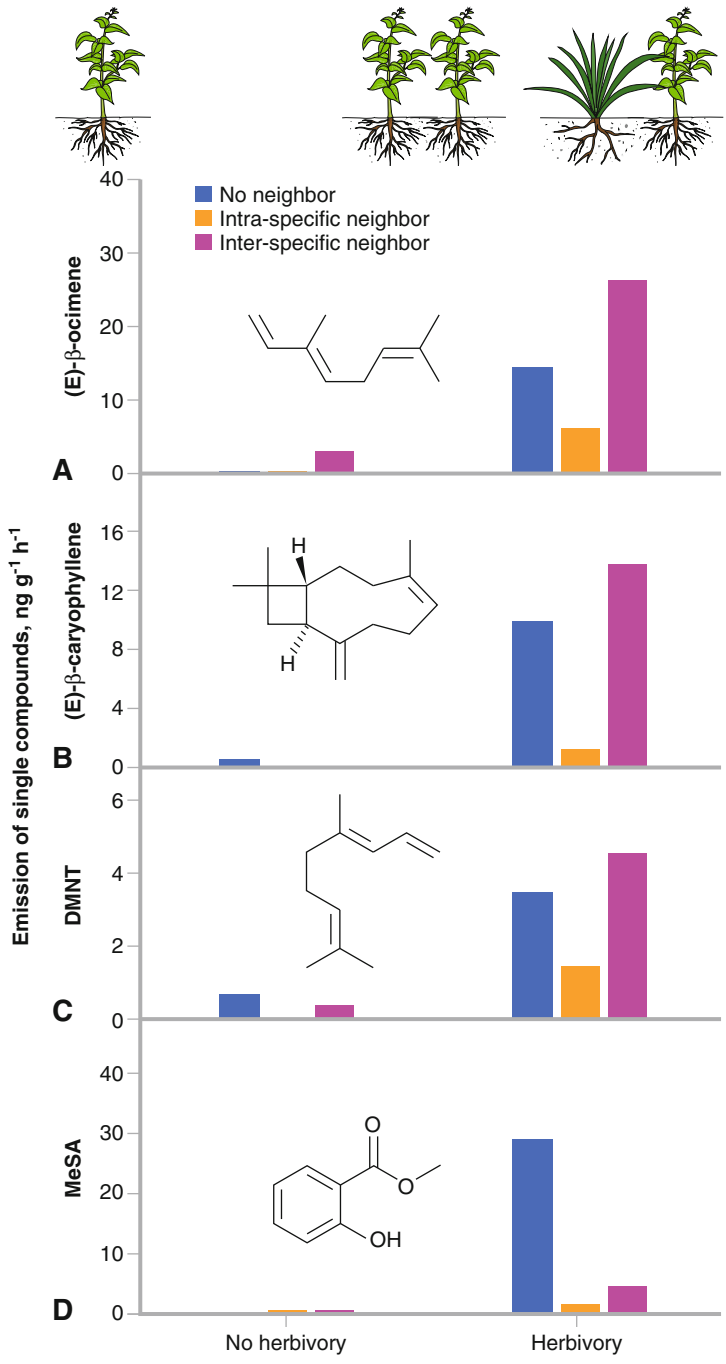

Fig. 16.2 (Top) Scheme of the experiment. The focal species, *Trifolium pratense* (strawberry clover), was grown alone, with another *Trifolium pratense* or with *Dactylis glomerata* (orchard grass). All plants were grown under the following treatments: (left) Control: individually grown *Trifolium pratense* plants. (right) Full contact: plants had both aboveground and belowground contact through openings in the pots and the bags. Half of the replicates were subjected to herbivory by caterpillar larvae (*Spodoptera littoralis*). Volatiles were collected immediately after 12 h of herbivory. (Bottom) Effects of herbivory by caterpillars (*Spodoptera littoralis*) and neighbor identity on emission of major herbivore-induced compounds of *Trifolium pratense* (strawberry

depend on neighboring plants for support, somehow perceive the presence of mechanical support. The elongation of tendrils is suppressed when they contact a supporting structure (Sect. 10.5.8). Some climbing plants seem to have a 'give-up' time concerning support finding. Darwin (1875) found that *Humulus lupulus* (twining hop) stops circumnutation after 5 days (37 revolutions) if it does not find a support. Other climbing plants show a similar response (Gianoli 2015). Long-lived species may have second chances: if a leader shoot of some lianas in a tropical rainforest fails to find a support, it either starts up a support nearer the ground or is replaced by another vertical leader (Putz 1984).

Plants can also respond to the presence of surrounding plants because of their neighbors' effect on above-ground microclimate, which is caused by differential heat exchange. This can have a tremendous effect on the outcome of competition (*e.g.*, in frost-prone areas). Tree seedlings may grow well in forest clearings for the first few years, but once a grassy groundcover establishes, the growth of the young trees becomes retarded and more susceptible to frosts. Although some of these effects might be due to competition for nutrients and water, this cannot account for their greater frost sensitivity. When seedlings of *Eucalyptus pauciflora* (snow gum) are surrounded by grass, the minimum air temperature experienced by seedlings decreases by as much as 2 °C, and they experience more frosts (Fig. 16.3; Ball et al. 1997). These effects cause greater photoinhibition, reduced growth, and a shorter growing season for seedlings surrounded by grass compared with those in bare patches. Thus, the microclimate above grass adversely affects spring growth of juvenile trees and may account for much of the competitive inhibition of tree seedling growth by grass during spring (Fig. 16.3).

There are clearly many ways in which plants perceive their neighbors, both above and below ground. Plants may respond in such a way as to avoid competition or in a manner that makes them superior competitors. That is, plants that are sufficiently **plastic** for certain traits may well be able to avoid their neighbors and grow in such a way as to tap resources not utilized by neighbors (Sect. 16.6). In the following Sections we explore what ecophysiological traits determine competitive success when plants compete for the same pool of limiting resources.

16.4 Relationship of Plant Traits to Competitive Ability

16.4.1 Growth Rate and Tissue Turnover

Species from high-resource environments exhibit a rapid **relative growth rate** (*RGR*), whereas species from low-resource environments compete most effectively by minimizing tissue loss (greater **tissue longevity**) more than by maximizing resource gain (Sects. 10.3 and 10.6). The ecological advantage of a high potential *RGR* seems straightforward: fast growth results in the rapid occupation of a large space which leads to the preemption of limiting resources (Grime 1977). Rapid growth may also lead to rapid completion of the plant's life cycle which is essential for **ruderals**, whose habitat does not persist for a

Fig. 16.2 (continued) clover). Depicted are results are expressed in ng (g dry weight)$^{-1}$ hour^{-1} for (**A**) the monoterpene (E)-β-ocimene, (**B**) the sesquiterpene (E)-β-caryophyllene, (**C**) the homoterpene (**E**)-4,8-dimethylnona-1,3,7-triene (DMNT), and (**D**) the aromatic compound, methyl salicylate (MeSA). Analysis includes the no neighbor, intraspecific, and interspecific treatments, where interactions involved simultaneous aboveground and belowground contact (Kigathi et al. 2013);

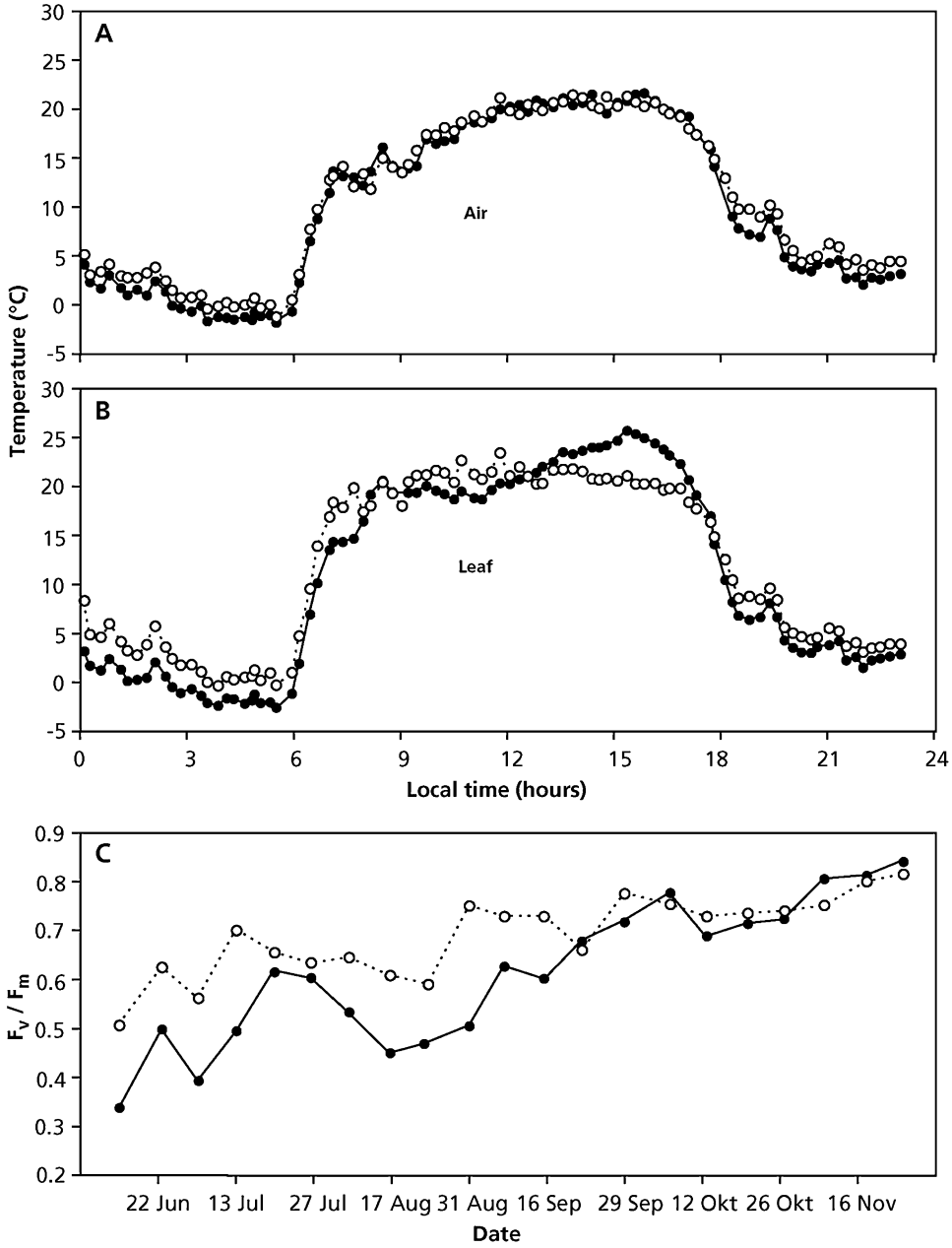

Fig. 16.3 Diurnal variation in (**A**) air temperature and (**B**) the temperature of the leaves of *Eucalyptus pauciflora* (snow gum) above an open patch (open symbols) and above grass (filled symbols), measured from midnight to midnight on a day in September (early spring). Temperatures were measured 10 cm above ground level for one leaf of a seedling; seedlings were about 2 m apart. (**C**) Seasonal changes in average weekly midday values for the fluorescence characteristic F_v/F_m, which is an indicator of the quantum yield of photosynthesis, for seedlings of *Eucalyptus pauciflora* grown in an open habitat (open symbols), or above grass (filled symbols) (Ball et al. 1997); © John Wiley & Sons Ltd.

long time. In growth analyses and in short-term competition experiments carried out at a limiting nutrient supply, potentially fast-growing species grow faster and produce more biomass than do slow-growing ones (Lambers and Poorter 1992). Even when growing naturally in a nutrient-poor

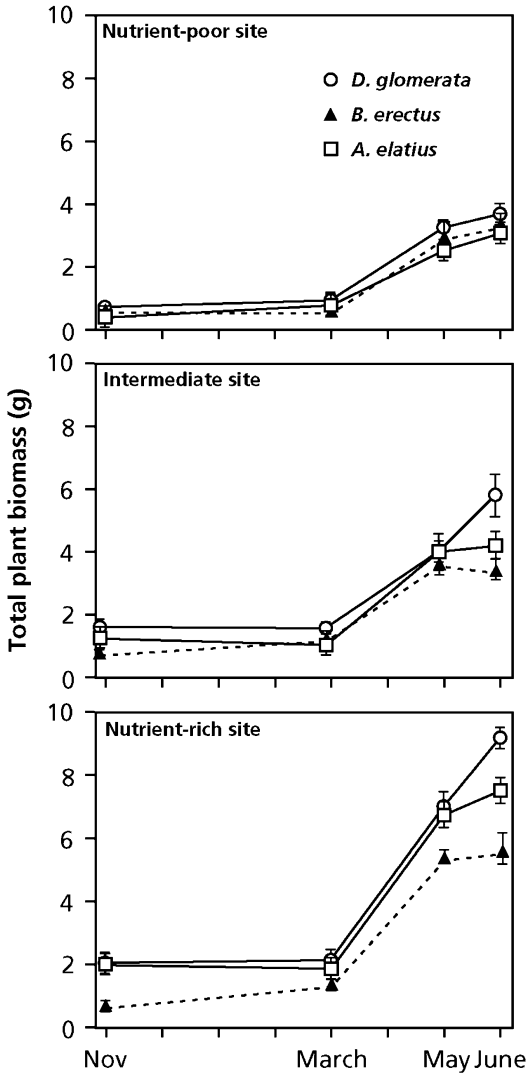

Fig. 16.4 Total biomass of three tussock-forming grasses, growing in three meadows that differ in nutrient availability. The grasses differ in their RGR_{max}, with *Bromus erectus* (upright brome; filled triangles) having the lowest RGR_{max}, *Arrhenaterum elatius* (oatgrass; open squares) an intermediate RGR_{max} and *Dactylis glomerata* (open circles) the highest (after Schläpfer and Ryser 1996).

meadow, in competition with surrounding plants, the species with the highest RGR_{max} grows fastest and produces most biomass in relatively short experiments (Fig. 16.4). The greater competitive ability in these short-term experiments is associated with a higher leaf area ratio (*LAR*), due to a lower leaf mass density (Lambers and Poorter 1992); it is also associated with a higher specific root length (*SRL*), due to thinner roots and a lower root mass density (Ryser and Lambers 1995).

Why do plants with a small root diameter and low tissue mass density (*i.e.* a high SRL) and with thin leaves and a low tissue mass density (*i.e.* a high specific leaf area, *SLA*) fail to dominate on nutrient-poor sites? For widely different species, including evergreen and deciduous ones, the low **tissue mass density** of fast-growing species is associated with a more rapid turnover of their leaves and a shorter **mean residence time of nutrients** (Sect. 9.4). In a comparison of ecologically contrasting grass species, slower-growing species from nutrient-poor habitats also tend to have a higher tissue mass density and slower turnover rates than do faster-growing ones from more productive sites (Ryser 1996). Turnover of plant parts inevitably causes some loss of nutrients from the plant and reduces the mean residence time of the nutrients (Sect. 9.4). Although rapid growth may therefore lead to a competitive advantage in the short term, even when the nutrient supply is severely limiting, there is a penalty associated with this trait in the long run (Berendse and Aerts 1987). That is, the losses associated with tissue turnover become so large that they cannot be compensated for by uptake of nutrients from the nutrient-poor environment. As a result, inherently fast-growing species are outcompeted by slower-growing ones, once the time scale of the experiment is long enough that differences in tissue loss and mean residence time influence the outcome of competition (Aerts and Van der Peijl 1993).

Why should a low tissue mass density be associated with faster turnover and shorter residence times? Part of the answer is straightforward: a high tissue mass density reflects a large investment in cell walls, sclerenchyma, and fibers, which reduce the **palatability** and **digestibility** of the tissue and allow the tissue to withstand abiotic stresses and deter herbivores. Or, as expressed by Eeyore in the house at Pooh Corner (Milne 1928): "Why do all plants which an animal likes, have the wrong sort of swallow or too many spikes" (Sect. 10.3.3).

Senescence is a highly programmed process of tissue death that also causes tissue turnover. The rate of tissue turnover or **life span** are quite separate from tissue mass density, though correlating with it for reasons that will become clear in this Section (Poorter et al. 2009; Osnas et al. 2018). This programming is obviously prolonged for leaves with a greater life span, even though we understand very little of the mechanisms underlying these differences. If the programming, however, is such that the leaves last a long time, the leaves must be constructed in such a way that biotic and abiotic factors do not prevent a long life span. In other words, natural selection for slow turnover and a large investment in defense should go together which explains the close correlation between the two, without there being a causal link (Lambers and Poorter 1992; Poorter et al. 2009).

There is a third reason for shorter nutrient residence times in faster-growing species at a low nutrient supply (Sect. 10.7). Species differ in the manner in which they respond to a limitation by nutrients in the environment: the typical response of a fast-growing species upon sensing nutrient shortage is to promote leaf senescence and so withdraw nutrients from older leaves and use these for its newly developing organs (Maillard et al. 2015). A slow-growing species that naturally occurs on nutrient-poor sites will slow down the production of new tissues, with less dramatic effects on leaf senescence and allocation pattern (Shane et al. 2003). When the leaves finally senesce, they remobilize for more nutrients, especially P, than do leaves of fast-growing species (Hayes et al. 2014). In other words, the environmentally induced senescence is much stronger in faster-growing species than it is in slower-growing ones. We again understand too little of a plant's physiology to fully account for these ecological observations, but the result is clear: the environmentally induced senescence of fast-growing species causes them to lose more nutrients, and gradually give way to more efficient slow-growing species.

16.4.2 Allocation Pattern, Growth Form, and Tissue Mass Density

There are a number of plant functional traits that affect the outcome of competition, dependent on environmental conditions. For example, under nutrient-rich conditions, *Lychnis flos-cuculi* (ragged robin) genotypes with an inherently high **leaf mass ratio** (LMR) achieve higher yields in competition with *Anthoxanthum odoratum* (sweet vernalgrass) and *Taraxacum hollandicum* (dandelion) than do genotypes with a lower LMR. At a low nutrient supply, however, this allocation pattern confers no advantage (Biere 1996). Increased N inputs cause shifts in plant community composition and plant functional traits in a grassland in eastern Nebraska, USA. Nitrogen addition increases community-weighted specific leaf area (*SLA*) by 19%, and decreases leaf dry matter content (*LDMC*) by 11% (Tatarko and Knops 2018). These results are consistent with the view that a selective advantage may accrue from either high or low values of individual *RGR* components, depending on habitat conditions, and that the selective advantage of low trait values in nutrient-poor environments may result in indirect selection for low *RGR* in these habitats. A high leaf area ratio (*LAR*), due to a high *LMR* and/or a high *SLA*, which is associated with a rapid growth rate, is advantageous in productive environments. On the other hand, a low *SLA*, which is associated with slow growth, confers a selective advantage in relatively unfavorable environments (Sects. 10.3.7 and 10.6.3; Lambers and Poorter 1992).

Just as *SLA* is an important above-ground trait for a plant's competitive ability, the **specific root length** (*SRL*) or **specific root area** (*SRA*) are important belowground traits, determining a plant's ability to compete for nutrients and water. This can be illustrated using two tussock grasses, competing with *Artemisia tridentata* (sagebrush) as an indicator species (Eissenstat and Caldwell 1988). *Agropyron desertorum* (desert wheatgrass) is an introduced species, with a

greater competitive ability than the native *Pseudoroegneria spicata* (formerly *Agropyron spicatum*; bluebunch wheatgrass). *Artemisia tridentata* plants that are planted among near-monospecific stands of one of the two tussock grasses show lower survival, less growth and reproduction, and a more negative water potential during part of the season when surrounded by *Agropyron desertorum* than they do when they compete with *Pseudoroegneria spicata*. *Agropyron desertorum* extracts water more rapidly from the soil profile, but it is remarkably similar in architecture, shoot phenology, root mass distribution in the soil profile, growth rate in various environments, and the efficiency of water and N use (Eissenstat and Caldwell 1987). Its roots are thinner, however, so that the SRL is about twice that of the less competitive *Pseudoroegneria spicata*. This allows the more competitive tussock grass (*i.e. Agropyron desertorum*) to extract water more rapidly from the profile. These traits likely contribute to the observation that *Artemisia tridentata*, growing side by side with the two tussock grasses, acquires 86% of all its absorbed labeled P from the interspace shared with *Pseudoroegneria spicata*, and only 14% from the interspace with *Agropyron desertorum*. Clipping of the tussock grasses enhances P uptake by *Artemisia tridentata* substantially, confirming that the grasses competed for resources from the soil before clipping (Caldwell et al. 1987). Because P is highly immobile in most soils (Sect. 9.2.1.3), roots of the competing plants or their associated mycorrhizal fungal hyphae must have been very close to each other.

In general, there are strong correlations among most root morphological traits, indicating the existence of a '**root economics spectrum**'. The main syndrome of root trait covariation is consistent at the different spatial scales and organizational levels, with soil nutrients and water availability being the main drivers of root trait variation (Fig. 16.5). Root trait variation is primarily aligned along a leading dimension related to resource economics (de la Riva et al. 2018). However, root traits are simultaneously constrained by various environmental drivers that are not necessarily related to resource acquisition, and mycorrhizal associations may offset selection for a root economics spectrum (Wen et al. 2019). Understanding and explaining belowground mechanisms and trade-offs that drive variation in root traits, resource acquisition, and plant performance across species, thus requires a fundamentally different approach than applied aboveground. This calls for studies that incorporate root traits involved in resource acquisition, the complex soil environment, and the various soil resource acquisition mechanisms, including the mycorrhizal pathway, in a multidimensional root trait framework (Weemstra et al. 2016).

16.4.3 Plasticity

Previous chapters provided numerous examples of the acclimation of photosynthesis, respiration, and biomass allocation to environmental factors such as irradiance and nutrient supply. A high capacity to acclimate reflects a genotype's **phenotypic plasticity** for a specific trait; however, a relatively small plasticity for one trait may result from a large plasticity in other traits. For example, the low morphological plasticity (stem length) of an alpine *Stellaria longipes* (Sect. 10.5.7) is a consequence of a high physiological plasticity (ethylene production). In addition, a large morphological plasticity in biomass allocation between roots and leaves in response to nutrient supply or irradiance results in a low plasticity of the plant's growth rate, so that this varies relatively little between different environments.

Interspecific differences in functional traits are a key factor for explaining the positive diversity-productivity relationship in plant communities. Modeling of an **intercropping** system of *Triticum aestivum* (wheat) and *Zea mays* (maize) as an example of mixed vegetation, shows that plasticity in plant traits is an important factor contributing to complementary light capture in species mixtures (Zhu et al. 2015). Light capture is 23% higher in the intercrop with plasticity than the expected value from monocultures, of which 36% is attributable to community structure and

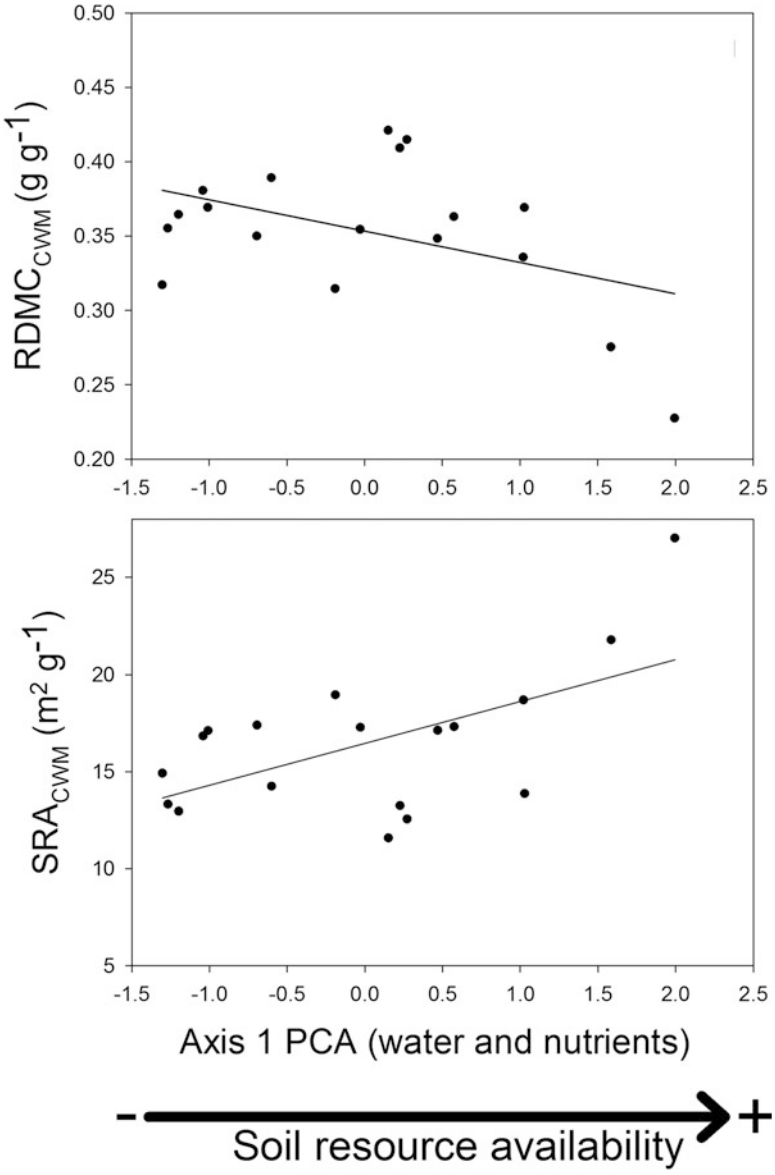

Fig. 16.5 Relationships between two community-level root traits traits), specific root area (SRA) and root dry matter content (RMDC) and the first axis of a Principal Component Analysis that represents soil resource availability (water and nutrients) (de la Riva et al. 2018).

64% to plasticity. For wheat, plasticity in tillering is the main reason for increased light capture, whereas for intercropped maize, plasticity induces a major reduction in light capture (Fig. 16.6). These results illustrate the potential of plasticity for enhancing resource acquisition in mixed stands, and indicate the importance of plasticity in the performance of species-diverse plant communities (Turcotte and Levine 2016).

There are certainly convincing examples of greater plasticity associated with competitive ability in a particular environment. A classic case is the response of stem elongation to shade light (Sects. 10.5.1 and 16.2). To confirm the importance of the **phytochrome system** for the perception of neighboring plants, Ballaré et al. (1994) used transgenic plants of *Nicotiana tabacum* (tobacco), overexpressing a phytochrome gene. These transgenics show a

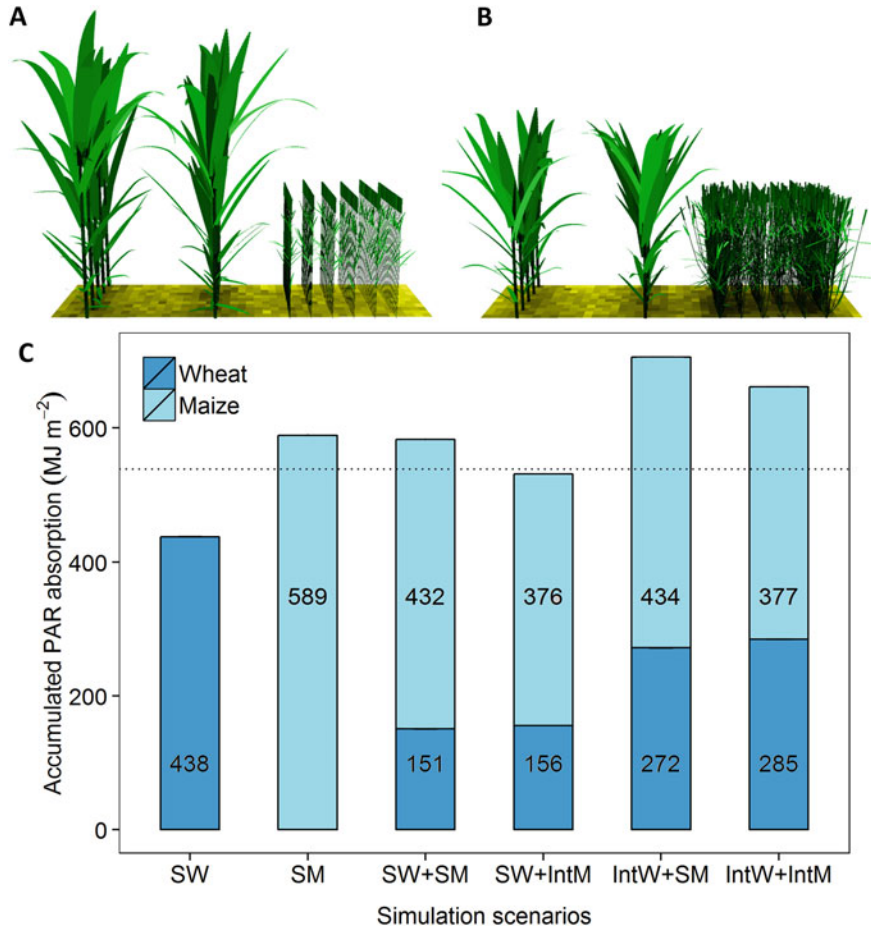

Fig. 16.6 Comparison of the architecture of different phenotypes of *Triticum aeastivum* (wheat) and *Zea mays* (maize) at wheat flowering stage (**A**) when assuming no plasticity, and (**B**) when assuming plastic responses to the intercrop situation. Thus, (**A**) depicts the empirically nonobservable modeled situation of plants with monoculture phenotype in a mixture setting. (**C**) Accumulated photosynthetically active radiation (PAR) capture over the season in different systems. SW, monoculture wheat; SM, monoculture maize; IW, intercrop wheat phenotype; IM, intercrop maize phenotype; SW + SM, a relay strip wheat–maize intercrop with phenotype of monoculture wheat and monoculture maize. Light capture in SW + SM represented a pure structure effect without a contribution from plant plasticity. The light capture, as indicated in the bar, for species in intercrops was expressed per m^2 of an intercrop area, in which the relative density of wheat is 1/3 and that of maize is 2/3. The horizontal dotted line represents the expected light capture (LC) in an intercrop without effects of structure or plant plasticity, calculated as $LC_{expected}$ = 1/3 LCSW +2/3 LCSM (Zhu et al. 2015); with permission of the New Phytologist Trust.

dramatically smaller response to the red/far-red ratio of the radiation and to neighboring plants. In a stand of such transgenics, the small plants of the population are rapidly suppressed by their neighbors. These results indicate that a high degree of plasticity in morphological parameters plays an important role in the competition with surrounding plants (Fig. 16.7).

With respect to variation in nutrient supply, a survey of a large number of species finds no correlation between relative growth rate and allocation (root mass ratio and stem mass ratio) (Reynolds and D'Antonio 1996). Plasticity for colonization by mycorrhizal fungi (Sect. 12.2) and release of root exudates (Sect. 9.2) are likely far more important.

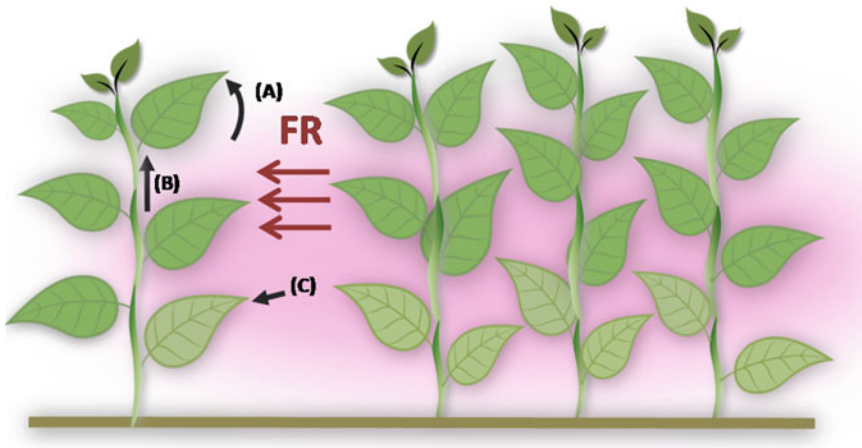

Fig. 16.7 Neighbor detection and local responses of plant organs to changes in the red:far Red (R:FR) ratios. Local responses to low R:FR ratios, such as those illustrated here, allow plants to shape their architecture to optimize light interception, and to retain those leaves that are important for whole-plant photosynthesis. (**A**) Local upward bending responses; (**B**) internode elongation responses triggered by stem-perceived FR radiation; and (**C**) local induction of leaf senescence and suppression of defense responses in leaves exposed to low R:FR ratios (Ballaré 2017); copyright Elsevier Science, Ltd.

In summary, it appears that fast-growing species from high-resource environments are more plastic for some traits, such as photosynthetic characteristics and the rate of stem elongation in response to shade, surrounding plants, and wind. When it comes to below-ground plant traits and morphological plasticity in response to the supply of nutrients, this conclusion is hard to substantiate, in part because plasticity in many traits (*e.g.*, nutrient uptake, root growth, and nutrient storage) can influence the response of allocation to nutrient supply. A full understanding of the relative role of plasticity in resource acquisition and plant performance requires a whole-plant (rather than 'single-trait') approach, taking into account that plants are integrated phenotypes.

16.5 Traits Associated with Competition for Specific Resources

16.5.1 Nutrients

We have shown the physiological basis for the trade-off between rapid growth and tolerance of low nutrient supply (Sect. 16.4). What evidence is there that species growing on infertile soils draw down resources below levels used by potential competitors, and what might be the processes responsible for such **resource draw-down**? Figure 9.13 shows that carboxylate-releasing P-mobilizing species have a greater capacity to access poorly available P than mycorrhizal species that do not release large quantities of such exudates. This strategy is also effective for other poorly mobile nutrients, *e.g.*, Fe and Zn (Sect. 9.2.6.2). For mobile nutrients, increasing transpiration would be more effective (Matimati et al. 2014).

What other nutritional traits might be involved in competition for nutrients? The **uptake kinetics** of species from infertile soils are unlikely to result in low soil solution concentrations. These species typically have a lower I_{max} of nutrient uptake and do not differ consistently in K_m from species that occur on fertile soils (Sect. 9.2.2.3.1). The influence of uptake kinetics on soil solution concentration should be greatest for mobile nutrients (*e.g.*, NO_3^-) and least pronounced for cations (*e.g.*, NH_4^+) and Pi (Sect. 9.2.1.2).

Nutrient-impoverished habitats, such as the campos rupestres in southeast Brazil, heathlands of southwest Australia and South Africa, are

among the most species-rich habitats in the world. How do so many species coexist where one might think that competition for nutrients must be critical for survival? There are some specialized root traits (cluster roots and their functional equivalent) that enable certain species to access P that is unavailable to other species (Sects. 9.2.2.4 and 9.2.2.5). Although species differ in preference for forms of N, most species have the physiological capability to tap all forms of soluble N and to adjust their capacities for uptake and assimilation, depending on supply (Sect. 9.2.1.2). Allelochemicals may inhibit **nitrification** (Sect. 13.2). Since NH_4^+ is far less mobile than NO_3^-, such inhibition may enhance the availability of N for plants whose roots release nitrification inhibitors. Ectomycorrhizas and ericoid mycorrhizas may break down **protein N** that would otherwise not be directly available to plants (Lambers et al. 2008). Most importantly, **facilitation** appears to be far more important than **competition** for nutrients (Muler et al. 2014; Wright et al. 2017). This, in combination with protection by mycorrhizal fungi against pathogens, accounts for t the coexistence of an outstanding number of species found on the sandplains in southwest Australia (Lambers et al. 2018). Their role in P acquisition is minor, in these systems, because very few hyphae can be found in the soil where colonized plants grow (Teste et al. 2016). Yet, the role of mycorrhizal fungi may be paramount, namely in protection against oomycetes (Fig. 16.8). It remains to be assessed how general these patterns are.

Facilitation based on P-mobilizing carboxylate release bu. neighbours can be assessed by measuring the concentration of **manganese** (Mn) in mature leaves (Gardner and Boundy 1983; Muler et al. 2014), because carboxylates not only mobilize P but also Mn (Fig. 9.13B; Lambers et al. 2015). Elevated leaf [Mn] in plants that do nor release carboxylates are likely partly accounted for by facilitation of P uptake by their carboxylate-releasing neighbors (Huang et al. 2017; Abrahão et al. 2018).

16.5.2 Water

The mechanism by which **desiccation-resistant plants** draw down soil moisture is well established. The lower the **water potential** that

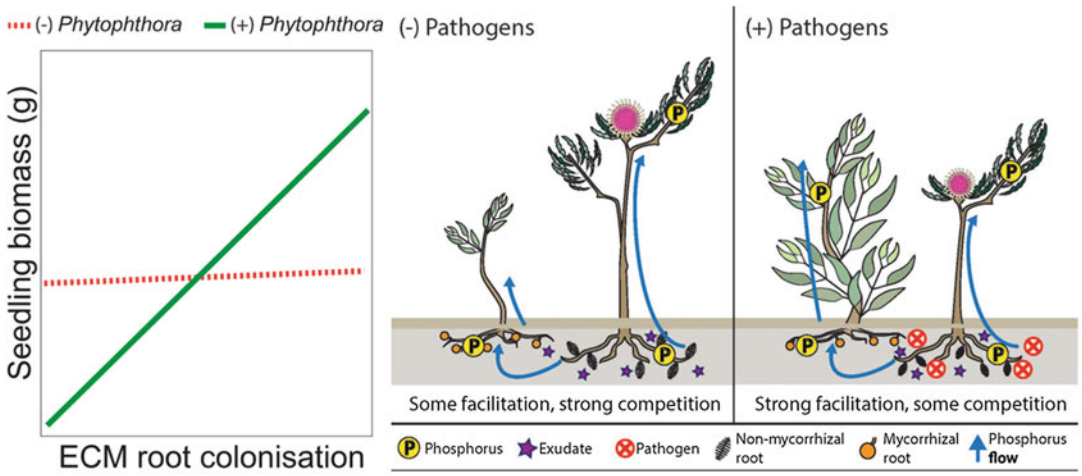

Fig. 16.8 (Left) Conceptual figure modified after Albornoz et al. (2017), showing the relationships between ectomycorrhizal root colonization and seedling biomass in the presence or absence of *Phytophthora* (an oomycete or slime mould) species. The solid green line indicates the presence of *Phytophthora* and a significant relationship, while the red dashed line indicates the absence of *Phytophthora* and a nonsignificant relationship. (Right) Diagram showing the net outcome of interaction between a mycorrhizal (plant on the left) and a non-mycorrhizal Proteaceae (plant on the right) in the absence (left panel) and presence (right panel) of native soil-borne pathogens. Drawing produced by Javier F. Tabima (Lambers et al. 2018).

a species can tolerate, the lower the level to which it can reduce soil moisture. When soil water potential falls below the minimum water potential tolerated by potential competitors, they can no longer withdraw water from the soil. The traits that enable a plant to maintain activity at a low water potential include osmotic or elastic adjustment, embolism-resistant xylem, and a stomatal conductance that is relatively insensitive to signals associated with a low root or leaf water potential (Sects. 5.4.1 and 5.5.4.1). This highlights a stark contrast with the mechanisms involved in competing for nutrients (Sect. 16.5.1).

Transpiration is the major avenue of water loss to the atmosphere, and therefore of soil drying in dense vegetation. In general, the species with greatest **desiccation resistance** have a suite of morphological and biochemical traits that enable them to conserve water (*e.g.*, CAM and C_4 photosynthesis, low stomatal conductance, low hydraulic conductance of the stem). When water is available, most plants maximize stomatal conductance and therefore water loss. In a mixed-species community, the species responsible for the greatest quantity of water loss are not those that are most resistant of water stress. The desiccation-resistant species are probably most important in the final stages of moisture drawdown, after less resistant species become dormant (Mitchell et al. 2008). The abundance of different life forms and physiological strategies in deserts indicates that competition for water may have selected divergent water-use strategies in dry environments, only some of which involve extreme resistance of low soil water potential. Other modes of competing effectively in deserts include phenological **avoidance** of drought and rapid growth when water is available such as observed in neotropical dry forests (Reich and Borchert 1984).

Competition for water becomes obvious when the understory is removed under a *Pinus sylvestris* (Scots pine) xeric forest in an Alpine valley in Switzerland. The removal of the understory increases soil water content, decreases tree water deficit, and increases mean annual radial growth 4.6-fold (Fig. 16.9). Reduced competition for soil water after removal of the understory vegetation is the primary cause of the increased performance of the overstory trees, since light was not a limiting factor before the understory

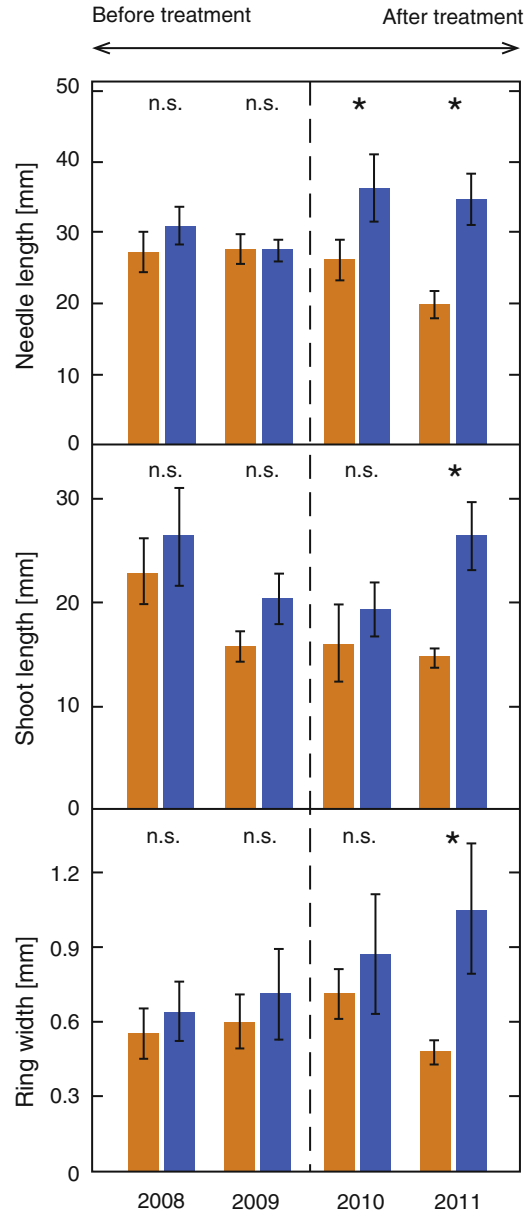

Fig. 16.9 Mean needle length, shoot length and tree-ring width of the treated (understory removal, blue) and the control (orange) overstory *Pinus sylvestris* (Scots pine) trees. The vertical dashed line divides the time in the period before (2008–2009) and after the understory removal in April 2010 (Giuggiola et al. 2018); copyright Elsevier Science, Ltd.

removal. Thus, increases in understory density due to altered forest management may have exacerbated drought-induced decline processes. The findings suggest decreasing understory density as a suitable management practice to increase overstory tree growth and vigor, and hence reduce mortality risk for a species like Scots pine in a drought-prone environment (Giuggiola et al. 2018).

A low conductance between roots and soil or of the soil might preclude substantial efflux of water from roots (Carminati and Vetterlein 2013). A nocturnal down-regulation of water-channels proteins (Sect. 5.5.2) might reduce water loss to dry soil. Although water efflux from roots into soil might be viewed as undesirable, there is no metabolic cost to **hydraulic lift**, and the water released at night is available for reabsorption during the day (Prieto et al. 2012). In addition, the moist soil may promote nutrient acquisition by roots and prolong the activity of symbiotic microorganisms such as mycorrhizal fungi in the upper soil layers. The moist soil may also prevent chemical signals that would otherwise originate from roots in contact with dry soil (Sect. 5.5.4.1). Grasses effectively take up water redistributed by East African *Vachellia tortilis* (formerly *Acacia tortilis*, umbrella thorn acacia) (Ludwig et al. 2004). When tree roots are experimentally removed, preventing access to redistributed water by grasses, the biomass of the grasses increases. Thus, although grasses effectively take up redistributed water, competition between tree and grasses outweighs the potential positive effect of hydraulic lift.

16.5.3 Light

Strong **competition for light** seldom coincides with strong competition for belowground resources for two reasons. First, high availability of below-ground resources is an essential prerequisite for the development of a leaf canopy dense enough to cause intense light competition, which is strongest under conditions where water and nutrients are not strongly limiting to plant growth. Second, trade-offs between shoot and root competition constrain the amount of biomass that can be simultaneously allocated to acquisition of above- and belowground resources (Brouwer 1963; Freschet et al. 2015). Those species that are effective competitors for light are trees with a high above-ground allocation.

As with water, the species that most strongly reduce light availability are not necessarily the species that are most tolerant of low light. Species that are tall and have a high **leaf area index** (LAI) have greatest impact on light availability, whereas understory plants and late-successional species are generally the most shade-tolerant. Because light is such a strongly directional resource, competition for light is generally quite asymmetric. The taller species having the greatest impact on the shorter ones, with often little detectable effect of adult understory species on the overstory, at least with respect to light competition. The **phytochrome** systems plays a major role in plant acclimation to shade (Sect. 16.4.3) (Ballaré 2017).

16.5.4 Carbon Dioxide

Carbon dioxide is relatively well mixed in the atmosphere; therefore, plant uptake creates less localized depletion of CO_2 than of nutrients, water, or light. Nonetheless, photosynthesis is often CO_2-limited, especially in C_3 plants. Plants with contrasting photosynthetic pathways may therefore differ in their competitive ability in relation to atmospheric CO_2 concentration. For example, one might expect the growth of C_4 plants, whose rate of photosynthesis is virtually saturated at current CO_2 concentrations of 400 μmol mol^{-1}, to respond less to the global rise in atmospheric CO_2 concentration than that of C_3 plants. To test this hypothesis, Johnson et al. (1993) compared the growth of **C_3 and C_4 plants**, while growing in competition at CO_2 concentrations, ranging from preindustrial levels to 350 μmol mol^{-1}, the prevalent CO_2 concentration at the time of the experiment. As expected, photosynthesis and growth were enhanced more by high levels of CO_2 in C_3 species than in C_4 species. Whereas the C_4 species outyield the C_3 plants at low CO_2

concentrations, the C_3 plants are superior competitors at elevated [CO_2]. How can we assess whether a change in competitive ability has indeed occurred? To address this question, the soil organic matter $\delta^{13}C$ of known age was analyzed to estimate changes in the relative abundance of C_3 and C_4 species between the late Pleistocene and the early Holocene in northern Mexico (Cole and Monger 1994). This showed an increase in abundance of C_3 species about 9000 years ago, a time when Antarctic ice cores show a rapid rise in atmospheric [CO_2]. Plant macrofossils from packrat middens show that this vegetation change coincided with an increase in aridity, which favors C_4 species. The vegetation change, therefore, was most likely caused by increased atmospheric [CO_2], rather than by climatic change.

Will C_3 species continue to conquer the world at the expense of C_4 species in years to come, while the concentration of CO_2 continues to rise? In experiments using around 340 and 620 μmol CO_2 mol^{-1} air, the competitive ability of *Triticum aestivum* (wheat) (C_3) is enhanced compared with that of *Echinochloa frumentacea* (Japanese millet) (C_4) (Wong and Osmond 1991). Drake and co-workers studied the effects of elevated [CO_2] on natural salt-marsh vegetation, consisting of both C_3 [predominantly *Scirpus olneyi* (olney threesquare)] and C_4 [mainly *Spartina patens* (salt hay grass)] sedges. After 4 years of exposure to elevated [CO_2], the biomass of *Scirpus olneyi* is greatly enhanced, both on sites where this species occurs as a pure stand and also where it grows in mixtures with *Spartina patens*. There is very little effect of elevated [CO_2] on the biomass of *Spartina patens* growing in a monospecific community, whereas it is reduced on sites where it grows in competition with the C_3 sedge (Arp et al. 1993).

C_4 plants have decreased in **competitive ability** since the beginning of the industrial revolution. They may well continue to lose ground with a further rise in atmospheric [CO_2]. Elevated CO_2 concentrations interact with temperature, however, and affect plant growth in a manner that may be quite different from a plant's response to elevated [CO_2] alone. The climate change caused by elevated [CO_2] may well have an opposite effect on competition between C_3 and C_4 species. Increased temperatures and drier climates might favor C_4 grasses and lead to an expansion of the area occupied by C_4 species.

Elevated atmospheric [CO_2] can alter availability of other environmental resources that can shift competitive balance in unpredictable ways. In a dry North American prairie, elevated [CO_2] causes an increase in soil moisture as a result of the reduction in stomatal conductance and transpiration. The improved soil moisture favors tall C_4 grasses over a subdominant C_3 grass which is opposite the result expected from direct photosynthetic response to CO_2 (Owensby et al. 1993).

Many of the published studies on competitive interactions of C_3 and C_4 species have been conducted in relatively fertile soils, where we would expect photosynthetic performance to have the strongest connection to growth and competitive ability. Nutrient limitation reduces plant growth response to elevated CO_2 (Edwards et al. 2005), and there is no consistent competitive advantage of C_3 or C_4 species at low nutrient availability. Therefore, **nutrient limitation** could reduce any competitive advantage that C_3 species might have with future increases in atmospheric CO_2. In summary, despite the greater photosynthetic responsiveness of C_3 plants to elevated CO_2, compared with that of C_4 species, this may not translate into a future competitive advantage (Reich et al. 2018).

16.6 Positive Interactions among Plants

Not all plant-plant interactions are competitive. Plants often ameliorate the environment of neighbors and increase their growth and survivorship (**facilitation**), particularly at the seedling stage and where the physical environment or water and nutrients strongly constrain growth (Fig. 16.10; Callaway 2007; Wright et al. 2017).

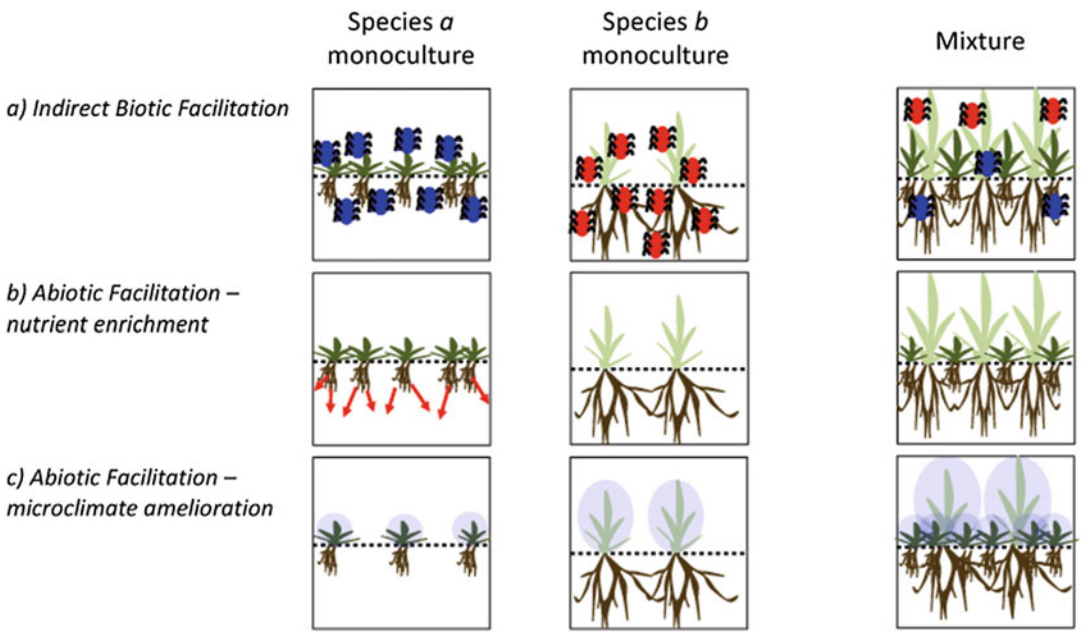

Fig. 16.10 Facilitative mechanisms that explain species-specific overyielding in biodiversity–ecosystem function (BEF) experiments. There are at least three facilitative mechanisms that can explain species-specific overyielding. First, indirect biotic facilitation can occur via diversity effects on species-specific pathogen loads (**A**), or through indirect competitive interactions increasing the productivity of a species growing in mixture. Here, all pathogens (fungal, bacterial, viral, *etc*.) are indicated with a drawing of an insect. When a single plant species grows alone in monoculture, it can accumulate species-specific pathogens over time. When these same species grow together in mixture, the species-specific pathogen load is reduced, and plants can grow more due to overall release from pathogenic attack. Second, facilitation of neighbors can result from abiotic effects on nutrient availability. In particular the legume-rhizobia symbiosis can directly increase nitrogen availability for neighboring plants (**B**). In (**B**) if species a is leguminous, it can have a positive effect on the growth of species b due to nitrogen inputs into the soil. Third, facilitation can be mediated through abiotic effects on microclimate conditions. For example, if species a is sensitive to irradiance or high temperatures, the microclimate effect provided by species b can improve the performance of species a in mixture of those species (**C**) (Wright et al. 2017);

16.6.1 Physical Benefits

In hot dry environments, seedlings often establish preferentially in the shade of other **nurse plants**. At the seedling stage, barrel cacti (*Ferocactus acanthodes*) suffer high mortality in deserts because of their small thermal mass. Seedlings in the shade of other plants are 11 °C cooler than they are in full sun and only survive in shade (Turner et al. 1966). Facilitation due to shading also occurs in oak savannas by reducing desiccation and overheating, and in salt marshes by reducing soil evaporation and therefore salt accumulation (Callaway 1995). Hydraulic lift by deep-rooted plants may increase water potential and growth of adjacent plants (Richards and Caldwell 1987; Sun et al. 2014). Other facilitative effects of plants include oxygenation of soils, stabilization of soils, physical protection from herbivores, and attraction of pollinators (Callaway 1995).

16.6.2 Nutritional Benefits

A second general category of facilitation involves enhanced **nutrient availability**. The most dramatic examples of this are establishment of N_2-fixing species in early-successional and other low-N habitats (Vitousek et al. 1987).

Decomposition of high-N litter of N_2-fixing plants increases N availability in these environments.

When P is limiting and most of it is sorbed onto soil particles, plants that access sorbed P due to the release of carboxylates from their roots, can benefit their neighbors that lack this ability, if these neighbors access it when it has been mobilized (Sect. 9.2.2.5). The neighbors may benefit because of the P-rich litter produced by facilitating species (Lambers et al. 2012). On calcareous soil, Fe uptake is restricted in calcifuge species, *e.g.*, *Arachis hypogaea* (peanut). When peanut is intercropped with *Zea mays* (corn), which releases phytosiderophores, peanut does not show signs of Fe deficiency and yields much better (Sect. 9.2.2.6.2) (Zuo et al. 2000; Zuo and Zhang 2008). These nutritional benefits can therefore be taken advantage of in **intercropping** systems in agriculture (Hauggaard-Nielsen and Jensen 2005; Hauggaard-Nielsen et al. 2008).

In the real world, plant-plant interactions involve complex mixtures of competitive and facilitative effects, which often occur simultaneously (Wright et al. 2017; Koffel et al. 2018). Symbionts may play a role as well, especially if plants are connected via mycorrhizal networks (Jakobsen and Hammer 2015; Wagg et al. 2015). Herbivores and pathogens may play a role as well, if the facilitating species is more sensitive to them (Lambers et al. 2018).

16.6.3 Allelochemical Benefits

As discussed in Sect. 13.2, some plants release allelochemicals that affect herbivores. For example, *Eragrostis curvula* (weeping lovegrass) releases chemicals that have a **nematicidal** effect. Such species may be used to manage nematodes in agriculture (Katsvairo et al. 2006).

In subsistence farming in Kenya, intercropping of *Zea mays* (corn) with the fodder legumes silverleaf (*Desmodium uncinatum*) and greenleaf (*Desmodium intortum*) dramatically reduce the infestation of maize by **parasitic witchweeds** such as *Striga hermonthica*, due to an allelochemicals released by the fodder legumes (Khan et al. 2002). Laboratory studies have shown that the allelochemical is a germination stimulant for *Striga hermonthica* as well as an inhibitor for haustorial development (Sects. 15.2.1 and 15.2.2; Fig. 16.11).

Certain plants release **stress signals**, even when undamaged, and these can cause defense responses in intact neighbors. These discoveries provide the basis for new crop protection strategies, either through conventional intercropping with plants that release stress signals or by genetic modification of plants (Pickett et al. 2003). Similar signaling discoveries within the **rhizosphere** offer potential to extend these approaches into new ways of controlling weeds and pests, by exploiting the potential of allelochemicals through signaling rather than by direct physiological effects (Sect. 13.4.3). '**Push-pull strategies**' involve the behavioral manipulation of pests and their natural enemies via the integration of stimuli that act to make the protected resource unattractive or unsuitable to the pests (push) while luring them toward an attractive source (pull) from where the pests are subsequently removed (Cook et al. 2007). The push and pull components are usually integrated with methods for population reduction, preferably biological control. While the use of intercrops as part of the push-pull strategy reduces the area available for the actual crop to a small extent, it greatly enhances the yield of the crop per unit area. The strategy is a valuable tool for **integrated pest management** aiming to reducing pesticide input and has been used successfully in subsistence farming in Africa (Hassanali et al. 2007).

These are just a few of numerous examples of chemical interactions between plants involving other organisms. They reveal an exciting eco-physiological complexity that we are only just beginning to appreciate. Possibilities for applications in agriculture are numerous, as alluded to above and in several other chapters.

16.7 Plant–Microbial Symbioses

Many woody species that appear in early phases of succession (*e.g.*, after a fire) are **N_2-fixing legumes**. These legumes tend to be

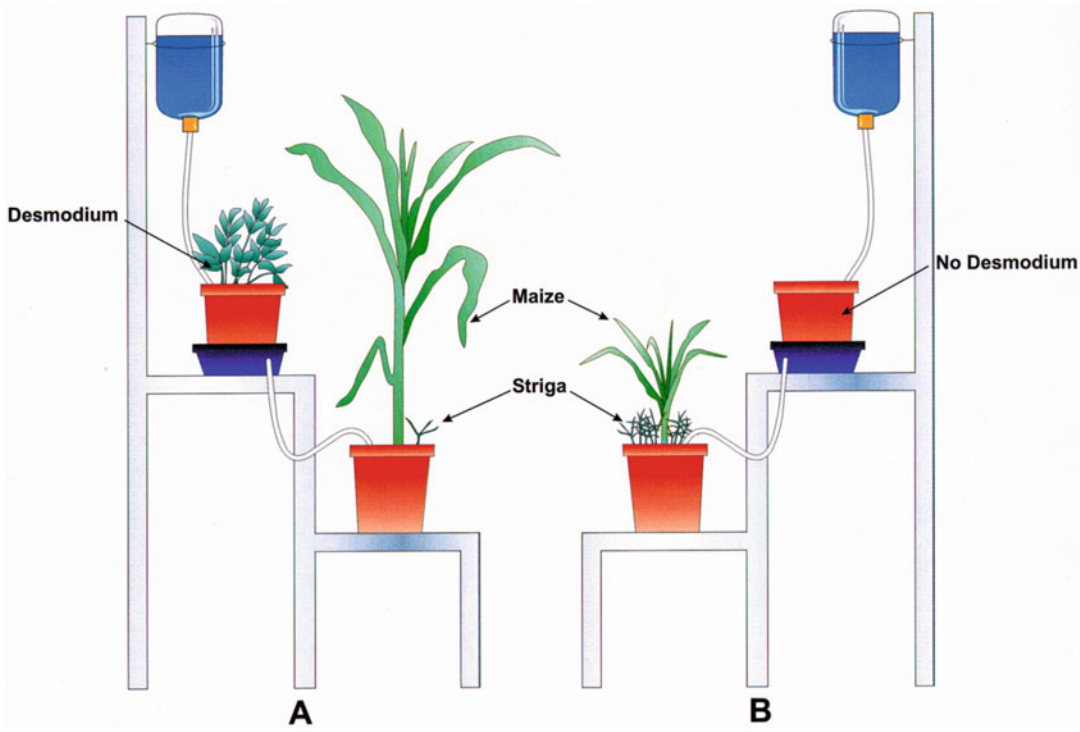

Fig. 16.11 Diagram of an experiment to investigate the allelochemical mechanism of the fodder legume *Desmodium uncinatum* (silverleaf) in suppressing *Striga hermonthica* (witchweed) infestation of *Zea mays* (corn). A comparison was made between corn plants irrigated by root eluates of *Desmodium uncinatum* (**A**) with those irrigated by water passing through pots containing only autoclaved soil (**B**) (after Khan et al. 2002).

P-demanding species, and would benefit from higher soil P concentrations after a fire (Butler et al. 2018). When the level of N in the soil increases and the P availability declines, their rates of N_2 fixation decline (Sect. 12.3.9). At later stages during succession, such pioneers may succumb to phytophagous arthropods or rust-forming galls arthropods [*e.g.*, *Acacia saligna* (orange wattle) in Australia (Wood and Morris 2007)]. The competitive success of this species, which was introduced into South Africa to stabilize sand dunes, is partly ascribed to its symbiotic association with rhizobia (Stock et al. 1995).

If competing plants are **mycorrhizal**, we also need to consider the ability of their external mycelium to capture nutrients. If they share a common external mycelium, via mycorrhizal networks (Simard et al. 2015; Wagg et al. 2015), then competition exists between the plants to acquire nutrients from that external mycelium. Can mycorrhizal infection alter the balance between different species? When seedlings of the AM grass *Festuca ovina* (sheep fescue) grow in nutrient-poor sand in competition with seedlings of other species, they grow less well in the presence of AM fungi than they do in their absence. Seedlings of many of their competitors, however, grow substantially better (with the exception of nonmycorrhizal species) in the presence of AM (Grime et al. 1987). The grass *Lolium perenne* (perennial ryegrass) and the dicot *Plantago lanceolata* (snake plantain) show similar values for *RGR* when the plants are grown separately, irrespective of their mycorrhizal status. When grown in competition, however, the mycorrhizal *Planceolata lanceolata* has a higher mean *RGR* than *Lolium perenne*, whereas the opposite occurs when the plants are nonmycorrhizal. This suggests that the

coexistence of *Plantago lanceolata* in grasslands depends on mycorrhizas (Newman et al. 1992).

Competitive interactions may become complicated when species differ in their mycorrhizal dependency (Sect. 12.2.1.2). For example, of two tallgrass prairie grasses, *Andropogon gerardii* (big bluestem) is highly dependent on the symbiosis, whereas *Koeleria pyranidata* (junegrass) is not. When competing in pairs, *Andropogon gerardii* dominates in the presence of mycorrhizal fungi, whereas *Koeleria pyranidata* does in the absence of the fungus (Hetrick et al. 1989).

Some herbaceous pioneers are **nonmycorrhizal** (Sect. 12.2.2), and these may grow well in the early phase of succession, because of their special ability to release P from sparingly available sources (Sect. 9.2.2.5) or because the P availability is high. At later stages, mycorrhizal species arrive and replace nonmycorrhizal species. When growing in competition with the nonmycorrhizal *Brassica nigra* (black mustard), growth and nutrient uptake of the mycorrhizal *Panicum virgatum* (switchgrass) are reduced when plants are of equal size. The presence of collembola that graze mycorrhizal fungi enhances the competitive advantage of the nonmycorrhizal black mustard. When seedlings of the nonmycorrhizal *Brassica nigra* have to compete with the mycorrhizal plants of *Panicum virgatum* that germinated 3 weeks earlier, the situation is reversed: *Brassica nigra* is negatively affected by competition, whereas the larger and older grass plants are not (Boerner and Harris 1991). This may account, in part, for the gradual replacement of nonmycorrhizal annuals by mycorrhizal perennials.

Allelochemicals released by mycorrhizal fungi may also be important in the replacement of nonmycorrhizal species (Sect. 12.2.2). Germination and seedling growth of nonmycorrhizal species are inhibited by the presence of mycorrhizal hyphae in the rhizosphere (Fig. 16.12). When P fertilization suppresses the mycorrhizal microsymbiont, the deleterious effects on root growth and functioning of nonmycorrhizal species become less pronounced. This might lead us to the erroneous conclusion that the growth of the plants whose biomass increases most strongly with P fertilization is more limited by P than is that of the mycorrhizal plants. If we go to the root of the problem, however, intricate allelochemical interactions that involve mycorrhizal fungi may well account for our field observations (Francis and Read 1994).

Mycorrhizal fungi can harm nonmycorrhizal plants, but the reverse also occurs. When *Glycine max* (soybean) is grown in the vicinity of the nonmycorrhizal species *Urtica dioica* (stinging nettle), infection of the soybean roots by the

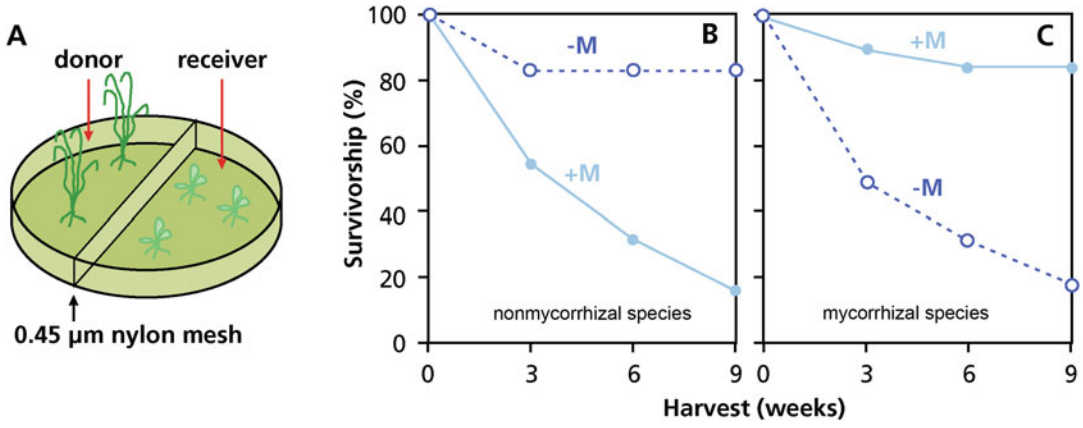

Fig. 16.12 (**A**) Experimental design to assess the effect of the presence of mycorrhizal hyphae on the survival of seedlings of mycorrhizal and nonmycorrhizal species. (**B**) Effects of mycorrhizal fungi on seedling survival of the nonmycorrhizal *Arenaria serpyllifolia* (thyme-leaved sandwort). (**C**) Effects of mycorrhizal fungi on seedling survival of the mycorrhizal *Centaurium erythraea* (common centaury) (after Francis and Read 1995).

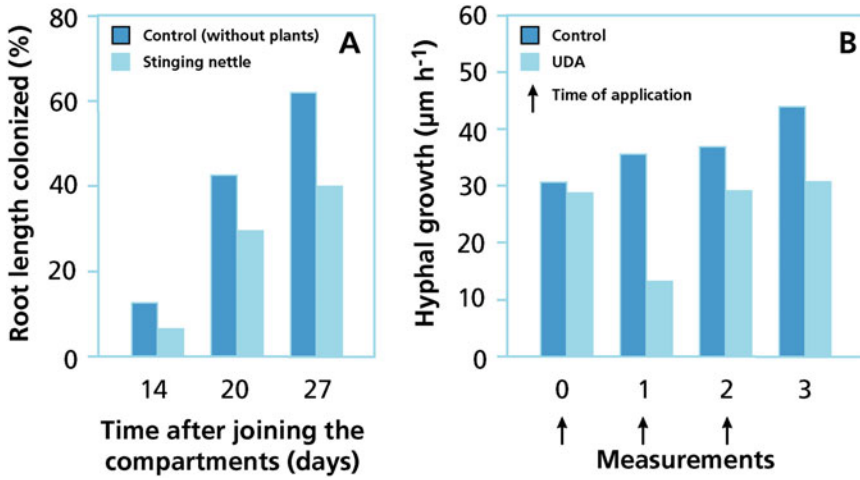

Fig. 16.13 (**A**) Spread of the mycorrhizal fungus *Glomus mosseae* across the rhizosphere of *Urtica dioica* (stinging nettle) or control soil, without stinging nettle. Uncolonized *Glycine max* (soybean) plants were used as acceptor plants. They were separated from well-colonized soybean plants (donor plants) by a test container of soil planted with stinging nettle or a container of soil without plants. (**B**) Effect of agglutinin from *Urtica dioica* on the hyphal growth of *Glomus mosseae*. The growth of hyphae of germinated spores was measured after application of small droplets of purified agglutinin. Application was repeated at 1 h intervals (arrows) (Vierheilig et al. 1996); copyright © 1996, Kluwer Academic Publishers.

mycorrhizal fungus *Glomus mosseae* is inhibited (Fig. 16.13A). A fungitoxic **lectin** (Sect. 12.2.2) inhibits the growth of fungal hyphae (Fig. 16.13B; Broekaert et al. 1989) which suggests that the lectin might be partly responsible for the effect of the presence of nonmycorrhizal species on the performance of mycorrhizal plants. Chitin-binding lectins in *Solanum integrifolium* (pumpkin tree) also have antifungal properties (Chen et al. 2018).

16.8 Succession and Long-Term Ecosystem Development

Successional changes in species composition following disturbance are the net result of different rates of **colonization**, **growth**, and **mortality** of early and late-successional species (Egler 1954; Li et al. 2016). Plant succession can be understood better when it is placed in the broadest possible temporal context (Walker and Wardle 2014). Plant succession can be central to the development of a framework that integrates a spectrum of ecological processes that occur over time scales ranging from seconds to millions of years (Fig. 16.14). Competition and facilitation both play roles in changes during succession and ecosystem development, especially in later stages. The resulting change in species composition through time is associated with predictable changes in plant functional traits (Fig. 9.1A).

During long-term soil development, soil N availability initially increases, and then declines, while soil P availability steadily declines (Sect. 9.2.1.1). Plant productivity initially increases during the progressive phase, and then declines during the retrogressive phase (Wardle et al. 2004). Leaf N:P ratios steadily decline, as plant productivity changes from primarily being N limited, via co-limitation by N and P, to increasingly P limited (Richardson et al. 2004; Hayes et al. 2014). Plant species richness steadily increases, as soil fertility declines (Fig. 16.15). There is a gradual shift in plant strategies as soils increase in age (Fig. 9.1 in Sect. 9.2.1) as well as an increase in diversity of nutrient-acquisition strategies (Zemunik et al. 2015, 2016). Although mycorrhizal species persist when soils are severely P-impoverished (Fig. 16.16), their role in nutrient acquisition becomes minor (Teste et al. 2016). However, they likely play a pivotal role in

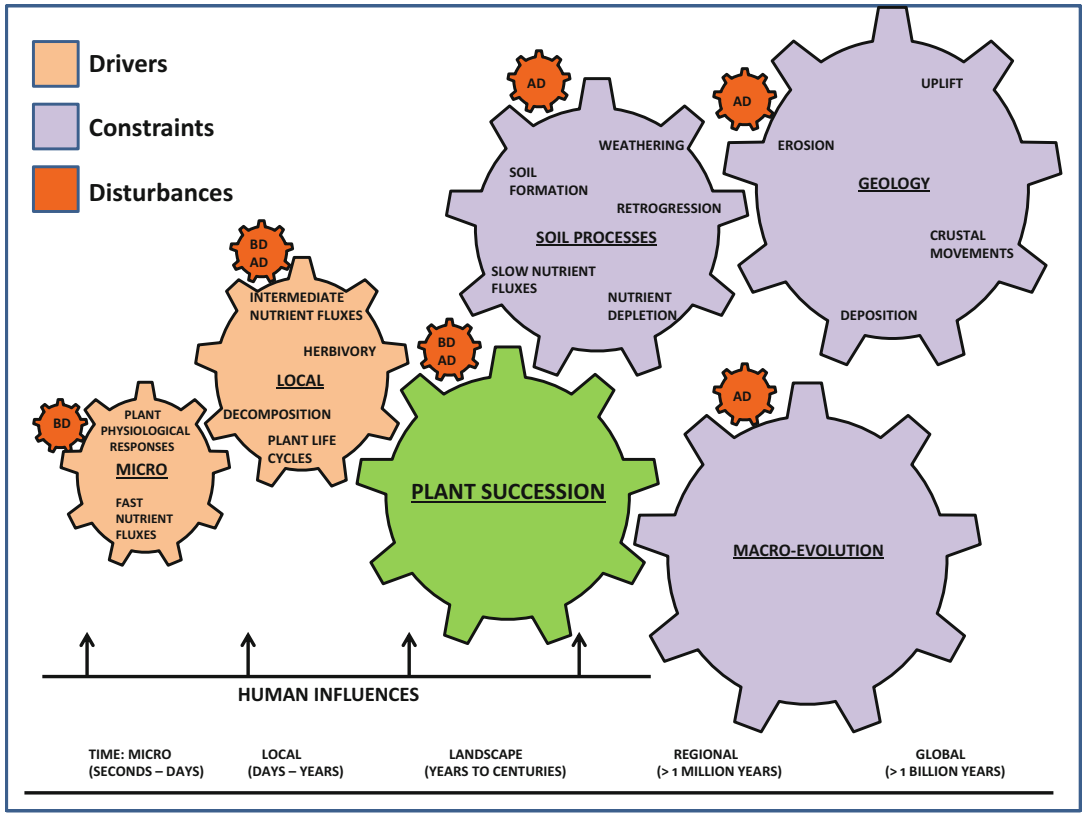

Fig. 16.14 Plant succession as an integrator of ecological processes. Placing plant succession (green) in a broader context can illustrate how succession is driven by shorter-term processes at micro and local scales (beige-colored drivers) and constrained by longer-term ones at regional and global scales (blue-colored constraints). Drivers provide mechanistic explanations and constraints provide boundaries to possible states (*e.g.*, trajectories) of succession; neither implies a directional influence on rates of succession. Spatial terminology is suitable for describing temporal scales because of the strong correlation between spatial and temporal scales. Categories of temporal scales are approximate because of the extensive overlap among ecological processes (*e.g.*, plant life cycles encompass weeks to centuries; soil formation occurs over years to millennia). Biotic (BD) and abiotic (AD) disturbances (dark-brown-colored) alter the influences of these processes on succession. Human influences both drive and constrain succession at many temporal scales (Walker and Wardle 2014); copyright Elsevier Science, Ltd.

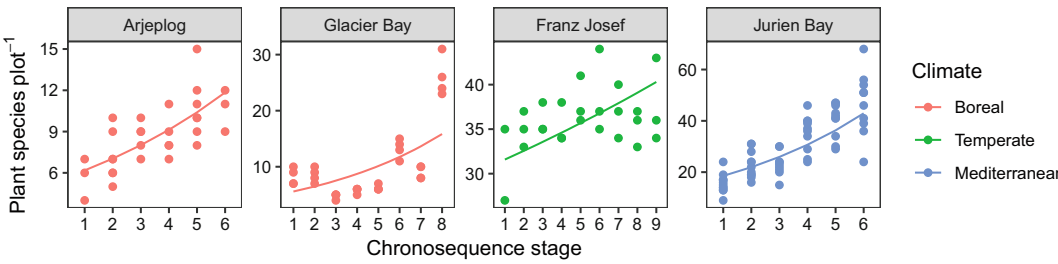

Fig. 16.15 Increases in plant species richness with soil age (represented by the ranked variable 'chronosequence stage') for four representative soil chronosequences from contrasting climates. All of these soil chronosequences include retrogressive stages. Red circles, boreal climate; green circles, temperate climate; blue circles, Mediterranean climate (Laliberté et al. 2013); copyright Elsevier Science, Ltd.

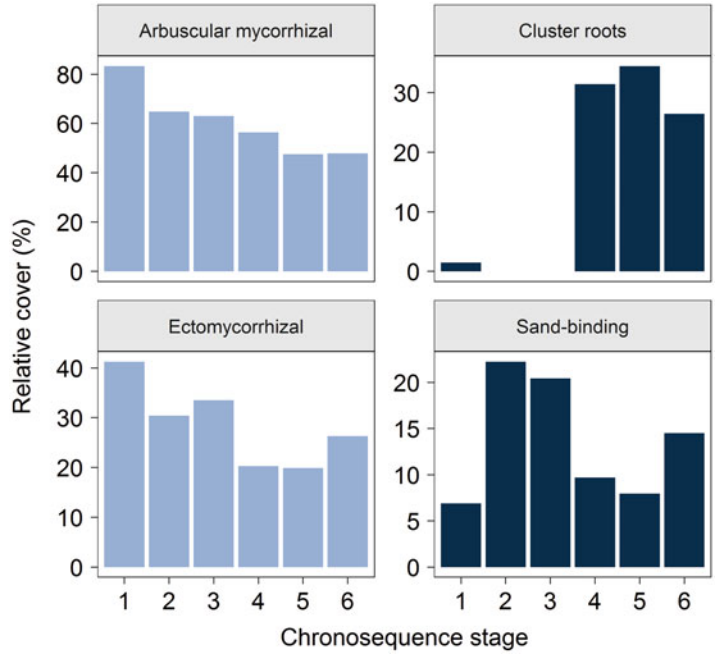

Fig. 16.16 Canopy cover of the four most-abundant plant nutrient-acquisition strategies along the Jurien Bay dune chronosequence. Relative cover declines for arbuscular mycorrhizal and ectomycorrhizal species, but increases for cluster-rooted species. Each of the four most-abundant strategies was treated in isolation from all other strategies; hence, total relative cover can sum to more than 100%. Mycorrhizal strategies are shaded with lighter grey bars, and nonmycorrhizal strategies with darker bars (Zemunik et al. 2015).

boosting the protection against pathogens (Fig. 16.8; Albornoz et al. 2017).

In summary, the changes in ecophysiological traits through long-term ecosystem development are identical to those described earlier in species that function effectively in high- *vs.* low-resource sites, explaining the change in plant performance that causes species replacement through succession.

16.9 What Do We Gain from This Chapter?

There is no single ecophysiological trait that gives a genotype competitive superiority. The outcome of competition may be due to the occurrence of an event, such as flooding, frost, fire, or drought. One genotype may be better able to cope with such a disturbance event, and therefore survive, whereas other genotypes may lose out. Superior traits in one environment (*e.g.*, a low tissue mass density, which is associated with rapid growth when nutrients are plentiful) may be inferior traits in a different environment, when a low tissue density is associated with relatively large losses of nutrients when nutrients are scarce. These trade-offs among suites of physiological traits are critical to understanding patterns of competitive success in different environments.

Competitive advantage may depend on a plant's secondary metabolism (*i.e.* the exudation of allelochemicals that harm other plants, excretion of compounds that solubilize sparingly available nutrients, or detoxify harmful soil components, production of chemicals that chelate metals, or the accumulation of defensive compounds that reduce the effects of herbivore attack and diseases). If plants did not produce such defense compounds, they might be able to grow faster in productive environments. In the longer term, however, such plants may succumb to pests or attack by a pathogenic bacterium, such as *Crataegus monogyna* (hawthorn) in Europe and many *Acacia* species in Australia. When released in a foreign environment, where such pests are absent, some species may become invasive [*e.g.*, *Acacia saligna* (orange wattle) from Australia, which was introduced into South Africa]. Other examples include *Prunus*

padus (bird cherry) from North America which was introduced into Western Europe, and *Salix* species (weeping willow) from Asia and *Rubus corylifolius* (blackberry) from Europe, both of which now invade river valleys in Australia.

A large phenotypic plasticity for various plant traits (*e.g.*, photosynthetic characteristics, nutrient acquisition, and stem elongation) may also contribute to competitive success. In addition, competitive advantage may be based on a profitable association with another organism, such as a symbiotic N_2-fixing microorganism, a mycorrhizal fungus, or a plant that happens to be a suitable host to parasitize.

References

Abrahão A, Ryan MH, Laliberté E, Oliveira RS, Lambers H. 2018. Phosphorus- and nitrogen-acquisition strategies in two *Bossiaea* species (Fabaceae) along retrogressive soil chronosequences in south-western Australia. *Physiol Plant* **163**: 323-343.

Aerts R, Van der Peijl M. 1993. A simple model to explain the dominance of low-productive perennials in nutrient-poor habitats. *Oikos* **66**: 144-147.

Albornoz FE, Burgess TI, Lambers H, Etchells H, Laliberté E. 2017. Native soil-borne pathogens equalise differences in competitive ability between plants of contrasting nutrient-acquisition strategies. *J Ecol* **105**: 549–557.

Arp WJ, Drake BG, Pockman WT, Curtis PS, Whigham DF. 1993. Interactions between C3 and C_4 salt marsh plant species during four years of exposure to elevated atmospheric CO_2. *Vegetatio* **104**: 133-143.

Aschehoug ET, Brooker R, Atwater DZ, Maron JL, Callaway RM. 2016. The mechanisms and consequences of interspecific competition among plants. *Annu Rev Ecol Evol Syst* **47**: 263-281.

Ball MC, Egerton JJG, Leuning R, Cunningham RB, Dunne P. 1997. Microclimate above grass adversely affects spring growth of seedling snow gum (*Eucalyptus pauciflora*). *Plant Cell Environ* **20**: 155-166.

Ballaré CL. 2017. Phytochrome responses: think globally, act locally. *Trends Plant Sci* **22**: 909-911.

Ballaré CL, Gross KL, Monson RK. 2013. Zooming in on plant interactions. *Oecologia* **171**: 601-603.

Ballaré CL, Scopel AL, Jordan ET, Vierstra RD. 1994. Signaling among neighboring plants and the development of size inequalities in plant populations. *Proc Natl Acad Sci USA* **91**: 10094-10098.

Ballaré CL, Scopel AL, Sánchez RA. 1995. Plant photomorphogenesis in canopies, crop growth, and yield. *HortSci* **30**: 1172-1181.

Barkman JJ 1988. New systems of plant growth forms and phenological plant type. In: Werger MJA, Van der Aart PJM, During HJ, Verhoeven JTA eds. *Plant Form and Vegetation Structure Adaptation, Plasticity and Relation to Herbivory*. The Hague: SPB Academic Publishing, 9-44.

Berendse F, Aerts R. 1987. Nitrogen-use-efficiency: a biologically meaningful definition? *Funct Ecol* **1**: 293-296.

Biere A. 1996. Intra-specific variation in relative growth rate: impact on competitive ability and performance of Lychnis flos-cuculi in habitats differing in soil fertility. *Plant Soil* **182**: 313-327.

Boerner REJ, Harris KK. 1991. Effects of collembola (arthropoda) and relative germination date on competition between mycorrhizal *Panicum virgatum* (Poaceae) and non-mycorrhizal *Brassica nigra* (Brassicaceae). *Plant Soil* **136**: 121-129.

Broekaert WF, Van Parijs J, F L, H J, Peumans WJ. 1989. A chitin-binding lectin from stinging nettle rhizomes with antifungal properties. *Science* **245**: 1100-1102.

Brouwer R. 1963. Some aspects of the equilibrium between overground and underground plant parts. *Meded Inst Biol Scheikd Onderz Landbouwgew* **1963**: 31-39.

Butler OM, Elser JJ, Lewis T, Mackey B, Chen C. 2018. The phosphorus-rich signature of fire in the soil–plant system: a global meta-analysis. *Ecol Lett* **21**: 335-344.

Caccianiga M, Luzzaro A, Pierce S, Ceriani RM, Cerabolini B. 2006. The functional basis of a primary succession resolved by CSR classification. *Oikos* **112**: 10-20.

Caldwell MM, Richards JH, Manwaring JH, Eissenstat DM. 1987. Rapid shifts in phosphate acquisition show direct competition between neighbouring plants. *Nature* **327**: 615.

Callaway RM. 1995. Positive interactions among plants. *The Botanical Review* **61**: 306-349.

Callaway RM. 2007. *Positive Interactions and Interdependence in Plant Communities. 1st edn*. Dordrecht: Springer.

Carminati A, Vetterlein D. 2013. Plasticity of rhizosphere hydraulic properties as a key for efficient utilization of scarce resources. *Ann Bot* **112**: 277-290.

Chave J, Coomes D, Jansen S, Lewis SL, Swenson NG, Zanne AE. 2009. Towards a worldwide wood economics spectrum. *Ecol Lett* **12**: 351-366.

Chen C-S, Chen C-Y, Ravinath DM, Bungahot A, Cheng C-P, You R-I. 2018. Functional characterization of chitin-binding lectin from *Solanum integrifolium* containing anti-fungal and insecticidal activities. *BMC Plant Biol* **18**: 3.

Cole DR, Monger HC. 1994. Influence of atmospheric CO_2 on the decline of C_4 plants during the last deglaciation. *Nature* **368**: 533-536.

Cook SM, Khan ZR, Pickett JA. 2007. The use of push-pull strategies in integrated pest management. *Annu Rev Entomol* **52**: 375-400.

Darwin C. 1875. *The Movements and Habits of Climbing Plants. 2d ed.* London: John Murray.

Dayrell RLC, Arruda AJ, Pierce S, Negreiros D, Meyer PB, Lambers H, Silveira FAO. 2018. Ontogenetic shifts in plant ecological strategies. *Funct Ecol* **32**: 2730-2741.

de la Riva EG, Marañón T, Pérez-Ramos IM, Navarro-Fernández CM, Olmo M, Villar R. 2018. Root traits across environmental gradients in Mediterranean woody communities: are they aligned along the root economics spectrum? *Plant Soil* **424**: 35–48.

Díaz S, Kattge J, Cornelissen JHC, Wright IJ, Lavorel S, Dray S, Reu B, Kleyer M, Wirth C, Colin Prentice I, Garnier E, Bönisch G, Westoby M, Poorter H, Reich PB, Moles AT, Dickie J, Gillison AN, Zanne AE, Chave J, Joseph Wright S, Sheremet'ev SN, Jactel H, Baraloto C, Cerabolini B, Pierce S, Shipley B, Kirkup D, Casanoves F, Joswig JS, Günther A, Falczuk V, Rüger N, Mahecha MD, Gorné LD. 2016. The global spectrum of plant form and function. *Nature* **529**: 167–171.

Edwards EJ, McCaffery S, Evans JR. 2005. Phosphorus status determines biomass response to elevated CO_2 in a legume : C_4 grass community. *Glob Change Biol* **11**: 1968-1981.

Egerton FN. 2001. A history of the ecological sciences, Part 2: Aristotle and Theophrastos. *Bull Ecol Soc Amer* **82**: 149-152.

Egler FE. 1954. Vegetation science concepts I. Initial floristic composition, a factor in old-field vegetation development. *Vegetatio* **4**: 412-417.

Eissenstat DM, Caldwell MM. 1987. Characteristics of successful competitors: an evaluation of potential growth rate in two cold desert tussock grasses. *Oecologia* **71**: 167-173.

Eissenstat DM, Caldwell MM. 1988. Competitive ability is linked to rates of water extraction. *Oecologia* **75**: 1-7.

Elhakeem A, Markovic D, Broberg A, Anten NPR, Ninkovic V. 2018. Aboveground mechanical stimuli affect belowground plant-plant communication. *PLoS ONE* **13**: e0195646.

Francis R, Read DJ. 1994. The contributions of mycorrhizal fungi to the determination of plant community structure. *Plant Soil* **159**: 11-25.

Francis R, Read DJ. 1995. Mutualism and antagonism in the mycorrhizal symbiosis, with special reference to impacts on plant community structure. *Can J Bot* **73**: 1301-1309.

Freschet GT, Swart EM, Cornelissen JHC. 2015. Integrated plant phenotypic responses to contrasting above- and below-ground resources: key roles of specific leaf area and root mass fraction. *New Phytol* **206**: 1247-1260.

Galán de Mera A, Hagen MA, Vicente Orellana JA. 1999. Aerophyte, a new life form in Raunkiaer's classification? *J Veg Sci* **10**: 65-68.

Gardner WK, Boundy KA. 1983. The acquisition of phosphorus by *Lupinus albus* L. IV. The effect of interplanting wheat and white lupin on the growth and mineral composition of the two species. *Plant Soil* **70**: 391-402.

Gianoli E. 2015. The behavioural ecology of climbing plants. *AoB PLANTS* **7**: plv013-plv013.

Giuggiola A, Zweifel R, Feichtinger LM, Vollenweider P, Bugmann H, Haeni M, Rigling A. 2018. Competition for water in a xeric forest ecosystem – Effects of understory removal on soil microclimate, growth and physiology of dominant Scots pine trees. *For Ecol Manag* **409**: 241-249.

Gommers CMM, Visser EJW, Onge KRS, Voesenek LACJ, Pierik R. 2013. Shade tolerance: when growing tall is not an option. *Trends Plant Sci* **18**: 65-71.

Grace JB 1990. On the relationship between plant traits and competitive ability. In: Grace JB, Tilman D eds. *Perspectives on Plant Competition*. San Diego: Academic Press, Inc, 51-65.

Grime J, Mackey J, Hillier S, Read D. 1987. Floristic diversity in a model system using experimental microcosms. *Nature* **328**: 420-422.

Grime JP. 1977. Evidence for the existence of three primary strategies in plants and its relevance to ecological and evolutionary theory. *Amer Nat* **111**: 1169-1194.

Grime JP 1994. The role of plasticity in exploiting environmental heterogeneity. In: Caldwell MM, Pearcy RW eds. *Exploitation of Environmental Heterogeneity by Plants: Ecophysiological Processes Above- and Below-ground*. New York: Academic Press, 1-19.

Grime JP. 2006. *Plant Strategies and Vegetation Processes*. Chichester: Wiley.

Hassanali A, Herren H, Khan ZR, Pickett JA, Woodcock CM. 2007. Integrated pest management: the push–pull approach for controlling insect pests and weeds of cereals, and its potential for other agricultural systems including animal husbandry. *Philosophical Transactions of the Royal Society of London B* **363**: 611-621

Hauggaard-Nielsen H, Jensen ES. 2005. Facilitative root interactions in intercrops. *Plant Soil* **274**: 237-250.

Hauggaard-Nielsen H, Jørnsgaard B, Kinane J, Jensen ES. 2008. Grain legume-cereal intercropping: the practical application of diversity, competition and facilitation in arable and organic cropping systems. *Renew Agric Food Syst* **23**: 3-12.

Hayes P, Turner BL, Lambers H, Laliberté E. 2014. Foliar nutrient concentrations and resorption efficiency in plants of contrasting nutrient-acquisition strategies along a 2-million-year dune chronosequence. *J Ecol* **102**: 396-410.

Hetrick BAD, Wilson GWT, Hartnett DC. 1989. Relationship between mycorrhizal dependence and competitive ability of two tallgrass prairie grasses. *Can J Bot* **67**: 2608-2615.

Huang G, Hayes PE, Ryan MH, Pang J, Lambers H. 2017. Peppermint trees shift their phosphorus-acquisition strategy along a strong gradient of plant-available phosphorus by increasing their transpiration. *Oecologia* **185**: 487-400.

Jakobsen I, Hammer E 2015. Nutrient dynamics in arbuscular mycorrhizal networks. In: Horton TR

ed. *Mycorrhizal Networks*: Springer Netherlands, 91-131.

Johnson HB, Polley HW, Mayeux HS. 1993. Increasing CO_2 and plant-plant interactions: effects on natural vegetation. *Vegetatio* **104**: 157-170.

Katsvairo TW, Rich JR, Dunn RA. 2006. Perennial grass rotation: an effective and challenging tactic for nematode management with many other positive effects. *Pest Manage Sci* **62**: 793-796.

Kattge J, Diaz S, Lavorel S, Prentice IC, Leadley P, Bönisch G, Garnier E, Westoby M, Reich PB, Wright IJ, Cornelissen JHC, Violle C, Harrison SP, Van Bodegom PM, Reichstein M, Enquist BJ, Soudzilovskaia NA, Ackerly DD, Anand M, Atkin O, Bahn M, Baker TR, Baldocchi D, Bekker R, Blanco CC, Blonder B, Bond WJ, Bradstock R, Bunker DE, Casanoves F, Cavender-Bares J, Chambers JQ, Chapin FS, Chave J, Coomes D, Cornwell WK, Craine JM, Dobrin BH, Duarte L, Durka W, Elser J, Esser G, Estiarte M, Fagan WF, Fang J, Fernández-Méndez F, Fidelis A, Finegan B, Flores O, Ford H, Frank D, Freschet GT, Fyllas NM, Gallagher RV, Green WA, Gutierrez AG, Hickler T, Higgins SI, Hodgson JG, Jalili A, Jansen S, Joly CA, Kerkhoff AJ, Kirkup D, Kitajima K, Kleyer M, Klotz S, Knops JMH, Kramer K, Kühn I, Kurokawa H, Laughlin D, Lee TD, Leishman M, Lens F, Lenz T, Lewis SL, Lloyd J, Llusiá J, Louault F, Ma S, Mahecha MD, Manning P, Massad T, Medlyn BE, Messier J, Moles AT, Müller SC, Nadrowski K, Naeem S, Niinemets Ü, Nöllert S, Nueske A, Ogaya R, Oleksyn J, Onipchenko V, Onoda Y, Ordoñez J, Overbeck G, Ozinga WA, Patiño S, Paula S, Pausas JG, Peñuelas J, Phillips OL, Pillar V, Poorter H, Poorter L, Poschlod P, Prinzing A, Proulx R, Rammig A, Reinsch Sabine , Reu B, Sack L, Salgado-Negret B, Sardans J, Shiodera S, Shipley B, Siefert A, Sosinski E, Soussana JF, Swaine E, Swenson N, Thompson K, Thornton P, Waldram M, Weiher E, White M, White S, Wright S, Joseph, Yguel B, Zaehle S, Zanne AE, Wirth C. 2011. TRY – a global database of plant traits. *Glob Change Biol* **17**: 2905-2935.

Khan ZR, Hassanali A, Overholt W, Khamis TM, Hooper AM, Pickett JA, Wadhams LJ, Woodcock CM. 2002. Control of witchweed *Striga hermonthica* by intercropping with *Desmodium* spp., and the mechanism defined as allelopathic. *J Chem Ecol* **28**: 1871-1885.

Kigathi RN, Weisser WW, Veit D, Gershenzon J, Unsicker SB. 2013. Plants suppress their emission of volatiles when growing with conspecifics. *J Chem Ecol* **39**: 537-545.

Koffel T, Boudsocq S, Loeuille N, Daufresne T. 2018. Facilitation- vs. competition-driven succession: the key role of resource-ratio. *Ecol Lett* **21**.

Laliberté E, Grace JB, Huston MA, Lambers H, Teste FP, Turner BL, Wardle DA. 2013. How does pedogenesis drive plant diversity? *Trends Ecol Evol* **28**: 331–340.

Laliberté E. 2017. Below-ground frontiers in trait-based plant ecology. *New Phytol* **213**: 1597-1603.

Lambers H, Albornoz F, Kotula L, Laliberté E, Ranathunge K, Teste FP, Zemunik G. 2018. How belowground interactions contribute to the coexistence of mycorrhizal and non-mycorrhizal species in severely phosphorus-impoverished hyperdiverse ecosystems. *Plant Soil* **424**: 11-34.

Lambers H, Bishop JG, Hopper SD, Laliberté E, Zúñiga-Feest A. 2012. Phosphorus-mobilization ecosystem engineering: the roles of cluster roots and carboxylate exudation in young P-limited ecosystems. *Ann Bot* **110**: 329-348.

Lambers H, Hayes PE, Laliberté E, Oliveira RS, Turner BL. 2015. Leaf manganese accumulation and phosphorus-acquisition efficiency. *Trends Plant Sci* **20**: 83-90.

Lambers H, Poorter H. 1992. Inherent variation in growth rate between higher plants: a search for physiological causes and ecological consequences. *Adv Ecol Res* **22**: 187-261.

Lambers H, Raven JA, Shaver GR, Smith SE. 2008. Plant nutrient-acquisition strategies change with soil age. *Trends Ecol Evol* **23**: 95-103.

Li Sp, Cadotte MW, Meiners SJ, Pu Z, Fukami T, Jiang L. 2016. Convergence and divergence in a long-term old-field succession: the importance of spatial scale and species abundance. *Ecol Lett* **19**: 1101-1109.

Li Y, Shipley B. 2017. An experimental test of CSR theory using a globally calibrated ordination method. *PLoS ONE* **12**: e0175404.

Ludwig F, Dawson TE, Prins HHT, Berendse F, De Kroon H. 2004. Below-ground competition between trees and grasses may overwhelm the facilitative effects of hydraulic lift. *Ecol Lett* **7**: 623-631.

Mahall BE, Callaway RM. 1992. Root communication mechanisms and intracommunity distributions of two Mojave Desert shrubs. *Ecology* **73**: 2145-2151.

Maillard A, Diquélou S, Billard V, Laîné P, Garnica M, Prudent M, Garcia-Mina J-M, Yvin J-C, Ourry A. 2015. Leaf mineral nutrient remobilization during leaf senescence and modulation by nutrient deficiency. *Front Plant Sci* **6**: 317.

Matimati I, Verboom GA, Cramer MD. 2014. Nitrogen regulation of transpiration controls mass-flow acquisition of nutrients. *J Exp Bot* **65**: 159-168.

McGill BJ, Enquist BJ, Weiher E, Westoby M. 2006. Rebuilding community ecology from functional traits. *Trends Ecol Evol* **21**: 178-185.

McIntire EJB, Fajardo A. 2014. Facilitation as a ubiquitous driver of biodiversity. *New Phytol* **201**: 403-416.

Milne AA. 1928. *The House at Pooh Corner*. New York: Dutton.

Mitchell PJ, Veneklaas EJ, Lambers H, Burgess SSO. 2008. Leaf water relations during summer water deficit: differential responses in turgor maintenance and

variation in leaf structure among different plant communities in south-western Australia. *Plant Cell Environ* **31**: 1791-1802.

Moles AT, Ackerly DD, Webb CO, Tweddle JC, Dickie JB, Westoby M. 2005. A brief history of seed size. *Science* **307**: 576-580.

Muler AL, Oliveira RS, Lambers H, Veneklaas EJ. 2014. Does cluster-root activity of *Banksia attenuata* (Proteaceae) benefit phosphorus or micronutrient uptake and growth of neighbouring shrubs? *Oecologia* **174**: 23-31.

Newman EI, Eason WR, Eissenstat DM, Ramos MIRF. 1992. Interactions between plants: the role of mycorrhizae. *Mycorrhiza* **1**: 47-53.

Oliveira RS, Galvão HC, de Campos MCR, Eller CB, Pearse SJ, Lambers H. 2015. Mineral nutrition of *campos rupestres* plant species on contrasting nutrient-impoverished soil types. *New Phytol* **205**: 1183-1194.

Osnas JLD, Katabuchi M, Kitajima K, Wright SJ, Reich PB, Van Bael SA, Kraft NJB, Samaniego MJ, Pacala SW, Lichstein JW. 2018. Divergent drivers of leaf trait variation within species, among species, and among functional groups. *Proc Natl Acad Sci USA*.

Owensby CE, Coyne PI, Ham JM, Auen LM, Knapp AK. 1993. Biomass production in a tallgrass prairie ecosystem exposed to ambient and elevated CO_2. *Ecol Appl* **3**: 644-653.

Pickett JA, Rasmussen HB, Woodcock CM, Matthes M, Napier JA. 2003 Plant stress signalling: understanding and exploiting plant-plant interactions. *Biochem Soc Trans* **31**: 123-127.

Pierce S, Brusa G, Vagge I, Cerabolini BEL. 2013. Allocating CSR plant functional types: the use of leaf economics and size traits to classify woody and herbaceous vascular plants. *Funct Ecol* **27**: 1002-1010.

Pierce S, Negreiros D, Cerabolini BEL, Kattge J, Díaz S, Kleyer M, Shipley B, Wright SJ, Soudzilovskaia NA, Onipchenko VG, van Bodegom PM, Frenette-Dussault C, Weiher E, Pinho BX, Cornelissen JHC, Grime JP, Thompson K, Hunt R, Wilson PJ, Buffa G, Nyakunga OC, Reich PB, Caccianiga M, Mangili F, Ceriani RM, Luzzaro A, Brusa G, Siefert A, Barbosa NPU, Chapin Iii FS, Cornwell WK, Fang J, Fernandes GW, Garnier E, Le Stradic S, Peñuelas J, Melo FPL, Slaviero A, Tabarelli M, Tampucci D. 2017. A global method for calculating plant CSR ecological strategies applied across biomes world-wide. *Funct Ecol* **31**: 444-457.

Pierik R, Mommer L, Voesenek LACJ. 2013. Molecular mechanisms of plant competition: neighbour detection and response strategies. *Funct Ecol* **27**: 841-853.

Poorter H, Niinemets Ü, Poorter L, Wright I, J, Villar R. 2009. Causes and consequences of variation in leaf mass per area (LMA): a meta-analysis. *New Phytol* **182**: 565-588.

Prieto I, Armas C, Pugnaire FI. 2012. Water release through plant roots: new insights into its consequences at the plant and ecosystem level. *New Phytol* **193**: 830-841.

Putz FE. 1984. The natural history of lianas on Barro Colorado Island, Panama. *Ecology* **65**: 1713-1724.

Raunkiaer C. 1934. *The Life Forms of Plants and Statistical Geography*. Oxford: Clarendon Press.

Reich PB. 2014. The world-wide 'fast–slow' plant economics spectrum: a traits manifesto. *J Ecol* **102**: 275-301.

Reich PB, Borchert R. 1984. Water stress and tree phenology in a tropical dry forest in the lowlands of Costa Rica. *J Ecol* **72**: 61-74.

Reich PB, Hobbie SE, Lee TD, Pastore MA. 2018. Unexpected reversal of C_3 versus C_4 grass response to elevated CO_2 during a 20-year field experiment. *Science* **360**: 317-320.

Reynolds HL, D'Antonio C. 1996. The ecological significance of plasticity in root weight ratio in response to nitrogen: Opinion. *Plant Soil* **185**: 75-97.

Richards JH, Caldwell MM. 1987. Hydraulic lift: substantial nocturnal water transport between soil layers by *Artemisia tridentata* roots. *Oecologia* **73**: 486-489.

Richardson S, Peltzer D, Allen R, McGlone M, Parfitt R. 2004. Rapid development of phosphorus limitation in temperate rainforest along the Franz Josef soil chronosequence. *Oecologia* **139**: 267-276.

Ryser P. 1996. The importance of tissue density for growth and life span of leaves and roots: a comparison of five ecologically contrasting grasses. *Funct Ecol* **10**: 717-723.

Ryser P, Lambers H. 1995. Root and leaf attributes accounting for the performance of fast- and slow-growing grasses at different nutrient supply. *Plant Soil* **170**: 251-265.

Saatkamp A, Cochrane A, Commander L, Guja Lydia K, Jimenez-Alfaro B, Larson J, Nicotra A, Poschlod P, Silveira FAO, Cross Adam T, Dalziell EL, Dickie J, Erickson TE, Fidelis A, Fuchs A, Golos PJ, Hope M, Lewandrowski W, Merritt DJ, Miller BP, Miller Russell G, Offord CA, Ooi MKJ, Satyanti A, Sommerville KD, Tangney R, Tomlinson S, Turner S, Walck JL. 2019. A research agenda for seed-trait functional ecology. *New Phytol* **221**: 1764-1775.

Schläpfer B, Ryser P. 1996. Leaf and root turnover of three ecologically contrasting grass species in relation to their performance along a productivity gradient. *Oikos* **75**: 398-406.

Shane MW, De Vos M, De Roock S, Cawthray GR, Lambers H. 2003. Effects of external phosphorus supply on internal phosphorus concentration and the initiation, growth and exudation of cluster roots in *Hakea prostrata* R.Br. *Plant Soil* **248**: 209-219.

Simard S, Asay A, Beiler K, Bingham M, Deslippe J, He X, Philip L, Song Y, Teste F 2015. Resource transfer between plants through ectomycorrhizal

fungal networks. In: Horton TR ed. *Mycorrhizal Networks*: Springer Netherlands, 133-176.

Stock WD, Wienand KT, Baker AC. 1995. Impacts of invading N_2-fixing *Acacia* species on patterns of nutrient cycling in two Cape ecosystems: evidence from soil incubation studies and ^{15}N natural abundance values. *Oecologia* **101**: 375-382.

Sun S-J, Meng P, Zhang J-S, Wan X. 2014. Hydraulic lift by *Juglans regia* relates to nutrient status in the intercropped shallow-root crop plant. *Plant Soil* **374**: 629-641.

Tatarko AR, Knops JMH. 2018. Nitrogen addition and ecosystem functioning: both species abundances and traits alter community structure and function. *Ecosphere* **9**: e02087.

Teste FP, Laliberté E, Lambers H, Auer Y, Kramer S, Kandeler E. 2016. Mycorrhizal fungal biomass and scavenging declines in phosphorus-impoverished soils during ecosystem retrogression. *Soil Biol Biochem* **92**: 119-132.

Tilman D. 1988. *Plant Strategies and the Dynamics and Function of Plant Communities*. Princeton: Princeton University Press.

Turcotte MM, Levine JM. 2016. Phenotypic plasticity and species coexistence. *Trends Ecol Evol* **31**: 803-813.

Turner RM, Alcorn SM, Olin G, Booth JA. 1966. The influence of shade, soil, and water on saguaro seedling establishment. *Bot Gaz* **127**: 95-102.

Verboom GA, Stock WD, Cramer MD. 2017. Specialization to extremely low-nutrient soils limits the nutritional adaptability of plant lineages. *Amer Nat* **189**: 684-699.

Vetaas OR. 2002. Realized and potential climate niches: a comparison of four *Rhododendron* tree species. *J Biogeog* **29**: 545-554.

Vierheilig H, Iseli B, Alt M, Raikhel N, Wiemken A, Boller T. 1996. Resistance of *Urtica dioica* to mycorrhizal colonization: a possible involvement of *Urtica dioica* agglutinin. *Plant Soil* **183**: 131-136.

Vitousek PM, Walker LR, Whiteaker LD, Mueller-Dombois D, Matson PA. 1987. Biological invasion by *Myrica faya* alters ecosystem development in Hawaii. *Science* **238**: 802-804.

Wagg C, Veiga R, van der Heijden MA 2015. Facilitation and antagonism in mycorrhizal networks. In: Horton TR ed. *Mycorrhizal Networks*: Springer Netherlands, 203-226.

Walker LR, Wardle DA. 2014. Plant succession as an integrator of contrasting ecological time scales. *Trends Ecol Evol* **29**: 504–510.

Wardle DA, Walker LR, Bardgett RD. 2004. Ecosystem properties and forest decline in contrasting long-term chronosequences. *Science* **305**: 509-513.

Weemstra M, Mommer L, Visser EJW, van Ruijven J, Kuyper TW, Mohren GMJ, Sterck FJ. 2016. Towards a multidimensional root trait framework: a tree root review. *New Phytol* **211**: 1159-1169.

Weiher E, Van der Werf A, Thompson K, Roderick M, Garnier E, Eriksson O. 1999. Challenging Theophrastus: a common core list of plant traits for functional ecology. *J Veg Sci* **10**: 609-620.

Wen Z, Li H, Shen Q, Tang X, Xiong C, Li H, Pang J, Ryan M, Lambers H, Shen J. 2019. Trade-offs among root morphology, exudation and mycorrhizal symbioses for phosphorus-acquisition strategies of 16 crop species. *New Phytol* **in press**.

Westoby M, Falster DS, Moles AT, Vesk PA, Wright IJ. 2002. Plant ecological strategies: some leading dimensions of variation between species. *Annu Rev Ecol Syst* **33**: 125-159.

Westoby M, Wright IJ. 2006. Land-plant ecology on the basis of functional traits. *Trends Ecol Evol* **21**: 261-268.

Wong S, Osmond C. 1991. Elevated atmosphere partial pressure of CO_2 and plant growth. III. Interactions between *Triticum aestivum* (C_3) and *Echinochloa frumentacea* (C_4) during growth in mixed culture under different CO_2, N Nutrition and irradiance treatments, with emphasis on below-ground responses estimated using the ^{13}C value of root biomass. *Funct Plant Biol* **18**: 137-152.

Wood AR, Morris MJ. 2007. Impact of the gall-forming rust fungus *Uromycladium tepperianum* on the invasive tree *Acacia saligna* in South Africa: 15 years of monitoring. *Biol Contr* **41**: 68-77.

Wright AJ, Wardle DA, Callaway R, Gaxiola A. 2017. The overlooked role of facilitation in biodiversity experiments. *Trends Ecol Evol* **32**: 383-390.

Wright IJ, Reich PB, Westoby M, Ackerly DD, Baruch Z, Bongers F, Cavender-Bares J, Chapin T, Cornelissen JHC, Diemer M, Flexas J, Garnier E, Groom PK, Gulias J, Hikosaka K, Lamont BB, Lee T, Lee W, Lusk C, Midgley JJ, Navas M-L, Niinemets Ü, Oleksyn J, Osada N, Poorter H, Poot P, Prior L, Pyankov VI, Roumet C, Thomas SC, Tjoelker MG, Veneklaas EJ, Villar R. 2004. The worldwide leaf economics spectrum. *Nature* **428**: 821-827.

Yang L, Callaway RM, Atwater DZ. 2015. Root contact responses and the positive relationship between intraspecific diversity and ecosystem productivity. *AoB PLANTS* **7**: plv053-plv053.

Zemunik G, Turner BL, Lambers H, Laliberté E. 2015. Diversity of plant nutrient-acquisition strategies increases during long-term ecosystem development. *Nat Plants* **1**: https://doi.org/10.1038/nplants.2015.1050.

Zemunik G, Turner BL, Lambers H, Laliberté E. 2016. Increasing plant species diversity and extreme species turnover accompany declining soil fertility along a long-term chronosequence in a biodiversity hotspot. *J Ecol* **104**: 792-805.

Zhu J, van der Werf W, Anten NPR, Vos J, Evers JB. 2015. The contribution of phenotypic plasticity to complementary light capture in plant mixtures. *New Phytol* **207**: 1213-1222.

Zuo Y, Zhang F. 2008. Effect of peanut mixed cropping with gramineous species on micronutrient concentrations and iron chlorosis of peanut plants grown in a calcareous soil. *Plant Soil* **306**: 23-36.

Zuo Y, Zhang F, Li X, Cao Y. 2000. Studies on the improvement in iron nutrition of peanut by intercropping with maize on a calcareous soil. *Plant Soil* **220**: 13-25.

Biotic Influences: Carnivory

17

17.1 Introduction

Around 75 years before Charles Darwin published his fundamental work on insectivorous plants, Scottish botanist Robert Brown observed that a small pitcher plant was an insect-catcher (Mithöfer 2017). Six years later, Labillardière described and named it as *Cephalotus follicularis*, the Albany pitcher plant, a species in its own genus and family, endemic to a small area in Southwest Australia (Cross et al. 2019).

Since the classic work of Charles and Francis Darwin (Darwin 1875, 1878) on the carnivorous habit of *Drosera rotundifolia* (common sundew), considerable information has accumulated on the significance of captured animal prey in the nutrition of carnivorous plants. **Carnivory** includes the catching and subsequent digestion of the freshly trapped prey. This is a common form of nutrition in the animal kingdom, but is rare in plants, with less than 600 known species from 10 families (Givnish 2014); that comprises only 0.2% of all vascular plant species (Table 17.1). We can find carnivorous plants worldwide, but they are generally restricted to sunny and nutrient-impoverished environments, with phosphorus being the key limiting nutrient. Many authors claim that the habitat of carnivorous plants is moist, but for many *Drosera* (sundew) species in southwestern Australia, where most of the species in this genus occur, the Mediterranean endemic *Drosophyllum lusitanicum* (Droseraceae), and *Philcoxia* species (Plantaginaceae) from Brazil, that is not invariably the case (Scatigna et al. 2017; Fleischmann et al. 2018; Skates et al. 2019). Their distribution pattern suggests that, under nutrient-impoverished sunny conditions, carnivory has a major **benefit** for plant survival. This benefit will be **nutritional** (Ellison and Adamec 2011). The restricted distribution of carnivorous plants, however, also suggests that the **costs** of carnivory exclude carnivores from most habitats. These costs include a reduced **photosynthetic capacity** of carnivorous tissues (Ellison and Farnsworth 2005; Givnish et al. 2018).

17.2 Structures Associated with the Catching of the Prey and Subsequent Withdrawal of Nutrients from the Prey

Carnivorous plants invariably have highly specialized structures (Ellison and Adamec 2018). These include **adhesive hairs** or **emergences** [*e.g.*, in *Pinguicula* (butterwort), *Drosera* (sundew), *Byblis* (rainbow plant) and *Philcoxia*], bladderlike **suction traps** [in *Utricularia* (bladderwort), **'lobster-pot'** or **eel traps** [in *Genlisea* (corkscrew plant)]. There are **snapping traps** [in *Dionaea* (Venus' fly trap) and *Aldrovanda* (waterwheel plant)], **catapult flytraps** [in some Australian *Drosera* (sundew) species], and **pitfalls** [*e.g.*, in *Nepenthes* (pitcher plant), *Sarracenia* (pitcher plant), and *Cephalotus*

H. Lambers, R. S. Oliveira, *Plant Physiological Ecology*, https://doi.org/10.1007/978-3-030-29639-1_17

Table 17.1 Carnivorous plant families and genera with their geographical distribution and trapping mechanisms.

Family	Genus	*N*	Geographical distribution	Trapping mechanism					Movement involved
				Eel trap	Suction trap	Snapping trap	Pitfall pitcher	Adhesive trap	
Nepenthaceae	*Nepenthes*	c. 120	Old World Palaeotropics (but not Africa)				x		
Sarraceniaceae	*Sarracenia*	11	Eastern and northern North America				x		
	Heliamphora	>15	Northern South America				x		
	Darlingtonia	1	Far west of North America				x		
Dioncophyllaceae	*Triphyophyllum*	1	W. Africa					x	
Droseraceae	*Drosera*	c. 250	Cosmopolitan			x		x	x
	Dionaea	1	N. and S, Carolina			x			
	Aldrovanda	1	Central Europe, Asia, N.E. Australia, Africa			x			x
Drosophyllaceae	*Drosophyllum*	1	Western Mediterranean					x	x
Byblidaceae	*Byblis*	7	Australia, New Guinea					x	
Roridulaceae	*Roridula*	2	South Africa					x	
Cephalotaceae	*Cephalotus*	1	Southwest Australia				x		
Lentibulariaceae	*Pinguicula*	46	Cosmopolitan					x	x
	Genlisea	21	Tropical America, Africa, Madagascar	x					
	Utricularia	c. 200	Cosmopolitan		x				x
Plantaginaceae	*Philcoxia*	7	Brazil					x	

Sources: Anderson and Midgley (2002); Chase et al. (2009); Givnish (2014); Scatigna et al. (2017); Fleischmann et al. (2018); information on snapping traps in some *Drosera* species is from Poppinga et al. (2012); Hartmeyer and Hartmeyer (2015)
Note: *N* is the number of species in each genus

(Albany pitcher plant)] (Fig. 17.1 and Table 17.1). The pitfall traps mostly contain water. In *Nepenthes* and *Cephalotus*, the trap secretes the fluid; the other genera collect rainwater. The pitchers are a habitat for protozoa, algae, and numerous small animals (Adlassnig et al. 2011).

Although it is strictly speaking not a carnivorous species, *Capsella bursa-pastoris* (shepherd's purse) has a mucous layer that surrounds the germinating seeds, which has the capacity to catch and digest nematodes, protozoa, and bacteria (Barber 1978). Other **protocarnivorous** species include *Geranium viscosissimum* (sticky purple geranium), and *Potentilla arguta* (glandular cinquefoil), which are common in the Pacific Northwest of the United States. Many 'sticky' plants show proteinase activity on their glandular surfaces, and digest proteins that are trapped on these surfaces. They subsequently absorb and translocate the breakdown products (Spomer 1999). Sticky plants have glands on their shoot surfaces that exude mucilage. This may have evolved as a defense against small arthropod herbivores (Levin 1973) or to avoid desiccation (Voigt and Gorb 2010). The mucilage hinders their movement, trapping them on the surface, where they die. Carnivorous species with adhesive surfaces [*e.g.*, *Drosera* (sundew), *Byblis* (rainbow plant), *Roridula* (fly bush), and *Pinguicula* (butterwort)] probably evolved from glandular or 'sticky' protocarnivores (Chase et al. 2009). Examples of other protocarnivores include tropical bromeliads, *Paepalanthus bromelioides* (Eriocaulaceae) from the Brazilian *campos rupestres* (Nishi et al. 2013) and *Dipsacus* (teasel), which have primitive 'pitfalls' (Christy 1923). Addition of dead dipteran larvae to leaf bases increases the seed set and seed mass:biomass ratio in *Dipsacus fullonum* by 30% (Shaw and Shackleton 2011).

Some carnivorous plants attract their prey by the production of nectar at the edge of the trap (Bauer et al. 2008; Bennett and Ellison 2009). The extrafloral nectar may also contain a range of amino acids, so there are also nitrogen (N) costs (Dress et al. 1997). In addition, the carnivorous plants secrete adhesive substances by special glands. These sticky compounds are either polysaccharide mucilage in Droseraceae, Lentibulariaceae, and their relatives, and terpenoid resins in Roridulaceae (Adlassnig et al. 2010). All carnivorous plants are green and capable of C_3 photosynthesis. Hence, carbon is unlikely to be a major element to be withdrawn from their prey, although it is certainly incorporated. Carnivorous species naturally occur on nutrient-poor, acidic soils, with the exception of *Pinguicula* (butterwort), which grows on a chalky substrate. Most species have a poorly developed root system, and many are nonmycorrhizal (Sect. 12.2.2; Adlassnig et al. 2005). It is generally assumed that carnivory is an adaptation to nutrient-poor soils and that inorganic nutrients are largely derived from the prey. There is a positive effect of supplementary feeding with prey on growth, even when this is done in the plant's natural habitat (Zamora et al. 1997). This growth response to prey addition also occurs at high soil-nutrient levels, suggesting that the roots of carnivorous plants have a very low capacity to acquire nutrients from soil (Karlsson and Pate 1992).

Nitrogen is a major element withdrawn from the prey (Ellison and Gotelli 2001; Millett et al. 2003). Relatively tall, erect, or climbing *Drosera* (sundew) species may derive approximately 50% of all their N from insect feeding, whereas species with a rosette habit derive less N from insects (12 to 32%, depending on site) (Schulze et al. 1991). The focus has been on N, because the availability of a stable isotope allows the feasibility of tracing experiments, but carnivorous plants also derive other elements from their prey. Given the P-impoverished nature of the habitat of most carnivorous plants, **phosphorus** is likely the most important (Tables 17.2 and 17.3; Pate and Dixon 1978; Ellison 2006). For *Nepenthes mirabilis* (pitcher plant), *Cephalotus follicularis* (Albany pitcher plant), and *Darlingtonia californica* (pitcher plant) the maximum fraction of N that is derived from insects is 62, 26, and 76%, respectively (Schulze et al. 1997). When insects are scarce (*e.g.*, in the severely nutrient-impoverished habitat of the tuberous sundew *Drosera erythrorhiza* (red ink sundew) in Western

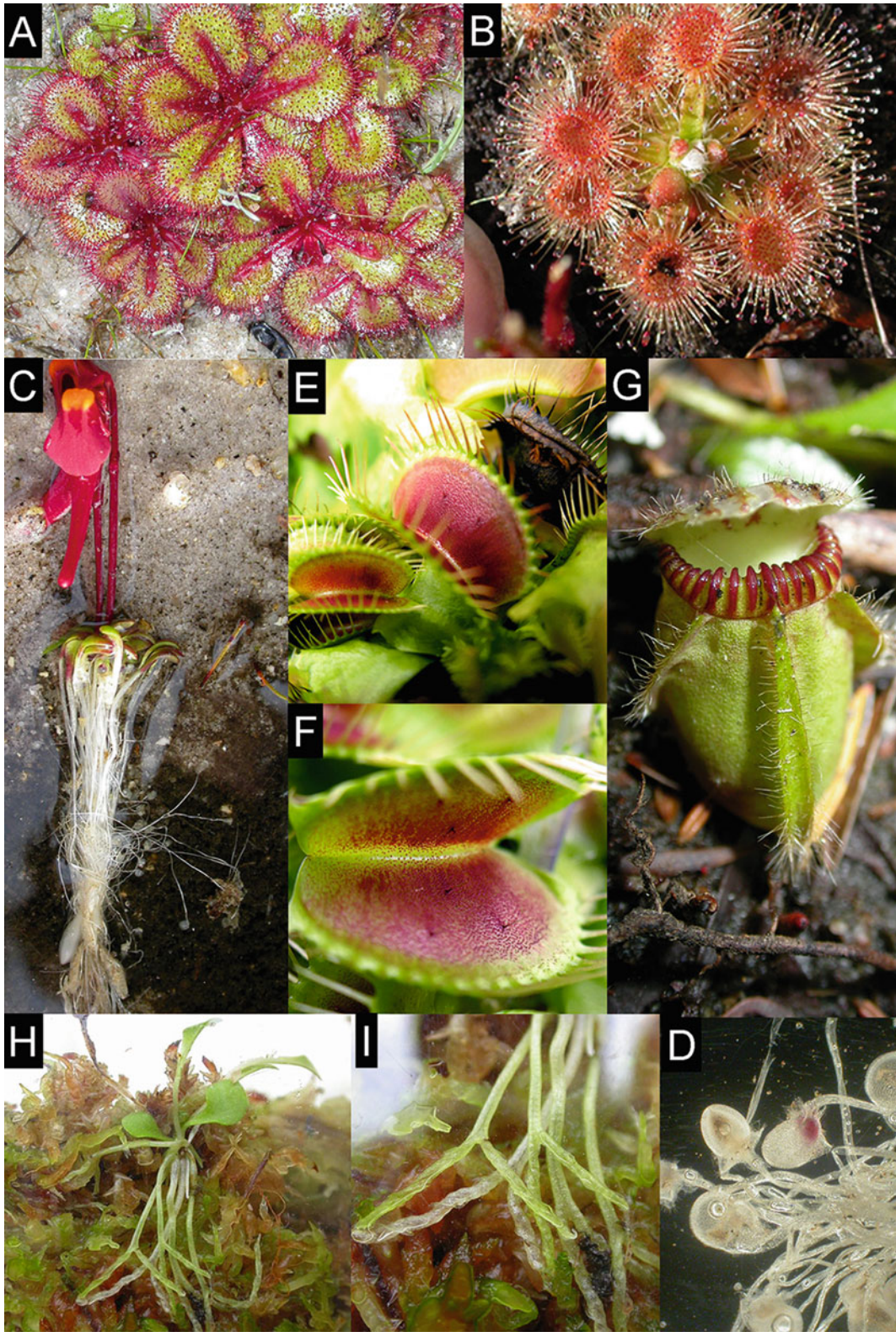

Fig. 17.1 Examples of carnivorous plants with different trapping structures. (**A** and **B**) *Drosera tubaestylus* and *Drosera pulchella* with adhesive hairs. (**C** and **D**) intact plant of *Utricularia menziesii* and detail of the trap of *Utricularia multifida* (bladderwort), with bladderlike suction traps. (**E** and **F**) *Dionaea muscipula* (Venus' flytrap),

Table 17.2 Response to feeding in the natural habitat of a mineral nutrient supplement or insects (16 *Drosophila* flies per plant) to individuals of a natural population of the annual *Drosera glanduligera* (pimpernel sundew).

	No *Drosophila* applied		*Drosophila* applied	
	No mineral nutrients applied	Mineral nutrients applied	No mineral nutrients applied	Mineral nutrients applied
Biomass (mg DM)	4.4	7.1	13.3	11.0
Nitrogen concentration (mmol N g^{-1} DM)	1.1	0.8	1.5	1.3
Total nitrogen content (μmol N $plant^{-1}$)	4.9	5.7	19.9	14.2
Phosphorus concentration (μmol P g^{-1} DM)	26	17	22	33
Total phosphorus content (nmol P $plant^{-1}$)	114	124	299	368

Source: Karlsson and Pate (1992)

Table 17.3 The effect of feeding *Utricularia gibba* (bladderwort) with *Paramecium* on magnesium (Mg) and potassium (K) deficiency.

	Internodes		
	Number	Length	
Media	(% of control)		Number of bladders formed
Complete medium (= control)	100	100	
Complete plus feeding	96	104	
Complete minus mg	38	33	85
Complete minus mg plus feeding	53	42	151
Complete medium (= control)	100	100	66
Complete plus feeding	136	139	86
Complete minus K	72	52	66
Complete minus K plus feeding	100	83	104

Source: Sorenson and Jackson (1968)

Australia), the input of N from the catch of arthropods by the glandular leaves may be very small. Isotopic tracer studies (^{15}N; Sects. 12.2.4 and 12.3.6) show that 76% of all N in the prey is transferred to the plant in *Drosera erythrorhiza*, but this constitutes only 11 to 17% of its total N requirement in its natural environment (Dixon et al. 1980). In this habitat, specialized small beetles that do not stick to the glandular emergences compete with the plant for food by consuming the prey stuck to the leaf hairs. The glandular emergences might therefore function primarily to deter herbivores. The efficiency of insect capture in *Sarracenia purpurea* (northern pitcher plant) (*i.e.* the number of captures per number of visits by potential preys) is also very low: less than 1% (Newell and Nastase 1998). *Nepenthes ampullaria* (tropical pitcher plant) plants growing under forest canopy derive 36% of their foliar N from leaf litter inputs (Moran

Fig. 17.1 (continued) with snapping trap and trigger hairs. (**G**) *Cephalotus follicularis* (Albany pitcher plant), with pitfall. (**H**) *Genlisea violacea* (corkscrew plant) with lobster-pot or eel traps. (**A**: courtesy M.D. Denton, Department of Primary Industries Victoria, Rutherglen, Australia; **B**, **C**, and **G**: photo **H**. Lambers; **D**: courtesy M.C. Brundrett, Western Australian Department of Biodiversity, Conservation and Attractions, Perth, Australia; **E** and **F**, courtesy the late M.W. Shane; **H** and **I**, reproduced with permission from http://www.exoticaplants.com/database/cps/genlisea/page/violacea.htm).

et al. 2003). These examples illustrate the importance of quantitative assessments in determining the actual significance of the carnivorous habit in acquiring nutrients from a prey in a natural habitat.

17.3 Some Case Studies

This section presents some more detailed ecophysiological studies of carnivorous plants.

17.3.1 *Dionaea muscipula*

One of the most fascinating traps is that of *Dionaea muscipula* (Venus' flytrap), which is a species endemic on sandy soils in the central southeastern coastal plain of North America (Fig. 17.1F). The trap consists of two lobes that are attached to a petiole. There are three **'trigger hairs'** on each lobe (Fig. 17.1F). Mechanical stimulation of these hairs leads to rapid closure of the trap. This is one of the fastest movements known in plants and is sufficiently rapid to catch even the most alert insects (Hodick and Sievers 1988, 1989). One of the six hairs inside the trap must be stimulated twice within 20 s; stimulation of two different hairs within the same time frame has the same effect (Fig. 17.2). Touching of one of the hairs leads to an **action potential**, which is propagated over the surface of one of the lobes (Fig. 17.3). At least two action potentials are required to close the trap. **Calcium** in the cell wall is a prerequisite for any action potential to develop (Hedrich and Neher 2018). Inhibitors of the cytochrome path, uncouplers (Sect. 3.2.3.3), and compounds that block Ca channels (*e.g.*, $LaCl_3$) also inhibit the trap's excitability.

Trap closure involves an increased **wall extensibility** of the lower epidermal cells (Table 17.4). Increased extensibility of the lower epidermis, in combination with the **tissue tension** (Sect. 5.4), leads to trap closure. The tissue tension is due to the relatively elastic walls of the mesophyll cells ('swelling tissue), compared with that of the epidermal cells. The presence of the relatively rigid upper and lower epidermal cells prevents the cells in the swelling tissue from reaching full turgor while the trap is open. The changes in extensibility that allow closure of the trap are not due to cell-wall acidification, as is the case when auxin induces similar changes in cell-wall properties (Sect. 10.2.2.2).

Closure of the trap occurs in two steps. The first step is a movement triggered by **mechanical** stimulation. If this is not followed by **chemical** stimulation, the trap gradually opens, due to the growth of the upper epidermis. If a chemical stimulus (in the form of chemical compounds from the hemolymph of the trapped insect) does occur, then the trap closes tightly and special glands begin to secrete **hydrolases** (*e.g.*, proteases, phosphatases, DNAase) and fluid. Trap opening is a much slower process, requiring extension (growth) of the upper epidermis. The opening and closing of the trap can occur only a few times, until both the upper and the lower epidermis have achieved their maximum length.

Snapping traps such as in *Dionaea muscipula* occur in only one other genus: the aquatic *Aldrovanda* (waterwheel plant) (Westermeier et al. 2018). Molecular studies have shown that *Aldrovanda* is sister to *Dionaea*, and that the pair is sister to *Drosera*. Snap-traps are derived from adhesive traps and have a common ancestry among flowering plants (Cameron et al. 2002).

17.3.2 The Suction Traps of *Utricularia*

The genus *Utricularia* (bladderwort), with over two hundred species, is the most widespread of all carnivorous plants (Chase et al., 2009). Many species from this rootless genus are aquatic or hygrophytic plants, occurring in nutrient-poor shallow water or waterlogged soil. Small bladders are produced on the shoots, either in water or in wet soil (Fig. 17.1C, D). A single trap is an ovoid bladder, up to 10 mm in length, with an entrance and a stalk (Fig. 17.4). The ventral part of the trap wall in the entrance forms the **threshold**. The inner surface of the trap is covered by four-armed hairs (quadrifids), which secrete **enzymes** that digest the captured prey. The inner surface of the threshold is covered by two-armed hairs

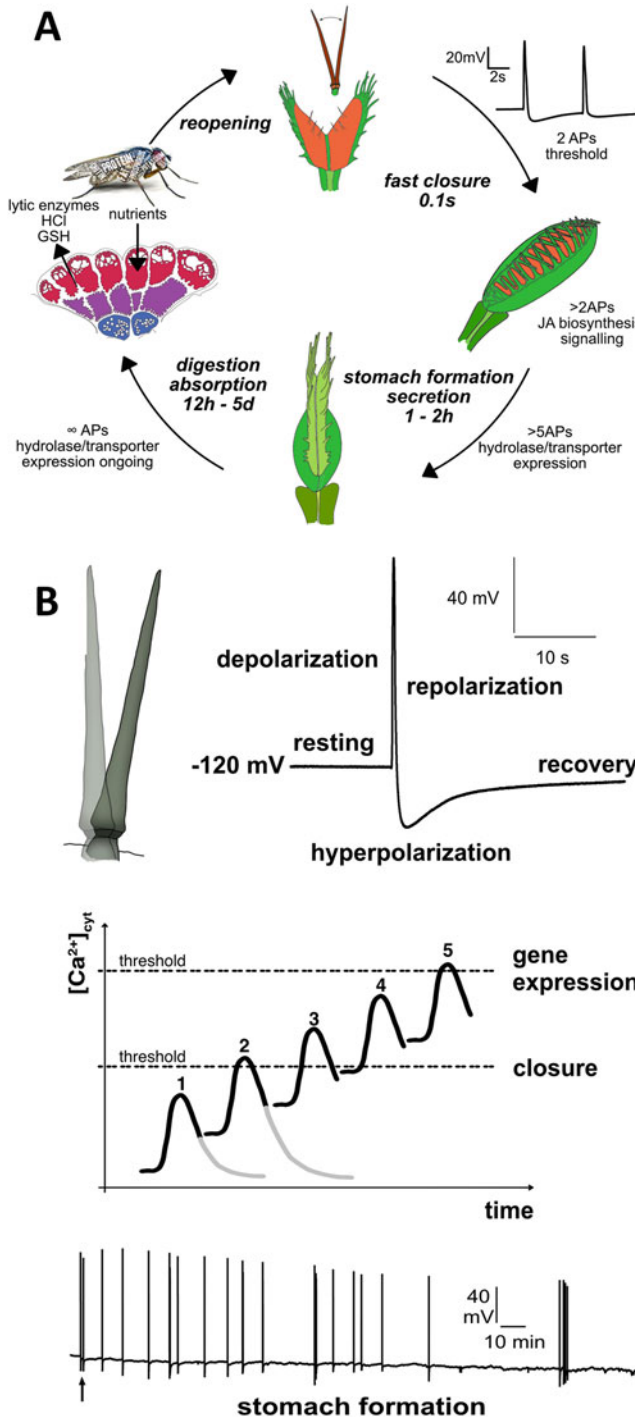

Fig. 17.2 (**A**) The hunting cycle of *Dionaea muscipula*, Venus; flytrap. The first mechano-electric stimulation of the trigger hair by a trap-visiting insect sets the trap in a 'poised to capture' mode. One touch-induced action potential is memorized by the trap but is insufficient for trap closure. A second action potential elicited within a given period (ca <30 s) is required for fast closure and prey capture. When trying to escape, a prey insect repeatedly touches the mechanosensors, thereby eliciting repetitive firing of action potentials. Three or more action potentials

(bifids), which mainly play a role in the movement of water out of the bladder lumen. Both types of hairs consist of a basal cell, a middle cell (which is a **transfer cell**), and terminal secretory cells. In the posterior part of the pavement epithelium there are hairs with terminal cells, whose cuticles ('velum') seal up the trap door. Commonly, there are glandular hairs near the trap entrance; these hairs produce mucilage for prey attraction. Thus the trap contains several types of hairs that are specialized to perform quite different functions (Płachno and Jankun 2004).

In some Utricularia species, small animals (*e.g.*, *Daphnia* species) touch one of the hairs of a trap door, causing the 'door' to snap open inward. In other species, spontaneous firings occur, which explains how phytoplankton and detritus enter traps, even when no prey is present (Adamec 2011; Vincent et al. 2011). The inside of the trap has a lower **hydrostatic pressure** than the outside (Adamec and Poppinga 2016), so water flows in when the trap opens, carrying the prey with it (Fig. 17.4). Then the trap door closes again. The entire process takes 10 to 15 milliseconds. The role of the hairs might be that of a 'lever', but action potentials may also play a role. The low hydrostatic pressure inside the bladder is the result of active transport of chloride (Cl^-) from the lumen of the bladder to the cells that surround it (across membrane A in Fig. 17.5). Sodium (Na^+) follows down an electrochemical potential gradient. Active transport is probably via 'two-armed glands' (Fig. 17.5). Transport of NaCl to the cells that surround the lumen of the bladder causes a gradient in water potential between the lumen and these cells. As a result, water flows from the lumen to these cells causing an increase in turgor which in turn promotes the transport of Na^+, Cl^-, and water out of the cells in the direction of the medium that surrounds the bladder. Suction traps only occur in *Utricularia* species.

Genlisea is sister to *Utricularia*, and the pair is sister to *Pinguicula* (Müller and Borsch 2005). *Genlisea* attracts its prey chemotactically, trapping them in its subterranean leaves (Barthlott et al. 1998; Płachno et al. 2008). *Genlisea* traps lack bifid glands that would be responsible for water pumping as in *Utricularia* traps. There is virtually no water in the traps of *Genlisea* species, showing that the traps are passive (Adamec 2003).

The oxygen concentration inside *Utricularia* and *Genlisea* traps is virtually zero, likely below the critical oxygen concentration for prey survival, and causes captured prey to die of suffocation (Adamec 2007). Under natural conditions, long periods of anoxia inside *Utricularia* traps can be interrupted by short periods of higher oxygen concentration after accidental trap firings. The very rapid respiration rate of internal glands may reduce the oxygen concentration to zero. Digestion of the prey in the bladders of *Utricularia* species requires the secretion of **enzymes**, as in other carnivorous plants (Sirová et al. 2003; Płachno et al. 2006). Apart from

Fig. 17.2 (continued) activate the jasmonic acid signaling pathway, and the capture organ becomes hermetically sealed. Glands covering the inner surface of the stomach start to express genes encoding hydrolase enzymes that decompose the prey into its nutrient building blocks, along with the expression of transporters for the uptake of prey-derived nutrients. In the latter processes, mechano-electric stimulation can be replaced by direct jasmonic acid hormone administration. The more often the trigger hairs are stimulated, action potentials are fired, and touch hormone is synthesized, the longer and greater the activity of the flytrap endocrine system, a process further stimulated by 'prey-derived molecular patterns'. By these means, the number of action potentials informs the plant about the size and nutrient content of the struggling prey. (**B**) A calcium (Ca^{2+}) clock provides a molecular counter. Sensory cells in the hinge region of the trigger hair (top left) convert mechano-sensation into an electrical signal. Trigger hair displacement results in a typical all-or-nothing action potential (top right) together with cytosolic Ca^{2+} transients. This Ca^{2+} clock (middle) provides the molecular basis for 'counting'. Two prey-evoked action potentials (arrow) trigger trap closure, while repetitive action potentials (bottom) drive the Ca^{2+} clock across defined threshold levels to control progression through individual steps of the hunting cycle. Abbreviation: cyt, cytoplasmic (Hedrich and Neher 2018); copyright Elsevier Science, Ltd.

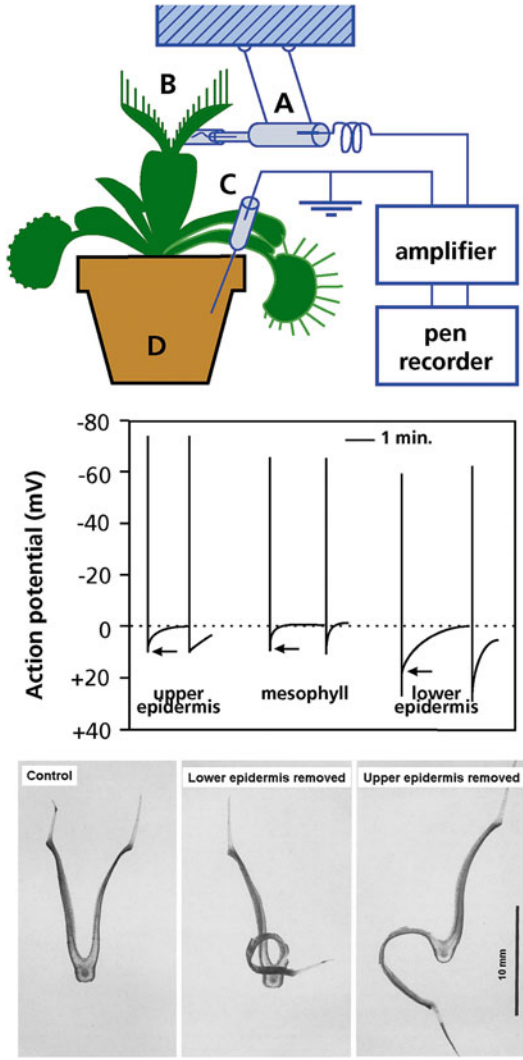

Fig. 17.3 (Top) A scheme of the experimental design to determine action potentials from the surface of *Dionaea muscipula* (Venus' flytrap). One electrode (**A**), suspended by a thread pendulum to maintain electrical contact with the leaf (**B**) during movement. The reference electrode (**C**) is inserted into the substratum and earthed. (Middle) Extracellular recordings of action potentials during trap closure (arrows). Trigger hairs (not shown), the upper and lower epidermis, as well as the mesophyll produce action potentials. (Bottom) Cross section of the Venus' flytrap, left intact. A similar cross section, but with the lower epidermis of the right-hand lobe removed, forcing the lobe to curl inward, illustrating what happens when the cells of the lower epidermis suddenly expand upon triggering of the sensitive hairs, as during trap closure. A similar cross section, but with the upper epidermis of the left-hand lobe removed, forcing the lobe to curl outward, illustrating what happens when the cells of the lower epidermis slowly expand during growth, as during trap re-opening (Hodick and Sievers 1988, 1989); copyright © 1988; 1989 Springer-Verlag.

Table 17.4 The relative extensibilities of the upper and lower sides of the trap of *Dionaea muscipula*, measured as reversible (elastic) and irreversible (plastic) extension, induced by the application of a constant load for 10 min.

	Upper side	Lower side
Trap closed		
Elastic extensibility	3.5	6.9
Plastic extensibility	1.6	11.4
Trap closed and then paralyzed		
Elastic extensibility	n.d.	8.1
Plastic extensibility	n.d.	12.6
Trap open and then paralyzed		
Elastic extensibility	3.5	2.7
Plastic extensibility	1.8	1.8

Source: Hodick and Sievers (1989)
Note: Tissue strips were extended perpendicularly to the midrib (n.d. = not determined). In some of the experiments, the trap was paralyzed with $LaCl_3$, which blocks Ca^{2+} channels and prevents excitability in whole leaves

captured prey, bladders also harbor communities of living algae, zooplankton, and associated debris (Koller-Peroutka et al. 2014; Płachno et al. 2014).

17.3.3 The Tentacles of *Drosera*

The organs of adhesive traps such as those of *Drosera* (sundew, (Fig. 17.1A, B) and *Pinguicula* (butterwort) can also move after mechanical and/or chemical triggering. The tentacles (emergences) on the leaves function in catching and digestion of the prey, so that the tentacles, or even the entire leaf, may surround the prey as a result of their movement. Some of these (faster) movements are triggered by **action potentials** (Williams and Spanswick 1976). Two action potentials within 1 min are required to trigger bending of a tentacle. The slower movements require a chemical stimulus (Williams 1976).

Drosera glanduligera (pimpernel sundew), a sundew from southern Australia (Poppinga et al. 2012), and several pygmy sundews in Southwest Australia (Hartmeyer and Hartmeyer 2015) produce sophisticated **catapult-flypaper traps**. Prey animals walking near the edge of the sundew trigger a touch-sensitive snap-tentacle, which swiftly catapults them onto adjacent sticky glue-

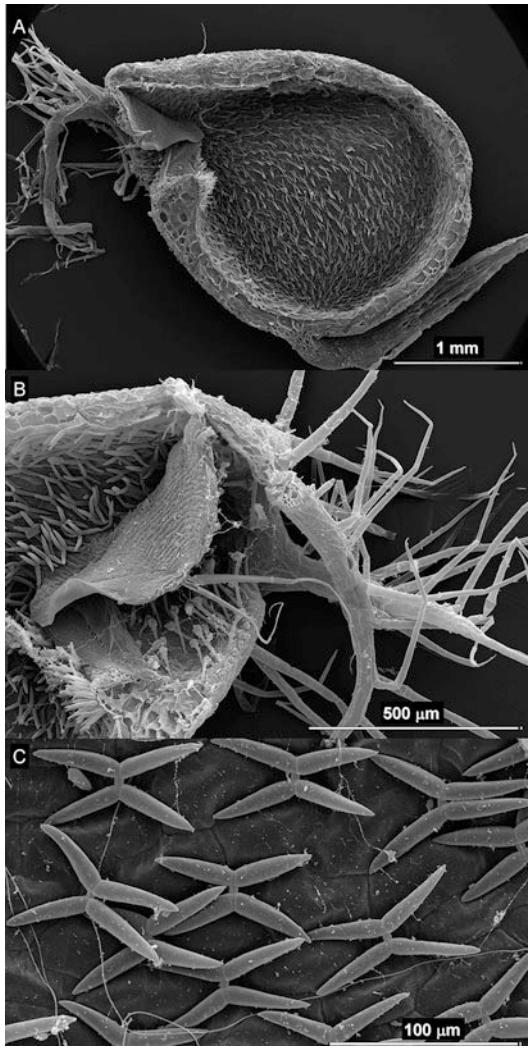

Fig. 17.4 (Top) Median section through a trap of *Utricularia intermedia*, showing antennae above the trap door at the left and numerous quadrifid (four-armed) and bifid (two-armed) hairs inside the lumen of the trap. A stalk attaches the trap to the rest of the plant (Płachno and Jankun 2004); copyright Polish Academy of Science. (Bottom, left) Detail of the trap door showing two sensitive hairs attached to the door, pointing toward the outside solution. Note the bifid hairs attached to the threshold of the door, and the quadrifid hairs at all other locations surrounding the lumen. (Bottom middle) Higher-magnification view of quadrifid hairs. (Bottom right) Higher-magnification view of quadrifid hairs (Courtesy B.J. Płachno, The Jagiellonian University, Cracow, Poland).

tentacles. There, the prey is gradually drawn within the concave trap leaf by sticky tentacles.

Both mechanical stimuli and live prey induce a fast, localized tentacle-bending reaction and enzyme secretion at the place of application in *Drosera capensis* (Cape sundew). By contrast, repeated wounding induce a nonlocalized convulsive tentacle movement and enzyme secretion in local, but also in distant systemic traps. Electrical signals are generated in response to wounding, and these partially mimic a mechanical stimulation of struggling prey and might trigger a false alarm, confirming that carnivory and plant defense mechanisms are related. To trigger the full enzyme activity, the traps must detect chemical stimuli from the captured prey (Krausko et al. 2016)

Digestion of the prey by carnivorous plants requires specific digestive enzymes, including **chitinases**, which hydrolyze the chitin in arthropod skeletons (Matušíková et al. 2005) and **phosphatases**, which release P from nucleic acids and other P-containing compounds (Płachno et al. 2006). Proteins in the pitcher fluid of the carnivorous plant *Nepenthes alata* (winged pitcher plant) probably have two roles in nutrient supply: digestion of prey and antibacterial (Hatano and Hamada 2012).

Species with adhesive or flypaper traps belong to different families (Table 17.1), and some of them are closely related to species with different trapping mechanism, offering clear examples of **divergent evolution** (Albert et al. 1992).

17.3.4 Pitchers of *Nepenthes*

Pitfall traps produced by *Nepenthes* (pitcher plant) species, like those of *Cephalotus follicularis* (Albany pitcher plants), are filled with fluid released by the walls of the pitcher, rather than rainwater (Buch et al. 2013). The traps produce **nectar** secreted from peristome nectaries. The presence of nectar on the peristome increases surface wetness, mainly by its hygroscopic properties, making the surface **slippery** (Bauer et al. 2013). The traps rely on slippery surfaces to capture insects, but *Nepenthes rafflesiana* (Raffles' pitcher plant) also produces fluid in its trap with a very high **viscoelasticity**. Most mountain *Nepenthes* species exhibit digestive fluids, while lowland species produce water-like fluids. Both characteristics contribute to

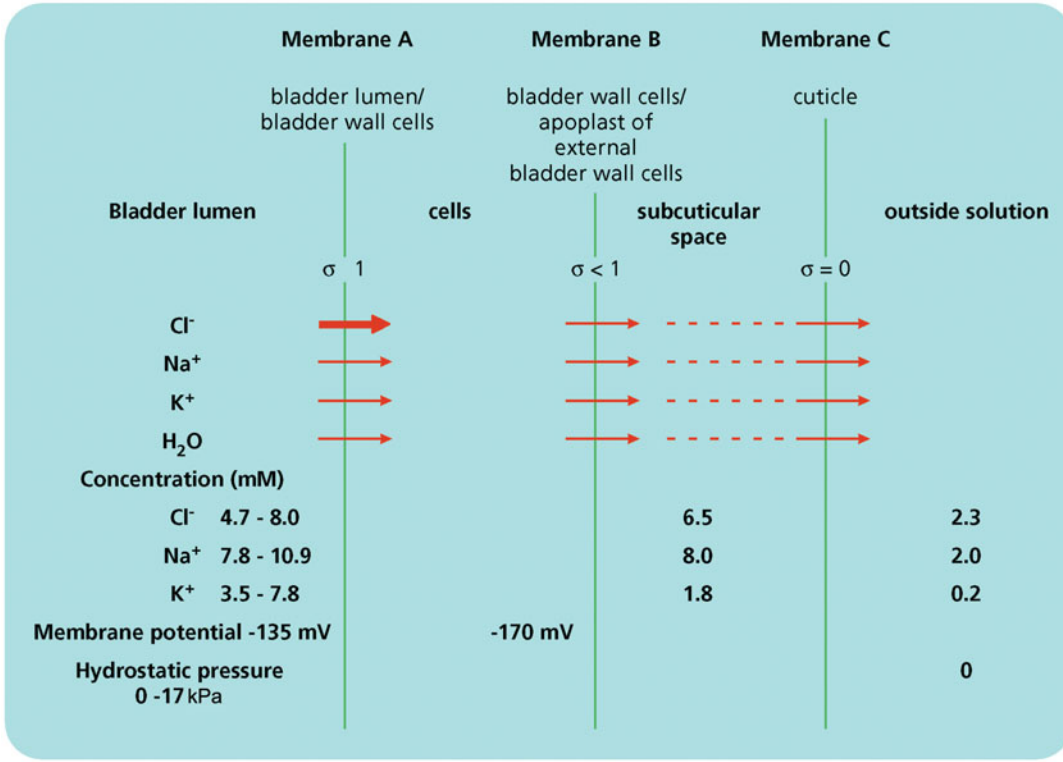

Fig. 17.5 A model of solute and water flow in the resetting of the bladder of *Utricularia* species. Heavy arrow: active transport; thin arrows: passive transport; dotted lines connecting the arrows: bulk flow of solution through the subcuticular space to the outside. The values of ionic concentrations and pressure in the bladder lumen show the range between triggered and reset bladder. The potential difference in the lumen, apart from a very rapid change at the time of triggering, is constant during resetting (After Sydenham and Findlay 1975).

insect trapping, but wax is more efficient at trapping ants, while viscoelasticity is key in trapping other insects, and is even more efficient than wax on flies (Bonhomme et al. 2011). *Nepenthes albomarginata* (picky pitcher plant) in Southeast Asia can catch thousands of termites, which eat a fringe of living white trichomes directly below the peristome. They lure and then trap the prey (Merbach et al. 2002).

The pitcher fluid is unsuitable as an environment for microbial growth, and *Nepenthes* plants effectively avoid and control the microbial colonization of their pitfall traps, and thereby reduce the need to compete with microbes for the prey-derived nutrients (Buch et al. 2013). A proteomic approach shows that the most abundant proteins in the secreted fluid are **proteases**, **nucleases**, **peroxidases**, **chitinases**, a **phosphatase**, and a **glucanase**. Nitrogen recovery involves a particularly rich complement of **proteases** (Lee et al. 2016). Transcription of proteases is strongly induced by ammonium, protein, and live prey; chitin induces transcription only very slightly (Saganová et al. 2018).

Nepenthes bicalcarata grows in Bornean peatswamp forests and has a mutualistic relationship with its **symbiotic ant**, *Camponotus schmitzi*. Plants inhabited by these ants produce more leaves of greater area and N content than unoccupied plants. The ants allow a 200% increase in foliar N to adult plants. Inhabited plants also produced more and larger pitchers containing more prey biomass (Bazile et al. 2012). A few *Nepenthes* species have mutualistic

relationships with mammals. *Nepenthes hemsleyana* gains N from a **bat**, *Kerivoula hardwickii*, while it roosts inside the pitchers. It uses urea from the bats' excrements, following secretion of **ureases**, which are necessary to degrade urea (Yilamujiang et al. 2017).

Nepenthes ampullaria (tropical pitcher plant) is commonly found under closed canopy forest and possesses morphological traits that indicate adaptation to trap leaf litter as a nutrient source. Comparing foliar N stable isotope composition ($\delta^{15}N$) between plants growing under forest canopy and those growing in open areas (no litterfall) in Borneo show foliar $\delta^{15}N$ values are significantly lower and total N concentrations are higher for plants with access to litter. *Nepenthes ampullaria* plants under forest canopy derive 36% of their foliar N from leaf litter inputs (Moran et al. 2003).

Though morphologically and functionally similar, pitcher plant genera belong to three distinctly separate families (Table 17.1). In particular, *Cephalotus follicularis* (Albany pitcher plant, Fig. 17.1G) is phylogenetically very distant. This offers another fascinating example of **convergent evolution** (Albert et al. 1992).

17.3.5 Passive Traps of *Philcoxia*

The recently described genus *Philcoxia* (Plantaginaceae) comprises seven species restricted to well-lit and low-nutrient soils in Southeast Brazilian (Scatigna et al. 2017). The morphological and habitat similarities of *Philcoxia* to those of carnivorous plants discussed in this chapter, along with observations of **nematodes** over its subterranean leaves, led to the suggestion that the genus is carnivorous. A unique capturing strategy of a plant that traps and digests nematodes with **underground adhesive leaves** (Fig. 17.6).

To test N acquisition from prey, nematodes labeled with ^{15}N were fed to to *Philcoxia minensis* (Pereira et al. 2012). Upon feeding, the labeled N is rapidly detectable in leaves: approximately 5% of the prey ^{15}N is in the leaves within 24 h and 15% after 48 h (Fig. 17.6). This conforms *Philcoxia* as a carnivorous genus, the first ever discovered in Plantaginaceae, and the rates of transfer are relatively high compared with those for other carnivorous species. The leaf N and P concentrations of *Philcoxia* are considerably higher than those of neighboring plants.

17.4 The Message to Catch

Carnivory is a rare trait in the plant world, found in only 0.2% of all vascular plant species. It is predominantly associated with nutrient-poor habitats. That is why carnivorous species are relatively common in ancient, severely nutrient-impoverished landscapes of Western Australia, Brazil, South Africa, and the Pantepui Highlands. Another center of diversity is the southeast of the United States, especially on nutrient-poor lateritic or sandy soils. There are **benefits** of the carnivorous habit, in that the prey or faeces provide an extra source of nutrients ('fertilizing effect'). There are also **costs** associated with secreting nectar, mucilage, and enzymes, but these would seem relatively small. The larger costs of the carnivorous habit are probably a reduced photosynthetic capacity, which would exclude carnivorous species from nutrient-rich sites where competition for light is important.

Carnivorous plants with adhesive surfaces probably evolved from protocarnivorous 'sticky' glandular plants. Protocarnivory is much more widespread than carnivory. If we were to engineer glandular crops with protocarnivorous capabilities, these might reduce the need for pesticides and even require a somewhat lower fertilizer input. The various trapping mechanisms of carnivorous plants offer great examples of both **convergent** and **divergent evolution**.

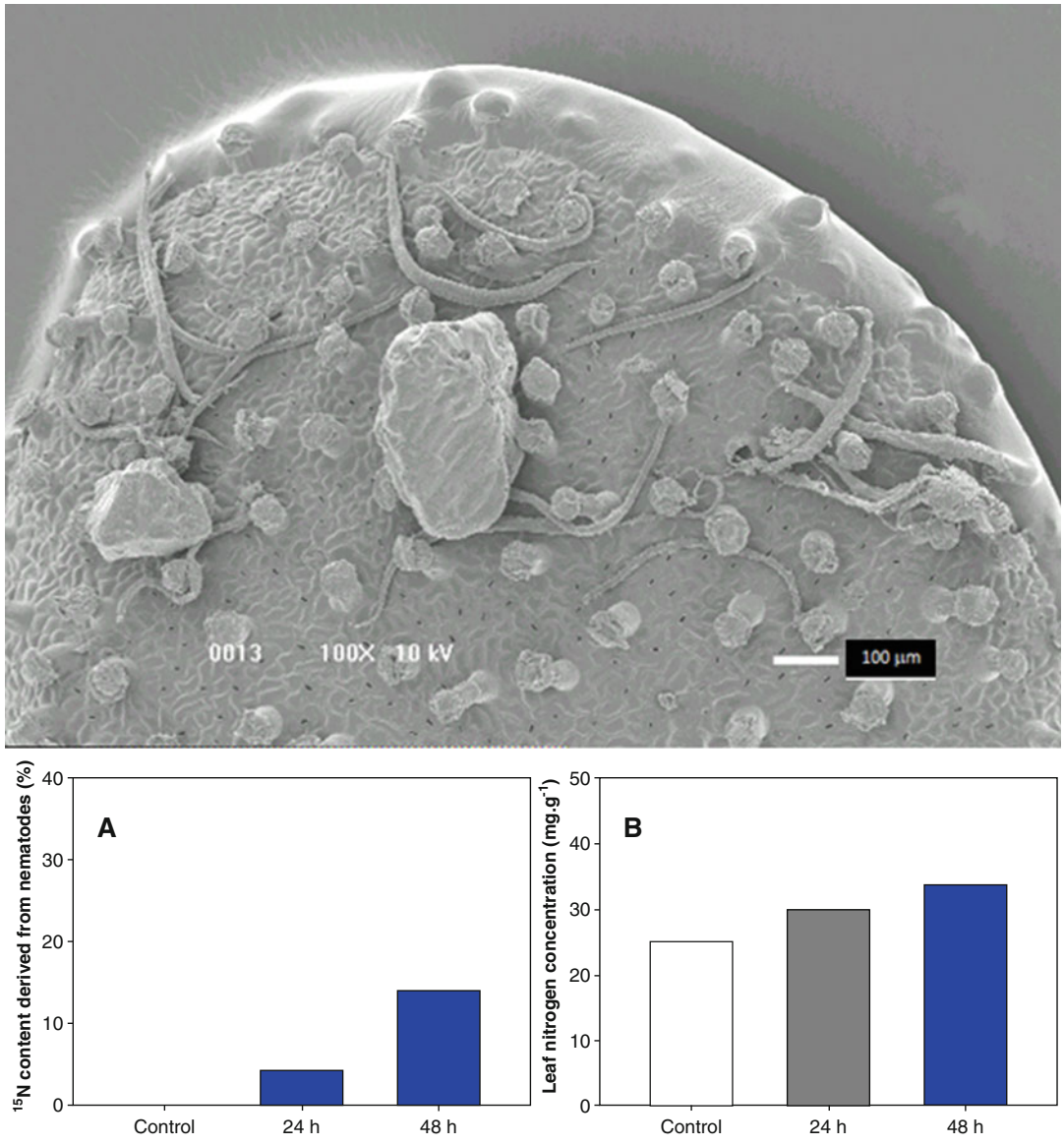

Fig. 17.6 (Top) Scanning electron microscopy image of the upper leaf surface of *Philcoxia minensis*, showing an abundance of nematodes, stalked glands, and adherent sand grains. Arrows point to nematodes and sand grains. (Bottom) Nitrogen (N) absorption in *Philcoxia minensis*. (**A**) ^{15}N absorption shown as mean values with standard error bars. Data show a significant difference in the isotope signature of the plants at 24 h and 48 h after placement of the nematodes onto the leaves compared with the control. (**B**) Average N absorption shown with standard error bars. Data show a tendency of increase at 24 h and a significant increase at 48 h after placement of the nematodes onto the leaves compared with the control. Pereira CG, Almenara DP, Winter CE, Fritsch PW, Lambers H, Oliveira RS. 2012. Underground leaves of *Philcoxia* trap and digest nematodes. *Proc Natl Acad Sci USA* **109**: 1154–1158.

References

Adamec L. 2003. Zero water flows in the carnivorous genus *Genlisea*. *Carniv Plants Newslett* **32**: 46–48.

Adamec L. 2007. Oxygen concentrations inside the traps of the carnivorous plants *Utricularia* and *Genlisea* (Lentibulariaceae). *Ann Bot* **100**: 849–856.

Adamec L. 2011. The comparison of mechanically stimulated and spontaneous firings in traps of aquatic carnivorous Utricularia species. *Aquat Bot* **94**: 44–49.

Adamec L, Poppinga S. 2016. Measurement of the critical negative pressure inside traps of aquatic carnivorous Utricularia species. *Aquat Bot* **133**: 10–16.

Adlassnig W, Lendl T, Peroutka M, Lang I 2010. Deadly glue – adhesive traps of carnivorous plants. In: von Byern J, Grunwald I eds. *Biological Adhesive Systems: From Nature to Technical and Medical Application*. Vienna: Springer Vienna, 15–28.

Adlassnig W, Peroutka M, Lambers H, Lichtscheidl IK. 2005. The roots of carnivorous plants. *Plant Soil* **274**: 127–140.

Adlassnig W, Peroutka M, Lendl T. 2011. Traps of carnivorous pitcher plants as a habitat: composition of the fluid, biodiversity and mutualistic activities. *Ann Bot* **107**: 181–194.

Albert VA, Williams SE, Chase MW. 1992. Carnivorous plants: phylogeny and structural evolution. *Science* **257**: 1491–1495.

Anderson B, Midgley JJ. 2002. It takes two to tango but three is a tangle: mutualists and cheaters on the carnivorous plant *Roridula*. *Oecologia* **132**: 369–373.

Barber JT. 1978. *Capsella bursa-pastoris* seeds. Are they 'carnivorous'? *Carniv Plants Newslett* **7**: 39–42.

Barthlott W, Porembski S, Fischer E, Gemmel B. 1998. First protozoa-trapping plant found. *Nature* **392**: 447–447.

Bauer U, Bohn HF, Federle W. 2008. Harmless nectar source or deadly trap: *Nepenthes* pitchers are activated by rain, condensation and nectar. *Proc R Soc B Biol Sci* **275**: 259–265.

Bauer U, Scharmann M, Skepper J, Federle W. 2013. 'Insect aquaplaning' on a superhydrophilic hairy surface: how *Heliamphora nutans* Benth. pitcher plants capture prey. *Proc R Soc B Biol Sci* **280**: 20122569.

Bazile V, Moran JA, Le Moguédec G, Marshall DJ, Gaume L. 2012. A carnivorous plant fed by its ant symbiont: A unique multi-faceted nutritional mutualism. *PLoS ONE* **7**: e36179.

Bennett KF, Ellison AM. 2009. Nectar, not colour, may lure insects to their death. *Biol Lett* **5**: 2009.0161.

Bonhomme V, Pelloux-Prayer H, Jousselin E, Forterre Y, Labat JJ, Gaume L. 2011. Slippery or sticky? Functional diversity in the trapping strategy of *Nepenthes* carnivorous plants. *New Phytol* **191**: 545–554.

Buch F, Rott M, Rottloff S, Paetz C, Hilke I, Raessler M, Mithöfer A. 2013. Secreted pitfall-trap fluid of carnivorous Nepenthes plants is unsuitable for microbial growth. *Ann Bot* **111**: 375–383.

Cameron KM, Wurdack KJ, Jobson RW. 2002. Molecular evidence for the common origin of snap-traps among carnivorous plants. *Am J Bot* **89**: 1503–1509.

Chase MW, Christenhusz MJM, Sanders D, Fay MF. 2009. Murderous plants: Victorian Gothic, Darwin and modern insights into vegetable carnivory. *Bot J Linn Soc* **161**: 329–356.

Christy M. 1923. The common teasel as a carnivorous plant. *J Bot* **61**: 33–45.

Cross A, Kalfas N, Nunn R, Conran J. 2019. *Cephalotus the Albany Pitcher Plant*. Poole, Dorset, England: Redfern Natural History Productions.

Darwin C. 1875. *Insectivorous Plants*. London: John Murray.

Darwin F. 1878. Experiments on the nutrition of *Drosera rotundifolia*. *J Linn Soc* **17**: 17–31.

Dixon KW, Pate JS, Bailey WJ. 1980. Nitrogen nutrition of the tuberous sundew *Drosera erythrorhiza* Lindl. with special reference to catch of arthropod fauna by its glandular leaves. *Aust J Bot* **28**: 283–297.

Dress WJ, Newell SJ, Nastase AJ, Ford JC. 1997. Analysis of amino acids in nectar from pitchers of *Sarracenia purpurea* (Sarraceniaceae). *Am J Bot* **84**: 1701–1706.

Ellison A, Adamec L, eds. 2018. *Carnivorous Plants: Physiology, Ecology, and Evolution*. Oxford: Oxford University Press.

Ellison AM. 2006. Nutrient limitation and stoichiometry of carnivorous plants. *Plant Biol* **8**: 740–747.

Ellison AM, Adamec L. 2011. Ecophysiological traits of terrestrial and aquatic carnivorous plants: are the costs and benefits the same? *Oikos* **120**: 1721–1731.

Ellison AM, Farnsworth EJ. 2005. The cost of carnivory for *Darlingtonia californica* (Sarraceniaceae): evidence from relationships among leaf traits. *Am J Bot* **92**: 1085–1093.

Ellison AM, Gotelli NJ. 2001. Evolutionary ecology of carnivorous plants. *Trends Ecol Evol* **16**: 623–629.

Fleischmann A, Cross AT, Gibson R, Gonella PM, Dixon KW 2018. Systematics and evolution of Droseraceae. In: Ellison AM, Adamec L eds. *Carnivorous Plants: Physiology, Ecology, and Evolution*. Oxford: Oxford University Press, 45–67.

Givnish TJ. 2014. New evidence on the origin of carnivorous plants. *Proc Natl Acad Sci USA* **112**: 10–11.

Givnish TJ, Sparks KW, Hunter SJ, Pavlovic A 2018. Why are plants carnivorous? Cost/benefit analysis, whole-plant growth, and the context- specific advantages of botanical carnivory. In: Ellison A, Adamec L eds. *Carnivorous Plants: Physiology, Ecology, and Evolution*. Oxford: Oxford University Press, 232–255.

Hartmeyer SRH, Hartmeyer I. 2015. Several pygmy sundew species possess catapult-flypaper traps with repetitive function, indicating a possible evolutionary change into aquatic snap traps similar to *Aldrovanda*. *Carniv Plants Newslett* **44**: 172–184.

Hatano N, Hamada T. 2012. Proteomic analysis of secreted protein induced by a component of prey in pitcher fluid of the carnivorous plant *Nepenthes alata*. *J Proteomics* **75**: 4844–4852.

Hedrich R, Neher E. 2018. Venus flytrap: how an excitable, carnivorous plant works. *Trends Plant Sci* **23**: 220–234.

Hodick D, Sievers A. 1988. The action potential of *Dionaea muscipula* Ellis. *Planta* **174**: 8–18.

Hodick D, Sievers A. 1989. On the mechanism of trap closure of Venus flytrap (*Dionaea muscipula* Ellis). *Planta* **179**: 32–42.

Karlsson PS, Pate JS. 1992. Contrasting effects of supplementary feeding of insects or mineral nutrients on the growth and nitrogen and phosphorous economy of pygmy species of *Drosera*. *Oecologia* **92**: 8–13.

Koller-Peroutka M, Lendl T, Watzka M, Adlassnig W. 2014. Capture of algae promotes growth and propagation in aquatic Utricularia. *Ann Bot* **115**: 227–236.

Krausko M, Perutka Z, Šebela M, Šamajová O, Šamaj J, Novák O, Pavlovič A. 2016. The role of electrical and jasmonate signalling in the recognition of captured prey in the carnivorous sundew plant Drosera capensis. *New Phytol* **213**: 1818–1835.

Lee L, Zhang Y, Ozar B, Sensen CW, Schriemer DC. 2016. Carnivorous nutrition in pitcher plants (*Nepenthes* spp.) via an unusual complement of endogenous enzymes. *J Proteome Res* **15**: 3108–3117.

Levin DA. 1973. The role of trichomes in plant defense. *Q Rev Biol* **48**: 3–15.

Matušíková I, Salaj J, Moravčíková J, Mlynárová L, Nap J-P, Libantová J. 2005. Tentacles of *in vitro*-grown round-leaf sundew (*Drosera rotundifolia* L.) show induction of chitinase activity upon mimicking the presence of prey. *Planta* **222**: 1020–1027.

Merbach MA, Merbach DJ, Maschwitz U, Booth WE, Fiala B, Zizka G. 2002. Mass march of termites into the deadly trap. *Nature* **415**: 36–37.

Millett J, Jones RI, Waldron S. 2003. The contribution of insect prey to the total nitrogen content of sundews (*Drosera* spp.) determined *in situ* by stable isotope analysis. *New Phytol* **158**: 527–534.

Mithöfer A. 2017. Plant carnivory: pitching to the same target. *Nat Plants* **3**: 17003.

Moran JA, Clarke CM, Hawkins BJ. 2003. From carnivore to detritivore? Isotopic evidence for leaf litter utilization by the tropical pitcher plant *Nepenthes ampullaria*. *Int J Plant Sci* **164**: 635–639.

Müller K, Borsch T. 2005. Phylogenetics of *Utricularia* (Lentibulariaceae) and molecular evolution of the trnK intron in a lineage with high substitutional rates. *Plant Syst Evol* **250**: 39–67.

Newell SJ, Nastase AJ. 1998. Efficiency of insect capture by Sarracenia purpurea (Sarraceniaceae), the northern pitcher plant. *Am J Bot* **85**: 88–91.

Nishi AH, Vasconcellos-Neto J, Romero GQ. 2013. The role of multiple partners in a digestive mutualism with a protocarnivorous plant. *Ann Bot* **111**: 143–150.

Pate JS, Dixon KW. 1978. Mineral nutrition of *Drosera erythrorhiza* Lindl. with special reference to its tuberous habit. *Aust J Bot* **26**: 455–464.

Pereira CG, Almenara DP, Winter CE, Fritsch PW, Lambers H, Oliveira RS. 2012. Underground leaves of *Philcoxia* trap and digest nematodes. *Proc Natl Acad Sci USA* **109**: 1154–1158.

Płachno BJ, Adamec L, Lichtscheidl IK, Peroutka M, Adlassnig W, Vrba J. 2006. Fluorescence labelling of phosphatase activity in digestive glands of carnivorous plants. *Plant Biol* **8**: 813–820.

Płachno BJ, Kozieradzka-Kiszkurno M, Swiatek P, Darnowski DW. 2008. Prey attraction in carnivorous *Genlisea* (Lentibulariaceae). *Acta Biol Cracov Ser Bot,* **50**: 87–94.

Płachno BJ, Wołowski K, Fleischmann A, Lowrie A, Łukaszek M. 2014. Algae and prey associated with traps of the Australian carnivorous plant *Utricularia volubilis* (Lentibulariaceae: *Utricularia* subgenus *Polypompholyx*) in natural habitat and in cultivation. *Aust J Bot* **62**: 528–536.

Płachno JB, Jankun A. 2004. Transfer cell wall architecture in secretory hairs of *Utricularia intermedia* traps. *Acta Biol Cracov Ser Bot,* **46**: 193–200.

Poppinga S, Hartmeyer SRH, Seidel R, Masselter T, Hartmeyer I, Speck T. 2012. Catapulting tentacles in a sticky carnivorous plant. *PLoS ONE* **7**: e45735.

Saganová M, Bokor B, Stolárik T, Pavlovič A. 2018. Regulation of enzyme activities in carnivorous pitcher plants of the genus *Nepenthes*. *Planta*.

Scatigna AV, Silva NGd, Alves RJV, Souza VC, Simões AO. 2017. Two new species of the carnivorous genus *Philcoxia* (Plantaginaceae) from the Brazilian cerrado. *Syst Bot* **42**: 351–357.

Schulze ED, Gebauer G, Schulze W, Pate JS. 1991. The utilization of nitrogen from insect capture by different growth forms of *Drosera* from Southwest Australia. *Oecologia* **87**: 240–246.

Schulze W, Schulze ED, Pate JS, Gillison AN. 1997. The nitrogen supply from soils and insects during growth of the pitcher plants *Nepenthes mirabilis*, *Cephalotus follicularis* and *Darlingtonia californica*. *Oecologia* **112**: 464–471.

Shaw PJA, Shackleton K. 2011. Carnivory in the teasel *Dipsacus fullonum* — the effect of experimental feeding on growth and seed set. *PLoS ONE* **6**: e17935.

Sirová D, Adamec L, Vrba J. 2003. Enzymatic activities in traps of four aquatic species of the carnivorous genus *Utricularia*. *New Phytol* **159**: 669–675.

Skates LM, Stevens JC, Paniw M, Ojeda F, Cross AT, Dixon KW, Gebauer G. 2019. An ecological perspective on 'plant carnivory beyond bogs': nutritional benefits of prey capture for the Mediterranean carnivorous plant *Drosophyllum lusitanicum*. *Ann Bot*.

Sorenson DR, Jackson WT. 1968. The utilization of paramecia by the carnivorous plant *Utricularia gibba*. *Planta* **83**: 166–170.

Spomer GG. 1999. Evidence of protocarnivorous capabilities in *Geranium viscosissimum* and *Potentilla arguta* and other sticky plants. *Int J Plant Sci* **160**: 98–101.

Sydenham PH, Findlay GP. 1975. Transport of solutes and water by resetting bladders of *Utricularia*. *Funct Plant Biol* **2**: 335–351.

Vincent O, Weißkopf C, Poppinga S, Masselter T, Speck T, Joyeux M, Quilliet C, Marmottant P. 2011. Ultra-fast underwater suction traps. *Proc R Soc B Biol Sci* **278**: 2909–2914.

Voigt D, Gorb S. 2010. Desiccation resistance of adhesive secretion in the protocarnivorous plant *Roridula gorgonias* as an adaptation to periodically dry environment. *Planta* **232**: 1511–1515.

Westermeier AS, Sachse R, Poppinga S, Vögele P, Adamec L, Speck T, Bischoff M. 2018. How the carnivorous waterwheel plant (*Aldrovanda vesiculosa*) snaps. *Proc R Soc B Biol Sci* **285**.

Williams SE. 1976. Comparative sensory physiology of the Droseraceae-the evolution of a plant sensory system. *Proc Amer Philos Soc* **120**: 187–204.

Williams SE, Spanswick RM. 1976. Propagation of the neuroid action potential of the carnivorous plant *Drosera*. *J Comp Physiol A* **108**: 211–223.

Yilamujiang A, Zhu A, Ligabue-Braun R, Bartram S, Witte C-P, Hedrich R, Hasabe M, Schöner CR, Schöner MG, Kerth G, Carlini CR, Mithöfer A. 2017. Coprophagous features in carnivorous *Nepenthes* plants: a task for ureases. *Sci Rep* **7**: 11647.

Zamora R, Gómez JM, Hódar JA. 1997. Responses of a carnivorous plant to prey and inorganic nutrients in a Mediterranean environment. *Oecologia* **111**: 443–451.

18 Role in Ecosystem and Global Processes: Decomposition

18.1 Introduction

Decomposition of plant litter involves the physical and chemical processes that reduce litter to CO_2, water, and mineral nutrients. It is a key process in the **nutrient cycle** of most terrestrial ecosystems, and the amount of carbon returned to the atmosphere by microbial decomposition of dead organic matter is an important component of the global carbon budget (Sect. 19.2.6; Freschet et al. 2013). In arid and semi-arid ecosystems, litter decomposition is primarily controlled by **photodegradation**, rather than microbial breakdown (Austin and Vivanco 2006). When litter builds up, fire may play a key role in nutrient cycling (Cornelissen et al. 2017).

Eventually, plant material that has not been consumed by herbivores or pathogens, or lost through a fire, is decomposed. Only a small proportion of recalcitrant organic matter and products of microbial decomposition become stabilized for thousands of years as **humus**. Most root-released material (exudates and other root-derived organic matter) is incorporated in the soil microbial biomass or lost as CO_2 within weeks, at least when there are sufficient inorganic nutrients and moisture. When nutrients limit growth, soil microorganisms utilize the root-derived material more slowly, because microbial growth is limited by nutrients, rather than by carbon (Schimel and Schaeffer 2012). In wet, anoxic environments, some of the plant litter may end up as peat, or even coal. In that case, carbon is temporarily removed from the global carbon cycle. The rate of **carbon sequestration** in peatlands is mainly determined by slow rates of decomposition of dead organic matter, rather than fast rates of primary production. Due to the relatively large peat cover on Earth, changes in the extent to which peatlands act as a CO_2-sink will affect the global carbon budget (Gorham 1991).

Nitrogen (N) and phosphorus (P) are released enzymatically during decomposition. Proteins and other N-containing polymers are broken down to monomers (amino acids, nucleotides) that can be absorbed by plants or soil microorganisms (Sect. 9.2.1.3). Under low-N conditions, plants and microorganisms (including mycorrhizal fungi) compete for this organic N. As N availability increases, this competition becomes less intense, and soil microorganisms become more energy-limited. Under these circumstances, they break down amino acids to meet their energy demands and convert N to inorganic forms (NH_4^+ and NO_3^-), which are excreted and can be absorbed by other microbes or plants (**N mineralization**) (Schimel and Bennett 2004). **Phosphorus mineralization** differs from that of N in that Pi is cleaved from P-containing polymers by plant or microbial **phosphatases** without breakdown of the associated carbon skeleton (Sect. 9.2.1.2).

H. Lambers, R. S. Oliveira, *Plant Physiological Ecology*, https://doi.org/10.1007/978-3-030-29639-1_18

18.2 Litter Quality and Decomposition Rate

18.2.1 Species Effects on Litter Quality: Links with Ecological Strategy

In a comparison of 125 British vascular plant species, which cover a wide range of life-forms, leaf habits, and taxa, the rate of leaf litter decomposition can be predicted from a small number of whole-plant traits (Fig. 18.1; Cornelissen et al. 1999). These traits include life form, deciduous *vs.* evergreen habit, leaf toughness, autumn coloration of the leaf litter, family, and a species' success in disturbed and productive habitats. In this wide comparison of species from the British Isles, there is a negative relationship between decomposition rate and **leaf life span**. For example, leaves of woody climbers and ramblers, which tend to have short-lived leaves with little investment in quantitative defense compounds, decompose readily. Leaves of subshrubs, which often inhabit infertile habitats and invest more in chemicals that reduce leaf digestibility and palatability, such as lignin and tannins decompose more slowly (Sect. 13.3.2) (Cornwell et al. 2008).

Across species and plant functional types, the **specific leaf area** (SLA) tends to correlate positively with the rate of leaf litter decomposition (Garnier et al. 2004; Reich 2014). Long-lived leaves, with relatively large investments in quantitatively important chemical defense, tend to have a lower SLA (Wright et al. 2005). This accounts for the positive correlation between rate of litter decomposition and SLA. Deviations from this relationship may be due to variation in other leaf traits that do not influence SLA much, but do have after-life effects on litter decomposition. Such traits include, for instance, cuticle structure, mobile secondary (defense) chemistry, and tissue pH (Cornelissen et al. 2006; Bradford et al. 2016). The association between autumn colors and decomposition is also a reflection of the leaf's secondary chemistry (Fig. 18.1; Cornelissen 1996). Brown colors are associated with phenolics, which slow down the rate of decomposition, in a manner similar to their effects on protein digestion (Sect. 13.3.2).

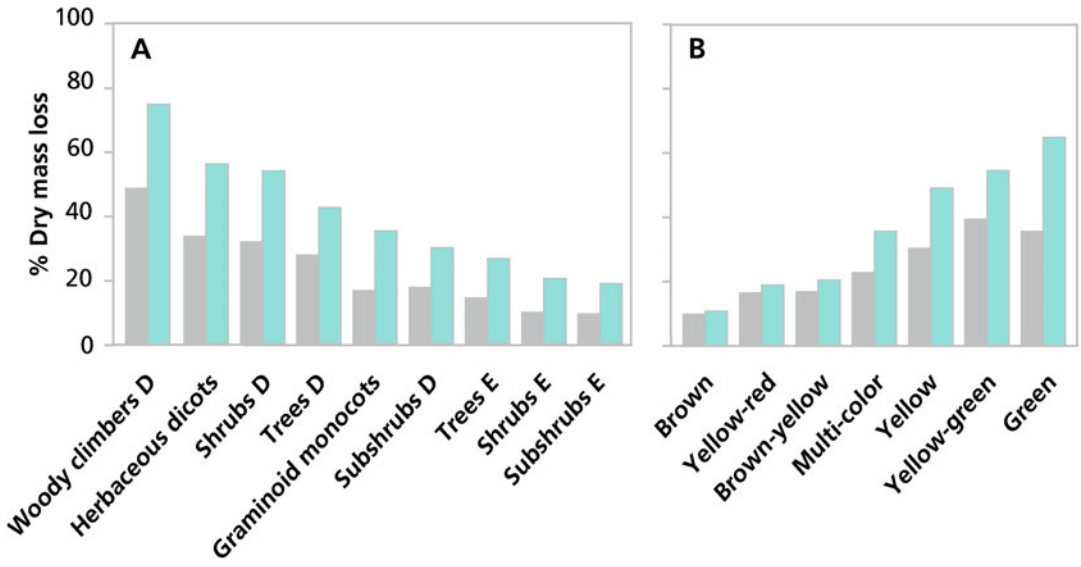

Fig. 18.1 Mass loss (% of original mass) of litter of 125 British species as related to (**A**) growth form and duration of decomposition period (8 weeks, grey bars; 20 weeks, blue bars) or (**B**) initial litter color (for deciduous woody species only) and mesh size of the bag that contained the litter (0.3 mm mesh, grey bars; 5 mm mesh, blue bars). D = deciduous; E = evergreen. Litter was buried in leaf mould near Sheffield, England. Means were calculated from mean values of individual species; based on information in Cornelissen (1996).

Litter turnover is also closely associated with mycorrhizal type. Species with **ericoid mycorrhizas** typically have low litter decomposability, compared with **ectomycorrhizal species**, whereas **arbuscular-mycorrhizal** plant show comparatively fast litter decomposition. Within a representative subset of a flora, ericoid and ectomycorrhizal strategies are linked with slow, and arbuscular-mycorrhizal species with fast ecosystem turnover (Cornelissen et al. 2001). Similarly, mycorrhizal type is closely associated with leaf traits linked to **flammability** measures, including SLA, leaf moisture content, and leaf chemistry (Powell et al. 2017). As discussed in Sect. 12.2.2, different mycorrhizal strategies dominate in contrasting habitats that differ in nutrient availability (Lambers et al. 2008). Slow decomposition and flammability are associated with slow growth and nutrient-conserving strategies, whereas we can expect fast decomposition and low flammability at the opposite resource-acquisitive end of the leaf economic spectrum (Wright et al. 2004).

To explain the biochemical basis of variation in leaf litter decomposition, we need information about **leaf chemistry**. High lignin concentrations reduce **microbial decomposition**, but increase **photodegradation** (Austin and Ballaré 2010). The lignin concentration in cellulose-lignin substrates consistently decrease in photodegradative incubations. Lignin clearly has a dual role affecting litter decomposition, depending on the dominant driver (biotic or abiotic) controlling carbon turnover. Under photodegradative conditions, light preferentially degrades lignin, because lignin acts as an effective light-absorbing compound over a wide range of wavelengths. Foliar concentrations of calcium (Ca) and magnesium (Mg) play an important role determining decomposition rates in broad comparisons, from forest floors and streams in the tropics to subarctic (García-Palacios et al. 2016). In addition to Ca and Mg, N, P, and potassium (K) are important predictors of decomposition rates in tropical forests, but each of these factors explains a very small amount of variance when considered in isolation (Waring 2012). Here, temperature and precipitation are relatively unimportant in regulating decomposition rates, except in montane forests where cool temperatures slow decay (Fig. 18.2; Bradford et al. 2016).

Tannins make up a significant portion of forest carbon pools, and foliage and bark may contain up to 40% tannin. Tannins function as herbivore deterrents (Sect. 13.3.2), but also play an important role in plant–litter–soil interactions. Tannins comprise a complex class of organic compounds whose concentration and chemistry differ greatly, both among and within plant species. They affect nutrient cycling by hindering decomposition rates, complexing proteins, inducing toxicity to microbial populations, and inhibiting enzyme activities (Kraus et al. 2003). As a result, tannins may reduce nutrient losses in infertile ecosystems and may alter N cycling to enhance the level of organic versus mineral N forms.

Species differences in **allocation** strongly influence decomposition, because of the strikingly different chemistry of leaves, wood, and roots. Stems and roots, with their high lignin and low N and P concentration, decompose more slowly than do leaves. Species differences in litter quality due to differences in allocation to wood *vs.* leaves often exceed differences due to variation in leaf quality (Hobbie 2015). Woody stems of slow-growing, late-successional species, with their higher concentrations of quantitative defenses, tend to decompose more slowly than do less dense woody stems of fast-growing species (Eaton and Lawrence 2006). Higher leaf N concentrations are associated with faster decomposition rate (Jo et al. 2016). However, litter chemical quality has a stronger effect on decomposer activity than tissue density and structure.

We know less about species differences in **root decomposition**, despite the large proportion of litter production that occurs below ground. Grasslands, which have more fine root biomass and root turnover compared with forests, also have faster rates of root decomposition (Solly et al. 2014). At a regional scale, fine root decomposition is influenced by environmental variables such as soil moisture, soil temperature and soil nutrient content. Root litter quality explains

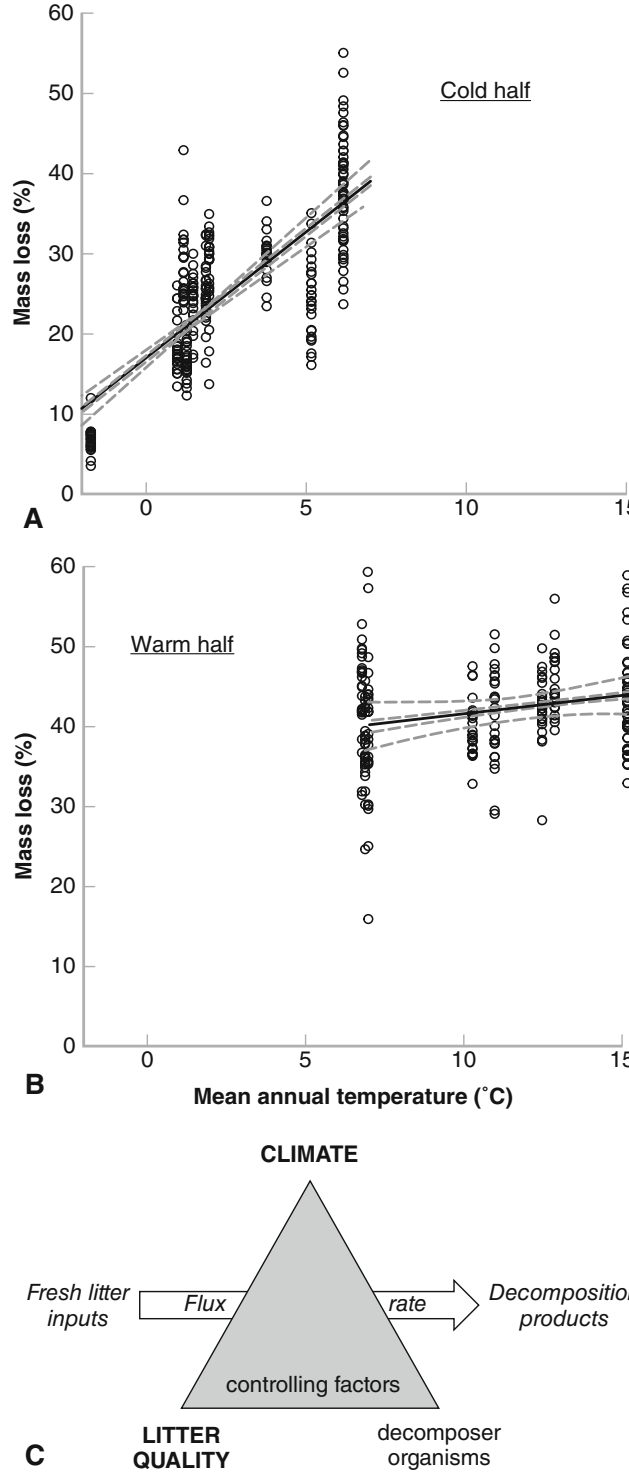

Fig. 18.2 Decomposition rates of *Pinus sylvestris* (Scots pine) needle litter, with the sites divided into colder (**A**) and warmer (**B**) locations. Climate explains more than half of the variation among cold sites, but has little explanatory power among warm sites. Black lines are the mean slope estimate and grey boundary lines the 95% confidence intervals. (**C**) The decomposition triangle is the conceptualization of the dominant factors regulating litter decomposition rates. Swift et al. (1979) separated physico-chemical controls into climatic and edaphic factors, emphasizing climate. Litter quality is instead the dominant control at broad spatial scales. The activities of decomposer organisms are regulated by climate and litter quality, and so do not exert independent control on decomposition rates. As such, the decomposer organisms appear in small grey font to emphasize that climate and litter quality are considered the dominant factors regulating the rate at which organic matter decomposes (Bradford et al. 2016); copyright © 2015, John Wiley and Sons.

additional variation. Decomposition rates of roots and leaf litter may vary greatly, due to the higher chemical recalcitrance of roots (Ma et al. 2016). Therefore, we need to consider roots and leaf litter separately when evaluating their role in plant–soil feedback.

18.2.2 Environmental Effects on Decomposition

Environment affects decomposition, both because of its effect on the quality of litter produced and its direct effects on microbial activity (Fig. 18.2). The direct effects of environment on microbial activity are strongest at low temperatures, and play a minor role at higher temperatures (Fig. 18.2). In anaerobic soils (*e.g.*, in peatlands), decomposition is more restricted than is plant production which results in substantial **carbon sequestration** (Sect. 18.1).

Microbial respiration associated with the decomposition of surface litter is often enhanced at night, because dew provides moisture for microbial activity, and decreases during the day as the litter dries out (Edwards and Sollins 1973). In dry environments, the moister conditions beneath vegetation may favor decomposition. In particularly sunny and dry environments, **photodegradation** are an important process for litter breakdown, dominating over microbial decay (Austin and Vivanco 2006).

Environment also affects tissue chemistry, and therefore litter quality. The higher tissue N and P concentrations in plants on fertile soils result in high litter nutrient concentrations (Table 9.19), and therefore fast rates of decomposition. Among woody plants, growth in infertile soils also increases **quantitative defenses**, further contributing to the slow decomposition of litter produced on these soils (Sect. 13.4.1). Reciprocal transplants of litter among forests that differ strongly in litter quality and environment often show that litter quality exerts a stronger effect on decomposition than do differences in temperature or moisture (Fig. 18.2).

18.3 The Link Between Decomposition Rate and Nutrient Supply

18.3.1 The Process of Nutrient Release

A major reason for interest in decomposition is its close link to **nutrient supply**. In most ecosystems the nutrients released during decomposition provide >90% of the N and P supply to plants (Table 9.1). Across herbaceous species in Britain, the best predictor of leaf litter decomposition rate is green-leaf total concentration of Ca, Mg, and K (Cornelissen and Thompson 1997). The relatively high litter pH associated with a high Ca concentration may favor microbial decomposition.

Phosphorus is partly ester-bonded to carbon skeletons in plant litter. However, its release is only indirectly linked to decomposition, because the ester bond is readily cleaved by **phosphatases**, without breakdown of the associated carbon skeleton. Phosphatases are produced by plant roots, ectomycorrhizal and ericoid **mycorrhizal fungi**, and **saprophytic microorganisms** (*i.e.* those microorganisms whose energy supply is derived from dead organic matter). Decomposition is indirectly linked to P release, because decomposition rate determines microbial demand for P, and therefore the rate of production of microbial phosphatases. In addition, decomposition of cell walls by fungi increases access of microbial phosphatases to P-containing compounds in plant litter.

Nitrogen is the nutrient whose release from plant litter is most tightly linked to decomposition, because, like decomposition, it requires the breakdown of organic compounds in plant litter. In many biomes, the first steps in decomposition are consumption by invertebrate **fauna** that reduce the size of litter particles. This step is important for **cuticle** damage, allowing access of microbes to the tissues and leaching of mobile **phenols** once membranes are ruptured (Swift et al. 1979). Subsequent N release involves the breakdown of **particulate organic N** (PON; polymers such as proteins and nucleic acids) to

dissolved organic N (DON), *i.e.* compounds that are small enough (*e.g.*, amino acids and nucleotides) to be absorbed by microbial cells (Fig. 18.3). DON production is catalyzed by microbial **exoenzymes** (enzymes that are secreted by microbial cells into the soil matrix) and is typically the rate-limiting step in N release from plant litter (Schimel and Schaeffer 2012). Both mycorrhizas (especially ectomycorrhizas) and saprophytes produce exoenzymes that convert PON to DON. DON can then be absorbed by saprophytes, plant roots, and their mycorrhizal partners. Under strongly N-limiting conditions (*e.g.*, tundra and peatlands), microbial growth is extremely N-limited, so all DON absorbed by microorganisms supports microbial growth, and negligible N mineralization occurs; under these circumstances, DON is the predominant form of N absorbed by all soil organisms, including plants (Schimel and Bennett 2004). In less N-limited environments (*e.g.*, conifer forests), some N mineralization occurs in N-rich microsites, where microbes are energy limited and use DON as an energy source, excreting NH_4^+ as a waste product (**N mineralization**), which diffuses into the bulk soil from these N-rich microsites. In these environments, plants and other microorganisms absorb both DON and NH_4^+ to meet their N demands. In extremely fertile soils, most soil microsites are N-rich, so breakdown of DON to NH_4^+ occurs abundantly and meets microbial energy demands. Some of this NH_4^+ is absorbed by nitrifying bacteria that use NH_4^+ as an energy source, and excrete NO_3^- as a waste product (**nitrification**). In summary, across a soil fertility gradient (which often correlates with a gradient in soil pH), the relative availability of N utilized by plants ranges from predominantly DON in infertile, often acidic soils to NH_4^+ in soils of intermediate fertility, to predominantly NO_3^- in fertile soils.

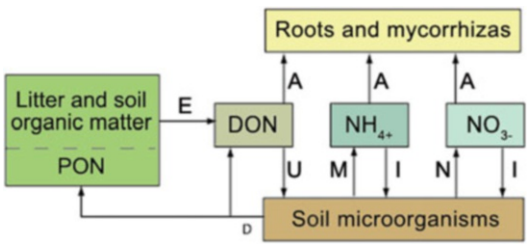

Fig. 18.3 Simplified diagram of microbially mediated nitrogen transformations in soils. Particulate organic nitrogen (PON) in plant litter and soil organic matter is broken down to dissolved organic nitrogen (DON) by exoenzymes (E); this is the rate-determining process in supplying plant-available nitrogen. Soil microorganisms take up (U) DON and use it to support their growth if they are nitrogen limited; they also immobilize (I) NH_4^+ and NO_3^-, if present. If microorganisms are carbon limited, they break down DON for energy, and excrete NH_4^+, during nitrogen mineralization (M), or NO_3^-, during nitrification (N). Plants and their mycorrhizal symbionts absorb (A) some combination of DON, NH_4^+, and NO_3^-, depending on relative availability.

Sulfur (S) is intermediate between N and P in terms of its linkage to decomposition, because some S is ester-bonded (like P) and can be released by **sulfatases** without decomposition, but other S atoms are covalently linked and require decomposition to dissolved organic forms before they can be absorbed and metabolized by soil microorganisms (Mitchell and Fuller 1988).

18.3.2 Effects of Litter Quality on Mineralization

When litter or soil organic matter contains nutrients in excess of microbial demands, N and P are excreted by soil microorganisms (net **mineralization**) during the decomposition process, and become available for plant uptake (Sect. 9.3.1; Fig. 9.2). On the other hand, if the organic matter is low in nutrients, microorganisms meet their nutrient demand by absorbing nutrients from the soil solution (net **immobilization**), resulting in competition for nutrients between soil microorganisms and plants. After nutrient resorption (Sect. 9.4.3.2), plant litter often has a higher C:N ratio than microbial biomass. Empirical observations suggest that, above a critical C:N ratio of about 20:1, microorganisms absorb nutrients from the soil solution, causing net N immobilization (Paul and Clark 1996). As microorganisms decompose the organic matter and respire carbon to meet respiratory demands for growth and maintenance, the C:N ratio of litter

declines. Net N mineralization occurs when the C:N ratio falls below the critical 20:1 ratio. The result is that fresh litter often initially increases in N concentration due to microbial immobilization, before net mineralization occurs. In many P-limited forest ecosystems, P is immobilized to a significantly greater extent than is N in the first stages of decomposition (Attiwill and Adams, 1996).

Net immobilization occurs to a greater extent and for a longer time where plants produce litter with low N and P concentrations. In those ecosystems where plant growth is N-limited, litter C:N ratios strongly govern decomposition and N immobilization, with P being mineralized more quickly, whereas in areas of heavy **N deposition**, C:P ratios exert stronger control over decomposition, and N is mineralized more quickly (Aerts and de Caluwe 1997). The high litter N and P concentrations of plants on fertile soils, with their fast growth rate and SLA, thus promote nutrient mineralization, whereas there is slower mineralization in ecosystems dominated by slow-growing plants with low SLA (Hobbie 2015).

If nutrient concentration affects mineralization so strongly, then will the low leaf nutrient concentrations caused by **elevated atmospheric CO_2 concentrations** reduce litter nutrient concentrations and therefore decomposition rate? In most cases studied to date, differences in leaf chemistry caused by elevated [CO_2] diminish during senescence, perhaps due to respiration of accumulated starch, so that litter quality and, therefore, decomposition and mineralization rates are similar for litter produced under elevated and ambient [CO_2] (Norby et al. 2001). Rising atmospheric [CO_2] only cause accumulation of soil carbon when N is added at rates well above typical atmospheric N inputs. Soil carbon sequestration under elevated [CO_2] is constrained both directly by N availability and indirectly by nutrients needed to support N_2 fixation (Sect. 12.3.8; Van Groenigen et al. 2006). Combining meta-analysis with data assimilation shows that atmospheric CO_2 enrichment stimulates both the input (+19.8%) and the turnover of carbon in soil (+16.5%). The increase in soil carbon turnover with rising [CO_2] leads to lower equilibrium soil carbon stocks than expected from the rise in soil carbon input alone, indicating that it is a general mechanism limiting carbon accumulation in soil (Fig. 18.4; Van Groenigen et al. 2014).

Species differences in the types of carbon compounds they contain magnify differences in mineralization rate due to litter nutrient concentration. The high concentrations of quantitative secondary metabolites in species with long-lived leaves (Sect. 18.2.1) slow down decomposition

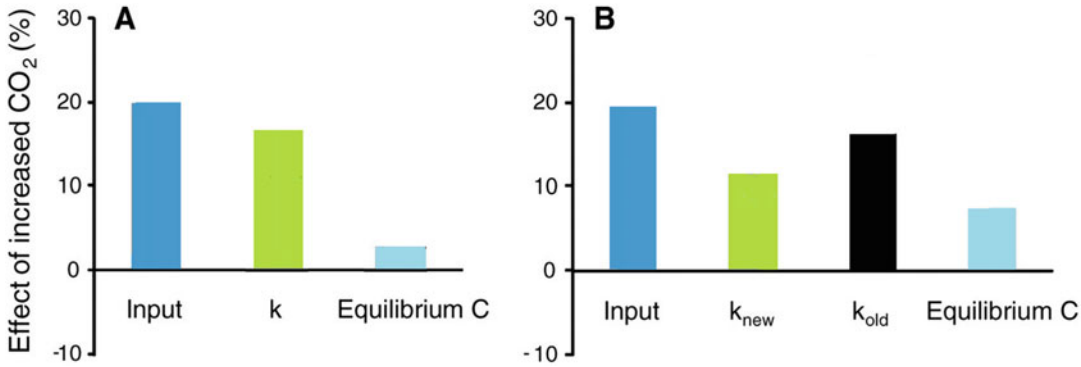

Fig. 18.4 Results of a meta-analysis on the response of soil carbon dynamics to increased levels of atmospheric CO_2. (**A**) The effect of increased CO_2 on soil carbon input (input), soil carbon turnover (k), and projected equilibrium soil carbon, based on a one-pool soil carbon model. (**B**) The effect of increased CO_2 on soil carbon input, new soil carbon turnover (k_{new}), old soil carbon turnover (k_{old}), and projected equilibrium soil carbon, based on a two-pool soil carbon model. Results are based on 53 experimental comparisons. Error bars represent 95% confidence intervals (Modified after Van Groenigen et al. 2014).

because of both the toxic effects on microorganisms and the difficulty of breakdown of secondary metabolites. **Phenolic** compounds that are decomposed slowly include lignin and tannin (Sect. 13.3.2). High tannin concentrations reduce the rate of **mineralization** of the litter, so that, for instance, most of the N in the boreal forest soil occurs as complexes of organic N and tannin, rather than as NO_3^-, NH_4^+, or amino acids (Northup et al. 1995). Tannins and other protein-binding phenolics also inhibit **nitrification**, the microbial conversion of ammonia, via NO_2^- to NO_3^- (Baldwin et al. 1983). Foliar N and P are resorbed less at N- and P-rich sites and under optimal climatic conditions than at N- and P-poor sites (Sect. 9.4.3). Thus, lower litter nutritional quality coincides with nutrient-poor sites and nonoptimal climatic conditions, constituting a positive feedback with negative consequences for the soil trophic web (Zechmeister-Boltenstern et al. 2015). In addition, lignin and tannin concentrations tend to be higher when nutrients limit plant productivity. As a result, the availability of N is even further reduced, at least for plants lacking mechanisms to release N from the tannin-organic N complexes (Sect. 12.2.4) (Northup et al. 1995).

Some **mycorrhizal fungi** produce enzymes that allow them to derive mineral nutrients and carbon from organic sources (Sect. 12.2.4). Especially, **ectomycorrhizas** and **ericoid mycorrhizas** are capable of using relatively complex organic N sources (Sect. 12.2.4), possibly including the complexes produced under pine stands growing under nutrient-poor conditions.

For nonmycorrhizal species in nutrient-poor environments, associations with mycorrhizal fungi cannot provide access to complexes of organic N with tannins. In nonmycorrhizal *Rhizophora mangle* (red mangrove) defenses are largely carbon-based (**quantitative**; Sect. 13.3.3). These plants have long been used for their high proanthocyanidin (condensed tannin) content of their wood, bark, and leaves. **Polyphenolics** account for approximately 23% of the total leaf dry mass. Interestingly, during leaf senescence, prior to leaf abscission, polyphenols largely disappear, leaving only the largest tannin polymers. The ecological significance of these changes may be that litter decomposition in the mangrove swamps would be greatly inhibited by the phenolic compounds that are broken down before leaf abscission. This breakdown would favor litter decomposition, rather than render the litter poorly available, as is the case for pine needles. Since mycorrhizal associations are not a strategy in mangrove swamps, breakdown of phenolic compounds before leaf abscission may be an alternative strategy to mycorrhizas accessing nutrients locked up in tannin complexes (Kandil et al. 2004). Indeed, leaf litter of *Rhizophora mangle* decomposes within 5 months (Middleton and McKee 2001).

In situations where the N availability is low because of plants that produce phenolics, invasion of grasses into nutrient-poor habitats dominated by ericaceous dwarf shrubs [*Calluna vulgaris* (Scottish heather) and *Erica tetralix* (crossleaf heath)] may enhance rates of **mineralization**. Such invasions are made possible by N deposition, due to **acid rain**. They may enhance the rate of N cycling in the system, because organic N contained in the litter of the grasses is mineralized faster than that in residues of woody species (Solly et al. 2014). Similarly, increased fire frequency in nutrient-poor Mediterranean woodlands may enhance P availability and weed invasion, which then further enhance the rate of nutrient cycling (Fisher et al. 2006, 2009).

18.3.3 Root Exudation and Rhizosphere Effects

The presence of living roots can greatly enhance litter decomposition and mineralization, by directly using organic matter in the litter through associations with ectomycorrhizal fungi (Sect. 12.4.2). Alternatively, the roots may provide a carbon source that either stimulates or retards the growth and activity of soil microorganisms and nematodes (Ehrenfeld et al. 2005). There may be either positive or negative effects of roots on mineralization, depending on environmental conditions.

Root exudates are released in response to a limiting supply of P or micronutrients, or to toxic levels of some metals (Sects. 9.2.25, 9.2.2.6, 9.3.1.3, and 9.3.3.4). They stimulate mineralization when microorganisms consume the exudates, and, in addition, decompose soil organic matter in the rhizosphere or are grazed by soil animals (Shahzad et al. 2015). Gram-negative bacteria with rapid growth rates, but a low capability to degrade complex substrates are generally the major microorganisms that are stimulated by exudation. For example, when *Triticum aestivum* (wheat) or *Secale cereale* (rye) plants are grown in soil with ^{14}C-labeled straw, only 6% of the microbial biomass is labeled with ^{14}C. This microbial biomass, however, is highly active in releasing $^{14}CO_2$, indicating a '**priming**' of decomposition by the exudates (Carney et al. 2007; Finzi et al. 2014). Under conditions of low nutrient availability, this priming effect is often less pronounced, because bacteria have insufficient nutrients to grow and attack soil organic matter (Zechmeister-Boltenstern et al. 2015), and because plants may intensely compete with soil microorganisms for nutrients under these conditions (Norton and Firestone 1996). This explains the **positive effect** of roots on N mineralization (Zhao et al. 2010; Meier et al. 2017), whereas these effects may be less pronounced or **negative** in infertile or highly organic soils (Parmelee et al. 1993). **Root exudates** may be effective in **priming** mineralization of fertile mull soil organic matter, because of its relatively labile carbon. By contrast, lignolytic activity may control soil N turnover in infertile mor soils, where bacteria stimulated by root exudates lack the enzymatic capacity to degrade lignin. Thus, soil fertility may determine the nutritional consequences of root exudation both through its effect on the carbon:nitrogen balance of bacteria and through effects on the recalcitrance of soil organic matter (Murphy et al. 2015).

Roots may also promote mineralization because of more intense grazing of bacteria by protozoa. The increased growth of bacteria in response to exudates in the rhizosphere attracts protozoa, which use the bacterial carbon to support their growth and maintenance; the protozoa excrete the mineralized nutrients, which are then available for uptake by the plant (Clarholm 1985; Geisen et al. 2018). We expect this nutrient release by bacterial grazers to be most pronounced in fertile soils, where bacterial growth rates would be fastest. The rapid bacterial growth in response to root exudates can also positively affect the plant by outcompeting microorganisms that have detrimental effects on plants.

There are major technical difficulties in studying the complex biotic interactions that may occur in the rhizosphere. However, recent molecular advances now enable the discovery of novel microorganisms with unforeseen metabolic capabilities, revealing new insight into the underlying processes regulating nutrient cycles at local to global scales. With the ability to sequence functional genes from the environment, molecular approaches now enable us to identify microorganisms and metabolic processes and develop an understanding of many globally important biogeochemical processes (Zak et al. 2006; Pepe-Ranney et al. 2016).

Elevated [CO_2] can influence mineralization through its effects on rhizosphere processes, but CO_2 effects on microbial processes vary, depending on the plant species present and soil fertility (Van Groenigen et al. 2006). Plant species composition influences how soil N cycling will respond to further increases in [CO_2] (Hungate et al. 2004; Carney et al. 2007). The nature of the rhizosphere community affects the quantity and quality of root exudates, with much faster exudation rates occurring in nutrient-poor soils than in common solution culture.

18.4 The End-Product of Decomposition

Decomposition of plant litter is a key process of the nutrient cycles of most terrestrial ecosystems. Rates of microbial decomposition strongly depend on chemical composition, with slower rates associated with acidic litter with a low base content, low concentrations of N or P, and high concentrations of phenolics (tannin, lignin). Photodegradation is faster when lignin

concentrations are higher. Since plants in nutrient-poor habitats tend to accumulate more quantitative secondary plant compounds and have low base and N and P concentrations, their litter is decomposed rather slowly by microorganisms, thus aggravating the low-nutrient status in these habitats. Some mycorrhizal associations appear pivotal in accessing N in litter containing high concentrations of phenolics. In semi-arid and arid ecosystems, microbial breakdown is less important than photodegradation, and fire plays a dominant role in nutrient cycling.

References

Aerts R, de Caluwe H. 1997. Nutritional and plant-mediated controls on leaf litter decomposition of *Carex* species. *Ecology* **78**: 244–260.

Attiwill PM, Adams MA 1996. Nutrient cycling in forests of southeastern Australia. In: Attiwill PM PP, Weston CJ, Adams MA ed. *Nutrition of Eucalypts*. Melbourne: CSIRO.

Austin AT, Ballaré CL. 2010. Dual role of lignin in plant litter decomposition in terrestrial ecosystems. *Proc Natl Acad Sci USA* **107**: 4618–4622.

Austin AT, Vivanco L. 2006. Plant litter decomposition in a semi-arid ecosystem controlled by photodegradation. *Nature* **442**: 555–558.

Baldwin IT, Olson RK, Reiners WA. 1983. Protein binding phenolics and the inhibition of nitrification in subalpine balsam fir soils. *Soil Biol Biochem* **15**: 419–423.

Bradford MA, Berg B, Maynard DS, Wieder WR, Wood SA, Cornwell W. 2016. Understanding the dominant controls on litter decomposition. *J Ecol* **104**: 229–238.

Carney KM, Hungate BA, Drake BG, Megonigal JP. 2007. Altered soil microbial community at elevated CO_2 leads to loss of soil carbon. *Proc Natl Acad Sci USA* **104**: 4990–4995.

Clarholm M. 1985. Interactions of bacteria, protozoa and plants leading to mineralization of soil nitrogen. *Soil Biol Biochem* **17**: 181–187.

Cornelissen JHC. 1996. An experimental comparison of leaf decomposition rates in a wide range of temperate plant species and types. *J Ecol* **84**: 573–582.

Cornelissen JHC, Aerts R, Cerabolini, Werger MJA, van der Heijden MGA. 2001. Carbon cycling traits of plant species are linked with mycorrhizal strategy. *Oecologia* **129**: 611–619.

Cornelissen JHC, Grootemaat S, Verheijen LM, Cornwell WK, Bodegom PM, Wal R, Aerts R. 2017. Are litter decomposition and fire linked through plant species traits? *New Phytol* **216**: 653–669.

Cornelissen JHC, Pérez-Harguindeguy N, Díaz S, Grime JP, Marzano B, Cabido M, Vendramini F, Cerabolini B. 1999. Leaf structure and defence control litter decomposition rate across species and life forms in regional floras on two continents. *New Phytol* **143**: 191–200.

Cornelissen JHC, Quested HM, van Logtestijn RSP, Pérez-Harguindeguy N, Gwynn-Jones D, Díaz S, Callaghan TV, Press MC, Aerts R. 2006. Foliar pH as a new plant trait: can it explain variation in foliar chemistry and carbon cycling processes among subarctic plant species and types? *Oecologia* **147**: 315–326.

Cornelissen JHC, Thompson K. 1997. Functional leaf attributes predict litter decomposition rate in herbaceous plants. *New Phytol* **135**: 109–114.

Cornwell WK, Cornelissen JHC, Amatangelo K, Dorrepaal E, Eviner VT, Godoy O, Hobbie SE, Hoorens B, Kurokawa H, Pérez-Harguindeguy N, Quested HM, Santiago LS, Wardle DA, Wright IJ, Aerts R, Allison SD, Van Bodegom P, Brovkin V, Chatain A, Callaghan TV, Díaz S, Garnier E, Gurvich DE, Kazakou E, Klein JA, Read J, Reich PB, Soudzilovskaia NA, Vaieretti MV, Westoby M. 2008. Plant species traits are the predominant control on litter decomposition rates within biomes worldwide. *Ecol Lett* **11**: 1065–1071.

Eaton JM, Lawrence D. 2006. Woody debris stocks and fluxes during succession in a dry tropical forest. *For Ecol Manag* **232**: 46–55.

Edwards NT, Sollins P. 1973. Continuous measurement of carbon dioxide evolution from partitioned forest floor components. *Ecology* **54**: 406–412.

Ehrenfeld JG, Ravit B, Elgersma K. 2005. Feedback in the plant-soil system. *Annu Rev Environ Res* **30**: 75–115.

Finzi AC, Abramoff RZ, Spiller KS, Brzostek ER, Darby BA, Kramer MA, Phillips RP. 2014. Rhizosphere processes are quantitatively important components of terrestrial carbon and nutrient cycles. *Glob Change Biol* **21**: 2082–2094.

Fisher JL, Loneragan WA, Dixon K, Delaney J, Veneklaas EJ. 2009. Altered vegetation structure and composition linked to fire frequency and plant invasion in a biodiverse woodland. *Biol Conserv* **142**: 2270–2281.

Fisher JL, Veneklaas EJ, Lambers H, Loneragan WA. 2006. Enhanced soil and leaf nutrient status of a Western Australian *Banksia* woodland community invaded by *Ehrharta calycina* and *Pelargonium capitatum*. *Plant Soil* **284**: 253–264.

Freschet GT, Cornwell WK, Wardle DA, Elumeeva TG, Liu W, Jackson BG, Onipchenko VG, Soudzilovskaia NA, Tao J, Cornelissen JHC. 2013. Linking litter decomposition of above- and below-ground organs to plant–soil feedbacks worldwide. *J Ecol* **101**: 943–952.

García-Palacios P, McKie BG, Handa IT, Frainer A, Hättenschwiler S. 2016. The importance of litter traits and decomposers for litter decomposition: a comparison of aquatic and terrestrial ecosystems within and across biomes. *Funct Ecol* **30**: 819–829.

Garnier E, Cortez J, Billès G, Navas M-L, Roumet C, Debussche M, Laurent G, Blanchard A, Aubry D, Bellmann A, Neill C, Toussaint J-P. 2004. Plant functional markers capture ecosystem properties during secondary succession. *Ecology* **85**: 2630–2637.

Geisen S, Mitchell EAD, Adl S, Bonkowski M, Dunthorn M, Ekelund F, Fernández LD, Jousset A, Krashevska V, Singer D, Spiegel FW, Walochnik J, Lara E. 2018. Soil protists: a fertile frontier in soil biology research. *FEMS Microbiol Rev* **42**: 293–323.

Gorham E. 1991. Northern peatlands: role in the carbon cycle and probable responses to climate warming. *Ecol Appl* **1**: 182–195.

Hobbie SE. 2015. Plant species effects on nutrient cycling: revisiting litter feedbacks. *Trends Ecol Evol* **30**: 357–363.

Hungate BA, Stiling PD, Dijkstra P, Johnson DW, Ketterer ME, Hymus GJ, Hinkle CR, Drake BG. 2004. CO_2 elicits long-term decline in nitrogen fixation. *Science* **304**: 1291.

Jo I, Fridley JD, Frank DA. 2016. More of the same? In situ leaf and root decomposition rates do not vary between 80 native and nonnative deciduous forest species. *New Phytol* **209**: 115–122.

Kandil FE, Grace MH, Seigler DS, Cheeseman JM. 2004. Polyphenolics in *Rhizophora mangle* L. leaves and their changes during leaf development and senescence. *Trees Struct Funct* **18**: 518–528.

Kraus TEC, Dahlgren RA, Zasoski RJ. 2003. Tannins in nutrient dynamics of forest ecosystems - a review. *Plant Soil* **256**: 41–66.

Lambers H, Raven JA, Shaver GR, Smith SE. 2008. Plant nutrient-acquisition strategies change with soil age. *Trends Ecol Evol* **23**: 95–103.

Ma C, Xiong Y, Li L, Guo D, Briones MJ. 2016. Root and leaf decomposition become decoupled over time: implications for below- and above-ground relationships. *Funct Ecol* **30**: 1239–1246.

Meier IC, Finzi AC, Phillips RP. 2017. Root exudates increase N availability by stimulating microbial turnover of fast-cycling N pools. *Soil Biol Biochem* **106**: 119–128.

Middleton BA, McKee KL. 2001. Degradation of mangrove tissues and implications for peat formation in Belizean island forests. *J Ecol* **89**: 818–828.

Mitchell M, Fuller R. 1988. Models of sulfur dynamics in forest and grassland ecosystems with emphasis on soil processes. *Biogeochemistry* **5**: 133–163.

Murphy CJ, Baggs EM, Morley N, Wall DP, Paterson E. 2015. Rhizosphere priming can promote mobilisation of N-rich compounds from soil organic matter. *Soil Biol Biochem* **81**: 236–243.

Norby RJ, Cotrufo MF, Ineson P, O'Neill EG, Canadell JG. 2001. Elevated CO_2, litter chemistry, and decomposition: a synthesis. *Oecologia* **127**: 153–165.

Northup RR, Yu Z, Dahlgren RA, Vogt KA. 1995. Polyphenol control of nitrogen release from pine litter. *Nature* **377**: 227–229.

Norton JM, Firestone MK. 1996. N dynamics in the rhizosphere of *Pinus ponderosa* seedlings. *Soil Biol Biochem* **28**: 351–362.

Parmelee RW, Ehrenfeld JG, Tate RL. 1993. Effects of pine roots on microorganisms, fauna, and nitrogen availability in two soil horizons of a coniferous forest spodosol. *Biol Fert Soils* **15**: 113–119.

Paul EA, Clark FE. 1996. *Soil Microbiology and Biochemistry, 2nd ed*. San Diego: Academic.

Pepe-Ranney C, Campbell AN, Koechli CN, Berthrong S, Buckley DH. 2016. Unearthing the ecology of soil microorganisms using a high resolution DNA-SIP approach to explore cellulose and xylose metabolism in soil. *Front Microbiol* **7**: 703.

Powell JR, Riley RC, Cornwell W. 2017. Relationships between mycorrhizal type and leaf flammability in the Australian flora. *Pedobiologia* **65**: 43–49.

Reich PB. 2014. The world-wide 'fast–slow' plant economics spectrum: a traits manifesto. *J Ecol* **102**: 275–301.

Schimel J, Schaeffer SM. 2012. Microbial control over carbon cycling in soil. *Front Microbiol* **3**.

Schimel JP, Bennett J. 2004. Nitrogen mineralization: challenges of a changing paradigm. *Ecology* **85**: 591–602.

Shahzad T, Chenu C, Genet P, Barot S, Perveen N, Mougin C, Fontaine S. 2015. Contribution of exudates, arbuscular mycorrhizal fungi and litter depositions to the rhizosphere priming effect induced by grassland species. *Soil Biol Biochem* **80**: 146–155.

Solly EF, Schöning I, Boch S, Kandeler E, Marhan S, Michalzik B, Müller J, Zscheischler J, Trumbore SE, Schrumpf M. 2014. Factors controlling decomposition rates of fine root litter in temperate forests and grasslands. *Plant Soil* **382**: 203–218.

Swift MJ, Heal OW, Anderson JM. 1979. *Decomposition in terrestrial ecosystems*. Oxford: Blackwell Scientific Publications.

Van Groenigen K-J, Six J, Hungate BA, De Graaff M-A, Van Breemen N, Van Kessel C. 2006. Element interactions limit soil carbon storage. *Proc Natl Acad Sci USA* **103**: 6571–6574.

Van Groenigen KJ, Qi X, Osenberg CW, Luo Y, Hungate BA. 2014. Faster decomposition under increased atmospheric CO_2 limits soil carbon storage. *Science* **344**: 508–509.

Waring BG. 2012. A Meta-analysis of climatic and chemical controls on leaf litter decay rates in tropical Forests. *Ecosystems* **15**: 999–1009.

Wright IJ, Reich PB, Cornelissen JHC, Falster DS, Groom PK, Hikosaka K, Lee W, Lusk CH, Niinemets Ü, Oleksyn J, Osada N, Poorter H, Warton DI, Westoby M. 2005. Modulation of leaf economic traits and trait relationships by climate. *Glob Ecol Biogeogr* **14**: 411–421.

Wright IJ, Reich PB, Westoby M, Ackerly DD, Baruch Z, Bongers F, Cavender-Bares J, Chapin T, Cornelissen JHC, Diemer M, Flexas J, Garnier E, Groom PK, Gulias J, Hikosaka K,

Lamont BB, Lee T, Lee W, Lusk C, Midgley JJ, Navas M-L, Niinemets Ü, Oleksyn J, Osada N, Poorter H, Poot P, Prior L, Pyankov VI, Roumet C, Thomas SC, Tjoelker MG, Veneklaas EJ, Villar R. 2004. The worldwide leaf economics spectrum. *Nature* **428**: 821–827.

Zak DR, Blackwood CB, Waldrop MP. 2006. A molecular dawn for biogeochemistry. *Trends Ecol Evol* **21**: 288–295.

Zechmeister-Boltenstern S, Maria KK, Mooshammer M, Peñuelas J, Richter A, Sardans J, Wanek W. 2015. The application of ecological stoichiometry to plant–microbial–soil organic matter transformations. *Ecol Monogr* **85**: 133–155.

Zhao Q, Zeng D-H, Fan Z-P. 2010. Nitrogen and phosphorus transformations in the rhizospheres of three tree species in a nutrient-poor sandy soil. *Appl Soil Ecol* **46**: 341–346.

19 Role in Ecosystem and Global Processes: Ecophysiological Controls

19.1 Introduction

In previous chapters, we emphasized the integration among processes from molecular to whole-plant levels and considered the physiological consequences of interactions between plants and other organisms. In this chapter, we move up in scale, to consider relationships between **plant ecophysiological processes** and those occurring at **ecosystem to global scales**. Plant species differ substantially in their responses to environment and to other organisms. It is not surprising that these physiological differences among plants contribute strongly to functional differences among ecosystems.

19.2 Ecosystem Biomass and Production

19.2.1 Scaling from Plants to Ecosystems

The supply rates of light, water and nutrients that govern ecosystem processes are functions of ground area and soil volume as well as leaf area. Therefore, a critical initial step in relating the processes in individual plants to those in ecosystems is to determine how **plant size and density** relate to **stand biomass**. In sparse stands of plants, there is no necessary relationship between size and density, so plants increase in mass without changes in density (Kays and Harper 1974). As plants begin to compete, however, mortality reduces plant density in a predictable fashion. In mid- and late-successional communities, plant density is determined more by mortality than by recruitment, and shows an inverse relationship between ln(biomass) and ln (density), with a slope of about −3/2. This **self-thinning line** was initially derived empirically for pure stands under cultivated and natural conditions (Yoda 1963). It has subsequently been observed in a wide array of studies, including mixed communities, both experimental and in the field, in ecosystems ranging from meadows to forests (Westoby 1984). The slope and intercept of the self-thinning line vary among species and experimental conditions (Weller 1987; Vandermeer and Goldberg 2013), but the relationship provides an empirical basis to extrapolate from individuals to stands of vegetation. Given that:

$$\ln(b) = -3/2 \ln(d) \tag{19.1}$$

it follows that

$$b = (d)^{-3/2} \text{or } d = (\text{b})^{-2/3} \tag{19.2}$$

$$B = b \times d = d^{-1/2} = b^{1/3} \tag{19.3}$$

where b is individual biomass (g plant $^{-1}$), d is density (plants m^{-2}), and B is stand biomass (g m^{-2}) for a single species growing in competition under specific conditions. These relationships indicate that, for a given plant

H. Lambers, R. S. Oliveira, *Plant Physiological Ecology*, https://doi.org/10.1007/978-3-030-29639-1_19

species and environment, increases in stand biomass are typically associated with increased plant size and reduced density. Biomass per individual can, in turn, be used as a basis for scaling metabolism to the ecosystem scale (Niklas and Enquist 2001).

19.2.2 Physiological Basis of Productivity

Net primary production (*NPP*) is the net biomass gain by vegetation per unit time. The main plant traits that govern *NPP* (g m^{-2} $year^{-1}$) are **biomass** (g m^{-2}) and **RGR** (g g^{-1} $year^{-1}$):

$$NPP = \text{Biomass} \times RGR \tag{19.4}$$

Most of the woody biomass of trees and shrubs consists of dead cells, so scaling productivity from individuals to stands in woody vegetation (or in vegetation comparisons that include woody species) generally uses leaf biomass rather than total biomass (Niklas and Enquist 2001). In many studies on tropical forests, aboveground biomass is estimated by measuring the diameter of all woody stems above some minimum size, and calculating each stem's biomass based on allometric relations from trees harvested nearby or in previous studies elsewhere (Clark et al. 2001). Woody biomass is important primarily as a way for plants to raise their leaves above those of neighbors.

At the **global scale**, **climate** and associated patterns of disturbance (*e.g.*, fire) are the major determinant of *NPP* (Fig. 19.1; Schimper 1898), because of constraints on both the growth of individual plants and the types of species that can compete effectively. Highest productivity occurs in rainforests, where warm moist conditions favor plant growth and development of a large plant size; lowest values are in desert and tundra, where low precipitation or temperature, respectively, constrains growth (Table 19.1; Huston and Wolverton 2009; Schlesinger and Bernhardt 2013). In the tropics, where temperature is not a constraint, rainforests have greater productivity than dry deciduous forests, which are more productive than savannas, *i.e.* productivity declines with reduced water availability and/or increases in disturbance by fire. Similarly, where moisture is less limiting to growth, productivity is governed by temperature, decreasing from tropical to temperate to boreal forests and finally to tundra. It is important to note that climatic variables may exert contrasting controls over productivity within biomes. For example, *NPP* of tropical forests may be limited by water

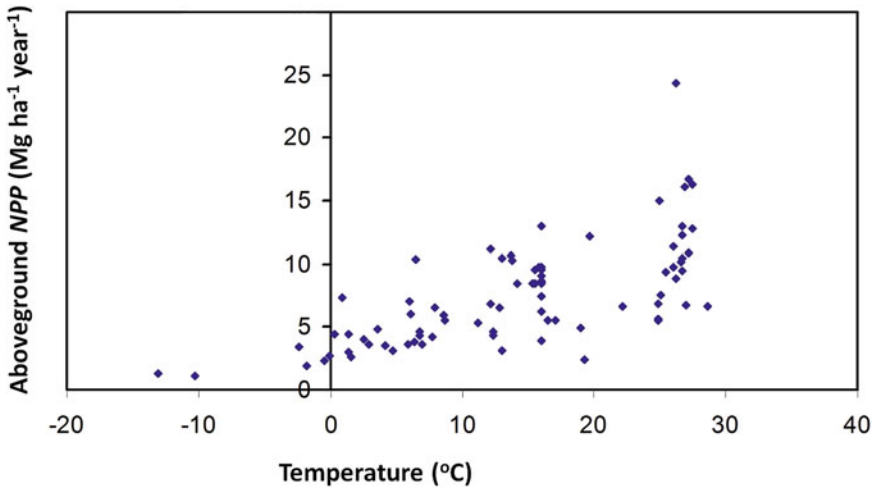

Fig. 19.1 The relationships between net primary production (*NPP*) and mean annual temperature (Schuur 2003). Copyright Ecological Society of America.

Table 19.1 Primary production and biomass estimates for the world.

Ecosystem type	Area (10^6 km^2)	Mean biomass (kg C m^{-2})	Total biomass (10^9 ton C)	Mean *NPP* (g C m^{-2} year^{-1})	Total *NPP* (Gt C year^{-1})[a]	*RGR* (year^{-1})
Tropical rainforest	17.0	20	340	900	15.3	0.045
Tropical seasonal forest	7.5	16	120	675	5.1	0.042
Temperate evergreen forest	5.0	16	80	585	2.9	0.037
Temperate deciduous forest	7.0	13.5	95	540	3.8	0.040
Boreal forest	12.0	9.0	108	360	4.3	0.040
Woodland and shrubland	8.0	2.7	22	270	2.2	0.100
Savanna	15.0	1.8	27	315	4.7	0.175
Temperate grassland	9.0	0.7	6.3	225	2.0	0.321
Tundra and alpine meadow	8.0	0.3	2.4	65	0.5	0.217
Desert scrub	18.0	0.3	5.4	32	0.6	0.107
Rock, ice, and sand	24.0	0.01	0.2	1.5	0.04	–
Cultivated land	14.0	0.5	7.0	290	4.1	0.580
Swamp and marsh	2.0	6.8	13.6	1125	2.2	0.165
Lake and stream	2.5	0.01	0.02	225	0.6	22.5
Total continental	149	5.5	827	324	48.3	0.058
Total marine	361	0.005	1.8	69	24.9	14.1
Total global	510	1.63	829	144	73.2	0.088

Source: Schlesinger (1997)
Note: [a]Gigatons (Gt) are 10^{15} g

availability when rainfall is < 2000 mm year^{-1}, and by radiation above this threshold (Wagner et al. 2016).

At **local to regional scales**, **climate** continues to be important, with strong differences in productivity associated with altitudinal gradients in temperature and precipitation and with temperature differences between north- and south-facing slopes. At regional scales, however, variation in soil moisture and nutrients, due to topographic variations in drainage and erosional transport of soils and to differences in **parent material** (the rocks that give rise to soils) become increasingly strong controls over productivity. For example, marshes are among the most productive habitats in most climate zones, due to high moisture and nutrient availability. Low-moisture and low-nutrient environments are typically dominated by slow-growing species with low specific leaf area (SLA), high leaf mass density, slow rates of photosynthesis per unit leaf mass, and low leaf area ratios (Sect. 10.3). These traits, sometimes combined with low plant density, result in low biomass and productivity.

At the local scale, there can still be important differences in biomass and productivity, due to differences in species traits, even with the same climate and parent material. Species introductions can result in strikingly different species dominating adjacent sites. For example, in California, *Eucalyptus globulus* (Tasmanian bluegum) plantations occur on sites that would otherwise be grasslands. The *Eucalyptus globulus* plantations have a biomass and productivity much

greater than that of the grassland, despite the same climate and parent material. The trees have deeper roots that tap water unavailable to the grasses, thus supporting the larger biomass and productivity (Robles and Chapin 1995). Once the grassland or forest is established, it is difficult for species of contrasting life forms to colonize. Consequently, there can be **alternative stable community types** with strikingly different biomass and productivity in the same environment. Greater water use by the trees compared with grasslands may have significant consequences for the availability of water elsewhere in the landscape. In deserts, deep-rooted **phreatophytes** can tap the water table and support a larger biomass and productivity than do shallow-rooted species. Thus, although climate and resource supply govern large-scale patterns of productivity (Schimper 1898), the actual productivity on a site depends strongly on historical factors that govern the disturbance regime and species present at a site (Sect. 1.3).

19.2.3 Disturbance and Succession

Stand age modifies environmental controls over biomass and productivity. After **disturbance**, the most common initial colonizers are herbaceous weedy species that have high reproductive allocation, effective dispersal and are commonly well represented in the buried seed pool (Sect. 11.3.1). There is initially an exponential increase in plant biomass, due to the exponential nature of plant growth (Sect. 10.2.1). Relative growth rate (RGR) declines as plants get larger and begin to compete with one another. In addition, as succession proceeds, there is often a replacement of fast-growing herbaceous species. Woody species that grow more slowly, are taller and shade out the initial colonizers take over. This causes a further decline in RGR (Table 19.2), despite the increase in biomass and productivity through time. In some ecosystems, productivity declines in late succession due to declines in soil nutrient availability and, in some forests, to declines in leaf area and photosynthetic capacity associated with reduced hydraulic conductance of old trees (Sect. 3.5.2.2; Sect. 5.5.1). Thus, changes in productivity through succession are governed initially by rates of colonization and RGR, followed by a gradual transition to a woody community that has lower RGR, but whose larger plant size results in further increases in productivity. Finally, over centuries to millennia, soil P availability declines, causing further decline in productivity (Sect. 9.2.1.1; Wardle et al. 2004). Frequent fire regimes can also have negative long-lasting effects on soil nutrient availability. Soils of tall and carbon-dense eucalypt forests in southern Australia that have been subjected to multiple fires have less available phosphorus and nitrate compared with undisturbed forests. These effects can persist for at least 80 years after the disturbance and strongly limit ecosystem recovery (Bowd et al. 2019).

Table 19.2 Aboveground biomass, production, and nitrogen (N) flux in major temperate ecosystem types, maximum height, and relative growth rate of species typical of these ecosystem types∗.

Parameter	Grassland	Shrubland	Deciduous forest	Evergreen forest
Above-ground biomass[a] (kg m^{-2})	0.3 (0.02)	3.7 (0.05)	15 (2)	31 (8)
Aboveground *NPP*[a] (kg m^{-2} $year^{-1}$)	0.3 (0.02)	0.4 (0.07)	1.0 (0.08)	0.8 (0.08)
N flux[a] (g m^{-2} $year^{-1}$)	2.6 (0.2)	3.9 (1.6)	7.5 (0.5)	4.7 (0.5)
Canopy height[b] (m)	1	4	22	22
Field *RGR* ($year^{-1}$)[c]	1.0	0.1	0.07	0.03
Laboratory *RGR*[b] (wk^{-1})	1.3	0.8	0.7	0.4

Source: Chapin (2003)
∗*Note*: Data are means (SE)
[a]Bokhari and Singh (1975); Cole and Rapp (1981); Gray and Schlesinger (1981); Sala et al. (1988)
[b]Grime and Hunt (1975); Tilman (1988)
[c]Aboveground production/aboveground biomass

Disturbance regime determines the relative proportion of early and late successional stands in a region. For example, **fire** is a natural agent of disturbance that is particularly common at intermediate moisture regimes. In deserts, there is often insufficient fuel to carry a fire, although grass invasions in moist deserts can increase fire probability. By contrast, in temperate and tropical ecosystems with high precipitation or in arctic ecosystems with low evapotranspiration, *i.e.* water loss from an ecosystem by transpiration and surface evaporation, naturally occurring vegetation is too wet to carry a fire in most years. In the tropics and at intermediate rainfall regimes (1000–2500 mm), both forests and savannas may be alternative stable states, and fire plays a role maintaining the low tree cover state (Staver et al. 2011). In grasslands and savannas, fire occurs so frequently that woody plants rarely establish, so the region is dominated by herbaceous vegetation with high RGR and modest productivity. These vegetation characteristics are favorable to mammalian grazers, which act as an additional disturbance to prevent colonization by woody plants (McNaughton et al. 1997).

Plant traits strongly influence the disturbance regime of ecosystems. In grasslands, grasses produce an abundant fine-structured fuel that burns readily when dry, because of the high SLA, high leaf production rate, and low leaf longevity. Abundant belowground reserves and meristem pools allow grasses to recover after grazing or fire. Thus, there is a common suite of **adaptations** that enable plants to tolerate fire and/or grazing in grasslands. Introduction of grasses into forests, shrublands, or deserts can increase fire frequency and cause a replacement of forest by savanna (D'Antonio and Vitousek 1992). Once the grasses create this disturbance regime with high **fire frequency**, tree and shrub seedlings can no longer establish. Thus, there is an increase in fire probability when succession is accompanied by changes in plant functional types. When species shifts do not occur, there is little or no change in flammability with increasing stand age (Schoennagel et al. 2004). The appearance of C_4 grasses in the late Miocene caused an increase in fire frequency in the tropics and allowed savanna expansion (Pagani et al. 1999; Beerling and Osborne 2006), clearly showing the role of plant traits in determining community composition and dynamics through their effects on fire regime.

19.2.4 Photosynthesis and Absorbed Radiation

One scaling approach is to extrapolate directly from leaf carbon exchange to the ecosystem level based on the relationship between photosynthesis and absorbed radiation. This approach was pioneered in agriculture (Monteith 1977) and has been extended to estimate patterns of carbon exchange in natural ecosystems (Field 1991). The fraction of incident photosynthetically active radiation that is absorbed by plants (***APAR***) is either converted to new biomass (*NPP*) or is respired. *APAR* depends on total leaf area as well as leaf angle, its vertical distribution and its photosynthetic capacity. Both light and leaf nitrogen (N) concentration decline in a predictable fashion through the canopy, with N preferentially allocated to the tops of canopies to maximize light utilization (Sect. 3.3.1; Box 8.1). Thus, as an initial simplification, the plant canopy can be treated as a **big leaf**, whose photosynthetic capacity depends on total canopy N (Sect. 8.2; Farquhar 1989; Field 1991). In unstressed crops, dry matter accumulation is roughly proportional to integrated radiation interception over the growing season, with a conversion efficiency of about 1.4 g MJ^{-1} (Monteith 1977). Natural ecosystems vary 10- to 100-fold in *NPP* (Table 19.1). Most of this variation is due to variation in *APAR*, rather than conversion efficiency, which varies about two-fold among studies. There are no striking ecological patterns in reported values of conversion efficiency, with much of the variation among studies likely due to differences in methodology, rather than inherent differences among ecosystems (Field 1991). Most of the variation in *APAR* is due to variation in **leaf area index** (*LAI*) (>50-fold variation among ecosystems), although leaf N concentration can vary nine-fold among ecosystems (Sect. 2.6.3; Reich and Oleksyn 2004). Thus, carbon gain and *NPP* are

low in unfavorable environments, due to the small amount of leaf biomass that can be supported and leaf N concentration that can be attained (Sect. 10.5).

The relatively consistent conversion of *APAR* into plant production among ecosystems provides a tool for estimating global patterns of *NPP*. We can estimate *APAR* from satellite-borne sensors, using the **normalized difference vegetation index** (***NDVI***):

$$NDVI = (NIR - VIS)/(NIR + VIS) \qquad (19.5)$$

where *NIR* (W m^{-2}) is reflectance in the near infrared, and *VIS* (W m^{-2}) is reflectance in the visible. *NDVI* uses the unique absorption spectrum of **chlorophyll** which differs from that of clouds, water, and bare soil to estimate absorbed radiation. Stands with fast rates of photosynthesis have a high *NDVI*, because they have low values of reflected *VIS* and high values of reflected *NIR*. *NDVI* is an excellent predictor of *APAR* and daily net photosynthesis in short-term plot-level studies (Fig. 19.2). It also provides good estimates of *NPP* using satellites (Fig. 19.3). The consistency of this relationship supports the argument that there may be a relatively constant efficiency of converting absorbed radiation into plant biomass. One reason for the modest variation in conversion efficiency between *APAR* and *NPP* may be the similarity of growth respiration across plant tissues and species (Sect. 3.5.2). From a pragmatic perspective, the strong relationship between NDVI and *NPP* is important, because it allows us to estimate *NPP* directly from satellite images (Fig. 19.3). In this way, we can estimate **regional and global patterns of *NPP*** in ways that avoid the errors and biases that are associated with the extrapolation of harvest data to the global scale.

Any factor that alters the leaf area of an ecosystem or the availability of water or N, changes the capacity of that ecosystem for carbon gain by moving vegetation along the generalized *APAR-NPP* relationship. **Climate** affects *LAI* and leaf N concentration (Reich and Oleksyn 2004). The physiological differences among plant species that we have discussed throughout the book also have pronounced effects on the leaf area and leaf N concentration that can be supported in any environment, as mediated by competitive interactions, herbivores, and pathogens. In general, the sorting of species among habitats by competition over the long term probably maximizes *APAR* and *NPP*, whereas pathogens and herbivores tend to reduce *APAR* and *NPP*. Disturbance regime also influences regional *APAR* and *NPP*, as does human land conversion of natural ecosystems to pastures and agriculture.

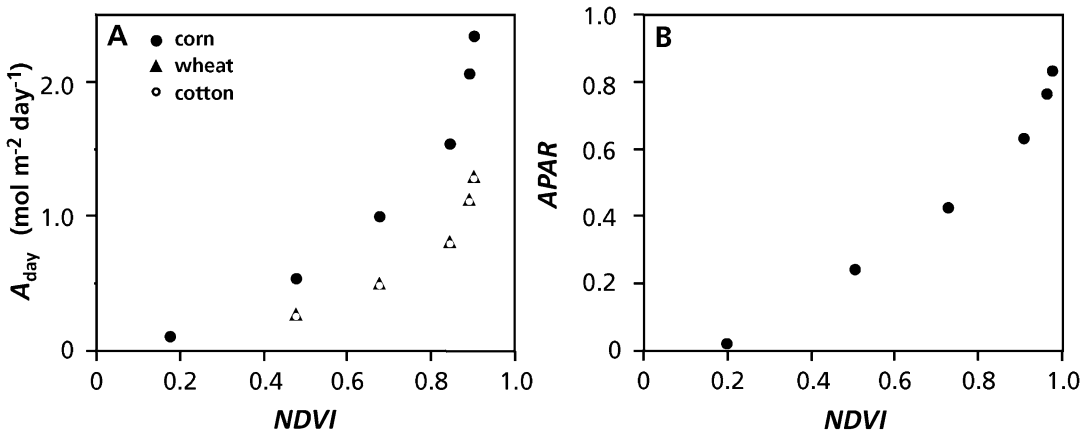

Fig. 19.2 Relationship of Normalized Difference Vegetation Index (*NDVI*) to daily net rate of CO_2 assimilation (A_{day}) and to the fraction of absorbed photosynthetically active radiation (*APAR*). These relationships were simulated based on data collected from *Triticum aestivum* (wheat), *Zea mays* (corn), and *Gossypium hirsutum* (cotton); after Field (1991), as redrawn from Choudhury (1987).

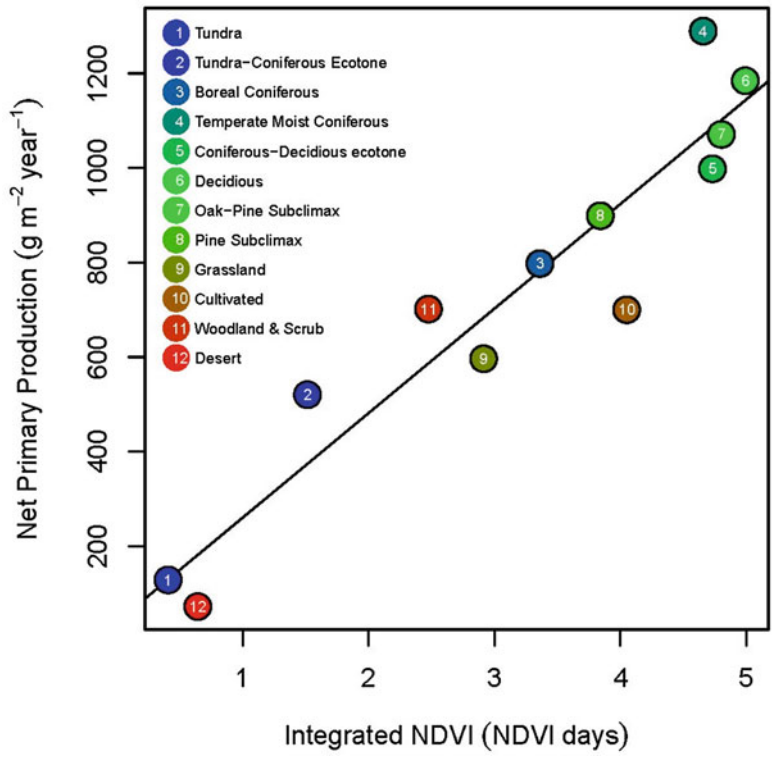

Fig. 19.3 Relationship between mean net primary production (*NPP*) for several biomes and the seasonally integrated Normalized Difference Vegetation Index (*NDVI*) measured from satellites. Each point represents a different biome; after Field (1991), as redrawn from Goward et al. (1985).

Satellite-based measurements of *NDVI* provide evidence for several large-scale changes in *NPP*. In the tropics and in the southern margin of the boreal forest, there have been decreases in *NDVI* associated with forest clearing and conversion to agriculture. The West African Sahel and Northern Mexico also show reductions in *NDVI* associated with land degradation due to overgrazing (Milich and Weiss 2000). At high latitudes, however, *NDVI* increased until about 1990, after which it continued increasing in tundra but declined in boreal forest (Goetz et al. 2005). These high-latitude changes in *NDVI* are caused by rapid arctic vegetation change because of global warming, including an increase in the cover and biomass of deciduous shrubs (McLaren et al. 2017). High-latitude warming may have increased *NPP* through increased length of growing season or direct temperature effects on growth. The declining *NDVI* in boreal forest may reflect warming-induced drought stress or reductions in biomass by insect outbreaks and wildfire (Goetz et al. 2005), which are increasing in areal extent (Kasischke and Turetsky 2006). Similar declining trends in *NDVI* have been observed in tropical forests associated with a long-term decline in precipitation (Zhou et al. 2014). Direct carbon emissions show an increase in Alaska and Canada during 1990–2012 compared with prior periods due to more extreme fire events, resulting in a large carbon source from these two regions. Among biomes, the largest carbon source is from the boreal forest, primarily due to large reductions in soil organic matter during, and with slower recovery after, fire events (Chen et al. 2017). The striking trends in changes in *NDVI* indicates that global *NPP* is changing substantially over broad regions of the globe.

19.2.5 Net Carbon Balance of Ecosystems

Net ecosystem production (*NEP*, g C m^{-2} year^{-1}) of carbon by an ecosystem depends on the balance between **net primary production**

(*NPP*, g C m^{-2} $year^{-1}$) and **heterotrophic respiration** (R_h, g C m^{-2} $year^{-1}$) or between **gross photosynthesis** (P_g, g C m^{-2} $year^{-1}$) and **total ecosystem respiration** (R_e, g C m^{-2} $year^{-1}$), which is the sum of R_h and plant respiration (R_p, g C m^{-2} $year^{-1}$).

$$NEP = NPP - R_h = P_g - R_e \qquad (19.6)$$

NEP is important, because it is usually the major determinant of **Net Ecosystem Carbon Balance (*NECB*)**, the change in carbon stored by an ecosystem.

$$NECB = P_g - R_e - \text{other C losses} \qquad (19.7)$$

Under some circumstances, however, additional carbon fluxes (*e.g.*, fire, harvest, leaching, lateral transfers of organic or inorganic carbon, and volatile emission of carbon in forms other than CO_2) are large enough to influence *NECB*, especially over long time periods (Chapin et al. 2006). We have discussed the plant physiological and environmental constraints on *NPP* (Sects. 19.2.2 and 19.2.4). **Decomposers** account for most of the heterotrophic respiration. Their respiration depends on moisture and temperature and on the quantity, quality, and location (above or below ground) of organic matter produced by plants (Sect. 18.3). In general, conditions that favor high *NPP* also favor high R_h. For example, both *NPP* and decomposition are greater in the tropics than in the arctic, and higher in rainforests than in deserts, due to similar environmental sensitivities of *NPP* and R_h. Similarly, species that are highly productive produce more litter or litter that more readily breaks down than do species of low potential productivity. Thus, habitats dominated by productive species are characterized by rapid decomposition rates (Sect. 18.3.2). There is also a necessary functional linkage between *NPP* and R_h. *NPP* provides the organic material that fuels R_h, and R_h releases the minerals that support *NPP* (Harte and Kinzig 1993). For all these reasons, *NPP* and R_h tend to be fairly closely matched in ecosystems at steady state (Odum 1966). Therefore, at steady state, by definition, *NEP* and changes in carbon storage are small, and show no correlation with *NPP* or R_h. In fact, **peat bogs**, which are among the least productive ecosystems, are ecosystems with the greatest long-term carbon storage. Exchangeable calcium strongly predicts soil organic matter content in water-limited, alkaline soils, whereas with increasing moisture availability and acidity, iron- and aluminum-oxyhydroxides are better predictors, demonstrating that the relative importance of soil organic matter stabilization mechanisms scales with climate and acidity (Rasmussen et al. 2018).

NEP is a small difference between two very large fluxes, $\boldsymbol{P_g}$ and $\boldsymbol{R_e}$ (Fig. 19.4). Although *NEP*, on average, is close to zero in ecosystems at steady state, it shows large enough seasonal variation to cause seasonal fluctuations in atmospheric CO_2 at the global scale (Fig. 2.55). The atmospheric CO_2 concentration ($[CO_2]$) decrease in the northern hemisphere during the summer, when terrestrial photosynthesis is greatest, and increases in winter, when terrestrial photosynthesis declines below the rate of ecosystem respiration. When P_g is low, in stressful environments, *NEP* is negative; in productive environments such as a vigorous, irrigated, and frequently harvested alfalfa field, *NEP* is positive (Baldocchi et al. 2015).

Over long time scales, factors other than *NEP* also influence *NECB*. The most clear-cut causes of ecosystem variation in *NECB* are successional cycles of disturbance and recovery. Most disturbances initially cause a negative *NECB*. Fire releases carbon directly by combustion (not part of *NEP*) and indirectly by producing conditions that are favorable for R_h (part of *NEP*) (Kasischke et al. 1995). For example, removal of vegetation typically reduces transpiration, causing an increase in soil moisture, and increases soil temperature due to greater radiation absorption (lower albedo and greater penetration of solar radiation to the soil surface) (Table 19.3). The warmer, moister soils enhance R_h, and the reduction in plant biomass reduces *NPP*, resulting in negative *NEP* for years after a forest wildfire. Eventually, however, photosynthesis exceeds R_h, leading to carbon accumulation in the ecosystem (a positive *NECB*). Agricultural tillage breaks up soil aggregates and increases access of soil

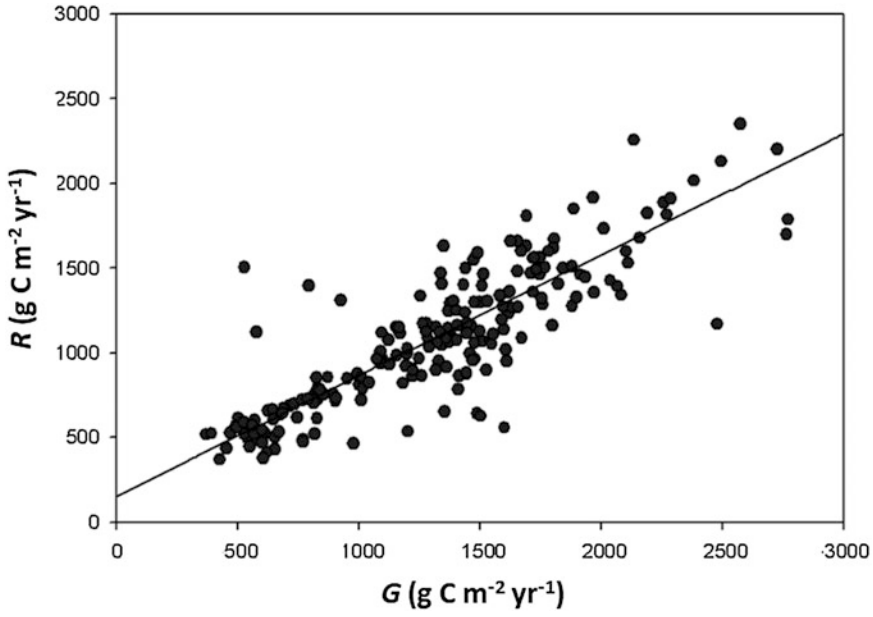

Fig. 19.4 Comparison of annual sums of canopy photosynthesis (P_g) and ecosystem respiration (R_e), based on 216 site years of data. Note the tight coupling between P_g and R_e on annual time scales. Climatic and physiological factors that reduce P_g also reduce R_e and *vice versa*. Increased root exudation as a result of a high P_g enhances soil respiration. All these processes are coupled as reflected in these results (Baldocchi et al. 2015); copyright Elsevier Science, Ltd.

Table 19.3 Shortwave (150–4000 nm) albedos for various surface types.

Surface type	Measured albedo
Clouds; cumulus	0.85
Clouds; cirrus	0.35
Snow; ice	0.7–0.90
Sands; dry	0.40–0.50
Sands; wet	0.20–0.25
Grasslands	0.15–0.35
Forests	0.10–0.20
Ocean	0.02–0.07

Source: Graetz (1991)

microbes to soil organic matter, resulting in a similar increase in R_h and negative *NEP* following conversion of natural ecosystems to agriculture. Tropical and temperate forest soils often lose about 35% of their soil carbon within one decade after conversion to agriculture (Wei et al. 2014).

NEP can also vary substantially among years, due to different environmental responses of photosynthesis and respiration. For example, a global carbon sink anomaly can be driven by growth of semi-arid vegetation in the southern hemisphere, with almost 60% of carbon uptake attributed to Australian ecosystems, where prevalent La Ninã conditions may cause up to six consecutive seasons of increased precipitation (Poulter et al. 2014). Since 1981, a 6% expansion of vegetation cover over Australia was associated with a four-fold increase in the sensitivity of continental net carbon uptake to precipitation. The faster turnover rates of carbon pools in semi-arid biomes are an increasingly important driver of global carbon cycle inter-annual variability. We need more research to identify to what extent the carbon stocks accumulated during wet years are vulnerable to rapid decomposition or loss through fire in subsequent years.

19.2.6 The Global Carbon Cycle

Recent large-scale changes in the global environment (*e.g.*, regional drought, N deposition, and elevated atmospheric [CO_2]) can alter *NEP*, if

they have differential effects on photosynthesis and respiration. For example, photosynthesis responds more strongly to atmospheric [CO_2] than does heterotrophic respiration, so the terrestrial biosphere might increase net CO_2 uptake in response to the increases in atmospheric [CO_2] caused by fossil fuel combustion and land-use change. NPP in most terrestrial ecosystems is nutrient-limited, however, strongly constraining the capacity of vegetation to respond to elevated [CO_2]. In relatively young landscapes, N is the key limiting nutrient (Sect. 9.2.1.1). Therefore, the clearest evidence for increases in *NPP* in response to elevated [CO_2] is in these landscapes with N deposition, where there are widespread increases in tree growth (Kauppi et al. 1992), even after N deposition declined by 25% (Binkley and Högberg 2016). *NPP* is only half the story, however: *NPP* must change more strongly than R_h and disturbance rate, if there is to be an increase in *NECB*. The metabolism of North America's oldest boreal trees, *Thuja occidentalis*, is strongly affected by rising [CO_2], with sharp increases in water use efficiency. However, its growth is not enhanced, suggesting that even in scenarios when there is a positive CO_2 fertilization effect, other mechanisms may prevent trees from assimilating and storing supplementary carbon as aboveground biomass (Giguère-Croteau et al. 2019).

Only 45% of the annual anthropogenic input of CO_2 remains in the atmosphere, with the rest being removed by the oceans or the terrestrial biosphere (Sect. 2.12). The location of this **missing sink** of atmospheric CO_2 is difficult to identify by direct measurement, because its global magnitude is 5.0 Gt C year^{-1} (Canadell et al. 2007), which is only 5% of global *NPP*. This is much smaller than measurement errors and typical interannual variability. Forests play an important role in regional and global carbon cycles. The sink of forests at the global scale is about 2.4 ± 0.4 Pg C year^{-1} for 1990–2007 (Pan et al. 2011). With extensive afforestation and reforestation efforts over the last several decades, forests in East Asia have largely expanded. Biomass carbon stocks of the forests in China, Japan, North Korea, South Korea, and Mongolia increased between the 1970s and the 2000s (Fang et al. 2014). Forest area and biomass carbon density increased from 179.78 × 106 ha and 38.6 Mg C ha^{-1} in the 1970s to 196.65 × 106 ha and 45.5 Mg C ha^{-1} in the 2000s, respectively. The C stock increased from 6.9 Pg C to 8.9 Pg C, with an averaged sequestration rate of 66.9 Tg C year^{-1}. Among the five countries, China and Japan are major contributors to the total region's forest carbon sink, with respective contributions of 71.1% and 32.9%. A reduction in forest land in both North Korea and Mongolia caused a carbon loss at an average rate of 9.0 Tg C year^{-1}, equal to 13.4% of the total region's carbon sink. Despite these vast increases over the last four decades, the biomass carbon sequestration by East Asia's forests offset only 5.8% of its contemporary fossil-fuel CO_2 emissions (Fang et al. 2014).

Isotopic fractionation in photosynthesis (Box 2.2) has provided an important key to identifying the magnitude and location of the missing sink. Atmospheric transport models can be run in 'inverse mode'. That is, opposite to the direction of cause to effect, to estimate the global distribution of CO_2 sources and sinks that are required to match the observed geographic and seasonal patterns of concentrations of CO_2 and $^{13}CO_2$ in the atmosphere (Fig. 2.55; Ciais et al. 1995). CO_2 uptake by the terrestrial biosphere can be distinguished from the CO_2 that dissolves in the ocean, because of the strong **isotopic fractionation** during photosynthesis. Similarly, atmospheric stoichiometry between CO_2 and O_2 separate biological from physical causes of changing atmospheric [CO_2]. Although there are still uncertainties, these models suggest that terrestrial ecosystems account for about 56% (2.8 Gt year^{-1}) of the missing sink, and that these terrestrial sinks are concentrated at mid to high northern latitudes (Canadell et al. 2007). Tropical forests also respond strongly to increased atmospheric [CO_2], but this is offset by rapid rates of deforestation, which release CO_2 to the atmosphere. Tropical land-use change represents a source of 1.3 ± 0.7 Pg C year^{-1}, which is the result of gross deforestation emission of 2.9 ± 0.5 Pg C year^{-1}, partially compensated by the forest regrowth carbon sink of 1.6 ± 0.5 Pg C

year^{-1}. Future agricultural productivity in the tropics is at risk from a deforestation-induced increase in mean temperature and the associated heat extremes, and from a decline in rainfall. Negative impacts on agriculture may extend well beyond the tropics (Lawrence and Vandecar 2014).

Human activities have caused the [CO_2] to increase 35% since 1750 (half of this increase since 1970), after about 10,000 years of relatively stable concentration. Atmospheric [CO_2] is now higher than any time in at least 650,000 years (Le Quéré et al. 2017). The capacity of ecosystems to sequester this anthropogenic CO_2 appears to be saturating for several reasons (Canadell et al. 2007). In part this is a logical consequence of the A-C_c curve (Fig. 2.6), which begins to saturate in most C_3 plants at the current [CO_2] (400 μmol mol^{-1}) of the atmosphere. However, growth is not simply determined by photosynthetic carbon assimilation. Growth constraints imposed by water shortage and low temperature are not resulting from reduced provision of carbon assimilates, but from impacts on leaf area formation. Similarly, effects of elevated [CO_2] on photosynthesis do not translate into growth stimulation if soil resources do not match enhanced demand which is unlikely in many natural systems (Körner 2013). This effect is amplified by declines in the photosynthetic capacity of ecosystems due to complex interactions among changes in nutrient and water availability, land-cover change, and pollution; the oceans exhibit an even greater decline in the capacity to sequester CO_2 (Canadell et al. 2007). This sobering observation suggests that we cannot depend on the terrestrial ecosystems to 'solve' the problem of rising atmospheric [CO_2], and that society must take serious measures to reduce CO_2 emissions, to prevent dangerous rates of climate warming. Physiological processes are now being incorporated into Dynamic Global Vegetation Models (DGVMs) to simulate the changes in competitive balance and species shifts expected to occur in response to climatic change (Cramer et al. 2001).

19.3 Nutrient Cycling

19.3.1 Vegetation Controls Over Nutrient Uptake and Loss

The controls over nutrient uptake and loss by stands of vegetation are basically the same as those described for individual plants (Sect. 9.2.2). Nutrient supply ultimately determines nutrient uptake at the stand level. However, individual plants influence their **acquisition of nutrients** directly by root biomass, the kinetics of ion uptake, and their nutrient-mobilizing capacity. **Root biomass**, including **mycorrhizas** is a major plant parameter governing stand-level nutrient uptake, because a large mycorrhizal root biomass is the major mechanism by which plants minimize diffusional limitations of nutrient delivery to the root surface (Sect. 9.2.2.1). The absolute magnitude of root biomass is probably greatest in high-resource environments, where there is a large total plant biomass (*e.g.*, forests; Table 19.2). Root biomass varies less across ecosystems (Table 5.5), however, than does total biomass, because proportional allocation to roots increases in low-resource environments (Sect. 10.5.4.4). I_{max} of ion uptake is generally greatest in plants that grow rapidly (a high plant demand for nutrients) and would therefore contribute to the rapid nutrient uptake in high-resource environments. In low-nutrient environments, vegetation maximizes nutrient acquisition through high root biomass (an acclimation response rather than adaptation), symbiotic associations (with mycorrhizal fungi and N_2-fixing microorganisms), and by solubilizing scarcely available P or organic N (Sect. 9.2.2; Sects. 12.2.3, 12.2.4, 12.2.5 and 12.3.7). Despite adaptations and acclimations of plants to maximize nutrient acquisition on infertile soils, there is a strong correlation between *NPP* and nutrient uptake by vegetation, because of the widespread occurrence of N or P limitation in most ecosystems (Augusto et al. 2017).

Annual **nutrient return** from vegetation to soils is greatest in high-nutrient environments.

Where *NPP* and biomass are high, there is a low mean residence time of nutrients in plants (rapid leaf and perhaps root turnover) and high nutrient concentrations in litter (Sect. 9.4.3.2). Phosphorus is more conservatively cycled, relative to N, particularly in systems where P is a major limiting nutrient, *e.g.*, in Amazon rainforests and Western Australian shrublands, and N is more conservatively cycled where N is limiting, *e.g.*, in a temperate deciduous forest in New Hampshire, United States (Fig. 19.5; Davidson et al. 2004). Thus, for both plant nutrient uptake and loss, the differences among ecosystems are the same as would be predicted by the patterns of acclimation and adaptation of individual plants, but they are more pronounced, because of the larger size of plants in favorable environments.

19.3.2 Vegetation Controls Over Mineralization

The effects of climate and resource availability on nutrient supply are similar to those described for decomposition (Sects. 9.2.5 and 9.2.1.1), with rapid rates of nutrient supply under favorable environmental conditions. Within these environmental constraints, however, **plant traits** strongly influence nutrient supply through their effects on root exudation, microenvironment, and litter quality. Litter quality differs among ecosystems and strongly influences microbial mineralization rates (Sect. 18.3.1). **Root exudates** provide a labile carbon source of sugars, organic acids, amino acids, and allelochemicals that can either enhance or reduce mineralization, depending on soil fertility (Sect. 18.3.3). Root exudates may also inhibit **nitrification** (Sect. 13.2; Lata et al. 2004; Coskun et al. 2017). Over longer time scales, successional development of vegetation modifies soil temperature (shading), soil moisture (transpiration), and the quantity and quality of organic matter inputs (litter and root exudates) (Sect. 18.2.2).

Over long time scales (decades to centuries), patterns of **nutrient input and loss** exert additional influences over nutrient supply. There is only fragmentary understanding of these long-term controls, although we know that abundance of N_2-fixing plants strongly influences N inputs (Vitousek and Howarth 1991). For example, introduction of the N_2-fixing shrub *Myrica faya* (candleberry myrtle) into the Hawaiian Islands greatly increased N inputs, N supply, and annual rates of N cycling (Vitousek 2004). Anthropogenic inputs of N from industrial fixation, emissions associated with burning of fossil fuel and planting of legume crops now exceeds inputs by natural fixation at the global scale (Vitousek et al. 1997), with substantial changes in the regulation of inputs and outputs of N in natural ecosystems (Elser et al. 2009; Högberg et al. 2017).

19.4 Ecosystem Energy Exchange and the Hydrological Cycle

19.4.1 Vegetation Effects on Energy Exchange

19.4.1.1 Albedo

Energy exchange at the ecosystem scale is influenced by the properties of individual leaves and stems (*e.g.*, albedo and the partitioning of dissipated energy between sensible and latent heat (Sect. 6.2.1) as well as by any contrasts between plant properties and those of the underlying surface. In addition, canopy complexity reduces albedo, because any incoming radiation that is initially reflected by a leaf or stem is more likely to encounter another surface, before being reflected back to space. When foliage is present, deciduous forest albedo can be more than twice that of evergreen conifers. Deciduous forest albedos are also more seasonally variable than evergreen forest albedos (Hollinger et al. 2010). The atmosphere is nearly transparent to the shortwave radiation emitted by the sun, so **air temperature** at local to global scales is primarily determined by the amount of energy absorbed and dissipated by the Earth's surface. Therefore, the influence of vegetation on surface reflectance (**albedo**) can have substantial effects on climate. For example, snow and white sand have higher albedos than vegetation, and therefore reduce

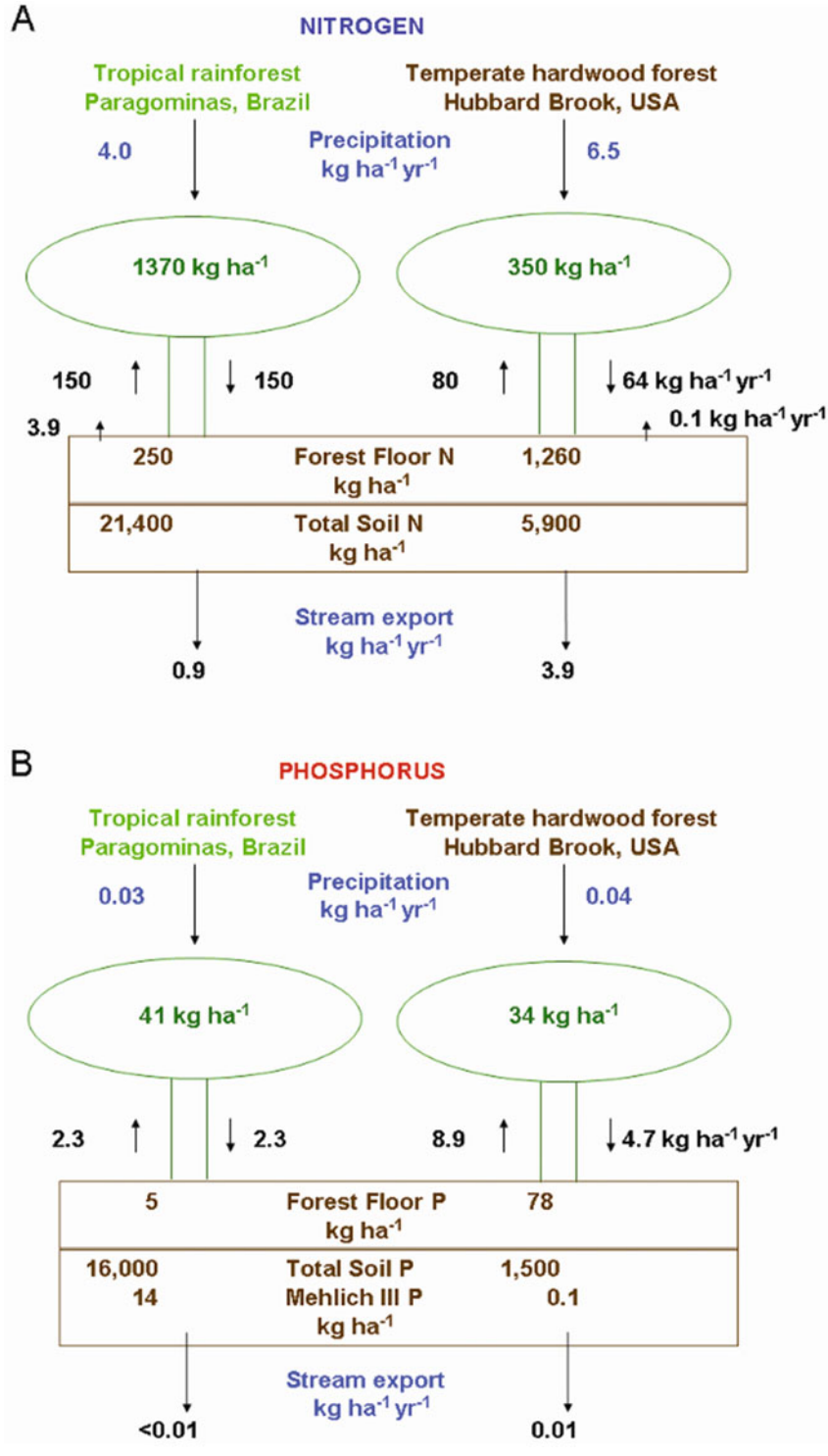

Fig. 19.5 Comparison of nutrient cycles at a mature moist tropical evergreen forest at Fazenda Vitória, Paragominas, Pará, Brazil and at a 55-year-old temperate mixed deciduous forest at Hubbard Brook, New Hampshire, United States. (**A**) Nitrogen (N) cycles. (**B**) Phosphorus cycles. Arrows indicate bulk precipitation inputs, plant uptake, litter and throughfall return to the soil, soil surface emissions of $NO+N_2O$, and stream export of total dissolved N. Soils stocks are to 8 m depth at Paragominas, whereas the soil depth averages about 0.5 m to the underlying glacial till at Hubbard Brook (after Davidson et al. 2004).

absorption of radiation at the surface (Table 19.3). In tundra, any increase in plant height relative to snow depth or increased density of tall shrubs or trees will mask the snow and reduce the albedo (*i.e.* increase absorbed energy and the energy dissipated to the atmosphere), thus raising the temperature of the overlying air (McGuire et al. 2006). Model simulations suggest that, when temperature warmed at the last thermal maximum, 6000 years ago, the **treeline** moved northward, reducing the regional albedo and increasing energy absorption (Foley et al. 1994). Approximately half of the **climatic warming** that occurred at that time is estimated to be due to the northward movement of treeline, with the remaining climate warming due to increased solar input (Fig. 19.6). Globally, tree lines that experience strong winter warming have advanced, and tree lines with a diffuse form are more likely to have advanced than those with an abrupt or Krummholz form. Diffuse treelines may be more responsive to warming because they are more strongly growth limited, whereas other treeline forms may be subject to additional constraints (Harsch et al. 2009). Shifts at treeline provide a positive feedback to regional warming. Thus, changes in vegetation height, relative to snow depth, exert a large effect on regional climate. Enhanced overall productivity and shifts in biomass allocation occur at the treeline, but individual species and functional groups will respond differently to these environmental changes, with consequences for ecosystem structure and functioning (Dawes et al. 2015).

Vegetation effects on albedo also influence regional climate in arid areas. For example, a 30-year drought in the Sahel at the end of the twentieth century reduced plant density, exposed more light-colored soil, and thus reduced absorbed radiation. This reduced heating and convective uplift of the overlying air, resulting in less advection of moisture from the Atlantic and reduced precipitation (Foley et al. 2003a). The resulting increase in drought, compounded by degradation of the land by **over-grazing**, acts as a positive feedback and further reduces plant production and biomass, stabilizing this pattern of regional drought. Similar results were obtained in a simulation on the effects of conversion of tropical savannas into grasslands and agricultural land. Decrease in precipitation was observed in all savanna regions converted to grasslands, and this decline in rainfall is attributable to changes in albedo and roughness length (Hoffmann and Jackson 2000).

Differences in albedo among vegetated surfaces are more subtle than those between vegetation and snow or soil. Vegetation albedo depends primarily on **phenology**. Leaf appearance in deciduous ecosystems increases albedo

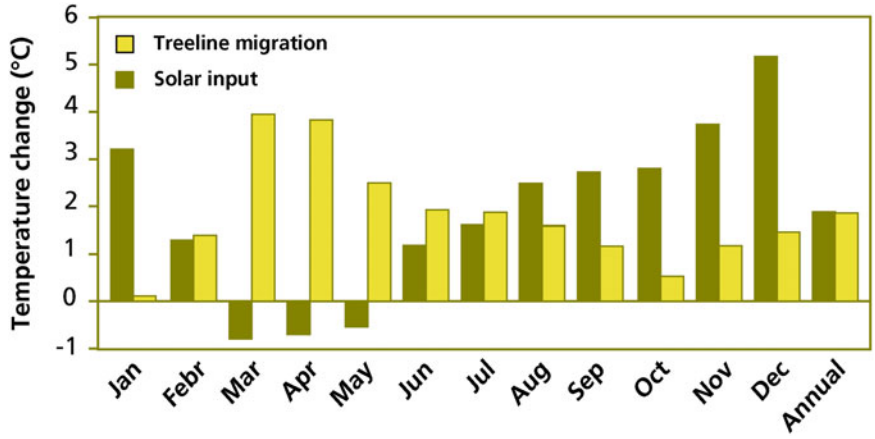

Fig. 19.6 The change in arctic air temperature at the last thermal maximum caused directly by changes in solar inputs and caused by the change in albedo associated with northward movement of treeline, as simulated by a general circulation model (redrawn from Foley et al. 1994).

if the soil surface is dark and reduces albedo over light-colored surfaces. Evergreen communities show minimal seasonal change in albedo (Hollinger et al. 2010). Even the small differences in albedo among plant species could be climatically important. For example, grasslands typically have higher albedo than forests, because of their more rapid leaf turnover and retention of dead reflective leaves in the canopy. Similarly, the higher albedo of deciduous than of conifer forests results in less energy absorption and transfer to the atmosphere (Hollinger et al. 2010). For this reason, forest fires that cause a replacement of late-successional conifers by early-successional herbs, shrubs, and deciduous trees act as a negative feedback to climate warming (Randerson et al. 2006). Policies that seek to promote ecosystem feedbacks to mitigate climate change have focused almost entirely on carbon sequestration associated with expanded forest extent and have ignored the large (and often contrasting) climate feedbacks caused by changes in **energy budget** (Betts 2000; Field et al. 2007). A valuable contribution of climate-change science to the policy arena would be a more comprehensive assessment of **ecosystem feedbacks** to the climate system. For example, the carbon sequestration effect (climate cooling) might prove to be strongest in the tropics, where warm moist conditions speed the carbon cycle, and changing cloudiness ameliorate the albedo effect. In contrast, the albedo effect (climate warming) of increased forest cover is most likely strongest at high latitudes, where there is a large albedo contrast between forests and snow-covered treeless lands. Therefore, efforts to reduce deforestation have most favorable climate consequences in the tropics, where they provide a simultaneous benefit of reducing biodiversity loss.

19.4.1.2 Surface Roughness and Energy Partitioning

The **roughness of the canopy** surface determines the degree of **coupling** between plants and the atmosphere and the extent to which stomatal conductance influences the partitioning between latent and sensible heat (Sect. 8.2; Baldocchi et al. 2004). Roughness is determined primarily by topography and vegetation structure. Tall uneven canopies have a high surface roughness that creates mechanical turbulence. The resulting eddies of air transport bulk air into the canopy and canopy air back to the free atmosphere. This increases the efficiency of water, gas, and energy exchange, relative to short-statured canopies such as those of most grasses or annual crops. The lower roughness of short-statured vegetation creates a thicker boundary layer and reduces the influence of stomatal regulation by individual leaves on overall conductance of the canopy to water loss, especially under moist conditions.

On average, the energy absorbed by an ecosystem must be balanced by energy returned to the atmosphere as sensible or latent heat flux. The ratio of sensible to latent heat flux (**Bowen ratio**) varies 100-fold among ecosystems, from less than 0.1 in tropical oceans to 10 in deserts, and depends primarily on climate and soil moisture. Ecosystems with abundant moisture have high rates of evapotranspiration (latent heat flux), and therefore a low Bowen ratio. Strong winds and rough canopies reduce temperature build-up at the surface which drives sensible heat flux, also leading to low Bowen ratios and high evapotranspiration. The Bowen ratio is important because it determines the strength of the linkage between energy exchange and the hydrological cycle. This linkage is strongest in moist ecosystems with low Bowen ratio, where most of the energy absorbed by the ecosystem is dissipated by water transfer to the atmosphere.

19.4.2 Vegetation Effects on the Hydrological Cycle

19.4.2.1 Evapotranspiration and Runoff

Climate clearly has a critical direct effect on the supply of water to ecosystems as a result of precipitation inputs. In addition, climate determines the rate at which water returns to the atmosphere due to climatic effects on soil moisture availability and the vapor pressure gradient that drives **evapotranspiration**. However, plant size, leaf area index (*LAI*), and stomatal conductance also exert strong controls over evapotranspiration**.** In

wet canopies, *LAI* determines the amount of water that can be intercepted and stored by the canopy, and plant size and canopy roughness determine the rate at which this water evaporates. Similarly, during winter, plant size and canopy roughness determine the amount of snow intercepted by the canopy and returned to the atmosphere by sublimation.

When canopies are dry, soil moisture, climate, and vegetation interact in complex ways to control evapotranspiration. Under moist-soil conditions, climate determines the driving forces for evapotranspiration (the net radiation that must be dissipated and the vapor pressure deficit of the bulk air), and plant size and canopy roughness determine the surface turbulence and boundary layer conductance that control how efficiently this water is transferred to the atmosphere. In general, the moisture content of the air (and the corresponding effect on stomatal conductance) is the most important climatic control over evapotranspiration in well coupled rough canopies, but net radiation (and the amount of energy to be dissipated) is the most important control in smooth canopies where atmosphere-canopy exchange is less tightly coupled to atmospheric conditions. *LAI* has surprisingly little influence on evapotranspiration under these moist-soil conditions; it simply determines the extent to which water evaporates from leaves *vs.* the moist soil surface (Kelliher et al. 1995). As soil moisture and soil surface evaporation decline, however, *LAI* and stomatal conductance exert increasing importance over evapotranspiration.

Plant biomass indirectly influences evapotranspiration, because of its correlation with the quantity of litter on the soil surface which influences the partitioning of water between surface **runoff** and **infiltration** into the soil:

$$dS = P - E - R - I \qquad (19.8)$$

where dS is change in soil water content, P is precipitation, R runoff, and I is infiltration. Surface **runoff** is negligible in forests and other communities with a well-developed litter layer, but can be substantial in dry ecosystems with minimal litter accumulation (Running and Coughlan 1988).

In dry environments, stomatal conductance and rooting depth exert additional influence over evapotranspiration. Desiccation-tolerant species keep their stomata open at times of lower water availability and thus support greater evapotranspiration during dry periods than do species typical of more mesic environments (Mitchell et al. 2013). Tall plants such as trees generally transpire more water than herbs, because of their more extensive root systems and greater leaf area and canopy roughness. Consequently, forest thinning reduces evapotranspiration and increases **runoff** (Saksa et al. 2017). This, in turns, increases river **streamflow** (Bosch and Hewlett 1982). Forest restoration, on the other hand, reduces run-off and streamflow (Filoso et al. 2017). In summary, plant size, which is a function of resource availability in the environment, is the major determinant of canopy water loss, although the response of stomatal conductance to plant water status becomes important under dry conditions. At the global scale, river runoff has increased during the twentieth century, primarily as a result of CO_2-induced reductions in stomatal conductance (Gedney et al. 2006).

The same plant traits that influence evapotranspiration influence **soil moisture**. In northern regions, species characteristic of steppe vegetation have faster rates of evapotranspiration than do mosses and other vegetation characteristic of tundra (Table 19.4). Either of these vegetation types can persist under the climate typical of tundra, with the faster transpiration rate of steppe plants maintaining the low soil moisture that favors these species and the slower transpiration rate of tundra species causing higher soil moisture that favors tundra species. Zimov et al. (1995) hypothesized that extirpation of mega-herbivores by humans at the end of the Pleistocene shifted the competitive balance from steppe species that tolerate grazing to tundra species. The resulting reduction in evapotranspiration would have increased soil moisture, contributing to the shift from dry steppe to mossy tundra that occurred at the end of the Pleistocene.

Table 19.4 Average evapotranspiration rate of tundra and steppe plants from weighing lysimeters under field conditions in northeast Siberia during July.

Surface type	Evapotranspiration rate (mm day^{-1})	
	Field capacity	Natural precipitation
Tundra plants		
Lichen	1.6	0.9
Moss	2.8	1.0
Steppe plants		
Agropyron	6.7	2.5
Eriophorum	5.3	3.0
Equisetum	4.0	1.6
Artemisia	6.1	2.3
Probability of tundra-steppe difference	0.03	0.02

Source: Zimov et al. (1995)
Note: Lysimeters were either maintained at field capacity by twice-daily watering or given access only to natural precipitation

19.4.2.2 Feedbacks to Climate

Species differences in **evapotranspiration** (ET) can have climatic consequences.

$$ET = T + E \tag{19.9}$$

where T is leaf transpiration and E soil surface evaporation. In most ecosystems, there is a close correlation of ET with P_g, because a high leaf area and high stomatal conductance promote both processes. In low-resource communities, however, canopies are sparse, and the soil or surface mosses contribute substantially to evapotranspiration. Below an LAI of 4, evapotranspiration becomes increasingly **uncoupled** from photosynthesis, due to proportional increase in surface **evaporation** (Schulze et al. 1994).

The increases in temperature associated with **deforestation** in the Amazon basin is likely around 1.4 °C, compared with a warming of approximately 2.0 °C expected from a doubling of atmospheric [CO_2] (Costa and Foley 2000). Simulations suggest that conversion of the Amazon basin from forest to pasture would cause a permanent warming and drying of South America (Foley et al. 2003b). Hotter and drier conditions would favor persistence of grasses, with low LAI. Transpiration contributes much of the water for rainfall over Amazonia. Satellite datasets show that rainforest transpiration enables an increase of shallow convection that moistens and destabilizes the atmosphere during the initial stages of the dry-to-wet season transition (Wright et al. 2017). This shallow convection moisture pump preconditions the atmosphere at the regional scale for a rapid increase in rain-bearing deep convection. Aerosols produced by late dry season biomass burning may alter the efficiency of this process. These results highlight the mechanisms by which interactions among land surface processes, atmospheric convection, and biomass burning may alter the timing of wet season onset, and provide a mechanistic framework for understanding how **deforestation** extends the dry season and enhances regional vulnerability to **drought**.

Environmental conditions could influence **vegetation feedbacks** to precipitation. For example, global warming caused by a doubling of atmospheric [CO_2] is predicted to increase precipitation by 8%. The reduction in stomatal conductance caused by this rise in [CO_2] (Sect. 2.1), however, reduces the magnitude of the expected precipitation increase to only 5% (Henderson-Sellers et al. 1995). Plant physiological responses to [CO_2] reduce predictions of future drought stress, and this reduction is captured by using plant-centric, rather than metrics from Earth system models (Swann et al. 2016). Atmosphere-centric models predict future increases in drought stress for more than 70% of global land area, but this drops to 37% with the use of precipitation minus evapotranspiration, a measure that represents the water flux available to downstream ecosystems and humans. On the other hand, increased plant growth and stomatal conductance caused by N deposition increases evapotranspiration and therefore precipitation. Thus, the interaction among environmental factors that influence plant growth and physiology modulate many of the terrestrial feedbacks to climate (Gedney et al. 2006).

The Amazon is one of very few continental regions where atmospheric aerosol particles and their effects on climate are dominated by natural, rather than anthropogenic sources. Fine particles,

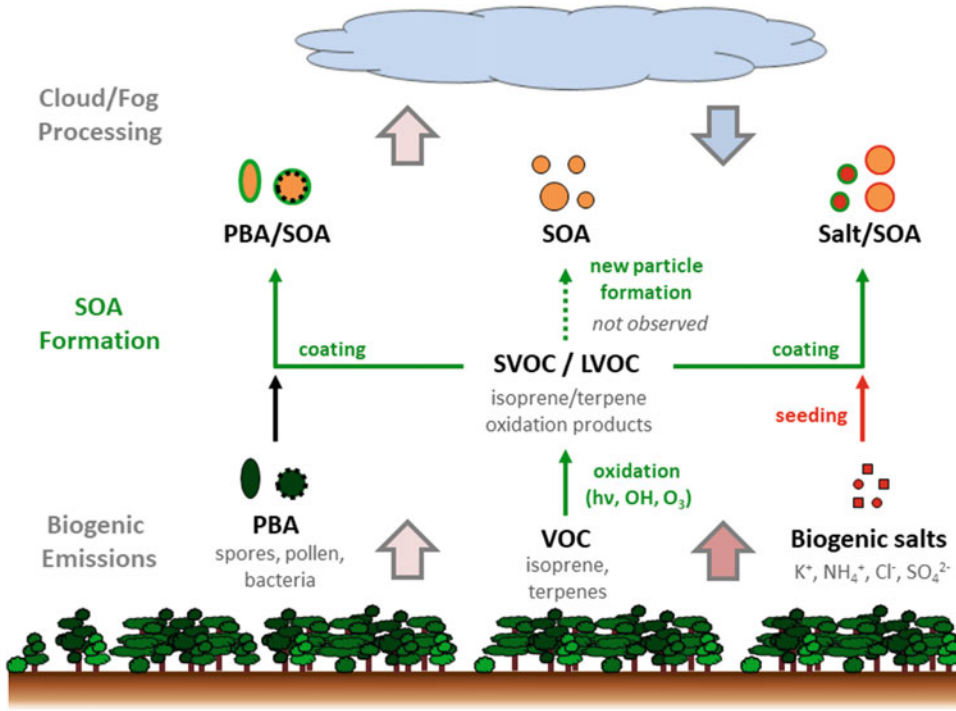

Fig. 19.7 Sources and processing of organic aerosol in pristine Amazonian boundary layer air. Formation of secondary organic aerosols (SOA) by photooxidation of volatile organic compounds (VOC) and condensation of semi- and low-volatile organic compounds (SVOC/LVOC) on primary biological aerosols (PBA) that dominate the coarse particle fraction (>1 mm), and on biogenic salt particles that serve as seeds for organic particles dominating the accumulation size range (0.1–1 mm) PBA (modified after Pöhlker et al. 2012).

predominantly composed of secondary organic material formed by oxidation of gaseous biogenic precursors, account for most cloud condensation nuclei. Minuscule particles, which are relevant as ice nuclei, consist mostly of primary biological material directly released from rainforest biota. The Amazon Basin appears to be a biogeochemical reactor, in which the biosphere and atmospheric photochemistry produce nuclei for clouds and precipitation sustaining the hydrological cycle. The prevailing regime of aerosol-cloud interactions in this natural environment is distinctly different from that in polluted regions (Pöschl et al. 2010). The origin of the particles that serve as cloud-condensation nuclei is not entirely clear, because there appears to be no new particle formation in the atmosphere. Pöhlker et al. (2012) reported that particles rich in potassium salts emitted by Amazonian vegetation can act as the seeds for the growth of organic aerosol particles that function as condensation nuclei for water droplets (Fig. 19.7). These biogenic salts provide a surface for the condensation of low- or semi-volatile organic compounds formed by the atmospheric oxidation of isoprene and terpenes, which are produced in great abundance by many plants (Sect. 7.3.3). These findings suggest that the primary emission of biogenic salt particles directly influences the concentration of cloud condensation nuclei and the microphysics of cloud formation and precipitation over the rainforest.

19.5 Moving to a Higher Level: Scaling from Physiology to the Globe

Physiological differences among species have important predictable consequences for ecosystem

and global processes. Environments with favorable climate and high resource availability support growth forms that are highly productive due to either large size or rapid growth, depending on time since disturbance. By contrast, unfavorable environments support slow-growing plants, whose well-developed defenses minimize herbivory and decomposition. Fast-growing plants have fast rates of photosynthesis and transpiration (on a mass basis), rapid tissue turnover, herbivory, and decomposition. Plant size is one of the major determinants of exchanges of carbon, nutrients, energy, and water. Vegetation differences in size and growth rate feed back to reinforce natural environmental differences, largely because large plants reduce soil moisture, and fast-growing plants produce litter that enhances nutrient availability.

At regional scales large plant size and high stomatal conductance promote evapotranspiration, and therefore precipitation. Small plant size or sparse vegetative cover dissipates more energy as sensible heat, leading to higher air temperatures. At high latitudes, large size reduces albedo by covering the snow with a dark surface, thereby promoting regional warming during winter and spring. The increasing recognition of the importance of plant traits in influencing ecosystem processes and climate provide a central role for physiological ecology in studies of ecosystem and global processes.

References

Augusto L, Achat DL, Jonard M, Vidal D, Ringeval B. 2017. Soil parent material—A major driver of plant nutrient limitations in terrestrial ecosystems. *Glob Change Biol* **23**: 3808–3824.

Baldocchi D, Sturtevant C, Contributors F. 2015. Does day and night sampling reduce spurious correlation between canopy photosynthesis and ecosystem respiration? *Agric For Met* **207**: 117–126.

Baldocchi DD, Xu L, Kiang N. 2004. How plant functional-type, weather, seasonal drought, and soil physical properties alter water and energy fluxes of an oak–grass savanna and an annual grassland. *Agric For Met* **123**: 13–39.

Beerling DJ, Osborne CP. 2006. The origin of the savanna biome. *Glob Change Biol* **12**: 2023–2031.

Betts RA. 2000. Offset of the potential carbon sink from boreal forestation by decreases in surface albedo. *Nature* **408**: 187–190.

Binkley D, Högberg P. 2016. Tamm Review: Revisiting the influence of nitrogen deposition on Swedish forests. *For Ecol Manag* **368**: 222–239.

Bokhari UG, Singh JS. 1975. Standing state and cycling of nitrogen in soil-vegetation components of prairie ecosystems. *Ann Bot* **39**: 273–285.

Bosch JM, Hewlett JD. 1982. A review of catchment experiments to determine the effect of vegetation changes on water yield and evapotranspiration. *J Hydrol* **55**: 3–23.

Bowd EJ, Banks SC, Strong CL, Lindenmayer DB. 2019. Long-term impacts of wildfire and logging on forest soils. *Nat Geosci* **12**: 113–118

Canadell JG, Le Quéré C, Raupach MR, Field CB, Buitenhuis ET, Ciais P, Conway TJ, Gillett NP, Houghton RA, Marland G. 2007. Contributions to accelerating atmospheric CO_2 growth from economic activity, carbon intensity, and efficiency of natural sinks. *Proc Natl Acad Sci USA* **104**: 18866–18870.

Chapin FS. 2003. Effects of plant traits on ecosystem and regional processes: a conceptual framework for predicting the consequences of global change. *Ann Bot* **91**: 455–463.

Chapin FS, Woodwell GM, Randerson JT, Rastetter EB, Lovett GM, Baldocchi DD, Clark DA, Harmon ME, Schimel DS, Valentini R, Wirth C, Aber JD, Cole JJ, Goulden ML, Harden JW, Heimann M, Howarth RW, Matson PA, McGuire AD, Melillo JM, Mooney HA, Neff JC, Houghton RA, Pace ML, Ryan MG, Running SW, Sala OE, Schlesinger WH, Schulze E-D. 2006. Reconciling carbon-cycle concepts, terminology, and methods. *Ecosystems* **9**: 1041–1050.

Chen G, Hayes DJ, McGuire AD. 2017. Contributions of wildland fire to terrestrial ecosystem carbon dynamics in North America from 1990 to 2012. *Glob Biogeochem Cycl* **31**: 878–900.

Choudhury BJ. 1987. Relationships between vegetation indices, radiation absorption, and net photosynthesis evaluated by a sensitivity analysis. *Rem Sens Environ* **22**: 209–233.

Ciais P, Tans PP, Trolier M, White JWC, Francey RJ. 1995. A large northern hemisphere terrestrial CO_2 sink indicated by the $^{13}C/^{12}C$ ratio of atmospheric CO_2. *Science* **269**: 1098–1102.

Clark DA, Brown S, Kicklighter DW, Chambers JQ, Thomlinson JR, Ni J, Holland EA. 2001. Net primary production in tropical forests: an evaluation and synthesis of existing field data. *Ecol Appl* **11**: 371–384.

Cole DW, Rapp M 1981. Elemental cycling in forest ecosystems. In: Reichle DE ed. *Dynamic Properties of Forest Ecosystems*. Cambridge: Cambridge University Press, 341–409.

Coskun D, Britto DT, Shi W, Kronzucker HJ. 2017. How plant root exudates shape the nitrogen cycle. *Trends Plant Sci* **22**: 661–673.

Costa MH, Foley JA. 2000. Combined effects of deforestation and doubled atmospheric CO_2 concentrations on the climate of Amazonia. *J Clim* **13**: 18–34.

Cramer W, Bondeau A, Woodward FI, Prentice IC, Betts RA, Brovkin V, Cox PM, Fisher V, Foley JA, Friend AD, Kucharik C, Lomas MR, Ramankutty N, Sitch S, Smith B, White A, Young-Molling C. 2001. Global response of terrestrial ecosystem structure and function to CO_2 and climate change: results from six dynamic global vegetation models. *Glob Change Biol* **7**: 357–373.

D'Antonio CM, Vitousek PM. 1992. Biological invasions by exotic grasses, the grass/fire cycle, and global change. *Annu Rev Ecol Syst* **23**: 63–87.

Davidson EA, Neill C, Krusche AV, Ballester VV, Markewitz D, Figueiredo RdO. 2004. Loss of nutrients from terrestrial ecosystems to streams and the atmosphere following land use change in Amazonia. *Geophys Monog Ser* **153**: 147–158.

Dawes MA, Philipson CD, Fonti P, Bebi P, Hättenschwiler S, Hagedorn F, Rixen C. 2015. Soil warming and CO_2 enrichment induce biomass shifts in alpine tree line vegetation. *Glob Change Biol* **21**: 2005–2021.

Elser JJ, Andersen T, Baron JS, Bergström A-K, Jansson M, Kyle M, Nydick KR, Steger L, Hessen DO. 2009. Shifts in lake N:P stoichiometry and nutrient limitation driven by atmospheric nitrogen deposition. *Science*: 835–837.

Fang J, Guo Z, Hu H, Kato T, Muraoka H, Son Y. 2014. Forest biomass carbon sinks in East Asia, with special reference to the relative contributions of forest expansion and forest growth. *Glob Change Biol* **20**: 2019–2030.

Farquhar GD. 1989. Models of integrated photosynthesis of cells and leaves. *Phil Trans R Soc Lond B* **323**: 357–367.

Field CB 1991. Ecological scaling of carbon gain to stress and resource availability. In: Mooney HA, Winner WE, Pell EJ eds. *Integrated Responses of Plants to Stress*. San Diego: Academic, 35–65.

Field CB, Lobell DB, Peters HA, Chiariello NR. 2007. Feedbacks of terrestrial ecosystems to climate change. *Annu Rev Environ Res* **32**: 1–29.

Filoso S, Bezerra MO, Weiss KCB, Palmer MA. 2017. Impacts of forest restoration on water yield: a systematic review. *PLoS ONE* **12**: e0183210.

Foley JA, Kutzbach JE, Coe MT, Levis S. 1994. Feedbacks between climate and boreal forests during the Holocene epoch. *Nature* **371**: 52–54.

Foley JA, Coe MT, Scheffer M, Wang G. 2003a. Regime shifts in the Sahara and Sahel: interactions between ecological and climatic systems in Northern Africa. *Ecosystems* **6**: 524–532.

Foley JA, Costa MH, Delire C, Ramankutty N, Snyder P. 2003b. Green surprise? How terrestrial ecosystems could affect Earth's climate. *Front Ecol Evol* **1**: 38–44.

Gedney N, Cox PM, Betts RA, Boucher O, Huntingford C, Stott PA. 2006. Detection of a direct carbon dioxide effect in continental river runoff records. *Nature* **439**: 835.

Giguère-Croteau C, Boucher É, Bergeron Y, Girardin MP, Drobyshev I, Silva LCR, Hélie J-F, Garneau M. 2019. North America's oldest boreal trees are more efficient water users due to increased [CO_2], but do not grow faster. *Proc Natl Acad Sci USA* **116**: 2749–2754.

Goetz SJ, Bunn AG, Fiske GJ, Houghton RA. 2005. Satellite-observed photosynthetic trends across boreal North America associated with climate and fire disturbance. *Proc Natl Acad Sci USA* **102**: 13521–13525.

Goward SN, Tucker CJ, Dye DG. 1985. North American vegetation patterns observed with the NOAA-7 advanced very high resolution radiometer. *Vegetatio* **64**: 3–14.

Graetz R. 1991. The nature and significance of the feedback of changes in terrestrial vegetation on global atmospheric and climatic change. *Clim Change* **18**: 147–173.

Gray JT, Schlesinger WH 1981. Nutrient cycling in Mediterranean type ecosystems. In: Miller PC ed. *Resource Use by Chaparral and Matorral*. New York: Springer-Verlag, 259–285.

Grime JP, Hunt R. 1975. Relative growth-rate: its range and adaptive significance in a local flora. *J Ecol* **63**: 393–422.

Harsch MA, Hulme PE, McGlone MS, Duncan RP. 2009. Are treelines advancing? A global meta-analysis of treeline response to climate warming. *Ecol Lett* **12**: 1040–1049.

Harte J, Kinzig AP. 1993. Mutualism and competition between plants and decomposers: implications for nutrient allocation in ecosystems. *Amer Nat* **141**: 829–846.

Henderson-Sellers A, McGuffie K, Gross C. 1995. Sensitivity of global climate model simulations to increased stomatal resistance and $C0_2$ increases. *J Clim* **8**: 1738–1756.

Hoffmann WA, Jackson RB. 2000. Vegetation–climate feedbacks in the conversion of tropical savanna to grassland. *J Clim* **13**: 1593–1602.

Högberg P, Näsholm T, Franklin O, Högberg MN. 2017. Tamm Review: On the nature of the nitrogen limitation to plant growth in Fennoscandian boreal forests. *For Ecol Manag* **403**: 161–185.

Hollinger DY, Ollinger SV, Richardson AD, Meyers TP, Dail DB, Martin ME, Scott NA, Arkebauer TJ, Baldocchi DD, Clark KL, Curtis PS, Davis KJ, Desai AR, Dragoni D, Goulden ML, Gu L, Katul GG, PallardY SG, Paw UKT, Schmid HP, Stoy PC, Suyker AE, Verma SB. 2010. Albedo estimates for land surface models and support for a new paradigm based on foliage nitrogen concentration. *Glob Change Biol* **16**: 696–710.

Huston MA, Wolverton S. 2009. The global distribution of net primary production: resolving the paradox. *Ecol Monogr* **79**: 343–377.

Kasischke ES, Christensen NL, Stocks BJ. 1995. Fire, global warming, and the carbon balance of boreal forests. *Ecol Appl* **5**: 437–451.

Kasischke ES, Turetsky MR. 2006. Recent changes in the fire regime across the North American boreal region—Spatial and temporal patterns of burning across Canada and Alaska. *Geophys Res Lett* **33**.

Kauppi PE, Mielikäinen K, Kuusela K. 1992. Biomass and carbon budget of European forests, 1971 to 1990. *Science* **256**: 70–74.

Kays S, Harper JL. 1974. The regulation of plant and tiller density in a grass sward. *J Ecol* **62**: 97–105.

Kelliher FM, Leuning R, Raupach MR, Schulze ED. 1995. Maximum conductances for evaporation from global vegetation types. *Agric For Met* **73**: 1–16.

Körner C. 2013. Growth controls photosynthesis – mostly. *Nov Acta Leopold* **114**: 273–283.

Lata J-C, Degrange V, Raynaud X, Maron P-A, Lensir R, Abbadie L. 2004. Grass populations control nitrification in savanna soils. *Funct Ecol* **18**: 605–611.

Lawrence D, Vandecar K. 2014. Effects of tropical deforestation on climate and agriculture. *Nat Clim Change* **5**: 27–36.

Le Quéré C, Andrew RM, Friedlingstein P, Sitch S, Pongratz J, Manning AC, Korsbakken JI, Peters GP, Canadell JG, Jackson RB, Boden TA, Tans PP, Andrews OD, Arora VK, Bakker DCE, Barbero L, Becker M, Betts RA, Bopp L, Chevallier F, Chini LP, Ciais P, Cosca CE, Cross J, Currie, Gasser T, Harris I, Hauck J, Haverd V, Houghton RA, Hunt CW, Hurtt G, Ilyina T, Jain AK, Kato E, Kautz M, Keeling RF, Klein Goldewijk K, Körtzinger A, Landschützer P, Lefèvre N, Lenton A, Lienert S, Lima I, Lombardozzi D, Metzl N, Millero F, Monteiro PMS, Munro DR, Nabel JEMS, Nakaoka S-i, Nojiri Y, Padin XA, Peregon A, Pfeil B, Pierrot D, Poulter B, Rehder G, Reimer J, Rödenbeck C, Schwinger J, Séférian R, Skjelvan I, Stocker BD, Tian H, Tilbrook B, Tubiello FN, Van der Laan-Luijkx IT, Van der Werf GR, Van Heuven S, Viovy N, Vuichard N, Walker AP, Watson AJ, Wiltshire AJ, Zaehle S, Zhu D. 2017. Global Carbon Budget 2017. *Earth Syst Sci Data* **10**: 405–448.

McGuire AD, Chapin FS, Walsh JEC, Wirth. 2006. Integrated regional changes in arctic climate feedbacks: implications for the global climate system. *Annu Rev Environ Res* **31**: 61–91.

McLaren JR, Buckeridge KM, Weg MJ, Shaver GR, Schimel JP, Gough L. 2017. Shrub encroachment in Arctic tundra: *Betula nana* effects on above- and belowground litter decomposition. *Ecology* **98**: 1361–1376.

McNaughton SJ, Banyikwa FF, McNaughton MM. 1997. Promotion of the cycling of diet-enhancing nutrients by African grazers. *Science* **278**: 1798–1800.

Milich L, Weiss E. 2000. GAC NDVI interannual coefficient of variation (CoV) images: Ground truth sampling of the Sahel along north-south transects. *Int J Rem Sens* **21**: 235–260.

Mitchell PJ, O'Grady AP, Tissue DT, White DA, Ottenschlaeger ML, Pinkard EA. 2013. Drought response strategies define the relative contributions of hydraulic dysfunction and carbohydrate depletion during tree mortality. *New Phytol* **197**: 862–872.

Monteith JL. 1977. Climate and the efficiency of crop production in Britain. *Phil Trans R Soc Lond B* **281**: 277–294.

Niklas KJ, Enquist BJ. 2001. Invariant scaling relationships for interspecific plant biomass production rates and body size. *Proc Natl Acad Sci USA* **98**: 2922–2927.

Odum EP. 1966. The strategy of ecosystem development. *Science* **164**: 262.270.

Pagani M, Freeman KH, Arthur MA. 1999. Late Miocene atmospheric CO_2 concentrations and the expansion of C_4 grasses. *Science* **285**: 876–879.

Pan Y, Birdsey RA, Fang J, Houghton R, Kauppi PE, Kurz WA, Phillips OL, Shvidenko A, Lewis SL, Canadell JG, Ciais P, Jackson RB, Pacala SW, McGuire AD, Piao S, Rautiainen A, Sitch S, Hayes D. 2011. A large and persistent carbon sink in the world's forests. *Science* **333**: 988–993.

Pöhlker C, Wiedemann KT, Sinha B, Shiraiwa M, Gunthe SS, Smith M, Su H, Artaxo P, Chen Q, Cheng Y, Elbert W, Gilles MK, Kilcoyne ALD, Moffet RC, Weigand M, Martin ST, Pöschl U, Andreae MO. 2012. Biogenic potassium salt particles as seeds for secondary organic aerosol in the Amazon. *Science* **337**: 1075–1078.

Pöschl U, Martin ST, Sinha B, Chen Q, Gunthe SS, Huffman JA, Borrmann S, Farmer DK, Garland RM, Helas G, Jimenez JL, King SM, Manzi A, Mikhailov E, Pauliquevis T, Petters MD, Prenni AJ, Roldin P, Rose D, Schneider J, Su H, Zorn SR, Artaxo P, Andreae MO. 2010. Rainforest aerosols as biogenic nuclei of clouds and precipitation in the Amazon. *Science* **329**: 1513–1516.

Poulter B, Frank D, Ciais P, Myneni RB, Andela N, Bi J, Broquet G, Canadell JG, Chevallier F, Liu YY, Running SW, Sitch S, van der Werf GR. 2014. Contribution of semi-arid ecosystems to interannual variability of the global carbon cycle. *Nature* **509**: 600–603.

Randerson JT, Liu H, Flanner MG, Chambers SD, Jin Y, Hess PG, Pfister G, Mack MC, Treseder KK, Welp LR, Chapin FS, Harden JW, Goulden ML, Lyons E, Neff JC, Schuur EAG, Zender CS. 2006. The impact of boreal forest fire on climate warming. *Science* **314**: 1130–1132.

Rasmussen C, Heckman K, Wieder WR, Keiluweit M, Lawrence CR, Berhe AA, Blankinship JC, Crow SE, Druhan JL, Hicks Pries CE, Marin-Spiotta E, Plante AF, Schädel C, Schimel JP, Sierra CA, Thompson A, Wagai R. 2018. Beyond clay: towards an improved set of variables for predicting soil organic matter content. *Biogeochemistry* **137**: 297–306.

Reich PB, Oleksyn J. 2004. Global patterns of plant leaf N and P in relation to temperature and latitude. *Proc Natl Acad Sci USA* **101**: 11001–11006.

Robles M, Chapin FS. 1995. Comparison of the influence of two exotic species on ecosystem processes in the Berkeley Hills. *Madroño* **42**: 349–357.

Running SW, Coughlan JC. 1988. A general model of forest ecosystem processes for regional applications I. Hydrologic balance, canopy gas exchange and primary production processes. *Ecol Model* **42**: 125–154.

Saksa PC, Conklin MH, Battles JJ, Tague CL, Bales RC. 2017. Forest thinning impacts on the water balance of Sierra Nevada mixed-conifer headwater basins. *Water Res Res* **53**: 5364–5381.

Sala OE, Parton WJ, Joyce LA, Lauenroth WK. 1988. Primary production of the central grassland region of the United States. *Ecology* **69**: 40–45.

Schimper AFW. 1898. *Pflanzengeographie und physiologische Grundlage*. Jena: Verlag von Gustav Fischer.

Schlesinger WH. 1997. *Biogeochemistry: An Analysis of Global Change, second edition*. San Diego: Academic.

Schlesinger WH, Bernhardt ES. 2013. *Biogeochemistry: An Analysis of Global Change, third edition*. New York: Elsevier/Academic press.

Schoennagel T, Veblen TT, Romme WH. 2004. The interaction of fire, fuels, and climate across Rocky Mountain forests. *BioSci* **54**: 661–676.

Schulze E-D, Kelliher FM, Körner C, Lloyd J, Leuning R. 1994. Relationships among maximum stomatal conductance, ecosystem surface conductance, carbon assimilation rate, and plant nitrogen nutrition: a global ecology scaling exercise. *Annu Rev Ecol Syst* **25**: 629–662.

Schuur EAG. 2003. Productivity and global climate revisited: the sensitivity of tropical forest growth to precipitation. *Ecology* **84**: 1165–1170.

Staver AC, Archibald S, Levin SA. 2011. The global extent and determinants of savanna and forest as alternative biome states. *Science* **334**: 230–232.

Swann ALS, Hoffman FM, Koven CD, Randerson JT. 2016. Plant responses to increasing CO_2 reduce estimates of climate impacts on drought severity. *Proc Natl Acad Sci USA* **113**: 10019–10024.

Tilman D. 1988. *Plant Strategies and the Dynamics and Function of Plant Communities*. Princeton: Princeton University Press.

Vandermeer JH, Goldberg DE. 2013. *Population Ecology: First Principles*. Princeton: Princeton University Press.

Vitousek PM. 2004. *Nutrient Cycling and Limitation: Hawai'i as a Model System*. Princeton, New Jersey: Princeton University Press.

Vitousek PM, Aber JD, Howarth RW, Likens GE, Matson PA, Schindler DW, Schlesinger WH, Tilman DG. 1997. Human alteration of the global nitrogen cycle: sources and consequences. *Ecol Appl* **7**: 737–750.

Vitousek PM, Howarth RW. 1991. Nitrogen limitation on land and in the sea: how can it occur? *Biogeochemistry* **13**: 87–115.

Wagner FH, Hérault B, Bonal D, Stahl C, Anderson LO, Baker TR, Becker GS, Beeckman H, Boanerges Souza D, Botosso PC, Bowman DMJS, Bräuning A, Brede B, Brown FI, Camarero JJ, Camargo PB, Cardoso FCG, Carvalho FA, Castro W, Chagas RK, Chave J, Chidumayo EN, Clark DA, Costa FRC, Couralet C, da Silva Mauricio PH, Dalitz H, de Castro VR, de Freitas Milani JE, de Oliveira EC, de Souza Arruda L, Devineau JL, Drew DM, Dünisch O, Durigan G, Elifuraha E, Fedele M, Ferreira Fedele L, Figueiredo Filho A, Finger CAG, Franco AC, Freitas Júnior JL, Galvão F, Gebrekirstos A, Gliniars R, Graça PMLDA, Griffiths AD, Grogan J, Guan K, Homeier J, Kanieski MR, Kho LK, Koenig J, Kohler SV, Krepkowski J, Lemos-Filho JP, Lieberman D, Lieberman ME, Lisi CS, Longhi Santos T, López Ayala JL, Maeda EE, Malhi Y, Maria VRB, Marques MCM, Marques R, Maza Chamba H, Mbwambo L, Melgaço KLL, Mendivelso HA, Murphy BP, O'Brien JJ, Oberbauer SF, Okada N, Pélissier R, Prior LD, Roig FA, Ross M, Rossatto DR, Rossi V, Rowland L, Rutishauser E, Santana H, Schulze M, Selhorst D, Silva WR, Silveira M, Spannl S, Swaine MD, Toledo JJ, Toledo MM, Toledo M, Toma T, Tomazello Filho M, Valdez Hernández JI, Verbesselt J, Vieira SA, Vincent G, Volkmer de Castilho C, Volland F, Worbes M, Zanon MLB, Aragão LEOC. 2016. Climate seasonality limits leaf carbon assimilation and wood productivity in tropical forests. *Biogeosciences* **13**: 2537–2562.

Wardle DA, Walker LR, Bardgett RD. 2004. Ecosystem properties and forest decline in contrasting long-term chronosequences. *Science* **305**: 509–513.

Wei X, Shao M, Gale W, Li L. 2014. Global pattern of soil carbon losses due to the conversion of forests to agricultural land. *Sci Rep* **4**: 4062.

Weller DE. 1987. A reevaluation of the −3/2 power rule of plant self-thinning. *Ecol Monogr* **57**: 23–43.

Westoby M. 1984. The self-thinning rule. *Adv Ecol Res* **14**: 167–225.

Wright JS, Fu R, Worden JR, Chakraborty S, Clinton NE, Risi C, Sun Y, Yin L. 2017. Rainforest-initiated wet season onset over the southern Amazon. *Proc Natl Acad Sci USA* **114**: 8481–8486.

Yoda K. 1963. Self-thinning in overcrowded pure stands under cultivated and natural conditions (Intraspecific competition among higher plants. XI). *J Biol Osaka City Univ* **14**: 107–129.

Zhou L, Tian Y, Myneni RB, Ciais P, Saatchi S, Liu YY, Piao S, Chen H, Vermote EF, Song C, Hwang T. 2014. Widespread decline of Congo rainforest greenness in the past decade. *Nature* **509**: 86–89-.

Zimov SA, Chuprynin VI, Oreshko AP, Chapin FS, Reynolds JF, Chapin MC. 1995. Steppe-tundra transition: a herbivore-driven biome shift at the end of the Pleistocene. *Amer Nat* **146**: 765–794.

Glossary

Words printed in *italic* are explained elsewhere in the Glossary

Abaxial located on the side furthest from the axis, *e.g.*, the lower side of a leaf

Abiotic not directly caused or induced by organisms

Absorptance the ratio of the radiant flux absorbed by a body to that incident upon it

Abscisic acid, ABA *phytohormone* (15-carbon compound that resembles the terminal portion of some *carotenoid* molecules) involved in *stress* responses; its name is derived from its involvement in leaf abscission; it reduces cell expansion and causes *stomatal* closure

Acclimation Increased tolerance to *stress* and/or improved plant performance as a result of structural and physiological adjustment by individual plants to specific environmental conditions (see also *plasticity*)

Accumulation build-up of storage products resulting from an excess of supply over *demand*; also termed interim deposition

Acidifuge avoiding acid soils; with a preference for a substrate that does not have a low pH

Active (or reactive) oxygen species (ROS) hydrogen peroxide (H_2O_2), superoxide radicals (O_2^-), and hydroxyl radicals ($OH^·$), the compounds can cause cell damage, but are also involved in *signal transduction*

Active transport transport of molecules across a *membrane* against an electrochemical gradient through expenditure of metabolic energy

Acyanogenic not releasing cyanide

Adaptation evolutionary adjustment of the genetic basis of a trait that enhances the performance in a specific environment

Adaxial located on the side nearest to the axis, *e.g.*, the upper side of a leaf

Adsorption binding of ions or molecules to a surface (*e.g.*, of a soil particle or a root)

Advection net horizontal transfer of gases

Aerenchyma tissue with large air spaces that facilitate transport of gases in plants

Agglutinin synonym for *lectin*

Albedo fraction of the incident short-wave radiation reflected by a surface (typically plant cover or bare soil or rock)

Alkaloid *secondary plant compound* (often toxic), characterized by its alkaline reaction and a heterocyclic ring (*e.g.*, nicotine, caffeine, and colchicine)

Allelochemical *secondary metabolite*, released by living plants or decomposing plant *litter* that (either negatively or positively) affects other organisms

Allelopathy suppression of growth of one plant by another of a different species due to the release of toxic substances

Allocation proportional distribution of products or newly acquired resources among different organs or functions in a plant

Alternative oxidase *mitochondria*l enzyme catalyzing the transfer of electrons from ubiquinol (the reduced form of ubiquinone) to O_2

H. Lambers, R. S. Oliveira, *Plant Physiological Ecology*, https://doi.org/10.1007/978-3-030-29639-1

Alternative pathway (of respiration) nonphosphorylating electron-transport pathway in the inner *membrane* of plant *mitochondria*, transporting electrons from ubiquinol (the reduced form of ubiquinone) to O_2, catalyzed by the *alternative oxidase*

Amphistomatous with *stomata* at both the *adaxial* (upper) and *abaxial* (lower) sides of a leaf

Amylase *starch*-hydrolyzing enzyme

Anion negatively charged ion

Anisotropic not equal in all directions; for example, the longitudinal walls of anisotropic cells have different chemical and biophysical properties from those of the radial walls

Anoxia absence of oxygen in (part of) a plant's environment

Annual species with a life cycle of less then a year; the short life cycle can be environmentally or developmentally determined

Antiport cotransport of one compound in one direction coupled to transport of another compound (mostly H^+) in the opposite direction

Apatite $Ca_5(PO_4)_3(OH,F)$; it accounts for 95% of the total P in igneous rock, and constitutes a major substrate for weathering, which releases inorganic phosphate for plants and microorganisms

Apoenzyme Enzymatic protein that requires a *coenzyme* to function

Apoplast (=apoplasm) space in a plant's tissue outside the space enclosed by plasma *membrane*s (*symplast*); it includes the *cell wall*s and the dead tissues of the xylem

Apoplastic (=apoplasmic) phloem loading transport of assimilates from *mesophyll* to the sieve tubes of the *phloem* occurring partly through the *apoplast*

Aquaporin water-channel protein in a *membrane*

Arbuscular mycorrhiza a type of *mycorrhiza* that forms arbuscules (highly branched exchange structures) within cortical cells of the root

Assimilation incorporation of an inorganic resource (*e.g.*, CO_2 or NH_4^+) into organic compounds (in the case of CO_2 assimilation also used as a synonym for *photosynthesis*)

ATPase enzyme catalyzing the *hydrolysis* of ATP, producing ADP and P_i; the energy from this hydrolysis is used to pump protons across a membrane (*e.g.*, plasma *membrane*, tonoplast), thus generating an electrochemical gradient

ATPase/ATP synthase enzyme complex in the inner *membrane* of *mitochondria* and the *thylakoid membrane* of *chloroplasts* catalyzing the formation of ATP, driven by the *proton-motive force* (pmf)

Autotoxicity deleterious effect of a chemical compound released by plants of the same species

Autotrophic growth increment in mass, volume, length, or area of plants or parts thereof which depend on carbon fixed in *photosynthesis* by the growing organism itself (see also *heterotrophic growth*)

Autotrophic respiration *respiration* by autotrophic plants and their associated *mycorrhizas* and *symbiotic N_2-fixing* structures (see also *heterotrophic respiration*)

Auxin *phytohormone* (indole-3-acetic acid) involved in growth promotion and meristem *differentiation* ; the name literally means enhancing, and is derived from its growth-promoting action; there are also synthetic auxins

Avoidance plant *strategy* of resisting adverse conditions by preventing deleterious effects of these conditions, *e.g.*, winter seed *dormancy*

Bacteroid state of *rhizobia* after they have penetrated the root and the *symbiosis* has been established

Bark Tissue with both a protective (outer bark) and transport (inner bark) function; inner bark consists of secondary *phloem* that carries sugars, amino acids and minerals from a *source* to a *sink*

Biennial species whose individuals typically live for two growing seasons, vegetative growth in the first year and continued growth and seed production in the second year; several species known as biennials can, however, have an extended vegetative period (*monocarpic perennial*), others are strictly biennial

Biomass Mass of plants (and other living organisms)

Biomass density dry mass of plant tissue per unit of fresh mass or volume (in the first case, the presence of intercellular air spaces is not taken into account)

Biotic caused or induced by organisms

Biotic filter *biotic* interactions, which eliminate species that would otherwise have survived the *abiotic* environment of a site

Blue-light receptors two classes of *photoreceptor*s, crytochromes and phototropins, that absorb in the blue region of the spectrum; the receptors are involved, *e.g.*, in the perception of irradiance and the directional component of light and thus affect *photomorphogenesis*

Bolting rapid extension of the flowering stalk

Boundary layer thin layer of air, water or soil around the leaf or root with reduced mass transport and increased reliance on *diffusion* for transport processes, conditions differ from those further away

Boundary layer conductance/resistance *conductance/resistance* for transport of CO_2, water vapor or heat between the leaf surface and the atmosphere measured across the *boundary layer*

Bowen ratio the ratio between sensible heat loss and heat loss due to *transpiration*

Bulk density mass of dry soil per unit volume

Bulk soil soil beyond the immediate influence of plant roots (see *boundary layer*)

Bundle sheath cells cells surrounding the vascular bundle of a leaf

C_3 photosynthesis photosynthetic pathway in which the first step of CO_2 *assimilation* is the *carboxylation* of Ribulose 1,5-bisphosphate (RuBP) by *Rubisco*; the first product is phosphoglyceric acid (PGA), a three-carbon intermediate

C_4 photosynthesis photosynthetic pathway in which the first step of CO_2 *assimilation* is the *carboxylation* of phophoenolpyruvate (PEP) by PEP carboxylase during the day; the first product is oxaloacetic acid (OAA) a four-carbon intermediate

Calcicole species with a preference for calcareous or high-pH soils

Calcifuge species that typically occupies acidic soils and is absent from calcareous or high-pH soils

Callose b-(1-3)-polymer of glucose, synthesized in sieve tube elements of the *phloem* in response to damage, sealing of the sieve tubes; callose is also produced in other cells upon microbial attack, thus providing a physical barrier

Calmodulin ubiquitous Ca^{2+}-binding protein whose binding to other proteins depends on the intracellular Ca^{2+} concentration; component of *signal-transduction pathways*

Calvin cycle (Calvin-Benson cycle, carbon reduction cycle) pathway of photosynthetic CO_2 *assimilation* beginning with *carboxylation* of RuBP by *Rubisco*

Canopy conductance/resistance *conductance/resistance* for transport of CO_2, water vapor or heat between the plant canopy and the atmosphere measured across the *boundary layer* of the canopy

Carbamylation reaction between CO_2 and an amino-group; in many species *Rubisco* is activated by carbamylation, catalyzed by *Rubisco activase*

Carbonic anhydrase enzyme catalyzing the interconversion of HCO_3^- and CO_2

Carboxylate organic acid minus its protons

Carboxylation binding of a CO_2 molecule to a CO_2-acceptor molecule

Carboxylation efficiency initial slope of the CO_2-response curve of *photosynthesis*

Carotenoid accessory photosynthetic pigment; carotenoids of the *xanthophyll cycle* play a role in dissipation of excess energy

Carrier protein involved in ion transport across a *membrane*

Caruncle (=*strophiole*) an outgrowth of a seed coat, near the *hilum*; preformed weak site in the seed coat

Casparian band/strip waxy suberin impregnation on the radial and transverse wall of *endodermis* and *exodermis* cells that renders the wall impermeable to water

Cation positively charged ion

Cavitation breakage of a water column in a xylem conduit due to a sudden phase change from liquid to vapor

Cellulose structural polymer of glucose; major component of plant *cell walls* giving tensile strength

Cell wall structural matrix surrounding plant cells; part of the *apoplast*

Cell-wall elasticity reversible change in *cell wall* dimensions

Cell-wall extensibility irreversible extension of *cell walls*, due to structural changes

Chaperones group of *stress proteins* that are encoded by a multigene family in the nucleus; chaperones bind to and stabilize an otherwise unstable conformation and, thus, mediate the correct assembly of other proteins

Chelate compound that combines reversibly, usually with high affinity, with a metal ion (*e.g.*, iron, copper or calcium)

Chelator *cation*-binding organic molecule, such as citric acid, malic acid and *phytosiderophores*

Chemiosmotic model theory accounting for the synthesis of ATP driven by a *proton-motive force*

Chilling injury/tolerance injury caused by exposure of plants or tissues to low temperatures (> 0°C); *tolerance* of such temperatures.

Chitin polymer of N-acetylglucosamine; component of the exoskeleton of arthropods and the *cell wall* of fungi, but not of plants

Chitinase chitin-hydrolyzing enzyme that breaks down fungal *cell walls*

Chlorenchyma tissue containing *chloroplasts*

Chlorophyll green pigment in the photosynthetic *membrane* (*thylakoid*) involved in light capture as the first step in *photosynthesis*

Chloroplast organelle (plastid) in which *photosynthesis* occurs

Chromophore light-absorbing constituent of a macromolecule (*photoreceptor*) that is responsible for light absorption

Citric acid cycle *Tricarboxylic acid cycle*

Climax species species that are confined to later stages of succession in a plant community; as opposite to *pioneer*

Clonal growth asexual production of physiologically complete plants; a form of vegetative reproduction

Cluster roots bottle-brush-like or Christmas-tree-like structures in roots with a dense packing of root hairs, releasing *carboxylates* into the *rhizosphere*, thus solubilizing poorly available nutrients (*e.g.*, phosphate) in the soil

CO_2-compensation point CO_2 concentration at which the rate of CO_2 *assimilation* by *photosynthesis* is balanced by the rate of CO_2 production by *respiration*

Coenzyme a nonproteinaceous organic substance that combines with a specific protein, the *apoenzyme*

Coevolution evolution of two (or more) species of which at least one depends on the other as a result of selection by mutual interactions

Cofactor inorganic ion or *coenzyme* required for an enzyme's activity

Cohesion theory accounts for the ascent of sap in the xylem due to the cohesive forces between ascending water molecules under high tension and the adhesive forces between water and capillaries in the wall of xylem conduits

Companion cell cell type in the *phloem*, adjacent to sieve element, involved in phloem loading

Compartmentation restriction of compounds or processes to specific cells, or parts of a cell, such as storage of *secondary metabolite*s in vacuoles

Compatible interaction response of a susceptible host to a virulent pathogen; positive interaction between pollen and pistil allowing guidance of the sperm cells toward the ovule

Compatible solute solute that has no deleterious effect on metabolism at high concentrations

Compensation point conditions (temperature, $[CO_2]$, light) where net CO_2 exchange by a leaf or plant is zero (*i.e. photosynthesis* equals *respiration*)

Competition interaction among organisms (of the same or different species), which utilize common resources that are in short supply (resource competition), or which harm one another in the process of seeking a resource, even if the resource is not in short supply (interference competition)

Competitive ability probability of winning in *competition* with another species in a particular environment

Conductance flux per unit driving force (*e.g.*, concentration gradient); inverse of resistance

Constitutive produced in constant amount (as opposed to regulated) (*e.g.*, for example, genes can be expressed constitutively)

Constitutive defense background level of plant defense in the absence of induction by herbivores or pathogens

Construction cost carbon and nutrients required to produce new tissue, including the *respiration* associated with the biosynthetic pathways

Contractile roots mature roots that decrease in length, while increasing in diameter, thus pulling the plant deeper in the soil, as in geophytes

Convective heat transfer direct transfer of heat (*e.g.*, from leaf to air) and further transport by turbulent movement

Convergent evolution process whereby, in organisms that are not closely related, similar traits evolve independently as a result of *adaptation* to similar environments or ecological niches

Coupling factor *ATP-synthetase* in thylakoid *membrane* of *chloroplasts* and inner membrane of *mitochondria*

Crassulacean acid metabolism photosynthetic pathway in which the first step of CO_2 *assimilation* is the *carboxylation* of phophoenolpyruvate (PEP) by PEP carboxylase; the first product is oxaloacetic acid (OAA) a four-carbon intermediate; in contrast to *C_4 photosynthesis*, in CAM *photosynthesis* the CO_2 assimilation occurs predominantly during the night with open *stomata*

Crista fold of the inner *mitochondrial membrane*

Critical daylength length of the night triggering flowering

Cross-resistance The phenomenon in which an organism that has acquired *resistance* to one pathogen or herbivore through direct exposure simultaneously has acquired resistance to other pathogens or herbivores to which it has not been exposed. Cross-resistance arises because the biological mechanism of resistance is the same and arises through identical genetic mutations.

Cross-talk Communication between different *signal transduction pathways*

Cryptochrome *blue- light-absorbing photoreceptor*, involved in *photomorphogenesis*

Cuticle waxy coating of external plant surfaces

Cuticular conductance/resistance *conductance/resistance* for transport of CO_2 or water vapor movement through the *cuticle*

Cutin waxy substances that are part of the *cuticle*; polymer consisting of many long-chain hydroxy fatty acids that are attached to each other by ester linkages, forming a rigid three-dimensional network

Cyanogenic releasing cyanide

Cytochrome colored, heme-containing protein that transfers electrons in the respiratory and photosynthetic electron transport chain

Cytochrome oxidase *mitochondrial* enzyme catalyzing the final step in the transfer of electrons from organic molecules to O_2

Cytochrome P-450 element in the synthesis of anthocyanins and in the detoxification of *xenobiotics*

Cytochrome pathway phosphorylating electron-transport pathway in the inner *membrane* of plant *mitochondria*, transporting electrons from NAD(P)H or $FADH_2$ to O_2, with *cytochrome oxidase* being the terminal oxidase

Cytokinin(s) a class of *phytohormones*, involved, *e.g.*, in the delay of leaf *senescence*, cell division, cell extension, release of *dormancy* of buds and *chloroplast differentiation*

Cytoplasm contents of a cell that are contained within its plasma *membrane*, but outside the vacuole and the nucleus

Cytosol cellular matrix in which *cytoplasmic* organelles are suspended

Dark reaction carbon fixation during *photosynthesis*; does not directly require light but uses the products of the light reaction (see also *Calvin cycle*)

Dark respiration processes in the *cytosol*, *plastids*, and *mitochondria* that break down carbon-containing compounds and generate ATP; it produces CO_2 and consumes O_2 when aerobic; when referring to gas exchange, all decarboxylation and O_2-consuming processes are included, apart form *photorespiration*

Deciduous Having leaves that fall off or are shed seasonally in response to specific environmental cues, such as occur during or preceding unfavorable seasons (see also *evergreen*)

Decomposition breakdown of organic matter through fragmentation, microbial and chemical alteration, and leaching

Defense compound *secondary metabolite* conferring some degree of protection from pathogens or herbivores

Dehydrins immunologically distinct family of proteins (*Lea* D11 family) that typically accumulate in plants during the late stages of embryogenesis or in response to any environmental influence that has a dehydrating effect

Delayed greening pattern of leaf development typical of shade-tolerant rain-forest species; leaves are initially white, red, blue, or light-green during the stage of leaf expansion, reflecting their low concentration of *chlorophyll* and associated photosynthetic proteins

Demand requirement; the term is used in the context of the control of the rate of a process (*e.g.*, nutrient uptake, CO_2 *assimilation*) by the amount needed

Demand function dependence of net CO_2 *assimilation* rate on the intercellular or *chloroplast* CO_2 concentration , irrespective of the supply of CO_2 at ambient atmospheric CO_2 concentration

Denitrification microbial conversion of nitrate to gaseous nitrogen (N_2 and N_2O); nitrate is used as an electron acceptor

Desiccation tolerance tolerance of extreme water *stress*, with recovery of normal rates of metabolism shortly following rehydration

Desorption the reverse of *adsorption*

Diaheliotropism solar tracking in which the leaf or flower remains perpendicular to incident radiation

Differentiation cellular specialization

Diffuse porous wood in which wide and narrow xylem *vessel*s are randomly distributed throughout each annual growth ring

Diffusion net movement of a substance along a concentration gradient due to random kinetic activity of molecules

Diffusion shell zone of nutrient depletion around individual roots caused by active nutrient uptake at the root surface and *diffusion* to the root from the surrounding soil (see also *boundary layer*)

Disulfide bond covalent linkage between two sulfhydryl groups on cysteines

Divergent evolution naturally selected changes in related species that once shared a common characteristic, but have come to be different during the course of their evolution

Dormancy a characteristic of bud or seed, the degree of which defines what conditions should be met to make a bud grow or seed germinate

Dorsiventral having structurally different upper and lower surfaces (see also *isobilateral*)

Down-regulation decrease of the normal rate of a process, sometimes involving suppression of genes encoding enzymes involved in that process

Ecophysiology study of the physiological mechanisms by which organisms cope with their environment

Ecosystem ecological system that consists of all the organisms in an area and the physical environment with which they interact

Ecosystem respiration sum of plant and *heterotrophic respiration*

Ecotone environmental gradient

Ecotype genetically differentiated population that is restricted to a specific habitat

Ectomycorrhiza *mycorrhizal* association in some trees in which a large part of the fungal tissue is found outside the root

Efficiency rate of a process per unit plant resource

Elastic modulus force needed to achieve a certain reversible change in cell volume

Embolism filling of the xylem with water vapor and/or air *cavitation*

Emissivity coefficient that describes the thermal radiation emitted by a body at a particular temperature relative to the radiation emitted by an ideal black body

Endocytosis uptake of material into a cell by an invagination of the plasma *membrane* and its internalization in a *membrane*-bound vesicle

Endodermis innermost layer of root cortical cells that surrounds the vascular tissue; these cells are surrounded by a suberized *Casparian strip* that blocks *apoplastic* transport

Ephemeral short-lived

Epidermis outermost cell layer of an organ, typically covered by a *cuticle*

Epinasty downward bending of a plant organ; see also *hyponasty*

Epiphyte plant living on another plant as a support, without a *symbiotic* or parasitic association

Ethylene ethene (C_2H_4); a gaseous *phytohormone*; ethylene is, *e.g.*, a signaling compound when roots are exposed to *hypoxia*, inducing *aerenchyma* formation and petiole extension

Evapotranspiration water loss from an *ecosystem* by *transpiration* and surface evaporation

Evergreen Bearing foliage that persists and remains throughout the year, as opposed to *deciduous*

Exaptation features that now enhances fitness, but was not built by natural selection for its current role Exclusionprevention of net entry of a molecule; it may be due to low permeability for a molecule or to its *extrusion*

Excretion active secretion of compounds (*e.g.*, salt from leaves)

Exodermis outer cortical cell layer in roots, immediately below the *epidermis*; these cells are surrounded by a suberized *Casparian strip* in the radial and transverse cell walls made of mainly lignin with a variable amount of suberin, and suberin lamellae deposited in between primary cell walls and the plasma membrane; the exodermis blocks *apoplastic* transport

Expansin cell-wall enzyme involved in cell expansion

Extensin rigid cell-wall glycoprotein, rich in hydroxyproline, that represents 5–10% of the dry weight of most primary *cell wall*s; significant component of the secondary walls of sclerenchyma cells

Extinction coefficient coefficient describing the exponential decrease in irradiance through a compartment that absorbs radiation (*e.g.*, a leaf, a canopy, or a pigment in solution)

Extrusion ion transport from root cells to the external medium, dependent on respiratory metabolism

Exudate compounds released by plants (mostly by roots); also xylem or *phloem* fluid that appears when the stem is severed from the roots or a cut is made in the stem

Exudation release of *exudates*, or the appearance of fluid from cut roots or stems

Facilitation positive effect of one plant on another

Facultative CAM plants plants that photosynthesize by *Crassulacean Acid Metabolism* (CAM) during dry periods and by C_3 or C_4 *photosynthesis* at other times

Feedback influence of a product of a later step in a chain on an earlier step; fluctuations in rate of the process or concentration of metabolites are minimized with negative feedbacks or amplified with positive feedbacks

Feedforward response in which the rate of a process is affected before any deleterious effect of that process has occurred; for example, the decline in *stomatal conductance* before the *water potential* in leaf cells has been affected

Fermentation anaerobic conversion of glucose to organic acids or alcohol

Field capacity water content that a soil can hold against the force of gravity

Flavanols, flavines, flavones families of *flavonoids*

Flavonoid one of the largest classes of plant *phenolics*, in which two aromatic rings are connected by a carbon link to a third phenyl ring; representatives of this class play a role in the *symbiosis* between *rhizobia* and legumes, as *phytoalexins*, as *antioxidants*, in the colors of flowers and as *defense compounds*

Fluence response response to a dosage of light

Fluorescence *photons* emitted when excited electrons return to the ground state

Frost hardening *acclimation* of a plant as a result of exposure to low temperatures that make it *frost tolerant* (*e.g.*, hardening in autumn)

Frost hardiness/tolerance physiological condition that allows exposure to subzero temperatures without cellular damage

Geotropism growth response of plant organs with respect to gravity

Germination (of a seed) emergence of a part of the embryo through the seed coat, normally the radicle

Gibberellin class of *phytohormones*; the first gibberellin was found in the fungus *Gibberella fujikora*, from which these phytohormones derive their name; gibberellins are involved, *e.g.*, in the promotion of seed *germination*, stem extension and *bolting*

Giga- prefix denoting 10^9

Glass Solidlike liquid with an extremely high viscosity; examples of a glass are macaroni and 'glass' as we know it from everyday life (which is not a solid, but a fluid, as apparent from the gradually changing properties of glass when it gets old); glass formation, rather than the formation of ice crystals, is essential to prevent damage incurred by the formation of ice crystals

Glaucousness shiny appearance (of leaves), due to the presence of specific wax compounds-Glucoside (or glycoside)compound in which a side chain is attached to glucose by an acetal bond

Glucosinolate secondary sulfur-containing metabolite in Brassicaceae (cabbage family) which gives these plants a distinct sharp smell and taste

Glutathione tripeptide (γ-glutamyl-cysteinyl-glycine) that acts as a reducing agent, protecting the cell against oxidative *stress*, and guards against chemical toxicity, via modification of (modified) *xenobiotics*

Glycolipid *membrane* lipid molecule with a short carbohydrate chain attached to a hydrophobic tail

Glycolysis ubiquitous metabolic pathway in the *cytosol* in which sugars are metabolized to pyruvate and/or malate with production of ATP and NADH (when pyruvate is the end-product)

Glycophyte species restricted to nonsaline soils

Glycoprotein any protein with one or more covalently linked oligosaccharide chainsGlycoside (or glucoside)compound in which a side chain is attached to a sugar by an acetal bond

G protein intracellular *membrane*-associated proteins activated by several receptors

Grana stacked region of photosynthetic *membranes* (*thylakoids*) in *chloroplasts* that contains *photosystem* II with its *light-harvesting complex*

Gross photosynthesis amount of carbon dioxide assimilated in *chloroplasts*; it is measured as net *photosynthesis* plus dark *respiration*

Growth increment in mass, volume, length, or area of plants or parts thereof

Growth respiration amount of *respiration* required per unit increment in *biomass*; it is not a rate

Guard cells specialized *epidermal* cells that surround the *stomata* and regulate the size of the *stomatal pore*

Guttation water *exuded* by leaves due to *root pressure*

Halophyte species that typically grows on saline soils

Hartig net hyphal network of *ectomycorrhizal* fungi that have penetrated intercellularly into the cortex of a higher plant

Haustorium organ that functions in attachment, penetration and transfer of water and solutes from a host to a parasitic plant

Heartwood central mass of xylem in tree trunks not functioning in water transport; it often contains substances that prevent decay and has a darker color than the surrounding *sapwood*

Heat-shock protein protein produced upon heat or other *stresses*

Heavy metal metal with a mass density exceeding 5 g mL^{-1}

Heliotropism solar tracking; movement of a leaf or flower that follows the angle of incident radiation

Heme cyclic organic molecule that contains an iron atom in the center which binds O_2 in leghemoglobin and carries an electron in *cytochromes*

Hemicellulose heterogeneous mixture of neutral and acidic polysaccharides, which consist predominantly of galacturonic acid and some rhamnose; these *cell-wall* polymers coat the surface of *cellulose* microfibrils and run parallel to them

Heterodimer protein complex composed of two different polypeptide chains

Heterotrophic growth *growth* of plants or parts thereof which depend on carbon supplied by another organism or organ of the plant (see also *autotrophic growth*)

Heterotrophic respiration *respiration* by nonautotrophic organisms (see also *autotrophic respiration*)

Hexokinase enzyme catalyzing the *phosphorylation* of hexose sugars while hydrolyzing ATP; a specific hexokinase is involved in *sugar sensing*

Hilum Seed scar where the funiculus (the stalk of the ovule) was once attached

Historical filter historical factors that prevent a species from arriving at a site

Homeostasis tendency to maintain constant internal conditions in the face of a varying external environment; this term is frequently used incorrectly when describing major internal changes

Homodimer protein complex composed of two identical polypeptide chains

Hormesis a stimulatory effect of sub-inhibitory concentrations of any toxic substances on any organism

Hormone organic compound produced in one part of a plant and transported to another, where it acts in low concentrations to control processes (*phytohormone*)

Humic substances high-molecular-weight polymers with abundant *phenolic* rings and variable side chains found in *humus*

Humus amorphous soil organic matter

Hydraulic lift upward movement of water from deep moist soils to dry surface soils through roots along a *water potential* gradient

Hydraulic redistribution movement of water from moist soils to dry soils through roots along a *water potential* gradient

Hydrenchyma water-storing tissue; during dehydration of a plant, water is predominantly lost from the cells in the hydrenchyma, while other cells lose relatively less water

Hydrolysis cleavage of a covalent bond with accompanying addition of water, -H being added to one product and -OH to the other

Hydrophyte plant that grows partly or wholly in water, whether rooted in the mud, as a lotus, or floating without anchorage, as the water hyacinth

Hygrophyte species typically occurring on permanently moist sites; see also *mesophyte* and *xerophyte*

Hydrotropism morphogenetic response (of roots) to a moisture gradient

Hypodermis outermost layer of the root cortex, just under the epidermis, comprising one or more layers in width

Hyponasty Upward bending of a plant organ (see also *epinasty*)

Hypostomatous with *stomates* at the *abaxial* (lower) side of the leaf only

Hypoxia low oxygen concentration in (part of) a plant's environment

Immobilization nutrient absorption from the soil solution and sequestering by soil microorganisms

Incompatible interaction response of a resistant host to a virulent pathogen; interaction between pollen and pistil preventing sperm cells from reaching the ovule

Induced defense increased levels of plant *secondary metabolites* in response to herbivory or pathogen attack

Infiltration movement of water into the soil

Infrared radiation radiation with wavelengths between approximately 740 nm and 1 mm; *short-wave infrared* is emitted by the sun (<3 μm), *long-wave infrared* is emitted at Earth temperatures (>3 μm)

Interception acquisition of nutrients by roots as a result of growing through soil; the nutrients contained in the soil volume displaced by the growing root; precipitation water remaining in a plant canopy that does not reach the soil

Intercrop one crop plant grown in combination with at least one other crop on the same plot at the same time (*e.g.*, an annual crop grown between trees)

Interference competition *competition* mediated by production of *allelochemicals* by a plant

Intermediary cell *phloem* cell in plants with a *symplastic* pathway of *phloem* loading; sucrose moves from the *mesophyll* into these cells, where it is processed to form oligosaccharides that move to the sieve tube

Internal conductance/resistance *conductance/resistance* for transport of CO_2 between the substomatal spaces and its *carboxylation* at the site of *Rubisco* in the *chloroplast*

Ion channel / ion-selective channel pore in a *membrane* made by a protein, through which ions enter single file; channels are specific and either open or closed, depending on *membrane* potential or the presence of regulatory molecules

Isobilateral having structurally similar upper and lower surfaces (see also *dorsiventral*)

Isohydric maintaining a constant water status

Isoprene small unsaturated hydrocarbon, containing five carbon atoms (2-methyl-1,3-butadiene); volatile compound, synthesized from mevalonic acid and precursor of other isoprenoids; can be produced in large amounts by photosynthesizing tissue at high temperatures

Isotope discrimination alteration of the isotopic composition of an element via processes of *diffusion*, evaporation, and chemical transformation, due to small differences in physical and chemical properties of isotopes; typically discrimination against the rare (heavy) isotope

Isotope effect end-result of various processes that have different rate constants for different isotopes of the same element

Isotope fractionation process that occurs when different isotopes of the same element have different rate constants for the same reaction or process, or chain of reactions or processes

Isotropic similar in all directions

Jasmonic acid *secondary plant compound* [3-oxo-2-(2′-*cis*-pentenyl)-cyclopropane-1-acetic acid], named after its scent from jasmine; *stress* signaling molecule in plants as well as between plants

Juvenile phase stage in the life cycle of a plant between the *seedling* and *reproductive* phases; the vegetative phase in herbaceous plants; typically a period of rapid *biomass* accumulation

k_{cat} catalytic constant of an enzyme: rate of the catalyzed reaction expressed in moles per mole catalytic sites of an enzyme (rather than per unit protein, as in V_{max})

K_i concentration of an inhibitor that reduces the activity of an enzyme to half the rate of that in the absence of that inhibitor

K_m substrate concentration at which a reaction proceeds at half the maximum rate

K strategy suite of traits that enable a plant to persist in a climax community

Kranz anatomy specialized leaf anatomy of *C_4* species with photosynthetic *bundle sheath cells* surrounding vascular bundles

Krebs cycle *tricarboxylic acid cycle*; metabolic pathway in the *matrix* of the *mitochondrion* oxidizing acetyl groups derived from imported substrates to CO_2 and H_2O

Latent heat energy consumed or released by evaporation or condensation, respectively, of water (enthalpy of transformation); it results in respectively loss and gain of heat

Law of the minimum obsolete concept that plant growth is always limited at any point in time by one single resource; it is not valid in this strict sense

Leaf area index total leaf area per unit area of ground

Leaf area ratio (LAR) ratio between total leaf area and total plant *biomass*

Leaf conductance/resistance *conductance/resistance* for transport of CO_2 or H_2O (vapor) of a leaf (it includes the conductance/resistance for the *stomatal* and the *boundary layer* pathways in the case of H_2O, and additionally for the *internal mesophyll* pathway in the case of CO_2)

Leaf-mass density leaf dry mass per unit of fresh mass or volume (in the first case, the presence of intercellular air spaces is not taken into account)

Leaf mass per unit leaf area (LMA) leaf mass expressed per unit leaf area

Leaf mass ratio (LMR), or leaf mass fraction (LMF) ratio of leaf and whole plant *biomass*

Leaf turnover replacement of *senescing* leaves by new ones, not accounting for a change in leaf area

Lectin protein with noncatalytic sugar-binding domains; lectins are involved in defense and cellular interactions

Leghemoglobin Hemoglobin-like protein in nodules that associates with O_2 by means of a bound *heme* group

Light-compensation point irradiance level at which the rate of CO_2 *assimilation* in *photosynthesis* is balanced by the rate of CO_2 production in *respiration*

Light-harvesting complex complex of molecules of *chlorophyll*, accessory pigments, and proteins in the *thylakoid membrane* that absorbs quanta and transfers the excitation energy to the reaction center of one of the *photosystems*

Light reaction transfer of energy from absorbed light to ATP and NADP(H) in the photosynthetic *membrane* (*thylakoid*)

Light saturation (of photosynthesis) range of irradiances over which the rate of CO_2 *assimilation* is maximal and insensitive to level of irradiance

Lignan *phenolic* compound with antifungal, antifeeding, and antitumor activity; minor component in most plants and tissues, but quantitatively more important in the wood of some tree species (*e.g.*, redwood)

Lignin large amorphous poly*phenolic* polymer that confers woodiness to stems

Litter dead plant material that is sufficiently intact to be recognizable

Litter quality chemical properties of *litter* that determine its susceptibility to *decomposition*, largely determined by concentrations of *secondary metabolite*s and nutrients

Lockhart equation equation that describes cell expansion in terms of *turgor* pressure and *cell-wall* properties

Long-day plant plant whose flowering is induced by exposure to short nights

Long-wave infrared radiation with wavelengths larger then approximately 3 μm emitted at Earth temperatures

Lumen cavity, such as the space surrounded by the *thylakoid membrane* or the trap of *Utricularia* surrounded by cells

Luxury consumption uptake of nutrients above the rate that enhances plant growth rate

Lysigenous aerenchyma Gas-transport tissue in plants that is formed from spatially selective death of expanded cells (see also *schizogenous aerenchyma*)

Macronutrients inorganic nutrients that a plant requires in relatively large quantities: K, Ca, Mg, N, S, P

Macrosymbiont larger partner (*i.e.* higher plant) in a *symbiosis* with a microorganism

Maintenance respiration *respiration* required to maintain the status quo of plant tissues

Mass flow movement of substances at equal rates as the fluid or gas in which they occur (*e.g.*, transport of solutes in flowing water and CO_2 in flowing air)

Matric potential component of the *water potential* that is due to the interaction of water with capillaries in large molecules (*e.g.*, clay particles in soil)

Matrix a substance in which other structures or organelles are embedded; used for the compartment inside *chloroplast*s or *mitochondria*, not including the *membrane* system; also used for the substance in which cell-wall macromolecules are embedded

Mean residence time (of a nutrient in a plant) time a nutrient remains in the plant, between uptake by the roots and loss (*e.g.*, due to leaf shedding, consumption by a herbivore)

Mega- prefix (M) denoting 10^6

Membrane (*phospholipid*) bilayer that surrounds cells (*plasmalemma*) cell organelles, and other cell compartmens

Membrane channel transmembrane protein complex that allows inorganic ions, small molecules, or water to move passively across the lipid bilayer of a *membrane*

Membrane fluidity loose term to describe the extent of disorder and the molecular motion within a lipid bilayer; fluidity is the inverse of viscosity

Mesophyll photosynthetic cells in a leaf; in a *dorsiventral* leaf often differentiated in *palisade* and *spongy parenchyma* cells

Mesophyte plant that typically grows without severe moisture *stress*es (see also *hygrophyte* and *xerophyte*)

Metallophyte species that typically grows in areas with high concentrations of certain heavy metals in the soil

Micro- prefix (μ) denoting 10^{-6}

Microclimate local atmospheric zone where the climate differs from the surrounding atmosphere. (*e.g.*, near a leaf , within a forest and near a body of water)

Microfibril structural component in *cell walls*, consisting of bundles of around 50 *cellulose* molecules, that provides the tensile strength of the wall

Metallothionein low-molecular-mass metal-binding protein

Micronutrients inorganic nutrients that a plant requires in relatively small quantities: Mo, Cu, Zn, Fe, Mn, B, Cl (see *macronutrients*)

Microsymbiont smaller partner (*i.e.* microorganism) in a *symbiosis* with a higher plant

Mimicry resemblance of an organism to another organism or object in the environment, evolved to deceive predators, prey, pollinators etc.

Mineralization breakdown of organic matter releasing inorganic nutrients in the process

Mistletoe xylem-tapping stem parasite

Mitochondrion organelle in which part of the respiratory process (*tricarboxylic acid cycle*, respiratory electron transport) occurs

Monocarpic life cycle that ends after a single seed production event; the plant flowers only once during its life time, which can be after several years or even decades of vegetative growthMycorrhiza (plural is mycorrhizae or mycorrhizas)structure arising from a symbiotic association between a mycorrhizal fungus and the root of a higher plant (from the Greek words for fungus and root, respectively)

Mycorrhizal dependency (of plant growth) the ratio of dry mass of mycorrhizal plants to that of plants of the same genotype grown without under the same environmental conditions

Nano- prefix (n) denoting 10^{-9}

Net assimilation rate (NAR) rate of plant *biomass* increment per unit leaf area; synonym is *unit leaf rate* (ULR)

Net ecosystem carbon balance (NECB) net change in *ecosystem* carbon content due to all processes, including *photosynthesis*, *respiration*, loss of *biomass*, leaching, and lateral movements and transfers

Net ecosystem production (NEP) organic carbon accumulation that equals gross *photosynthesis* minus *ecosystem respiration* or *net primary production* minus *heterotrophic respiration*

Net primary production (NPP) quantity of new plant material produced annually per unit ground area including lost plant parts; equals *gross photosynthesis* minus *autotrophic respiration*

Nitrification microbial process that transforms ammonia, via nitrite, into nitrate

Nitrogen assimilation incorporation of inorganic nitrogen (nitrate, ammonium) into organic compounds

Nitrogen fixation reduction of dinitrogen gas to ammonium by specialized microorganisms

Nod factor product of *nod* genes required for successful *nodulation* in the legume-*rhizobium symbiosis*

***Nod* gene** *rhizobial* gene involved in the process of *nodulation*

Nodulation formation of nodules in symbiotic N_2-fixing plants

Nodulins class of plant proteins that are synthesized in legumes upon infection by *rhizobia*

Normalized difference vegetation index (NDVI) greenness index used to estimate above-ground net primary production from satellites, based on *reflectance* in the visible and near-*infrared*

Nuclear magnetic resonance (NMR) spectroscopy technique used to make a spectrum of molecules with a permanent magnetic moment, due to nuclear spin; the spectra are made in a strong magnetic field that lines up the nuclear spin in all the molecules; it can, for instance, be used to measure the pH in different cellular compartments in vivo because the site of the peak in a spectrum depends on the pH around the molecule

Nutrient productivity rate of plant *biomass* increment per unit nutrient in the plant

Nutrient resorption withdrawal of nutrients from a plant part during *senescence* before shedding

Nutrient-use efficiency growth per unit of absorbed plant nutrient which equals nutrient productivity times mean residence time of the nutrient; *ecosystem* nutrient-use efficiency is the ratio of *litter*fall mass to *litter*fall nutrient content (*i.e.* the amount of *litter* produced per unit of nutrient lost in *senescence*)

Opportunity costs diminished growth resulting from diversion of resources from alternative functions that might have yielded greater growth

Osmoregulation adjustment of the concentration of osmotic solutes in plant cells in response to changes in soil *water potential*

Osmosensor system involved in sensing a change in the concentration of solutes in cells; osmosensors were first extensively studied in yeasts and subsequently also identified in plants

Osmotic potential component of the *water potential* that is due to the presence of osmotic solutes; its magnitude depends on solute concentration

Oxidative pentose phosphate pathway metabolic pathway that oxidizes glucose and generates NADPH for biosynthesis

Oxidative phosphorylation formation of ATP (from ADP and P_i) coupled to a respiratory electron-transport chain in *mitochondria* and driven by a proton-motive force

Oxygenation the binding of O_2 to a substrate, without changing the redox state of O (*e.g.*, ribulose-1,5-bisphosphate by *Rubisco*); it also refers to the addition of O_2 to a medium (*e.g.*, water)

P50 the plant water potential corresponding to 50% loss of hydraulic conductivity of the xylem

Palisade mesophyll transversally oriented elongated photosynthetic cells at the *adaxial* side of a *dorsiventral* leaf

PAR *photosynthetically active radiation* (400–700 nm)

Paraheliotropism leaf movement that positions the leaf more or less parallel to the incident radiation throughout the day

Parent material rock and other substrates that generate soils through weathering

Pectin *cell-wall* polymer rich in galacturonic acid

Perennial species whose individuals typically live more than two years; the length of the life cycle can be indeterminate or end after a single seed production event (*monocarpic*)

Peribacteroid membrane plant-derived *membrane* that surrounds one or more bacteroids in root nodules

Pericarp matured ovulary wall in a seed

Pericycle layer of outermost stelar cells, adjacent to the *endodermis*

Permanent wilting point soil *water potential* at which a plant can no longer absorb water from the soil; it is species-specific but is generally taken to be −1.5 MPa

Peta- prefix (P) denoting 10^{15}

Phenol compound that contains a hydroxyl group on an aromatic ring

Phenolics aromatic hydrocarbons, many of which have antimicrobial and antiherbivore properties

Phenology time course of periodic developmental events in an organism that are typically seasonal (*e.g.*, budbreak or flowering)

Phenotypic plasticity range of variation of a trait in a genotype as a result of growth in contrasting environmental conditions

Phenylalanine ammonia lyase enzyme that catalyzes the fist step in the conversion of the amino acid phenylalanine into *phenolics*

Phloem long-distance transport system in plants for *mass flow* of carbohydrates and other solutes

Phosphatase enzyme hydrolyzing organic phosphate-containing molecules

Phospholipid major category of *membrane* lipids, generally composed of two fatty acids linked through glycerol phosphate to one of a variety of polar groups

Phosphorylation process involving the covalent binding of a phosphate molecule; many enzymes change their catalytic properties when phosphorylated

Photodamage/photodestruction damage to / destruction of components of the photosynthetic apparatus as a result of exposure to high irradiance, frequently in combination with other *stress* factors; the result is *photoinhibition*

Photoinhibition decline in *photosynthetic efficiency* upon exposure to high irradiance; the decline can be transient (less than 24 hours), which is related to protection of the photosynthetic apparatus, or it can be longer lasting, which implies *photodamage*

Photomorphogenesis Plant development affected by light; generally under control of *photoreceptors*

Photon discrete unit of light that describes its particle-like properties (quantum); light also has wavelike properties

Photon flux density (PFD) A measure of the level of irradiance in the (near) visible spectral region; it is expressed as *photon*s incident on a (horizontal) plane per unit of time; photosynthetic *photon* flux density (PPFD) refers to the *photosynthetically active* part of the spectrum; see also *quantum flux density*

Photoperiod length of the daylight period each day

Photoperiodic responding to the length of the night

Photoreceptor A protein with chromophore that absorbs light in a specific spectral region; it is typically the start of a *signal-transduction pathway* leading to *photomorphogenetic* events

Photorespiration production of CO_2 in the metabolic pathway that metabolizes the products of the *oxygenation* reaction catalyzed by *Rubisco*; see also *respiration*

Photosynthesis process in which light energy is used to reduce CO_2 to organic compounds; occurs in *chloroplast*s in higher plants and algae

Photosynthetic efficiency *efficiency* of the use of light for *photosynthesis* (*quantum yield*); mostly used in conjunction with *chlorophyll fluorescence*

Photosynthetic nitrogen-use efficiency rate of *photosynthesis* expressed per unit (organic) nitrogen in the photosynthesizing tissue

Photosynthetic quotient ratio between CO_2 uptake and O_2 release in *photosynthesis*

Photosynthetic water-use efficiency ratio between photosynthetic carbon gain and *transpiration*al water loss

Photosynthetically active radiation (PAR) radiation used to drive *photosynthesis* (400–700 nm); the spectral region is similar to that of visible light, but the spectral sensitivity is different from that of the human eye.

Photosystem unit comprising pigments and proteins where the excitation energy derived from absorbed *photon*s is transferred to an electron; there are two types of photosystems (I and II) that are embedded in the photosynthetic *membrane* (*thylakoid*)

Phototropism growth of plant organs in response to the directional component of light perceived by the *blue-light photoreceptor* phototropin

Phreatophyte plant species that accesses deep layers of water

Phyllosphere immediate surroundings of a leaf

Phylogenetic constraint genetic constitution of a population or taxon that restricts evolutionary change; it can prevent the development of particular traits

Physiological filter physiological limitations due to intolerance of the physical environment, which prevent survivorship of plant species that arrive at a site

Phytate calcium salt of *myo*-inositol hexakisphosphate; organic P-storage compound in seeds and *endodermis* of some plant species and major fraction of organic P in soils

Phytoalexin plant defense compound against microorganism, whose synthesis is triggered by components of microbial origin

Phytoanticipin *constitutive*ly produced plant *defense compound* against microorganism

Phytochelatin sulfur-rich peptide which binds (heavy) metals

Phytochrome *photoreceptor* absorbing red or far-red radiation (depending on its configuration); this pigment is involved in the perception of the presence of light, light quality and daylength

Phytohormone plant compound produced in one part of the plant and having its effect in another part at minute concentrations (nanomolar and picomolar range)

Phytomining Extracting naturally occurring metals from soils, by utilizing the uptake capacity of plants that accumulate these metals

Phytoremediation use of green plants to remove, contain, or render harmless environmental contaminants

Phytosiderophore iron-chelating organic molecule in grasses

Pico- prefix (p) denoting 10^{-12}

Pioneer species that is a major component of a vegetation at early stages of *succession*; used in contrast to *climax species*

Pit narrow channel through the thick secondary walls of *vessel* elements in xylem

Pit-membrane relatively thin structure in each *pit* which is formed from the primary *cell wall* and consists of a dense network of hydrophilic *cellulose* polymers

Plant-soil feedback a plant response involving (i) species-specific changes to soils caused by plants, and (ii) plant species-specific responses to these changes; the feedback can be positive or negative

Plasmalemma plasma *membrane*; external membrane surrounding the *cytoplasm*

Plasmodesma(ta) minute *membrane*-lined channels that traverse the plant *cell wall* to provide a *cytoplasm*ic pathway for transport of substances between adjacent cells

Plasmolysis separation of the *cytoplasm* from the *cell wall* due to water loss; only happens in water, not in air

Plasticity the ability of an organism to adjust depending on the external environment

Pneumatophore specialized portion of the root that emerges from water-logged soils, believed to be used for gas exchange

Poikilohydric plants or plant parts (seeds, pollen) that can dry out without losing their capacity to function upon rehydration

Post-illumination CO_2 fixation CO_2 fixation that occurs briefly after a light pulse

ppb part per billion; 1 nmol mol^{-1}; 1 ng g^{-1}; nl l^{-1} (not an acceptable SI unit)

ppm part per million; 1 μmol mol^{-1}; 1 μg g^{-1}; μl l^{-1} (not an acceptable SI unit)

Pressure chamber chamber in which a plant or part thereof can be pressurized; it is, among others, a part of the equipment used to determine the *water potential* in the xylem of plant stems

Pressure potential pressure component of the *water potential*; it is positive in nonplasmolyzed living plant cells (*turgor*) and negative in the xylem of transpiring plants (suction)

Pressure probe microcapillary that is injected in a living cell to measure cell *turgor*

Protease/proteinase protein-hydrolyzing enzyme

Protein turnover breakdown and synthesis of proteins that does not account for a change in protein concentration

Proteoid root (=cluster root) cluster root; a short-lived dense package of root hairs that exudes nutrient solubilizing compounds; the name stems from the family of the Proteaceae

Protocarnivory capability of plants to digest arthropods or other organic items that are trapped on sticky surfaces or in "tank" traps and absorb the breakdown products of the trapped material

Proton cotransport transport mechanism that allows movement of a compound against the electrochemical gradient for that molecule, using the *proton-motive force*

Proton-motive force driving force across cell *membrane*s due to a membrane potential and/or proton gradient

Protoplasmic streaming flow of the *cytoplasm*, mediated by the cytoskeleton

Protoplast cell *membrane* with *cytoplasm* and cell organelles inside; it is isolated after enzymatic removal of the *cell wall*

Pulvinus 'joint' in a petiole that allows the movement of a leaf, due to transport of ions between cells in the pulvinus, followed by changes in *turgor* (*e.g.*, in many legumes)

Q_{10} change in rate of a reaction in response to a 10°C change in temperature

Qualitative defense compound highly toxic secondary plant metabolite that protects against attack by herbivores at low concentration

Qualitative long-day plant plant that will not flower unless the length of the night gets below a critical value

Qualitative short-day plant plant that will not flower unless the length of the night gets above a critical value

Quantitative defense compound secondary plant metabolite that gives some protection against attack against a broad range of herbivores when present in large amounts

Quantitative long-day plant plant whose flower induction is promoted by exposure to short nights

Quantitative short-day plant plant whose flower induction is promoted by exposure to long nights

Quantum flux density a measure of the level of irradiance; it is expressed as quanta incident on a (horizontal) plane per unit of time; see also *photon flux density*

Quantum yield moles of CO_2 fixed or O_2 evolved in *photosynthesis*, or electrons transported in the photosynthetic *membrane*, per mole of quanta absorbed; in the context of gas exchange often restricted to the linear, light-limited part of the *photosynthesis* – irradiance curve; when measuring chlorophyll fluorescence it refers to the full range of photosynthetic irradiance

Recalcitrant organic matter soil organic matter that takes a long time to be decomposed

Recalcitrant seeds seeds that do not tolerate desiccation and are consequently difficult to store for longer periods; they typically germinate shortly after dispersal without first going through a phase of *dormancy*

Receptor protein with a high affinity and specificity for a signaling molecule (*e.g.*, a *phytohormone*), which is the start of a *signal-transduction pathway*)

Reductive pentose phosphate pathway metabolic pathway that utilizes NADPH produced in the light reaction of *photosynthesis* and produces triose phosphate

Reflectance fraction of radiation incident on a surface that is reflected (*e.g.*, a leaf, or the Earth surface)

Relative humidity water vapor concentration of air relative to the maximum water vapor concentration at that temperature

Relative water content water content of a plant tissue relative to the water content at full hydration

Reserve formation build-up of storage products that result from diversion of plant resources to storage from alternative *allocations*, such as growth

Resistance (against stress) plant capacity to minimize the impact of *stress* factors in the environment, either by the presence of tolerance mechanisms or by *avoidance* of the stress

Resorption translocation of nutrients and soluble organic compounds from senescing tissues prior to abscission

Resource competition use of the same pool of growth-limiting resources by two or more plants

Respiratory quotient ratio between CO_2 release and O_2 consumption in *dark respiration*

Resurrection plant plant that withstands complete dehydration and resumes functioning upon rehydration

Rheology study of the deformation of matter at a mesoscopic or macroscopic scale

Rhizobia collective term for bacteria that fix N_2 in *symbiosis* with legumes or *Parasponia* of the genera *Rhizobium*, *Bradyrhizobium, Sinorhizobium, Mesorhizobium* and *Azorhizobium*

Rhizosphere zone of soil influenced by the presence of a root

Ring porous wood in which xylem *vessel*s produced early in the growing season are longer and wider than those produced in late wood, adding to the distinction of annual growth rings

Rock phosphate Inorganic phosphate compound with very low solubility

Root density total root length per unit soil volume

Root-mass density see *biomass density*

Root mass ratio (RMR) ratio between root *biomass* and total plant biomass, synonym is root mass fraction (RMF)

Root pressure positive *water potential* in the xylem due to ion transport into the xylem of roots and subsequent osmotic uptake of water

Root shoot ratio ratio between root and shoot *biomass*

Root turnover replacement of (old) roots by new ones, not accounting for a change in the total amount of roots

Roughness unevenness of a surface that creates turbulence and enhances convective exchange between the surface and the atmosphere

Ribosomal RNA the major organic P fraction in leaves that is associated with ribonucleic acids (RNA) in ribosomes

Rubisco ribulose-1,5-bisphosphate carboxylase/oxygenase; enzyme catalyzing the primary step in the Calvin-cycle, the attachment of CO_2 to the CO_2-acceptor molecule Ribulose-1,5-bisphorphate (RuBP); also catalyses the *oxygenation* of RuBP

Rubisco activase protein catalyzing the carbamylation of *Rubisco* that regulates its activity; chaperone protein protecting the catalytic sites of Rubisco at extreme temperatures and in darkness

Ruderal species species that flourish on disturbed sites and complete their life cycle relatively rapidly

Run-off gravitational water loss from an *ecosystem*; the difference between precipitation and evapotranspiration (surface and groundwater run-off)

Saline soils soils with high salt concentration

Salt gland group of cells involved in salt *excretion*

Saponin secondary plant compound with soap-like properties

Sapwood most recent wood in the xylem of a tree trunk, with open xylem conduits that still function in water transport; it has often a lighter color than the innermost *heartwood*

Scarification breaking, scratching or softening the seed coat to allow moisture penetration

Schizogenous aerenchyma Gas-transport tissue in plants that is the outcome of highly regulated and species-specific patterns of cell separation and differential cell expansion that creates spaces between cells (see also *lysigenous aerenchyma*)

Sclerenchyma tissue that can consist of two types of cells: sclereids and fibers, which both have thick secondary walls and are frequently dead at maturity

Scleromorph containing a relatively large amount of *sclerenchyma*

Sclerophyllous leaves that are *scleromorph*; they are thick, tough and have a thick *cuticle*

Secondary metabolites compounds produced by plants that are not essential for normal growth and development; they are frequently involved in the interaction with a plant's *biotic* and *abiotic* environment

Seed quiescence state of seeds that occurs when it fails to germinate, because the external environmental conditions are unfavorable; this is different from true seed *dormancy*

Seedling phase recently germinated plants that still have their cotyledons attached

Self-thinning reduction in plant density due to increased mortality as a result of *competition*

Senescence programmed series of metabolic events that involve metabolic breakdown of cellular constituents and transport of the breakdown products out of the senescing organ that ultimately dies

Serotinous state of cones on a tree that remain closed with release of seeds delayed or occurring gradually

Serpentine soil soils that naturally contain high levels of various heavy metals and magnesium, but low concentrations of calcium, nitrogen, and phosphate

Short-day plant plants whose flowering is induced by exposure to long nights

Signal-transduction pathway chain of events by which a chemical messenger (*e.g.*, a *phytohormone* or other signaling molecule) or physical (*e.g.*, radiation) signal is sensed and relayed into a chain of molecular events that lead to a response; it can operate at the cellular or whole-plant level, involving long-distance transport of the signal

Sink part of the plant that shows a net import of a compound (*e.g.*, a root is a sink for carbohydrates and a leaf is a sink for inorganic nutrients); see also *source*

Soil texture particle size distribution in a soil, e.g. the relative proportions of sand, silt, and clay

Solar tracking movement of a leaf or flower that positions this organ at a more or less constant angle relative to the incident radiation throughout the entire day

Source part of a plant that shows a net export of a compound (*e.g.*, a leaf is a source for carbohydrates and a root is a source for inorganic nutrients); see also *sink*

Specific leaf area (SLA) leaf area per unit leaf dry mass

Specific leaf mass leaf dry mass per unit leaf area (LMA)

Specific root length (SRL) root length per unit root dry mass

Spongy mesophyll loosely packed photosynthetic cells at the *abaxial* side of a *dorsiventral* leaf

Stomata structures in the leaf *epidermis* formed by specialized epidermal cells; mostly the term refers to the pores, as well as to the stomatal apparatus

Stomatal pore opening in the leaf *epidermis* between two guard cells of *stomata*

Starch polymer of glucose; storage compound in plastids

Stomatal conductance/resistance *conductance/resistance* for transport of CO_2 or water vapor through the stomata

Storage build-up of a metabolically inactive pool of compounds that can subsequently serve to support growth or other physiological functions; see *reserve formation*

Strategy complex suite of traits allowing *adaptation* to a particular environment

Stratification breaking of seed *dormancy* by exposure of moist seeds to low temperatures

Stress environmental factor that reduces plant performance

Stress protein protein that is produced only or in greater quantities upon exposure to *stress*

Stress response the immediate detrimental effect of *stress* on a plant process causing reduced plant performance

Stroma *matrix* within the *chloroplast* containing Calvin-cycle enzymes and in which the *thylakoid membrane* system is suspended

Strophiole (=caruncle) an outgrowth of a seed coat, near the *hilum*; preformed weak site in the seed coat that allows entry of water when sufficiently weathered

Suberin polymer containing long-chain acids, hydroxy acids, alcohols, dicarboxylic acid and *phenol*s; the exact structure is not fully understood; cell-wall component in many locations (*e.g.*, *Casparian strip*, corky periderm)

Subsidiary cell epidermal cell type around many stomata, located distally and laterally to a guard cell

Succession directional change in plant species composition resulting from biotically driven changes in resource supply

Succulence thick fleshy state of herbaceous tissues due to high water content; it is quantified as the volume of water in the leaf at a *relative water content* of 100% divided by the leaf area

Succulent plant with tissue of high degree of *succulence*

Sugar sensing the perception of internal sugar concentrations that is at the start of a *signal-transduction pathway*

Summer annual species whose seeds germinate after winter and completes its life cycle before the start of the next winter

Sunfleck short period of high irradiance that interrupts the background of low diffuse radiation in and under leaf canopies caused by direct sunlight that penetrates small holes in the canopy

Supercooling refers to the noncrystalline state of water at sub-zero temperatures

Supply function equation describing CO_2 *diffusion* from the atmosphere into the leaf, supplying substrate for *photosynthesis*

Symbiosis intimate association between two organisms of different species (in this text the term is used when both symbionts derive a long-term selective advantage)

Symbiosome *membrane*-surrounded space containing one or more *rhizobia* in an infected cell of a root nodule in a legume

Symplast space comprising all the cells of a plant's tissues connected by plasmodesmata and surrounded by a plasma *membrane*.

Symplastic phloem loading occurs in plants in which photosynthates moves from the *cytoplasm* of the *mesophyll* cells of the leaves, via *plasmodesmata*, to intermediary cells; after chemical transformation into oligosaccharides, these move, again via plasmodesmata, to the sieve tubes

Symport cotransport of one compound in one direction coupled to transport of another compound (mostly H^+) in the same (uniport) or opposite (*antiport*) direction

Systemic resistance *resistance* that is induced by a herbivore or a microorganism at a location that differs from the plant part that has been primarily affected; the organisms that induce the resistance may be parasitic or have a growth-promoting effect

Tannin class of protein-precipitating polymeric *phenolic* secondary plant compound; typically a *quantitative defense compound*

TCA cycle *Tricarboxylic acid cycle*

Terpenoid class of *secondary plant compounds* containing C and H, produced from the precursor mevalonic acid

Testa seed coat

Thermogenic respiration *respiration* that increases the temperature of an organ, such a the flowers of *Arum* lilies

Thigmomorphogenesis altered growth of plant organs in response to a physical force (touch, wind, vibrations, rain, turbulent water flow)

Thylakoid photosynthetic *membrane* suspended in the *stroma* in *chloroplast*s; it encloses a lumen and contains the photosynthetic pigments, electron-transport chain components and *ATP-synthase*

Tissue-mass density dry mass per unit volume of a tissue

Tissue tension result of differences in *turgor* and/or *cell wall* elasticity between different cells in a tissue or organ; the tension is relaxed when the organ is cut, resulting in deformation; tissue tension plays an important role in the closing mechanism of the carnivorous Venus fly trap (*Dionaea*)

Tolerance endurance of unfavorable environmental conditions

Tracheid cell type in the xylem

Trade-off balancing of investment in mutually exclusive traits (*e.g.*, protective structures *vs.* photosynthetic machinery in leaves)

Transfer cell cell involved in transport that has a proliferation of the plasma *membrane* causing surface enlargement (*e.g.*, in the *phloem* of plants using the *apoplast*ic *phloem*-loading pathway, in the *epidermis* of aquatic plants using bicarbonate)

Translocation transport of solutes through the *phloem*

Transmittance fraction of radiation incident on a body that passes through the body; mostly used with reference to leaves

Transpiration water loss from leaves or whole plants due to evaporation from within a leaf or other plant parts

Tricarboxylic acid cycle (TCA cycle) conversion of malate or pyruvate to CO_2 within the *mitochondria*

Trichome epidermal hair on a leaf or stem

Trypsin protein-hydrolyzing enzyme (in animals)

Turgor positive hydrostatic pressure in live plant cells

Uncoupler chemical compound that enhances the *membrane conductance* for protons and so uncouples electron transport from *phosphorylation*

Unit leaf rate (ULR) synonym for *net assimilation rate (NAR)*

Up-regulation increase in the normal rate of a process, sometimes involving increased transcription of genes encoding enzymes involved in that process

V_{max} substrate-saturated rate of a chemical conversion catalyzed by an enzyme (expressed per unit protein, rather than per mole catalytic sites as in k_{cat})

Vacuole *membrane*-bound cell compartment filled with water and solutes; among others used for storage of sugars, nutrients, and *secondary metabolite*s

Vapor pressure deficit (VPD) difference in actual vapor pressure and the vapor pressure in air of the same temperature and pressure that is saturated with water vapor

Vapor pressure difference (Δw) difference in vapor pressure between the intercellular spaces and the atmosphere

Vegetative reproduction asexual reproduction of plants though detachment of a part that develops into a complete plant; clonal growth

Vegetative storage protein proteins accumulating in vegetative plant parts (leaves and hypocotyls) at a high supply of nitrogen (*e.g.*, in *Glycine max*)

Vernalization induction of flowering by exposure to low temperatures (from the Latin word ver = spring)

Vessel water-conducting element of the xylem

Viscoelastic creep mixture of viscous and elastic processes during *cell-wall* expansion; also unsavory character met in dark alleys

Viviparous seeds seeds that germinate prior to abscission from the maternal plant (*e.g.*, mangrove species)

Wall loosening refers to the process during which covalent or noncovalent bonds between *cellulose* microfibrils and other macromolecules are broken, so that the cell under *turgor* can expand

Water channel pore for water transport in *membrane*s consisting of a specialized protein (*aquaporin*); water moves single file

Water potential chemical potential of water divided by the molar volume of water, relative to that of pure water at standard temperature and pressure

Water status loose term referring to aspects of the plant's *relative water content*, *turgor*, *water potential*, etc.

Water stress *stress* due to shortage of water

Water-use efficiency ratio between the gain of (above-ground) *biomass* in growth or CO_2 in *photosynthesis* and *transpiration*al water loss

Wilting point *water potential* at which *turgor* pressure is zero

Winter annual species whose seeds germinate before or in winter and completes its life cycle before the start of the next summer; typically found in Mediterranean-type climates

Xanthophyll cycle chemical transformations of a number of carotenoid molecules in the *chloroplast* that avoid serious damage by excess radiation

Xenobiotic potentially toxic chemical that is found in an organism where it is normally not occurring; can be restricted to synthetic compounds, but is also used in a wider sense

Xerophyte plant that typically grows in dry environments, see also *mesophyte* and *hygrophyte*

Yield coefficient a proportionality constant in the Lockhart equation that refers to the plasticity of *cell wall*s

Yield threshold minimum *turgor* pressure for cell expansion

Zeatin a *phytohormone* belonging to the *cytokinins*, the name stems from *Zea mays* (corn), from which it was first isolated

Index

H. Lambers, R. S. Oliveira, *Plant Physiological Ecology*, https://doi.org/10.1007/978-3-030-29639-1